

ENERGY: SOURCES, CONVERSION & UTILIZATION

Ahmed Ghoniem

Lecture # 1

Feb 3, 2020

- Subject Themes
- Sources and consumption, now and then
- Environmental Impact, CO₂
- Solutions and Scaling
- Technologies

Ghoniem, A.F., Needs, resources and climate change: Clean and efficient conversion technologies, *Progress Energy Combust Science*, 37, 2011, pp. 15-51. <http://dx.doi.org/10.1016/j.pecs.2010.02.006>

Ghoniem, A.F., Energy Conversion Engineering, Chapter 1.

FUNDAMENTALS OF ADVANCED ENERGY CONVERSION

2.60 (U), 2.62 (G), 10.390J (U) 10.392J (G), 22.40J (G)

Instructor: Ahmed Ghoniem

TA: Omar Labban

Spring 2020, MW 12:30-2:30 PM

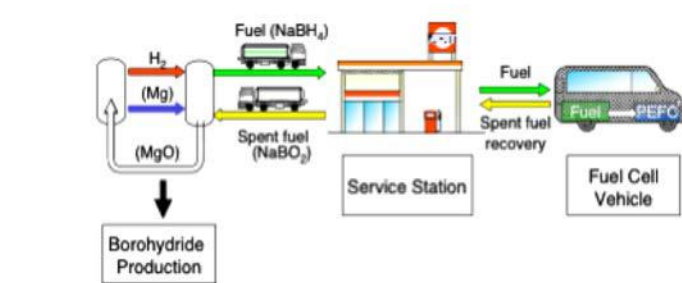
Fundamentals of Energy conversion
Engineering: processes and systems utilizing fossil and renewable energy (solar, wind biomass, geothermal) and nuclear resources, with emphasis on efficiency and environmental impact especially CO₂.

Prereq.: 2.006/equivalent or permission of instructor.

Grading: Homework and term project

U and G students are graded separately.

Energy conversion engineering: power for electricity production; conventional, renewable and hybrid. Direct conversion & fuel cells, Synthetic and biofuels. Solar, wind and biomass. Storage. “Hydrogen & electric economies”. CO₂ capture and reuse. Life Cycle Analysis: efficiency and emissions.



SUBJECT THEMES 1

We cover concepts and tools used to analyze conversion of energy sources into useful forms, primarily electricity and fuels, using different technologies. For instance, the conversion of the chemical energy to carbon free (H_2) fuels for transportation, or biomass to ethanol.

We discuss converting chemical energy to electricity, covering fuel cells and turbines. We compare options, e.g., biomass to electricity for electric cars, or biomass to ethanol for a flex fuel engines. Comparisons are based on overall efficiency and CO_2 emissions (WTW or LCA).

An important theme is “ CO_2 ” and what to do about it: use carbon capture, reuse and storage, nuclear or renewables?

We discuss capturing heat from the sun, geothermal wells or nuclear reactors, and how it is used to produce electricity or fuels.

We discuss hydrogen production using thermolysis or electrolysis.

SUBJECT THEMES 2

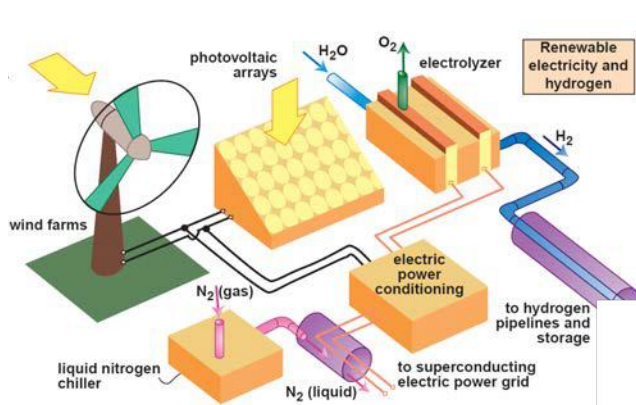
We discuss fundamentals of battery technology for electricity storage.

We discuss the challenges for hydrogen as a transportation fuel and how it can be enabled.

We talk about carbon capture in power and fuel production, the technical advantages using different technology pathways.

We cover integrated and hybrid systems and how combining different conversion technologies can improve efficiency : combined cycles, hybrid solar-NG, etc., also how integrating storage can further improve the system.

We talk about the difference between concentrated generation and distributed generation,

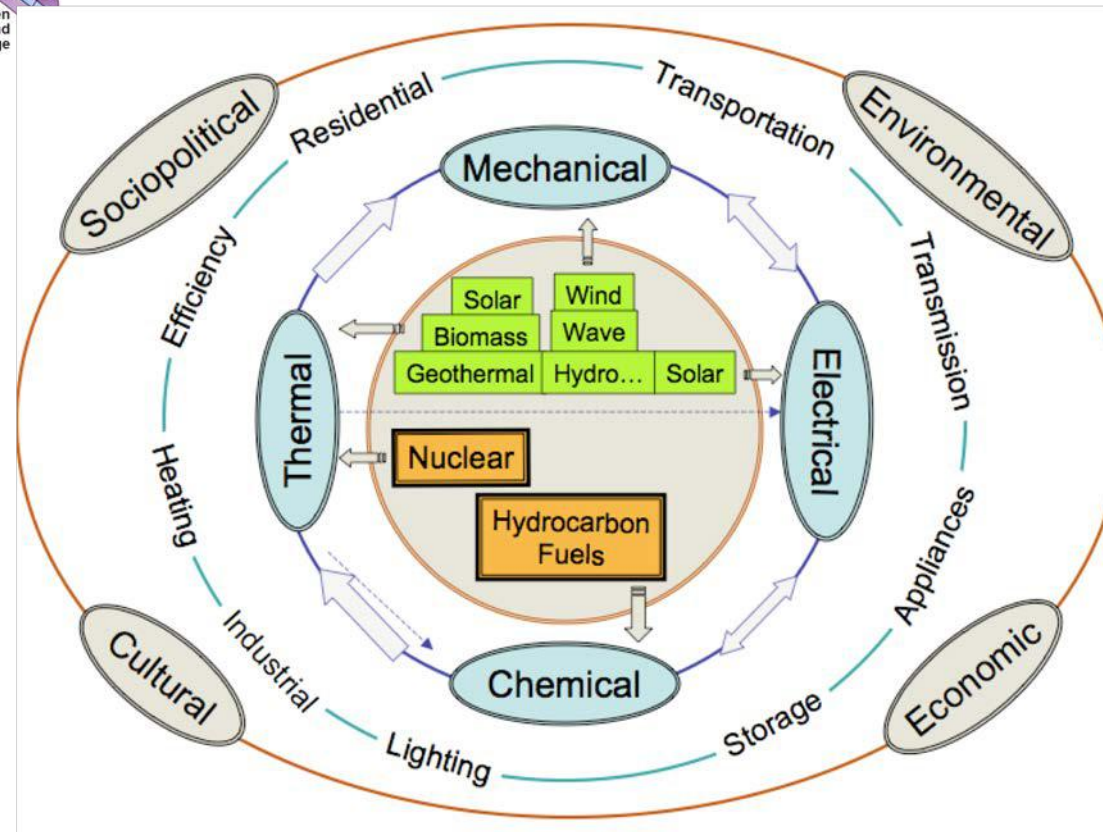


Hoffert et al., Science, 298 (2002)

© AAAS. All rights reserved. This content is excluded from our Creative Commons license. For more information, see <https://ocw.mit.edu/fairuse>.

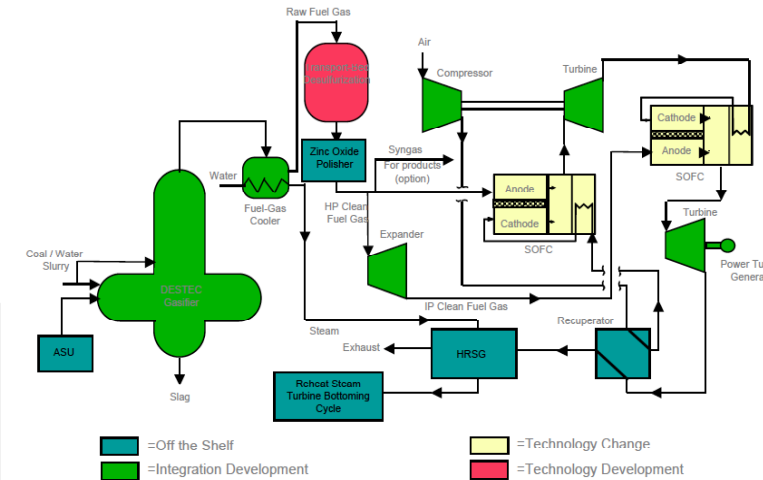


Thermodynamics of the Corn-Ethanol Biofuel Cycle



© Informa UK Limited. All rights reserved. This content is excluded from our Creative Commons license. For more information, see <https://ocw.mit.edu/fairuse>.

Tad W. Patzek (2004) "Thermodynamics of the Corn-Ethanol Biofuel Cycle", *Critical Reviews in Plant Sciences*, 23:6, 519-567, DOI: [10.1080/07352680490886905](https://doi.org/10.1080/07352680490886905).



Fuel cell handbook. Office of fossil energy.

Image courtesy of DOE.

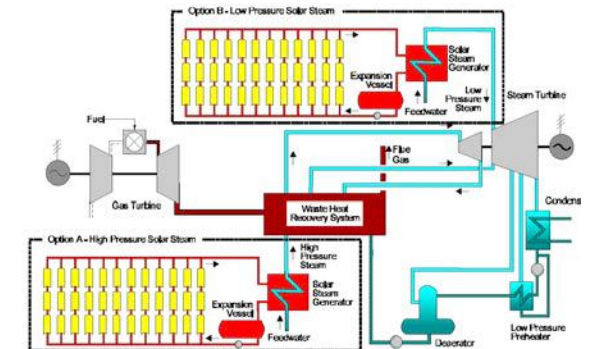


Figure 2. Integrated Solar Combined Cycle System [1].

Mancini TR. An overview of concentrating solar power.

Image courtesy of DOE.

#	Date	Topic		HW	Project
1	M 02/03	Introduction, Energy Challenges			
2	W 02/5	Thermodynamics, Availability	}		
3	M 02/10	Mixtures and Separation		HW 1, posted	
4	W 02/12	Applications, EES-1	}		Project posted
5	T 02/18	Chemical Thermodynamics		HW 1, DUE	
6	W 02/19	Conversion and Equilibrium		HW 2, posted	
7	M 02/24	Gasification, Reforming, EES-2	}		projects selected
8	W 02/26	Electrochemistry		HW 2, DUE	
9	M 03/02	Fuel Cells		HW 3, posted	
10	W 03/04	Electrolysis, H ₂ & Storage	}		
11	M 03/09	Batteries		HW 3, DUE	
12	W 03/11	Photovoltaics		HW 4, posted	
13	M 03/16	Power plants I	}		
14	W 03/18	Power Plants II		HW 4, DUE	

#	Date	Topic		HW	Project
15	M 03/30	Geothermal/Solar Thermal	}		Mid Terms Report
16	W 04/01	System Modeling & Aspen		HW 5, posted	
17	M 04/06	Energy & Materials			
18	W 04/08	Gas separation	}	HW 5, Due	
19	M 04/13	CCS I		HW 6, posted	
20	W 04/15	CCS II			
21	W 04/22	Wind		HW 6, DUE	
22	M 04/27	Biomass I			
23	W 04/29	Biomass II			
24	M 05/04	Storage			
25	W 05/06	Nuclear Energy			Final Report due, 05/08
26	M 05/11	PROJECT PRESENTATIONS			

Please note that, from experience, some small changes in the ordering of the lectures or the topics may be used during the semester according to the pace and coverage, but the HW and project schedule will remain fixed.

- Lectures are 2x50 min (with a break in between)
- PPTs will be posted lecture by lecture
- HW every other week, last two weeks of the semester dedicated to finishing the project

Grading policy:

U & G are graded separately.

66% Homework (6x11) + 34% Project (total).

Term project: 9% midterm report + 20% final report + 5% presentation

ENERGY CONVERSION ENGINEERING
FOR LOW CO₂ POWER & FUELS:
FUNDAMENTALS AND SYSTEMS FOR CCS AND RENEWABLES;
WITH FOCUS ON EFFICIENCY AND INTEGRATION

1. Low carbon Energy?
2. Thermodynamics: Availability
3. Chemical Thermodynamics:
4. Electrochemical Thermodynamics,
5. Gas Turbine Cycles
6. Rankine Cycles
7. Fuel Cells, SOFCs
8. Combined and Hybrid Cycles
9. Solar Thermal & Geothermal
10. Gas Separation
11. Low CO₂, NG
12. Coal
13. Low CO₂, Coal
14. Biomass

ENERGY STUDIES MINOR

Did you know?

2.60J Fundamentals of Advanced Energy Conversion fulfills an Engineering in Context requirement

The world's energy and climate challenges require innovative problem-solvers like you!

*Discover and prepare for an exciting
career leading the transition to
a clean energy future.*

CORE CURRICULUM

Science Foundations

Choose one of the following options:

Option 1 (one subject)

8.21 Physics of Energy¹

Option 2 (two subjects)

select a combination from the following list (subject titles below):

3.012 and 6.007

3.012 and 12.021

6.007 and 2.005

6.007 and 5.60

6.007 and 12.021

12.021 and 2.005

12.021 and 5.60

2.005 Thermal-Fluids Engineering I

3.012 Fundamentals of Materials Science and Engineering

5.60 Thermodynamics and Kinetics

6.007 Electromagnetic Energy: From Motors to Solar Cells

12.021 Earth Science, Energy, and the Environment

Technology/Engineering In Context

Choose one of the following:

2.60J Fundamentals of Advanced Energy Conversion

4.42J Fundamentals of Energy in Buildings¹

22.081J Introduction to Sustainable Energy

Social Science Foundations

Required subjects:

select one of the following:

14.01 Principles of Microeconomics

15.0111 Economic Analysis for Business Decisions

Choose one of the following options:

Option 1 (one subject)

select one of the following:

14.44J Energy Economics and Policy

15.031J Energy Decisions, Markets, and Policies¹

Option 2 (two subjects)

select one subject from each of the following groups:

GROUP A

14.42 Environmental Policy and Economics

15.026J Global Climate Change:
Economics, Science, and Policy

GROUP B

1.801J Environmental Law, Policy, and Economics:
Pollution Prevention and Control¹

11.162 Politics of Energy and the Environment¹

22.04J Social Problems of Nuclear Energy

Students who take more than the required subjects from any of the core curriculum subject lists may count the additional coursework toward the elective requirement.

A Perpetual Concern

“Matter and Energy” (1912)

Frederick Soddy, Noble Prize, Chemistry, 1921.

“The laws expressing the relations between energy and matter are not solely of importance in pure science. they control the rise or fall of political systems, the freedom or bondage of nations, the movements of commerce and industry, the origin of wealth and poverty and the physical welfare of the race.”

*The Terawatt Challenge:
R. Smalley, Noble Prize,
Chemistry 1997*

- ♦ ENERGY
- ♦ WATER
- ♦ FOOD
- ♦ ENVIRONMENT
- ♦ POVERTY
- ♦ TERRORISM, WAR
- ♦ DISEASE
- ♦ EDUCATION
- ♦ DEMOCRACY
- ♦ POPULATION

Needs: Energy Consumption

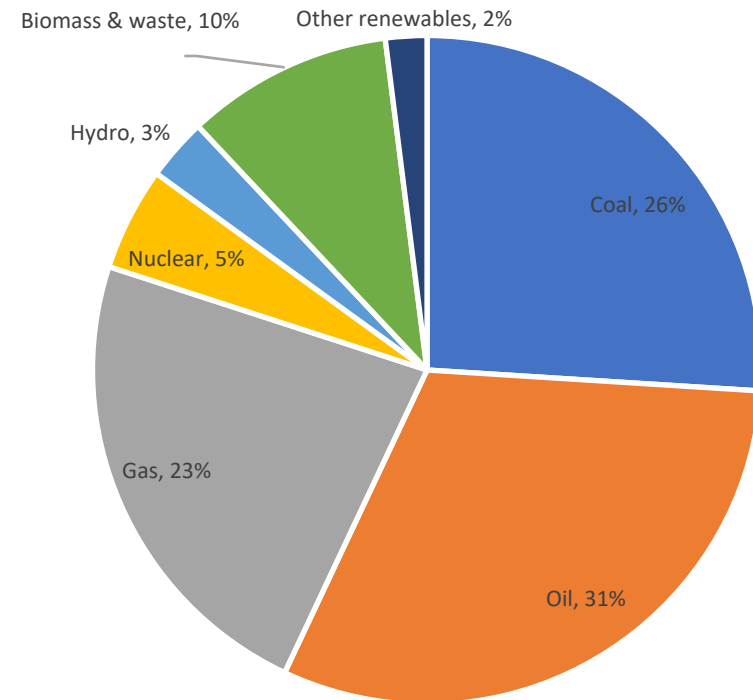
~ 600 EJ (~ 440 EJ in early 2000's) produced by close to 18 TW Power (6.1 TW for electricity generation)

The breakdown of the World primary energy consumption in 2014. The total is 13,558 Mtoe (million tonne oil equivalent) (was 11,059 Mtoe in 2006). Except for hydropower, primary energy measures the thermal energy equivalent in the fuel that was used to produce a useful form of energy, e.g., thermal energy (heat), mechanical energy, electrical energy, etc. When energy is obtained directly in the form of electricity, efficiency is used to convert it to equivalent thermal energy.

1 toe ~ 42 GJ.

IEA World Energy Outlook 2015, p57.

Breakdown in 2018



© IEA. All rights reserved. This content is excluded from our Creative Commons license. For more information, see <https://ocw.mit.edu/fairuse>.

US resources, consumption and patterns ~100 EJ annually in 2018,

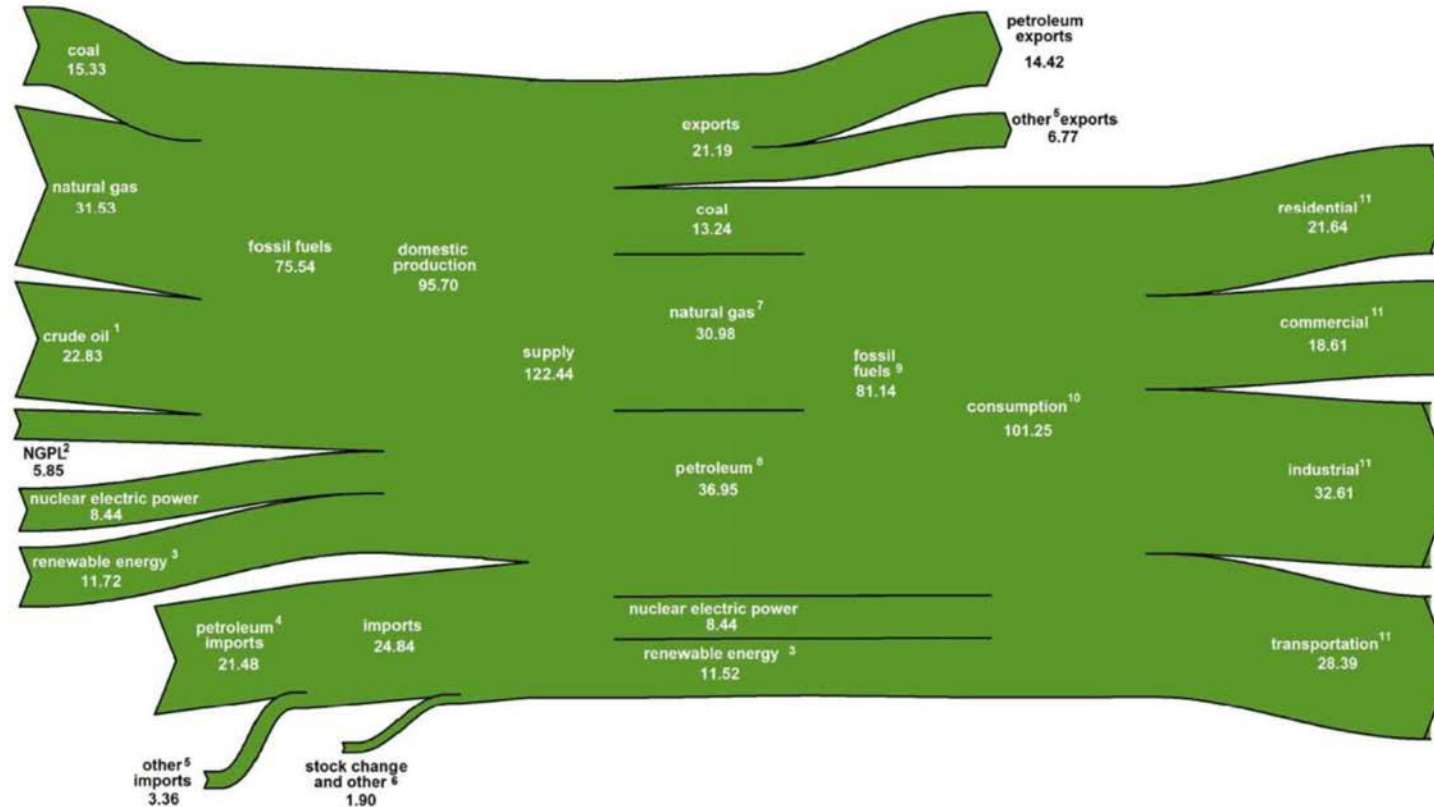
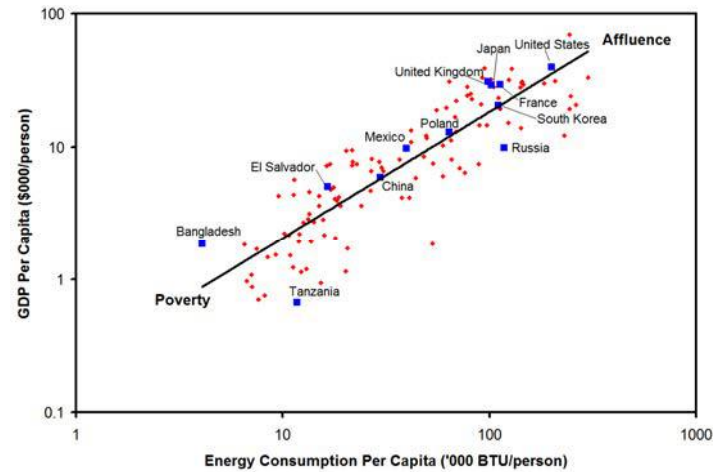


Image courtesy of U.S. Energy Information Administration.

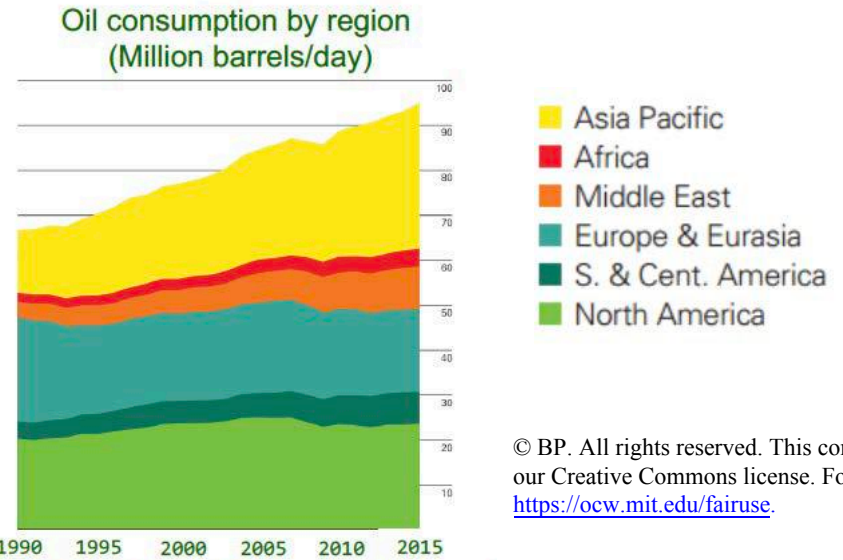
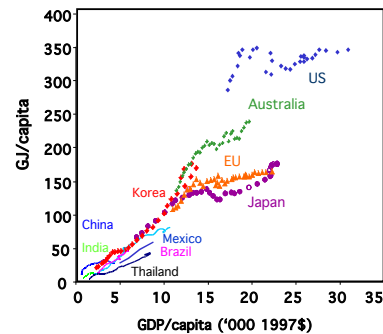
https://www.eia.gov/totalenergy/data/monthly/pdf/flow/total_energy.pdf

Who uses how much?

Per capita energy consumption and GDP. (Produced from data from the United Nations Development Programme (UNDP) Human Development Report (HDR) 2006.

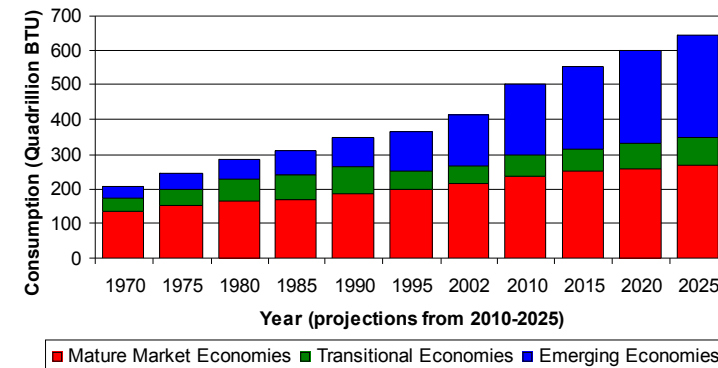


Reference: GDP per capita data for 2004 from Table 1, pages 283-286. Energy consumption per capita found by dividing GDP per capita data for 2004 (Table 1, pages 283-286) by GDP per unit of energy use for 2003 (Table 21, pages 353-356). GDP per unit of energy use for 2003 is expressed in dollars for the year 2000.



© BP. All rights reserved. This content is excluded from our Creative Commons license. For more information, see <https://ocw.mit.edu/fairuse>.

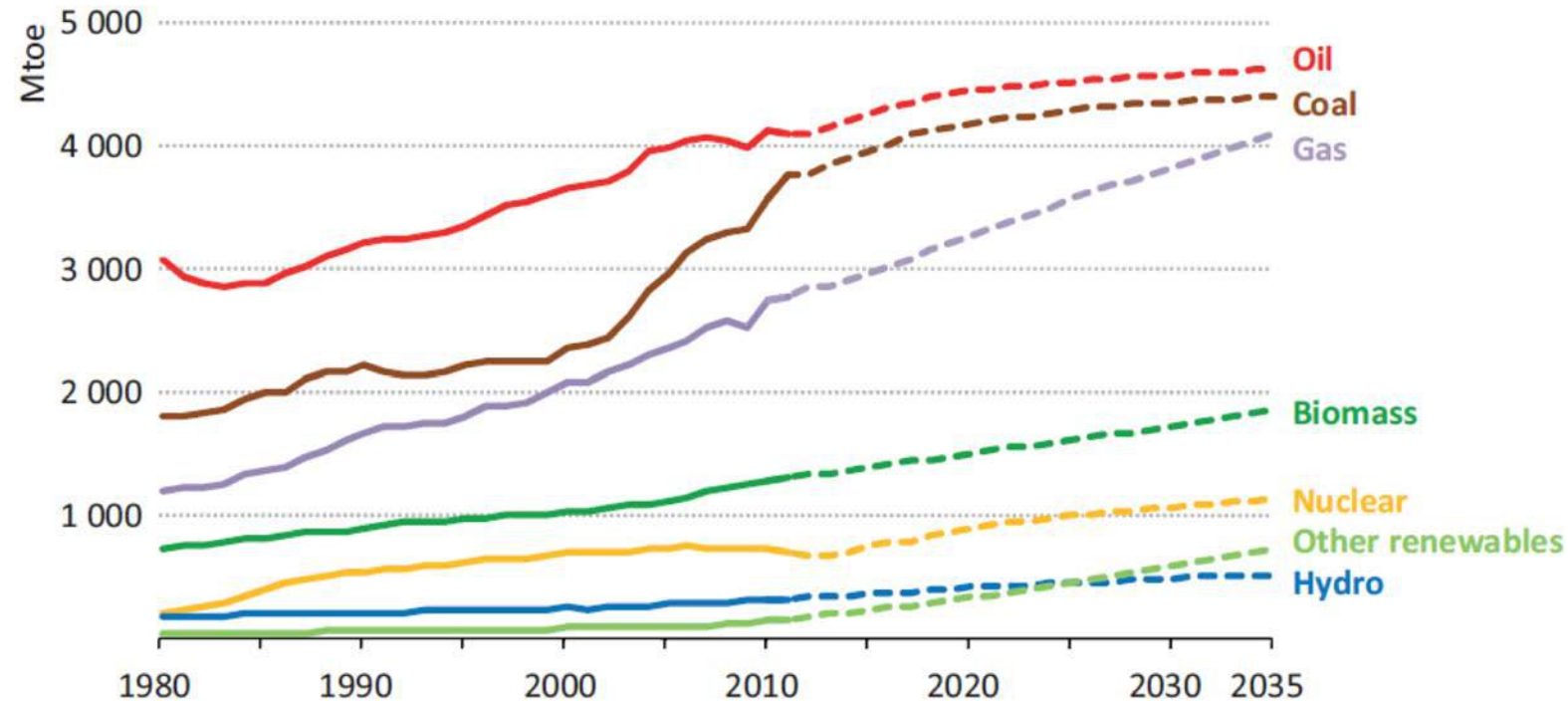
BP 2016 Statistical Review of World Energy



© IEA. All rights reserved. This content is excluded from our Creative Commons license. For more information, see <https://ocw.mit.edu/fairuse>.

Energy demand by economic status for the past three decades, and projects for the next three on the basis of the current trends (IEA Energy Outlook, 2005)

World primary energy demand by fuel



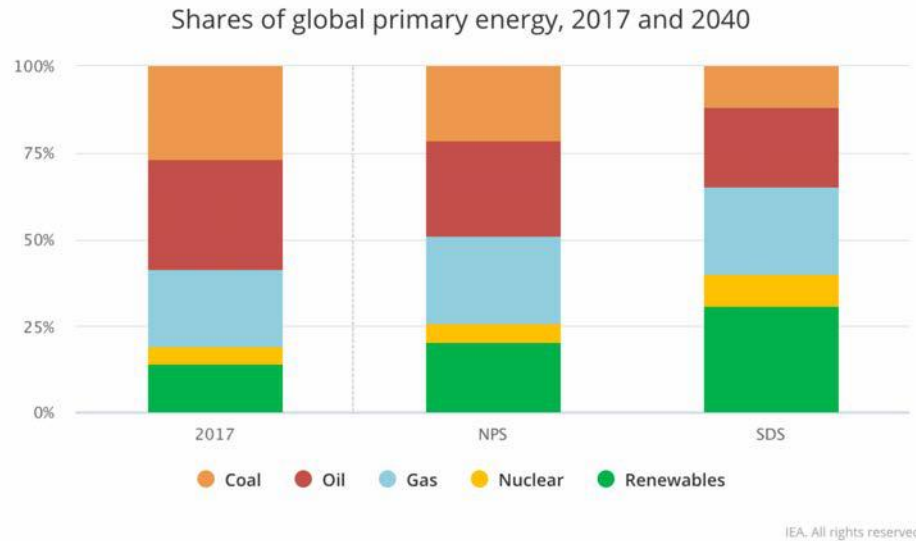
Predicted based on the continuation of existing policies and measures as well as cautious implementation of policies that have been announced by governments but are yet to be given effect (mid-2013).

Source: IEA world energy outlook 2013, P63

© IEA. All rights reserved. This content is excluded from our Creative Commons license. For more information, see <https://ocw.mit.edu/fairuse>.

Shares of global primary energy, 2017 and 2040

Source: <https://www.iea.org/weo2018/fuels/>



© IEA. All rights reserved. This content is excluded from our Creative Commons license. For more information, see <https://ocw.mit.edu/fairuse>.

New Policies Scenario (NPS): Global oil demand growth slows but does not peak before 2040.

Sustainable Development Scenario (SDS): Determined policy interventions to address climate change lead to a peak in global oil demand around 2020 at 97 mb/d.

Global Greenhouse Gas Emissions by Economic Sector (2015)

https://www.epa.gov/sites/production/files/2016-05/global_emissions_sector_2015.png

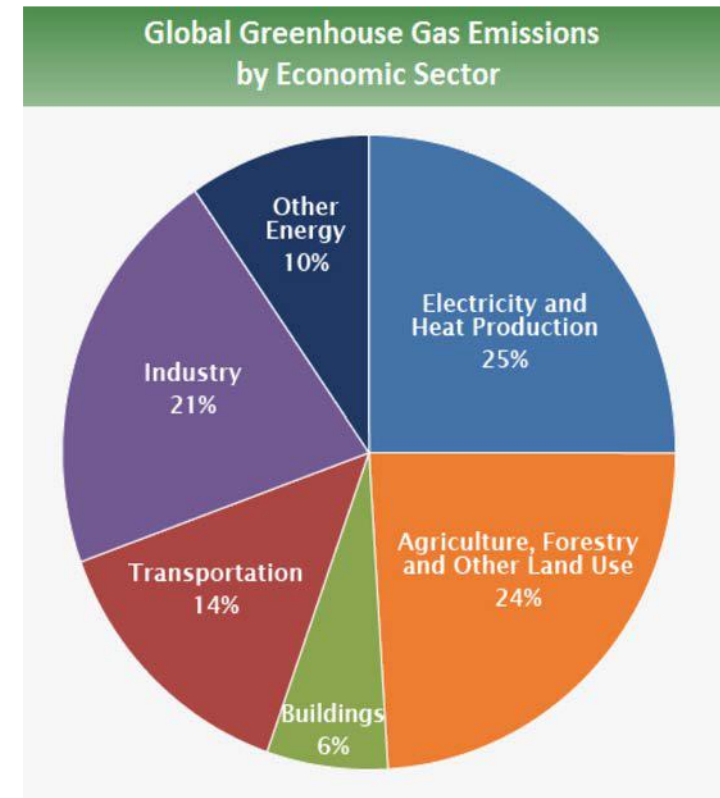
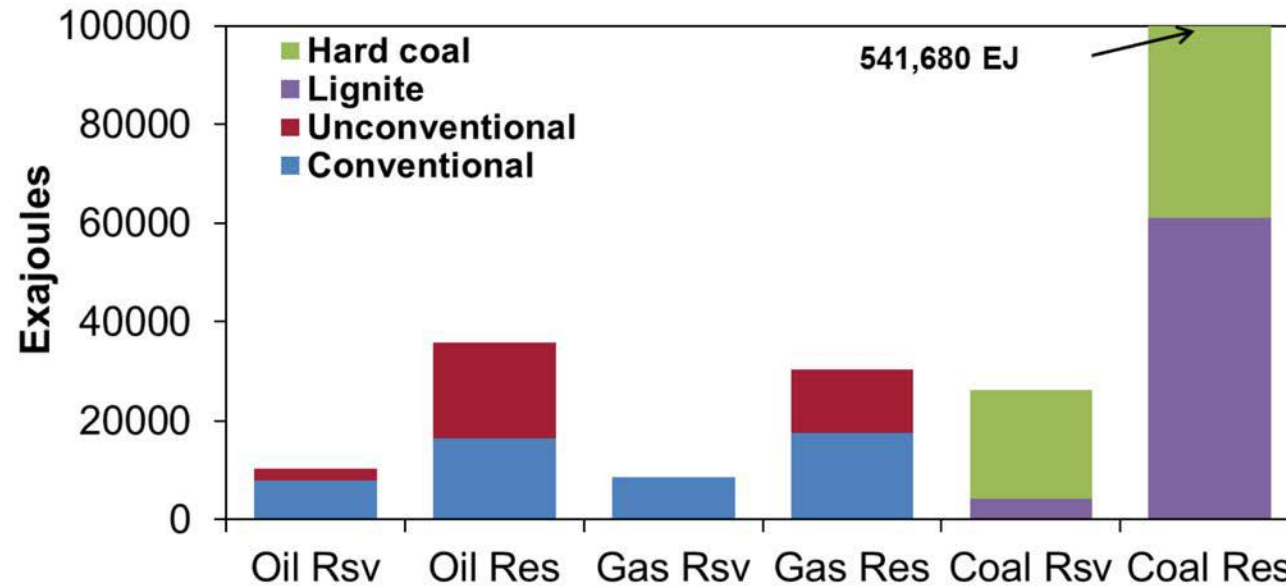


Image courtesy of EPA.

Fuel Reserves and Resources

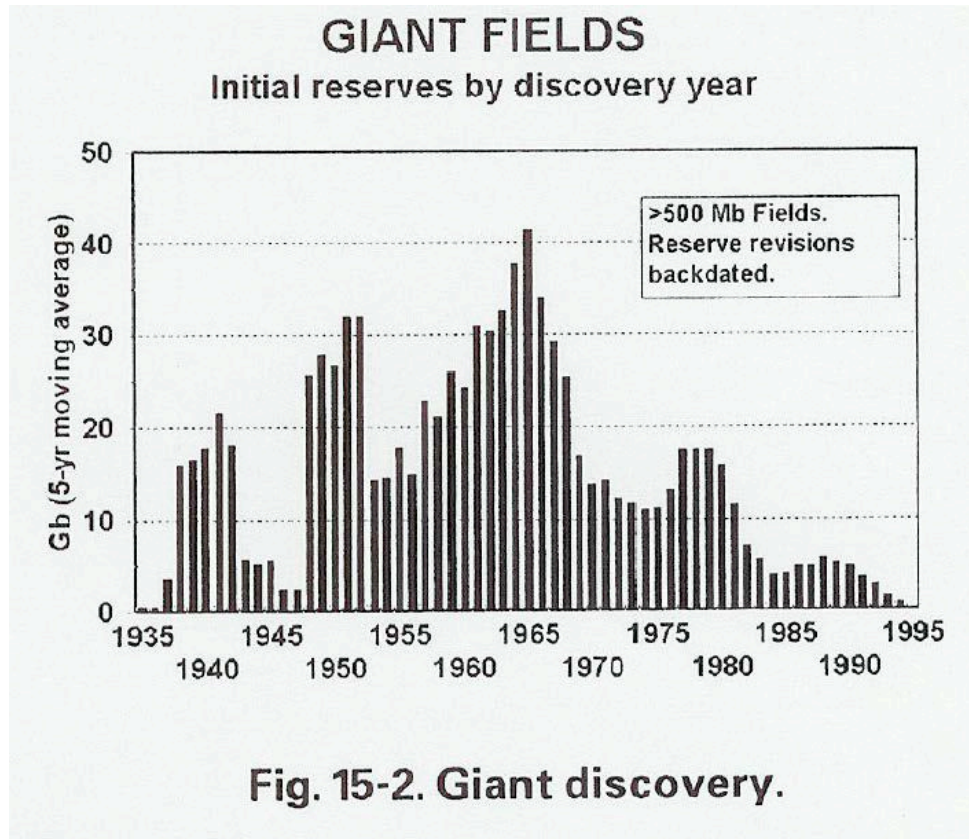
there is plenty of Hydrocarbons, but ..



© IEA. All rights reserved. This content is excluded from our Creative Commons license. For more information, see <https://ocw.mit.edu/fairuse>.

Reserves/(2013 Consumption/yr)		Resource/(2013 Consumption/yr)	
Oil	44 – 58	93 – 203	
Gas	70	145 – 250	
Coal	133 – 158	3282 - 3652	

Care should be exercised when projecting?



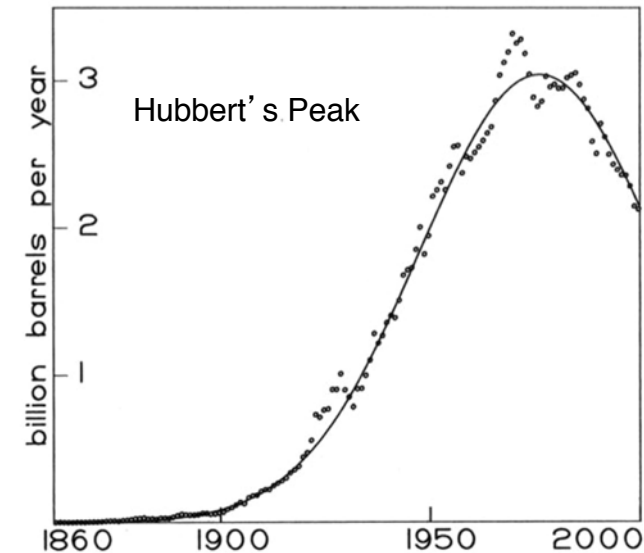
© Source unknown. All rights reserved. This content is excluded from our Creative Commons license. For more information, see <https://ocw.mit.edu/fairuse>.

US production

Predicted _____

Actual

In 2015, US production was 3.4 BBy

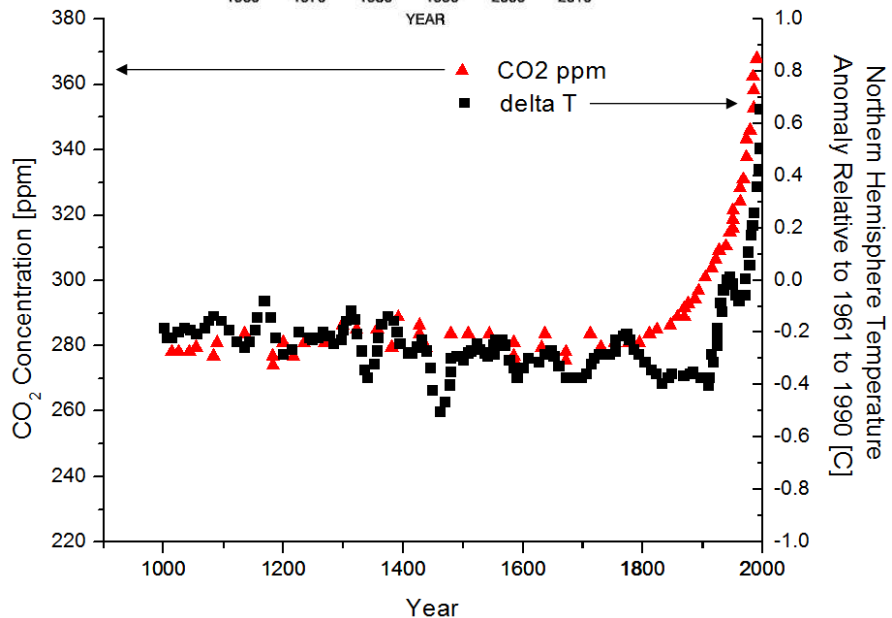
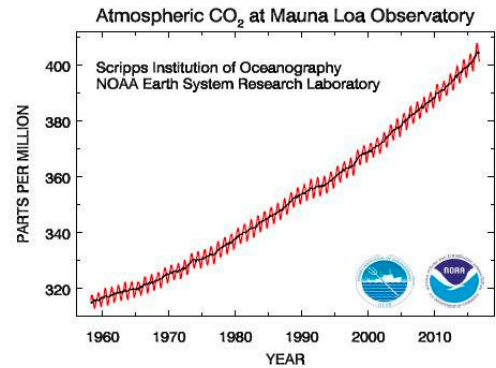


Campbell, the Coming Oil Crisis, 1998

© Multi-Science Publishing Co. Ltd. All rights reserved. This content is excluded from our Creative Commons license. For more information, see <https://ocw.mit.edu/fairuse>.

The US is now the largest oil producer (thanks to fracking)

CO₂ emissions and Climate Change!



Intergovernmental Panel on Climate Change record of temperature over Antarctica, atmospheric concentration of CO₂ and methane during the past 420,000 years

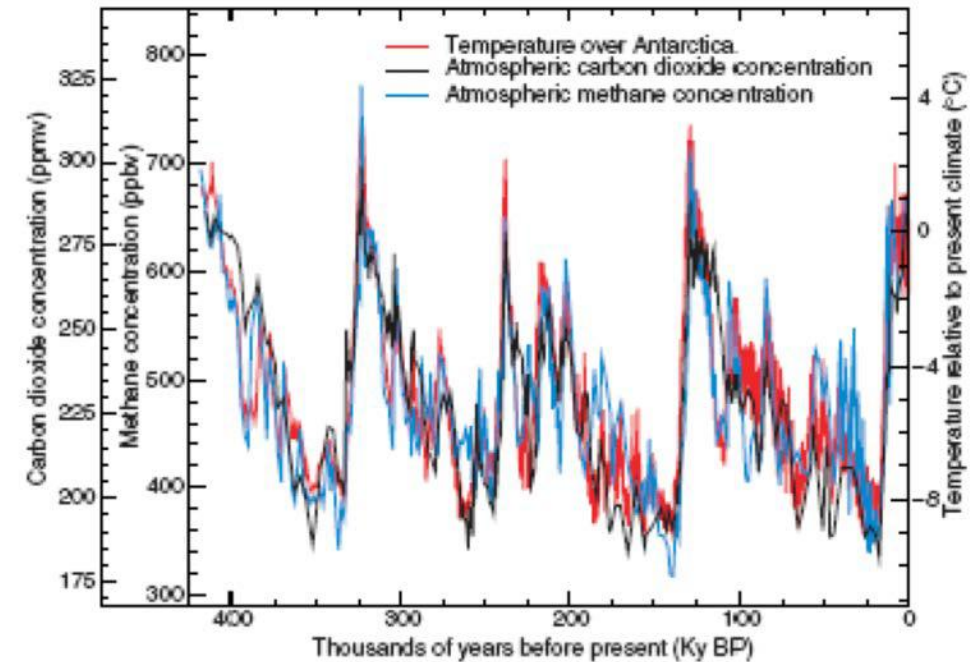


Figure 2.22: Variations of temperature, methane, and atmospheric carbon dioxide concentrations derived from air trapped within ice cores from Antarctica (adapted from Sowers and Bender, 1995; Blunier *et al.*, 1997; Fischer *et al.*, 1999; Petit *et al.*, 1999).

© IPCC. All rights reserved. This content is excluded from our Creative Commons license. For more information, see <https://ocw.mit.edu/fairuse>.

Reference: IPCC Third Assessment Report (2001), Working Group I, Ch. 2, Figure 2.22, page 137. Variations of temperature, methane, and atmospheric carbon dioxide concentrations derived from air trapped within ice cores from Antarctica.

Greenhouse gases are: CO₂, CH₄ and N₂O and CFCs (H₂O and aerosols are also GH gases)

Arrhenius predicted CO₂ impact on global T' back in 1896

Greenhouse gases absorb part of the outgoing radiation, with water molecules absorbing in the 4-7 and at 15 microns wavelength, and carbon dioxide absorbing in 13-19 micron.

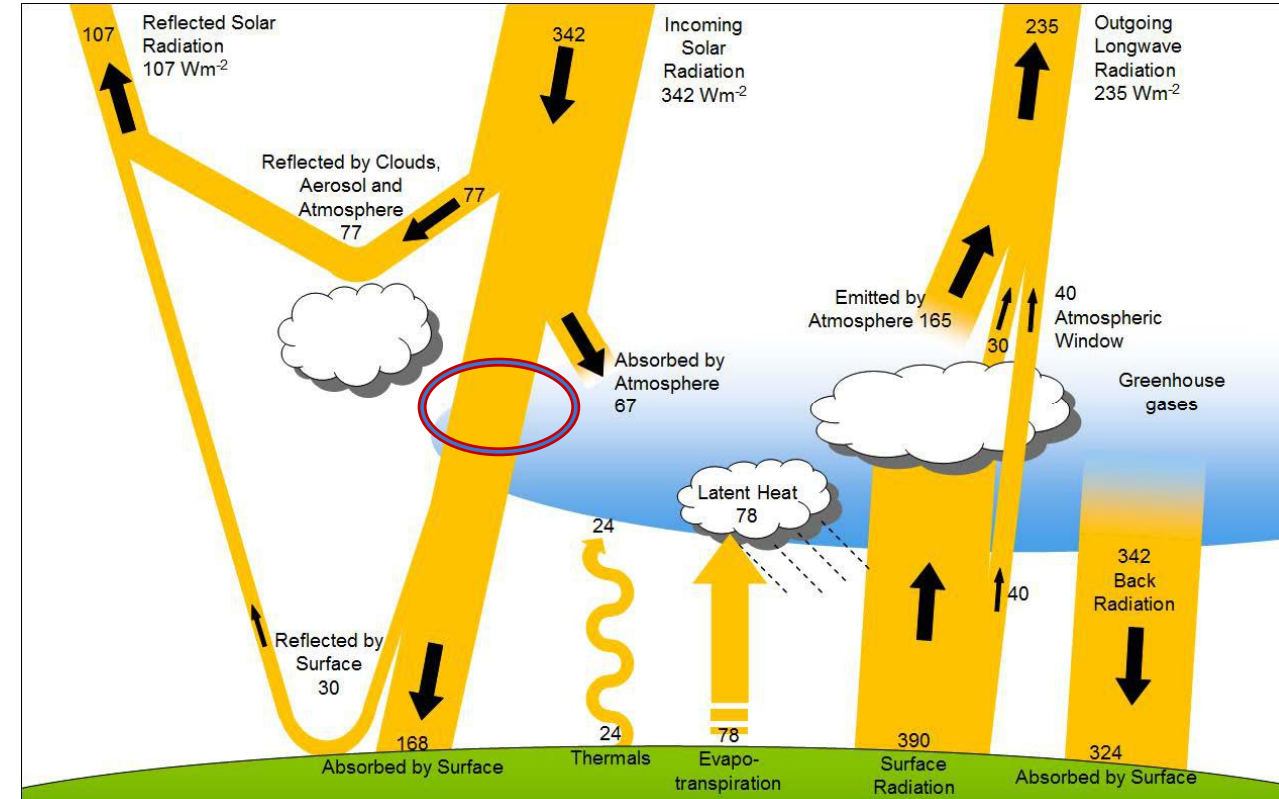
A fraction of this energy is radiated. The change of the energy balance due to this greenhouse gas radiation is known as *the radiation forcing*, and its contribution to the Earth energy balance depends on their concentration.

The net effect of absorption, radiation and re-absorption keep the Earth surface warm, at average temperature ~ 15 C. Without it the surface temperature could fall to ~ -19 C.

Because of its concentration, carbon dioxide has the strongest radiation forcing, except for that of water. However water concentration is least controlled by human activities.

The global energy balance

The Green House Effect



Solar energy flux, how much of it reaches the Earth's surface; the radiation emitted by the ground, and the balance that is re-radiated back to the surface. All numbers are in units of Wm^{-2} . Adapted from Intergovernmental Panel on Climate Change, Working Group 1: The Physical Basis of Climate Change, Chapter 1, Historical Overview of Climate Change Science, page 96, FAQ 1.1, Figure 1 (2007).

© IPCC. All rights reserved. This content is excluded from our Creative Commons license. For more information, see <https://ocw.mit.edu/fairuse>.

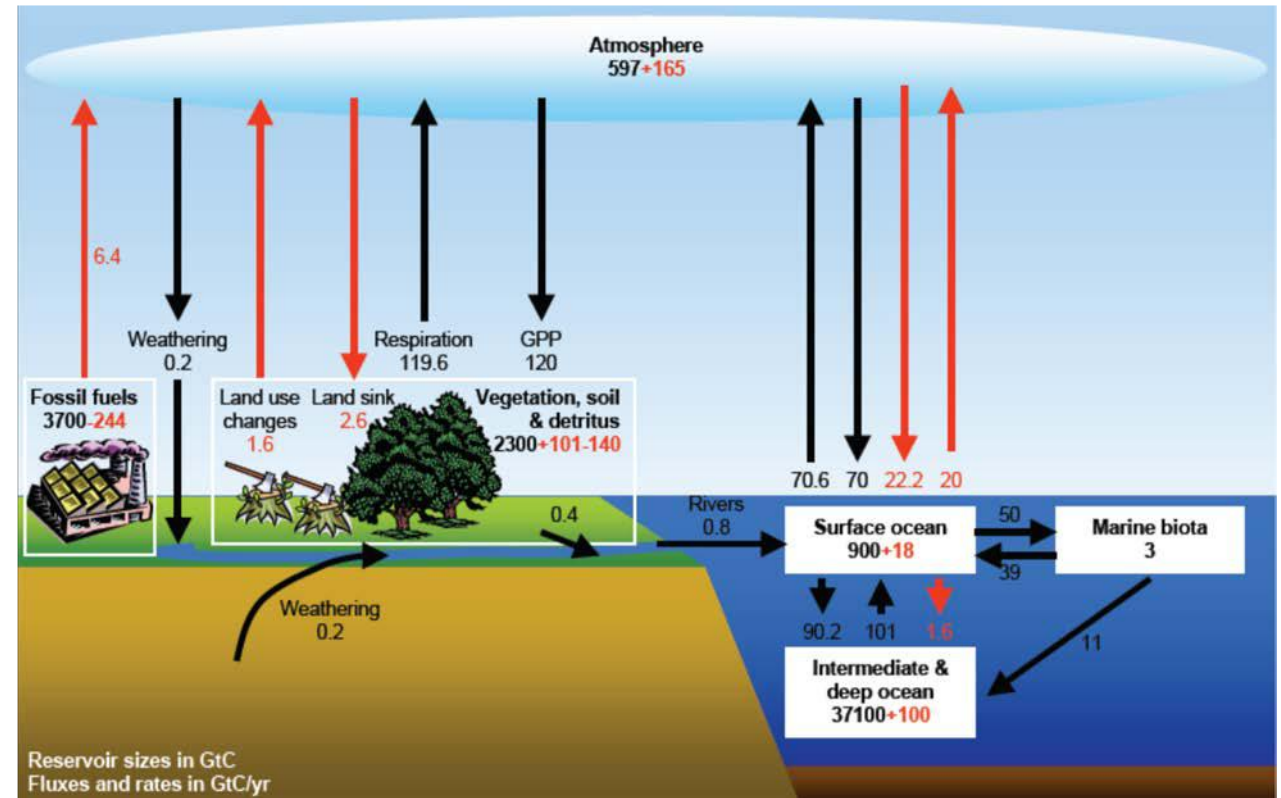
The carbon balance

Fossil fuel:

- 3700 GtC was available at onset of the industrial revolution.
- 244 GtC has been used so far.
- 6.6 GtC is being burnt and emitted each year.

GPP (Gross Primary Production) accounts for photosynthesis ($\text{CO}_2 + \text{H}_2\text{O} + \text{Sun photons}$)

Other activities show a sink of $\sim 3.4 \text{ GtC/y}$



Fluxes of CO_2 are shown in terms the equivalent C

Courtesy Elsevier, Inc., <http://www.sciencedirect.com>. Used with permission.

Source: <http://dx.doi.org/10.1016/j.pecs.2010.02.006>

Fossil fuel combustion produces $\sim 6 \text{ GtC/y}$ (1 GtC is $= 44/12 = 3.667 \text{ GtCO}_2$).

- Carbon dioxide is injected into the atmosphere through *respiration* and the *decomposition of biomass*, and is removed by *absorption* during photosynthesis and by the phytoplankton living in the oceans.
- Respiration produces $\sim 60 \text{ GtC/y}$, while photosynthesis removes $\sim 61.7 \text{ GtC/y}$, with a balance of a sink of 1.7 GtC/y .
- The surfaces of the Oceans act as a sink, net uptake of 2.2 GtC/y , a source/sink balance between production of 90 and consumption of 92.2 GtC/y .
- Changing land use (deforestation) and ecosystem exchange adds/removes $1.4/1.7 \text{ GtC/y}$, for a net balance of a sink of 0.3 GtC/y .

The overall net gain of CO_2 in the atmosphere is estimated to be around 3.5 GtC/y .

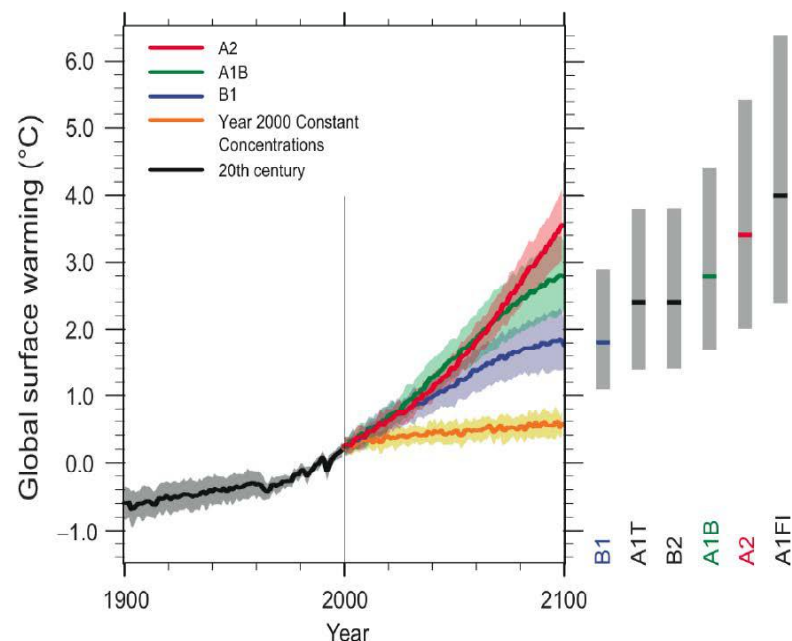
It is relative these balances that the contribution of fossil fuel combustion (and cement production) appears significant.

These numbers are uncertain and that there is $1\text{-}2 \text{ GtC/y}$ unaccounted for in the overall balance (in ways that are not well understood).

For each 2.1 GtC introduced in the atmosphere, CO_2 concentration rises by 1 ppm (the average lifetime of CO_2 in the atmosphere is 100-200 years).

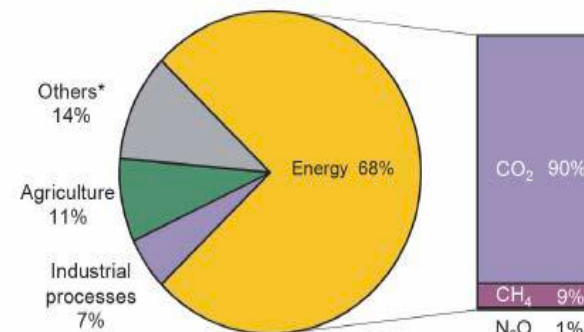
How warm will it get

Climate sensitivity: change in global temperature as CO₂ doubles, estimates: 1.5-4.5 °C

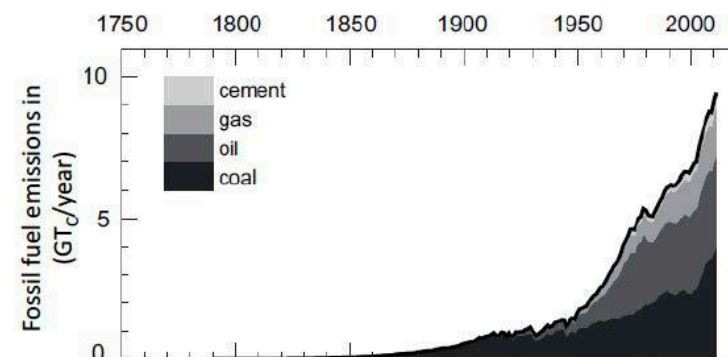


Prediction of the temperature rise during the 21st century, according to different models that account for scenarios for the introduction of CO₂ into the atmosphere and its response. Source: IPCC WGI Fourth Assessment Report, Summary for Policymakers, Figure SPM-5, page 14, Multi-model Averages and Assessed Ranges for Surface Warming.

Emissions by Source



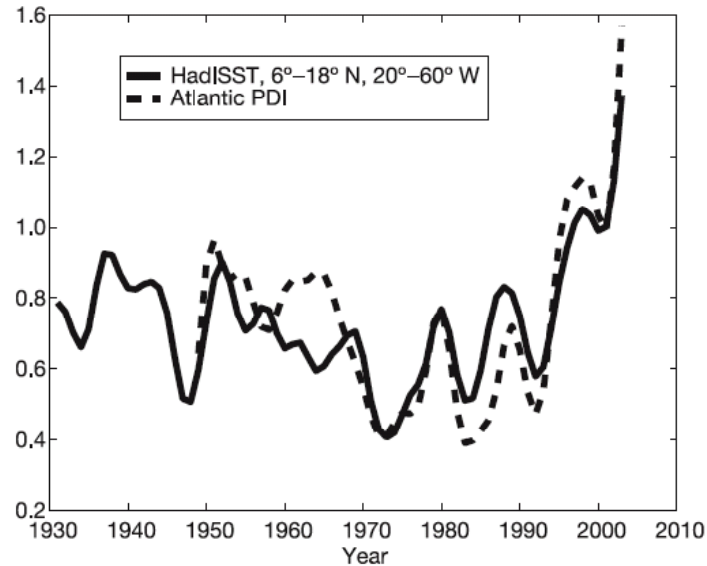
International Energy Agency, CO₂ Emissions from Fuel Combustion, 2016 Highlights



GHG emission by fuel and cement production, reached 9.8 GTC by 2014, 1/3 is transportation (oil based)

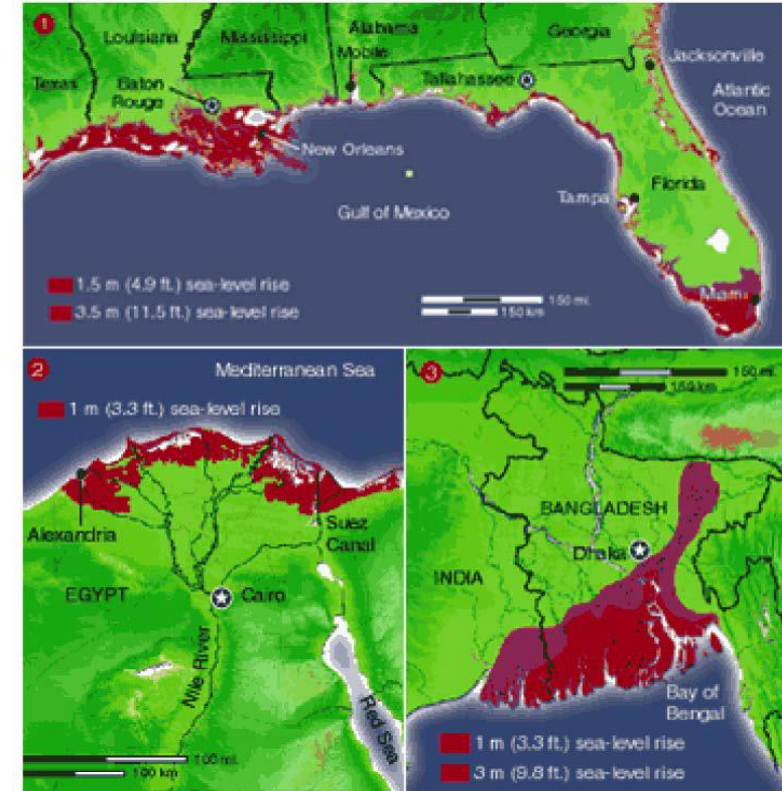
IPCC 2014 Technical Summary, IEA, 2015 CO₂ emissions from fossil fuels

Global Warming Impacts



© Springer Nature Limited. All rights reserved. This content is excluded from our Creative Commons license. For more information, see <https://ocw.mit.edu/fairuse>.

A measure of the total power dissipated annually by tropical cyclones in the north Atlantic (the power dissipation index PDI) compared to September sea surface temperature (SST), measured over the past 70 years. The PDI has been multiplied by 2.1×10^{-12} and the SST, is averaged over 6-18° N latitude and 20-60° W longitude. North Atlantic hurricane power dissipation has more than doubled in the past 30 years. Emanuel, K., Increasing destructiveness of tropical cyclones over the past 30 years, Nature Letters, Vol 436/4, August 2005.



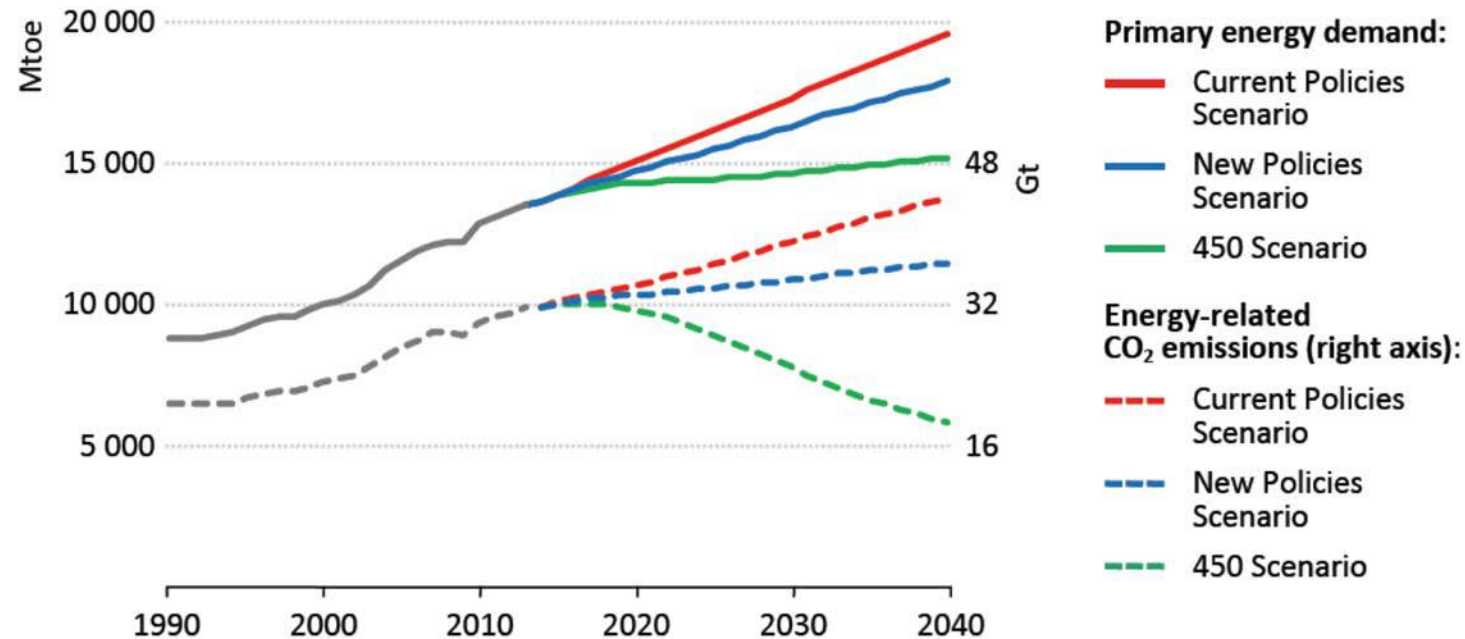
Courtesy Elsevier, Inc., <http://www.sciencedirect.com>. Used with permission.

Source: <http://dx.doi.org/10.1016/j.peccs.2010.02.006>

Rising sea levels

>> Rise in ocean acidity

Extrapolation Into the Near Future



© IEA. All rights reserved. This content is excluded from our Creative Commons license. For more information, see <https://ocw.mit.edu/fairuse>.

New policies scenario: takes into account the policies and implementing measures affecting energy markets that had been adopted as of mid-2015 (as well as the energy-related components of climate pledges in the run-up to COP21, submitted by 1 October)

450 scenario: depicts a pathway to the 2° C climate goal that can be achieved by fostering technologies that are close to becoming available at commercial scale.

Source: IEA world energy outlook 2015, P55

WHILE TIME SCALES ARE UNCERTAIN:

1. Fossil fuel Reserves are limited, 50-300 years.
2. CO₂ and climate change are correlated.

BUT, WE MUST ACT WITHIN CONSTRAINTS:

1. Inertia, big numbers and many stakeholders.
2. Economic, and country dependent scenarios.
3. Social; old habits diehard or do not die at all.
4. Environmental constraints and CO₂ ...
5. Political: let us not even get there!

SCALE MATTERS

Pacala & Socolow, Stabilizing Wedges: Solving the Climate Problem for the Next 50 Years with Current Technologies...
Science, Aug 2004,

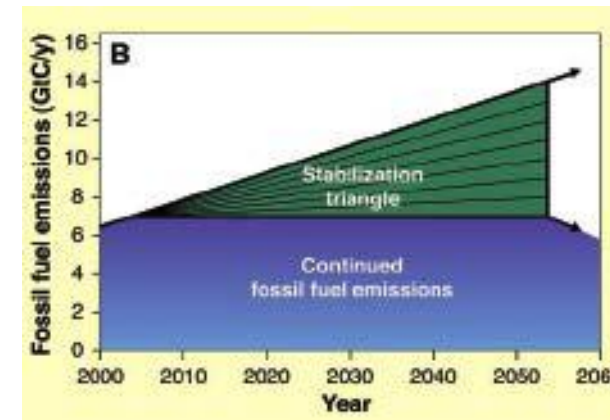
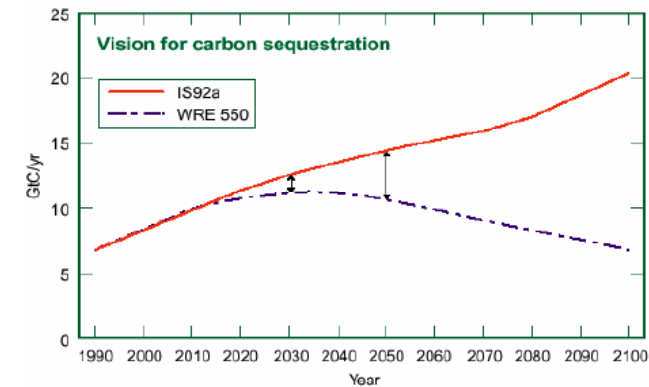
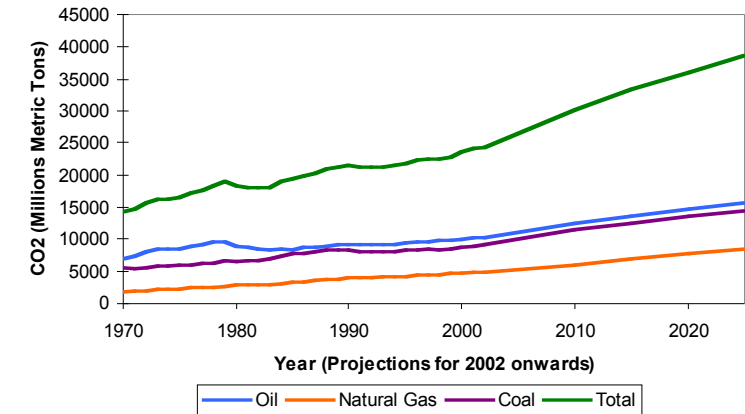
- Goal: Stabilizing CO₂ @ ~ 550 ppm by mid century.
- How: hold emission @ 7 GtC/y (1990 level)
- (BAU will double to 14 GtC/y in 50 years growing at the rate of @ 1.5% /y).
- A stabilization “wedge” prevents 1 GtC/y by mid century. Need 7 wedges!

1 GtC/y is produced by:

750 GWe coal at efficiency (32-36%)

1500 GWe NG plants @ efficiency (38-55%)

Many assumptions and some number are confusing but



© AAAS. All rights reserved. This content is excluded from our Creative Commons license. For more information, see <https://ocw.mit.edu/fairuse>.

SCALE MATTERS, NEED A PORTFOLIO

of solutions that offer such wedges, how are they equivalent?

Economy-wide carbon-intensity reduction (CO₂/\$GDP)	Raise global reduction goal by 0.15%/y (in US raise reduction from 1.96% to 2.11%/y)	>>> policy and challenges
1. Efficient vehicles	Raise fuel economy for 2B cars 30 to 60 mpg	Engine options, size and power, hybrid, electric
2. Less use of vehicles	2B cars @ 30 mpg travel 5000 instead of 10,000 mile/y	Transit options
3. Efficient buildings	1/4th less emissions: efficient lighting, appliances, etc.	Construction cost!
4. Efficient coal plants	Raise thermal efficiency from 32% to 60%	technical

SCALE MATTERS EVEN MORE

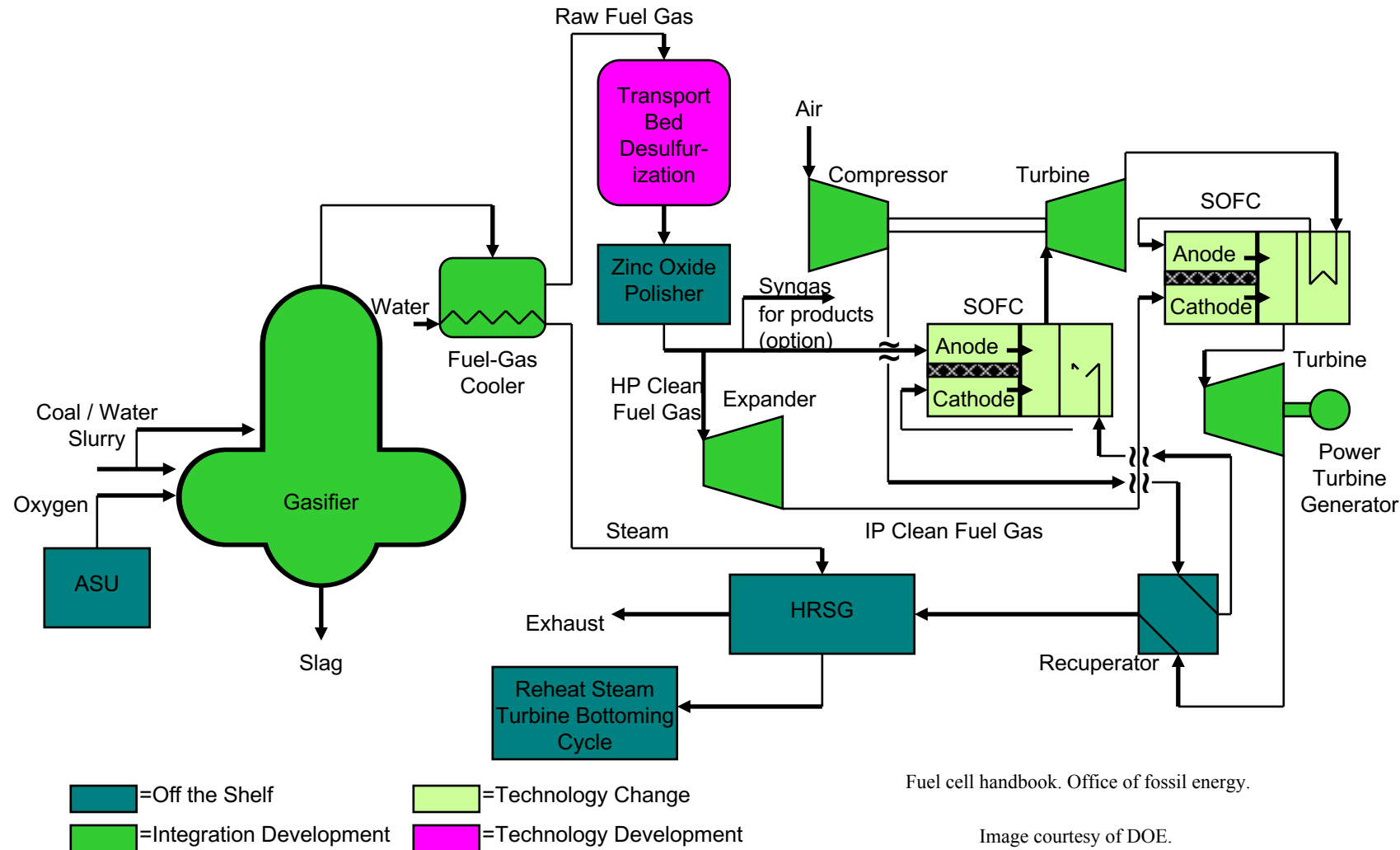
Fuel shift:		
5. NG instead of coal for electricity	Replace 1.4 TWe coal with gas (4X of 2004 NG plant capacity)	Price of NG
Capture CO₂ (CCS):		
6. In power plants	CCS in 0.8 TW coal or 1.6 TW gas	Improved technology
7. In H ₂ production for transportation	CCS in coal plants producing 250 MtH ₂ /y or NG plants producing 500 MtH ₂ /y	Technology and H ₂ issues
8. In coal to Synfuel plants	CCS in plants producing 30 Mbarrel/day (200X current Sasol capacity) from coal	Technology and price

YES SCALES ARE BIG AND MUST BE CONSIDERED

9. Nuclear instead of coal for electricity	700 GW fission plants (2X of 2004 capacity)	Security and waste
Renewable Sources:		
10. Wind instead of coal for electricity	Add 2 M 1-MW peak turbines (30×10^6 ha, sparse and off shore)	Land use, material, off shore tech.
11. PV instead of coal for electricity	Add 2 TW peak PV (2×10^6 ha)	Cost and material
12. Wind for H ₂ (for high efficiency vehicles)	Add 4 M 1-MW peak turbines	H ₂ infrastructure
13. Biomass for fuel	Add 100X of 2004 Brazil (sugar cane) or US (corn) ethanol. (250×10^6 ha. 1/6 of total world cropland)	Land use

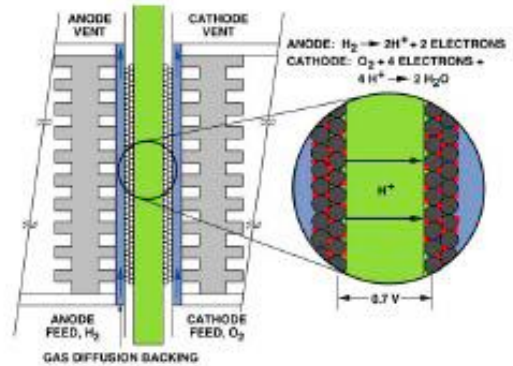
HIGH EFFICIENCY POWER PLANTS

Layout of an integrated-gasification combined cycle power plant, in which the conventional gas turbine-steam turbine combined cycle is equipped with “topping” high temperature fuel cells



Fuel Cells

DOE
Fuel Cell Handbook, 2004
Download new version, very useful



Also known as membrane-electrode-assembly (MEA), and made of one “physical” plate with anode and electrode material “sprayed” on both side.

The membrane is a polymer (nafion) for low T cells and a ceramic plate for high T cells.

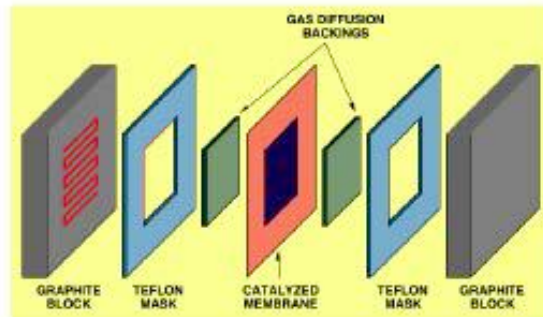
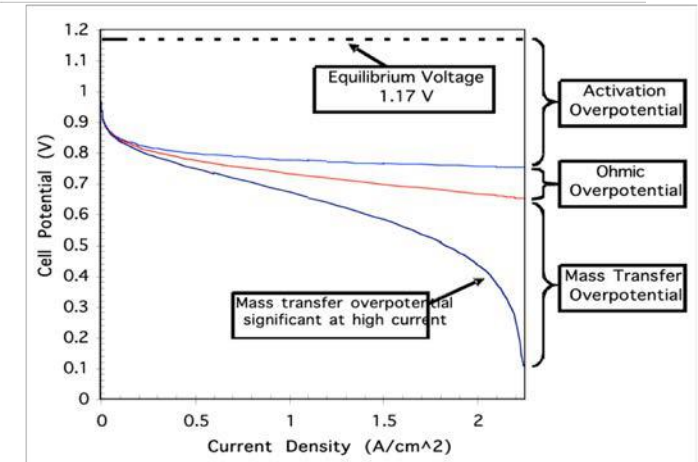
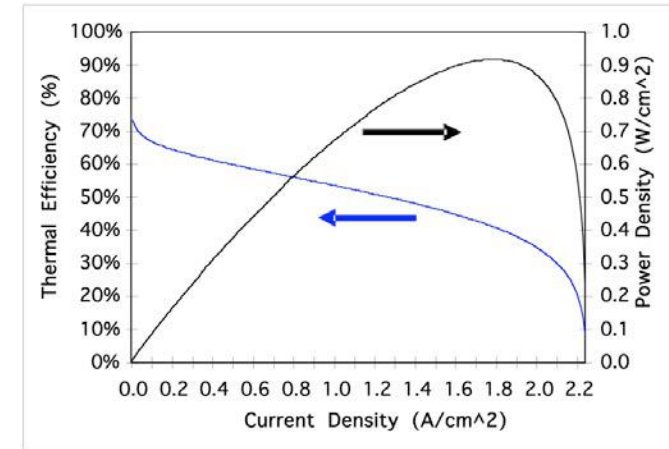


Figure 3-1 (a) Schematic of Representative PEFC (b) Single Cell Structure of Representative PEFC(1)

Image courtesy of DOE.



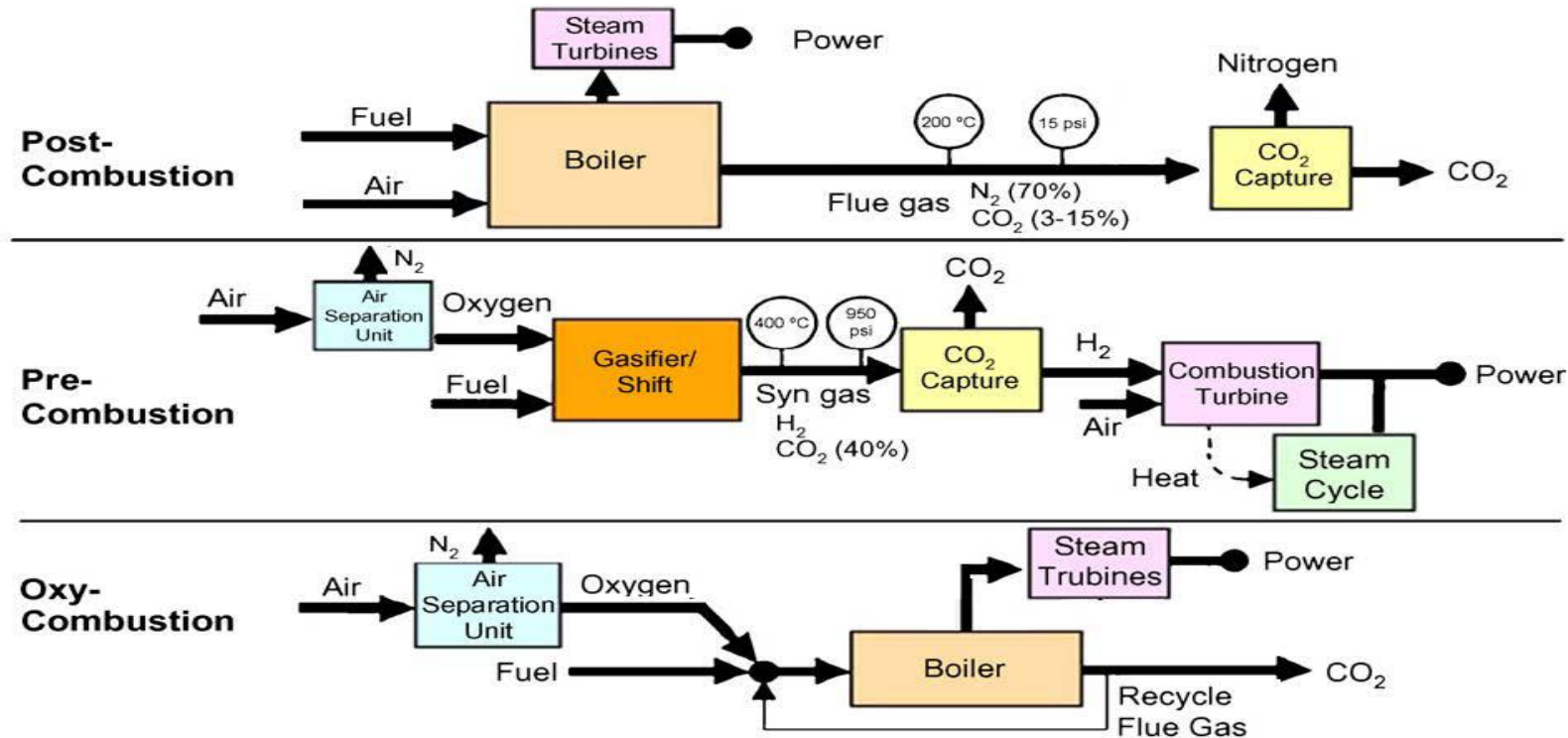
$$\eta_{FU} = \frac{\mathcal{P}}{(\dot{n}_f)_{\text{sup}} \Delta \hat{h}_{R,f}} = \frac{IV}{(\dot{n}_f)_{\text{sup}} \Delta \hat{h}_{R,f}} = \frac{I}{n_e \mathcal{S}_a (\dot{n}_f)_{\text{sup}}} \frac{V}{V_{OC}} \frac{\zeta V_{OC}}{\Delta \hat{h}_{R,f}}$$

$$= \eta_{far} \eta_{rel} \eta_{OC}$$

$$\eta_{OC} = \frac{\Delta G_R}{\Delta H_R}$$

Mome Power Cycle for CO₂ Capture

Penalty in efficiency, minimized with novel technology and system integration....



© IEEE. All rights reserved. This content is excluded from our Creative Commons license. For more information, see <https://ocw.mit.edu/fairuse>.

- (1) *Post combustion: chemical scrubbing of CO₂ from exhaust.*
- (2) *Oxy-ocmbustion: burning with O₂ first.*
- (3) *Precombustion: IGCC, burn in O₂, separate and then burn H₂.*

CO_2 Capture (Reuse!) and Storage

B

Fossil fuel	Energy content [TW-yr]	Carbon content [GtC]	(E_{fuel}/C) [TW-yr/GtC]	(E/C) [TW-yr/GtC]	Sequestration rate [GtC/yr]
Gas	1200	570	2.1	1.9 - 1.6	5 - 6
Oil	1200	750	1.6	1.4 - 1.2	7 - 8
Coal	4800	3690	1.3	1.2 - 1.0	9 - 10

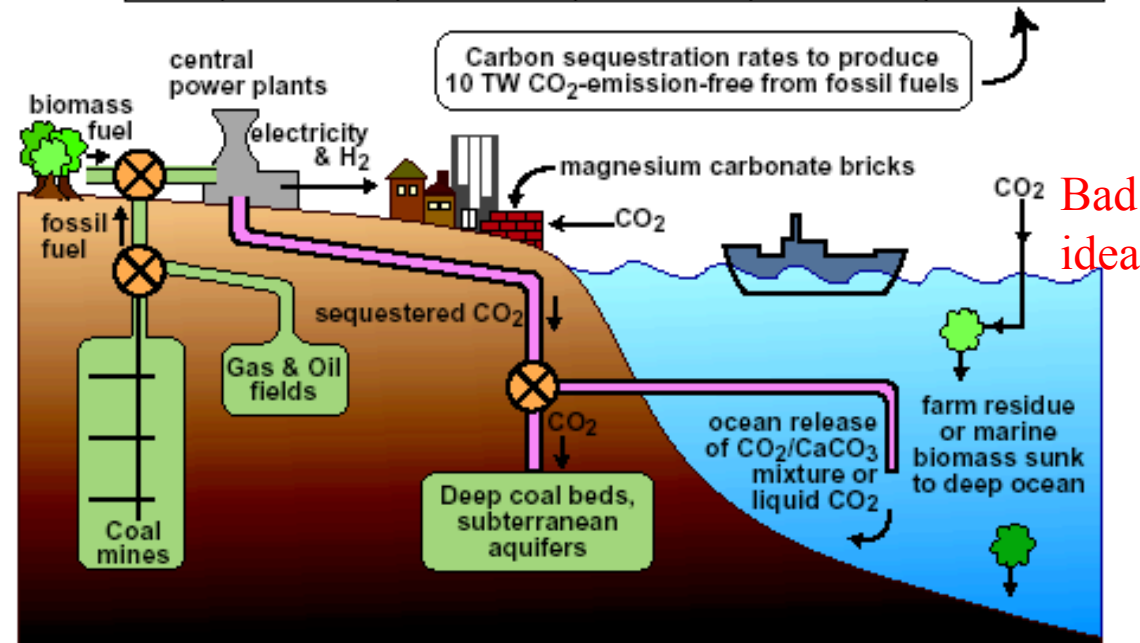


Fig. 1. (A) Fossil fuel electricity from steam turbine cycles. (B) Collecting CO_2 from central plants and air capture, followed by subterranean, ocean, and/or solid carbonate sequestration, could foster emission-free electricity and hydrogen production, but huge processing and sequestration rates are needed (5 to 10 GtC year⁻¹ to produce 10 TW emission-free assuming energy penalties of 10 to 25%).

© AAAS. All rights reserved. This content is excluded from our Creative Commons license. For more information, see <https://ocw.mit.edu/fairuse>.

Source: M.I. Hoffert et al., *Science* 298, 981 (2002)

© by Ahmed F. Ghoniem

Separation Technology and its impact on efficiency

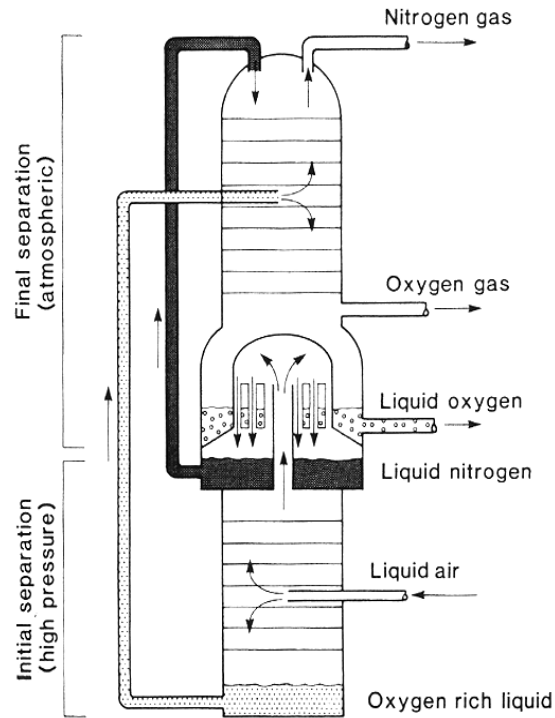


Figure 5.6 Distillation column for fractional separation of liquid air (after Ref. 11).

Probstien, Synthetic Fuels.

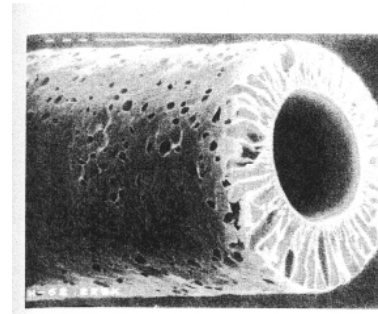
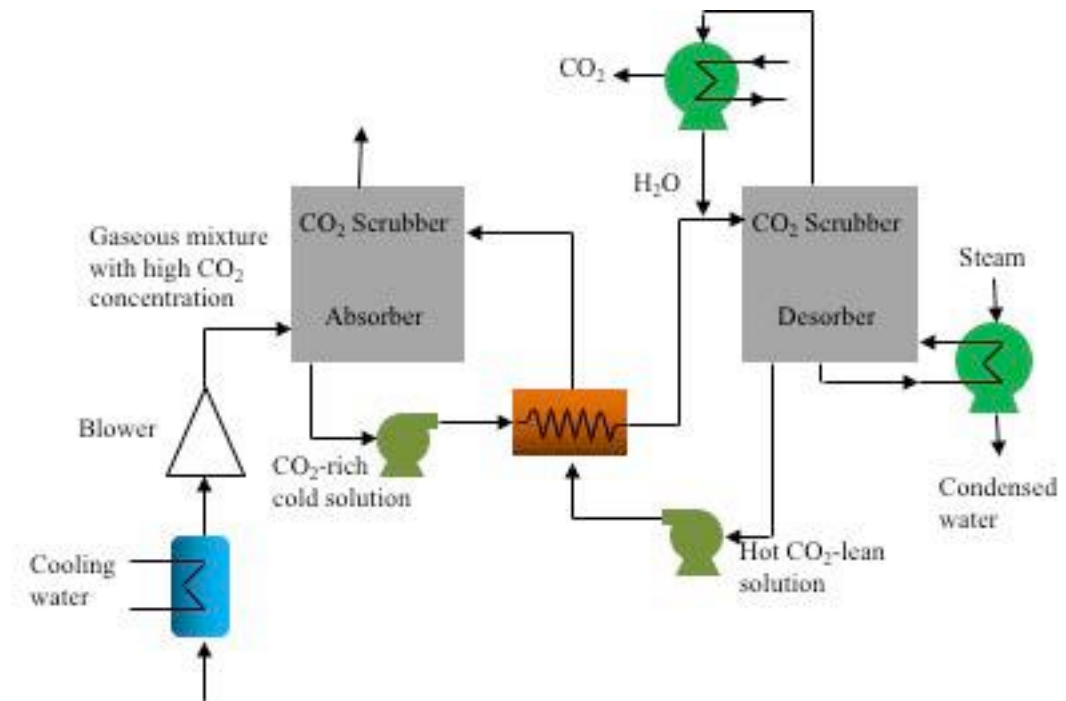


FIGURE 26.3
Capillary ultrafiltration membrane.
Electron micrograph (150 \times) of a
DIAFLO™ hollow fiber. (Courtesy
of Millipore Corporation)

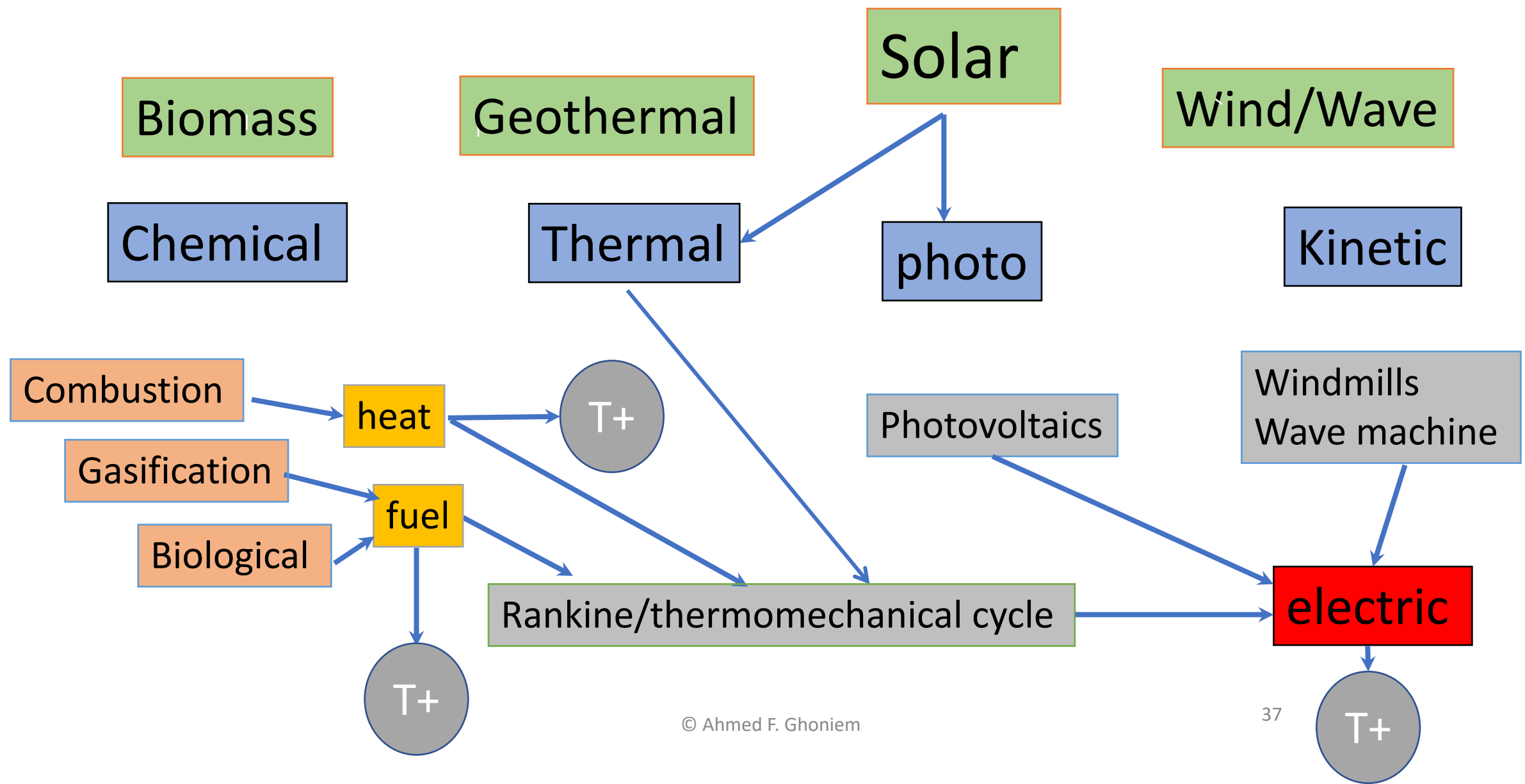
McCabe et al, unit
operation of Che. Eng.

© McGraw-Hill Education. All rights reserved.
This content is excluded from our Creative
Commons license. For more information, see
<https://ocw.mit.edu/fairuse>.



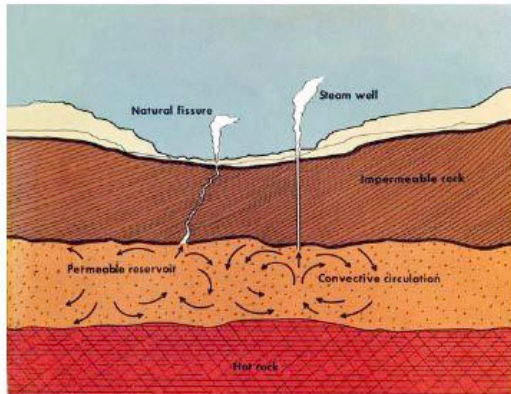
© Source unknown. All rights reserved. This content is excluded from our Creative Commons license. For more information, see <https://ocw.mit.edu/fairuse>.

Renewable Sources and Their Utilization

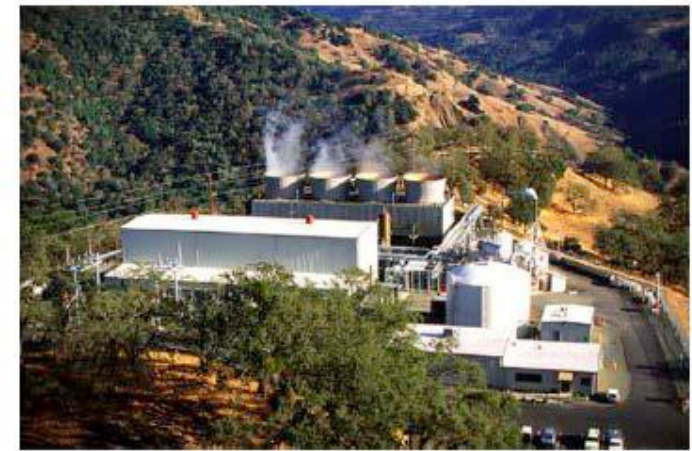
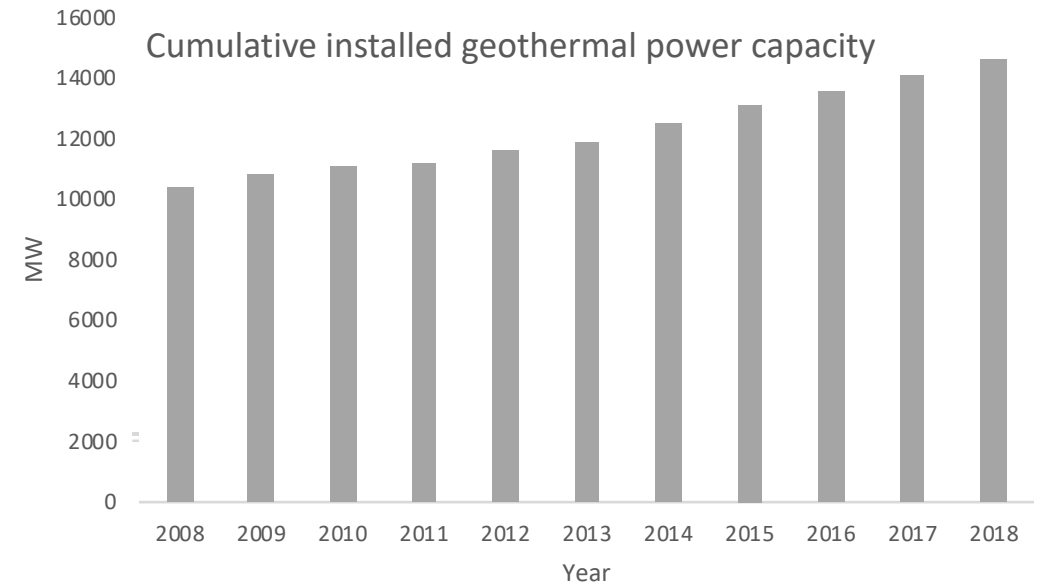


Geothermal Energy

- Nearly emissions free and dispatchable.
- Uses conventional technology (thermal efficiency is low), and prices are closer to fossil electricity.
- Well life is relatively short, resources are localized and distributed.
- Needs alternative drilling technology.
- 2016 capacity worldwide ~ 30 GWe.



© Source unknown. All rights reserved. This content is excluded from our Creative Commons license. For more information, see <https://ocw.mit.edu/fairuse>.



© Geothermal Education Office. All rights reserved. This content is excluded from our Creative Commons license. For more information, see <https://ocw.mit.edu/fairuse>.

Wind Utilization is rising fast ..

Explore technology pathways for installing and operating large wind power facilities in water depths greater than 30 meters.

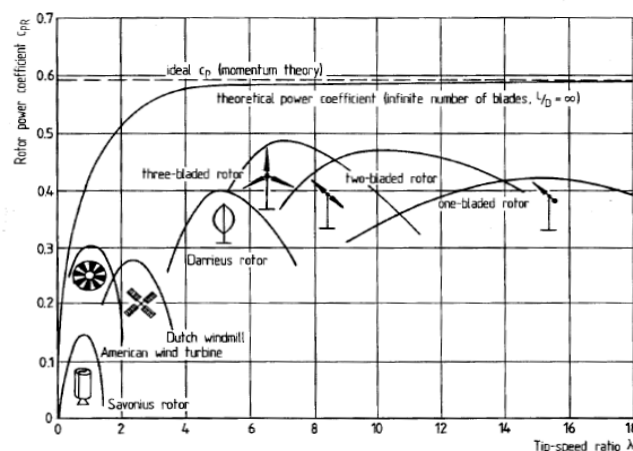
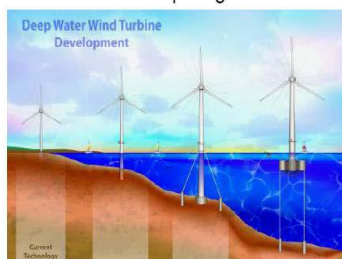


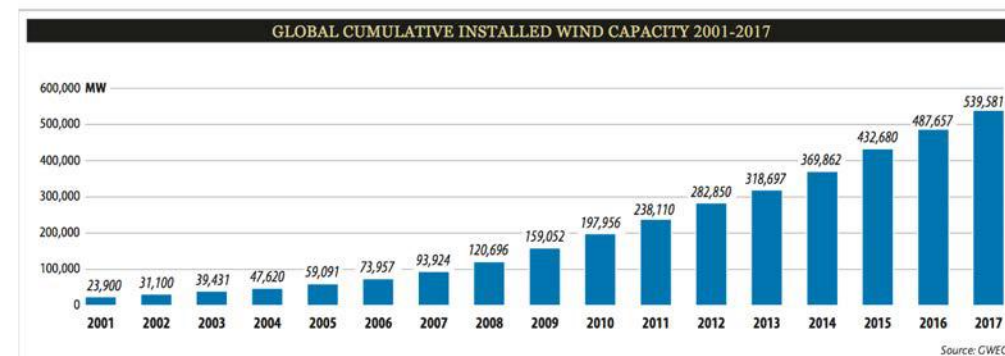
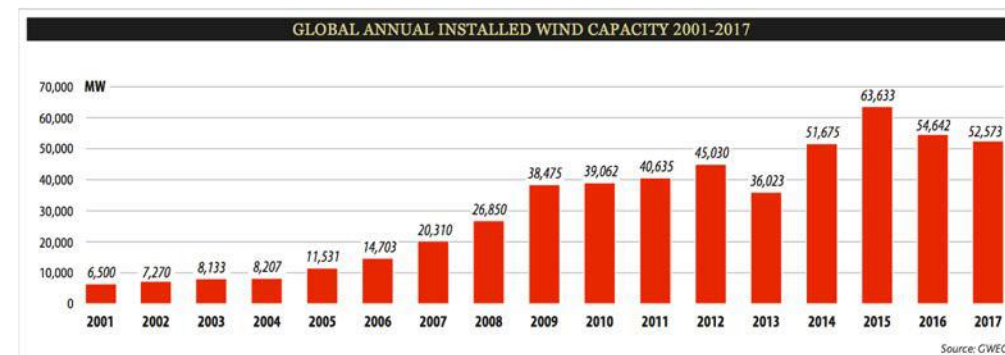
Fig. 5.10. Power coefficients of various of wind rotors [2]

$$F_V = \left(L - \frac{V}{U} D \right) \frac{U}{V_r} = \frac{1}{2} \rho U \left(C_L - \frac{V}{U} C_D \right) V_r A_{bl}$$

$$\mathcal{P}_{bl} = F_V V = \frac{1}{2} \rho U^3 A_{bl} \left(C_L - \frac{V}{U} C_D \right) \frac{V}{U} \sqrt{1 + \left(\frac{V}{U} \right)^2}$$

C_L and C_D change with $\left(\frac{V}{U} \right)$

Two bar charts © GWEC and the other images © source unknown. All rights reserved. This content is excluded from our Creative Commons license. For more information, see <https://ocw.mit.edu/fairuse>.



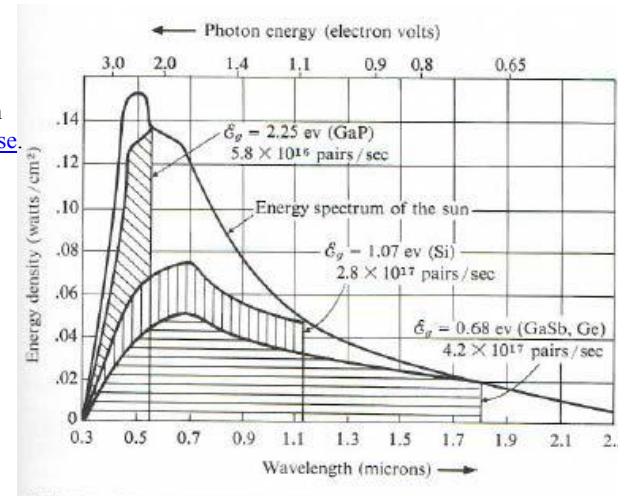
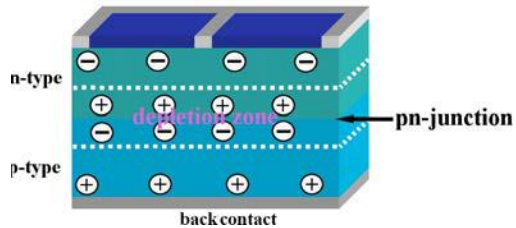
Source: https://gwec.net/wp-content/uploads/vip/GWEC_PRstats2017_EN-003_FINAL.pdf



Solar PVs

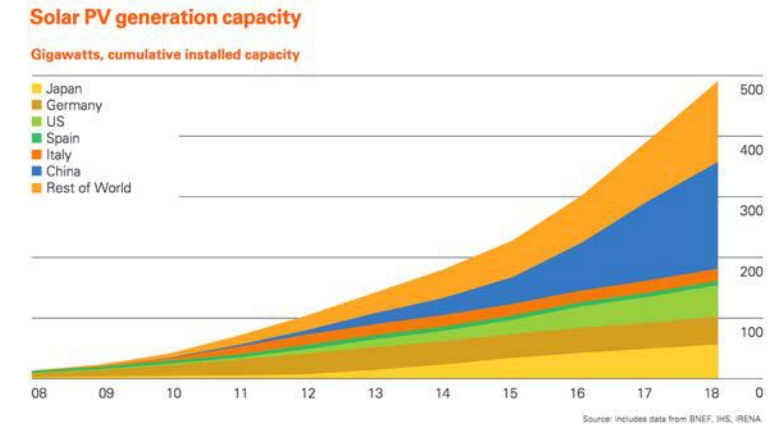


© Informationsbüro Haustechnik. All rights reserved. This content is excluded from our Creative Commons license. For more information, see <https://ocw.mit.edu/fairuse>.



© Source unknown. All rights reserved. This content is excluded from our Creative Commons license. For more information, see <https://ocw.mit.edu/fairuse>.

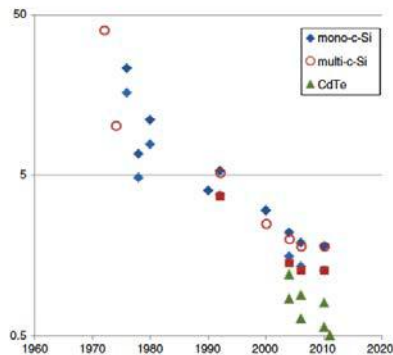
Global PV installed capacity in GW



© BP. All rights reserved. This content is excluded from our Creative Commons license. For more information, see <https://ocw.mit.edu/fairuse>.

Source: <https://www.bp.com/content/dam/bp/business-sites/en/global/corporate/pdfs/energy-economics/statistical-review/bp-stats-review-2019-renewable-energy.pdf>

© SPECMAT, Inc. All rights reserved. This content is excluded from our Creative Commons license. For more information, see <https://ocw.mit.edu/fairuse>.



Energy payback period for different PV technologies, low numbers are for insolation of 2,400 kWh/m²/y, high are for 1,700 kWh/m²/y

© Source unknown. All rights reserved. This content is excluded from our Creative Commons license. For more information, see <https://ocw.mit.edu/fairuse>.

$$j = j_s - j_0 \left(\exp \left(\frac{e_0 V}{nkT} \right) - 1 \right) \approx j_s - j_0 \exp \left(\frac{e_0 V}{nkT} \right)$$

j_s : zero voltage (short circuit) current $V = 0$

j_0 : current in the absence of illumination)

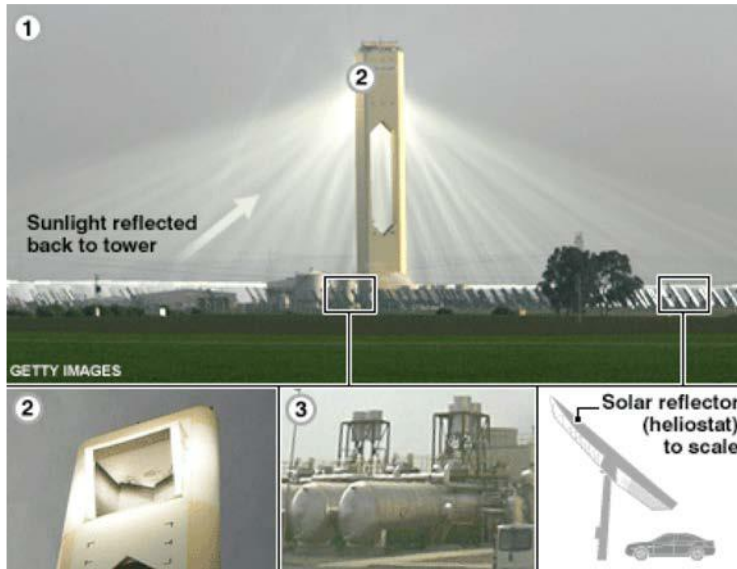
e_0 : electron charge = $1.602 \cdot 10^{-19}$ Coulombs

V : voltage

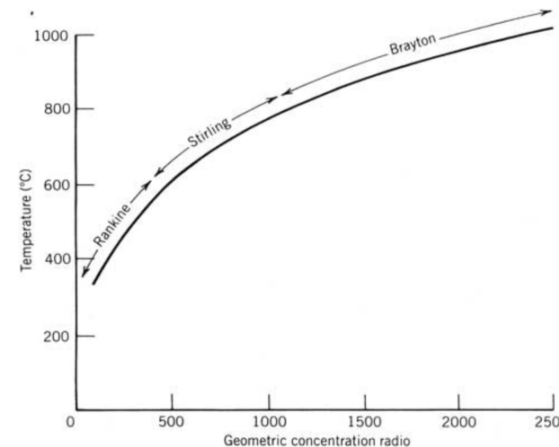
n : =1-2 (known as the diode ideality factor)

k : Boltzman constant= $1.381 \cdot 10^{-23}$ J/K

Solar Energy Generating System (SEGS) Plant Can Be Used To Satisfy Percentage From Renewable Sources



- Thermal Efficiency may reach 54-58%
- Annual average solar-to-electric 10-14%.
- “hybridizable” for dispatchability (25%)
- Storage Ready.

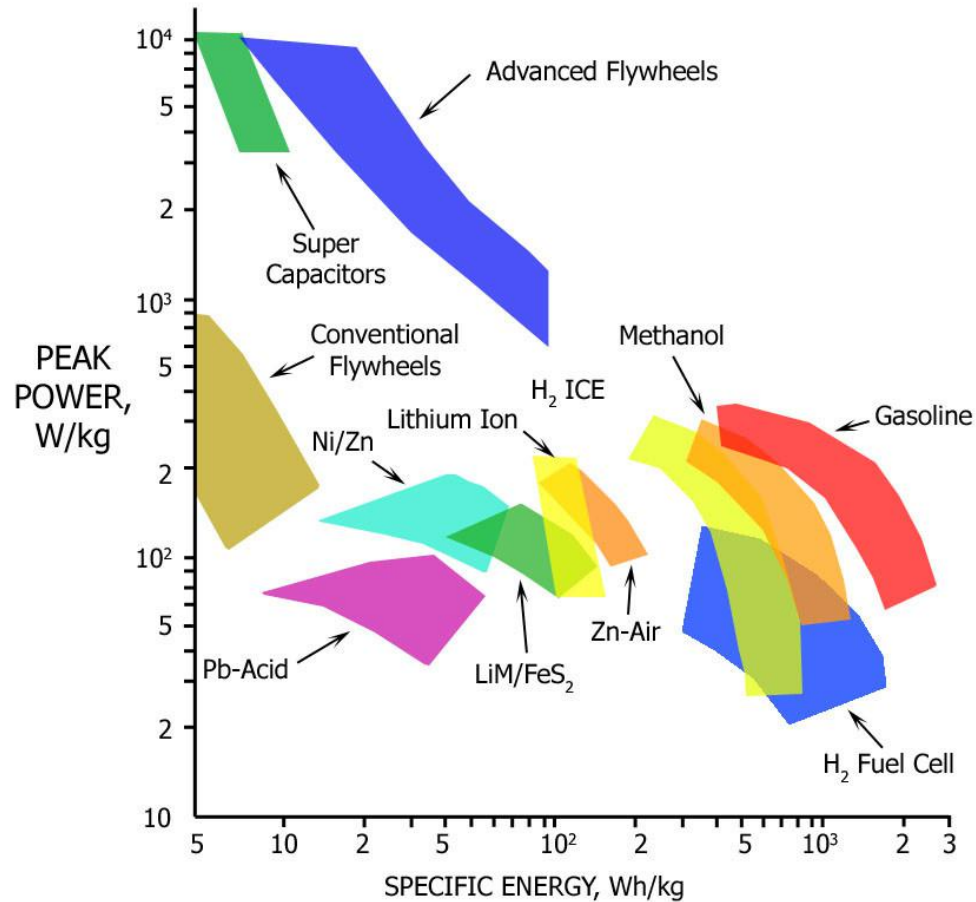


- Total reflective area > 2.3 M. m²
- More than 117,000 HCEs
- 30 MW increment based on regulated power block size

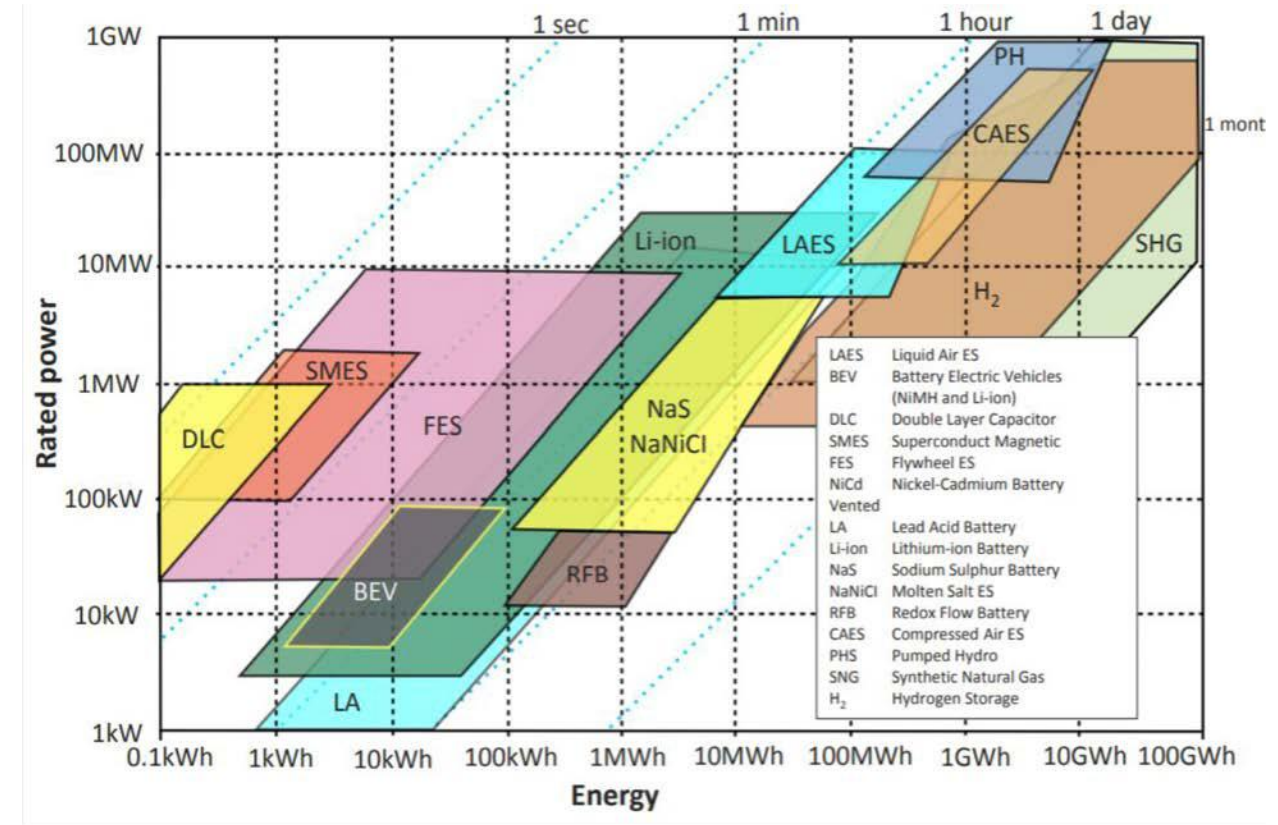
© John Wiley & Sons, Inc. All rights reserved. This content is excluded from our Creative Commons license. For more information, see <https://ocw.mit.edu/fairuse>.

T. R. Mancini, Concentrating Solar Power ,SNL, Albuquerque, New Mexico, USA

Storage; for all forms of energy



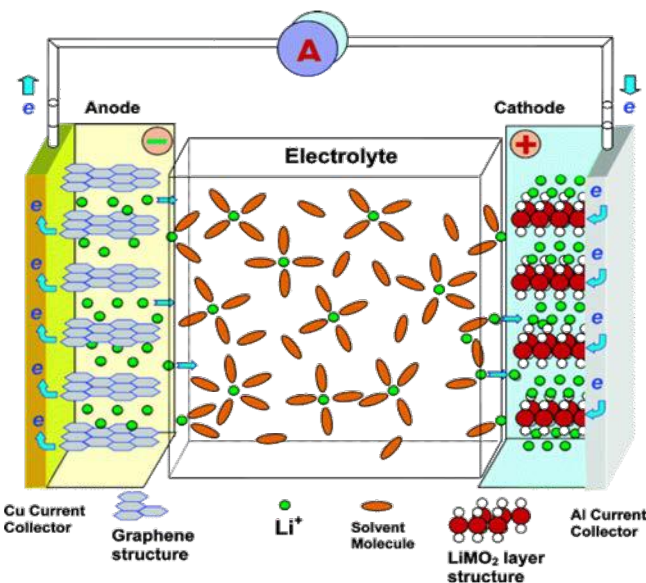
© Walter de Gruyter GmbH. All rights reserved. This content is excluded from our Creative Commons license. For more information, see <https://ocw.mit.edu/fairuse>.



© Source unknown. All rights reserved. This content is excluded from our Creative Commons license. For more information, see <https://ocw.mit.edu/fairuse>.

Ragone plot of power density versus energy density

Batteries



Xu, K. Electrolytes and interphases in Li-ion batteries and beyond. *Chem. Rev.* **114**, 11503–11618 (2014).

© ACS Publications. All rights reserved. This content is excluded from our Creative Commons license. For more information, see <https://ocw.mit.edu/fairuse>.

- During operation, reversible Li^+ intercalation (insertion) into the layered electrode materials

$$\text{Li}_x\text{C}_6 + \text{Li}_{1-x}\text{CoO}_2 \leftrightarrow \text{C}_6 + \text{LiCoO}_2$$
- Forward reaction: discharge ($\Delta G < 0$), Li^+ move towards cathode, as shown in figure
- Reverse reaction: charge ($\Delta G > 0$)

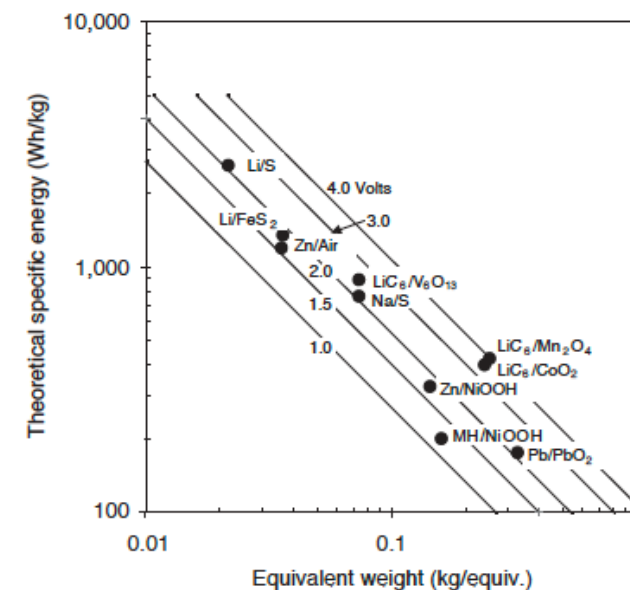
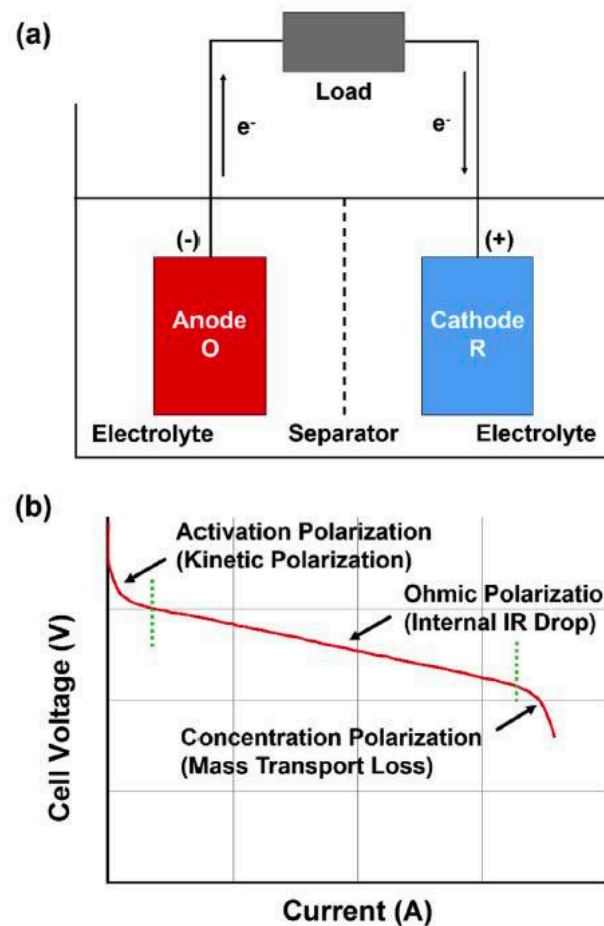


FIGURE 1 Theoretical specific energy for various cells as a function of the equivalent weights of the reactants and the cell voltage.

© Source unknown. All rights reserved. This content is excluded from our Creative Commons license. For more information, see <https://ocw.mit.edu/fairuse>.

Biomass & Biofuels



Thermodynamics of the Corn-Ethanol Biofuel Cycle

© Informa UK Limited. All rights reserved. This content is excluded from our Creative Commons license. For more information, see <https://ocw.mit.edu/fairuse>.

Tad W. Patzek (2004) "Thermodynamics of the Corn-Ethanol Biofuel Cycle", *Critical Reviews in Plant Sciences*, 23:6, 519-567, DOI: [10.1080/07352680490886905](https://doi.org/10.1080/07352680490886905).

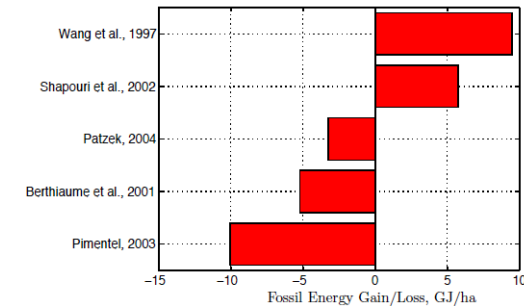
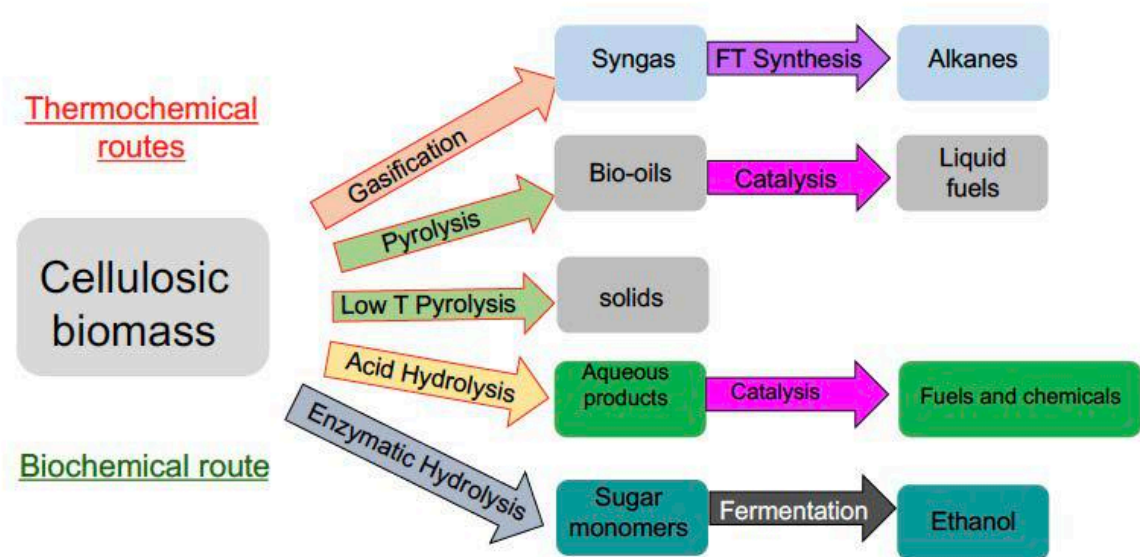
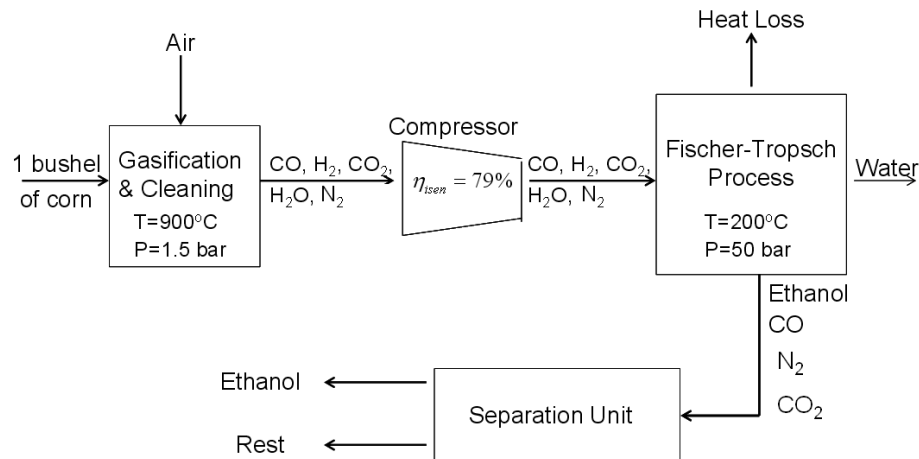
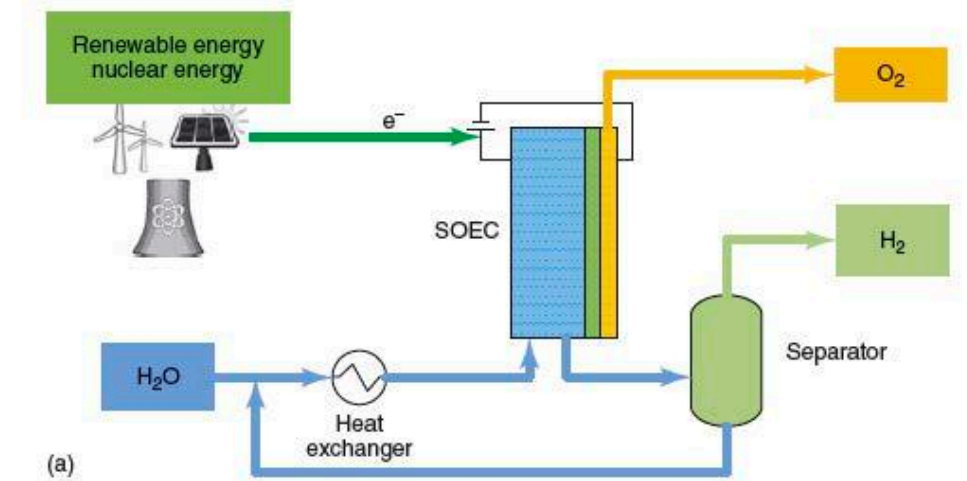


Figure 19: Fossil energy gain/loss in corn ethanol production. Note that the dubious energy credits described in Section 4.4 do not eliminate the use of fossil fuels in the first place, but present alternative useful outcomes of this use.

© Source unknown. All rights reserved. This content is excluded from our Creative Commons license. For more information, see <https://ocw.mit.edu/fairuse>.

HYDROGEN

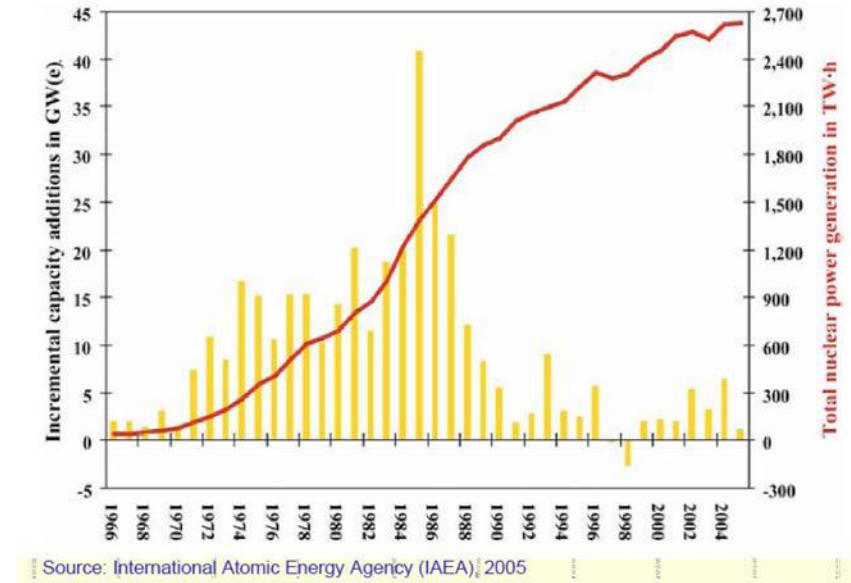
- Like electricity: expensive to produce, not easy to store.
- Produced by:
 - @ Oxygen or steam Reforming of hydrocarbon, or,
 - @ Splitting water electrolytically or thermochemically .
- Has low volumetric by high gravimetric energy density.
- Storage: metal fiber tanks, cryogenic container, in metal hydrides (solids) through physical or chemical sorption.
- It is a “lower grade” of energy than electricity.
- Must be regarded as an energy storage medium.
- Ideal fuel for Low T Fuel Cell: PEMFC



Nuclear Energy; Potential @ CO₂ price



© Source unknown. All rights reserved. This content is excluded from our Creative Commons license. For more information, see <https://ocw.mit.edu/fairuse>.

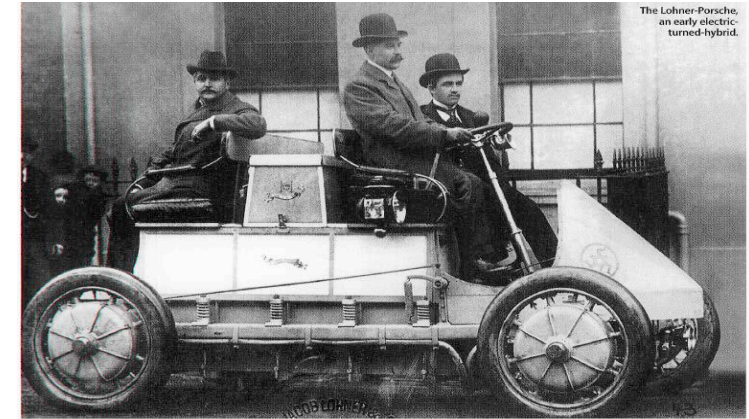


© IAEA. All rights reserved. This content is excluded from our Creative Commons license. For more information, see <https://ocw.mit.edu/fairuse>.

Transition is not new in this business



Figure 3-11 BMW's Hydrogen-Powered Internal Combustion Vehicle



The Lohner-Porsche, an early electric-converted hybrid.

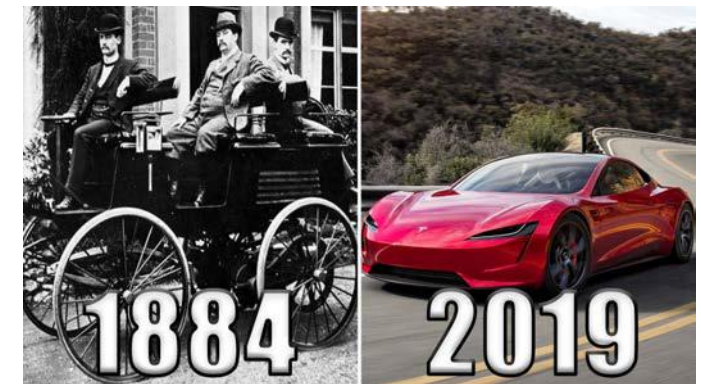
Prescient Porsche

The legendary car designer's earliest autos featured an innovation that took off 100 years later. **BY DAN CHO**

drive mechanisms of the day. He installed electric motors in each of a car's front wheel hubs, eliminating the shafts, gears, and chains needed for ordinary transmission systems. The Lohner-Porsche auto debuted at the 1900 Paris Exposition, taking the event's Grand Prix. Over the next couple years, Porsche would win both races and wide acclaim with his car.

This image is in the public domain.

Source: https://commons.wikimedia.org/wiki/File:Lohner_Porsche.jpg



© Source unknown. All rights reserved. This content is excluded from our Creative Commons license. For more information, see <https://ocw.mit.edu/fairuse>.

THE ELECTRIC CAR PAST AND FUTURE



World's first hybrid electric car invented

1901

Thomas Edison works to develop better EV batteries

1832

First crude EVs developed

1900-1912

EVs reach their heyday

1920-1935

Cheap Texas crude oil fuels decline in electric vehicles

1971

Electric lunar rover is first manned vehicle to drive on moon

1973

General Motors unveils prototype for urban EV

1974-1977

U.S. carmaker Sebring-Vanguard produces more than 2,000 CitiCar EVs, which have range of 80-97km



1990-1992

New U.S. environmental regulations renew interest in EVs

1997

Toyota introduces Prius, world's first mass-produced hybrid



1996

GM releases EV1, first mass-produced EV by major automaker



2008

Tesla launches commercial production of Roadster EV



2009-2013

U.S. government installs 18,000 residential, commercial, public chargers

China's BYD Auto releases F3DM, world's first plug-in hybrid

2010

Nissan releases all-electric Leaf



2014

Tesla breaks ground on massive Gigafactory 1 battery plant in U.S. state of Nevada

2016

GM releases Chevy Bolt, its first electric car

Chinese Finance Minister Lou Jiwei says country will totally phase out subsidies for green energy vehicles by 2021

2017

MARCH India's power minister suggests country aims for EV-only sales by 2030

JULY

France, U.K. say they will end sales of gasoline, diesel vehicles by 2040

2020

Tesla targets annual sales of 1 million cars

2025

VW targets annual sales of 2-3 million EVs by this year

OCTOBER

GM says it will launch at least 20 new electric, fuel-cell vehicles by 2023

2030

Up to 200 million EVs projected to be in circulation

2040

EVs projected to account for 32% of global auto sales

Prius photo by Reuters, others by Getty Images
Sources: International Energy Agency's Global EV Outlook 2017 report, U.S. Department of Energy

Prof. Ferdinand Porsche Created the First Functional Hybrid Car



© Porsche Museum. All rights reserved. This content is excluded from our Creative Commons license. For more information, see <https://ocw.mit.edu/fairuse>.

© Teslarati.com. All rights reserved. This content is excluded from our Creative Commons license. For more information, see <https://ocw.mit.edu/fairuse>.

<https://www.pinterest.com/pin/380272762280612514/>

MIT OpenCourseWare
<https://ocw.mit.edu/>

2.60J Fundamentals of Advanced Energy Conversion
Spring 2020

For information about citing these materials or our Terms of Use, visit: <https://ocw.mit.edu/terms>.

Lecture # 2

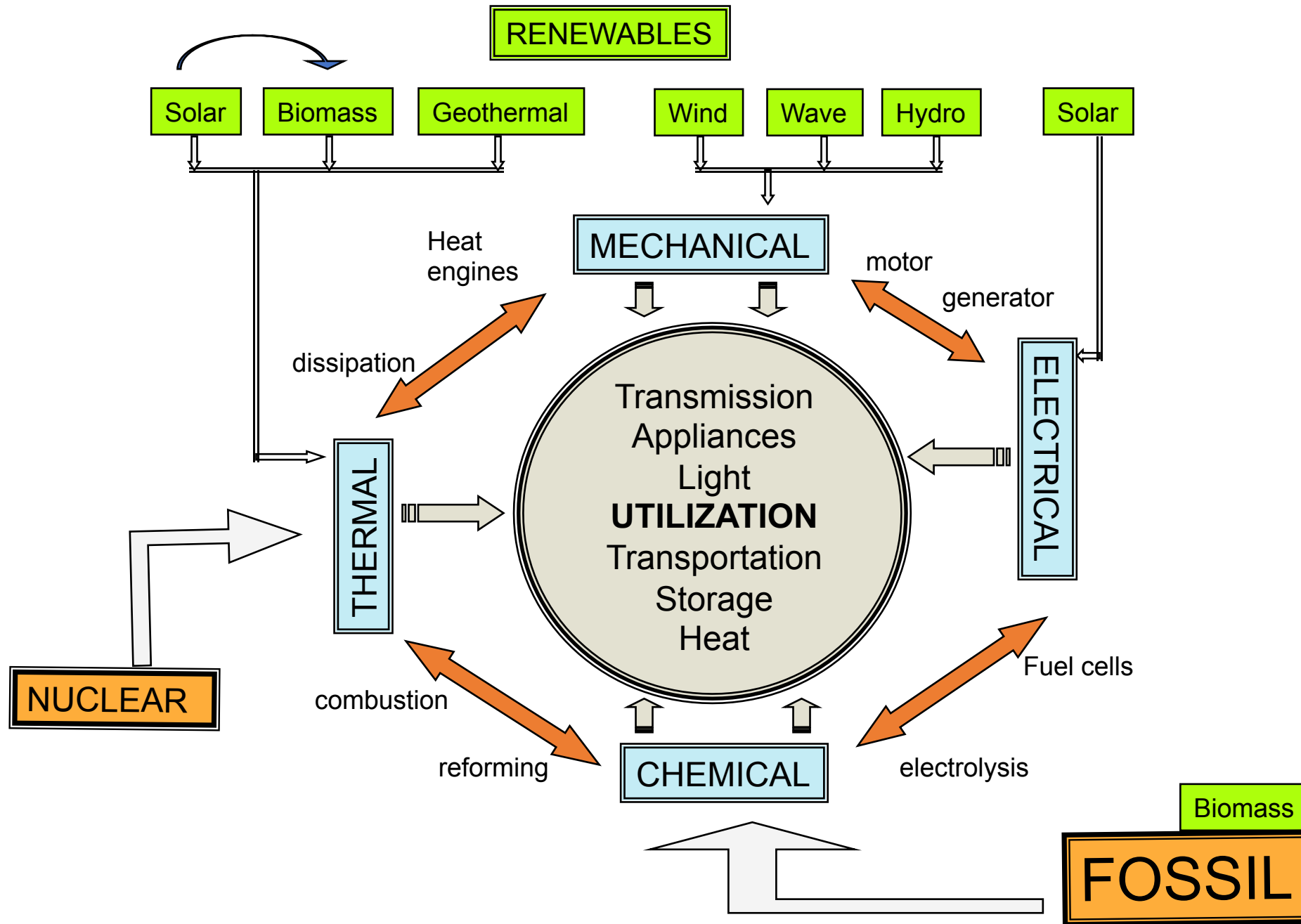
Thermodynamics and Tools to Analyze Conversion Efficiency

Ahmed Ghoniem

Feb 5, 2020

- Conservation laws
- Limits on conversion
- Availability
- Efficiency

Ghoniem, AF Energy Conversion Engineering, Chapter II, Thermodynamics.

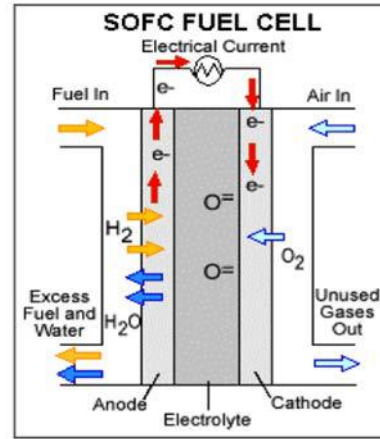
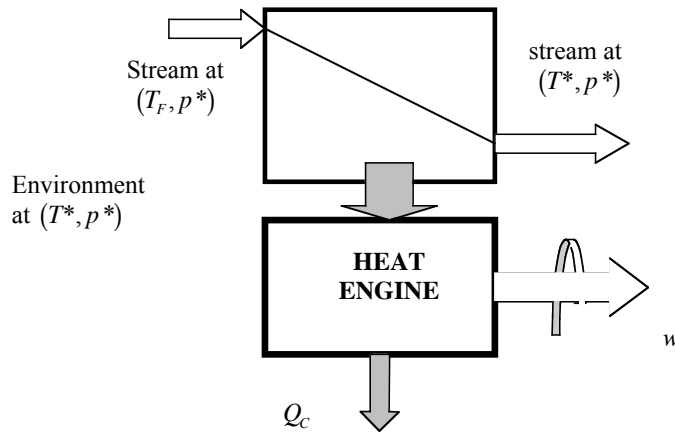


Some Thermodynamics

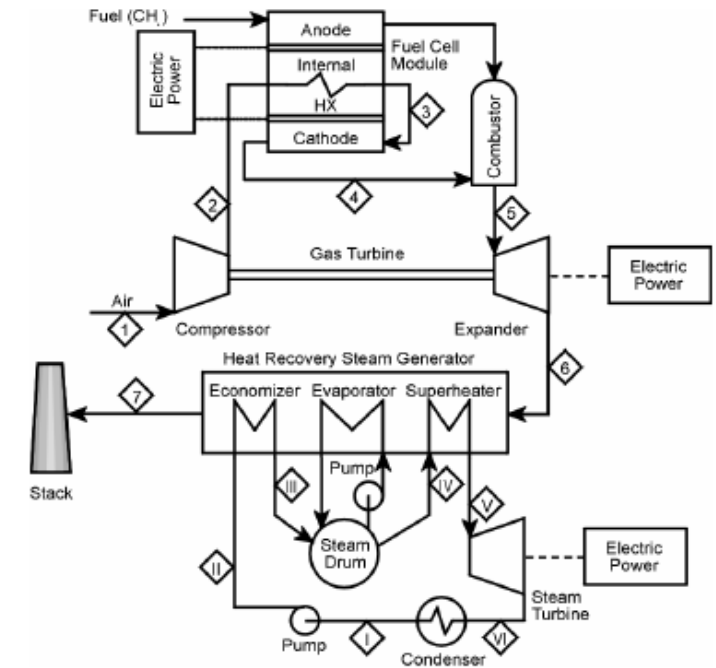
“Classical Thermodynamics is the only physical theory of universal content which, ... within the framework of its basic notions, will never be toppled.” *Albert Einstein.*

- Energy conversion is governed by conservation principles, and often involves “availability” loss.
- This translates to the all important “efficiency”.
- How to maximize conversion efficiency, identify sources of loss and minimize them?

Heat Engine & Fuel Cell, Efficiency?



Integration of Thermomechanical and Electrochemical Systems



$$\eta_{car} = 1 - \ln \frac{T_F}{T^*} / \left(\frac{T_F}{T^*} - 1 \right)$$

$$= 70\% \text{ for } T_F / T^* = 8$$

$$\mathcal{E}(T, p, X_i) = \mathcal{E}^o(T) + \frac{\Re T}{2\mathfrak{S}} \left(\frac{1}{2} \ln p + \ln \left(\frac{X_{H_2} X_{O_2}^{1/2}}{X_{H_2O}} \right) \right)$$

$$\eta_{OC} = \frac{w_{\max}}{\Delta H_{R, H_2O}^o} = \frac{\Delta G_{R, H_2O}}{\Delta H_{R, H_2O}^o}$$

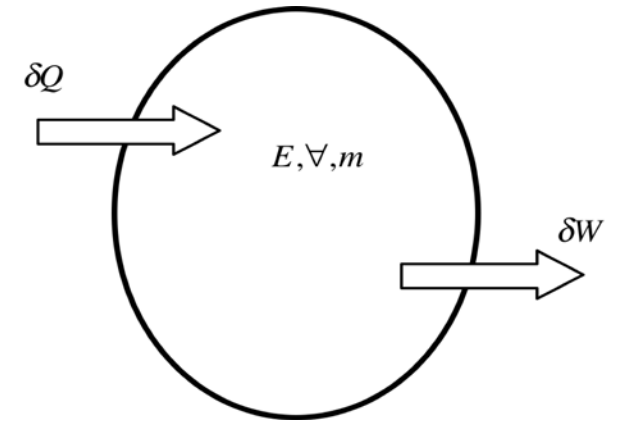
Ideal thermomechanical vs. electrochemical systems, governing principles and efficiency, and their integration for maximizing the latter

First Law: Energy Conversion, heat and work transfer, control mass

$$\Delta Q - \Delta W = E_2 - E_1$$

Stored Energy (in terms of state properties, V , $u = U / m$, Z , ζ , ...)

$$E = \underbrace{\frac{1}{2}m\mathbf{V}^2}_{KE} + \underbrace{mg_r Z}_{PE} + \underbrace{U}_{U_{th} + U_{ch}} + \underbrace{\frac{1}{2}k_s x^2}_{E_{elas}} + \underbrace{\epsilon \zeta}_{E_{elect}} + E_{mag} + E_{nuc}$$



$$-\delta W_{mech} = \vec{F} \cdot d\vec{x} = -p d\forall$$

$$-\delta W_{el} = \mathcal{E} d\zeta$$

$$-\delta W_{mag} = H dM_g$$

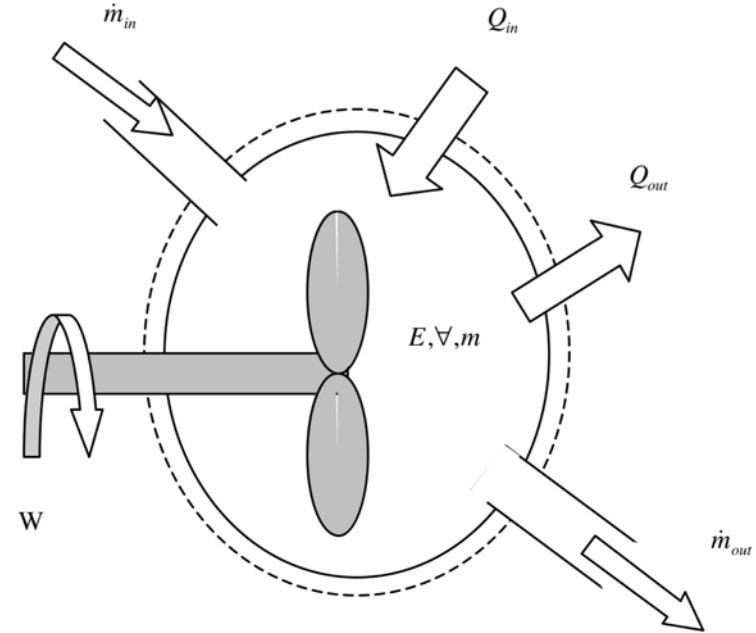
Control Volume:

Need mass conservation as well

$$\frac{dm_{CV}}{dt} = \sum_{in} \dot{m}_i - \sum_{out} \dot{m}_i$$

$$\frac{dE}{dt} = \dot{Q} - \dot{W} + \sum_{in} \dot{m}_i (h + ke + pe + \dots) - \sum_{out} \dot{m}_i (h + ke + pe + \dots)$$

$$E_2 - E_1 = Q - W + \sum_{in} \dot{m}_i (h + ke + pe + \dots) - \sum_{out} \dot{m}_i (h + ke + pe + \dots)$$



Second Law: Entropy

Control mass

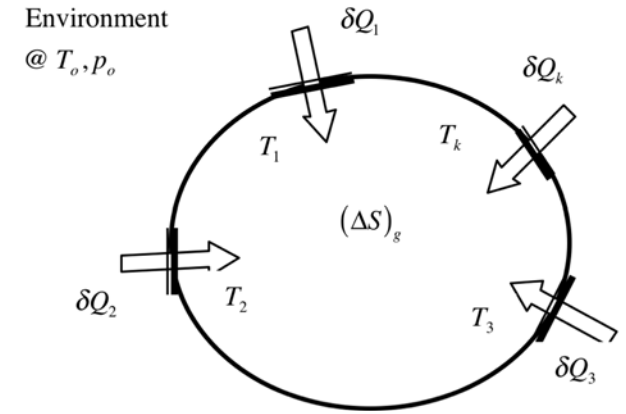
$$S_2 - S_1 = \int_1^2 \frac{\delta Q}{T} + (\Delta S)_g \quad \text{or} \quad S_2 - S_1 = \sum_{k=1}^K \frac{\Delta Q_k}{T_k} + (\Delta S)_g$$

Entropy is generated when:

- Heat is transferred across a finite temperature gradient
- Fluid expands across a finite pressure drop
- Mixing of different fluids (or same fluid volumes with different T)
- Chemical reactions causing temperature rise (or drop)

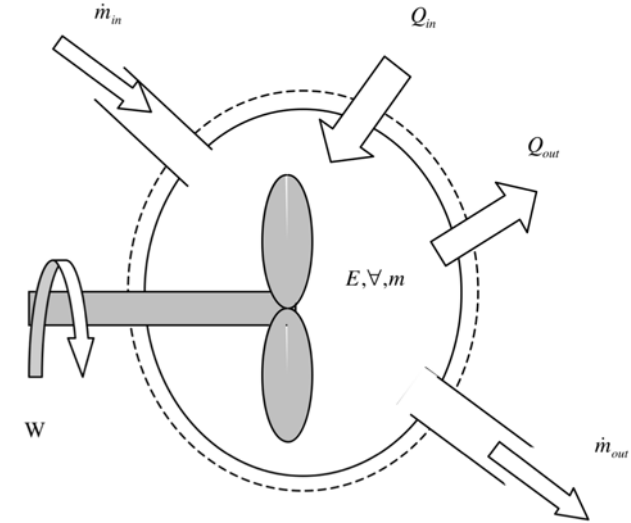
Informally: entropy is generated when a process is performed without work transfer when work could have been obtained (or when it is less than the maximum possible).

One of the original statements: a cyclic machine cannot be used to convert heat into work at 100% efficiency.



Second Law: Entropy Control volume

$$\frac{dS_{cv}}{dt} = \int_1^2 \frac{\delta \dot{Q}}{T} + \sum_{in} s_i \dot{m}_i - \sum_{out} s_i \dot{m}_i + \left(\frac{dS}{dt} \right)_g$$
$$(S_2 - S_1)_{CV} = \sum \frac{\Delta Q_i}{T_i} + \sum_{in} s_i m_i - \sum_{out} s_i m_i + (\Delta S)_g$$



Entropy generation is a quantitative measure of “loss of work”!?

The lost work is measured by the “availability” or “exergy” loss.

Maximum Work, Availability and limits on energy conversion:

System (with fixed mass)

“Add” the first and second laws

For a system with heat transfer at fixed temperatures

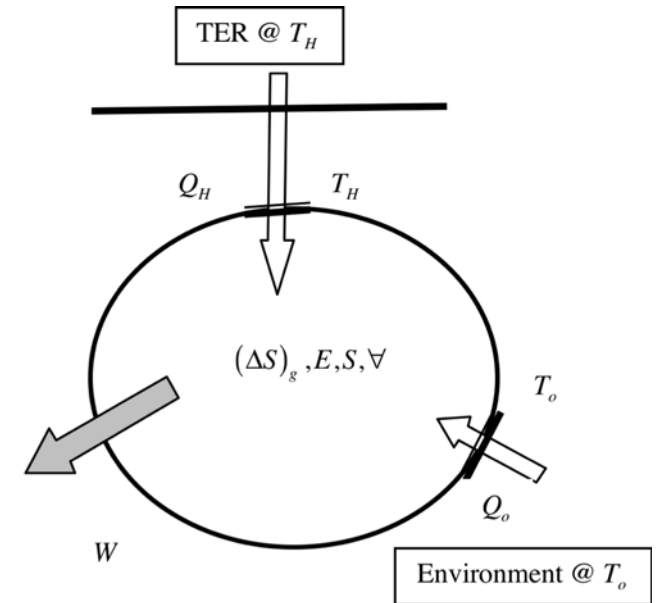
$$W_{use} = Q_H \left(1 - \frac{T_o}{T_H} \right) + \Xi_1 - \Xi_2 - I_{ir}.$$

system availability is:

$$\Xi = (E - U_o) + p_o(\forall - \forall_o) - T_o(S - S_o).$$

Changes in internal energy, volume or entropy can produce work

$$I_{ir} = T_o(\Delta S)_g \rightarrow \text{internal irreversibility or lost work}$$



Examples:

Heat Engine, work produced by heat transfer only:

2 TER*, high TER fixed at T_H

$$W_{\max} = \left(1 - \frac{T_o}{T_H}\right) Q_H = W_{car}$$

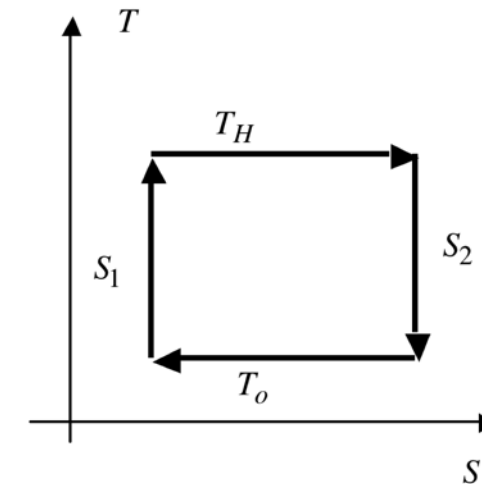
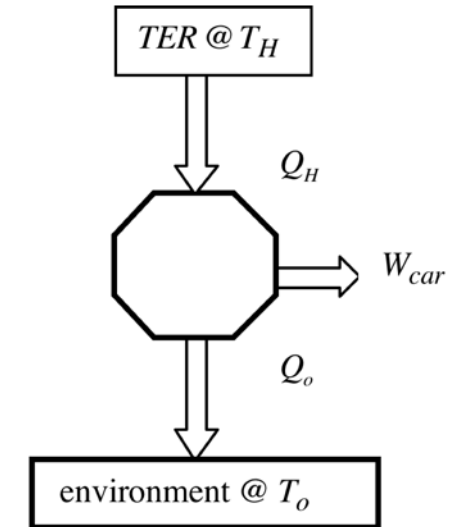
* it is easy to fix T_o , but not T_H

Can only be realized with:

- Isothermal heat transfer from sources (with zero ΔT)
- Ideal expansion/compression

The Carnot cycle is an ideal heat engine

(as well as the Stirling and Ericsson cycles)



For a control volume

Fixed Mass interacting with single TER@ T_o :

$$\begin{aligned} W_{\max} &= (E_1 - T_o S_1 + p_o \forall_1) - (E_2 - T_o S_2 + p_o \forall_2) \\ &= \Xi_1 - \Xi_2 \end{aligned}$$

Ξ : total exergy or availability difference

in case only internal energy is utilized, $E = U$

with no change of chemical state, $U = U_{th}$.

For $\max|W_{\max}|$, final state (2) must be in equilibrium

with environment (restricted dead state), $T_2 = T_o, p_2 = p_o$

$$\begin{aligned} \dot{W}_{cv} &= \sum_{TERs} \left(1 - \frac{T_o}{T_i} \right) \dot{Q}_i - \left(\frac{d\Xi_{cv}}{dt} - p_o \dot{\forall}_{cv} \right) \\ &\quad + \sum_{in} \dot{m}_i \xi_i - \sum_{out} \dot{m}_i \xi_i - \dot{I}_{ir} \\ \xi &= (\tilde{h} - h_o) - T_o (s - s_o) \\ &\quad \text{(flow exergy/availability per unit mass)} \\ \tilde{h} &= h + ke + pe \end{aligned}$$

for an ideal gas, fixed c_p

$$\Delta h = c_p (T_2 - T_1),$$

$$\Delta s = c_p \ln \left(\frac{T_2}{T_1} \right) - \Re \ln \left(\frac{p_2}{p_1} \right)$$

For steady operation of a CV interacting with 2 TER and stream:

$$\dot{W}_{cv} = \underbrace{\left(1 - \frac{T_o}{T_H}\right) \dot{Q}_H}_{\text{Carnot Engine heat availability}} + \underbrace{\dot{m}(\xi_{in} - \xi_{out})}_{\text{flow stream flow availability}} - \dot{I}_{ir} \quad \xi = (\tilde{h} - h_o) - T_o(s - s_o)$$

For maximum work:

- zero irreversibility, $\dot{I}_{ir} = 0$
- equilibrium with environment, $\xi_{out} = \xi_{env}$

For steady operation of a CV interacting with a stream only: $\dot{Q}_H = 0$

Entropy and exergy analysis serve the same purpose, they are interchangeable

Either can be used to determine the source of inefficiency in a complex system

Example 2.8. (subcooled) Water at 200 kPa and 100°C is expanded in an adiabatic throttle valve to a final pressure of 20 kPa. The process does not involve any work transfer. An inventor claims to have designed a device that generates work of 10 kJ/kg of water while maintaining the same inlet and outlet conditions of the throttle and exchanging heat with the environment at 25°C. Is this claim feasible?



assume steady operation, neglect changes in the kinetic and potential energies.

At 200 kPa and 100 °C, $h_1 = h_{f@100^\circ\text{C}} = 419.17 \text{ kJ/kg}$ and $s_1 = s_{f@100^\circ\text{C}} = 1.3072 \text{ kJ/kg-K}$.

energy balance across an adiabatic throttle is: $h_2 = h_1 = 419.17 \text{ kJ/kg}$.

The final state is determined by knowing the final pressure, p_2 , and the final enthalpy, h_2 . Since the enthalpy falls between the saturated liquid and the saturated vapor values at 20 kPa, $h_{f@20\text{kPa}} = 251.42 \text{ kJ/kg}$ and $h_{g@20\text{kPa}} = 2608.9 \text{ kJ/kg}$,

the quality of the mixture is $x_2 = (h_2 - h_f) / h_{fg} = 0.0712$,

and the entropy is $s_2 = s_f + x_2 s_{fg} = 0.8320 + 0.0712 \times 7.9073 = 1.3354 \text{ kJ/kg-K}$.

maximum work is the difference between the availability between initial and final states:

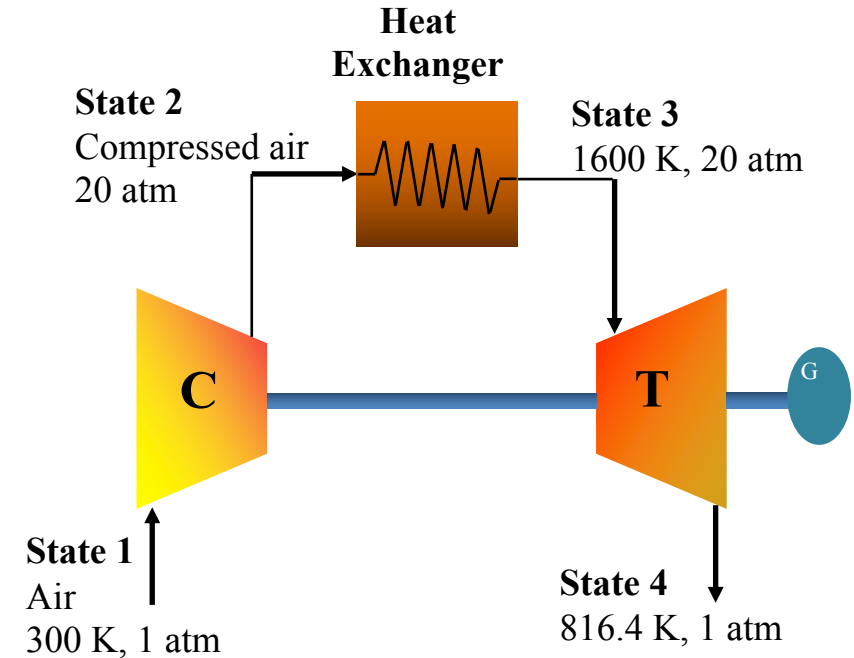
$$w_{\max} = (h_1 - T_o s_1) - (h_2 - T_o s_2) = T_o (s_2 - s_1) = 8.417 \text{ kJ/kg}$$

work output claimed by the inventor is higher than maximum value, not possible.

Using exergy analysis to determine the performance of a system and how to improve it

A closed-cycle gas turbine power plant, shown in the following figure, operates with air as a working fluid. Conditions are shown in figure. Analyze the losses and propose improvements

State	$T(K)$	p (atm)	h (kJ/kg.K)	ξ (kJ/kg)
1	300	1	0	0
2	808.3	20	510.4	469.8
3	1600	20	1305.2	1058.9
4	816.4	1	519.4	217.5



Energy (and availability) are added (from outside) in process 2-3 only.
For maximum work all availability added should be used as work
How much is lost in each component and with the exit stream?

To determine performance

of individual components:

For a flow process:

$$Q - W = \Delta h$$

Maximum work

= change in availability

$$(W_{\max})_{\text{turbine}} = \xi_4 - \xi_3, \quad (W_{\max})_{\text{compr}} = \xi_2 - \xi_1,$$

$$(W_{\max})_{\text{exitstream}} = \xi_4 - \xi_1,$$

state 1 taken as reference

to find maximum work by system

$$W_{\text{sys}} = \left(1 - \frac{T_o}{T_i}\right) Q_i + \xi_1 - \xi_4 - I_{\text{ir}}$$

for max work, ξ_4 should be equal to ξ_1

$$\text{and } I_{\text{ir}} = 0. \quad W_{\text{sys},\max} = \left(1 - \frac{T_o}{T_i}\right) Q_i$$

to determine the RHS, apply the same to HX, with $I_{\text{ir}} = 0$:

$$0 = \left(1 - \frac{T_o}{T_i}\right) Q_i + \xi_2 - \xi_3, \text{ and substitute: } W_{\text{sys},\max} = \xi_3 - \xi_2$$

	Enthalpy change (kJ/kg)	Availability change (kJ/kg)
Heat Exchanger	$h_3 - h_2 = 794.8$	$\xi_3 - \xi_2 = \mathbf{589.1}$
Compressor	$W_c = 510.4$	-469.8
Turbine	$W_t = 785.8$	841.4
Net Work	$(h_3 - h_4) - (h_2 - h_1) = \mathbf{275.4}$	
Air out at 4	$h_4 - h_1 = 519.4$	$\mathbf{217.5}$

First law efficiency is $275.4/794.8 = 34.6\%$

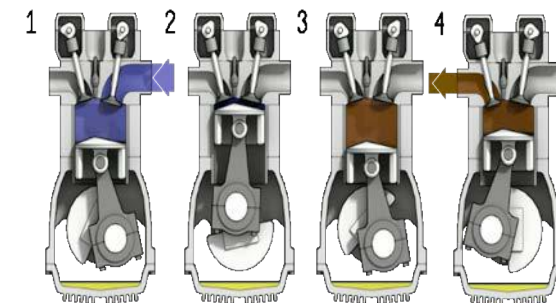
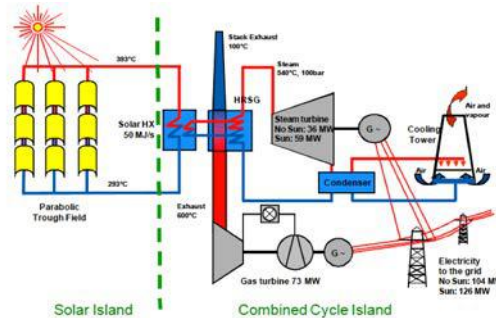
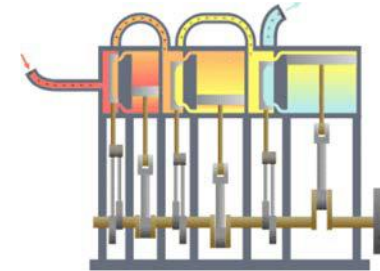
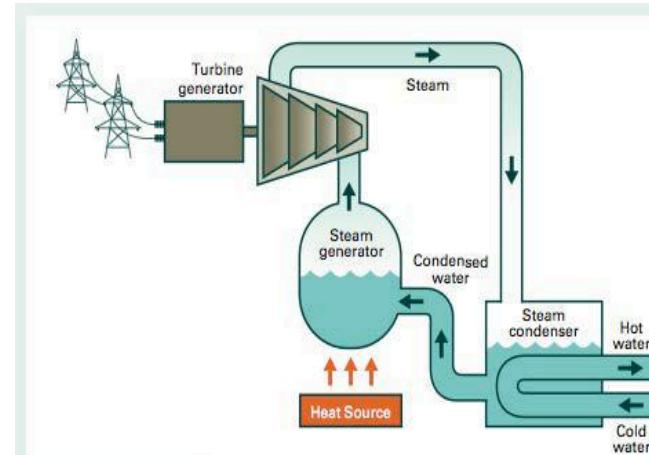
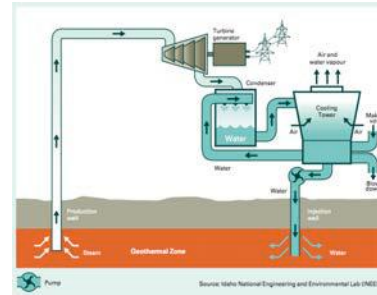
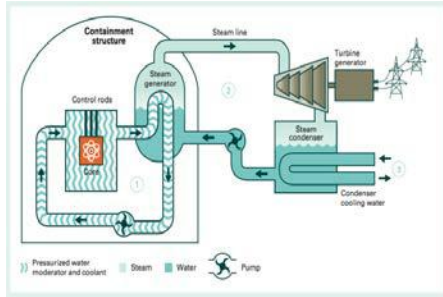
Second law efficiency is $275.4/589.1 = 46.7\%$

Compressor irreversibility $\frac{\dot{I}}{\dot{m}} = -\frac{\dot{W}}{\dot{m}} + \xi_1 - \xi_2 = \mathbf{40.6 \text{ kJ/kg}}$

Turbine irreversibility $\frac{\dot{I}}{\dot{m}} = -\frac{\dot{W}}{\dot{m}} + \xi_3 - \xi_4 = \mathbf{55.6 \text{ kJ/kg}}$

losses with exit stream = $\mathbf{217.5 \text{ kJ/kg}}$

Many Heat Engines since ...



Gas turbine engines and turbo jet engine



GENx Engine 53,000-75,000 pounds thrust |

Rumford birthplace (1753) and museum, Elm St, Woburn MA

Benjamin Thompson/Lord Rumford established the equivalency of heat and work, worked on cannons, invented the modern fireplace, drip coffee maker, etc., his bust in Rhode Island (and a historical society named after him)

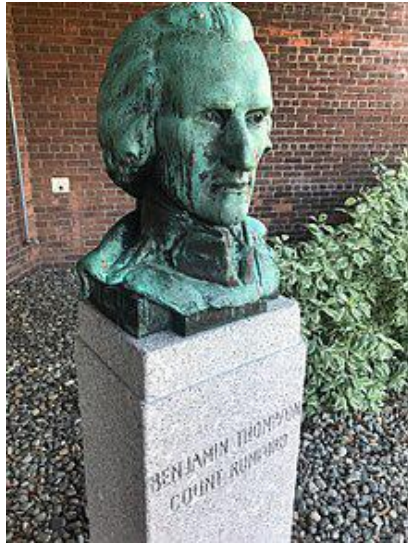


Image courtesy of Mass.gov.

Benjamin Thompson born 1753 in Woburn, MA, educated in Harvard, married Sarah Rolfe from Concord NH, then called Rumford. Worked on boring cannons, helped the British during the revolutionary war, and ran to England, where became Lord Rumford, eventually moved to Munich and contributed much to physics and thermodynamics.

© Babbage on [Wikimedia](#). CC BY-SA 4.0. This content is excluded from our Creative Commons license. For more information, see <https://ocw.mit.edu/fairuse>.

The inverse of a heat engine is refrigerators and air conditioners, arguably the most important invention of engineering in the 20th century.

Power Plant Efficiency

Do we have an Energy or an Entropy Crisis?

What have engineers been doing over the past 200 years?

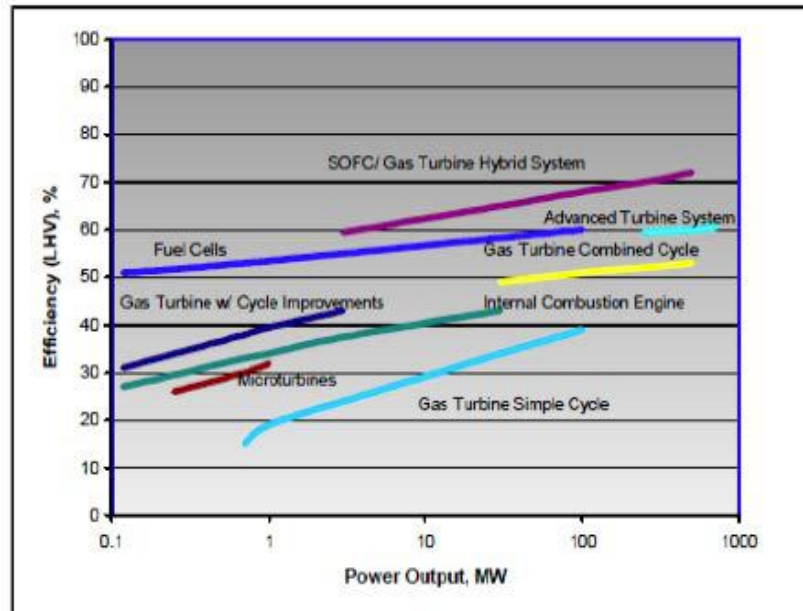
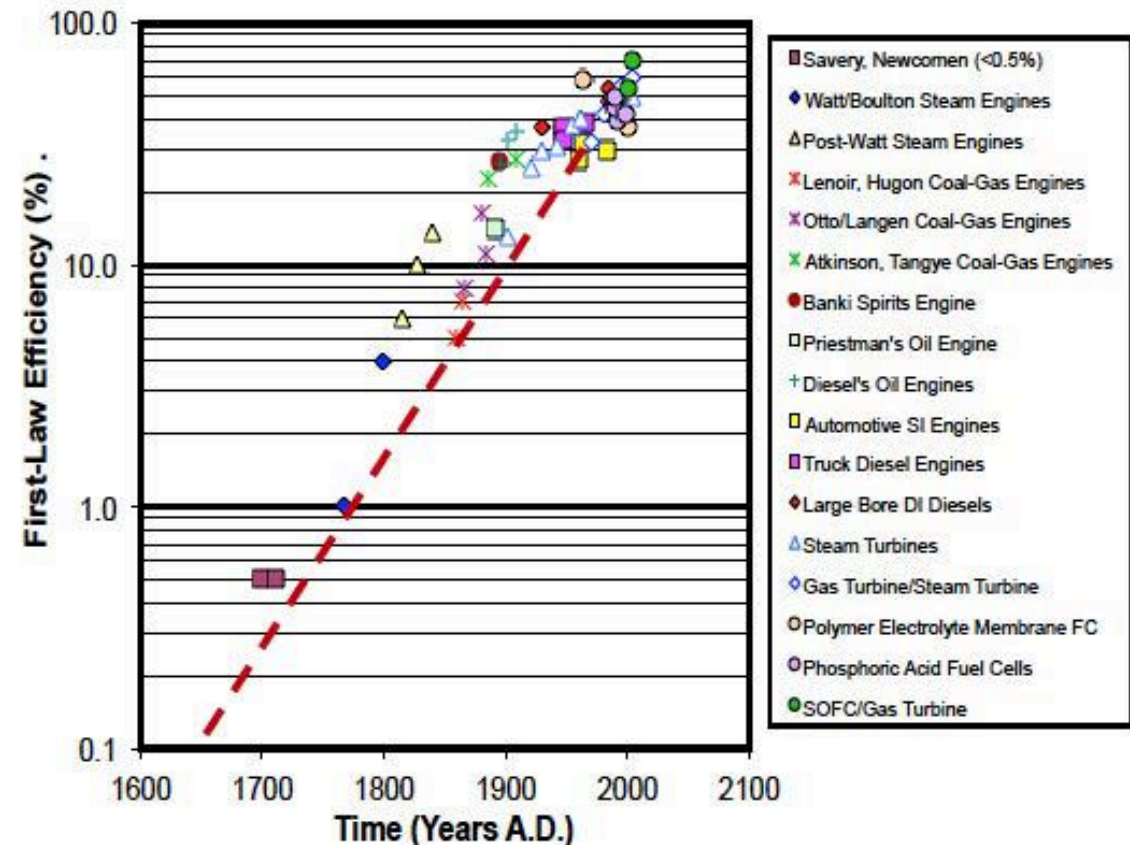


Figure 8-41 Estimated performance of Power Generation Systems

Image courtesy of DOE.

Fuel Cell Handbook, 7th Ed., by EG&G Technical Services, U.D. DOE, Office of Fossil Energy, NETL, Morgantown, W Va, Nov 2004, p. 8-91.



The best **heat engine** (**thermal to mechanical**) is a Carnot engine operating between two fixed temperatures:

the (thermo-mechanical) conversion efficiency of the engine is

$$\eta_I = \frac{W_{net}}{Q_H} = 1 - \frac{Q_o}{Q_H}, \text{ also called the first law efficiency}$$

$$\eta_{car} = 1 - \frac{T_o}{T_H}$$

temperatures are in absolute, e.g., in K=273+C

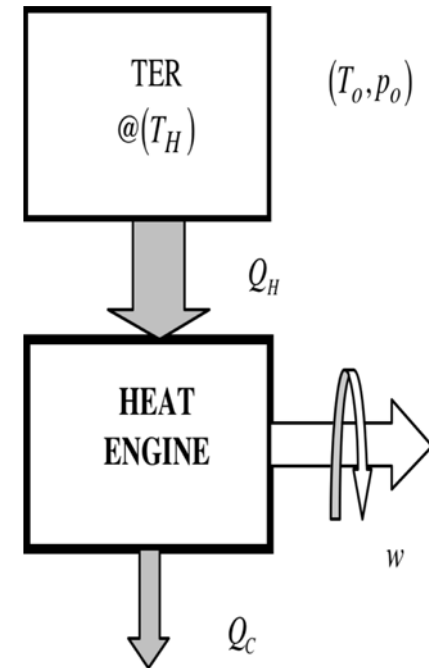
$$T_o \sim 300 \text{ K},$$

maximum fuel combustion temperature $\sim 1800\text{-}2400 \text{ K}$

$$T_H / T_o = 6 - 8, \quad \eta_{car} = 84 - 88\%$$

the efficiency depends critically on T of the heat source!

also on the cold side T



A heat engine operating between a continuous stream starting at a high temperature and the environment has a lower efficiency.

If the stream pressure is fixed:

$$W_{\max} = \int_{T_o}^{T_H} \left(1 - \frac{T_o}{T} \right) dQ = \int_{T_o}^{T_H} \left(1 - \frac{T_o}{T} \right) C dT$$

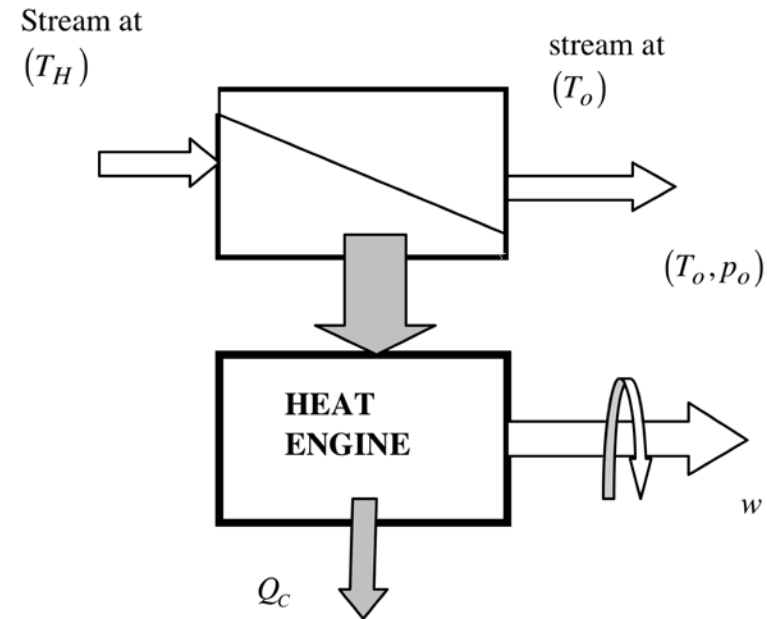
$$= C \left[(T_H - T_o) - T_o \ln \frac{T_H}{T_o} \right]$$

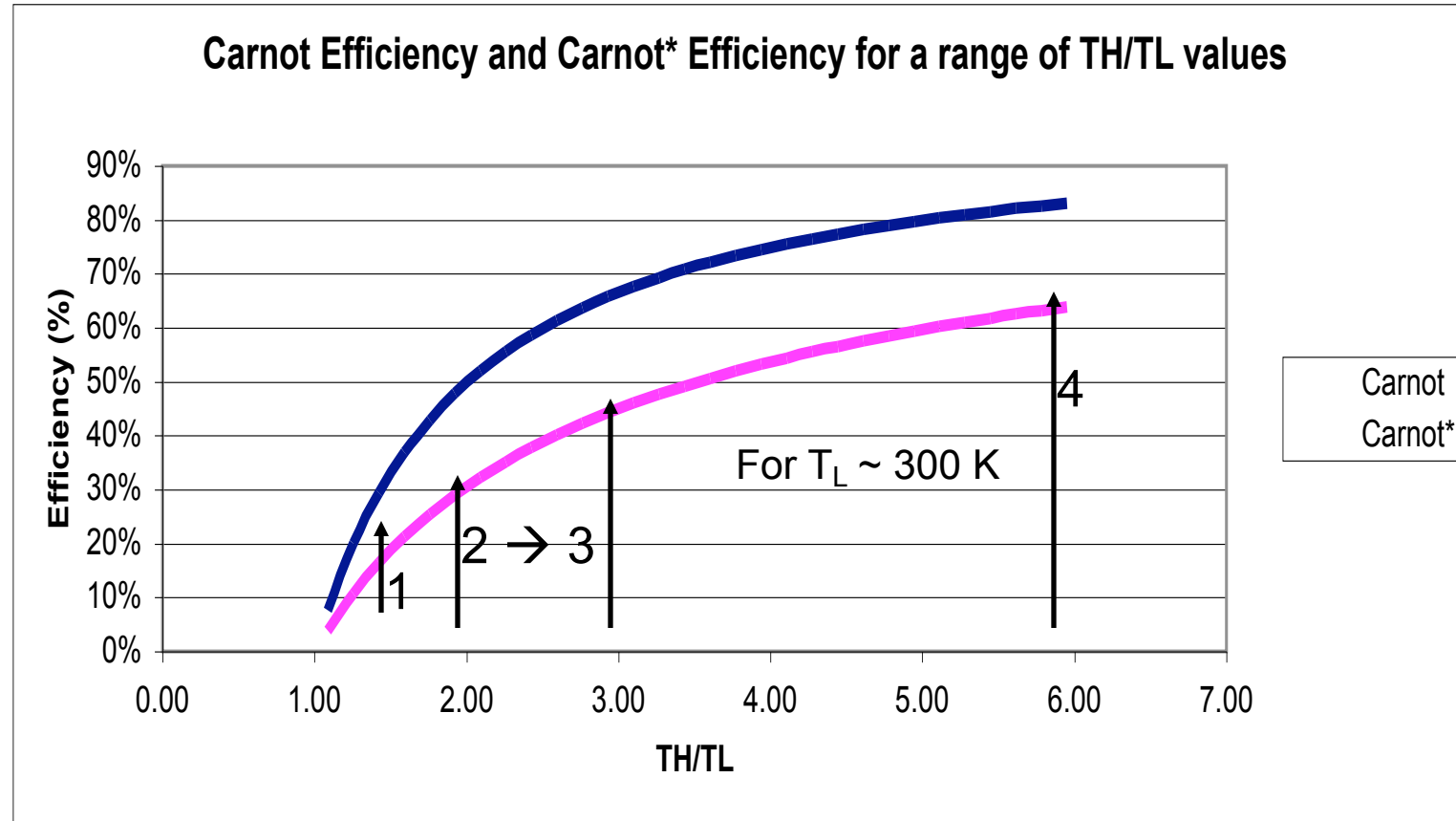
OR (since streams at same p_o)

$$W_{\max} = \xi_H - \xi_o = (H_H - H_o) - T_o (S_H - S_o)$$

$$\eta_{car}^* = 1 - \ln \left(\frac{T_H}{T_o} \right) / \left(\frac{T_H}{T_o} - 1 \right)$$

$$T_H / T_L = 6 - 8, \eta_{car}^* = 70\%$$

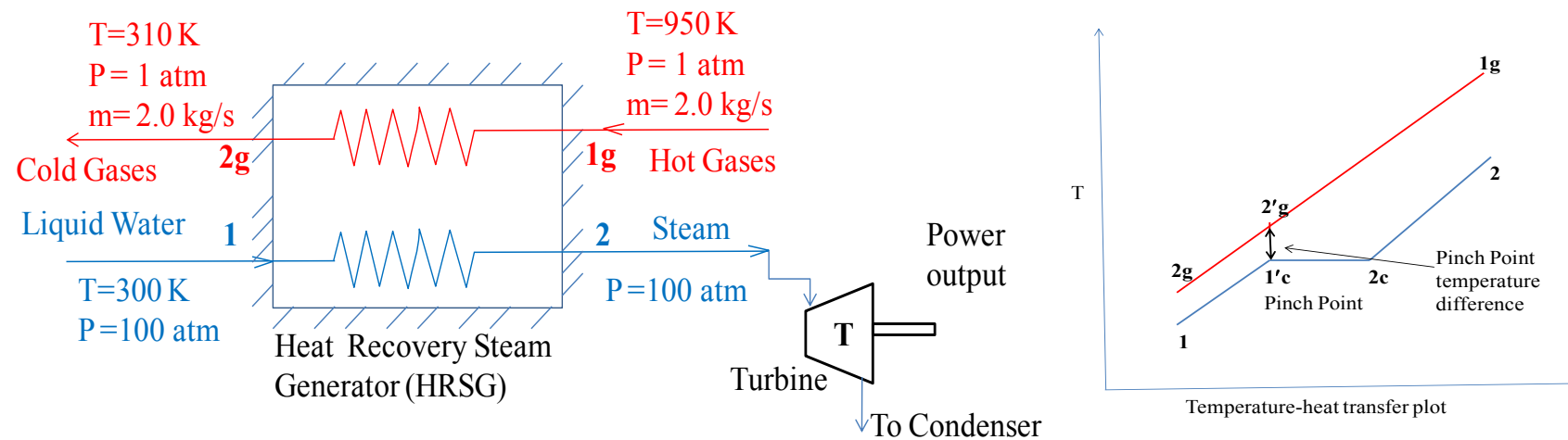




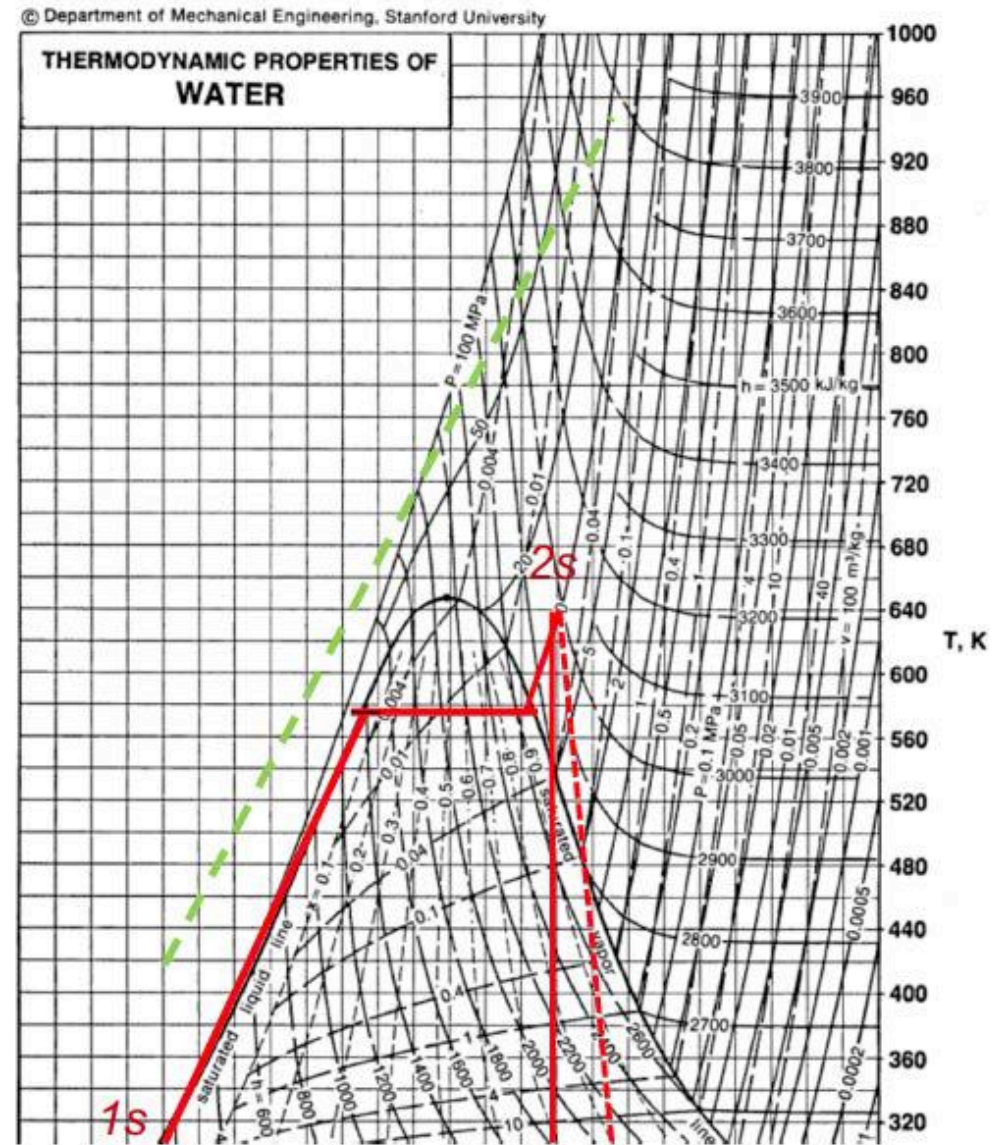
1. Geothermal heat @ $T_H \sim 100$ - 150 C
2. Solar concentrators produce heat @ $T_H \sim 300$ - 600 C
3. Nuclear reactors $T_H \sim 300$ - 600 C
4. Combustion, only limited by material, $T_H \sim 1400$ - 2100 C.

Example 2.10

An industrial plant requires high temperature heat, which it generates by burning kerosene. After extracting the “useful” high temperature heat from the combustion products, the plant discharges gases at 950 K and 1 atm. The flow rate of combustion gases is 2.0 kg/s. A waste heat-recovery system (WHRS) is proposed for the utilization of the energy in the hot exhausted gases. It consists of a steam generator, the heat recovery steam generator (HRSG) and a steam turbine. The isentropic efficiency of the turbine is 94%, and steam exits the turbine at 40 °C. Assume the pinch point temperature difference of 10 °C. Atmospheric conditions are at 1 atm. and 300 K. Assume the hot combustion products as an ideal gas with the same properties as air, specific heat is $c_{p,GAS} = 1.048 \text{ kJ/kg}\cdot\text{K}$. Calculate the exergy losses in this system.



Green, gas
Red, steam



Maximum work from the stream is obtained using the availability of the hot gases:

$$\text{Maximum Work} = \dot{\Xi}_{GASES} = \dot{\Xi}_{1g} = \dot{m}_{1g}[(h_{1g} - h_{0g}) - T_0(s_{1g} - s_{0g})] = 638.1 \text{ kW}$$

Now we calculate the mass flow rate of turbine water (do not yet know exit conditions of steam): energy balance between the two streams from the cold side of HRSG to pinch point (PP),

$$\dot{m}_{1g}(h_{2'g} - h_{2g}) = \dot{m}_w(h_{1'c} - h_1)$$

from tables, specific enthalpy of saturated water at 100 atm: $h_{1'c} = 1413.0 \text{ kJ/kg}$.
Looking at enthalpy of water at $T = 300 \text{ K}$ and $p = 101325 \text{ kPa}$: $h_1 = 121.8 \text{ kJ/kg}$.
From the steam tables, the saturation temperature $T_{1'c}$ at 10132.5 kPa is 585.2 K.

Pinch point temperature difference is 10 K. $T_{2'g} = T_{1'c} + 10 = \underline{595.2 \text{ K}}$

Therefore, mass flow of water is:

$$\dot{m}_w = \frac{\dot{m}_{1g} C_{P,GAS} (T_{2'g} - T_{2g})}{(h_{1'c} - h_1)} = \frac{2.01.048(595.2 - 310)}{(1413 - 121.8)} = \mathbf{0.4629 \text{ kg/s}}$$

After knowing mass flow rate of water, we apply energy equation for the entire HRSG

$$\dot{m}_{1g}(h_{1g} - h_{2g}) = \dot{m}_w(h_2 - h_1)$$

This gives $h_2 = 3020 \text{ kJ/kg}$.

With $h_2 = 3020 \text{ kJ/kg}$ and $p_2 = 100 \text{ atm}$, from steam tables, we get $T_2 = 650.7 \text{ K}$.

Loss of work/irreversibility in HRSG:

$$0 = \sum \left(1 - \frac{T_0}{T_j} \right) \dot{Q}_j - \dot{W}_{CV} + \dot{\Xi}_{1g} - \dot{\Xi}_{2g} + \dot{\Xi}_1 - \dot{\Xi}_2 - \dot{\Xi}_{DESTRUCTION}$$

First two terms are zeros

$$\text{Irreversibility} = \dot{\Xi}_{DESTRUCTION} = 637.7 - 549.8 = 87.48 \text{ kW}$$

For the turbine, exit temperature $T = 273 + 40 = 313 \text{ K}$ (we know it is 2 phase), from tables, saturation pressure is 7.323 kPa .

$T_2 = 650.7 \text{ K}$, $p_2 = 10132.5 \text{ kPa}$, $h_2 = 3020 \text{ kJ/kg}$ and $s_2 = 6.091 \text{ kJ/kg-K}$

Isentropic conditions of steam exiting turbine are: $p_3 = 7.323 \text{ kPa}$, $s_{3s} = s_2 = 6.091 \text{ kJ/kg-K}$.

From steam tables, isentropic enthalpy is $h_{3s} = 1895 \text{ kJ/kg}$.

The actual conditions (enthalpy) of steam exiting turbine can be found from

$$\eta_T = \frac{(h_2 - h_3)}{(h_2 - h_{3s})} \Rightarrow 0.94 = \frac{(3020 - h_3)}{(3020 - 1895)}$$

This gives $h_3 = 1962$ kJ/kg. Using h_3 and p_3 and $T_3 = 313$ K, from steam tables: $s_3 = 6.307$ kJ/kg-K (less than $s_{3sat \text{ steam}}$, verifying it is a two-phase flow mixture).

Turbine work rate is 489.5 kW.

But $0 = -\dot{W}_{turbine} + \dot{\Xi}_{in} - \dot{\Xi}_{out} - \dot{I}$

Change of Availability in the turbine is:

$$\Delta \dot{\Xi} = \dot{m}_w \left[(h_2 - h_3) - T_o (s_2 - s_3) \right] =$$

$$0.4629 \left[(3020 - 1962) - 300 (6.091 - 6.307) \right] = 519.4 \text{ kW}$$

Exergy loss is the difference between change and work, **29.88 kW**

This is much less than exergy destroyed in HRSG.

Thermodynamic Efficiencies

Conversion Efficiency or first law efficiency $\eta_I = \frac{\text{All what you get}}{\text{All what you pay}}$

heat engines $\eta_I = \frac{\text{net work out}}{\text{Heat in}}$

Electrochemical Efficiency for battery or fuel cell $\rightarrow \frac{\text{Work (Electrical Energy) out}}{\text{Chemical Energy in/used}}$

electrochemical efficiency for charging battery or electrolyzer $\rightarrow \frac{\text{Chemical Energy stored}}{\text{electrical Energy in}}$

Co-generation efficiency(bad definition but it is used) $\rightarrow \frac{\text{Work} + \text{Heat}}{\text{Chemical Energy}}$

a better definiton is $\rightarrow \frac{\text{Work} + (1 - \frac{T_o}{T_H})Q_H}{\text{Chemical Energy}}$

Thermodynamic Efficiencies

$$\text{Conversion Efficiency or first law efficiency } \eta_I = \frac{\text{Work/Energy/Heat OUT}}{\text{Heat/Energy/Work IN}}$$

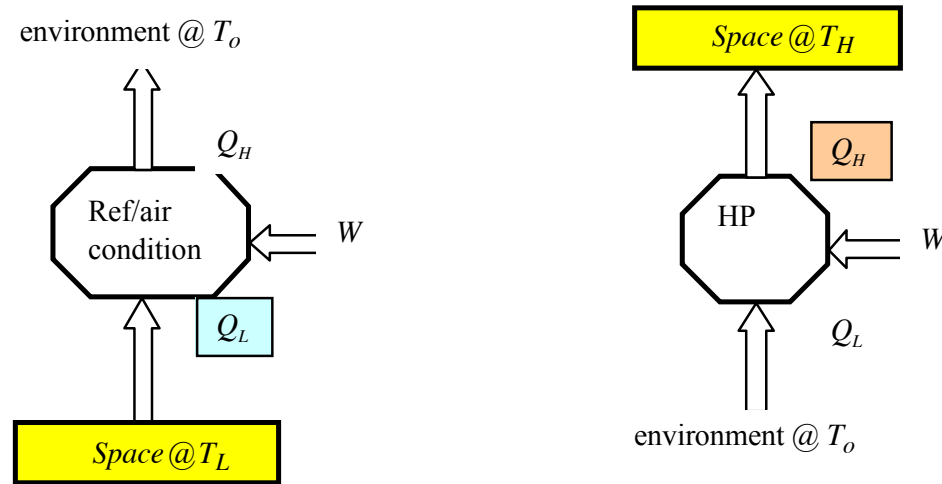
$$\text{Thermomechanical Efficiency of a Heat Engine} \rightarrow \frac{\text{Work (Mechanical)}}{\text{Heat}}$$

$$\text{Combustion Efficiency} \rightarrow \frac{\text{Thermal Energy}}{\text{Chemical Energy}}$$

$$\text{Reforming Efficiency} \rightarrow \frac{\text{Chemical Energy Out}}{\text{Chemical Energy In}}$$

$$\text{Fuel Utilization Efficiency of a combustion engine} \rightarrow \frac{\text{Power (Mechanical)}}{\text{Rate of Chemical Energy in}}$$

In heating and cooling equipment, we define:
 The Coefficient of Performance (can be larger than 1)



$$\beta_{ref/aircondition} = \frac{Q_L}{W}$$

$$\beta_{HeatPump} = \frac{Q_H}{W}$$

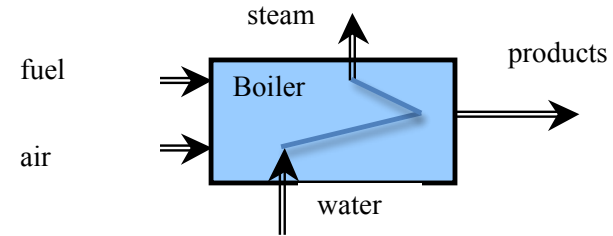
Carnot like expressions still define
 the best performance

In combustion
we use the stored chemical energy to define efficiencies:

Boiler efficiency:

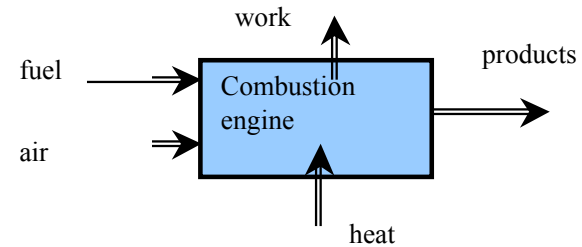
$$\eta_{Boiler} = \frac{\dot{m}_{steam} |\Delta H_{steam}|}{\dot{m}_{fuel} |\Delta H_{r,fuel}|}$$

$|\Delta H_{r,fuel}|$ is the energy (thermal) gained by
converting a unit mass of fuel to products



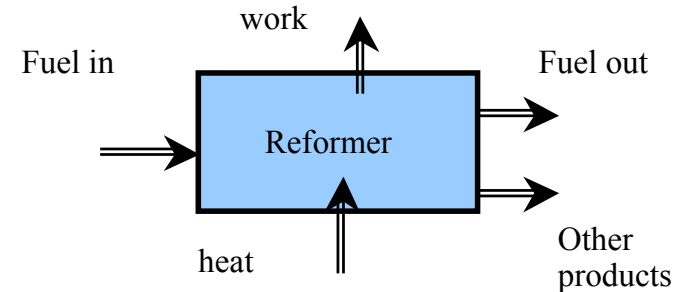
Combustion engine:

$$\eta_{fuelutilization} = \frac{P_{out}}{\dot{m}_{fuel} |\Delta H_{r,fuel}|}$$



Reformer

$$\eta_{reformer} = \frac{\dot{m}_{fuelout} |\Delta H_{r,fuelout}|}{\dot{m}_{fuelin} |\Delta H_{r,fuelin}|}$$

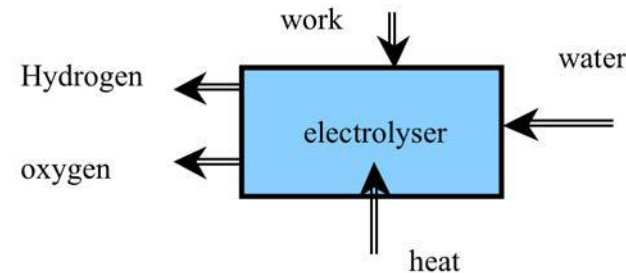
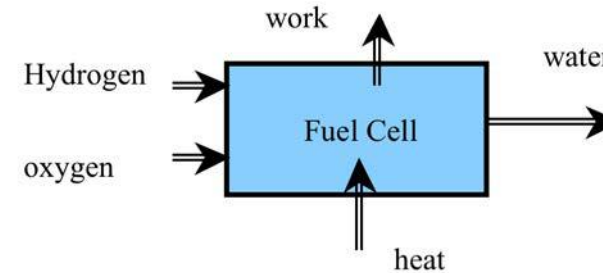


In direct conversion between chemical and electrical energy (fuel cells and electrolysis), we use the stored chemical energy of the fuel to define efficiencies:

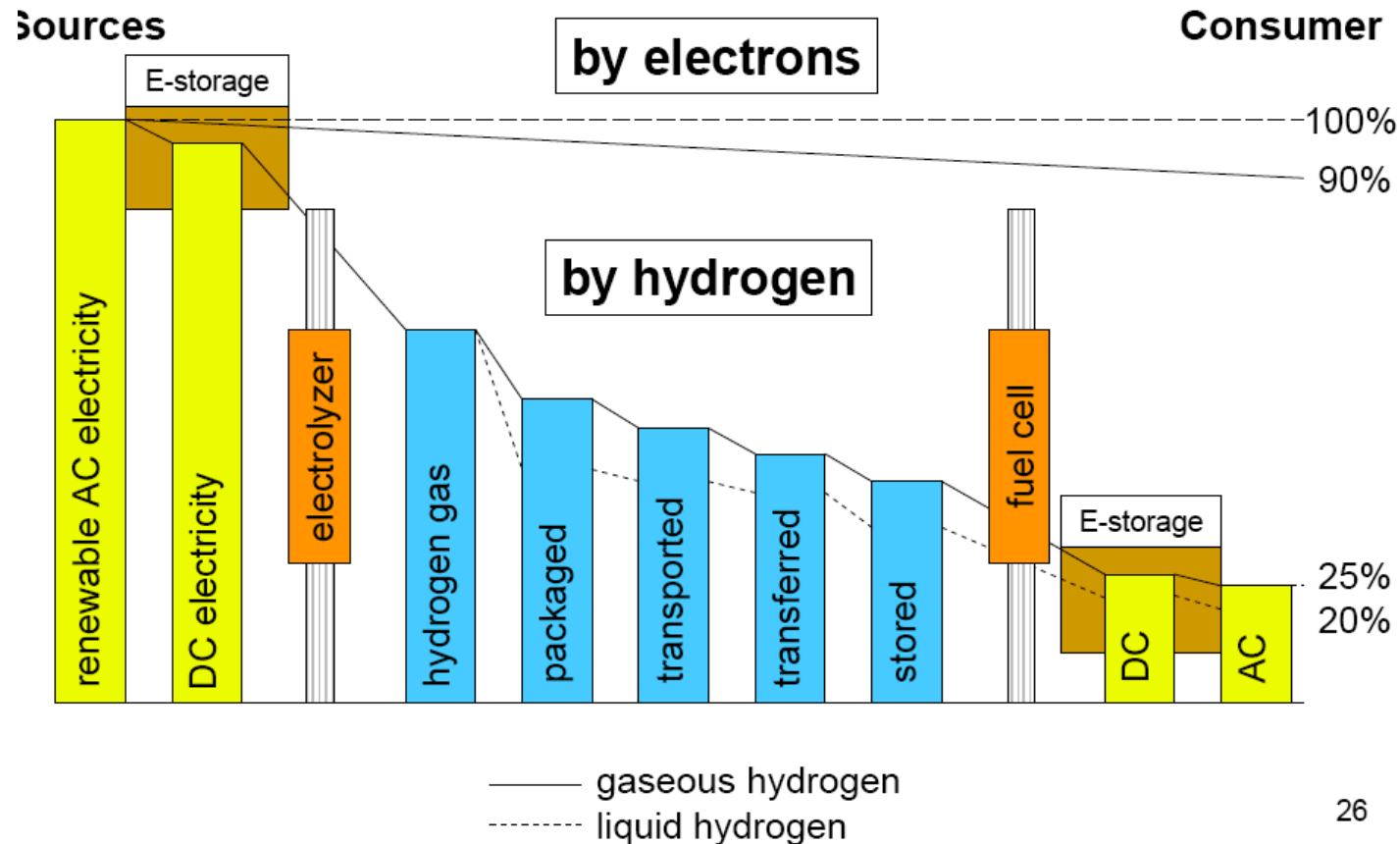
$$\eta_{FC} = \frac{P_{out}}{\dot{m}_{H_2} |\Delta H_{r,H_2}|}$$

$$\eta_{electrolysis} = \frac{\dot{m}_{H_2} |\Delta H_{r,H_2}|}{P_{in}}$$

$|\Delta H_{r,H_2}|$ is the energy (thermal) gained by converting a unit mass of hydrogen to water



WTW or LCA requires knowledge of process efficiency and overall integration of processes and systems ...



© Source unknown. All rights reserved. This content is excluded from our Creative Commons license. For more information, see <https://ocw.mit.edu/fairuse>.

Bossel, Towards a Sustainable Energy Future, Oct 2004

© by Ahmed F. Ghoniem

Effectiveness, or Second Law Efficiency = $\frac{\text{actual efficiency}}{\text{maximum efficiency}} = \frac{\text{work}}{\text{maximum work}}$

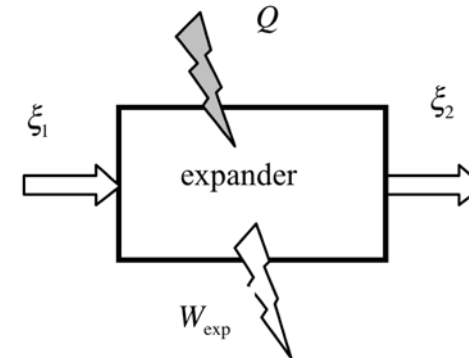
System interacting with 2 TER only: $\eta_{II} = \frac{W_{net}}{W_{max}} = \frac{W_{net} / Q_H}{1 - T_L / T_H}$

System processing a stream: $\eta_{II} = \frac{W_{net}}{W_{max}} = \frac{W_{net}}{\Delta \Xi} \rightarrow$ work producing cycle (system)

Device expanding a stream: $\eta_{II} = \frac{w_{net}}{w_{max}} = \frac{w_{net}}{\Delta \xi} \rightarrow$ work producing cycle

In an isothermal process with an ideal gas:

$$\hat{w}_{max} = \Delta \hat{\xi} = \Delta \hat{h} - T_o \Delta \hat{s} = \Re T_o \ln \left(\frac{p}{p_o} \right)$$



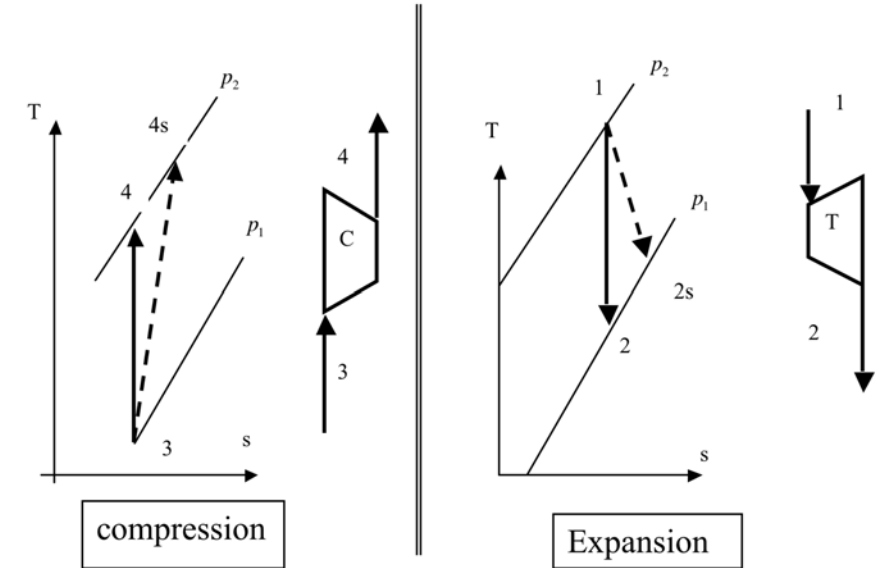
other important efficiencies (related to the second law)

$$\text{turbine isentropic efficiency } \eta_T = \frac{W}{W_{\max}} = \frac{W}{W_{is}}$$

note that for an adiabatic turbine,

$$W_{\max} = \xi_1 - \xi_2 = (h_1 - h_2) - T_o((s_1 - s_2)) = (h_1 - h_2)$$

$$\text{compressor isentropic efficiency } \eta_T = \frac{W_{\min}}{W} = \frac{W_{is}}{W}$$



MIT OpenCourseWare
<https://ocw.mit.edu/>

2.60J Fundamentals of Advanced Energy Conversion
Spring 2020

For information about citing these materials or our Terms of Use, visit: <https://ocw.mit.edu/terms>.

Lecture # 3

Thermodynamics of Ideal Gas Mixtures and Separation

Ahmed Ghoniem

February 10, 2020

1. Ideal Gas Mixtures
2. Entropy of mixing
3. Ideal separation work
4. Air separation for O₂ production
5. CO₂ separation from products and air.

Ideal Gas Mixture

mass fraction $Y_i = m_i / m$, $m = \sum_{i=1}^N m_i$ where mass of component is m_i

number of moles $n_i = m_i / \widetilde{M}_i$, where \widetilde{M}_i is molecular weight, and mole fraction $X_i = n_i / n$, $n = \sum_{i=1}^N n_i$

mass and mole fractions are related $X_i = \frac{(Y_i / \widetilde{M}_i)}{\left(\sum_{i=1}^N (Y_i / \widetilde{M}_i) \right)}$, $Y_i = \frac{(X_i \widetilde{M}_i)}{\sum_{j=1}^N (X_j \widetilde{M}_j)}$

Equation of state: $p\forall = n\Re T$, for an ideal gas.

partial pressure: $p_i\forall = n_i\Re T$, $p_i = X_i p$ (all components occupy same total volume \forall)

partial volume: $\forall_i = \frac{n_i\Re T}{p}$, and $\forall_i / \forall = \frac{n_i}{n} = X_i$ (as if all components were at same p)

Component	Molecular weight M_i	Mole fraction X_i	Vol. fraction \forall_i / \forall	Partial pressure $p_i = X_i p$	Mass fraction
N ₂	28.016	0.7803	0.7803	0.7803	0.7546
O ₂	32.000	0.2099	0.2099	0.2099	0.2319
Ar	39.944	0.0098	0.0098	0.0098	0.0135

Ideal Gas Mixture

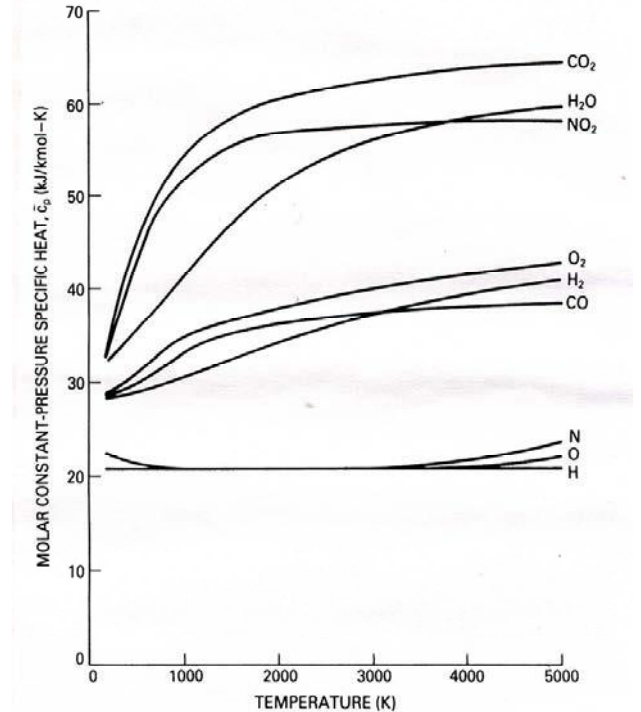
for ideal mixture (and gases)

mixing does not affect the properties of individual components
(enthalpy of mixing = 0)

Enthalpy of a mixture: $h = \sum_{i=1}^N Y_i h_i(T)$

$$\hat{h} = \sum_{i=1}^N X_i \hat{h}_i(T),$$

$$h_i = h_i^o + \int_{T^o}^T c_{p,i}(T) dT, \quad \hat{h}_i = \hat{h}_i^o + \int_{T^o}^T \hat{c}_{p,i}(T) dT$$



Entropy of a Mixture

entropy of ideal gas: $\hat{s}(T, p) = \hat{s}^o(T) - \Re \ln \frac{p}{p^o}$,

$$\hat{s}^o(T) = \hat{s}^{oo} + \int_{T^o}^T \frac{\hat{c}_p(T)}{T} dT$$

$$\begin{aligned} \text{Entropy of a mixture: } \hat{s}(T, p) &= \sum_{i=1}^N X_i \hat{s}_i(T, p_i) = \sum_{i=1}^N X_i \left\{ \hat{s}_i^o(T) - \Re \ln \frac{p_i}{p^o} \right\} \\ &= \underbrace{\sum_{i=1}^N X_i \hat{s}_i^o(T) - \Re \ln \frac{p}{p^o}}_{\text{entropy before mixing}} - \Re \sum_{i=1}^N X_i \ln X_i \end{aligned}$$

entropy before mixing

(when all gases were at p and their partial volume)

$$\text{Entropy of Mixing: } (\Delta \hat{s})_g = (\hat{s}_{\text{after mixing}} - \hat{s}_{\text{before mixing}}) = -\Re \sum_{i=1}^N X_i \ln X_i \quad (\text{always positive})$$

Spontaneous mixing of gases at same T and p

p, T, \forall_1 n_1, h_1, s_1	p, T, \forall_2 n_2, h_2, s_2	p, T, \forall_3
--------------------------------------	--------------------------------------	-------------------

$p, T, \sum \forall, p_i = X_i p, X_i = \forall_i / \forall$ $H = \sum n_i \hat{h}_i, S = \sum n_i \hat{s}_i(T, p_i)$

Entropy is generated as gases, with initial volumes \forall_i but same (T, p) mix at constant T and "total" p . Following mixing $\forall = \sum_i \forall_i$.

Thus, during mixing, each component expands freely, lowering its pressure from p to $p_i = \forall_i / \sum \forall_i = X_i p$, without doing work. The lost work, $T_o (\Delta \hat{s})_g$, is the "chemical potential" for doing work. It is also the "chemical availability", more on that later.

Ideal Work of Separation, steady continuous flow:

First Law: $\dot{Q} - \dot{W} + \dot{n}_1 \hat{h}_1 - (\dot{n}_a \hat{h}_{a2} + \dot{n}_b \hat{h}_{b3}) = 0$

Second Law: $\frac{\dot{Q}}{T_0} + \dot{n}_1 \hat{s}_1 - (\dot{n}_a \hat{s}_{a2} + \dot{n}_b \hat{s}_{b3}) + \dot{S}_g = 0$

$$-\dot{W} = \left[\dot{n}_a (\hat{h}_{a2} - T_0 \hat{s}_{a2}) + \dot{n}_b (\hat{h}_{b3} - T_0 \hat{s}_{b3}) \right] - \dot{n}_1 (\hat{h}_1 - T_0 \hat{s}_1) + T_0 \dot{S}_g$$

per one mole of original mixture, $w = \dot{W} / \dot{n}_1$, $X_a = \dot{n}_a / \dot{n}_1$, $X_b = \dot{n}_b / \dot{n}_1$

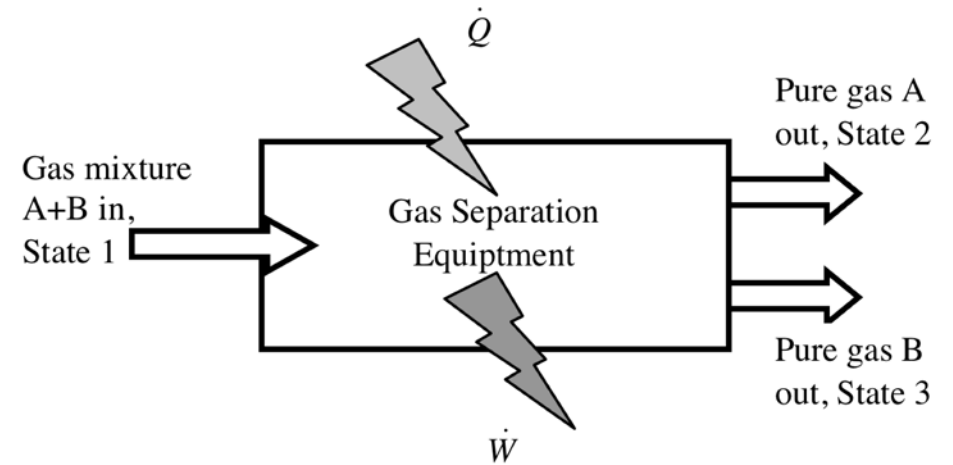
$$-\hat{w}_{\min} = X_a \left[(\hat{h}_{a2} - \hat{h}_{a1}) - T_0 (\hat{s}_{a2} - \hat{s}_{a1}) \right] + X_b \left[(\hat{h}_{b3} - \hat{h}_{b1}) - T_0 (\hat{s}_{b3} - \hat{s}_{b1}) \right]$$

For "least" minimum work, (1) out streams must be in thermal equilibrium with environment,

$$T_1 = T_2 = T_3 = T_0, \quad \frac{\hat{w}_{\min}}{\Re T_0} = X_a \ln \left(X_a \frac{p_1}{p_{a2}} \right) + X_b \ln \left(X_b \frac{p_1}{p_{b3}} \right)$$

and (2) out stream must be in mechanical equilibrium with environment,

$$p_1 = p_2 = p_3 = p_0, \quad \frac{\hat{w}_{\min}}{\Re T_0} = X_a \ln X_a + X_b \ln X_b = \sum_N X_i \ln X_i$$



For a mixture with "two" components, X_1 and $(1-X_1)$,
minimum work per mole of mixture:

$$\hat{w}_{mole\ of\ mixture} = -\Re T_o \left(X_1 \ln X_1 + (1 - X_1) \ln(1 - X_1) \right)$$

work per mole of component 1 is:

$$\hat{w}_{mole\ of\ X_1} = \frac{\hat{w}_{mole\ of\ mixture}}{X_1} = -\Re T_o \left(\ln X_1 + \frac{(1 - X_1)}{X_1} \ln(1 - X_1) \right)$$

EXAMPLE: Production of argon by separating it from air:

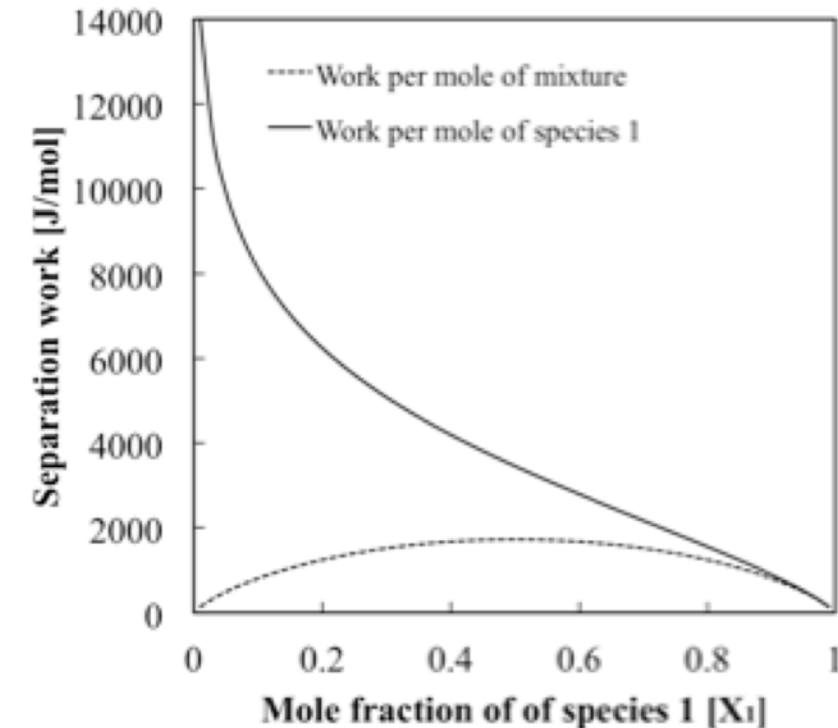
Air contains 0.9% argon, and 99.1% of nitrogen and oxygen, by volume,

that is: $X_{Ar} = 0.009$ and $X_{O_2+N_2} = 0.991$.

$$\hat{w}_{mole-mixture} = -\Re T_o \left(X_1 \ln X_1 + (1 - X_1) \ln(1 - X_1) \right) \approx -\Re T_o X_1 \ln X_1$$

Substituting, at 25°C, we get -0.127 MJ/kmol of air, **or -14.3 MJ/kmol of argon.**

Work of separation, at $T = 300$ K.



Work Done in an Air Separation Unit:

@1 atm and 25 C. mole fractions are 0.21 of O₂ and 0.79 of N₂.

$$\hat{w}_{mole-mixture} = -\mathcal{R}T_o \left(X_1 \ln X_1 + (1 - X_1) \ln (1 - X_1) \right), \mathcal{R} = 8.314 \text{ kJ/kmol.K}$$

Minimum work per kmol of air is -1.273 MJ/kmol of air.

OR 1.611 MJ/kmol of N₂, **OR 6.061 MJ/kmol of O₂**

(Available technology consumes ~ 30 MJ/kmol of O₂)

Second law efficiency of separation is low: 10-30%.

Enthalpy of reaction of methane (LHV) ~ 800 MJ/kmol methane

(with 50% efficiency, work is ~ 400 MJ/kmol methane)

2 moles of oxygen are required for each mole of methane:

Separation energy penalty in oxy-combustion of gas

$$(\text{in \%}) \text{ is } \frac{2.0 \times 6.06}{(\eta_{II} = 0.2) \times 400} \approx 15\% \text{ of original energy}$$

Need better air separation technology



© Source unknown. All rights reserved. This content is excluded from our Creative Commons license. For more information, see <https://ocw.mit.edu/fairuse>.

Direct Air Capture (DAC)

Work for separating CO₂ from air with 500 ppm:

Take: $X_{CO_2} \sim 0.0005$ and $X_{O_2+N_2} = 0.9995$.

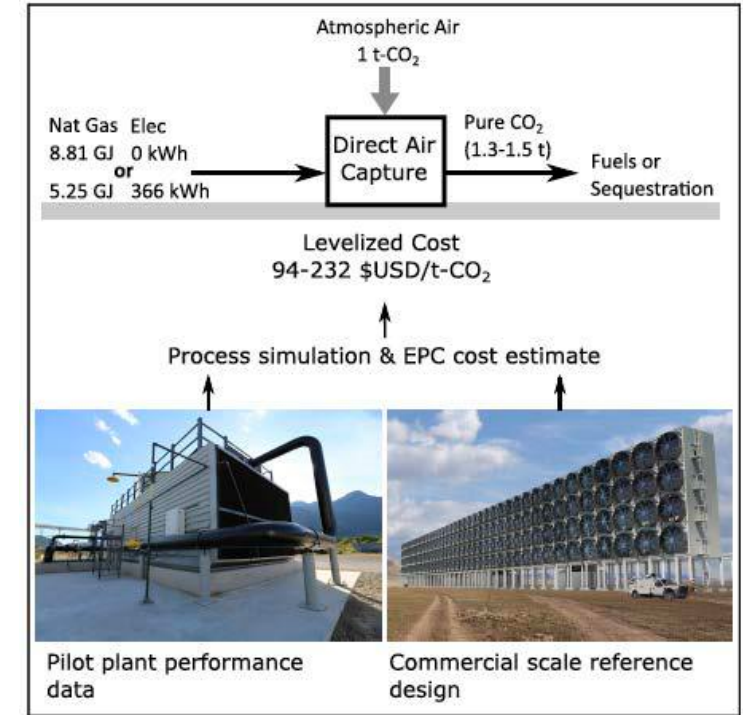
$$\hat{w}_{unitCO_2} \approx -\mathcal{R}T_o \ln X_1, \mathcal{R} = 8.314 \text{ kJ/kmol.K}$$

At 25°C, we get 18.415 MJ/kmol CO₂ or 0.418.5 MJ/kg CO₂

Recent paper (Keith et al., Joule, 2, 2018. Company: Carbon Engineering) claims 8.8 GJ_{th}/ton CO₂ (from methane burning). Assuming 50% efficiency, equivalent work is 4.4 MJ_e/kg CO₂.

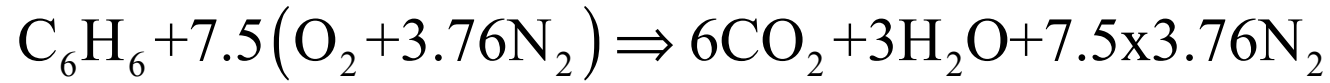
It seems that the second law efficiency of this technology is ~ 10%

This is not unreasonable since it accounts for the process inefficiencies (plenty, will be discussed later), the work of sucking all this air as well compressing CO₂ to storage conditions (~ 150 bar!).



Keith et al., Joule, 2, 2018

Courtesy Elsevier, Inc., <http://www.sciencedirect.com>. Used with permission.



Ideal Work for CO₂ Separation from combustion products (post combustion capture):

The concentrations are: $X_{\text{CO}_2} = 0.16$ and $X_{\text{H}_2\text{O}+\text{N}_2} = 0.84$. At $T_0 \sim 300\text{K}$,

$$\begin{aligned} w_{\min} &= \Re T_o (X_1 \ln X_1 + (1 - X_1) \ln (1 - X_1)) = 1.107 \text{ MJ/Kmol mix} \\ &= 6.92 \text{ MJ/Kmol CO}_2 = 0.16 \text{ MJ/kg CO}_2 \end{aligned}$$

Also: the work is **41.1 MJ/kmol of benzene**.

The enthalpy of reaction of benzene is 3171 MJ/kmol.

Taking 40% efficient cycle, the “useful” work produced is **1268.4 MJ/kmol of benzene**.

There is a penalty of 3.25% for the separation of CO₂ at $T = 27^\circ\text{C}$.

Actual separation processes require more work (5-10 times) due to irreversibility.

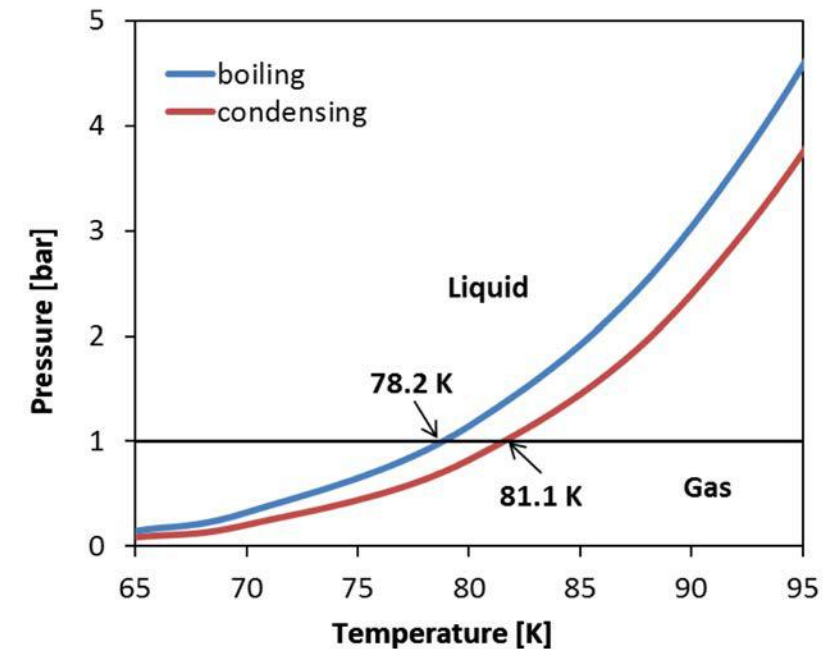
Thus, efficiency penalty can be as large as **32.5% of the original work**.

Air Liquefaction

(used extensively in air separation,
and could be a good large scale storage option)

At atmospheric pressure, the boiling/condensation temperature of oxygen is 90 K (-183 C) and of nitrogen is 77 K (-196 C) (nitrogen is more volatile than oxygen as it evaporates at lower temperature).

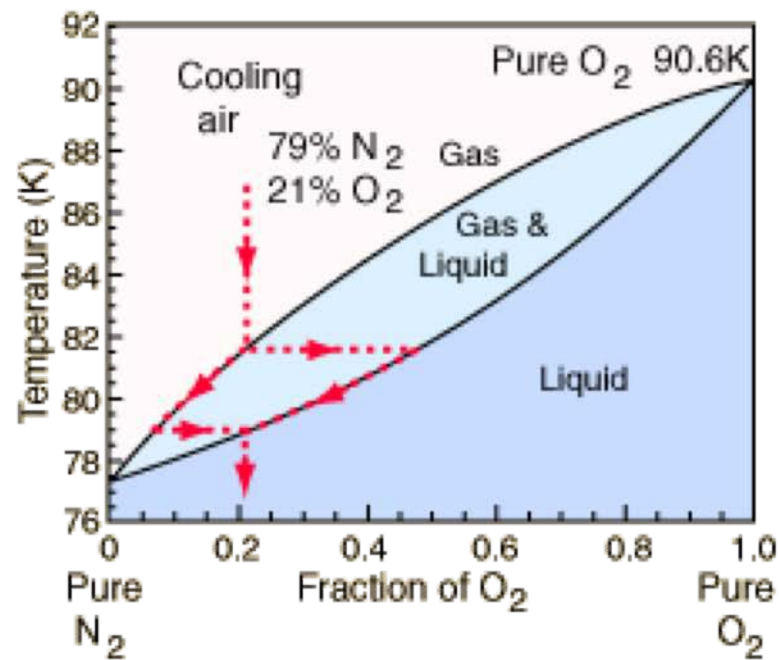
When air is cooled at atm. pressure, it remains gas till 81.6 K. and completely liquefy at 79 K (inverse when heated)



© THERMOPEDIA. All rights reserved. This content is excluded from our Creative Commons license. For more information, see <https://ocw.mit.edu/fairuse>.

Ref: <http://www.thermopedia.com/content/553/>

Air Liquefaction Process



after Schroeder

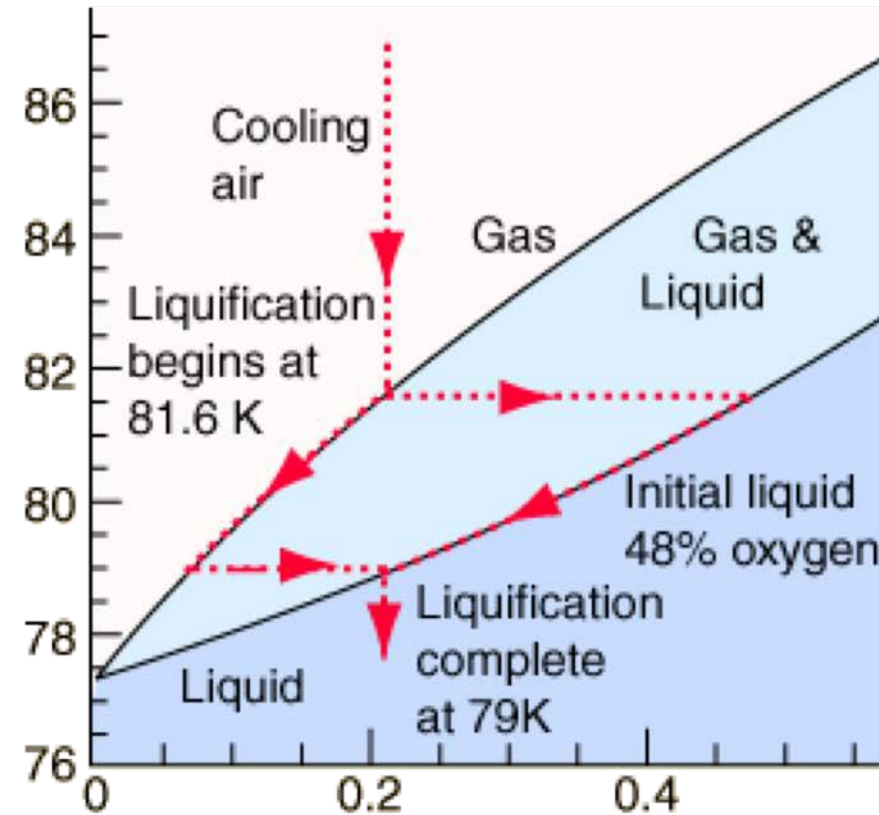


Image courtesy of C. R. Nave, HyperPhysics, Department of Physics and Astronomy, Georgia State University. Used with permission.

Ref: <http://hyperphysics.phy-astr.gsu.edu/hbase/thermo/liqair.html>

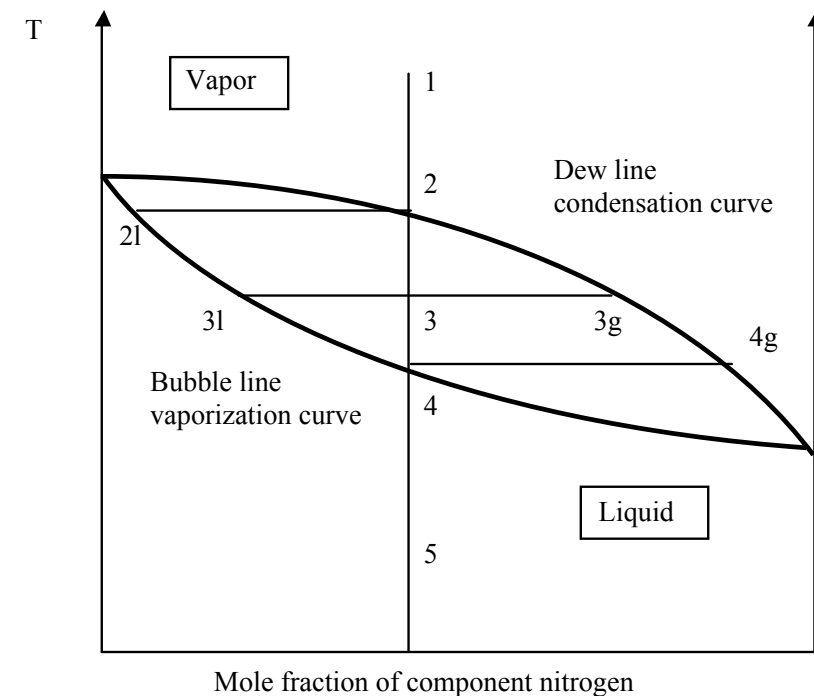
Introduction to binary mixture phase diagram

When cooling a mixture starting at 1, we see the following:

2 is where condensation starts, with 2l being the liquid mixture composition of the first element to condense, it is mostly oxygen

@ 3, 3l is the liquid mixture composition (still mostly oxygen) and 3g is the gas mixture composition (mostly nitrogen).

4 is the last gas element, 4g is that gas mixture composition (left after condensation), it is mostly nitrogen.



MIT OpenCourseWare
<https://ocw.mit.edu/>

2.60J Fundamentals of Advanced Energy Conversion
Spring 2020

For information about citing these materials or our Terms of Use, visit: <https://ocw.mit.edu/terms>.

Lecture # 4



Liquefaction and Gas Storage

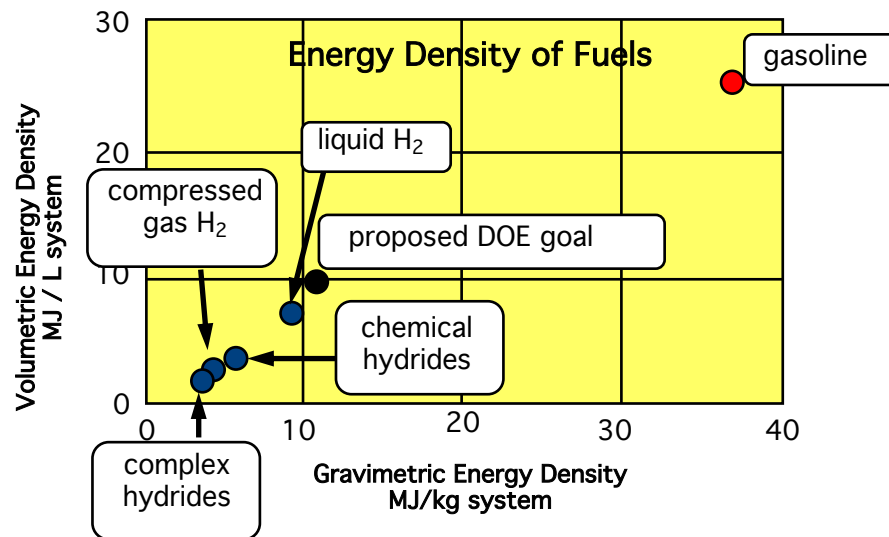
Ahmed Ghoniem

February 12, 2020

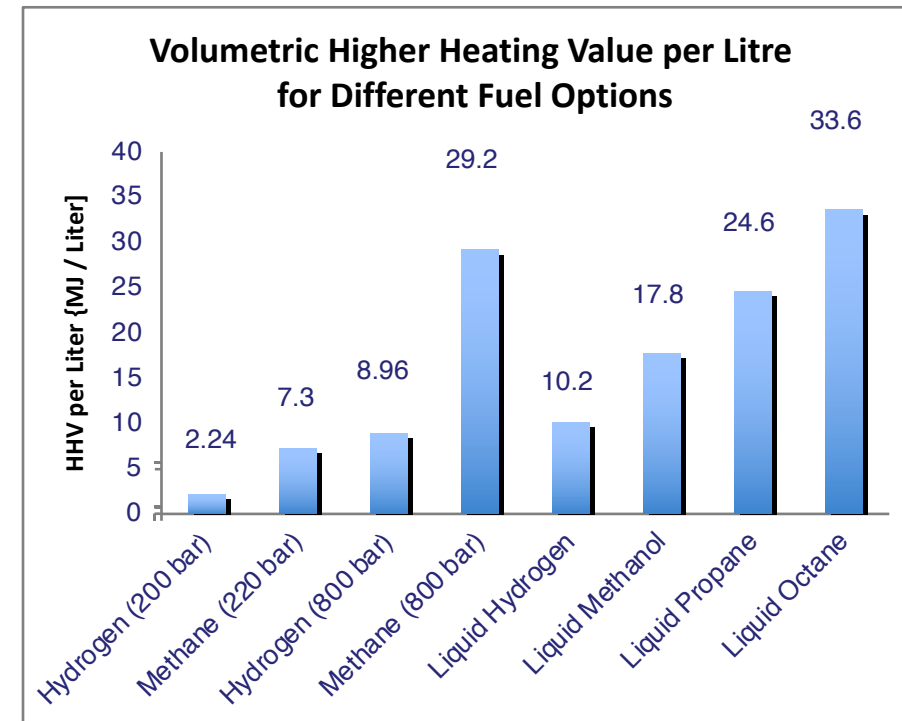
1. Ideal liquefaction work.
2. Liquefaction work for hydrogen and storage
3. Losses in actual processes.
4. Air liquefaction and large scale storage.

Liquefaction Work, Ideal and “Actual”

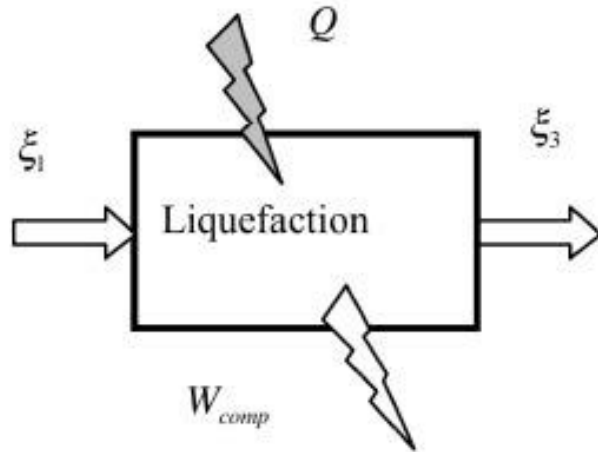
- Some gas separation processes require cooling and liquefaction.
- Highest “storage density” for Hydrogen is in the liquid form.
- Liquefied natural gas is becoming important for transporting it.
- For CCS, CO₂ must be in liquid form for injection.



Lithium rechargeable Batteries:
0.54 MJ/kg Or 150 Wh/kg



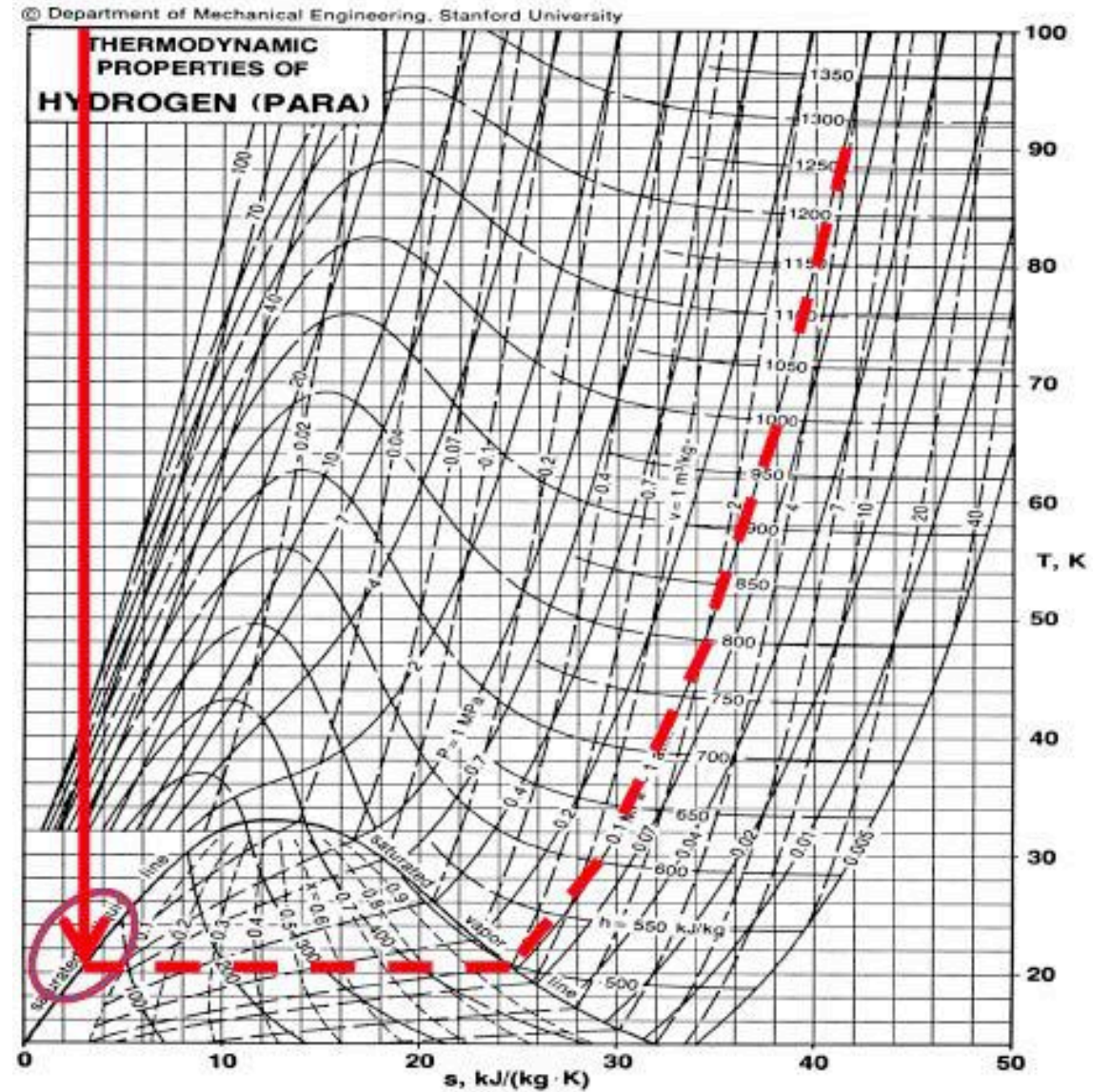
Minimum Liquefaction Work



Use availability equation :

$$\dot{W}_{cv} = \underbrace{\left(1 - \frac{T_o}{T_H}\right) \dot{Q}_H}_{(Q_H = 0)} + \dot{m}(\xi_{in} - \xi_{out}) - \underbrace{\dot{I}_{ir}}_{0 \text{ for min work}}$$

$$\hat{w}_{min} = -[(h_3 - h_1) - T_o(s_3 - s_1)]$$



© Department of Mechanical Engineering, Stanford University. All rights reserved. This content is excluded from our Creative Commons license. For more information, see <https://ocw.mit.edu/fairuse>.

The critical point of hydrogen is 33.3 K, 1.3 MPa

Calculate the ideal liquefaction work for hydrogen starting at 1 atm and 298 K:

$$s_1 = 53.436 \text{ kJ/kgK}, h_1 = 3929.6 \text{ kJ/kg},$$

The liquid hydrogen temperature at 1 atm is 20 K.

$$s_3 = -0.02 \text{ kJ/kgK}, h_3 = -0.44 \text{ kJ/kg}$$

$$w_{\min} = 11.870 \text{ MJ/kg H}_2.$$

Actual values ~ 4-10 times, 40-110 MJ/kg H₂
(low second law efficiency).

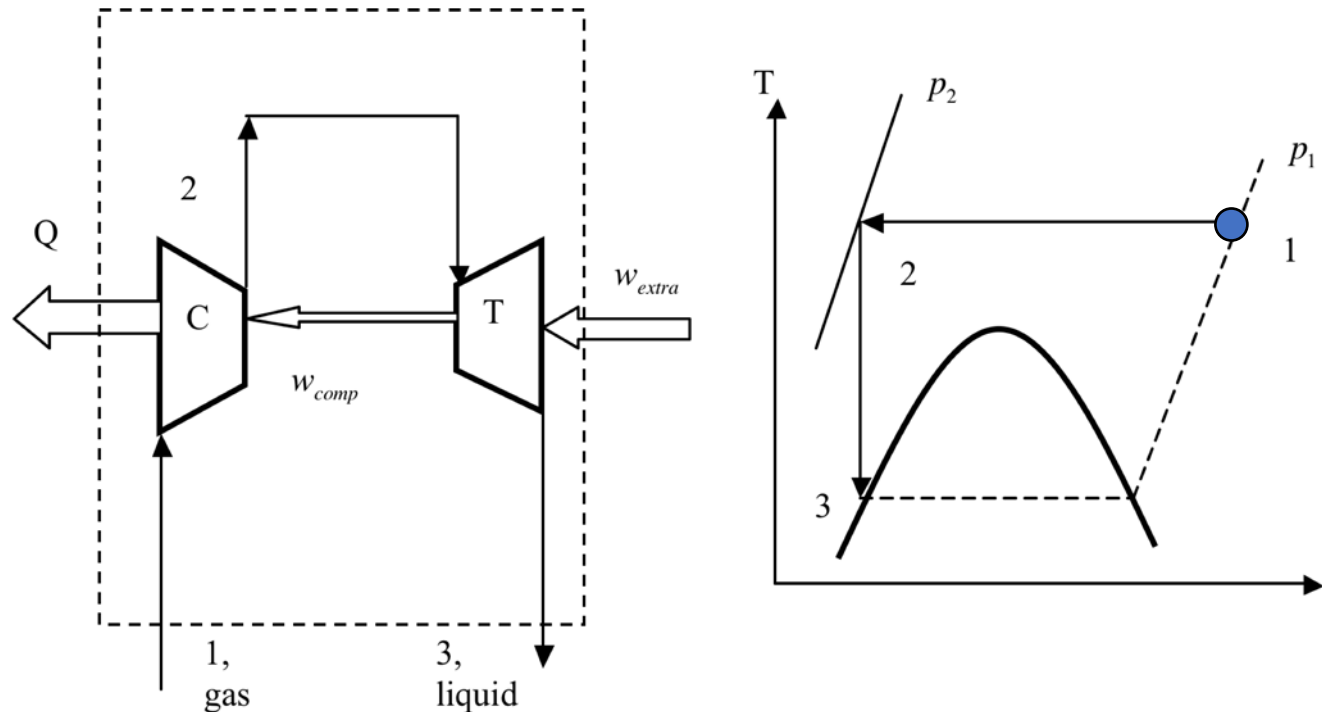
The lower heating value LHV of hydrogen is 120.9 MJ/kg
Liquefaction work is 30-100% of the LHV (or more)

Useful work produced by an engine running at 40% efficiency is ~ 50 MJ/kg
The numbers do not look good!

Minimum Liquefaction Work $\hat{w}_{\min} = -\left[(h_3 - h_1) - T_1(s_3 - s_1)\right]$

Realization of the ideal Linde Liquefaction process:

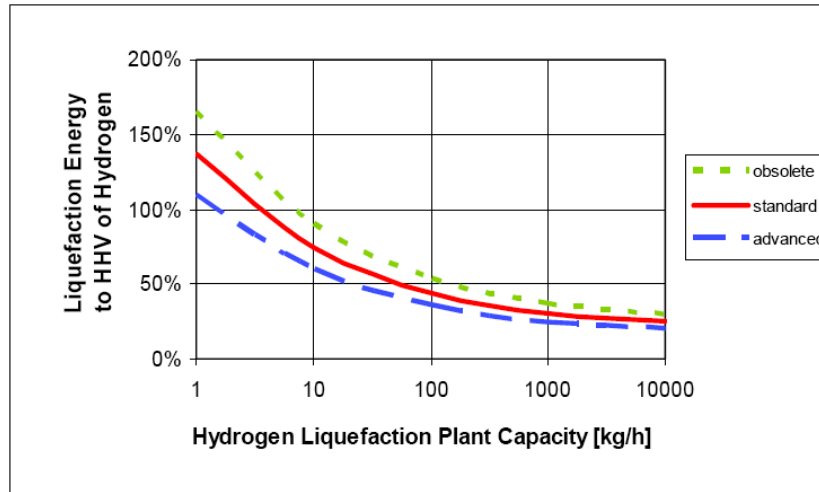
All processes must be reversible: isothermal heat exchange and isentropic work transfer, thus Isothermal compression and isentropic expansion



Storage and Packaging of Hydrogen

Plant size determines the quality of the equipment and integration of processes

Liquefaction of Hydrogen: Liquefaction Energy in HHV-% of H₂

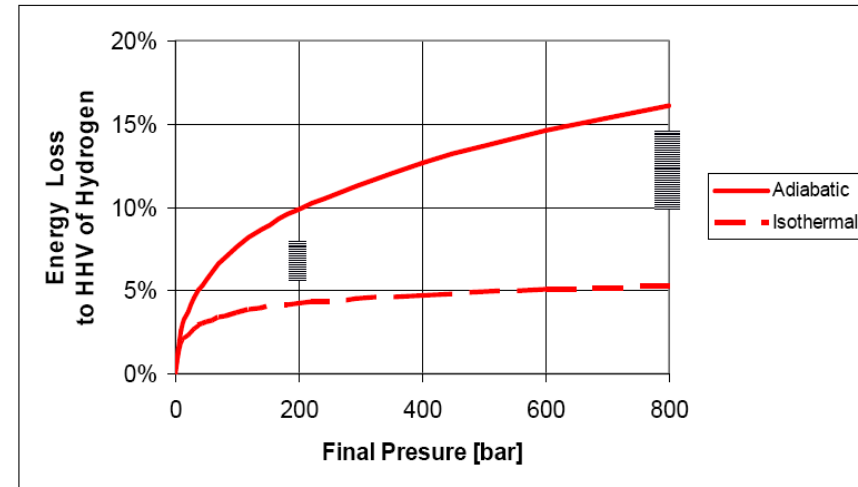


for an ideal gas, the min work is

$$w_{isothermal} = \Re T_o \ln(p_2 / p_1)$$

$$w_{isentropic} = c_p T_o \left((p_2 / p_1)^{\frac{k-1}{k}} - 1 \right)$$

Adiabatic and Isothermal Compression: Compression Energy in HHV-% of H₂



Compression energy CE of H₂ = 8 x CE of natural gas or 15 x CE of air

© EFCF. All rights reserved. This content is excluded from our Creative Commons license. For more information, see <https://ocw.mit.edu/fairuse>.

The Future of the Hydrogen Economy, Bright or Bleak” Eliasson, and Bossel, 2003.

Compressed/Liquid H₂ Storage

Compressed H₂ Storage

- Composite tanks are available at 5,000 psi (350 bar)
- Prototype 10,000 psi tanks demonstrated



Liquid H₂ Storage

- BMW has demonstrated automotive liquid H₂ storage
- Liquefying H₂ requires substantial energy (40% of total energy content of H₂ fuel)
- Boil-off is an issue for non-pressurized insulated tanks
- Pressurized cryogenic tanks are being developed by LLNL.



Both images © Source unknown. All rights reserved. This content is excluded from our Creative Commons license. For more information, see <https://ocw.mit.edu/fairuse>.

For compressed and liquid storage, packaging volume is still a concern.

Leap forward ~ 10 years, Toyota Mirai



Fuel cell-powered 113 kW (152 hp)
Battery 1.6 kWh Nickel-metal hydride
Range 502 km (312 mi) (EPA)

This image is in the public domain.



Electric
(traction)
motor

Fuel cell stack
(115 kW)

H2 storage tanks @ 700 bar
(70 MPa or 10,000 psi) for 5
kg of H2.

Nickel-metal hydride
battery (1.6 kWh)

© Source unknown. All rights reserved. This content is excluded from our Creative Commons license. For more information, see <https://ocw.mit.edu/fairuse>.

Natural gas is liquefied for its transportation

(Critical point of methane is 191.1 K and 4.74 MPa)

Liquefy methane between $p_I = 1$ atm, $T_I = 273$ °K, and $p_f = 2.6$ atm and $T_f = 110$ °K

$$w_{\min} = -\left[(h_f - h_I) - T_0(s_f - s_I)\right]$$

From NIST web site, the thermodynamic properties of methane:

$$\begin{aligned} h_I &= 854.5 \text{ kJ/kg} & s_I &= 6.48 \text{ kJ/kgK} \\ h_f &= -5.55 \text{ kJ/kg} & s_f &= -0.053 \text{ kJ/kgK} \end{aligned}$$

$$w_{\min} = -\left[(-5.55 - 854.5) - 273(-0.053 - 6.48)\right] = -923.46 \text{ kJ/kg}_{\text{methane}}$$

If the second law efficiency of 25%, $w^{\text{actual}} = -3693.84 \text{ kJ/kg}_{\text{methane}}$

LHV of methane is 50 MJ/kg

Methane engine running at 40% efficiency produces 20 MJ/kg

Number look a lot better!

Linde-Hampson Process

Replace (expensive) isentropic expansion with a throttle valve

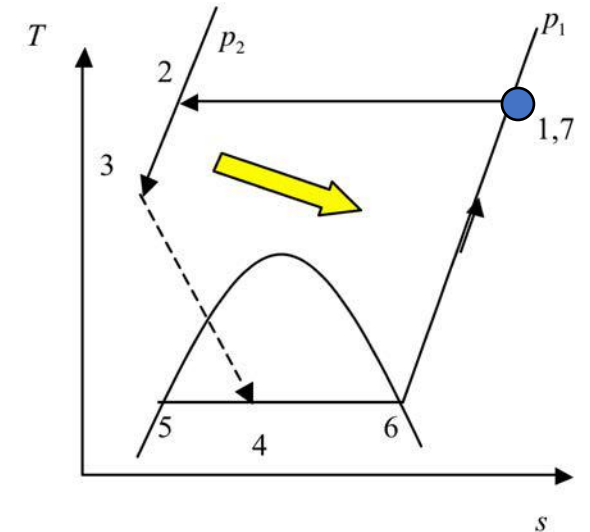
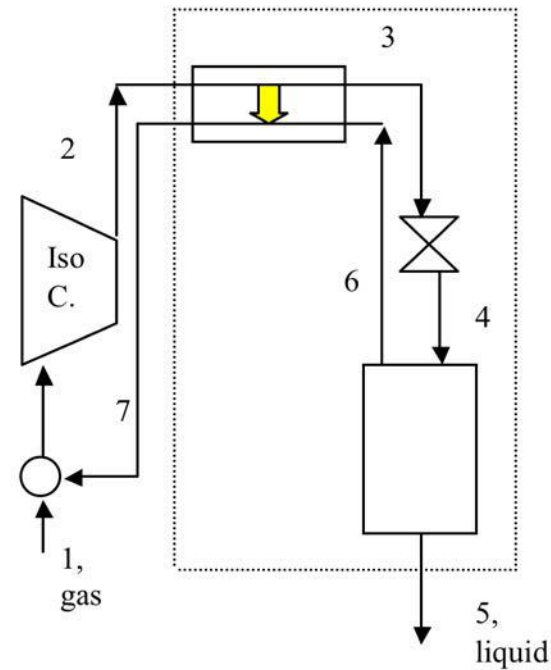
Keep isothermal compression, but use recuperation and (constant enthalpy) throttle valve, also called Joule-Thompson valve

energy balance over (broken line) CV

$$m_2 h_2 = m_5 h_5 + (m_2 - m_5) h_1, \quad \rightarrow \quad Y_l = \frac{m_5}{m_2} = \frac{h_1 - h_2}{h_1 - h_5}$$

isothermal compression: $w = T_1(s_2 - s_1) - (h_2 - h_1)$

$$w_l = \frac{w}{Y_l} = \frac{h_1 - h_5}{h_1 - h_2} [T_1(s_2 - s_1) - (h_2 - h_1)]$$



Liquid nitrogen is used extensively ...

the critical point of nitrogen is 126.2 K and 3.4 MPa.

The properties of nitrogen at (STP) 1 atm and 298 K (state 1): $h_1 = 311.1$ kJ/kg and $s_1 = 6.84$ kJ/kg.K.

the properties of nitrogen at 1 atm at saturated liquid (state 3): $h_3 = -122.1$ kJ/kg, $s_3 = 2.83$ kJ/kg.K and $T_3 = 77$ K.

ideal liquefaction work: $w_{\min} = -769.4$ kJ/kg N

Linde-Hampson using: $p_2 = 20$ MPa: $h_2 = 279.0$ kJ/kg and $s_2 = 5.16$ kJ/kg.K

$w = -6354.3$ kJ/kg N

Second law efficiency of Linde Hampson, it or figure of merit,

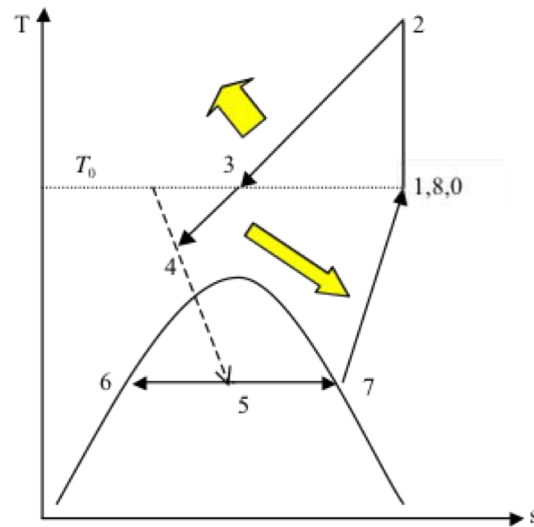
$769.4/6354.3 = 0.121$ (very low).

Actual Linde-Hampson plants have even lower efficiency because they may use adiabatic instead of isothermal compression

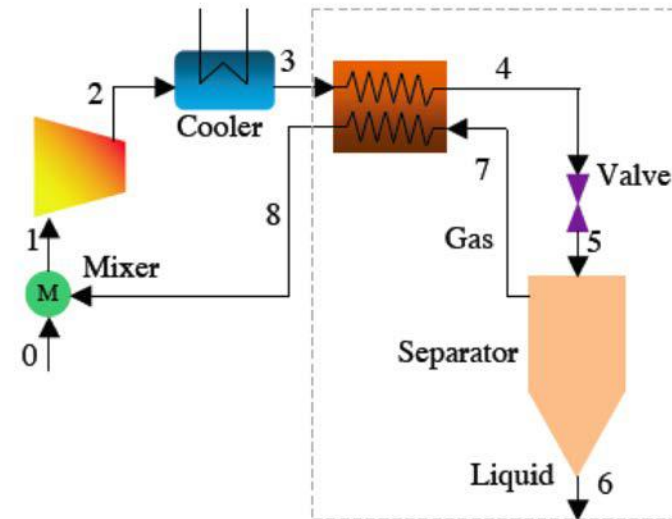
Multi stage compression with intercooling is used to approach the isothermal limit.

An expander can also be used to recover some of the expansion energy

Improvements make sense only in larger plants when larger capital costs are justifiable.



The T-s diagram of the adiabatic-compression liquefaction cycle shown above, utilizing a cooler to reduce the gas temperature between 2 and 3, and a regenerator to further reduce the gas temperature between 3 and 4 (while heating up the separated vapor between 7 and 8).



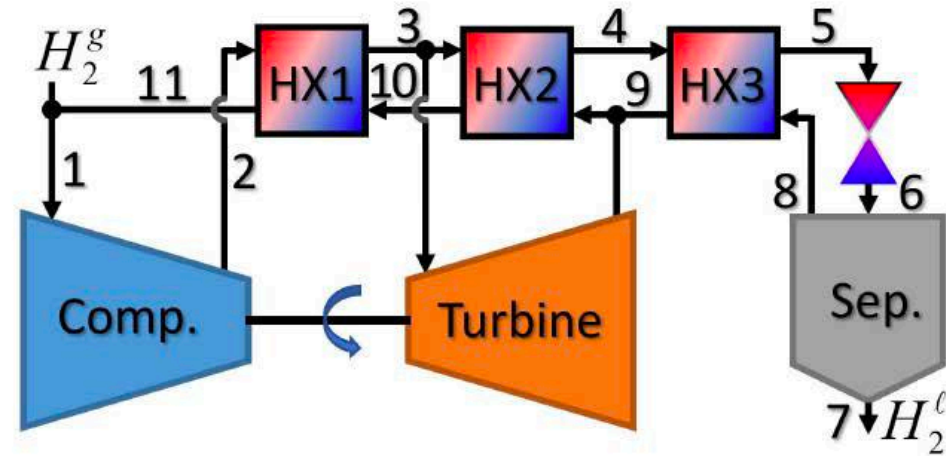
Liquefaction cycle with adiabatic compression and a separate cooler.

Claude Cycle uses
expanded H_2 to:

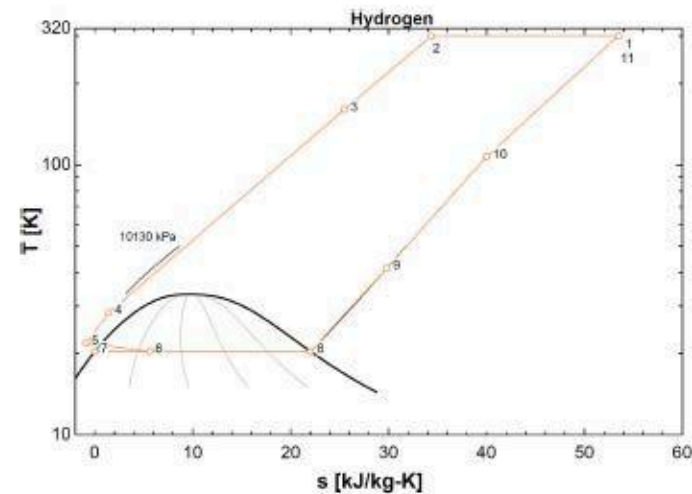
- reduce work input
- prechill without LN_2

30% Efficient
(7% of H_2 Exergy)

½ Entropy generation
caused by throttling



State	T_i [K]	P_i [kPa]	h_i [kJ/kg]	s_i [kJ/(kg·K)]
1	300	101.3	3958	53.46
2	300	10130	4006	34.38
3	160	10130	2011	25.46
4	50.76	10130	466.1	8.881
5	39.98	10130	308.3	5.4
6	20.37	101.3	308.3	15.14
7	20.37	101.3	0.06483	0.003021
8	20.37	101.3	448.7	22.03
9	41.39	101.3	678.2	29.82
10	125	101.3	1594	41.79
11	300	101.3	3958	53.46



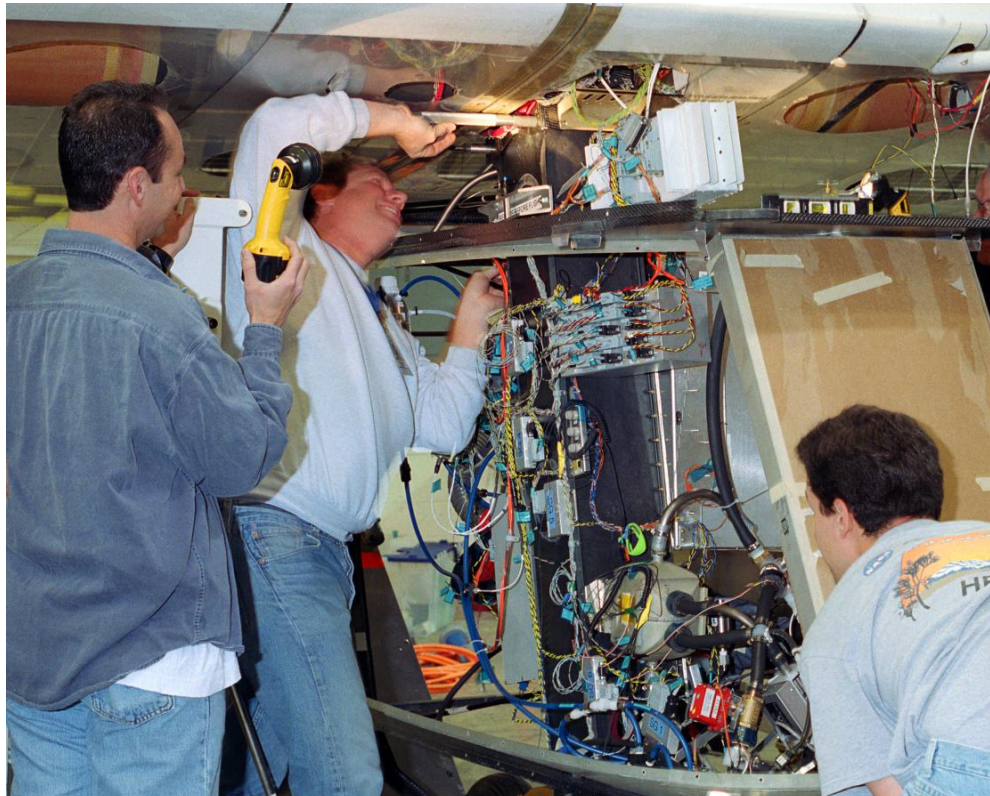
Images and table © Oxford University Press. All rights reserved. This content is excluded from our Creative Commons license. For more information, see <https://ocw.mit.edu/fairuse>.

Using H₂ to power a fuel cell for Helios



Image courtesy of NASA.

© by Ahmed F. Ghoniem



NASA Dryden flight Research Center Photo Collection
<http://www.dfrc.nasa.gov/gallery/photo/index.html>
 NASA Photo: EC03-0058-2 Date: March 4, 2003

Aerovironment technicians line up attachments as a fuel cell electrical system is installed on the Helios Prototype solar powered flying wing.



NASA Dryden flight Research Center Photo Collection
<http://www.dfrc.nasa.gov/gallery/photo/index.html>
 NASA Photo: EC03-0058-6 Date: March 4, 2003

Technicians for AeroVironment, Inc., jack up a pressure tank to the wing of the Helios Prototype solar-powered flying wing.

Images courtesy of NASA.

Liquid Air Energy Storage
Good material in Chris Nutty and Scott Seo
2019 student term report
The Claude cycle, etc.

MIT OpenCourseWare
<https://ocw.mit.edu/>

2.60J Fundamentals of Advanced Energy Conversion
Spring 2020

For information about citing these materials or our Terms of Use, visit: <https://ocw.mit.edu/terms>.

Lecture # 5

Chemical Thermodynamics 1

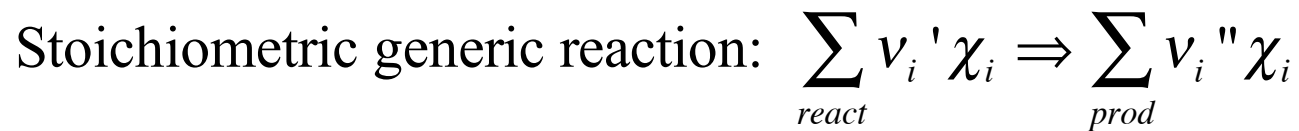
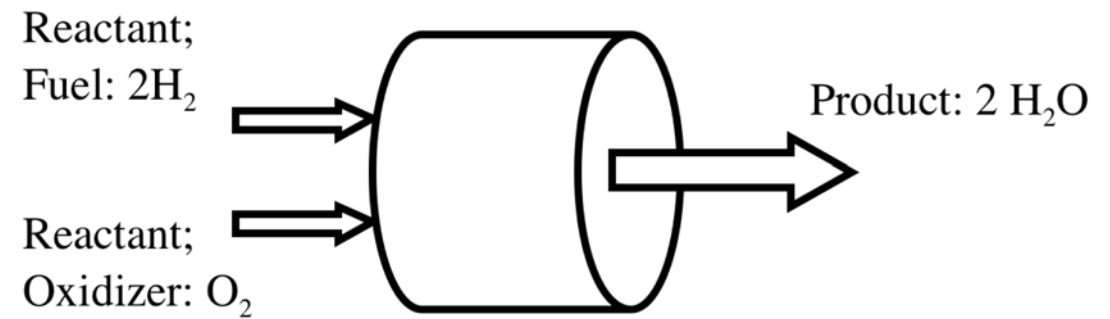
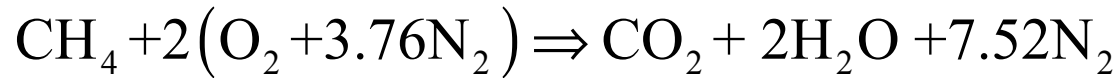
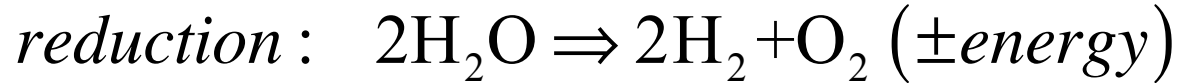
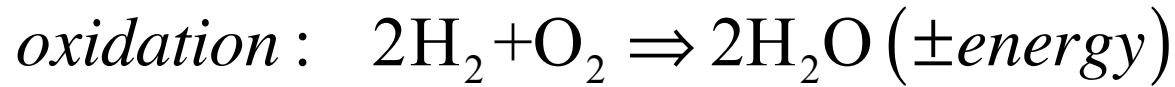
Ahmed Ghoniem

February 18, 2020

- Mass conservation in chemical reactions
- Energy conservation in chemical reactions
- Fuels and chemical energy carriers
- Combustion and Flame temperature.

Stoichiometry (element conservation) & Mass Conservation

Complete oxidation (burning) or reduction of “chemical energy carriers”:



ν_i' and ν_i'' are the stoichiometric coefficient satisfying conservation of element.

mass or elemental balance: $\sum_{react} \nu_i' \nu_{ij}^* = \sum_{prod} \nu_i'' \nu_{ij}^*$, or $\sum_{react} \nu_i \nu_{ij}^* = 0$ for $j = 1, J$

ν_{ij}^* is the number of j atom in i molecule.

The molar stoichiometric air-fuel ratio:

$$\widehat{AF}_{ST} = \left(\frac{n_{air}}{n_{fuel}} \right)_{ST} = \left(\frac{n_{oxygen} + n_{nitrogen}}{n_{fuel}} \right)_{ST} = \frac{v'_{oxygen} + v'_{nitrogen}}{v'_{fuel}} \quad (\text{a mole has } N_a = 6.022 \cdot 10^{23} \text{ molecules})$$

for methane-air: $\widehat{AF}_{ST} = 2(1+3.76) = 9.52$

The mass-based stoichiometric air-fuel ratio $AF_{ST} = \left(\frac{m_{air}}{m_{fuel}} \right)_{ST} = \frac{v'_{oxygen} M_{oxygen} + v'_{nitrogen} M_{oxygen}}{v'_{fuel} M_{fuel}}$

For methane-air: $AF_{ST} = 2(32+3.76 \times 28)/(12+4) = 17.16$

For non stoichiometric reactions/combustion: $\widehat{AF} = \left(\frac{n_{air}}{n_{fuel}} \right) = \left(\frac{n_{oxygen} + n_{nitrogen}}{n_{fuel}} \right)$

The ratio between the actual and stoichiometric is: the excess air ratio is:

$$\tilde{\lambda} = \frac{AF}{AF_{ST}}, \quad \text{and the equivalence ratio: } \phi = \frac{1}{\tilde{\lambda}}$$

(Fuel) Lean and rich burn

Lean Burning, $\phi < 1$ (in many power plants, burners and diesel engines).

Likely to lead to complete combustion, low NO_x formation (because of low T):



Rich Burning, $\phi > 1$, used in partial oxidation, fuel reforming and production of syngas, hydrogen, etc,

Example: partial oxidation (exothermic) for coal gasification/biochar: $\text{C} + \frac{1}{2}\text{O}_2 \Rightarrow \text{CO}$,



Not all reactions involve fuel oxygen!

Reforming (endothermic) can also be steam gasification $\text{C} + \text{H}_2\text{O} \Rightarrow \text{CO} + \text{H}_2$



More hydrogen can be produced by the "water-gas shift": $\text{CO} + \text{H}_2\text{O} \Rightarrow \text{CO}_2 + \text{H}_2$

Thermodynamic Properties of Fuel Combustion at 25 C and 1 atm Pressure

Fuel	Chemical symbol	Molecular weight kg/kmol	FHV MJ/kg_fuel	A/F	$H_r - H_p$ MJ/kg_product	Δg MJ/kg_fuel	FHV MJ/kg_C
hydrogen	H ₂	2.016	119.96	34.28	3.4	117.63	NA
Carbon (graphite)	C _{solid}	12.01	32.764	11.51	2.619	32.834	32.764
Methane	CH ₄	16.04	50.040	17.23	2.745	51.016	66.844
Carbon monoxide	CO	28.01	10.104	2.467	2.914	9.186	23.564
Ethane	C ₂ H ₆	30.07	47.513	16.09	2.780	48.822	59.480
Methanol	CH ₄ O	32.04	20.142	6.47	2.696	22.034	53.739
Propane	C ₃ H ₈	44.10	46.334	15.67	2.779	47.795	56.708
Ethanol	C ₂ H ₆ O	46.07	27.728	9.000	2.773	28.903	53.181
Isobutane	C ₄ H ₁₀	58.12	45.576	15.46	2.769		53.142
Hexane	C ₆ H ₁₄	86.18	46.093	15.24	2.838		54.013
Octane	C ₈ H ₁₈	114.2	44.785	15.12	2.778		53.246
Decane	C ₁₀ H ₂₂	142.3	44,599	15.06	2.778		52.838
Dodecane	C ₁₂ H ₂₆	170.3	44.479	15.01	2.778		52.567
Hexadecane	C ₁₆ H ₃₄	226.4	44.303	14.95	2.778		52.208
Octadecane	C ₁₈ H ₃₈	254.5	44.257	14.93	2.778		52.102

FHV=LHV (water in the products in the vapor phase)

Δg is the Gibbs free energy of reaction (maximum work under isothermal reaction conditions).

Last column: the heating value/carbon = FHV*molecular weight of fuel/molecular weight of carbon.

Fossil/Organic/Hydrocarbon Fuels

COAL, OIL, NATURAL GAS.

OIL SHALE, TAR SANDS, PEAT.

“BIOMASS” .. Young, “renewable”.

- Formed due to the fossilization of *organic* matter, underground (although evidence of earth mantle inorganic (abiogenic) methane is rising).
- All formed of carbon and hydrogen, some with little oxygen, plus sulfur, mercury and other minerals, and non combustibles.
- Most require some form of processing: sulfur removal, grinding and washing, oil refining, gas desulfurization.

Energy Balance in Chemical Reactions

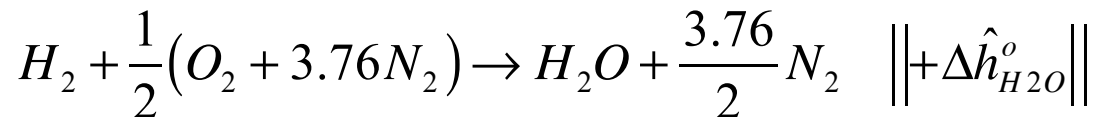
$$\frac{dE}{dt} = \dot{Q} - \dot{W} + \left(\sum_{react} \dot{m}_i (h_i + \mathbf{V}_i^2 + g_v z_i) - \sum_{prod} \dot{m}_i (h_i + \mathbf{V}_i^2 + g_v z_i) \right)$$

$$h_i = h_{i,thermal} + h_{i,chemical} = \int_{T^o}^T c_{p,i} dT + h_{i,chemical}^o$$

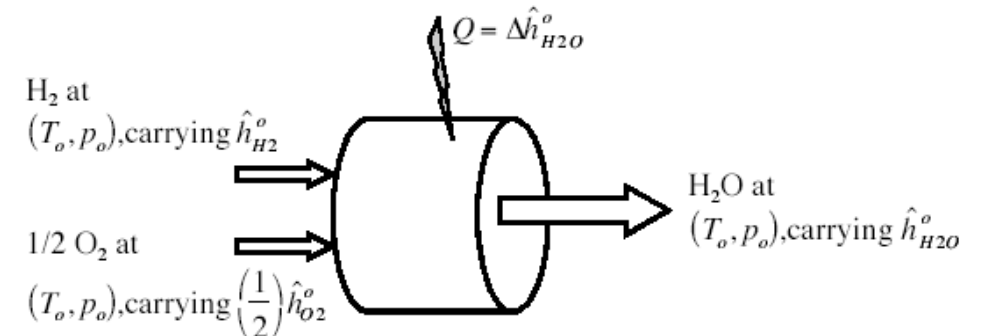
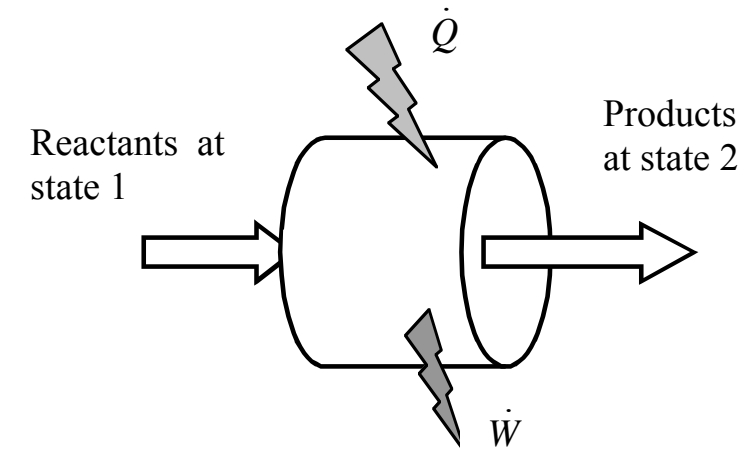
Steady, constant pressure and temperature, one mole of fuel:

$$Q = \sum_{prod} n_i \hat{h}_i - \sum_{react} n_i \hat{h}_i \quad (\equiv \text{heating value of the fuel})$$

- heat transfer out of the reaction, at constant p and T is *the enthalpy of reaction*.



$$\Delta\hat{h}_{fuel}^o = \sum_{prod} \nu_i'' \hat{h}_i^o - \sum_{react} \nu_i' \hat{h}_i^o, \quad \nu_i \text{ is the stoichiometric coefficient}$$



- Need to define a reference for the enthalpies.

Reference Enthalpy, Enthalpy of Formation

$$H = \sum_{i=1}^N m_i h_i(T, p_i) = \sum_{i=1}^N n_i \hat{h}_i(T, p_i)$$

$$h_i = h_{f,i}^o + \int_{T^o}^T c_{p,i}(T) dT, \text{ and } \hat{h}_i = \hat{h}_{f,i}^o + \int_{T^o}^T \hat{c}_{p,i}(T) dT$$

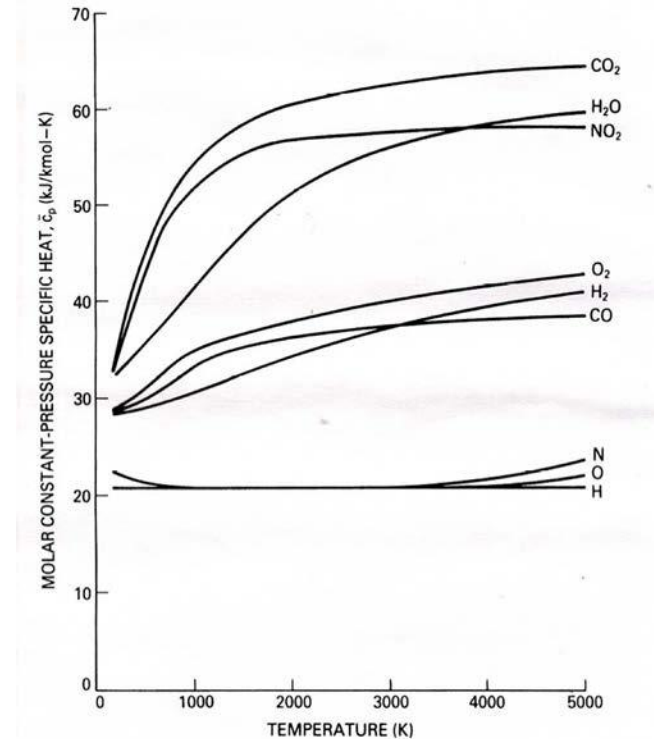
$$\hat{h}_f^o \equiv \Delta \hat{h}_f^o$$

Reference Entropy

$$\hat{s} = \sum_{i=1}^N X_i \hat{s}_i(T, p_i)$$

$$= \sum_{i=1}^N X_i \left(\hat{s}_i^{oo} + \int_{T^o}^T \frac{\hat{c}_{p,i}(T)}{T} dT \right) - \Re \sum_{i=1}^N X_i \ln \frac{p_i}{p^o}$$

$$\hat{s}_i^{oo} \equiv \Delta \hat{s}_f^o$$

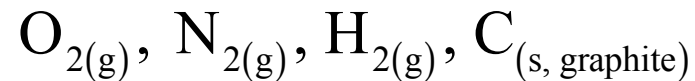


Enthalpy of Formation

Formation Reaction: $\sum_i \nu_i \chi_i \Rightarrow \chi_{comp}$

$$\Delta \hat{h}_R^o = \hat{h}_{comp}^o - \sum_i \nu_i \hat{h}_i^o = \hat{h}_{comp}^o \text{ for formation reaction ...}$$

Enthalpy of reaction of stable molecules, in their phase at STP, is taken to be zero:



Formation reaction of methane: $\text{C}_{(s)} + 2\text{H}_{2(g)} \Rightarrow \text{CH}_{4(g)}$

Energy of formation accounts for the net energy required to form or break bonds in a complex molecule.

Types of bonds: single, double, ... depending on the number of shared electrons. C has four bonds.

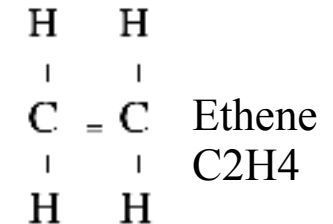
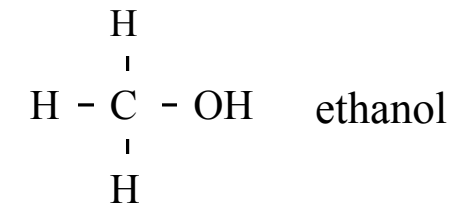
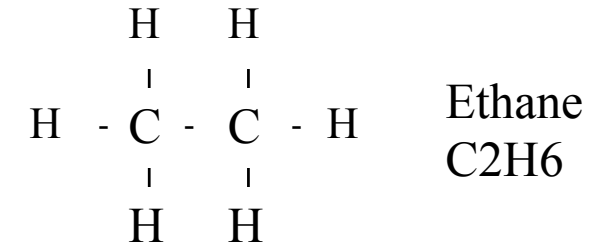
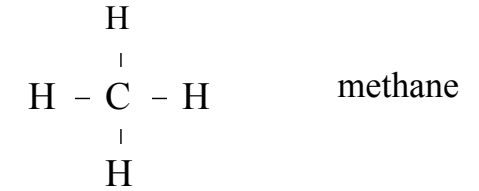
A saturated HC, like methane and methanol, use the four C bonds to attach another atom (H or C or a functional group (OH))

Unsaturated HC use multiple bond to connect C atoms

Single C – C bond 248 MJ/kmol
 Double C=C bond 615 MJ/kmol
 Triple 812 MJ/kmol

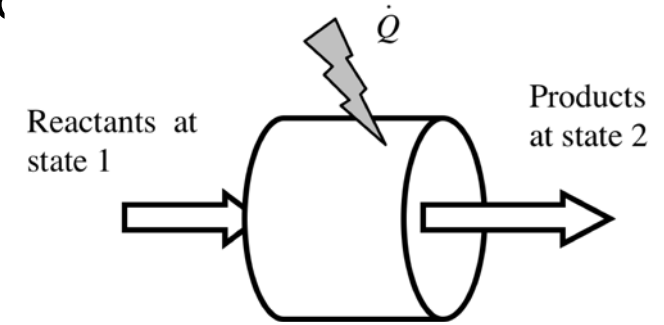
O-H bond 463 MJ/kmol
 Single O-O 139 MJ/kmol
 Double O=O 498 MJ/kmol
 ...

O-OH 498 MJ/kmol
 H-O2 196 MJ/kmol



Substance	Formula	Δh_f° MJ/kmol	Δg_f° MJ/kmol	Δs_f° kJ/kmol K
Ammonia	NH ₃	-45.7	-16.2	-99.1
Argon	Ar	0	0	0
Benzene	C ₆ H ₆	83.0	129.7	-156.9
Carbon	C	0	0	0
Carbon dioxide	CO ₂	-393.8	-394.6	2.9
Carbon monoxide	CO	-110.6	-137.4	89.7
Ethane	C ₂ H ₆	-84.7	-33.0	-173.7
Ethanol	C ₂ H ₅ OH	-235.0	-168.4	-223.3
Ethylene	C ₂ H ₄	52.3	68.2	-53.1
Hydrogen	H ₂	0	0	0
Hydrogen (atomic)	H	218.0	203.3	49.4
Hydroxyl	OH	39.5	34.3	17.4
Isooctane	C ₈ H ₁₈	-224.3	13.7	-798.6
Methane	CH ₄	-74.9	-50.9	-80.6
Methanol	CH ₃ OH	-201.3	-162.6	-129.8
Nitrogen	N ₂	0	0	0
Nitrogen (atomic)	N	472.8	455.6	57.6
Nitrogen dioxide	NO ₂	33.9	52.0	-60.8
n-Octane	C ₈ H ₁₈	-208.6	16.4	-754.6
Oxygen	O ₂	0	0	0
Water	H ₂ O	-242.0	-228.8	-44.4

Enthalpy of Reaction, Steady, constant p, zero work, etc



Arbitrary mixture

$$Q = H_{out}(T_{out}) - H_{in}(T_{in}) = \sum_{prod} n_i \hat{h}_i - \sum_{react} n_i \hat{h}_i$$

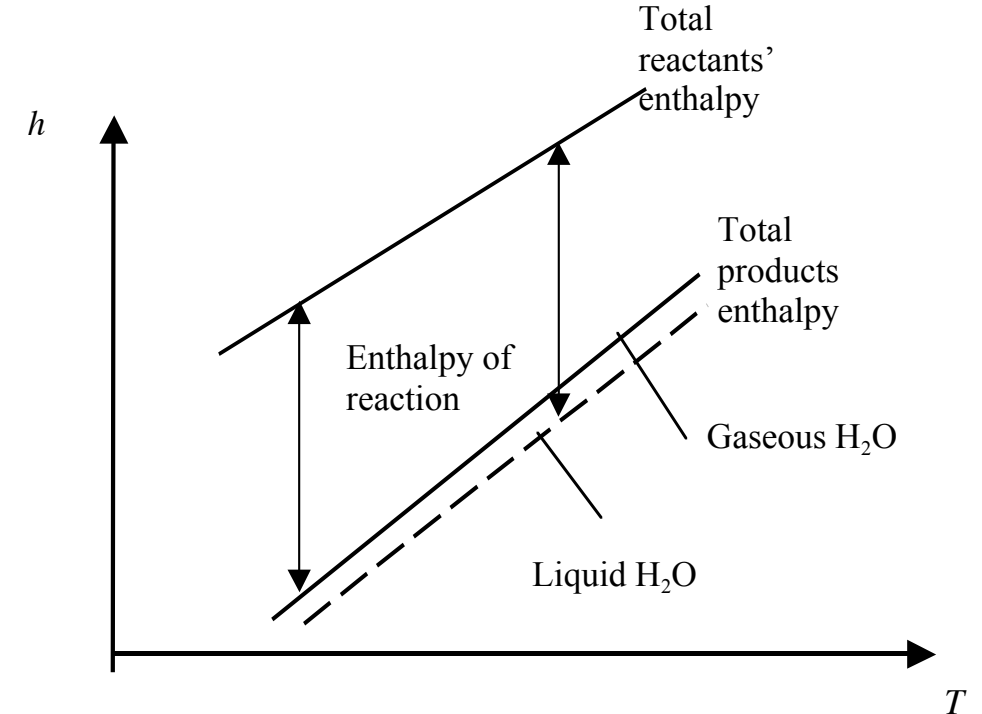
stoichiometric at STP (same T^o)

$$\Delta H_R^o = \sum_{prod} \nu_i'' \hat{h}_i^o - \sum_{react} \nu_i' \hat{h}_i^o$$

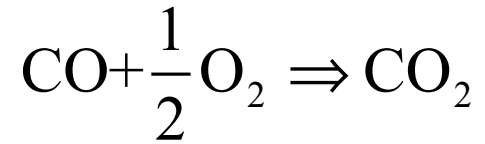
stoichiometric at arbitrary T

$$\Delta H_R(T) = \sum_{prod} \nu_i'' \hat{h}_i(T) - \sum_{react} \nu_i' \hat{h}_i(T) = \sum_{species} \nu_i \hat{h}_i(T)$$

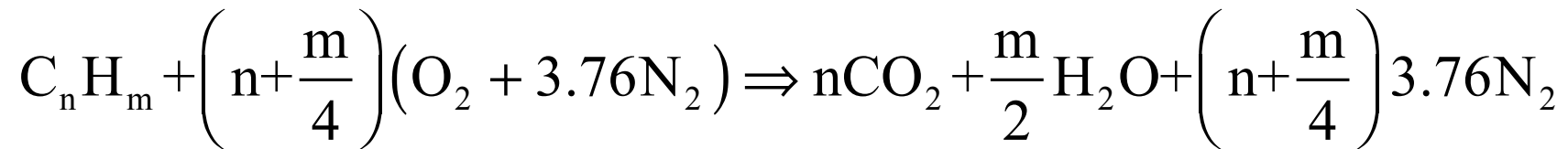
$$\nu_i = \nu_i'' - \nu_i'$$



Examples:



$$Q^o = \hat{h}_{\text{CO}_2}^o - \left(\hat{h}_{\text{CO}}^o + \frac{1}{2} \hat{h}_{\text{O}_2}^o \right) = -393 - (-110.6 + 0) = -282.5 \text{ kJ/gmol of CO}$$



$$\Delta \hat{H}_{R, \text{C}_n\text{H}_m}^o = n \hat{h}_{\text{CO}_2}^o + \frac{m}{2} \hat{h}_{\text{H}_2\text{O}}^o - \hat{h}_{\text{C}_n\text{H}_m}^o = \Delta \hat{h}_{R, \text{C}_n\text{H}_m}^o$$

For methane-air combustion, the "standard" enthalpy of reaction is:

$$\Delta \hat{h}_{\text{CH}_4}^o = -393.8 + 2(-242) - (-74.9) = -802.9 \text{ MJ/kgmol of methane}$$

Thermodynamic Properties of Fuel Combustion at 25 C and 1 atm Pressure

Fuel	Chemical symbol	Molecular weight kg/kmol	FHV MJ/kg_fuel	A/F	$H_r - H_p$ MJ/kg_product	D_g MJ/kg_fuel	FHV MJ/kg_C
hydrogen	H ₂	2.016	119.96	34.28	3.4	117.63	NA
Carbon (graphite)	C _{solid}	12.01	32.764	11.51	2.619	32.834	32.764
Methane	CH ₄	16.04	50.040	17.23	2.745	51.016	66.844
Carbon monoxide	CO	28.01	10.104	2.467	2.914	9.186	23.564
Ethane	C ₂ H ₆	30.07	47.513	16.09	2.780	48.822	59.480
Methanol	CH ₄ O	32.04	20.142	6.47	2.696	22.034	53.739
Propane	C ₃ H ₈	44.10	46.334	15.67	2.779	47.795	56.708
Ethanol	C ₂ H ₆ O	46.07	27.728	9.000	2.773	28.903	53.181
Isobutane	C ₄ H ₁₀	58.12	45.576	15.46	2.769		53.142
Hexane	C ₆ H ₁₄	86.18	46.093	15.24	2.838		54.013
Octane	C ₈ H ₁₈	114.2	44.785	15.12	2.778		53.246
Decane	C ₁₀ H ₂₂	142.3	44.599	15.06	2.778		52.838
Dodecane	C ₁₂ H ₂₆	170.3	44.479	15.01	2.778		52.567
Hexadecane	C ₁₆ H ₃₄	226.4	44.303	14.95	2.778		52.208
Octadecane	C ₁₈ H ₃₈	254.5	44.257	14.93	2.778		52.102

FHV=LHV (water in the products in the vapor phase)

D_g is the Gibbs free energy of reaction (maximum work under isothermal reaction conditions).

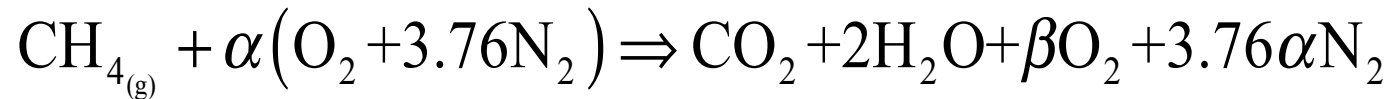
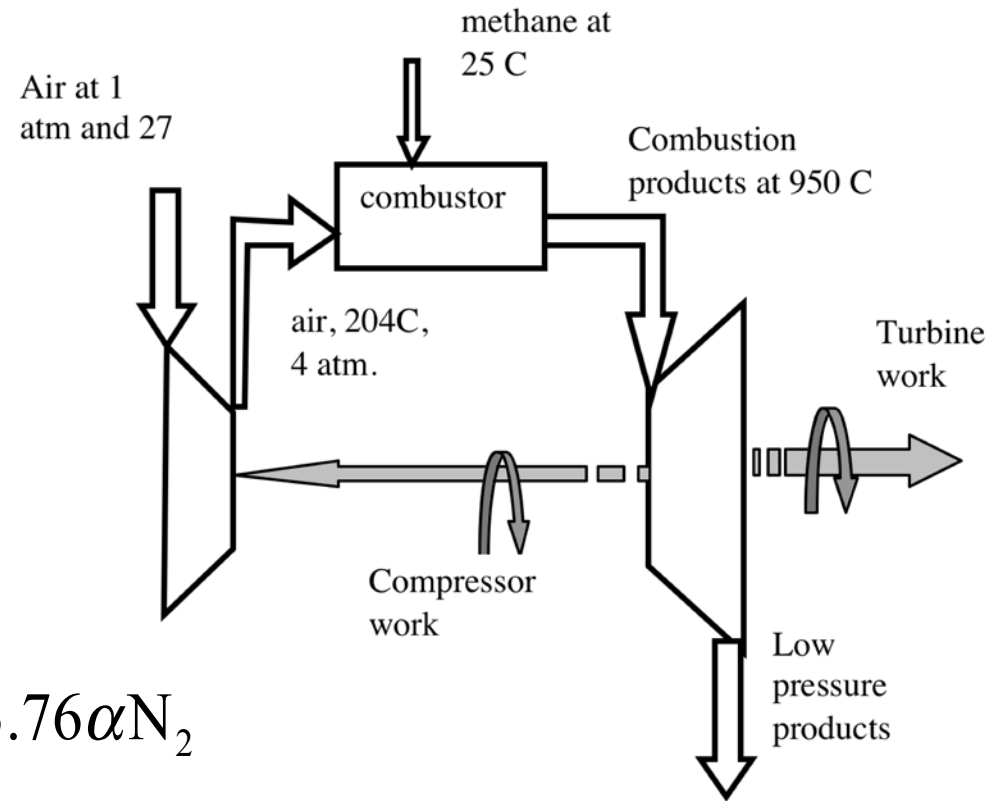
Last column: the heating value/carbon = FHV*molecular weight of fuel/molecular weight of carbon.

The Heating Value of a fuel is |enthalpy of reaction| per mole,
The table shows the LHV (water in vapor form).

HHV is obtained when water comes out in liquid form.

Fuel (phase)	LHV (kJ/mol)	HHV (kJ/mol)	$-\Delta G_R^{oo}(T^o, p^o)$ (kJ/mol)	$\hat{\xi}_{ch}^o$ (kJ/mol)
Hydrogen (g), H ₂	241.8	285.9	228.6	235.2
Carbon (s), C	393.5	393.5	394.4	410.5
<i>Paraffin (alkane) Family, C_n H_{2n+2}</i>				
Methane (g), CH ₄	802.3	890.4	818	830.2
Ethane (g), C ₂ H ₆	1427.9	1559.9	1467.5	1493.9
Propane (g), C ₃ H ₈	2044	2220	2108.4	2149
Butane (g), C ₄ H ₁₀	2658.5	2878.5	2747.8	2802.5
Pentane (g), C ₅ H ₁₂	3272.1	3536.1	3386.9	3455.8
Pentane (l), C ₅ H ₁₂	3245.5	3509.5	3385.8	3454.8
Hexane (g), C ₆ H ₁₄	3886.7	4194.8	4026.8	4110
Hexane (l), C ₆ H ₁₄	3855.1	4163.1	4022.8	4106
Heptane (g), C ₇ H ₁₆	4501.4	4853.5	4667	4764.3
Heptane (l), C ₇ H ₁₆	4464.9	4816.9	4660	4757.3
Octane (g), C ₈ H ₁₈	5116.2	5512.2	5307.1	5418.6
Octane (l), C ₈ H ₁₈	5074.6	5470.7	5297.2	5408.7

How much fuel is needed to raise the temperature of the products to 950 C, starting with air at 204 C and methane at 25C.



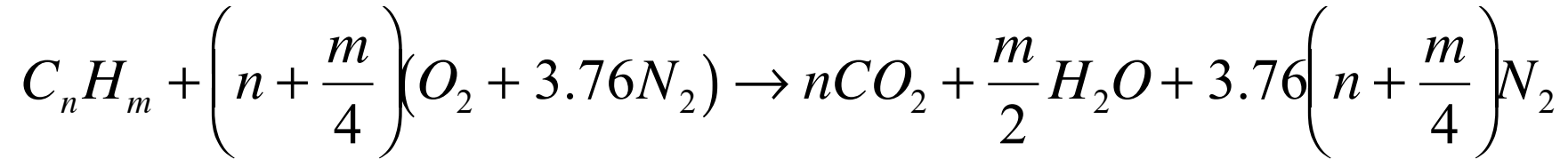
complete combustion: $\beta = \alpha - 2$

adiabatic combustion:

$$\hat{h}_{\text{CH}_4}^{27\text{C}} + \alpha(\hat{h}_{\text{O}_2}^{205\text{C}} + 3.76\hat{h}_{\text{N}_2}^{205\text{C}}) = \hat{h}_{\text{CO}_2}^{950\text{C}} + 2\hat{h}_{\text{H}_2\text{O}}^{950\text{C}} + (\alpha - 2)\hat{h}_{\text{O}_2}^{950\text{C}} + 3.76\alpha\hat{h}_{\text{N}_2}^{950\text{C}}$$

solve using enthalpy expressions: $\alpha = 7.428$ (for stoichiometric: $\alpha=2$)

Hydrocarbon Combustion in Air



- Hydrocarbons store energy in their chemical bonds. Highest energy storage per unit mass or unit volume (in liquid/solid forms).
- Chemical Energy is converted into thermal energy during combustion, or to other forms of chemical energy during refining and reforming (processes that may require energy).
- In complete, *stoichiometric* combustion of hydrocarbons, the products are water and carbon dioxide.

The table shows the LHV (water in vapor form), in MJ/kg fuel.

Commercial Fuels

Natural gas			36-42
Gasoline			47.4
Kerosene			46.4
No. 2 oil			45.5
No. 6 oil			42.5
Anthracite coal			32-34
Bituminous coal			28-36
Subbituminous coal			20-25
Lignite			14-18

Biomass Fuels

Wood (fir)			21
Grain			14
Manure			13

COAL

(fossilized vegetations)

lignite, subbituminous, bituminous, anthracite.

- Coal is carbon + hydrogen (CH_m , $m < 1$) + sulfur (up to 10% by weight) + nitrogen + oxygen + ash (non combustibles).
- Heating value per unit mass increases from lignite to anthracite, as the carbon ratio grow (and moisture, volatile matter including H_2 ratio, and sulfur decrease).
- Some sulfur can be washed away before combustion, but mostly is scrubbed from combustion products using limestone.
- In gasification, rich burning in oxygen and water forms syngas ($\text{CO} + \text{H}_2$), desulfurization before combustion or gas separation.

OIL

(or petroleum, liquid rock, fossilized marine life. algae)

- Made up of many organic compounds + hydrogen + nitrogen + sulfur. Sweet and sour refer to the amount of sulfur. CH_m , $1 < m < 2$.
- “Light oil” is generally composed of three hydrocarbon families:
 - Saturated hydrocarbons: normal alkanes (paraffins), $\text{C}_n\text{H}_{2n+2}$, with gas, $n = 1-4$, liquid, $n = 5-15$, and solids, $n > 15$.
 - Unsaturated hydrocarbons, and aromatics like benzene, C_6H_6 , toluene, C_7H_8 and naphthalene, C_{10}H_8 .
 - Resin and asphaltenes, heavier hydrocarbons rich in nitrogen, oxygen, sulfur and vanadium.
- Refining: distillation (separation of lighter components), catalytic cracking (heating) and reforming (with steam or hydrogen). Products are typically refinery gas, LPG, gasoline (mostly octane C_8H_{18}), aviation fuels (JPx), diesels, heating and lube oils

A Large Demand for Hydrogen is due to the Declining Quality of Available Crude Oil

ORNL DWG 2001-107R2

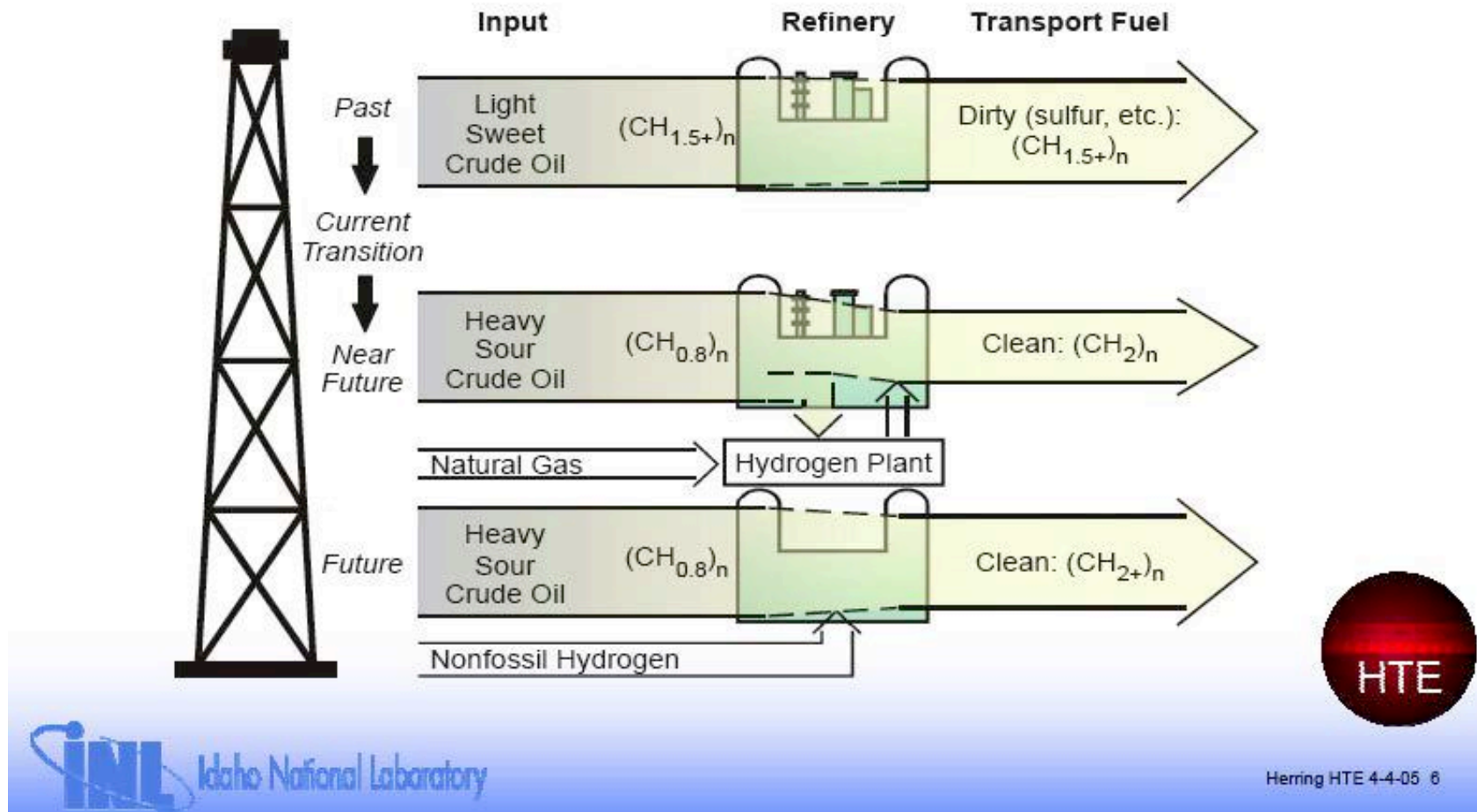


Image courtesy of Idaho National Laboratory, DOE.

Non-Conventional “Heavy” Oil

(all require intensive processing)

Oil Shale:

impermeable hard rock containing (organic, non petroleum) *kerogen* (pre-oil), which pyrolyzes into oil + (organic, petroleum) *bitumen* that liquefies with heating.

Tar and Tar Sands:

a mixture of sand and *bitumen* (coal-like), the bitumen is extracted by heating and steam, and it can be refined into oil components.



Courtesy of [Lindsey G](#) on [Wikimedia](#). License: CC BY.

After slowing down in 2016, U.S. shale oil is expected to ramp up again in 2017, continuing a decade-long surge. Constructed by Lucas Davis (UC Berkeley) using EIA data.

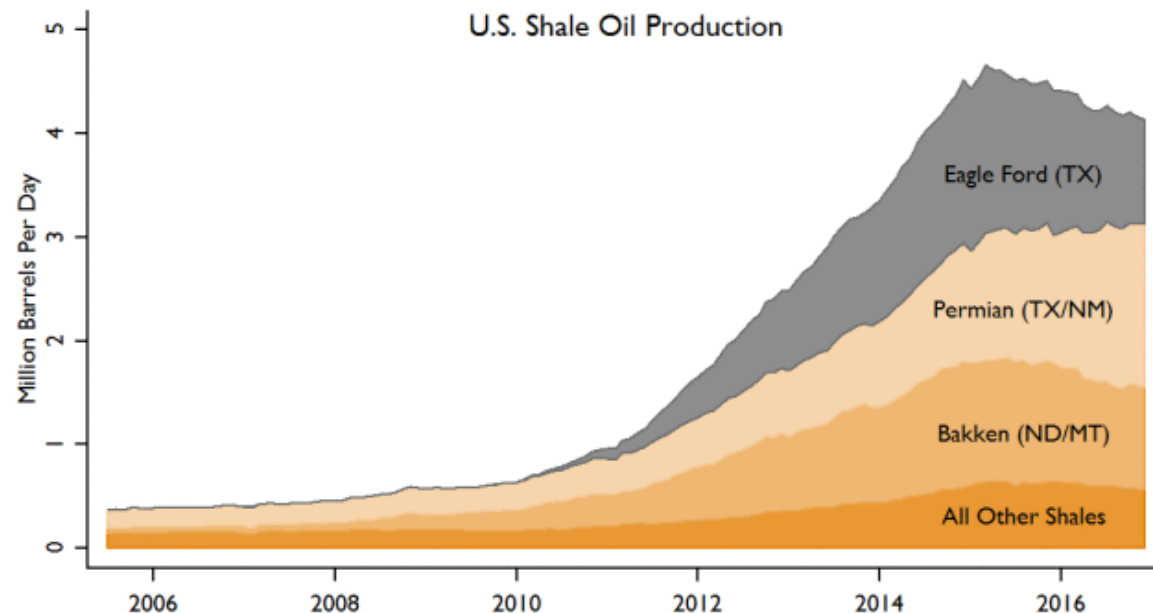


Figure courtesy of Lucas Davis, UC Berkeley. Used with permission.

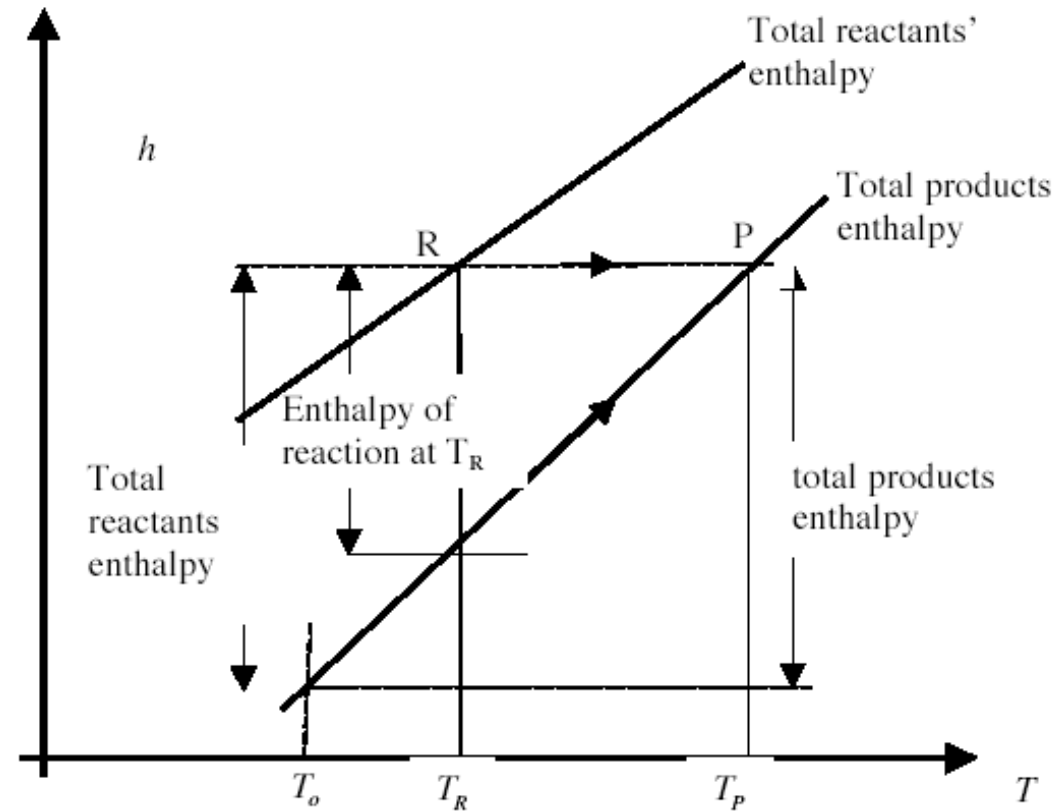
U.S. oil production in 2015 reached its highest level in decades, driven large increases in production from shale oil. Ford, Permian, and Bakken, but other areas have grown rapidly as well, and shale oil now represents almost half of all U.S. production.

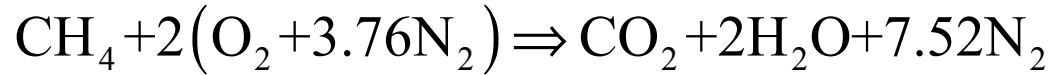
NATURAL GAS

- Mostly methane, CH_4 , ethane C_2H_6 , some propane, C_3H_8 , and little butane, C_4H_8 , with small fractions of higher hydrocarbons, may contain sulfur, oxygen, CO_2 at small quantities.
- Requires least processing.
- Biogenic Gas: near surface, difficult to exploit.
- **Methane hydrides/hydrates**, found in deep oceans, and permafrost, encapsulated in water (estimated to exceed 2 orders of magnitude of proven gas reserves) in ice like structures.
- Shale gas, like shale oil.
- Abiogenic gas, deep underground, non organic

Adiabatic Flame Temperature

$$\sum_{react} n_i \hat{h}_i(T_r) = \sum_{prod} n_i \hat{h}_i(T_p)$$





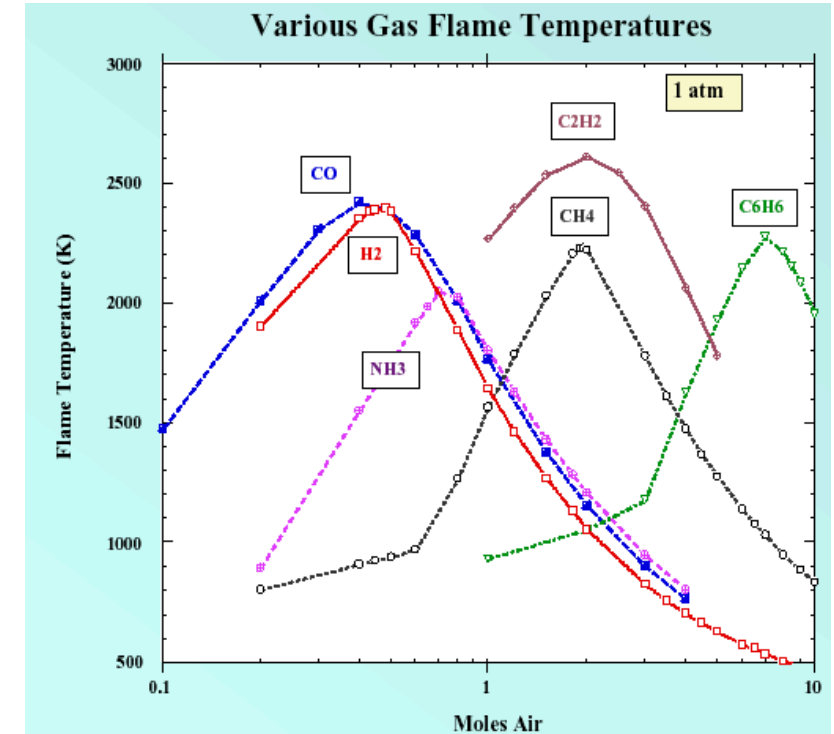
starting with $T = 298 \text{ K}$

$$\sum_{\text{react}} \nu_i \hat{h}_i(298) = \hat{h}_{\text{methane}}^o = -74,831 \text{ kJ/kgmole}$$

$$\hat{h}_{\text{CO}_2}(T_p) + 2\hat{h}_{\text{H}_2\text{O}}(T_p) + 7.52\hat{h}_{\text{N}_2}(T_p) = \sum_{i=1}^3 n_i \hat{h}_i^o + \sum_{i=1}^3 n_i \int_{T_o}^{T_p} \hat{c}_{p,i} dT$$

By iteration: $T = 2340 \text{ K}$.

The adiabatic flame temperature is highest at conditions slightly richer than stoichiometric (because of dissociation). Most fuels peak around 2300-2400 K, hydrogen's and CO are higher, and acetylene is the highest. *Lean* and *rich* burn, or lower and higher equivalence ratios, lead to lower flame temperature, with the latter containing fuel fragments. Oxy-combustion is much higher.



© Source unknown. All rights reserved. This content is excluded from our Creative Commons license. For more information, see <https://ocw.mit.edu/fairuse>.

Combustion in a Closed Volume

$$\begin{aligned}
 Q - W &= \Delta U = U_p - U_r \\
 &= H_p - H_r - \left((p\forall)_p - (p\forall)_r \right) \\
 &= \sum_{prod} n_i \hat{h}_i(T_p) - \sum_{react} n_i \hat{h}_i(T_r) - (n_p \Re T_p - n_r \Re T_r)
 \end{aligned}$$

“Standard” Internal Energy of Reaction

$$\begin{aligned}
 \Delta \hat{U}_R^o &= \sum_{prod} \nu_i \hat{h}_i(T^0) - \sum_{react} \nu_i \hat{h}_i(T^0) - (\nu_p - \nu_r) \Re T^0 \\
 &= \Delta \hat{H}_R^o - (\nu_p - \nu_r) \Re T^0
 \end{aligned}$$

$$\nu_p = \sum \nu'', \quad \nu_r = \sum \nu'$$

The complete combustion of various hydrocarbons in a **perfectly insulated constant-volume combustion chamber**, stoichiometric mixture with dry air starting at 298 C and 1 atm. from Gyftopoulos and Beretta

Fuel	Formula	T_b <i>K</i>	p_b <i>atm</i>
Hydrogen	H ₂	2870.8	8.33
Carbon	C	2677.9	7.58
Methane	CH ₄	2655.4	9.02
Acetylene	C ₂ H ₂	3009.7	10.00
Ethylene	C ₂ H ₄	2811.0	9.63
Ethane	C ₂ H ₆	2691.1	9.42
Propane	C ₃ H ₈	2698.7	9.56
<i>n</i> -Butane	C ₄ H ₁₀	2702.7	9.64
Benzene	C ₆ H ₆	2767.6	9.61
<i>n</i> -Heptane	C ₇ H ₁₆	2707.6	9.75
<i>n</i> -Octane	C ₈ H ₁₈	2706.9	9.76
Isooctane	C ₈ H ₁₈	2702.6	9.74

Efficiency

Combustion: $(\eta_{comb})_I = \frac{\sum_{prod} n_i \hat{h}_i - \sum_{react} n_i \hat{h}_i}{-\hat{h}_{R,f}} = \frac{Q_H}{HV_{fuel}} < 1$, (incomplete combustion; heat losses)

For engines and FC (chemical engines: $\eta_{fuel-utiliz} = \frac{\dot{W}_{net}}{\dot{m}_{fuel} HV_{fuel}}$

OR: $\eta_{fuel-utiliz} = \frac{W_{net}}{W_{max}} \frac{W_{max}}{Q_H} \frac{Q_H}{HV_{fuel}} = \eta_{II} \cdot \eta_{car} \cdot \eta_{comb}$

For fuel production: $(\eta_{reform})_I = \frac{\text{Energies Out}}{\text{Energies In}} = \frac{\text{Chemical Energy Out}}{\text{Chemical Energy In}} = \frac{(\dot{n}_f \Delta \hat{h}_f)_{out}}{\sum_{in} (\dot{n}_f \Delta \hat{h}_f)}$

MIT OpenCourseWare
<https://ocw.mit.edu/>

2.60J Fundamentals of Advanced Energy Conversion
Spring 2020

For information about citing these materials or our Terms of Use, visit: <https://ocw.mit.edu/terms>.

Lecture # 6

Chemical Thermodynamics 2

Ahmed F Ghoniem

February 19, 2020



Mass conservation determines the products composition if the number of components equals the number of distinct element.

Energy conservation determines the temperature, or the heat and work interactions.

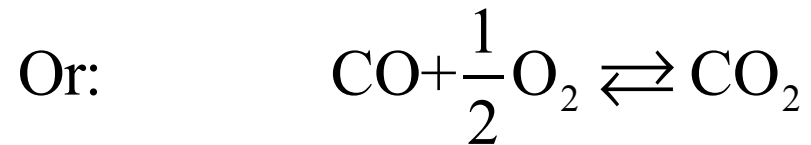
What defines the product composition if the number of components is larger than the number of elements (rich burning, reforming, dissociation)?

Or how to determine the extent of the reaction (at equilibrium) as function of the conditions (T,p) and elemental composition?

complete oxidation: $C + O_2 \rightarrow CO_2$, partial oxidation: $C + O_2 \rightarrow CO + \frac{1}{2}O_2$

in general: $C + O_2 \rightarrow \alpha CO + \beta CO_2 + \gamma O_2 + \dots$

Chemical reactions can move both ways, forward and backward:



that is the mixture of three components (CO , O_2 , CO_2) can co-exist
the fractions depend on the thermodynamic state, e.g., (p, T)

The composition, or final state depends on the conditions, that is, pressure, temperature and amount originally existing in the mixture (elemental composition).

We need to find the rules of “Equilibrium”.

How about Entropy

$$\frac{dS}{dt} = \sum_k \frac{\dot{Q}_k}{T_k} + \sum_{react} \dot{n}_i \hat{s}_i - \sum_{prod} \dot{n}_i \hat{s}_i + \dot{S}_g$$

$$\hat{s}_i(T, p, X_i) = \left(\hat{s}_i^{oo} + \int_{T^o}^T \frac{\hat{c}_{p,i}(T)}{T} dT \right) - \left(\Re \ln \frac{p}{p^o} + \Re \ln X_i \right)$$

For steady adiabatic reactions: $\Delta S_R = \Delta S_g = \sum_{prod} \nu_i'' s_i(T, p, X_i) - \sum_{react} \nu_i' s_i(T, p, X_i)$

For "spontaneous" reactions at constant (H and p), ΔS_g must be positive ..

General Condition for Equilibrium

Expressed in terms of Entropy Generation

the combined statement of the 1st and 2nd law

$$T dS_g = T dS - dU - p d\forall \geq 0$$

At constant (given) $(U, \forall) : dS = dS_g$

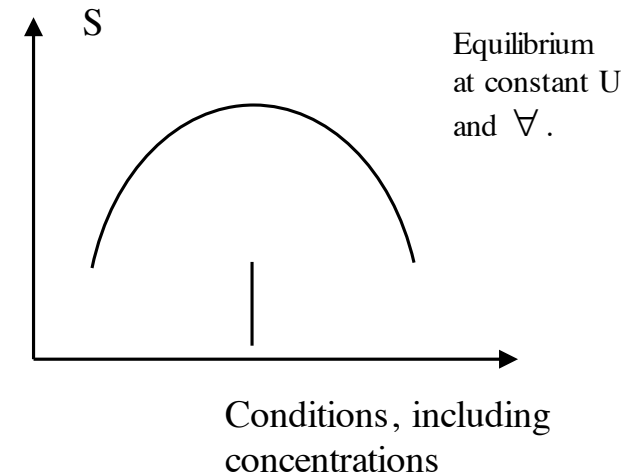
and hence in terms of properties

$$dS \geq 0 \quad \text{at constant } (U, \forall)$$

$$S = \sum n_i \hat{s}_i(T, p_i), \quad p_i = X_i p$$

For a mixture undergoing a chemical reaction:

Mass transfer among the components maximizes S



Under different constraints, other conditions should be used:

$$H = U + p\forall$$

$$T dS_g = T dS - dH + \forall dp \geq 0 \rightarrow \text{at constant } (p, H): dS \geq 0$$

$$G = H - TS$$

$$T dS_g = -dG + \forall dp - S dT \geq 0 \rightarrow \text{at constant } (p, T): dG \leq 0$$

$$A = U - TS$$

$$T dS_g = -dA - p d\forall - S dT \geq 0 \rightarrow \text{at constant } (T, \forall): dA \leq 0$$

Maximizing (or minimizing a function (with mass conservation constraints) is used extensively in computer codes.

The Element Potential Method for Equilibrium Calculations

Maximize (or minimize) a function (with respect to the concentrations of the components) subject to constraints of Mass Conservation and two Thermodynamic properties (this approach is used in equilibrium computer codes)

e.g., for constant internal energy and volume, maximize the entropy,

$$S = \sum_N n_i \left[\hat{s}^o + \int_{T_o}^T \frac{\hat{c}_p(T)}{T} dT - \Re \left(\ln \frac{p}{p_o} + \ln X_i \right) \right] \rightarrow \max \text{ w.r.t. } X$$

subject to mass conservation and:

$$U = \sum_N n_i \hat{u}_i = \text{Constant}, \quad \forall = \sum_N n_i \hat{v}_i = \text{Constant}$$

It is best to use codes like CANTERA, CHEMKIN or EES.

Another Approach relies on *the Chemical Potential*

Gibbs Fundamental Relation With Mass Transfer

$$T dS = dU + p d\forall - \sum_N \mu_i dn_i$$

μ_i associated with change in S at constant U and \forall
as we change n_i by dn_i . In finite form:

$$U = TS - p\forall + \sum_N \mu_i n_i,$$

Define Gibbs function again: $g = h - Ts$,

$$\text{or } G = H - TS$$

$$G = U + p\forall - TS = \sum_N \mu_i n_i$$

But $G = \sum_N n_i \hat{g}_i$, and hence $\mu_i = \hat{g}_i(T, p_i)$

For an Ideal Gas Mixture $\mu_i = \hat{g}_i(T, p_i) = \hat{g}_i^o(T) + \Re T \ln p_i$

$$\mu_i = \hat{g}_i^o(T) + \Re T \ln p + \Re T \ln X_i,$$

where $\hat{g}^o(T) = \hat{g}^{oo} + \Im n(T)$,

\hat{g}^{oo} is standard Gibbs free energy (of formation)

Equilibrium in terms of Chemical Potential

The general expression of entropy generation with mass transfer

$$T dS_g = T dS - dU - p d\forall \quad (\geq 0 \text{ for equilibrium}),$$

combined with the Gibbs Fundamental relation:

$$T dS = dU + p d\forall - \sum_N \mu_i dn_i,$$

$$\text{we get: } T dS_g = - \sum_N \mu_i dn_i, \quad (\text{entropy generation due to mass transfer})$$

and hence **the general condition for mass transfer equilibrium**

$$\sum_N \mu_i dn_i \leq 0$$

**chemical potential drives mass transfer, similar to T driving heat transfer
and p driving work transfer (mass flux is proportional to $\nabla \mu$)**

The Equilibrium Constant of A Reaction

The condition for equilibrium is:

$$\sum_N \mu_i dn_i = 0$$

When applied to the chemical reaction:

$$\sum_{react} \nu_i' \chi_i \Rightarrow \sum_{prod} \nu_i'' \chi_i,$$

For which ($\nu_i = \nu_i'' - \nu_i'$): $dn_i / \nu_i = \text{constant} = d\xi$

We get:

$$\sum_{species} \nu_i \mu_i = 0,$$

the Law of Mass Action

$$\sum_{prod} \nu_i'' \mu_i - \sum_{react} \nu_i' \mu_i = 0$$

The Equilibrium Constant of A Reaction

$$\sum_{prod} \nu_i'' \mu_i - \sum_{react} \nu_i' \mu_i = 0$$

$$\text{with } \mu_i = \hat{g}_i(T, p_i) = \hat{g}_i^o(T) + \Re T \ln \frac{p_i}{p_o}$$

$$\frac{\prod_{prod} p_i^{\nu_i''}}{\prod_{react} p_i^{\nu_i'}} = K_p(T), \quad p_o = 1 \text{ atm}, p_i \text{ in atm}$$

with the Equilibrium Constant

$$K_p(T) = \exp\left(-\frac{\Delta G_R^o(T)}{\Re T}\right)$$

$$\Delta G_R^o(T) = \sum_{prod} \nu_i'' \hat{g}_i^o(T) - \sum_{react} \nu_i' \hat{g}_i^o(T) = \sum_{species} \nu_i \hat{g}_i^o(T)$$

$\Delta G_R^o(T)$ is the Gibbs free energy of reaction @ T

it is a function of

the stoichiometric coefficients of the reaction and T

The equilibrium constant is defined as $K_p(T) = \frac{X_3^{v_3} X_4^{v_4}}{X_1^{v_1} X_2^{v_2}} \left(\frac{p}{p_o} \right)^{-v_1 - v_2 + v_3 + v_4}$

in which $P_o = 1$ atm: $v_1 A_1 + v_2 A_2 \rightleftharpoons v_3 A_3 + v_4 A_4$

table shows log K

$H_2O \rightleftharpoons$ $OH + \frac{1}{2}H_2$	$\frac{1}{2}O_2 + \frac{1}{2}N_2 \rightleftharpoons$ NO	$CO_2 \rightleftharpoons$ $CO + \frac{1}{2}O_2$	$CO_2 + H_2 \rightleftharpoons$ $CO + H_2O$	T, K
-143.8	-46.453	-143.2	-19.6	100
-46.137	-15.171	-45.066	-5.018	298
-26.182	-8.783	-25.025	-2.139	500
-11.309	-4.062	-10.221	-0.159	1000
-8.811	-3.275	-7.764	+0.135	1200
-7.021	-2.712	-6.014	+0.333	1400
-5.677	-2.290	-4.706	+0.474	1600
-4.631	-1.962	-3.693	+0.577	1800
-3.793	-1.699	-2.884	+0.656	2000
-3.107	-1.484	-2.226	+0.716	2200
-2.535	-1.305	-1.679	+0.764	2400
-2.052	-1.154	-1.219	+0.802	2600
-1.637	-1.025	-0.825	0.833	2800
-1.278	-0.913	-0.485	+0.858	3000
-0.559	-0.69	+0.19	+0.902	3500
-0.022	-0.524	+0.692	+0.930	4000
+0.397	-0.397	+1.079	+0.946	4500
+0.731	-0.296	+1.386	+0.956	5000
+1.004	-0.214	+1.635	+0.960	5500
+1.232	-0.147	+1.841	+0.961	6000

Chemical reactions are algebraically additive:

$$R = R_1 + R_2 + R_3 \dots$$

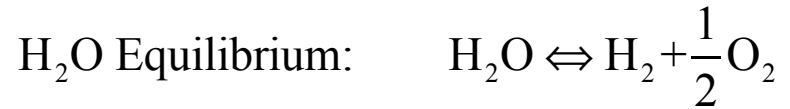
with $\Delta G_{R,1}^o$, $\Delta G_{R,2}^o \dots$ and $K_{p,1}$, $K_{p,2}$

$$\begin{aligned} \ln K_p &= -\frac{1}{\Re T} (\Delta G_R^o(T)) \\ &= -\frac{1}{\Re T} (\Delta G_{R,1}^o(T) + \Delta G_{R,2}^o(T) + \Delta G_{R,3}^o(T) + \dots) \\ &= \ln(K_{p,1}) + \ln(K_{p,2}) + \ln(K_{p,3}) + \dots \\ &= \ln(K_{p,1} K_{p,2} K_{p,3} \dots) \end{aligned}$$

Example: Water Dissociation At High Temperature

1 mole of water becomes:

$$\left((1-\alpha)H_2O + \alpha H_2 + \frac{\alpha}{2}O_2 \right)$$



mole fractions: $n_{total} = \sum_{mixture} \alpha_i, \quad X_i = \frac{\alpha_i}{n_{total}}$

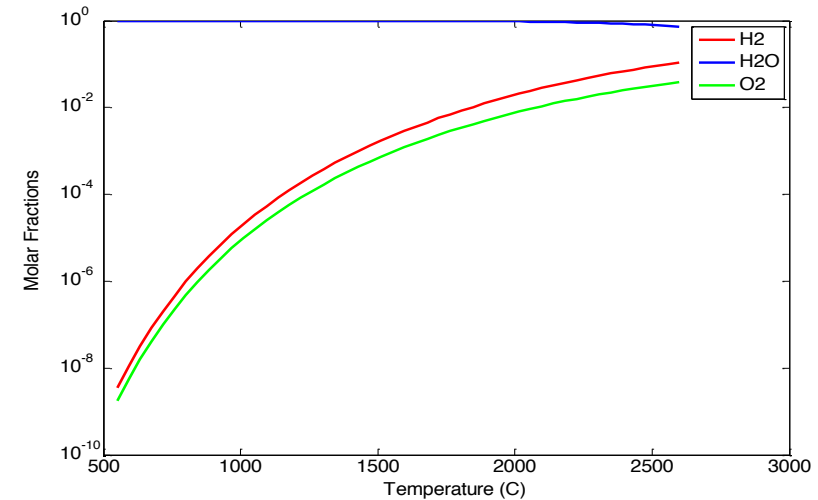
$$\frac{X_{H_2} X_{O_2}^{1/2}}{X_{H_2O}} = \frac{K_{p,H_2O}}{\sqrt{p}},$$

$$K_{p,H_2O \rightarrow H_2 + \frac{1}{2}O_2}(T) = \exp\left(-\frac{\Delta G_{R,H_2O}^o(T)}{\Re T}\right)$$

$$\frac{\alpha}{1-\alpha} \left(\frac{\alpha}{2+\alpha} \right)^{1/2} = \frac{K_{p,H_2O}}{\sqrt{p}}$$

at 3000 K, $X_{H_2O} = 0.794$, $X_{H_2} = 0.137$, and $X_{O_2} = 0.069$.

Equilibrium limitation for water splitting

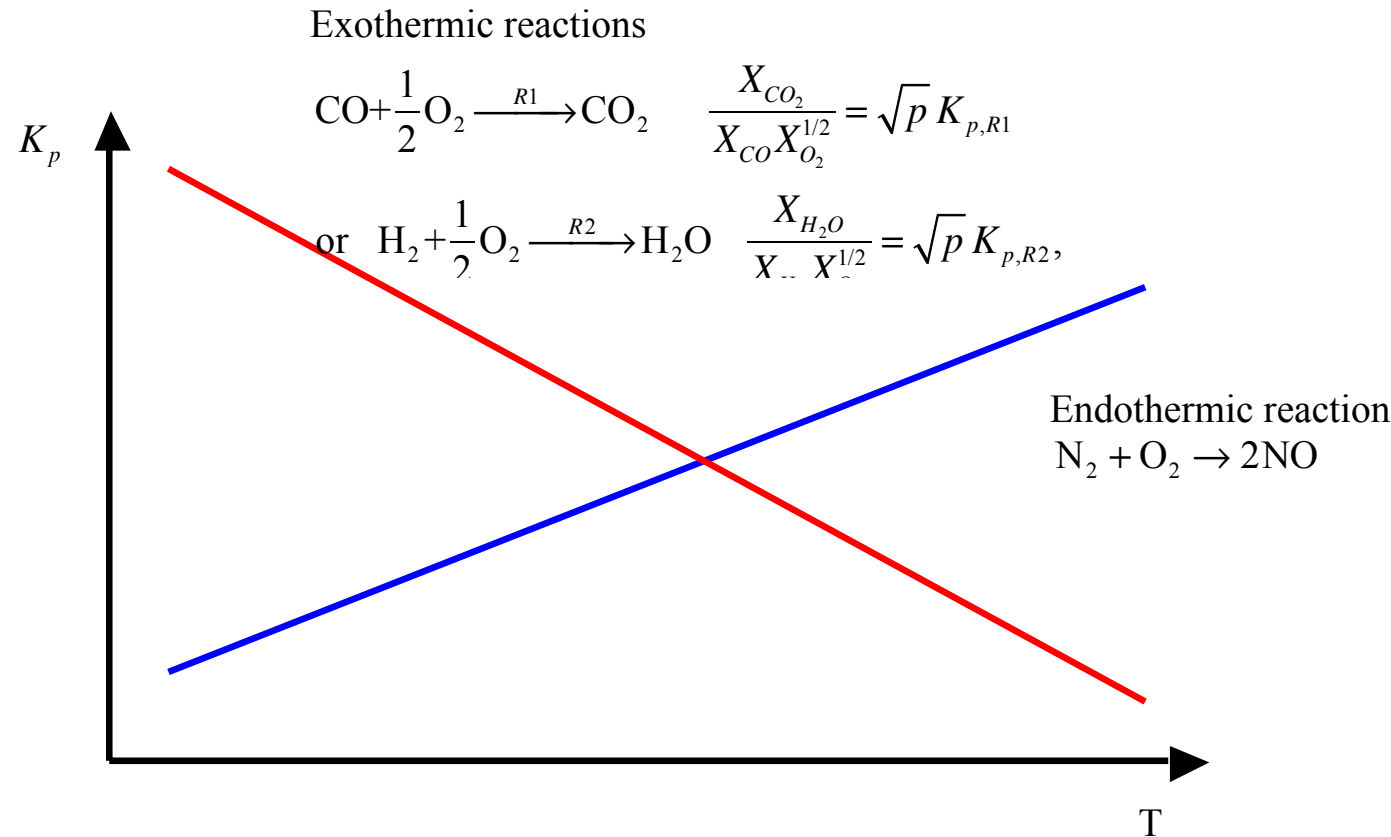


Temperature Dependence of Equilibrium Composition

The van't Hoff Equation: $\frac{d(\ln K_p)}{d(1/T)} = -\frac{\Delta H_R}{\mathfrak{R}}$

and $K_p \approx \bar{K}_p^o \exp\left(-\frac{\Delta H_R^0}{\mathfrak{R}T}\right)$

- The “partial pressure” of a solid is one.
- The reverse reaction has the inverse equilibrium constant.
- Additive reactions have multiplicative equilibrium constant.



Example: CO₂ reduction to CO at high T

Heating CO₂ from 298 K to 2800 K, while p drops:

mass conservation: mixture is $\left((1-\alpha)CO_2 + \alpha CO + \frac{\alpha}{2}O_2 \right)$,

$$n_{total} = \sum_{mixture} \alpha_i, \quad X_i = \frac{\alpha_i}{n_p}$$

CO₂ Equilibrium: $CO_2 \rightleftharpoons CO + \frac{1}{2}O_2$, $\frac{X_{CO}X_{O_2}^{1/2}}{X_{CO_2}} = \frac{K_{p,CO_2}}{p^{1/2}}$,

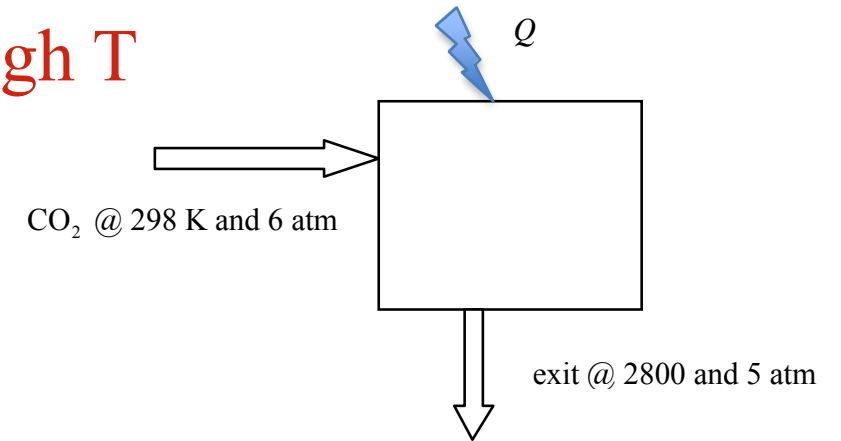
$$\frac{K_p^2}{p} = \frac{\alpha^3}{(1-\alpha)^2(2+\alpha)}$$

@ 2800K, $\alpha = 0.1867$, or 18.7% carbon dioxide dissociation.

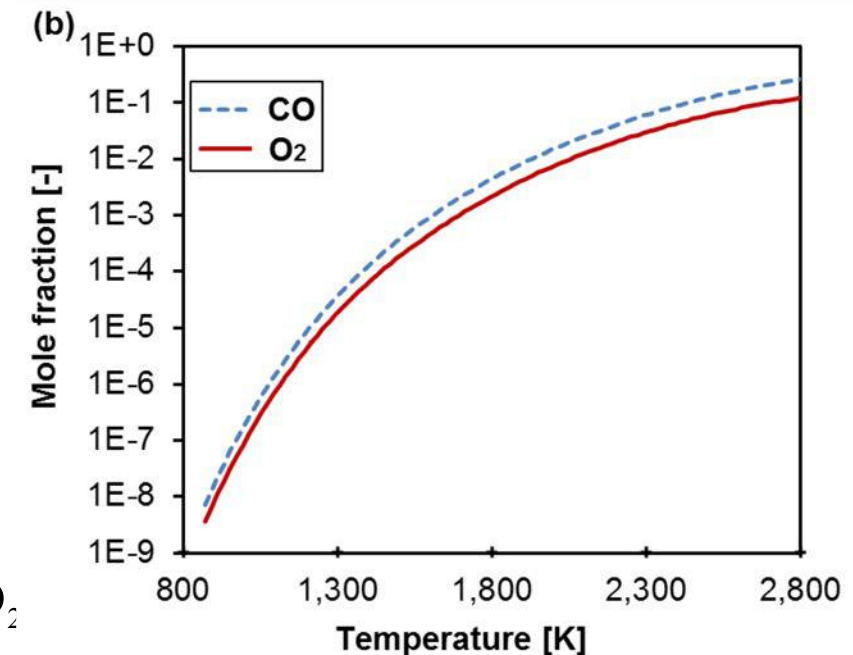
how much thermal energy is needed:

Energy Conservation: $Q = \left[(1-\alpha)\hat{h}_{CO_2}^{2800} + \alpha\hat{h}_{CO}^{2800} + \frac{\alpha}{2}\hat{h}_{O_2}^{2800} \right] - \hat{h}_{CO_2}^{298}$.

and $Q = 192$ MJ/kmolCO₂. If dissociation was neglected, $Q = 140$ MJ/kmolCO₂



Equilibrium limitation for CO₂ reduction



Pressure Dependence of Equilibrium Composition

$$\frac{\prod_{prod} X_i^{v_i''}}{\prod_{react} X_i^{v_i'}} = \frac{K_p(T)}{p^\sigma} \quad \text{where} \quad \sigma = \sum_{prod} v_i'' - \sum_{react} v_i'$$

Complete oxidation of coal: $\text{C} + \text{O}_2 \rightarrow \text{CO}_2$ is pressure independent.

Partial Oxidation: $\text{C} + \frac{1}{2}\text{O}_2 \rightarrow \text{CO}$ favors reactants at high p

$$\frac{X_{\text{CO}}}{X_{\text{O}_2}} = \frac{K_{p, \text{C} + \frac{1}{2}\text{O}_2 \rightarrow \text{CO}}(T)}{\sqrt{p}}$$

So does steam reforming of coal: $\text{C} + \text{H}_2\text{O} \rightarrow \text{CO} + \text{H}_2$

$$\frac{X_{\text{CO}} X_{\text{H}_2}}{X_{\text{H}_2\text{O}}} = \frac{K_{p, \text{C} + \text{H}_2\text{O} \rightarrow \text{CO} + \text{H}_2}(T)}{p}$$

Example 3.9. Formation of NO in hot Air

When heated, air may partially dissociate and yield NO. Assume air is made up of 21% of O₂ and 79% of N₂. Consider the dissociation of air at 1500 and 2000 K at 1 atmosphere. Determine the concentration of NO at these two conditions.

Solution:

The equilibrium reaction for the dissociation of NO from O₂ and N₂ is: $N_2 + O_2 \rightleftharpoons 2 NO$. We can alternatively choose the equilibrium reaction, which corresponds to NO formation: $1/2 N_2 + 1/2 O_2 \rightleftharpoons NO$. We will use the first equilibrium reaction to show how one can relate the equilibrium constant of this reaction to that of the formation reaction. The actual global reactions relating air (the reactants) and its products (air and dissociation of air) may be written, per mole of O₂ in air, as: $O_2 + 3.76 N_2 \rightleftharpoons a O_2 + b N_2 + c NO$. The atom balance yields 2 equations for the elements N and O:

$$O: \quad 2 = 2a + c$$

$$N: \quad 3.76 \times 2 = 2b + c$$

However, we have 3 unknowns, a , b and c , and an additional equation is needed to find all of them. This equation will be based on the equilibrium reaction $N_2 + O_2 \rightleftharpoons 2 NO$ whose rate constant can be related to the partial pressures of the species in the products of the global reaction:

$$K_p(T) = \frac{P_{NO}^2}{P_{N_2} P_{O_2}} = \frac{X_{NO}^2 P^2}{(X_{N_2} P)(X_{O_2} P)} = \frac{X_{NO}^2}{X_{N_2} X_{O_2}}.$$

The mole fractions are expressed as: $X_{\text{O}_2} = \frac{a}{a+b+c}$, $X_{\text{N}_2} = \frac{b}{a+b+c}$, $X_{\text{NO}} = \frac{c}{a+b+c}$, which after substitution of b and c in terms of a from the above elemental balance yields:

$$X_{\text{O}_2} = \frac{a}{4.76}, X_{\text{N}_2} = \frac{2.76+a}{4.76}, X_{\text{NO}} = \frac{2(1-a)}{4.76}.$$

Substituting these mole fractions into the expression for the equilibrium constant above yields:

$$K_p(T) = \frac{4(1-a)^2}{a(2.76+a)}.$$

We can formulate the expression for the unknown a in terms of a quadratic equation:

$$(4 - K_p) a^2 - (8 + 2.76 K_p) a + 4 = 0$$

with the only valid root for a that corresponds to a positive value. The equilibrium constants at 1500 K and 2000 K are: 1.0617×10^{-5} and 3.9945×10^{-4} , respectively. Increasing the equilibrium constant between 1500 and 2000 K indicates a higher amount of dissociation of heated air at the higher temperature.

Solving the above quadratic equation at 1500 K gives $a = 0.997$, $b = 3.769$ and $c = 6.306 \times 10^{-3}$. On the other hand, at 2000 K, we get $a = 0.981$, $b = 3.741$ and $c = 3.831 \times 10^{-3}$. Thus, the concentration of NO at 1500 K and 2000 K is 0.13% and 0.8%, respectively.

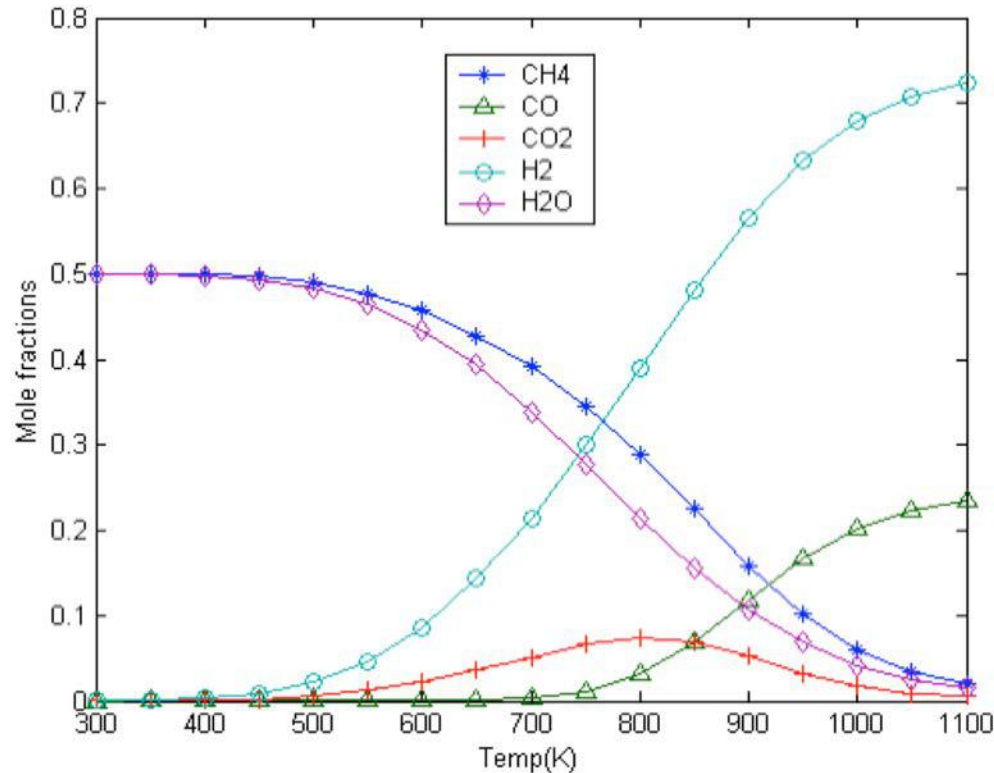
Methane-steam Reforming for Hydrogen production



Start with one mole of methane and one mole of water

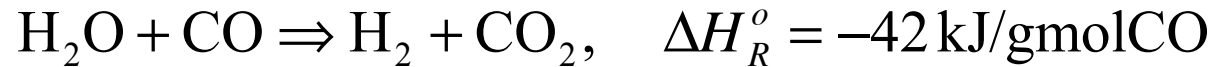
Determine the equilibrium of Mixture: $(\text{CH}_4, \text{CO}, \text{CO}_2, \text{H}_2, \text{H}_2\text{O})$

3 mass conservations, and two equilibrium:

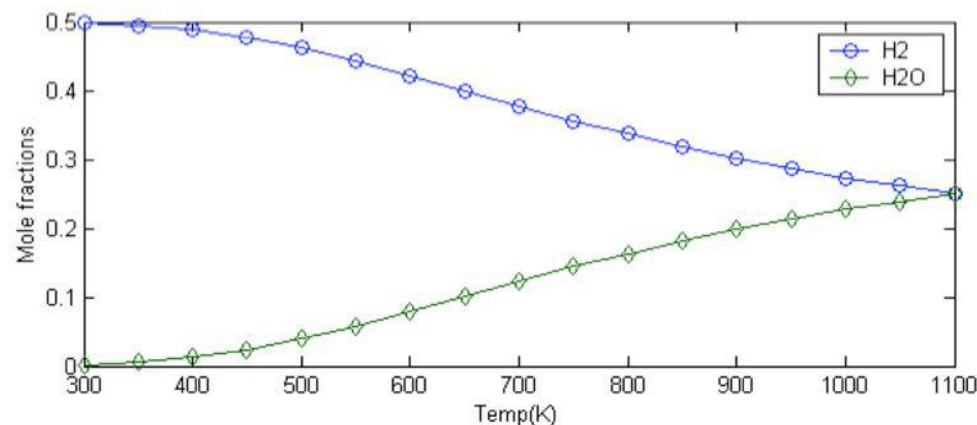
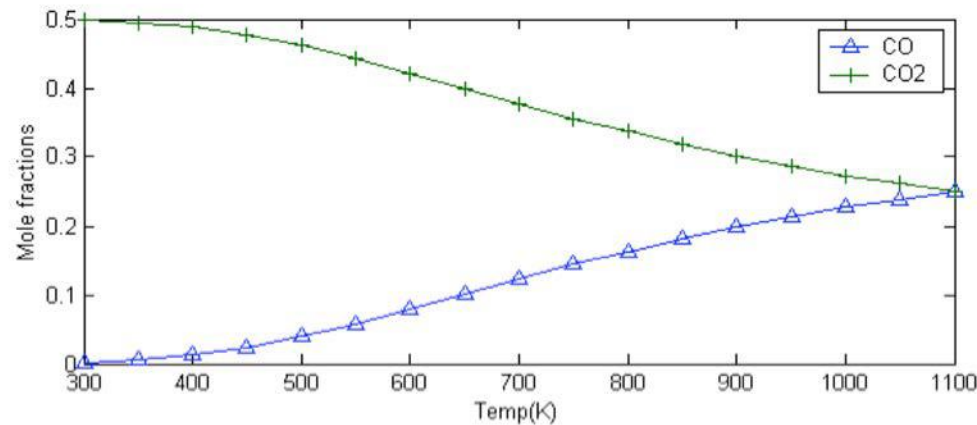


- Run at high T to maximize H_2 yield (equilibrium shift).
- Works better (shift towards H_2) at lower p .
- Needs catalysis (to speed up kinetics) even at these T .
- More endothermic at higher T .
- Fast quench (sudden drop in T) can freeze the mixture composition.

Water-Gas Shift to remove CO and increase H₂ concentration



(start with equal volumes of CO, CO₂, H₂ and H₂O @ 1100 K)

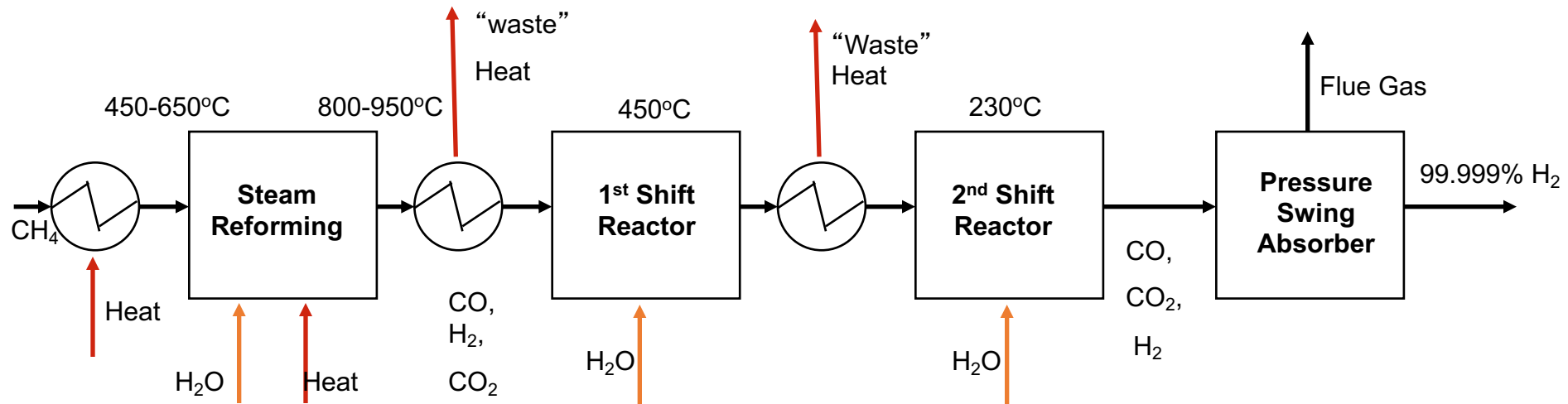


- Weakly endothermic at higher T (water in liquid phase).
- Should run at low T to maximize H₂ yield, two steps are often used (keep kinetics fast at high T).
- Need a catalyst to speed up the reactions (nickel and copper).
- Heat should be recycled to improve efficiency.

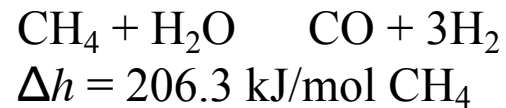
Application: Hydrogen Production by Steam Reforming

Define reactor conditions to achieve maximum conversion

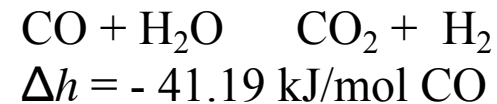
Temperature must be raised to shift equilibrium away from methane, then lowered to shift equilibrium towards hydrogen



Steam Reforming

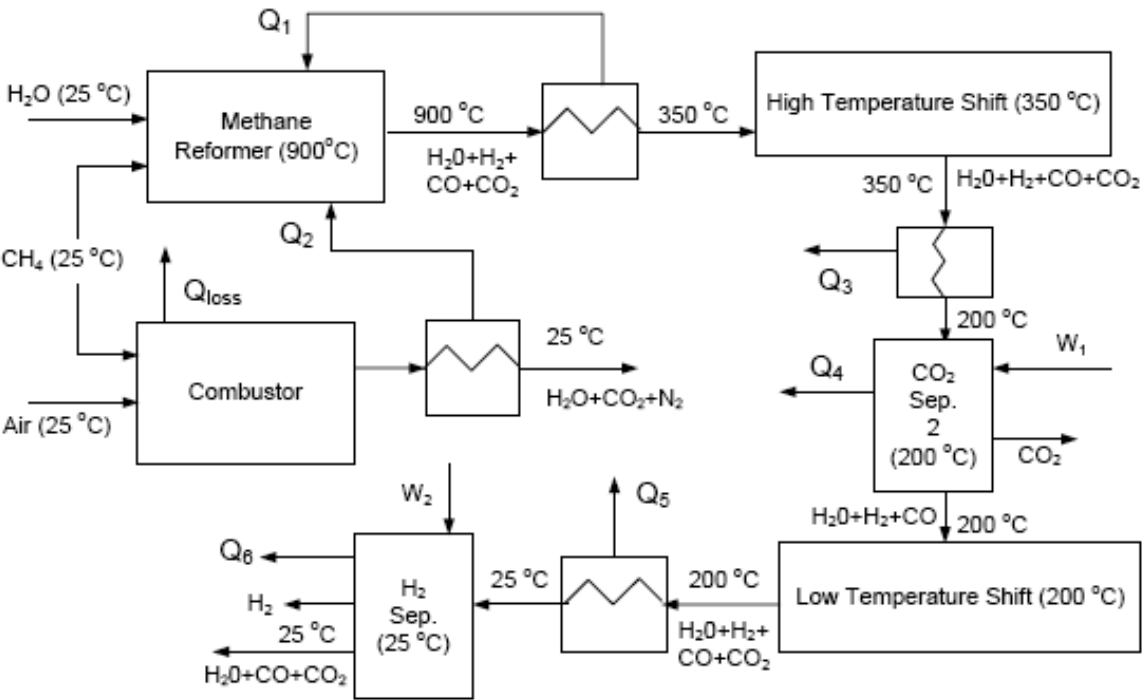


Water Gas Shift Reaction



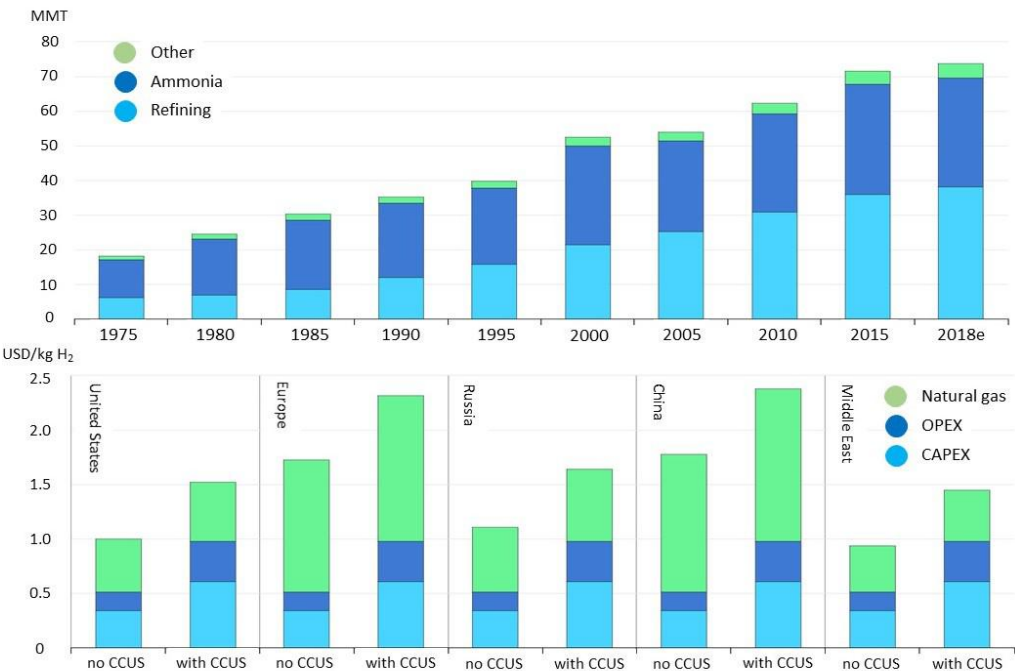
Max Efficiency = 85% if some "waste heat" can be used internally
Efficiency = 60 to 70% for on-site reforming, up to 85% with integration

A Practical Scheme for Methane Reforming



Hydrogen

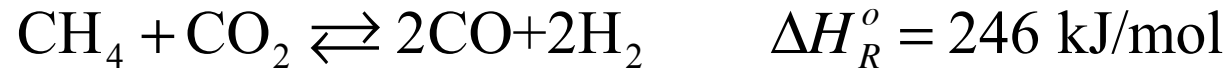
Worldwide production and cost based on SMR



© IEA. All rights reserved. This content is excluded from our Creative Commons license. For more information, see <https://ocw.mit.edu/fairuse>.

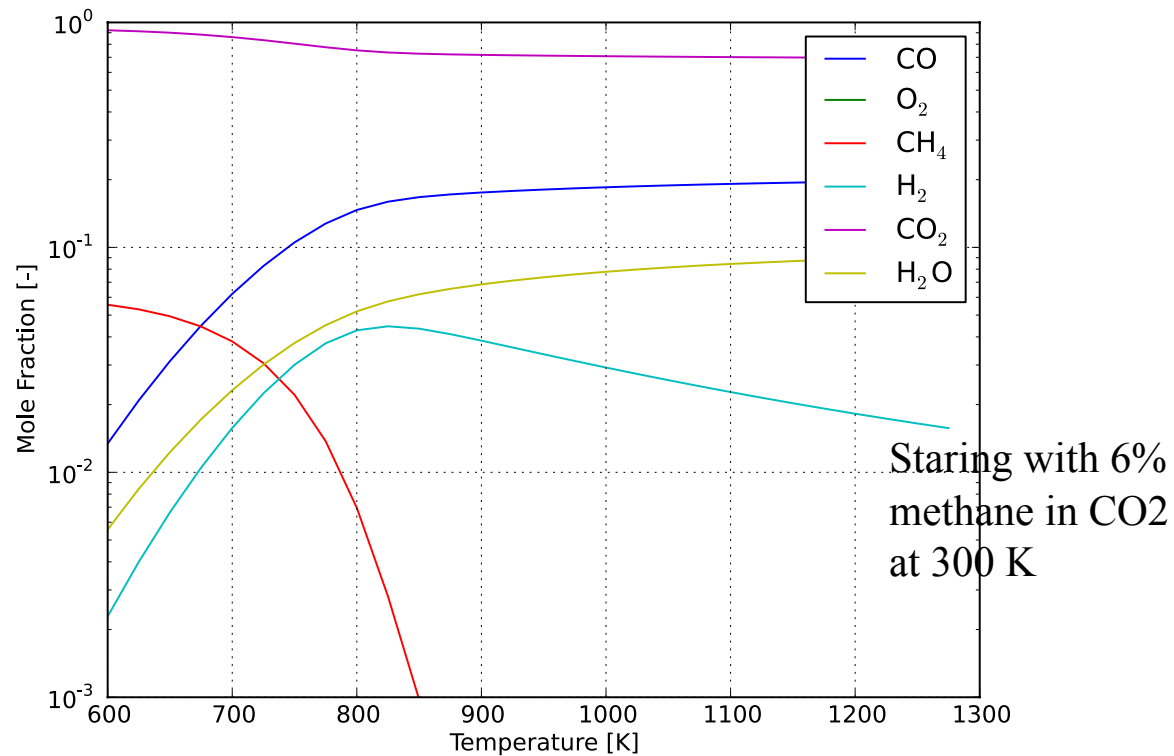
IEA Technology Report, June 2019,
<https://www.iea.org/reports/the-future-of-hydrogen>.

Methane (dry) reforming in CO₂



allowing for the co-existence of CH₄, CO₂, CO, H₂, O₂, and H₂O

Minimize Gibbs free energy .



- Proposed for the generation of Solar Fuels, and /or recycling CO₂.
- The syngas stores the solar energy in chemical bonds.
- If products are continuously removed, the equilibrium can be shifted towards more products.
- Significant fraction of “dead” products: H₂O and CO₂

Or impose equilibrium of the reforming reaction + the water-gas shift (without O₂) + 3 conservation equations.

Direct Irradiation Systems

Elysia Sheu's



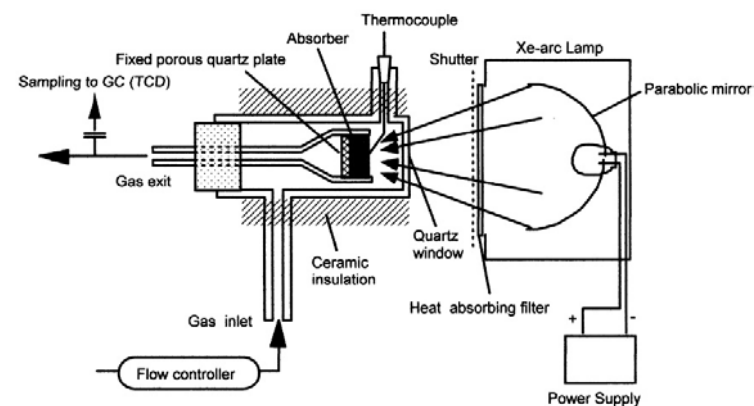
Anikeev et al. *Solar Energy*, 1998



Buck et al. *Solar Energy Materials*, 1991

Courtesy Elsevier, Inc., <http://www.sciencedirect.com>. Used with permission.

- Two main components:
 - Solar receiver
 - Chemical reactor
 - Absorber matrix
- Typically reaction rate limited



Kodama et al. *Energy & Fuels*, 2003

Because of the number of heat transfer processes, system integration is very important for raising the overall reforming efficiency ...

$$\eta_{reform} = \frac{\text{chemical energy out (+ thermal !)}}{\text{chemical (and thermal) energy in + separation energy}}$$
$$= \frac{\left(\dot{n}_f \Delta \hat{h}_f \right)_{out} + \dot{Q}_{out}}{\sum_{in} \left(\dot{n}_f \Delta \hat{h}_f \right) + \dot{Q}_{in} + E_{sep}}$$

A number of high efficiency heat exchangers are needed ...

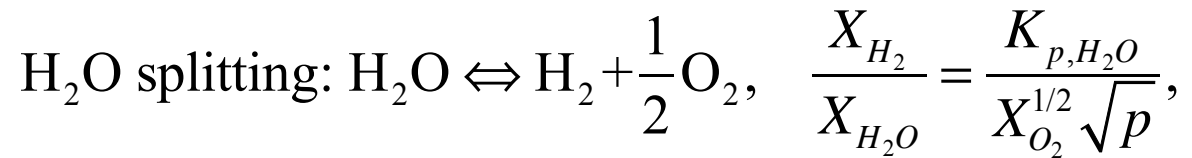
Cost is a concern, perhaps more justifiable for large production facility.

Less so for local operation or mobile applications ..

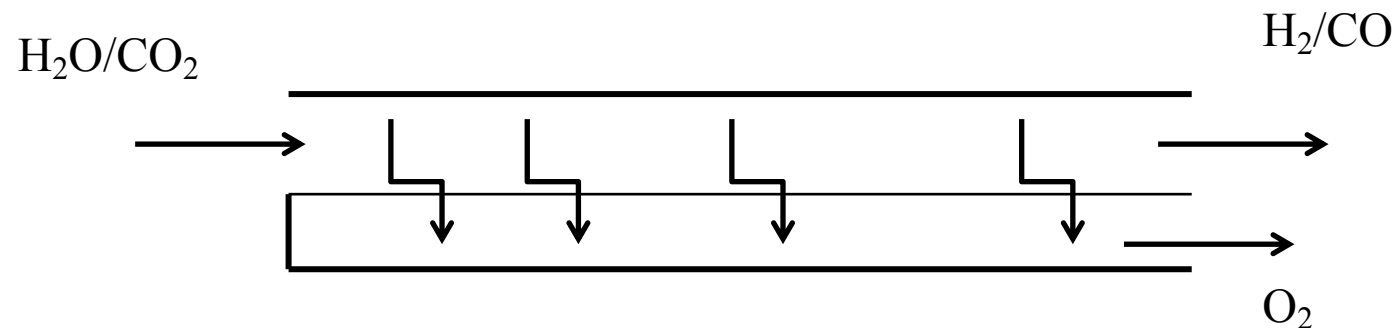
Progress and innovation ARE underway ...

How to beat equilibrium limitations?

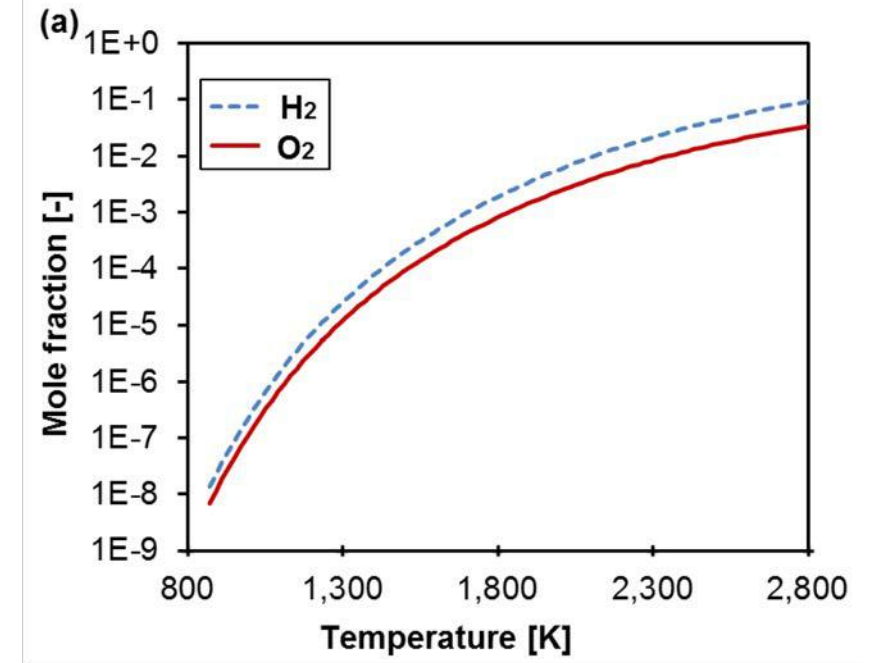
Continuously remove the products (one or both) from the mixture. An ion transport membrane can remove O₂ at T (750-1000 C)



Thus, by removing O₂ (across a membrane) and reducing its mole fraction in the mixture, the equation shows X_{H_2} will increase, removing oxygen encourages more dissociation of water.



Equilibrium limitation for water splitting



$$p_{\text{feed}} \gg p_{\text{sweep}}$$

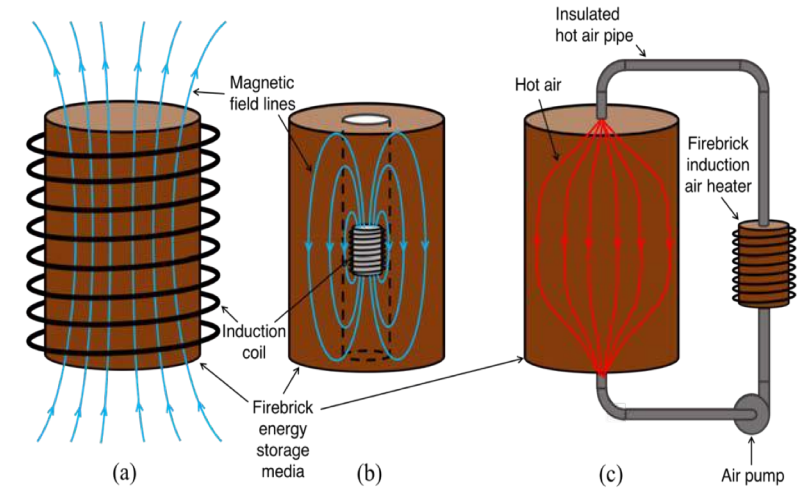
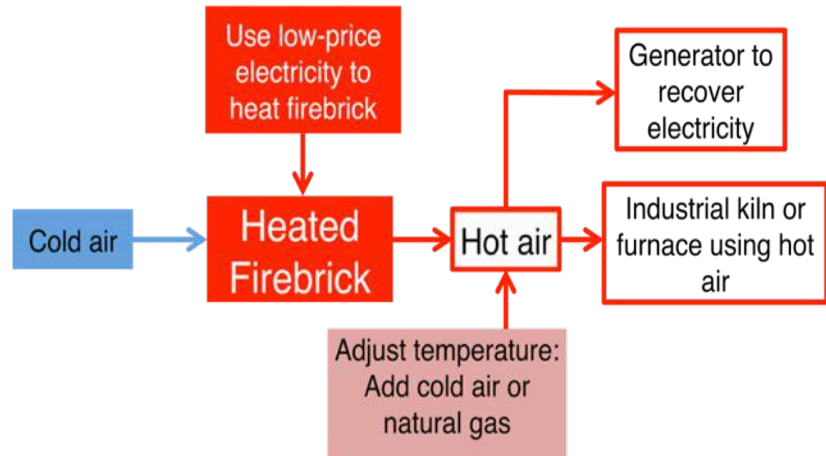
$$J_{\text{O}_2} \approx A e^{E_a/\mathcal{R}T} \left(\sqrt{p_{\text{O}_2,\text{feed}}} - \sqrt{p_{\text{O}_2,\text{sweep}}} \right)$$

Projects ...

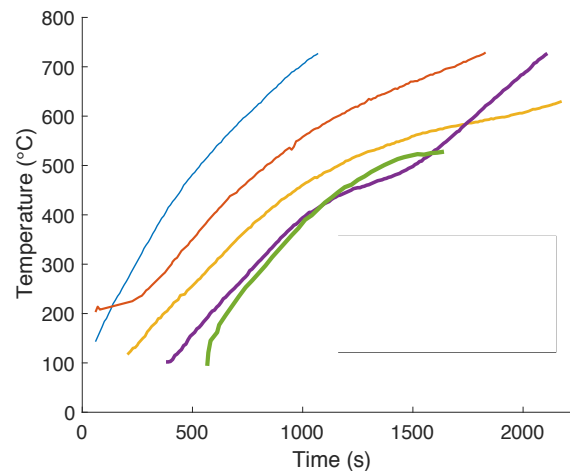
Induction Heating of Firebrick for Electricity-to-High-Temperature Stored Heat for Industry and Power

R. T. Ibekwe, C. W. Forsberg, A. F. Ghoniem

Massachusetts Institute of Technology



Schematic diagram of a firebrick energy storage system

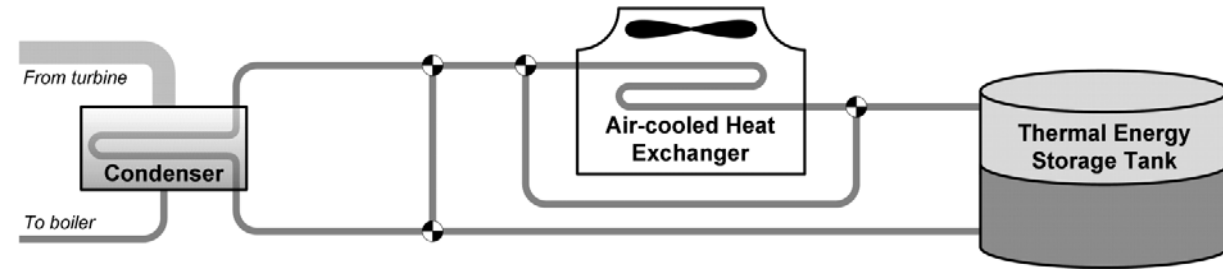


Three proposed design concepts for an induction-heated firebrick energy storage system. Concept (a) is the one investigated in this work.

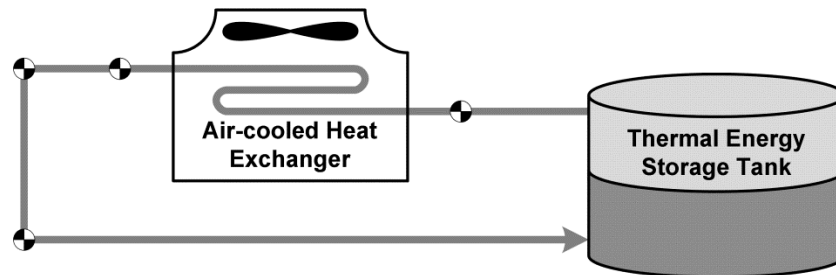
Plots of temperature against time for various firebricks under induction heating.

Cold-Side Thermal Energy Storage for Dry-Cooled Concentrating Solar Power Plants

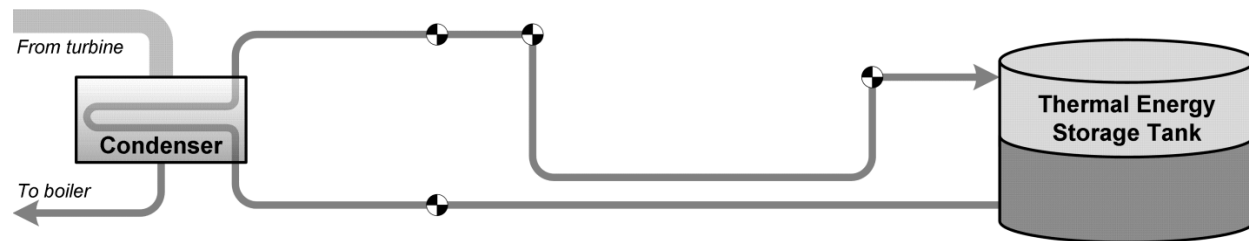
Michael J. Rutberg and Ahmed F. Ghoniem



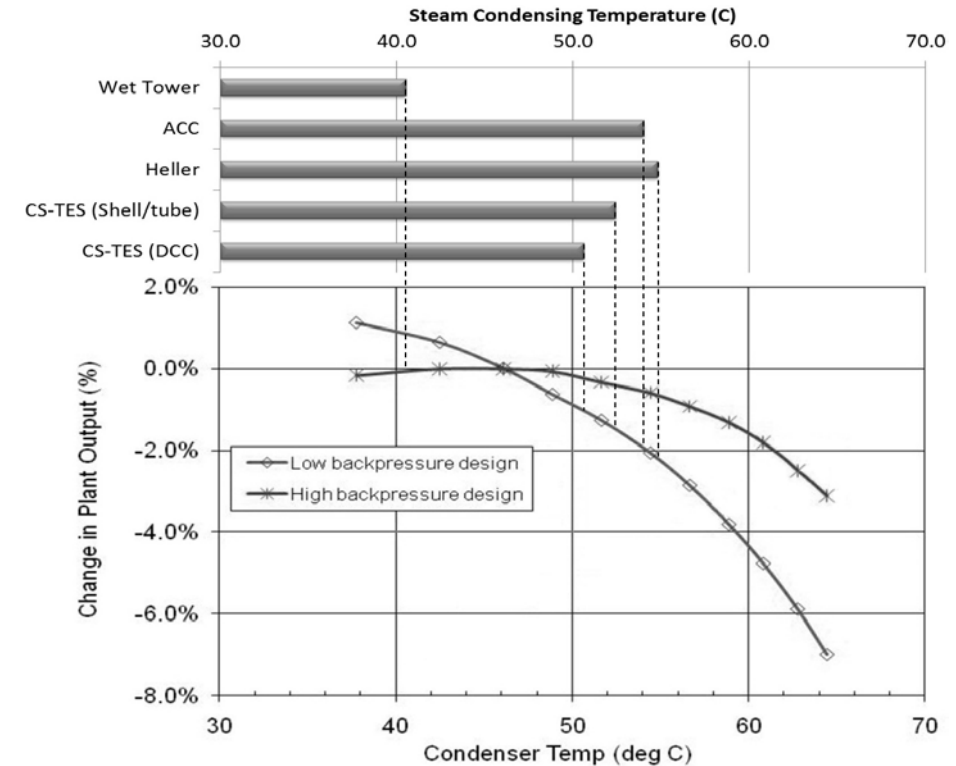
The cold-side thermal energy storage (CS-TES) cooling system architecture



CS-TES operational mode: Overnight cooling



CS-TES operational mode: Daytime operation

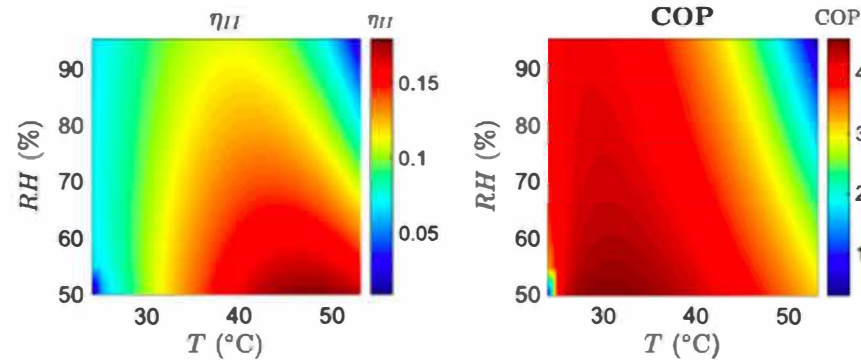
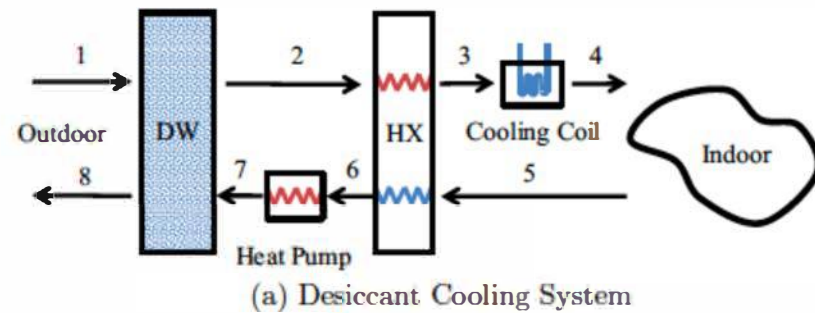


Case study steam condensing temperatures, optimized with NPV of cooling system costs constant at \$41m (except wet tower: \$13m); typical turbine output curves (Turchi et al., 2010) are shown for reference

Next-generation HVAC: Prospects for and limitations of desiccant and membrane-based dehumidification and cooling



Omar Labban^{a,1}, Tianyi Chen^{a,1}, Ahmed F. Ghoniem^{a,2}, John H. Lienhard V^{a,2}, Leslie K. Norford^{b,*,2}



(b) Efficiency of the DCS with cooling coil system

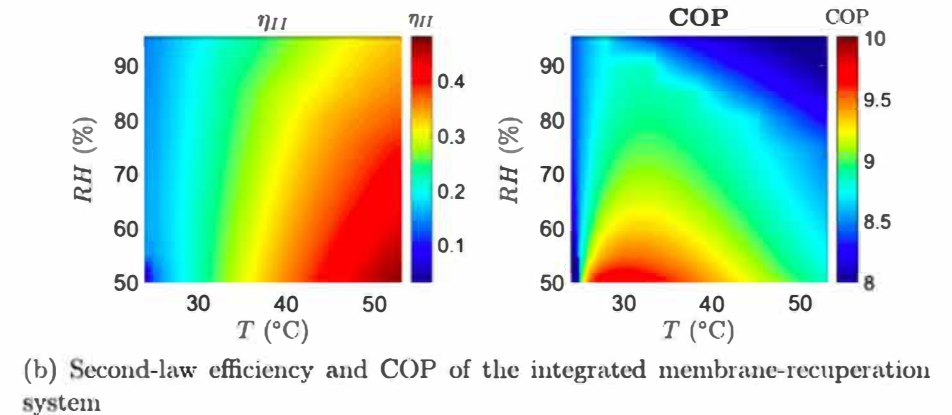
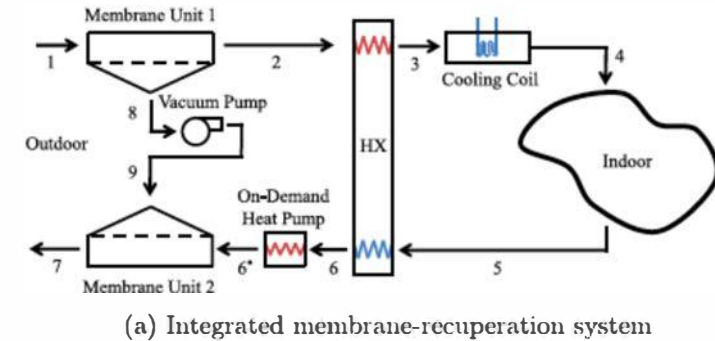


Fig. 11. Performance of the integrated membrane-recuperation system.

MIT OpenCourseWare
<https://ocw.mit.edu/>

2.60J Fundamentals of Advanced Energy Conversion
Spring 2020

For information about citing these materials or our Terms of Use, visit: <https://ocw.mit.edu/terms>.

Lecture # 7

Chemical Thermodynamics 3

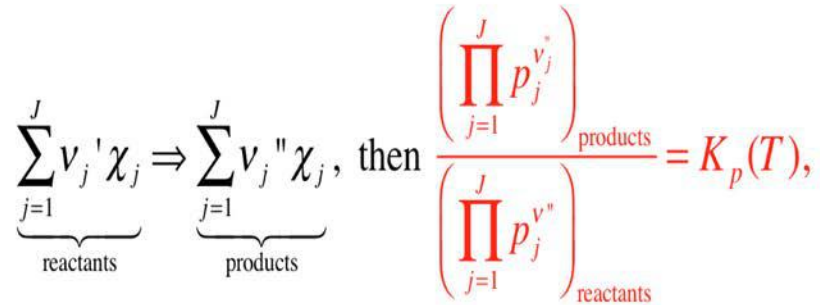
Ahmed F. Ghoniem

February 24, 2020

- Adiabatic Combustion
- Gasification
- Availability Loss in adiabatic combustion
- Combustion Engine Efficiency
- Maximum possible efficiency using chemical energy

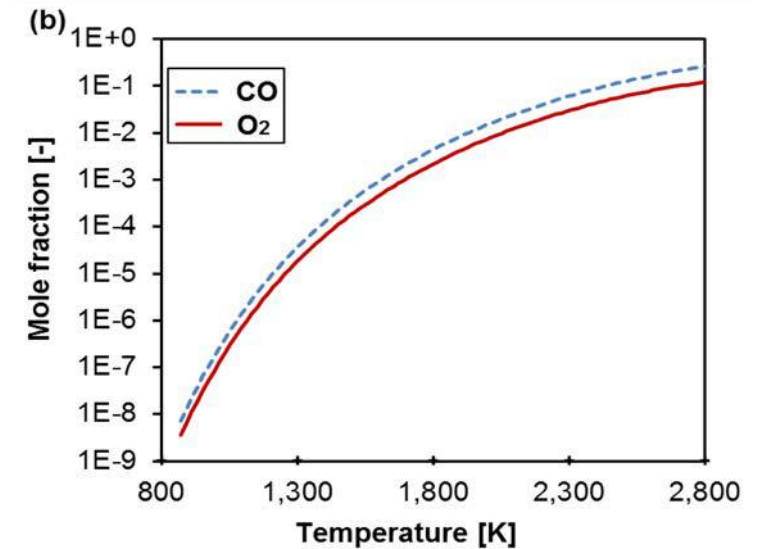
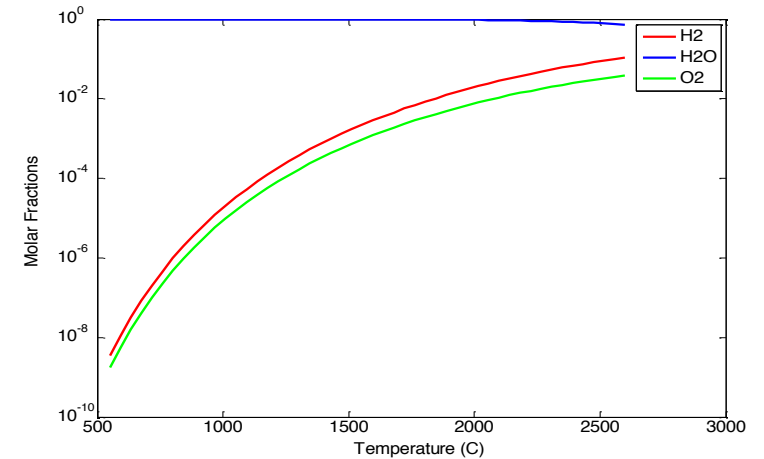
Mixtrure has: $\chi_1, \chi_2, \chi_3, \dots, \chi_n$

Some components can participate in one or more reactions:

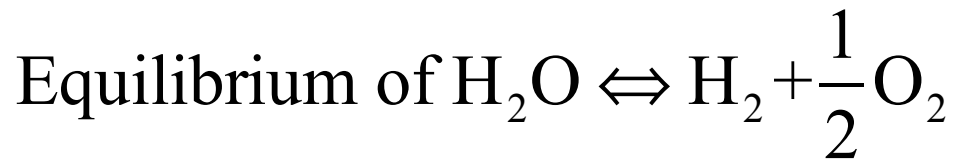
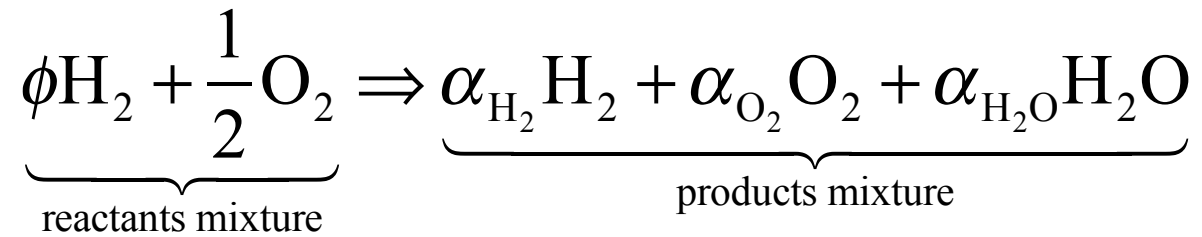


$$\frac{\prod_{\text{prod}} X_j^{\nu_j''}}{\prod_{\text{react}} X_j^{\nu_j'}} = \frac{K_p(T)}{p^\sigma} \quad \text{where} \quad \sigma = \sum_{\text{prod}} \nu_j'' - \sum_{\text{react}} \nu_j'$$

Equilibrium driven dissociation of H_2O (top) and of CO_2 (bottom) at high T

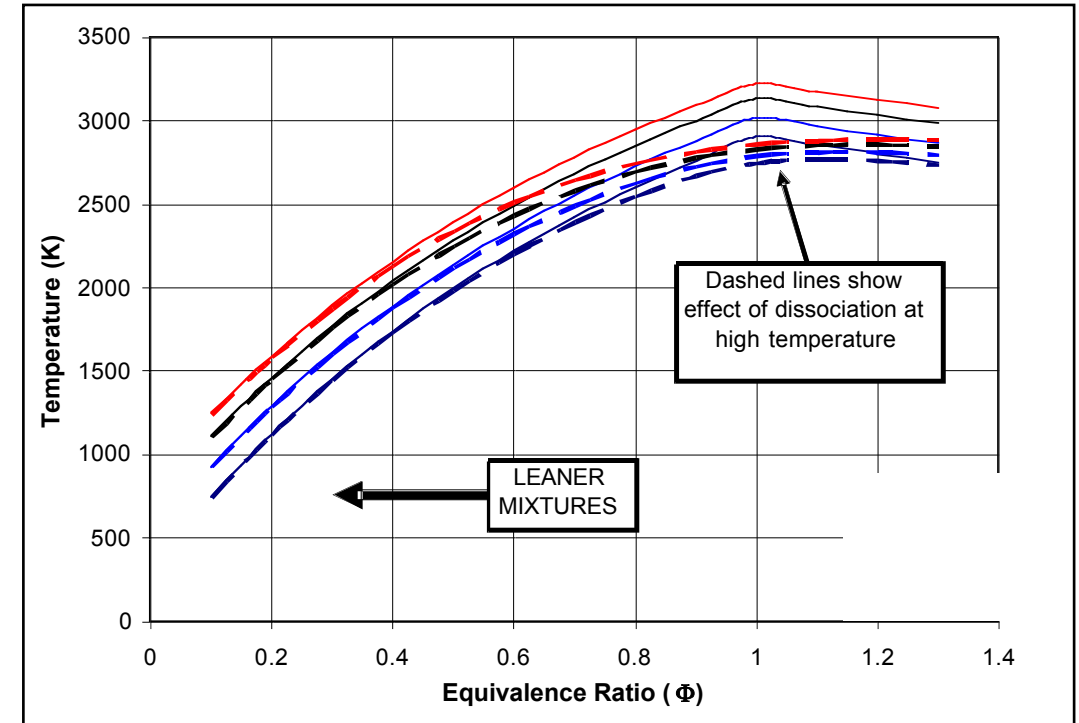


Adiabatic Combustion of Hydrogen-Oxygen, and their Flame temperature

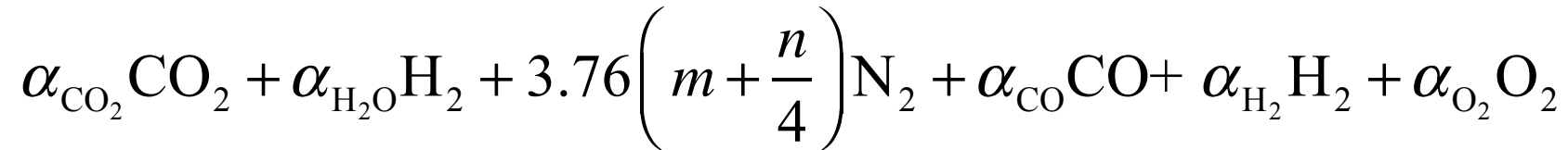
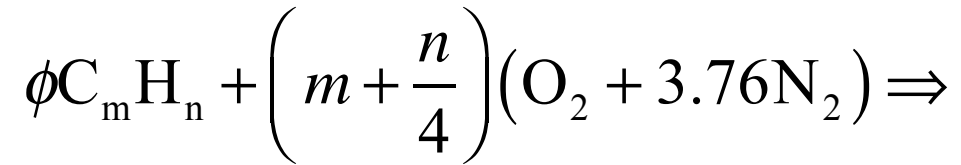


and + the energy equation ...

$$\sum_{\text{react mix}} n_i \hat{h}_i(T_r) = \sum_{\text{prod mix}} n_i \hat{h}_i(T_p)$$



Computing products of combustion of HC combustion using equilibrium constants



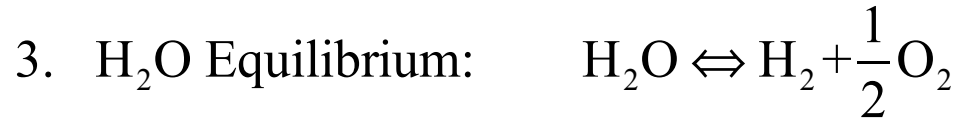
six unknowns (including T):

1. Mass conservation (3 equations) $m = \alpha_{CO_2} + \alpha_{CO}$, and $n = 2(\alpha_{H_2O} + \alpha_{H_2})$

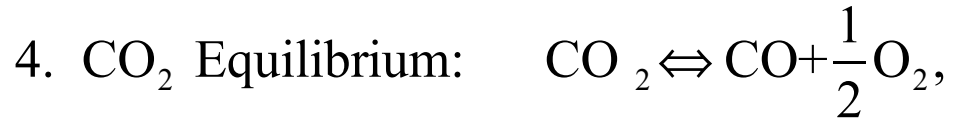
and $\left(m + \frac{n}{4} \right) = \alpha_{CO_2} + \frac{1}{2} \alpha_{CO} + \frac{1}{2} \alpha_{H_2O} + \alpha_{O_2}$ (note that: $X_i = \alpha_i / \sum \alpha_i$)

2. Energy Conservation (constant H): $\sum_{react} \nu_i \hat{h}_i(T_1) = \sum_{prod} \alpha_i \hat{h}_i(T_p)$

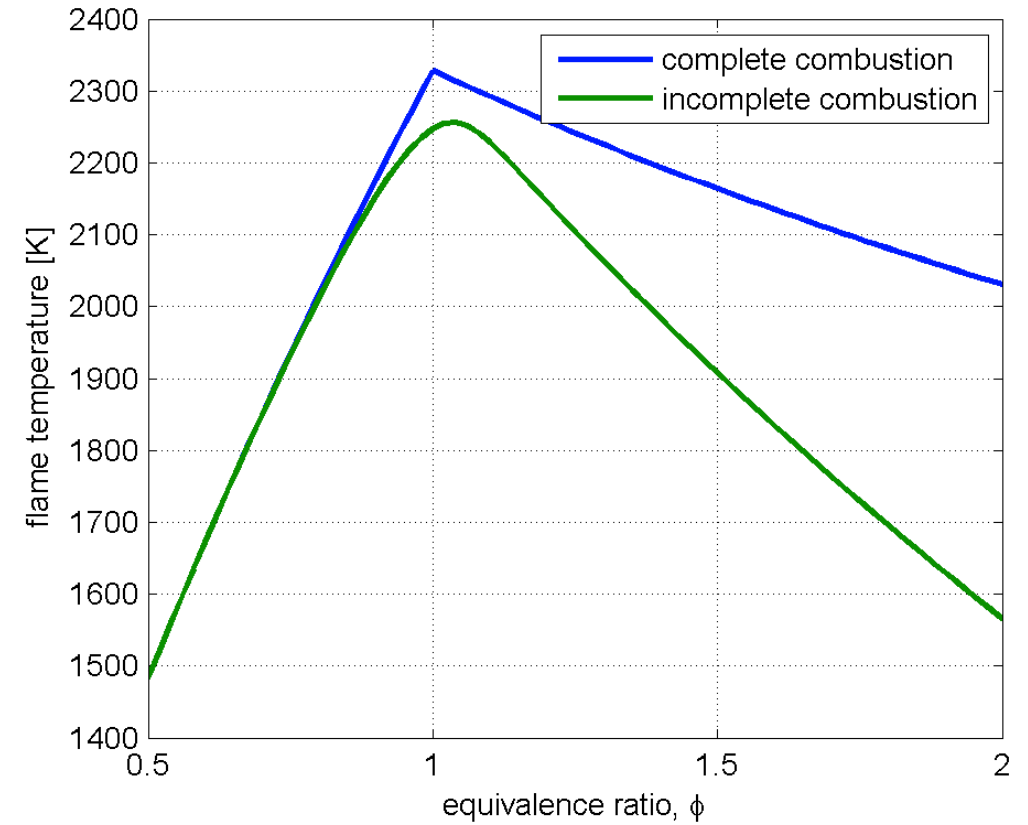
Important Reactions



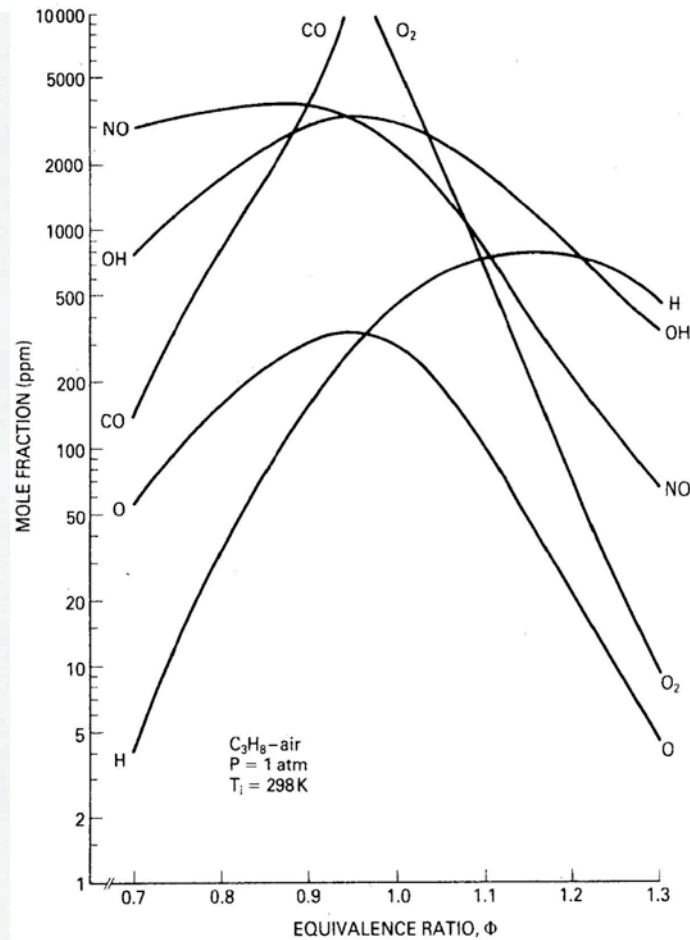
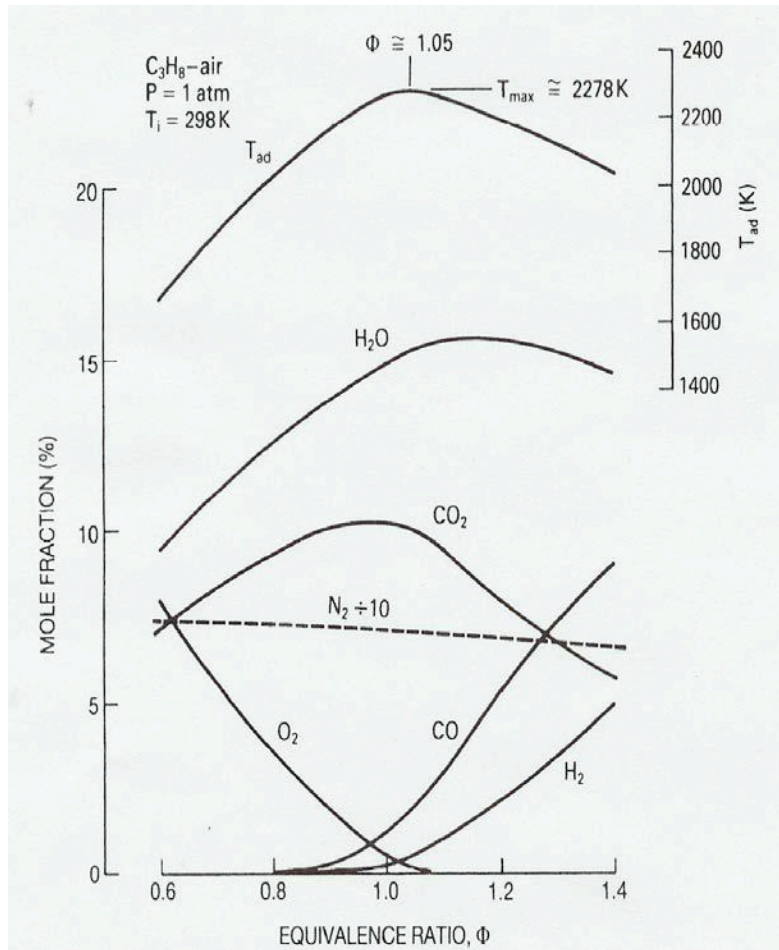
$$\frac{X_{\text{H}_2} X_{\text{O}_2}^{1/2}}{X_{\text{H}_2\text{O}}} = \frac{K_p}{\sqrt{p}}, \quad K_p(T) = \exp\left(-\frac{\Delta G_{R, \text{H}_2\text{O} \rightleftharpoons \text{H}_2 + \frac{1}{2}\text{O}_2}^o(T)}{\Re T}\right)$$



$$\frac{X_{\text{CO}} X_{\text{O}_2}^{1/2}}{X_{\text{CO}_2}} = \frac{K_p}{p^{1/2}}, \quad K_p(T) = \exp\left(-\frac{\Delta G_{R, \text{CO}_2 \rightleftharpoons \text{CO} + \frac{1}{2}\text{O}_2}^o(T)}{\Re T}\right)$$



Methane combustion in air



If oxygen is not present in products,
or is negligible ($\phi \geq 1$)

then one reaction is sufficient:

Homogeneous water-gas equilibrium:



$$\text{and } \frac{X_{\text{H}_2} X_{\text{CO}_2}}{X_{\text{H}_2\text{O}} X_{\text{CO}}} = K_p,$$

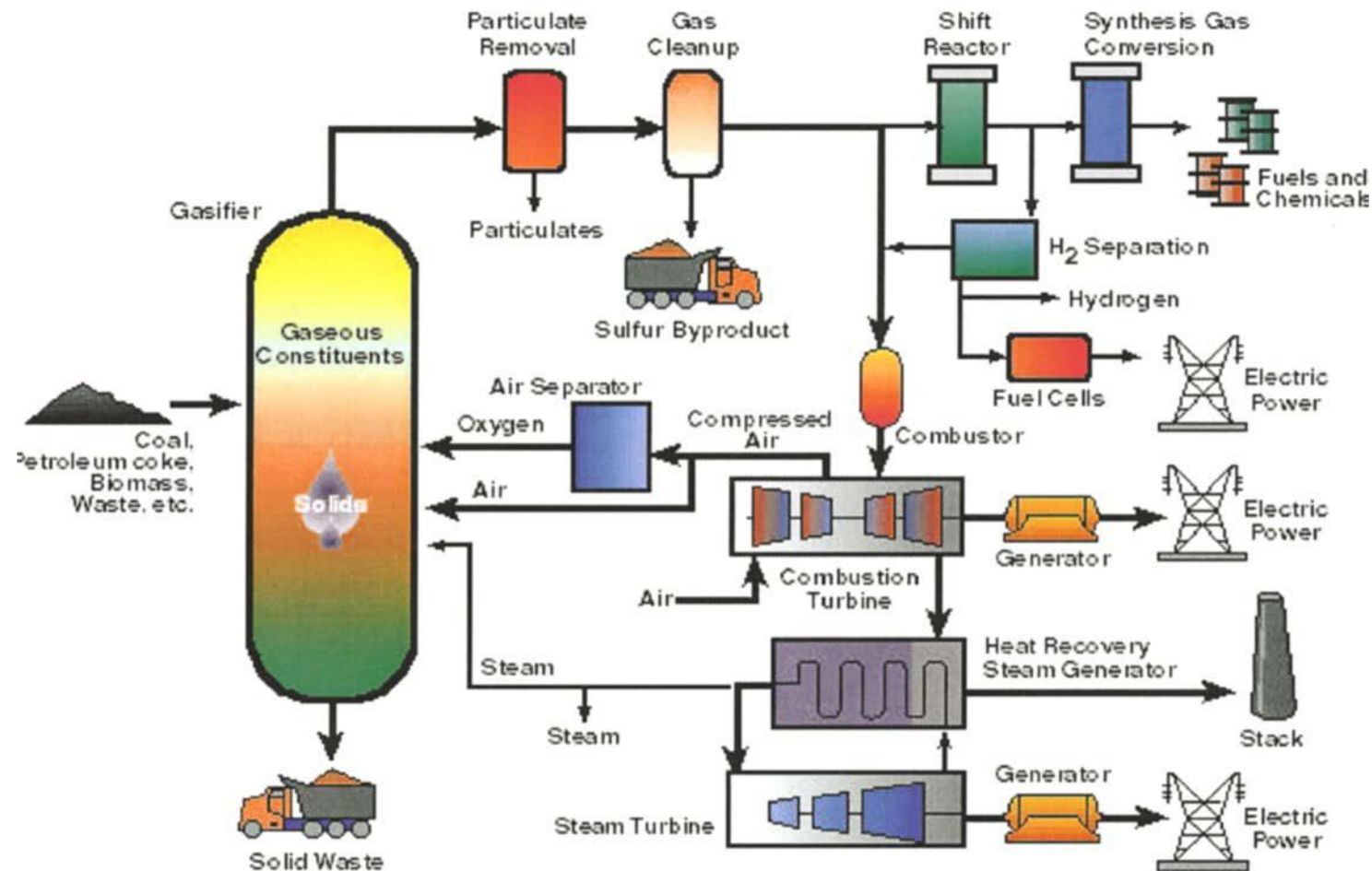
with $K_{p, \text{H}_2\text{O} + \text{CO} \rightleftharpoons \text{H}_2 + \text{CO}}(T) =$

$$\exp \left(- \frac{\Delta G_{R, \text{H}_2\text{O} + \text{CO} \rightleftharpoons \text{H}_2 + \text{CO}}^o(T)}{\mathfrak{R}T} \right)$$

For NO, $\frac{1}{2} \text{O}_2 + \frac{1}{2} \text{N}_2 \rightleftharpoons \text{NO},$

But NO hardly reaches equilibrium

Coal Gasification and IGCC (also “Clean Coal!”) and pre-combustion CO₂ Capture



© Source unknown. All rights reserved. This content is excluded from our Creative Commons license. For more information, see <https://ocw.mit.edu/fairuse>.

Coal Gasification Reactions

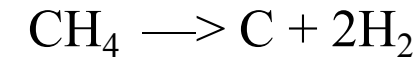
Heating value of coal, 14-35 MJ/kg, or
168-420 MJ/kmol depends on its type

		MJ/kgmol	
Partial oxidation $C + \frac{1}{2} O_2 \rightarrow CO$	← with p ↑	-123.1	Provides gasification heat
combustion $C + O_2 \rightarrow CO_2$		-393.6	Provides more gasification heat
Boudouard reaction $C + CO_2 \rightarrow 2CO$	← with p ↑ → with T ↑	159.9 1	Gasification reaction
Heterogeneous shift reaction $C + H_2O \rightarrow CO + H_2$	← with p ↑ → with T ↑	118.5	Gasification reaction
methane formation $C + 2H_2 \rightarrow CH_4$	→ with p ↑ ← with T ↑	-87.5	
Homogeneous shift reaction $CO + H_2O \rightarrow CO_2 + H_2$	← with T ↑	-40.9	
Methanation reaction $CO + 3H_2 \rightarrow CH_4 + H_2O$	→ with p ↑ ← with T ↑	-205.9	

Gottlicher, The Energetics of Carbon Dioxide Capture in Power Plants, DOE, 2004

Courtesy of DOE.

Methane Pyrolysis (for C and H₂ production)



- One kmol of CH₄ (LHV=800 MJ/kmol) results in 2 kmol H₂ (total LHV=2x240=480 MJ) and 1 kmol of C (HV=394 MJ) and requires ~ 80 MJ/kmol (difference between the products and reactants total enthalpy).
- Total H₂ energy (480 MJ) is 60% of what we had originally.

Because of heat transfer processes and gas separation in synthetic fuel production, system integration is important for raising the overall reforming efficiency ...

$$\eta_{reform} = \frac{\text{chemical energy out (+ thermal !)}}{\text{chemical (and thermal) energy in+separation work}}$$

$$= \frac{(\dot{n}_f \Delta \hat{h}_f)_{out} + \dot{Q}_{out}}{\sum_{in} (\dot{n}_f \Delta \hat{h}_f) + \dot{Q}_{in} + \dot{E}_{sep}}$$

\dot{E}_{sep} should be measured in terms of "heat equivalent"

- High efficiency heat exchangers are needed.
- Cost is high, integration justifiable for large production.
- Less so for local operation or mobile applications.
- Progress and innovation are underway.

Efficiency of Synthetic Fuel Production

Fuel	Product	Efficiency
Coal	syngas	72-87%
Coal	methane	61-78
Coal	Methanol	51-59
Coal	Hydrogen	62
Oil	Hydrogen	77
Methane	Hydrogen	70-79
Coal/Oil/Gas	Hydrogen (E)	20-30
Oil Shale	Oil/Gas	66-72
Methanol	Oil/gas	86
Wood	Gas	90
Corn	Ethanol	46
Manure	Gas	90

Fay and Colomb, Energy and the Environment, 2000.

Courtesy of EPA.

1. Chemical energy can be converted to thermal energy or heat at nearly 100% efficiency (some equilibrium limitations).
2. Chemical Energy can be converted to other forms of chemical energy, typically conversion is limited by equilibrium which is T (and p) dependent, but at $< 100\%$ due to losses in the system. If other chemicals are produced, separation energy further reduces the output.
3. Chemical energy can be converted to work in
 1. Combustion engine, entropy loss in combustion lowers efficiency.
 2. Directly, through electrochemical reaction, nearly isothermally, lowering entropy generation. What is this?

IMPACT OF ENTROPY GENERATION IN REACTIONS

Adiabatic Combustion involves entropy generation and loss of availability, but raises the temperature to values suitable for the operation of heat engines.

For adiabatic reactions:

$$\Delta S_R = \Delta S_g = \sum_{\text{prod mix}} n_i \hat{s}_i(T, p, X_i) - \sum_{\text{react mix}} n_i \hat{s}_i(T, p, X_i)$$

OR $\Delta S_g = S_p(T_F, p_p) - S_r(T^*, p^*)$

adiabatic flame temperature, pressure, entropy generation, and composition of some of the product gases for combustion of isooctane, C_8H_{18} , in a **perfectly insulated constant-volume combustion chamber**, Gyftopoulos and Beretta

	T_b	p_b	$\frac{T_o S_{irr}}{(-n_{1a} \Delta g^o)}$	CO_2	CO	H_2
λ	K	atm	%	$\frac{kmol}{MJ}$	$\frac{mol}{MJ}$	$\frac{mol}{MJ}$
1.0	2912	44.8	20.8	1.17	357	73.8
1.1	2843	43.2	21.5	1.30	230	44.9
1.2	2758	41.5	22.1	1.39	143	27.6
1.3	2667	39.9	22.8	1.44	86.8	17.0
1.4	2577	38.4	23.4	1.48	52.1	10.5
1.5	2489	37.0	23.9	1.50	31.4	6.60
1.6	2408	35.7	24.5	1.51	19.0	4.19
1.7	2332	34.5	25.0	1.52	11.7	2.70
1.8	2262	33.4	25.4	1.52	7.28	1.78
1.9	2198	32.4	25.9	1.53	4.61	1.19
2.0	2138	31.4	26.3	1.53	2.96	0.78

mixture of isooctane and dry air is at $T_a = 700$ K and $p_a = 10$ atm.

Work interaction in a Process undergoing Chemical Reaction

steady state, flow process

$$Q - W = H_{out} - H_{in}$$

$$0 = \frac{Q}{T^*} + S_{in} - S_{out} + \Delta S_g$$

$$W_{chem.eng.} = (H_1 - T^* S_1) - (H_2 - T^* S_2) - T^* \Delta S_g$$

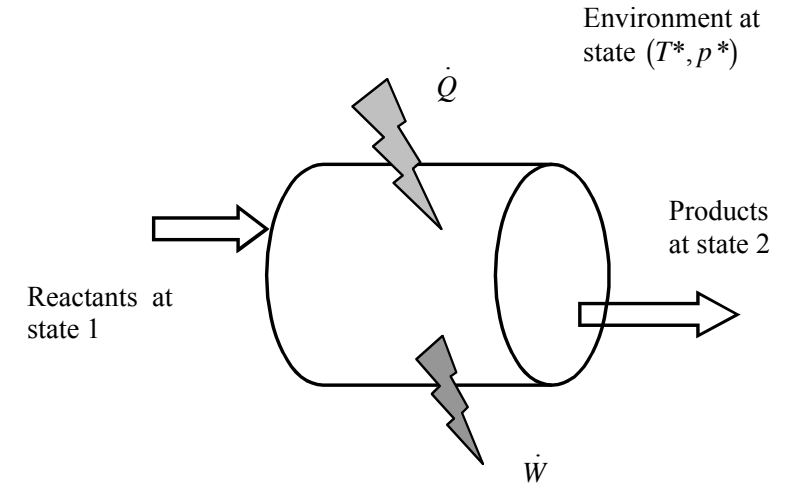
(availability-Irreversibility)

reactants at state 1 and products at state 2:

$$W = \sum_{react} n_i \left(\hat{h}_i(T_1) - T^* \hat{s}_i(T_1, p_{i,1}) \right) - \sum_{prod} n_i \left(\hat{h}_i(T_2) - T^* \hat{s}_i(T_2, p_{i,2}) \right) - T^* \Delta S_g$$

Maximum Work, $\Delta S_g \rightarrow 0$

$$W_{max.chem.eng} = \sum_{react,1} v_i' (\hat{h}_i - T^* \hat{s}_i) - \sum_{prod,2} v_i'' (\hat{h}_i^* - T^* \hat{s}_i^*)$$



"Largest" Maximum work:

exit stream at mechanical, thermal
and chemical equilibrium with environment,
If inlet and exit streams are both at
mechanical and thermal equilibrium

with the environment $(T_o, p_o) = (T^o, p^o)$:

$$\begin{aligned} w_{\max} &= \sum_{\text{react}} \nu_i' \left(\hat{h}_i(T_o) - T_o \hat{s}_i(T_o, p_{o,i}) \right) \\ &\quad - \sum_{\text{prod}} \nu_i'' \left(\hat{h}_i(T_o) - T_o \hat{s}_i(T_o, p_{o,i}) \right) \\ &= -\Delta G_R^o(T_o, p_{o,i}) = -\Delta G_R^{\text{avail}}(T_o, p_{o,i}) \end{aligned}$$

Since $p_o = 1 \text{ atm}$,

$$\begin{aligned} (-\Delta G_R^{\text{avail}}) &= (-\Delta G_R^{oo}(T_o)) + \Re T_o \ln \left(\prod_{\text{react}} X_i^{\nu_i'} / \prod_{\text{prod}} X_i^{\nu_i''} \right) \\ &\approx \Delta G_R^{oo} \end{aligned}$$

Calculations show that $\Delta G_R^{oo} \approx \Delta H_{R,LHV}^o$

Fuel (phase) ^b	$-\Delta H_R^o$ (for LHV) kJ/mol	$-\Delta H_R^o$ (for HHV) kJ/mol	$-\Delta G_R^{oo}(T^o, p^o)$ (kJ/mol)	$\hat{\xi}_{fuel}^o$ (kJ/mol)
Hydrogen (g), H ₂	241.8	285.9	228.6	235.2
Carbon (s), C	393.5	393.5	394.4	410.5
<i>Paraffin (alkane) Family, C_n H_{2n+2}</i>				
Methane (g), CH ₄	802.3	890.4	818	830.2
Ethane (g), C ₂ H ₆	1427.9	1559.9	1467.5	1493.9
Propane (g), C ₃ H ₈	2044	2220	2108.4	2149
Butane (g), C ₄ H ₁₀	2658.5	2878.5	2747.8	2802.5
Pentane (g), C ₅ H ₁₂	3272.1	3536.1	3386.9	3455.8
Pentane (l), C ₅ H ₁₂	3245.5	3509.5	3385.8	3454.8
Hexane (g), C ₆ H ₁₄	3886.7	4194.8	4026.8	4110
Hexane (l), C ₆ H ₁₄	3855.1	4163.1	4022.8	4106
Heptane (g), C ₇ H ₁₆	4501.4	4853.5	4667	4764.3
Heptane (l), C ₇ H ₁₆	4464.9	4816.9	4660	4757.3
Octane (g), C ₈ H ₁₈	5116.2	5512.2	5307.1	5418.6
Octane (l), C ₈ H ₁₈	5074.6	5470.7	5297.2	5408.7

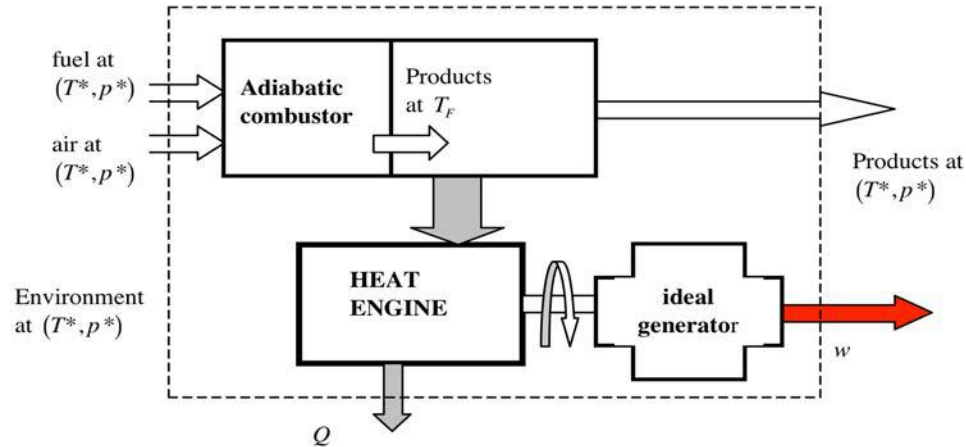
$$\hat{\xi}_{fuel}^o = (-\Delta G_R^{oo}) + \Re T_o \ln \left(\prod_{\text{react} \neq \text{fuel}} (X_i^o)^{\nu_i'} / \prod_{\text{prod}} (X_i^o)^{\nu_i''} \right) \approx (-\Delta G_{R,fuel}^{oo})$$

X_i^o are evaluated for standard concentrations (except for the fuel)

Bejan, Advanced Eng. Thermo., Wiley 1988 and Moran, Availability Analysis, Prentice Hall 1982

© Prentice Hall, Inc. All rights reserved. This content is excluded from our Creative Commons license. For more information, see <https://ocw.mit.edu/fairuse>.

Combustion Engine Work and Efficiency



Another model uses:

$$\eta_{car} = 1 - \ln \frac{T_F}{T^*} / \left(\frac{T_F}{T^*} - 1 \right)$$

$$= 70\% \text{ for } T_F / T^* = 8$$

$$W_{\max} = \eta_{car} |\Delta H_R|$$

A Possible Model:

$$\begin{aligned} W_{\max, \text{comb. eng.}} &= W_{\max, \text{chem. eng.}} - T^* \Delta S_{\text{ad. comb}} \\ &= (H_1 - T^* S_1) - (H_2 - T^* S_2) - T^* \Delta S_g \\ &= (H_1 - T^* S_1) - (H_2 - T^* S_2) - T^* (S_F - S_1) \\ &= (H_F - T^* S_F) - (H_2 - T^* S_2) (= W_{car}(T_F, T^*)) \end{aligned}$$

$$(\eta_{\text{best. comb}})_{\text{sec Law}} = \frac{W_{\max, \text{comb. eng.}}}{\Delta G_R^o} = \frac{W_{\max, \text{chem. eng.}}^*}{\Delta G_R^o} - \left| \frac{T_o \Delta S_{\text{ad. comb}}}{\Delta G_R^o} \right|$$

$$(\eta_{\text{best. comb}})_{\text{sec Law}} \approx \frac{W_{\max, \text{chem. eng.}}^*}{\Delta G_R} - \underbrace{\left| \frac{T_o \Delta S_{\text{ad. comb}}}{\Delta G_R^o} \right|}_{\text{See Tables}}$$

- The choice of T_F is tricky, its max is the adiabatic stoichiometric flame T , but the actual value depends on the equipment
- Another model uses the log mean temperature Carnot efficiency (T_F and T^*) and enthalpy of reaction for max W .
- Again the choice of T_F is tricky!

MIT OpenCourseWare
<https://ocw.mit.edu/>

2.60J Fundamentals of Advanced Energy Conversion
Spring 2020

For information about citing these materials or our Terms of Use, visit: <https://ocw.mit.edu/terms>.

Lecture # 8

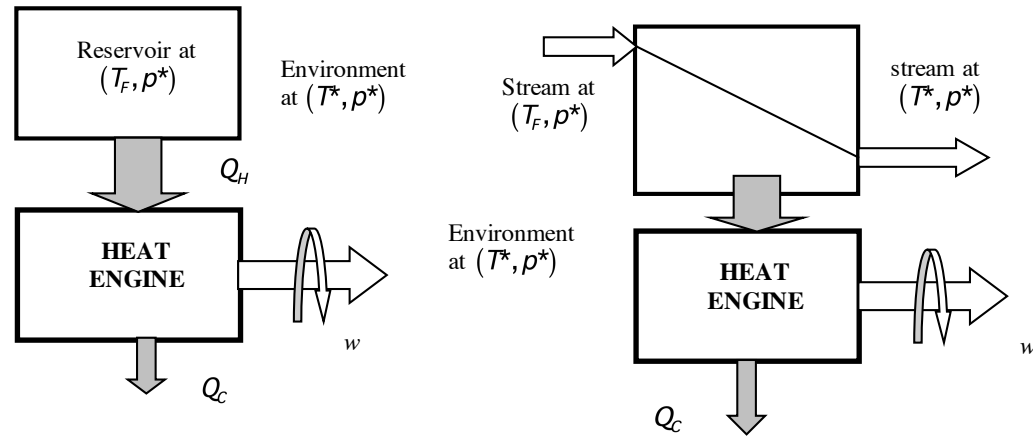
Electrochemical Thermodynamics 1

Ahmed F. Ghoniem

February 26, 2020

- Electrochemical reactions
- Electrodes and electrolytes
- Fuel cell components
- Work generated by a fuel cell
- Voltage and Ideal Efficiency

Heat engine (heat to work) efficiency



$$\eta_{car} = 1 - \frac{T_L}{T_H}$$

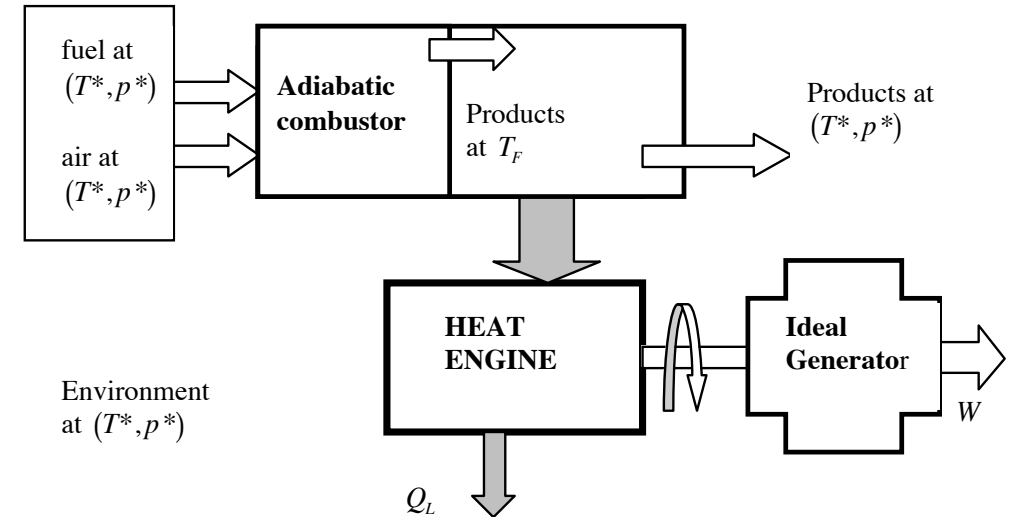
$$= 87.5\% \text{ for } T_H / T_L = 8$$

$$\eta_{car} = 1 - \ln \frac{T_F}{T^*} / \left(\frac{T_F}{T^*} - 1 \right)$$

$$= 70\% \text{ for } T_F / T^* = 8$$

Ideal thermo-mechanical efficiency using practically achievable/manageable temperatures is 70-85%!

Engines running on adiabatic combustion



$$w_{\max . \text{adiab. comb. eng.}} = w_{\max . \text{chem. eng.}} - T^* \Delta S_{\text{ad. comb}}$$

$$\left(\eta_{\text{best adiabatic. comb}} \right) \approx \frac{w_{\max . \text{comb. eng.}}}{\Delta G_R}$$

$$\approx \frac{w_{\max . \text{chem. eng.}}}{\Delta G_R} - \left| \frac{T^* \Delta S_{\text{ad. comb}}}{\Delta G_R} \right|$$

$$= 75\%$$

Keeping the reaction isothermal and in equilibrium with the environment produces maximum work

$$Q - W = H_{out} - H_{in} = \Delta H_R$$

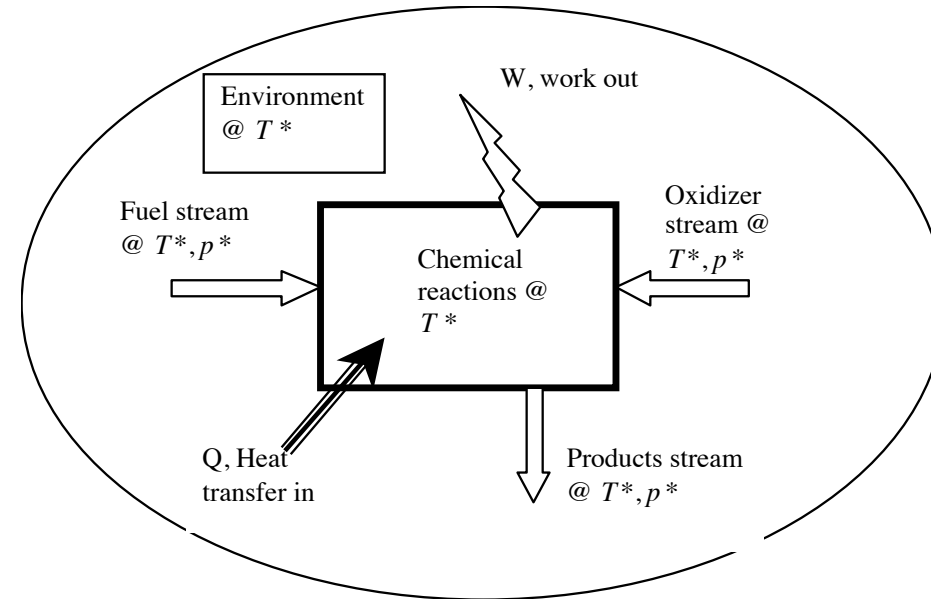
$$\frac{Q}{T^*} = S_{out} - S_{in} = \Delta S_R$$

$$Q = T\Delta S_R \quad \text{heat added}$$

$$\begin{aligned} -W &= (H - TS)_{out} - (H - TS)_{in} \\ &= \Delta H_R - T\Delta S_R \end{aligned}$$

$$W = -\Delta G_R \quad \text{work produced.}$$

The isothermal reaction produces work = Gibbs free energy of reaction, and rejects heat = $T \cdot$ entropy of reaction



$$T\Delta S_R = \Delta H_R - \Delta G_R = Q$$

for typical exothermic reactions,

both ΔH_R and $\Delta G_R < 0$

and heat is mostly rejected

(but can also be added) depending on T

How can we perform such an isothermal reaction with work transfer?

The overall Reaction: $\text{H}_2 + \frac{1}{2}\text{O}_2 \Rightarrow \text{H}_2\text{O}$

can be performed in a Redox Pair (reduction-oxidation), or two electrochemical "half reactions", across an electronically non-conducting material, leading to the formation of charged species;

Hydrogen Oxidation: $\text{H}_2 \Rightarrow 2\text{H}^+ + 2\text{e}^-$ Hydrogen loses e^-

Hydrogen Reduction: $\frac{1}{2}\text{O}_2 + 2\text{e}^- + 2\text{H}^+ \Rightarrow \text{H}_2\text{O}$ Reactants gain e^-

H^+ ions diffuse through the electrolyte (acidic, +ve ion (proton) transport medium (PEMFC))

e^- moves through an external resistance

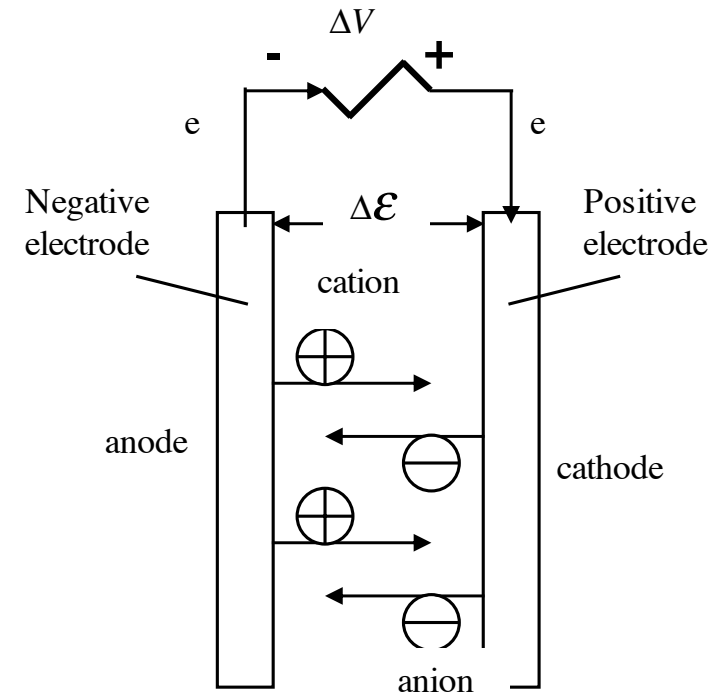
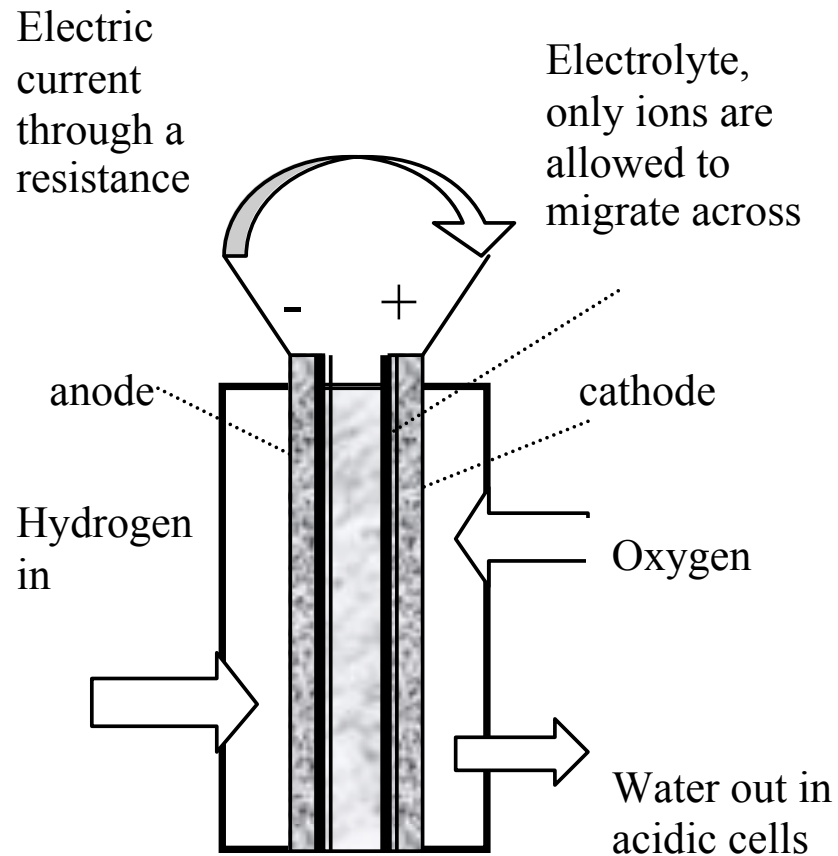
A useful note: the general definition of oxidation and reductions:

Oxidation is Loss of electron (loss of -ve charge or becoming positive)

Reduction is Gain of electron (gain of -ve charge or becoming negative)

Hydrogen Oxidation: $\text{H}_2 \Rightarrow 2\text{H}^+ + 2\text{e}^-$ Hydrogen loses e^-

Hydrogen Reduction: $\frac{1}{2}\text{O}_2 + 2\text{e}^- + 2\text{H}^+ \Rightarrow \text{H}_2\text{O}$ Reactants gain e^-

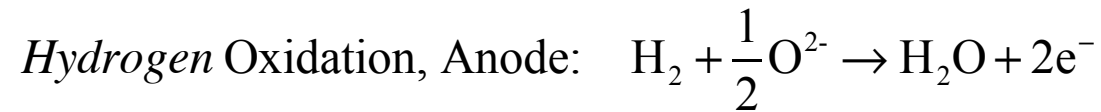
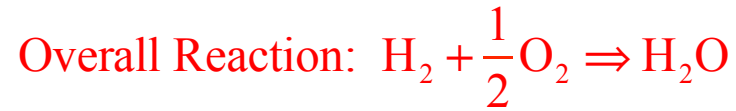


Galvanic or voltaic cell.

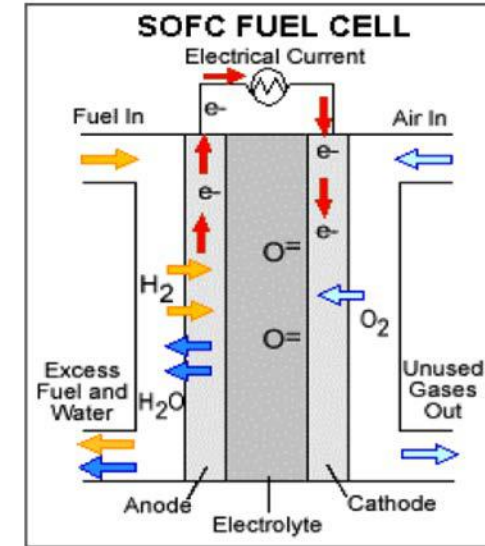
At finite current, $\Delta V < \Delta \mathcal{E}$.

In galvanic cells the anode is the -ve electrode and the cathode is the +ve electrode.

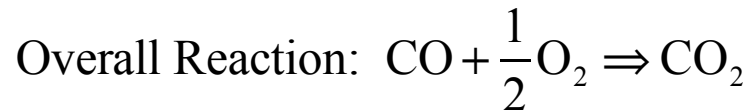
Another redox pair uses an alkaline electrolyte (transports -ve ions):



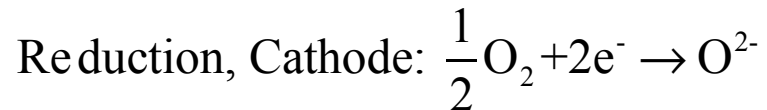
O^{2-} ions move through the electrolyte from the cathode to the anode



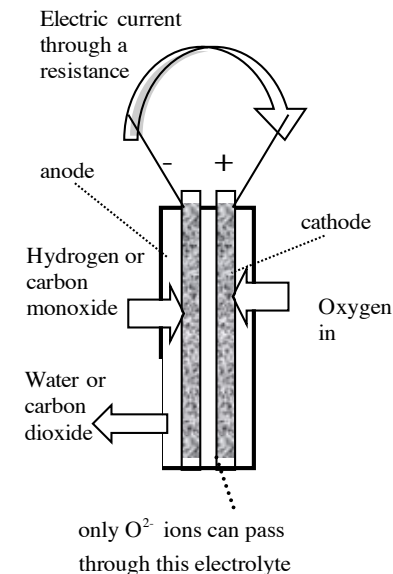
CO Electrochemical Oxidation



The Redox Pair (two half reaction)



Can combine H_2 and CO in a single cell



Open circuit Work:

$$\begin{aligned} (-\Delta G_R(T^*, p^*)) &= \sum_{react} \nu_i' \left(\hat{h}_i(T^*) - T^* \hat{s}_i(T^*, p^*) \right) - \sum_{prod} \nu_i'' \left(\hat{h}_i(T^*) - T^* \hat{s}_i(T^*, p^*) \right) \\ &= \left(-\Delta G_R^o(T^*) \right) - \sigma \Re T^* \ln \left(\frac{p^*}{p^o} \right) - \Re T^* \ln \left(\frac{\prod_{prod} X_i^{\nu_i''}}{\prod_{react} X_i^{\nu_i'}} \right) \end{aligned}$$

$$\Delta G_R^o(T^*) = \sum_{react} \nu_i' \left(\hat{h}_i(T^*) - T^* \hat{s}_i^o(T^*) \right) - \sum_{prod} \nu_i'' \left(\hat{h}_i(T^*) - T^* \hat{s}_i^o(T^*) \right)$$

Important remarks:

1. Reactants are introduced separately.
2. Products mix with one of the reactant stream
3. Or products leave separately through the electrolyte.

Fuel (phase)	LHV (kJ/mol)	$-\Delta G_R^o(T^o, p^o)$ (kJ/mol)
Hydrogen (g), H ₂	241.8	228.6
Carbon (s), C	393.5	394.4
Methane (g), CH ₄	802.3	818
Ethane (g), C ₂ H ₆	1427.9	1467.5
Propane (g), C ₃ H ₈	2044	2108.4
Butane (g), C ₄ H ₁₀	2658.5	2747.8

Equilibrium or Open-circuit Efficiency:

$$\eta_{OC} = \frac{W_{\max}}{\Delta H_{R, H_2O}^*} = \frac{\Delta G_{R, H_2O}^*}{\Delta H_{R, H_2O}^*}$$

For separate streams for hydrogen, oxygen and water: All at 1 atm

$$\Delta G_R^o(T) = \left(\hat{h}^o(T) - T\hat{s}^o(T) \right)_{\text{H}_2\text{O}} - \left[\left(\hat{h}^o(T) - T\hat{s}^o(T) \right)_{\text{H}_2} + \frac{1}{2} \left(\hat{h}^o(T) - T\hat{s}^o(T) \right)_{\text{O}_2} \right]$$

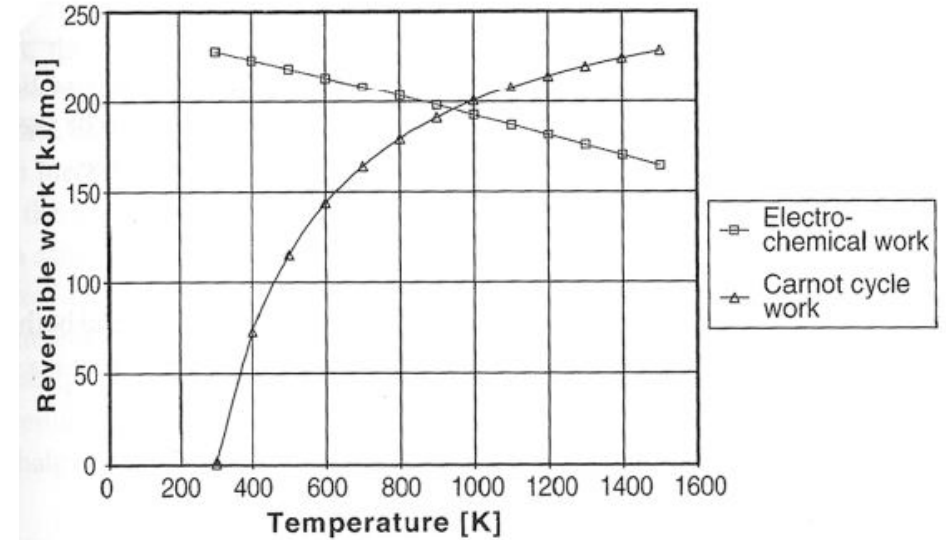
$$\hat{s}^o(T) = \hat{s}(T, p = 1 \text{ atm})$$

$$\eta_{OC} = \frac{\Delta G_{R, \text{H}_2\text{O}}^*}{\text{HHV}_{\text{H}_2\text{O}}}$$

@ T = 300 K: water leaving as liquid: $\eta_{OC} = 237/286 = 83\%$
 (water leaving as vapor: $\eta_{OC} = 228/242 = 94\%$)

@ T = 500 K: water leaving as vapor: $\eta_{OC} = 219 / 242 = 76.5\%$

@ T = 1000 K: water leaving as vapor: $\eta_{OC} = 193 / 245 = 67.3\%$



© Source unknown. All rights reserved. This content is excluded from our Creative Commons license. For more information, see <https://ocw.mit.edu/fairuse>.

- Reversible work produced by H₂/O₂ cell and a simple Carnot engine.
- Based on the HHV (284 kJ/mol H₂). Cross over point is 950 K.
- Comparison is not necessarily meaningful.

Open Circuit Cell Potential:

$$\hat{w}_{\max} = \Delta \hat{g}_R = \Delta \mathcal{E} \, \varsigma \text{ (work of moving charge } \varsigma \text{ across a potential difference } \Delta \mathcal{E})$$

$$\varsigma = n_e \varsigma_{e^-} N_a = n_e \mathfrak{F}_a$$

n_e : number of electrons produced when oxidizing one fuel molecule

$$N_a = 6.023 \times 10^{23} \text{ mole}^{-1} \text{ (Avogadro's number)}$$

$$\varsigma_{e^-} = -1.602 \times 10^{-19} \text{ Coulombs/electron}$$

$$\mathfrak{F}_a = \varsigma_{e^-} N_a = 9.6485 \times 10^4 \text{ Coulombs/mole (Faraday's number)}$$

for the hydrogen-oxygen, $n_e = 2$, and $\varsigma = 2\varsigma_{e^-} N_a = 2\mathfrak{F}_a$,

@ 300K, $\Delta \mathcal{E} = 1.18$ volts with water leaving in vapor form

$\Delta \mathcal{E} = 1.23$ volts with water leaving in liquid form.

For the methanol-oxygen reaction, $\Delta \mathcal{E}_o = 1.21 \text{ V}$.

The Nernst Equation: effect of pressure and fuel concentration

$$\Delta\mathcal{E}(p^*, T^*) = \Delta\mathcal{E}^O(T^*) - \frac{\Re T^*}{n_e \mathcal{S}} \ln \left(\frac{\prod_{prod} (p_i^*)^{v_i''}}{\prod_{react} (p_i^*)^{v_i'}} \right) = \Delta\mathcal{E}^O(T^*) - \frac{\sigma \Re T^*}{n_e \mathcal{S}_a} \ln \left(\frac{p^*}{p_o} \right) - \frac{\Re T^*}{n_e \mathcal{S}_a} \ln \left(\frac{\prod_{prod} X_i^{v_i''}}{\prod_{react} X_i^{v_i'}} \right)$$

$$= \Delta\mathcal{E}^O(T^*) + \Delta\mathcal{E}_p(p^*, T^*) + \Delta\mathcal{E}_{conc}(X_i, T^*) \quad \text{where } \sigma = \sum_{prod} v_i'' - \sum_{react} v_i'$$

for a hydrogen-oxygen cell: $\Delta\mathcal{E}_{conc} = \frac{\Re T^*}{2 \mathcal{S}_a} \left(\ln(X_{H_2})_{fuel} + \frac{1}{2} \ln(X_{O_2})_{oxy} - \ln(X_{H_2O})_{sep/fuel/oxy} \right)$

Equation applied at one point (under equilibrium, things are subtle).

Lower reactants concentrations decrease the OC potential, especially at higher T.

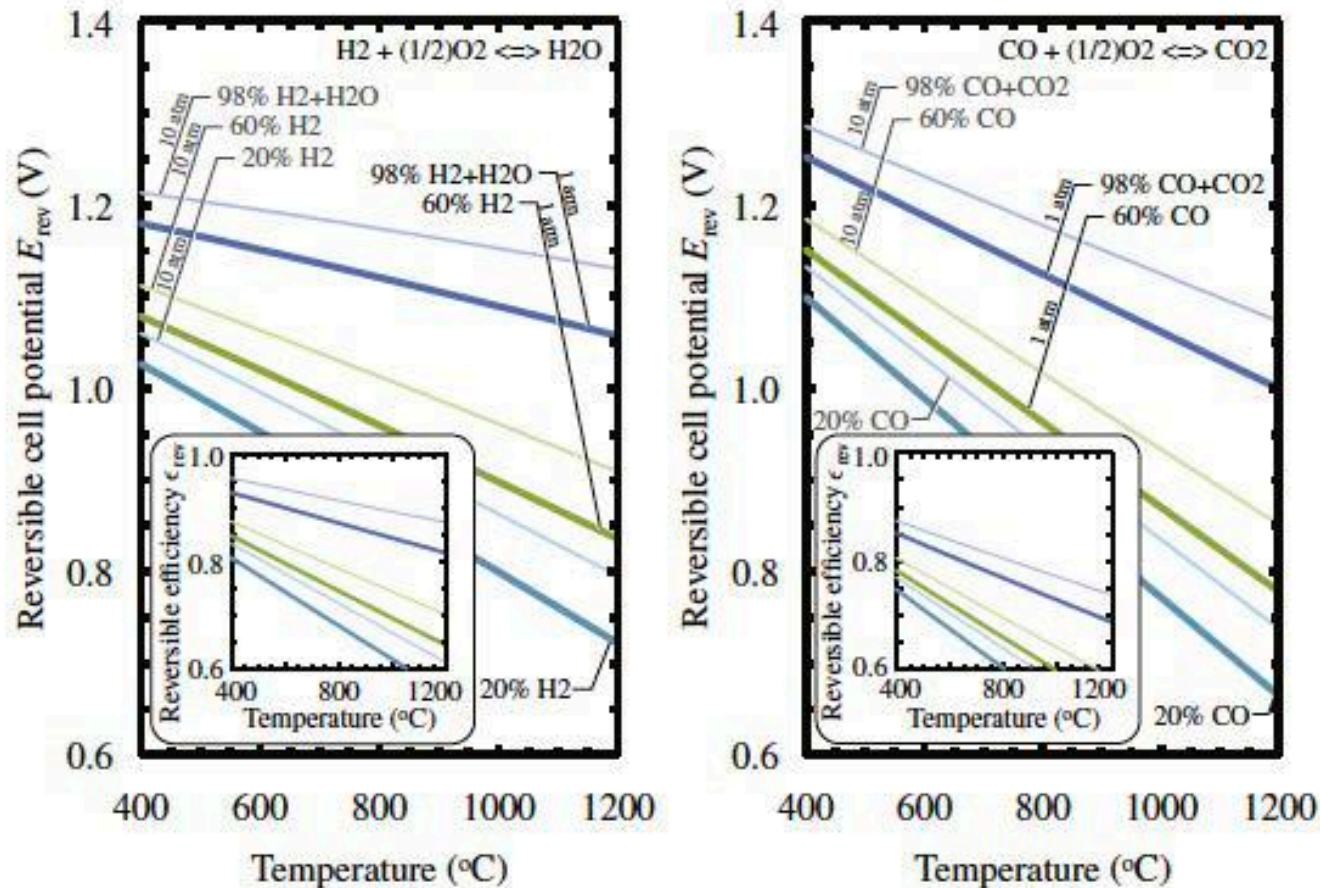
Using air instead of oxygen also penalizes the potential, $\Delta\mathcal{E}_{conc, O_2} = 2.15 \times 10^{-5} T^* \ln(0.21) = -0.012 @ 350K$

Using products of methane reforming as fuel: $CH_4 + 2H_2O \rightarrow CO_2 + 4H_2$

$$X_{H_2} = 0.8, \quad \Delta\mathcal{E}_{conc} = 2.15 \times 10^{-5} T^* \ln(0.8)$$

this reduces the OC by $\Delta\mathcal{E}_{conc, H_2} = 0.00168V (@350K)$

Impact of fuel, concentration, temperature and pressure



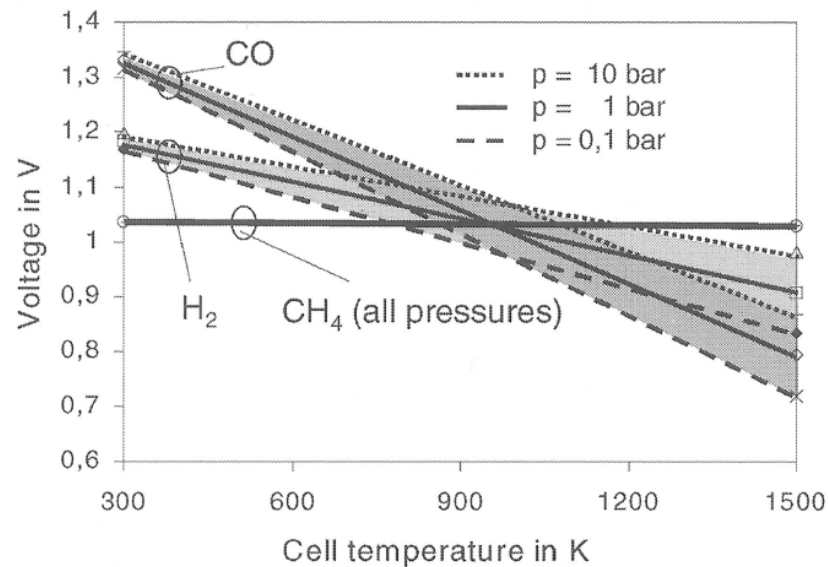
$P=1$, thick lines
 $P=10$ thin line

Colors for different
fuel concentrations

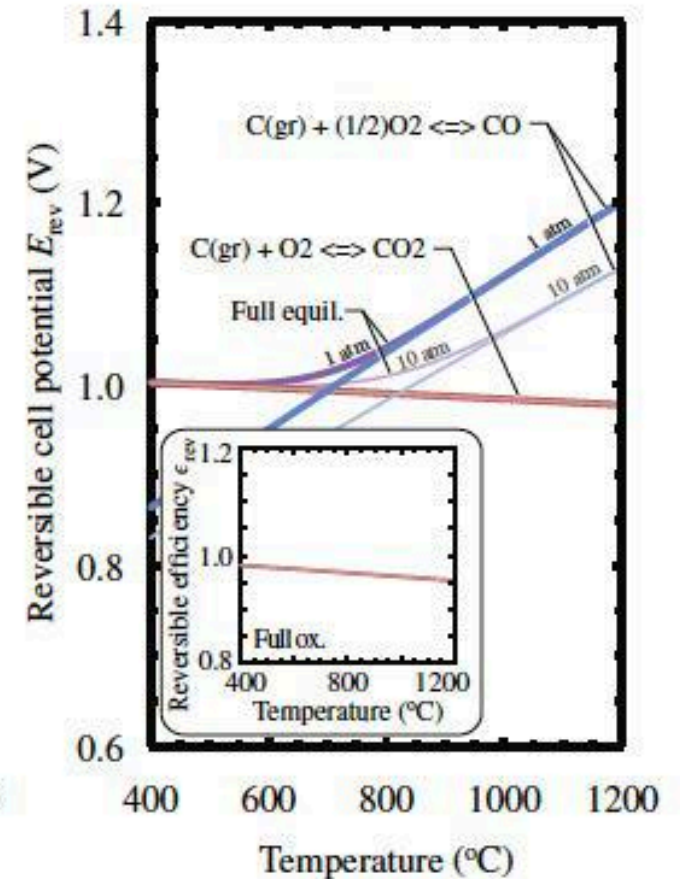
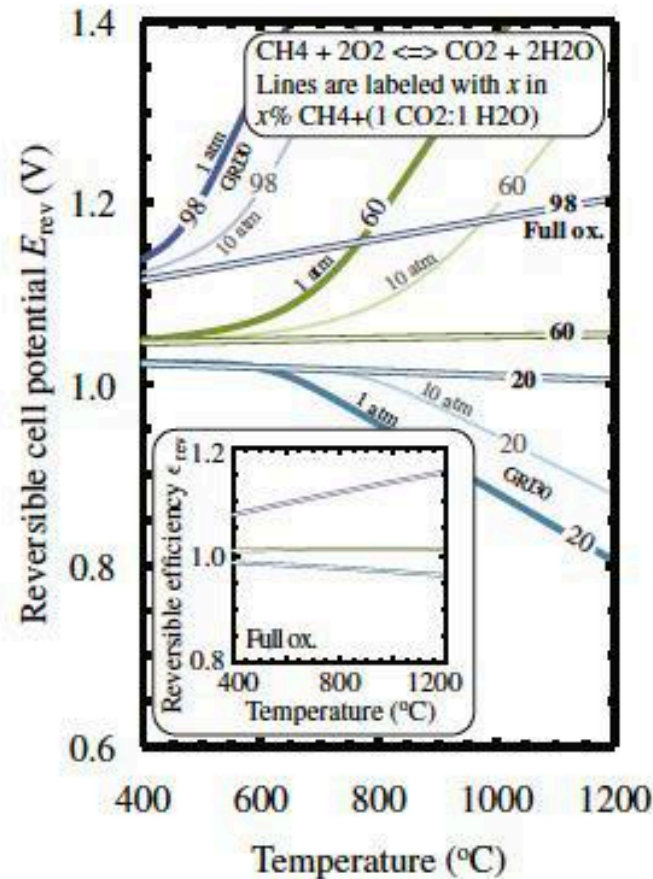
© PECS. All rights reserved. This content is excluded from our Creative Commons license. For more information, see <https://ocw.mit.edu/fairuse>.

Hanna, Lee, Shi, and Ghoniem, PECS, 40 (2014) 74-111

Impact of fuel, concentration, temperature and pressure



© Source unknown. All rights reserved. This content is excluded from our Creative Commons license. For more information, see <https://ocw.mit.edu/fairuse>.



© PECS. All rights reserved. This content is excluded from our Creative Commons license. For more information, see <https://ocw.mit.edu/fairuse>.

Hanna, Lee, Shi, and Ghoniem, PECS, 40 (2014) 74-111

Fuel Cell Components

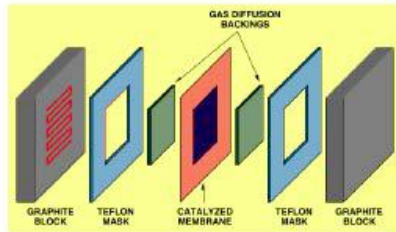
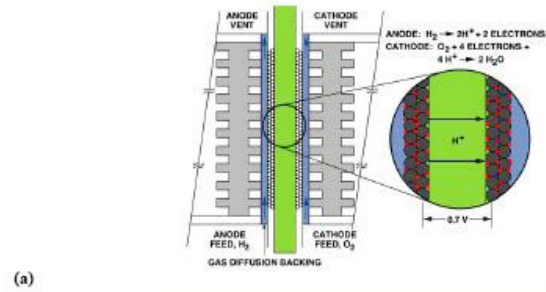
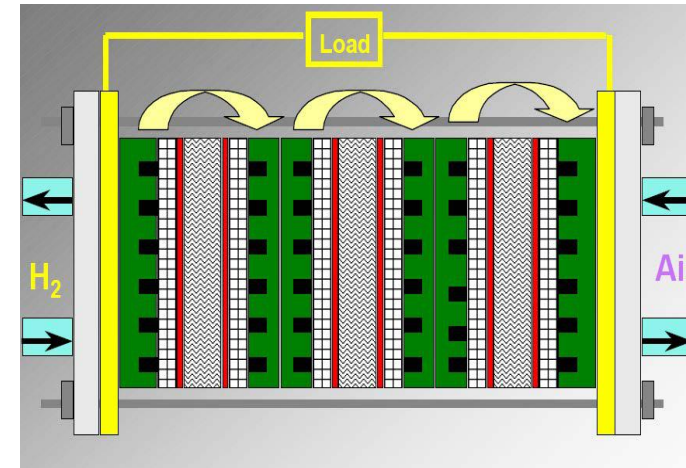
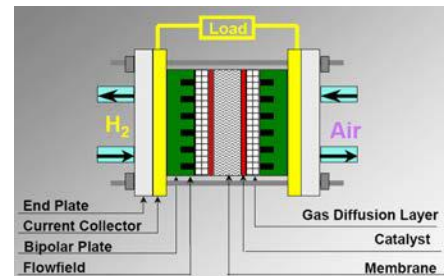


Figure 3-1 (a) Schematic of Representative PEFC (b) Single Cell Structure of Representative PEFC(1)



Also known as membrane-electrode-assembly (MEA), and made of one “physical” plate with anode and electrode material deposited on both side.

The membrane is a polymer (nafion) for low T cells and a ceramic plate for high T cells.

Images courtesy of DOE.

Electrochemical Reactions and Types of Fuel Cells

Overall Reaction: $\text{H}_2 + \frac{1}{2}\text{O}_2 \Rightarrow \text{H}_2\text{O}$

(A) $\text{H}_2 \Rightarrow 2\text{H}^+ + 2\text{e}^-$ and (C) $\frac{1}{2}\text{O}_2 + 2\text{H}^+ + 2\text{e}^- \Rightarrow \text{H}_2\text{O}$, acidic electrolyte (PEM cell)

(A) $\text{H}_2 + \text{O}^{2-} \Rightarrow \text{H}_2\text{O} + 2\text{e}^-$ and (C) $\frac{1}{2}\text{O}_2 + 2\text{e}^- \Rightarrow \text{O}^{2-}$, alkaline electrolyte (SOFC cell)

(A) $\text{H}_2 + 2\text{OH}^- \Rightarrow 2\text{H}_2\text{O} + 2\text{e}^-$ and (C) $\frac{1}{2}\text{O}_2 + \text{H}_2\text{O} + 2\text{e}^- \Rightarrow 2\text{OH}^-$, alkaline electrolyte (Alkaline cell with humidified air)

Overall Reaction: $\text{CO} + \frac{1}{2}\text{O}_2 \Rightarrow \text{CO}_2$

(A) $\text{CO} + \text{O}^{2-} \Rightarrow \text{CO}_2 + 2\text{e}^-$ and (C) $\frac{1}{2}\text{O}_2 + 2\text{e}^- \Rightarrow \text{O}^{2-}$, alkaline electrolyte (SOFC cell)

Overall Reaction: $\text{CH}_4 + 2\text{O}_2 \Rightarrow \text{CO}_2 + 2\text{H}_2\text{O}$

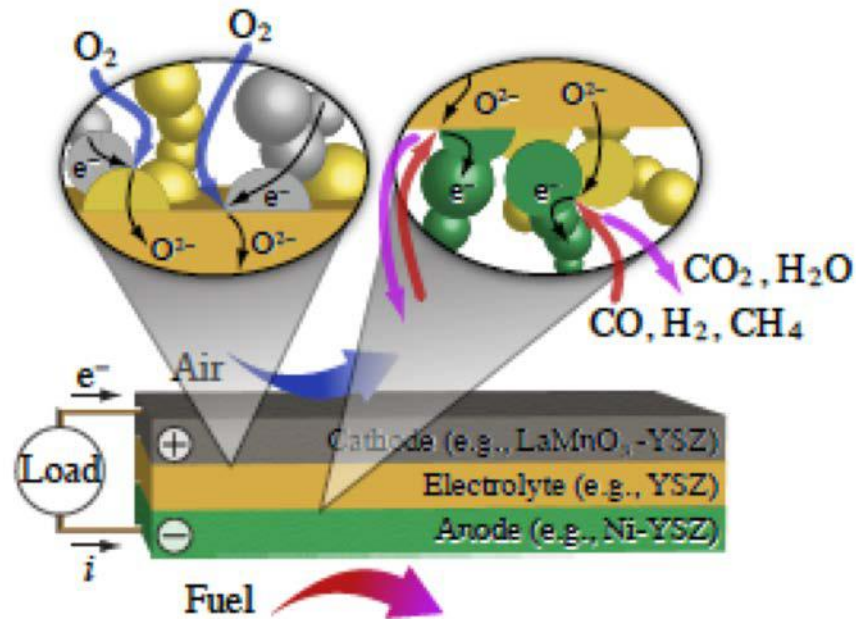
(A) $\text{CH}_4 + 4\text{O}^{2-} \Rightarrow \text{CO}_2 + 2\text{H}_2\text{O} + 8\text{e}^-$ and (C) $2\text{O}_2 + 8\text{e}^- \Rightarrow 4\text{O}^{2-}$, alkaline electrolyte (SOFC cell)

in all, two electrons are produced per oxygen atom.

Fuel Cell Types

Fuel cell	Proton Exchange	Alkaline	Phosphoric Acid	Molten Carbonate	Solid Oxide
Electrolyte	Polymer ion exchange membrane	potassium hydroxide in asbestos	liquid phosphoric acid in SiC	liquid molten carbonate in LiAlO_2	Perovskites
Electrode	Carbon	Transition metals	Carbon	Nickels and nickel oxides	perovskites/ metal cermet
Catalyst	Platinum	Platinum	Platinum	Electrode material	Electrode material
Interconnect	Carbon or metal	Metal	Graphite	Stainless steel of nickel	Nickel, ceramics
Temperature	40 - 80 °C	65 - 220 °C	205 °C	650 °C	600 -1000 °C
Charge Carrier	H^+	OH^-	H^+	$\text{CO}_3^{=}$	$\text{O}^=$
fuel	Hydrogen	Hydrogen	Hydrogen	Hydrocarbon	hydrocarbon

Materials for Solid Oxide Fuel Cells



In the left bubble, oxygen is reduced at the cathode and oxygen ions are conducted through the electrolyte. Oxygen ions move into the anode (right bubble), where they are used to oxidize the fuel at the three-phase boundary TPB). Electrons released in the charge-transfer reactions are conducted through the anode (metal), to the external circuit.

© PECS. All rights reserved. This content is excluded from our Creative Commons license. For more information, see <https://ocw.mit.edu/fairuse>.

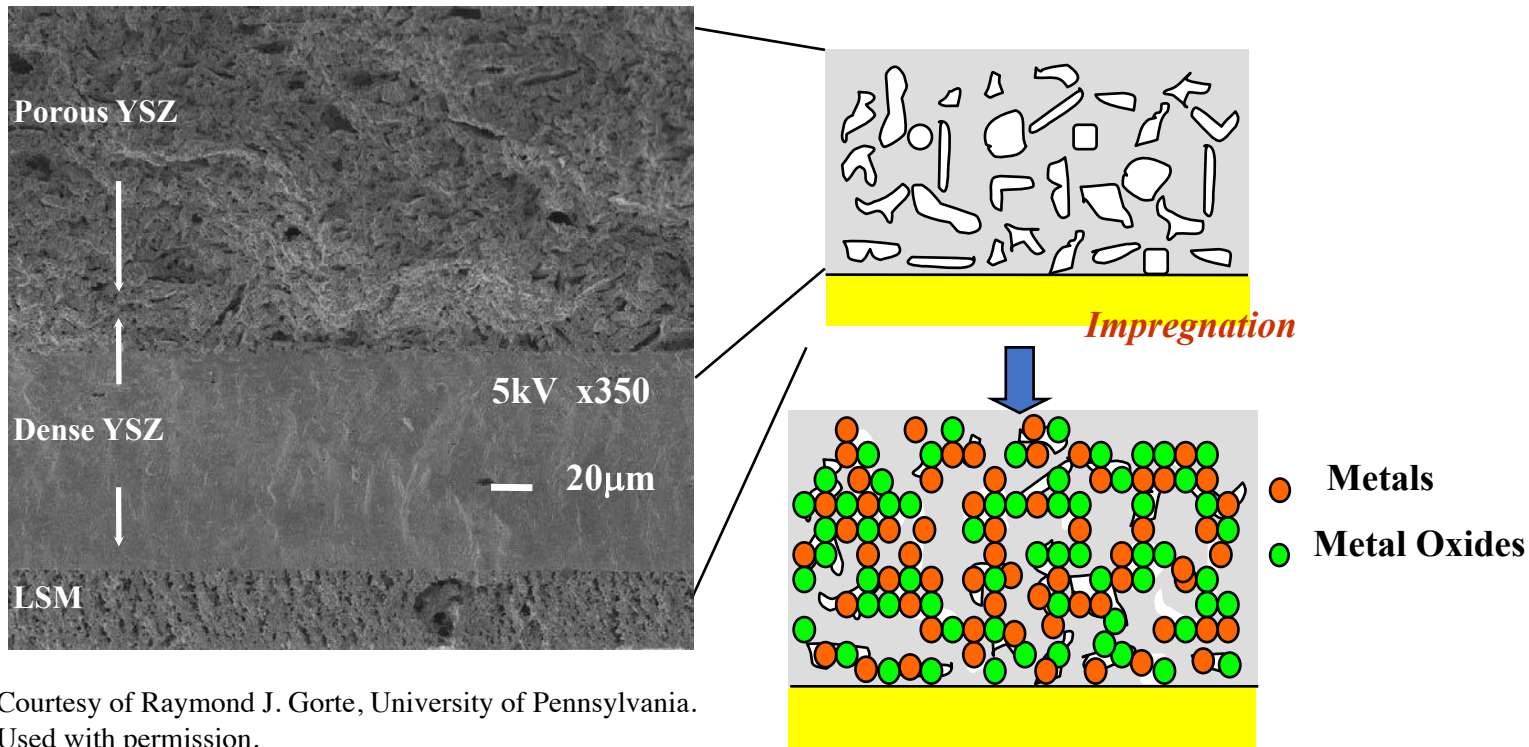
LaMnO_3 (lanthanum manganese oxide) is used to catalyze the oxygen reduction reaction on the cathode side
YSZ (Yttria stabilized zirconia) is used as an ion transport membrane
Ni (nickel) is used to catalyze the fuel oxidation reaction on the anode side.

Solid Oxide Fuel Cells

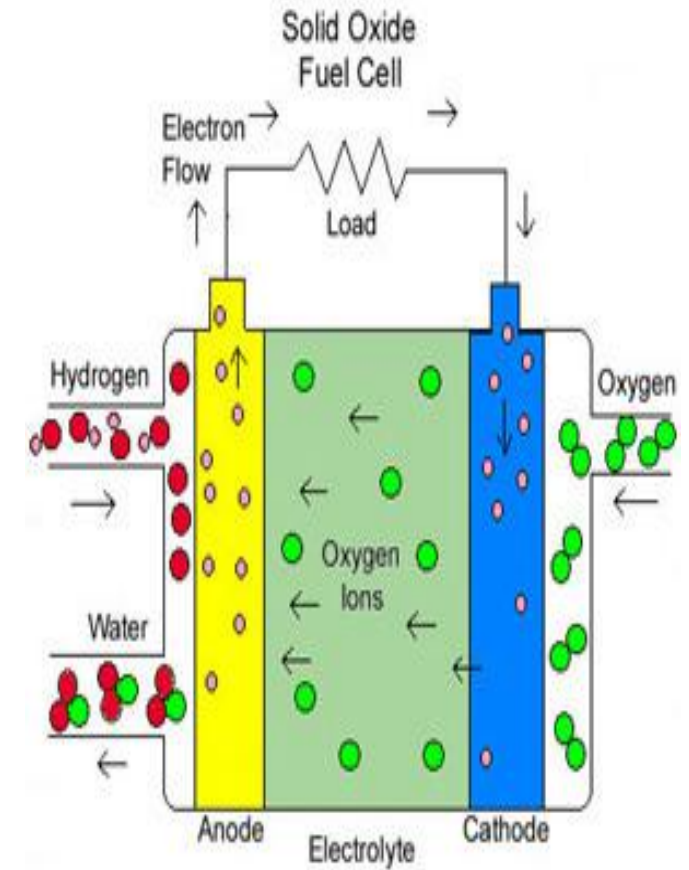
High T cells use regular metals as catalysts

Electrolyte: YSZ, Anode: Ni-YSZ, Cathode: Sr-doped LaMnO₃

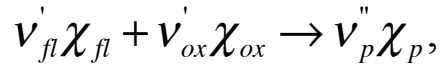
YSZ = yttria – stabilized zirconia



Courtesy of Raymond J. Gorte, University of Pennsylvania.
Used with permission.



Fuel Utilization and its impact on the Open Circuit Potential and Cell Efficiency



$$\Delta\mathcal{E} = \Delta\mathcal{E}^{(o)} - \frac{\sigma \Re T^*}{n_e \mathfrak{I}_a} \ln\left(\frac{p}{p_o}\right) + \frac{\Re T}{n_e \mathfrak{I}_a} \ln\left(\frac{X_{fl} X_{ox}^{\nu'_o}}{X_p^{\nu''_p}}\right)$$

concentrations of fuel and oxidizer decrease between inlet and outlet
as both are consumed according to their stoichiometric ratio

Partial Fuel utilization: $\varphi = \frac{n_{fl1} - n_{fl2}}{n_{fl1}}$

@ Inlet: $X_{fl1} = \frac{1}{1 + n_{d1}}, \quad X_{ox1} = 0.21,$

@ exit: $X_{fl2} = \frac{1 - \varphi}{1 - \varphi + n_{d1} + \nu''_p \varphi}, \quad X_{ox2} = \frac{(1 - \varphi) \nu'_{ox}}{3.76 \nu'_{ox} + (1 - \varphi) \nu'_{ox}}$

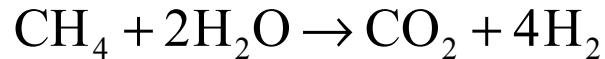
using values at exit gives lower $\Delta\mathcal{E}$

For a SOFC where products form
in the fuel channel



Open Circuit potential for different fuel utilization and for 50% oxygen utilization, cell is fueled by hydrogen produced by SMR (Fuel Cell Explained, Laramie et al.)

If products of methane-water reforming are used:



The fuel mixture *has* $X_{\text{H}_2} = 0.8$

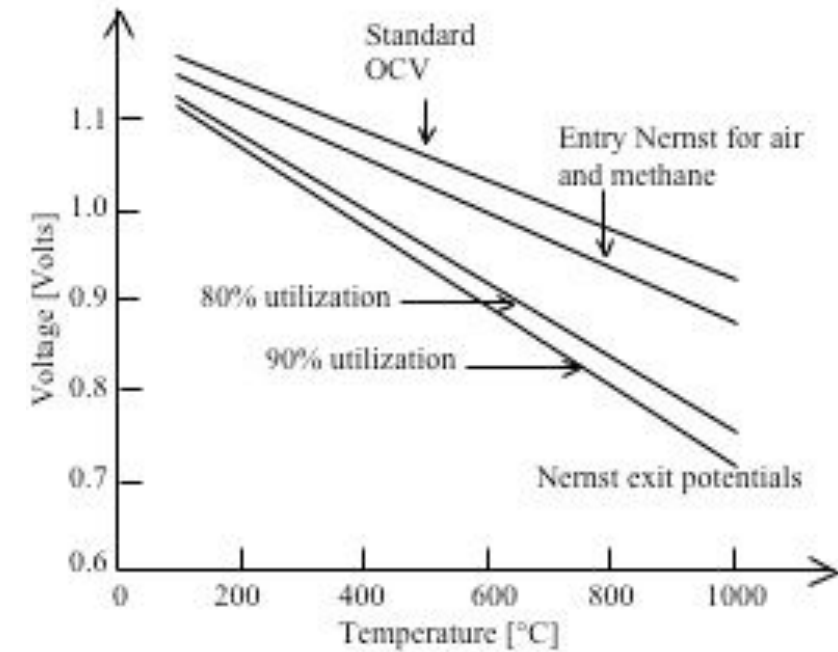
Oxidizer is air, $X_{\text{O}_2-\text{inlet}} = 0.21$

Much air is flown to ensure that

oxidation is not limited by oxygen

Assume that @ exit, 50% utilized of oxygen,

$$X_{\text{O}_2-\text{exit}} = 0.105$$



There advantages to running the cell at low T, but chemistry is slow and we need a precious metal catalyst, which make it expensive and sensitive to fuel impurities.

- In this example, products are mixed with fuel in the fuel channel, reducing the fuel concentration towards the exit.
- Methane can also be "naturally" reformed internally, hydrogen and CO are more electro-chemically active

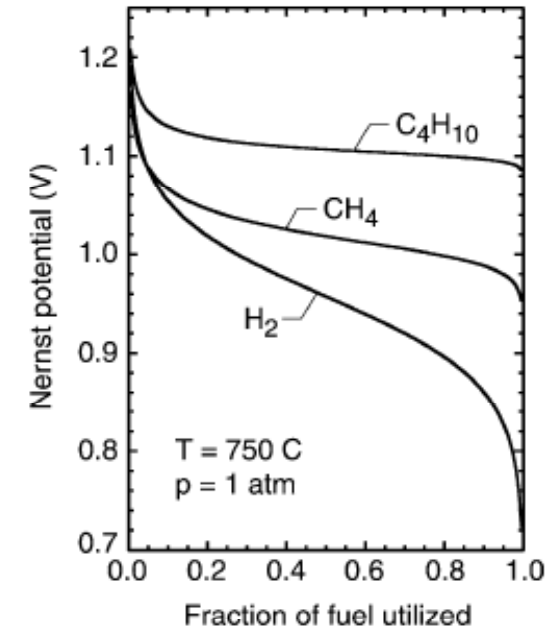
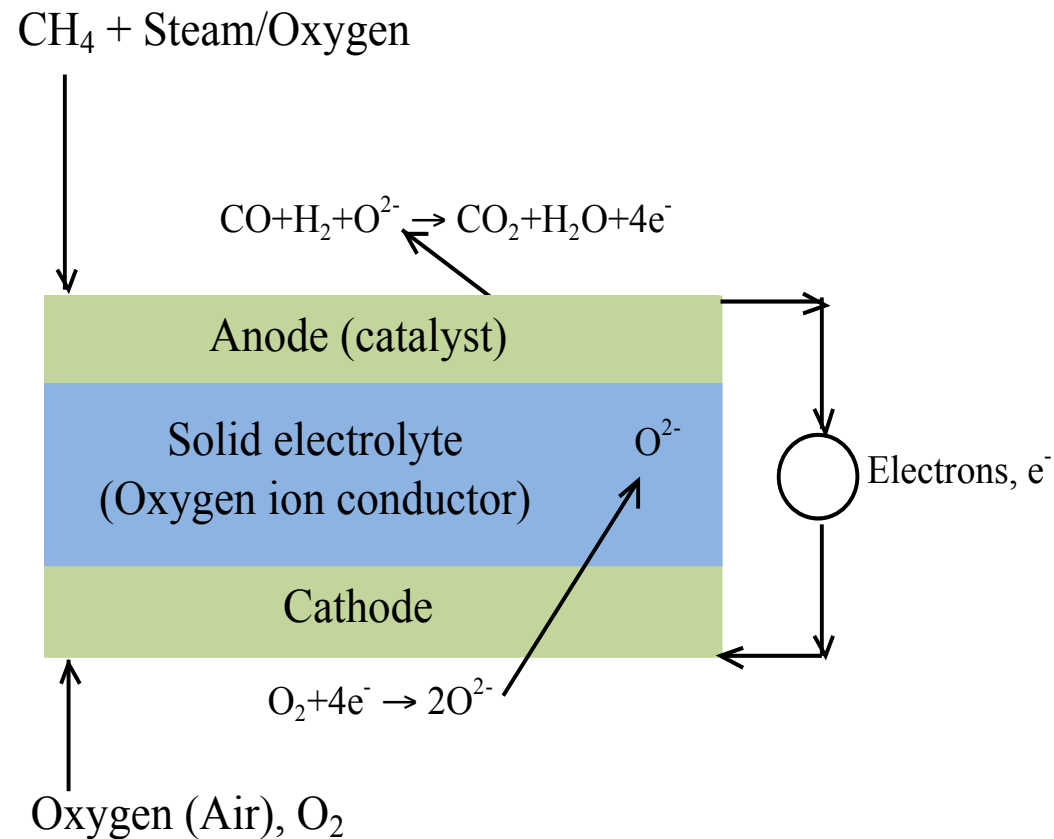
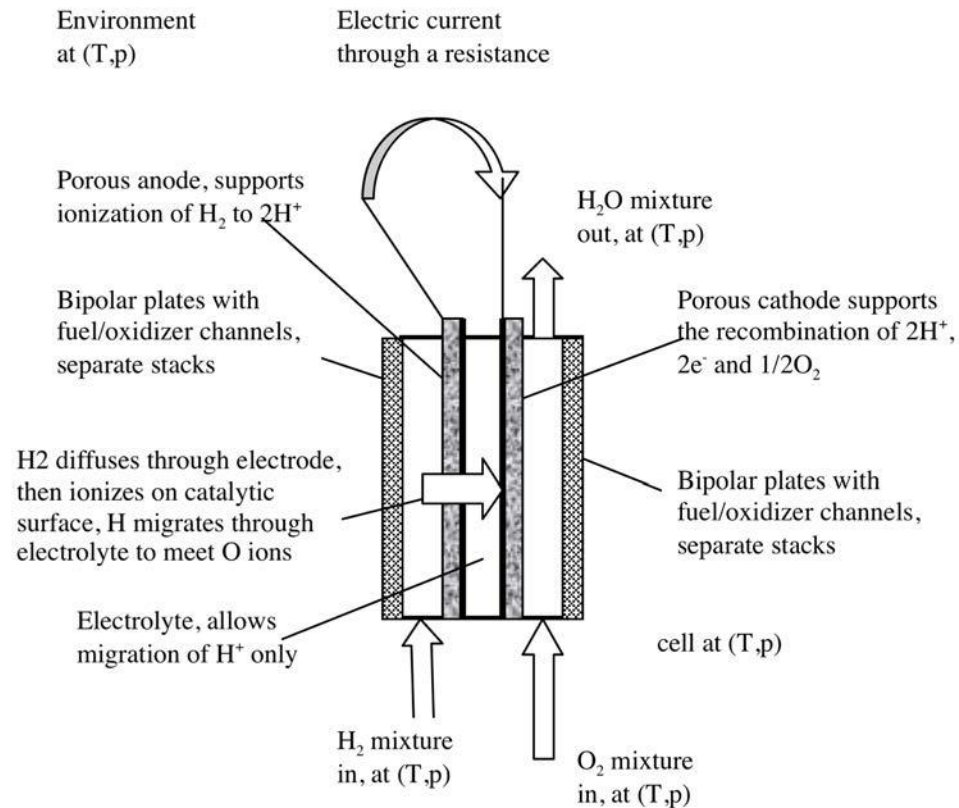


Fig. 3. Nernst potential for three fuels-air systems as a function of percentage of the fuel utilization. As the fuel is "utilized" it is converted to stoichiometric products that dilute the fuel on the anode side. The air is not depleted in this system.

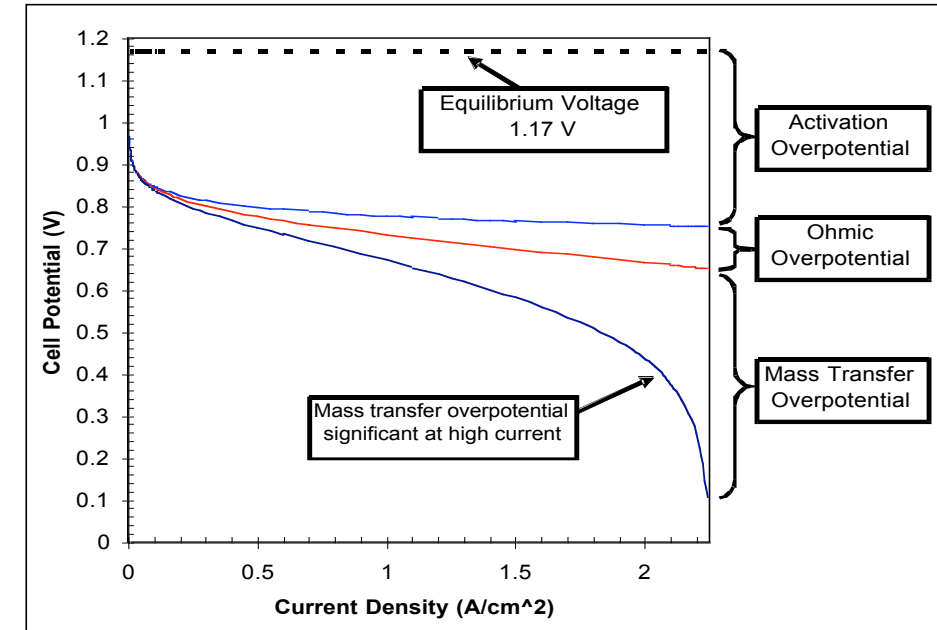
Courtesy Elsevier, Inc., <http://www.sciencedirect.com>. Used with permission.

Fuel Cell Performance at Finite Current (Power) Conditions

$$\text{Faraday's Law: } I = n_e \mathfrak{F}_a \dot{n}_f \quad \text{or} \quad i = n_e \mathfrak{F}_a j_f$$



Components of a PEMFC



Relative contributions depend on design and operating conditions:

- Catalysis, type and density.
- Thickness of electrodes and membrane.
- Water management (in PEM cells).

MIT OpenCourseWare
<https://ocw.mit.edu/>

2.60J Fundamentals of Advanced Energy Conversion
Spring 2020

For information about citing these materials or our Terms of Use, visit: <https://ocw.mit.edu/terms>.

Lecture 9

Fuel Cells at Finite Current

Ahmed Ghoniem

March 2, 2020

Loss mechanisms in fuel cells

Kinetics of electron transfer reactions, activation overpotential

Transport Processes and transport overpotential

Total losses and overall efficiency

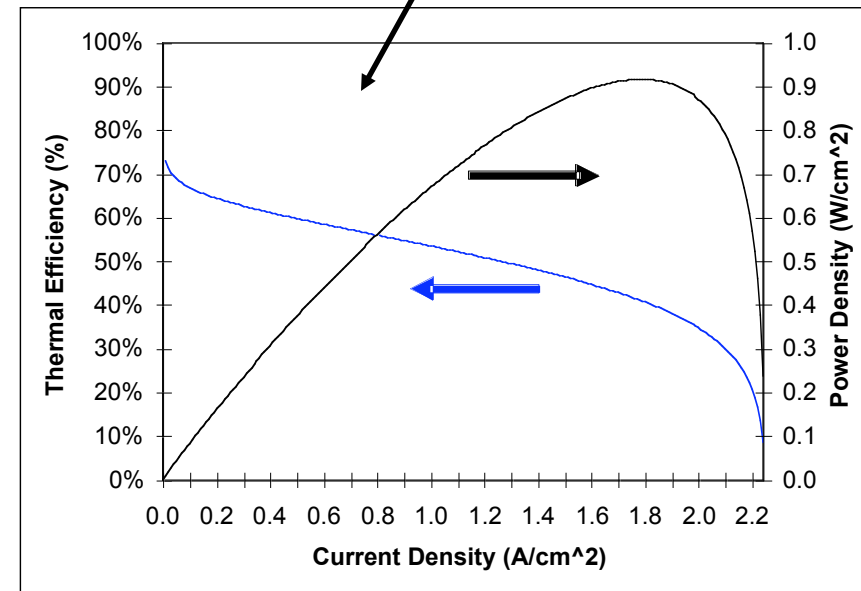
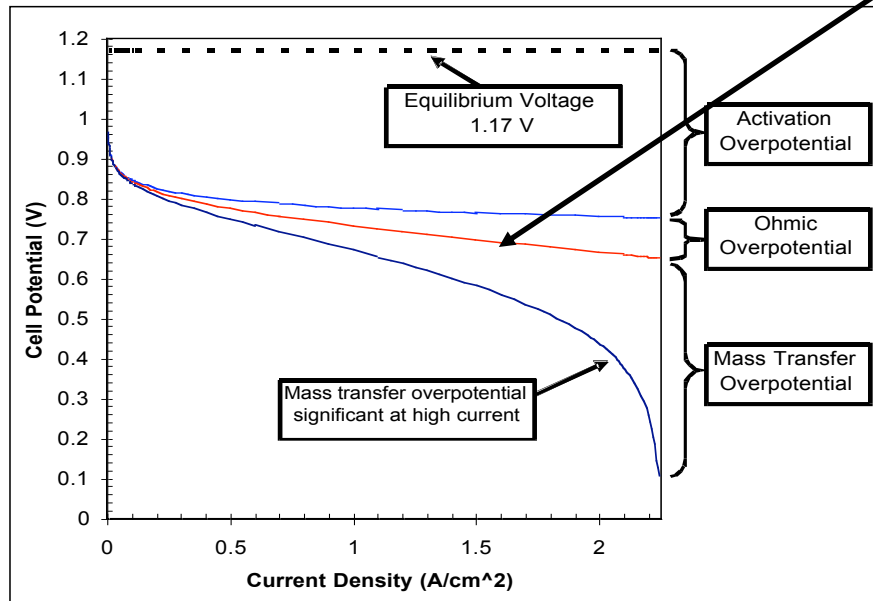
Faraday's Law: $I = n_e \mathfrak{Z}_a \dot{n}_f$, rate of fuel utilization is $\dot{n}_f \leq (\dot{n}_f)_{\text{sup}}$

$$\eta_{FU} = \frac{\wp}{(\dot{n}_f)_{\text{sup}} \Delta \hat{h}_{R,f}} = \frac{IV}{(\dot{n}_f)_{\text{sup}} \Delta \hat{h}_{R,f}} = \frac{I}{n_e \mathfrak{Z}_a (\dot{n}_f)_{\text{sup}}} \left(\frac{V}{V_{OC}} \right) \left(\frac{\xi V_{OC}}{\Delta \hat{h}_{R,f}} \right)$$

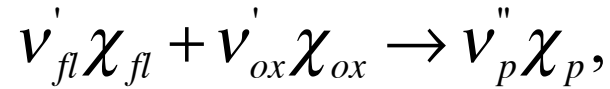
$$= \eta_{far} \eta_{rel} \eta_{OC}$$

$$\eta_{OC} = \frac{\Delta G_R}{\Delta H_R}$$

Max power (at lower efficiency), $\sim 2.0 \text{ kW/m}^2$



Finite-Current Performance of HTFC's



$$\Delta\mathcal{E}^{act} = \Delta\mathcal{E}^{(o)} - \frac{\sigma \Re T^*}{n_e \mathfrak{I}_a} \ln\left(\frac{p}{p_o}\right) + \frac{\Re T}{n_e \mathfrak{I}_a} \ln\left(\frac{X_{fl} X_{ox}^{v'_o}}{X_p^{v''_p}}\right)^{act}$$

must calculate concentrations where chemistry occurs

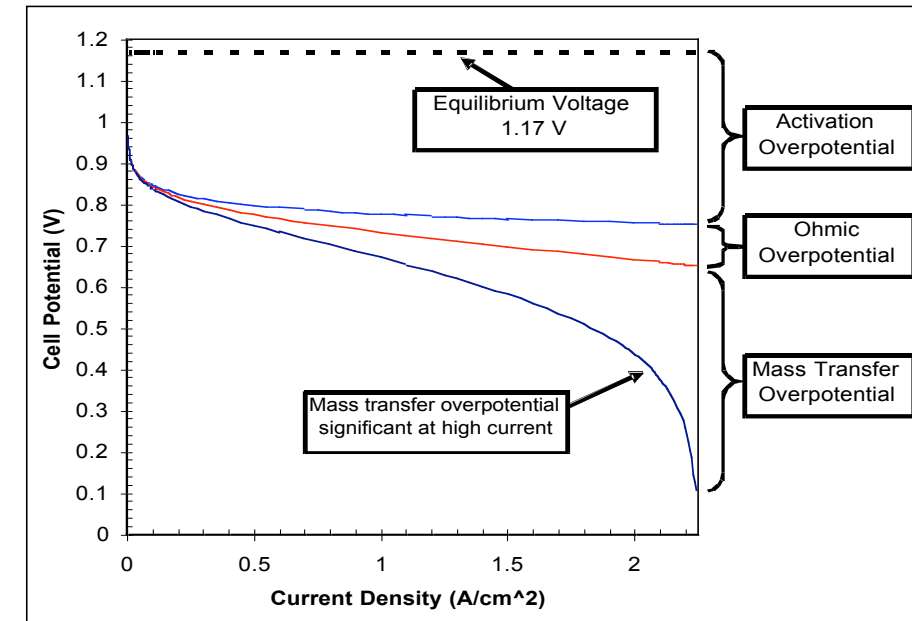
$$\Delta\mathcal{E} = \Delta\mathcal{E}^o$$

$$+\tilde{\eta}_{a,act} + \tilde{\eta}_{a,conc} + \tilde{\eta}_{a,FU}$$

$$+\tilde{\eta}_{el,oh}$$

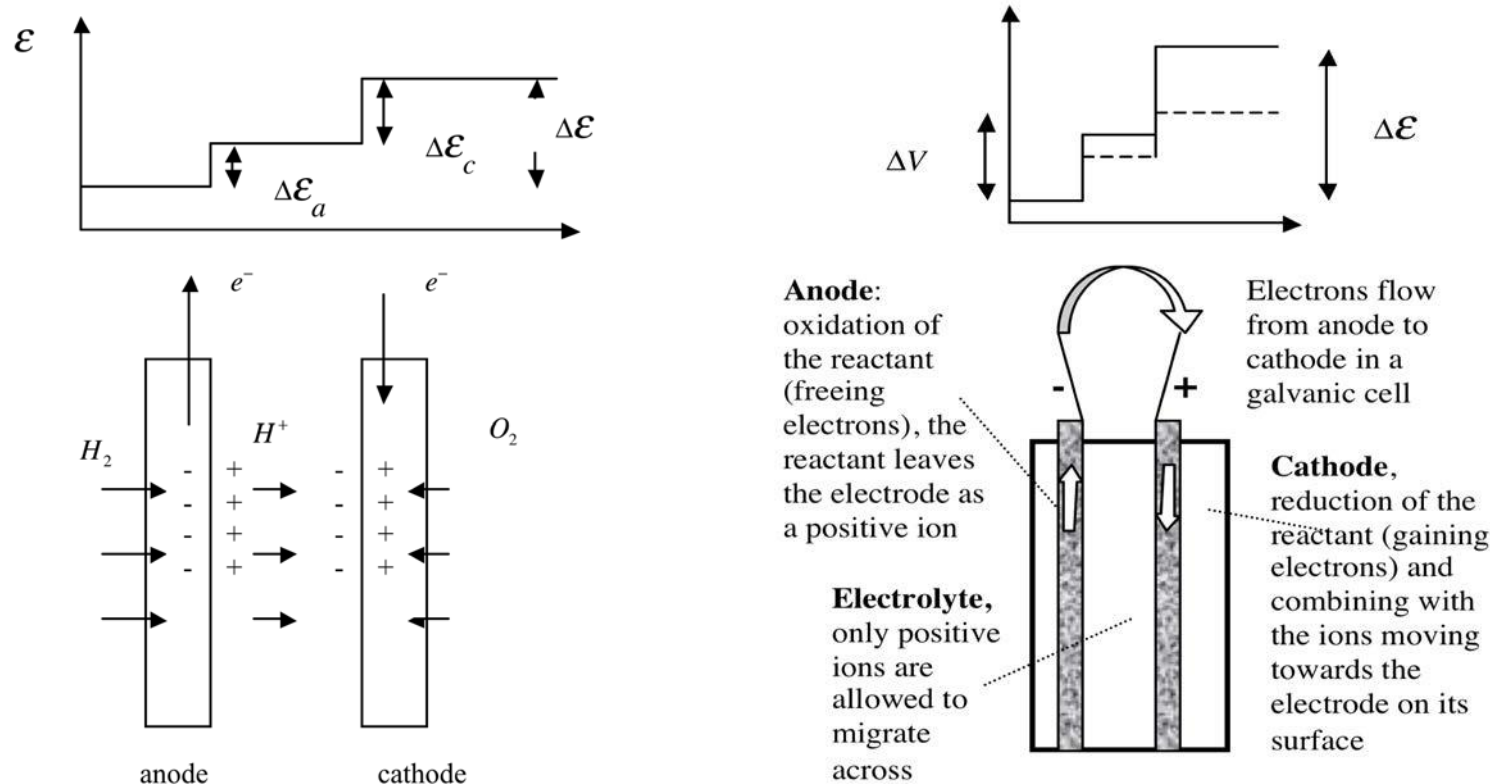
$$+\tilde{\eta}_{c,act} + \tilde{\eta}_{c,conc} + \tilde{\eta}_{c,FU}$$

$$\tilde{\eta} \equiv \text{overpotential}$$



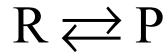
An electrochemical cell at equilibrium (left) and one producing finite current (right).

Notice the charge separation at the interface between the electrode and electrolyte (the electric double layer). The thickness of the layer is nanometer. At finite current, only the charge with higher free energy (overpotential) can overcome the potential difference across the double layer.



An (oversimplified) Introduction to Chemical kinetics

Rate of chemical
(thermochemical)
reaction:



$$\frac{d[P]}{dt} = [R]k_{f0}e^{-\frac{E_f}{\Re T}} - [P]k_{b0}e^{-\frac{E_b}{\Re T}} = -\frac{d[R]}{dt} \quad (\text{Arrhenius expression})$$

E_j : the activation energy and [-] is the concentration
molecules must have excess energy to react!

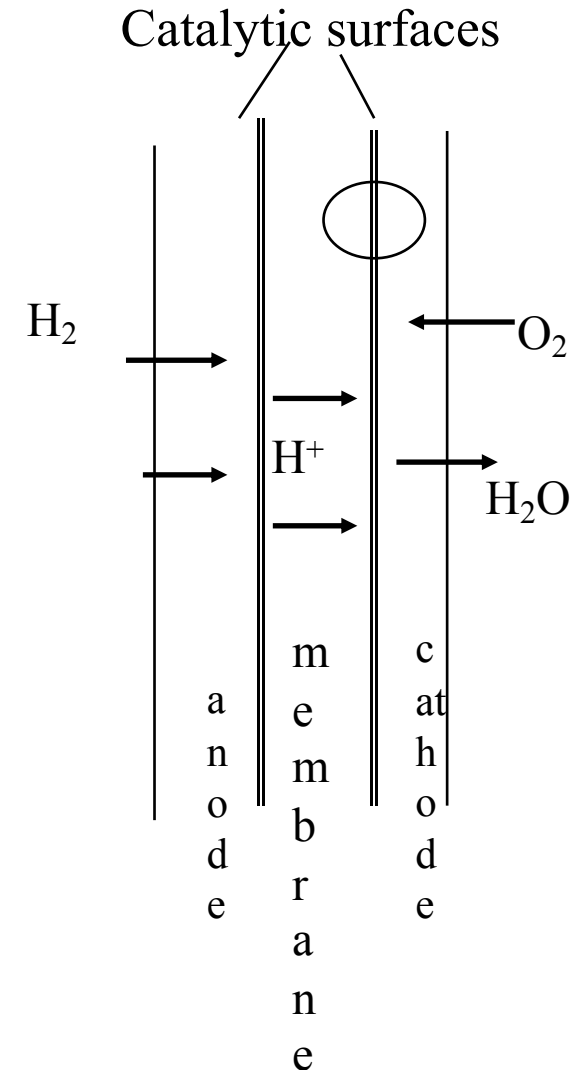
Rate of
electrochemical
(charge transfer)
reaction:



$$\frac{d[P]}{dt} = [R]\tilde{k}_{f0}e^{-\frac{\Im_a \tilde{\eta}_f}{\Re T}} - [P]\tilde{k}_{b0}e^{-\frac{\Im_b \tilde{\eta}_b}{\Re T}} = -\frac{d[R]}{dt} = i$$

$\tilde{\eta}$: the activation "overpotential", or the difference between the actual potential of the charge and the equilibrium value, that charged

species must have to jump across the layer. $\tilde{k}_{f0} = k_{f0}e^{-\frac{E_{af}}{\Re T}}$



Electrochemical Reaction Kinetics

Consider the reversible oxidation reaction at an electrode: $\text{R} \xrightleftharpoons[k_b]{k_f} \text{P}^+ + \text{e}^-$

The net current = current leaving a surface

- current arriving (the reverse reaction)

$$= \mathfrak{I}_a \left(\tilde{k}_f C_R^{(s)} \exp \left(-\frac{\mathfrak{I}_a \tilde{\eta}_f}{\Re T} \right) \right) - n \mathfrak{I}_a \left(\tilde{k}_b C_P^{(s)} \exp \left(-\frac{\mathfrak{I}_a \tilde{\eta}_b}{\Re T} \right) \right)$$

The "free" energy required to drive the reaction *changes* by $\mathfrak{I}_a \tilde{\eta}$.

This energy is divided between the two layers

using a transfer coefficient, α :

$$\Delta G_{af}^\# = \Delta G_{af}^{\#0} + \alpha \mathfrak{I}_a \tilde{\eta}, \quad \text{and} \quad \Delta G_{ab}^\# = \Delta G_{ab}^{\#0} - (1 - \alpha) \mathfrak{I}_a \tilde{\eta},$$

$$\tilde{k}_f = \hat{A}_f \exp \left(-\frac{\Delta G_{af}^{\#0}}{\Re T} \right) \exp \left(-\alpha \frac{\mathfrak{I}_a \tilde{\eta}}{\Re T} \right) = k^0 \exp \left(-\alpha \frac{\mathfrak{I}_a \tilde{\eta}}{\Re T} \right)$$

$$\tilde{k}_b = \hat{A}_b \exp \left(-\frac{\Delta G_{ab}^{\#0}}{\Re T} \right) \exp \left((1 - \alpha) \frac{\mathfrak{I}_a \tilde{\eta}}{\Re T} \right) = k^0 \exp \left((1 - \alpha) \frac{\mathfrak{I}_a \tilde{\eta}}{\Re T} \right)$$

Define the exchange current density as:

$$i_0 = \frac{I_0}{A_e} = n \mathfrak{I}_a k^0 C_O^{(s)*} = n \mathfrak{I}_a \hat{A}_f \exp \left(-\Delta G_{af}^{\#0} / \Re T \right) C_O^{(s)*}$$

Substitute in the net current equation we get:

$$i = i_0 \left\{ \exp \left(\alpha \frac{n \mathfrak{I}_a \tilde{\eta}}{\Re T} \right) - \exp \left(-(1 - \alpha) \frac{n \mathfrak{I}_a \tilde{\eta}}{\Re T} \right) \right\},$$

$$i = i_0^* \left\{ \frac{C_O^{(s)}}{C_O^{(s)*}} \exp \left(\alpha_a \frac{n \mathfrak{I}_a \tilde{\eta}}{\Re T} \right) - \frac{C_P^{(s)}}{C_P^{(s)*}} \exp \left(-\alpha_c \frac{n \mathfrak{I}_a \tilde{\eta}}{\Re T} \right) \right\}$$

This is the Butler Volmer Equation. An implicit relation between the overpotential (loss of potential) and the current from the electrode

$$i = i_0^* \left\{ \frac{C_O^{(s)}}{C_O^{(s)*}} \exp\left(\alpha_a \frac{n\mathcal{S}_a \tilde{\eta}}{\mathcal{R}T}\right) - \frac{C_P^{(s)}}{C_P^{(s)*}} \exp\left(-\alpha_c \frac{n\mathcal{S}_a \tilde{\eta}}{\mathcal{R}T}\right) \right\}$$

exchange current density

$$\frac{I_0}{A_e} = n\mathcal{S}_a \hat{A}_f \exp(-\Delta G_f^{\#0} / \mathcal{R}T) C_O^{(s)*}$$

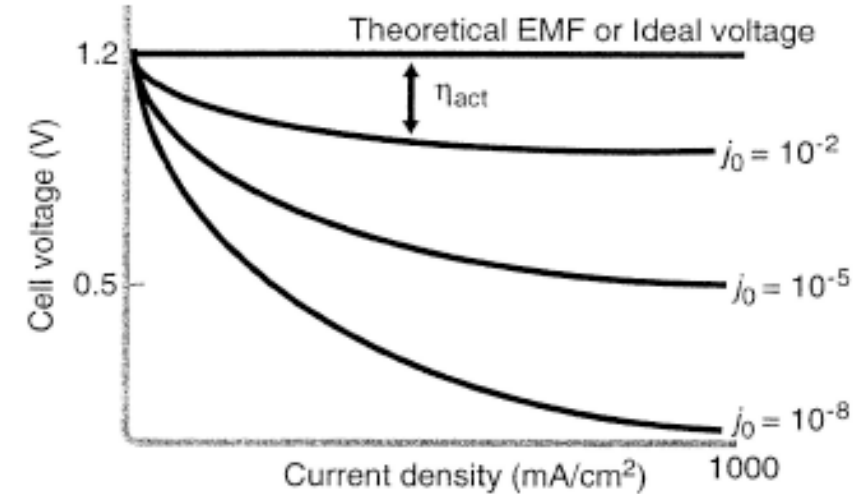


Figure 3.11. Effect of activation overvoltage on fuel cell performance. Reaction kinetics typically inflicts an exponential loss on a fuel cell's i – V curve as determined by the Butler–Volmer equation. The magnitude of this loss is influenced by the size of j_0 . (Curves calculated for various j_0 values with $\alpha = 0.5$, $n = 2$, and $T = 298.15$ K.)

© Source unknown. All rights reserved. This content is excluded from our Creative Commons license. For more information, see <https://ocw.mit.edu/fairuse>.

High exchange current density is important for reducing activation overpotential by:

1. Raising the cell temperature (see next figure) ... opposite to T 's impact on OC potential.
2. Using an active catalyst, and more of it.
3. Using a rough surface (nanostructured).
4. Increasing reactants concentrations
5. Raising the pressure.

Proton Exchange Membrane Fuel Cell (low temperature)

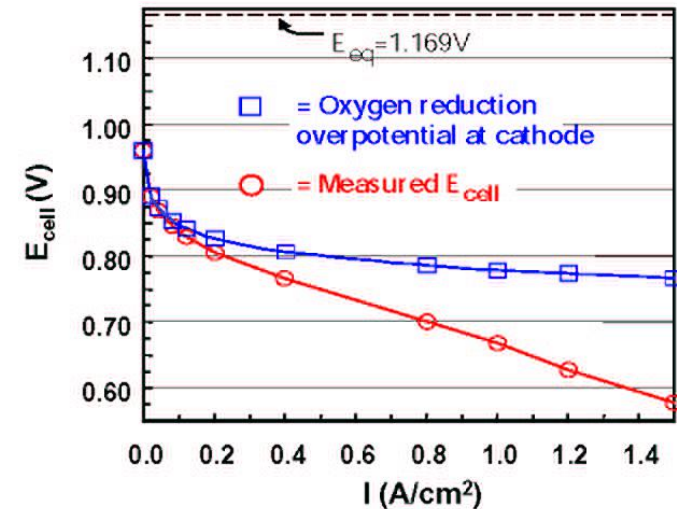
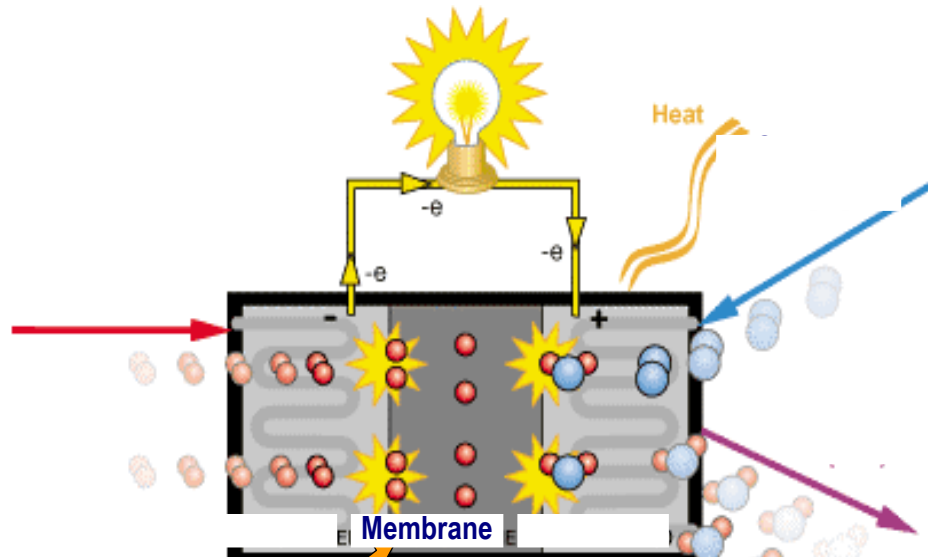
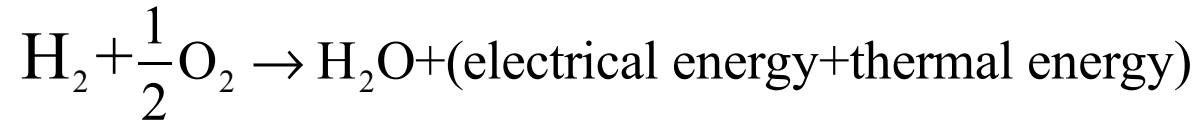


Figure 10 (Lower curve) Cell Voltage (E_{cell}) of a State-of-the-art H_2/Air Membrane Electrode Assembly Operated at 80°C versus the Current Drawn from the Cell (in amp/cm^2) (Gasteiger and Mathias 2002) (The equilibrium [theoretical] cell voltage [1.169 V] is shown by the dashed line at the top of the figure.) (Upper curve) Reduction from the Theoretical Value Caused by the Oxygen Reduction Overpotential at the Cathode Alone (Note that the overpotential is large at all but the very lowest currents. The remaining loss in potential at a given current is caused by internal resistance in the cell and to O_2 gas transport limitations through the air in the porous cathode composite.)

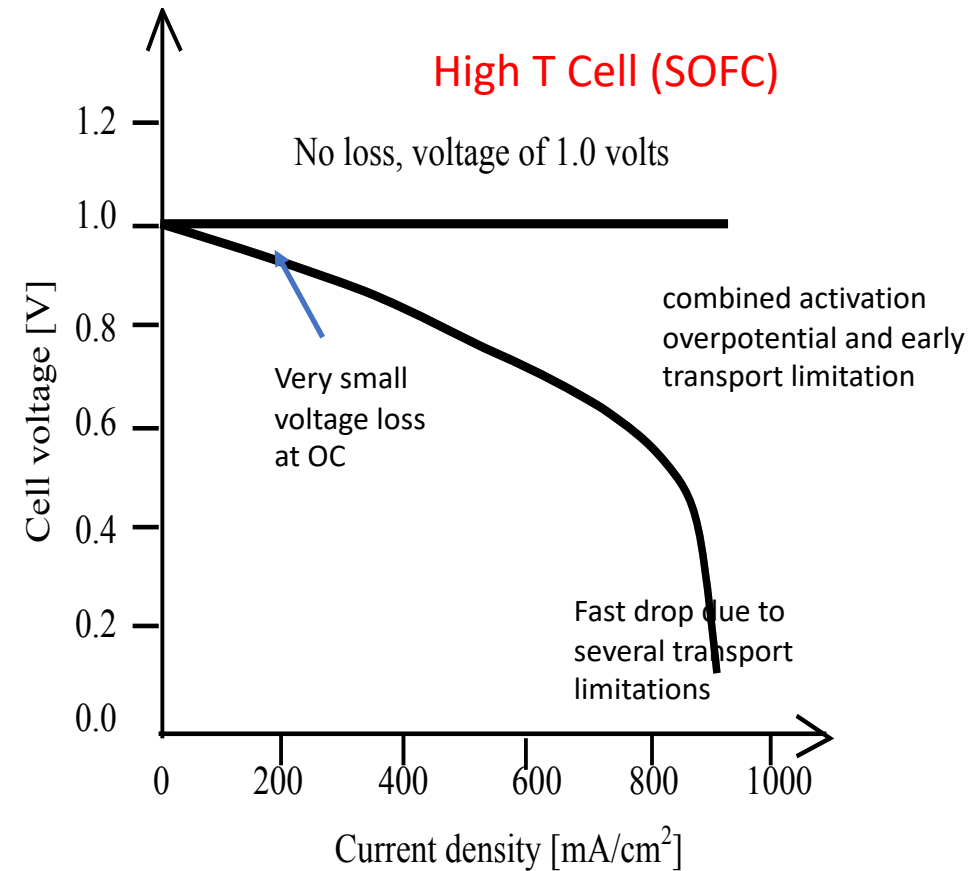
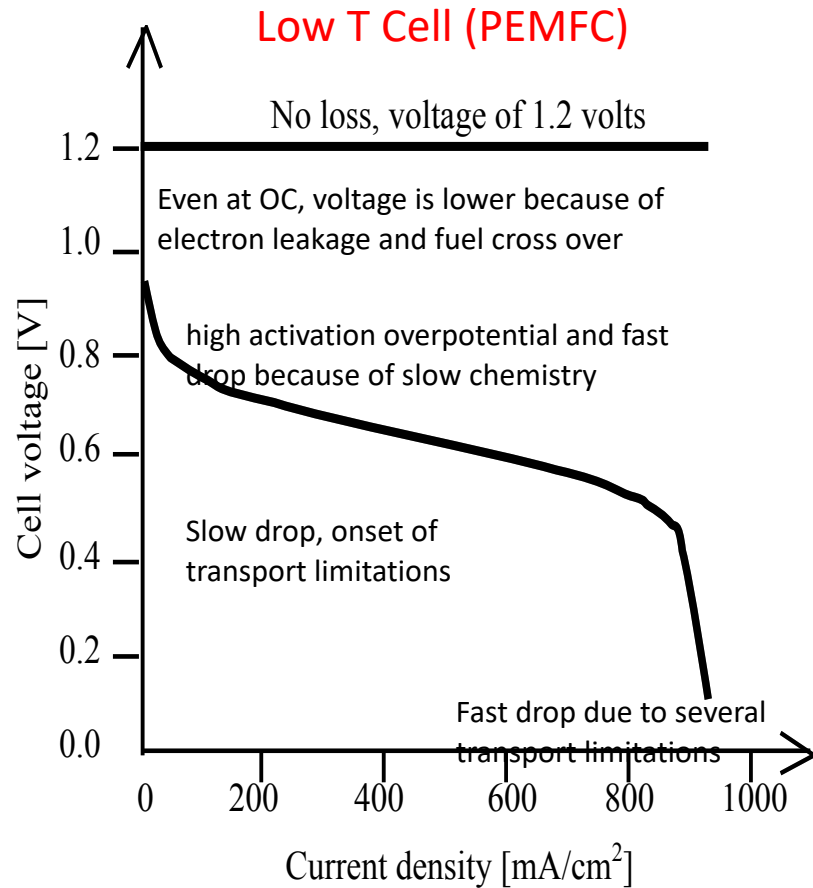
- Ideal for Transportation.
- Uses H_2 Only.
- Uses Platinum as a catalyst.
- Efficiency depends on power, $\sim 40\text{-}50\%$, surface power density (IV) $\sim 0.7 \text{ kW}/\text{m}^2$.

Both images © Source unknown. All rights reserved. This content is excluded from our Creative Commons license. For more information, see <https://ocw.mit.edu/fairuse>.

Effect of Cell Temperature on activation overpotential

Low T cells (left) suffer more from sluggish kinetics than high T cells (right)

for small current and overpotential: $\tilde{\eta}_{act} \approx \frac{RT}{\alpha n_e \mathfrak{I}} \left(\ln \frac{i + i_n}{i_o} \right)$ i_n is the "leakage" ..



- The B-V equation applies to the anode and cathode. Should add both overpotentials to determine the total.
- Oxygen has sluggish kinetics, and higher overpotential, and dominates kinetic overpotential loss.
- Exchange current density for O_2 is $O(10^{-9} \text{ A/cm}^2)$ for Pt-acid electrolyte, vs. $O(10^{-3})$ for H_2 .
- The concentration used in the B-V equation is at *the electrode-electrolyte* interface.
- Use of air increases activation overpotential (lower oxygen concentration).

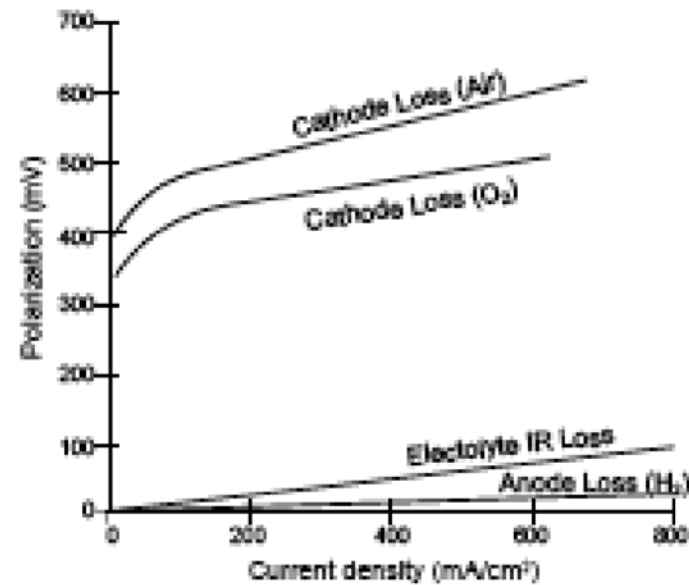


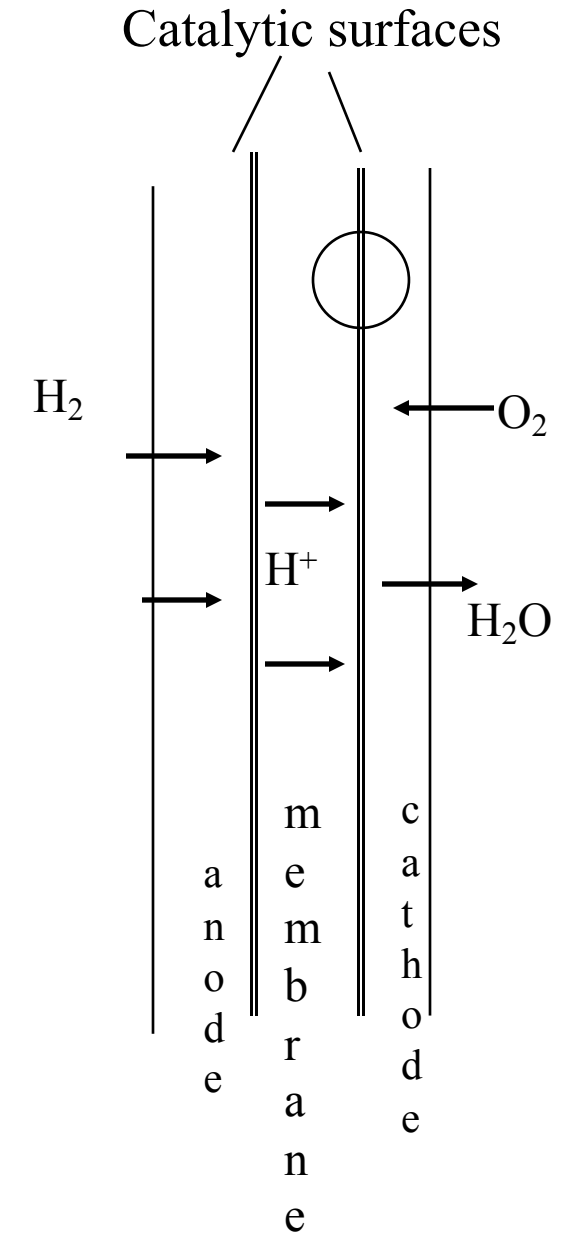
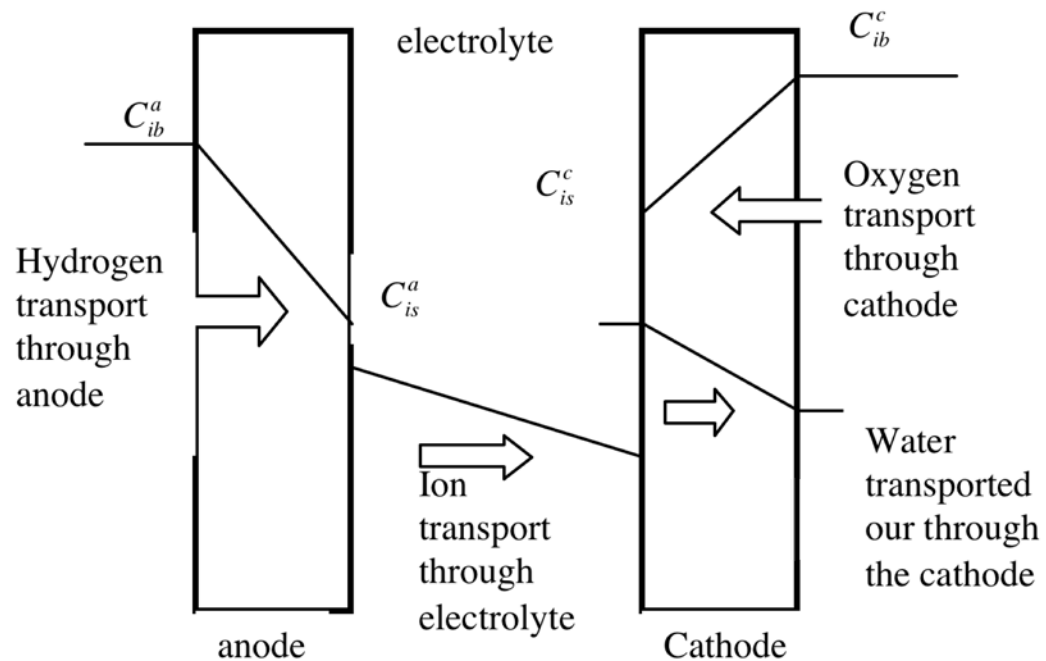
Image courtesy of DOE.

Electrochemical Cell Transport

Fick's Law of mass diffusion: $j_i = -D_i \frac{dC_i}{dx}$

Diffusion is associated with the presence of a species gradient!

very similar to heat diffusion (conduction) where $q = -\lambda \frac{dT}{dx}$



Overpotentials occur due to concentration drop across several layers,

$$\Delta \mathcal{E}(T, p_i) = \Delta \mathcal{E}^o(T) + \frac{\Re T}{2\mathfrak{I}_a} \left(\frac{1}{2} \ln p \right) + \frac{\Re T}{2\mathfrak{I}} \left(\ln X_{H_2} + \frac{1}{2} \ln X_{O_2} - \ln X_{H_2O} \right)$$

Concentrations should be evaluated at the reactive surfaces of the electrodes,

The drop of concentrations is due to transport.

The difference in concentrations across each layer creates an overpotential.

Take one concentration: based on concentrations at interface: $\Delta \mathcal{E}_{act} = \Delta \bar{\mathcal{E}}^o + \frac{\Re T}{n_e \mathfrak{I}_a} \ln C_i^{(act)}$,

But based on concentration in the supply channel: $\Delta \mathcal{E}_{sup} = \bar{\mathcal{E}}^o + \frac{\Re T}{n_e \mathfrak{I}_a} \ln C_i^{(sup)}$

difference is concentration overpotential: $\tilde{\eta}_{conc} = \Delta \mathcal{E}_{act} - \Delta \mathcal{E}_{sup} = \frac{\Re T}{n_e \mathfrak{I}_a} \ln \frac{C_i^{(act)}}{C_i^{(sup)}}$

or: $\Delta \mathcal{E}_{act} = \Delta \mathcal{E}_{sup} + \tilde{\eta}_{conc}$

Transport Overpotentials across an electrode in terms of limiting current density

$$\tilde{\eta}_{conc} = \frac{\Re T}{n_e \mathfrak{I}_a} \left(\ln \frac{C_{is}}{C_{ib}} \right) \quad \{C_{is} < C_{ib}\}$$

Fick's law of diffusion: $j_i = -D_i \frac{dC_i}{dx},$

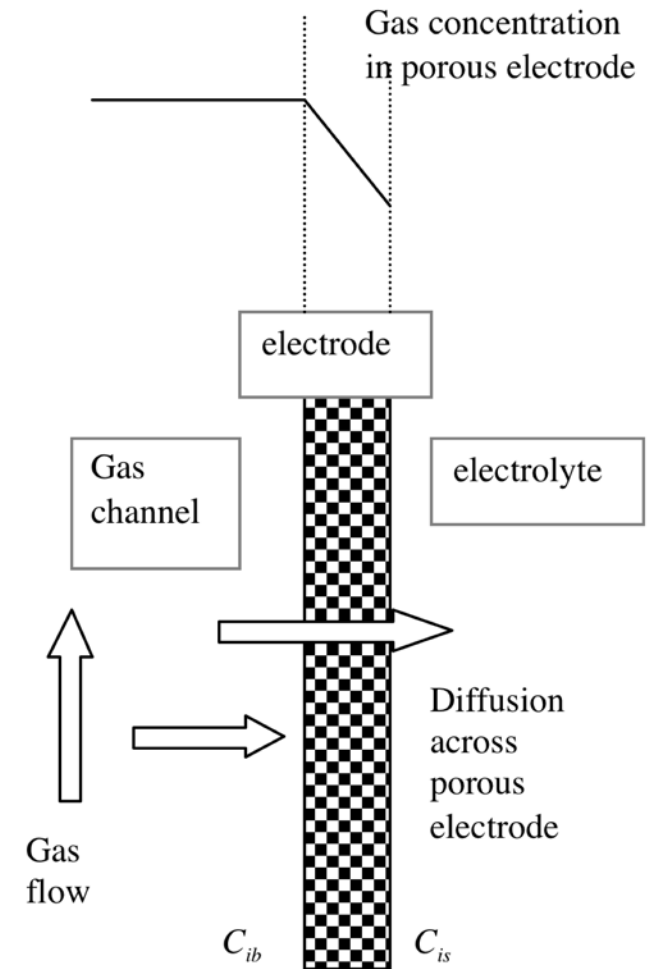
and $C_{ib} - C_{is} = \frac{\delta_{electrode}}{D_{electrode}} j_i$

At limiting conditions $C_{is} = 0$: $C_{ib} = \frac{\delta_{electrode}}{D_{i,electrode}} j_{i,lim}$

this is limiting current: $i_{lim} = n_e \mathfrak{I}_a j_{i,lim} = n_e \mathfrak{I}_a \frac{D_{electrode}}{\delta_{electrode}} C_{ib}$

Thus the concentration ratio for any current is $\frac{C_{is}}{C_{ib}} = 1 - \frac{i}{i_{lim}}$

the electrode diffusion overpotential: $\tilde{\eta}_{el,conc} = \frac{\Re T}{n_e \mathfrak{I}_a} \ln \left(1 - \frac{i}{i_{lim}} \right)$



$$i_{\text{lim}} = n_e \mathfrak{S}_a D_i \frac{C_{ib}}{\delta_{el}}$$

Most cell designs have $i_{\text{lim}} = O(1 \text{ A/cm}^2)$. Why:

- $n_e = 1 - 2$,
- $\mathfrak{S}_a = 98,487 \text{ Coulombs/mol}$,
- $D_i \sim 10^{-5} - 10^{-6} \text{ m}^2/\text{s}$,
- $C_{ib} \sim 10 \text{ mol/m}^3$ (for oxygen in air at SAP),
- $\delta_{el} = 10^{-4} \text{ m}$.

The limiting current density can be raised by:

- Increasing the effective diffusivity of the reactants through the electrodes;
- Increasing the reactants concentrations in the supply channels; and,
- Decreasing the thickness of the electrodes.

Expression must be corrected for concentration drop
across the boundary layer in the gas channel
(in case a carrier gas is used)

$$j_i = h_{conc} (C_{i\infty} - C_{ib}) = -D_{el} \frac{C_{i\infty} - C_{ib}}{\delta_{electrode}}$$

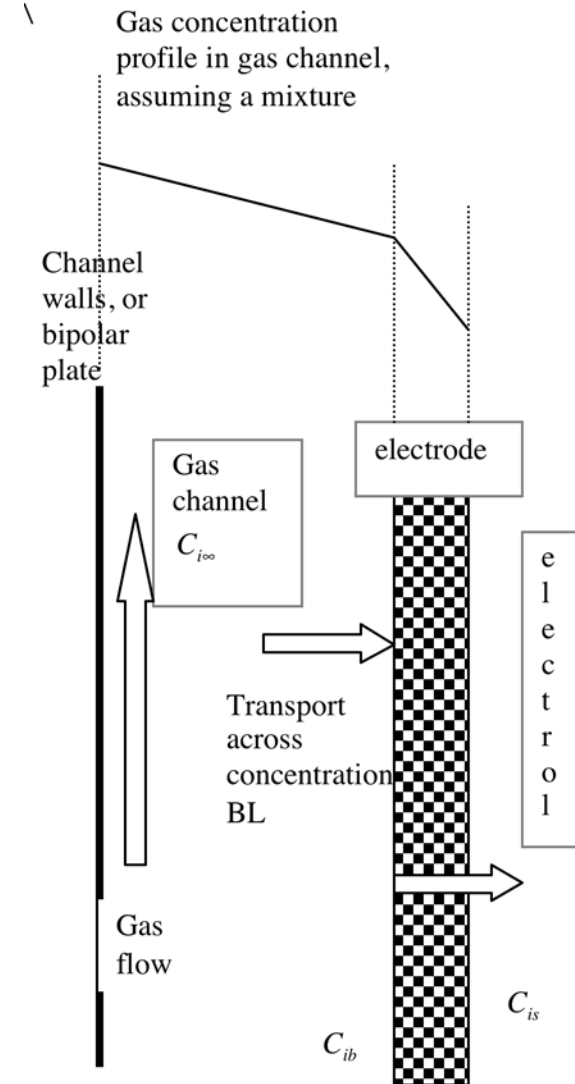
Sherwood number for mass transfer: $Sh = \frac{h_{conc} d_h}{D_{gas}} = O(3-5)$

Eliminate C_{ib} and use Faraday's law:

$$i = n_e \mathcal{S}_a j_i = n_e \mathcal{S}_a \frac{C_{i\infty} - C_{is}}{\left(\frac{\delta_{el}}{D_{el}} + \frac{1}{h_{conv}} \right)}$$

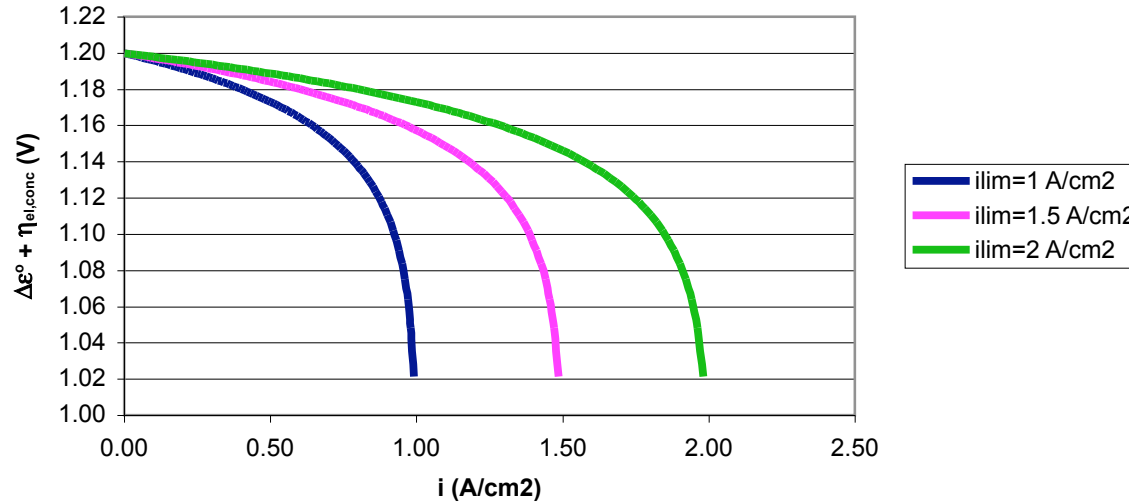
$$i_{lim} = n_e \mathcal{S}_a \frac{C_{i\infty}}{\left(\frac{\delta_{el}}{D_{el}} + \frac{1}{h_{conv}} \right)}$$

the total electrode transport overpotential: $\tilde{\eta}_{el,transpot} = \frac{\mathcal{R}T}{n_e \mathcal{S}_a} \ln \left(1 - \frac{i}{i_{lim}} \right)$



Recall that the kinetic overpotential depends on the concentration

at the electrode surface, hence:
$$\tilde{\eta}_{el,conc,tot} = \frac{\Re T}{n_e \mathfrak{S}} \left(1 + \frac{1}{\alpha} \right) \ell n \left(1 - \frac{i}{i_{lim}} \right)$$



In a porous electrode: $D_{ij}^{eff} \approx D_{ij} \frac{\epsilon}{\tau}$

ϵ : porosity = $\frac{\text{pore volume}}{\text{total volume}}$

τ : tortuosity = $\frac{\text{pore length}}{\text{thickness}}$

Ohmic Overpotetial:

Voltage drop due to resistance to charged species flow

Within electrolyte, resistance to ion flow

Within electrodes, resistance to electron flow:

$$\tilde{\eta}_{oh} = -(R_{electrodes} + R_{electrolyte}) I$$

$$\text{and } I = i A_{electrolyte}$$

$$R_{electrolyte} = \frac{t_{electrolyte}}{A_{electrolyte} \sigma_{electrolyte}},$$

where the conductivity is: $\sigma = |z_i| \mathfrak{S}_a C_i \tilde{u}_i$

and the charge mobility is

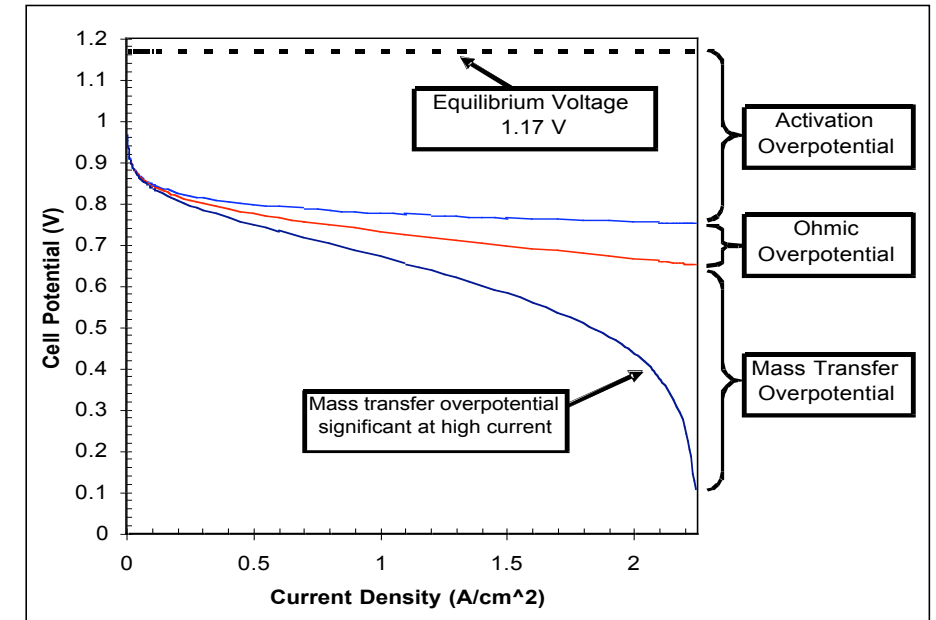
$$\tilde{u}_i = \frac{|z_i| \mathfrak{S}_a D_i}{\Re T} \text{ and } D_i \text{ the Diffusivity.}$$

Diffusivity depends on electrolyte material, water content (in polymer electrolytes), temperature and concentration.

Finite-Current Performance of HTFC's

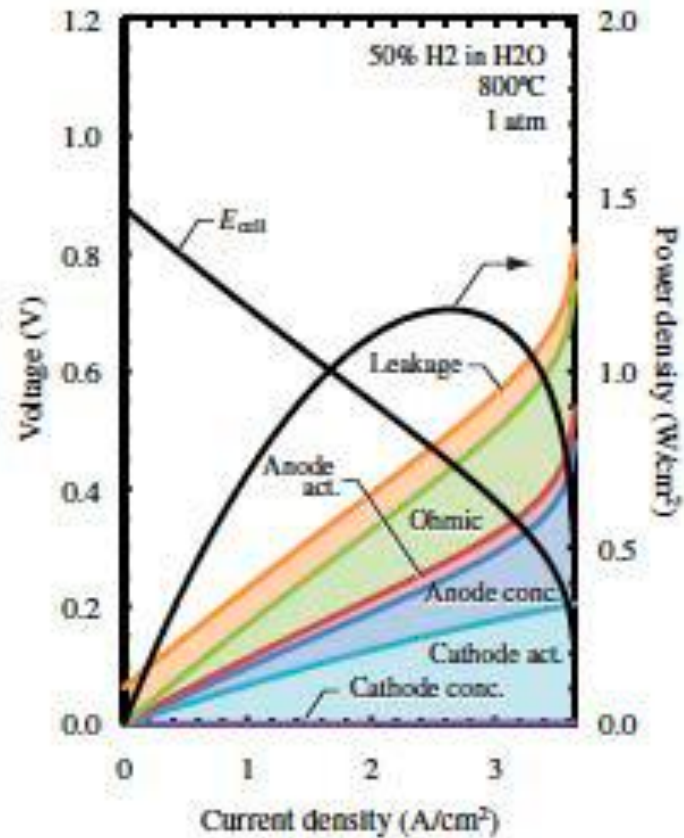
Fuel cells suffer significant irreversibility due to finite-rate processes.

$$\begin{aligned}\Delta \mathcal{E} = & \Delta \mathcal{E}^o \\ & + \tilde{\eta}_{a,act} + \tilde{\eta}_{a,conc} + \tilde{\eta}_{a,FU} \\ & + \tilde{\eta}_{el,oh} \\ & + \tilde{\eta}_{c,act} + \tilde{\eta}_{c,conc} + \tilde{\eta}_{c,FU}\end{aligned}$$



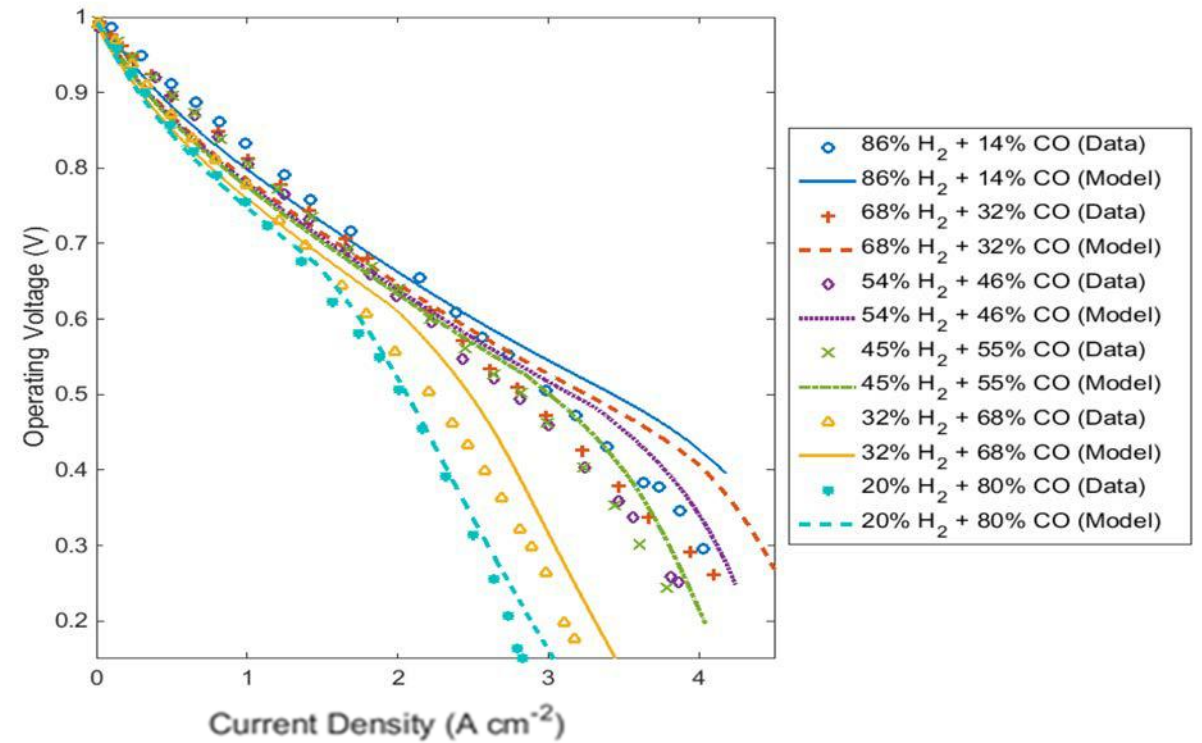
$$\eta = \frac{\text{Power Out}}{\text{Rate of Chemical Enthalpy}} = \frac{I \cdot V}{\dot{n}_f \Delta H_R^o} = \eta_{OC} \cdot \underbrace{\frac{\eta_{rel}}{V}}_{V_{OC}} \cdot \underbrace{\frac{\eta_{Far}}{I}}_{n_e \mathfrak{I} \dot{n}_{fuel}}$$

Finite-Current Performance of SOFC'



Different voltage losses in a typical SOFC running on hydrogen, losses are shown cumulatively starting with cathodic concentration overpotential, cathodic activation overpotential, etc. (Hanna, Shi and Ghoniem, PECS, 40 (2014))

© PECS. All rights reserved. This content is excluded from our Creative Commons license. For more information, see <https://ocw.mit.edu/fairuse>.

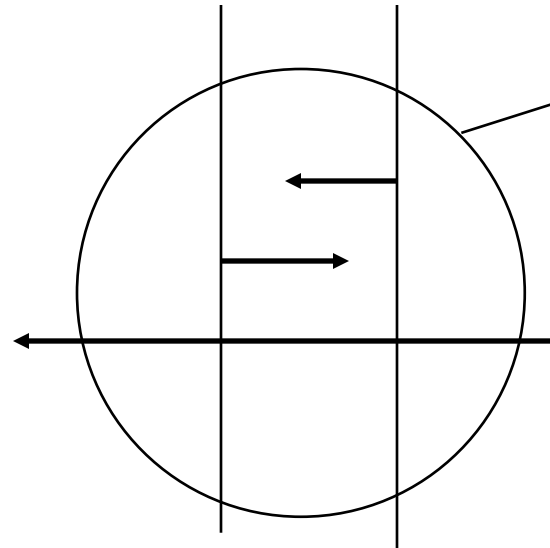


Polarization curve for an SOFC running on syngas with different concentration of H₂ to CO. CO electrochemistry is more sluggish and hence the fast drop. Ong and Ghoniem, IJHE, 41(2016)

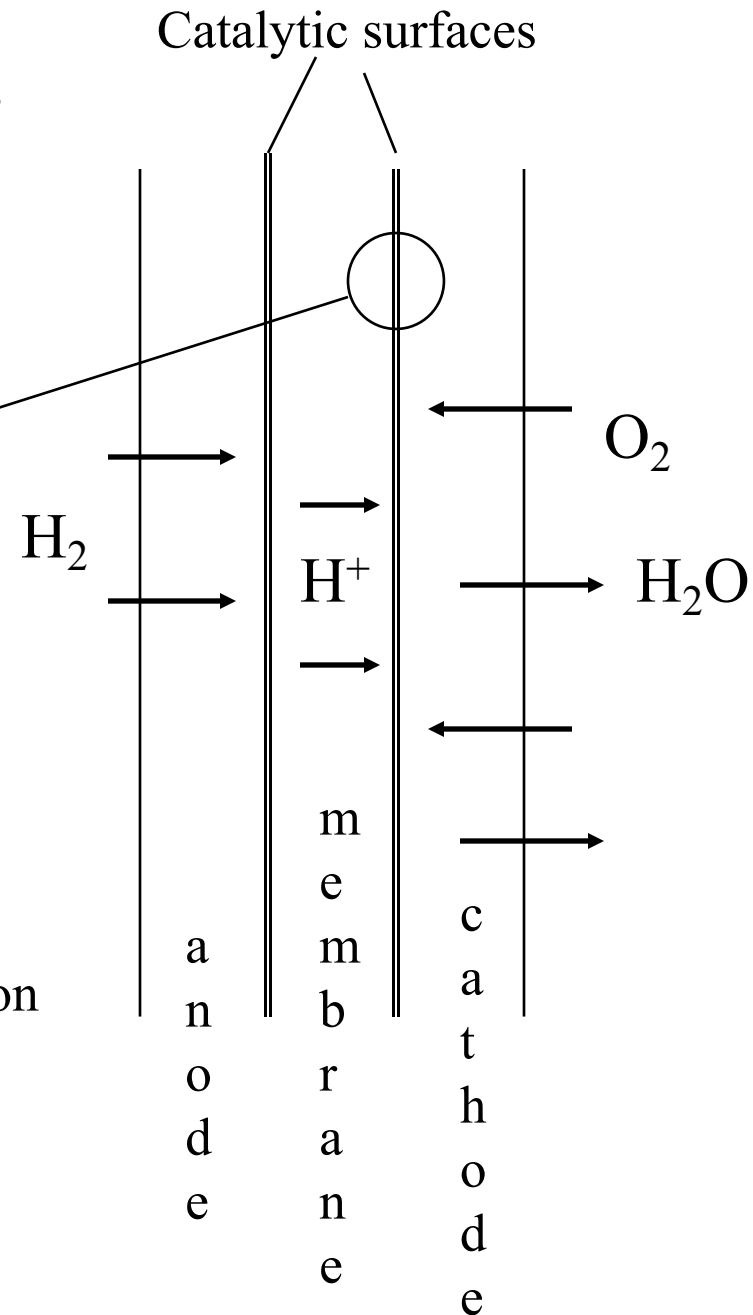
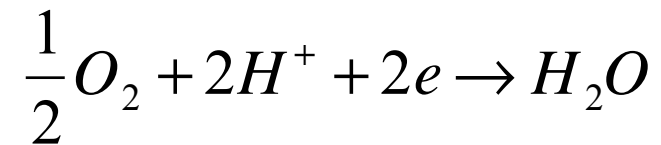
© UHE. All rights reserved. This content is excluded from our Creative Commons license. For more information, see <https://ocw.mit.edu/fairuse>.

Electrochemical Cell Kinetics

One electrochemical (electron transfer) reaction on each side



Overall cathodic (charge transfer) reaction

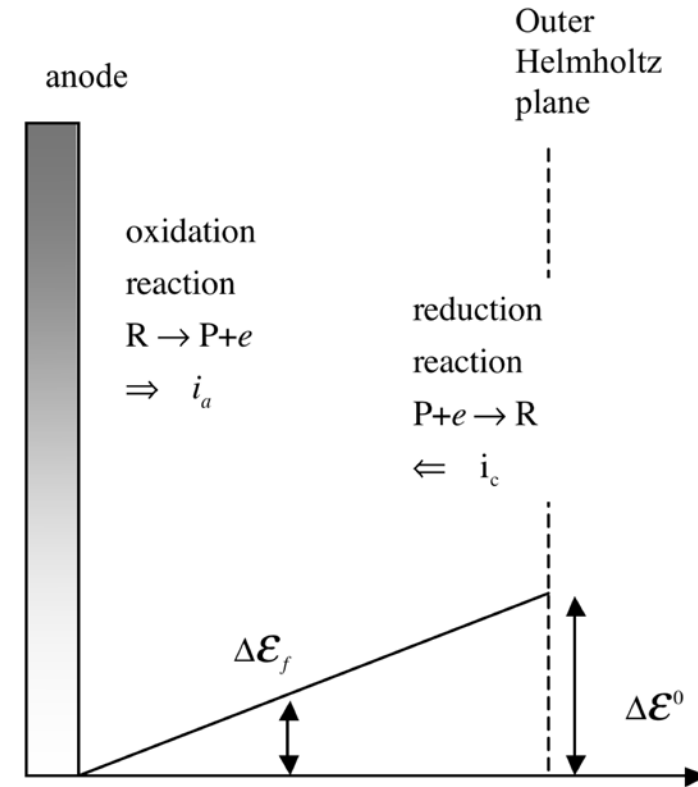


Electrochemical Reaction Kinetics

- The electrochemical reaction on each electrode separates the charge, forming an electric double layer.
- The chemical free energy of the reaction is stored in the electric field.

At Equilibrium, on the electrode surface,

- the chemical free energy and the electrical energy are equal.
- the charge concentrations are equal at the surface and outer plane.
- the net current out of the surface is zero.



The free energy associated with the forward reaction equals the work done to separate the charge

Electrochemical Reaction Kinetics

consider the oxidation reaction:

$$\text{R} \xrightleftharpoons[k_b]{k_f} \text{P} + e$$

the current leaving a surface is $i_a = \mathfrak{S}_a \left(k_f C_R^{(s)} \right)$

on the outer plan, the reverse reaction occurs; $i_c = \mathfrak{S}_a \left(k_b C_p^{(s)} \right)$

the net current is the balance of the two reactions; $i = i_a - i_c$

The reaction rate constant depends on the free energy available to drive the reaction

$$k_{f/b} = \hat{A}_{f/b} \exp \left(-\frac{\Delta G_{f/b}^{\#}}{\mathfrak{R}T} \right)$$

In electrochemistry, we should use total available Gibbs free energy

$$\Delta \hat{G}^{\#} = \Delta \hat{G} + n_e \mathfrak{S}_a \Delta \mathcal{E} \quad \text{where } \Delta \mathcal{E} \text{ is the local electric potential.}$$

the second term is energy consumed in moving the charge through the potential.

Under finite current, nonequilibrium conditions, the net current between the two layers is associated with a potential $\tilde{\eta}$, the "overpotential" And the "*free*" energy available to drive the reaction changes by $\mathfrak{I}_a \tilde{\eta}$. The change of energy is divided between the two layers according to the transfer coefficient, α , $0 \leq \alpha \leq 1$:

$$\Delta G_{af}^{\#} = \Delta G_{af}^{\#0} + \alpha \mathfrak{I}_a \tilde{\eta},$$

$$\Delta G_{ab}^{\#} = \Delta G_{ab}^{\#0} - (1 - \alpha) \mathfrak{I}_a \tilde{\eta},$$

$$k_f = \hat{A}_f \exp\left(-\frac{\Delta G_{af}^{\#0}}{\mathfrak{R}T}\right) \exp\left(-\alpha \frac{\mathfrak{I}_a \tilde{\eta}}{\mathfrak{R}T}\right) = k^0 \exp\left(-\alpha \frac{\mathfrak{I}_a \tilde{\eta}}{\mathfrak{R}T}\right)$$

$$k_b = \hat{A}_b \exp\left(-\frac{\Delta G_{ab}^{\#0}}{\mathfrak{R}T}\right) \exp\left((1 - \alpha) \frac{\mathfrak{I}_a \tilde{\eta}}{\mathfrak{R}T}\right) = k^0 \exp\left((1 - \alpha) \frac{\mathfrak{I}_a \tilde{\eta}}{\mathfrak{R}T}\right)$$

MIT OpenCourseWare
<https://ocw.mit.edu/>

2.60J Fundamentals of Advanced Energy Conversion
Spring 2020

For information about citing these materials or our Terms of Use, visit: <https://ocw.mit.edu/terms>.

Lecture # 10



Electrolysis & Energy Storage

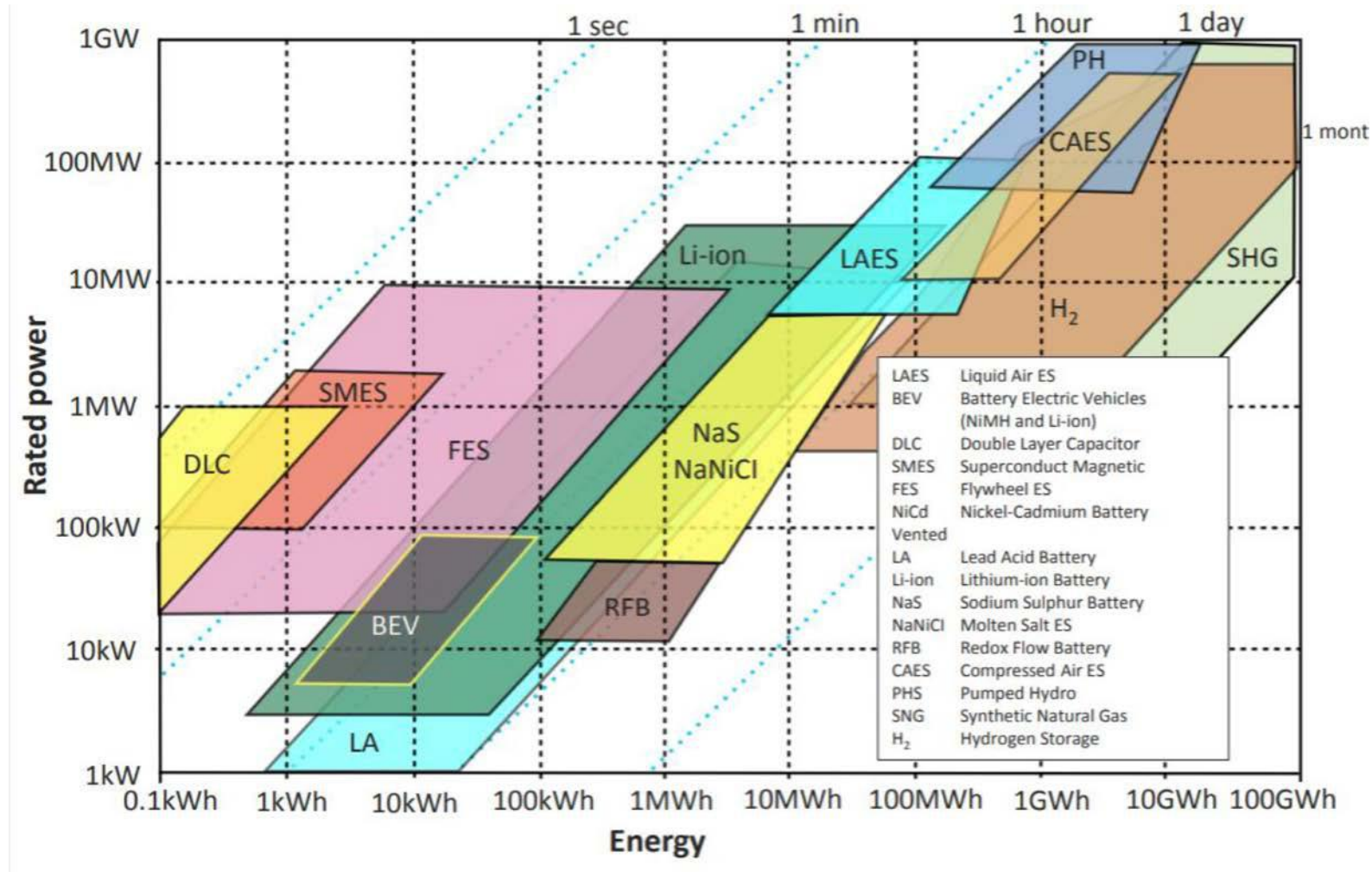
Ahmed F. Ghoniem

March 4, 2020

- Storage technologies, for mobile and stationary applications..
- Fuel Cells and Electrolysis, some more electrochemistry..
- CO₂ reduction/reuse via electrolysis

Shi, Yu et al in Literature/Luo Yu Electrolysis

Energy Storage Capacity



© Source unknown. All rights reserved. This content is excluded from our Creative Commons license. For more information, see <https://ocw.mit.edu/fairuse>.

Hydrogen Production

Hydrogen

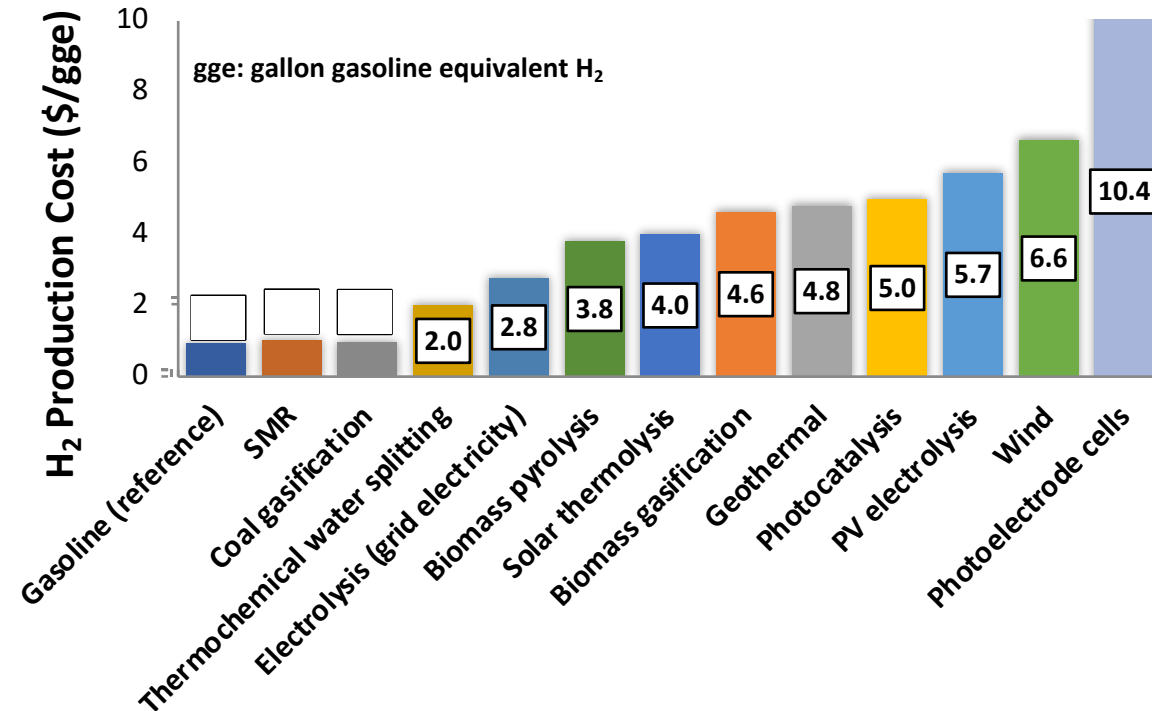
Market of \$152.1B by 2021 ^[1]

Important for oil refining especially heavy and sour crude

Future clean fuel

DOE threshold^[1] (by 2020):
<\$2.00 /gge

IEA suggests^[2] commercial cost target: \$0.3/gge



- Steam reforming has reached peak efficiency (70-85%)
- Novel technology needs to be developed to reach the goal
- Alternatives needed for zero CO₂ emissions

[1] Hydrogen production technical team roadmap, US DRIVE, June 2013.

[2] Hydrogen production and storage: R&D priorities and gaps, IEA 2006

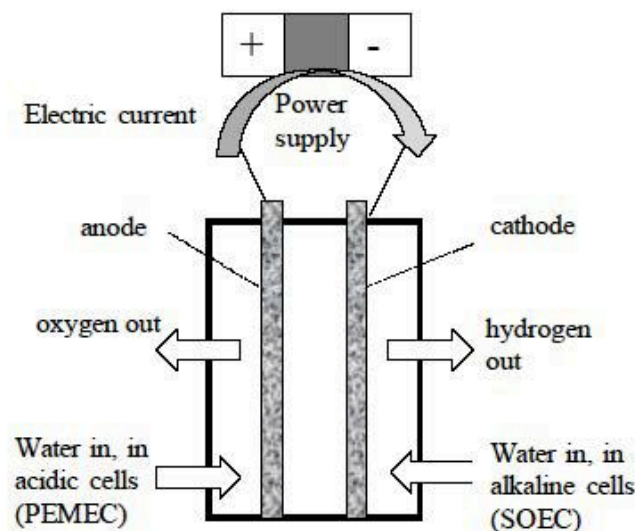
[3] Hosseini (2016) Renew. Sust. Energ. Rev.

[4] **(Photon-based methods):** Dincer (2015) Int. J. Hydro. Energ.;

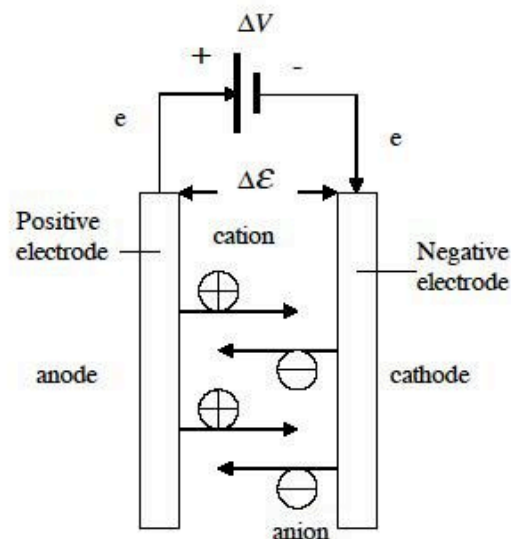
[5] **Geothermal:** Yuksel (2016) Int. J. Hydro. Energ

*All prices exclude compressing, storage, and dispensing costs

In an electrolyzer: a potential difference is externally imposed to force the reversal of the oxidation reactions and reduce water back to H_2 . Under finite current, a potential difference higher than the ideal/OC must be externally imposed to overcome the internal losses or overpotentials.

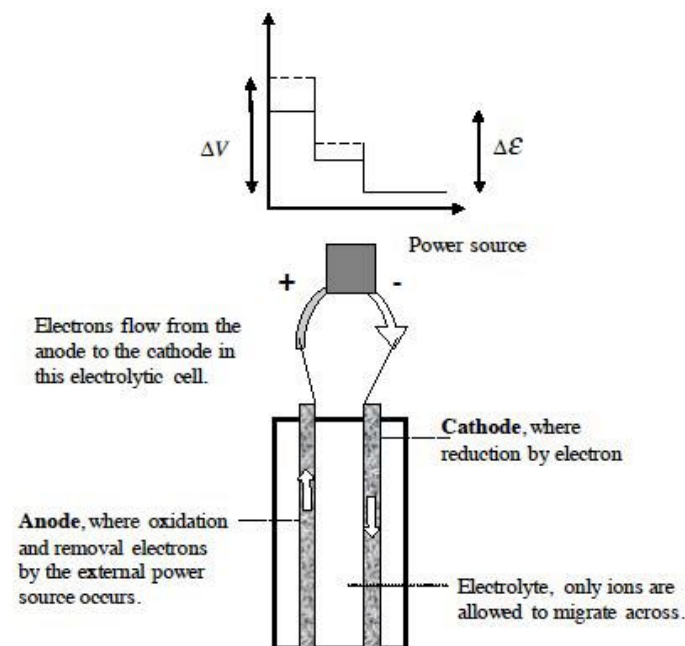


A schematic diagram of an electrolysis cell splitting water into pure oxygen and hydrogen. In an acidic (PEMEC) cell, the electrolyte conducts positive ions, water is introduced on the anode side and hydrogen leaves on the other side. In an alkaline (SOEC) cell, the electrolyte conducts negative ions, water is introduced on the cathode side and hydrogen leaves on the same side.



Electrolytic cell.

A source of electricity is connected to supply a potential to overcome the equilibrium potential of the reaction, $DV > D_e$. The cathode is now negatively charged, supplied externally with electrons, while the anode is positively charged.

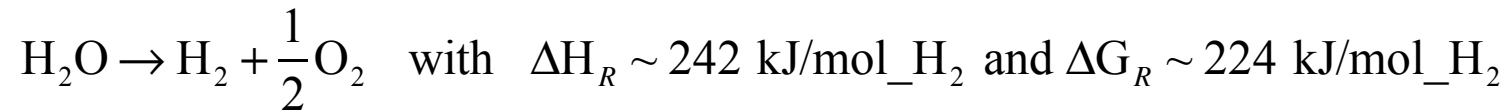


A simple electrolytic cell. Often neutral species are removed from both electrodes. The solid lines in the potential diagram show the equilibrium potential differences, and the broken lines show the case under finite current operation.

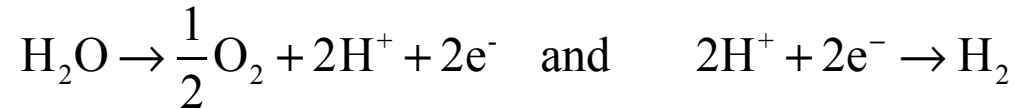
Electrolysis reduces water back to H₂

Can be used to store an “infinite” amount of energy (from electricity) in the form of chemical energy
Operates as the reverse of a fuel cell

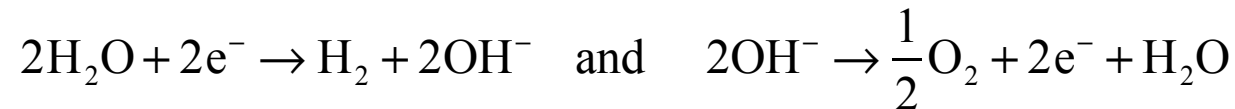
Overall Reaction:



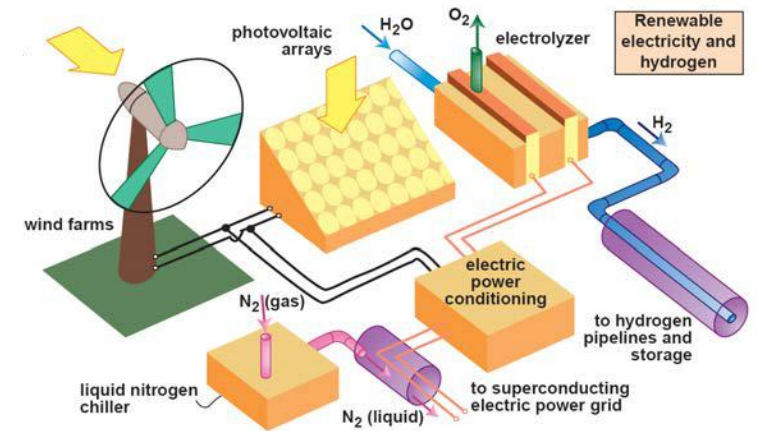
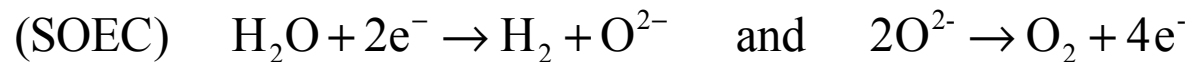
In an acidic (electrolyte transporting +ve ions) cell (PEM):



In an alkline (electrolyte transporting -ve ions) cell:

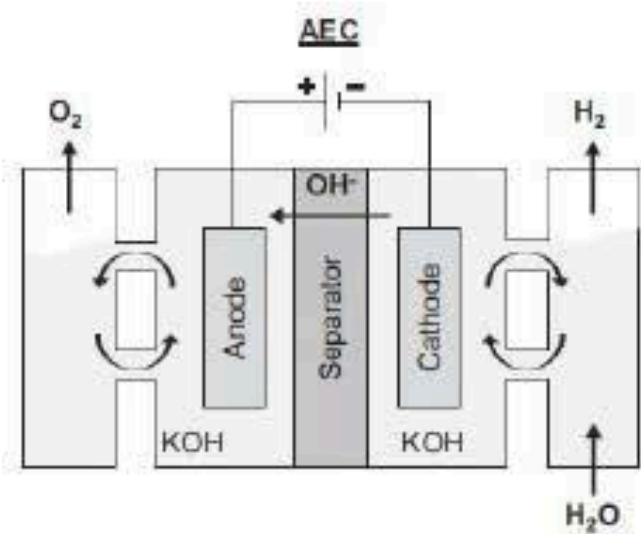
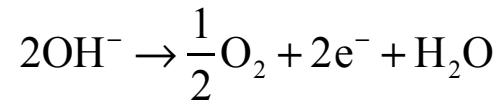
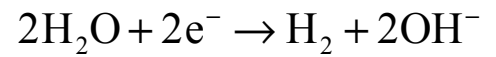


In Solid Oxide (electrolyte transporting -ve ions) cells:

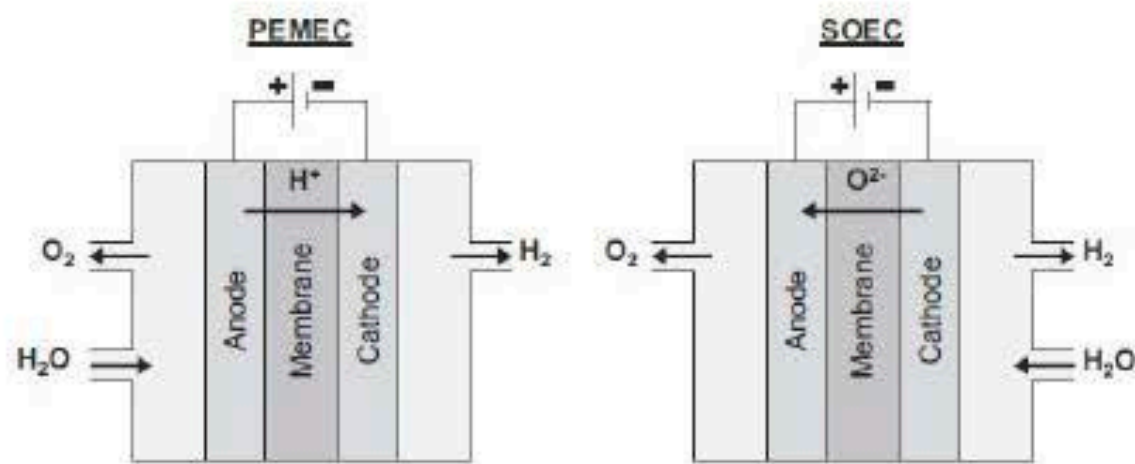
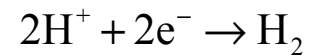
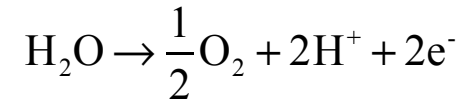


© Source unknown. All rights reserved. This content is excluded from our Creative Commons license. For more information, see <https://ocw.mit.edu/fairuse>.

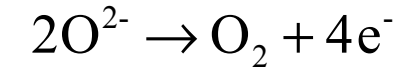
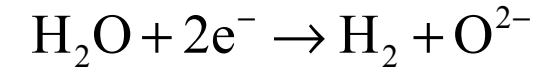
(AEC)



(PEM):



(SOEC)

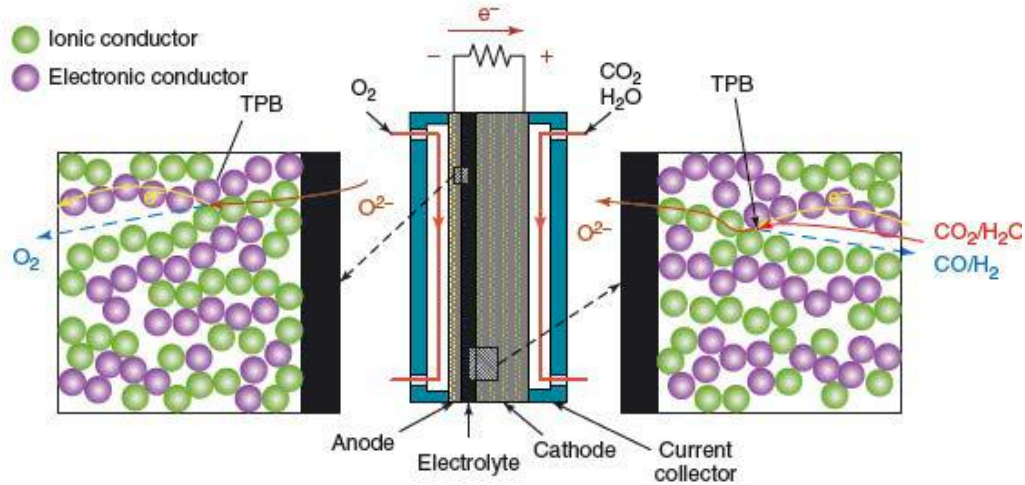


Schmidt, A. 2017, Int. J. Hydrog. Energy

Courtesy Elsevier, Inc., <http://www.sciencedirect.com>. Used with permission.

	Alkaline (AEC) (~\$1/W)	Polymer (PEMEC) (~\$2/W)	Solid Oxide (SOEC) (>\$2/W)
Pros	Widely Deployed No rare materials Long Life	High Pressure High Power Density Fast response	Least Electricity Required Fast Kinetics No rare materials
Cons	Low Power Density	Rare Materials (Pt, Ir)	Less deployed/ more risk

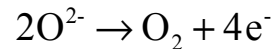
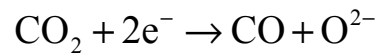
CO₂ Reuse



Electrolysis can be used to split water and/or CO₂
 But similar to SOFC's the high T solid oxide type is more compatible with CO₂ splitting



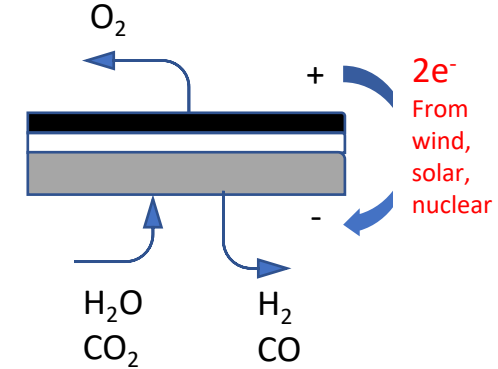
In an alkalyine (electrolyte transporting -ve ion) SOEC cell:



Solid Oxide Electrolysis and Fuel Cells

Oxygen electrode
 $\text{O}^{2-} \rightarrow \frac{1}{2}\text{O}_2 + 2\text{e}^-$

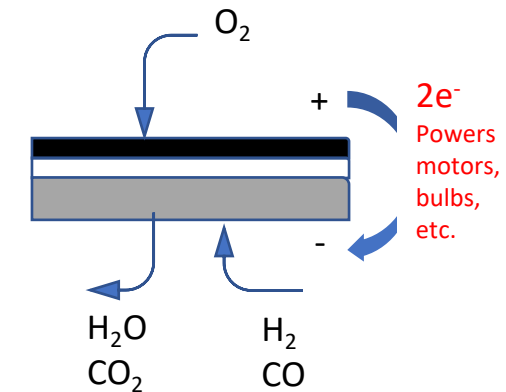
Fuel electrode
 $\text{H}_2\text{O} + 2\text{e}^- \rightarrow \text{H}_2 + \text{O}^{2-}$
 $\text{CO}_2 + 2\text{e}^- \rightarrow \text{CO} + \text{O}^{2-}$



SOEC

Oxygen electrode
 $\frac{1}{2}\text{O}_2 + 2\text{e}^- \rightarrow \text{O}^{2-}$

Fuel electrode
 $\text{H}_2 + \text{O}^{2-} \rightarrow \text{H}_2\text{O} + 2\text{e}^-$
 $\text{CO} + \text{O}^{2-} \rightarrow \text{CO}_2 + 2\text{e}^-$



SOFC

Electrolysis reduces water back to H₂

Can be used to store an “infinite” amount of energy (from electricity) in the form of chemical energy

Operates as the reverse of a fuel cell

The thermodynamics are very similar to that of a fuel cell

$$Q - W = H_{out} - H_{in} = \Delta H_R \quad \text{and} \quad \frac{Q}{T^*} = S_{out} - S_{in} = \Delta S_R$$

$$-W = (H - TS)_{out} - (H - TS)_{in} = \Delta H_R - T\Delta S_R$$

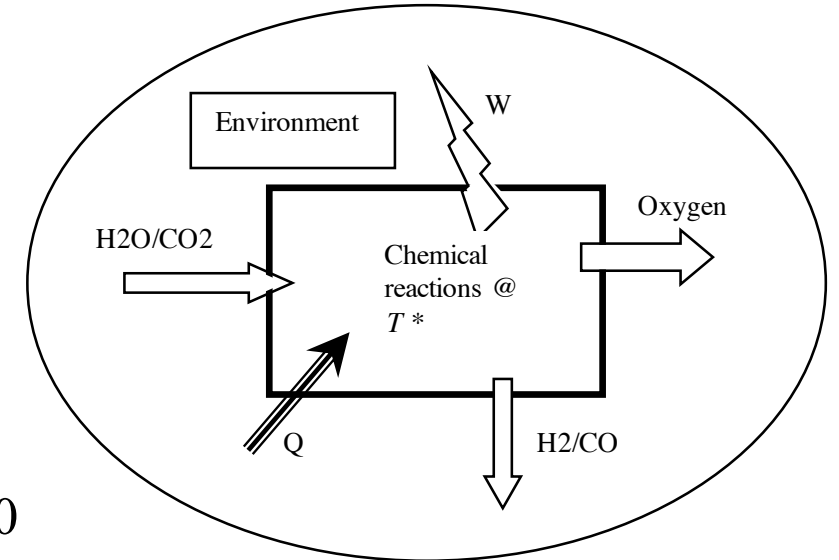
$$W = -\Delta G_R \quad \text{and} \quad Q = T\Delta S_R$$

$$Q = T\Delta S_R = \Delta H_R - \Delta G_R$$

reversing the original (FC) reaction, we have $\Delta H_R > 0$ and $\Delta G_R > 0$

In electrolysis, both work is added and heat is added (when $\Delta H_R > \Delta G_R$)

A fuel cell produces work and rejects heat, an electrolyzer needs both



$$W = -\Delta G_R \quad (\text{electricity})$$

$$Q = T\Delta S_R = \Delta H_R - \Delta G_R \quad (\text{heat})$$

In electrolysis, both work and heat are added

at 400 °K, $\Delta H_R \sim 242$ and $\Delta G_R \sim 224$ kJ/mol,
thus, $W = -224$ and $Q = 18$ kJ/mol.

at 1000 °K, $\Delta H_R \sim 245$ and $\Delta G_R \sim 193$ kJ/mol,
thus, $W = -193$ and $Q = 52$ kJ/mol

At higher temperature, need less work & more heat!

Open circuit voltage (similar to fuel cells),

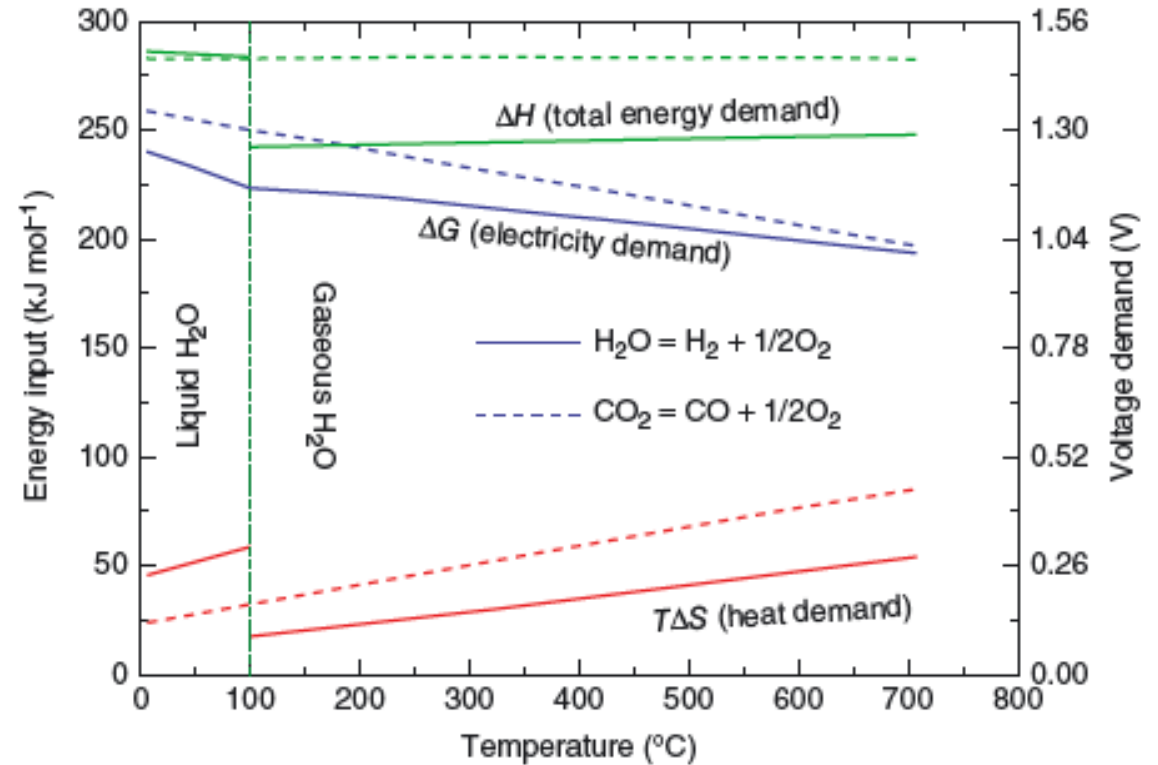
$$-W = \Delta G_R = -\Delta \mathcal{E} \zeta = -\Delta \mathcal{E} n_e \mathfrak{I}_a$$

$\mathfrak{I}_a = e^- N_a = 9.6485 \times 10^4$ Coulombs/mole
for water splitting,

at 400 °K, $\Delta \mathcal{E} \sim 1.1$ V,

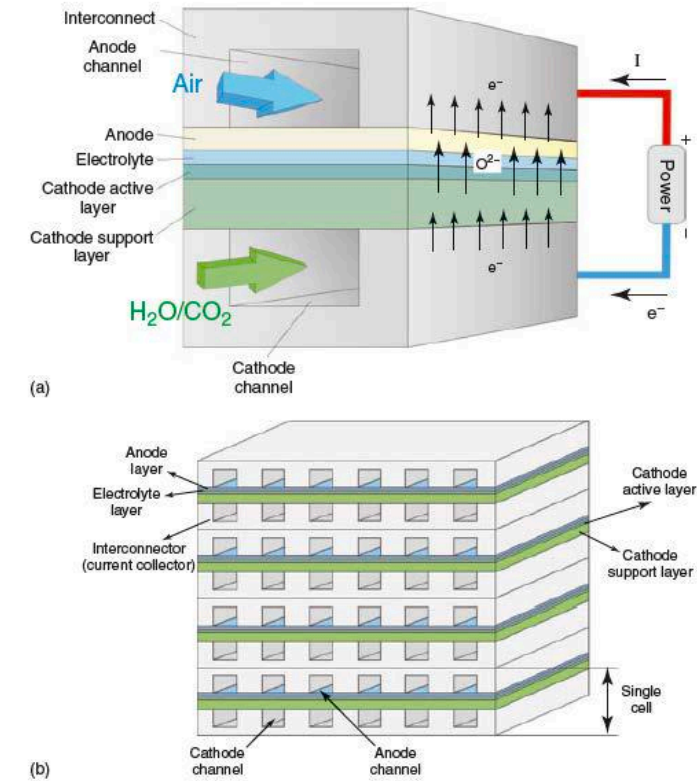
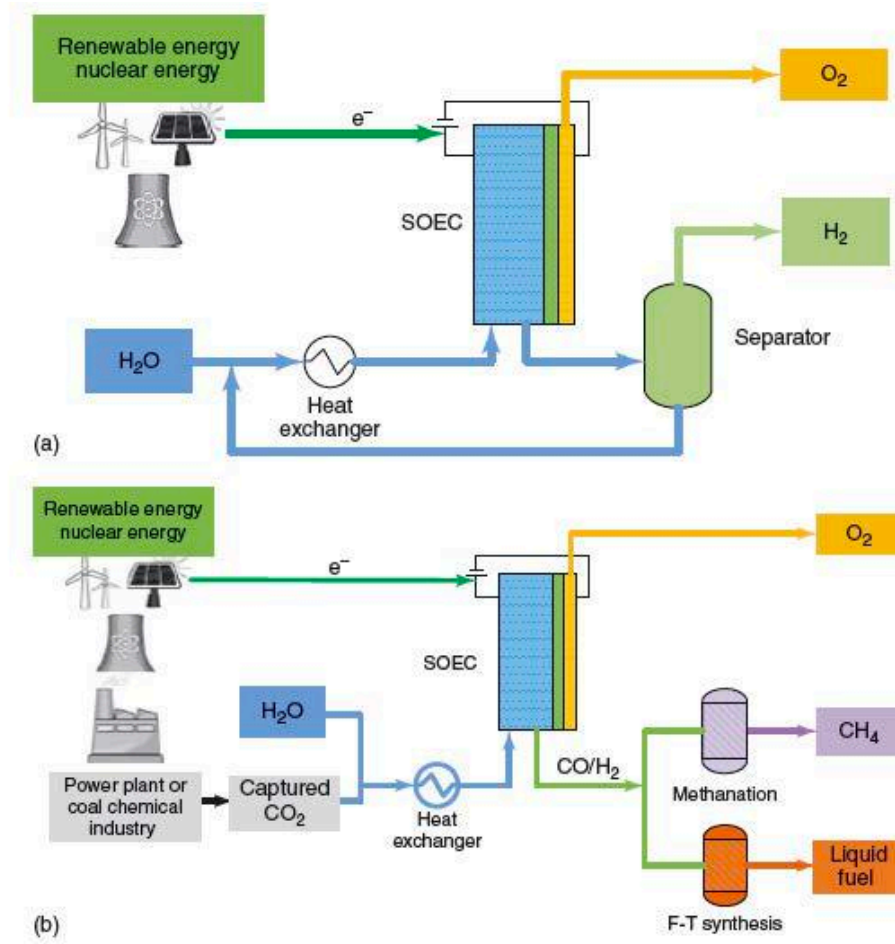
at 1000 °K, $\Delta \mathcal{E} \sim 0.86$ V.

Thermodynamics of Eletrolysis



- In electrolysis, work demand decreases while heat demand increases with temperature
- Electrolysis can also be used to reduce CO₂ back to CO (but there are material challenges). The energy requirements are higher.

Electrolysis for production of H₂ and/or co-production of H₂/CO and synthesis fuels



(a) Single element
(b) A stack

© Wiley. All rights reserved. This content is excluded from our Creative Commons license. For more information, see <https://ocw.mit.edu/fairuse>.

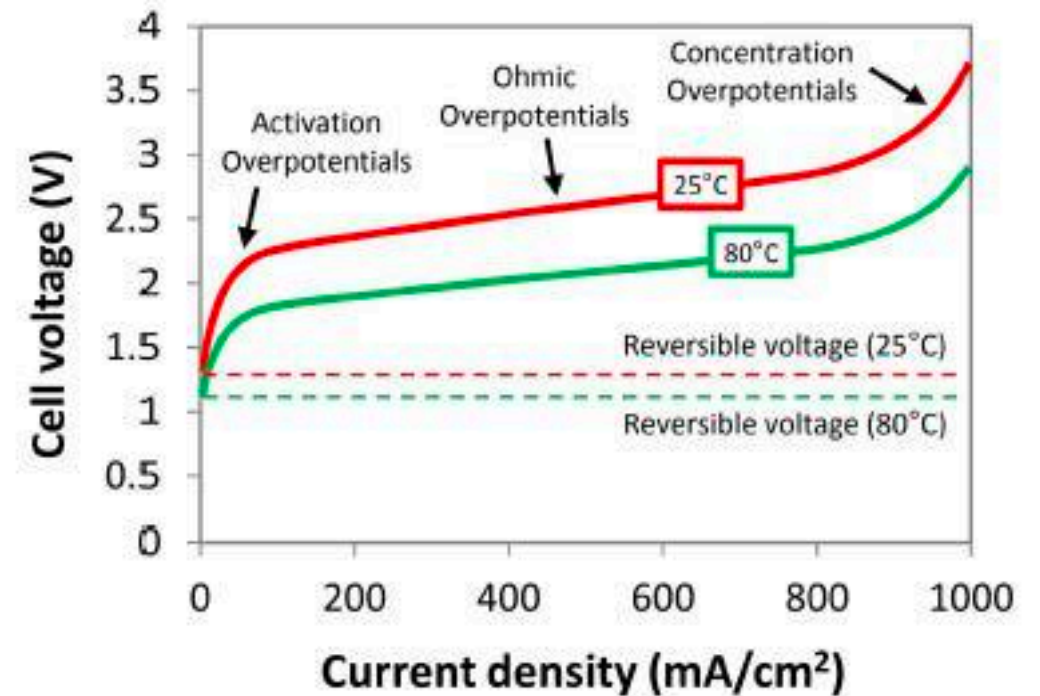
At finite current, an electrolyzer suffers from the same losses as a FC, generating positive internal voltage drop that must be compensated for externally,

$$\Delta \mathcal{E}_{EC} = \Delta \mathcal{E}^o + \tilde{\eta}_{a,act} + \tilde{\eta}_{a,conc} + \tilde{\eta}_{a,FU} + \tilde{\eta}_{el,oh} + \tilde{\eta}_{c,act} + \tilde{\eta}_{c,conc} + \tilde{\eta}_{a,FU}$$

$\tilde{\eta} \equiv$ (positive) overpotential

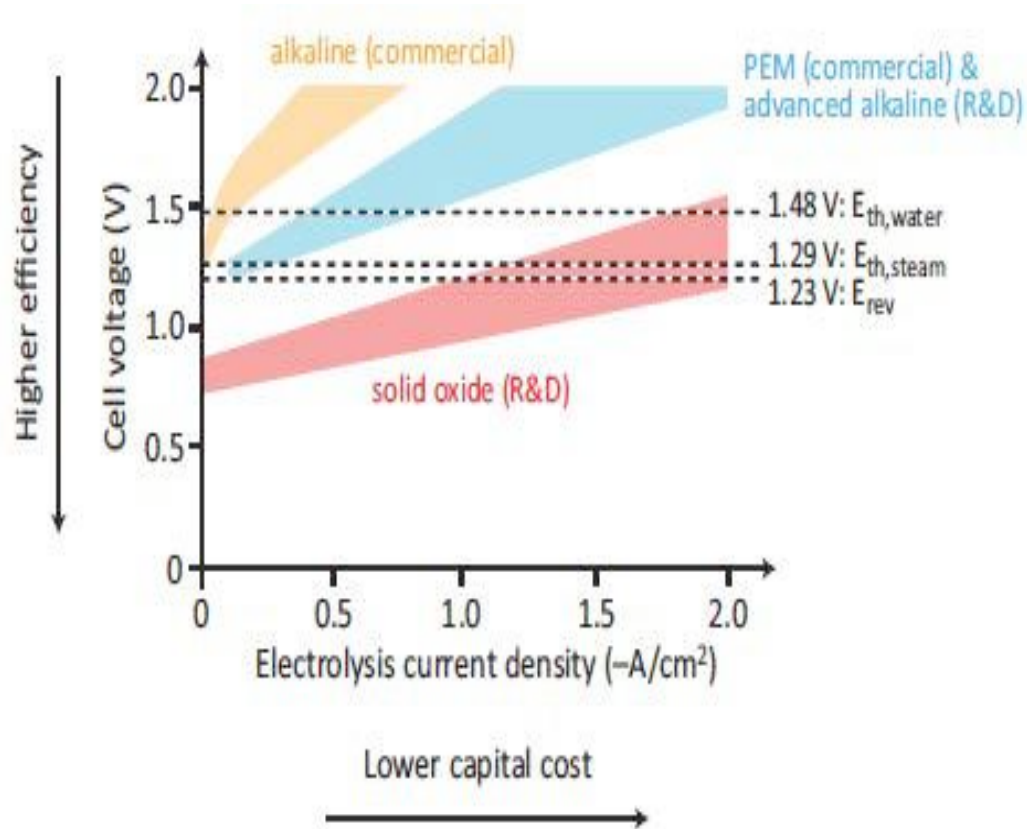
Therefore, the imposed external potential difference in electrolysis must be higher than the open circuit potential. The difference between the actual imposed potential difference and the open circuit values are expected to be of the same order of magnitude to those in fuel cells, at the same current (see two sides arrows in figure).

In this case, the difference between the ideal work and actual work is heat dissipated in the cell, which is typically the heat required by first law analysis.



B

Reversible voltage (zero current) and actual voltage of an electrolyzer at finite current at different T. Lower T reduces the OC voltage, but at finite current, kinetics are sluggish and diffusivity is lower leading to more losses and higher operating voltage



Typical I-V curve of a number of electrolyzers for water splitting, including low T commercial and advanced alkaline (PEM transporting OH^- ions) and solid oxide (SOEC). These are more complex than FC I-V curves, especially for SOEC because of the use of internal dissipation to supply thermal energy

From Luo et al. Applied Energy, 215 (2018).
Note the “negative” current increasing towards the left.

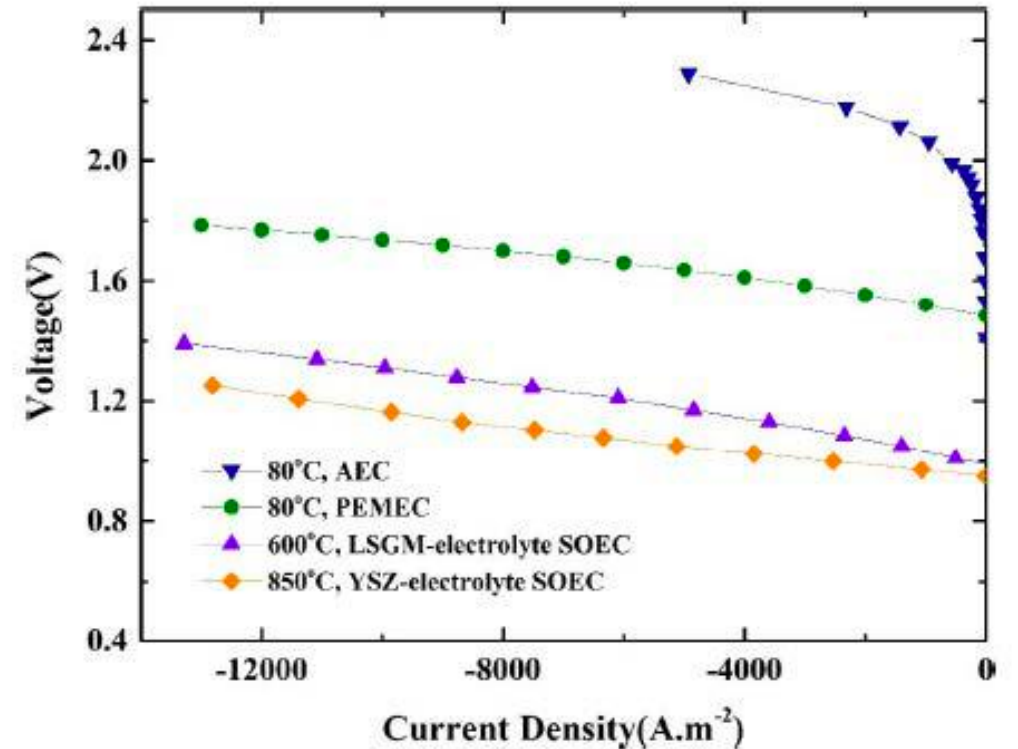


Fig. 3. Typical polarization curves of PEMEC, AEC, LSGM-electrolyte SOEC, and YSZ-electrolyte SOEC [32,33,35,36] for H_2O electrolysis.

- [32] Ebbesen SD, Graves C, Mogensen M. Int J Green Energy 2009;6:646–60.
- [33] Wendel CH, Gao Z, Barnett SA, Braun RJ. J Power Sources 2015;283:329–42.
- [35] Han B, Mo J, Kang Z, Zhang FY. Electrochim Acta 2016;188:317–26.
- [36] Miles MH, Kissel G, Lu PWT, Srinivasan SJ Electrochem Soc 1976;123:332–6.

Both images courtesy Elsevier, Inc., <http://www.sciencedirect.com>. Used with permission.

At finite current, it is *not* necessary to supply heat to the electrolysis cell externally, internal dissipation is sufficient to generate the necessary heat. Therefore only electricity is needed, at the *actual* potential (including the overpotentials) required to run the electrolysis reactions. The heat generation rate is $I(V-V_{oc})$.

Several efficiencies are usually defined: a second law efficiency, and a first law like efficiency which can be based on either the enthalpy or Gibbs free energy of the produced hydrogen:

$$\eta_{II} = \frac{\Delta \varepsilon_{OC}}{\Delta \varepsilon}$$

$$\eta_{thermal} = \frac{J_{H_2} \cdot \Delta \hat{h}_{R,H_2}}{i \cdot \Delta \varepsilon}$$

$$\eta_{work} = \frac{J_{H_2} \cdot \Delta G_{R,H_2}}{i \cdot \Delta \varepsilon}$$

Anode	Cathode	Electrolyte	T (C)	Cell Voltage (V)	η_{th}	η_{II}	
IrO ₂					89.70%	74.55%	
Ir _{0.6} Ru _{0.4} O ₂		Nafion 115	90	1.567	94.45%	78.49%	
IrO ₂		Nafion 112	80	1.63	90.80%		
Ir _{0.5} Ru _{0.5} O ₂		Nafion 112	80	1.65	89.70%		
Ir		Nafion 112	80	1.72	86.05%		
Ru		Nafion 112	80	1.79	82.68%		
IrO ₂ nano film		Nafion 117	80	1.83	80.87%		
Ir Black		Nafion 115	90	1.7	87.06%		
Ir Black		Nafion 115	90	1.67	88.62%		
Ir Black		Nafion 115	90	2.45	60.41%		
Ir Black		Nafion 115	90	2	74.00%		
20%RuO ₂ /ATO (SnO ₂)							

Efficiency of a number of PEMEC. Note that the conditions at which these efficiency were determined could be very different, that is, the current or hydrogen production rate. The thermal efficiency is higher than the voltage efficiency because of the internal use of the heat generated by dissipation (Le Chang).

$$\eta_{II} = \frac{\Delta \varepsilon_{OC}}{\Delta \varepsilon}$$

$$\eta_{thermal} = \frac{J_{H_2} \cdot \Delta \hat{h}_{R,H_2}}{i \cdot \Delta \varepsilon}$$

$$\eta_{current} = \frac{J_{H_2}}{n_e \mathfrak{I}_a i}$$

recall that under ideal conditions

$$J_{H_2} = n_e \mathfrak{I}_a i$$

Anode Electrolyte Cathode	T°C	Voltage (V)	Current Density (A/cm ²)	Hydrogen Production Rate (umol/s cm ²)	$\eta_{current}$	η_{II}
YSZ Y ₂ O ₃ +Zr/YSZ LaMnO ₃				1.73		
Ni-YSZ YSZ LaCoO		1.31	0.13	0.35		
Y-ZrO ₃ ScSZ LSM		1.4	0.38	1.94		
Ni-CGO Y _{0.2} Ce _{0.8} O _{1.9} LSCF		1.22	0.4	2.04		
Ni+YSZ YSZ LSM+YSZ		1.3	0.32	1.58		
LSM-YSZ YSZ LSCM-YSZ		1.6	1.25	6.36		
Ni-YSZ YSZ LaSrCrMnO ₃						

Performance of solid oxide electrolysis cells, shown in terms of the current efficiency (less than 100% due to leakage, etc.), and the second law efficiency. Different values were determined under different conditions (not always defined clearly in publications). The “thermal” efficiency can be higher because more heat is generated and used in the reactions, but the values are somewhat arbitrary Le Chang)!

MIT OpenCourseWare
<https://ocw.mit.edu/>

2.60J Fundamentals of Advanced Energy Conversion
Spring 2020

For information about citing these materials or our Terms of Use, visit: <https://ocw.mit.edu/terms>.

Lecture # 11



Batteries & Energy Storage

Ahmed F. Ghoniem

March 9, 2020

- Storage technologies, for mobile and stationary applications ..
- Batteries, primary and secondary, their chemistry.
- Thermodynamics and electrochemistry
- Performance,

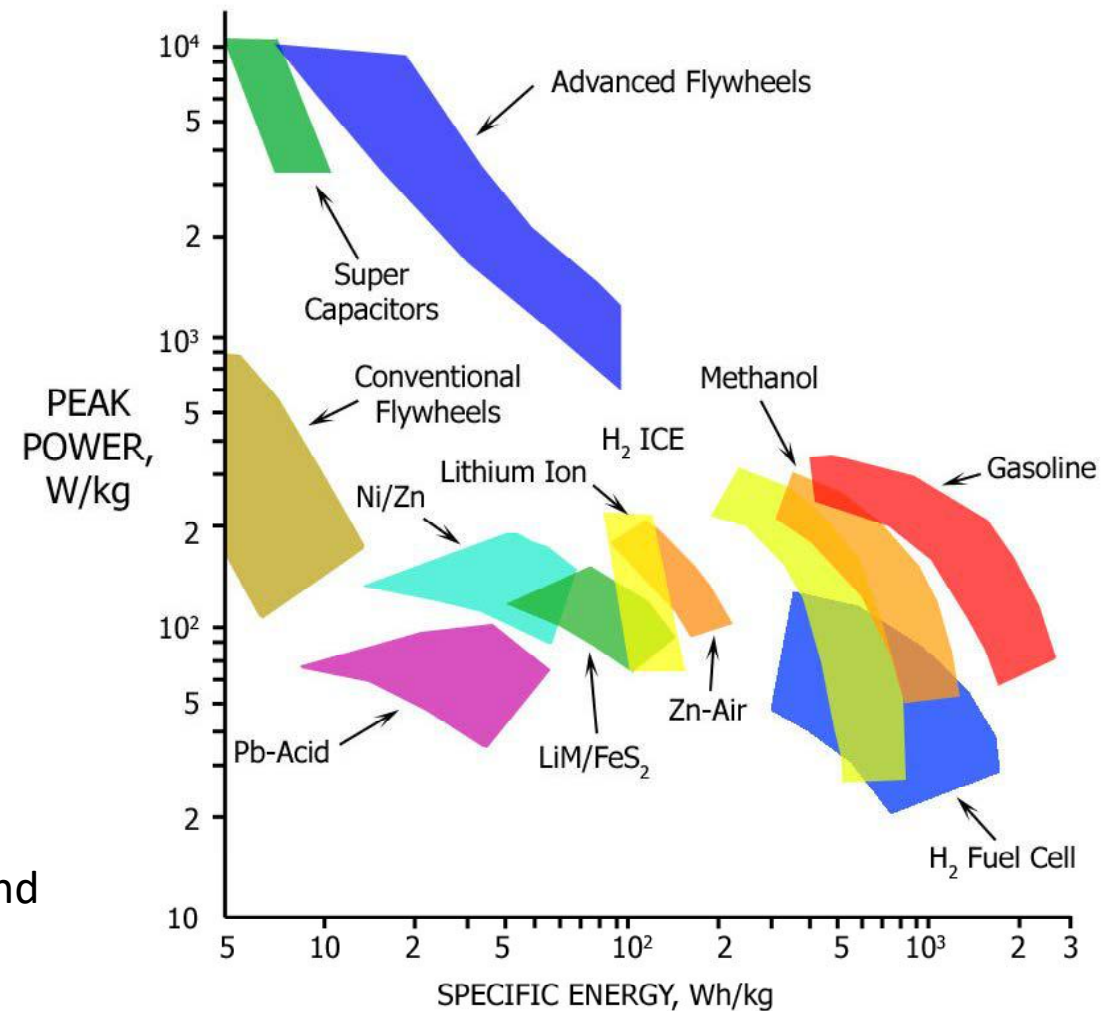
THE RAGONE DIAGRAM is more applicable to mobile applications.
Electric mobility is totally dependent on battery storage.

an important definition:

Round trip efficiency:

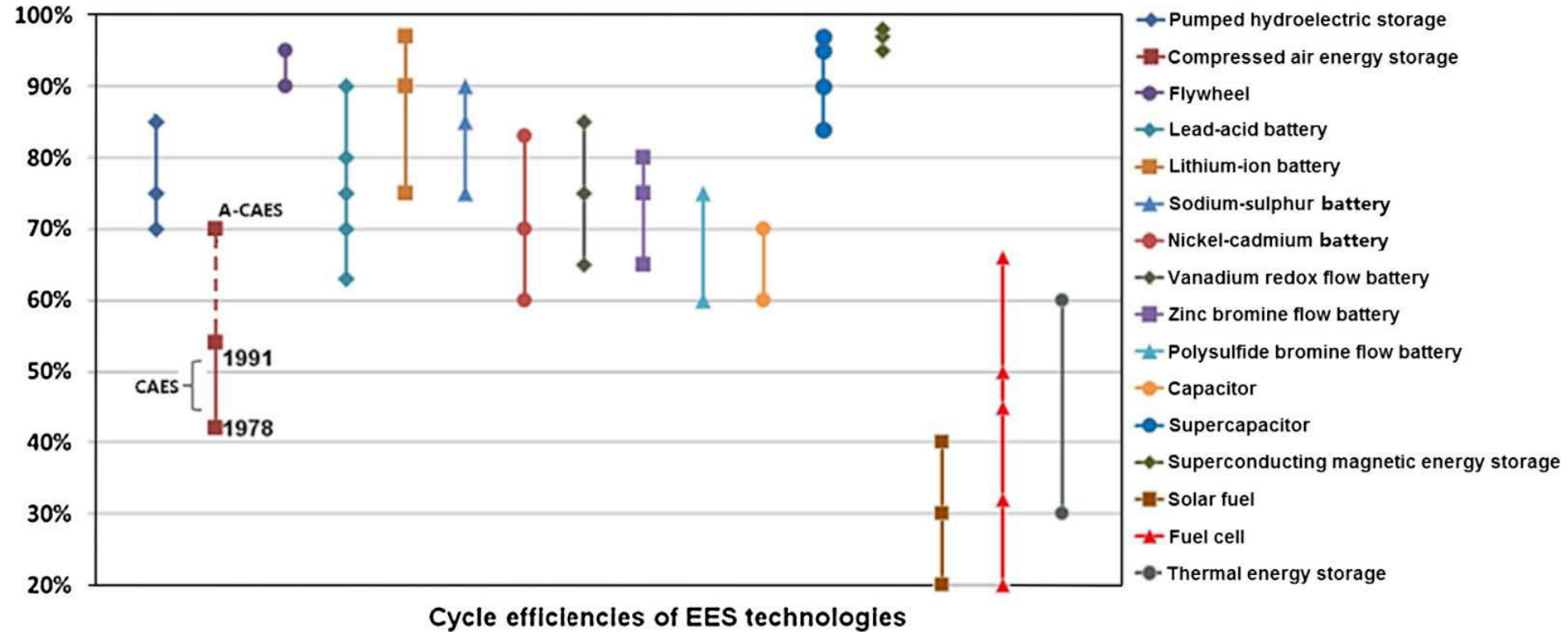
$$\eta_{round} = \eta_{charge} \eta_{discharge}$$

For stationary applications, criteria for selection and hence technologies can be very different.



© Source unknown. All rights reserved. This content is excluded from our Creative Commons license. For more information, see <https://ocw.mit.edu/fairuse>.

THE RAGONE DIAGRAM. Figure shows approximate estimates for peak power density and specific energy for a number of storage technology mostly for mobile applications.



Round-trip efficiency of electrical energy storage technologies. Markers show efficiencies of plants which are currently in operation.

Courtesy Elsevier, Inc., <http://www.sciencedirect.com>. Used with permission.

Xing Luo, et al. Applied energy, 137:511–536, 2015.
 Niklas Hartmann, et al. Applied Energy, 93:541–548, 2012.
 Behnam Zakeri and Sanna Syri. 42:569–596, 2015.

Energy Storage: Overview and other options

The table shows technologies for stationary and mobile applications including mechanical and electrochemical. Capacitors are integral parts of mobile storage!

Not inclusive and other options are available and under development.

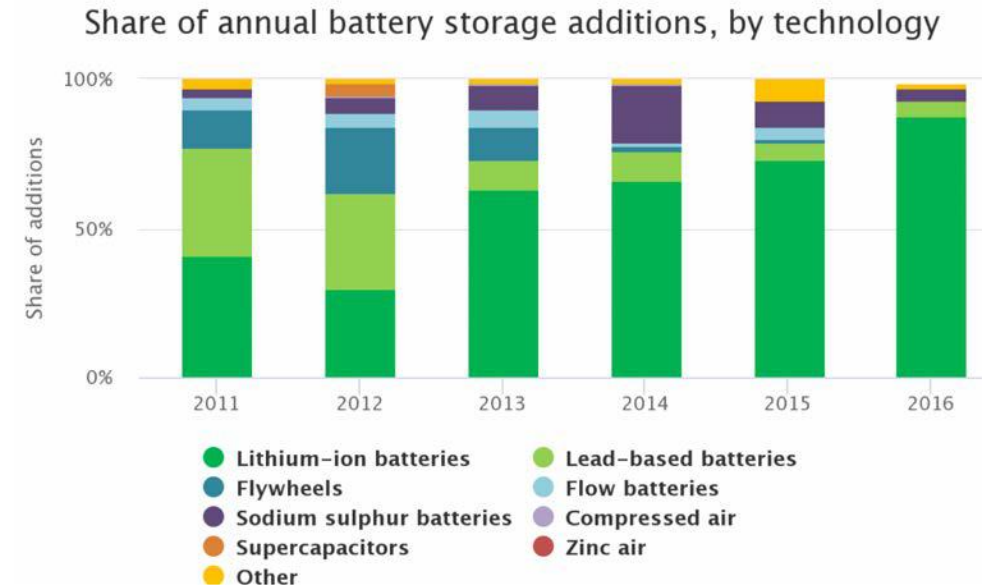
Does not show thermal (storage) and chemical (hydrogen, fuels and thermochemical) options which are very important.

Prices change constantly but comparison is still reasonable.

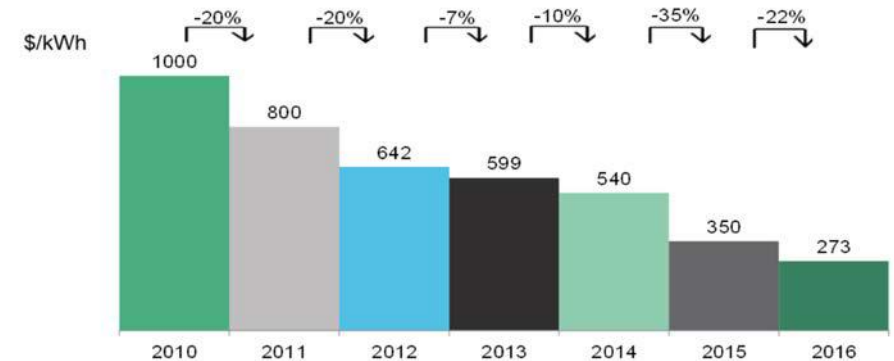
Characteristic	PHS	CAES	Batteries	Flywheel
<i>Energy Range (MJ)</i>	1.8x10 ⁶ - 36x10 ⁶	180,000- 18x10 ⁶	1,800 – 180,000	1 – 18,000
<i>Power Range (MW)</i>	100-1000	100-1000	0.1 – 10	1-10
<i>Overall Cycle Efficiency</i>	64-80%	60-70%	~75%	~90%
<i>Charge/Discharge Time</i>	Hours	Hours	Hours	Minutes
<i>Cycle Life</i>	10,000	10,000	2,000	10,000
<i>Footprint/Unit Size</i>	Large if above ground	Moderate if under ground	Small	Small
<i>Siting Ease</i>	Difficult	Difficult- Moderate	N/A	N/A
<i>Maturity</i>	Mature	Development	Mature except for flow type	Development
<i>Estimated Capital Costs - Power (\$/kWe)</i>	600 – 1,000	500-1,000	100-200 (LA)	200 - 500
<i>Estimated Capital Costs - Energy (\$/kWh)</i>	10 - 15	10 - 15	150-300	100 - 800

Batteries

- Similar to fuel cells in that they convert chemical to electrical energy directly, and the secondary type can reverse the reactions
- But they store their chemicals internally in their electrodes (except for flow batteries)
- Have seen a very wide range of applications, at many scales for centuries!
- Still relatively expensive for large scales storage deployment, although convenient.
- Also heavier than ideal in mobile application.
- Must be carefully managed thermally to avoid thermal run away and fires.

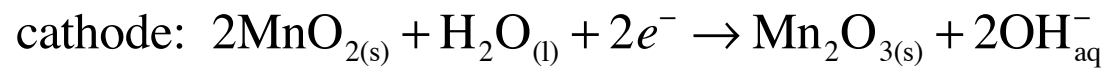
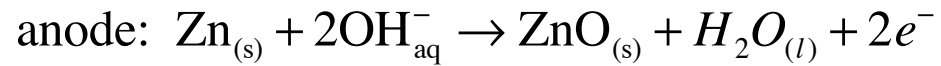
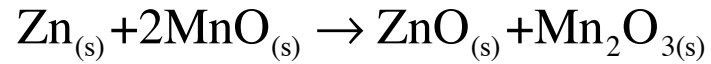


BNEF lithium-ion battery price survey, 2010-16 (\$/kWh)



Both images © Source unknown. All rights reserved. This content is excluded from our Creative Commons license. For more information, see <https://ocw.mit.edu/fairuse>.

Primary Batteries: the alkaline dry cell

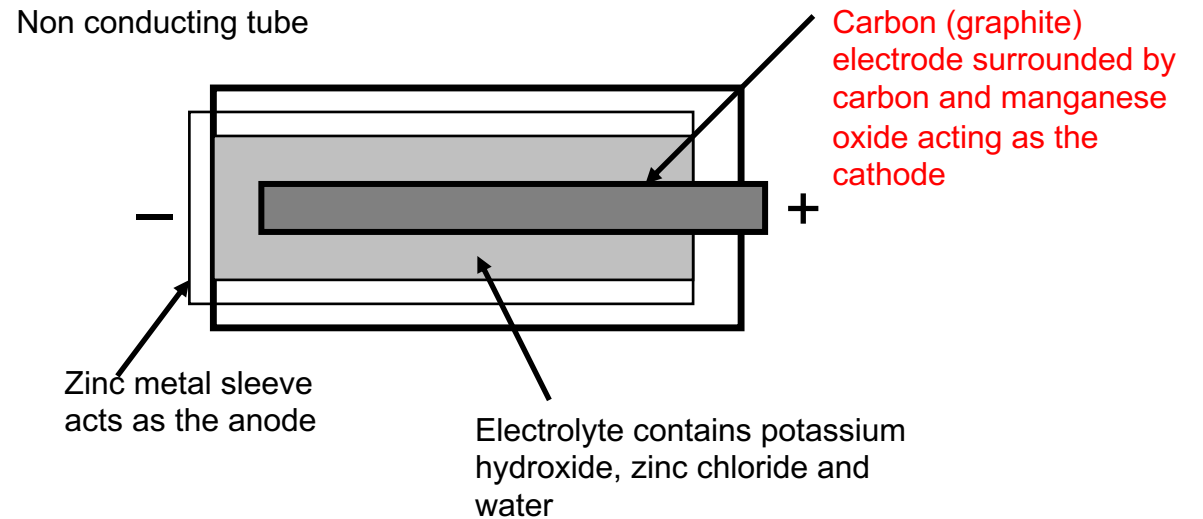


$$\Delta G_R^o = -277 \text{ kJ/mol}, \quad n_e = 2$$

$$\Delta \mathcal{E}_o = \frac{277000}{96485 \times 2} = 1.44 \text{ V}$$

Zn: Zink

Mn: Manganese



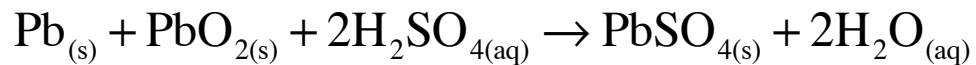
A schematic drawing showing the internal detail of an alkaline battery

Secondary Batteries: The Lead Acid Battery

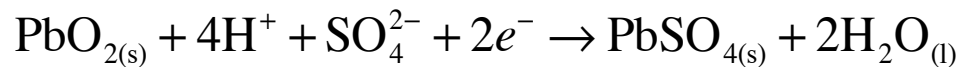
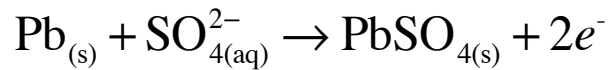
(look under the hood)

a lead electrode and a lead oxide electrode are immersed in sulfuric acid-water solution

During discharge:



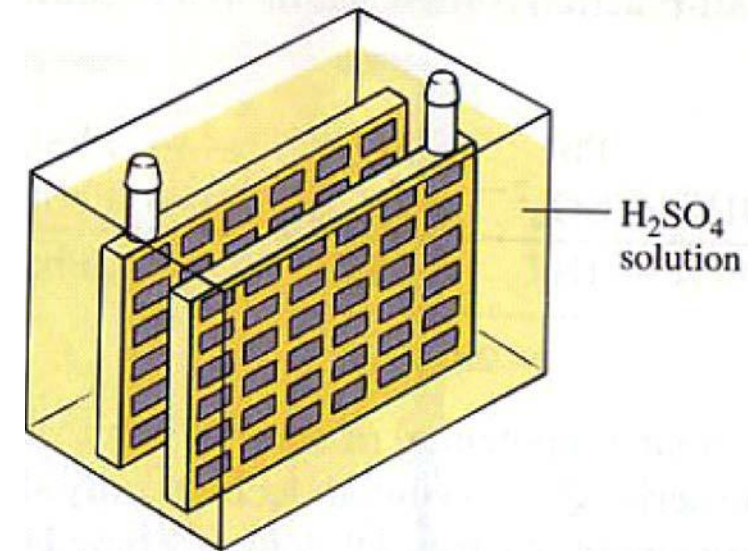
The Redox reactions:



$$\Delta\mathcal{E} = 2.04\text{V}$$

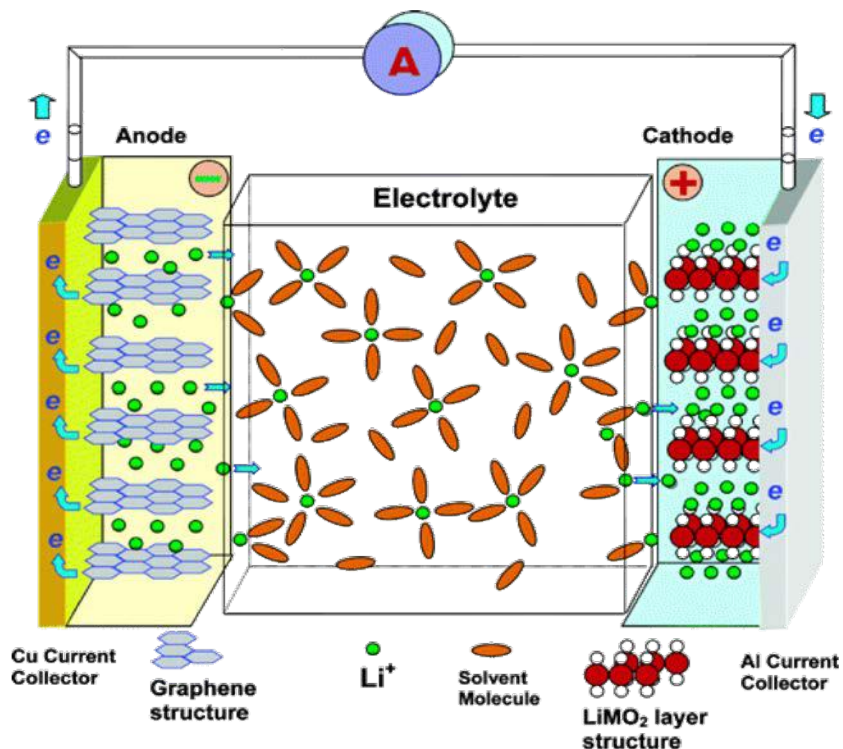
During charging, the above reactions are reversed by applying an external voltage.

Lead acid batteries charge below this value to prevent water electrolysis
can be dangerous but used extensively in cars, etc.



© Source unknown. All rights reserved. This content is excluded from our Creative Commons license. For more information, see <https://ocw.mit.edu/fairuse>.

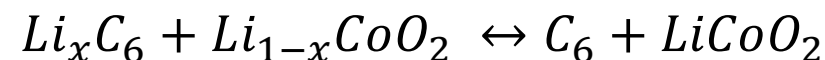
Lithium-ion batteries



Xu, K. Electrolytes and interphases in Li-ion batteries and beyond. *Chem. Rev.* **114**, 11503–11618 (2014).

© American Chemical Society. All rights reserved. This content is excluded from our Creative Commons license. For more information, see <https://ocw.mit.edu/fairuse>.

- During operation, reversible Li^+ intercalation (insertion) into the layered electrodes' materials (leaving graphite anode during discharge).
- The overall reaction, where x is the fraction of the anode Li leaving and joining the cathode lithium cobalt oxide:

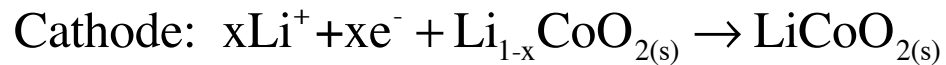
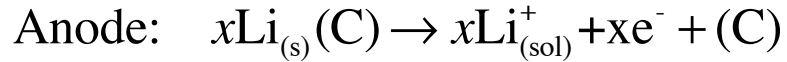


- Forward reaction: discharge ($\Delta G < 0$), Li^+ move towards cathode, as shown in figure
- Reverse reaction: charge ($\Delta G > 0$)

- Anode (-ve electrode, electrons leaving): Li metal and graphite
- Cathode (+ve electrode, electrons returning): Metal oxides (MnO_2 , CoO_2 , LiFePO_4)
- Electrolyte: Organic solvents, carbonates and lithium salts (LiPF_6)
- Current collectors, Cu on the anode side and Al on the cathode side.

Lithium-ion batteries

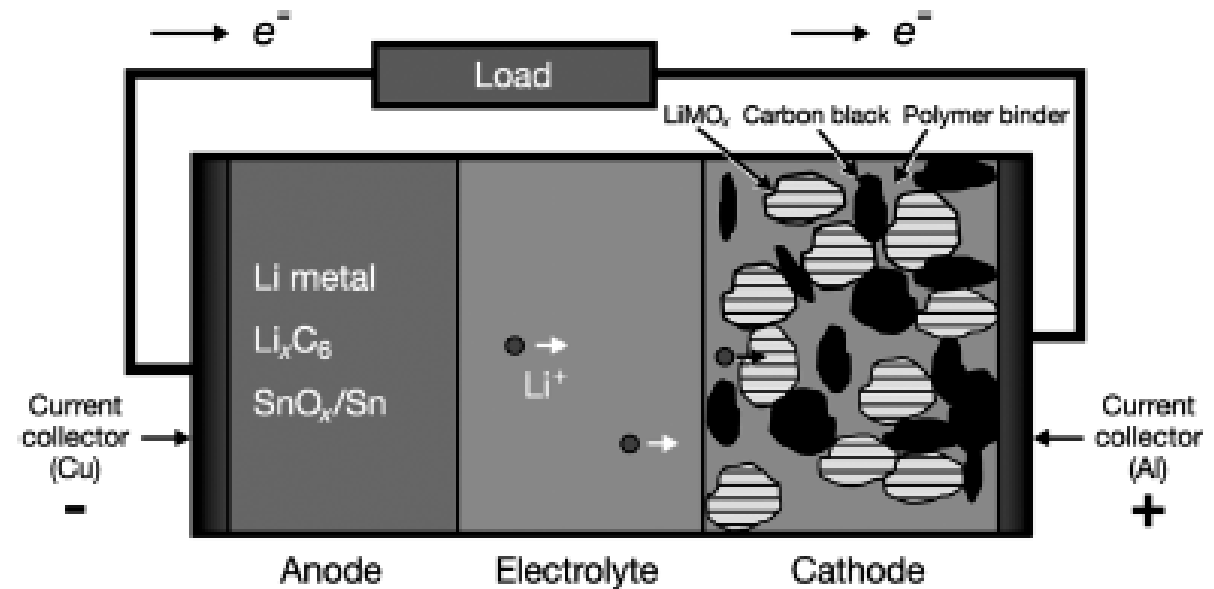
During discharge (cobalt cathode):



The backward reactions occur during charging.

Material	Theoretical Voltage V	Theoretical specific energy Wh/kg
Li/CoO ₂	3.6	570
Li/Mn ₂ O ₄		

Lithium is single valent, giving up a single electron during discharging (more advanced batteries would use multi valent metal such as magnesium).



Courtesy Elsevier, Inc., <http://www.sciencedirect.com>. Used with permission.

Li-Mn battery during discharge:
Li ions move from –ve electrode (anode)
to +ve electrode (cathode)
through solid or liquid electrolyte

Specific Energy

The theoretical specific energy is $-\Delta G_R / \sum M_i$ where the sum is taken over all the reactants (and products) in the redox reaction.

This expression ignores the mass of the battery housing, inert electrode material and electrolytes.

Actual specific energy is 20-35% of this value because of the weight of these components and the energy losses

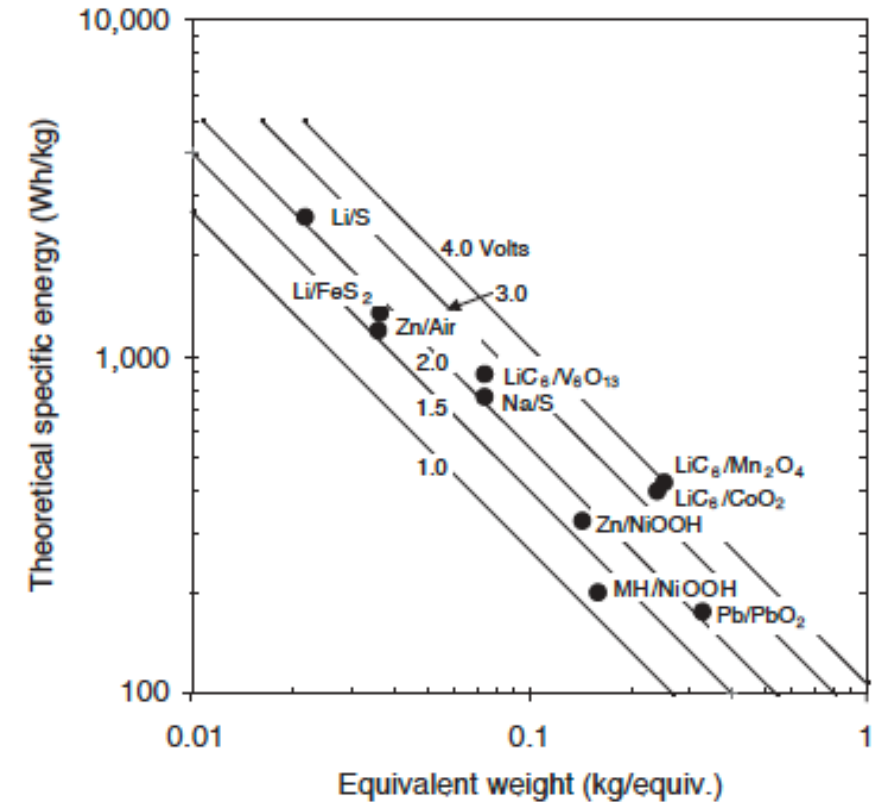


FIGURE 1 Theoretical specific energy for various cells as a function of the equivalent weights of the reactants and the cell voltage.

(Elton j Cairns, "Batteries, Overview, Encyclopedia of Energy, Vol 1, 2004 , Elsevier Inc)

Courtesy Elsevier, Inc., <http://www.sciencedirect.com>. Used with permission.

Battery Materials

Electrode materials are selected to maximize the theoretical specific energy of the battery, using reactants/reactions with a large (-ve) ΔG and light weight (small ΣM).

- Negative electrode (anode) reactants that can give up electrons easily have large (-ve) ΔG . These elements are located on the LHS of the periodic table.
- Elements with a low MW are located toward the top of the periodic table.
- Positive electrode (cathode) reactants (oxides) should readily accept electrons. These elements are located on the RHS of the periodic table.

(Elton j Cairns, “Batteries, Overview, Encyclopedia of Energy, Vol 1, 2004 , Elsevier Inc)

Periodic Table of the Elements

© Todd Helmenstine. All rights reserved. This content is excluded from our Creative Commons license. For more information, see <https://ocw.mit.edu/fairuse>.

<h1>Periodic Table of the Elements</h1>																	
<p>© Todd Helmenstine. All rights reserved. This content is excluded from our Creative Commons license. For more information, see https://ocw.mit.edu/fairuse.</p>																	
1 H Hydrogen 1.01																	2 He Helium 4.00
3 Li Lithium 6.94	4 Be Beryllium 9.01											5 B Boron 10.81	6 C Carbon 12.01	7 N Nitrogen 14.01	8 O Oxygen 16.00	9 F Fluorine 19.00	10 Ne Neon 20.18
11 Na Sodium 22.99	12 Mg Magnesium 24.31											13 Al Aluminum 26.98	14 Si Silicon 28.09	15 P Phosphorus 30.97	16 S Sulfur 32.06	17 Cl Chlorine 35.45	18 Ar Argon 39.95
19 K Potassium 39.10	20 Ca Calcium 40.08	21 Sc Scandium 44.96	22 Ti Titanium 47.88	23 V Vanadium 50.94	24 Cr Chromium 51.99	25 Mn Manganese 54.94	26 Fe Iron 55.85	27 Co Cobalt 58.93	28 Ni Nickel 58.69	29 Cu Copper 63.55	30 Zn Zinc 65.38	31 Ga Gallium 69.72	32 Ge Germanium 72.63	33 As Arsenic 74.92	34 Se Selenium 78.97	35 Br Bromine 79.90	36 Kr Krypton 84.80
37 Rb Rubidium 85.47	38 Sr Strontium 87.62	39 Y Yttrium 88.91	40 Zr Zirconium 91.22	41 Nb Niobium 92.91	42 Mo Molybdenum 95.95	43 Tc Technetium 98.91	44 Ru Ruthenium 101.07	45 Rh Rhodium 102.91	46 Pd Palladium 106.42	47 Ag Silver 107.87	48 Cd Cadmium 112.41	49 In Indium 114.82	50 Sn Tin 118.71	51 Sb Antimony 121.76	52 Te Tellurium 127.6	53 I Iodine 126.90	54 Xe Xenon 131.29
55 Cs Cesium 132.91	56 Ba Barium 137.33	57-71 Lanthanides	72 Hf Hafnium 178.49	73 Ta Tantalum 180.95	74 W Tungsten 183.85	75 Re Rhenium 186.21	76 Os Osmium 190.23	77 Ir Iridium 192.22	78 Pt Platinum 195.08	79 Au Gold 196.97	80 Hg Mercury 200.59	81 Tl Thallium 204.38	82 Pb Lead 207.20	83 Bi Bismuth 208.98	84 Po Polonium [208.98]	85 At Astatine 209.98	86 Rn Radon 222.02
87 Fr Francium 223.02	88 Ra Radium 226.03	89-103 Actinides	104 Rf Rutherfordium [261]	105 Db Dubnium [262]	106 Sg Seaborgium [266]	107 Bh Bohrium [264]	108 Hs Hassium [269]	109 Mt Meitnerium [278]	110 Ds Darmstadtium [281]	111 Rg Roentgenium [280]	112 Cn Copernicium [285]	113 Nh Nihonium [286]	114 Fl Flerovium [289]	115 Mc Moscovium [289]	116 Lv Livermorium [293]	117 Ts Tennessine [294]	118 Og Oganesson [294]

Alkali Metal Alkaline Earth Transition Metal Basic Metal Metalloid Nonmetal Halogen Noble Gas Lanthanide Actinide

Lead-acid, nickel-metal (Cd/Fe/Mn) hydride and Zinc batteries.

- The round-trip efficiency of batteries ranges between 70% for nickel/metal hydride and more than 90% for lithium-ion batteries.
- This is the ratio between electric energy out during discharging to the electric energy in during charging.
- The battery efficiency can change on the charging and discharging rates because of the dependency of losses on the current.

Some rechargeable aqueous batteries

System	Cell voltage [V]	Theoretical specific energy [Wh/kg]	Actual specific energy [Wh/kg]	Specific power [W/kg]	Cycle life
Pb/PbO ₂	2.1	175	30-45	50-100	>700
Cd/NiOOH	1.2	209	35-55	400	2000
Fe/NiOOH	1.3	267	40-62	70-150	500-2000
H ₂ /NiOOH	1.3	380	60	160	1000-2000
Zn/NiOOH	1.74	326	55-80	200-300	500
Zn/Air	1.6	1200	65-120	<100	300

Courtesy Elsevier, Inc., <http://www.sciencedirect.com>. Used with permission.

Elton j Cairns, "Batteries, Overview, Encyclopedia of Energy, Vol 1, 2004 , Elsevier Inc

The power density is ~ 0.2 (20 kW/100kg), need ~ 500 kg to power a 100 kW motor.

Lithium Ion batteries

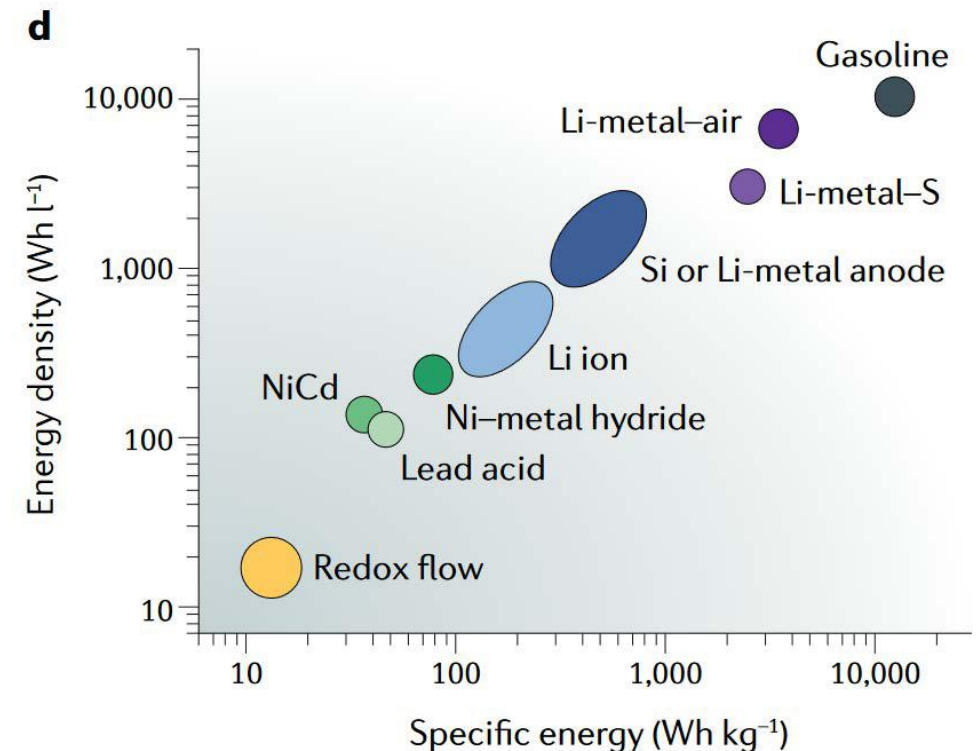
The open circuit potential of a LiCoO_2 battery is ~ 4.2 V. Specific energy is $\sim 3\text{-}5\text{X}$, specific power is 2X higher than lead-acid. **Table** shows the characteristics of lithium ion batteries with different positive electrode (cathode) materials: Co (cobalt), Mn (manganese), Fe (iron), Ti (titanium), or S (sulfur), etc., for improved stability, specific energy and power.

Nonaqueous Rechargeable Battery Chemistries

Material	Voltage [V]	Theoretical specific energy [Wh/kg]	Actual Specific energy [Wh/kg]	Specific power [W/kg]
Li/CoO ₂	3.6	570	125	>200
Li/Mn ₂ O ₄	4	593	150	200
Li/FePO ₄	3.5	621	120	100
Li/V ₆ O ₁₃	2.4	890	150	200
Li/TiS ₂	2.15	480	125	65
Li/S	2.1	2600	300	200

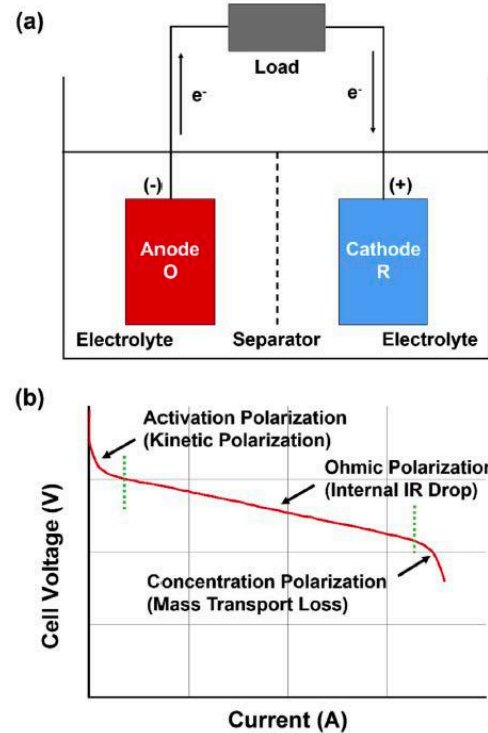
Courtesy Elsevier, Inc., <http://www.sciencedirect.com>. Used with permission.

“Batteries, Overview” by E Cairns, Encyclopedia of Energy, V 1, 2004, Elsevier.



Lopez, Jeffrey, et al. "Designing polymers for advanced battery chemistries." *Nature Reviews Materials* 4.5 (2019): 312-330.

finite current performance



© PECS. All rights reserved. This content is excluded from our Creative Commons license. For more information, see <https://ocw.mit.edu/fairuse>.

The i-V curve of a battery resembles that of a fuel cell, with similar loss mechanisms affecting the performance at higher currents.

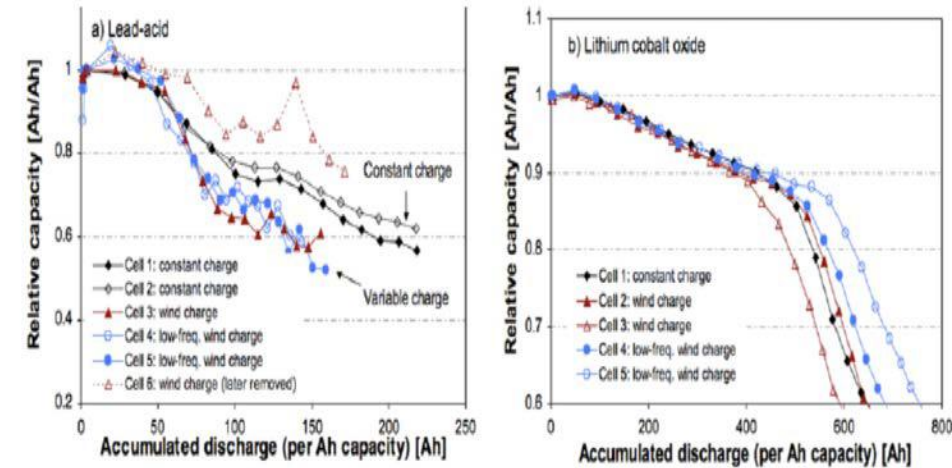


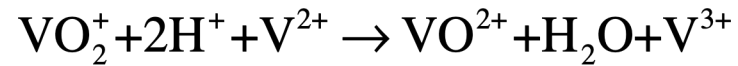
Figure 1: Capacity fade as a function of normalized discharge throughput in a lead-acid and a lithium-ion battery. Lead-acid batteries show rapid capacity fade compared to the lithium-ion batteries. [Source: Krieger et al. 2013⁴]

© Source unknown. All rights reserved. This content is excluded from our Creative Commons license. For more information, see <https://ocw.mit.edu/fairuse>.

- Since all the reactants are stored internally, performance can change with degree of discharge.
- As more current is drawn from a battery, the reactants concentrations drop (and products concentrations increase) leading to significant increase in concentration overpotential and performance degradation under deep discharge conditions.

Redox Flow Batteries, the All-Vanadium design

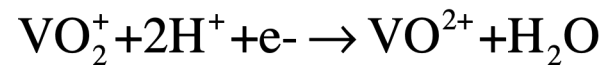
Overall



On the negative electrode side:

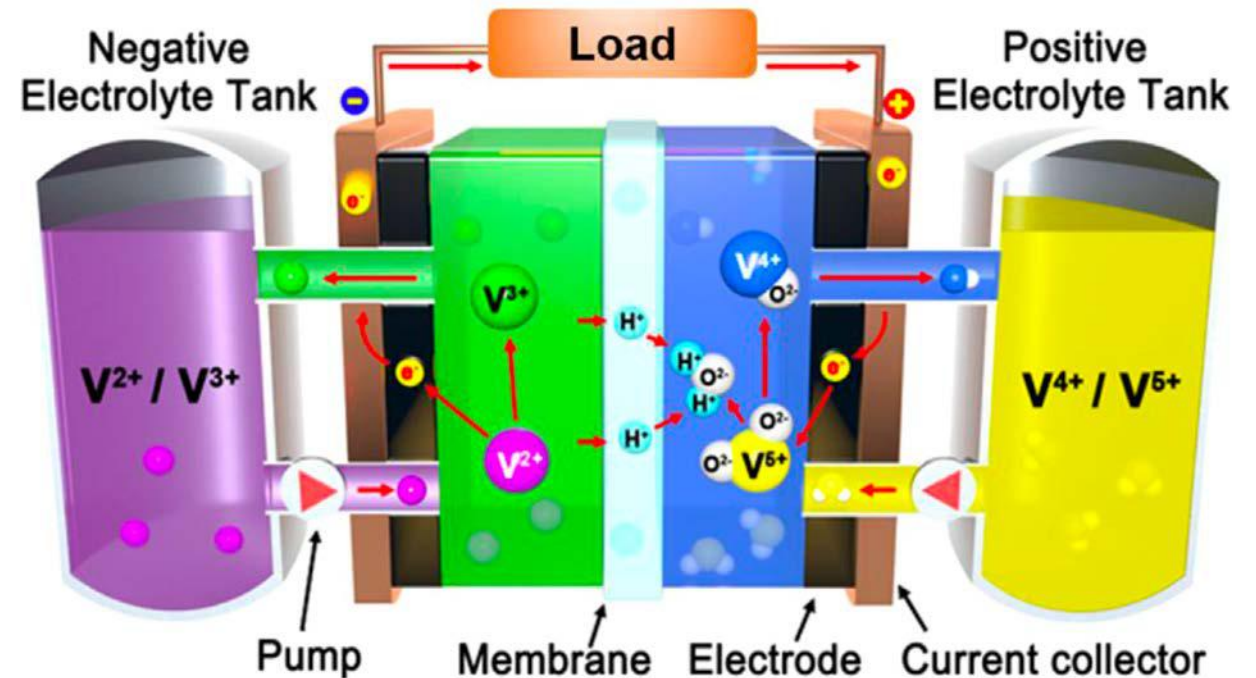


On the positive electrode side



Open circuit voltage is $\sim 1.26\text{V}$.

Observed efficiency (round trip!) $\sim 85\%$.



© PECS. All rights reserved. This content is excluded from our Creative Commons license. For more information, see <https://ocw.mit.edu/fairuse>.

Cho et al., PECS 48 (2013) 84

MIT OpenCourseWare
<https://ocw.mit.edu/>

2.60J Fundamentals of Advanced Energy Conversion
Spring 2020

For information about citing these materials or our Terms of Use, visit: <https://ocw.mit.edu/terms>.

Lecture # 12



Solar Photovoltaics

Ahmed F. Ghoniem

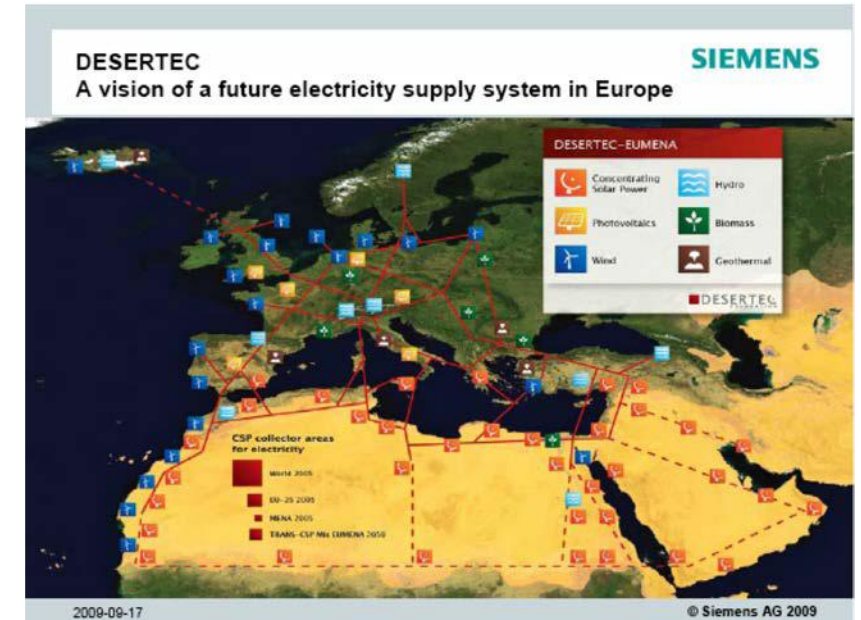
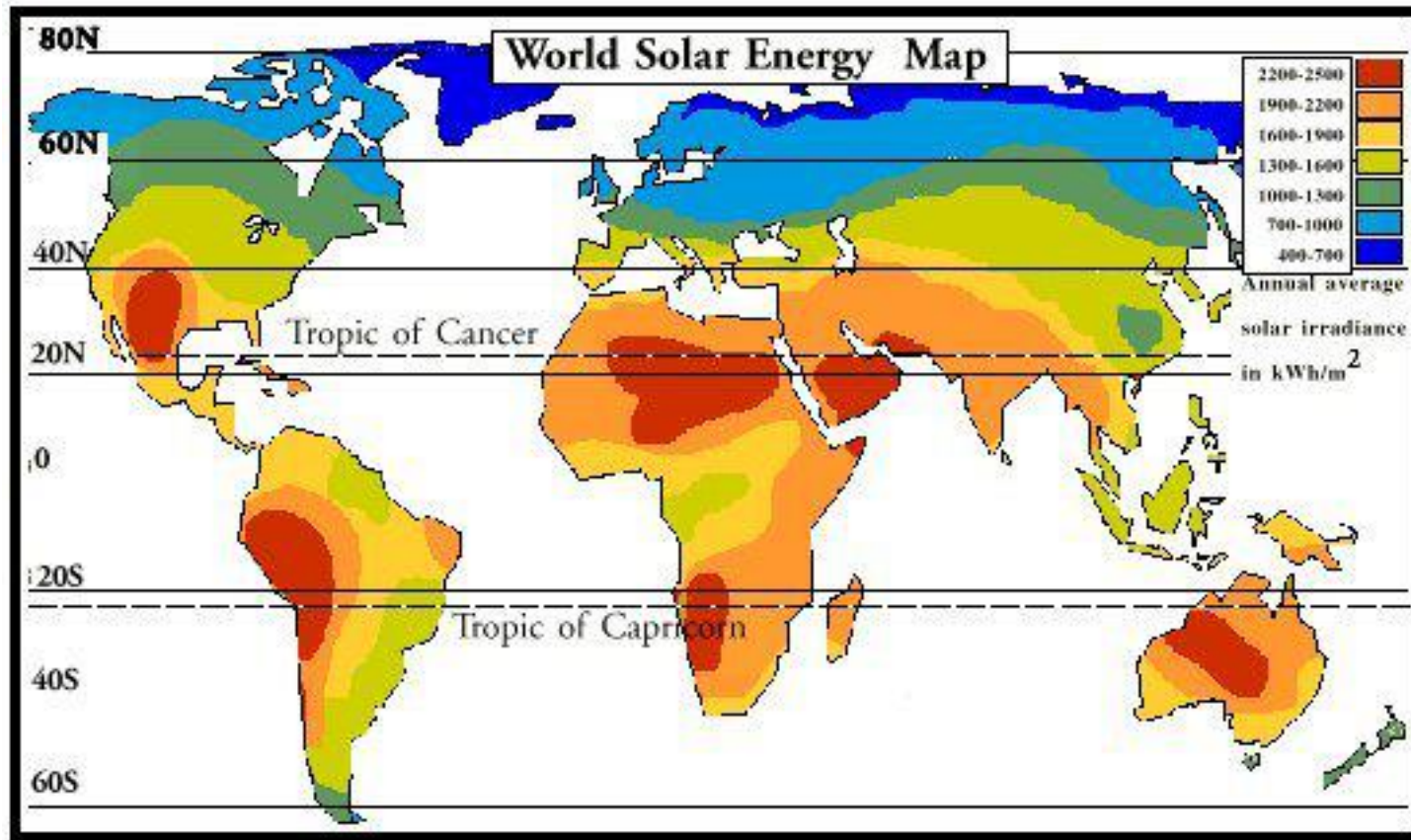
March 11, 2020

Solar resources, potential, progress, pricing ..

Semiconductor physics, p-n junction, bandgap, efficiency ..

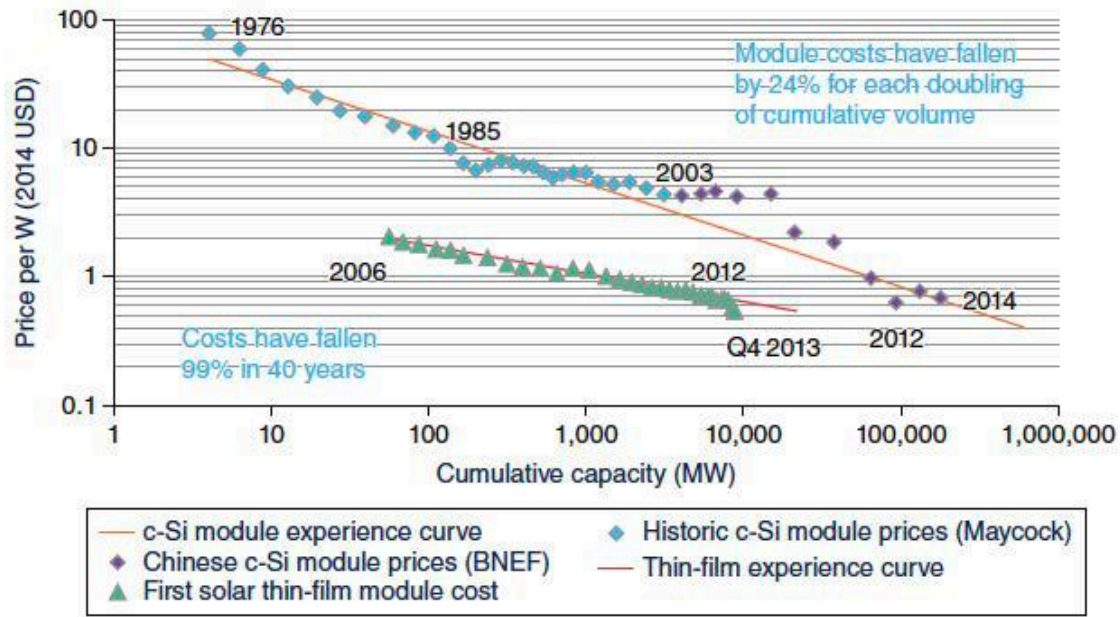
Solar panels, fabrication, variety, farms, systems

Solar Energy is “Everywhere”.
Opportunities vary.
Distribution networks may look different



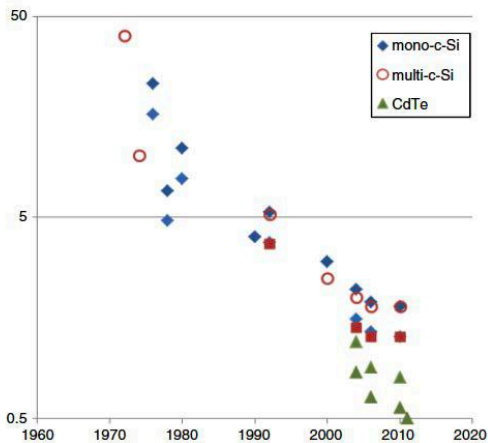
© Siemens AG. All rights reserved. This content is excluded from our Creative Commons license. For more information, see <https://ocw.mit.edu/fairuse>.

c-Si dominates the market (cheaper and mostly more efficient)

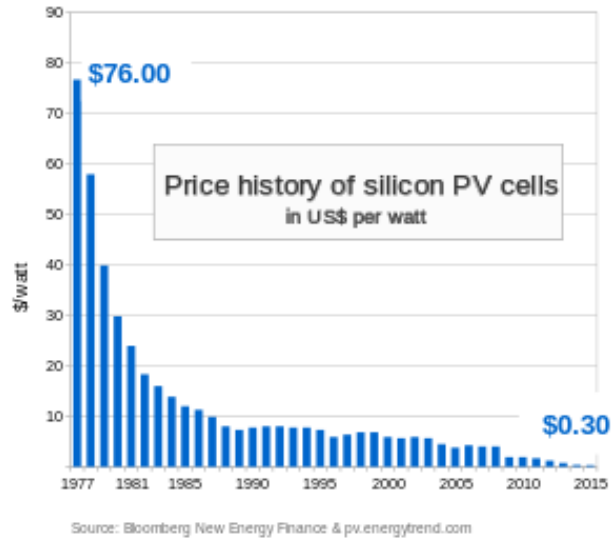


Photovoltaic Solar Energy, Reinder et al, Ed., Wiley, 217

© Wiley. All rights reserved. This content is excluded from our Creative Commons license. For more information, see <https://ocw.mit.edu/fairuse>.



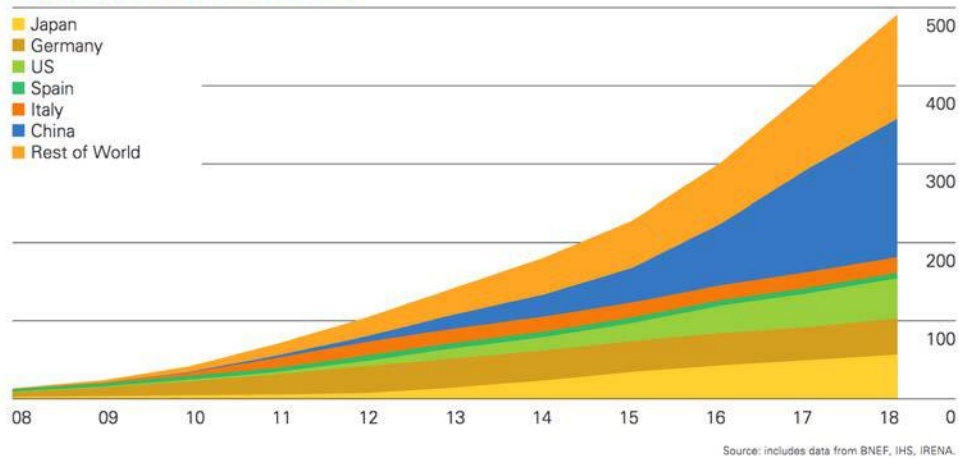
Energy payback period for different PV technologies, low numbers are for insolation of 2,400 kWh/m²/y, high are for 1,700 kWh/m²/y



© Bloomberg Finance L.P. All rights reserved. This content is excluded from our Creative Commons license. For more information, see <https://ocw.mit.edu/fairuse>.

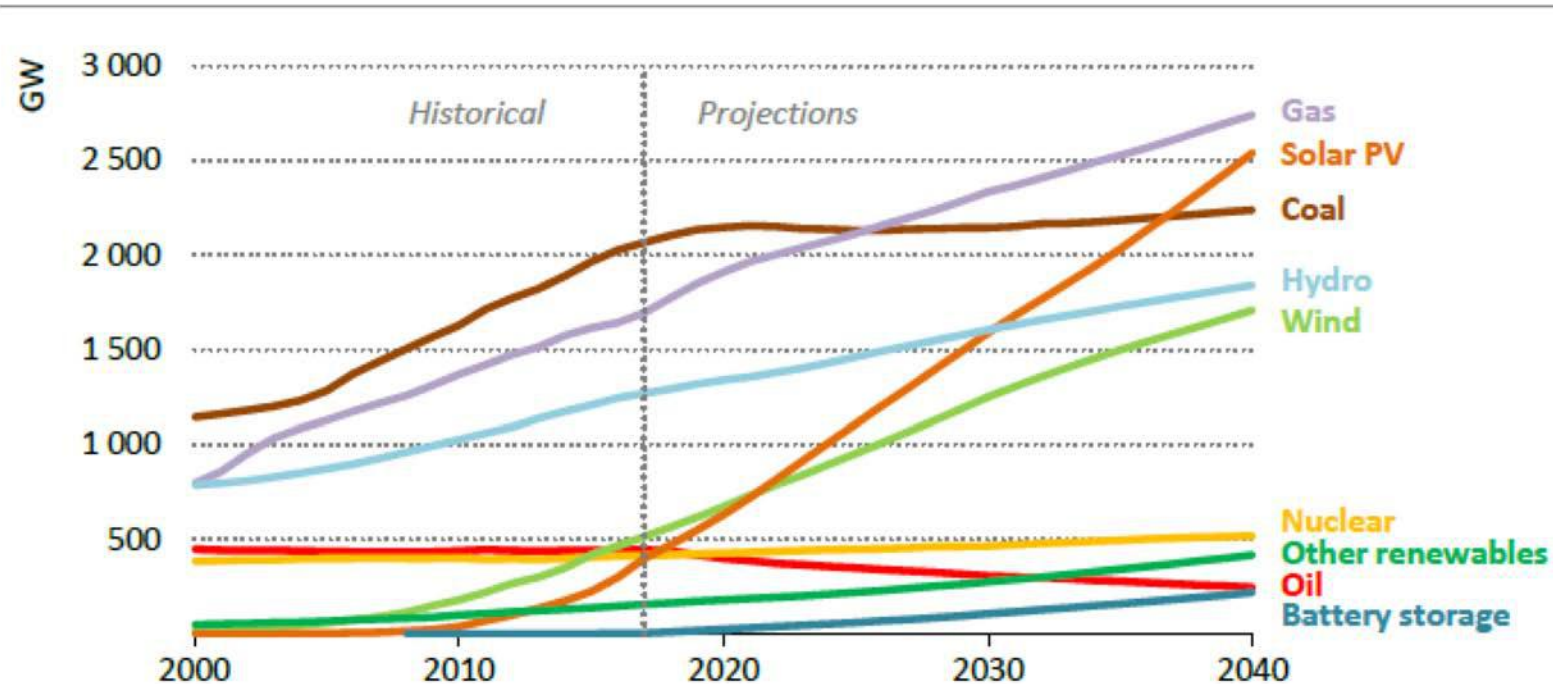
Solar PV generation capacity

Gigawatts, cumulative installed capacity



© Source unknown. All rights reserved. This content is excluded from our Creative Commons license. For more information, see <https://ocw.mit.edu/fairuse>.

Installed power generation capacity worldwide by source and prediction in the new policies scenario

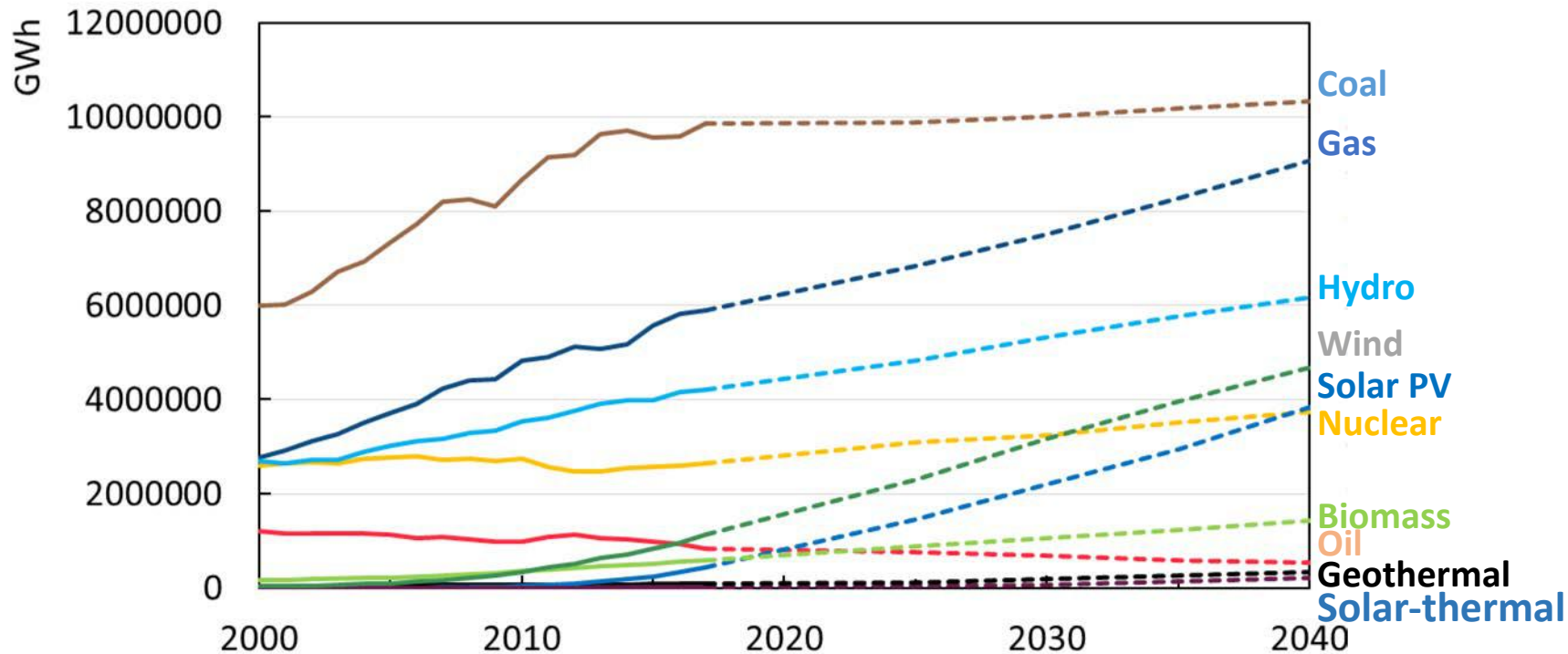


With more than 180 GW under construction, coal fuels the most capacity until the mid-2020s when natural gas overtakes it, and renewables are on the rise

© IEA. All rights reserved. This content is excluded from our Creative Commons license. For more information, see <https://ocw.mit.edu/fairuse>.

World electricity production by source

only electricity generated is accounted, no matter what source is from



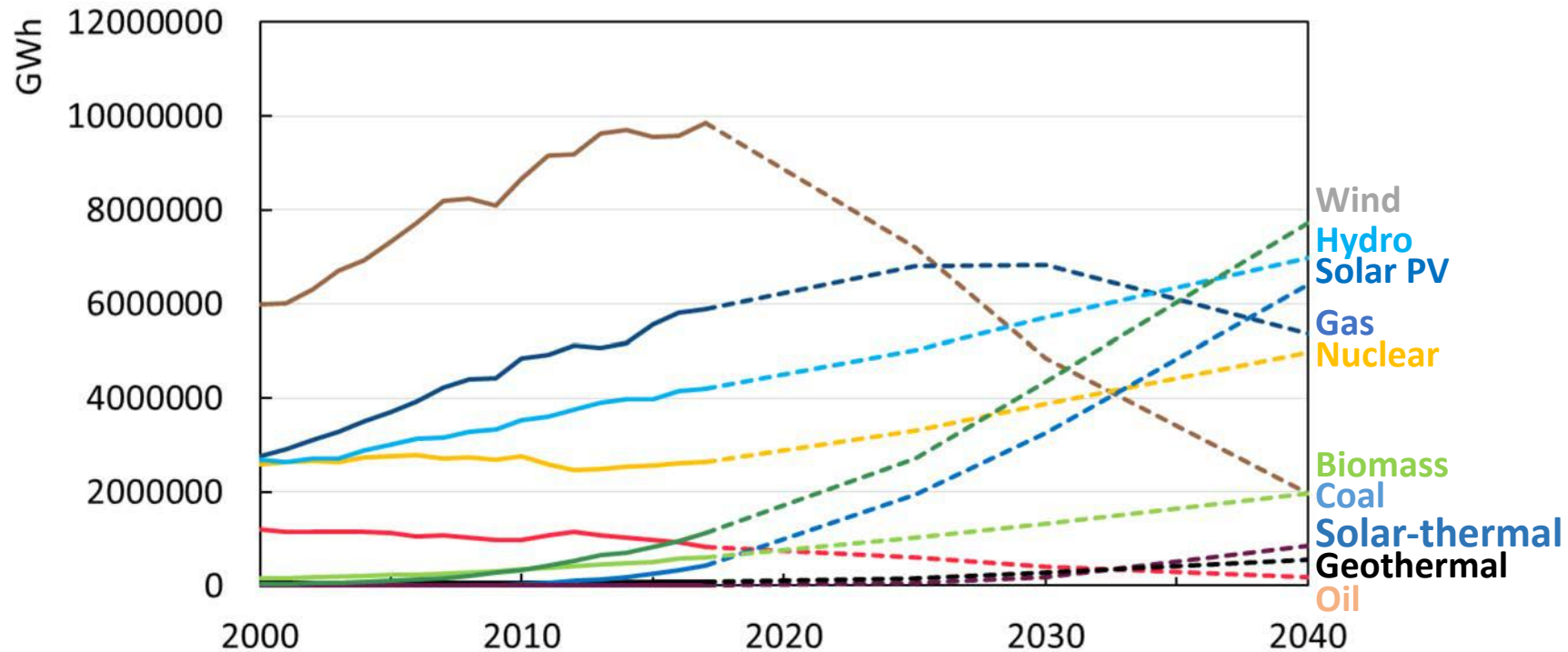
The dotted line is the prediction based on new policies to be implemented

Source: historic data from IEA website (up to 2017)

prediction data from IEA world energy outlook 2018, P528

World electricity production by source

only electricity generated is accounted, no matter what source is from

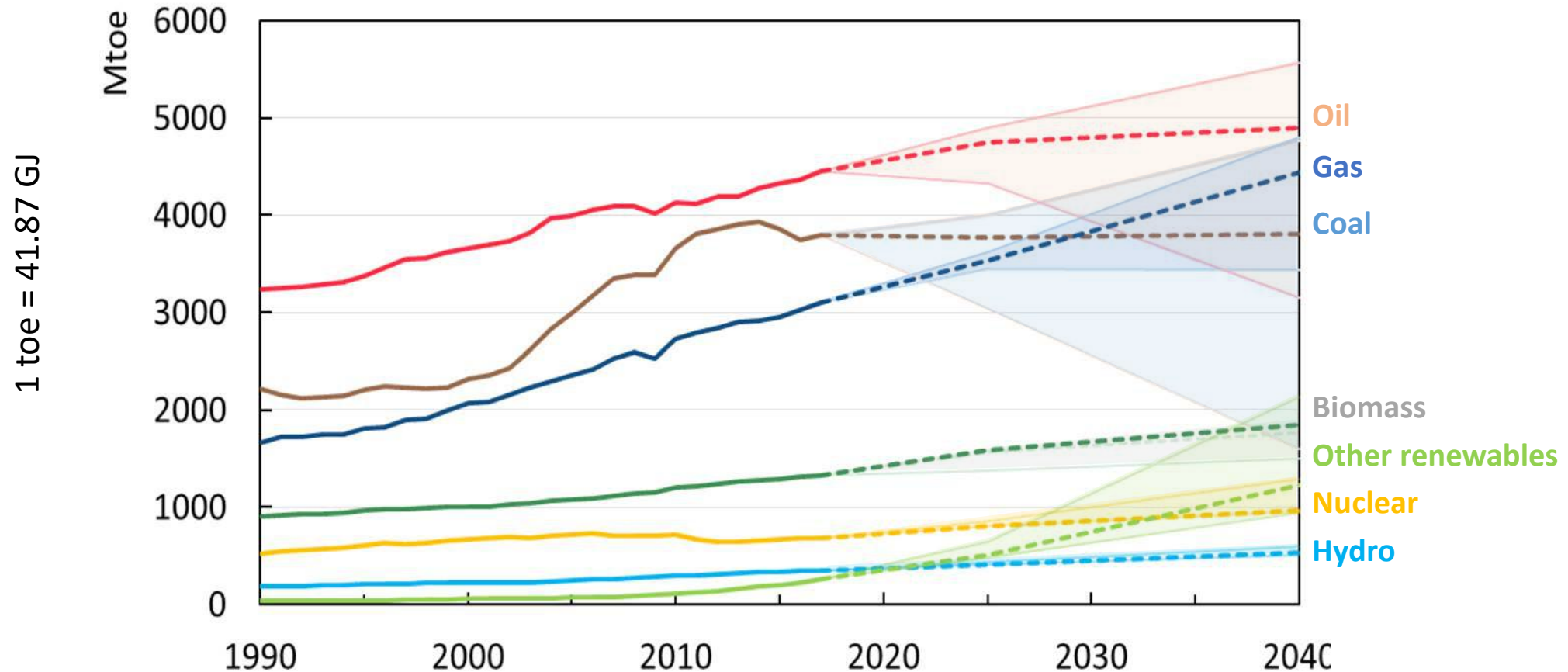


The dotted line is the prediction based on sustainable development goals

Source: historic data from IEA website (up to 2017)

prediction data from IEA world energy outlook 2018, P529

World primary energy supply by fuel/source*

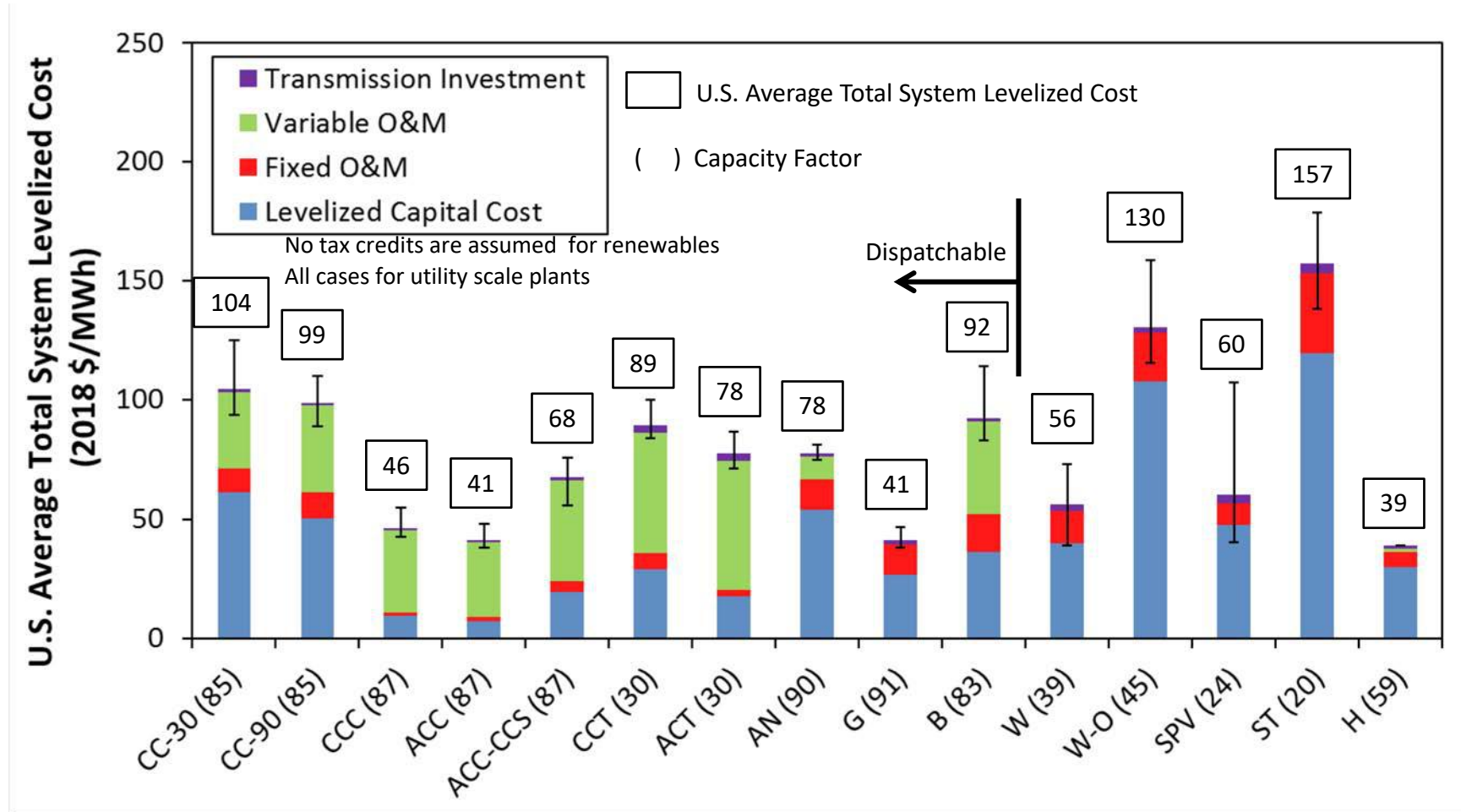


The dotted line is the prediction based on new policies to be implemented. The shaded areas show the possible scenarios between current policies and sustainable development. Source: IEA world energy outlook 2018, P38

© IEA. All rights reserved. This content is excluded from our Creative Commons license. For more information, see <https://ocw.mit.edu/fairuse>.

* When it comes to electricity from non-combustible sources, the IEA, in line with IRES, adopts a coherent principle across sources – the “physical content method” – by measuring the primary energy equivalent at the first point downstream in the production process for which multiple energy uses are practical. This means that hydro, wind and solar become “energy products” in the statistical sense at the point of generation of electricity, and that their “primary energy equivalent” is computed as the electricity generated in the plant, while the kinetic energy of the wind or the water does not enter the “energy balance”, although being “energy” in a scientific sense.

Estimated (in 2019) Levelized Cost of Electricity Generation Plants in 2023



CC-30: Coal with 30% CCS
 CC-90: Coal with 90% CCS
 CCC: Conventional Combined Cycle
 ACC: Advanced Combined Cycle
 ACC-CCS: Advanced CC with CCS

CCT: Conventional Combustion Turbine
 ACT: Advanced Combustion Turbine
 AN: Advanced Nuclear
 G: Geothermal
 B: Biomass

W: Wind – Onshore
 W-O: Wind – Offshore
 SPV: Solar PV
 ST: Solar Thermal
 H: Hydroelectric

Image courtesy of U.S. Energy Information Administration (EIA).

Source: U.S. Energy Information Administration, Annual Energy Outlook 2019, Feb 2019.

Solar Radiation Spectrum

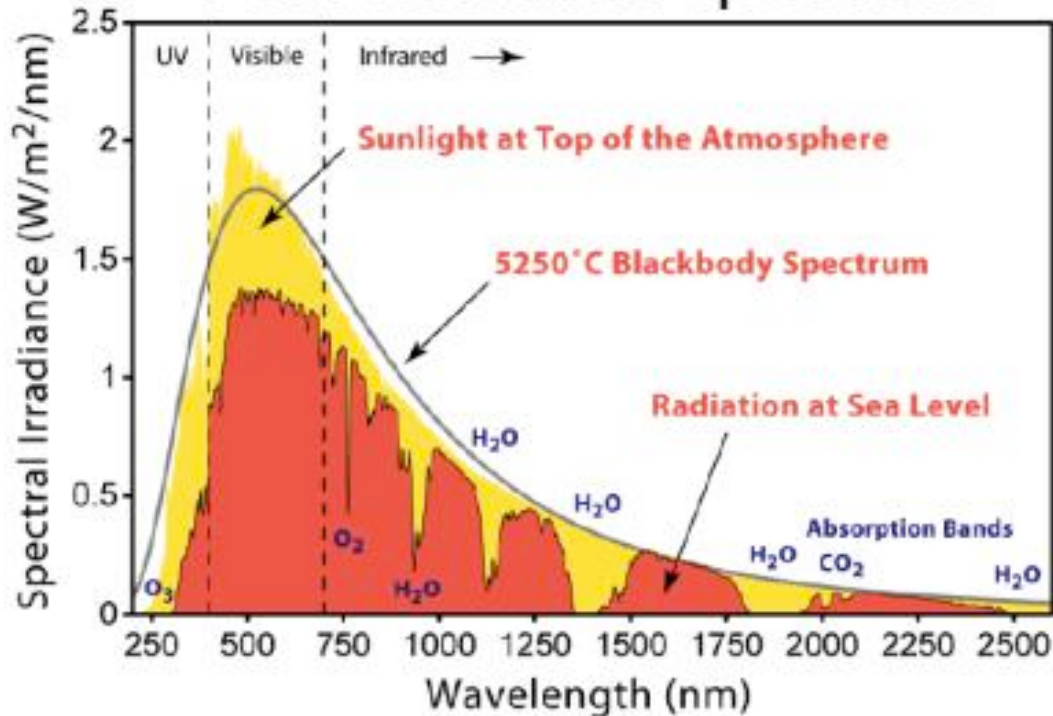
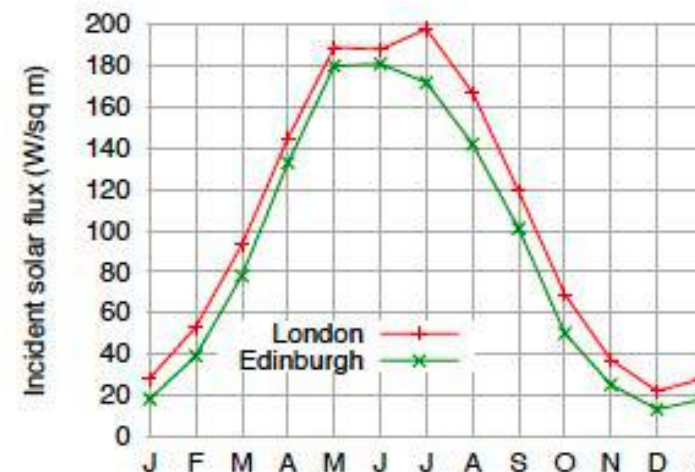


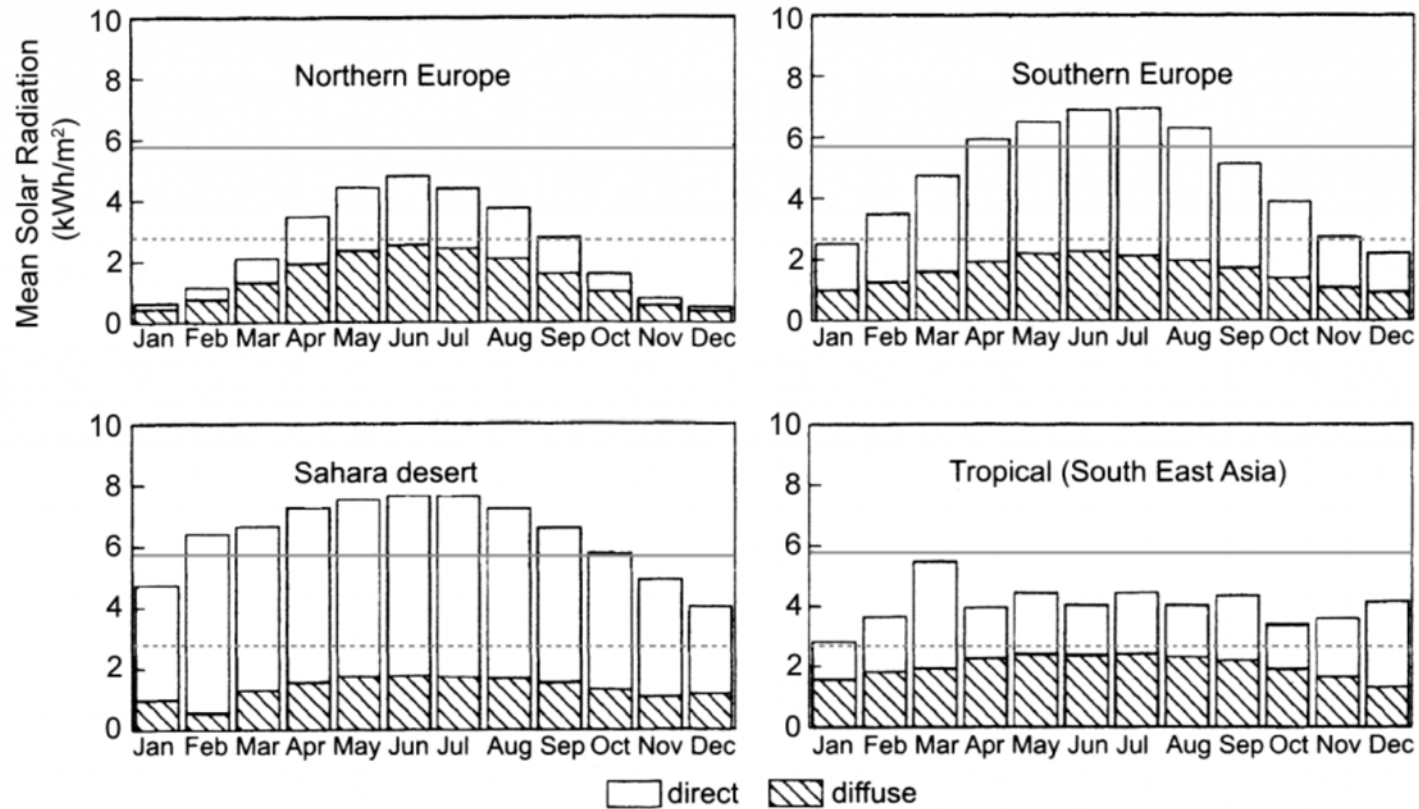
Figure 3: The solar spectrum above the atmosphere and at sea level

© Source unknown. This content is excluded from our Creative Commons license. For more information, see <https://ocw.mit.edu/fairuse>.

- Extra-terrestrial total irradiance (insolation: incident solar radiation) $\sim 1367 \text{ W/m}^2$
- Irradiance at Earth's surface is made of beam (direct) and diffuse components
- Total terrestrial irradiance depends on location (north, south ..), hours/days of sun, cloud coverage, etc. When averaged over one day:
 - Clear $\sim 590 - 1000 \text{ W/m}^2$
 - Cloudy days $\sim 120 \text{ W/m}^2$
 - Average $\sim 300 \text{ W/m}^2$ (strong function of location)

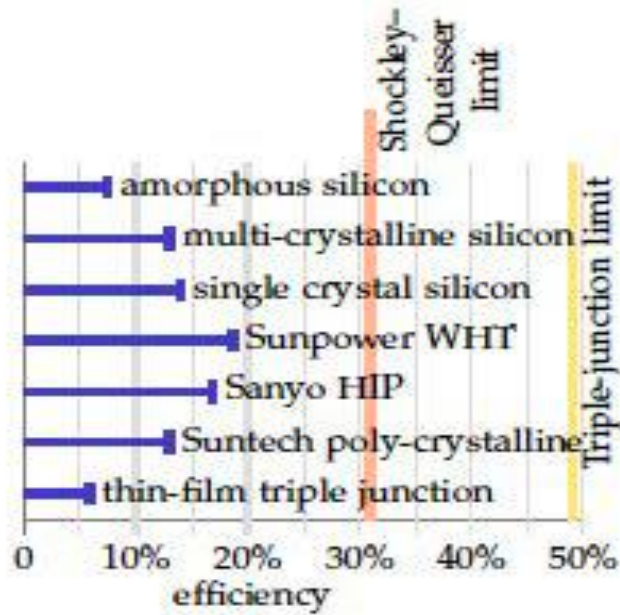


In London, solar intensity, average over the year is $\sim 100 \text{ W/m}^2$ MacKay



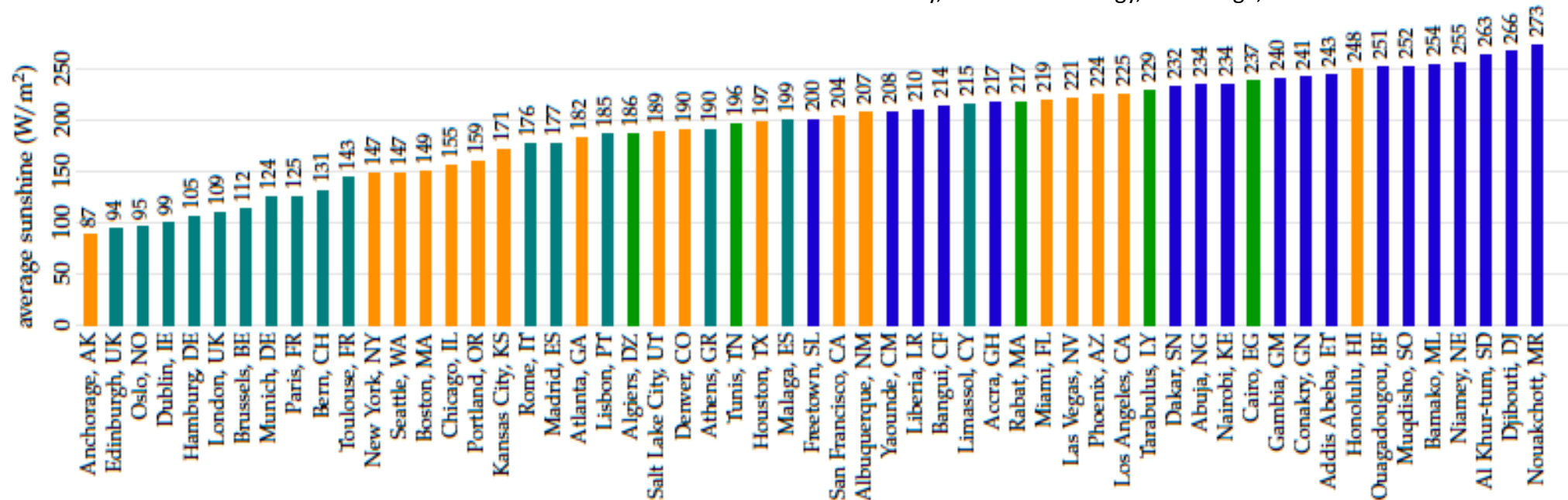
© ITACA. All rights reserved. This content is excluded from our Creative Commons license. For more information, see <https://ocw.mit.edu/fairuse>.

The yearly variation of the mean total daily solar radiation (total per day) for different locations, the dashed lines is at 2.88 kWh/m².day and solid line is at 5.75 kWh/m².day, showing both direct and diffuse radiation. Location affects number of hours/day of sun, solar angle, weather conditions, ..



With an average solar power of 100 W/m^2 , and PV efficiency of 15%, electric power production is 15 W/m^2 (much higher than sun-to-biomass-to electricity, which would be less than 1 W/m^2)

Mackay, Sustainable Energy, Cambridge, 2009



Semiconductors

- Electrons orbit the nucleus at different bands, the outer-most band is typically called the *valence band*.
- It takes energy to move an electron outwards from one band to the next.
- The energy required to pull electrons from the valence band to the *conduction band* is called the *bandgap*. Electrons in the (electrical or thermal) conduction band are free to move within the semiconductor.

- *Intrinsic semiconductors* have intermediate bandgap values (< 3 eV). They have average number of valence electrons (4 in the case of silicon)
- When *doped* with other metal, they can increase or decrease the number of electron in their valence band depending on the dopant.

Photovoltaic Solar Energy, Reinder et al, Ed., Wiley, 217

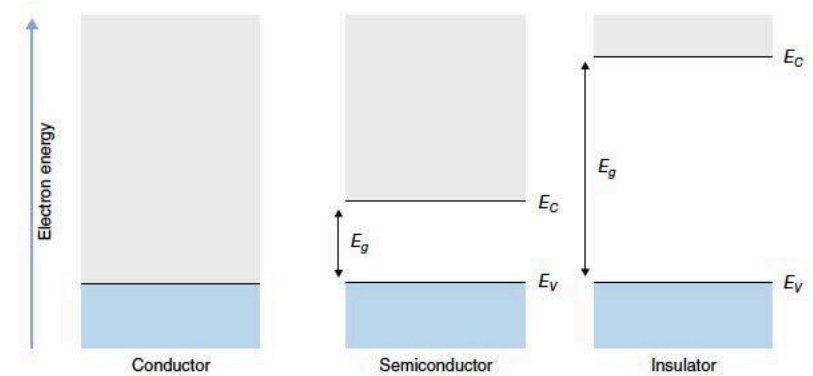


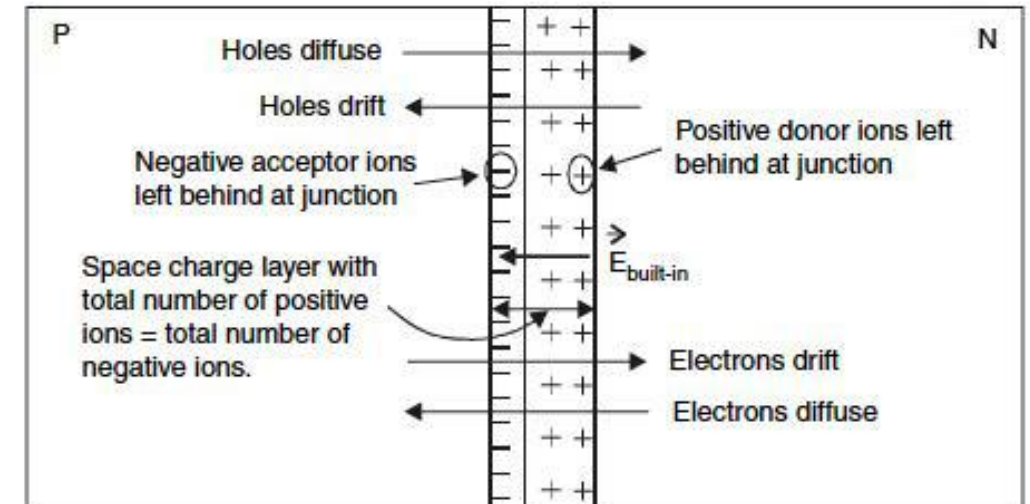
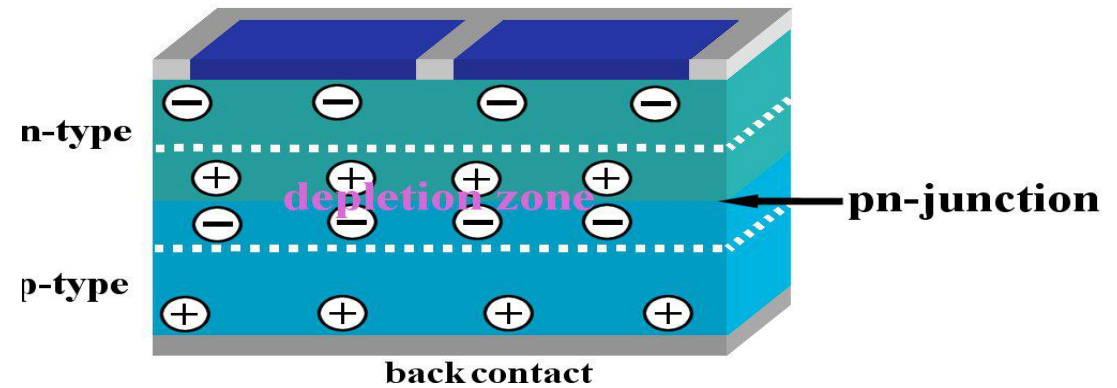
Figure 2.1.3 Energy band diagrams for a conductor, a semiconductor and an insulator

© Wiley. All rights reserved. This content is excluded from our Creative Commons license. For more information, see <https://ocw.mit.edu/fairuse>.

The electron volt [eV] is the energy required to move an electron (charge) across a 1 V potential, $eV = 1.6 \times 10^{-19}$ J

A p-n junction

- *n-type semiconductors* have more valence electrons than Si (phosphorous has 5).
- *p-type* have less valence electrons than Si (boron has 3).
- At a *p-n junction*, the interface region between the two doped semiconductors, some electrons from the n-side move to the p-side (leaving an electron *hole* behind) hence giving the structure more uniform electron distribution, and creating *charge separation* at the interface (diode effect) and an associated *potential difference*.

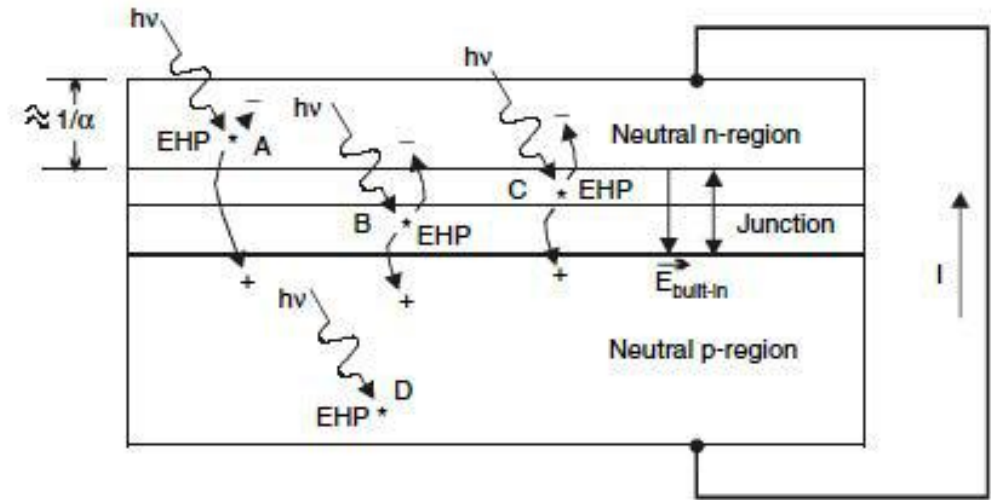


© CRC Press, LLC. All rights reserved. This content is excluded from our Creative Commons license. For more information, see <https://ocw.mit.edu/fairuse>.

A typical p-n junction showing charge separation by the migration of electrons across the interface

An “illuminated” p-n junction

- An electron in the valence band on the n-type side can absorb an *energetic photon (whose energy is $> e_{bg}$)* raising its energy and moving it to the conduction band (where it moves freely) if the photon energy is higher than the *bandgap energy* of the semiconductor.
- In a p-n junction this free electron can leave the semiconductor (if the thickness of the n-type layer is sufficiently small), generating an *external current*.
- Typical thicknesses of the two layers on the two sides of the junction are microns or less.
- The electron can also move across the junction towards the p-type.



© CRC Press, LLC. All rights reserved. This content is excluded from our Creative Commons license. For more information, see <https://ocw.mit.edu/fairuse>.

The illuminated p-n junction showing the formation of electron-hole pair by the adsorption of a photon (EHP: electron-hole pair)

The Photoelectric Effect

light is made of photons whose energy is given by:

$$\varepsilon_{ph} = h_{Planck} \nu_{ph} = h_{Planck} C_{light} / \lambda_{ph},$$

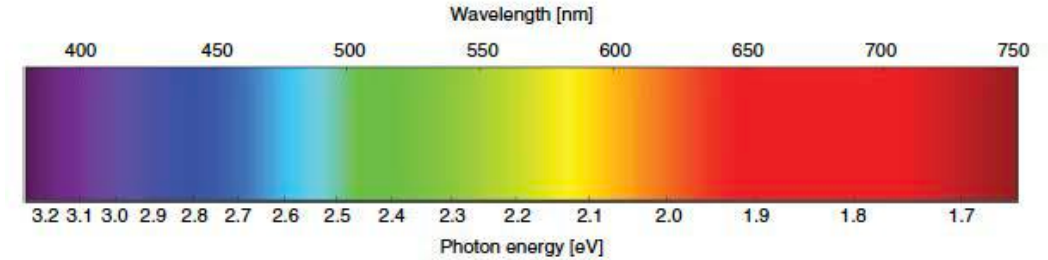
$$h_{Planck} = 6.62 \cdot 10^{-34} \text{ J.s},$$

$$\text{and } C_{light} = 3 \cdot 10^8 \text{ m/s}$$

$$\varepsilon_{ph} = 1.24 / \lambda_{ph} \text{ [eV]},$$

with λ_{ph} measured in μm ,

$$\text{eV} = 1.6 \cdot 10^{-19} \text{ J}.$$



The wavelength/color of visible light and its energy

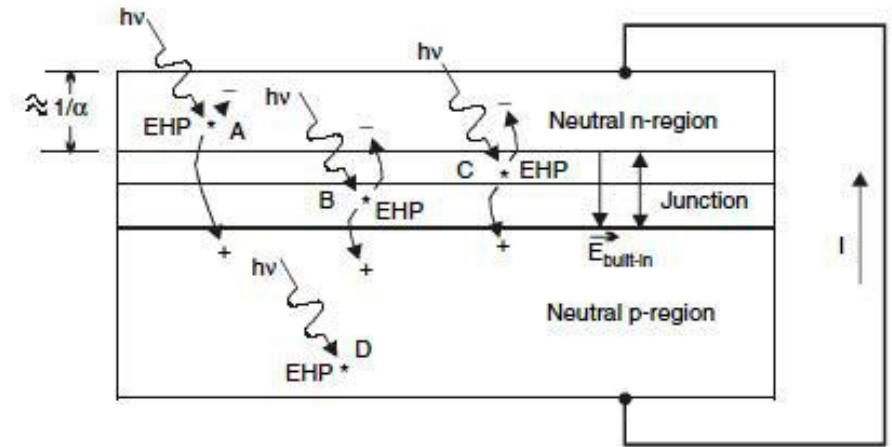
© Wiley. All rights reserved. This content is excluded from our Creative Commons license. For more information, see <https://ocw.mit.edu/fairuse>.

Photovoltaic Solar Energy, Reinder et al, Ed., Wiley, 217

- For Si, the **bandgap energy** is $e_{bg} \sim 1.1 \text{ eV}$, and adsorbed photons with $\lambda < \lambda_{bg} = 1.13 \mu\text{m}$ (near the infrared part of the solar spectrum) can move an electron to the conduction band (where it is free to move within the semiconductor).
- An adsorbed photon with energy $< e_{bg}$ (wavelength $> \lambda_{bg}$) dissipates its energy

The Photoelectric Effect

- An adsorbed photon with energy $> e_{bg}$ (wavelength $< \lambda_{bg}$) still moves a *single* electron to the conduction band (one electron/ photon), with the remaining energy dissipating into heat.
- The photon-induced current, which is proportional to the incident photon intensity, can move *across* the junction or to an *external circuit*.
- Freed electron (and electron holes) could be reabsorbed within the material unless the distance between the junction and the circuit is less than the diffusion length of electrons.



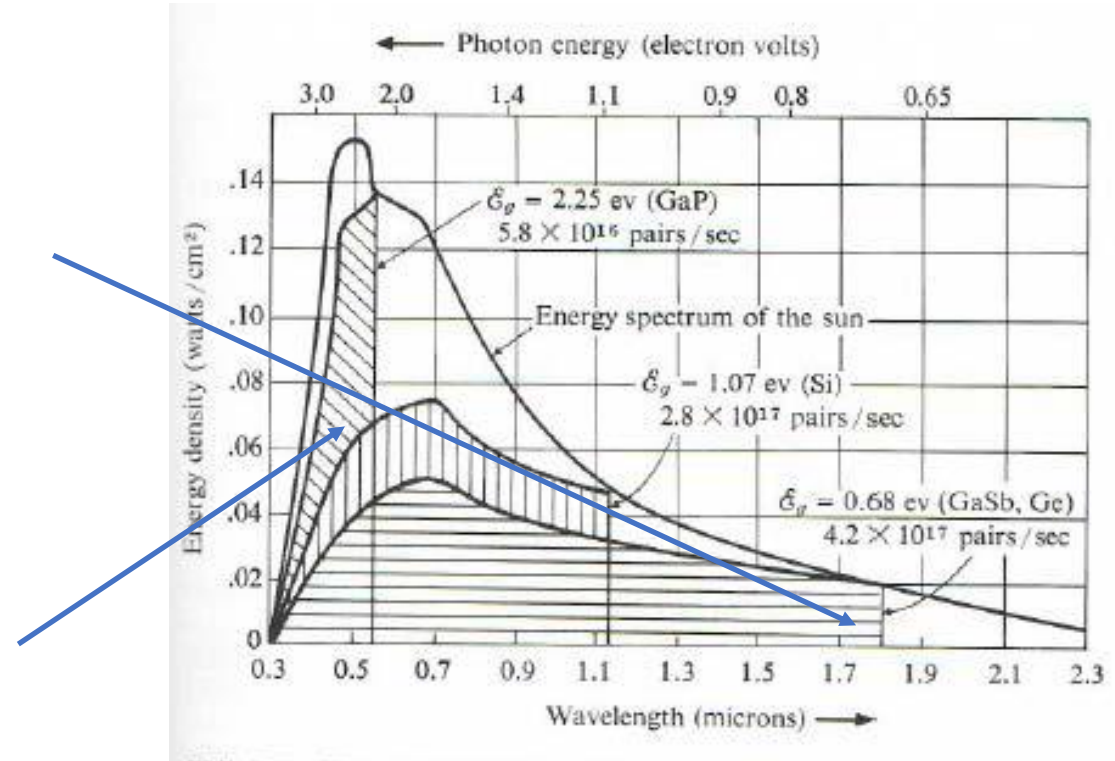
© CRC Press, LLC. All rights reserved. This content is excluded from our Creative Commons license. For more information, see <https://ocw.mit.edu/fairuse>.

The illuminated p-n junction showing the formation of electron-hole pair by the adsorption of a photon

Impact of Band Gap Width on efficiency:

- Different semiconductors have different efficiency, depending on their **bandgap e_{bg} or λ_{bg}**
- Semiconductors with low bandgap energy e_{bg} (or high λ_{bg}) take advantage of most of the solar spectrum, but their efficiency can be low because of the high dissipation from the more energetic electrons (the electron only captures the semiconductor e_{bg}).
- Semiconductors with high bandgap energy (low λ_{bg}), take advantage of a smaller fraction of the spectrum.

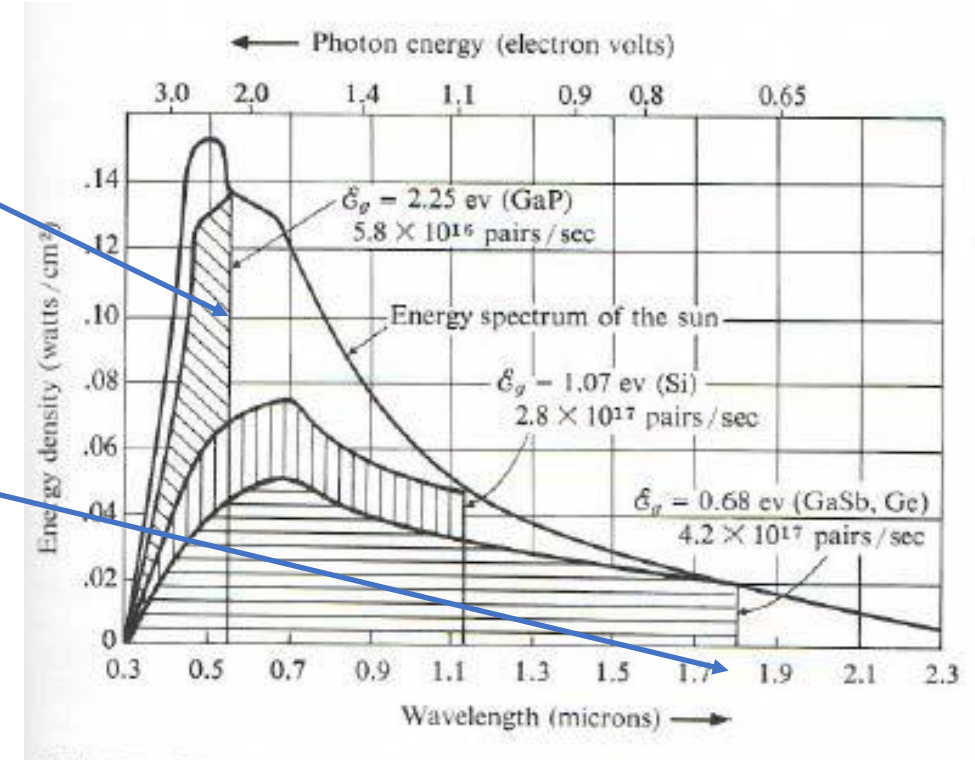
$$\varepsilon_{ph} = 1.24 / \lambda_{ph} \text{ [eV]}$$



© Source unknown. All rights reserved. This content is excluded from our Creative Commons license. For more information, see <https://ocw.mit.edu/fairuse>.

Impact of Band Gap Width on efficiency:

- Moreover, semiconductors with high bandgap energy (low λ_{bg}), have higher cell voltage ($V_{bg} = e_{bg} / \epsilon_0$ and ϵ_0 is the charge of an electron) but produce less electrons.
- While semiconductors with low bandgap have low cell voltage and produce more electrons.
- It is not possible to capture the full spectrum using a single semiconductor, and the maximum theoretical efficiency using a single or “homo” junction $\sim 30\%$ (the Shockley limit)



© Source unknown. All rights reserved. This content is excluded from our Creative Commons license. For more information, see <https://ocw.mit.edu/fairuse>.

- Hetero or multi junction (layered homojunctions) could be used to overcome this limit (semiconductor layers with different bandgaps can capture photons with different wavelength).

Impact of Band Gap Width on efficiency:

alloy	Bandgap eV	alloy	bandgap
c-Si	1.12	Zn ₃ P ₂	1.5
a-Si	1.7	CuInSe ₂	1.04
GaAs	1.43	CuGaSe ₂	1.68
InP	1.34	Cu(In,Ga)Se ₂	1.2
CuS	1.2	CuInS ₂	1.57
CdTe	1.45	Cu(In,Ga)(S,Se) ₂	1.36

c-Si: crystalline silicon

a-Si: amorphous silicon

Si: silicon

Zn: zink

Ga: gallium

P: phosphorus

As: arsenide

In: indium

Cu: copper

Se: selenium

S: sulfur

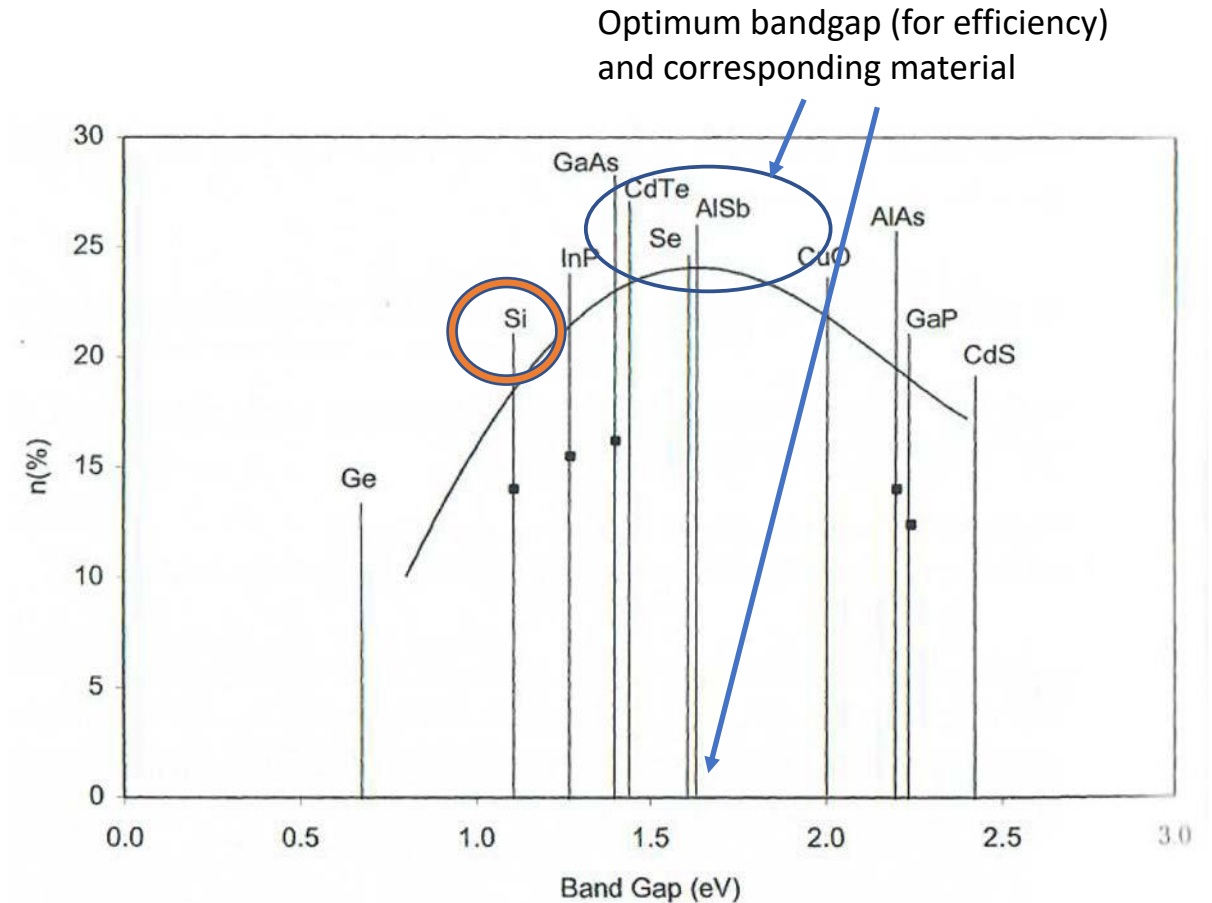
Ge: germanium

Cd: cadmium

Sb: antimony

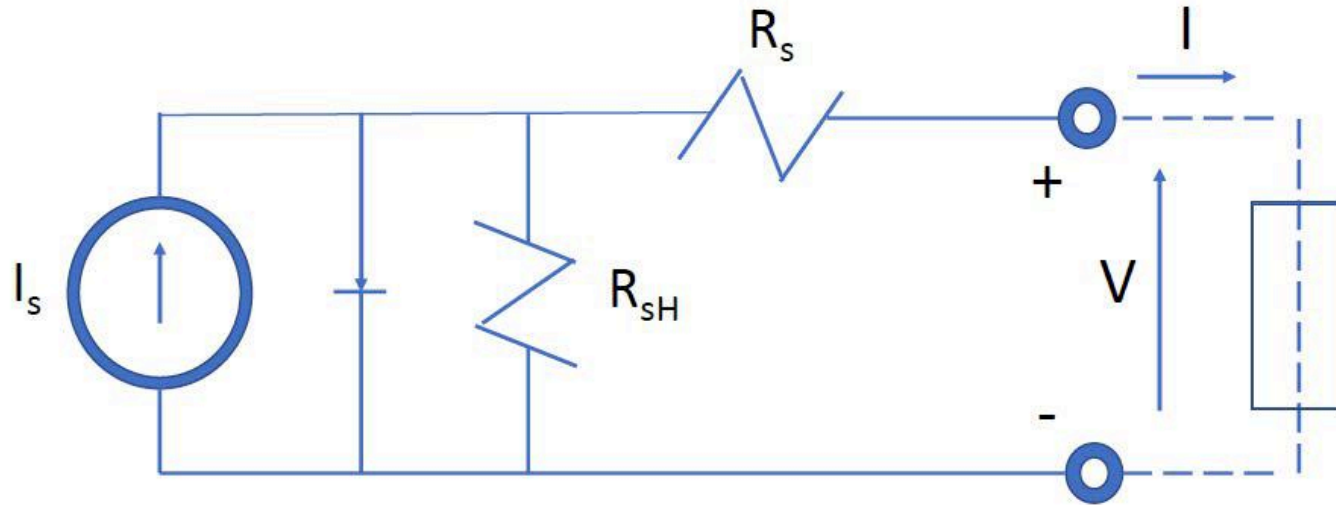
Te: telluride

Al: aluminum



The curve shows the ideal maximum (extraterrestrial) solar energy conversion efficiency as a function of the semiconductor bandgap. The measured value is shown by a solid square.

$$\eta = \int \eta_{\lambda} I_{\lambda} d\lambda / \int I_{\lambda} d\lambda$$



R_s is the zero series resistance ($=0$ under ideal conditions)

R_{sH} is the shunt resistance ($=\infty$ under ideal conditions)

For the following slides describing the modeling of the cell, See

Ginley and Cahen, Fundamentals of materials for energy and environmental sustainability, Cambridge, 2011.

Chen, Physics of Solar Energy, Wiley, 2011

Also Aliza Khurram 2019 term paper on Mars Mission

The external current density-voltage, J-V, relation of an illuminated p-n junction is:

$$j = j_s - j_0 \left(\exp\left(\frac{e_0 V}{nkT}\right) - 1 \right) \approx j_s - j_0 \exp\left(\frac{e_0 V}{nkT}\right)$$

j_s : zero voltage (short circuit) current $V = 0$

(also known as the photogenerated current).

j_o : dark current (current in the absence of illumination)

e_0 : electron charge = $1.602 \cdot 10^{-19}$ Coulombs (J/V)

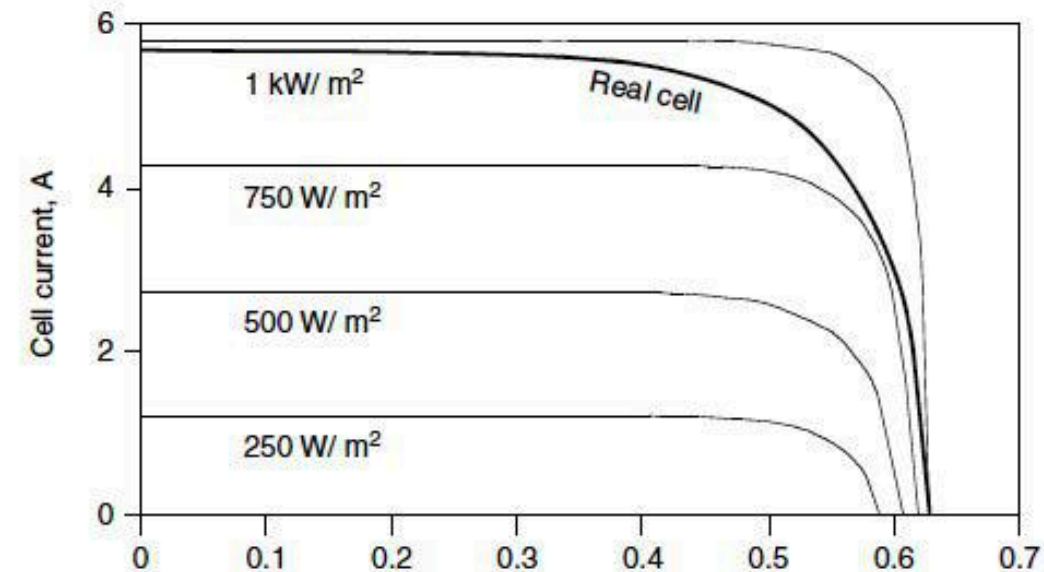
V : voltage

n : =1-2 (known as the diode ideality factor)

k : Boltzman constant= $1.381 \cdot 10^{-23}$ J/K

At zero current, $I = 0$,

$$V_{oc} = \frac{nkT}{e_0} \ln\left(\frac{j_s}{j_0} + 1\right) \approx \frac{nkT}{e_0} \ln \frac{j_s}{j_0}$$



© CRC Press, LLC. All rights reserved. This content is excluded from our Creative Commons license. For more information, see <https://ocw.mit.edu/fairuse>.

The I-V curve of a real PV cell (dark), and the ideal curves for a cell subjected to different illumination levels (or photon flux)

$$j_0 = A \exp\left(-\varepsilon_o \frac{E_g(T)}{kT}\right)$$

$A \sim 1.5 \cdot 10^8 \text{ mA/cm}^2$ (empirically determined)

$$E_g(T) \sim E_g(0) - \left(\frac{\alpha T^2}{T + \beta}\right): \text{bandgap energy}$$

$$j_s = \varepsilon_o \int_0^{\infty} \eta_{\lambda}(\lambda) \phi(\lambda) d\lambda$$

η_{λ} : is the quantum efficiency

$\phi(\lambda)$; is the spectral flux

j_s is often measured experimentally

material	Eg(0) in eV	$\alpha \cdot 10^{-4}$ in eV K ⁻¹	β in K
Si	1.1557	7.021	1108
Ge	0.7412	4.561	210
GaAs	1.5216	8.871	572

$$V_{OC} \approx \frac{nkT}{e_0} \ln \frac{j_s}{j_0} \sim V_{OCn} + \frac{nkT}{e_0} \ln \frac{G}{G_n}$$

V_{OCn} : open circuit voltage under normal conditions

G and G_n : solar irradiance under actual and normal conditions

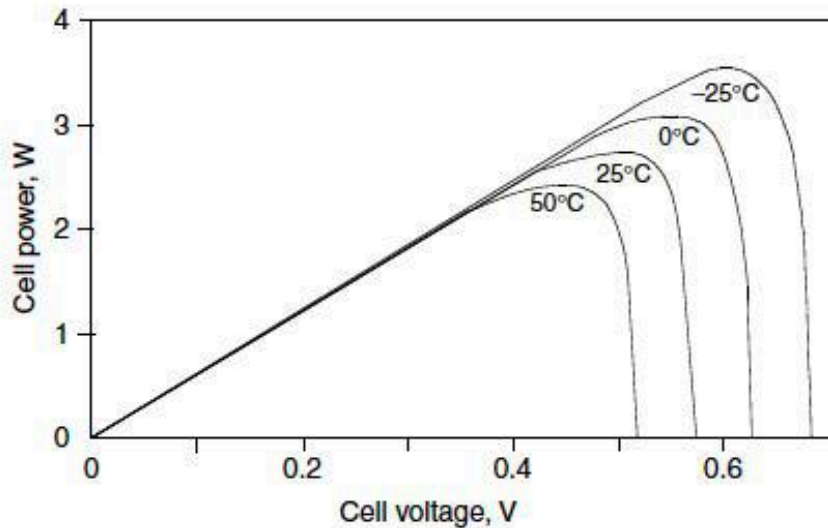
the fill factor measure the quality of the cell

$$FF = \frac{P_{\max}}{P_{th}} = \frac{j_{MP} V}{j_s V_{OC}}$$

j_{MP} : current at max power

$$\text{The conversion efficiency is: } \eta = \frac{P_{\max}}{P_{in}} = \frac{FF j_s V_{OC}}{G}$$

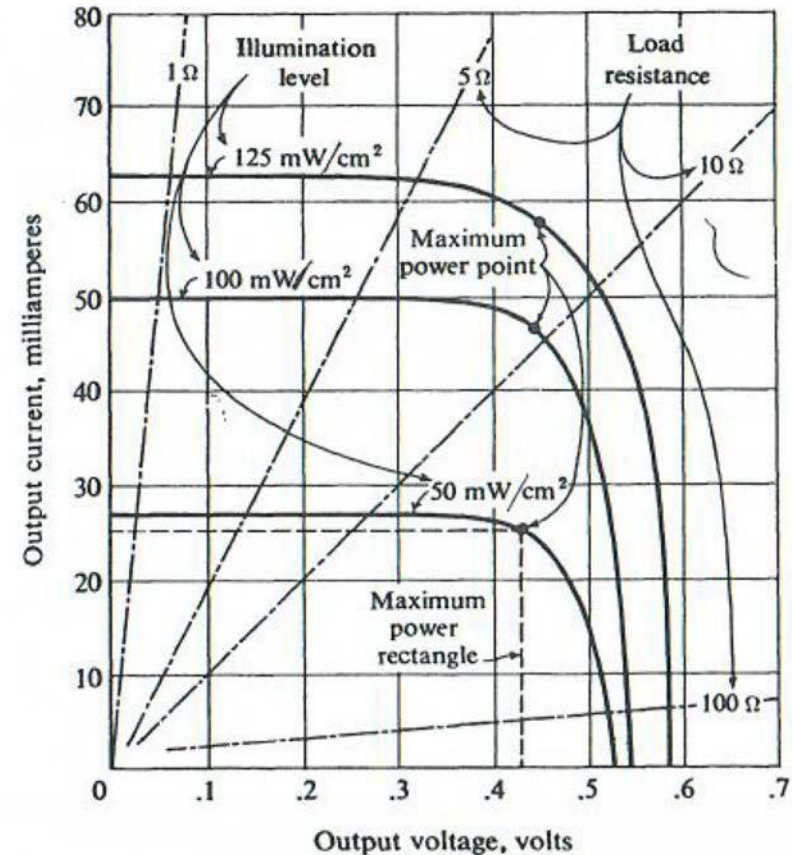
Impact of operating temperature on Power-Voltage curve of a PV cell.



© CRC Press, LLC. All rights reserved. This content is excluded from our Creative Commons license. For more information, see <https://ocw.mit.edu/fairuse>.

Goswami and Kreith, Energy Conversion, CRC Press, 2008.

Typical I-V curve of a Si cell showing the effect of illumination and load resistance

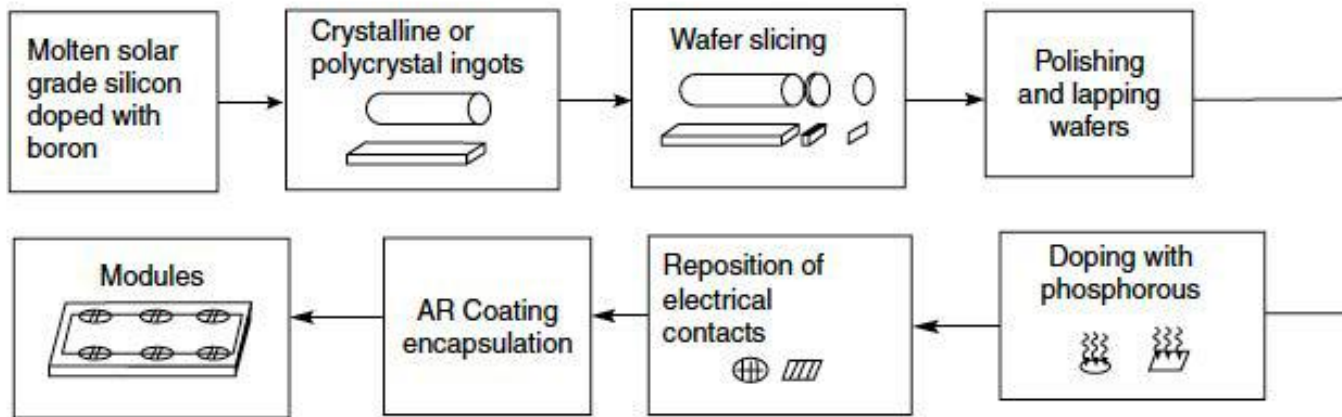


© Allyn and Bacon. All rights reserved. This content is excluded from our Creative Commons license. For more information, see <https://ocw.mit.edu/fairuse>.

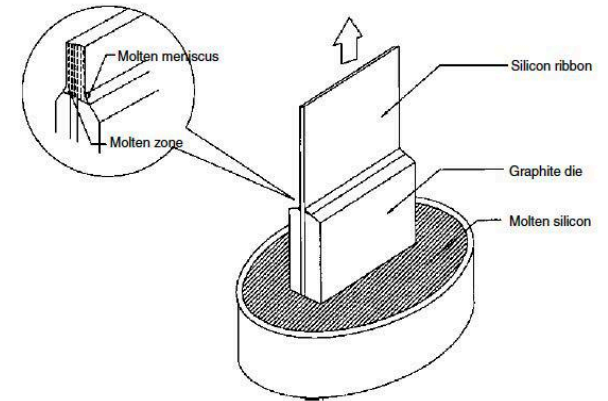
Angrist, Direct Energy conversion, 1976.

Some solar cell manufacturing techniques

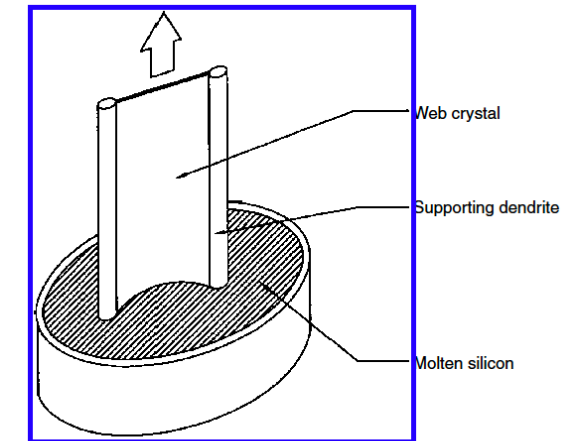
- PV cells use purified silicon (produced by reducing silicon oxides) but not necessarily electronic grade.
- All methods start with a molten solar grade silicon (doped with different impurities to produce the p or n semiconductor, or to pacify some of the defects).
- Production of solar cells is energy intensive (with some pay-back energy period).



Processes involved in manufacturing crystalline and polycrystalline PV cells by slicing 250 micron wafers and fusing n-layer into the p-layer.



Edge-define film-fed growth (EFG) methods for growing thin films



String-ribbon production of a thin-film cell

The cell and the panel

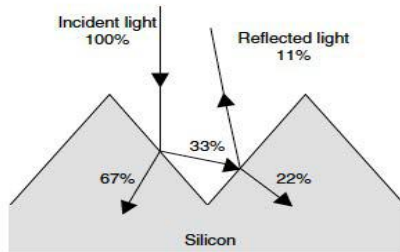


Figure 3.2.2 Effect of a textured surface on the reflectivity of silicon

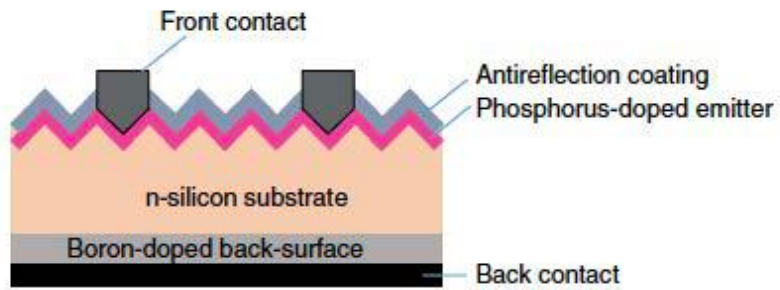


Figure 3.2.8 n-type rear emitter silicon solar cell

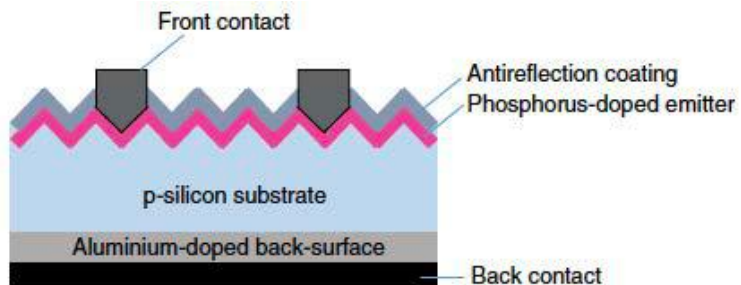


Figure 3.2.4 Screen-printed silicon solar cell

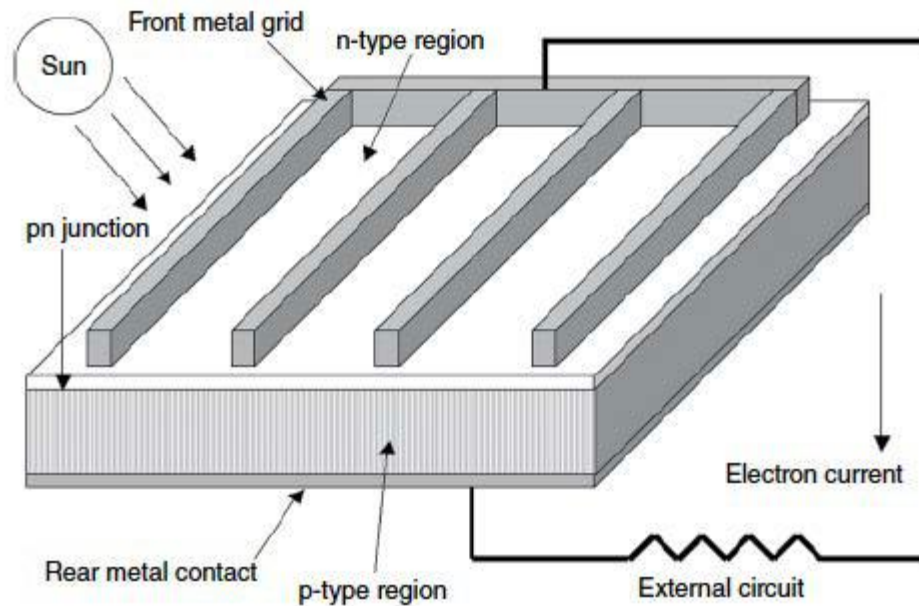
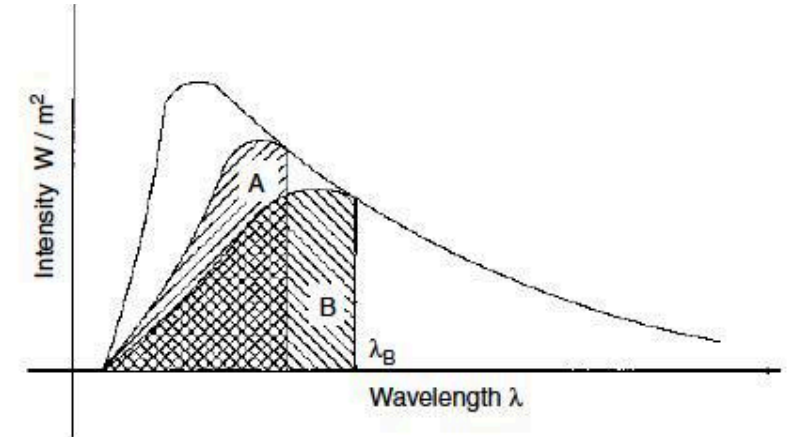


Figure 3.2.1 Schematic of a typical solar cell

Heterojunction Devices

- Efficiency can be improved using multi layer cells (tandem devices), with high bandgap material at top and low bandgap material below (low frequency radiation penetrates better).
- The open circuit voltage of the stack is the sum of the open circuit voltages of the individual cells.
- Multijunction devices using Silicon and Gallium Arsenide are the most efficient solar cells to date, reaching as high as 39% efficiency. They are also the most expensive.

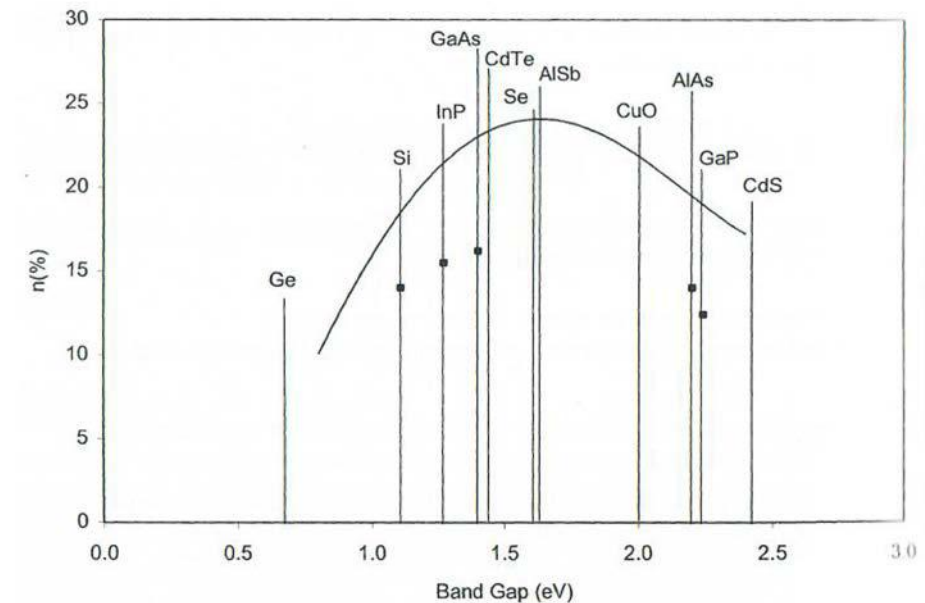


Part of the spectrum captured by a two layered tandem cell

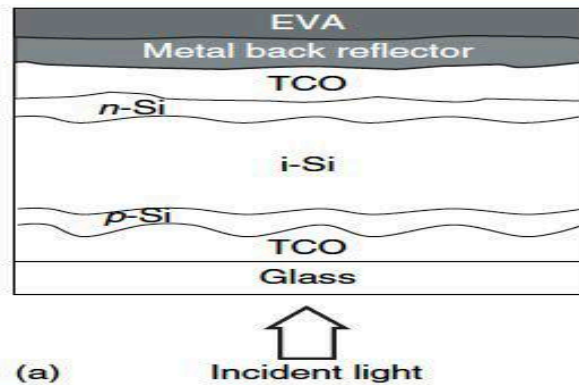
© CRC Press, LLC. All rights reserved. This content is excluded from our Creative Commons license. For more information, see <https://ocw.mit.edu/fairuse>.

Thin film technology

- Material with bandgap close to 1.5 eV should be used to achieve higher efficiency (than Si), but they are expensive (CdTi, GaAs, InP, Zn₃P₂, ...)
- Can only be used in thin film form to be economical
- Because of the thin film (few microns), material should also have high optical absorption coefficient to achieve high efficiency.
- And because they are used in thin film, it is possible to build tandem or heterojunction cells
- But they need good substrate to deposit the thin film on



A single p-i-n junction thin film a-Si with transparent conduction oxide (TCO), metal and glass as outer layers and a vinyl acetate (EVA) cover.



© CRC Press, LLC. All rights reserved. This content is excluded from our Creative Commons license. For more information, see <https://ocw.mit.edu/fairuse>.

- Si has also been used with thin film technology, with and intrinsic (i) layer between the p- and n-, and transparent conducting oxides (TCO) between the p-n junction and the outer layers.
- **Crystalline Si** has better conversion efficiency than **amorphous Si** but less optical absorption. The efficiency of a-Si is improved by hydrogen alloying (Si:H).

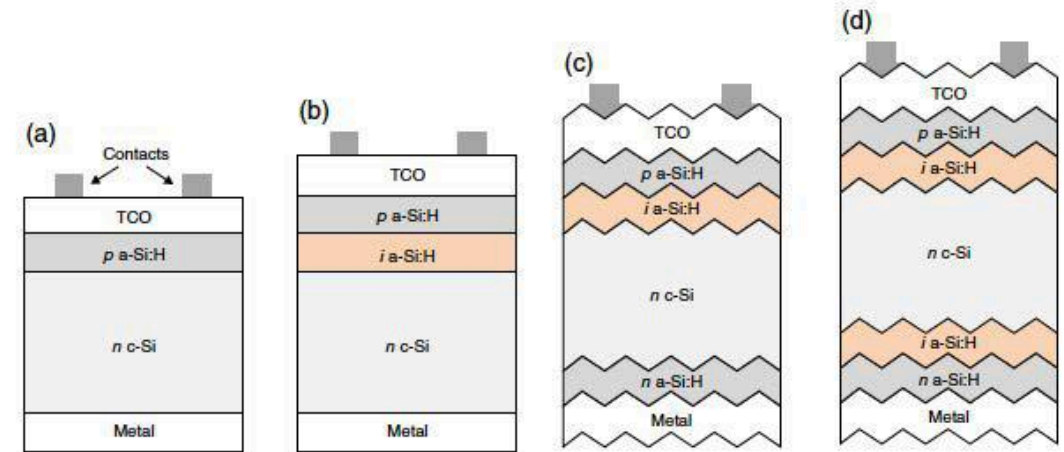
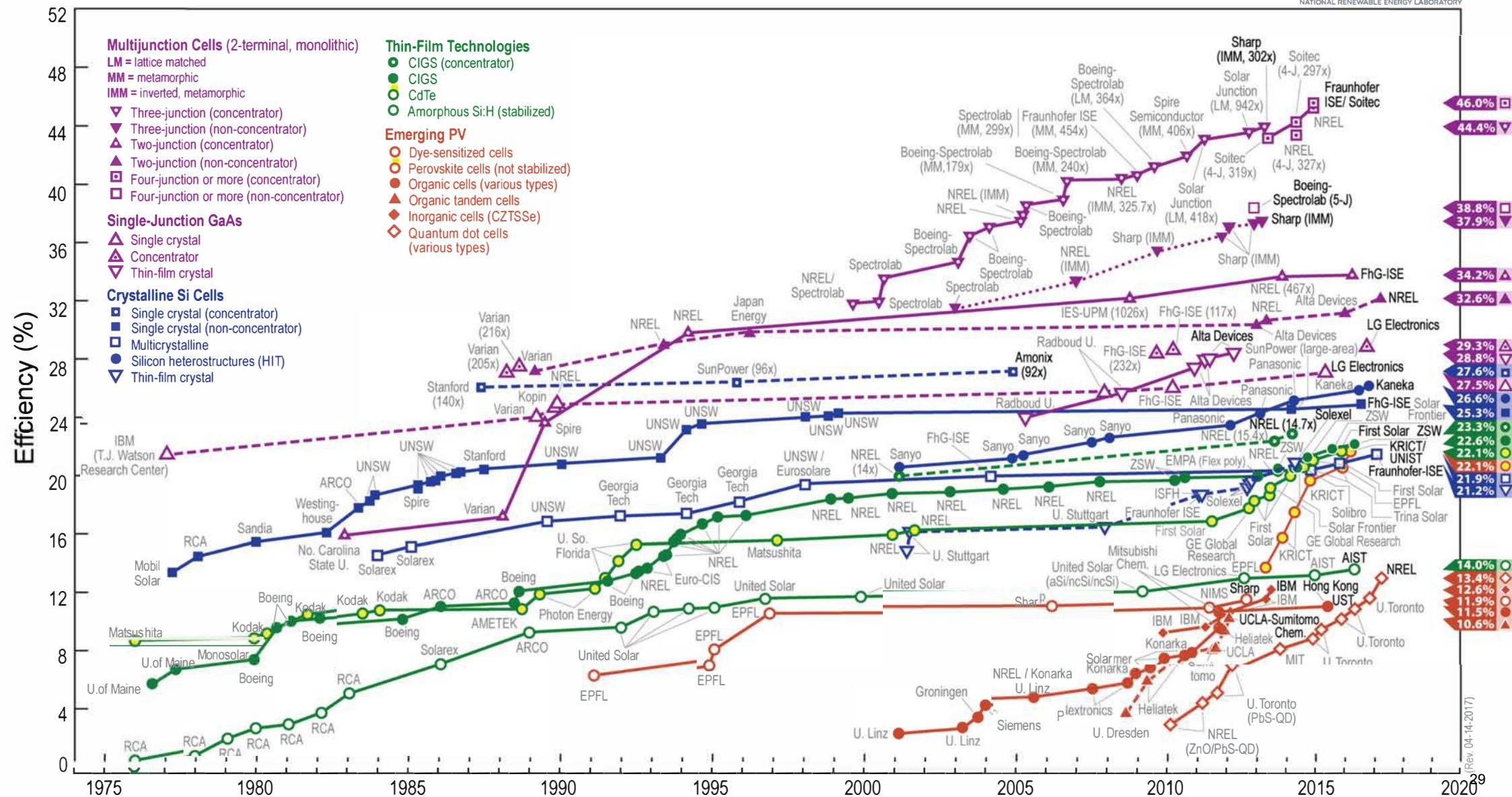


Figure 3.4.3 Schematic structure of heterojunction a-Si:H/c-Si solar cells. (a) basic structure with transparent conductive oxide and metal as top and back contact; (b) idem, with intrinsic a-Si:H layer sandwiched between p a-Si:H and n c-Si; (c) idem, with textured interfaces and back-surface field layer of n a-Si:H; (d) idem, with additional i a-Si:H. Note, drawings are not to scale

© Wiley. All rights reserved. This content is excluded from our Creative Commons license. For more information, see <https://ocw.mit.edu/fairuse>.

Best Research-Cell Efficiencies



PV Farms

Fixed tilt systems:

Least expensive. Ideal tilt for annual production is the site azimuth angle (determined by latitude) $\pm 15\text{--}20$ degrees. Wind loading, etc., tends to favor tilts less than azimuth angle.

Single-axis Tracking (N-S) axis:

Energy capture is enhanced as much as 25% over fixed tilt systems. Simpler and less expensive than two-axis tracking systems. Typical tracker rotation range is 45 degrees East and West.

Two-axis tracking:

Maximum power: keep the PV plane normal to the sun direct beam throughout the day and seasonally. Energy yield is as high as 40% over fixed tilt systems. High structural, space, and cost requirements.



Figure 11.1.5 PV systems with (a) a single-axis horizontal tracker, and (b) a single-axis tilted tracker. Sources: (a) NEXTracker™ (2015); (b) Nellis AFB (2007)

“Soiling”

Modules covered by dirt, dust, and other particulates can cause annual energy production losses up to 10% or more if not cleaned periodically



Benban 150 MW plant, Aswan Egypt

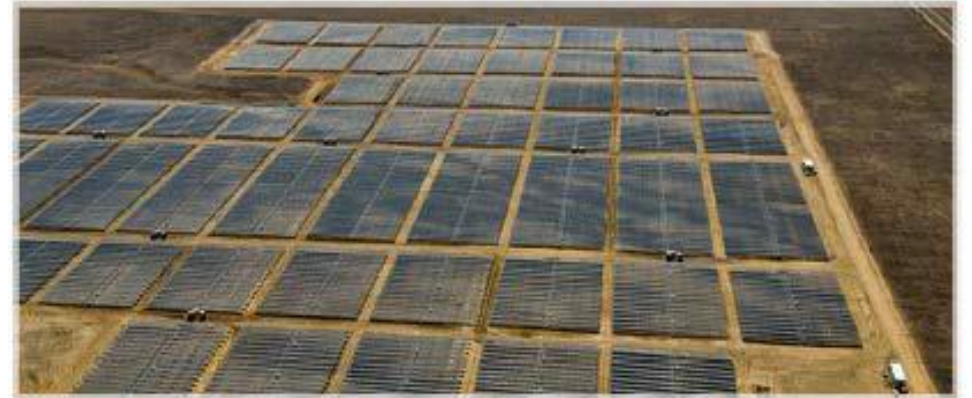


Figure 11.1.6 250 MWac ground-mounted system in California. Source: SunPower



Figure 13.1.3 Solar tracking system with robotic cleaning

© Source unknown. All rights reserved. This content is excluded from our Creative Commons license. For more information, see <https://ocw.mit.edu/fairuse>.

© Wiley. All rights reserved. This content is excluded from our Creative Commons license. For more information, see <https://ocw.mit.edu/fairuse>.

Inverter efficiency:

Inverter DC-AC conversion efficiency is important to the overall system efficiency. Typical range is 94–98% and expressed in terms of peak and weighted output efficiency. Inverter maximum power point tracking (MPPT) efficiency typically can result in additional 0.5–1% loss (see next slide).

Transformer losses:

Additional external transformers are sometimes required to interconnect with utility distribution or transmission systems. Losses on an annual basis typically in range of 0.5–1.5%.

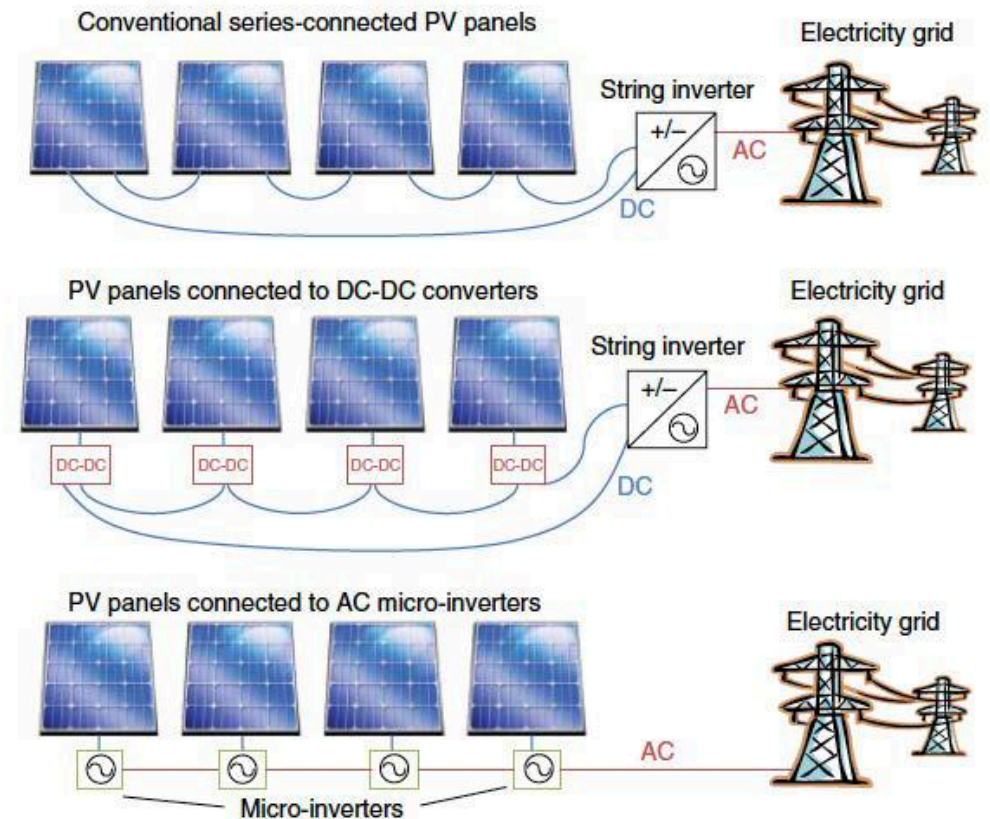


Figure 11.2.1 Schematic of conventional single-string PV system (top), DC-DC converter-equipped “Smart Modules” (middle), and AC micro-inverter-equipped PV system (bottom). (See insert for color representation of the figure)

An additional consideration for inverter MPPT is mismatch caused by partial shading. In the P&O strategy described above, the algorithm operates around a local maximum point,

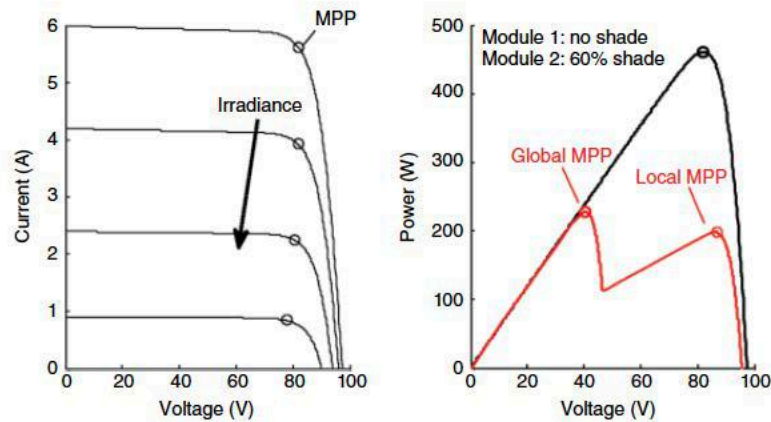


Figure 11.2.5 Comparison of MPP voltage and current with change in irradiance (left). Partial shading (right) can result in multiple local maxima, potentially affecting the MPPT operation

© Wiley. All rights reserved. This content is excluded from our Creative Commons license. For more information, see <https://ocw.mit.edu/fairuse>.

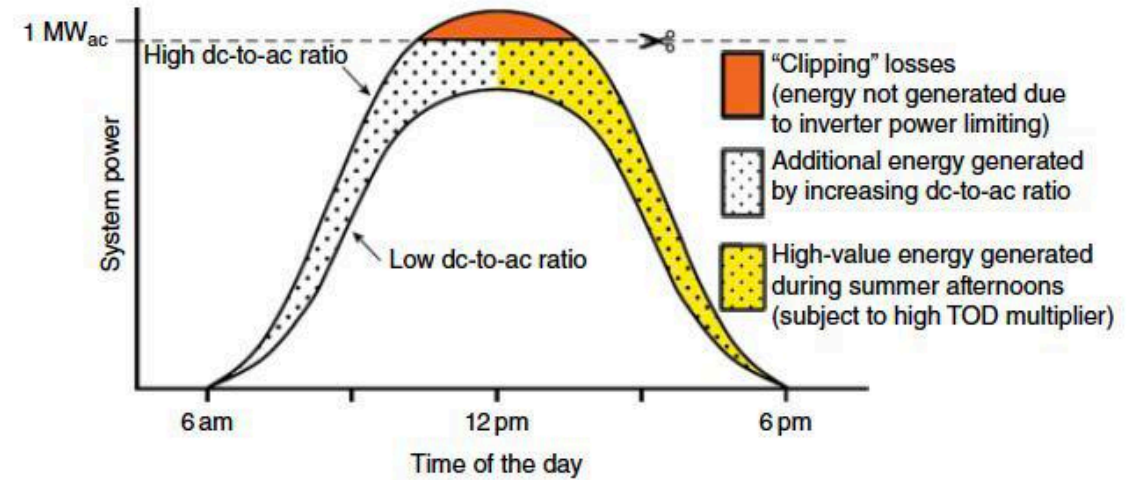
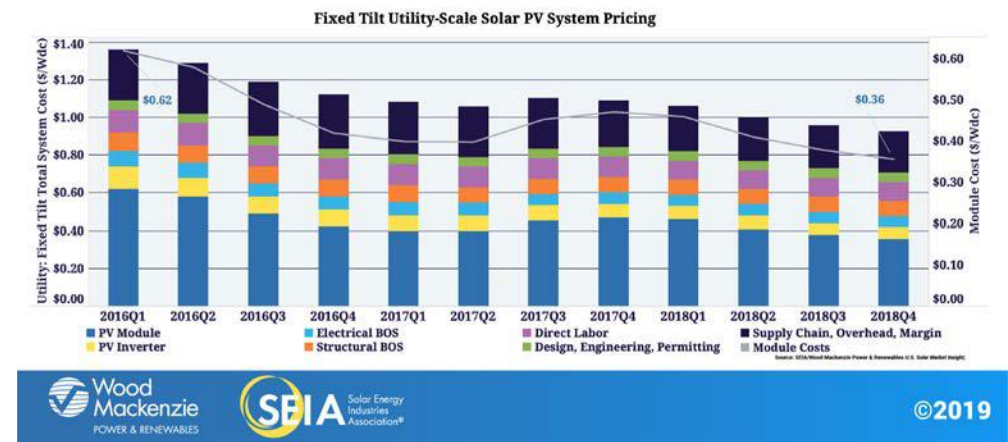
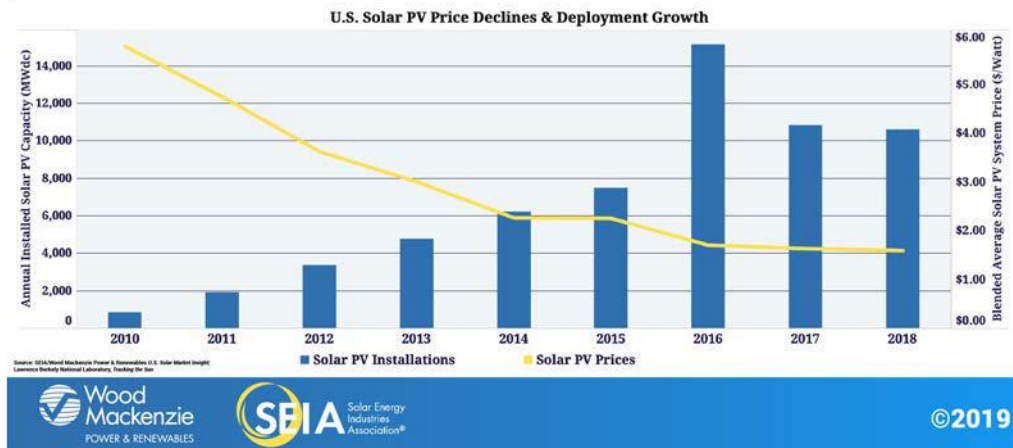
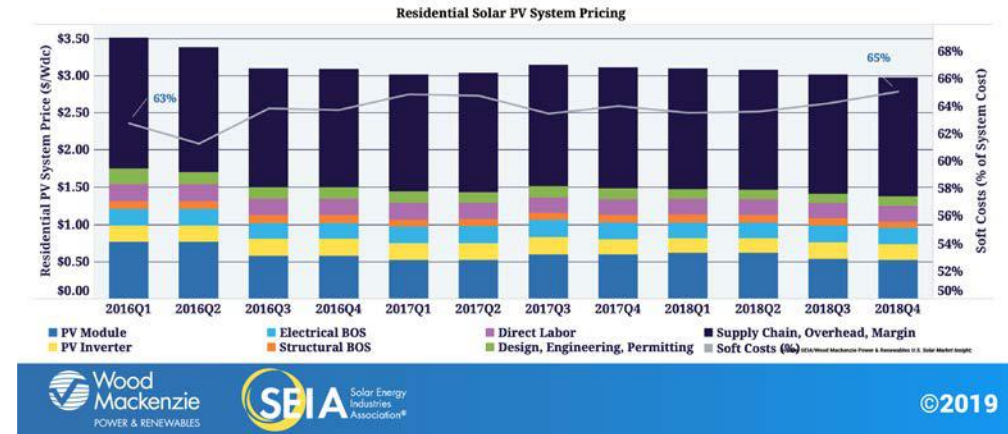
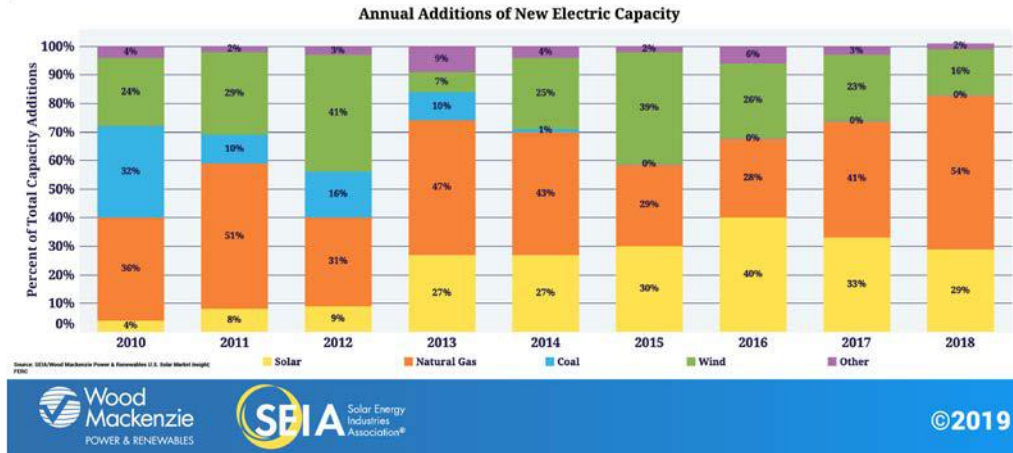


Figure 11.1.7 Impact of varying PV system DC/AC ratio. Source: *SolarPro Magazine* (2013)

© SolarPro. All rights reserved. This content is excluded from our Creative Commons license. For more information, see <https://ocw.mit.edu/fairuse>.

Changes in the US Electricity markets



© Solar Energy Industries Association. All rights reserved. This content is excluded from our Creative Commons license. For more information, see <https://ocw.mit.edu/fairuse>.

MIT OpenCourseWare
<https://ocw.mit.edu/>

2.60J Fundamentals of Advanced Energy Conversion
Spring 2020

For information about citing these materials or our Terms of Use, visit: <https://ocw.mit.edu/terms>.

Lecture # 15

Thermo-mechanical Conversion

Gas Turbine Power Plants

Ahmed Ghoniem
March 30, 2020

1. Why Gas Turbines
2. High T gas turbine cycles.
3. Recuperation.
4. Recovery of exhaust energy in HAT
5. Recovery of exhaust energy in chemical recuperation

Scenarios: Generation in kWh, now and in 2040

How to achieve certain targets (total electricity production) given constraints.

Without CO₂ constraints, coal remains the largest source for electricity production but NG grows significantly. Renewables (hydropower, wind and solar) grow.

With CO₂ constraints, coal dies and NG and renewables grow much faster, with added nuclear.

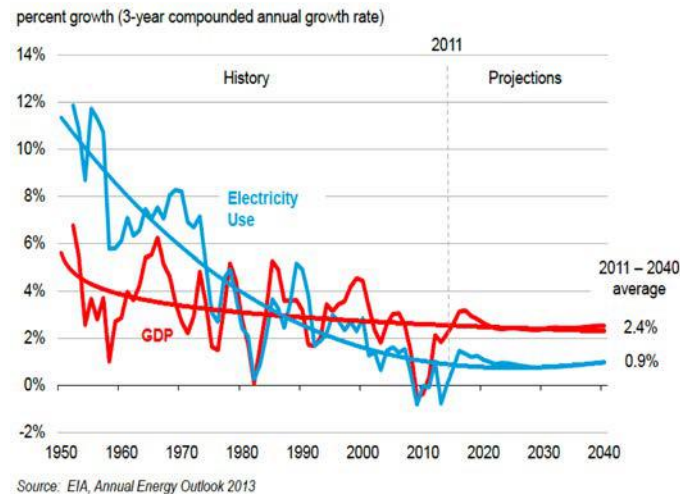


Image courtesy of Energy Information Administration (EIA).

US annual growth of electricity demand and GDP, indicating significant efficiency improvement

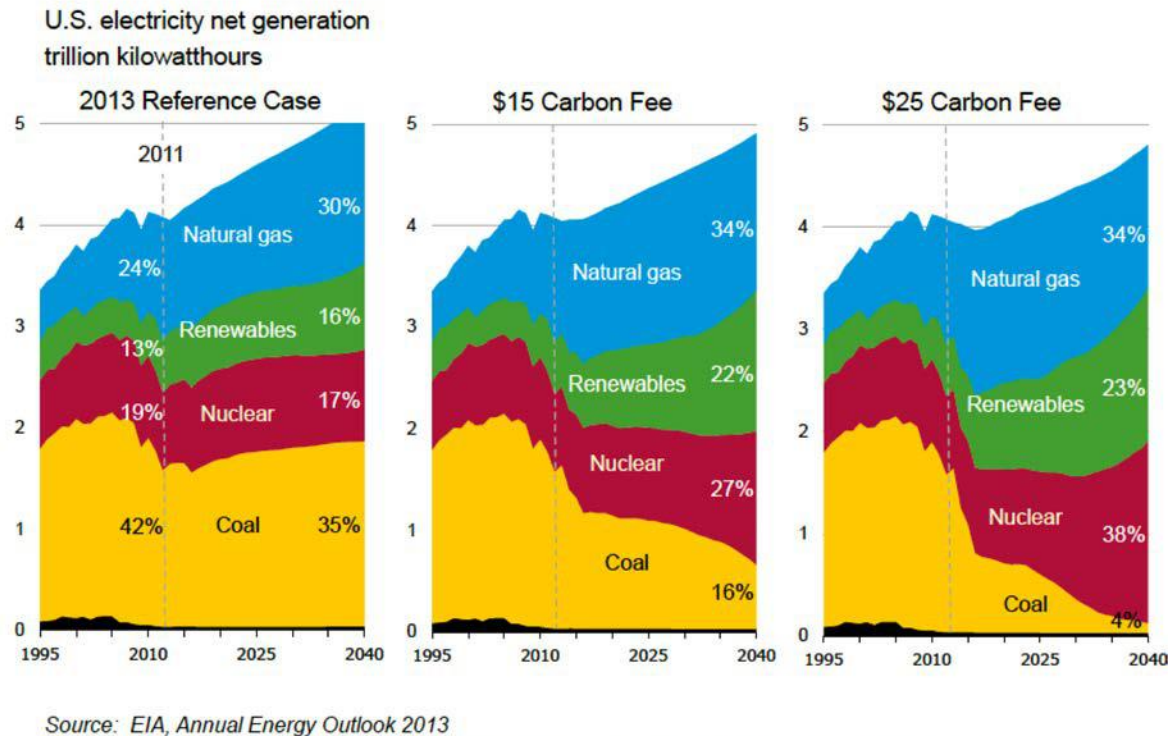


Image courtesy of Energy Information Administration (EIA).

NG, Nuclear and renewables benefit significantly from CO₂ prices

MARCH 8, 2019

New U.S. power plants expected to be mostly natural gas combined-cycle and solar PV

Source: U.S. Energy Information Administration, [Annual Energy Outlook 2019](#)

EIA's long-term projections show that most of the electricity generating capacity additions installed in the United States through 2050 will be natural gas combined-cycle and solar photovoltaic (PV). Onshore wind looks to be competitive in only a few regions before the legislated phase-out of the production tax credit (PTC), but it becomes competitive later in the projection period as demand increases and the cost for installing wind turbines continues to decline.

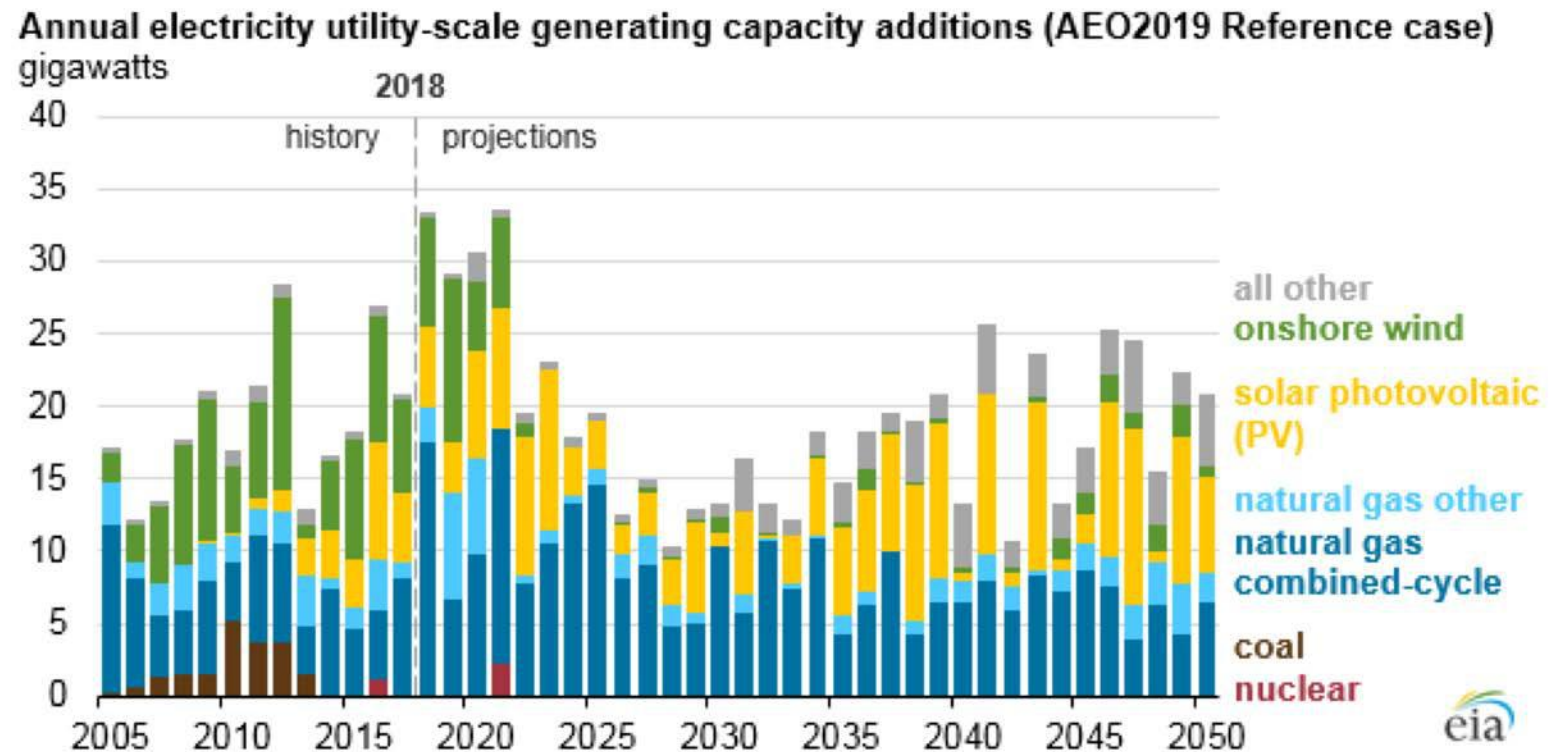


Image courtesy of Energy Information Administration (EIA).

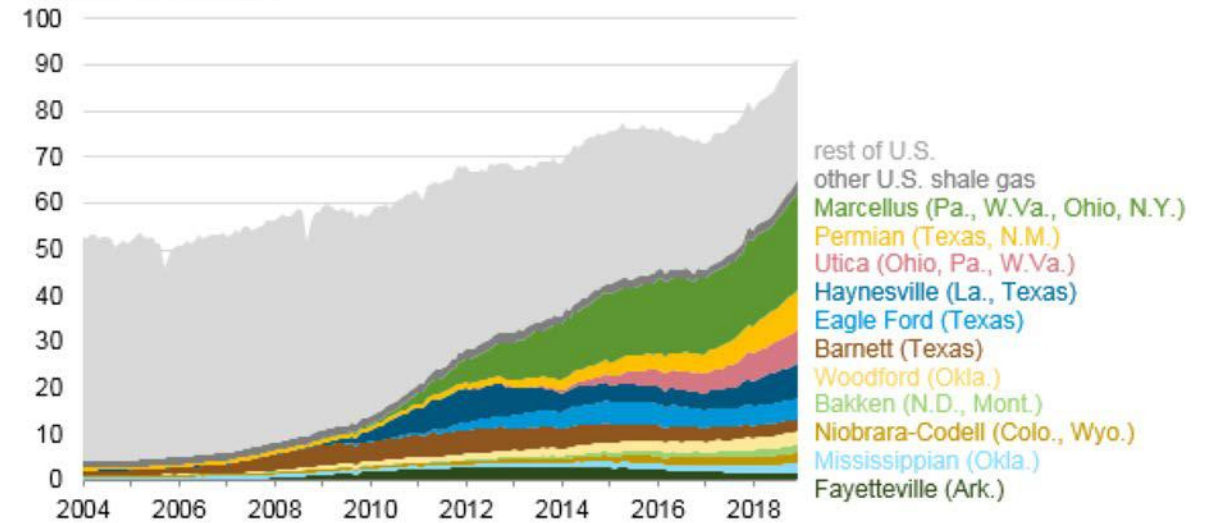
EIA adds new play production data to shale gas and tight oil reports

Source: U.S. Energy Information Administration, [Natural Gas Monthly](#), [Petroleum Supply Monthly](#), and [Short-Term Energy Outlook](#), and DrillingInfo

Impact of fracking on US oil and gas production

Monthly U.S. dry natural gas production (2004-2018)

billion cubic feet per day



Monthly U.S. crude oil production (2004-2018)

million barrels per day

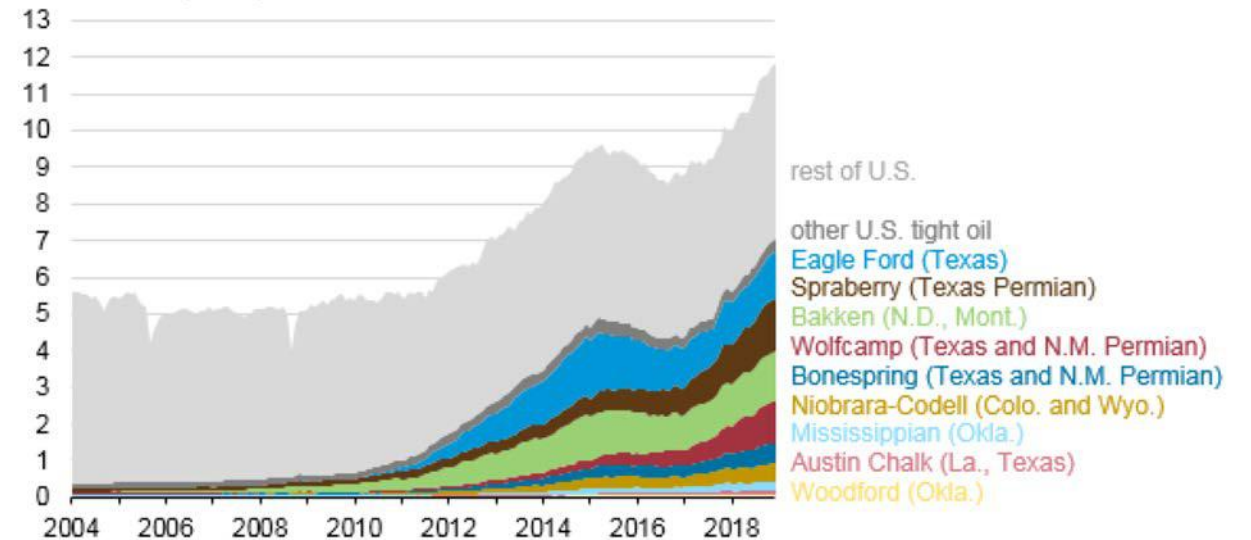


Image courtesy of Energy Information Administration (EIA).

<https://www.eia.gov/todayinenergy/detail.php?id=38372>

Estimated (in 2019) Levelized Cost of Electricity Generation Plants in 2023

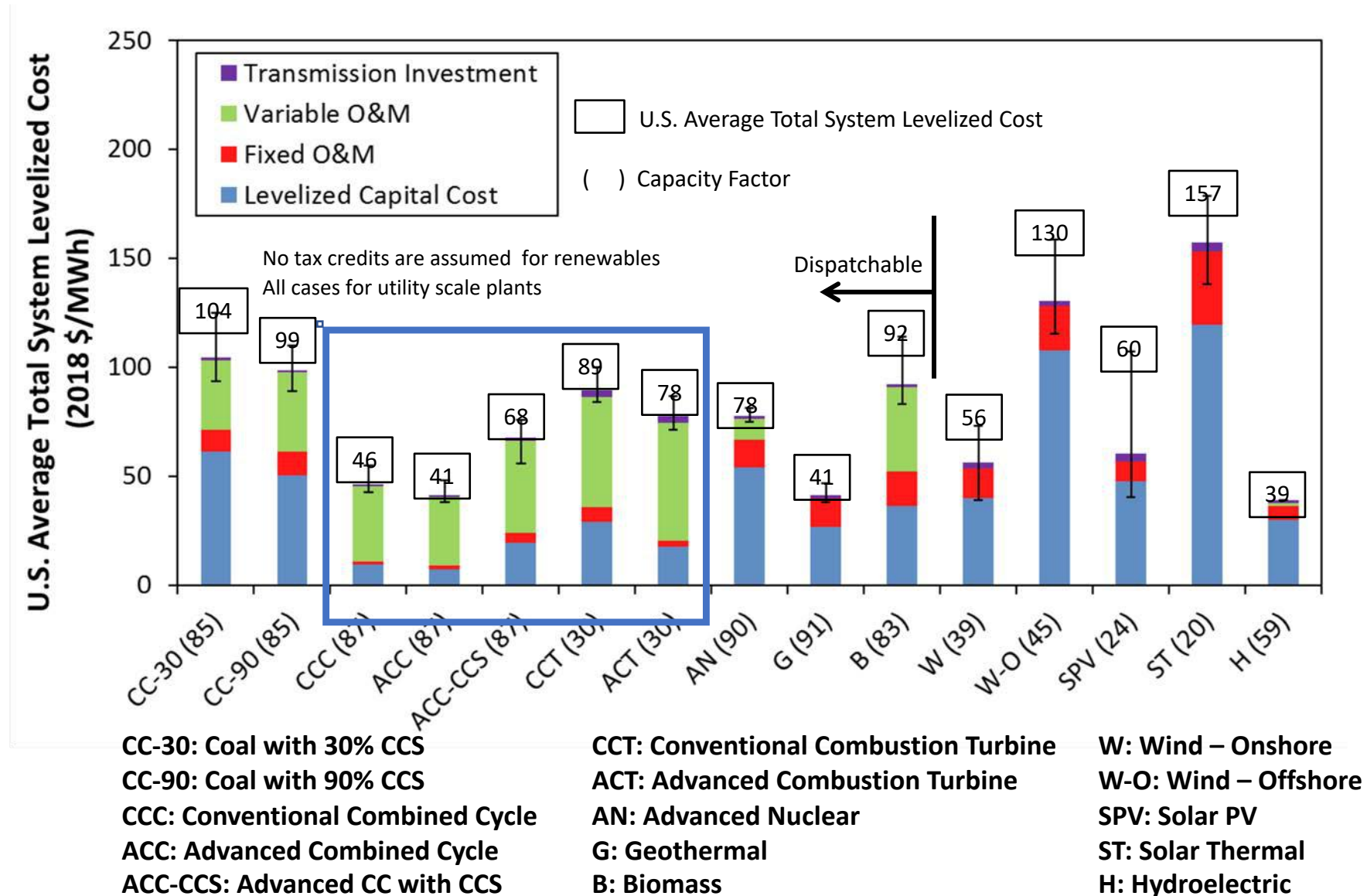


Image courtesy of Energy Information Administration (EIA).

Source: U.S. Energy Information Administration, Annual Energy Outlook 2019, Feb 2019.

Carbon dioxide production in electricity generation: for each mole of fuel we produce:

$|\Delta \hat{h}_{R,f}|$ MJ of thermal energy, $\eta_e |\Delta \hat{h}_{R,f}|$ MJ_e electricity and $\nu_{CO_2} M_{CO_2}$ kg-CO₂

or in short: $\frac{\nu_{CO_2} M_{CO_2}}{\eta_e |\Delta \hat{h}_{R,f}|}$ kgCO₂ / MJ_e

ν_{CO_2} number of moles of CO₂ per mole of fuel burned (=1 for coal or methane),

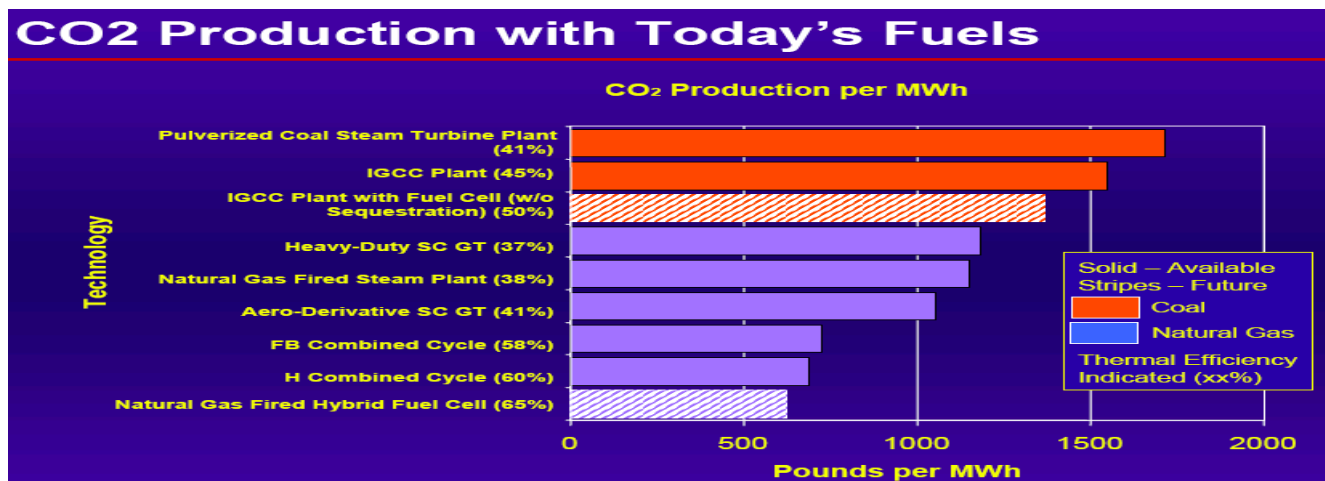
$M_{CO_2} = 44$ molecular weight of CO₂,

η_e is the plant efficiency (0.4 for coal and 0.55 for methane),

$\Delta \hat{h}_{R,f}$ the molar enthalpy of reaction of the fuel (~360 for coal and 800 for methane).

For methane, in a combined gas-steam cycle with 55% efficiency, 0.1 kgCO₂/MJ_e.

For coal, in a simple steam cycle with 35% efficiency, 0.3 kgCO₂/MJ_e.



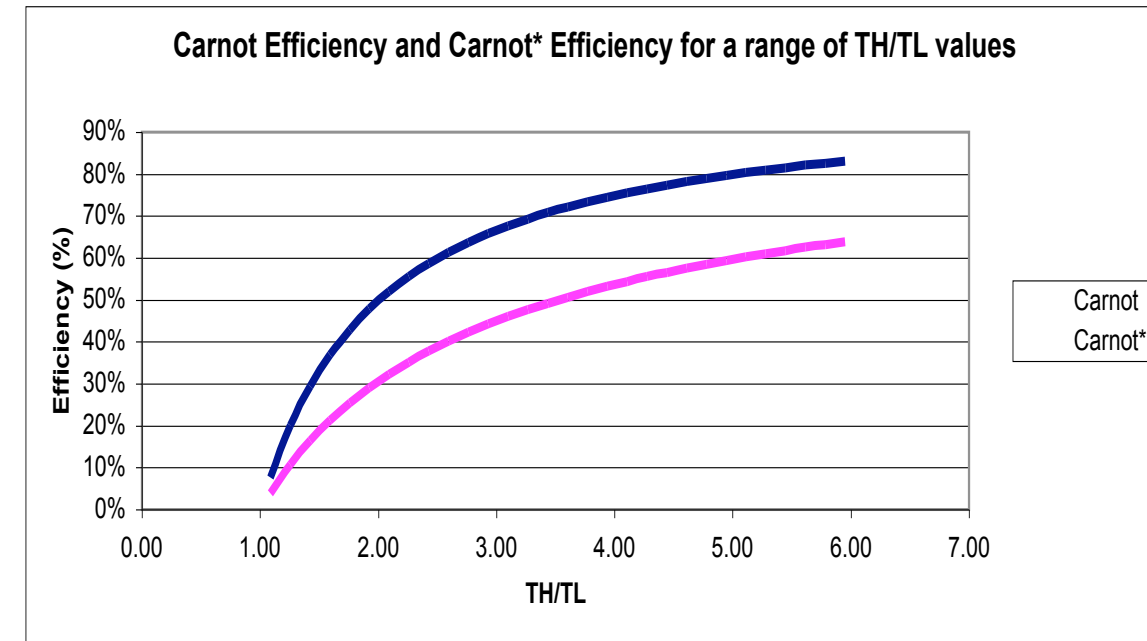
To convert to kgCO₂/MJ_e, multiply the number given in the plot by 0.12 10⁻³

© Source unknown. All rights reserved. This content is excluded from our Creative Commons license. For more information, see <https://ocw.mit.edu/fairuse>.

Alan Walker, GE Power Systems, H2 Symposium, MIT, Sep 2003. SC: Simple Cycle.

Thermomechanical efficiency depends on “heat source” Temperature

Power plant	T_H in C	T_H/T_L
Pressurized heavy water reactor (PHWR)	260-280	1.8-2.0
Boiling water reactors (BWR),	280-290	1.8-2
Pressurized water reactors (PWR	300-350	2.0-2.1
Metal cooled reactors	550	3
Compressed gas reactors (CGR	700-800	3-4
Solar thermal with troughs	280-350	2-2.2
Solar thermal with towers	Up to 500	3
Solar thermal with dishes	750	3.5
Geothermal plants	100-200	1.5
Gas turbine with NG	900-1400	4-5



Thermodynamic Models of Gas Turbine Brayton Open Cycles

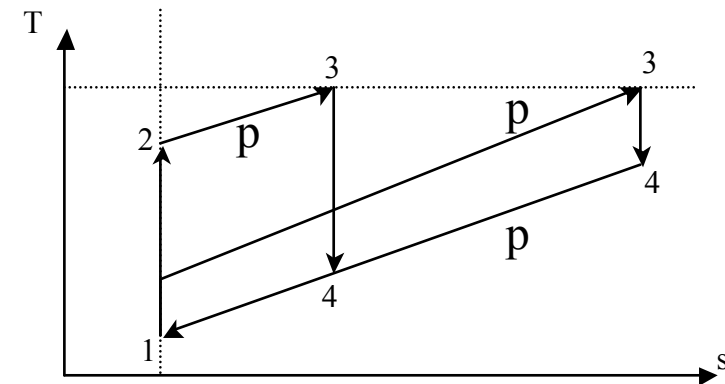
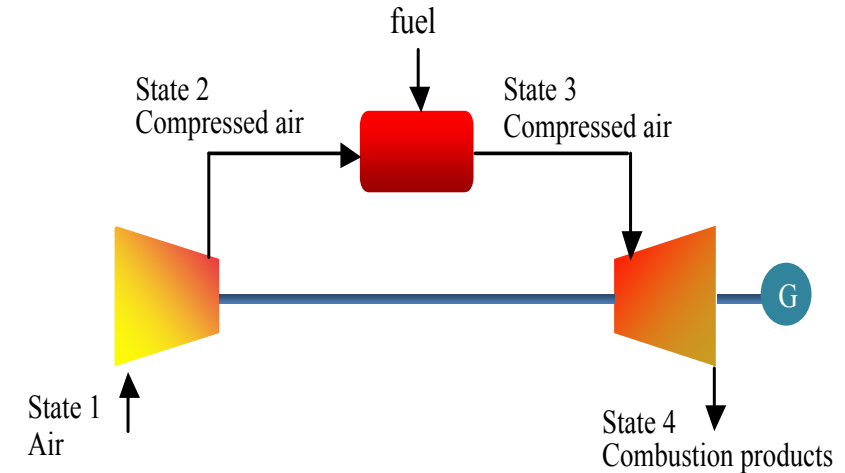
$$\eta_I = \frac{\text{net work out}}{\text{heat transfer in}} \quad \text{and} \quad \eta_{II} = \frac{\text{net work out}}{\text{maximum work}}$$

$$\eta_{\text{fuel-utilization}} = \frac{\wp}{\dot{m}_f \cdot \xi_f^o} \approx \frac{\wp}{\dot{m}_f \cdot LHV}$$

Ideal simple Brayton cycle: $\eta_I = 1 - \left(\frac{1}{\pi_p} \right)^{(k-1)/k} = 1 - \frac{1}{\vartheta_{2s}}$

π_p = pressure ratio across compressor, $\vartheta_{2s} = T_{2s} / T_1$.

at higher π_p , less fraction of the heat is rejected (see schematic)



Ideal gases, air standard cycle ...

$$\frac{T_{2s}}{T_1} = \left(\frac{p_2}{p_1} \right)^{\frac{k-1}{k}}, \text{ and } \eta_C = \frac{h_{2s} - h_1}{h_2 - h_1} = \frac{T_{2s} - T_1}{T_2 - T_1},$$

$$\text{hence: } T_2 = T_1 + \frac{T_{2s} - T_1}{\eta_C}$$

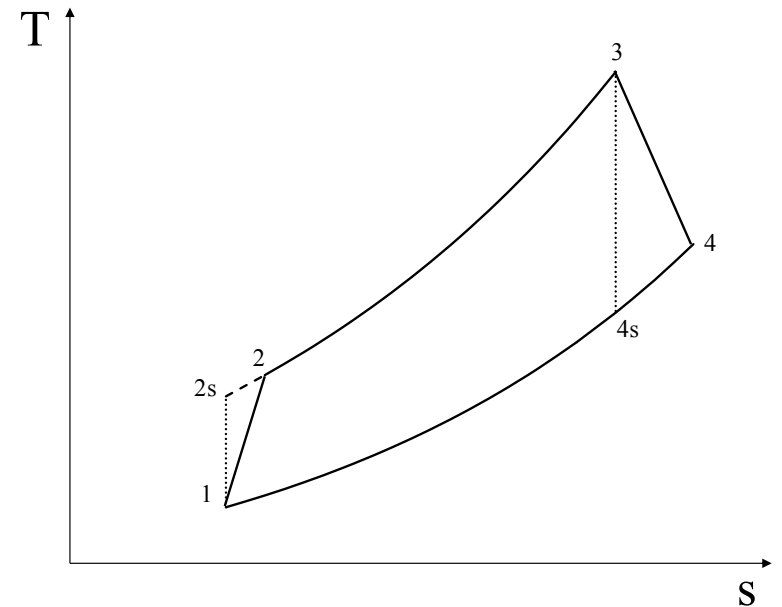
$$\frac{T_3}{T_{4s}} = \left(\frac{p_3}{p_4} \right)^{\frac{k-1}{k}} = \left(\frac{p_2}{p_1} \right)^{\frac{k-1}{k}}, \text{ and } \eta_T = \frac{h_3 - h_4}{h_3 - h_{4s}} = \frac{T_3 - T_4}{T_3 - T_{4s}},$$

$$\text{hence: } T_4 = T_3 - \eta_T (T_3 - T_{4s})$$

$$Q_{in} = h_3 - h_2 = c_p (T_3 - T_2)$$

$$W_{net} = (h_3 - h_4) - (h_2 - h_1) = c_p [(T_3 - T_4) - (T_2 - T_1)]$$

$$\eta_{cycle} = \frac{W_{net}}{Q_{in}}$$



Compressor efficiency is key ...
 $T_{max} < 1000 \text{ C}$, Modern designs, $T_{max} \sim 1400 \text{ C}$.

compressor work: $w_c = \frac{c_p T_1}{\eta_c} \left[\pi_p^{(k-1)/k} - 1 \right]$

Turbine work: $w_t = \eta_T c_p T_3 \left[1 - \frac{1}{\pi_p^{(k-1)/k}} \right]$

Tables are for the following:

$T_{min} = 20\text{C}$, $T_{max} = 800\text{C}$,

Carnot efficiency = 62.5%

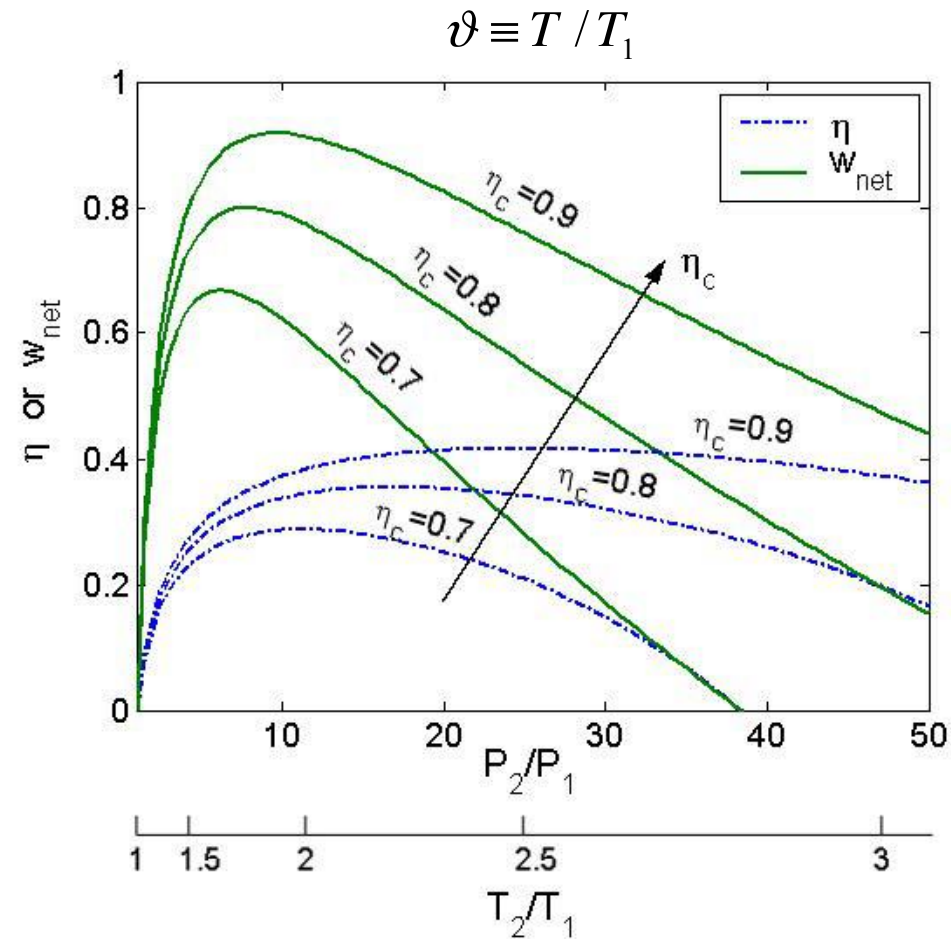
Turbine isentropic efficiency = 90%

Air, $\pi_p = 4$	W_C	W_T	W_{net}	Q_H	η	$T_4 \text{ (K)}$
Ideal	143.0	352.3	209.3	640.2	0.327	722.1
Real, $\eta_c=0.85$	168.2	317.1	148.9	614.9	0.242	757.2
Real, $\eta_c=0.65$	219.9	317.1	97.2	563.2	0.173	757.2
With regeneration $\eta_c=0.85$					0.412	

Air, $\pi_p = 8$	W_C	W_T	W_{net}	Q_H	η	$T_4 \text{ (K)}$
Ideal	238.7	482.6	243.9	544.4	0.448	592.3
Real, $\eta_c=0.85$	280.8	434.3	153.5	502.3	0.306	640.4
Real, $\eta_c=0.65$	367.2	434.3	67.1	415.9	0.161	640.4
With regeneration, $\eta_c=0.85$					0.345	

Figure 4. The impact of the compressor efficiency on the Brayton cycle efficiency and specific work, for $\vartheta_3 = 4.5, \eta_T = 90\%, \beta = 1$.

- Compressor performance, or isentropic efficiency, is key.
- Note how the the specific power peaks at a certain pressure ratio.
- Also the efficiency peaks more sharply as the compressor efficiency decreases.



Closed Cycles: Not currently in use ...

- ▲ Closed cycles allow flexibility in choosing working fluid;
- ▲ they need cooling, and turbine can exhaust at p lower than atmosphere
(this may not be an advantage since compressor work increases)
- ▲ They can also use "dirty fuels" or nuclear (or renewable) heat.

$$\eta_I = 1 - \left(\frac{1}{\pi_P} \right)^{(k-1)/k}$$

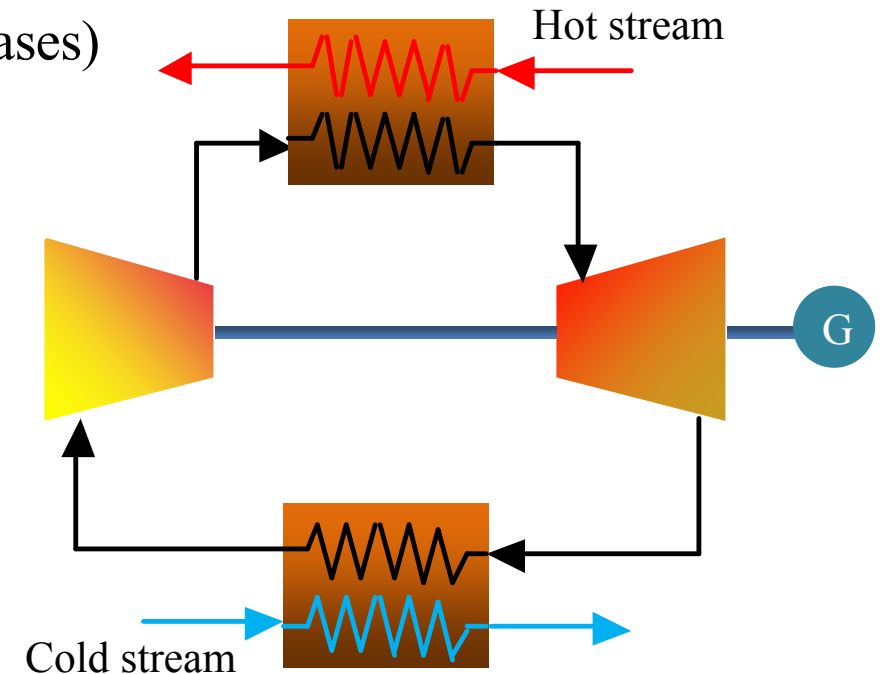
Helium has:

higher $k = 1.67$, higher temperature @ low pressure ratio

Thus higher efficiency.

higher heat capacity, $c_{p,He} / c_{p,air} = 5$

but it is less dense, i.e., high flow velocities needed.

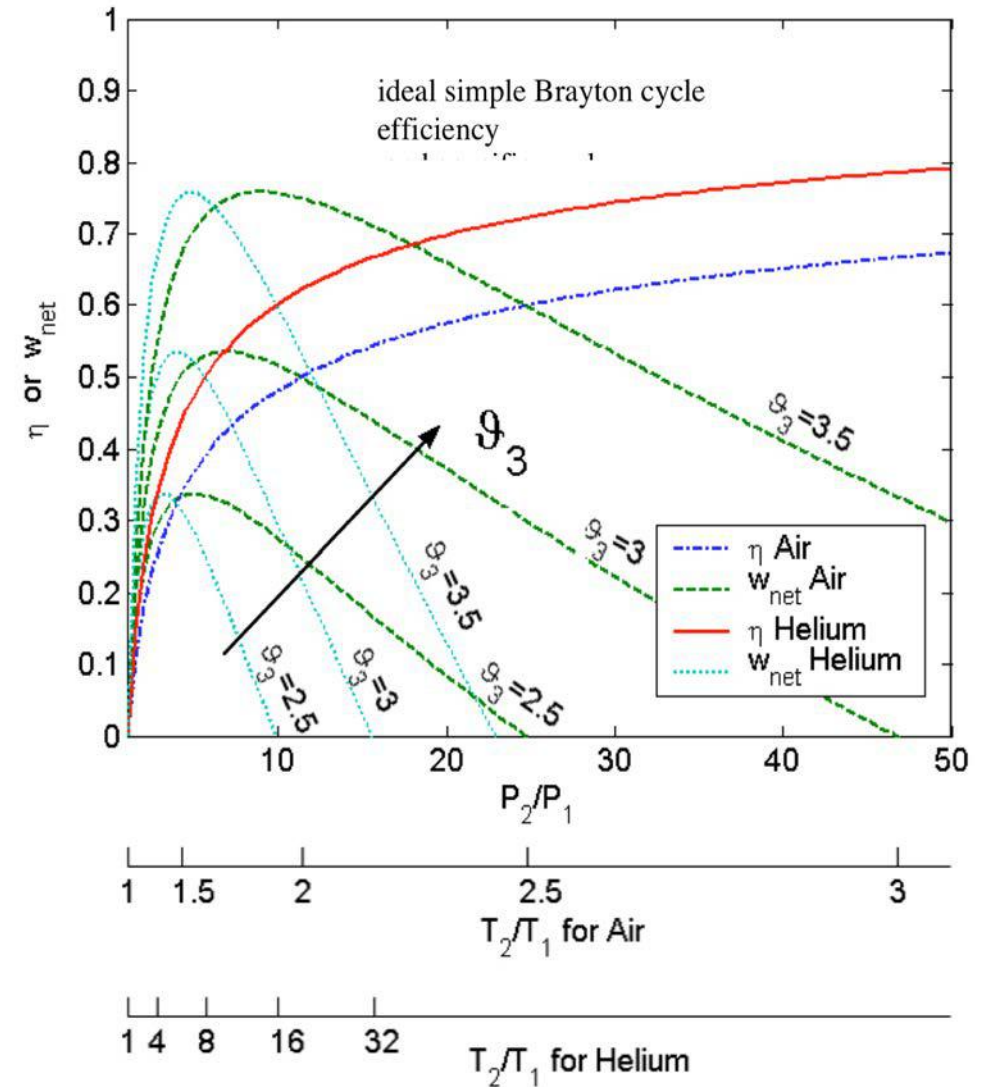


Ideal cycle performance:

Impact of maximum turbine temperature on specific work:

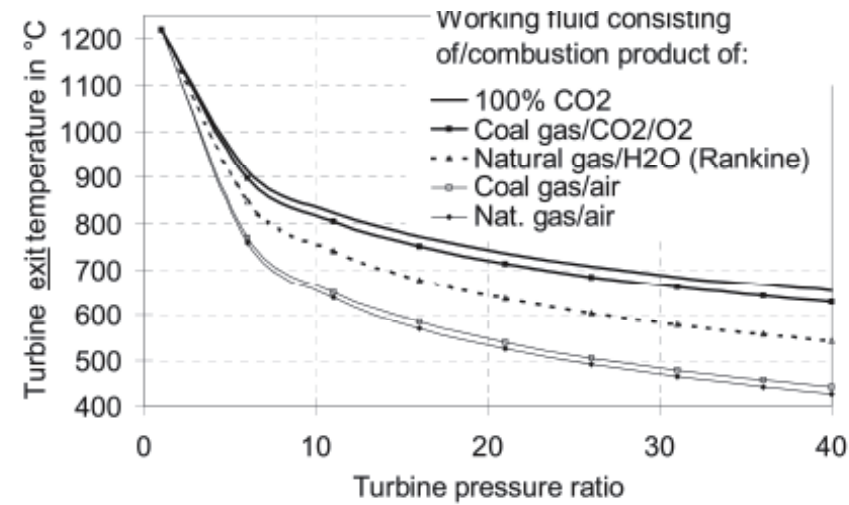
Impact of working fluid on efficiency and maximum work conditions.

- Choice of design point.
- Compromise between hardware cost (initial and running), and fuel cost, CO₂ emissions, etc.



$$\frac{T_3}{T_{4s}} = \left(\frac{p_3}{p_4} \right)^{\frac{k-1}{k}} = \left(\frac{p_2}{p_1} \right)^{\frac{k-1}{k}},$$

$$\eta_I = 1 - \left(\frac{1}{\pi_P} \right)^{(k-1)/k}$$



2.15: Turbine exit temperature calculated for different working fluids in dependence on pressure ratio at a turbine inlet temperature of 1200°C²².

© Source unknown. All rights reserved. This content is excluded from our Creative Commons license. For more information, see <https://ocw.mit.edu/fairuse>.

The gas turbine exit temperature calculated for different working fluids and pressure ratios across the turbine, for turbine inlet temperature of 1200 C. The working fluid consists of either pure CO₂, or is the combustion products of the fuel and the oxidizer list in the figure, with stoichiometry adjusted to give the specified inlet temperature. The essential difference between the different gases is the effective isentropic index. The curve for helium is lower than that for NG/air because of the higher isentropic index of helium. Lower exit temperatures for the working fluid lead to higher overall cycle efficiency. But regeneration and combined cycles can be used to correct that!

Pressure losses during combustion can impact efficiency:

$$\beta_H = p_3 / p_2, \beta_L = p_1 / p_4, \beta^* = (\beta_L \beta_H)^{\frac{k-1}{k}}, \pi_P^* = \pi_P^{(k-1)/k}$$

$$\eta = \frac{\eta_T \vartheta_{\max} \left(1 - \frac{1}{\beta^* \pi_c^*} \right) - \frac{1}{\eta_C} (\pi_c^* - 1)}{\vartheta_{\max} - \left(1 + \frac{\pi_c^* - 1}{\eta_C} \right)}$$

$$w_{net} = \vartheta_{\max} \eta_T \left(1 - \frac{1}{\beta^* \pi_c^*} \right) - \frac{1}{\eta_C} (\pi_c^* - 1)$$

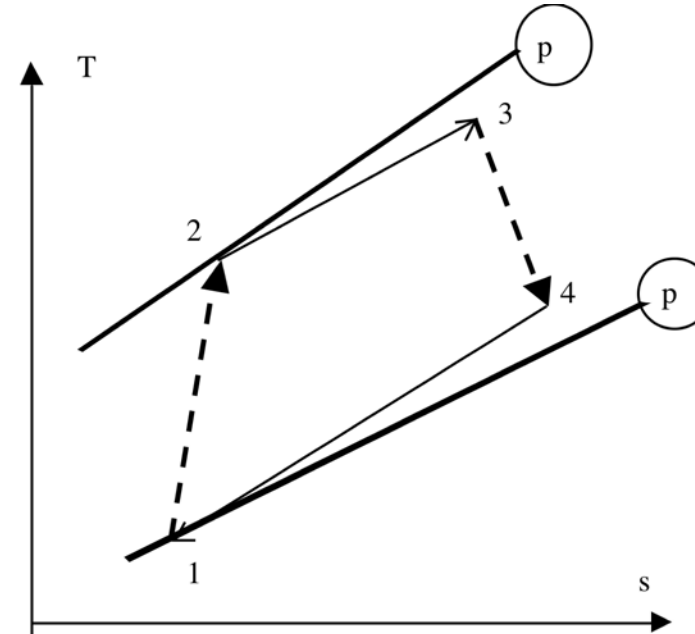
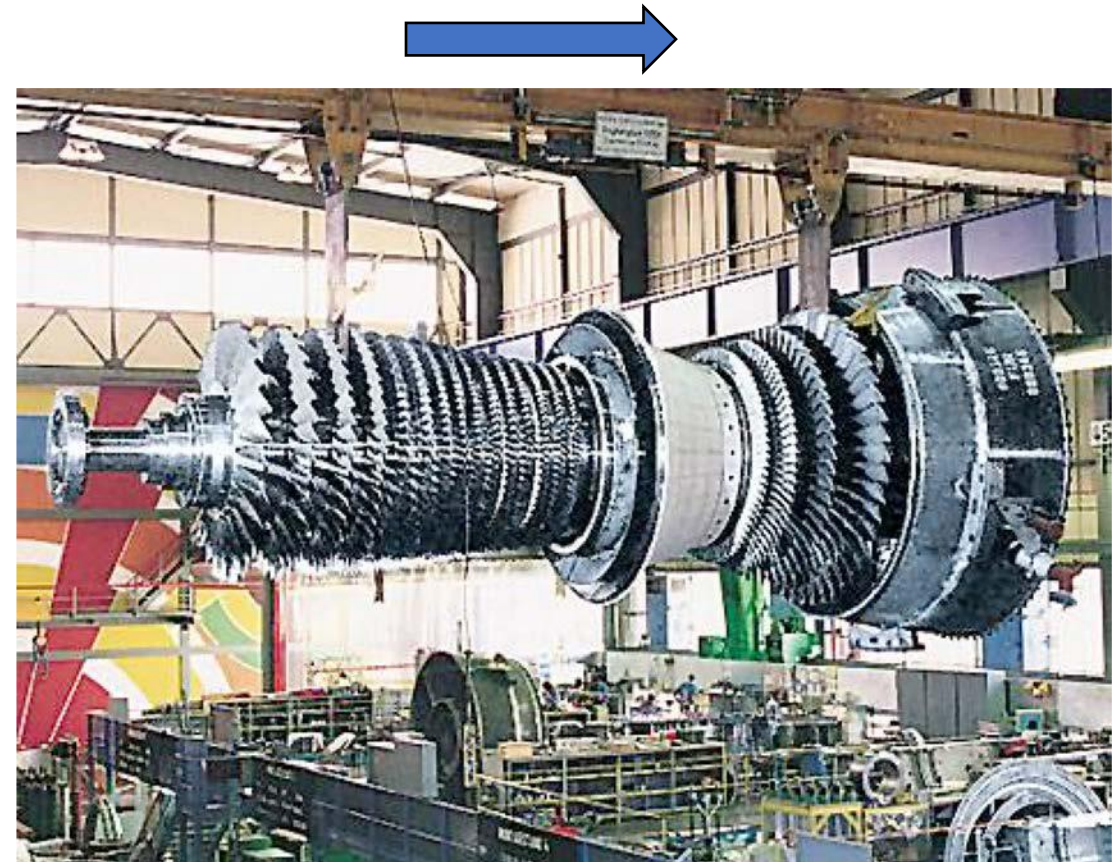


Figure 6. The temperature entropy diagram of a simple Brayton cycle, with isentropic efficiencies for the work transfer components, and pressure drop across the heat transfer components.

- Annular, walk-in combustion chamber with 24 hybrid burners
- Advanced cooling technology
- Ceramic combustion chamber tiles
- Optional multiple fuels capability
- 15-stage axial flow compressor with optimized flow distribution (controlled diffusion airfoils)
- Low-NOx combustion system
- Single-crystal turbine blades with thermal barrier coating and film cooling



SIEMENS: SGT5-4000F
(278 MW, 50Hz)

© Siemens. All rights reserved. This content is excluded from our Creative Commons license. For more information, see <https://ocw.mit.edu/fairuse>.

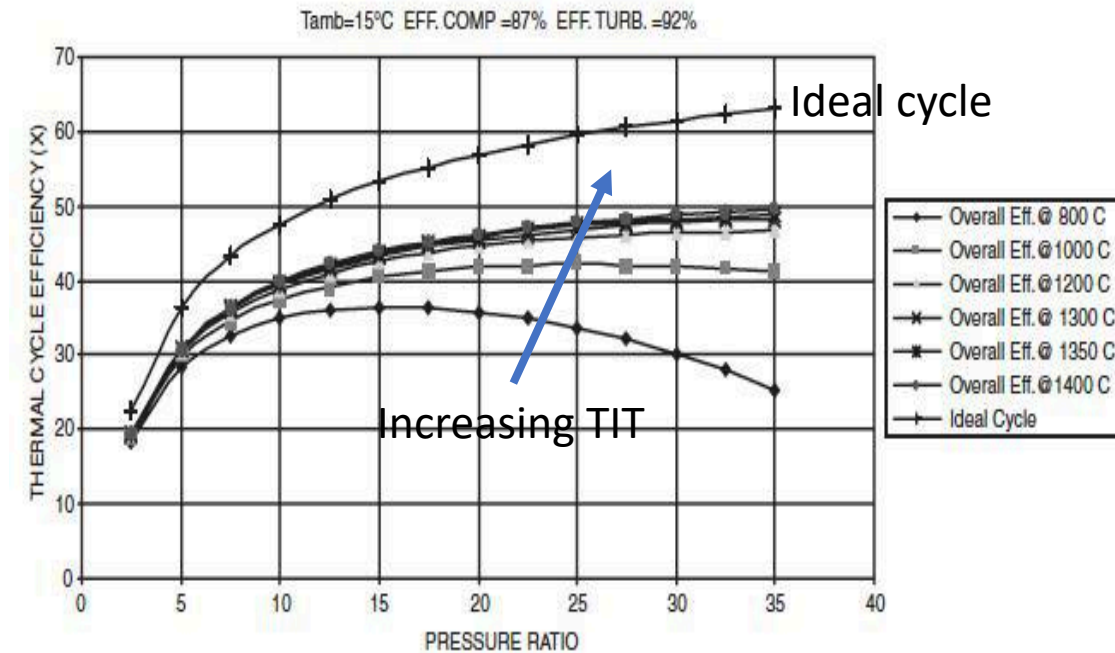
THE USE OF GAS TURBINES IN POWER GENERATION INCREASED FIVE FOLDS BETWEEN 1990 AND 2000, . Why?

Table 1. Westinghouse Combustion Turbine Fleet

	501A	501B	501D	501D5	501DA	501F	501G	ATS
Commercial year	1968	1973	1976	1982	1994	1992	1997	2000
Power (Simple cycle, MWe)	45	80	95	107	120	160	230	290
Pressure ratio	7.5	11.2	12.6	14.0	15.0	15.0	19.2	28.0
Rotor inlet temperature, °C (°F)	879 (1615)	993 (1819)	1096 (2005)	1132 (2070)	1177 (2150)	1277 (2330)	1417 (2583)	1510 (2750)
Exhaust temperature, °C (°F)	474 (885)	486 (907)	513 (956)	527 (981)	540 (1004)	584 (1083)	593 (1100)	593 (1100)
Efficiency – Simple (%)	27.1	29.4	31.2	34.0	34.5	35.5	38.5	--
Efficiency – Combined (%)	37.9	46.4	46.4	48.4	48.6	53.1	58.0	60.0

“Advanced NG Fire Gas Turbine Systems” DOE contract DE-FG21-95MC32071, Westinghouse Electric .

Image courtesy of DOE.

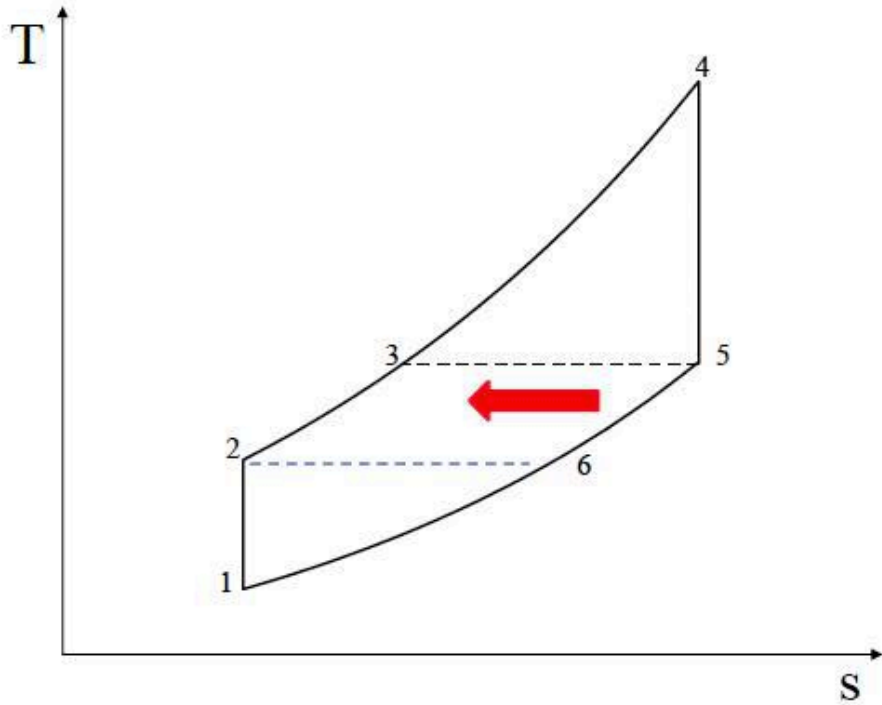


Impact of pressure ratio and turbine inlet temperature on overall cycle efficiency.

Boyce, *Gas turbine Handbook, 2nd Edition*. 2002.

© Gulf Professional Publishing. All rights reserved. This content is excluded from our Creative Commons license. For more information, see <https://ocw.mit.edu/fairuse>.

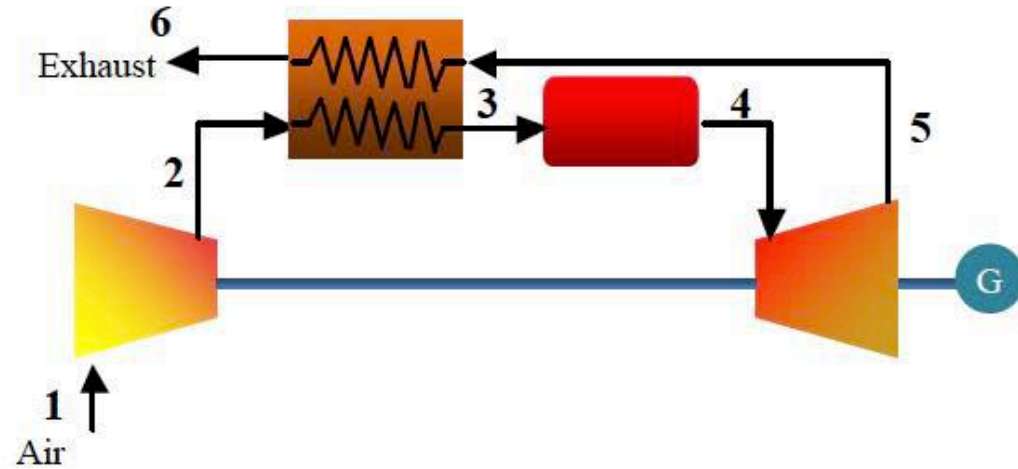
Exhaust heat recovery: Regenerative Cycles:



with ideal recuperation,

$$T_3 = T_5$$

$$\eta = 1 - \pi_P^{\frac{k-1}{k}} / \vartheta_4$$

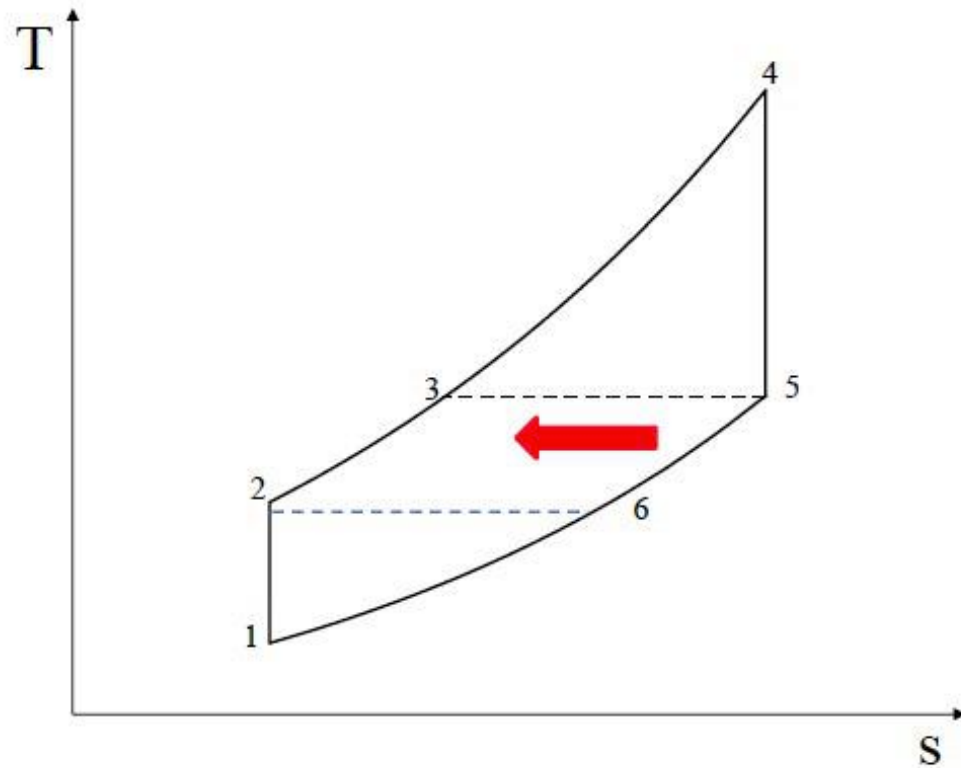


With 85% temperature recovery, $T_3 - T_{2s} = 0.85(T_{5s} - T_{2s})$,
and 85% compressor and turbine efficiencies:

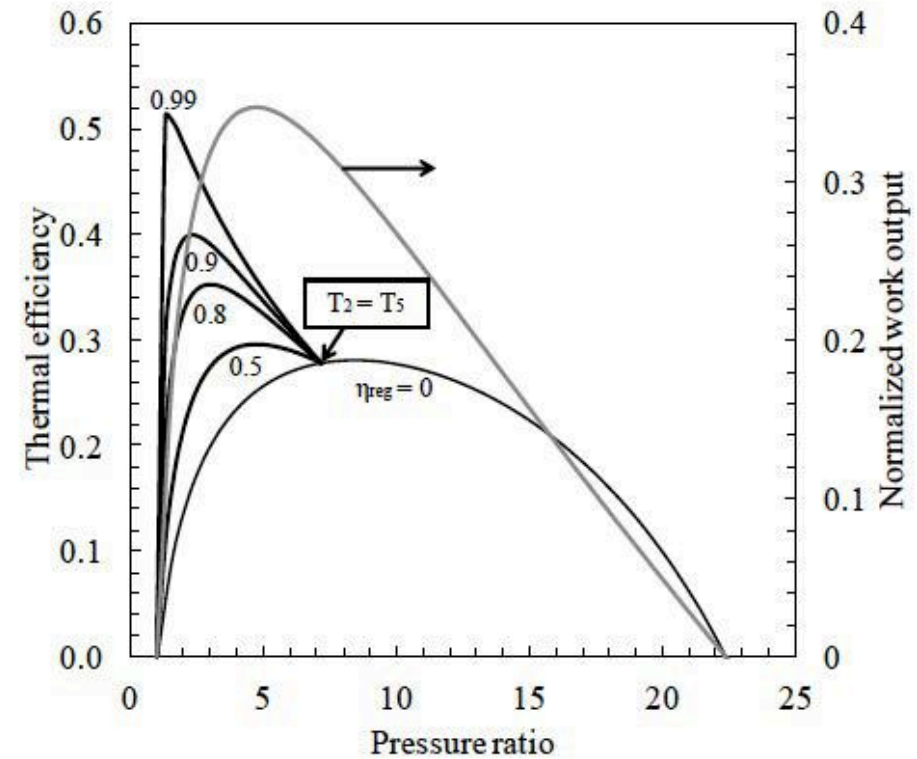
For $\pi_c = 4$: $\eta = 41.2\%$ vs. 24.2% for a simple cycle.

For $\pi_c = 8$: $\eta = 34.5\%$ vs. 30.6% for a simple cycle.

- Regeneration works best for low-p ratio, $T_5 \gg T_2$.
- Intercooling and reheating improve performance.

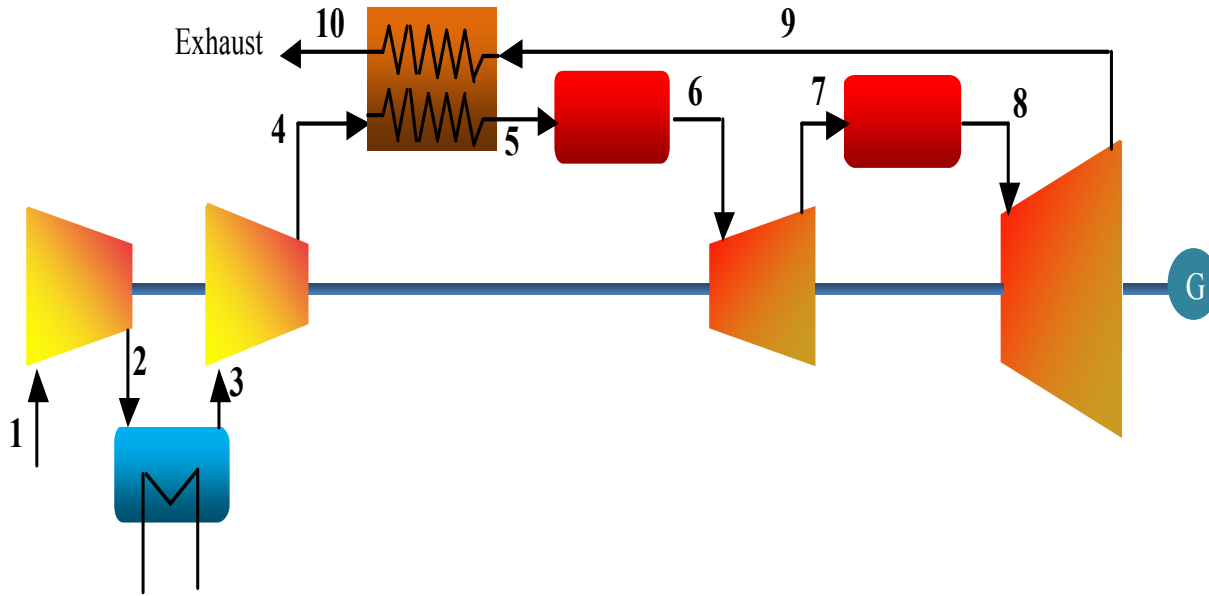


With regeneration, we recover some of the exhaust energy, making it possible to reduce the added heat (heat demand) and adding that heat at the highest possible T , resulting in a low exhaust temperature.



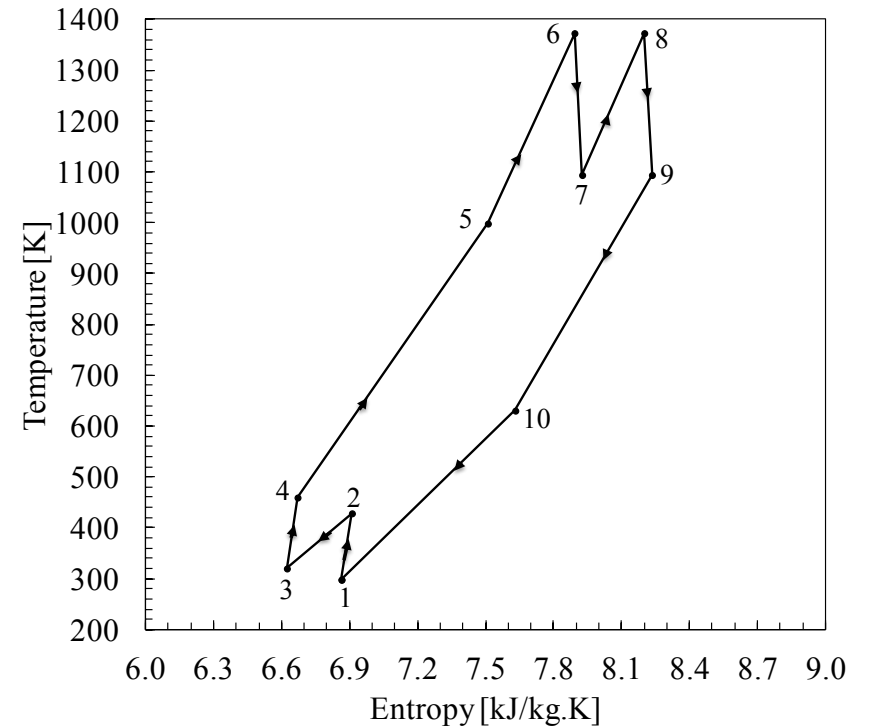
Impact of regeneration efficiency on the Brayton cycle efficiency, $\eta_T = \eta_C = 0.90$, $\vartheta_{max} = 3$, $\beta = 1$. Numbers on the lines show the regeneration efficiency, defined as $((T_5 - T_2)/(T_5 - T_6))$

Intercooling and Reheating: Near Isothermal Heating and Cooling:



compressor work: $w_c = \frac{c_p T_1}{\eta_c} \left[\pi_p^{(k-1)/k} - 1 \right]$ increases with T_1

Turbine work: $w_t = \eta_T c_p T_3 \left[1 - \frac{1}{\pi_p^{(k-1)/k}} \right]$ increases with T_3



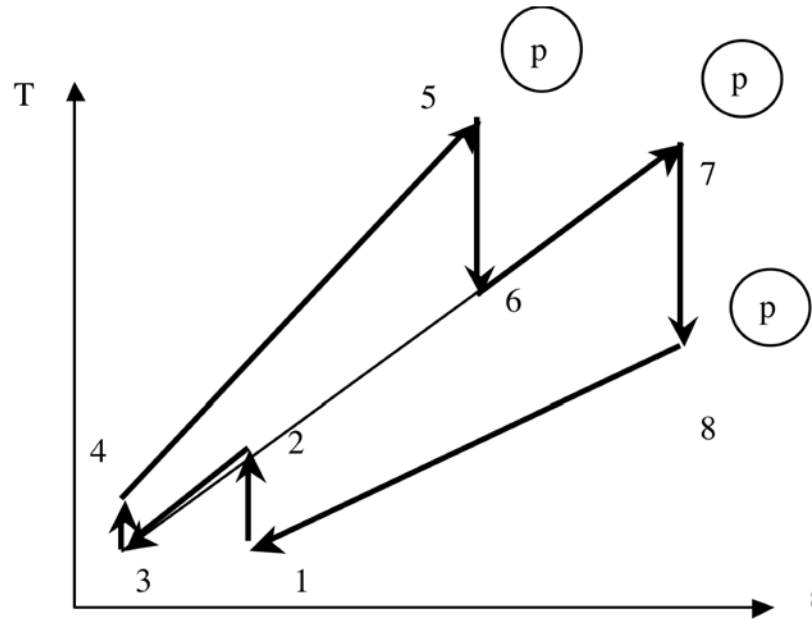


Figure 10. Ideal Brayton cycle with one intercooling stage and one reheating stage.

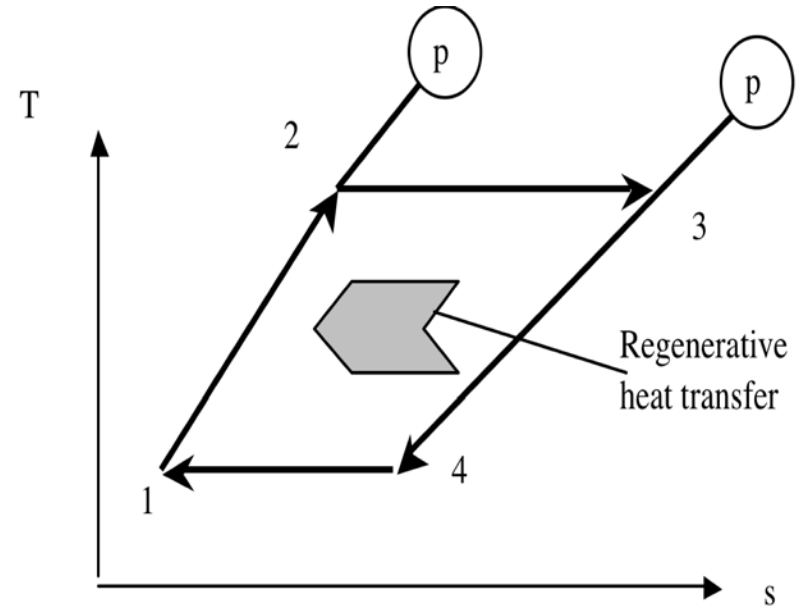
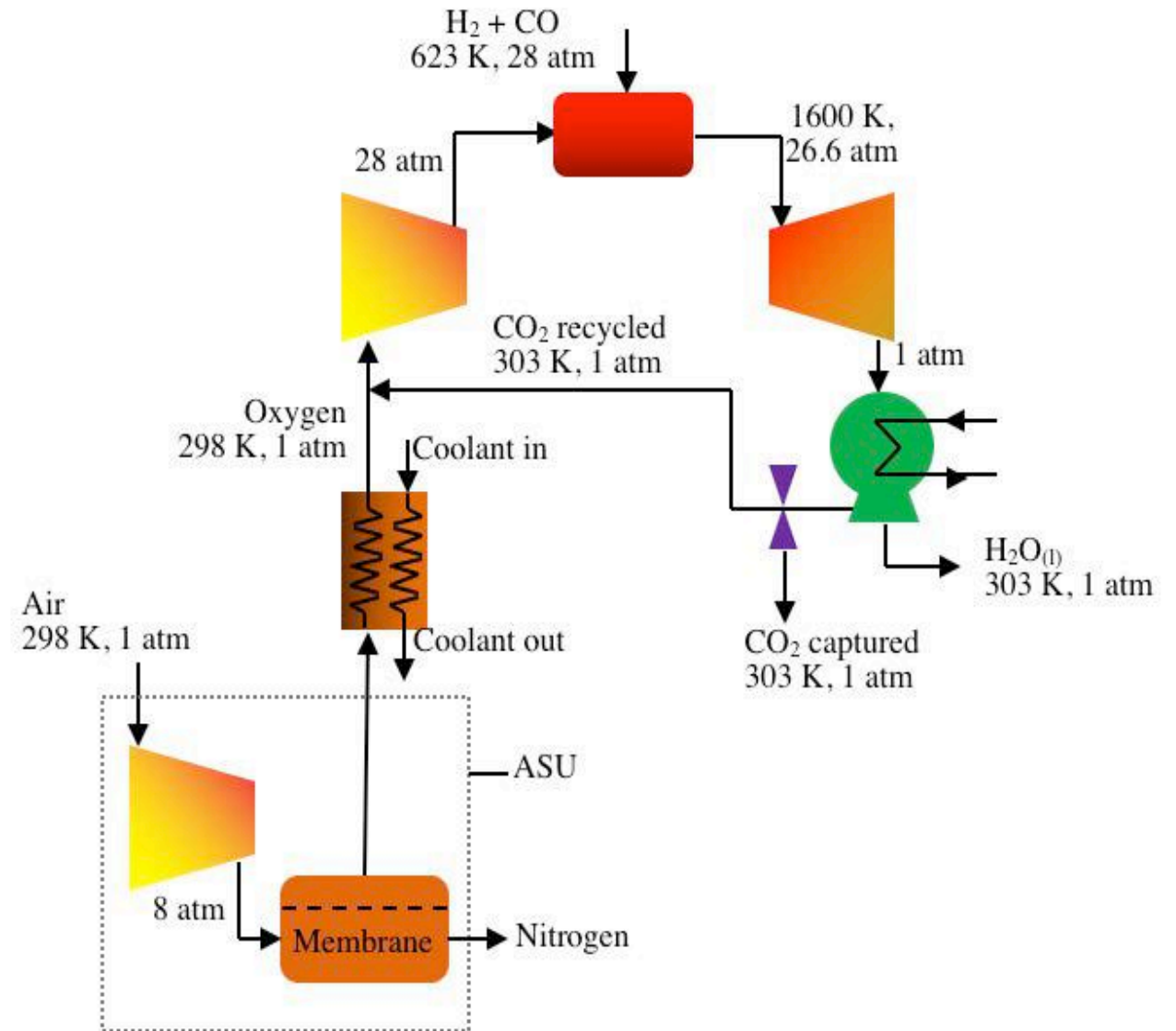


Figure 11. The ideal Ericsson cycle.

- **Intercooling** decreases compressor work, asymptotes to isothermal compression .. Minimum compression work
- **Reheat** increases power output and efficiency (work at high T).
- Both work better with **regeneration** (high turbine exit T and lower compressor inlet T).
- Asymptotes to **Ericsson Cycle**, has Carnot cycle efficiency (but with regeneration in the constant p processes).

Example 5.3 A gas turbine power plant operates with oxy-fuel combustion and uses syngas (a mixture of 1 mole of hydrogen and 1 mole of carbon monoxide) as a fuel. Air at 25 °C and 1 atm is pressurized to 8 atm within an ASU, which produces oxygen at 1 atm. Oxygen is cooled to 30 °C (303 K not 298 K shown in fig.) before mixing with recycled CO_2 . The mixture of oxygen and carbon dioxide is compressed to 28 atm. The syngas is burned adiabatically (and completely), and the products exit at 1600 K. The pressure drop within the combustor is 5%. The combustion products expand in the turbine whose isentropic efficiency is 90%. The turbine exhaust is cooled to 30 °C to condense water. Some of the CO_2 is recycled. Assume an isentropic efficiency of 80% for the compressors. How much CO_2 recycle is needed? Calculate the net power and thermal efficiency of the plant.

Solution is in notes



We begin the analysis from the first compressor where air is compressed for separation within the ASU. The air temperature at the compressor outlet is

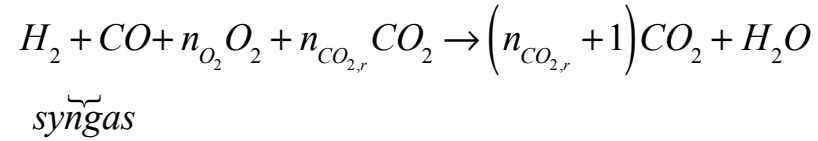
$$T_1' = T_0 \left[1 + \frac{(p_1' / p_0)^{k-1/k} - 1}{\eta_c} \right] = 298 \times \left[1 + \frac{8^{0.4/1.4} - 1}{0.8} \right] = 600.3 K$$

Next, we calculate the temperature of the oxygen and carbon dioxide mixture at the exit of the gas turbine cycle compressor. We assume that the specific heat ratio of the O₂-CO₂ mixture is that of carbon dioxide and that they are at the same temperature (the figure shows oxygen at 298 K incorrectly). This will be verified later. Hence,

$$k_{mix} = k_{CO_2} = 1.289$$

$$T_2 = T_1 \left[1 + \frac{(p_2 / p_1)^{k-1/k} - 1}{\eta_c} \right] = 303 \times \left[1 + \frac{28^{0.342/1.342} - 1}{0.8} \right] = 723.7 K$$

The combustion reaction can be written as:

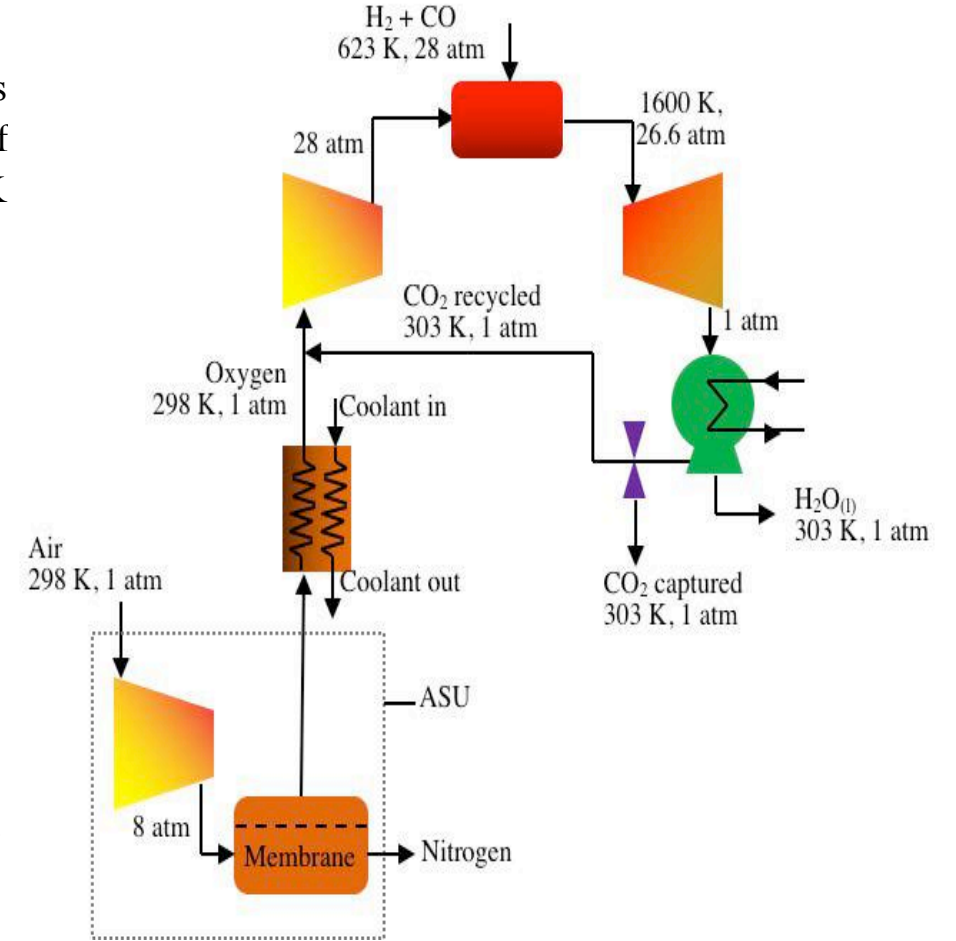


where $n_{CO_2,r}$ is the number of CO₂ moles recycled.

From oxygen balance, we find $n_{O_2} = 1$. Applying energy conservation to the adiabatic combustor,

$$\hat{h}_{H_2}^{623K} + \hat{h}_{CO}^{623K} + \hat{h}_{O_2}^{723.7K} n_{CO_2,r} \hat{h}_{CO_2}^{723.7K} = (n_{CO_2,r} + 1) \hat{h}_{CO_2}^{1600} + \hat{h}_{H_2O}^{1600}$$

The enthalpies of gases are calculated as follows.



$$\hat{h}_{H_2}^{623K} = \hat{h}_{f,H_2}^0 + \hat{c}_{p,H_2} (623 - 298) = 0 + 28.6 \times 325 = 9295 \text{ kJ / kmol}$$

Similarly: $\hat{h}_{CO}^{623K} = \hat{h}_{f,CO}^0 + \hat{c}_{p,CO} (623 - 298) = -101072.5 \text{ kJ / mol}$

$$\hat{h}_{O_2}^{723.7K} = 12517 \text{ kJ / kmol}, \quad \hat{h}_{CO_2}^{809.7K} = -377963 \text{ kJ / kmol}$$

$$\hat{h}_{H_2O}^{1600} = 202419.2 \text{ kJ / kmol}, \quad \hat{h}_{CO_2}^{1600} = 345365.6 \text{ kJ / kmol}$$

Substituting into the equation above and solving for $n_{CO_2,r}$, we find $n_{CO_2,r} = 14.4$

Next, we calculate the exit temperature of the turbine.

$$T_4 = T_3 \left\{ 1 - \eta_t \left[1 - \left(p_4 / p_3 \right)^{k-1/k} \right] \right\} = 1600 \left\{ 1 - 0.9 \left[1 - \left(1 / 26.6 \right)^{\frac{0.289}{1.289}} \right] \right\} = 850.1 \text{ K}$$

The specific heat ratio of CO₂ is used because over 90% of the mixture is carbon dioxide. work of the gas turbine is obtained as follows.

$$\begin{aligned} W_t &= (n_{CO_2} \hat{c}_{p,CO_2} + n_{H_2O} \hat{c}_{p,O_2}) (1600 - 850.1) = (15.4 \times 37.2 + 1 \times 30.4) (1600 - 850.1) \\ &= 451.668 \text{ kJ} \end{aligned}$$

Similarly, the work of the O₂-CO₂ compressor is calculated

$$W_c = (n_{CO_2,r} \hat{c}_{p,CO_2} + n_{O_2} \hat{c}_{p,O_2}) (723.7 - 303) = (14.4 \times 37.2 + 1 \times 29.4) \times 420.7 = 237.333 \text{ kJ}$$

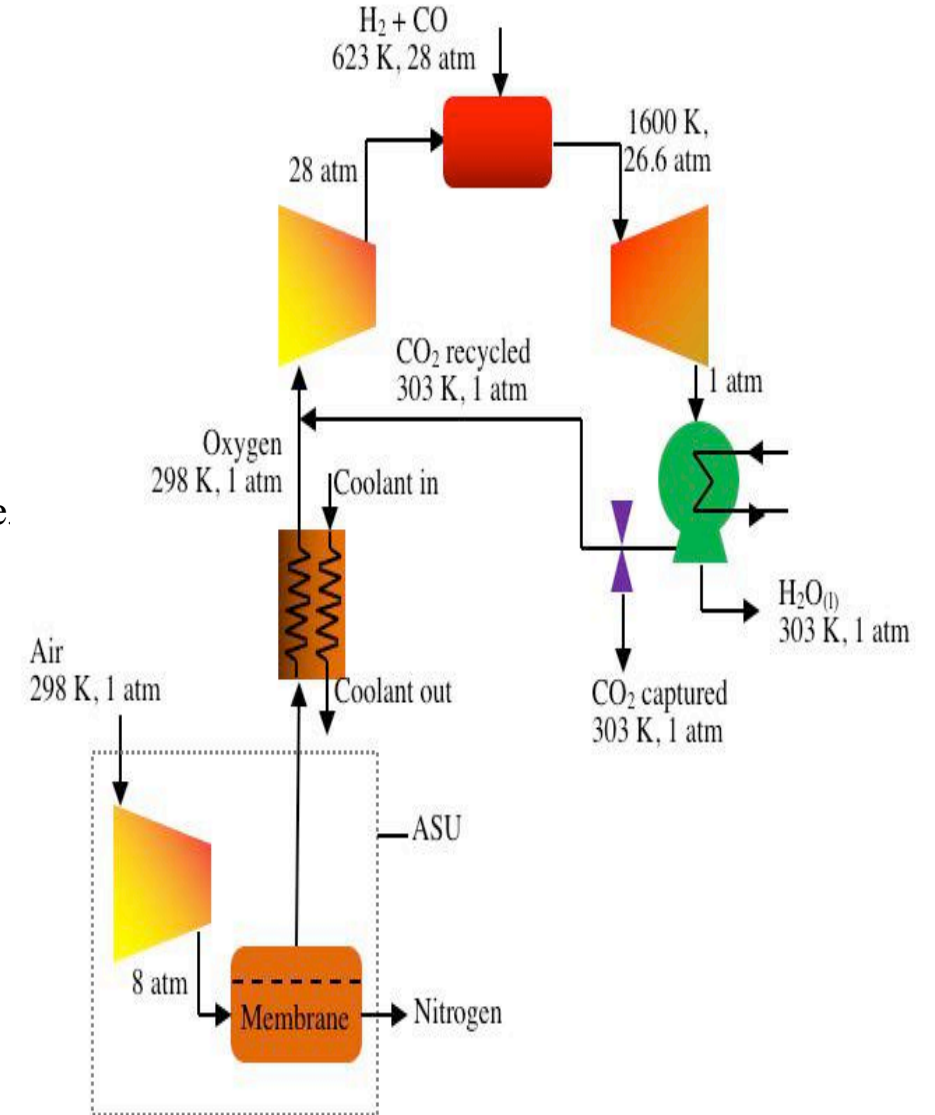
Moreover, the work requirement of the ASU compressor is

$$W_{c,ASU} = (29.4 + 3.76 \times 29.1) (600.3 - 303) = 41.265 \text{ kJ}$$

The net work produced by the power plant is therefore

$$W_{net} = W_t - W_c - W_{c,ASU} = 173.070 \text{ kJ}$$

The thermal efficiency of the power plant is $n_{th} = \frac{W_{net}}{LHV_{H_2} + LHV_{CO}} = \frac{173070}{242000 + 283270} = 0.33$

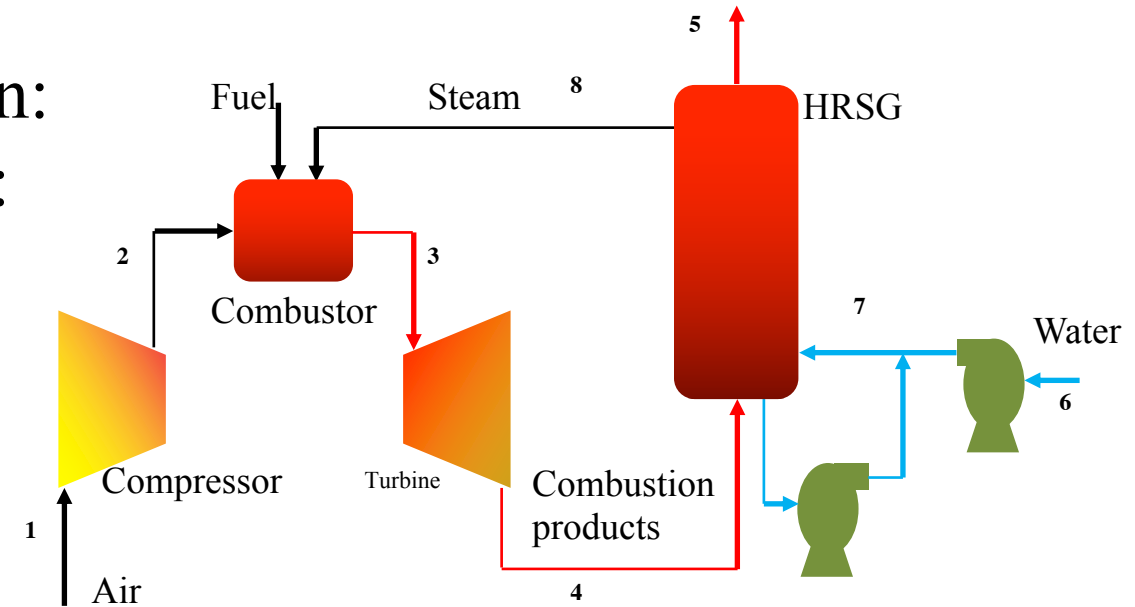


Exhaust Heat Recovery:

Humid Air Cycles, alternative to regeneration:

1. Steam injection and heat recovery cycle:

- Similar to regenerative cycles.
- Recovers some of the turbine exhaust energy.
- 20% of turbine mass flow is water.
- Limited by condensation pressure at turbine exit T.
- Needs purified water
- Has materials' issues.
- Can have NOx emissions' advantages.



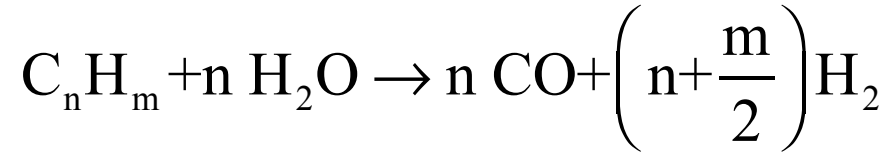
Performance data	Simple cycle	CC	HAT
Gas turbine type		AD	
Pressure ratio		46	
TIT °C		1500	
Water consumption, kg/kWh		0.74	0.72
Efficiency, %			

Ad: aeroderivative

Water/air ~ 15% (water/(air+NG) ~ 13%)

In HAT water/products ~ 20%

2. Thermochemical Recuperation (TCR):



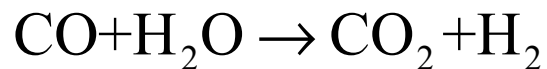
for methane,

$$\Delta H_{\text{reforming}} = 226 \text{ kJ/mole of methane}$$

The HV of methane is $\sim 800 \text{ MJ/kmol}$

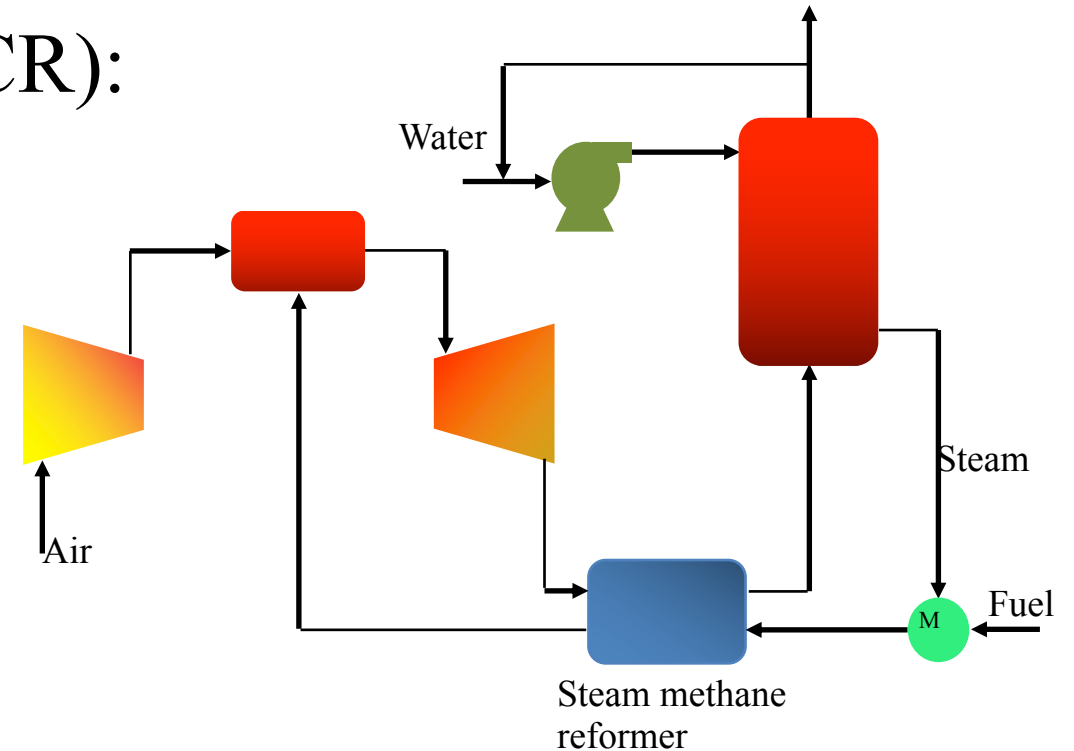
thus reforming to syngas raises the HV by $\sim 25\%$

further reforming is also possible:



$$\Delta H_R = 41 \text{ kJ/mole}$$

3. Combined Cycle, next chapter



	TCR	SC	CC
Steam to NG ratio by mass		NA	
Air to NG ratio by mass		42.7	
Makeup water, kg/kWh		0	
Stack gas temperature, °C		590	
Net cycle power, MW		166	264
Cycle efficiency, %			

Water/air $\sim 15\%$ (water/(air+NG) $\sim 13\%$)

SC: simple cycle,

CC Combined Cycle

Gas turbines have advantages in power generation:

- They operate at high temperatures.
- They can be started, turned down, and stopped relatively easily and within a short period of time, i.e. can load-follow and are capable of meeting peak load demands.
- They are compact and easy to operate, and they take advantage of ongoing developments in the aerospace, sea and some ground propulsion applications.
- They operate at relatively low pressures, compared to steam turbines, and this simplifies the plumbing of the plant.

Advantages of combustion turbines:

- Installations, for a wide range of loads, have been built and operated over the past couple of decades, mostly burning natural gas, or in dual fuel mode NG and oil.
- Gas turbines do not handle wet gases like steam turbines do, and are not as vulnerable to corrosion as steam turbines.
- Open cycle, or combustion gas turbines do not require heat transfer equipment on the low-temperature side, and no coolant either, and hence can be built and operated in hot dry areas.

limitations:

- They may have relatively low thermodynamic efficiency, the maximum temperature is limited by the blade material can handle, even with cooling.
- Their Second Law efficiency is low, because of the high compressor work; and the low efficiency of compressors.
- Open cycle turbines are limited by the relatively high exhaust pressure, which limits the work transfer of the turbine.
- They cannot be used with “dirty” fuels, e.g., coal, since sulfur oxides damage the blades.

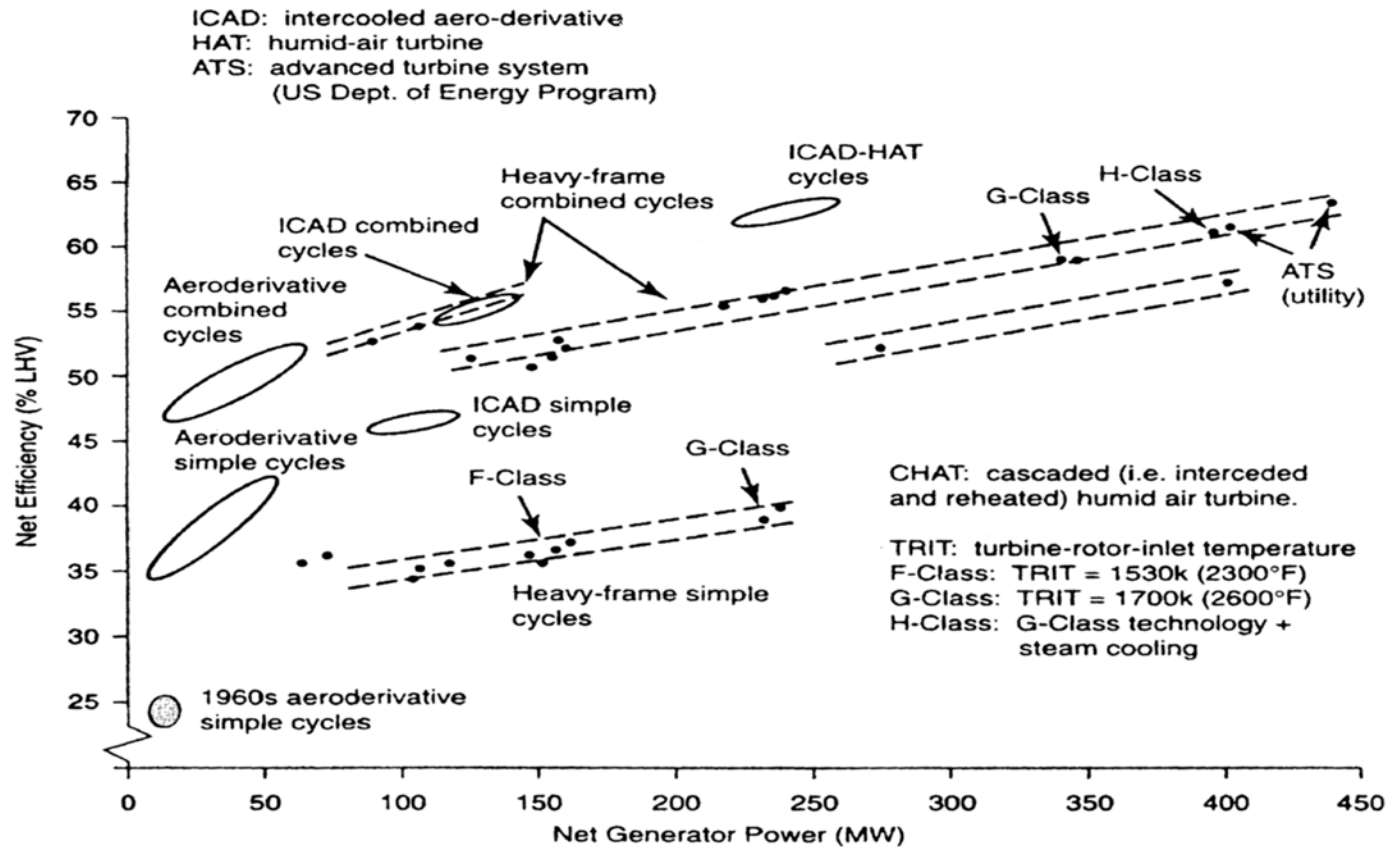
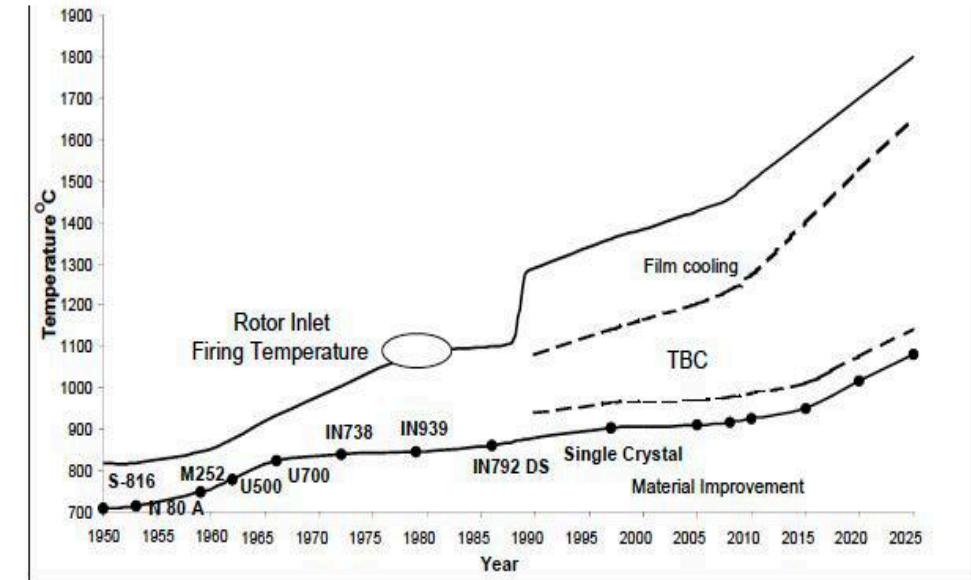


Figure 3. Thermal efficiency versus power of different turbines, and combined cycles (Wilson, and Korakianitis, 1998).

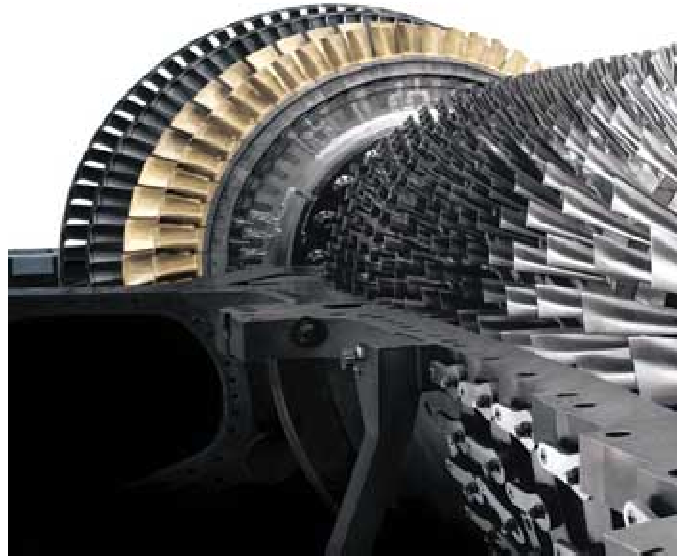
© Source unknown. All rights reserved. This content is excluded from our Creative Commons license. For more information, see <https://ocw.mit.edu/fairuse>.



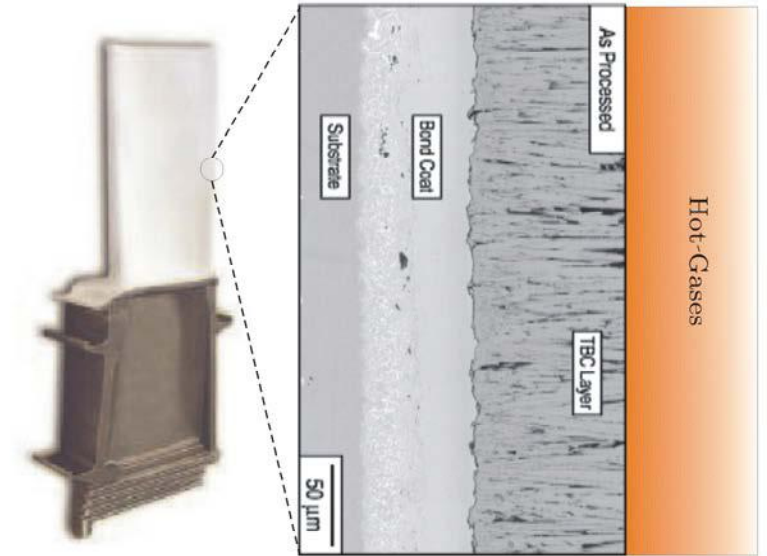
Impact of turbine blade metal, thermal barrier coating (TBC) and film cooling on the turbine inlet temperature (A. Rao, "Advanced Bryton Cycles," 2002).

Image courtesy of DOE.

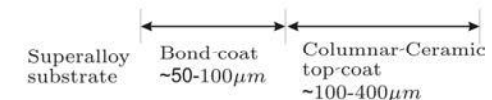
Current GE H-System NGCC Turbine Technology (Natural Gas Combined-Cycle Plants, 400MW ~60% Efficiency)



© Source unknown. All rights reserved. This content is excluded from our Creative Commons license. For more information, see <https://ocw.mit.edu/fairuse>.



- Turbine inlet temperatures --- ~ 1430C
- Single Crystal superalloy blades. Melting temperature ~ 1300C
- Active cooling so that blade temperatures do not exceed ~ 1050C (~0.8 T_m of blade material)
- Ceramic thermal barrier coatings (TBCs) to accommodate blade surface temperatures of ~1275C



© Source unknown. All rights reserved. This content is excluded from our Creative Commons license. For more information, see <https://ocw.mit.edu/fairuse>.

Advanced turbines are manufactured using composite materials and “superalloys” of nickel (Ni) and cobalt (Co), mixed with molybdenum, tungsten, titanium, aluminum (Al) and chromium (Cr). The blades are hollowed for cooling.

A combination of high temperature and oxygen-rich gases make gas turbine blade vulnerable to corrosion. The blades are coated with chromium, or at higher temperature, with XCrAlY, where X stands for cobalt or nickel, and Y is yttrium, mixed in a dense aluminum oxide layer on the blade surface. This is part of the thermal barrier coating (TBC) applied to the blade surface, which is often a ceramic layer of zirconia (ZrO_2) stabilized with yttria and a bonding of a metallic layer of XCrAlY. The ceramic layer has low thermal conductivity. Advanced manufacturing techniques, including physical vapor deposition or plasma vapor deposition are used in applying these coats.

Cooling techniques are also used. These include air and steam cooling using jet impingement, inner extended surfaces and cooling films on the surface.

**The latest generation of gas turbines offered by different manufacturers,
showing pressure ratio, the maximum temperature and simple cycle efficiency**

		Westinghouse Fiat, MHI			ABB							General Electric Nuovo Pignone			Siemens Ansaldo	
Performance data		TG50 D5S6	FMW 701F	MW 501 F	GT13 E2	GT11 N2	GT2 6	GT2 4	V84. 3A	Performance data		MS90 01FA	MS7 001 FA	MS9001 EC	V94.3 A	V84. 3A
Power	output, MW	143	237	153	164	109	254	173	170	Power		226.5	159	219	240	170
Simple	cycle efficiency, %	38.5	37.2	35.3	35.7	34.2	38.3	38.0	38.0	Simple	cycle efficiency, %	35.7		34.9	38.0	38.0
Exhaust	gas flow rate, kg/s	454	666		525	375	562	390	454	Exhaust	gas flow, kg/s	615		507	640	454
Turbine	inlet temp, °C	1250	1350		1100	1085				Turbine	inlet temp, °C	1235		1290	1204-1340	
Exhaust	gas temp, °C	528	550		525	524	608	610		Exhaust	gas temp, °C	589		558	562	
Compressor	pressure ratio	14.1	15.9	16	15		30			Compressor	p. ratio	15		14.2	16	

Khartchenko, N.V., Advanced Energy Systems,
Taylor & Francis, 1998, xix+218

© Informa UK Limited. All rights reserved. This content is excluded from our
Creative Commons license. For more information, see <https://ocw.mit.edu/fairuse>.

Table 5.1. Operating data of aeroderivative based gas turbine power plants

Performance data	Value
Power output, MW	40-50
Turbine inlet temperature, °C	1280-1350
Compressor pressure ratio	30-60
Net specific work output, kJ/kg	350-370
Thermal efficiency, %	39.0-39.9
Air mass flow, kg/s	115-135
Gas turbine outlet temperature, °C	450-470

Khartchenko, N.V., Advanced Energy Systems, Taylor & Francis, 1998, xix+218

© Informa UK Limited. All rights reserved. This content is excluded from our Creative Commons license. For more information, see <https://ocw.mit.edu/fairuse>.

Power Systems for the 21st Century – “H” Gas Turbine Combined-Cycles

R.K. Matta
G.D. Mercer
R.S. Tuthill
GE Power Systems
Schenectady, NY

Some steam is injected into the GT to cool blade and increase power (HAT)

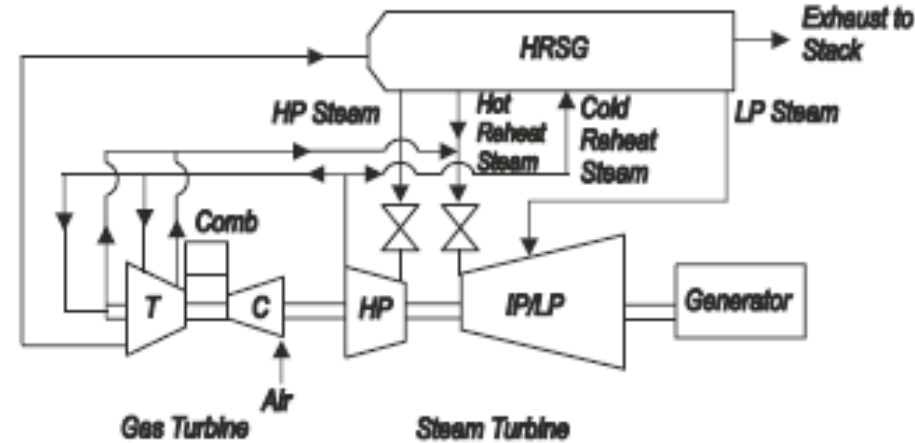
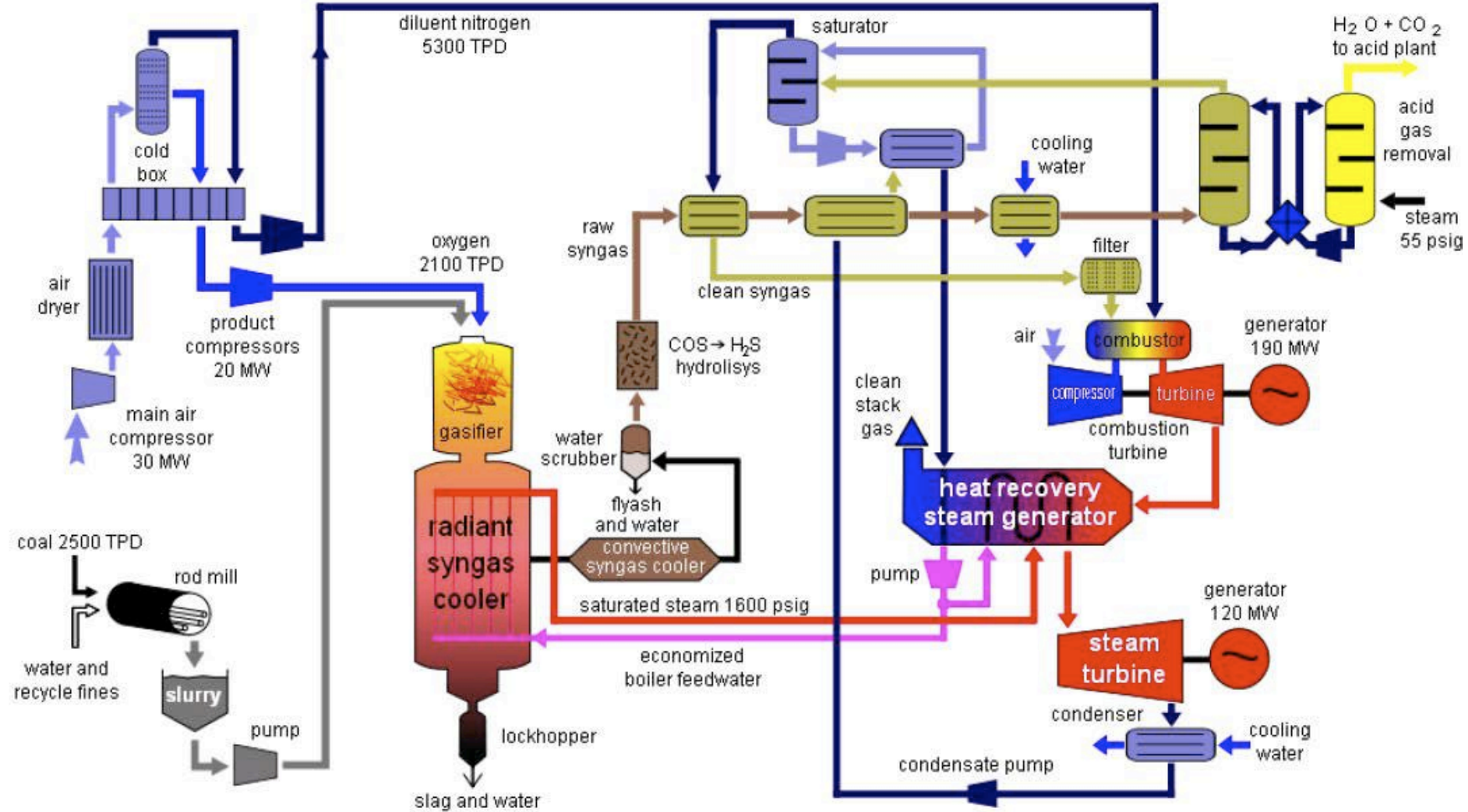


Figure 3. H Combined-cycle and steam description

	<i>7FA</i>	<i>7H</i>
Firing Temperature Class, F (C)	2400 (1316)	2600 (1430)
Air Flow, lb/sec (kg/sec)	953 (433)	1230 (558)
Pressure Ratio	15	23
Combined Cycle Net Output, MW	263	400
Net Efficiency, %	56.0	60
NO_x (ppmvd at 15% O₂)	9	9

Table 2. H Technology performance characteristics (60 Hz)

Using Gas Turbines with Coal Gasification is necessary



© Stan Zurek on [Wikimedia](https://commons.wikimedia.org/wiki/File:Coal_gasification_process_flow_diagram.png). License: CC BY-SA 3.0. This content is excluded from our Creative Commons license. For more information, see <https://ocw.mit.edu/fairuse>.

MIT OpenCourseWare
<https://ocw.mit.edu/>

2.60J Fundamentals of Advanced Energy Conversion
Spring 2020

For information about citing these materials or our Terms of Use, visit: <https://ocw.mit.edu/terms>.

Lecture # 16
Thermomechanical Conversion II
Two-Phase Cycles and Combined Cycles

Ahmed Ghoniem
April 1, 2020

Rankine Cycle: two phase region

Superheat and Ultra-superheat Cycles. Reheating. Recuperation.

Supercritical Cycles. Hypercritical Cycles (CO_2 as working fluid)

Water requirements.

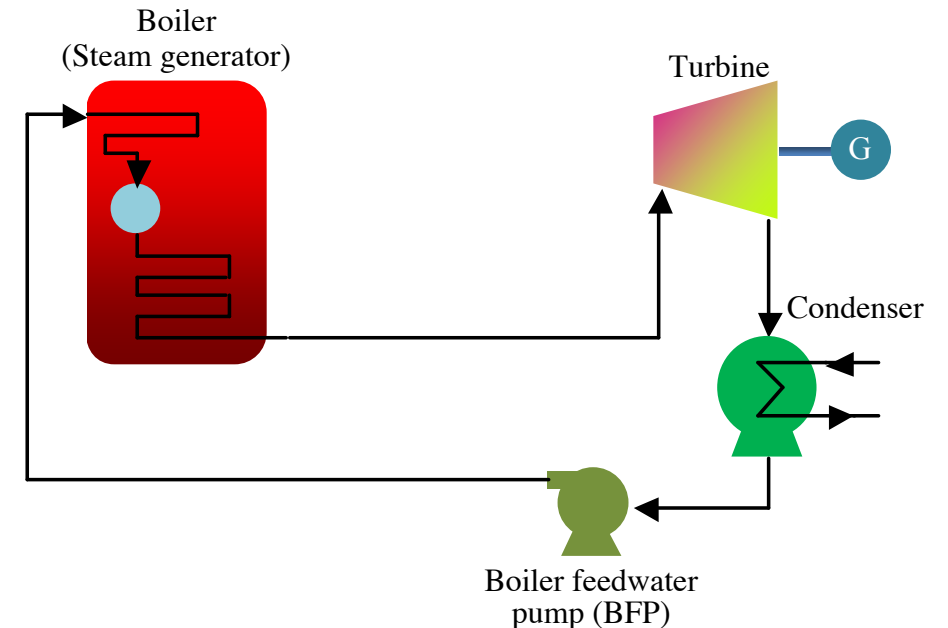
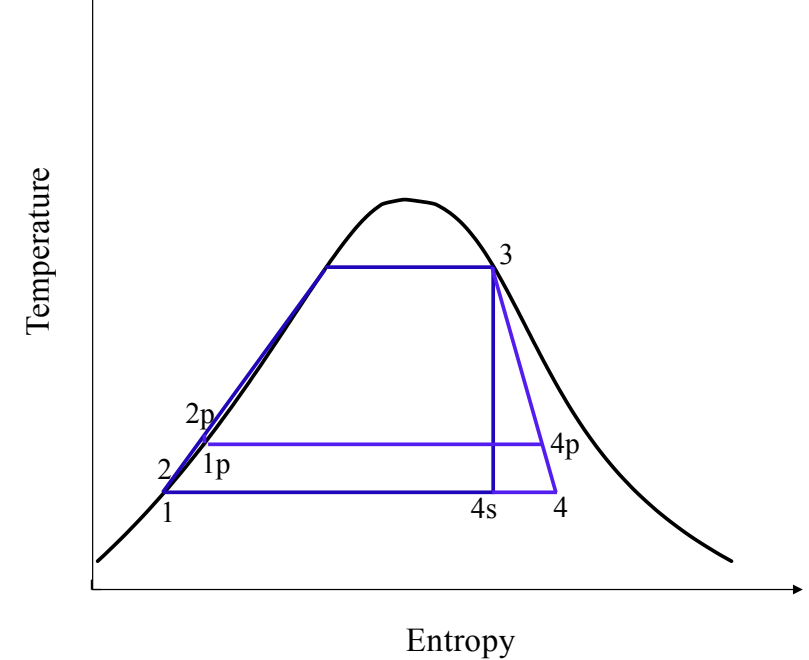
Simple Rankine Cycles: open and closed

Critical point for Water: $T_c = 374\text{ C}$, $p_c = 22.088\text{ MPa}$

@ $T = 15\text{ C}$, $p_{sat} = 5.63\text{ kPa}$

@ $p = 1\text{ atm}$, $T_{sat} = 100\text{ C}$.

- Rankine cycles operate at relatively lower high temperature.
- They take advantage of the low pumping work of an incompressible liquid and high expansion work of the compressible gas.
- Operating in a closed cycle (to recirculate the working fluid), the turbine exhausts into vacuum, the pressure is determined by the cold temperature (condensation).
- Otherwise the efficiency is unacceptably low.



Simple ideal Rankine Cycle:

$$w_{pump,ideal} = h_{2s} - h_1 = v(p_2 - p_1)$$

$$w_{T,ideal} = h_3 - h_{4s}$$

$$q_H = h_3 - h_2$$

$$\eta_I = \frac{w_T - w_{pump}}{q_H}$$

In a real cycle:

$$w_{pump} = \frac{v(p_2 - p_1)}{\eta_{is}}$$

$$w_T = \eta_{T,is} (h_3 - h_{4s})$$

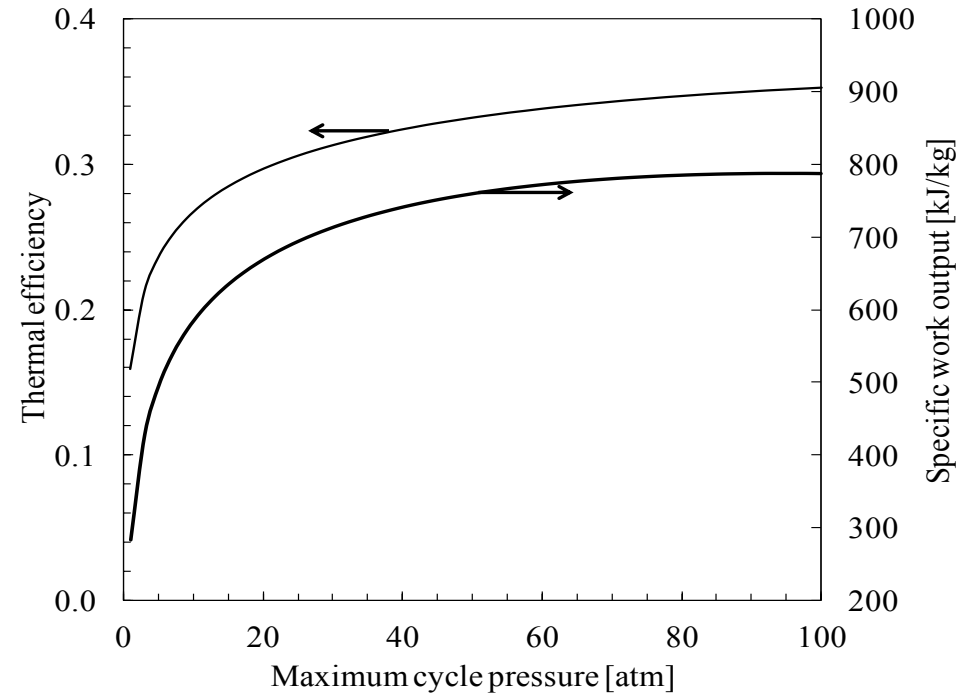
$$q_H = h_3 - h_2$$

Simple saturated cycle efficiency,
Pressure Ratio = 8,
Pump = 65%, turbine 90%.

	Conventional	
	Tmin=20 Closed cycle	Pmin=1 atm Open cycle
w_{pump} (kJ/kg)	1.23	1.12
w_t (kJ/kg)	736	316
w_{net} (kJ/kg)	735	315
η	27.4 %	13.4%
η_{ideal}	30.4%	14.9%
η_{car}	33.9%	15.8%
X_4	0.794	0.8856

- low pumping work, for an incompressible fluid; $\Delta h = v \Delta p$ (the fluid temperature does not rise).
- Generally, lower *high T* requirements (compatible with nuclear, solar thermal, geothermal and lower quality fuel sources) but needs *high p*. Also good for waste heat recovery (using organic working fluids)
- Good efficiency: small pumping work and near isothermal heat interactions.
- Large heat transfer (latent heat).

Simple closed cycle efficiency, saturated state
 Pump = 65%, turbine 90%, condenser $T = 30\text{ }^{\circ}\text{C}$



Both work and efficiency increase monotonically
 because of small pumping work

Superheat Cycles

From Dave Burke, 2.611

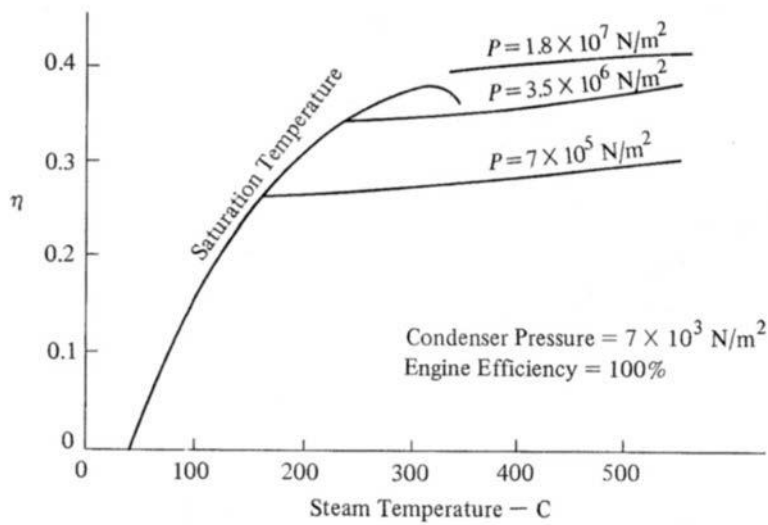
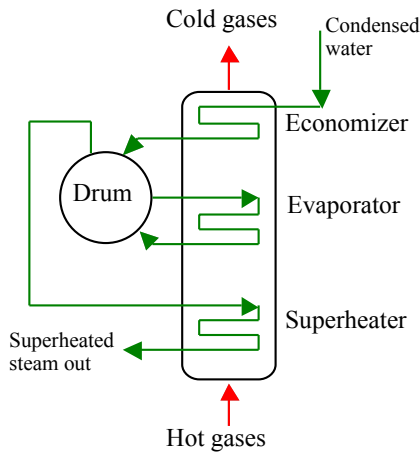
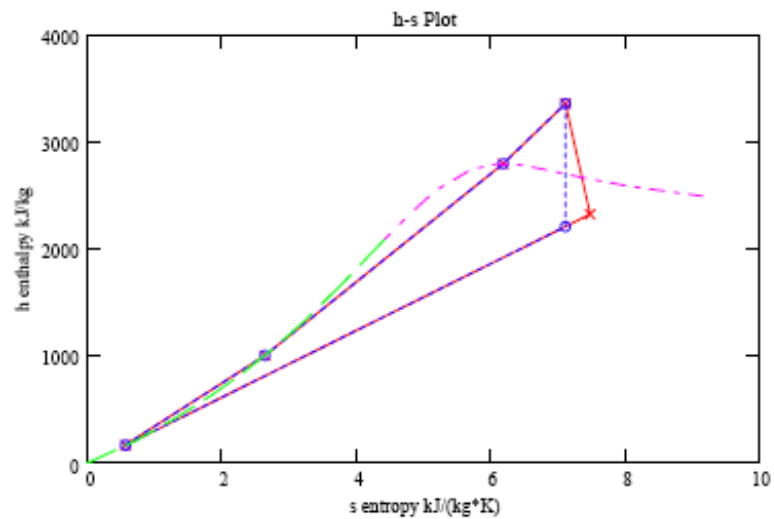
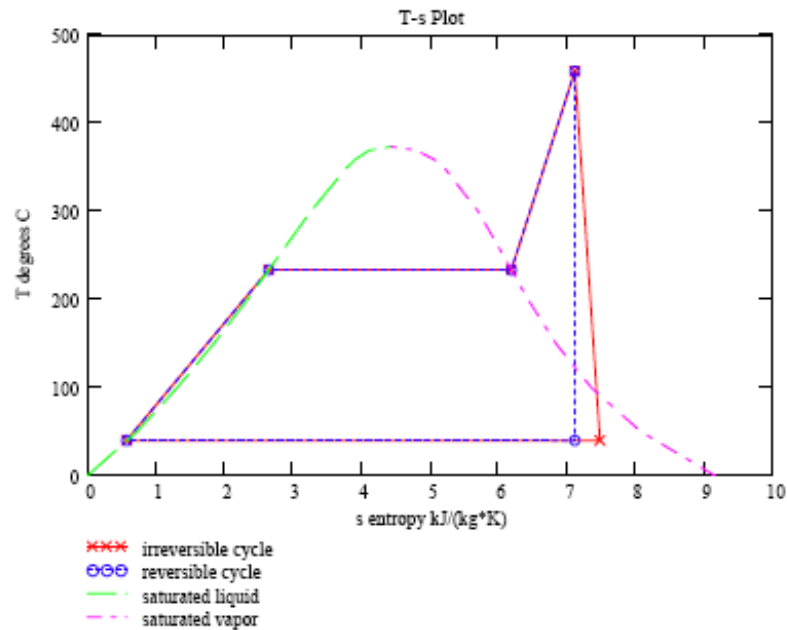


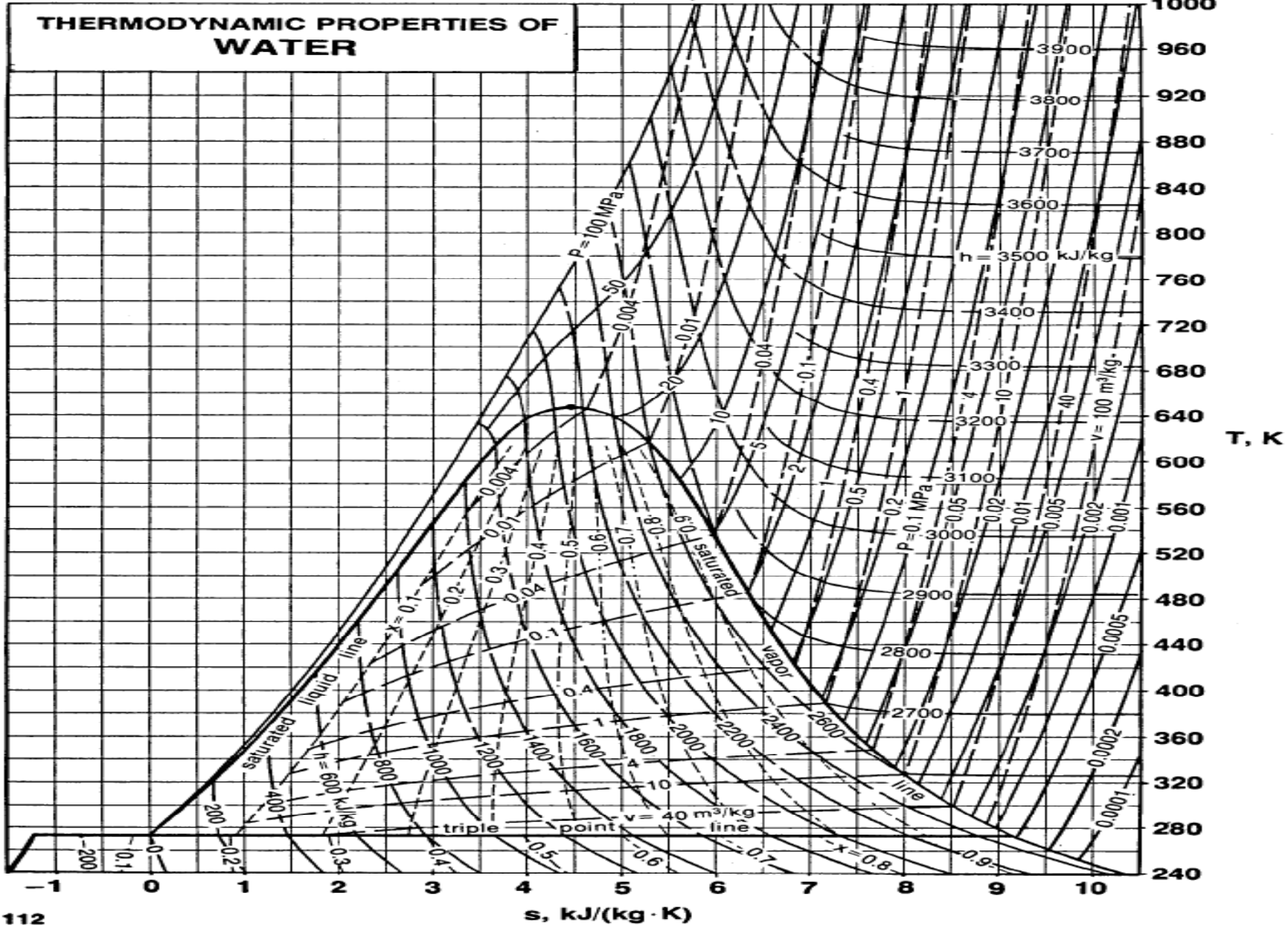
Figure 12.4 Influence of superheat on Rankine cycle efficiency



From Smith and Cravalho,
Engineering Thermodynamics

		Superheat +100
	Tmin=20	
w_{pump} (kJ/kg)	1.23	1.23
w_t (kJ/kg)	736	818
w_{net} (kJ/kg)	735	817
η	27.4 %	28.1 %
η_{ideal}	30.4 %	
η_{car}	33.9 %	46.0 %
X_4	0.794	0.8517

© Pitman. All rights reserved. This content is excluded from our Creative Commons license. For more information, see <https://ocw.mit.edu/fairuse>.



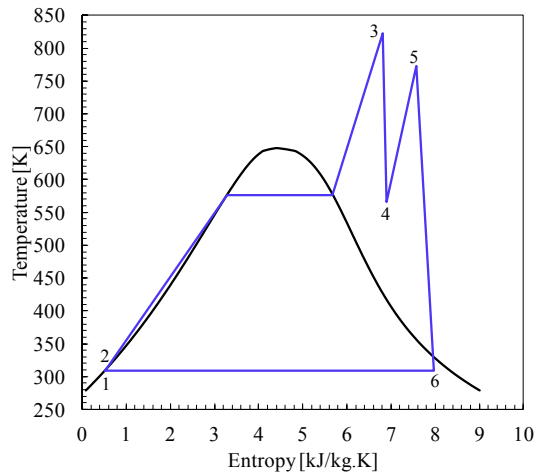
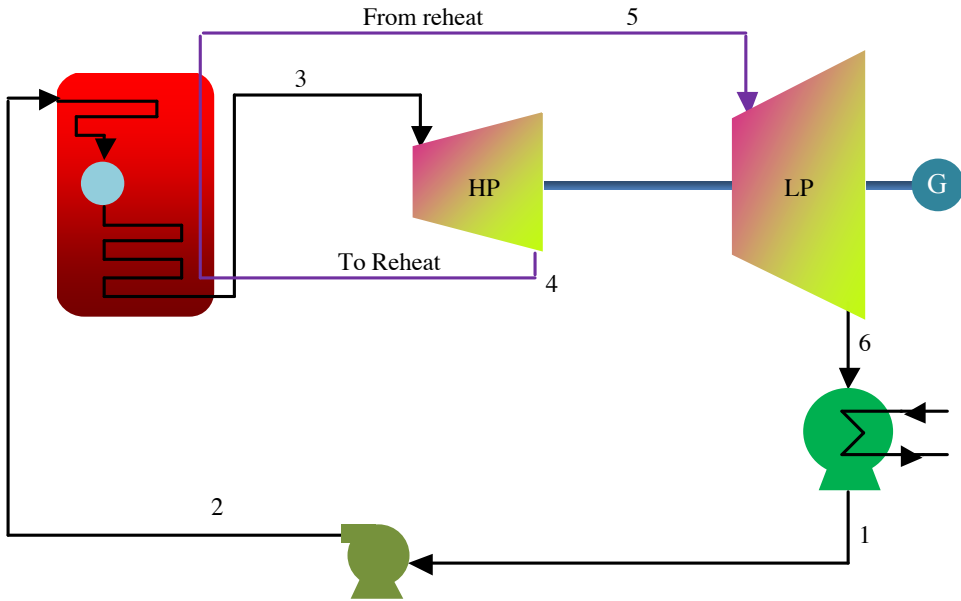
Concentrated solar thermal (CSP) and hybrid concentrated solar thermal (Hy-CS) power plants



Florida Power (FPL) is adding 75 MW (peak) solar increment to its 3800 MG NG plant (Hybrid Concentrated Solar, or HyCS) to boost the fraction of renewable energy generation. HyCS reduces the cost and does not require storage, another costly item in solar plants.

© The New York Times Company. All rights reserved. This content is excluded from our Creative Commons license. For more information, see <https://ocw.mit.edu/fairuse>.

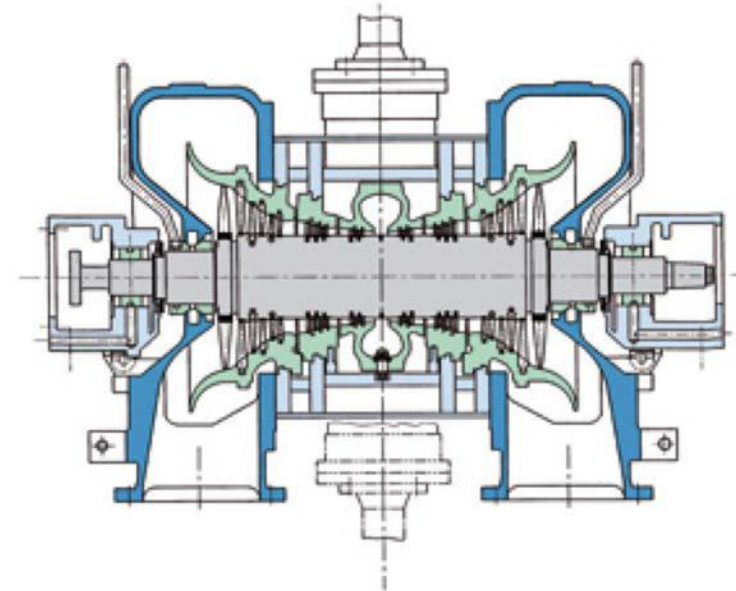
Reheat Cycle



Better efficiency and steam quality at end of expansion

	Reheat Cycle			
	Tmin=20	+100	+200	+300
w_{pump} (kJ/kg)	1.23	1.23	1.23	1.23
w_t (kJ/kg)	736	947.2	1086	1400
w_{net} (kJ/kg)	735	946	1085	1398
η	27.4 %	28.1%	30.3%	35.5%
η_{ideal}	30.4%			
η_{car}	33.9%	46.0%	54.4%	60.6%
X_6	0.794	0.9583	Vapor	Vapor

SIEMENS SST-500



Technical Data

© Siemens. All rights reserved. This content is excluded from our Creative Commons license. For more information, see <https://ocw.mit.edu/fairuse>.

All data are approximate and project-related

Output range	up to	85 MW
live steam conditions		
temperature	up to	540C / 1000F
pressure	up to	140 bar / 2000 ps
Bleed	up to	2 at various pressure level
Controlled extraction		
temperature	up to	350C / 662F
pressure	up to	30 bar / 435 ps

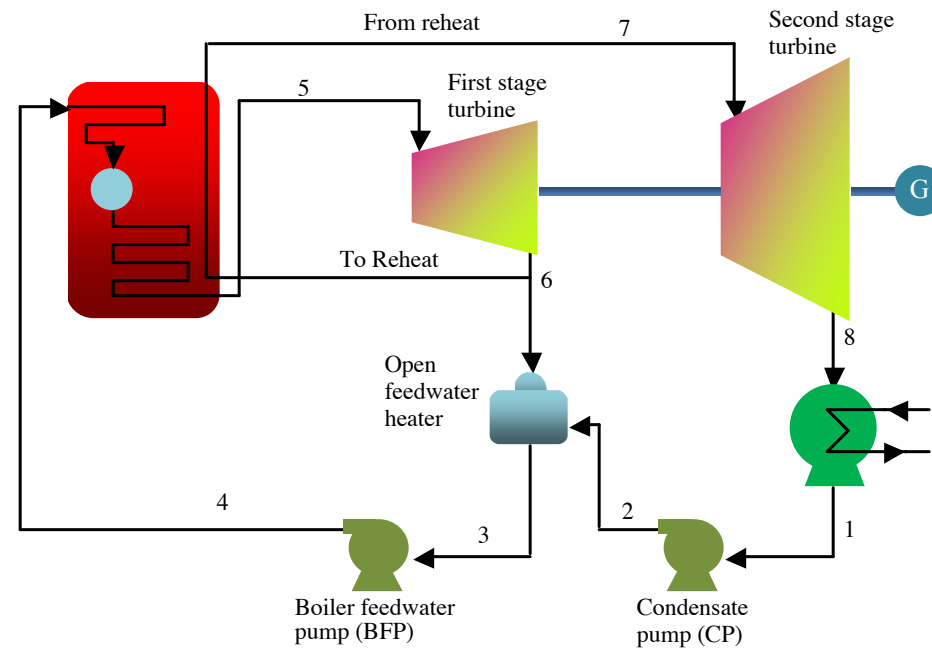
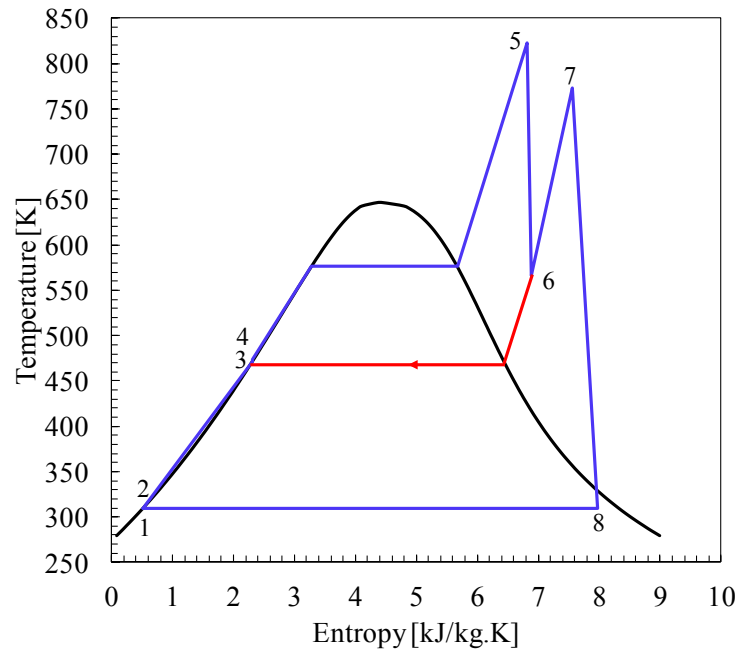
Typical plant layout for a SST-500 Steam Turbine

Dimensions

Length (L) 10m/32.8 ft. to 19m/62.3 ft.
Width (W) 4.0m/13.1 ft. to 6.0m/19.7 ft.
Height (H) 3.5m/11.5 ft. to 5.0m/16.5 ft.

Regenerative Cycles

1. Direct Contact (open) Feedwater Heater



Best feedwater heater arrangement from the efficiency viewpoint, but requires an extra pump.

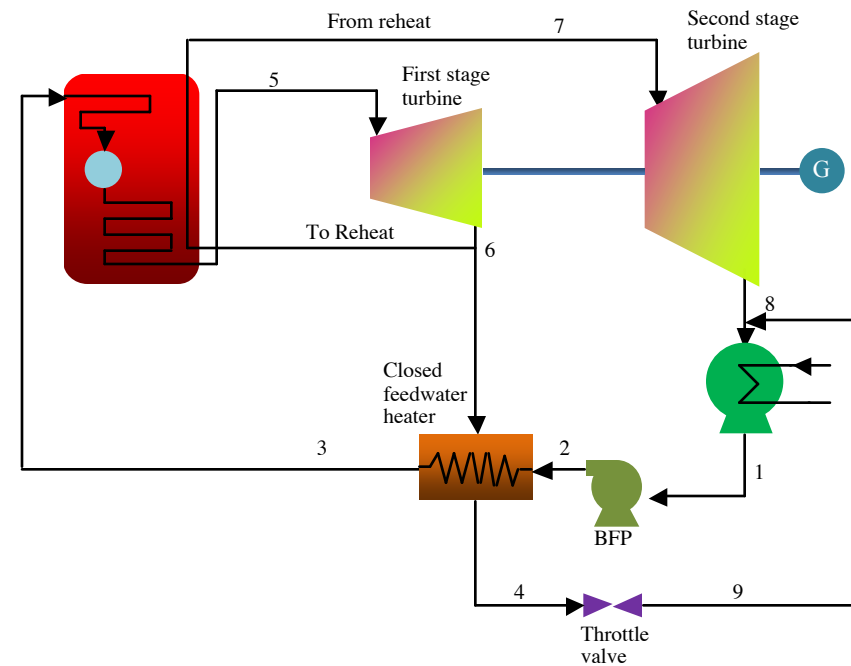
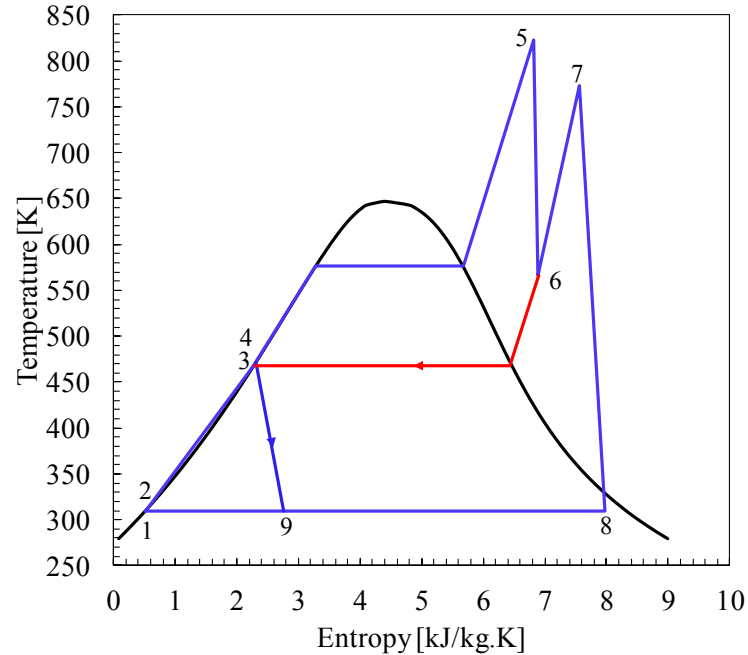
α is extracted from the turbine at state 6 is given by: $\alpha h_6 + (1 - \alpha) h_2 = h_3$

condenser sees only $(1 - \alpha)$ of the flow

Pump = 65%, turbine 90%, Pressure ratio = 8

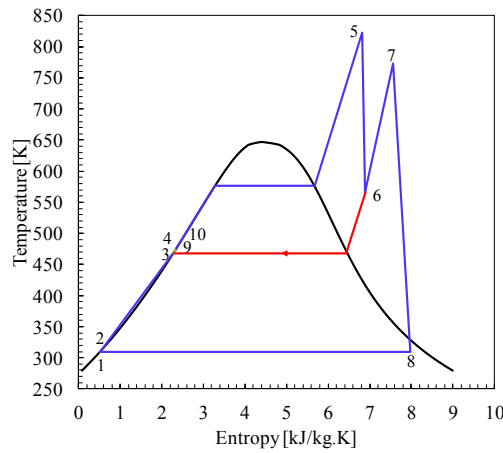
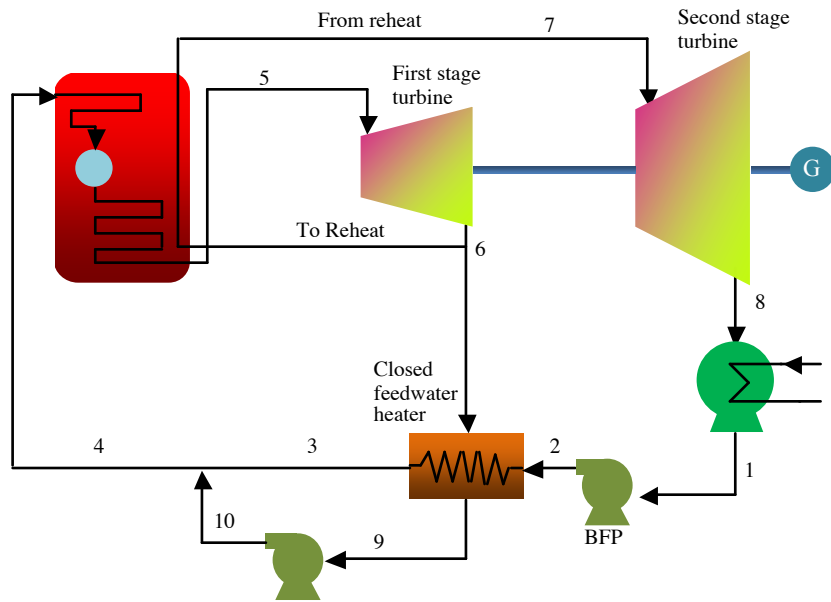
		Reheat Cycle	Regenerative Cycle +100
	Tmin=20	+100	
w_{pump} (kJ/kg)	1.23	1.23	1.26
w_t (kJ/kg)	736	947.2	774
w_{net} (kJ/kg)	735	946	773
η	27.4 %	28.1%	29.4%
η_{ideal}	30.4%		
η_{car}	33.9%	46.0%	46.0%
X_4	0.794	0.9583	N/A

2. Cascading Backward, Closed Feedwater Heater

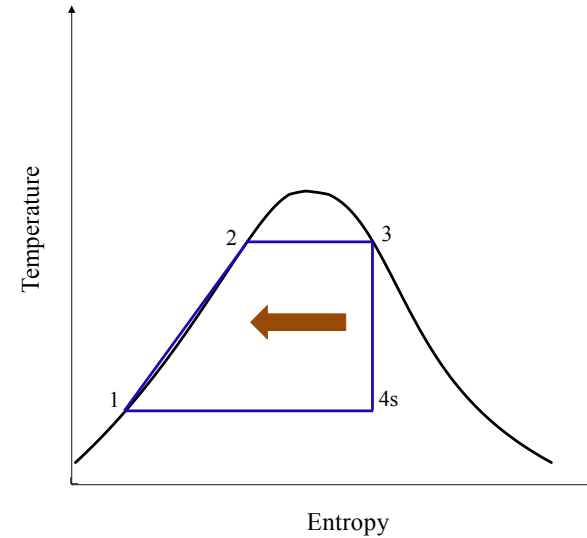


Less efficient because of throttling and some heat rejection in condenser, but only one pump is required .

3. Cascading Forward, Closed Feedwater Heater



Ultimate Regenerative Cycle:



Ultimate Regenerative Cycle:

1. Internally heat the feedwater using extracted steam.
2. Amount of extracted steam is small, latent heat \gg sensible heat.
3. External heat transfer is isothermal.
4. Cycle efficiency = Carnot efficiency.

Using a small pump after heater avoids rejecting extra heat in extracted steam

SUPERCRITICAL CYCLES

$p_{boiler} > p_c$, for Water: $T_c = 374\text{ C}$, $p_c = 22.088\text{ MPa}$

> Raises the cycle temperature

> Reduces ΔT between source and steam

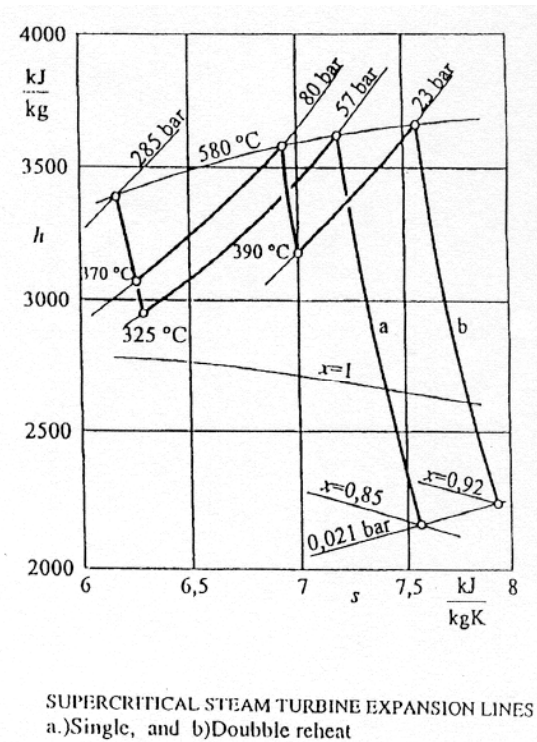
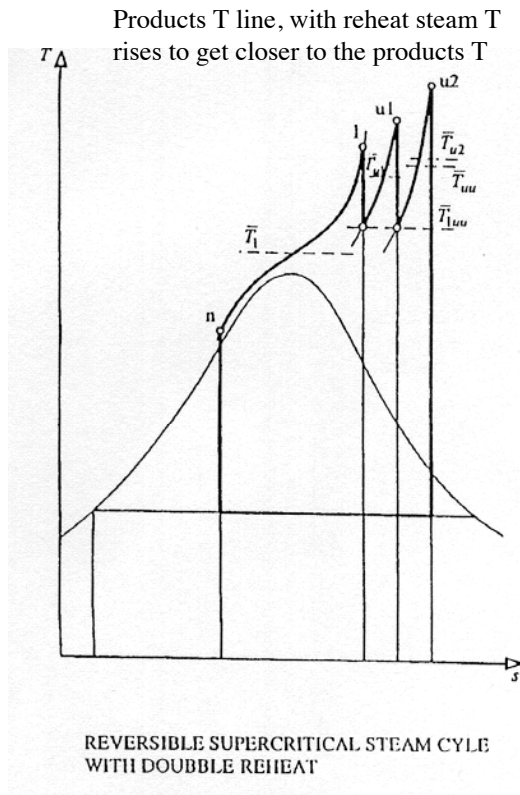


Table 1.3 USC steam plants in service or under construction globally

Power station	Cap. MW	Steam parameters	Fuel	Year of Comm.	Eff% LHV
Matsuura 2	1000	255bar/598°C/596°C	PC	1997	
Skaerbaek 2	400	290bar/580°C/580°C/580°C	NG	1997	49
Haramachi 2	1000	259bar/604°C/602°C	PC	1998	
Nordjylland 3	400	290bar/580°C/580°C/580°C	PC	1998	47
Nanaoota 2	700	255bar/597°C/595°C	PC	1998	
Misumi 1	1000	259bar/604°C/602°C	PC	1998	
Lippendorf	934	267bar/554°C/583°C	Lignite	1999	42.3
Boxberg	915	267bar/555°C/578°C	Lignite	2000	41.7
Tsuruga 2	700	255bar/597°C/595°C	PC	2000	
Tachibanawan 2	1050	264bar/605°C/613°C	PC	2001	
Avedere 2	400	300bar/580°C/600°C	NG	2001	49.7
Niederaussen	975	290bar/580°C/600°C	Lignite	2002	>43
Isogo 1	600	280bar/605°C/613°C	PC	2002	
Neurath	1120	295bar/600°C/605°C	Lignite	2008	>43%

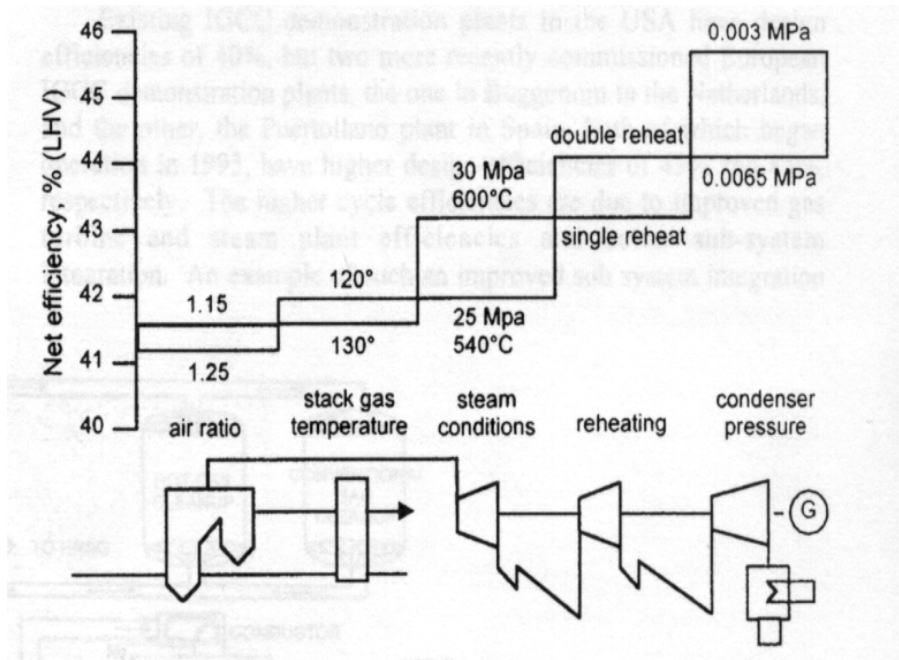
(Blum and Hald and others)

Coal plans are less efficient than NG plants
because of exhaust gas clean up

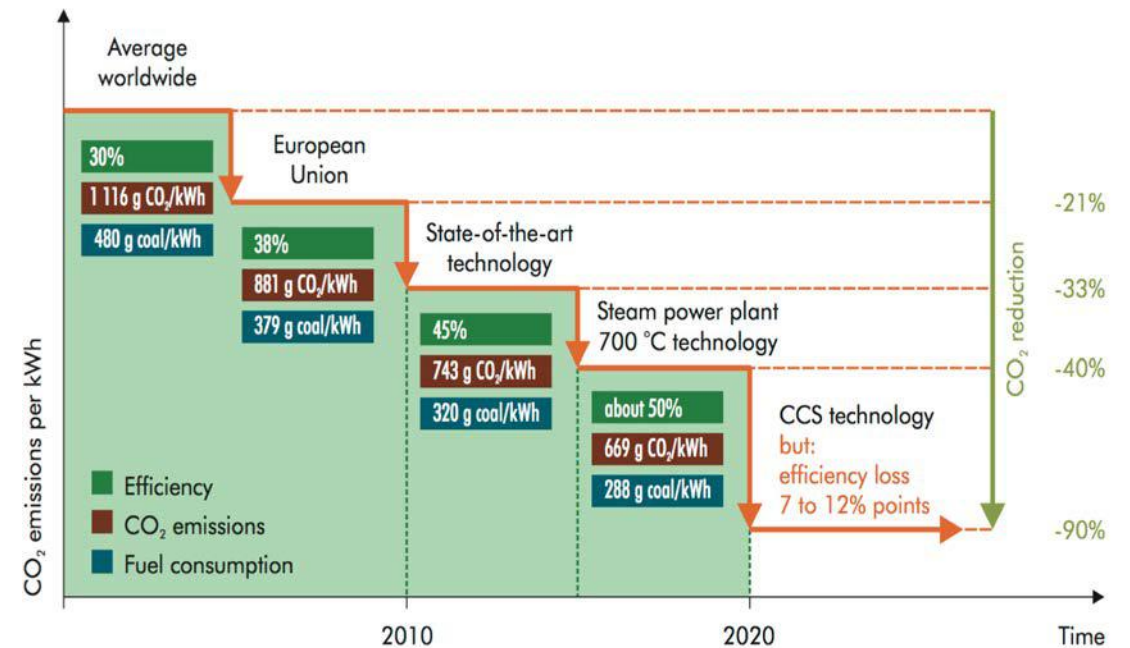
T-s and h-s diagram representations of supercritical steam cycle with reheat
(3.Büki G.,Magyar Energiatechnika 1998;6:33-42)

Efficiency Improvements and CO₂ Emissions

Effect of various measures for improving the efficiency (LHV) of pulverized coal fired power generating plant (Schilling,H.D.:VGB Kraftwerkstechnik 1993;73(8)pp.564-76 (English Edition))



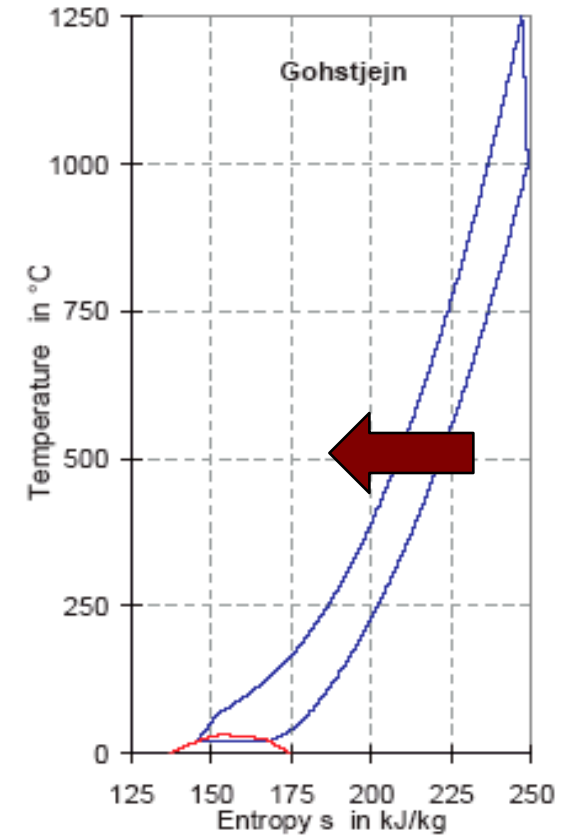
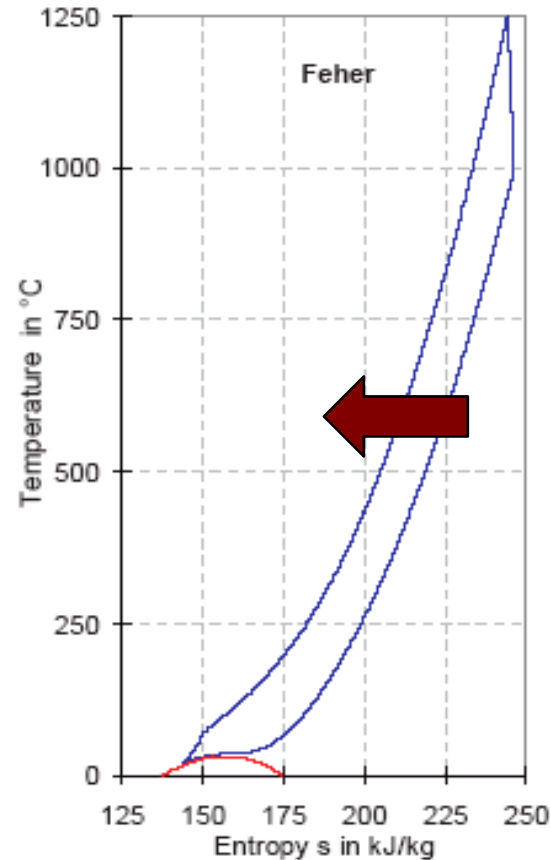
Limits of Efficiency improvement on CO₂ emissions and Role of CCS



Source: VGB (2009). Reprinted by permission of the publisher. © VGB PowerTech e.V., 2009.

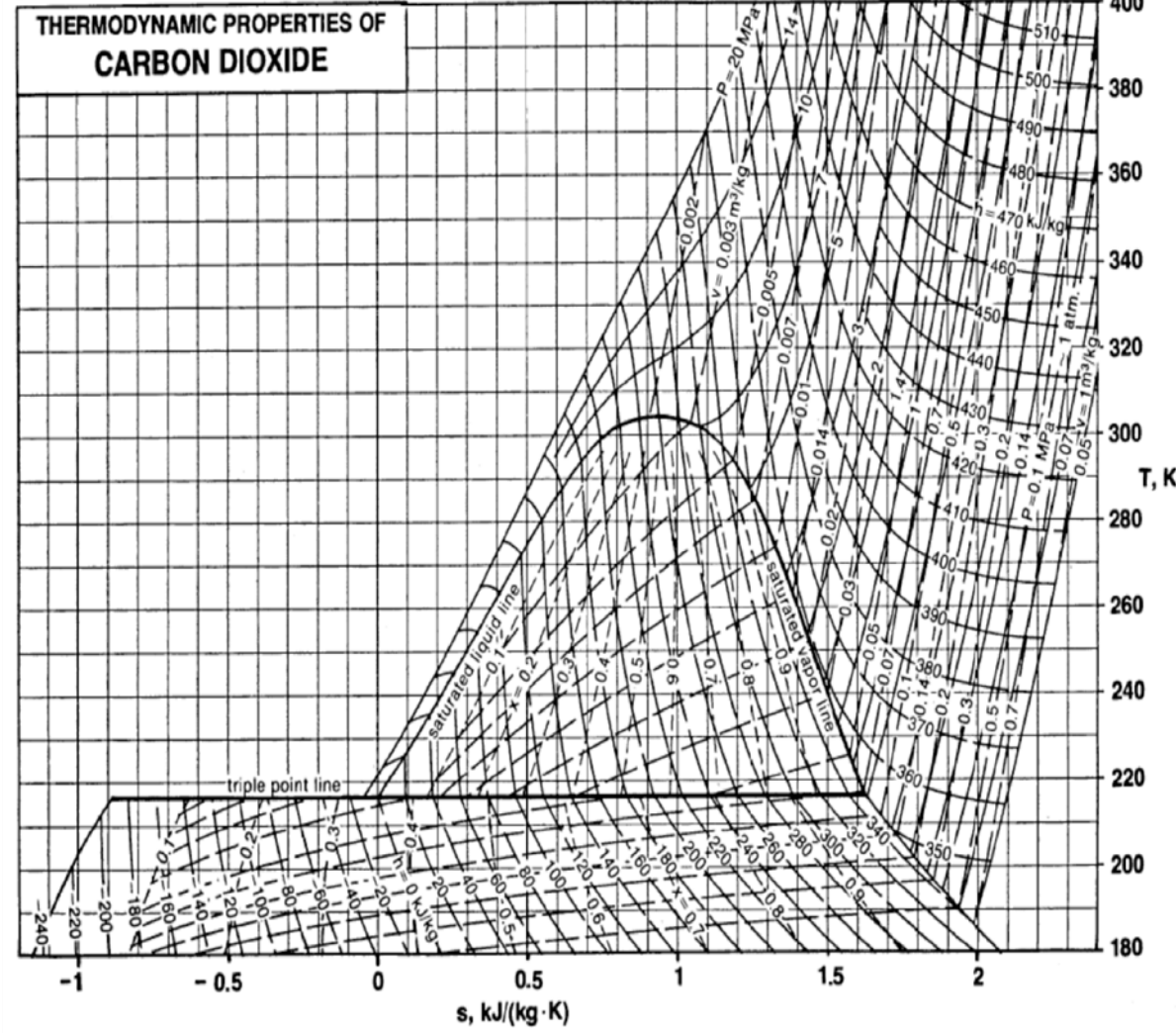
Hypercritical closed CO₂ “Gas” Cycles

- $p_{\text{crit}} = 7.39 \text{ MPa}$, and $T_{\text{crit}} = 30.4 \text{ C}$.
- Can take advantage of benefits of supercritical cycles without the need for very high p (typical pressure ratio is 4 but can go up to 10)).
- High T is used to improve efficiency.
- Regeneration improves the efficiency significantly, see diagrams.
- Low compression work (near critical point, more pumping than compression)
- Under consideration for nuclear plants.
- Also for oxy-combustion cycles

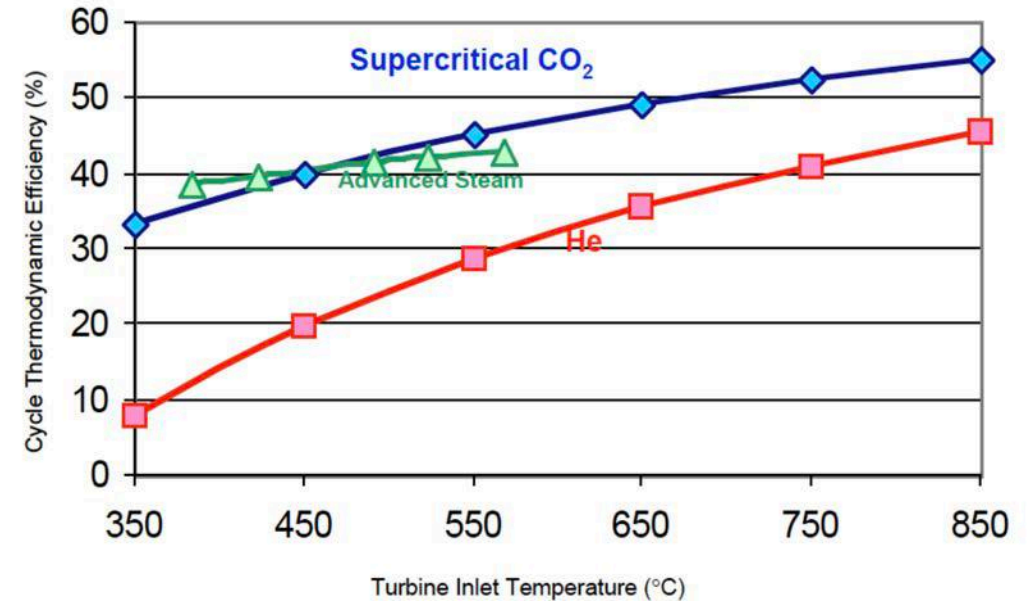


Courtesy of USGS.

From Gottlicher, the Energetics of Carbon Sequestration in Power Plants



See Chapter 6 for more detail, especially the impact of regeneration and split compression to achieve impressive efficiency in CO₂ cycles



- Thermal efficiency of a number of cycles within the low temperature range.
- Helium cycles are Brayton cycles, which can only achieve low efficiency at these low temperatures.
- Advanced steam cycles are superheated or supercritical steam cycles.
- Supercritical CO₂ are “hypercritical” cycles.

Rankine cycles:

1. Fuel flexible, works well with coal and other dirty fuels (closed cycle).
2. Have high efficiency, low pumping power.
3. Require lower flow rate (latent enthalpy).
4. Run at lower high T (work well with renewable sources), but high p.
5. Works well with nuclear energy:

BUT ...

1. High inertia, good for base load but not for load following.
2. Require cooling, big condensers, ..
Water ...

- Condenser adds cost, needs vacuum and allows air leakage.
- Must remove air to maintain low pressure in condenser.
- Condenser needs large surface area and large water flow.
- Superheat increases efficiency and specific work.
- Superheat improves steam quality in late stages of turbine, reduces material damage.
- Reheat helps efficiency and steam quality.
- Recuperation increases efficiency at the cost of hardware complexity.

COMBINED CYCLES

$$Q_{in} = Q_{GT},$$

$$W_{GT} = \eta_{GT} Q_{GT},$$

$$Q_{ST} \approx (1 - \eta_{GT}) Q_{GT},$$

$$W_{ST} = \eta_{ST} (1 - \eta_{GT}) Q_{GT}$$

$$W = W_{GT} + W_{ST},$$

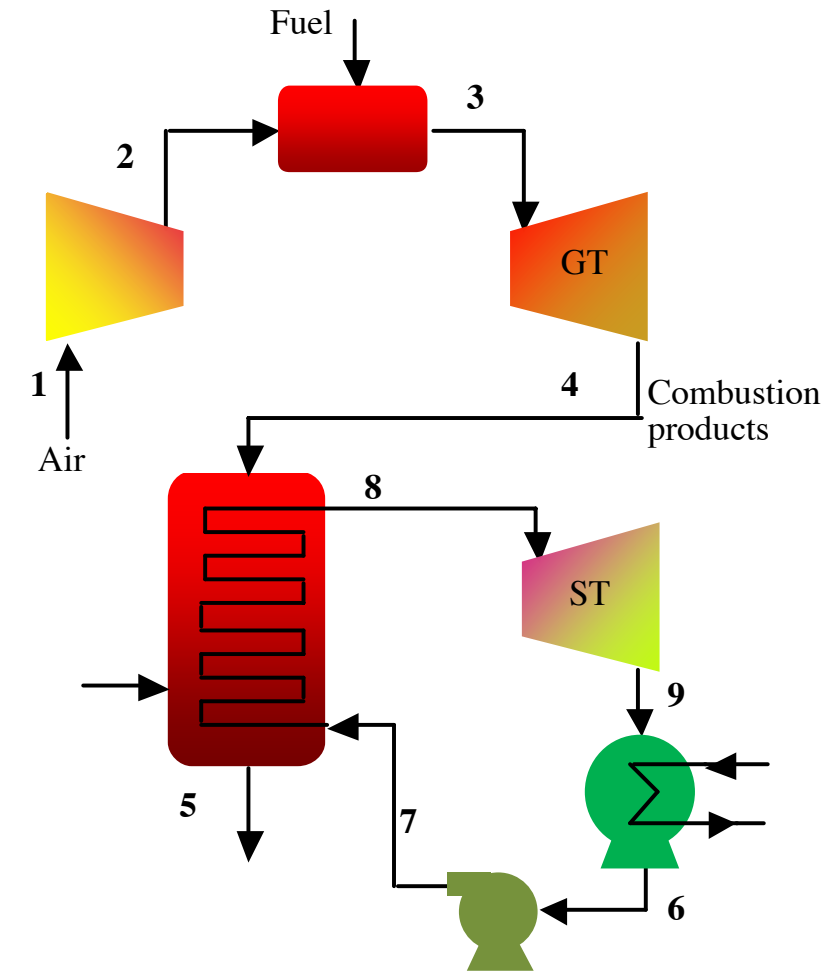
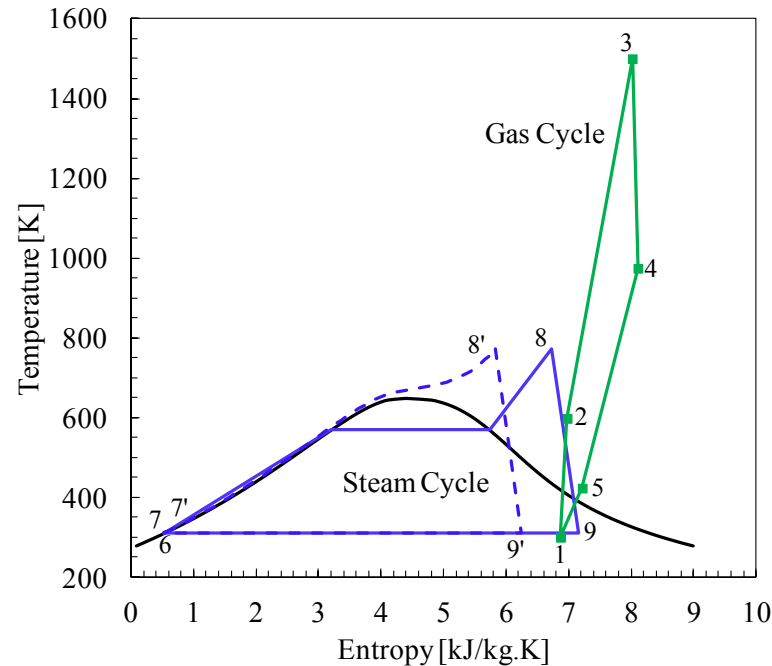
$$\eta_{CC} = \eta_{GT} + \eta_{ST} (1 - \eta_{GT})$$

$$\eta_{GT} = 0.25, \text{ and } \eta_{ST} = 0.4,$$

$$\eta_{GT} = 0.3, \text{ and } \eta_{ST} = 0.28,$$

$$\eta_{GT} = 0.38, \text{ and } \eta_{ST} = 0.25,$$

$$\eta_{GT} = 0.38, \text{ and } \eta_{ST} = 0.40,$$



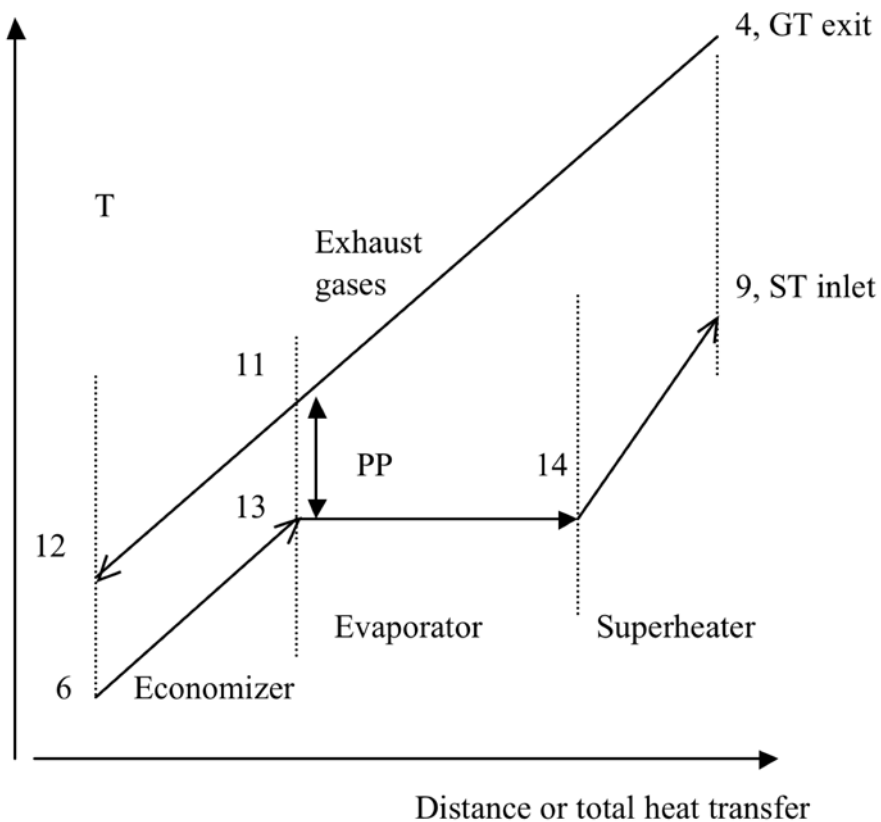
$$\eta_{CC} = 0.55$$

$$\eta_{CC} = 0.5$$

$$\eta_{CC} = 0.535$$

$$\eta_{CC} = 0.628$$

Mass flow rates are not arbitrary, Pinch-point analysis and impact on efficiency:



T_4 is determined by gas turbine exit conditions

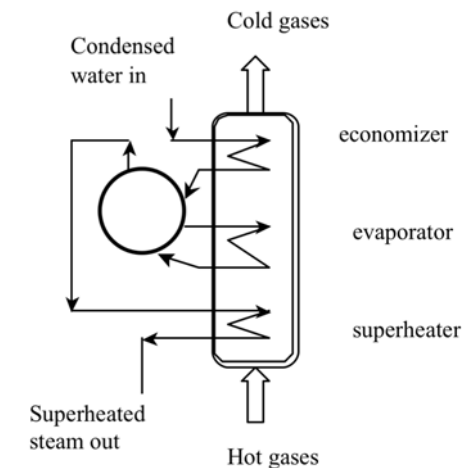
T_{13} is determined by steam cycle high pressure

$T_{11} = T_{13} + PP$ for good heat transfer rates: $PP = O(10 - 15 \text{ C})$

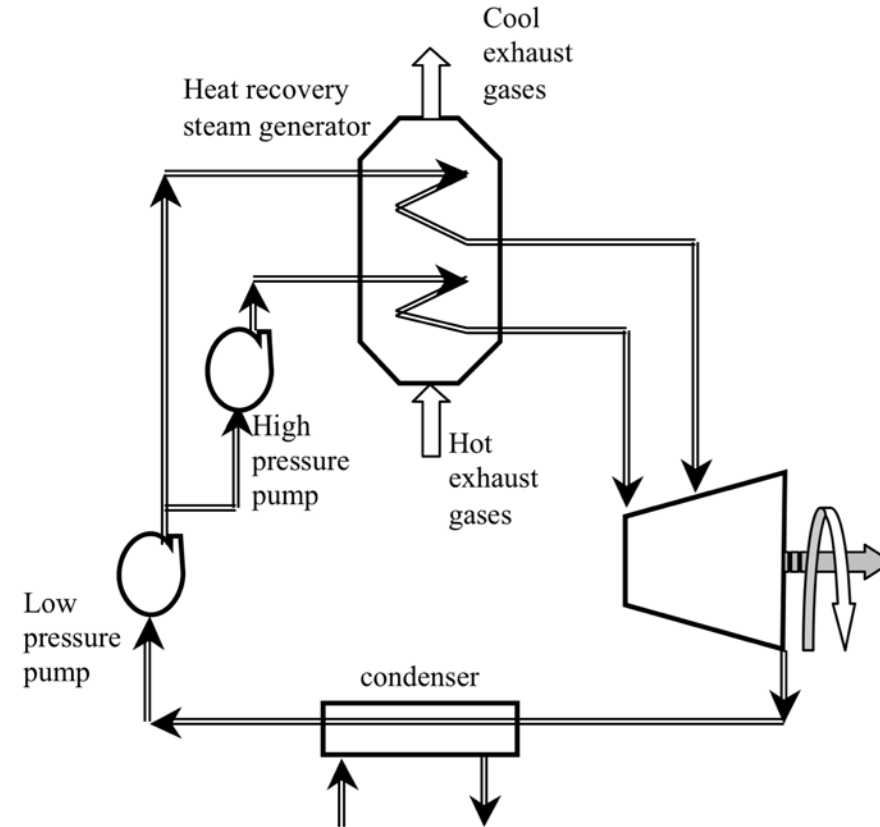
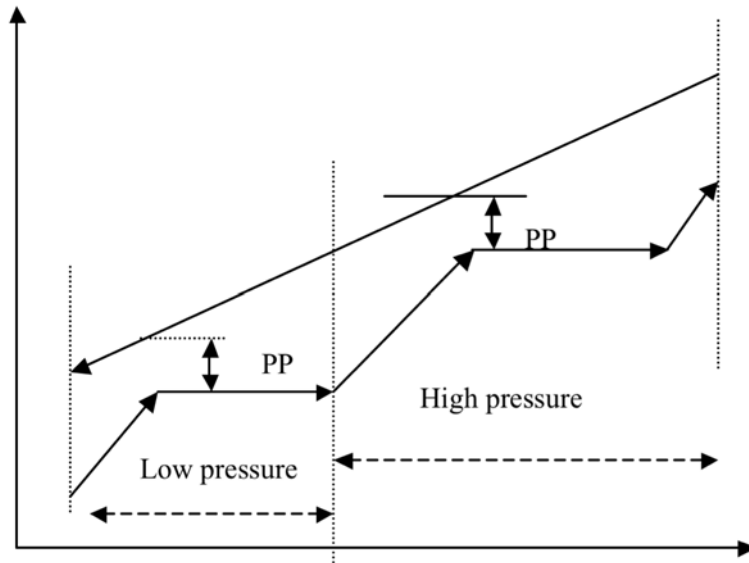
T_9 is determined by steam cycle design

Therefore:

$$\dot{m}_{st} = \dot{m}_g \frac{c_{pg} (T_4 - T_{11})}{(h_9 - h_{13})}$$



Temperature difference between streams can be reduced by employing dual or triple pressure steam cycles:

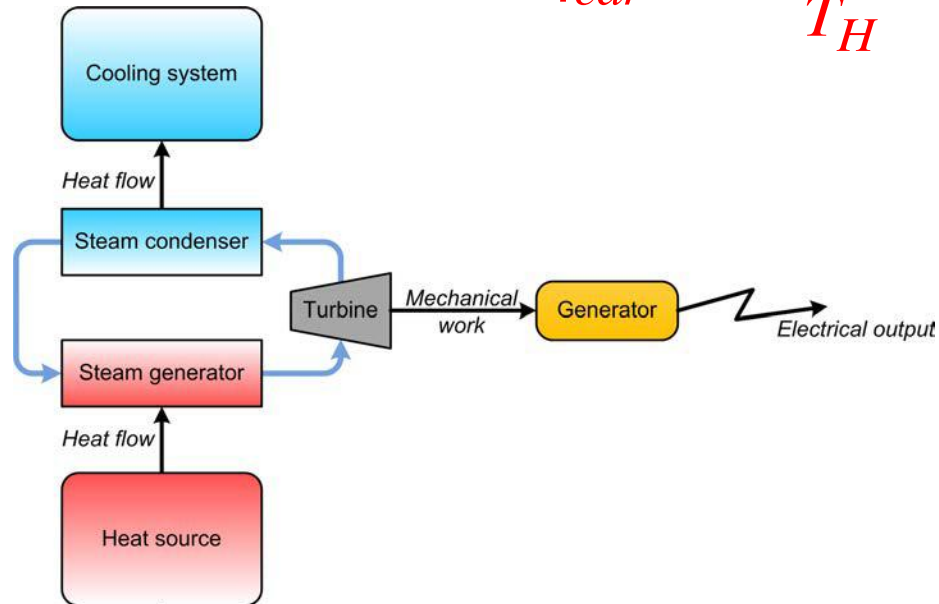


Leading to 2-3 percentage points in efficiency gain.

Steam power plant energy balance

more complex than just the efficiency

$$\eta_{car} = 1 - \frac{T_o}{T_H}$$



Solar thermal, geothermal and nuclear plants run at lower temperatures than combustion plants, have lower thermal efficiencies and higher water footprints – but lower carbon footprints!

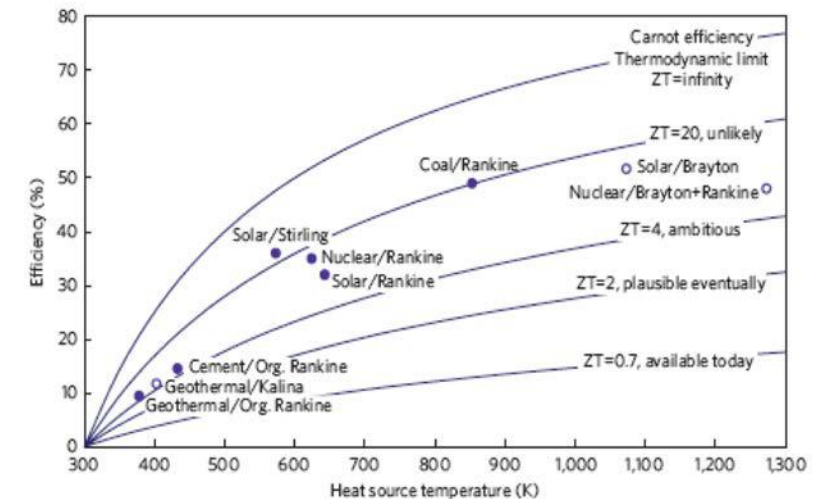
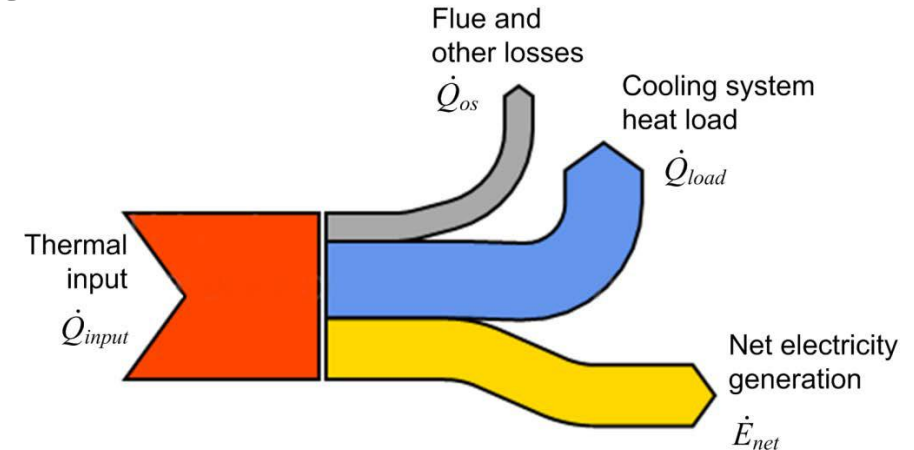
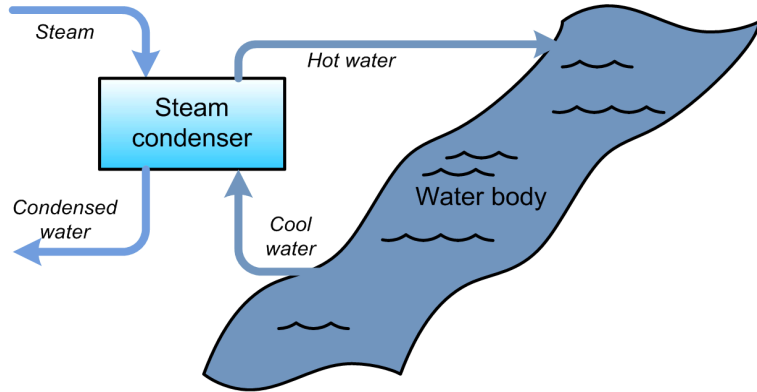


Figure 2 | Assessing thermoelectrics. Efficiency of 'best practice' mechanical heat engines compared with an optimistic thermoelectric estimate (see main text for description).

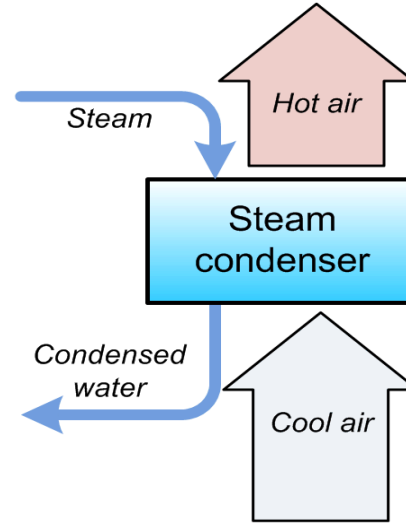
© Source unknown. All rights reserved. This content is excluded from our Creative Commons license. For more information, see <https://ocw.mit.edu/fairuse>.

Cooling system types and tradeoffs

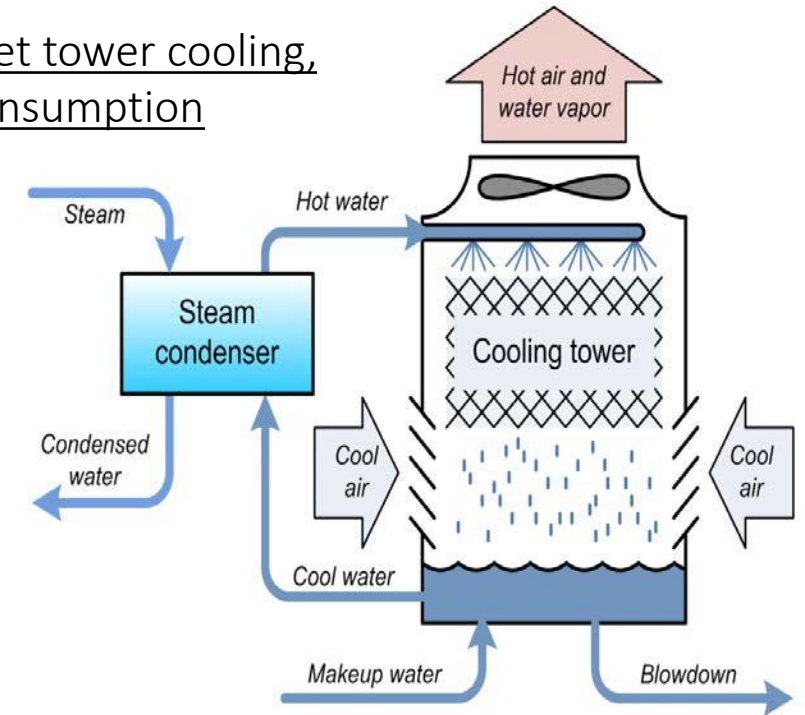
Once-through cooling, withdrawal



Dry cooling



Wet tower cooling, consumption



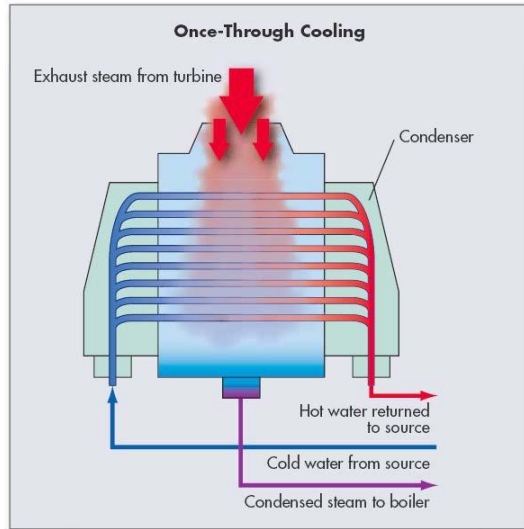
exit T is the dew point of water at its partial p in the exit air.

*All of these →
also depend on local water
and weather conditions!*

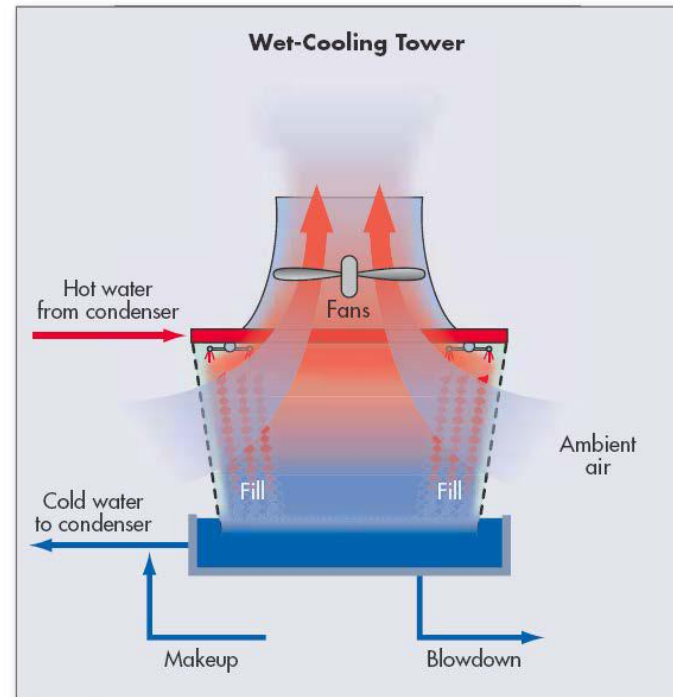
	H2O withdrawal	H2O consumption	Capital cost	Plant efficiency	Ecological impact
Once-through cooling:	Red	Yellow	Green	Green	Red
Wet tower cooling:	Yellow	Red	Yellow	Green	Green
Dry or hybrid cooling:	Green	Green	Red	Red	Green

Cooling system types

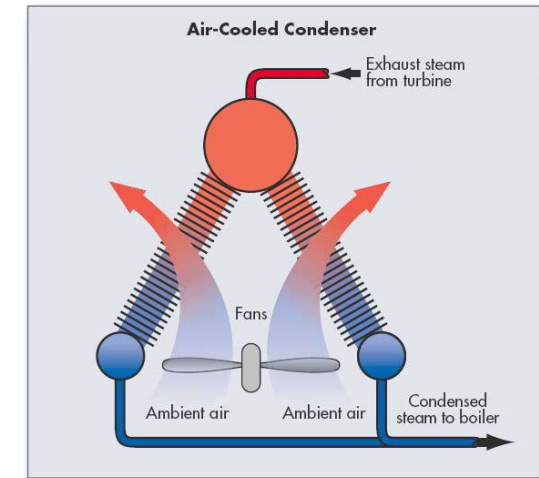
Image: EPRI Journal Summer 2007 "Running Dry at the Power Plant"



- Simple, low-cost
- Condensate temp approaches source temp
- High withdrawal but low consumption, about 1% of withdrawal,
- Ecological issues: organism entrainment and impingement, hot effluent
- Use being phased out in the US under Clean Water Act

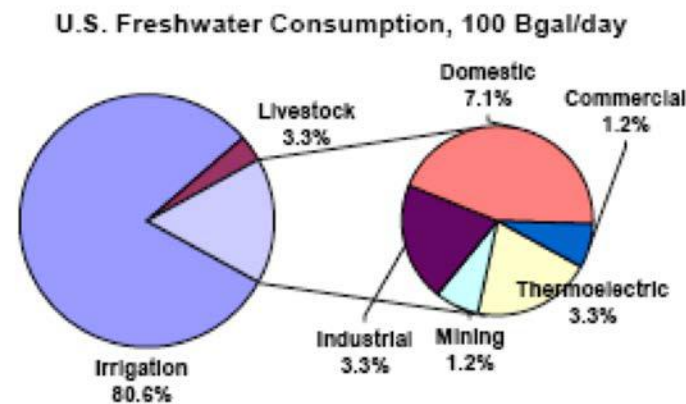
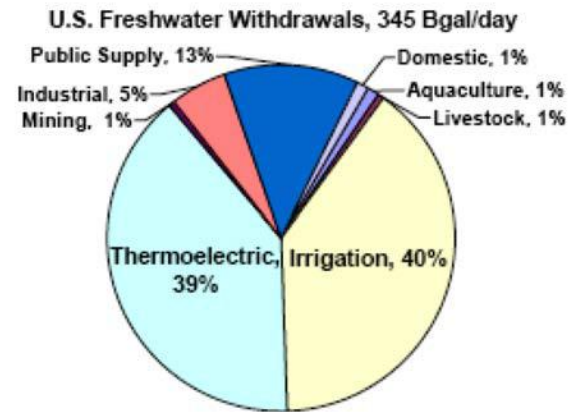
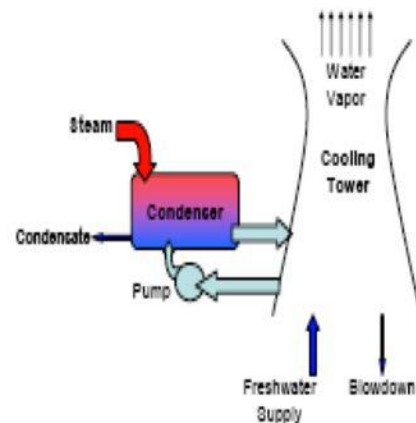
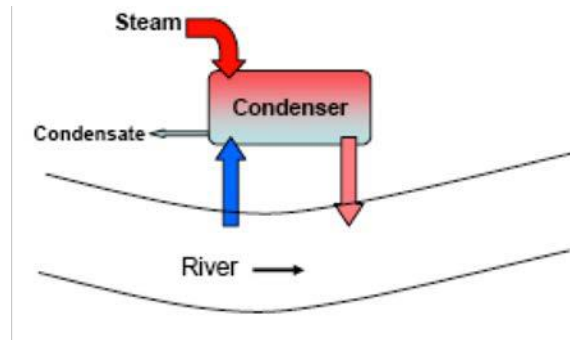


- More complex and costly
- Cooling water temp approaches ambient wet-bulb temp
- Lower withdrawal, 2 orders of magnitude less
- High consumption



- Very expensive, 3-4x more than evaporative
- Condensate temp approaches ambient dry-bulb temp, poor efficiency on hot days
- Zero withdrawal and consumption

In late 90ies, 59 BGPD seawater and 136 BGPD fresh water were withdrawn for thermoelectric power plant* (39% of total)*, only 3.3 BGPD were consumed (~20% of non agri consumption)*, other returned at higher T (causes further evaporation, estimated at 1%). About 30 % of US plants use open loop cooling*. Most plants after 1970 utilize closed loop cooling



Electricity is as thirsty as the livestock or industrial use



GEBZE & ADAPAZARI 3 x 777 MW_e CCGP commissioned in 2002 (Turkey)
EPC-Contractor: BECHTEL-ENKA JV, End-user: INTERGEN
The world's largest dry cooled combined cycle power plant

13

The Advanced Heller System, by A. Balogh and Z. Szabo, EPRI Conference on Advanced Cooling Strategies/Technologies, June 2005, Sacramento, CA

Working fluids requirements:

1. High T_c for efficiency but low p_c for simplicity
2. Large enthalpy of evaporation
3. Non toxic, non flammable, non corrosive, cheap ..

Water: $p_c=22.088$ MPa $T_c=374$ C, most common

CO₂: $p_c=7.39$ MPa, $T_c=30.4$ C (low p)

Can also use a bottoming cycle (Binary Cycle) to avoid strong vacuum, but need exotic fluids (mercury...)

Renewable sources (low to very low T for solar and geothermal):

Ammonia: $p_c=11.63$ MPa, $T_c=132$ C.

Propane: $p_c= 4.26$ MPa, $T_c= 97$ C

Isobutane, Freon

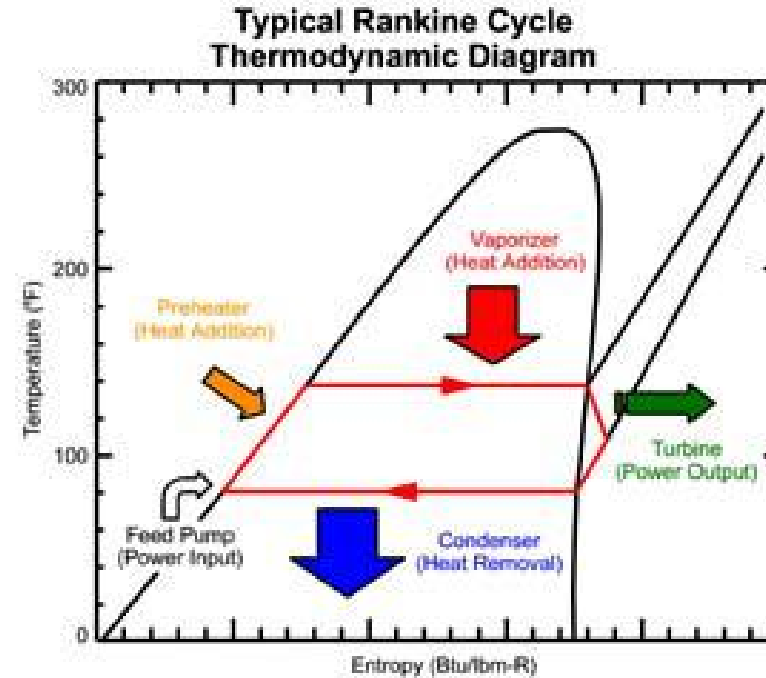
Organic Rankine Cycles

Solar Energy Applications:

When flat plate collectors are used, maximum heat transfer fluid temperature is ~ 150 C.

When geothermal heat sources are used, maximum temperature is below 200 C.

In both case, working fluid critical temperature should be lower. An example these “organic” working fluids, used in “Organic Rankine Cycles” is shown:



Ha Teboho Village, Lesotho
Matt Orosz, Liz Wyman et al.

MIT OpenCourseWare
<https://ocw.mit.edu/>

2.60J Fundamentals of Advanced Energy Conversion
Spring 2020

For information about citing these materials or our Terms of Use, visit: <https://ocw.mit.edu/terms>.

Lecture # 17

Solar Thermal Energy

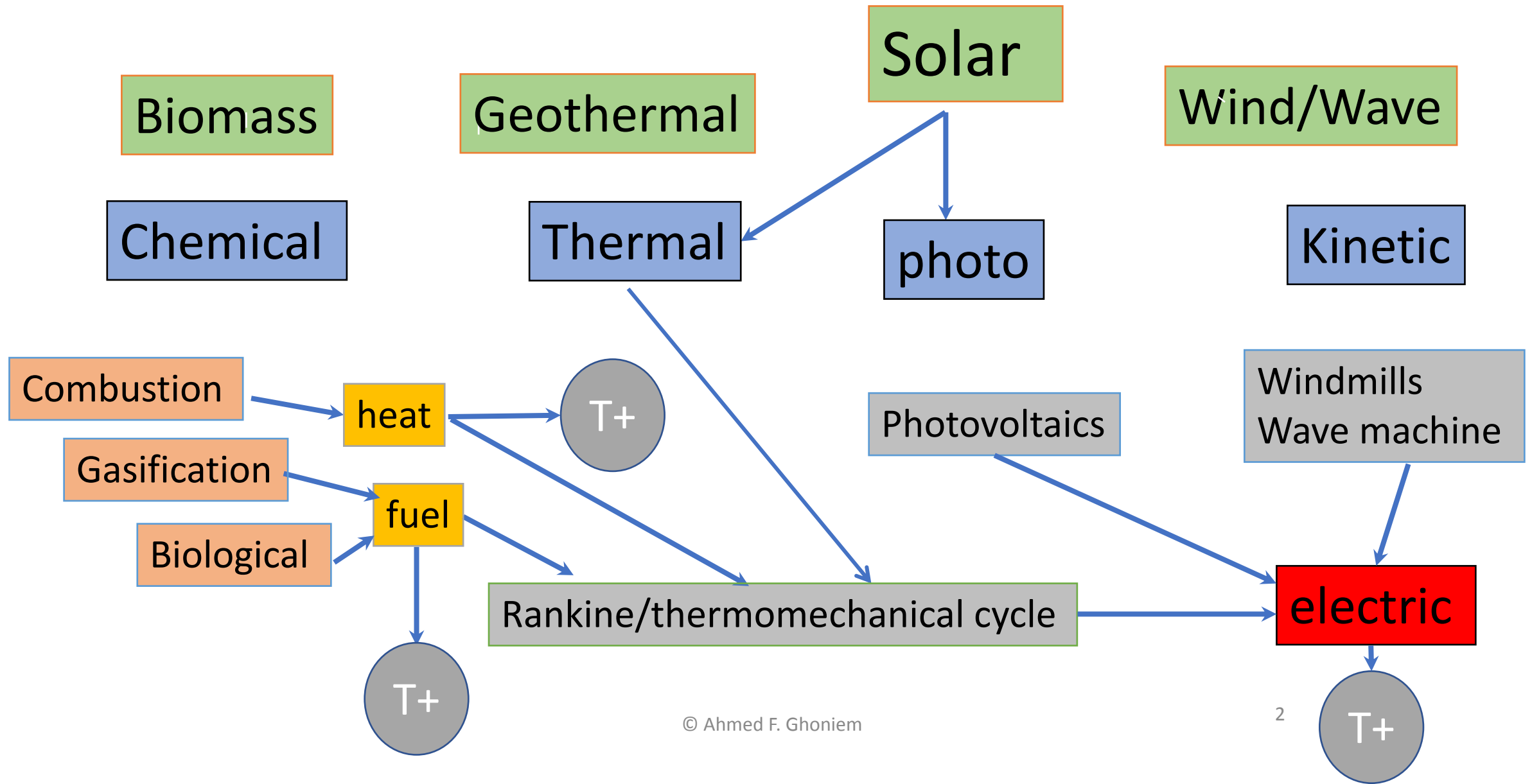
Ahmed Ghoniem
April 6, 2020

Renewables: Some characteristics and specifics.

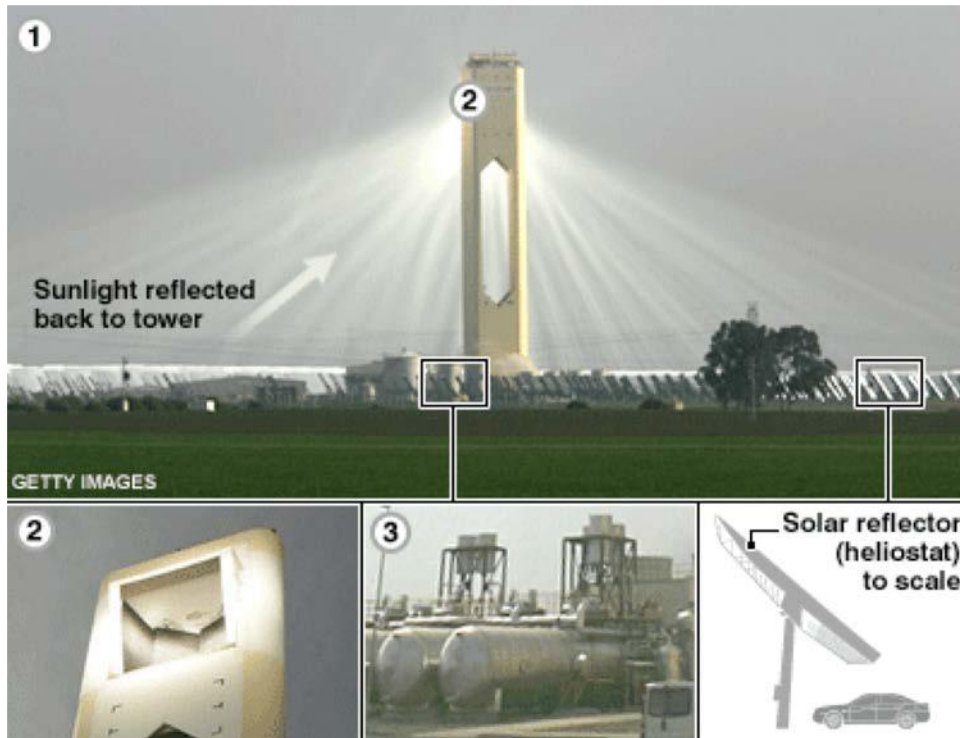
Historical Trends ...

Solar Thermals: Concentrators and Plants

Renewable Sources and Their Utilization



Solucar, Outside Seville, 2007, 600 mirrors generate 11 MWe,



1. The solar tower is 115m (377ft) tall and surrounded by 600 steel reflectors (heliostats). They track the sun and direct its rays to a heat exchanger (receiver) at the top of the tower
2. The receiver converts concentrated solar energy from the heliostats into steam
3. Steam is stored in tanks and used to drive turbines that, eventually, will produce enough electricity for up to 6,000 homes

© Getty Images. All rights reserved. This content is excluded from our Creative Commons license. For more information, see <https://ocw.mit.edu/fairuse>.



Aerial view of PS10 11MW solar plant

Designed for 10 MW, central receiver, to deliver 20-25 GWh/y (25-30% capacity)
Located in Sanlucar La Mayor (best area in Spain for solar), built and operated by Abengoa.

© Solucar. All rights reserved. This content is excluded from our Creative Commons license. For more information, see <https://ocw.mit.edu/fairuse>.

www.solucar.es

Cost estimated to be 3X higher
Capital cost: E3000/KWe

Saturated steam is generated at the receiver tower, fed directly to the turbine, or some stored in hot water tank for extending the hours of operation. The receiver is a forced circulation radiant boiler receiving ~ 55 MWt of concentrated solar radiation. Storage capacity is 20 MWht, sufficient to operate the turbines for 50 minutes at 50% capacity.

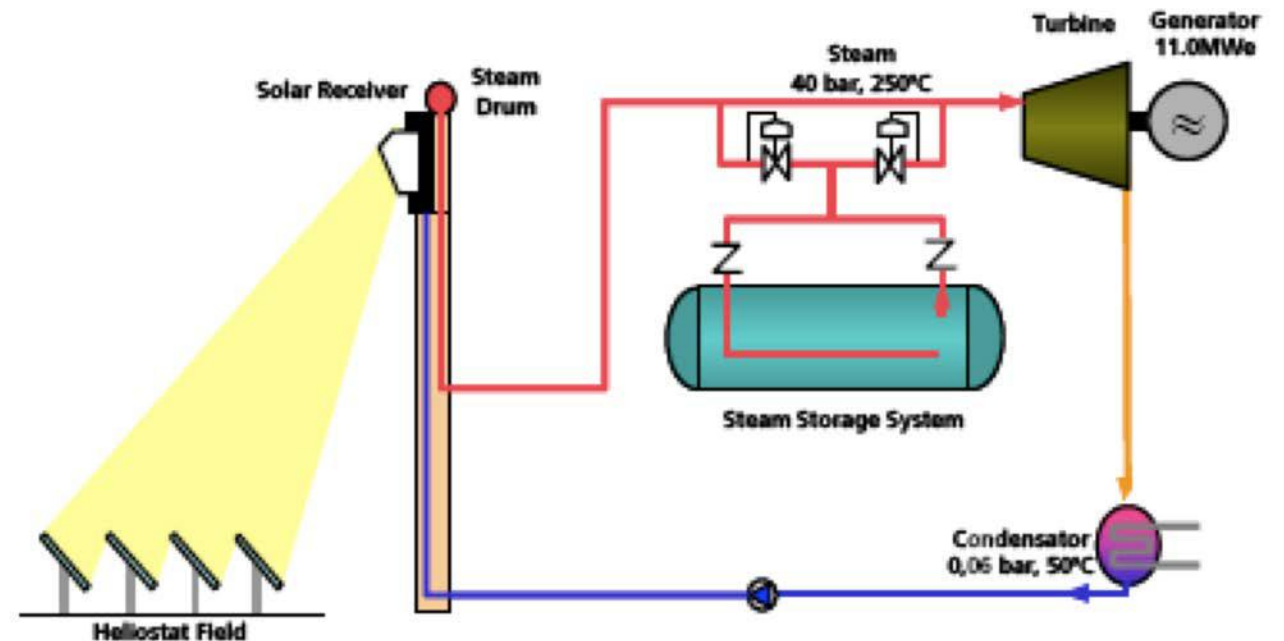


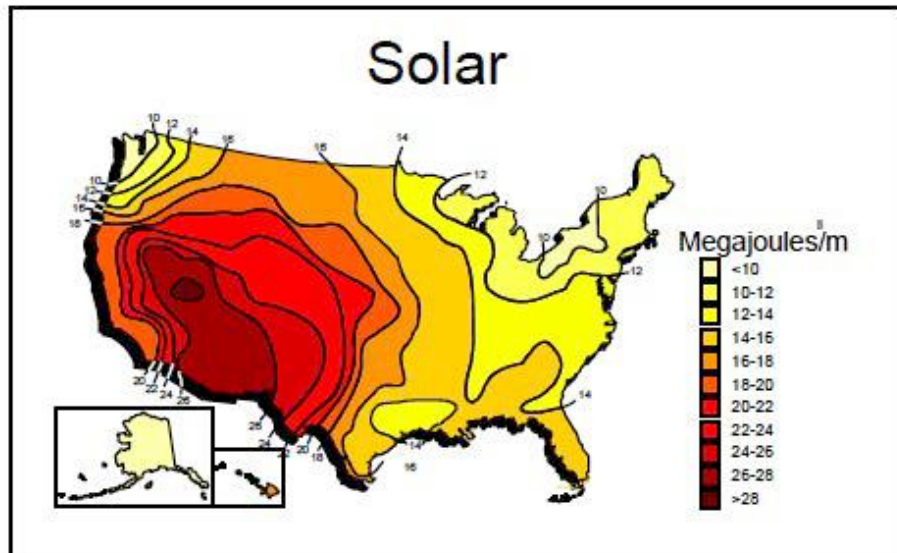
Image courtesy of DOE.

General characteristics of Renewable Sources (does not apply to hydropower and some geothermal):

1. Ubiquitous, certainly with solar, less so with wind (more wind off-shore).
2. Low energy density, mostly surface area dependent, lower grade heat and low heating value for biomass.
3. Mostly intermittent, especially for solar, wind and wave, less so for hydropower and biomass (which has seasonal intermittency instead of daily).
4. Fuel cost is negligible (except for biomass and geothermal), but capital cost to collect the energy can be significant.
5. Carbon neutral (if all is kept renewable).

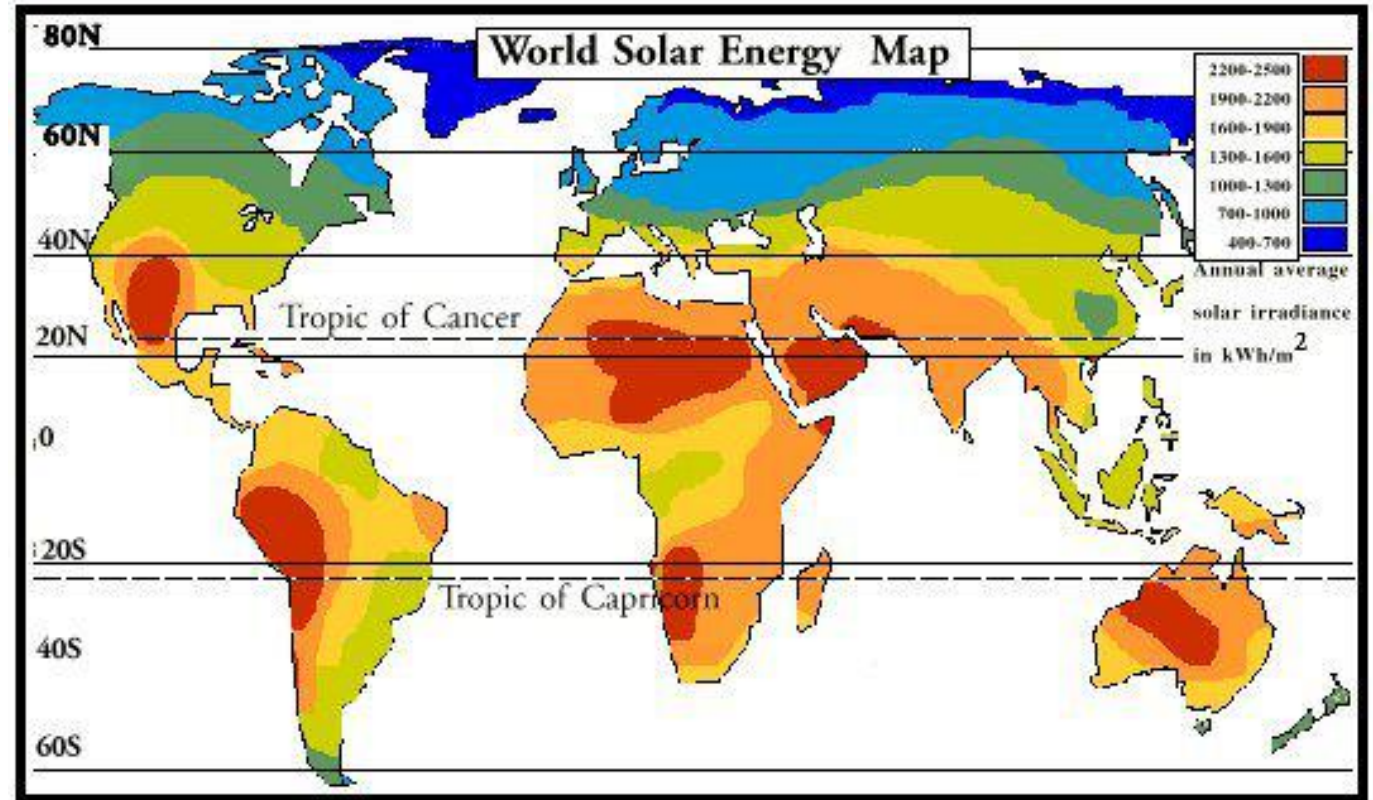
Solar Energy is “Everywhere”, But Opportunities Vary

Distribution networks may have to look different



Average daily total irradiance on a horizontal surface in a clear day Source: US DOE

Image courtesy of DOE.



© Source unknown. All rights reserved. This content is excluded from our Creative Commons license. For more information, see <https://ocw.mit.edu/fairuse>.

Historical Notes

In 1780, 95% of total power used in commercial applications was from natural sources (wind and water). By 1911, all but 2% of power was generated from burning coal and harnessing steam.

“Within a few generations at most, some other energy than that of combustion of fuel must be relied upon to do a fair share of the work of the civilized world.” *Robert H. Thurston - 1901, the Smithsonian Institution annual report.*

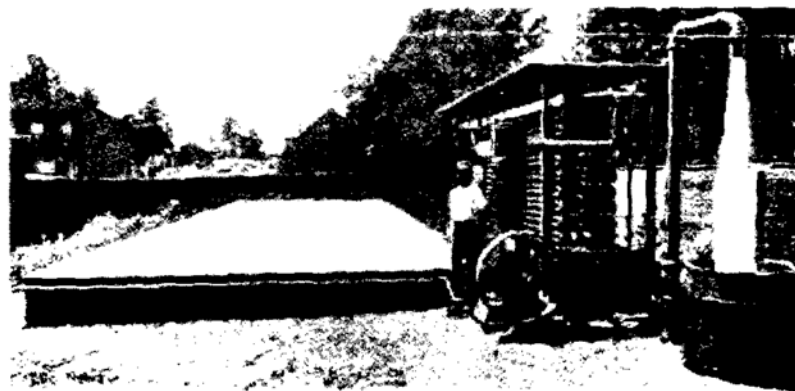
“... the human race must finally utilize direct sun power or revert to barbarism because eventually all coal and oil will be used up. I would recommend all far-sighted engineers and inventors to work in this direction to their own profit, and the eternal welfare of the human race”
Frank Shuman – 1914

The conversion of solar energy into mechanical power was attempted as a commercial venture by **the Sun Power Company** in Pennsylvania by Frank Shuman, 1910. “The fact that ... no fuel is required is such an enormous advantage as to entirely offset the increased initial cost, and in addition cause great profits.” *Frank Shuman - 1911.*

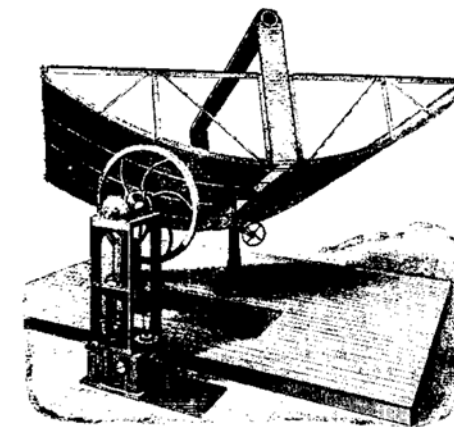
Source: The power of Light by Frank T. Kryza, McGraw Hill, 2003



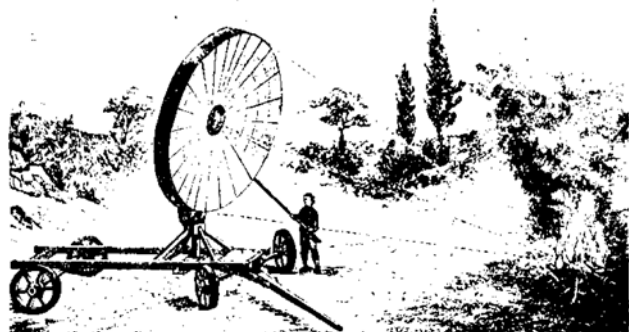
Leonardo Da Vinci and his drawing of a 4-mile burning mirror to be set in the ground.



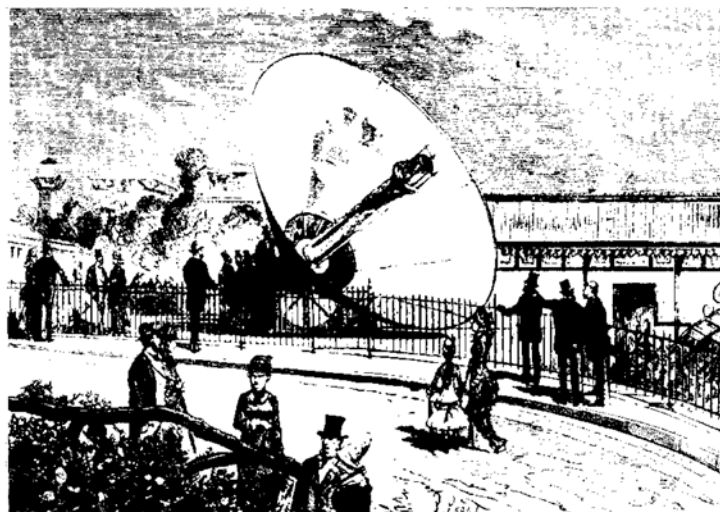
Shuman's first Tacony solar plant. Note the water gushing out of the pipe at right.



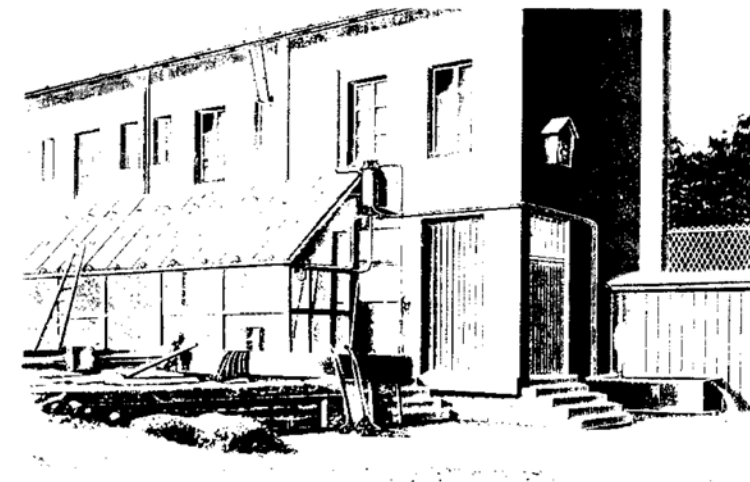
John Ericsson's solar motor, the first to use a "parabolic trough" collector (the curved shape that looks like a section of metal barrel). Frank Shuman later enlarged and adapted this design for his solar machine in Egypt.



A large, lightweight German burning mirror of the late 1700s being used to set fire to a pile of wood at a distance of about 30 feet. This compound parabolic mirror used scores of flat pieces of thin brass plate nailed onto a parabolic armature or frame made of wood. Mirrors of this type, often 10 feet or more in diameter, were by far the most powerful solar reflectors yet developed and could focus the concentrated rays of the sun on a target area less than 1 inch in diameter. Wood burst into flame almost instantly. Copper ore melted in 1 second, lead in the blink of an eye.

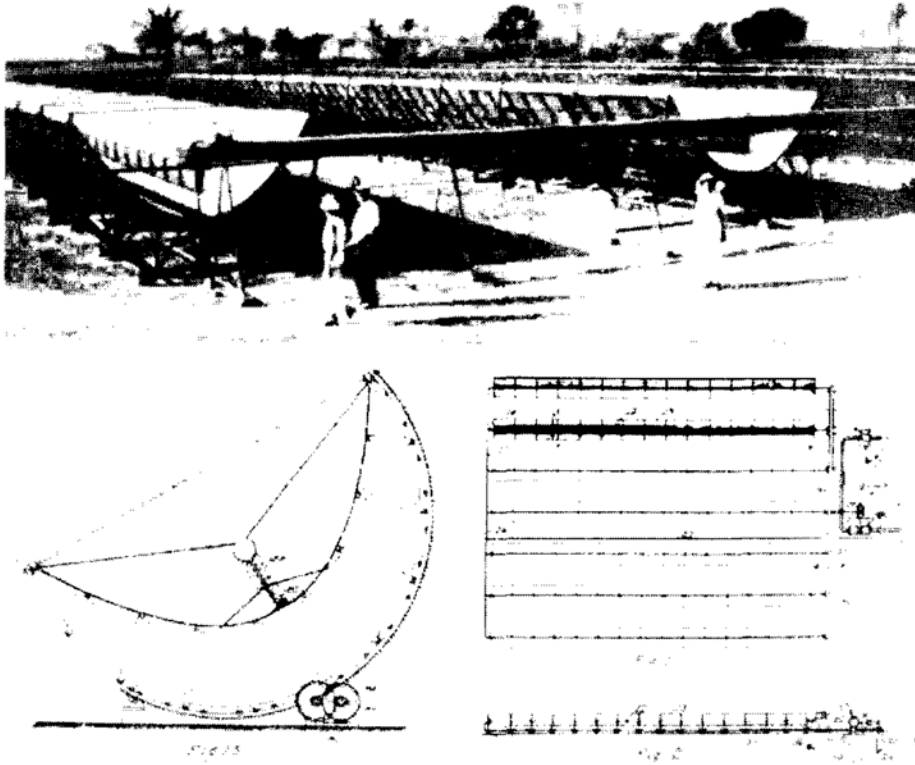


One of the largest Mouchot devices ever built on display at the Universal Exposition in Paris in 1878 on the banks of the Seine. It was a prototype of this device that so intrigued Napoleon III in 1867 and spurred him to provide Mouchot with financing.

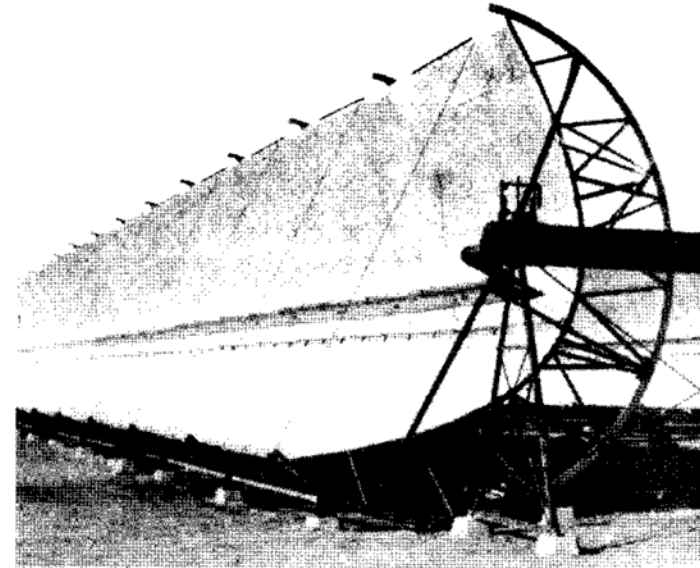


Large cast-iron solar hot boxes (numbered 1 through 10 in the diagram) built on the side of Charles Tellier's Paris workshop. The thick metal plates were needed because the working fluid was ammonia under pressure. Tellier hooked up the pump powered by the ammonia to lift water from his well.

Solar Powered Irrigation in Egypt -1913



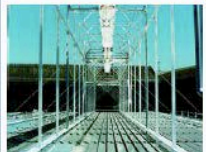
Frank Shuman's Maadi plant in Egypt, with cutaway diagram of the parabolic trough collectors.



Frank Shuman's Maadi parabolic troughs, close up.

Fast forward to 21st Century



	Collector Type	Operating Temperature [°C]	Heat Transfer Medium	Contact person within Task 33/IV	Page
	Fix Focus Trough	100 - 200	water, steam, thermal oil, air	Klaus Hennecke DLR Institute for Technical Thermodynamics D-51170 Köln Germany	21
	Linear Concentrating Fresnel Collector	100 - 400	Water, steam, thermal oil	Andreas Häberle PSE Solar Info Center 79072 Freiburg Germany	22
	CHAPS Combined Heat and Power Solar collector	80 - 150	Water	Joe Coventry The Australian National University Centre for Sustainable Energy Systems Department of Engineering, Canberra ACT 0200 Australia	24

The Combined Heat and Power Solar (CHAPS) collector

Authors:

Dr Joe Coventry
Prof Andrew Blakers

Research Institution(s) involved in the development

The Australian National University
Centre for Sustainable Energy Systems
Department of Engineering
Canberra ACT 0200 Australia



Prototype CHAPS system



300m² Bruce Hall system under construction

Description of collector, operating temperature range and stagnation temperature

The CHAPS collector is a parabolic trough system consisting of glass-on-metal mirrors that focus light onto high efficiency monocrystalline silicon solar cells to generate electricity. Water, with anti-freeze and anti-corrosion additives, flows through a conduit at the back of the cells to remove most of the remaining energy as heat. The

thermal energy may be used via a heat exchanger for industrial applications, building heating and domestic hot water.

Operating temperature level:

The operating temperature of the collector is limited by the inclusion of solar cells. The electrical efficiency of the system reduces as operating temperature increases. Therefore the system is ideally suited to lower temperature applications (<80°C) where electrical system efficiency is maintained above 10%; however, temperatures up to around 150°C are feasible, with electrical efficiency still in the order of 8%.

Stagnation temperature:

Not applicable. The receiver is destroyed well below the stagnation temperature, so preventative measures are included to avoid the possibility of stagnation conditions occurring. For example, the tracking system uses a dc actuator with battery backup. This is combined with automatic collector 'parking' in case of over-temperature conditions.

Dimensions of the prototype collectors

Width of single trough: 1.55 m
Length of single trough: 24 m
Focal length: 0.85 m

Collector parameters based on aperture area

The thermal efficiency parameters are estimated, but based on data measured at operating temperatures lower than 80°C. It is assumed that the insulation is improved for higher temperature applications. Efficiencies are based on DNI (direct normal irradiation) and on the total aperture area of the mirror.

	Thermal efficiency	Electrical efficiency ¹
η_0	0.56	0.126
a_{1s}	0.0325 W/(m ² K)	0.355
a_{2s}	0.00313 W/(m ² K ²)	

¹ Although it is not strictly correct to plot electrical efficiency on the same axes as for a thermal efficiency curve, this has been done for the sake of comparison. The parameters are based on 1000 W/m² assuming ambient temperature of 25°C. Actually, the absolute temperature of the receiver is what matters for electrical performance, so technically the temperature difference (T_m-T_{amb}) should be in reference to a baseline T_{amb}.

Linear Concentrating Fresnel Collector

Authors:

A. Häberle, PSE GmbH
Christaweg 40
D-79114 Freiburg
E-mail: ah@pse.de

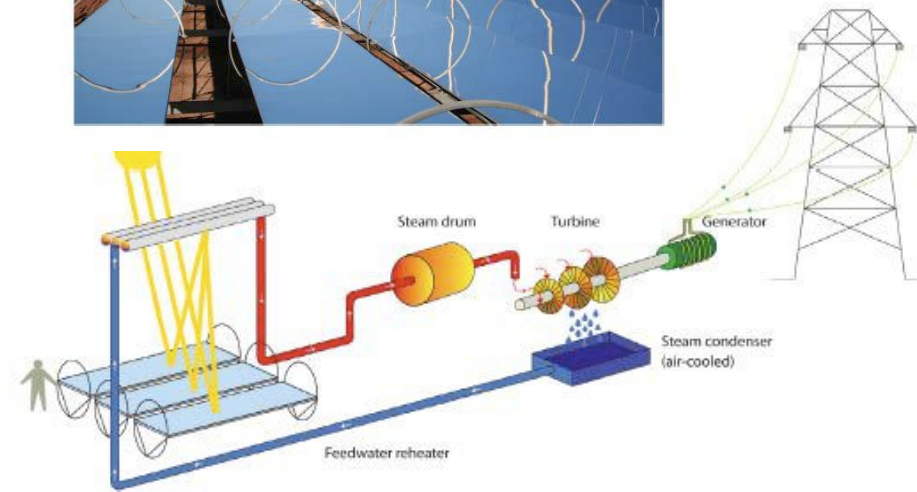
Research Institution(s) involved in the development

Fraunhofer ISE
Heidenhofstrasse 2
D-79110 Freiburg, Germany

DLR
Institute for Technical Thermodynamics
Lindner Höhe
51170 Köln, Germany

Companies involved in the development

Solarmundo, PSE GmbH
A similar concept is being pursued by the Australian company SHP (Solar Heat and Power) and SHP-Europe in co-operation with the University of Sydney.



Copyright © 2007 Ausra, Inc. All Rights Reserved.

9/07

Ausra's CLFR technology builds on the experience with troughs and towers. Ausra's core technology, the Compact Linear Fresnel Reflector (CLFR) solar collector and steam generation system, was originally conceived in the early 1990s by Ausra's founders in Australia. The CLFR system retains a key advantage of troughs – fewer foundations and positioning motors per square meter of mirror – and a key advantage of the PS-10 tower system – direct steam generation and energy storage. Compared to trough systems, the CLFR system reduces costs by replacing special heat-curved reflectors with standard flat glass, and keeps all mirrors close to the ground, lowering wind loads and steel usage.

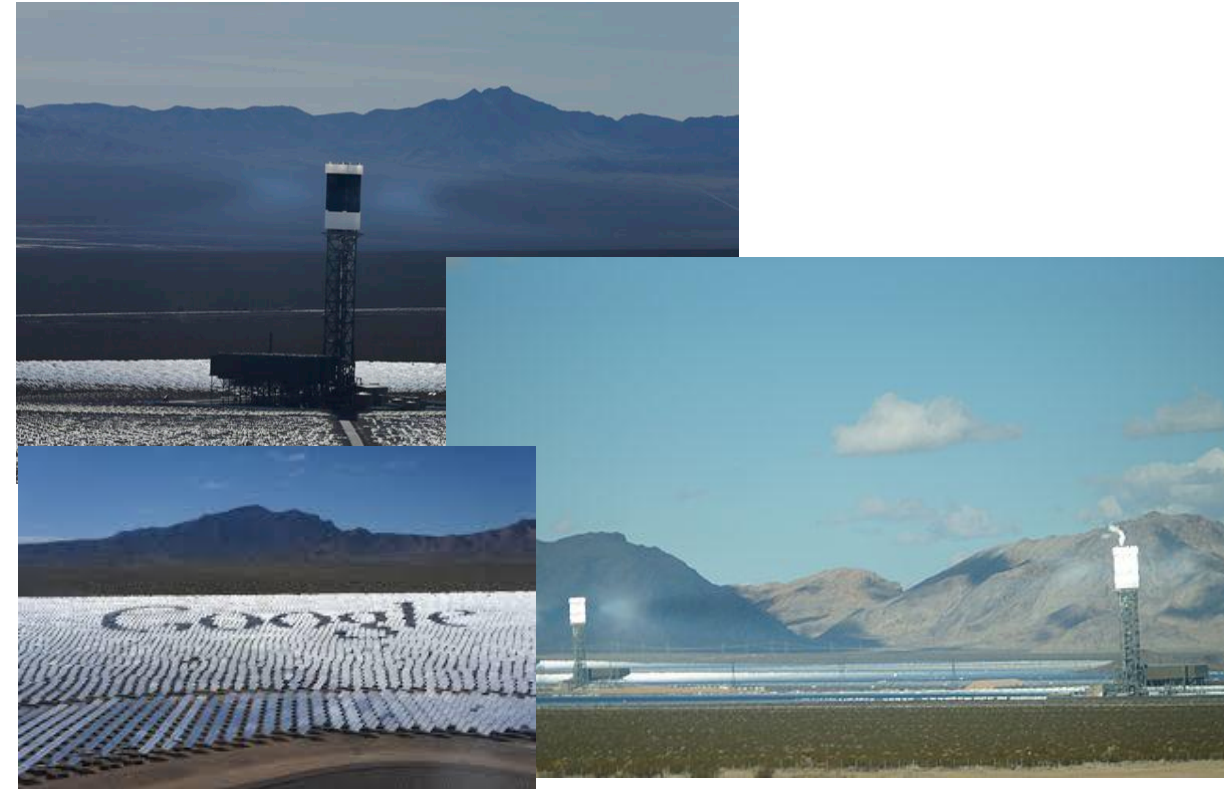
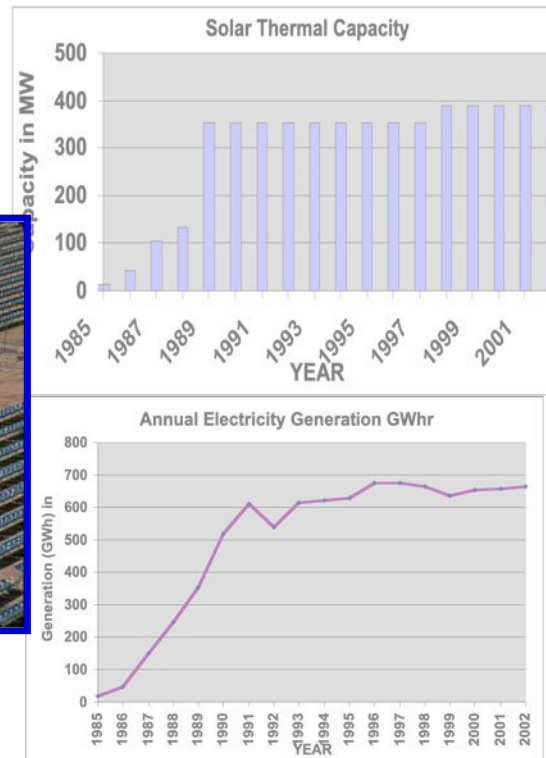
Solar Thermal Electric Generation Stations (SEGS) 1985-2002

Modern plants 2006-2014

Nine SEGS Plants in the Mojave Desert (350MW)



Image courtesy of NREL.



- In 2006, Nevada Solar 1 was commissioned, 64 MWe, built over 250 acres (1.3 sq km), using 760 troughs. Expected power 130 million kWh/y, capacity factor ~ 25%). Cost \$250M (~\$110M for IGCC and ~\$35M for NGCC).
- Ivanpah solar plant (2014), Dry Lake, CA, world largest CSP, 392 MW, capacity factor 28.72% . 4000 acres, 173,500 heliostats, \$2.2 B (\$1.6 B loan guarantees, total cost \$2.2B), doubles US solar electricity

Solar Radiation Spectrum

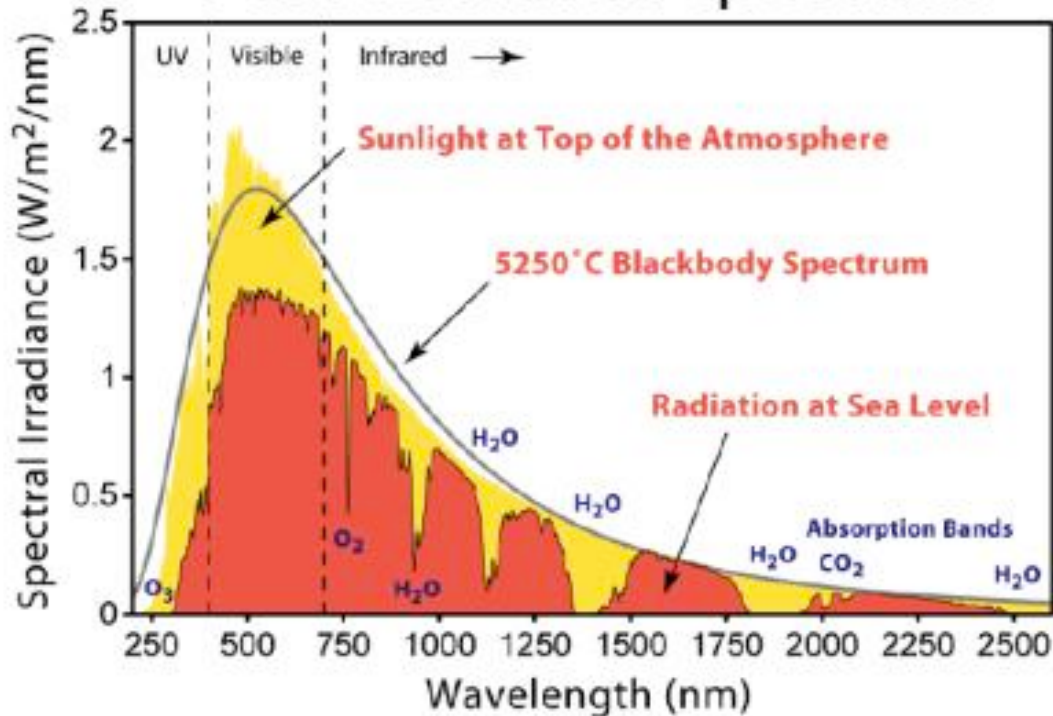
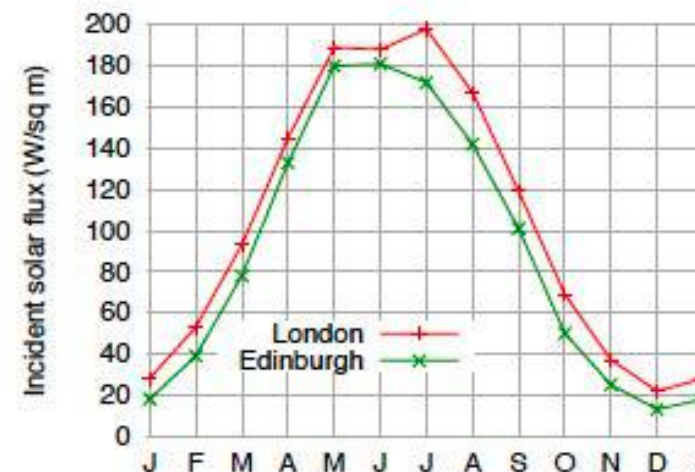


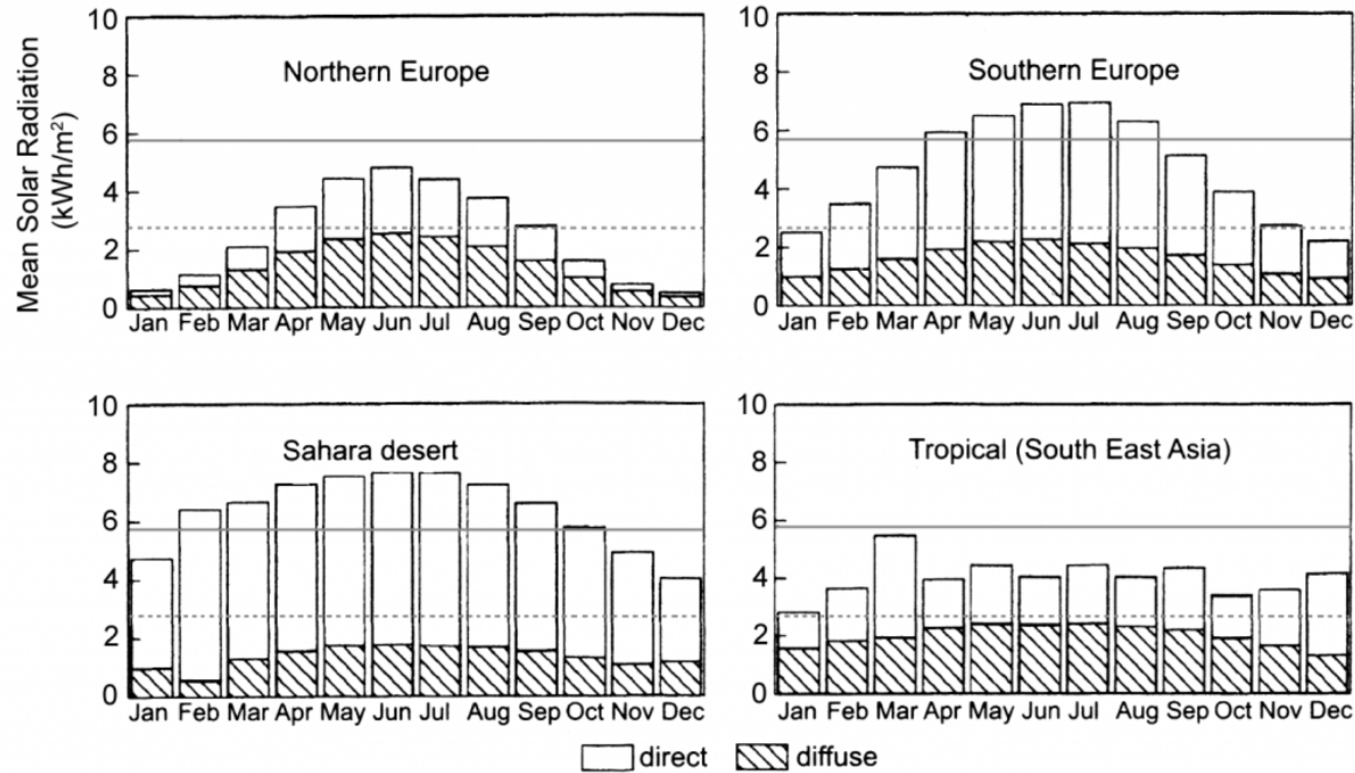
Figure 3: The solar spectrum above the atmosphere and at sea level

© Source unknown. This content is excluded from our Creative Commons license. For more information, see <https://ocw.mit.edu/fairuse>.

- Extra-terrestrial total irradiance (insolation: incident solar radiation) $\sim 1367 \text{ W/m}^2$
- Irradiance at Earth's surface is made of beam (direct) and diffuse components
- Total terrestrial irradiance depends on location (north, south, ..), hours/days of sun, cloud coverage, etc. When averaged over one day:
 - Clear $\sim 590 - 1000 \text{ W/m}^2$
 - Cloudy days $\sim 120 \text{ W/m}^2$
 - Average $\sim 300 \text{ W/m}^2$ (strong function of location)



In London, solar intensity, average over the year is $\sim 100 \text{ W/m}^2$ from MacKay



© ITACA. All rights reserved. This content is excluded from our Creative Commons license. For more information, see <https://ocw.mit.edu/fairuse>.

The yearly variation of the mean total daily solar radiation (total per day) for different locations, the dashed lines is at 2.88 kWh/m²day, and solid line is at 5.75 kWh/m²day, showing both direct and diffuse radiation. Location affects number of hours/day of sun, solar angle, weather conditions, ..

Intermittency is tricky! Role of storage, backup and multiple sources/technologies

How Much? On average
2.7 MWh/m²/y total incident radiation
~ 7 kWh/m²/day total
~ 0.3 kW/m² total

@ ~ 15% conversion efficiency,
~ 0.05 kW/m², therefore for a house
using ½ kW, you need ~ 10 m².

@ 20% (overall: field x cycle) efficiency
(CSP), generate 60 MW/km², for a
power plant)

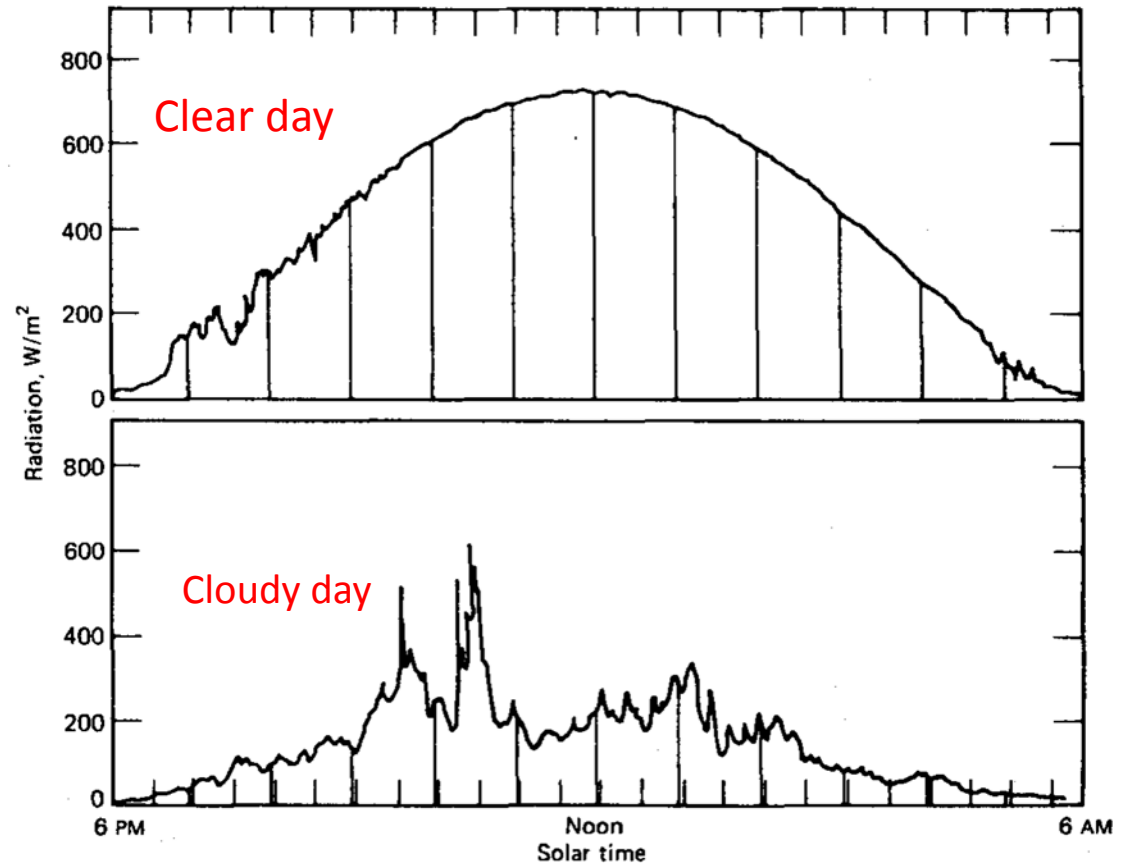


Figure 2.5.1 Total (beam and diffuse) solar radiation on a horizontal surface vs. time for clear and largely cloudy day, latitude 43°, for days near the equinox.

© Source unknown. All rights reserved. This content is excluded from our Creative Commons license. For more information, see <https://ocw.mit.edu/fairuse>.

Energy Balance of collectors and their fluid temperature

(1) Flat Collectors:

$$q = \beta I - \hat{h}(T_c - T_a)$$

q net flux collected by a fluid passing through the collector

I Irradiance $< 1 \text{ kW} / \text{m}^2$

β fraction absorbed, depends on orientation & transmissivity < 0.8

\hat{h} overall heat transfer coefficient

T_c collector T

T_a environment T

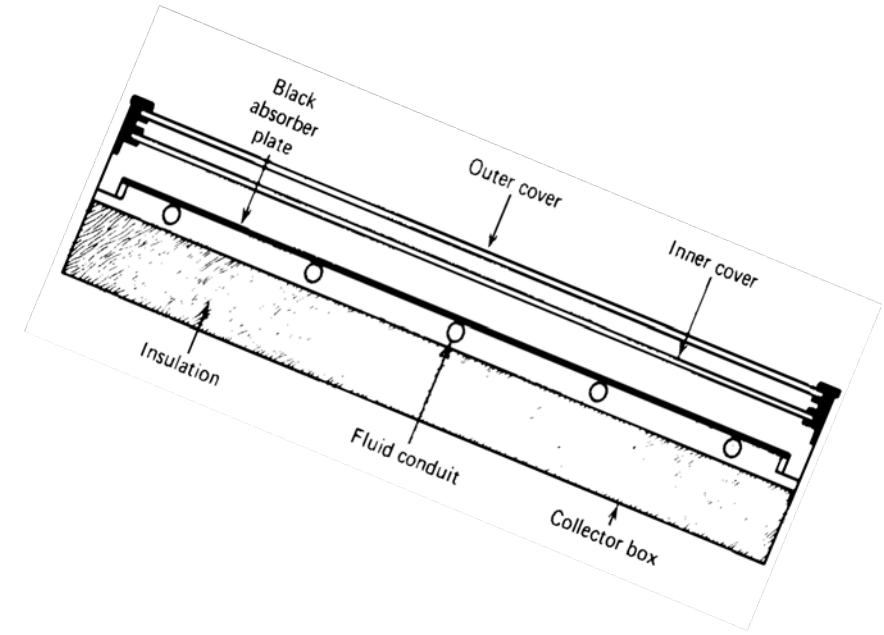
$$\text{at } q = 0 \quad (T_c)_{\max} = T_a + \frac{\beta I}{\hat{h}}$$

for high $(T_c)_{\max}$, \hat{h} must be very low (insulation $< 0.1 \text{ kW/m}^2\text{K}$)

Typical value $T_c \sim 80 \text{ C}$

$$\eta_{\text{col}} = \frac{q}{I} = \beta - \frac{\hat{h}(T_c - T_a)}{I} \leq \beta$$

goes down linearly with temperature! must limit heat loss



© Source unknown. All rights reserved. This content is excluded from our Creative Commons license. For more information, see <https://ocw.mit.edu/fairuse>.

Flat collectors:

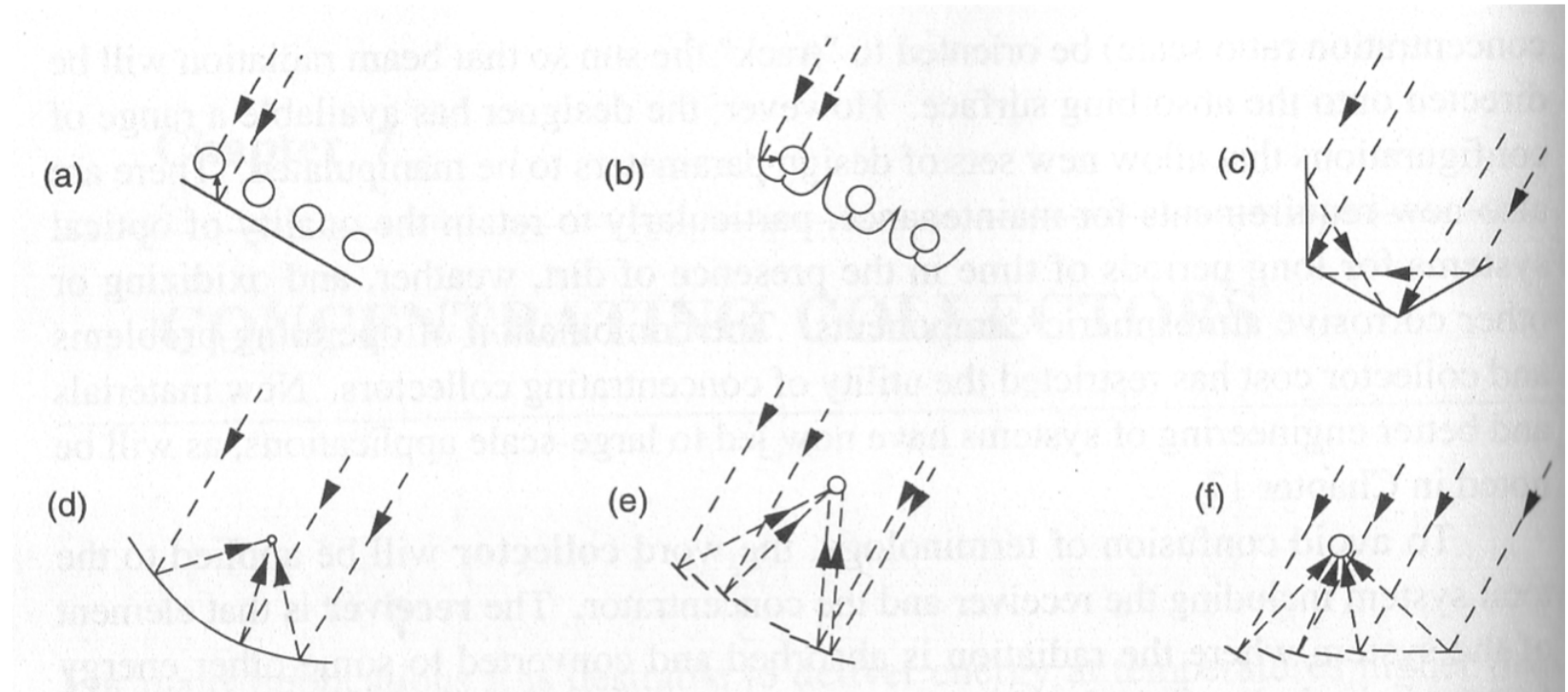
limit heat transfer fluid temperature.

Typical values of β , is 80%,

Collection efficiency at $T_c \sim 60 \text{ C}$, $\sim 50\%$.

Concentrating Collectors:

1. Trough
2. Tower
3. Cone



© Source unknown. All rights reserved. This content is excluded from our Creative Commons license. For more information, see <https://ocw.mit.edu/fairuse>.

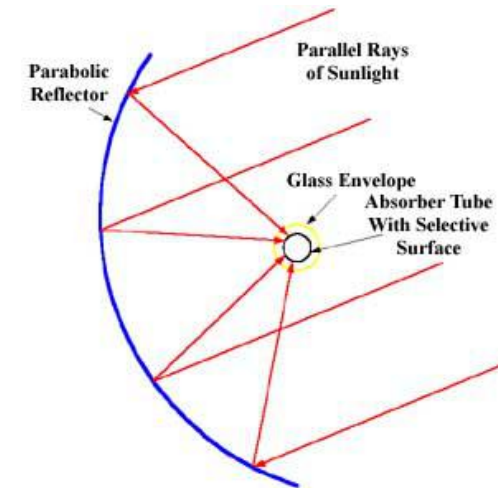
- (a) Flat collector, (b) with local curved mirrors, (c) concave, (d) parabolic,
(e) Fresnel reflector (f) Array of heliostats with central receiver
Goal: Increasing the flux of radiation on receivers

Focusing Collectors : **increases the collector temperature and collection efficiency:**

- Project the collected energy onto a small area (from Sun to mirror/reflector to collector) to increase T.
- Energy is collected from the *large area of the concentrator*, and lost from the *small area of the collector* only.
- Concentration Ratio C_R is the ratio between irradiance on the collector (at the focal point of the concentrator) and incident irradiance, I , is (also the area ratio):

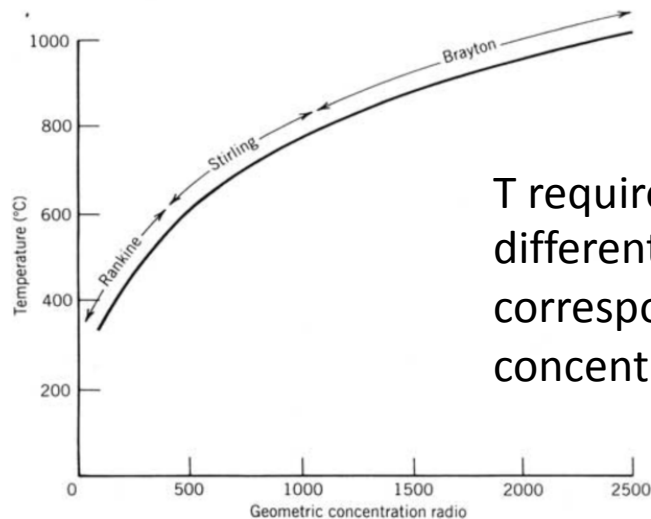
$$C_R = 107.5 \frac{D_m}{F} \text{ for cylindrical}$$
$$= 11560 \left(\frac{D_m}{F} \right)^2 \text{ for spherical}$$

D_m : mirror dimension, F : focal length



Concentrating Collectors

- Thermal energy at T higher than those possible with flat-plate collector; using a concentrator and a receiver.
- Increasing the concentration ratio: the ratio of collector area to absorber area, raises T at which energy is delivered.
- Spherical (3D) collectors deliver higher T than cylindrical (2) collectors.



T requirements for different engines and the corresponding concentration ratio

net absorbed flux: $qA_{col} = \beta A_{conc} I - \hat{h} A_{col} (T_c - T_a)$

define: $C_R = A_{conc} / A_{col}$

then: $q = \beta C_R I - \hat{h} (T_c - T_a)$

β depends on reflective and transmissive properties of glass cover and absorptive properties of collector surface $\sim 80\%$ (best)

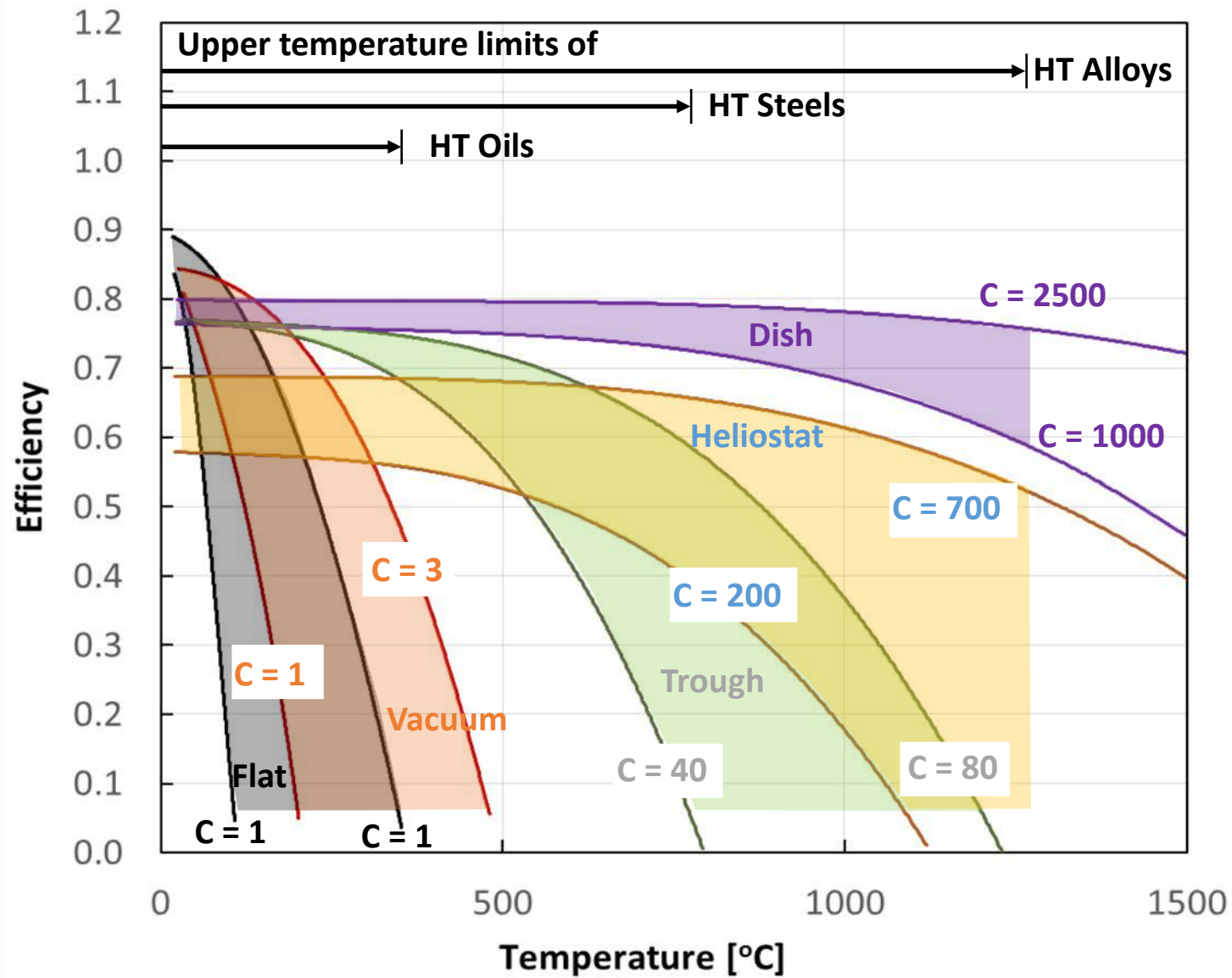
maximum collector/fluid temperature is when $q = 0$,

$$(T_c)_{\max} = T_a + \frac{\beta I C_R}{\hat{h}}$$

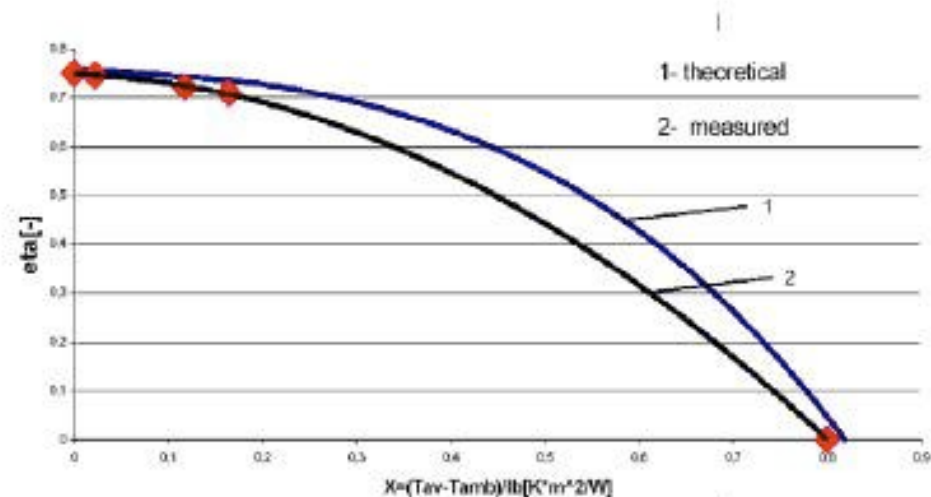
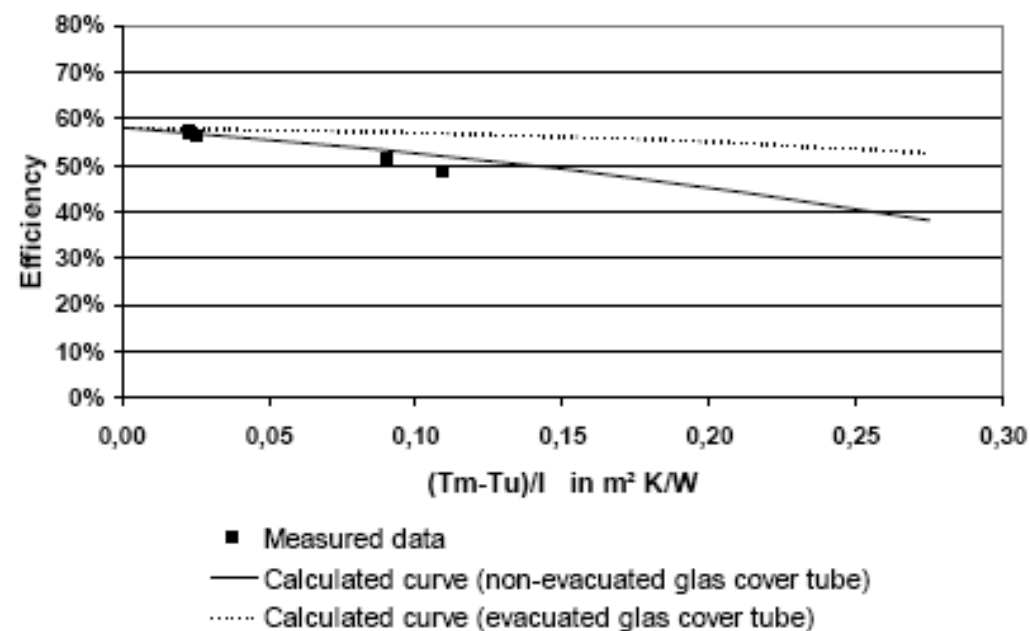
collector efficiency: $\eta_{col} = \frac{qA_{col}}{IA_{conc}} = \frac{q}{IC_R} = \beta - \frac{\hat{h}(T_c - T_a)}{IC_R}$

note how it increases with the concentration ratio

Solar field efficiency:



C: concentration ratio



$$\eta_0 = 0,75$$

$$a_{1a} = 0,1123 \text{ W}/(m^2 K)$$

$$a_{2a} = 0,00128 \text{ W}/(m^2 K^2)$$

$$\eta = \eta_0 - a_{1a} \cdot \frac{\Delta \bar{T}}{DNI} - a_{2a} \cdot \frac{\Delta \bar{T}^2}{DNI}$$

The power is about 1 kW. The efficiency curve is shown in figure 2. The collector has an efficiency of around 60% at a radiation of 800 W/m² and a temperature of 300°C.

Optimizing the Solar Field-Power Block System

Using oil as a heat transfer fluid.
Or direct steam generation in the collectors.

By X.G. Casala, Jan 2000, "Modeling and Optimizing the use of Parabolic Trough Technology with Rankine Cycles for Electricity Productions" Escala Tecnica Superior de Ingeniera, Madrid.

DSG: direct steam generation

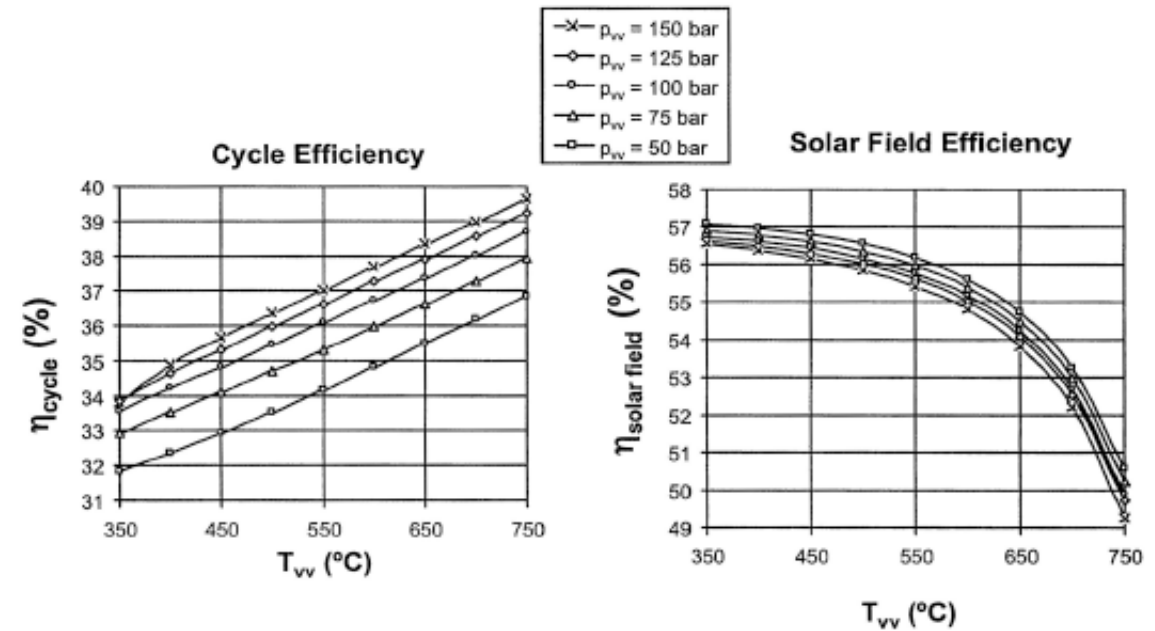


Fig.27: Effect of turbine inlet pressure on cycle and solar field efficiencies. Rankine water cooled.

$$\eta_{col} = \frac{q}{I} = \beta - \frac{\hat{h}(T_c - T_a)}{I C_R} \leq \beta$$

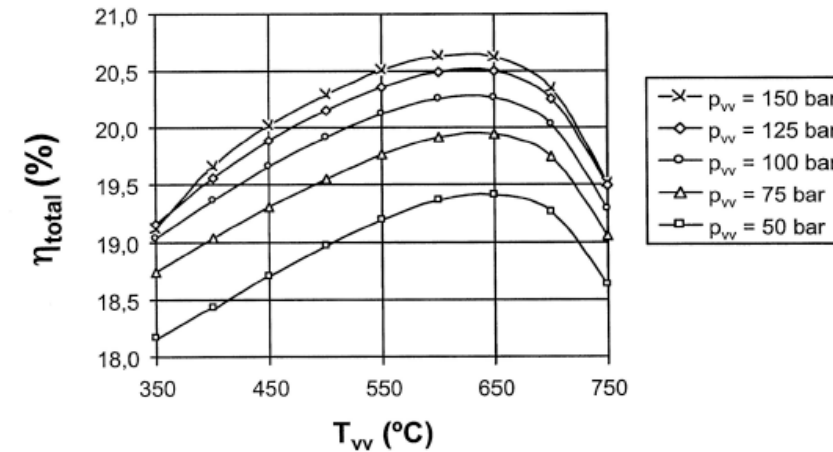
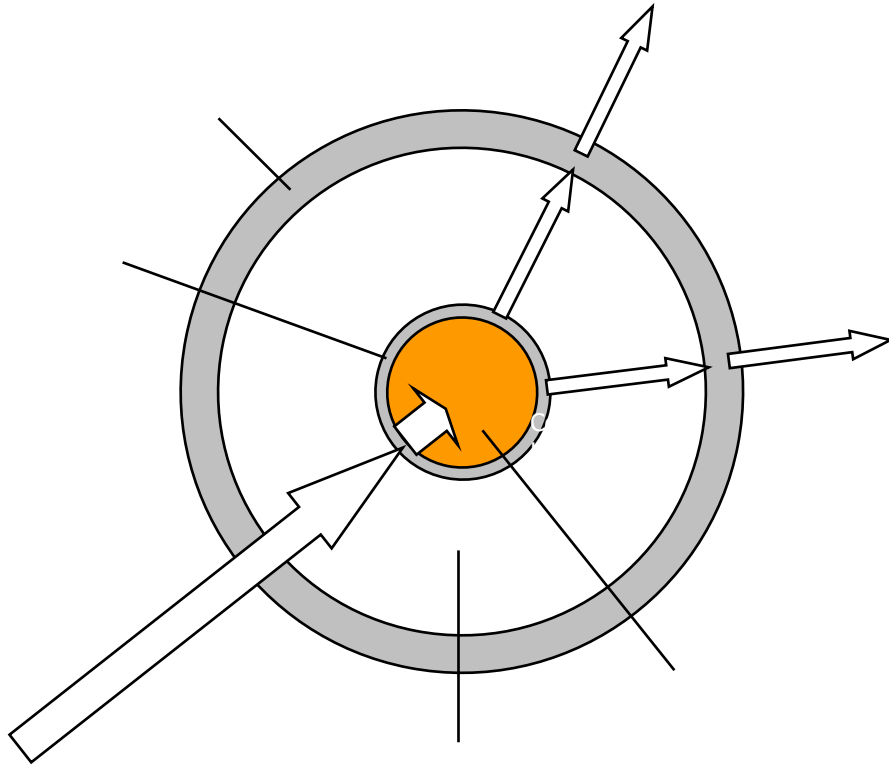


Fig.28: Total conversion efficiency as function of turbine inlet temperature and pressure. Rankine cycle water cooled.

Heat-Collection Element (HCE)

Space between absorber pipe and glass shield is evacuated

- Reduces convective losses



Glass shield has a spectrally selective coating

- Lets solar radiation in
- Blocks thermal radiation

Solar thermal Electric Power systems

Source: US DOE 2005

Characteristics of solar thermal electric power systems.

	Parabolic Trough	Power Tower	Dish/Engine
Size	30-320 MW*	10-200 MW*	5-25 kW*
Operating Temperature (°C/°F)	390/734	565/1,049	750/1,382
Annual Capacity Factor	23-50%*	20-77%*	25%
Peak Efficiency	20%(d)	23%(p)	29.4%(d)
Net Annual Efficiency	11(d')-16%*	7(d')-20%*	12-25%*(p)
Commercial Status	Commercially Available	Scale-up Demonstration	Prototype Demonstration
Technology Development Risk	Low	Medium	High
Storage Available	Limited	Yes	Battery
Hybrid Designs	Yes	Yes	Yes
Cost			
\$/m ²	630-275*	475-200*	3,100-320*
\$/W	4.0-2.7*	4.4-2.5*	12.6-1.3*
\$/W _p [†]	4.0-1.3*	2.4-0.9*	12.6-1.1*

* Values indicate changes over the 1997-2030 time frame.

† \$/W_p removes the effect of thermal storage (or hybridization for dish/engine).

(p)=predicted; (d) = demonstrated; (d') = has been demonstrated, out years are predicted values

Table courtesy of DOE.

Parabolic-Trough Technology

Parabolic Trough systems use parabolic trough-shaped mirrors to focus sunlight on thermally efficient receiver tubes that contain a heat transfer fluid (Figure 1). This fluid is heated to 390°C (734°F) and pumped through a series of heat exchangers to produce superheated steam which powers a conventional turbine generator to produce electricity. Nine trough systems, built in the mid to late 1980's, are currently generating 354 MW in Southern California. These systems, sized between 14 and 80 MW, are hybridized with up to 25% natural gas in order to provide dispatchable power when solar energy is not available.



Developed by Luz Int., and installed in Kramer Junction in 1991, company failed commercially in 92 (low NG prices), but plant is still in operation.

Image courtesy of DOE.

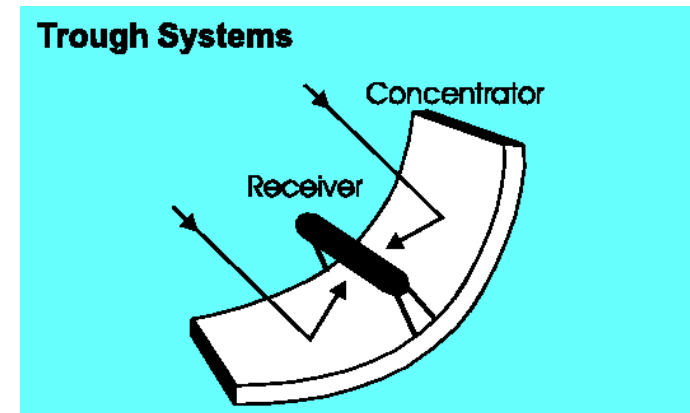


Image courtesy of DOE.

Solar Energy Generating System (SEGS)

- Nine SEGS Plants in the Mojave Desert (350MW)
- Parabolic-Trough Collectors, single axis tracking.
- Hybrid Design with Auxiliary Boiler
- Conversion Efficiency
 - 24% Peak
 - 8%-13% Annualized
- Levelized Cost of Electricity
 - 13 ¢/kWh (Hybrid)
 - 17 ¢/kWh (Solar Only)



Image courtesy of DOE.

Hybrid Combined Cycle SEGS Plant

- Would boost thermal efficiency to 54-58%
- Total annual average solar-to-electric efficiency at 10-14%.
- Plants use conventional equipment and are “hybridized” for dispatchability (25%)



Image courtesy of NREL.

- Total reflective area $> 2.3 \text{ M. m}^2$
- More than 117,000 Heat Collecting Elements
- 30 MW increment based on regulated power block size

Hybridized Parabolic-Trough System

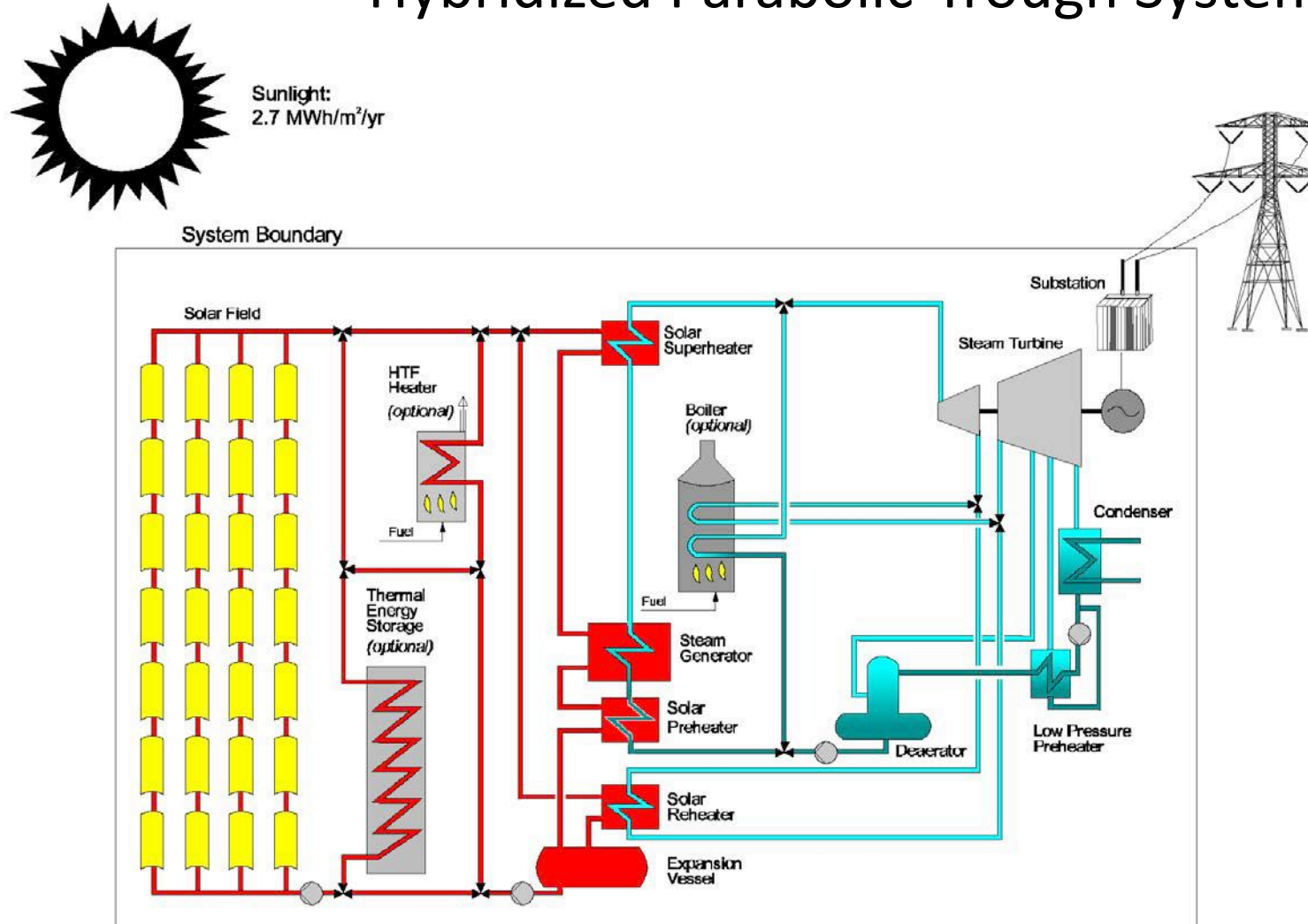


Figure 1. Solar/Rankine parabolic trough system schematic [1].

Image courtesy of DOE.

Critical to keep the reflectors clean

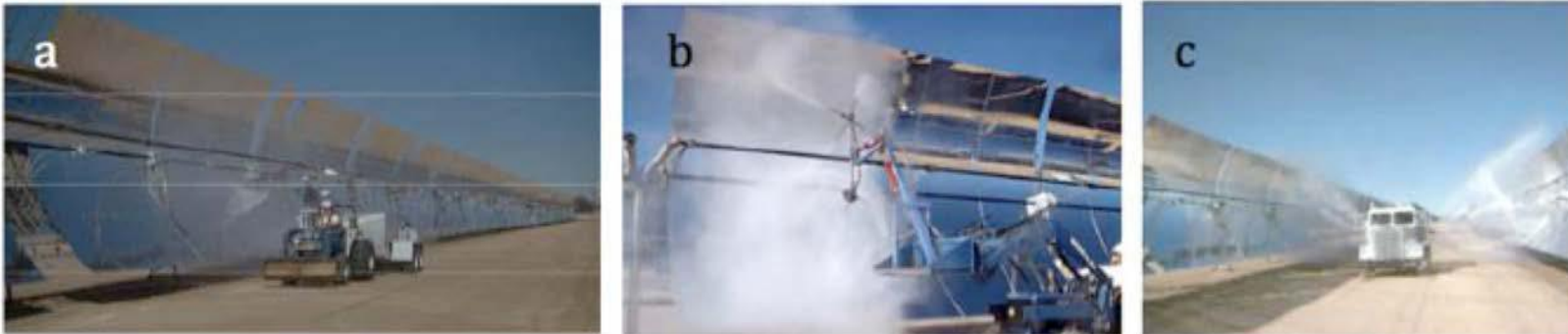
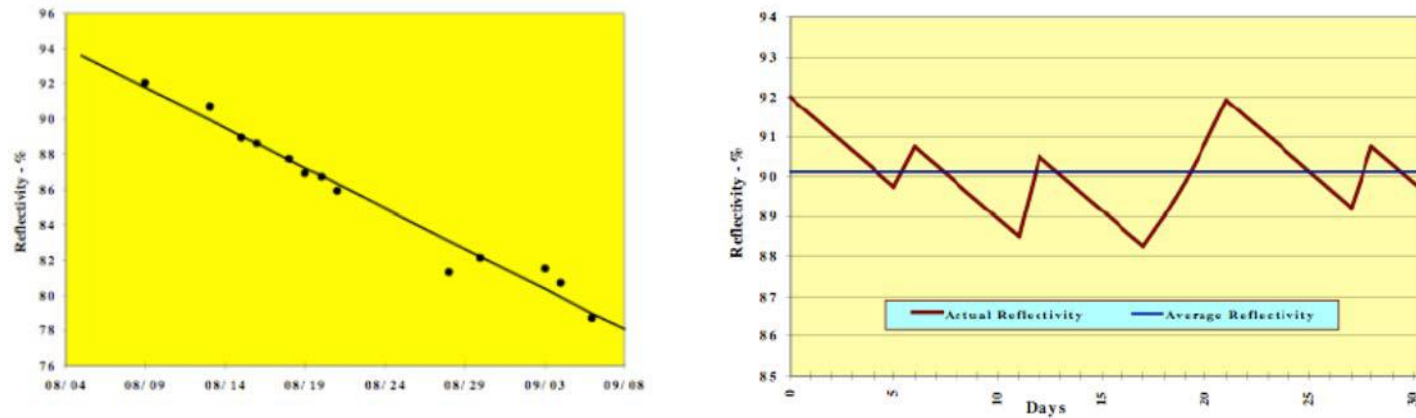


Figure 2: Water wash methods used in the solar-thermal industry [1]. (a) Traditional spray (b) High-pressure spray (c) Deluge-type cleaning

© Sandia Lab. All rights reserved. This content is excluded from our Creative Commons license. For more information, see <https://ocw.mit.edu/fairuse>.

[1] G.E. Cohen, D.W. Kearney, and G.J. Kolb, "Final Report on the Operation and Maintenance Improvement Program for Concentrating Solar Power Plants," Sandia Lab Report on CSP SAND99-1290.

Power Tower Technology



During daylight hours, 2000 mirrors at Solar Two track the sun and store its energy as heat in molten salt. This energy can then be used to generate electricity when needed, such as during periods of peak demand for power.

Image courtesy of DOE.

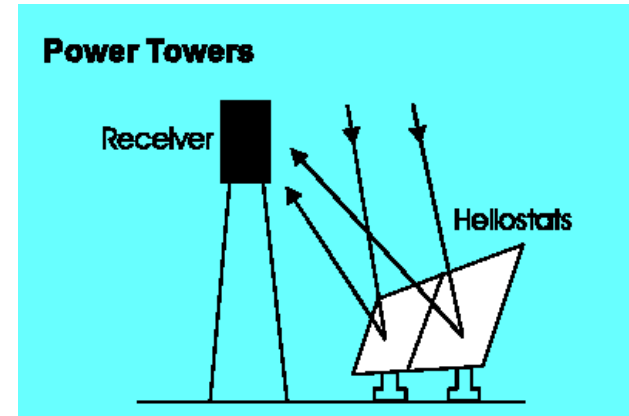


Image courtesy of DOE.

Power Tower systems use a circular field array of heliostats (large individually-tracking mirrors) to focus sunlight onto a central receiver mounted on top of a tower (Figure 2). The first power tower, Solar One, which was built in Southern California and operated in the mid-1980's, used a water/steam system to generate 10 MW of power. In 1992, a consortium of U.S. utilities banded together to retrofit Solar One to demonstrate a molten-salt receiver and thermal storage system.

The addition of this thermal storage capability makes power towers unique among solar technologies by promising dispatchable power at load factors of up to 65%. In this system, molten-salt is pumped from a “cold” tank at 288°C (550°F) and cycled through the receiver where it is heated to 565°C (1,049°F) and returned to a “hot” tank. The hot salt can then be used to generate electricity when needed. Current designs allow storage ranging from 3 to 13 hours.

“Solar Two” first generated power in April 1996, and is scheduled to run for a 3-year test, evaluation, and power production phase to prove the molten-salt technology. The successful completion of Solar Two should facilitate the early commercial deployment of power towers in the 30 to 200 MW range.

Dispatchable Power Requires Storage

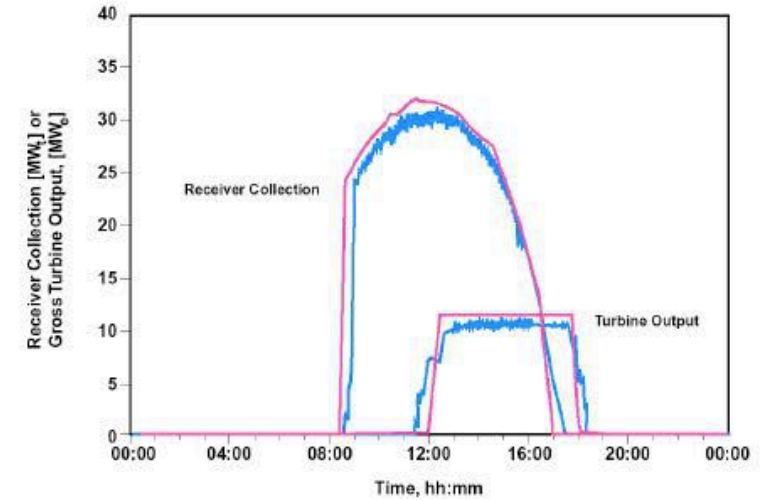
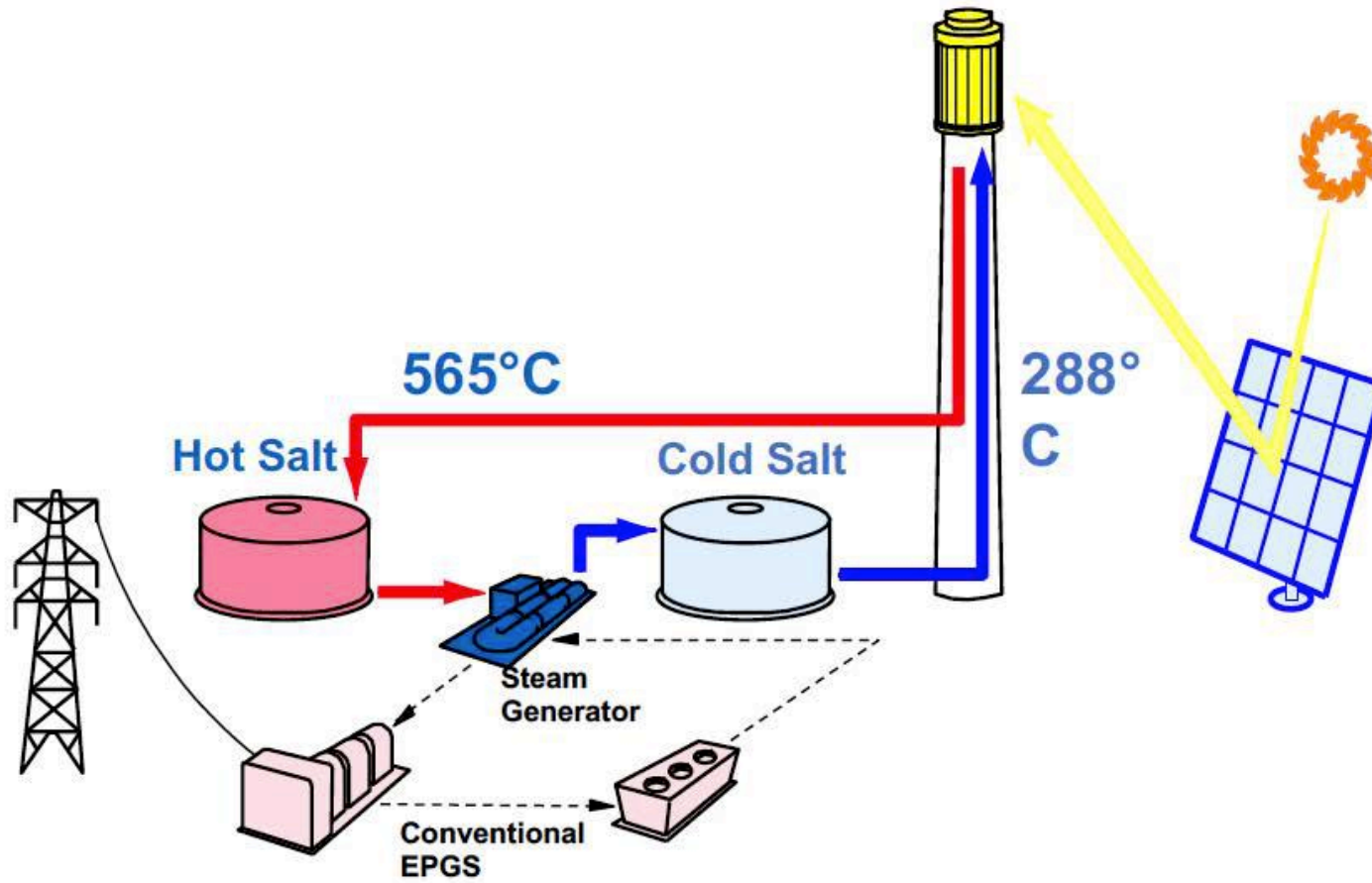


Image courtesy of DOE.

2009, Near Lancaster, CA

The eSolar Module

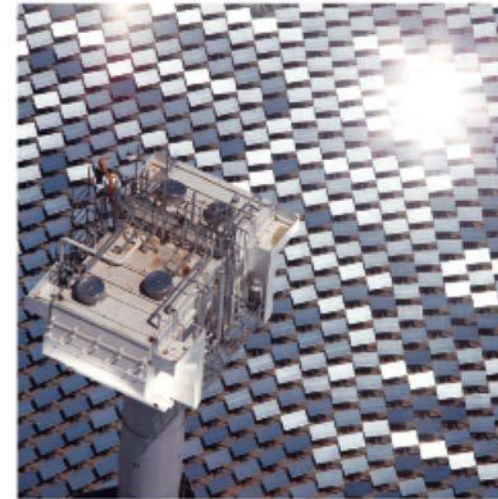
- 10 acres
- 1 tower
- 1 thermal receiver
- 12,000 mirrors reflecting the power of 10,000 suns
- 2.5 MW powering 2,000 households with clean, renewable energy

Sierra SunTower Quick Facts

- 2 modules
- 20 acres
- 2 towers
- 2 65-ton thermal receivers
- 1 refurbished 1947 GE steam turbine generator
- 24,000 mirrors reflecting the power of 20,000 suns
- 5 MW of clean, renewable energy supplied to 4,000 Southern California Edison households through a power purchase agreement
- Only operating solar thermal power tower plant in the US



eSolar is a responsible steward of our shared natural resources.



Solar Dish + Stirling Engine/Micro turbine

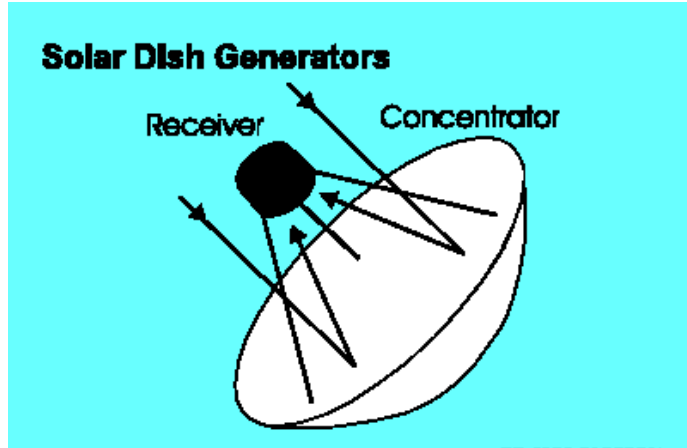
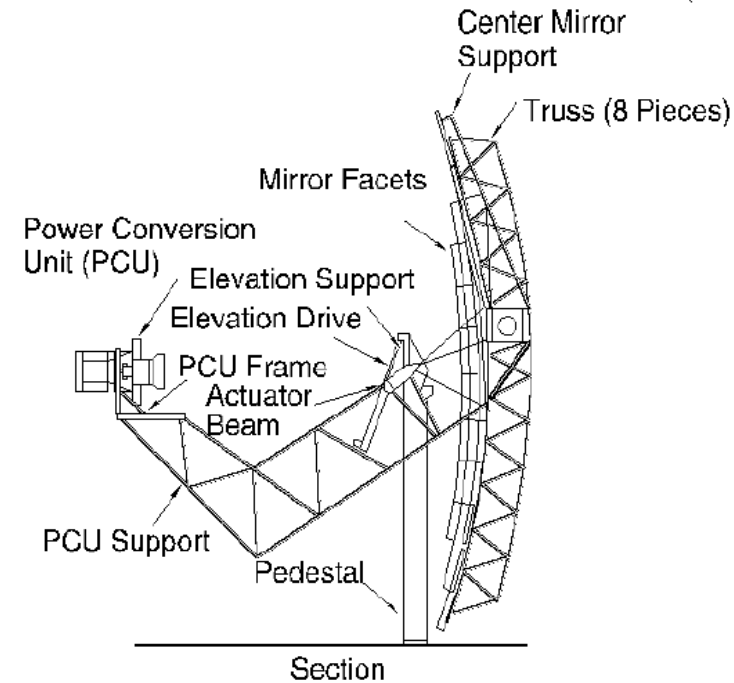


Image courtesy of DOE.

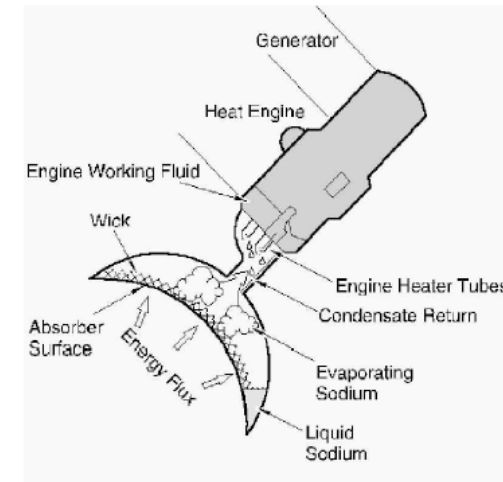


© Source unknown. All rights reserved. This content is excluded from our Creative Commons license. For more information, see <https://ocw.mit.edu/fairuse>.

A parabolic dish mirror concentrates the energy onto the engine hot side. $T \sim 750\text{ C}$ is achievable. Stirling engines or micro gas turbine could be used with 10-25 kW. Overall efficiency close to 30%

CSP Dish/Converter Systems

- ♦ *Technology Features:*
 - *High efficiency (Peak > 30% net solar-to-electric)*
 - *Modularity (10, 25kW)*
 - *Autonomous operation*
 - *Hybrid capabilities (no storage)*
 - *Stirling and, in future, Brayton engines and CPV*



DESERTEC

A vision of a future electricity supply system in Europe

SIEMENS



2009-09-17

© Siemens AG 2009

The solar potential in the MENA Region

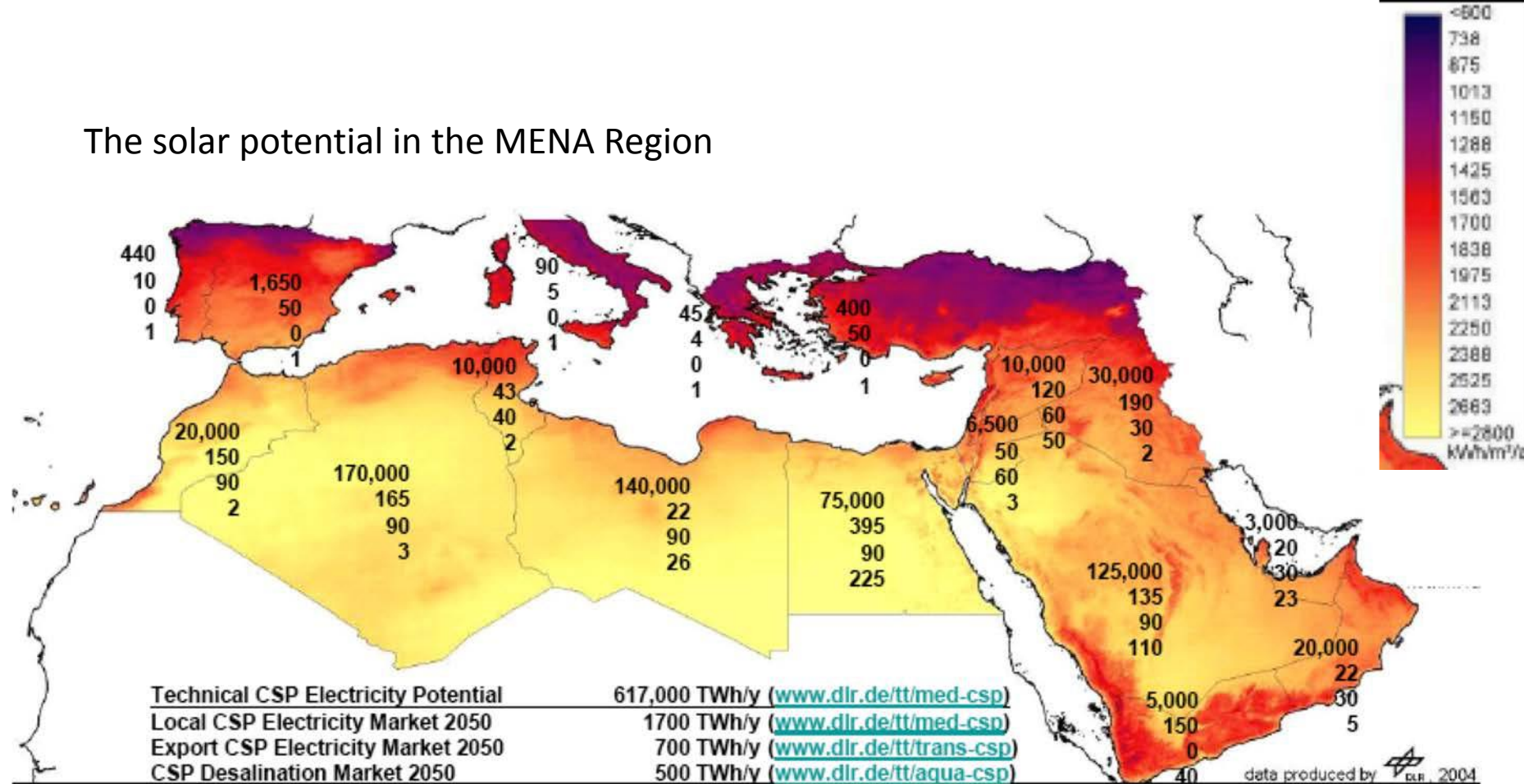


Figure 4-1: Concentrating Solar Power Potentials until 2050 in TWh/y. Techno-economic supply-side potential (top), potential for local electricity (second from top), potential for electricity export from MENA to Europe (third from top) and potential for seawater desalination (bottom). For better comparison, desalination potentials have been converted to electricity required by reverse osmosis. Background: Fig. 1-13.

AQUA-CSP: Concentrating solar power for seawater desalination
 German Aerospace Center (DLR) <http://www.dlr.de/tt/aqua-csp>

Operating Hybrid Combined Cycle Solar Plant

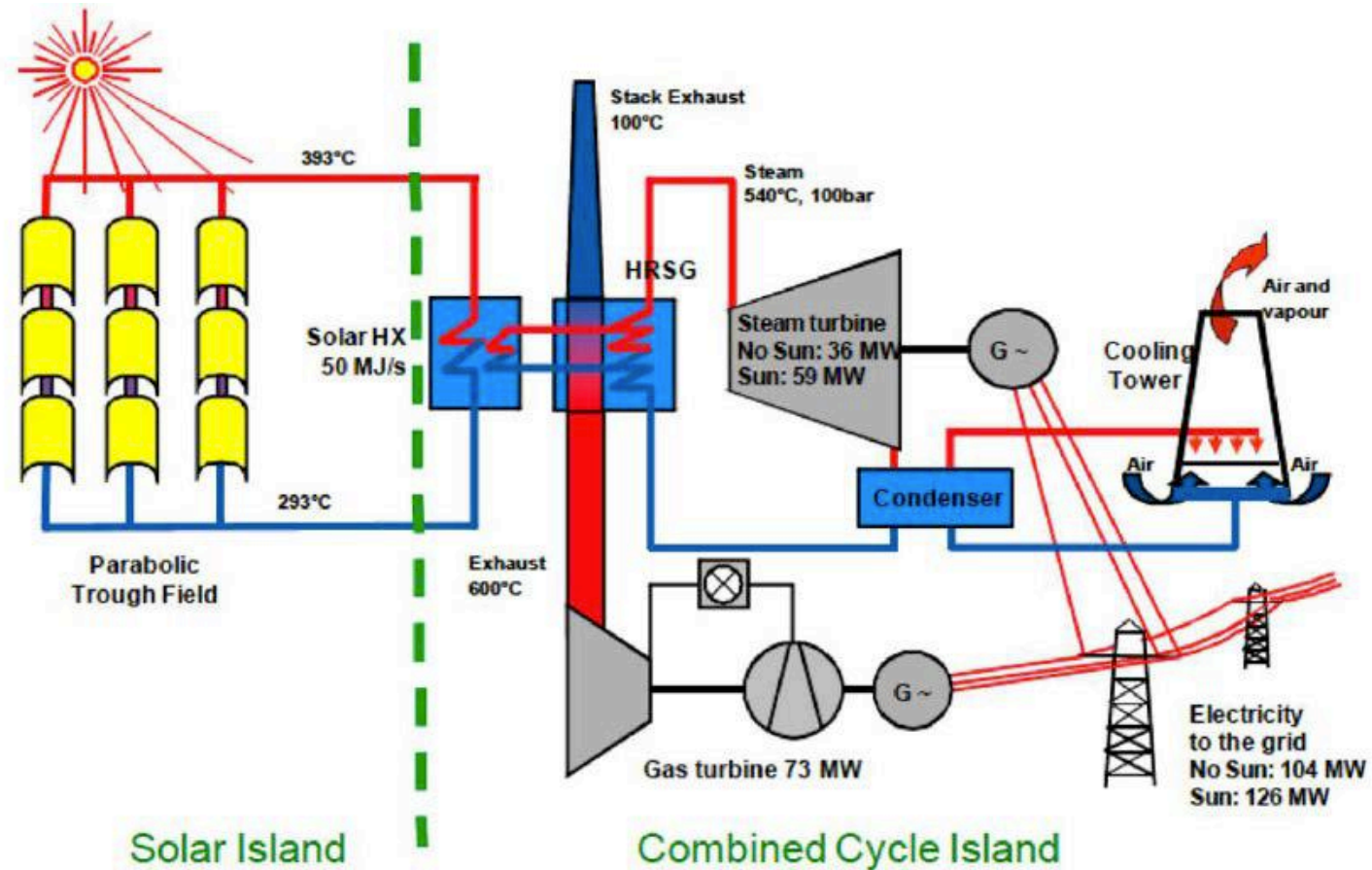


Figure 3-1 Scope Split and General Concept of the ISCC Kuraymat

© DCSP. All rights reserved. This content is excluded from our Creative Commons license. For more information, see <https://ocw.mit.edu/fairuse>.

Table 1 shows the technical key data for the ISCC Kuraymat according to the EPC contract and the latest construction design. The design thermal power of the Solar Island will be reached for DNI values between 700 and 800 Watt/m² depending on incident angle and status of the solar field (Number of loops in operation, tracking accuracy, mirror reflectivity etc.).

Key Technical Data	Unit	Value
Solar Field total Aperture Area	m ²	130800
Number of Collectors	N°	160
Number of Collector Loops	N°	40
Design Irradiation	W/m ²	700
Solar Field Design Thermal Power at Reference Conditions	MJ/s	50
Hot Leg HTF Temperature	°C	393
Cold Leg HTF Temperature	°C	293
Gas Turbine Generator Rated Power Output	MWe	74,4
Steam Turbine Generator Rated Power Output	MWe	59,5

Table 1 Key Technical Data

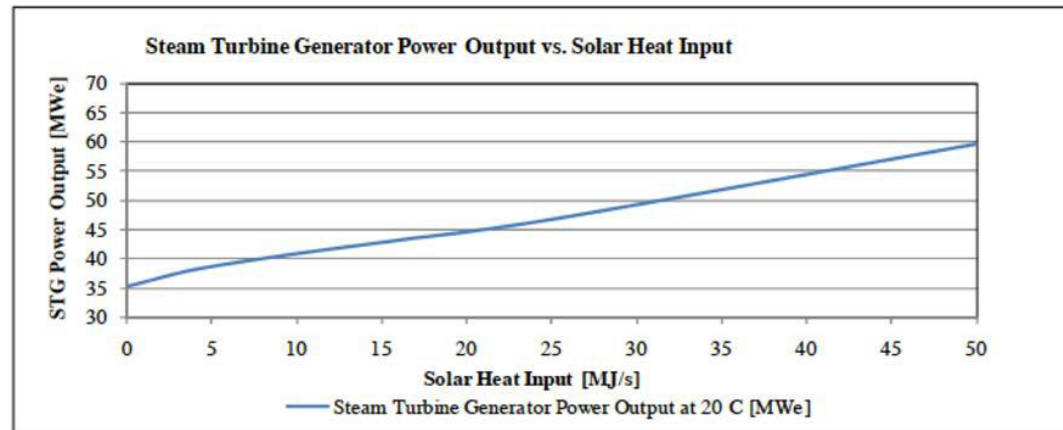


Figure 5-1 Steam Turbine Generator Output vs. Solar Heat Input¹

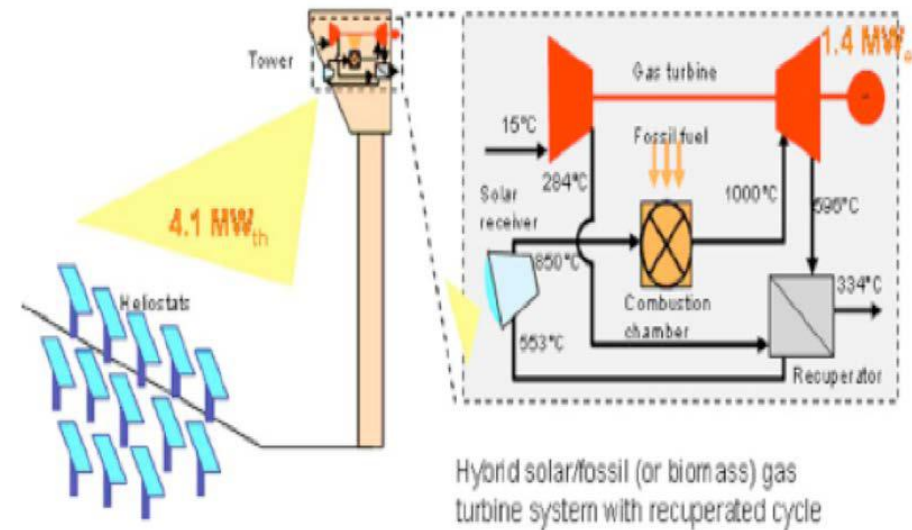
Table and figure © SolarPACES. All rights reserved. This content is excluded from our Creative Commons license. For more information, see <https://ocw.mit.edu/fairuse>.



Israel

AORA solar gas turbine hybrid system
 100 kW electricity
 170 kW heat

No longer operating, problems with
 the concentrator and heliostat



© Source unknown. All rights reserved. This content is excluded from our Creative Commons license. For more information, see <https://ocw.mit.edu/fairuse>.



© Source unknown. All rights reserved. This content is excluded from our Creative Commons license. For more information, see <https://ocw.mit.edu/fairuse>.

Located in the Western Region of Abu Dhabi, the 100-megawatt, grid connected power plant generates clean energy to power 20,000 homes in the UAE **(2012)**.

Shams 1 was designed and developed by Shams Power Company, a joint venture between Masdar (60 percent), Total (20 percent) and Abengoa Solar (20 percent).

Covering an area of 2.5 km² – or 285 football fields – Shams 1 incorporates the latest in parabolic trough technology and features more than 258,000 mirrors mounted on 768 tracking parabolic trough collectors.

The CSP project reduces the UAE's carbon emissions, displacing approximately 175,000 tonnes of CO₂ per year, an equivalent to planting 1.5 million trees, or taking 15,000 cars off the road.

Solar Chimney

the Hydroelectric Power for the desert”



Courtesy Elsevier, Inc., <http://www.sciencedirect.com>. Used with permission.

Operated in Spain, 1982-89
From Encyclopedia of Physical Science and Technology, 2000
Article by J Schlaich and W Schiel

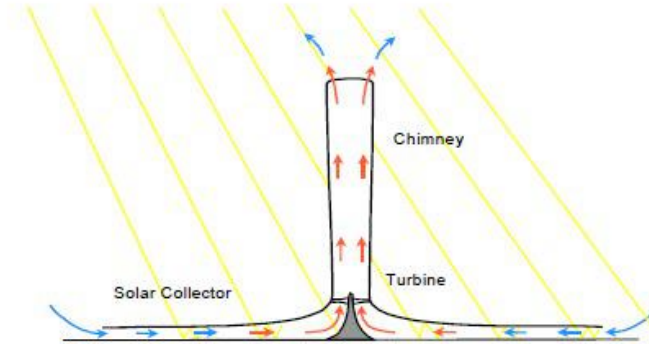


Fig. 1. Principle of the solar chimney: glass roof collector, chimney tube, wind turbines.

$$V_{ch} = \sqrt{\frac{\Delta T}{T}} 2gH_{ch}$$

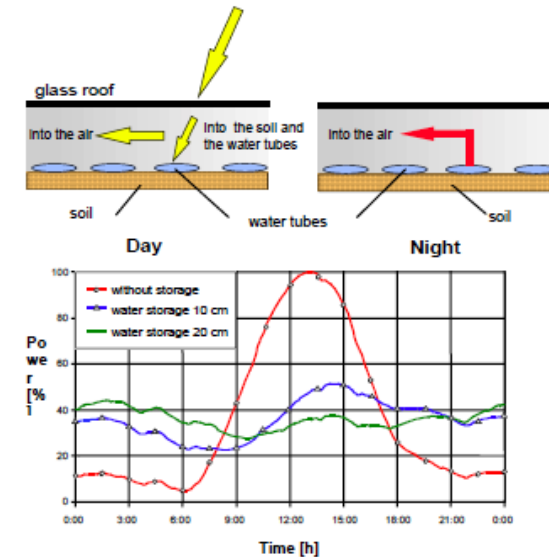


Fig. 2. Principle of heat storage underneath the roof using water-filled black tubes.

Figures 1 and 2 © Source unknown. All rights reserved. This content is excluded from our Creative Commons license. For more information, see <https://ocw.mit.edu/fairuse>.

The principle dimensions and technical data for the facility are:

Chimney height: $HT = 194.6$ m

Chimney radius: $RT = 5.08$ m

Mean collector radius: $RC = 122.0$ m

Mean roof height: $HC = 1.85$ m

Number of turbine blades: 4

Blade: length 5 m, profile FX W-151-A tip-
to-wind speed ratio: 1 : 10

Transmission ratio: 1 : 10

Operation: stand-alone or grid connection
mode

Heating in collector: $\Delta T = 20^\circ \text{C}$

Nominal output: 50 kW

Roof covered with plastic: 40,000 m²

Roof covered with glass: 6000 m²

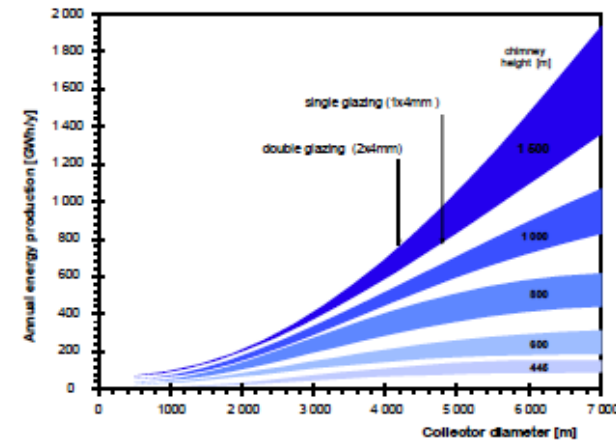


Fig. 3. Annual energy production by a Solar Chimney (at 2300kwh/m²/a global insolation) dependent on collector diameter and chimney height.

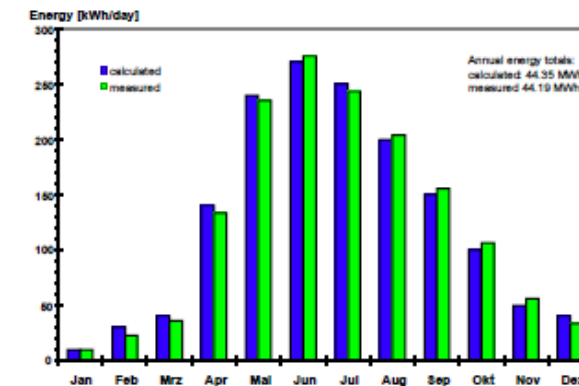
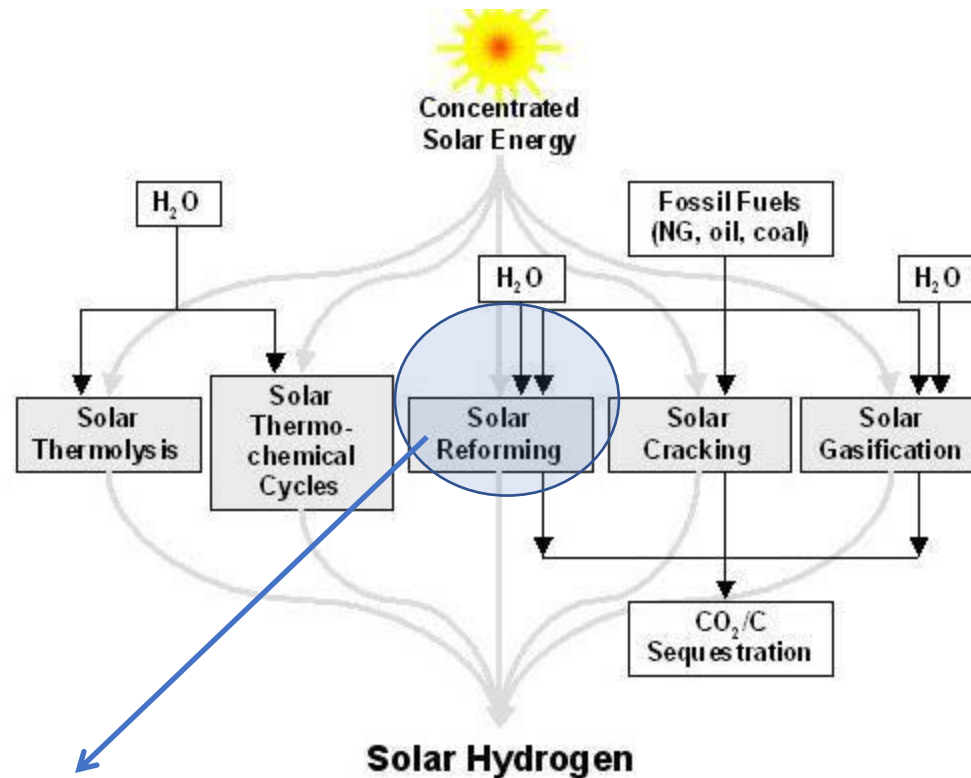


Fig. 9. Comparison of measured and calculated monthly energy outputs for the Manzanares plant.

Figures 3 and 9 © Source unknown. All rights reserved. This content is excluded from our Creative Commons license. For more information, see <https://ocw.mit.edu/fairuse>.

Many trends in Solar Chemical Hybrid Systems

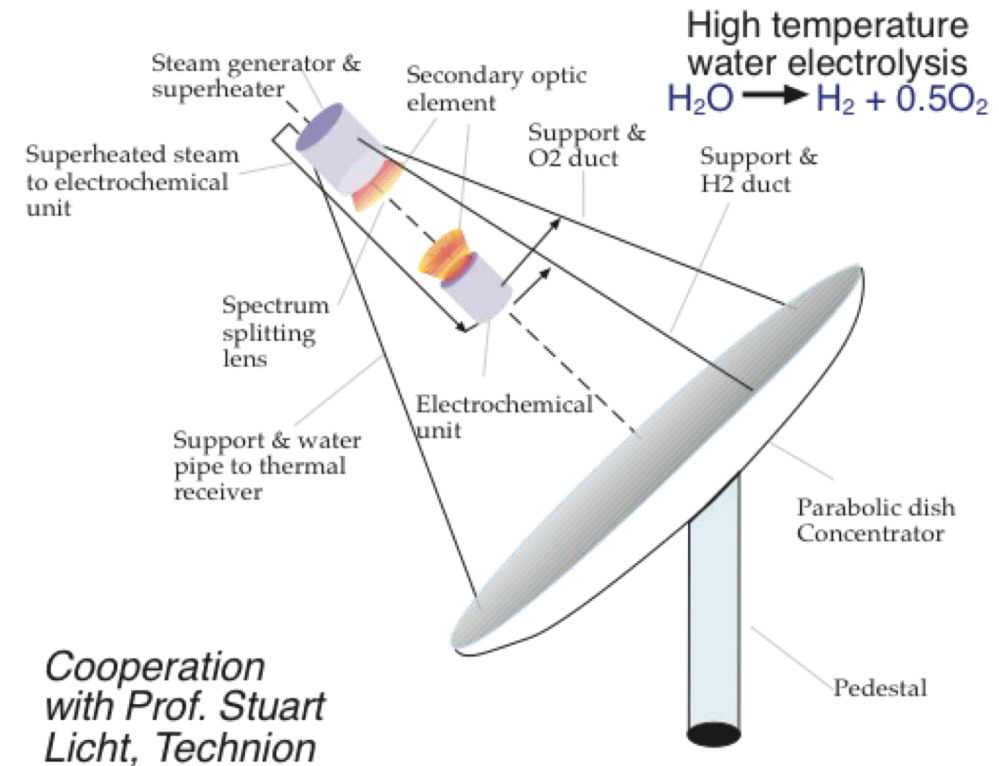
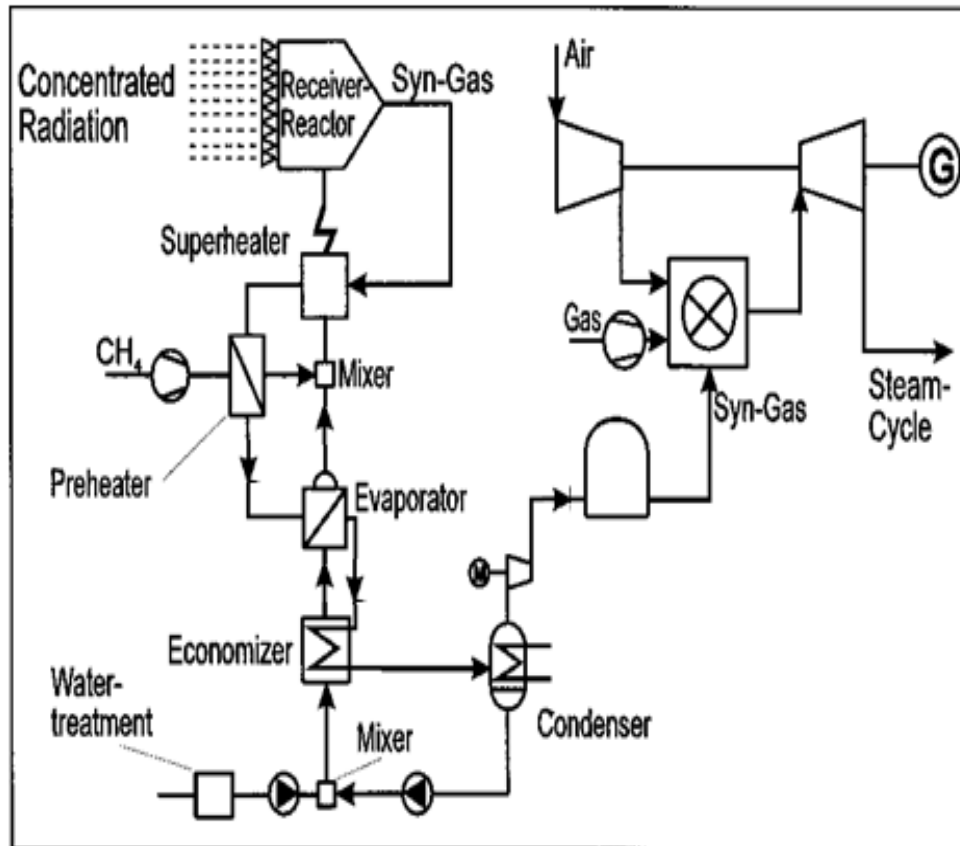
Water splitting using solar heat, or steam reforming, cracking or gasification of fuels (gas, liquid and solids).



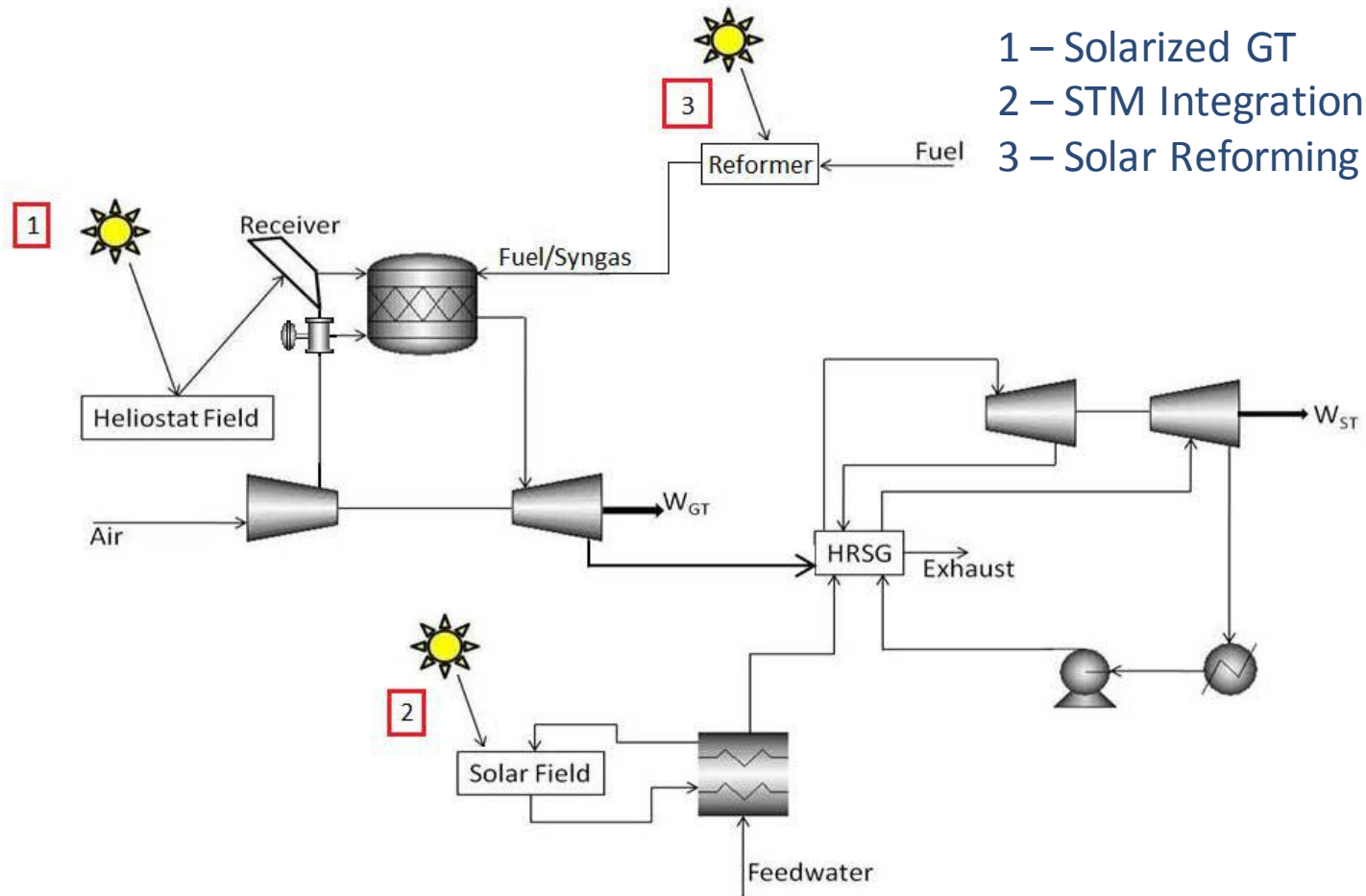
“Solar fuels” is a very active research area in many leading institutions and the subject on newly awarded large centers in the US>

Potential: Low temperature solar thermal chemical process

H₂ or Syngas Production Using Solar Energy



Three Hybridization Schemes



Courtesy Elsevier, Inc., <http://www.sciencedirect.com>. Used with permission.

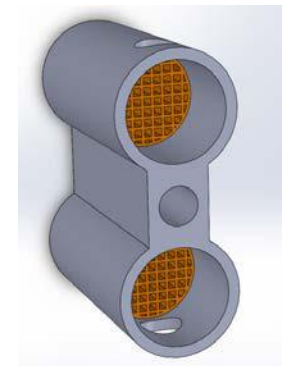
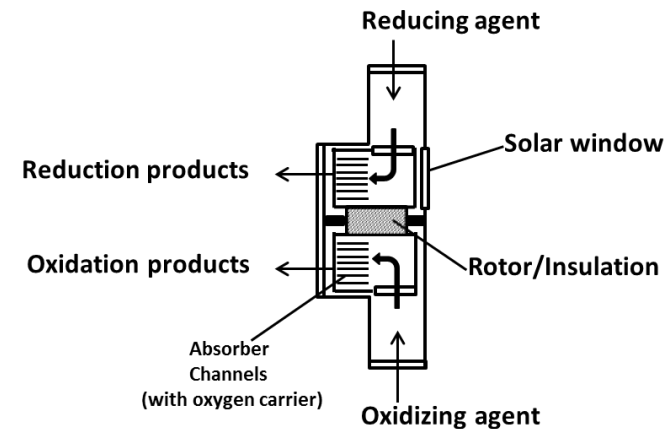
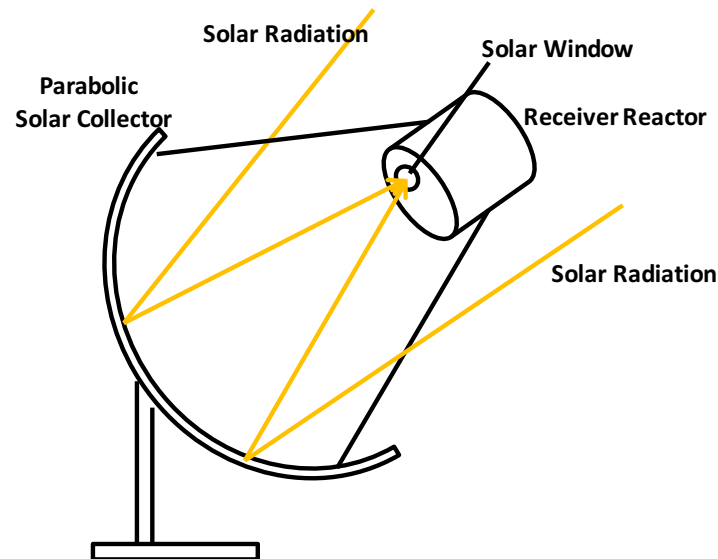
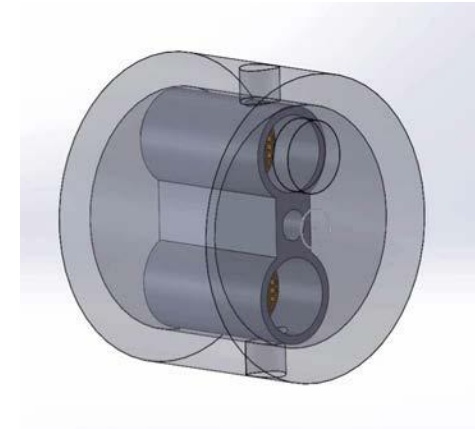
J. Sheu and A. F. Ghoniem. *International Journal of Hydrogen Energy*, 39(27): 14817-14833, 2014

E. J. Sheu, E. M. A. Mokheimer, and A. F. Ghoniem, *Journal of Hydrogen Energy*, 40(7): 2939-2949, 2015

Solar Fuels?

Metal	Reduction/oxidation reactions
Copper	$\text{CuO} + \text{CH}_4 \rightarrow \text{Cu} + \text{CO} + 2\text{H}_2 \quad \Delta H^\circ = 120.40 \text{ kJ/mol}$ $\text{Cu} + \text{H}_2\text{O}(v) \rightarrow \text{CuO} + \text{H}_2 \quad \Delta H^\circ = 85.77 \text{ kJ/mol}$
Nickel	$\text{NiO} + \text{CH}_4 \rightarrow \text{Ni} + \text{CO} + 2\text{H}_2 \quad \Delta H^\circ = 204.03 \text{ kJ/mol}$ $\text{Ni} + \text{H}_2\text{O}(v) \rightarrow \text{NiO} + \text{H}_2 \quad \Delta H^\circ = 2.125 \text{ kJ/mol}$
Iron	$\frac{1}{4}\text{Fe}_3\text{O}_4 + \text{CH}_4 \rightarrow \frac{3}{4}\text{Fe} + \text{CO} + 2\text{H}_2 \quad \Delta H^\circ = 243.93 \text{ kJ/mol}$ $\frac{3}{4}\text{Fe} + \text{H}_2\text{O}(v) \rightarrow \frac{1}{4}\text{Fe}_3\text{O}_4 + \text{H}_2 \quad \Delta H^\circ = -37.77 \text{ kJ/mol}$

Novel, looping based reformer



Courtesy Elsevier, Inc., <http://www.sciencedirect.com>. Used with permission.

MIT OpenCourseWare
<https://ocw.mit.edu/>

2.60J Fundamentals of Advanced Energy Conversion
Spring 2020

For information about citing these materials or our Terms of Use, visit: <https://ocw.mit.edu/terms>.

Lecture# 18

Geothermal Energy

Ahmed F. Ghoniem
April 8, 2020

Material in this lecture is based on Prof J Tester's (previously at MIT and currently at Cornell) lecture on the same subject.

Geothermal energy resources

- Hydrothermal: liquid and superheated water
- Hydrothermal: Vapor and dry steam
- Geopressure: methane, hydraulic and thermal energy
- Magma: Hot dry rock or Enhance Geothermal Systems

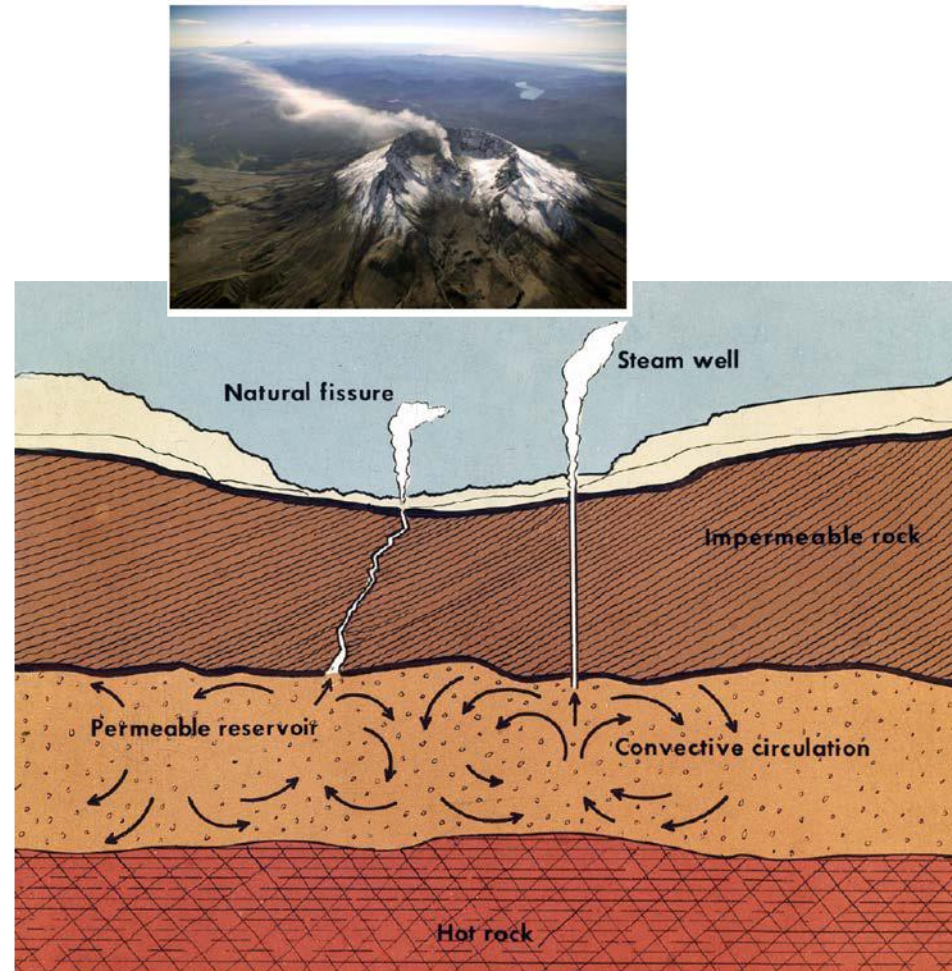
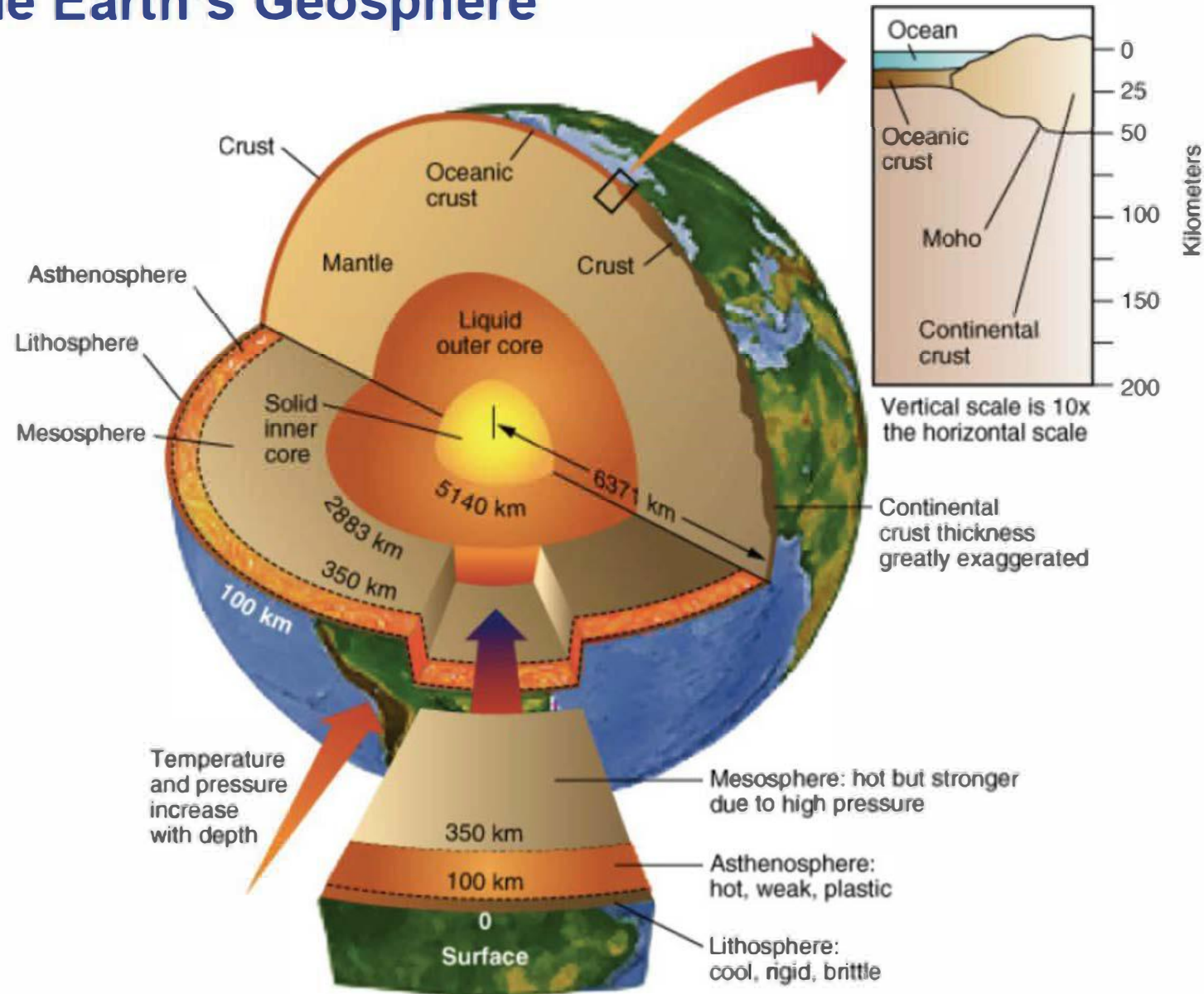


Image courtesy of Idaho National Laboratory.

Looking to “inner space” for opportunities in the Earth’s Geosphere



Copyright 1999 John Wiley and Sons, Inc. All rights reserved.

Geothermal energy:

- Renewable, non depleteable on a short time scale (renewal time \sim 2-3 time depletion time)
- Reasonably well distributed: available everywhere at 6 km depth, and at shallower depths (3-6 km) in “high-grade” regions
- Provides low grade heat, 100-200 C.
- Scalable: 5-50 MW modules
- Dispatchable: high capacity factor (90%) suitable for base load, no need for storage
- Clean energy, low emission, low footprint
- Uses of-the-shelf power plant equipment
- Cost competitive especially for high grade hydrothermal systems
- BUT EGS require deep drilling

Classification of geothermal resources and reserves

Note that 40 C/km
is high quality
geothermal energy!

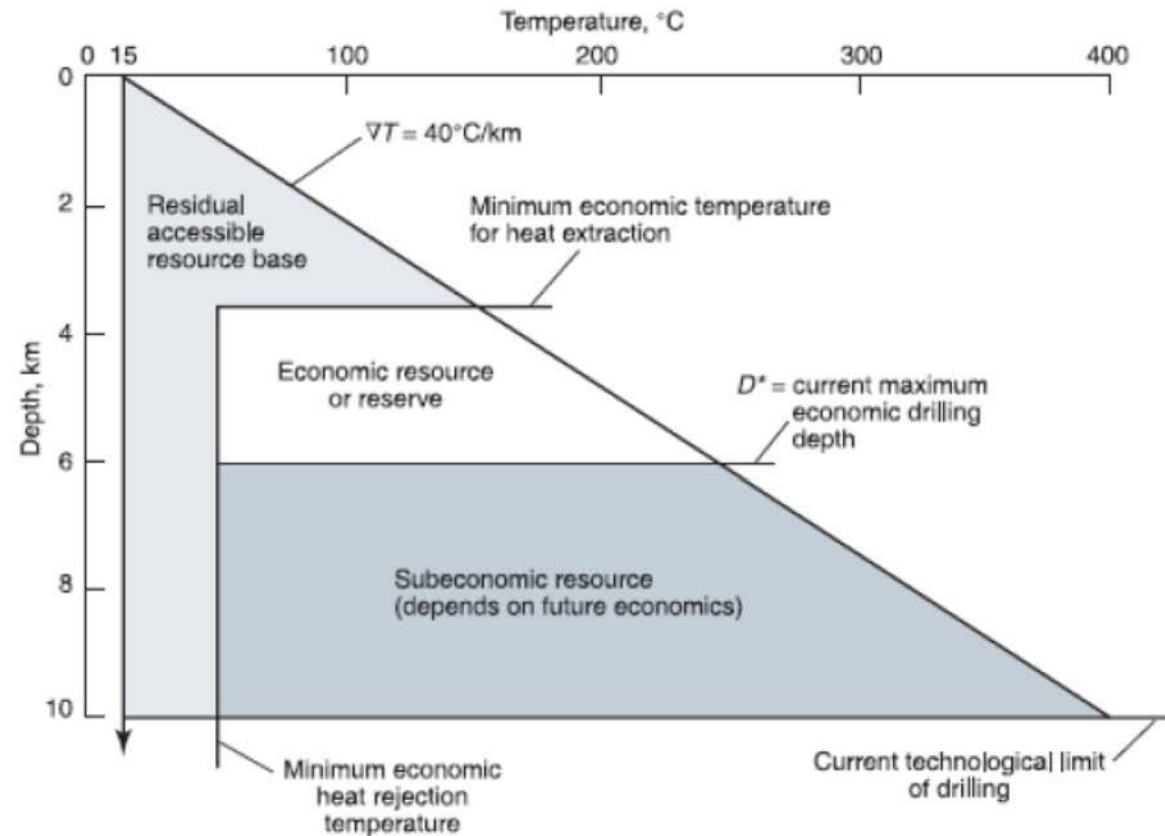
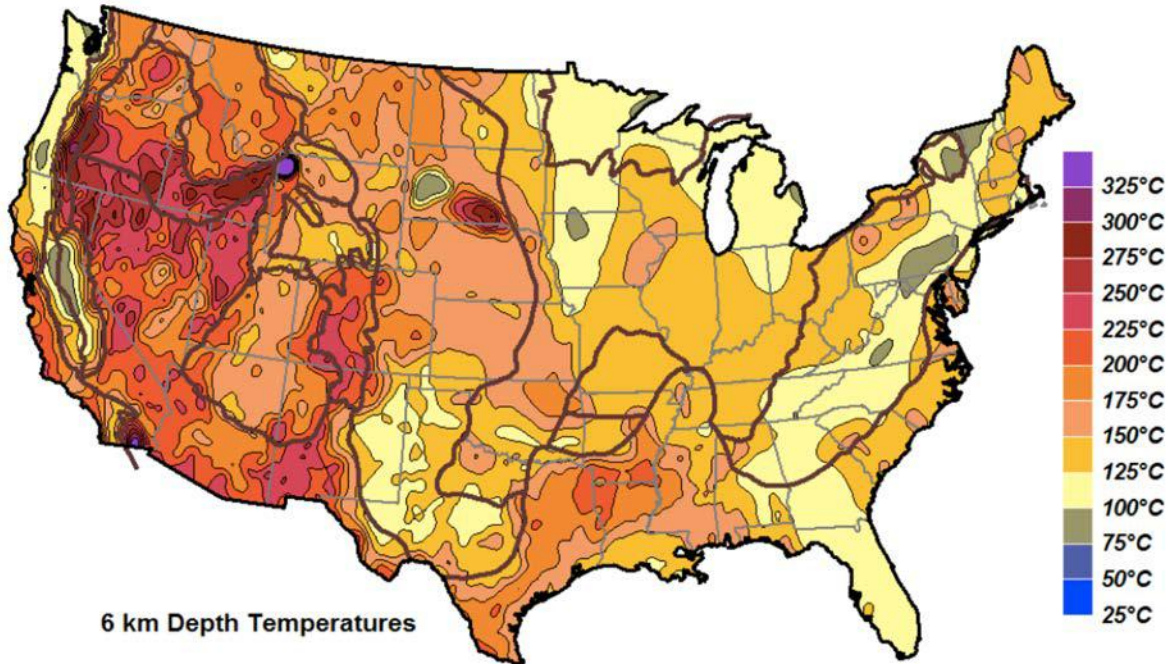
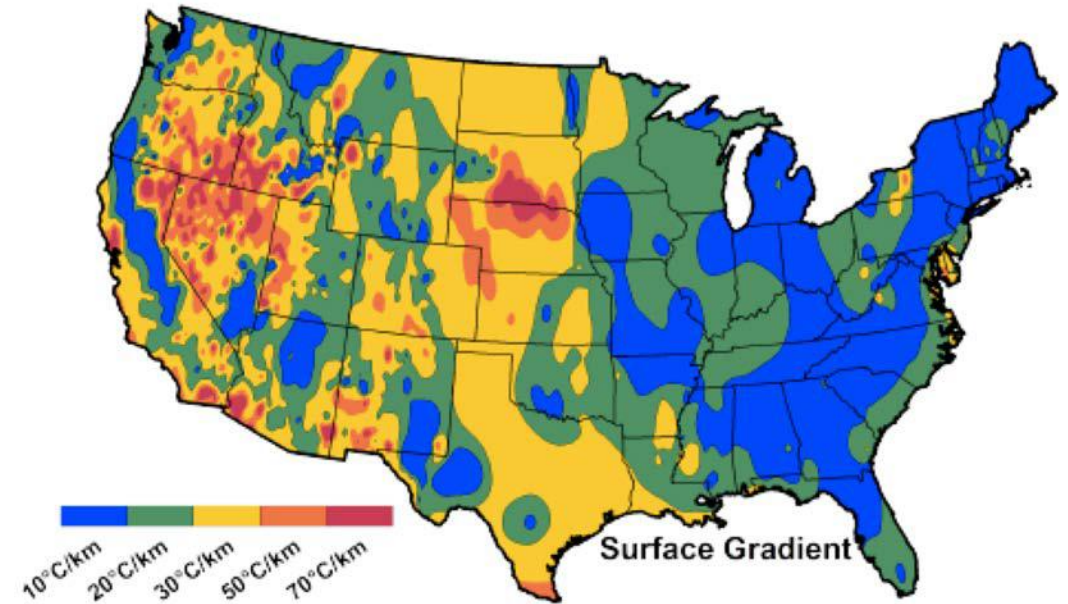


Figure 11.4. Idealized depth versus temperature profile for a hypothetical 40°C/km geothermal resource. The resource base and economic resource or reserve regions are shaded in different tones to illustrate the factors limiting the portion of the total resource base that can be economically produced with a specified set of technologies and economic factors. Adapted from Tester and Grigsby (1980). Reprinted with permission of John Wiley & Sons.

The temperature gradient is the most critical factor!



From Blackwell and Richards (June, 2007)

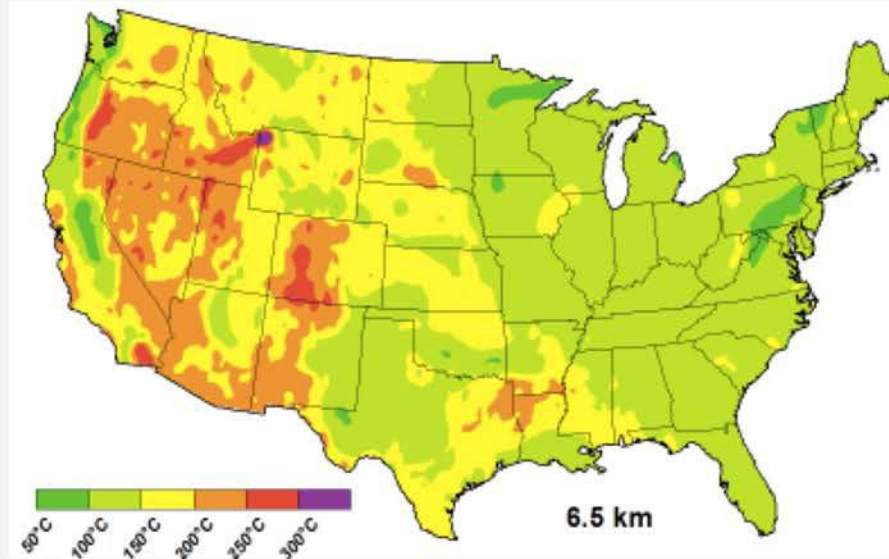
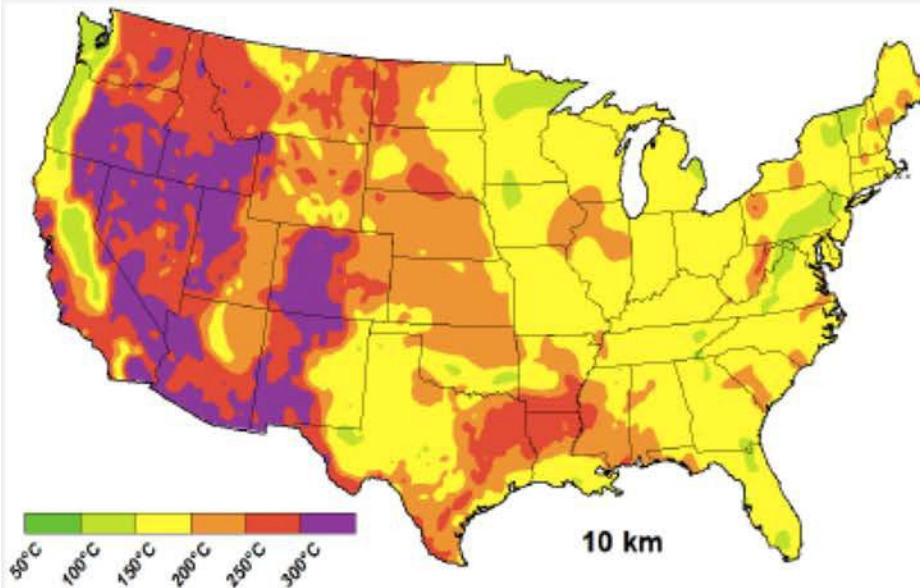
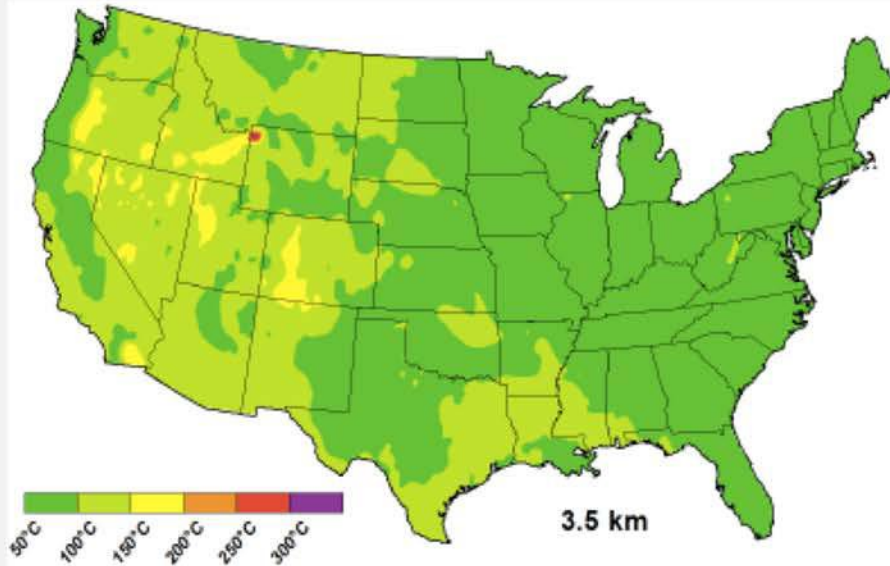


**Average surface geothermal gradient
from Blackwell and Richards, SMU (2006)**

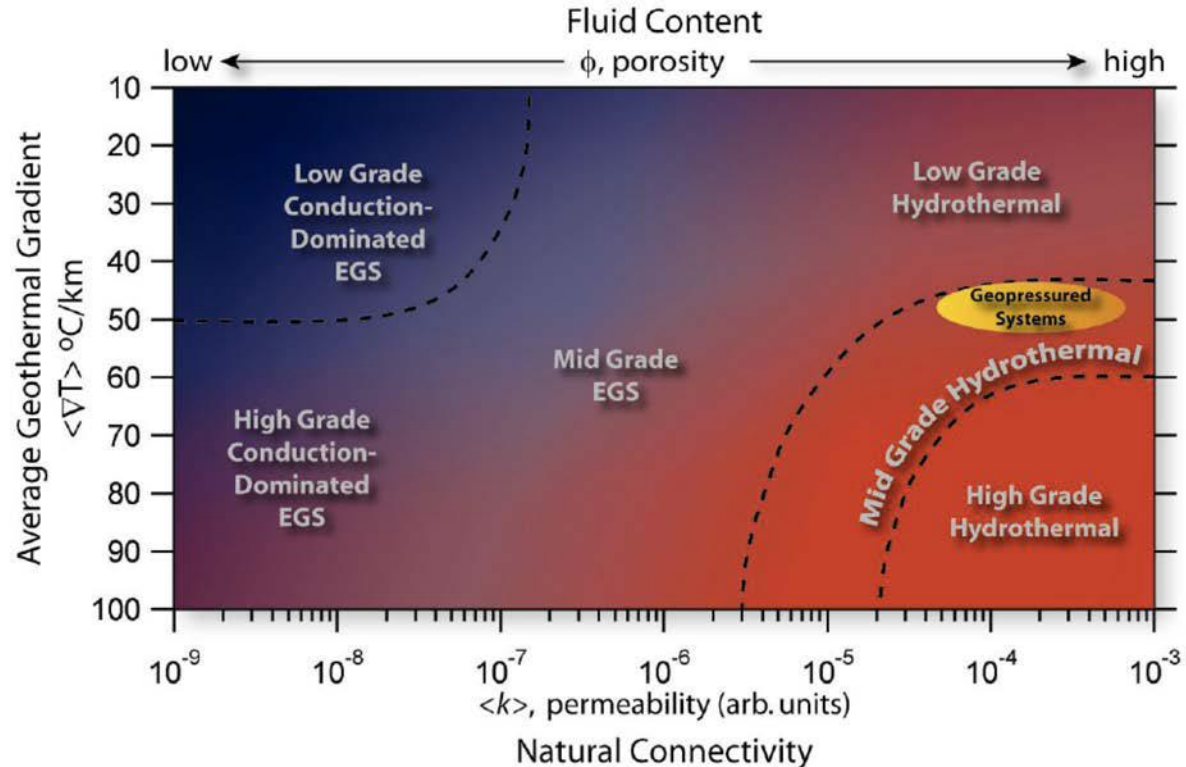
© Blackwell and Richards, SMU. All rights reserved. This content is excluded from our Creative Commons license. For more information, see <https://ocw.mit.edu/fairuse>.

6 km is the limit of economic drilling, mostly used for oil and gas

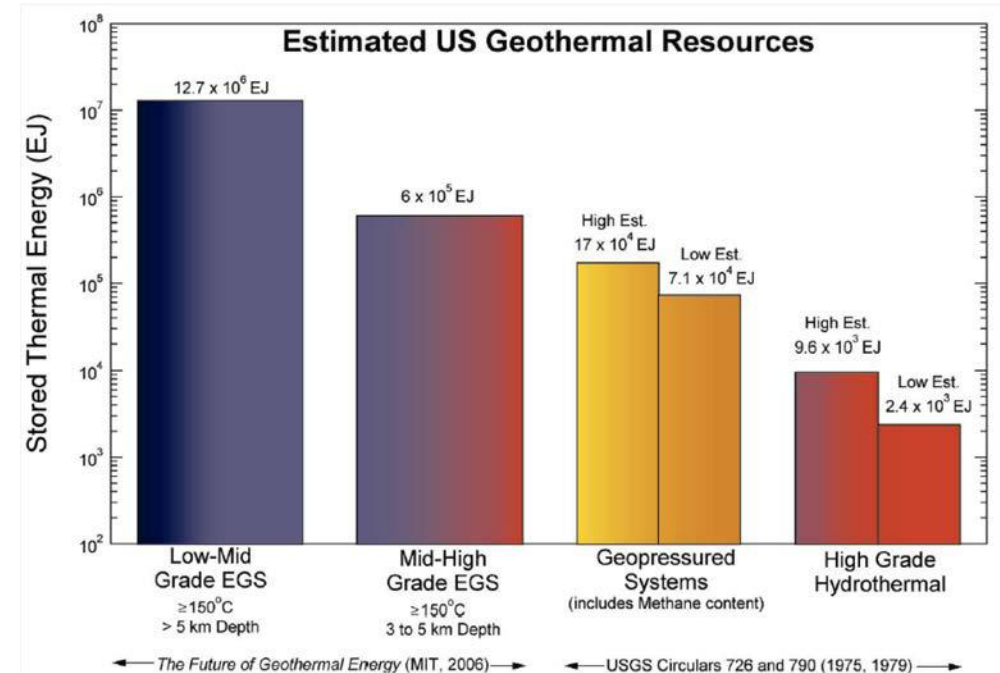
Estimated Temperatures at Specific Depths



The geothermal continuum – from high-grade hydrothermal to high and low grades of EGS



US Annual use ~ 100 EJ



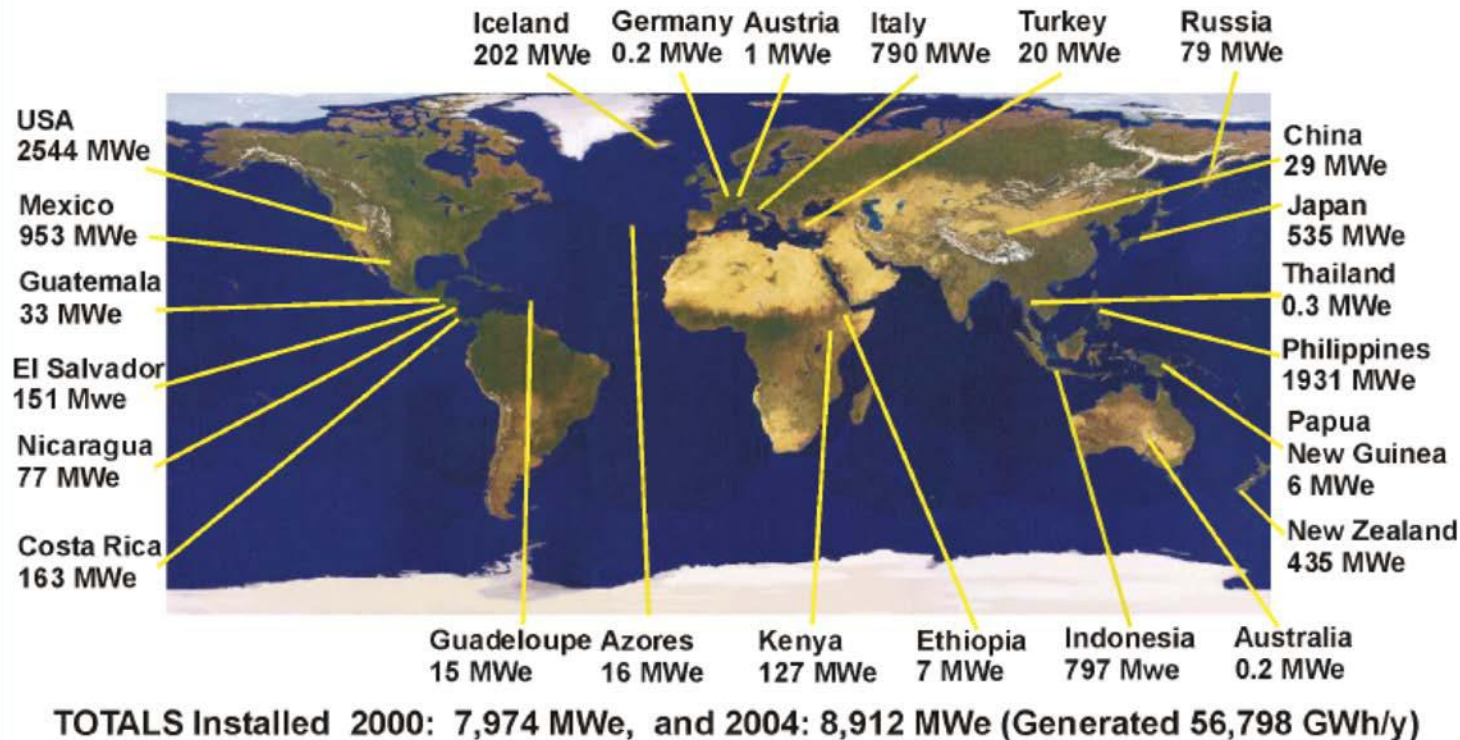
Figures courtesy of Hildigunnur Thorsteinssona, Chad Augustinea, Brian J. Andersonb, Michal C. Moorec, and Jefferson W. Tester. Used with permission.

- Hydrothermal resources depend on high permeability to naturally bring hot water and steam to the well. Water comes up under its own pressure.
- EGS: Enhanced Geothermal Systems, futuristic systems that rely on heat conduction to heat up a fractured well where water is injected to recover the heat and brings it to the surface.

Today there are over 10,000 MWe on-line or under construction

Iceland -- 440 MWe up from 202 MWe in 2005

USA -- 6304 MWe up from 2544 MWe in 2005



© Tony Batchelor, 2005

© Tony Batchelor. All rights reserved. This content is excluded from our Creative Commons license. For more information, see <https://ocw.mit.edu/fairuse>.

Geothermal energy in Iceland is a significant part of their energy sources.

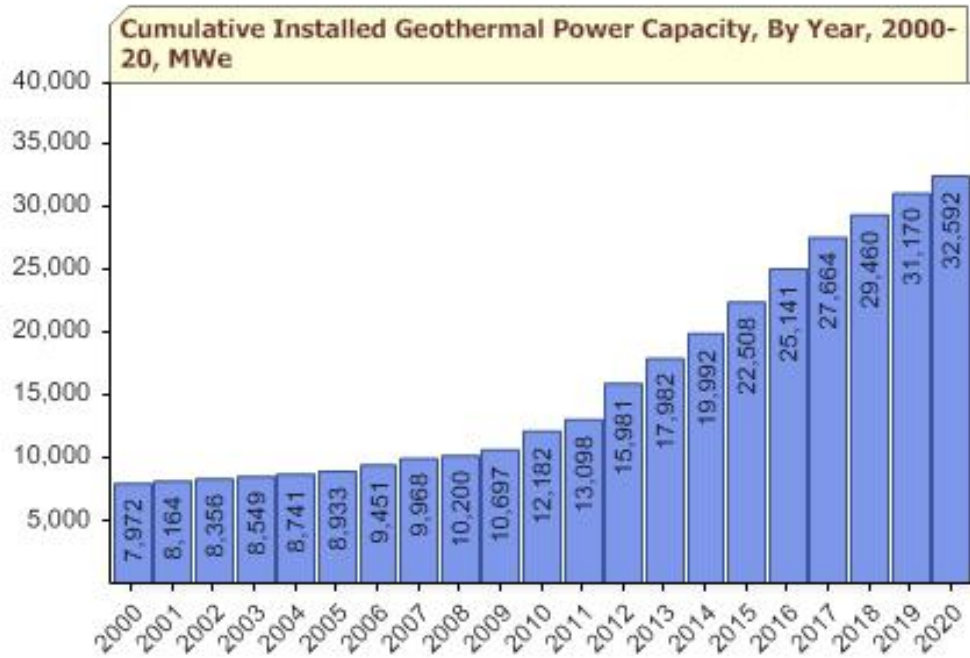


Courtesy Elsevier, Inc., <http://www.sciencedirect.com>. Used with permission.

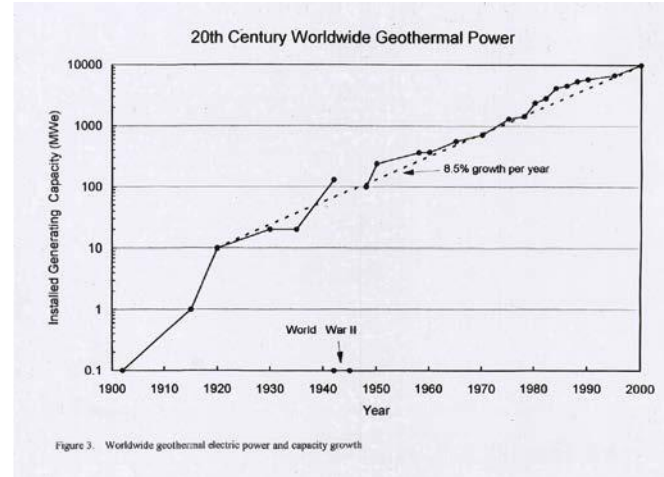


© Source unknown. All rights reserved. This content is excluded from our Creative Commons license. For more information, see <https://ocw.mit.edu/fairuse>.

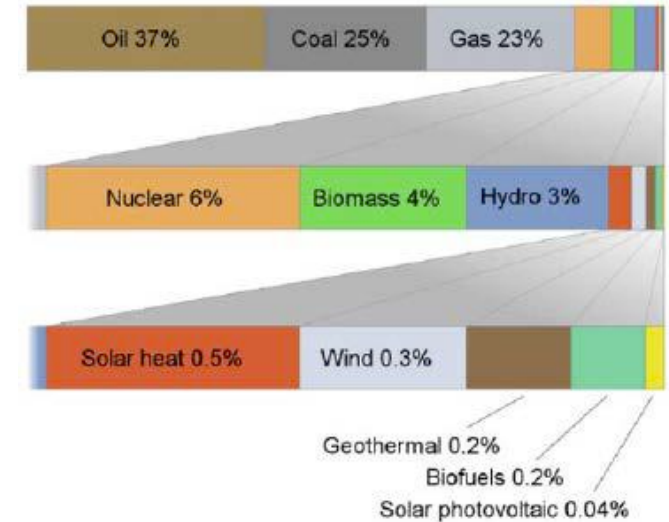
**Larderello started producing on 1904
.... Still going strong!**



© GlobalData Plc. This content is excluded from our Creative Commons license. For more information, see <https://ocw.mit.edu/fairuse>.



© Source unknown. This content is excluded from our Creative Commons license. For more information, see <https://ocw.mit.edu/fairuse>.



© [Omegatron](https://ocw.mit.edu/fairuse). License: CC BY-SA. This content is excluded from our Creative Commons license. For more information, see <https://ocw.mit.edu/fairuse>.

- Geothermal electricity generates a good fraction of the standard renewables (GWS), more than solar but less than wind.
- It is also used for heating (probably less than solar).
- It enjoys a high capacity factor.
- It has grown steadily but less than wind and solar, which enjoy 20-30%/y over the past few years because of the price drop.

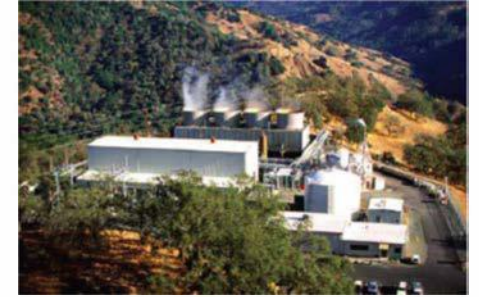
Geothermal energy today for heat and electricity

- From its beginning in the Larderello Field in Italy in 1904, nearly 10,000 MWe of capacity worldwide today
- Additional capacity with geothermal heat pumps (e.g. >100,000 MWt worldwide)
- Current costs -- 7–10¢/kWh
- Attractive technology for dispatchable base load power for both developed and developing countries



Condensers and cooling towers, The Geysers, being fitted with direct contact condensers developed at NREL

Image courtesy of NREL.

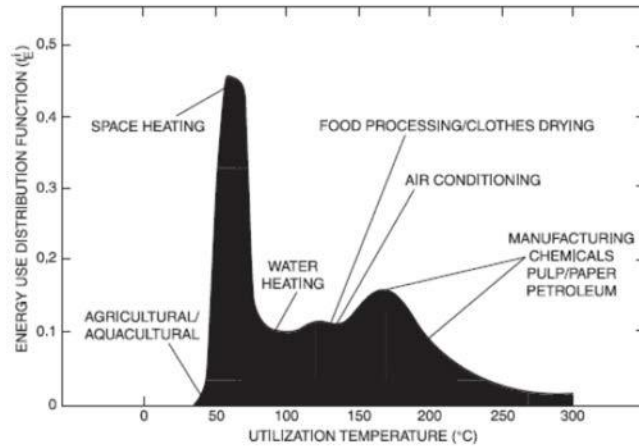


© Geothermal Education Office. All rights reserved. This content is excluded from our Creative Commons license. For more information, see <https://ocw.mit.edu/fairuse>.



© Source unknown. All rights reserved. This content is excluded from our Creative Commons license. For more information, see <https://ocw.mit.edu/fairuse>.

The non-electric portion of energy use is large and at relatively low temperatures



In the US over 30% of our primary energy is actually used at temperatures < 200°C

Figure 11.5. Fractional energy use distribution as a function of end-use temperature for non-electric applications below 300°C. The function f'_2 at T_i is simply the derivative of the cumulative energy use at that specific temperature T_i . Source: Tester (1982).

© Source unknown. All rights reserved. This content is excluded from our Creative Commons license. For more information, see <https://ocw.mit.edu/fairuse>.

Geothermal energy, like low grade solar thermal energy, works well for heating applications.

More than 30% of the US primary energy is used at $T < 200^\circ\text{C}$

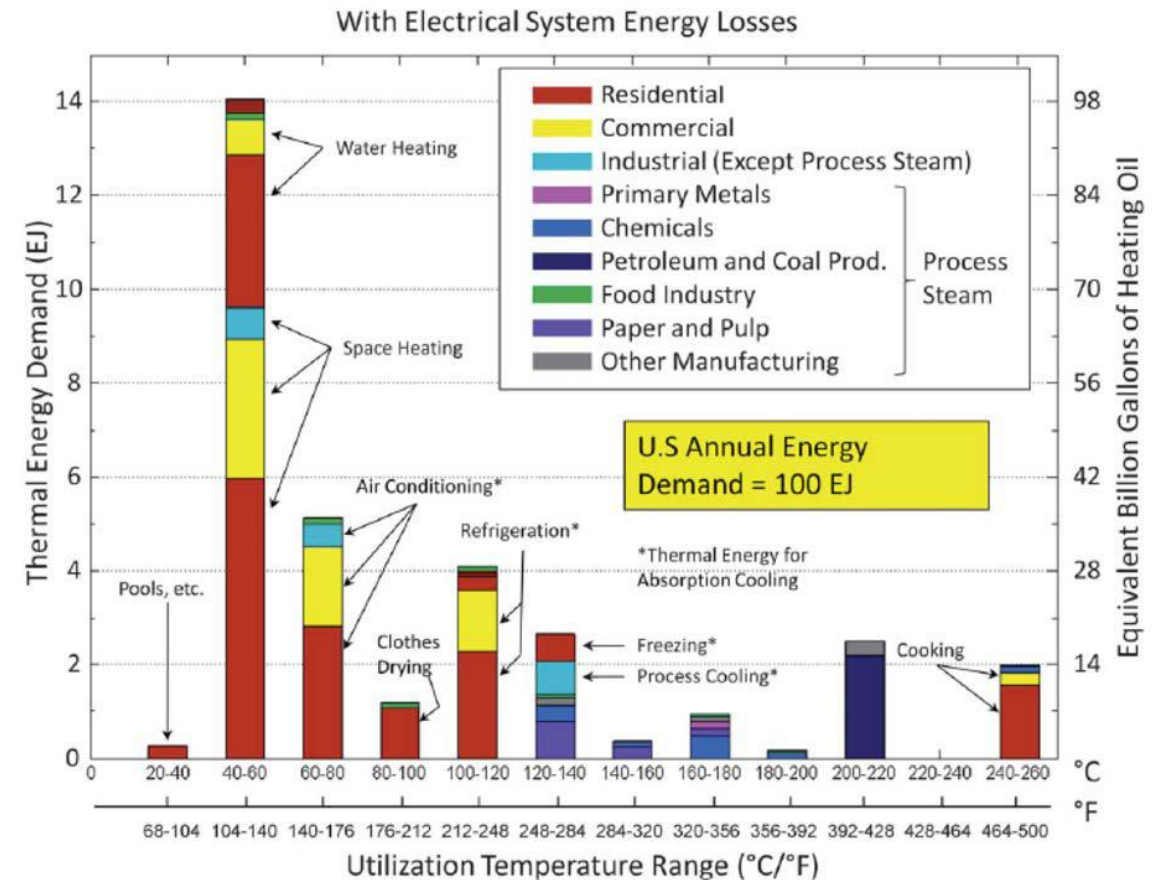
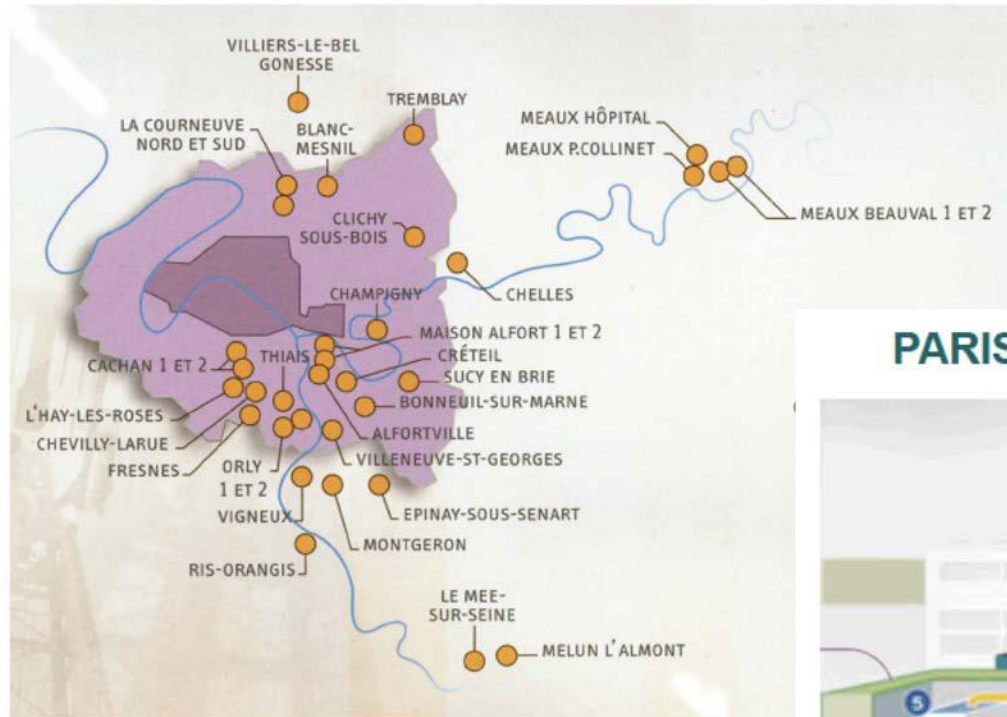


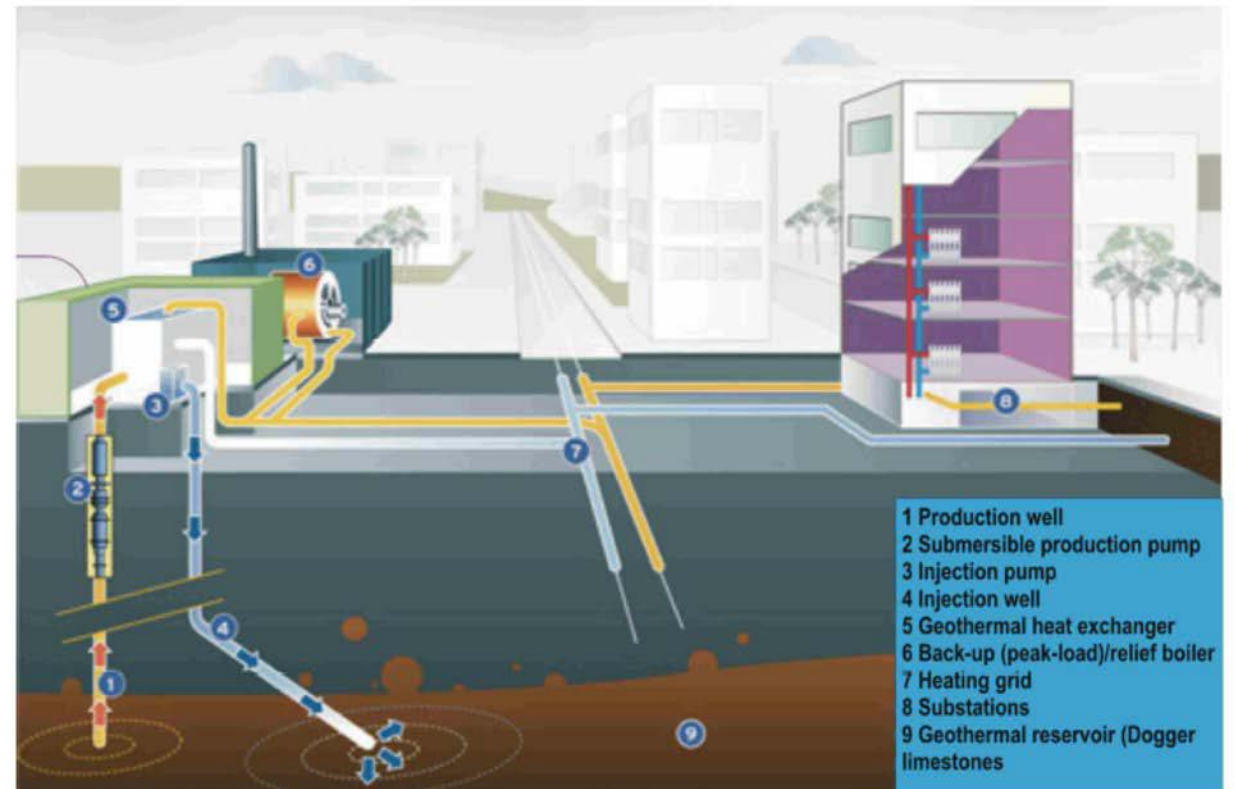
Fig. 1 Estimated thermal energy consumed in America below 260°C (500°F).

Location of Paris Basin geothermal district heating doublets 2006 status (source ADEME)



Very effective use of Geo resources
Central/district heating

PARIS BASIN GDH SCHEME



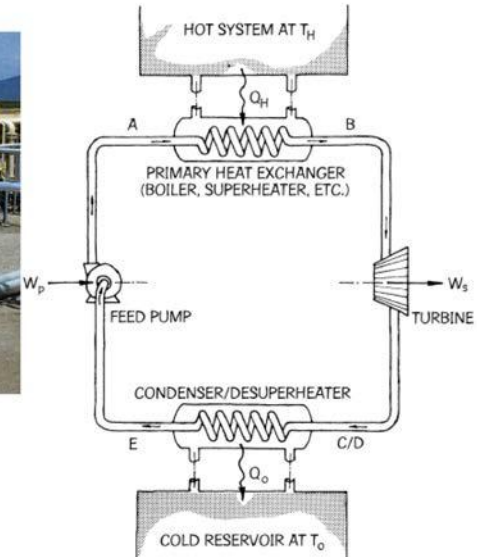
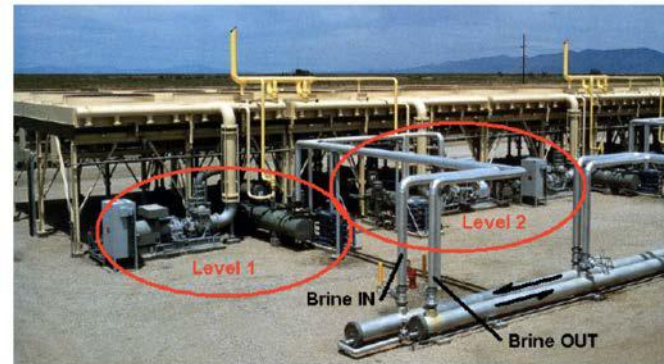
5 MWe organic binary cycle in Nevada using isobutane as a working fluid with no cooling water consumption!



Geothermal power plants tend to be small, 20-80 MWe. Some are smaller!

Stillwater, Nevada Organic Rankine Cycle Plant

With low T resource, ORC are ideal.



Working fluids requirements for Rankine Cycles:

1. High T_c for efficiency but low p_c for simplicity
2. Large enthalpy of evaporation
3. Non toxic, non flammable, non corrosive, cheap ..

Water: $p_c=22.088$ MPa $T_c=374$ C, most common

CO₂: $p_c=7.39$ MPa, $T_c=30.4$ C (low p)

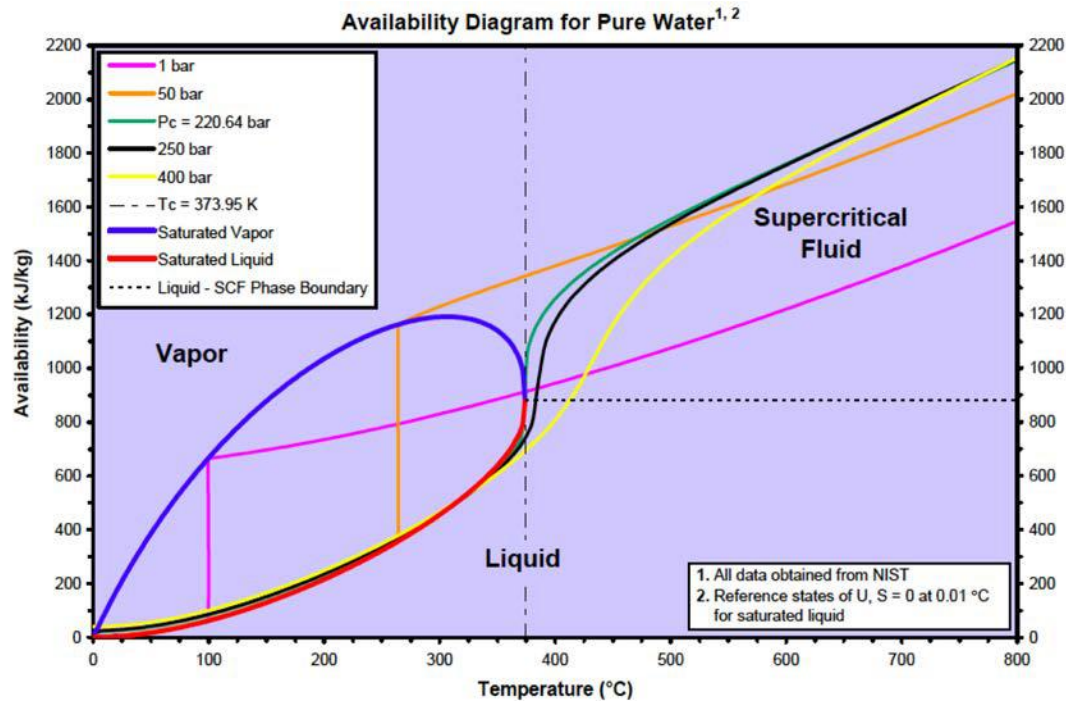
Renewable sources (low to very low T for solar and geothermal):

Ammonia: $p_c=11.63$ MPa, $T_c=132$ C.

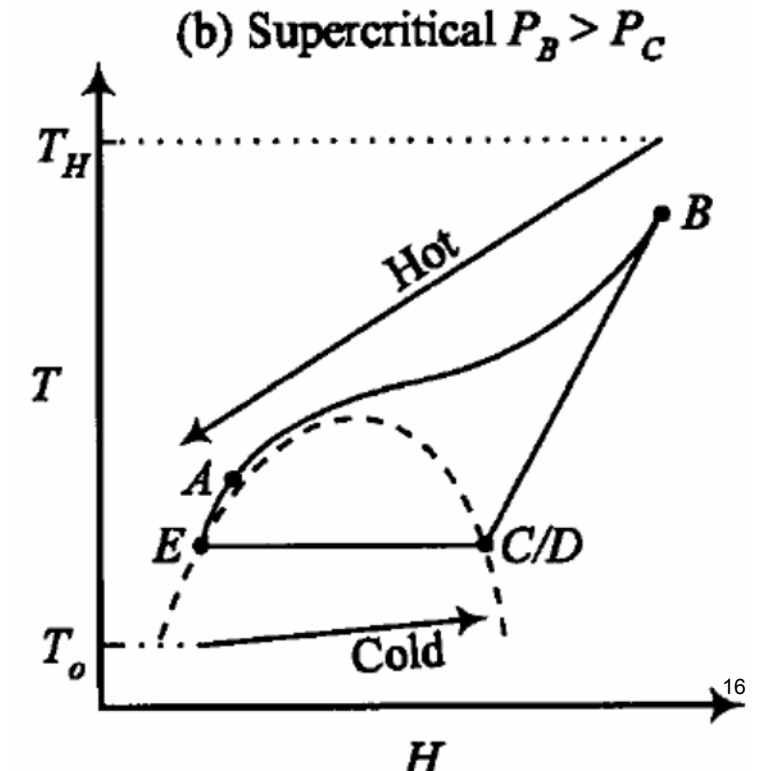
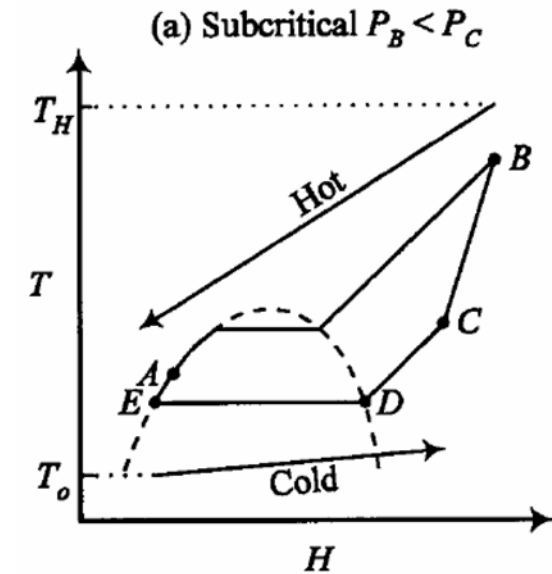
Propane: $p_c= 4.26$ MPa, $T_c= 97$ C

Isobutane, Freon

Max T is low, and Supercritical Cycles must be used to improve efficiency



- Availability of working fluid increases sharply when heat is added at constant T, and in the supercritical region.
- Supercritical operation reduces availability loss between source (geo fluid) and working fluid.

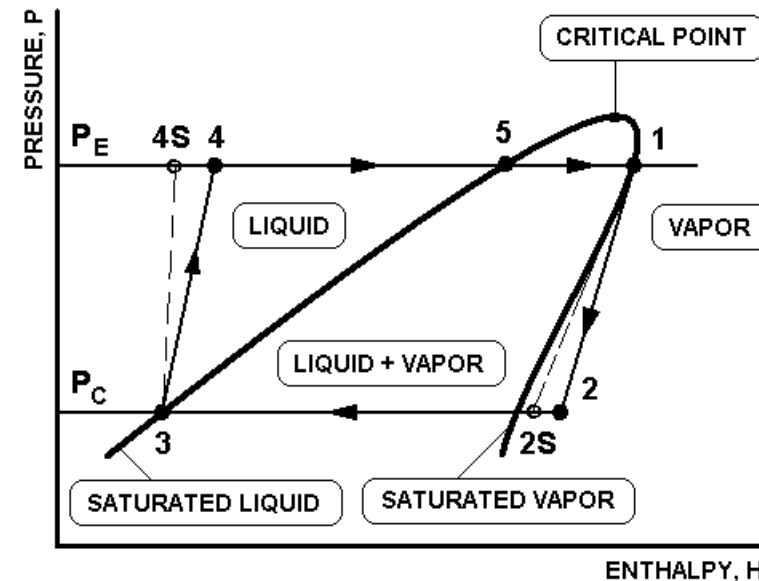
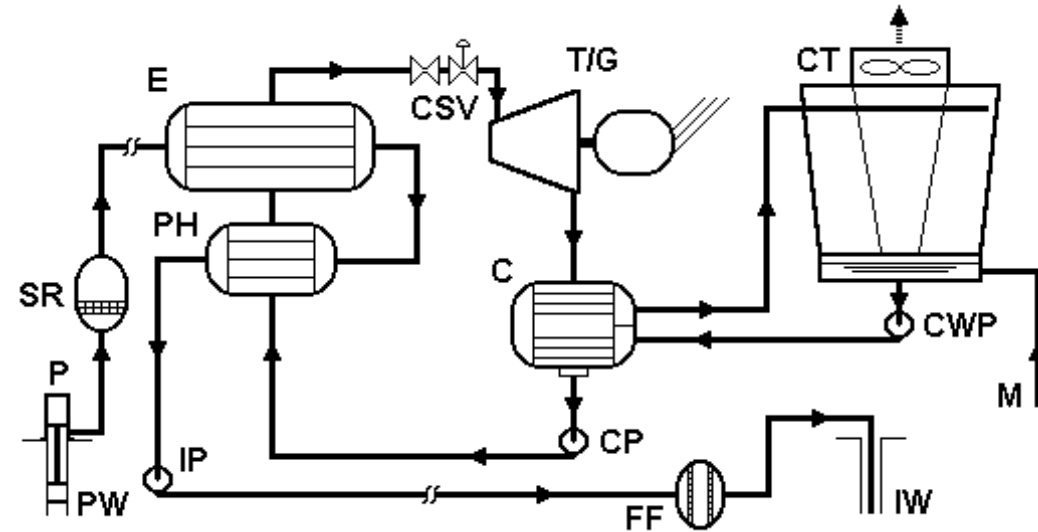


Surface Plant: Binary

An ordinary Rankine cycle with an organic fluid used as a working fluid.

The working fluid is heated in two stages (E and PH), expanded in a turbine, condensed and pumped back.

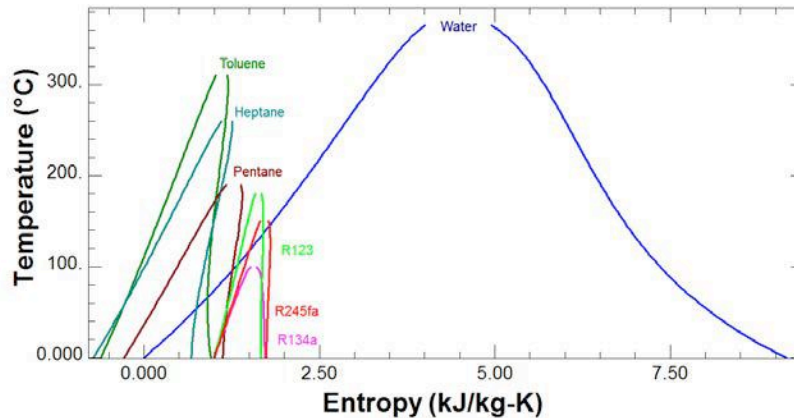
The Geo fluid is used to supply heat to the working fluid (E and PH) and is returned back to well.



Organic Rankine Cycles

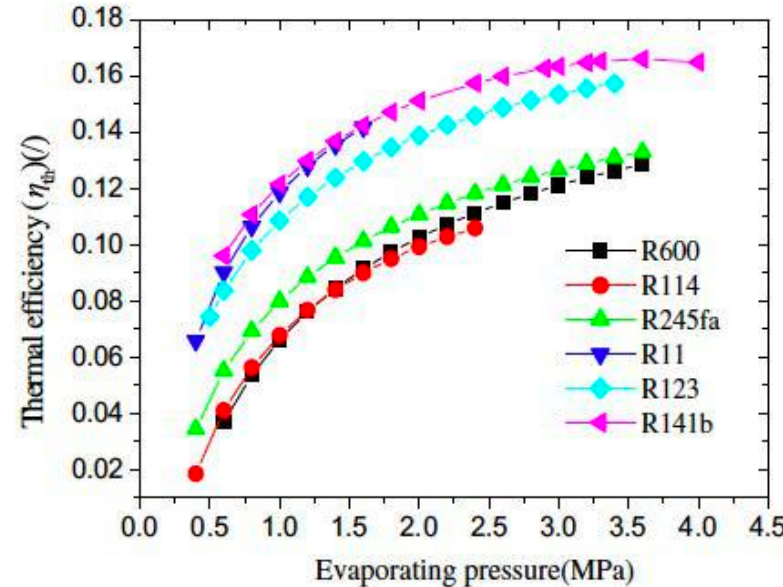
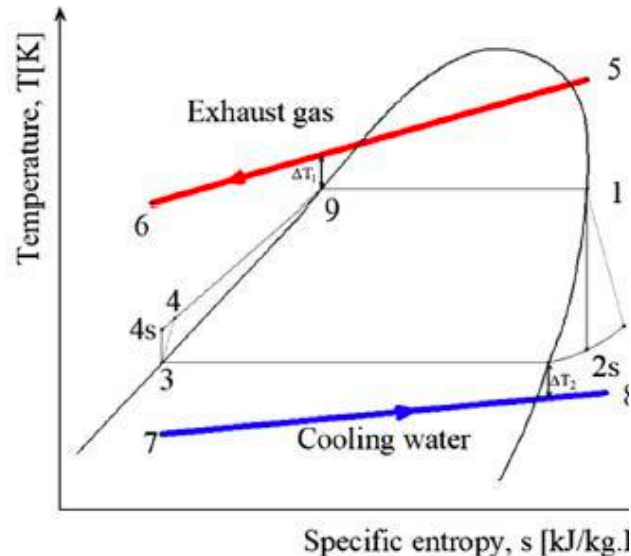
Used in Waste Heat Recovery” as well

T-s diagram for different organic fluids, normal and “overhang”



All are Refrigerants, T_b : the boiling point, ODP: Ozone Depletion Potential, GWP Global warming potential
 Tchanché et al, Fluid selection for a low temperature solar organic Rankine cycle, Applied Thermal Eng., 29:2468-2476 (2009)

Substance		Physical Data				Environmental Data		
								GWP (100 y)
1	R123	152.93	27.8	183.7	3.668	1.3	0.020	77
2	R134a	102.03	26.1	101	4.059	14	0	1430
3	R152a	66.05	-24	113.3	4.520	1.4	0	124
4	R245fa	134.05	15.3	154.05	3.640	7.6	0	950
5	R290	44.10	42.10	96.68	4.247	0.041	0	~ 20
6	R600	58.12	-0.5	152	3.796	0.018	0	~ 20



(left) The T - s diagram of an ORC using a fluid with an overhang saturation curve, and (right) using a number of different working fluids. The analysis applied realistic models for the different cycle components and working fluid equation of state. The cycle operates on engine exhaust 250 °C. Results show the impact of the cycle high pressure Tian et al., *Energy*, 47, 125–136, 2012.

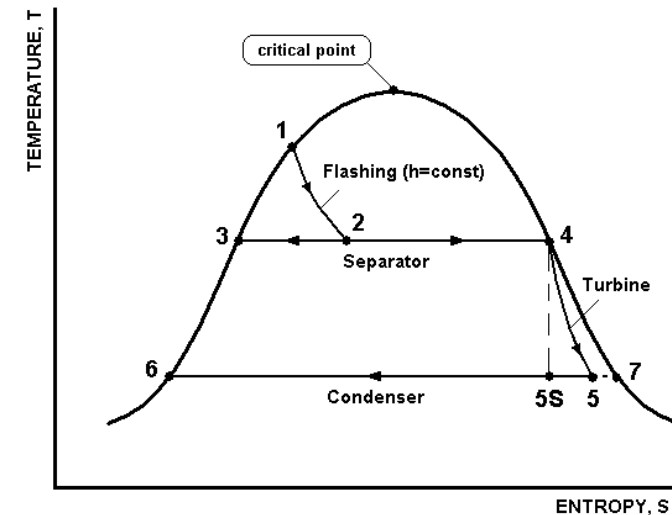
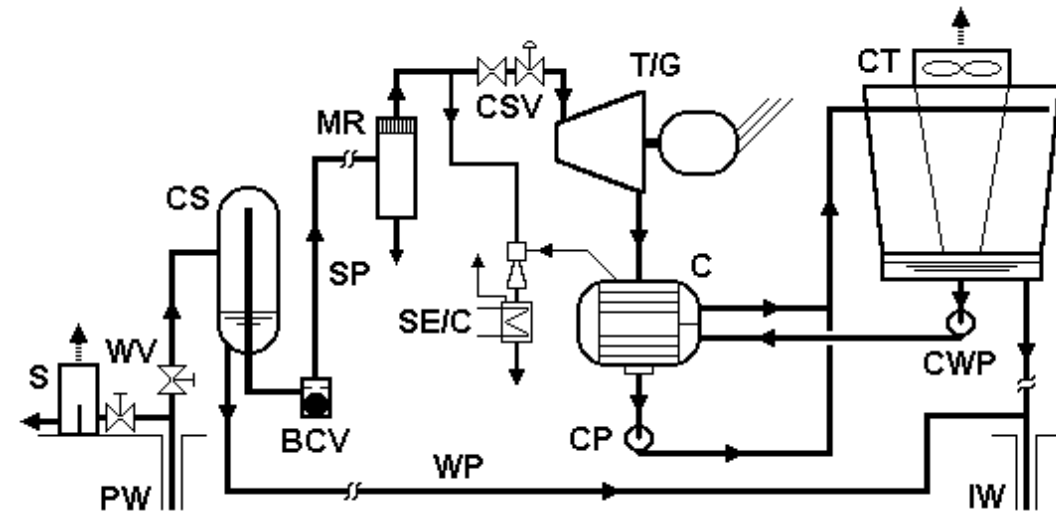
Surface Plant: Flash

A simpler cycle in which the Geo fluid is used as a working fluid.

First it is flashed to a lower pressure, with steam then expanded in the turbine, condensed, pumped back and returned to the well.

The water remaining after flashing is returned to the well directly.

The geo steam is conditioned before expansion.



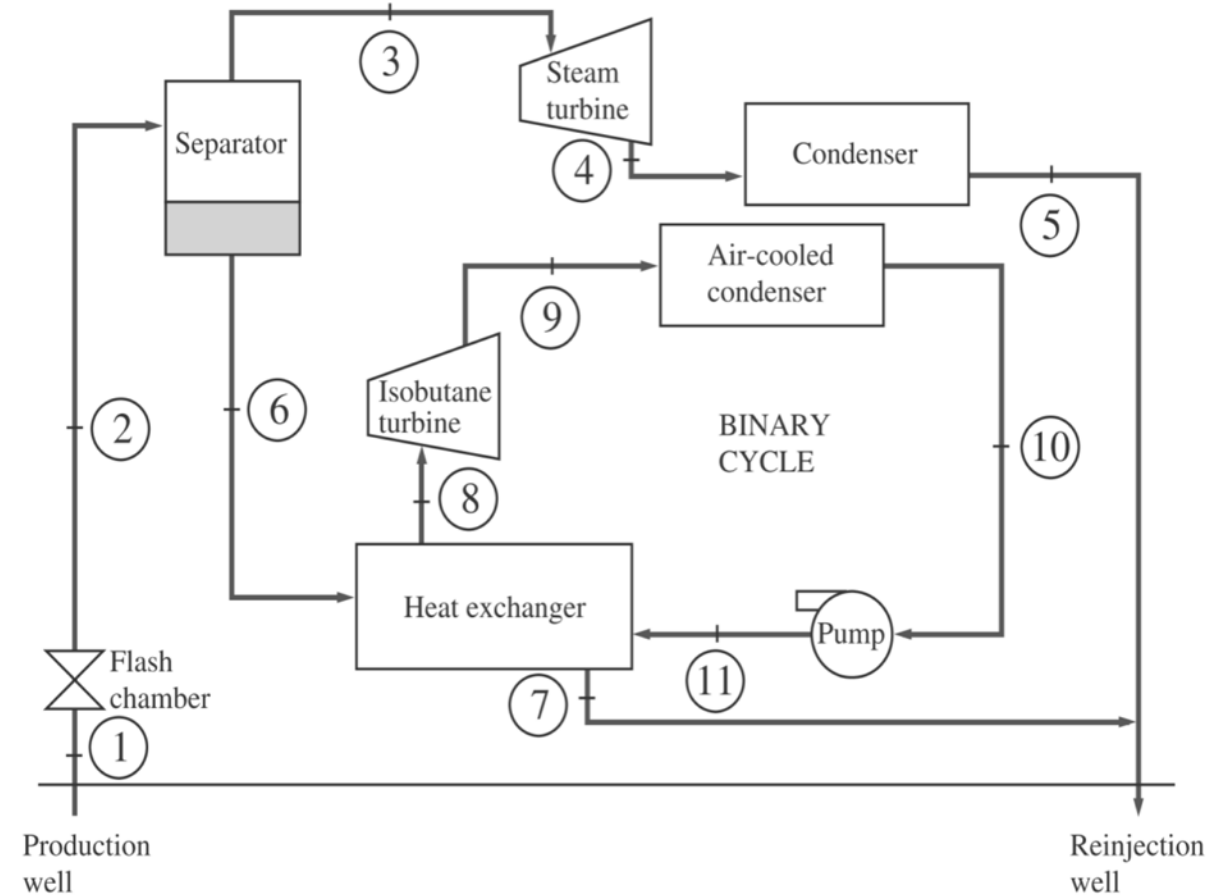
Example 9.1

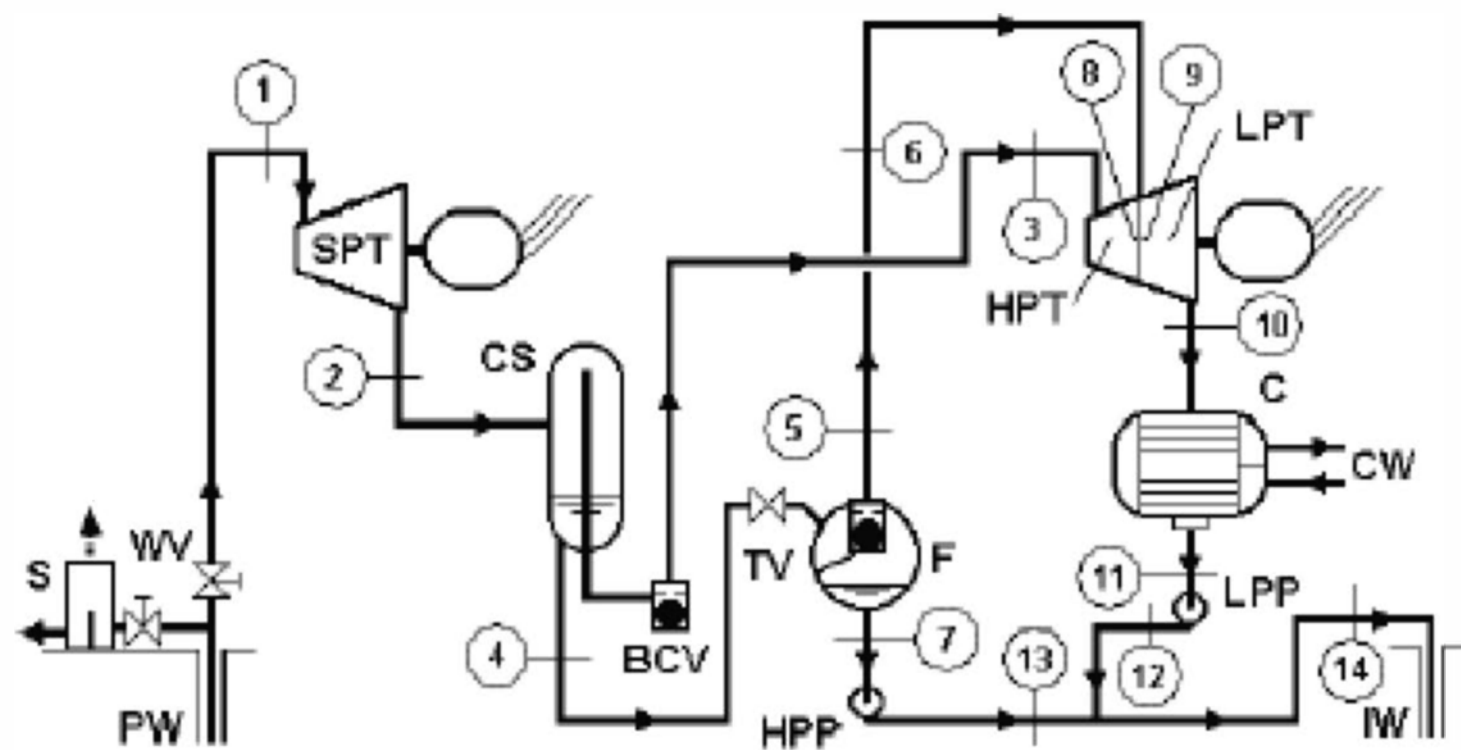
- Hybrid plant: single flash to separate the geo-fluid into steam and liquid.
- A steam turbine extracts work from the steam.
- A binary cycle (iso-butane) heated by the liquid produces more work.

See solution.

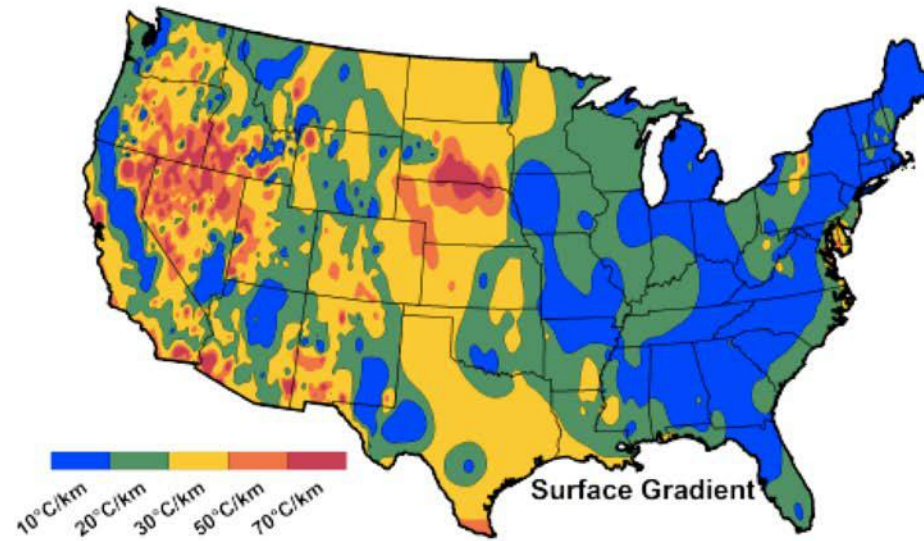
Efficiency of steam by itself is 7.6%

Efficiency of hybrid plant is 10.6%

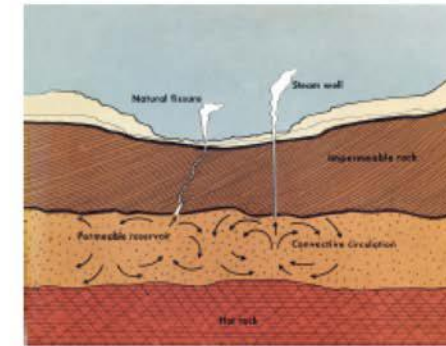




Is there a feasible path from today's hydrothermal systems with 3000 MWe capacity to tomorrow's Enhanced Geothermal Systems (EGS) with 100,000 MWe or more capacity by 2050 ?



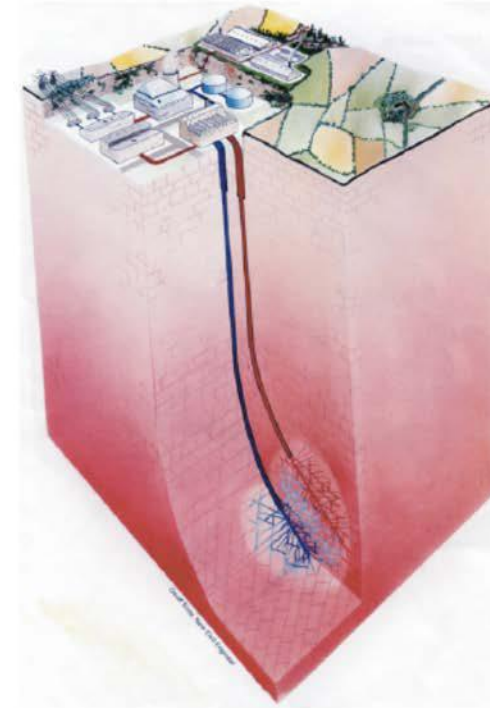
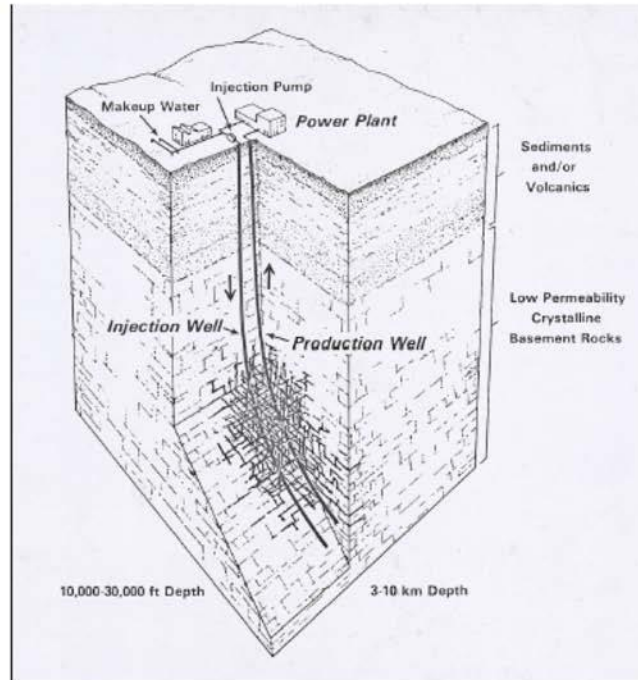
Average surface geothermal gradient
from Blackwell and Richards, SMU (2006)



© Source unknown. All rights reserved. This content is excluded from our Creative Commons license. For more information, see <https://ocw.mit.edu/fairuse>.

Significant fraction of the land area has 20 C/km gradient or higher. At 6 km deep, it is possible to recover heat at 120 C or higher that can be used in low grade geothermal plant. However, there is little fluid down there!

Enhanced/Engineered Geothermal Systems (EGS)



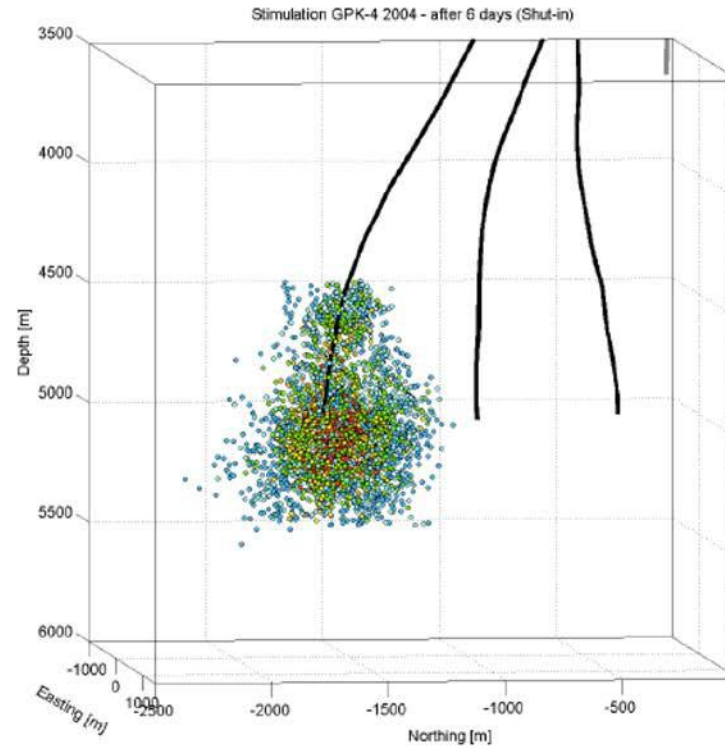
© Source unknown. All rights reserved. This content is excluded from our Creative Commons license. For more information, see <https://ocw.mit.edu/fairuse>.

“fracking is necessary: crack the rock by drilling deeps well, first vertically then horizontally, inject water (and sand and possibly some chemicals) to further fracture the rock and keep the small cracks open Now inject cold water and recover it as warm water from another well”

Developing stimulation methods to create a well-connected reservoir

The critical challenge technically is how to engineer the system to emulate the productivity of a good hydrothermal reservoir

Connectivity is achieved between injection and production wells by hydraulic pressurization and fracturing



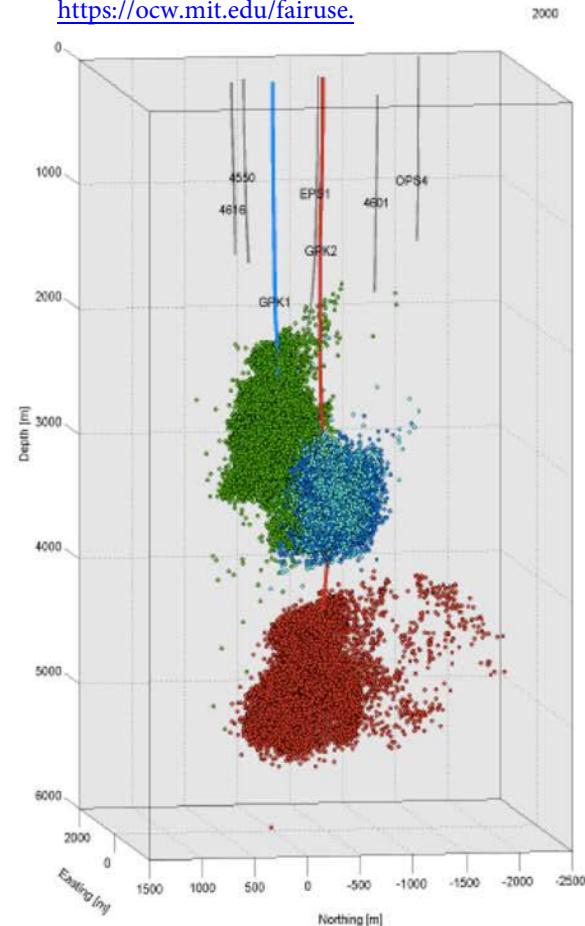
“snap shot” of microseismic events during hydraulic fracturing at Soultz from Roy Baria

© Source unknown. All rights reserved. This content is excluded from our Creative Commons license. For more information, see <https://ocw.mit.edu/fairuse>.

Drilling deep holes may cause micro seismic events (and sometimes more than micro that can lead to shutting down the operation).

R&D focused on developing technology to create reservoirs That emulate high-grade, hydrothermal systems

© Source unknown. All rights reserved. This content is excluded from our Creative Commons license. For more information, see <https://ocw.mit.edu/fairuse>.



Soultz, France from Baria, et al.

30+ years of field testing at

- Fenton Hill, Los Alamos US project
- Rosemanowes, Cornwall, UK Project
- Hijori, et al , Japanese Project
- Soultz, France EU Project
- Cooper Basin, Australia Project, et al.

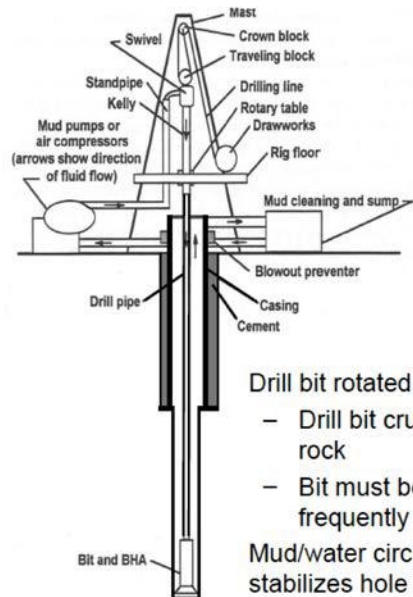
has resulted in much progress and many lessons learned

- directional drilling to depths of 5+ km & 300+°C
- diagnostics and models for characterizing size and thermal hydraulic behavior of EGS reservoirs
- hydraulically stimulate large >1km³ regions of rock
- established injection/production well connectivity within a factor of 2 to 3 of commercial levels
- controlled/manageable water losses
- manageable induced seismic and subsidence effects
- net heat extraction achieved

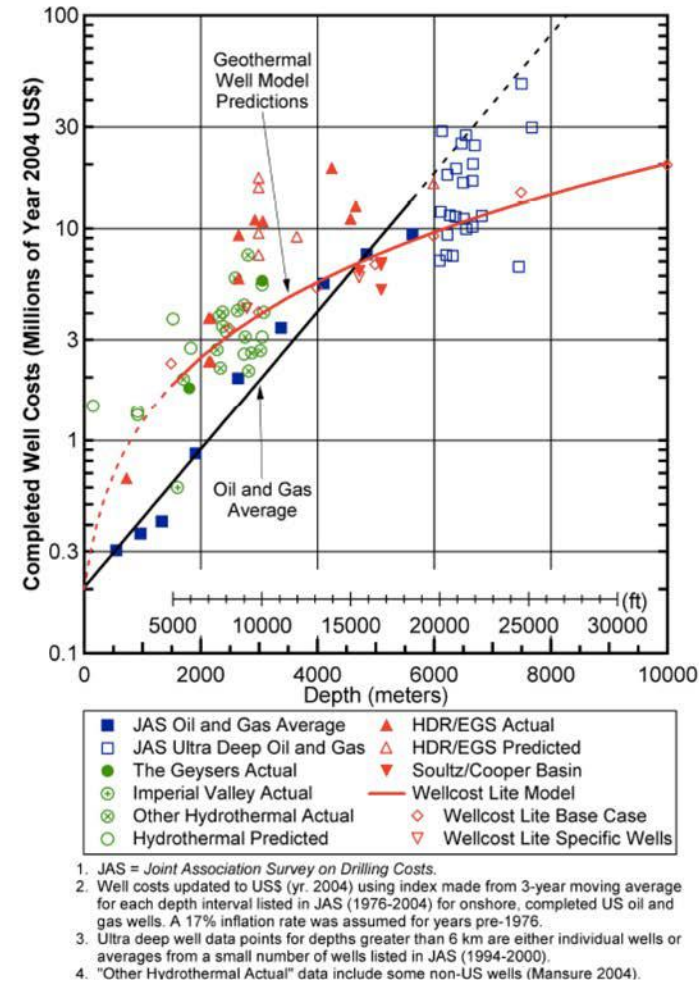


**17 March 2008 --
Wellhead flow rate 18 kg/s
at 275 bar, 208°C and rising**

Today's Conventional Rotary Drilling



- Drill bit rotated by drill string
 - Drill bit crushes and grinds rock
 - Bit must be replaced frequently
- Mud/water circulation cleans bit, stabilizes hole
 - Steel casing and cement used to secure hole



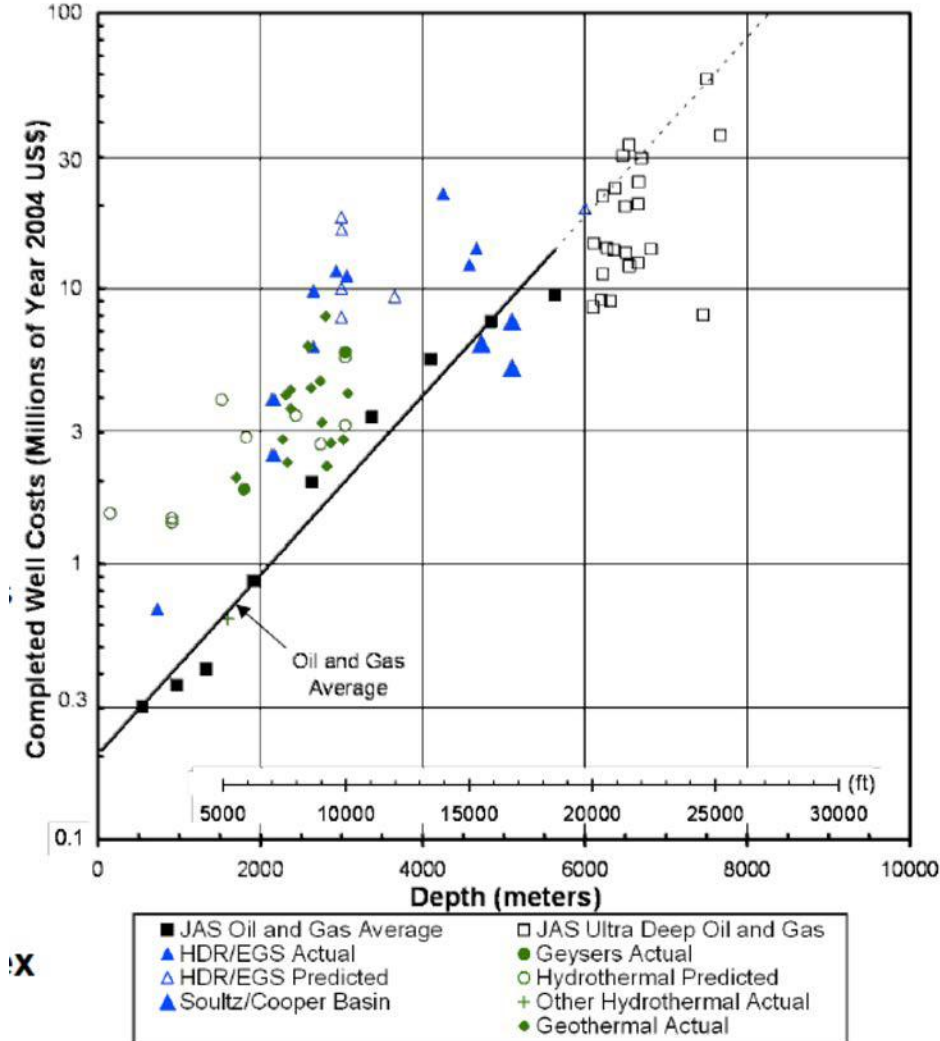
Drilling costs for geothermal wells compared to oil and gas wells



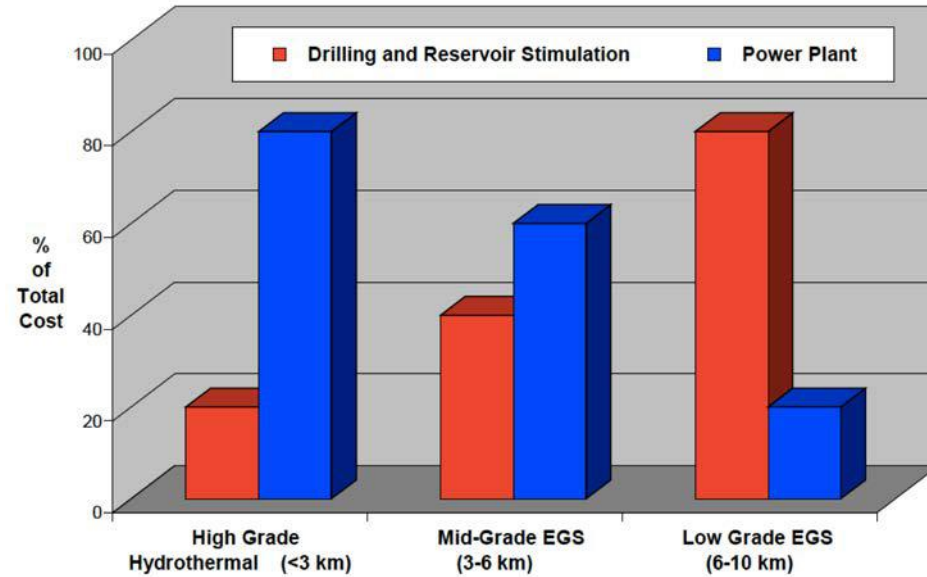
Two photos (same image with different sizes) of geothermal energy plant © Warren Gretz. All rights reserved. This content is excluded from our Creative Commons license. For more information, see <https://ocw.mit.edu/fairuse>.

All the other images © Source unknown. All rights reserved. This content is excluded from our Creative Commons license. For more information, see <https://ocw.mit.edu/fairuse>.

Cost depends on nature of rock, location, formations, etc.



As EGS resource quality decreases,
drilling and stimulation costs dominate



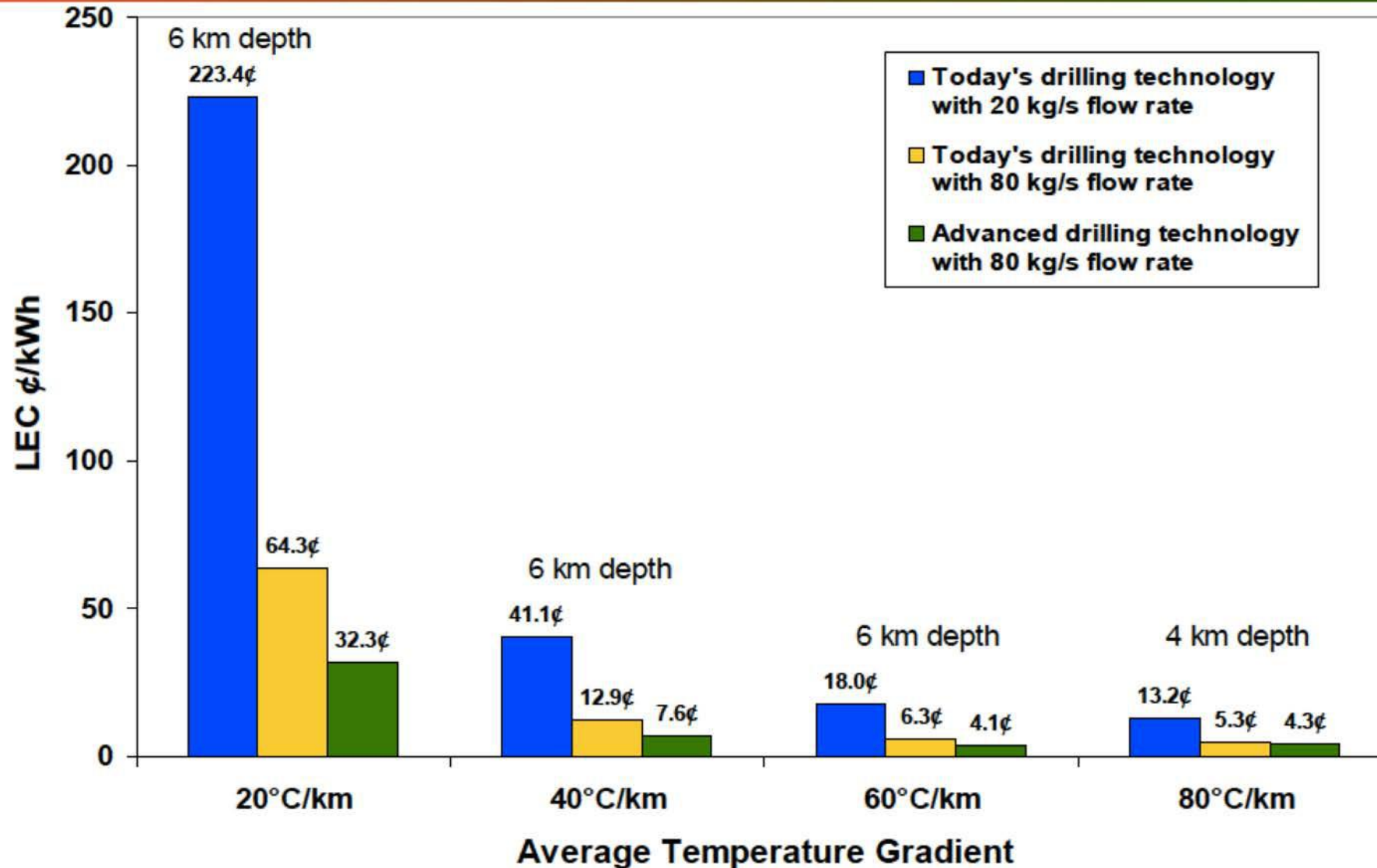
The "Laws" Geothermal Economics

1st Law -- Completed well cost increases exponentially with depth

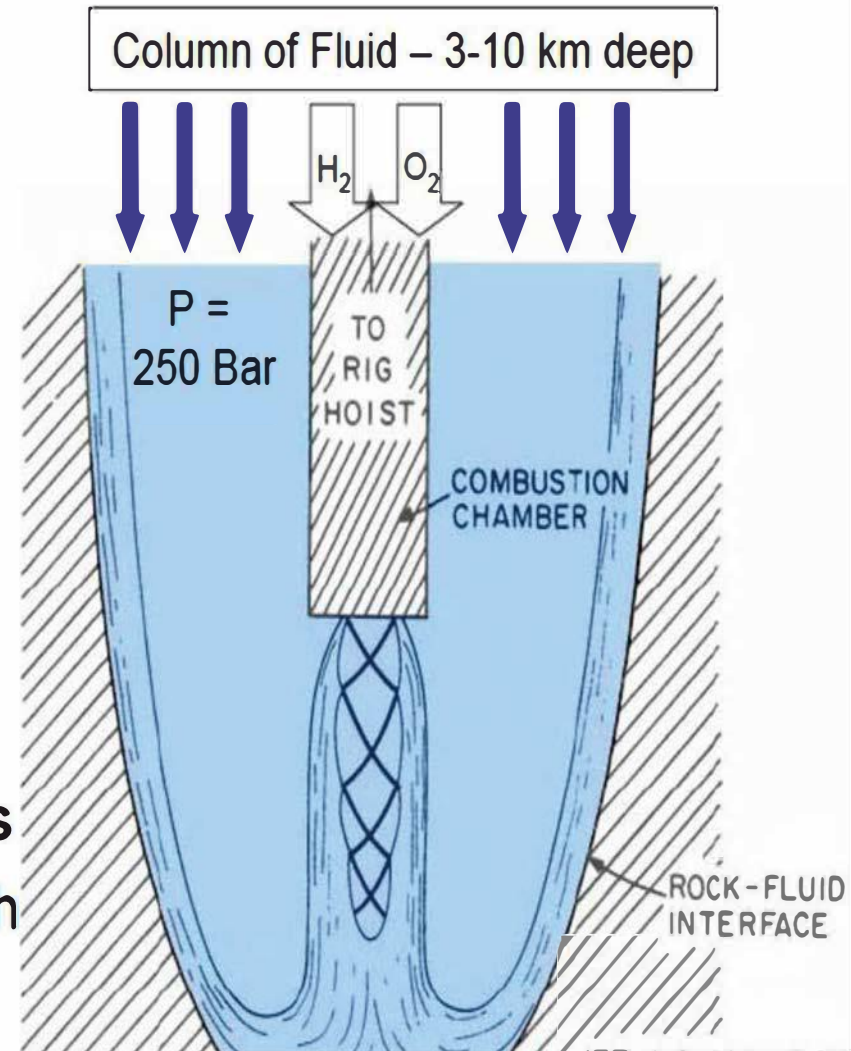
2nd Law -- Power plant cost decreases linearly with temperature

3rd Law -- As resource quality decreases drilling costs dominate

Levelized energy costs vary with resource grade and reservoir productivity and drilling costs



- **Supercritical water**
 - Pressures of > 220 bar
 - Temperatures of over 2500 K
- **Heat and momentum Transport**
 - Turbulent flow
 - Jet impinging against rock
- **Detailed chemical kinetics**
 - $\text{H}_2\text{-O}_2$ combustion at high pressures \rightarrow kinetic mechanisms unknown



© Source unknown. All rights reserved. This content is excluded from our Creative Commons license. For more information, see <https://ocw.mit.edu/fairuse>.

MIT OpenCourseWare
<https://ocw.mit.edu/>

2.60J Fundamentals of Advanced Energy Conversion
Spring 2020

For information about citing these materials or our Terms of Use, visit: <https://ocw.mit.edu/terms>.

Lecture # 19

GAS SEPARATION TECHNOLOGIES

And their Application to CO₂ CAPTURE

Ahmed Ghoniem
April 13, 2020

Classification of separation processes:

- Chemical Absorption (using liquid solvent)
- Physical Absorption (using liquid solvent)
- Physical Adsorption (using a solid solvent)
- Distillation (using refrigeration)
- Membranes (molecules moving across a filter)

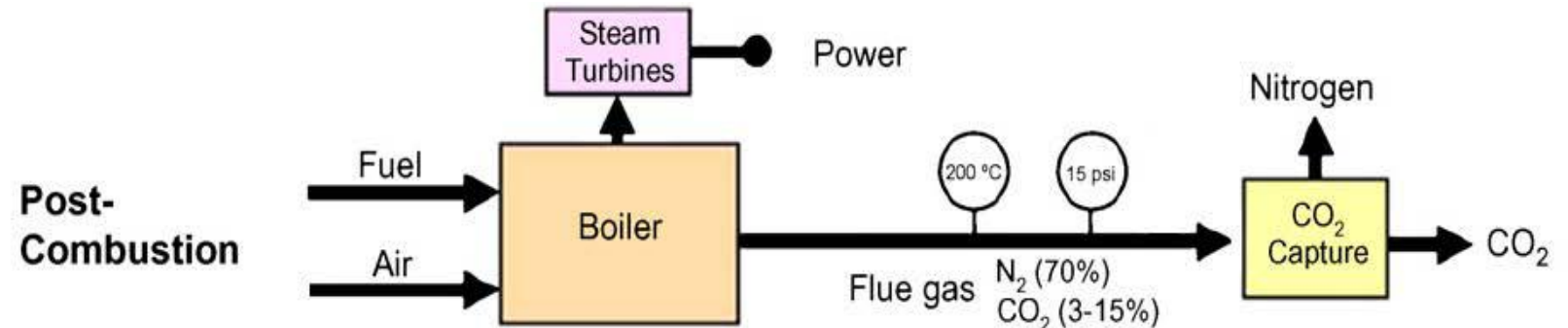
Average thermal efficiency and CO₂ production in (steam, pulverized) coal fired and (combined cycle) natural gas fired electricity generation plant, MJ_e and MW_e is the electricity generated.

	Pulverized coal (steam)	Natural gas (CC)
Efficiency	35-40%	55-60%
Heating value, MJ/kg _{fuel}	~30	~50
CO ₂ production, kg/MW _e	~1200	~400
CO ₂ specific energy, MJ _e /kgCO ₂	~3	~9

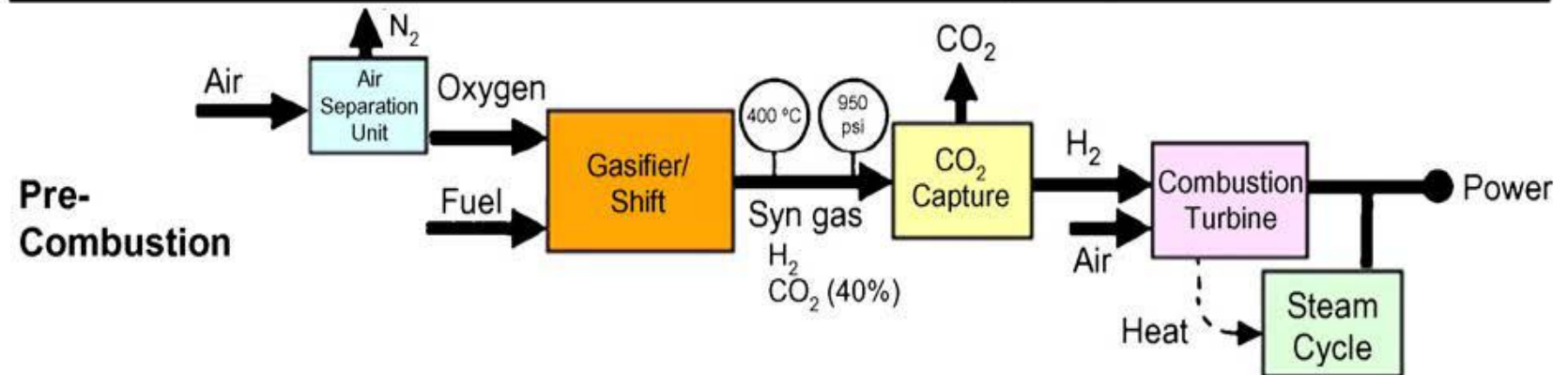
Approaches for CO₂ capture

(shown for coal used in steam cycle plants)

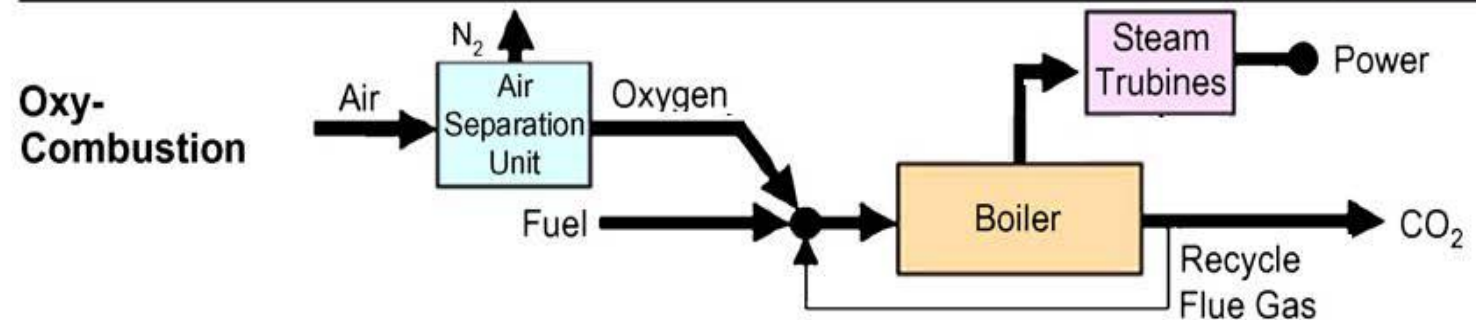
Separate CO₂ from CO₂+N₂



Separate CO₂ from CO₂+H₂

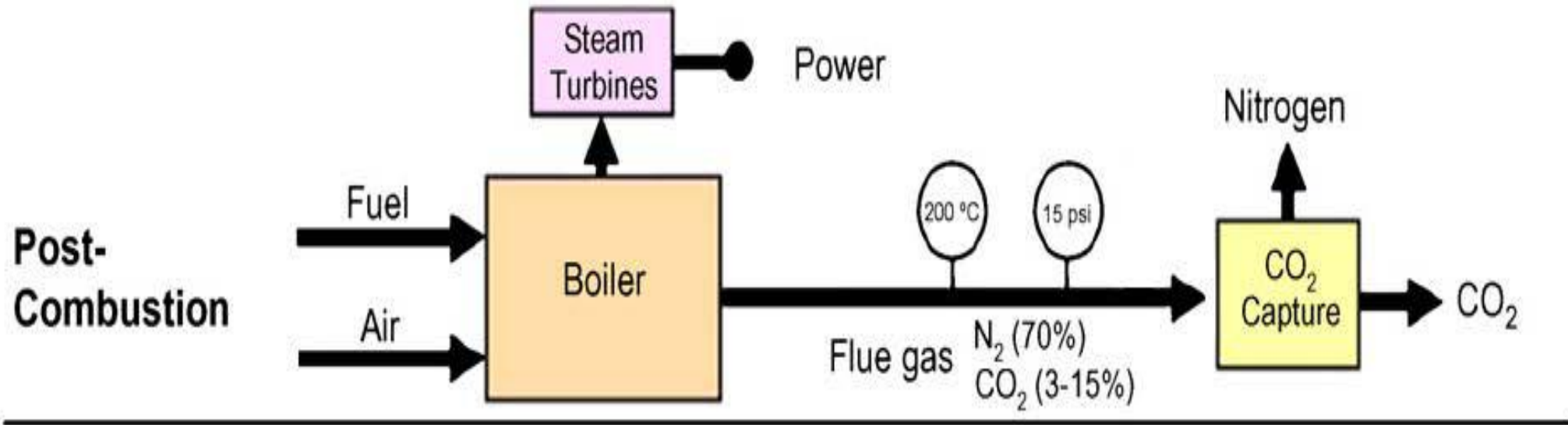


Separate O₂ from O₂+N₂



Post combustion Separation or Capture

Separate CO_2 from $\text{CO}_2 + \text{N}_2$



Courtesy Elsevier, Inc., <http://www.sciencedirect.com>. Used with permission.

The Petra Nova Project

Petra Nova plant has been operating since Jan 2017, it is the world's largest coal-fired power plant post-combustion carbon dioxide (CO₂) capture system. Since coming online it has **captured over 3.9 million short (US) tons of CO₂**, which was used to **produce over 4.2 million barrels of oil (from West ranch oil field)** through enhanced oil recovery (EOR).



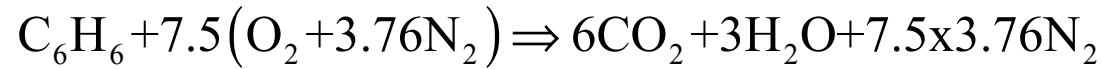
Image courtesy of DOE.

Partially funded by the U.S. DOE and managed NETL. Owned and operated by NRG Energy, Inc. and JX Nippon Oil and Gas Exploration Corporation, the Petra Nova project successfully retrofit carbon-capture technology onto a unit at the coal-fired W.A. Parish Generating Station located southwest of Houston, TX.

Petra Nova is designed to capture approximately 90 percent of the CO₂ from a 240-megawatt equivalent flue gas slipstream—which is approximately 1.6 million tons of CO₂ per year. The captured CO₂ is compressed, dried, and transported to the West Ranch Oil Field in Jackson County, TX. Then, the CO₂ is used in EOR to boost oil production.

<https://www.energy.gov/fe/articles/happy-third-operating-anniversary-petra-nova>

Estimate of the ideal and actual Work required for CO₂ Separation from combustion products in a post combustion capture process



The concentrations are: $X_{\text{CO}_2} = 0.16$ and $X_{\text{H}_2\text{O}+\text{N}_2} = 0.84$

Minimum CO₂ separation work equation: $-0.137 T_0$ MJ/kmol of benzene

At $T_0 = 300\text{K}$, the work is **41.1 MJ/kmol of benzene**.

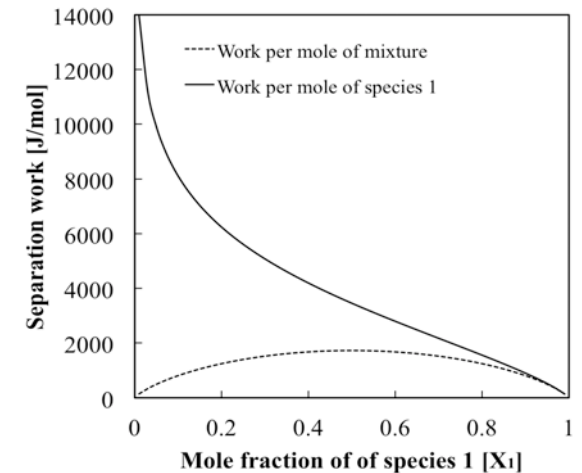
The enthalpy of reaction of benzene is 3171 MJ/kmol.

Taking 40% efficient cycle, the “useful” work produced is **1268.4 MJ/kmol of benzene**.

There is a penalty of 3.25% for the separation of CO₂ at $T = 27^\circ\text{C}$.

Actual separation processes require more work (5-10 time) due to irreversibility.

Thus, WORK penalty can be as large as **32.5% of the original work**.



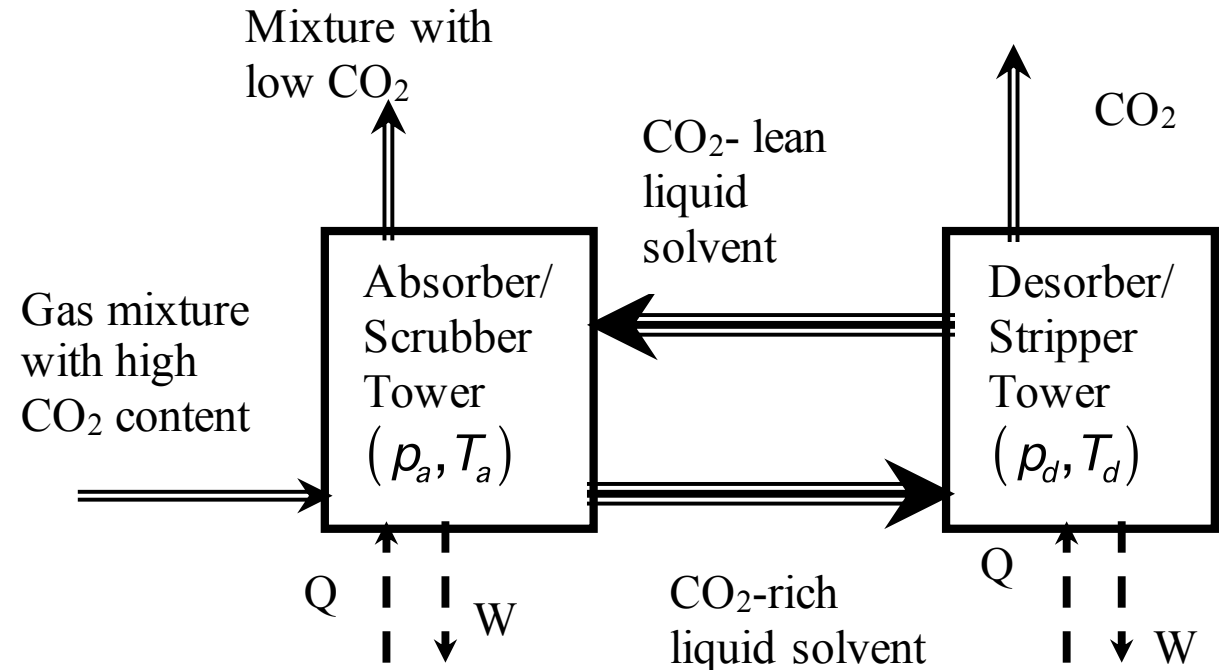
$$\dot{w}_{\text{mole of mixture}} = -\Re T_o \left(X_1 \ln \frac{X_1}{1-X_1} + \ln(1-X_1) \right)$$

$$\dot{w}_{\text{mole of } X_1} = -\Re T_o \left(\ln \frac{X_1}{1-X_1} + \frac{\ln(1-X_1)}{X_1} \right)$$

Separation or “capture” of CO₂ by absorption or adsorption

Relies on how much gas (CO₂) can be absorbed/adsorbed, chemically or physically, into a liquid/solid at a given temperature and/or pressure. The sorbent must be regenerated/brought back to its original form by releasing CO₂ in a different vessel and under different temperature and/or pressure.

- Separation of CO₂ by continuous absorption & desorption using a looping solvent, between two vessels (at different T/p).
- The liquid solvent can bind with CO₂ chemically or physically.
- The temperature and pressure are different in the two vessels, leading to favorable conditions for absorbing and desorbing CO₂ as the solvent loops between them



(1) SEPARATION By Chemical Absorption in a liquid solution

Works well for separating CO₂ from combustion products (mixture of N₂+CO₂)

use a reversible reaction whose equilibrium is temperature dependent

for an "amine solution" $2\text{R-NH}_2 + \text{CO}_2 \leftrightarrow \text{R-NH}_3^+ + \text{R-NH-COO}^-$

or $\text{CO}_2\text{-lean chemical solvent} + \text{CO}_2 \xrightleftharpoons[\text{desorber @ high T}]{\text{absorber @ low T}} \text{CO}_2\text{-rich chemical solvent}$

o forward absorption reaction is exothermic and lower temperatures favor absorption (products)

$$\frac{[\text{R-NH-COO}^-]}{[\text{R-NH}_2]} \text{ is proportional to } K_p(T) = \exp\left(-\frac{\Delta G_R}{\Re T}\right) = e^{\Delta S_R/\Re} \exp\left(\frac{|\Delta H_R|}{\Re T}\right) \uparrow \text{ as } T \downarrow$$

o lower T ~ 50 C, equilibrium favors products' formation or CO₂ absorption into the amine solution

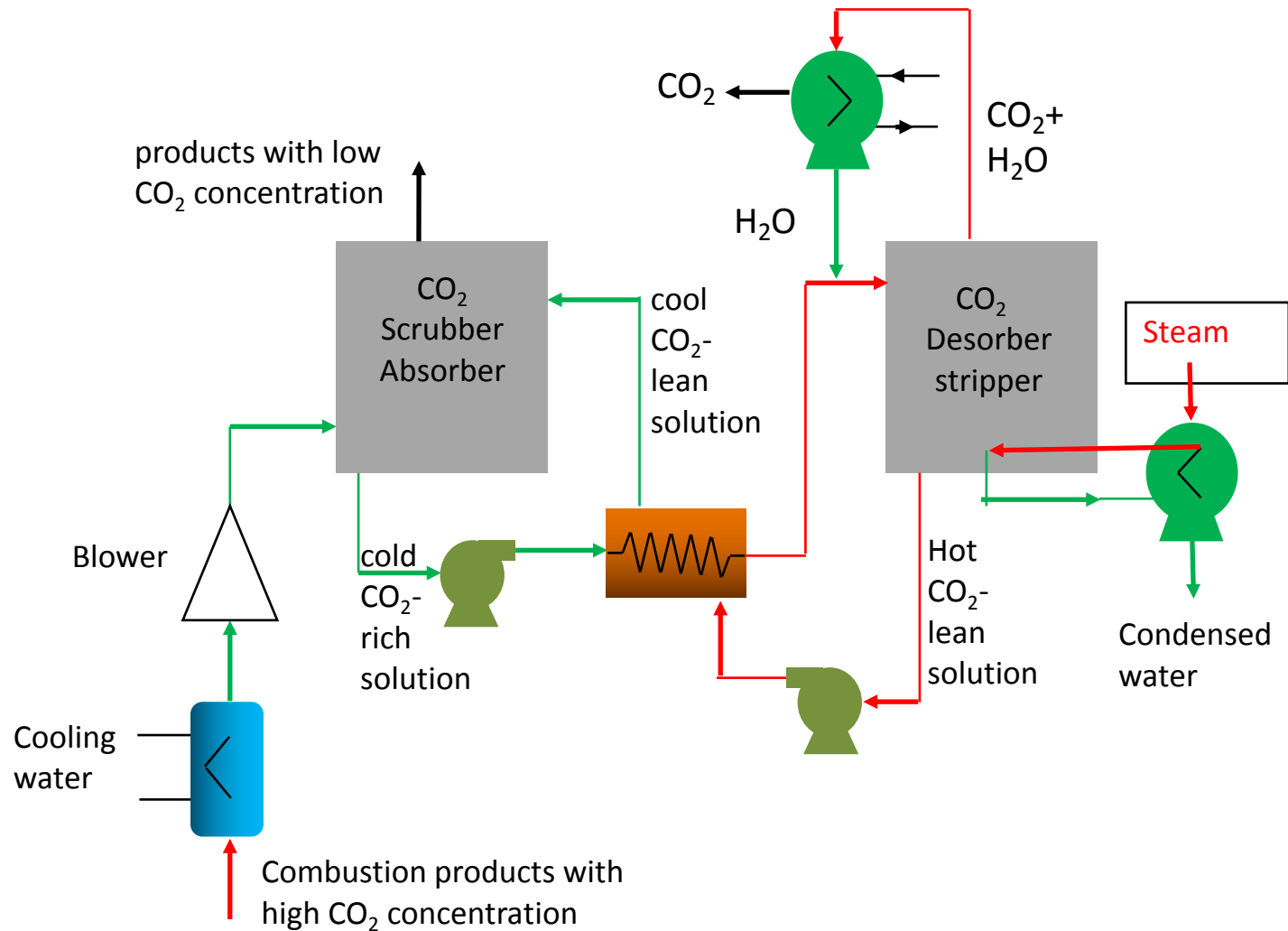
Must keep the absorber "tower" cool (reject "low quality" heat) to increase CO₂ in the amine phase.

o opposite is true at higher T ~ 150 C, the reaction reverses, and CO₂ is desolved from the solution

Need to heat up the solvent to release CO₂ and regenerate the solvent.

for $\text{R} \equiv (-\text{CH}_2\text{CH}_2\text{OH})$, monoethanolamine (MEA), $\Delta H_R = -1.919 \text{ MJ/kgCO}_2$

Using heat recuperation to reduce the heat required in the desorber (heat duty)



Energy required by the separation plant:

energy for separation

= enthalpy of the desorption reaction
 + thermal enthalpy of solution (water)
 + enthalpy of evaporation of vaporized water
 + enthalpy of evaporation of vaporized absorbent
 + enthalpy of desolution of CO₂ from water
 + *pumping work*

Most important components are:

$$Q_{\text{recovery}} = n_{\text{solution}} \ddot{Q}_{\text{solution}} \Delta T + n_{\text{water}} \Delta \ddot{H}_{\text{evap}} + n_{\text{sorbent}} \left(\Delta \ddot{H}_{\text{desorption}} + \Delta \ddot{H}_{\text{CO}_2, \text{sol}} \right)$$

Total heat required for separation (simplified calculations)

Burning 1 kmole of coal generates one kmole of CO₂, and ~ 360 MJ of heat.

For each kmole of CO₂, 2 kmoles of MEA are needed. With 10% sorbent molar concentration in water (or 0.27 by mass, MW_{sorb}=61), one needs 7.3 kmoles solvent.

The reaction energy of desorption is 1.919 MJ/kgCO₂, or (1.919x44)= **84.5 MJ** for 1 kmole CO₂.

But some water evaporates, $\Delta h_{\text{evap}} \sim 2.25$ MJ/kg_{water}. Assume ~ 1 kmole of water evaporates per mole CO₂ removed, we need (2.25x18)= **40 MJ**.

Thus, the total thermal energy in the reboiler is ~ 84.5+40= **124.5 MJ**.

Thus ~ (124/36) or one third of the original thermal energy is needed for CO₂ capture.

More energy is used to raise the solvent T (some comes from regeneration), and for pumping the solvent through the loop. The work penalty is less because this is “lower quality heat”.

APPLICATIONS: Chemical scrubbing of CO₂ from flue gases has been used extensively:

During 1982-1986, an aqueous solution of MEA was used in: Lubbock Power plant, Texas, NG was fired in a 50 MW plant, producing near 1000 t/d of CO₂ (for EOR)

And in a coal-steam generator in Carlsbad NM producing 113 t/d (also EOR)

Since 1991, CO₂ scrubbing using 15-20% MEA solutions in the 300 MW Shady Point CHP Plant in Oklahoma, producing nearly 400 t/d CO₂, used in food industry and EOR.

Norway Sleipner Vest gas field separates CO₂ from the recovered natural gas to reduce CO₂ concentration in the produced gas from 95% to 2.5%. The separated CO₂ is then injected back into a 250 m deep aquifer located 800 m below the ocean surface.

A similar project in Indonesia in which the CO percentage of CO₂ in the recovered gas will be reduced from 71 to almost zero.

In Algeria, the In Salah field

Malaysia



North Dakota



Figure TS.4. (a) CO₂ post-combustion capture at a plant in Malaysia. This plant employs a chemical absorption process to separate 0.2 MtCO₂ per year from the flue gas stream of a gas-fired power plant for urea production (Courtesy of Mitsubishi Heavy Industries). (b) CO₂ pre-combustion capture at a coal gasification plant in North Dakota, USA. This plant employs a physical solvent process to separate 3.3 MtCO₂ per year from a gas stream to produce synthetic natural gas. Part of the captured CO₂ is used for an EOR project in Canada.

© Source unknown. All rights reserved. This content is excluded from our Creative Commons license. For more information, see <https://ocw.mit.edu/fairuse>.

EOR and the Dakota Gasification Company

250 million cu.ft. per day CO₂ by-product of coal gasification

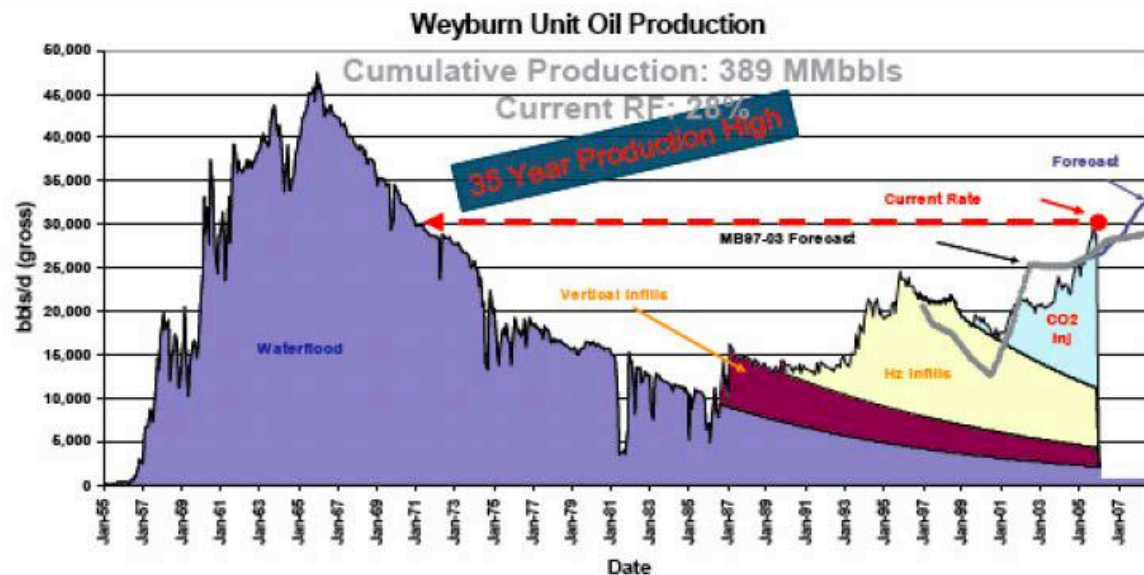
95 million cu.ft. per day contracted for Weyburn project

320 km pipeline

CO₂ purity 95%

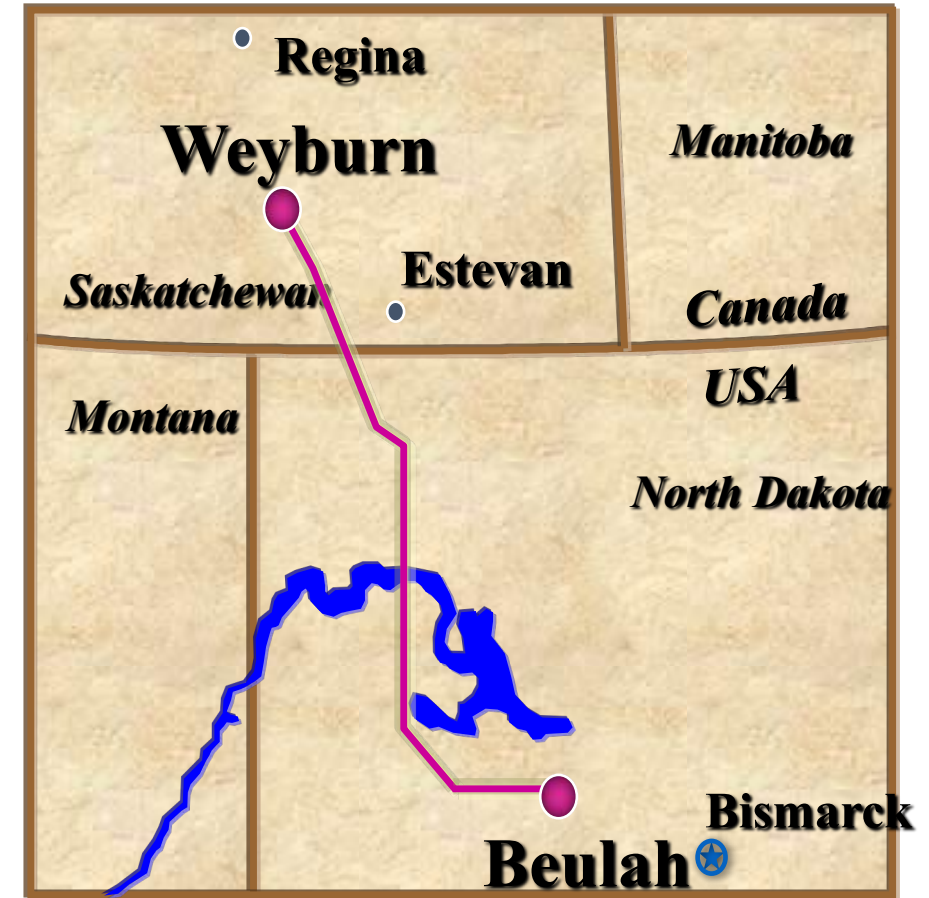
CO₂ pressure 14MPa

Weyburn Oil Production

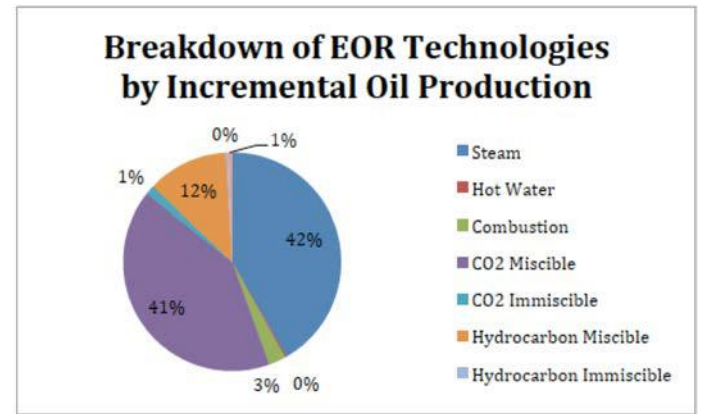
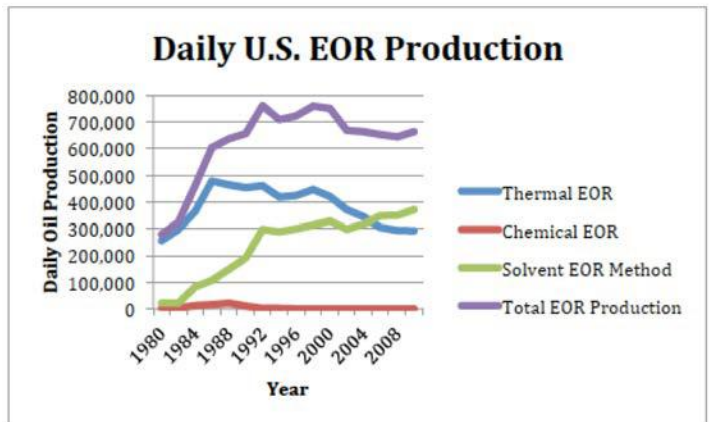
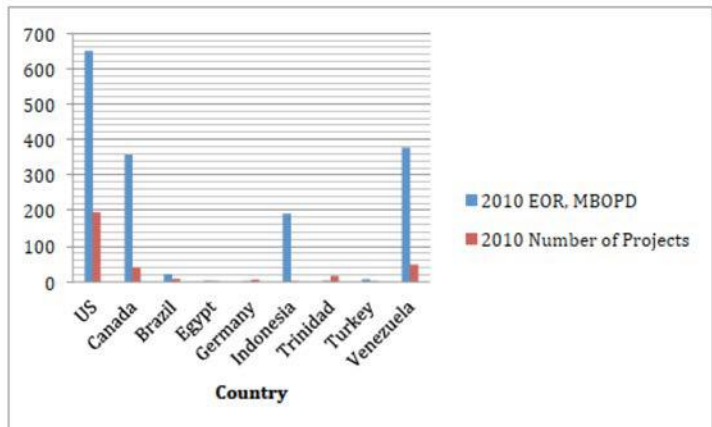


Source: EnCana Corporation (via Don Langley, B&W)

© EnCana Corporation. All rights reserved. This content is excluded from our Creative Commons license. For more information, see <https://ocw.mit.edu/fairuse>.



© Source unknown. All rights reserved. This content is excluded from our Creative Commons license. For more information, see <https://ocw.mit.edu/fairuse>.



Koottungal "Special Report: 2010 worldwide EOR survey," the oil and gas J., 14 (2010)

© Endeavor Business Media, LLC. All rights reserved. This content is excluded from our Creative Commons license. For more information, see <https://ocw.mit.edu/fairuse>.

Carbon Dioxide Pipelines in Operation in North America

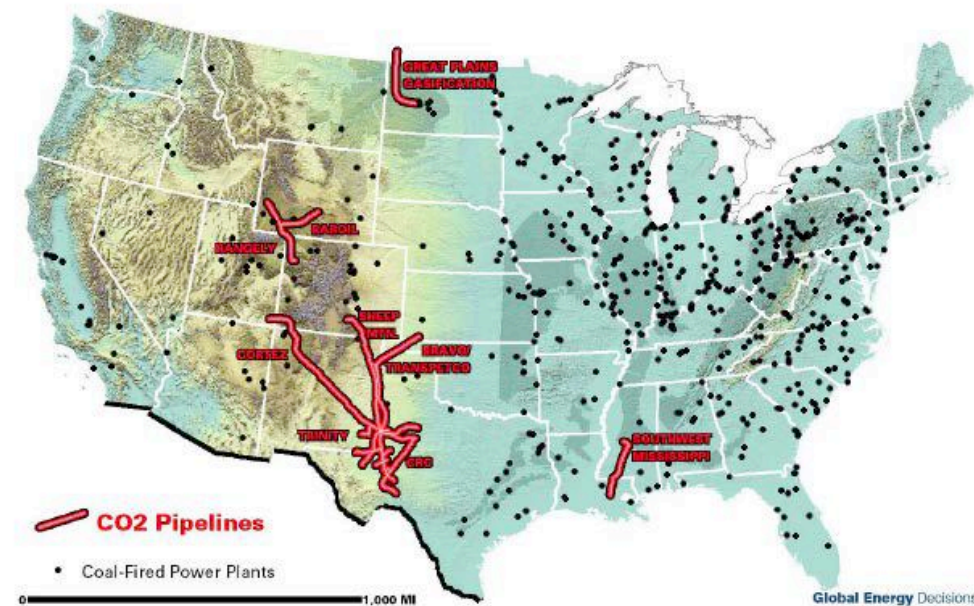
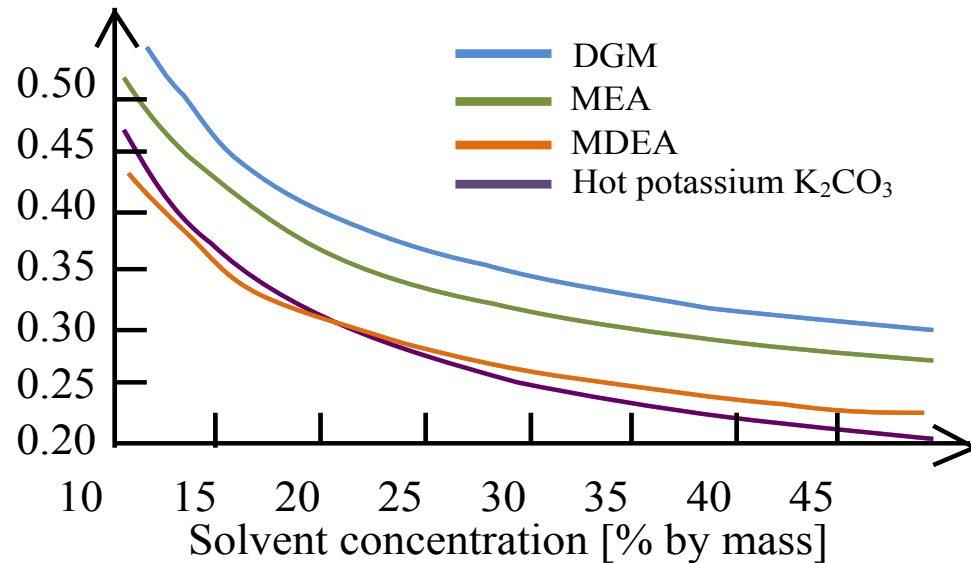


Figure 6.3

Coal: America's Energy Future, The National Coal Council, March 2006.

© Global Energy Decisions LLC. All rights reserved. This content is excluded from our Creative Commons license. For more information, see <https://ocw.mit.edu/fairuse>.

Sorbents with lower desorption reaction enthalpy are under development

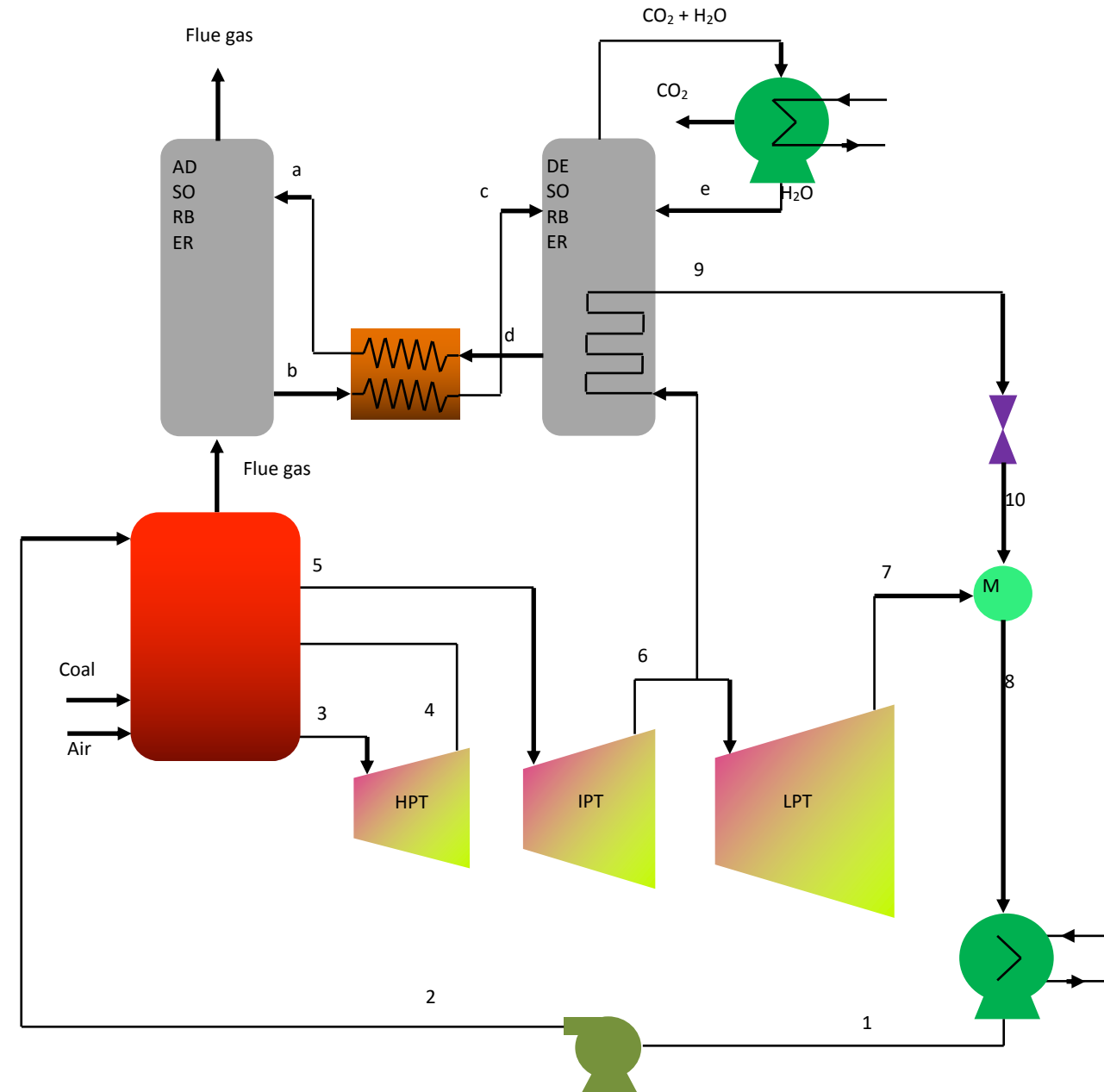


		MJ/kg_CO2
Monoethanolamine (MEA)	$R \equiv (-CH_2CH_2OH)$	1.919
Diethanolamine (DEA)	$R = (-CH_2CH_2OH)_2$	1.519
Triethanolamine (TEA),		0.989
Methyldiethanolamine (MDEA),		1.105

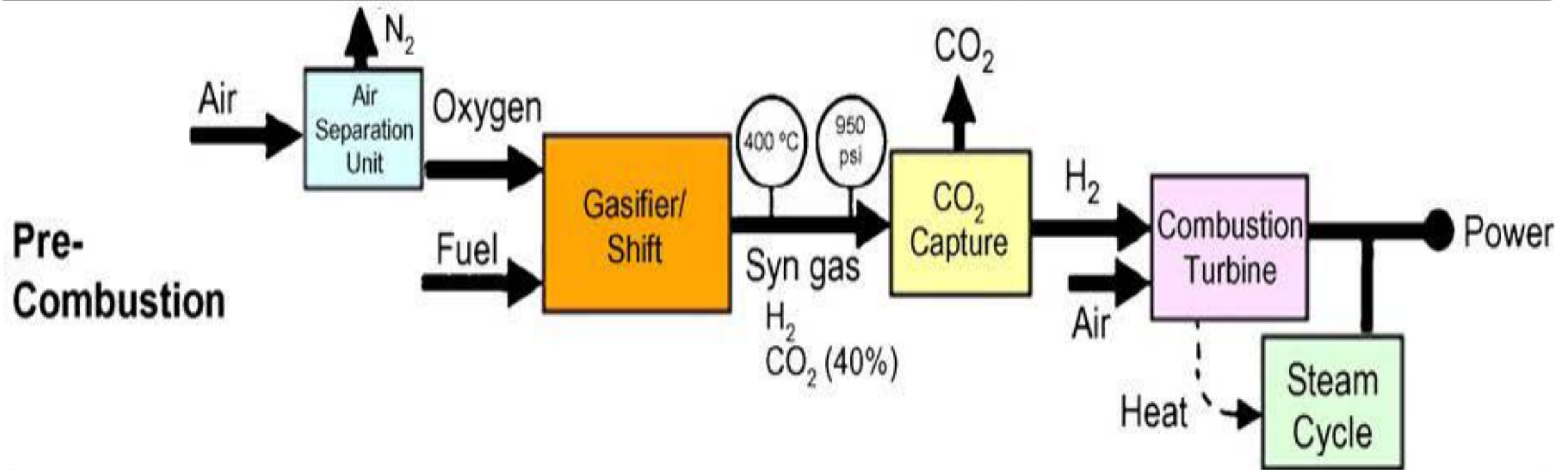
Energy penalty for CO₂ separation using chemical absorption expressed as work (exergy) or reduction of electricity production in kWh/kgCO₂. Increasing the concentration of the sorbent in the solution reduces the energy required for CO₂ removal. With higher sorbent concentration, more energy is expended in the desorption reaction enthalpy than in heating and evaporating the solvent. However, higher sorbent concentration can be corrosive, and mass concentrations below 30% have been recommended (kWh = 3.6 MJ). DGA is known as Econamine (n diglycolamine in aqueous solution), MDEA is 2n mythyldiethanolamine.

Integration of Separation with the Power Cycle

- Works by extracting steam at lower T (~ 150 C), i.e., from lower pressure sections of steam turbine, to reduce exergy losses in the cycle.
- MAE works with (in the presence of) SO_x .
- For monoethanolamine, or MEA, a SO_x level of less than 10 ppmv is desired for the Fluor Daniel EconamineTM process.
- A level of 50-100 ppmv can be tolerated by the KEPCO/MHI process



Approaches for CO₂ capture: pre-combustion capture



Separate CO₂ from CO₂+N₂

(2) SEPARATION by Physical Absorption (in a liquid)

Works well for separating H₂+CO₂ mixture (pre-combustion capture)

- In a given solvent, different gases have different solubility (different values of Henry's constant), and hence get absorbed at different fractions by the liquid solvent.
- "Selectivity" is measured by the relative value of the solubility, or He.
- Higher pressure and lower temperature favors absorption.
- Lowering the pressure or raising the temperature of the solvent causes the gas to escape.

In gas-liquid equilibrium (at low concentration)

$$X_{L,j} = \frac{p_j}{He_j} = \frac{p}{He_j(T)} X_{V,j}$$

$X_{L,j}$ Mole fraction of gas "j" dissolved in liquid

p_j Gas "j" partial pressure in the gas phase

p Total pressure of gas mixture in contact with liquid

$X_{V,j}$ "j" mole fraction in gas mixture in contact with liquid

He_j Henry's constant of gas "j" in the liquid

Henry's constant for a number of gases in methanol, measured in **MPa/(mol/kg methanol)**, at two different temperatures. It decreases rapidly with T

gas	- 40 C	- 70 C
Hydrogen sulfide H ₂ S	0.28	0.026
Carbon dioxide	1.4	0.31
methane	70	30
hydrogen	670	930

A continuous separation process using physical absorption

the fraction of CO_2 in liquid is: $X_{L,\text{CO}_2} = \frac{p_{\text{CO}_2}}{He_{\text{CO}_2}} = \frac{X_{V,\text{CO}_2}}{He_{\text{CO}_2}} p$

this fraction increases significantly at high p and low T (low He)

If all the CO_2 (fraction $X_{V,\text{CO}_2,\text{in}}$) in the gas stream $\dot{n}_{\text{prod},\text{in}}$ is absorbed by solvent \dot{n}_{sol} (leaving with $X_{L,\text{CO}_2,\text{out}}$):

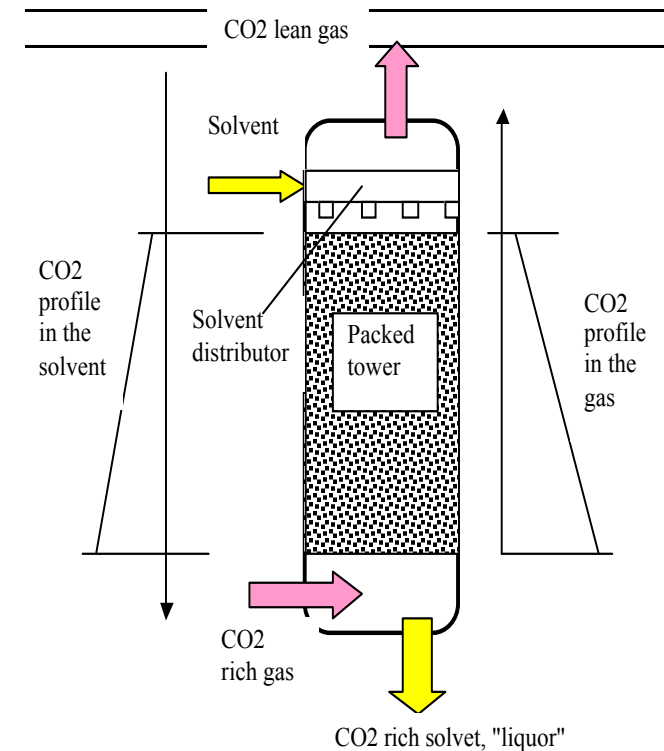
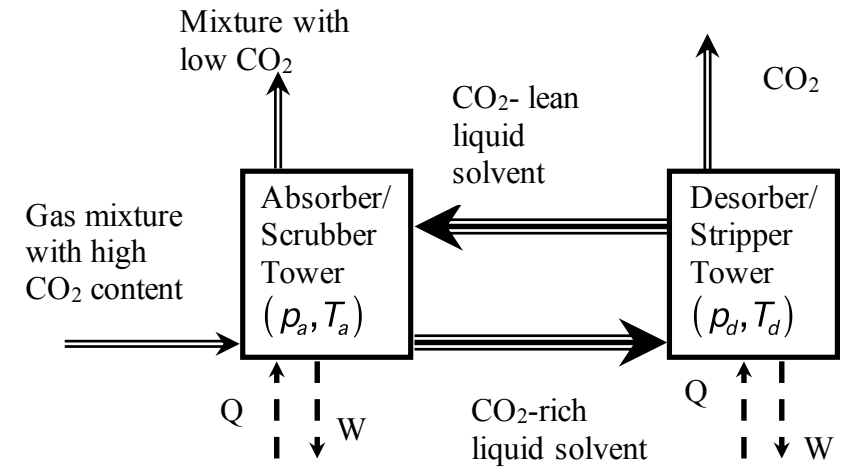
$$\dot{n}_{\text{prod},\text{in}} X_{V,\text{CO}_2,\text{in}} = \dot{n}_{\text{sol}} X_{L,\text{CO}_2,\text{out}}$$

The required solvent flow rate (from the two equations):

$$\dot{n}_{\text{sol}} = \frac{He}{p} \dot{n}_{\text{prod},\text{in}}$$

Power required to move fluid: $\wp_{\text{pump}} = \dot{V}_{\text{sol}} \frac{\Delta p}{\eta_{\text{pump}}}$

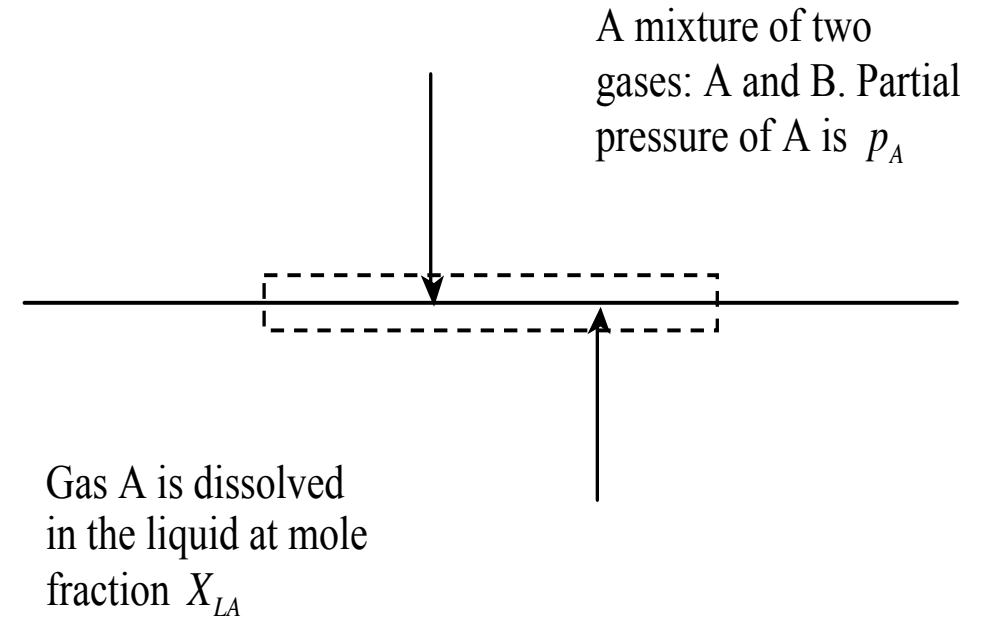
$$\Delta p_{\text{total}} = \Delta p_{\text{between tanks}} + \Delta p_{\text{across Absorber}} + \Delta p_{\text{across Desorber}}$$



$$X_{L,A} = \frac{p_A}{He_A} = \frac{p}{He_A(T)} X_{V,A}$$

Henry's constant (in bars) in water at low to moderate pressures

Solute	290 K	300 K	310 K	320 K	330 K	340 K
H ₂ S	440	560	700	830	980	1140
CO ₂	1280	1710	2170	2720	3220	-
O ₂	38000	45000	52000	57000	61000	65000
H ₂	67000	72000	75000	76000	77000	76000
CO	51000	60000	67000	74000	80000	84000
Air	62000	74000	84000	92000	99000	104000
N ₂	76000	89000	101000	110000	118000	124000



- Higher He means that less gas is absorbed in the liquid at the given temperature
- As T decreases, more gas is absorbed, and vice versa (temperature swing processes)
- Water absorbs a lot more CO₂ than nitrogen, i.e., it is more selective to CO₂.
- Gas can also be desorbed from the liquid by reducing the pressure (pressure swing processes)

Changing the pressure to release the gas, Pressure Swing Absorption (PSA):

@ 10 atm and -70 C , a gas mixture in which the molar concentration of CO_2 is 10% is in equilibrium with a methanol solvent in which the molar concentration of CO_2 is (He is in MPa/(mol/kg_methanol) is:

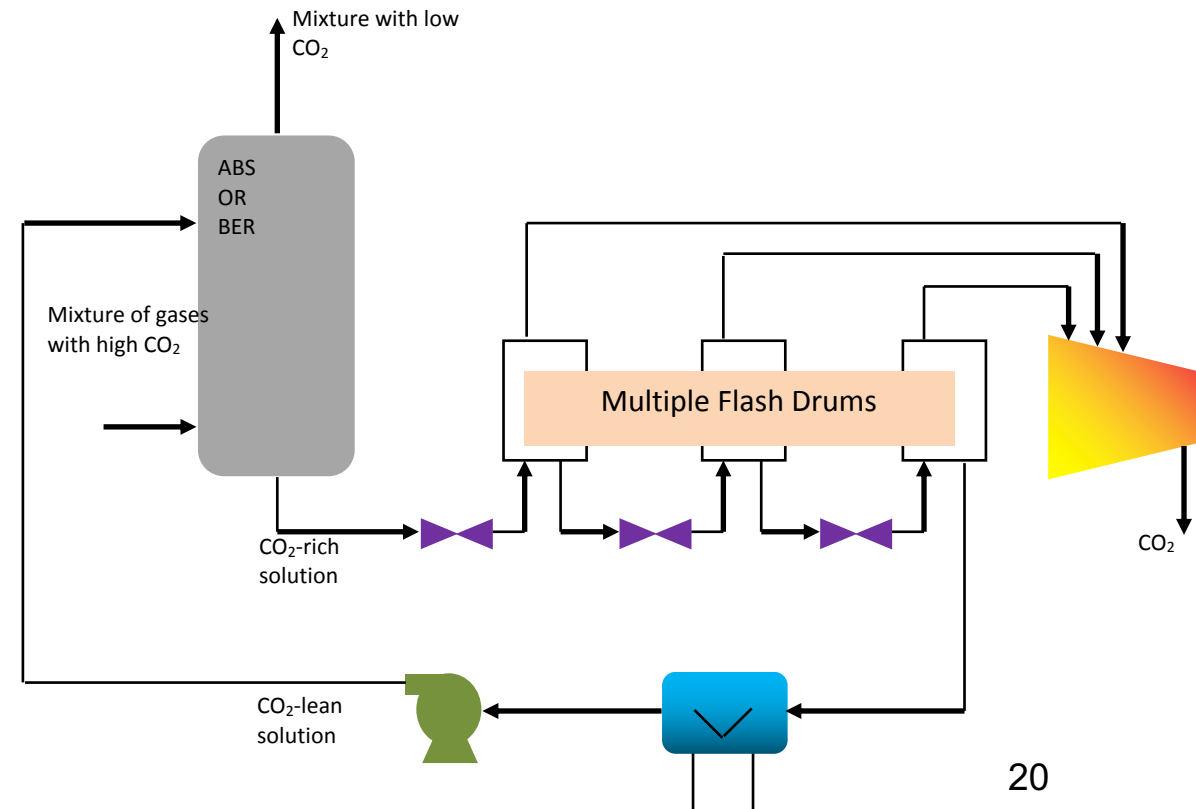
$$X_{L,\text{CO}_2}(1\text{ MPa}, -70\text{ C}) = \frac{X_{V,\text{CO}_2} = 0.1 \cdot p = 1}{He = 0.31} = 0.32\text{ mol/kg_methanol}.$$

If this solvent is transported to another vessel in which the pressure is 0.1 atm (pure CO_2 , $X_{V,\text{CO}_2}=1$), the equilibrium concentration of CO_2 in methanol drops to

$$X_{L,\text{CO}_2}(0.01\text{ MPa}, -70\text{ C}) = \frac{X_{V,\text{CO}_2} = 1 \cdot p = 0.01}{He = 0.31} = 0.032\text{ mol/kg_methanol}$$

and 0.288 mol of CO_2 per kg of solvent is released.

- (1) Methanol, used in **the Rectisol process**;
- (2) N-methyl-2-pyrrolidone (NMP), used in **the Purisol process**;
- (3) Dimethylether polyethylene glycol (DMPEG), used in **the Selexol process**.



Changing the pressure and temperature to release the gas

@ 10 atm and -70 C , a gas mixture in which the molar concentration of CO_2 is 10% is in equilibrium with a methanol solvent in which the molar concentration of CO_2 is

$$X_{L,\text{CO}_2}(1\text{ MPa}, -70\text{ C}) = \frac{X_{V,\text{CO}_2} = 0.1 \cdot p = 1}{He = 0.31} = 0.32 .$$

If pressure is reduced to 1 atm and the temperature is raised to -40 C , the new equilibrium concentration of CO_2 in the solvent is,

$$X_{L,\text{CO}_2}(0.1\text{ MPa}, -40\text{ C}) = \frac{p = 0.1}{He = 1.4} = 0.071 ,$$

and 0.249 moles CO_2 is released per kg_methanol.

This is the pressure-temperature swing separation (PTSA).

(3) Physical Separation by Adsorption (in a solid) with Pressure or Temperature Swing

Langmuir Isotherm for gas-solid surface equilibrium

$$\theta_i = \frac{p_i}{1 / K_i(T) + p_i}$$

θ_i : fraction of occupied sites by gas "i" on solid surface.

p_i : partial pressure of gas "i" in contact with solid surface.

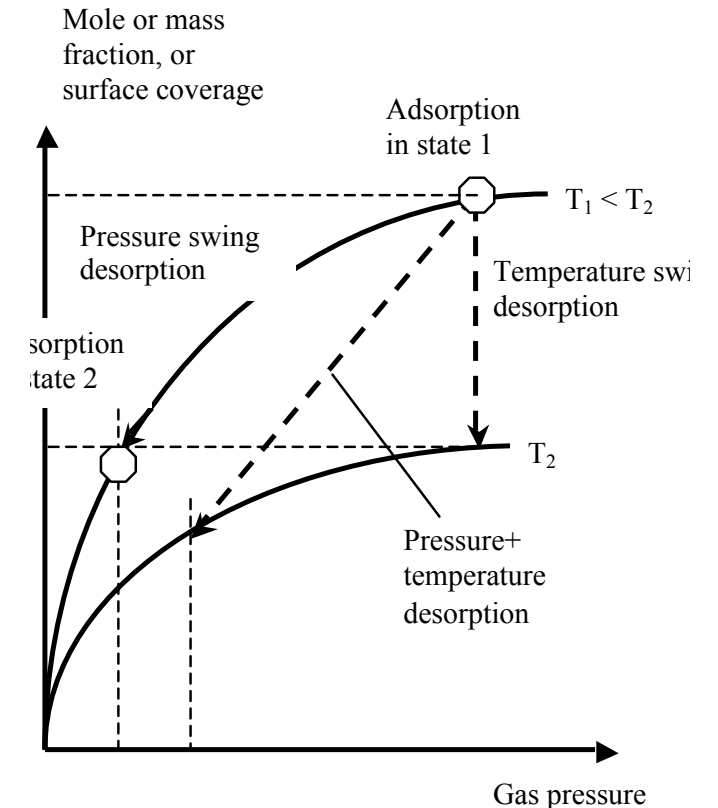
At low p_i , $\theta_i \approx K_i(T) p_i$ and at high p_i , $\theta_i \approx K_i(T)$

In terms of C_i is the concentration of gas in solid,

$$C_i = \frac{\alpha_s p_i}{1 / K_i(T) + p_i} = \frac{\alpha_s X_i}{1 / p K_i(T) + X_i}, \text{ where } \alpha_s = (A_s / \nabla) \tilde{\Gamma} / N_a$$

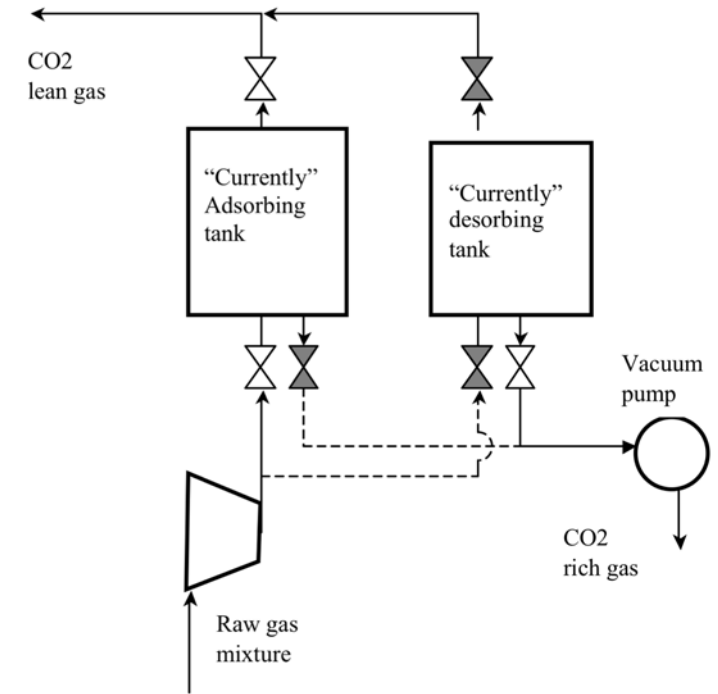
A_s / ∇ : surface area/volume, and $\tilde{\Gamma}$: number of site/area

the gas concentration on the solid depends on $K_i(T)$ and p



Solid Absorbers

- **Activated carbon**, manufactured from carbonaceous matter such as coal, petroleum coke and wood, are used in the powder form.
- Activation involves carbonization, i.e., elimination of volatile matter and partial gasification to develop the porosity and enlarge surface area.
- The pore surface area is high, 300-2500 m²/g, largest among all known adsorbents.
- The pore diameter in activated carbon is 10-35 Å.
- The heat of adsorption of activated carbon is generally lower than that of other adsorbents, and stripping the adsorbate requires less energy.
- Activated carbon is nearly hydrophobic to low humidity mixtures, and hence can be used in separating humid gas mixtures.



Compatible with availability of high p stream as in IGCC, pre-combustion capture application.

- **Molecular sieves carbon (MSC)** is produced by carbonization of polymers such as cellulose and sugar, and other methods.
- The pore structure and pore diameter depends on the original material and the carbonization temperature. Pore diameters in the range of 2-8 Å have been demonstrated.
- These are used in ASU's and in other applications in the chemical industry.
- Carbon (3%) deposited into the pores of lignite char by cracking methane at 855 °C produces MSC that shows significant molecular sieving between CO₂ (admitted) and N₂ (hindered). CO₂ is a linear molecule that is thought to have a diameter of 3.7 Å.

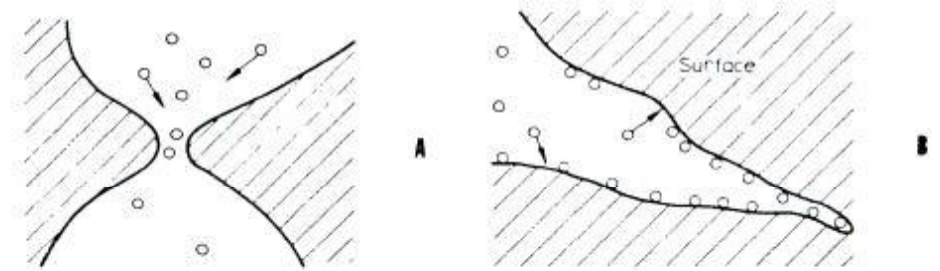


Figure 2.5 Molecular-sieve carbons made by Bergbau-Forschung: (A) Type CMSN2 with bottlenecks near 5 Å formed by coke deposition at the pore mouth; (B) Type CMSH2 formed by steam activation. Source: Jüntgen, Knoblauch, and Harder [34]. Reprinted with permission.

© Imperial College Press. All rights reserved. This content is excluded from our Creative Commons license. For more information, see <https://ocw.mit.edu/fairuse>.

Yang, R.T., Gas Separation by Adsorption Processes, Imperial College Press, 1997

- **Zeolites** are crystalline aluminosilicates of alkali or alkali earth elements such as sodium, potassium and calcium.
- The basic structure of zeolite is an aluminosilicate skeleton, with a window aperture of 3-10 Å.
- Sorption into zeolites can occur with great selectivity because of the size of the window, and they can also act as molecular sieve.
- Zeolites come in a variety of structures (see figure) depending on how they are manufactured.
- They have been used in hydrogen purification and air separation.

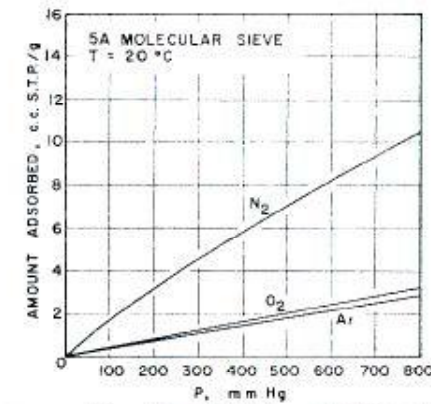


Figure 7.20 Isotherms on 5A zeolite [57]. The selectivity ratio for N_2/O_2 declines gradually to slightly less than 2 as the pressure is increased to 8 atm [58]. Source: Lee and Stahl [20]. Reprinted with permission.

Gottlicher, G., The Energetics of Carbon Dioxide Capture in Power Plants, The US DOE, Office of Fossil Energy, NETL, Feb 2004

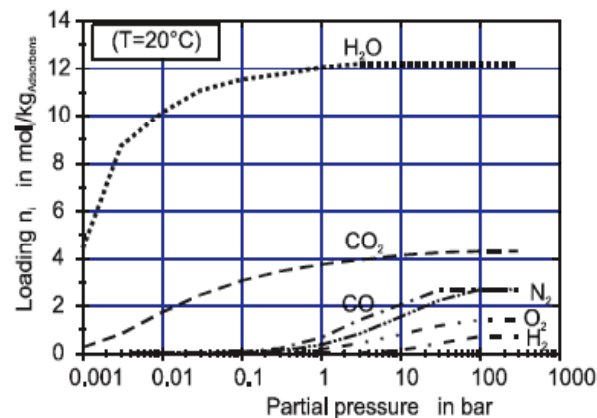
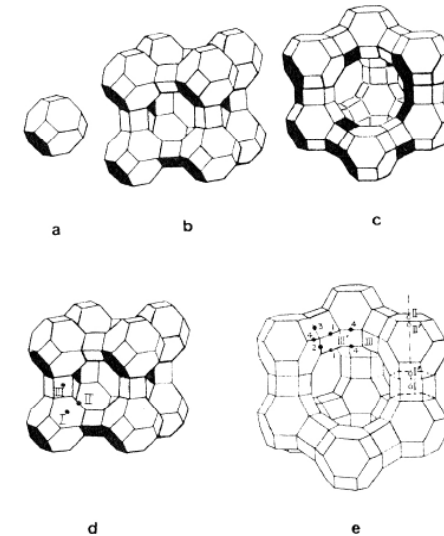


Image courtesy of DOE.

Figure 3.17: Adsorption isotherms of the pure components for zeolite 5A molecular sieve at 20°C ⁴²

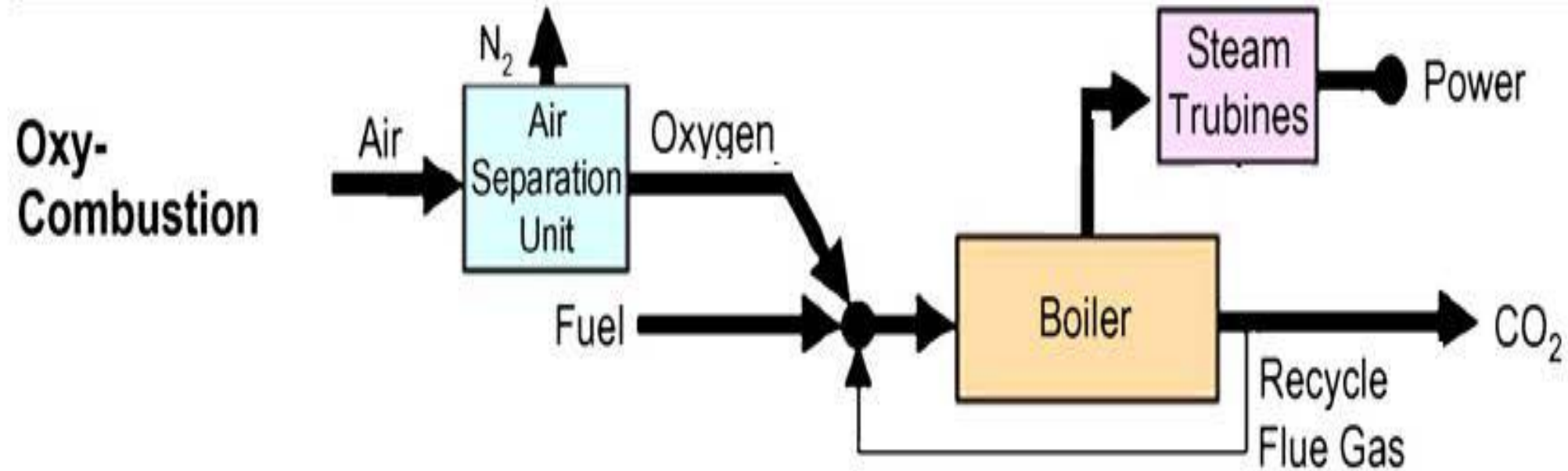
Amount of gas adsorbed in zeolite molecular sieve, in mol/kg_adsorbent @ 20 C for different partial pressure of the adsorbed gas. Trends follow Langmuir isotherm and show CO₂-H₂ selectivity.



© Imperial College Press. All rights reserved. This content is excluded from our Creative Commons license. For more information, see <https://ocw.mit.edu/fairuse>.

Yang, R.T., Gas Separation by Adsorption Processes, Imperial College Press, 1997

Approaches for CO₂ capture: Oxy-combustion capture



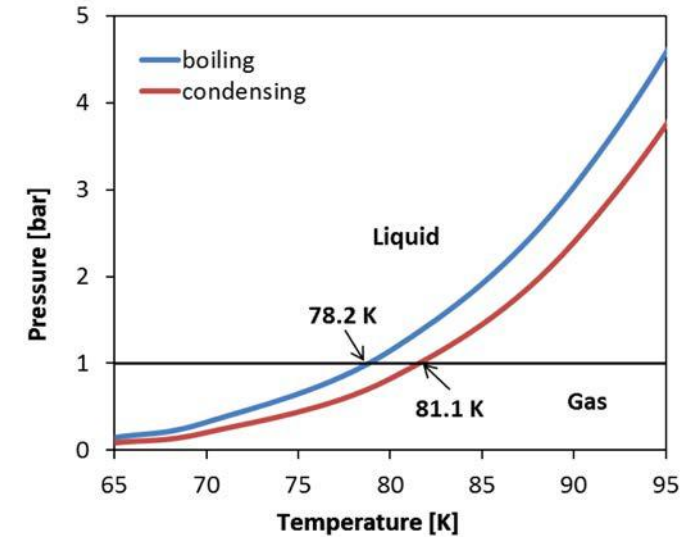
Separate O₂ from O₂+N₂

Liquefaction & Cryogenic Air Separation

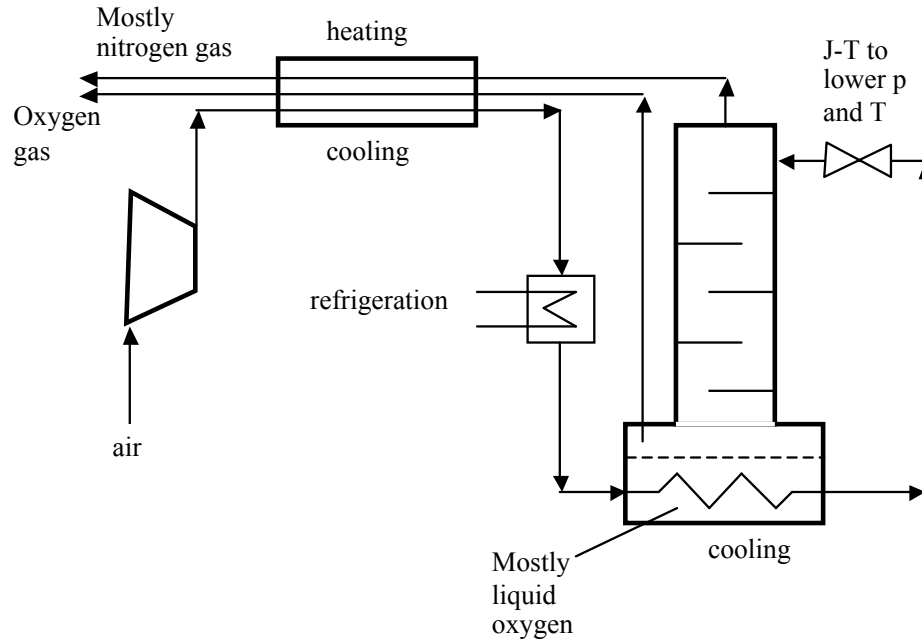
Ref: <http://www.thermopedia.com/content/553>

At atmospheric pressure, the boiling/condensation temperature of oxygen is 90 K (-183 C) and of nitrogen is 77 K (-196 C) (nitrogen is more volatile than oxygen as it evaporates at lower temperature).

When air is cooled at atm. pressure, it remains gas till 81.6 K. and completely liquefy at 79 K (inverse when heated)



Two figures have been removed due to copyright restrictions. Please see the figures on page: <http://hyperphysics.phy-astr.gsu.edu/hbase/thermo/liqair.html>.



A column distillation cycle for air separation. Air is compressed, then cooled in a regeneration unit using the separation products (N_2 and O_2), and a refrigeration unit. A Joule-Thompson valve lowers p and T , i.e., flashes air into a distillation column to separate oxygen and nitrogen. Energy expended is in air compression and refrigeration.

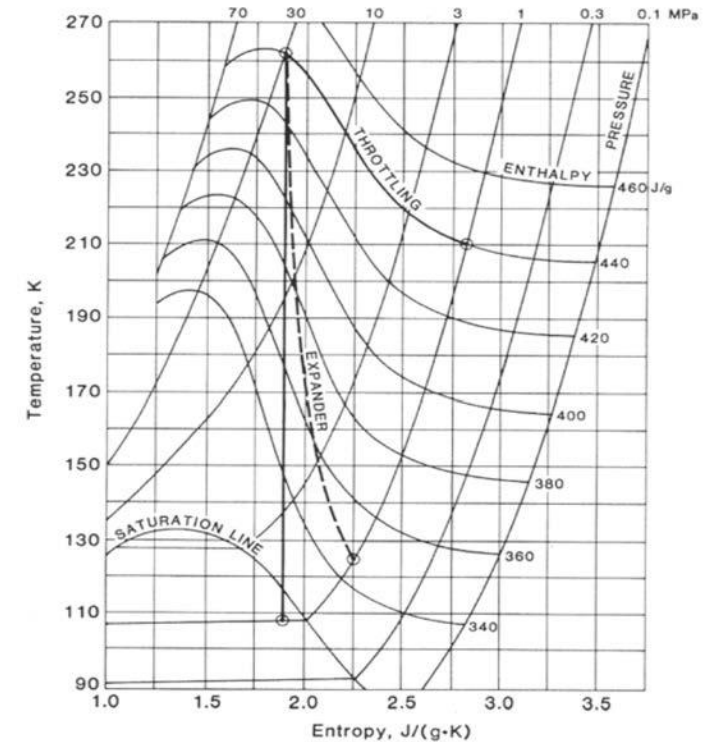
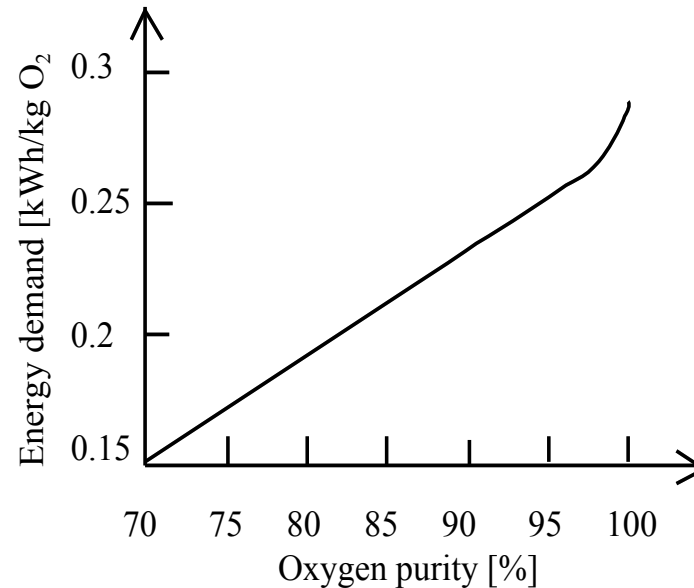


Figure 5.4 Comparison for air of Joule-Thomson cooling with cooling by a mechanical expander.

© Source unknown. All rights reserved. This content is excluded from our Creative Commons license. For more information, see <https://ocw.mit.edu/fairuse>.

Air Separation energy ~ 1 MJ/kg_O2

The energy requirement for air separation depends strongly on the purity of the products streams. To achieve 90% oxygen purity (volume fraction) air must be pressurized to 5 bars. Higher purity requires pressure up to 10 bar. The products are delivered at pressures and temperatures close to the atmospheric values.



Energy required to produce oxygen in a large scale double column facility.

Gotticher, G., The Energetics of Carbon Dioxide Capture in Power Plants, The US DOE, Office of Fossil Energy, NETL, Feb 2004

Image courtesy of DOE.

Ideal work for air separation is 0.104 kWh/kg_O2, or 0.374 MJ/kg_O2. Air separation efficiencies in cryogenic plants are low, 15-30%.

R.F. Probstein and R. E. Hicks, *Synthetic Fuels*,

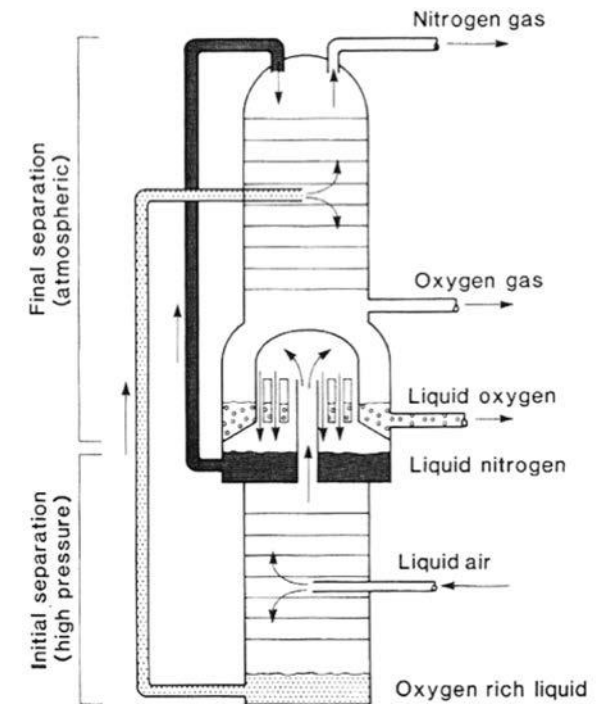
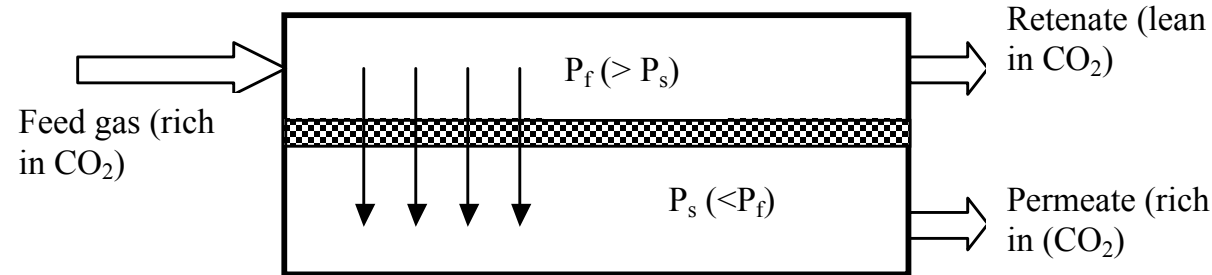


Figure 5.6 Distillation column for fractional separation of liquid air (after Ref. 11).

© Source unknown. All rights reserved. This content is excluded from our Creative Commons license. For more information, see <https://ocw.mit.edu/fairuse>.

(2) Membrane Separation



For porous membranes, the flux of one gas is

$$J_i = \frac{D_{ei}}{\mathfrak{RT} \ell} \Delta p_i = \tilde{Q}_i (p_{i,f} - p_{i,s}) = \tilde{Q}_i (X_{i,f} p_f - X_{i,s} p_s) = \frac{\tilde{q}}{\ell} (X_{i,f} p_f - X_{i,s} p_s)$$

D_{ei} is the effective diffusivity of gas component i

\tilde{Q} is permeability, ℓ is the membrane thickness, \tilde{q} is permeability coefficient

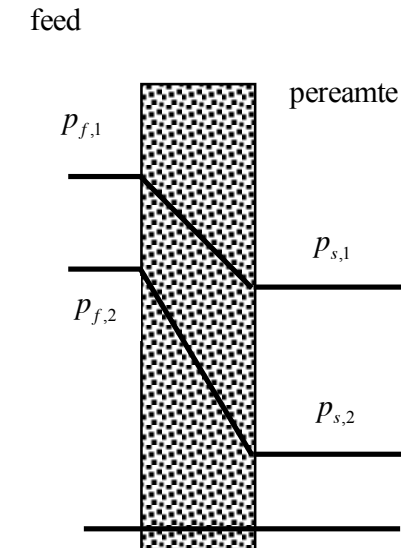
f and s (or p) correspond to feed and sweep (or permeate) sides

Most gases can diffuse across porous and polymer membranes,

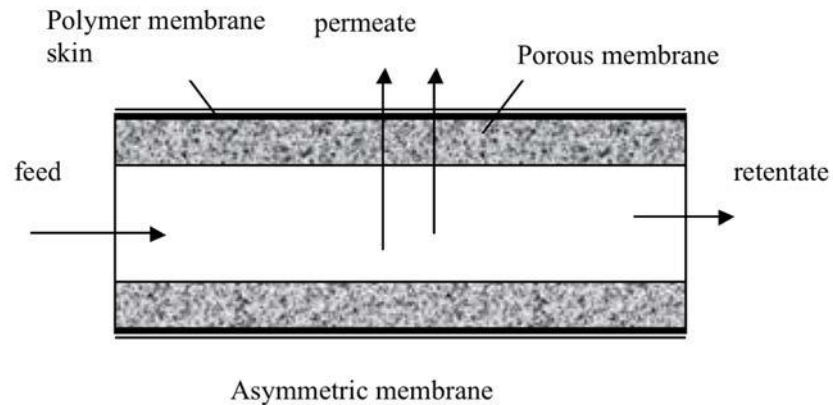
But they diffuse at different rates depending on their value of D_{ei}

The selectivity, $\alpha_{ij} = \frac{\tilde{Q}_i}{\tilde{Q}_j}$, is the ratio of permeabilities of two gases

The selectivity determines the effectiveness of separation



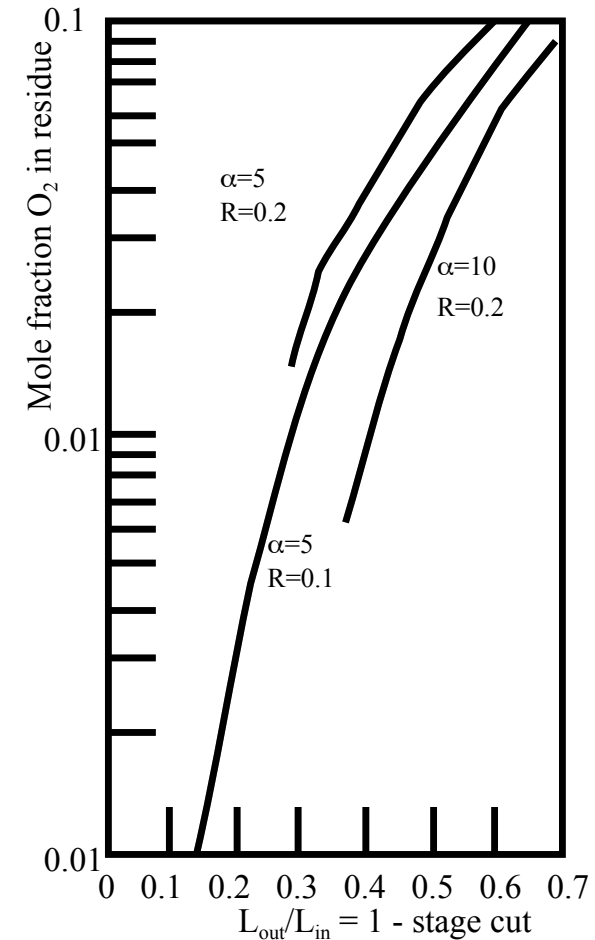
For a porous membrane



Permeability, Q , in $m_N^3 m^{-2} Pa^{-1} s^{-1}$ of the main components of coal gas at 40 °C for the Ube membrane.

Hydrogen	1374
Carbon monoxide	23
Carbon dioxide	461
Nitrogen	13
Argon	31

McCabe, W.L., Smith, J.C., and Harriott, P., Unit Operations of Chemical Engineering, 7th Edition, McGraw Hill, 2005



The production of nitrogen from air in a counter flow membrane separator, showing the residual oxygen in the nitrogen stream as function of the flow rate ratio. α is the membrane selectivity (Q_{O_2}/Q_{N_2}), R is the pressure ratio across the membrane, L is the feed rate.

$$\wp_c = \frac{1}{\eta_c} n \frac{k\Re}{k-1} \left(\left(\frac{p_{out}}{p_{in}} \right)^{\frac{k-1}{nK}} - 1 \right) J_c$$

J_c is the molar flux through the compressor,

n is the number of compression stages,

T_o is the temperature before each compression stage

p_{out} is the pressure after a compression stage,

p_{in} is the pressures before a compression stage,

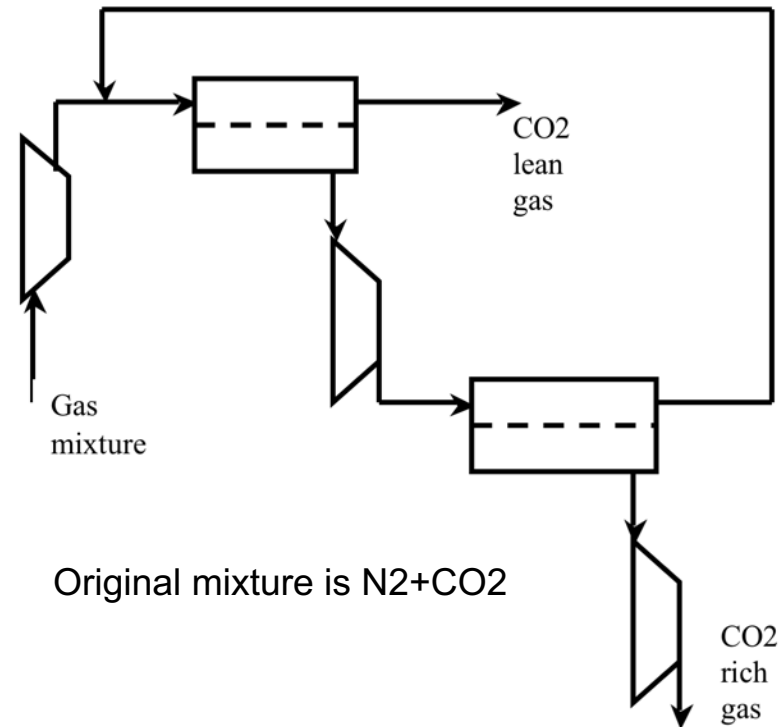
K is the isentropic index of the gas through the stage

η_c is the isentropic efficiency of the compressor.

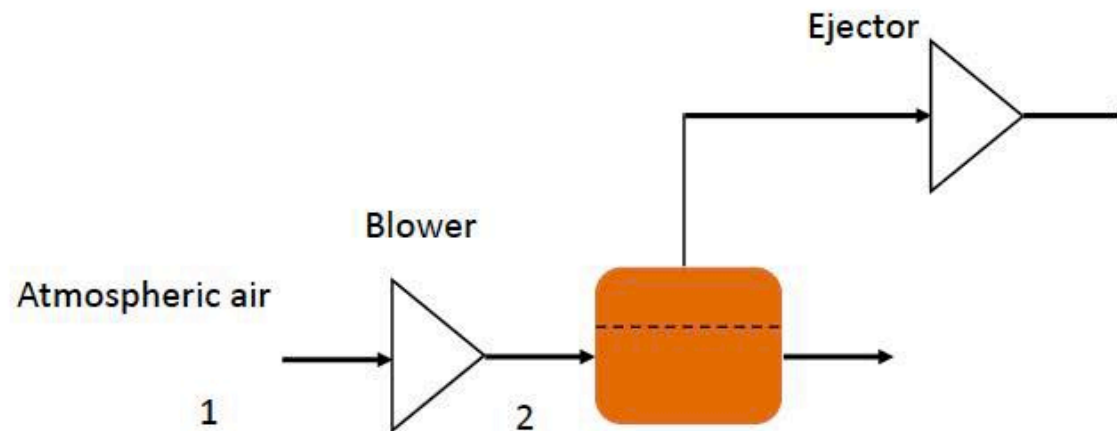
$\Re = 8.314 \text{ J / mol K}$

Because of finite permeability of different gases, producing near pure gases requires multi stages, significantly increasing the work.

Energy Requirements:



Example 9.5. An air separation unit (ASU) consisting of a blower, a membrane and an ejector, is shown below. Atmospheric air at 30 °C and 1 atm is sucked through the blower and fed to the membrane at 1.1 atm. The oxygen mole fraction at the permeate side is 35%. The ejector maintains a pressure of 0.3 atm on the permeate side. The membrane is made of a special silicon rubber with 1.5 μm thickness and 10 m^2 area. The permeability coefficient of oxygen is 500 Barrer (at STP). The behavior of gas in all parts of the system can be approximated as an ideal gas. (a) Assuming perfect mixing at the feed and the permeate sides, determine the daily production of the oxygen-enriched stream. (b) Take an isentropic efficiency of 75% for the blower and ejector, and that ; calculate the energy requirement of this unit.



permeability coefficient is $\tilde{p}_{O_2} = 500 \text{ Barrer} = 500 \times 7.500.5 \times 10^{-18} \text{ m}^2 / (\text{s Pa})$

$$J_{O_2} = \frac{\tilde{p}_{O_2}}{t_m} (X_{f,O_2} p_f - X_{p,O_2} p_p) = 3.191 \times 10^{-5} \text{ m}^3 / (\text{m}^2 \cdot \text{s})$$

$$\dot{V}_p = \frac{J_{O_2} A}{X_{p,O_2}} = 0.000912 \text{ m}^3/\text{s} \quad \text{and}$$

$$\dot{m}_p = \left(X_{p,O_2} M_{O_2} + X_{p,N_2} M_{N_2} \right) \frac{p \dot{V}_p}{\Re T} = 0.001078 \text{ kg} / \text{s}$$

total per day is 93.2 kg

$$\dot{W} = \dot{m} c_p \left(\frac{T_{2s} - T_1}{\eta} \right) \quad \text{and} \quad T_{2s} = T_1 \left(\frac{p_2}{p_1} \right)^{\frac{k-1}{k}}$$

$$\dot{W}_{blower} = 241.4 \text{ W} \quad \text{and} \quad \dot{W}_{ejector} = 183.7 \text{ W}$$

MIT OpenCourseWare
<https://ocw.mit.edu/>

2.60J Fundamentals of Advanced Energy Conversion
Spring 2020

For information about citing these materials or our Terms of Use, visit: <https://ocw.mit.edu/terms>.

Lecture # 20

CO₂ CAPTURE and STORAGE Mostly NG but with some Coal

Ahmed Ghoniem

April 15, 2020

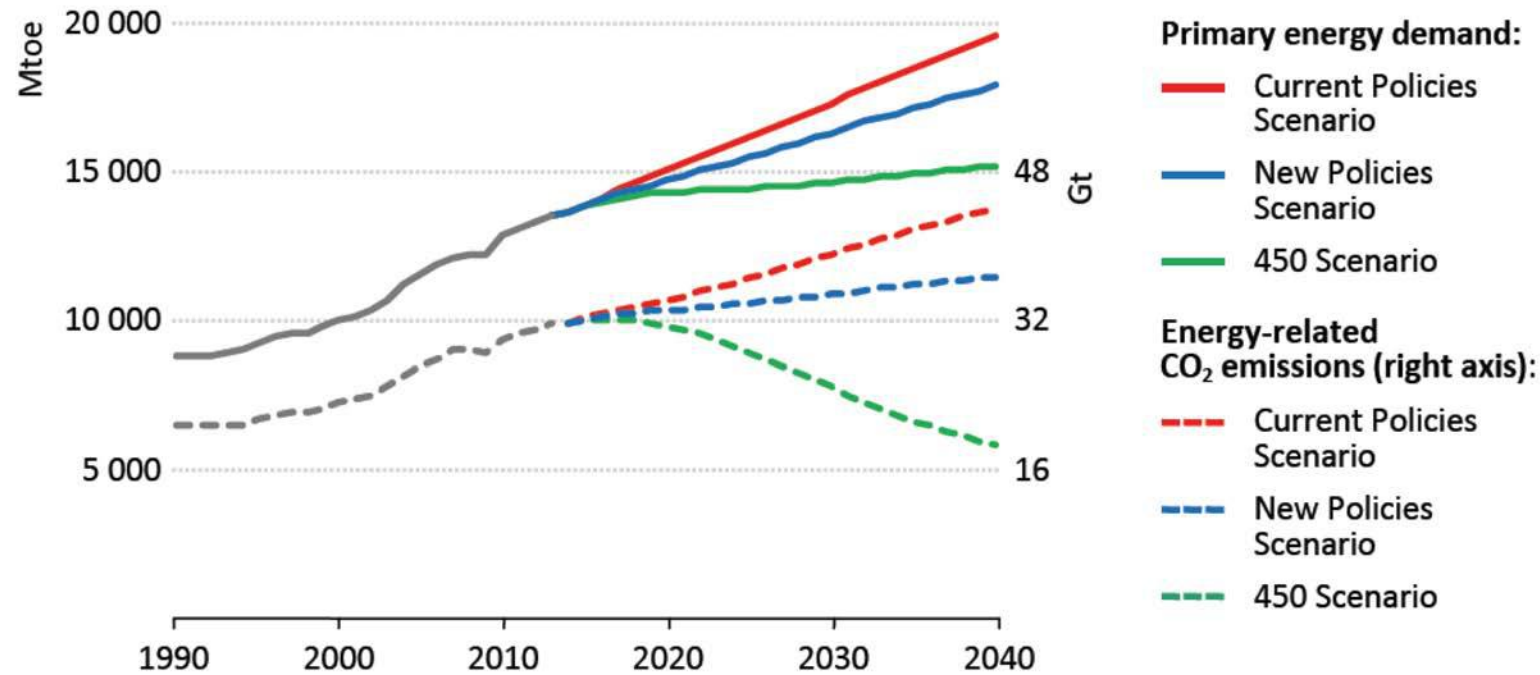
CO₂ reduction and improved efficiency

CO₂ Capture Schemes

CO₂ Capture Enabled Cycles

CO₂ Sequestration

COP21

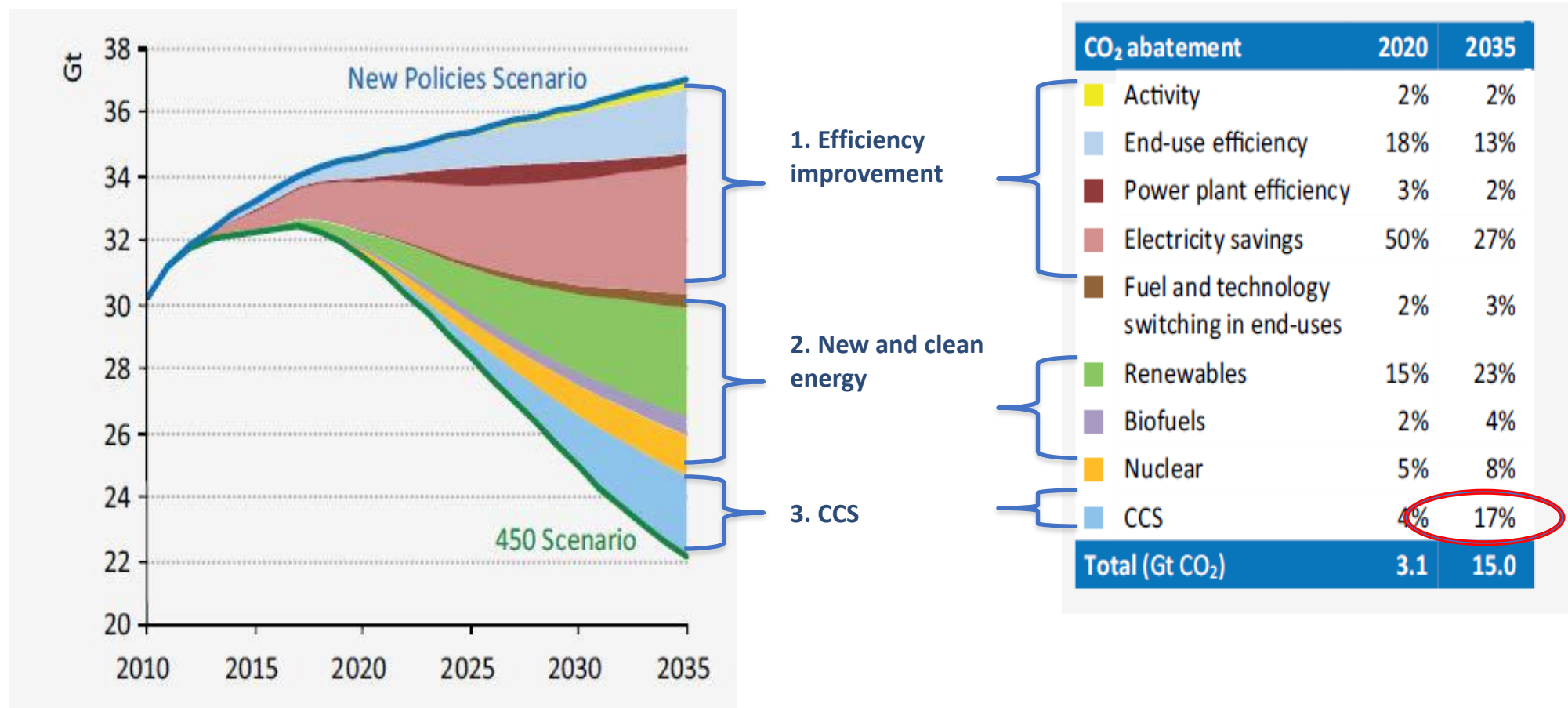


© IEA. All rights reserved. This content is excluded from our Creative Commons license. For more information, see <https://ocw.mit.edu/fairuse>.

- New policies scenario: takes into account the policies and implementing measures affecting energy markets that had been adopted as of mid-2015 (as well as the energy-related components of climate pledges in the run-up to COP21)
- 450 scenario: depicts a pathway to the 2° C climate goal that can be achieved by fostering technologies that are close to becoming available at commercial scale.

Source: IEA world energy outlook 2015, P55

Energy-related CO₂ emission's reduction



© IEA. All rights reserved. This content is excluded from our Creative Commons license. For more information, see <https://ocw.mit.edu/fairuse>.

Estimated (in 2019) Levelized Cost of Electricity Generation Plants in 2023

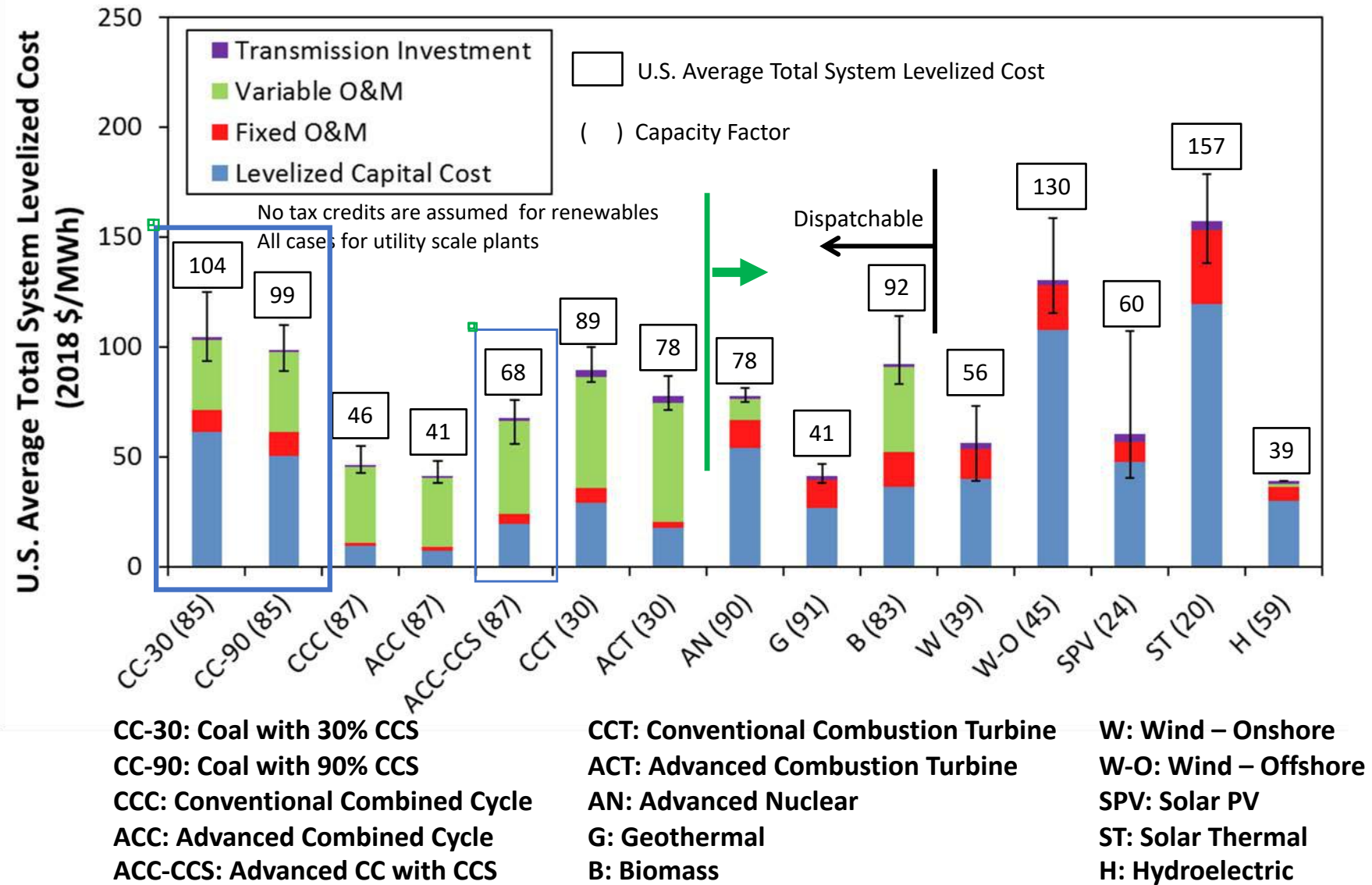


Image courtesy of U.S. Energy Information Administration.

Source: U.S. Energy Information Administration, Annual Energy Outlook 2019, Feb 2019.

Proposed CO₂ emissions Regulations on Coal and NG

Coal plant at 35% efficiency, 1 mole CO₂/mole of coal.
Take 32 MJ/kg as coal heating value, plant produces $(0.35 \times 32 \times 12 / 44) = 3.05$ MJe/kgCO₂
or ~ 1,180 kg CO₂/MWhe. (proposed 1100 lb/MWhe)

NG plant at 55% efficiency, 1 mole CO₂/mole CH₄,
with 45 MJ/kg NG heating value, generates $(0.55 \times 45 \times 16 / 44) = 9$ MJe/kgCO₂
or ~ 400 kgCO₂/MWhe. (proposed 1000 lb/MWhe)

Coal can not meet these without CCS ..

Petra Nova!

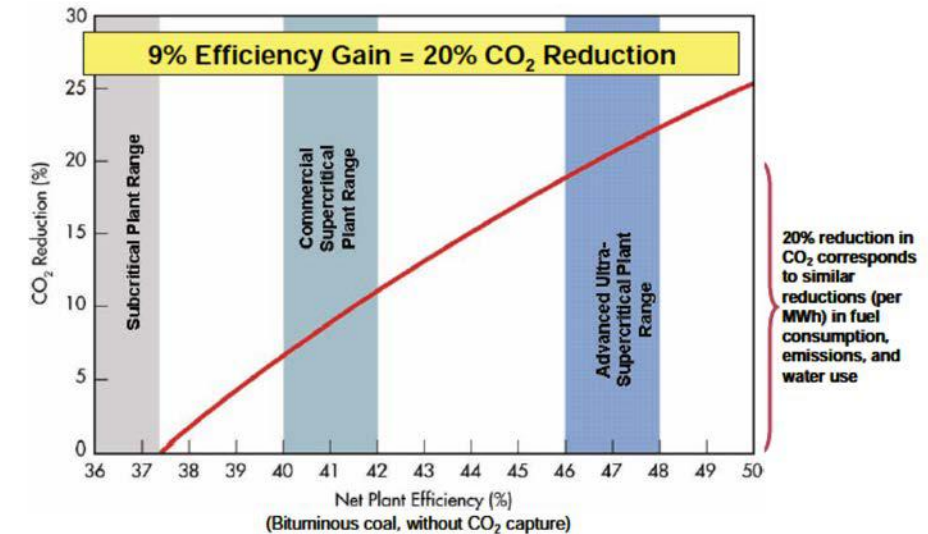


Figure 1-4
High-Efficiency Advanced Pulverized Coal Power Plants Substantially Reduce Fuel Costs and CO₂ and Other Emissions^a

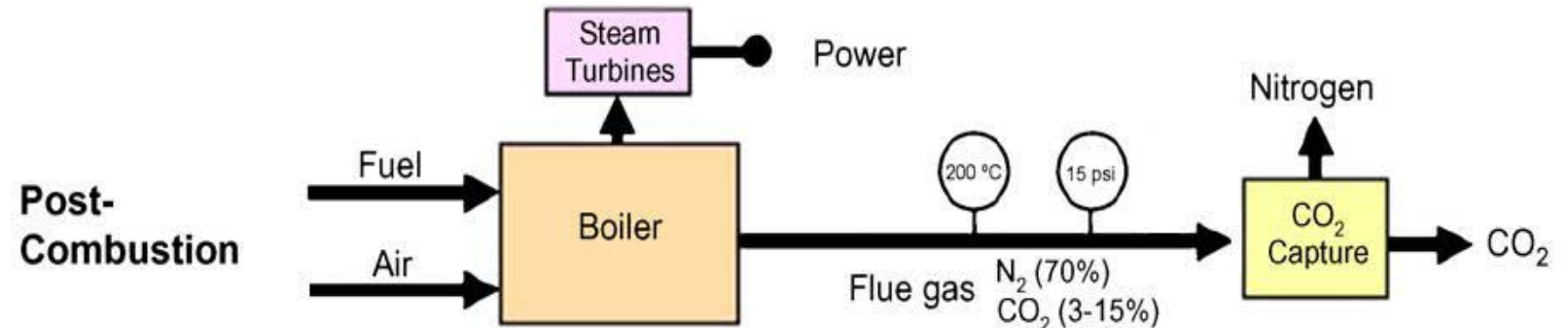
© EPRI. All rights reserved. This content is excluded from our Creative Commons license. For more information, see <https://ocw.mit.edu/fairuse>.

Efficiency improvements reduce
CO₂ emissions, with limits

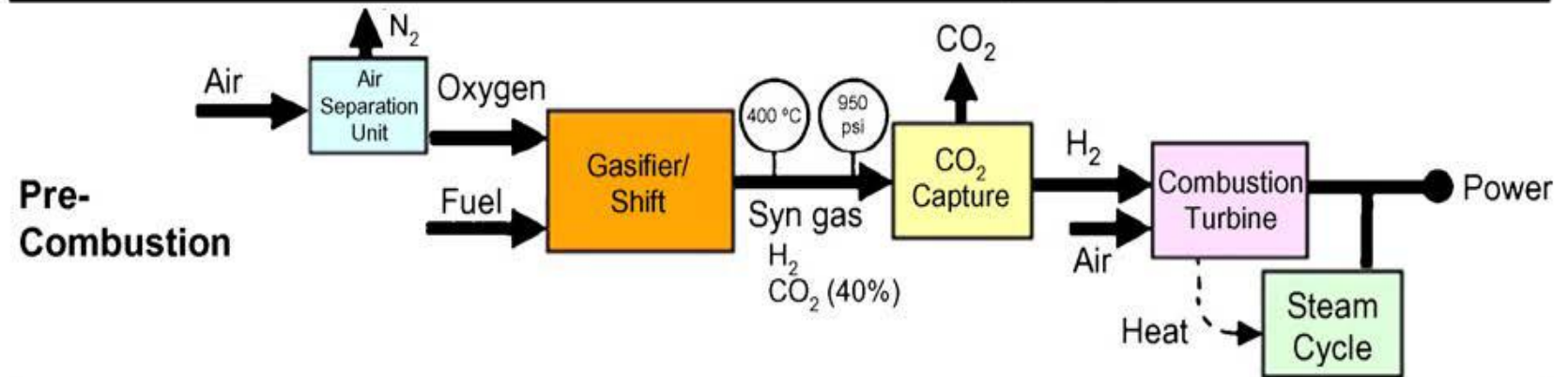
Approaches for CO₂ capture

(shown for coal used in steam cycle plants)

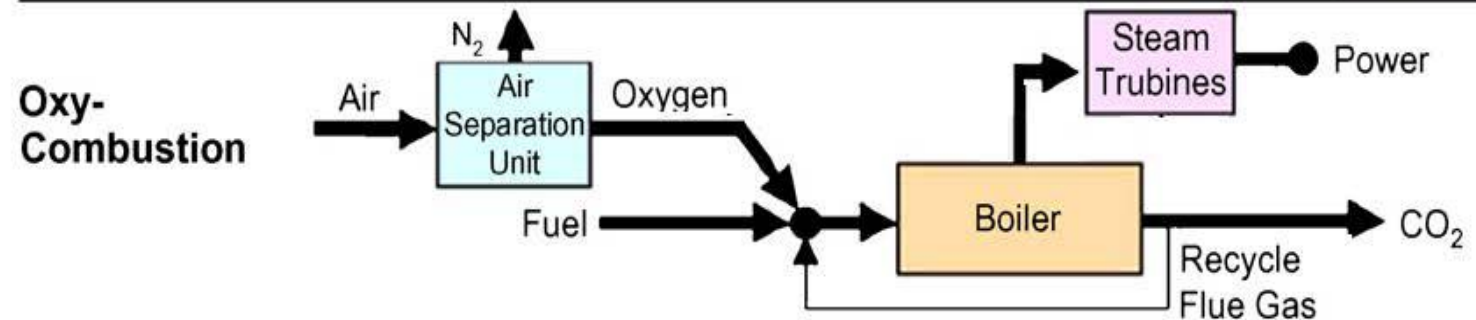
Separate CO₂ from CO₂+N₂



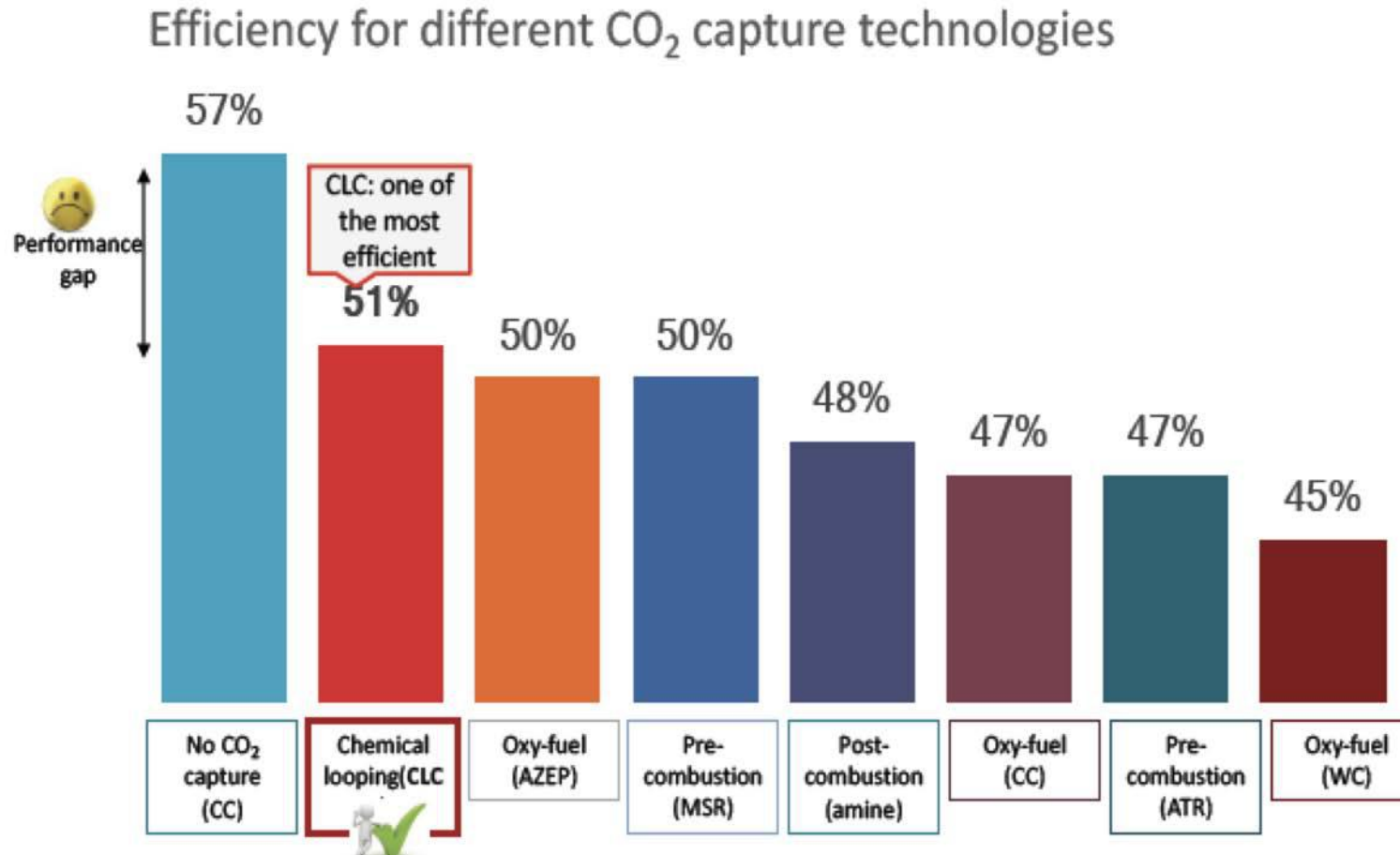
Separate CO₂ from CO₂+H₂



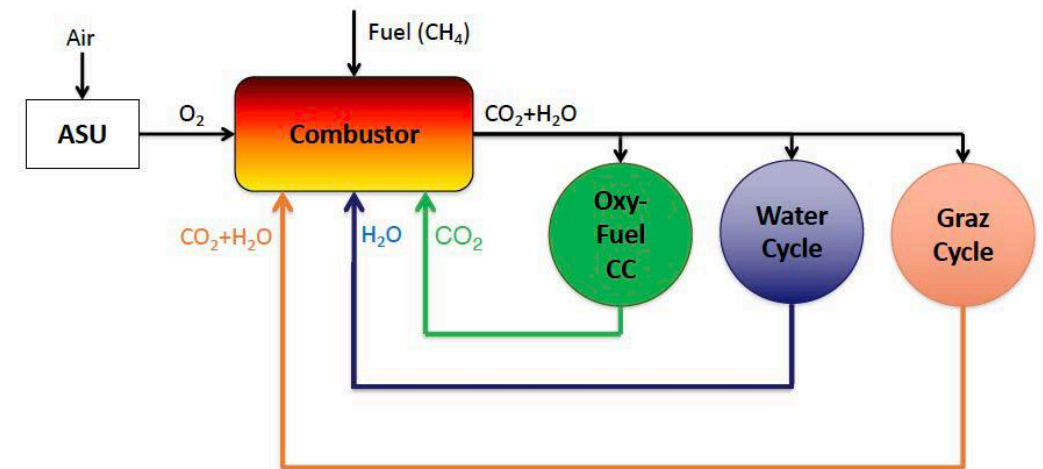
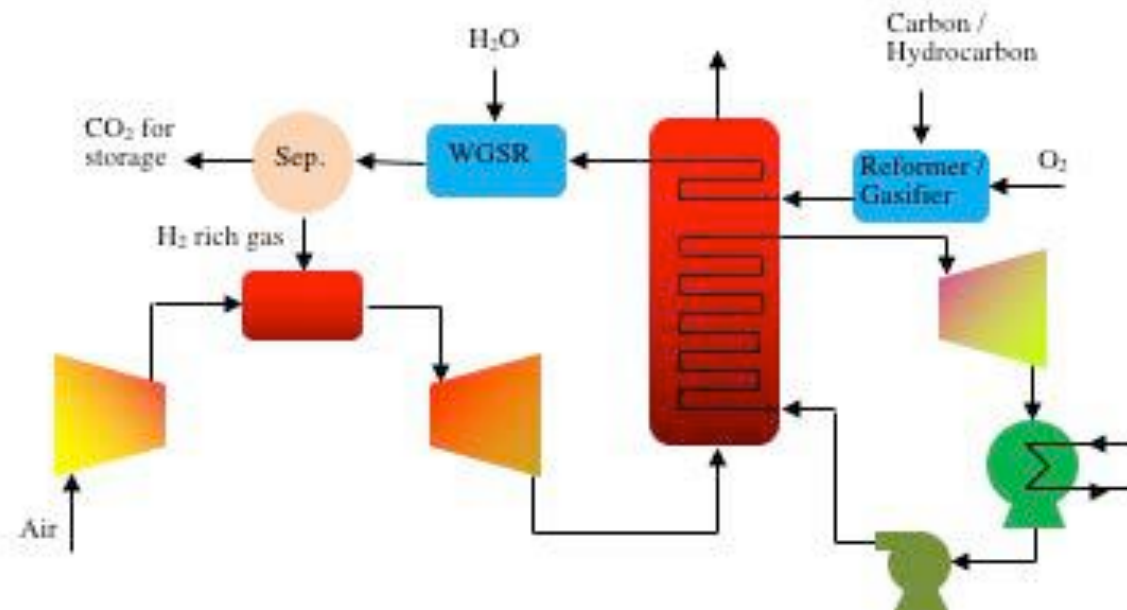
Separate O₂ from O₂+N₂



System level analysis for NG (ASPEN BASED ANALYSIS)

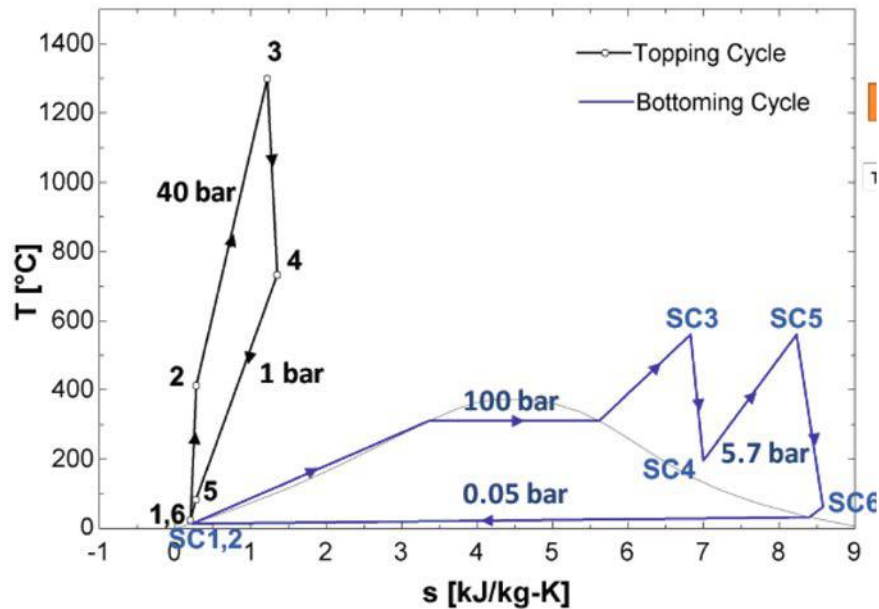


NG OXY-COMBUSTION CAPTURE SCHEME



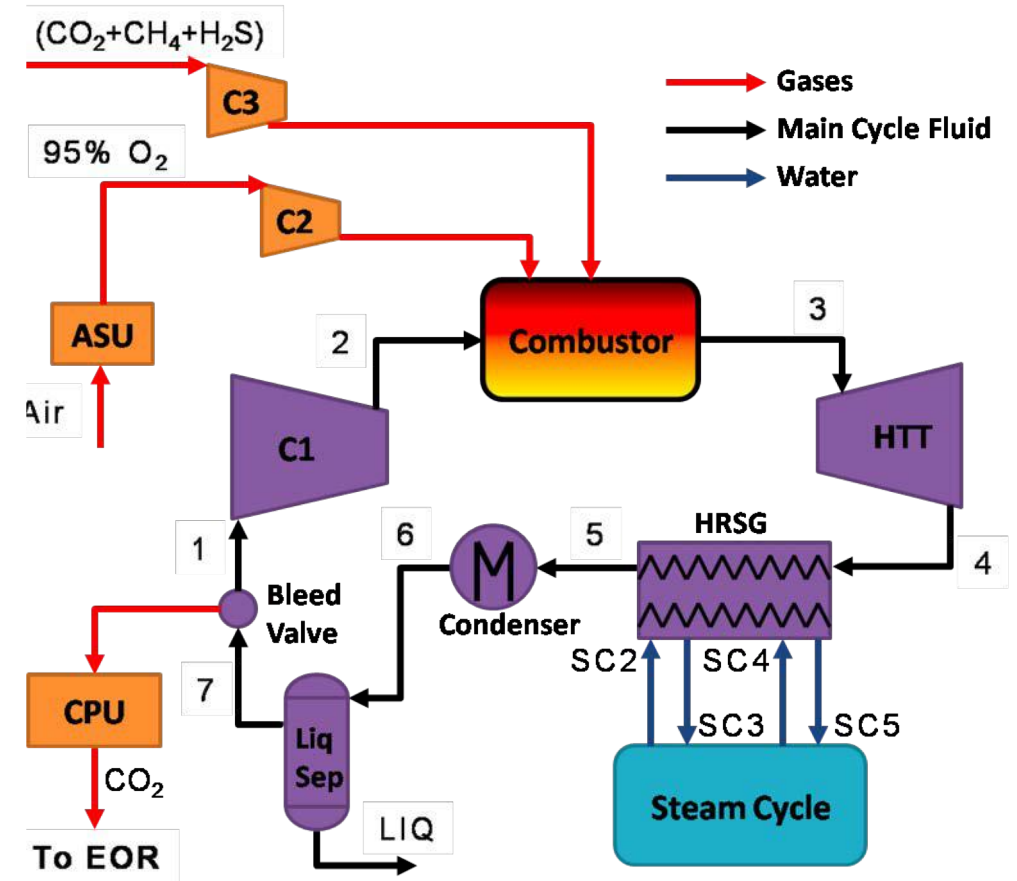
Oxyfuel combustion. An air separation unit is used. Estimated efficiency penalty for syngas and NG are 5-12% points and 6-9% points, respectively. This amounts to increasing the fuel use by 24-27 % and 22-28 %. Broken line for a PC plant.

NG Oxy-combustion Combined cycle



Courtesy Elsevier, Inc., <http://www.sciencedirect.com>. Used with permission.

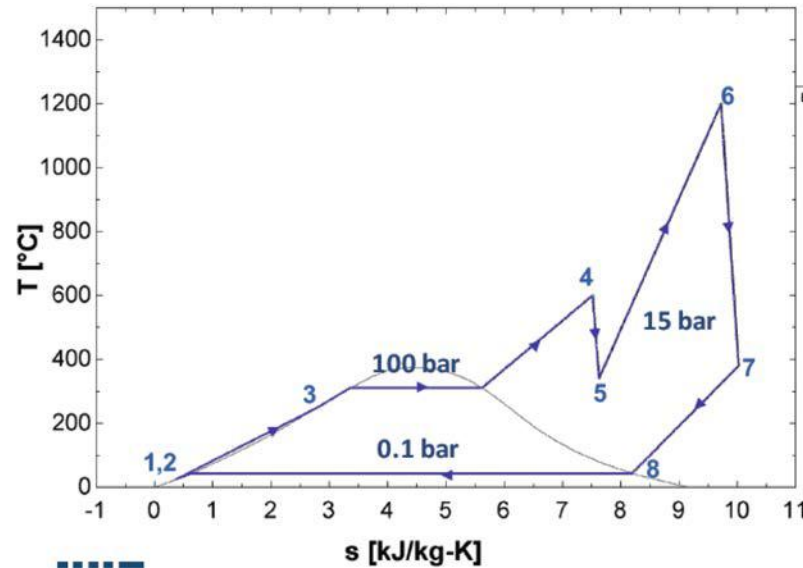
- Working Fluid: Mainly CO₂ (78%)
- CO₂ is recycled back to the combustor in order to moderate temperatures (93%)
- **Net Efficiency: 45.9%**
- 100 MW_e SCOC-CC demonstration plant, partnership of Siemens , Nebb Engineering, SINTEF & Lund University.



Courtesy Elsevier, Inc., <http://www.sciencedirect.com>. Used with permission.

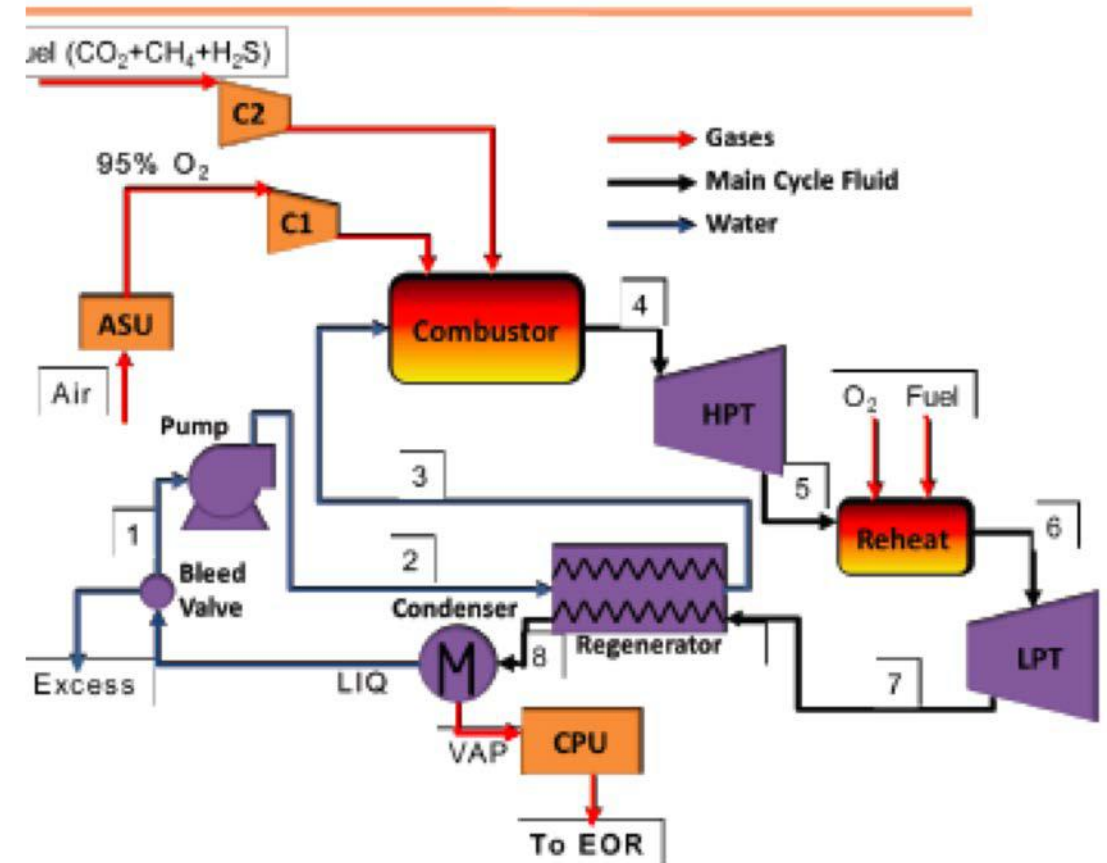
Chakroun, N. W. and Ghoniem, A.F., *Int. J. Greenhouse Control*, 36 (2015) 1-12.
Chakroun, N.W. and Ghoniem, A.F., *Int. J. Greenhouse Control*, 41 (2015) 163-173.

NG Oxy-Combustion Water cycle



Courtesy Elsevier, Inc., <http://www.sciencedirect.com>. Used with permission.

- Working Fluid: Mainly H_2O (94%)
- **Liquid** water is recycled to the combustor to moderate temperatures (83%)
- **Net Efficiency: 41.4%**
- This cycle has been implemented since 2005 by Clean Energy Systems (CES) in a 5MW test plant in Kimberlina, CA (world's first zero emission power plant)



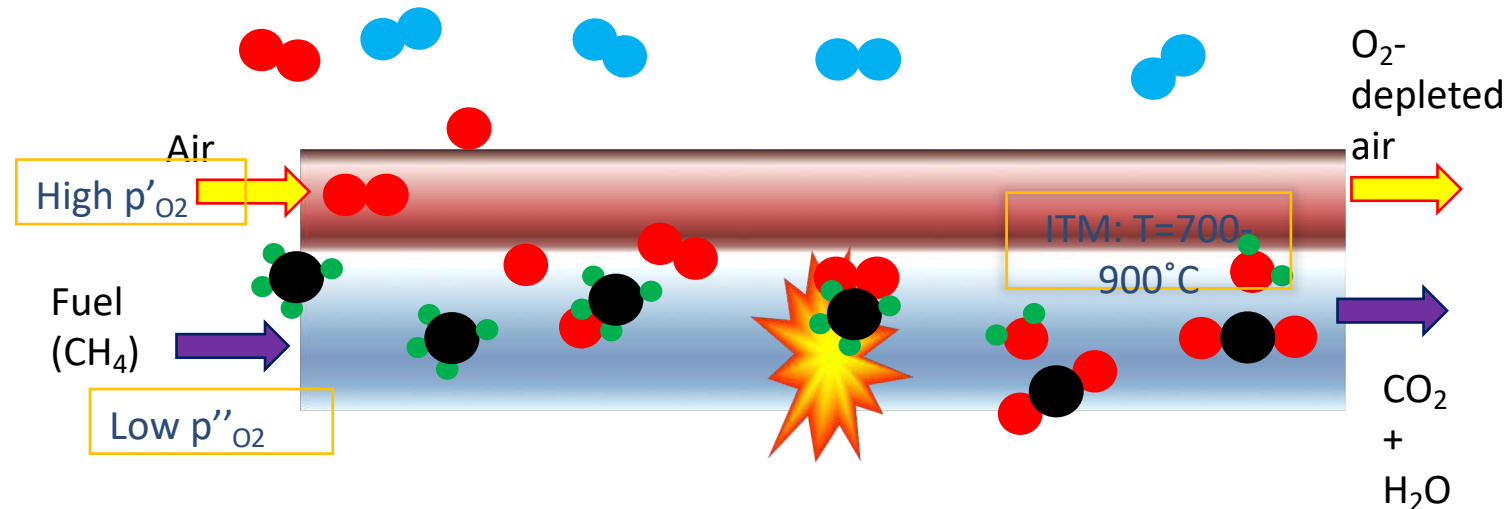
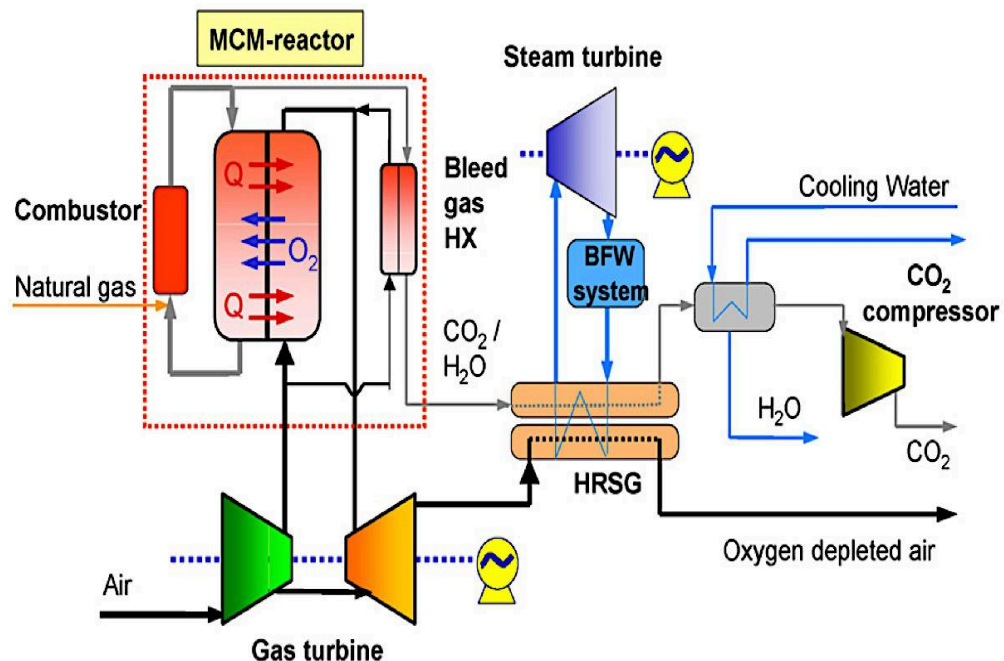
Courtesy Elsevier, Inc., <http://www.sciencedirect.com>. Used with permission.

Oxygen Penalty

		SCOCC-CC	Water Cycle	Graz Cycle
Working Fluid Composition (% vol.)				
		13%	94%	
Operating P (bar)			100	
Efficiency Ranges			40-49%	
Cycle Power Breakdown (% heat input)	Turbine		62%	
	Compressors, Pumps		2.2%	
	ASU		9.1%	
	CO ₂ Compression		6.1%	
Turbine Technologies		<ul style="list-style-type: none"> ➤ New designs of current gas turbine machinery needed, due to unusual working fluid (CO₂ & H₂O) and high T's 	<ul style="list-style-type: none"> ➤ Steam turbine technologies available for HPT and LPT, from CES, for this cycle up to certain temperatures 	<ul style="list-style-type: none"> ➤ Needs development of advanced turbine technology, for HTT, due to unusual working fluid (H₂O & CO₂) & high T's
Cycle Implementation		<ul style="list-style-type: none"> ➤ Cycle not been implemented in real life but layout of cycle is similar to CC's so modifications may be practical ➤ A new oxy-fuel power plant w/ supercritical CO₂ cycle is being developed by NET Power and a test plant should be completed by 2015 	<ul style="list-style-type: none"> ➤ Cycle has been built and implemented in real-life by CES at the Kimberlina Power Plant 	<ul style="list-style-type: none"> ➤ Cycle not been implemented yet b/c of complexity & unusual working fluid makes it economically unviable (so far) & needs new turbo-machinery design

MIEC MEMBRANES (ITM) FOR GAS SEPARATION AND FOR OXY-COMBUSTION

DOE's cycle, non reactive MSU

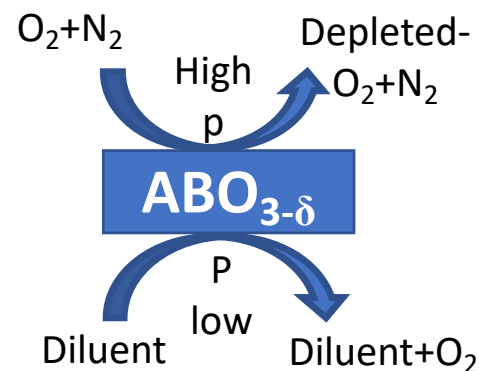


$$J_{O_2} = \frac{\frac{k_r}{k_f} (P_{O_2, sweep}^{-0.5} - P_{O_2, feed}^{-0.5})}{R_{interface}^{feed} + R_{bulk} + R_{interface}^{sweep}}$$

- At intermediate T and high Δp_{O_2} , ITMs produces high purity O_2 at reduced energy penalty
- Use reactive sweep gas to maintain low p''_{O_2} and perform air separation and oxy-combustion in same unit

ITM based ASU (MSRU)/Syngas Production

- Large penalty in ASU technology
 - Cryogenic: $0.36 \text{ kWh}_{el}/\text{m}^3 \text{ STP } O_2$
 - Small PSA $\sim 0.9 \text{ kWh}_{el}/\text{m}^3 \text{ STP } O_2$
- Ion Transport Membranes (ITM):
 - ❑ Oxygen purity: near 100%
 - ❑ O_2 separation/reaction combined in a single unit
 - ❑ Energy $\sim 0.2 \text{ kWh}_{el}/\text{m}^3 \text{ STP } O_2$ (Fraunhofer IKTS)

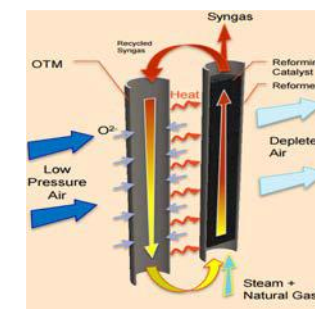


ITM stacks by Air Products

In our Labs, we have fabricating some of the best performing pervoskite membranes (L_{CF}, L_{SCF}, B_{ZF}, L_{SCo}, L_{SCrCo}, including biphasic and bilayer, novel morphology, etc. for different applications)

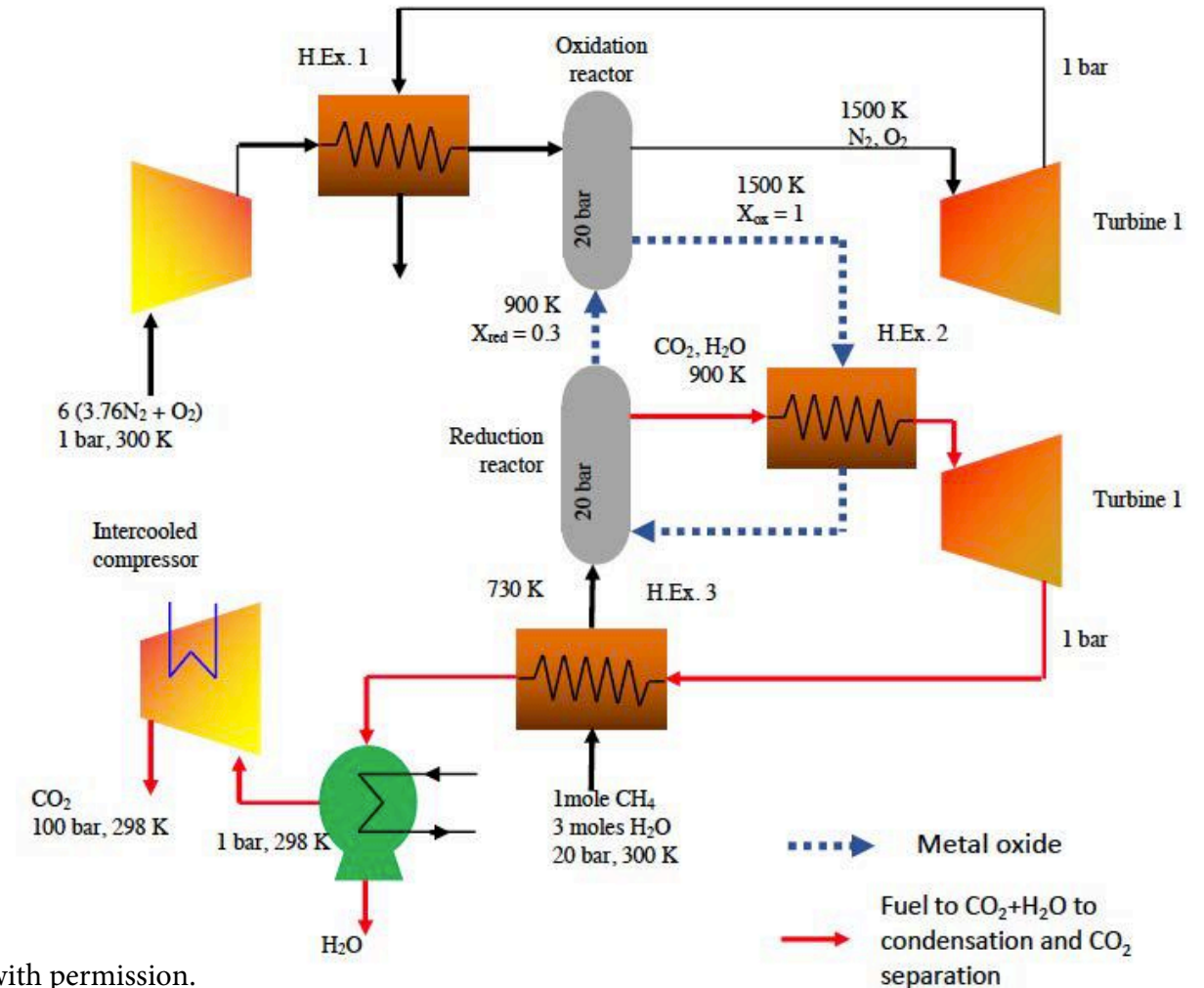
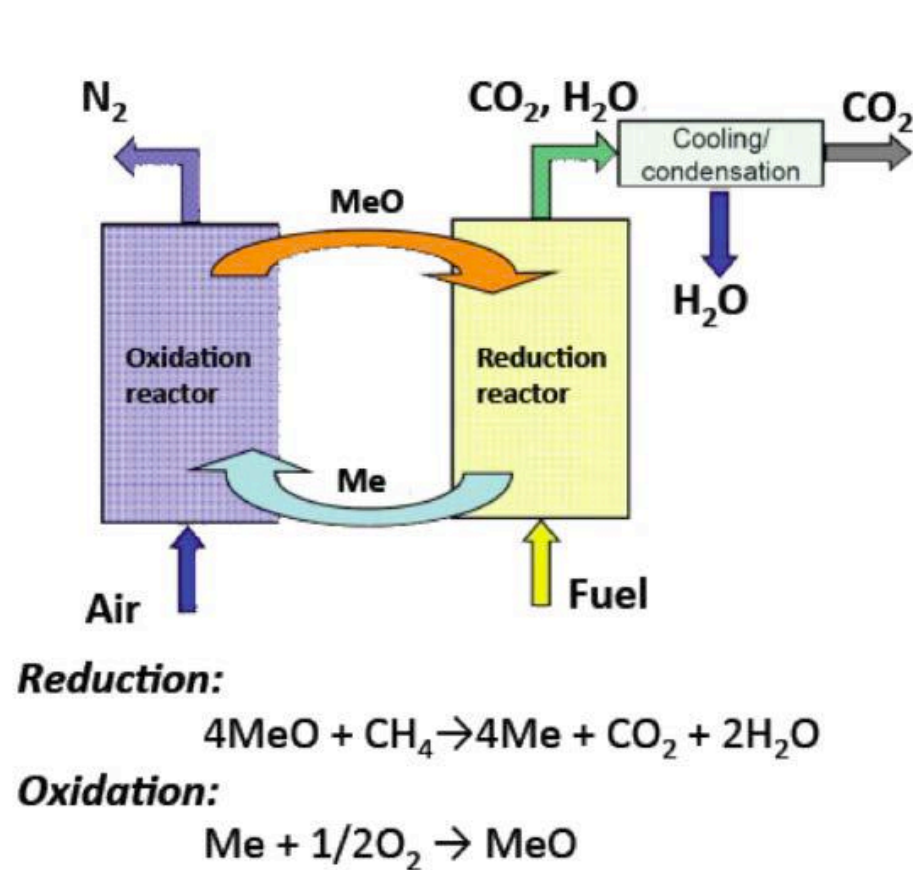


Fraunhofer Institute, $Ba_{0.5}Sr_{0.5}Co_{0.8}Fe_{0.2}O_{3-\delta}$, uses tubular membranes, heat recovery to achieve $0.14 \text{ kWh/kg}_{O_2}$



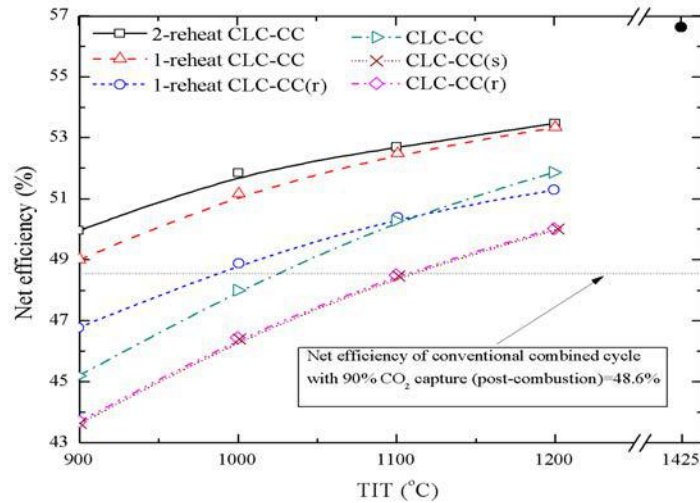
OTM Syngas module by Praxair

Chemical Looping for Oxy-combustion



Courtesy Elsevier, Inc., <http://www.sciencedirect.com>. Used with permission.

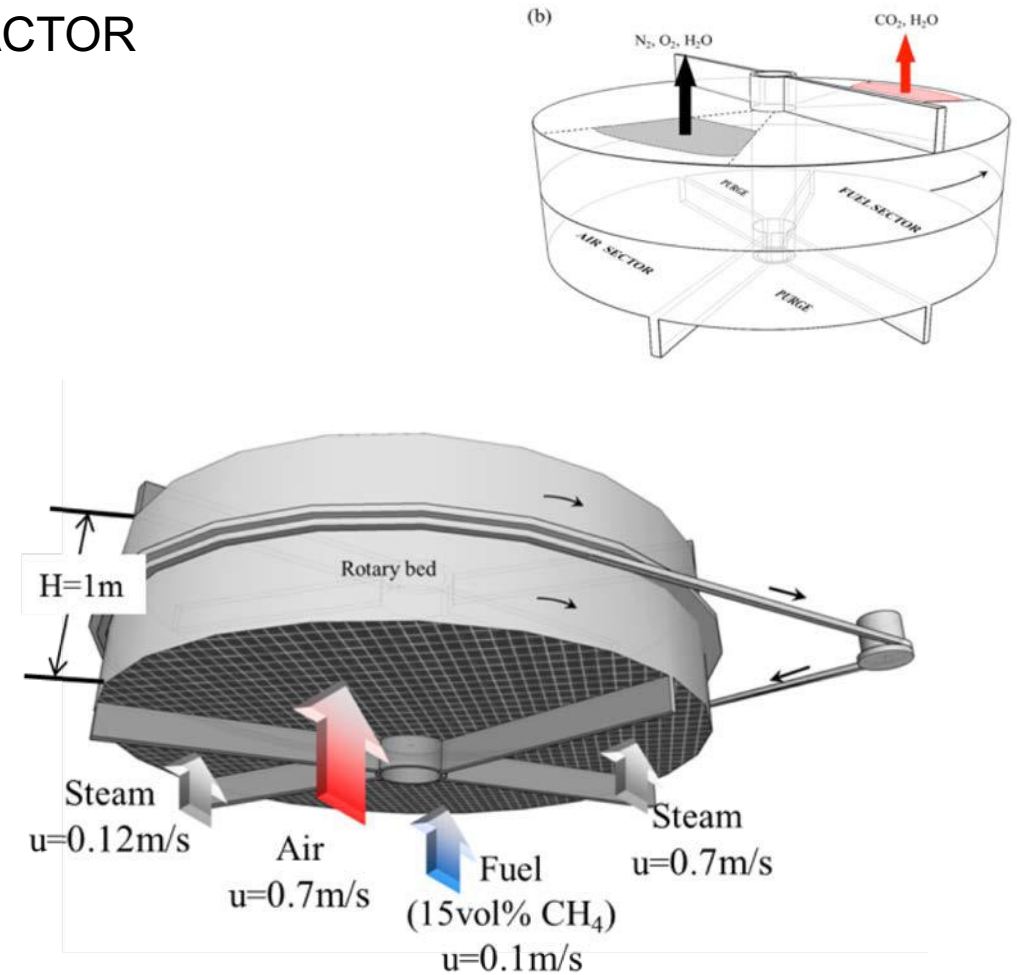
CHEMICAL LOOPING COMBUSTION USING OXYGEN METAL CARRIERS IN REDOX REACTIONS AND AN ISOTHERMAL ROTARY REACTOR



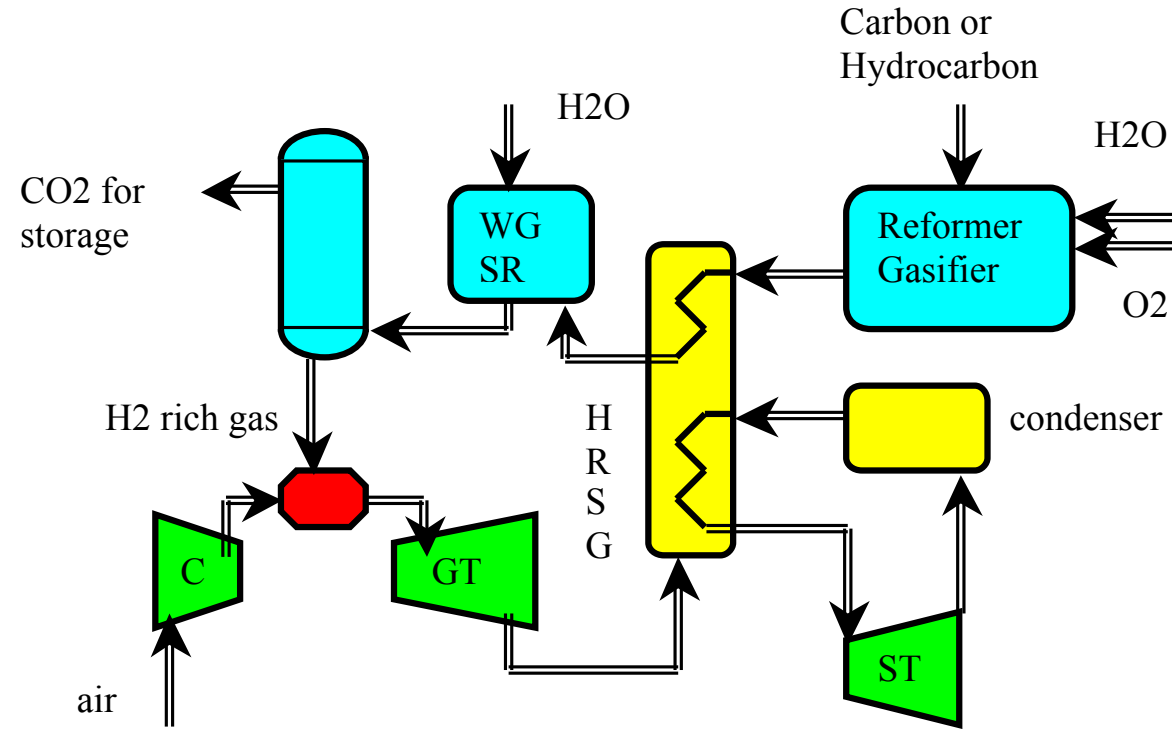
Comparison of multi-stage combined cycle designs. The solid circle on the top right-hand corner is for the combined cycle without CCS. CLC-CC with no reheat, 1 or 2 reheat. CLC-CC(r) is the CLC combined cycle with FR flue gas recuperation (no reheat and a single reheat); CLC-CC(s) is the CLC combined cycle with FR flue gas powering a bottom steam cycle. The TIT plays a very important role in determining the efficiency

© ACS Publications. All rights reserved. This content is excluded from our Creative Commons license. For more information, see <https://ocw.mit.edu/fairuse>.

Zhao, Z.L., Chen, T.J., and Ghoniem, A.F., Energy & Fuels, 2013.

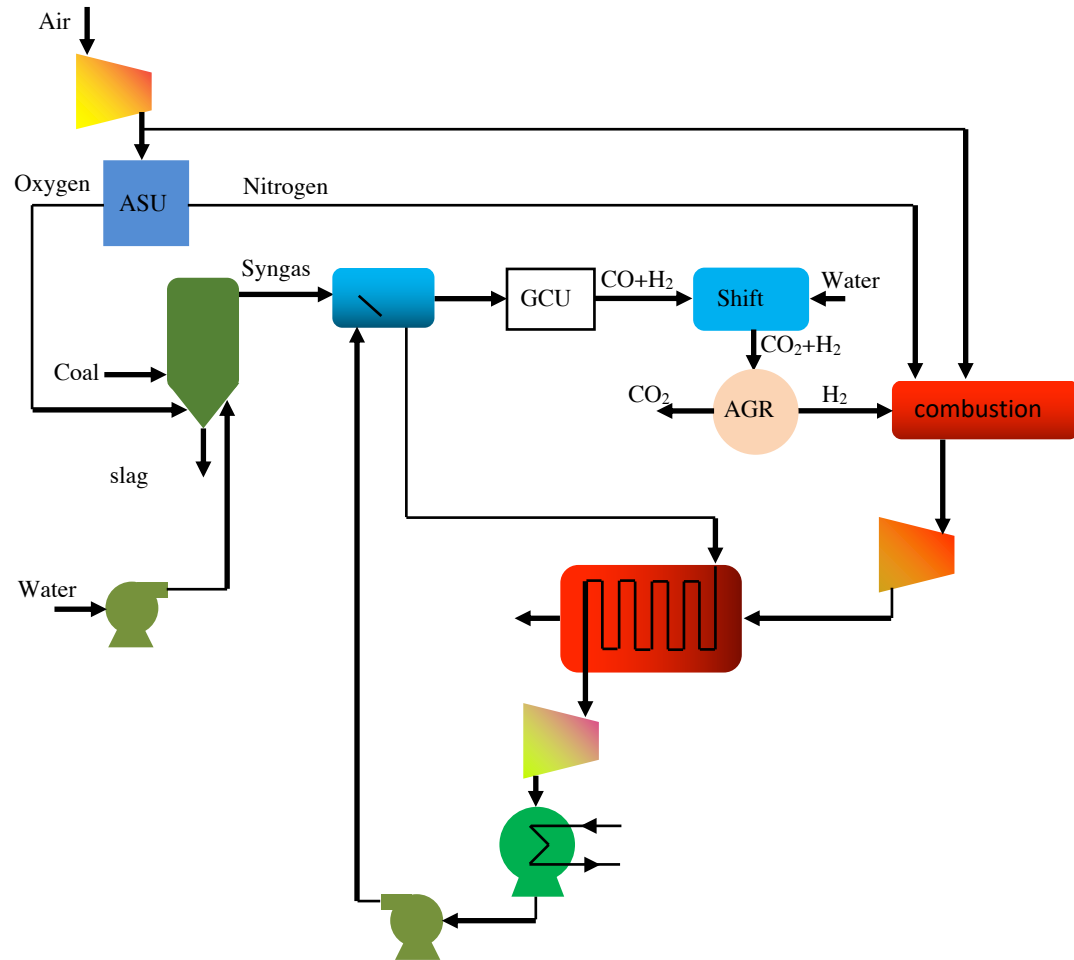


PRE-COMBUSTION CO₂ CAPTURE, NGCC or IGCC



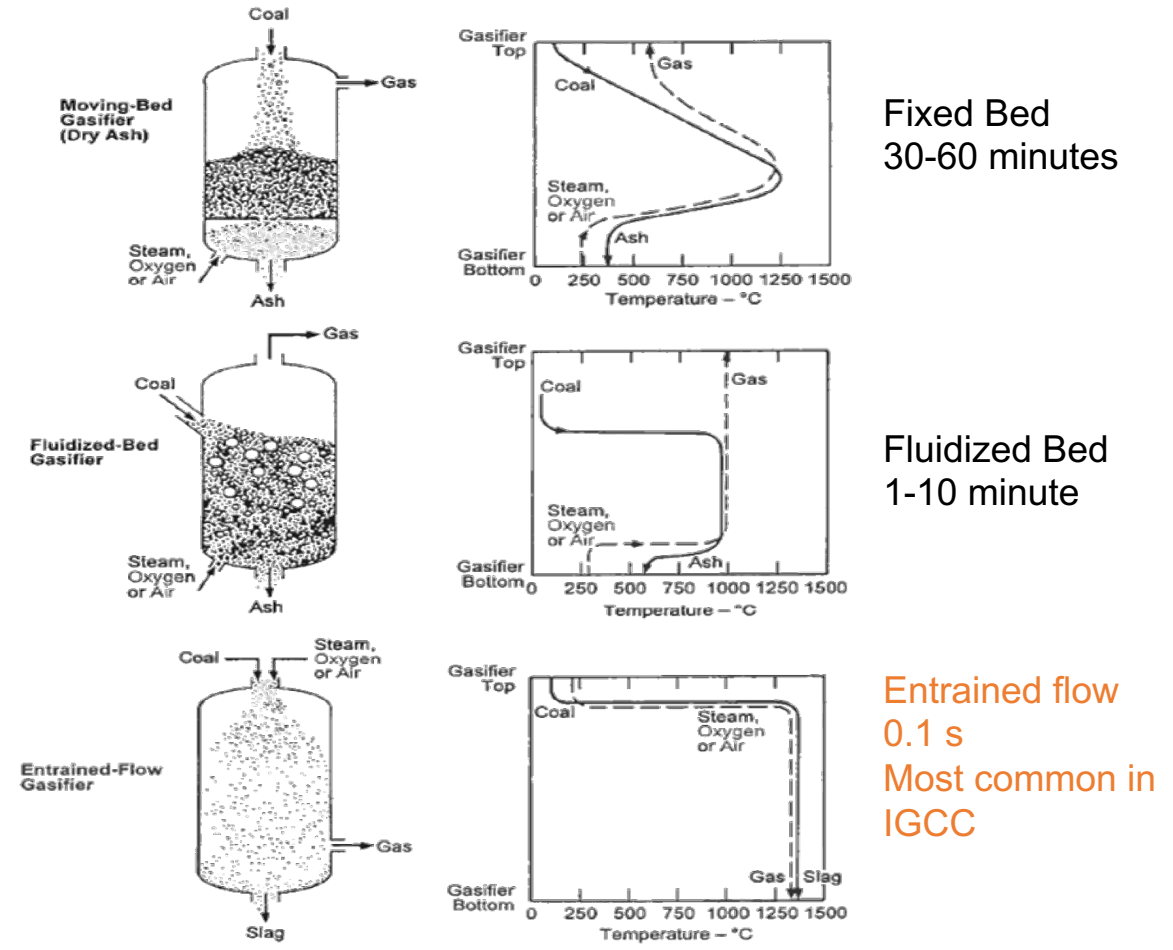
CO₂ pre-combustion capture. Reformed fuel is shifted and CO₂. Estimated efficiency penalty for syngas and NG are 7-13% points and 4-11% points, respectively. Given current efficiencies of coal and NG plants, this amounts to increasing the fuel use by 14-25 % and 16-28 %, respectively.

Integrated Gasification Combined Cycle Coal Plants



GCU: Gas Cleanup Unit
AGR: Acid Gas Removal to separate CO_2

Gasifier Types and the exit gas temperature



© Source unknown. All rights reserved. This content is excluded from our Creative Commons license. For more information, see <https://ocw.mit.edu/fairuse>.

TEMPE ELECTRIC POLK IGCC POWER PLANT

250 MW, 35.3 % efficiency, 2500 TPD coal,
200 TPD sulfuric acid, built 1996, \$600M

Why add oxygen in gasification ???

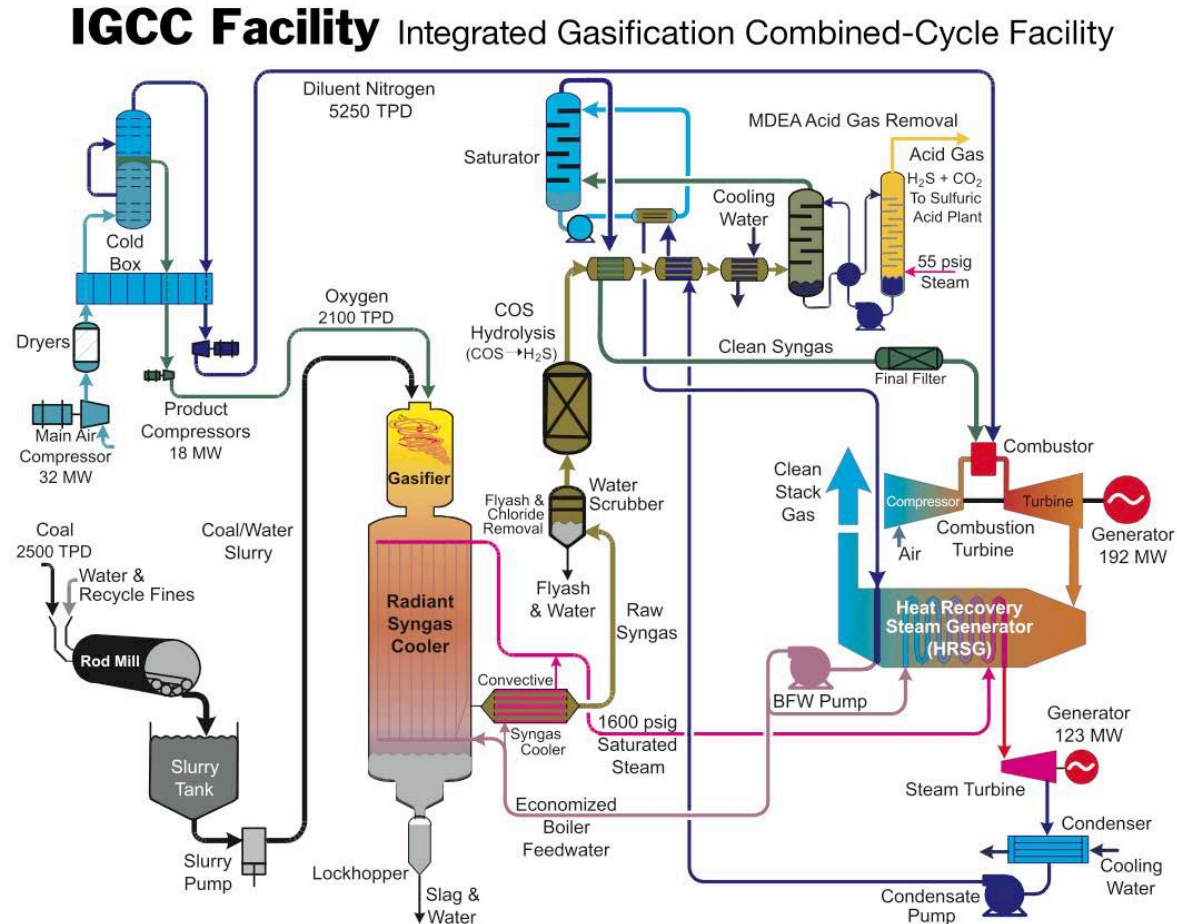


Image courtesy of DOE.

© Ahmed F. Ghoniem

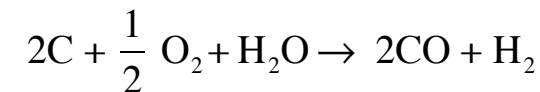
steam gasification: $C + H_2O \rightarrow CO + H_2$

is endothermic $\Delta \hat{h}_r = 118 \text{ MJ/kgmol C}$ (1)

partial oxidation: $C + \frac{1}{2} O_2 \rightarrow CO$

is exothermic $\Delta \hat{h}_r = -123 \text{ MJ/kgmol C}$ (2)

Add (1)+(2) makes the gasification nearly autothermal:

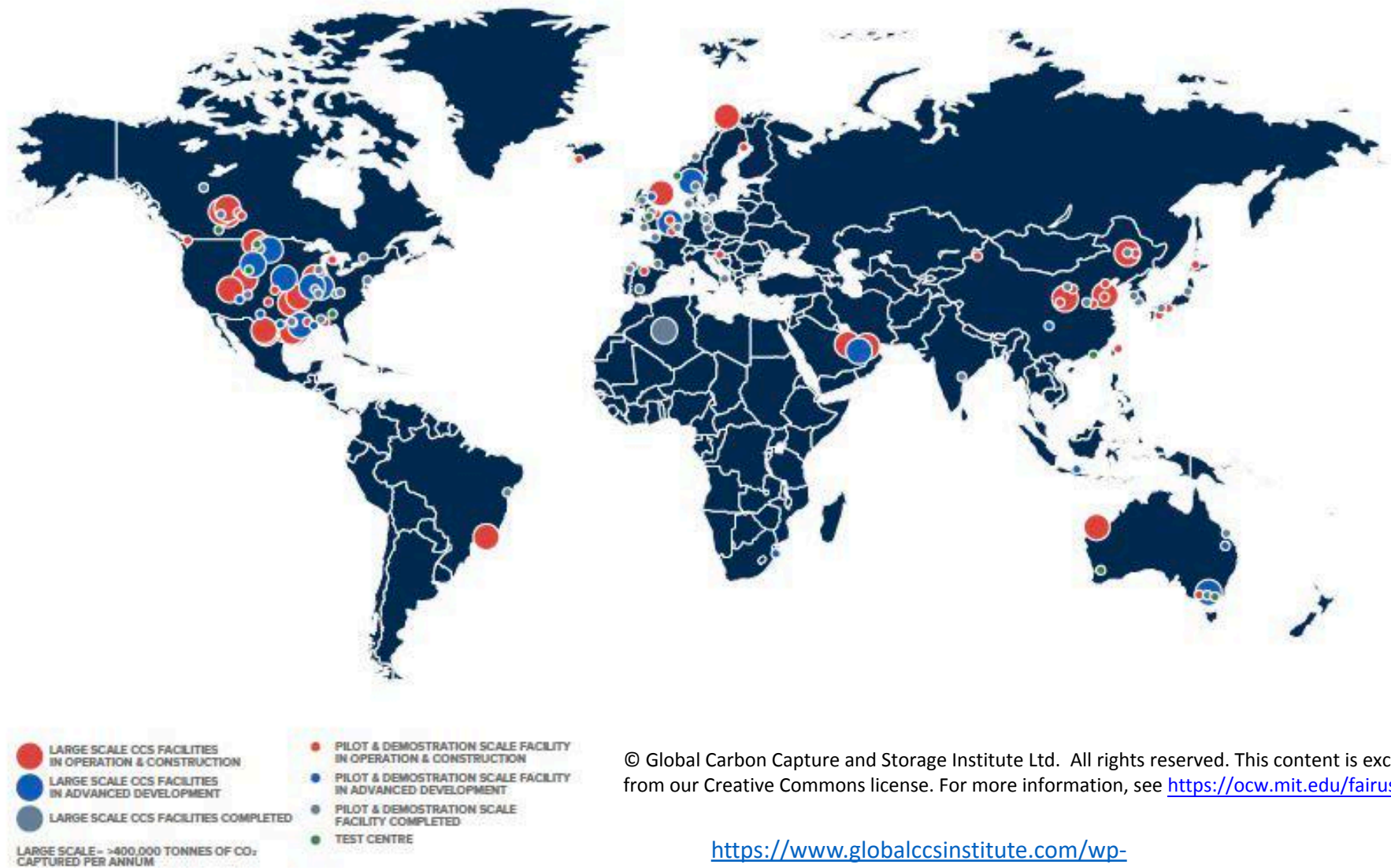


$\Delta \hat{h}_r = -5 \text{ MJ/2 kgmol C}$

⇒ cold gas efficiency:

chemical energy in syngas/chemical energy in coal is ~100%
(practical values are lower because of heat losses)

GLOBAL CCS FACILITIES UPDATE



© Global Carbon Capture and Storage Institute Ltd. All rights reserved. This content is excluded from our Creative Commons license. For more information, see <https://ocw.mit.edu/fairuse>.

https://www.globalccsinstitute.com/wp-content/uploads/2019/12/GCC_GLOBAL_STATUS_REPORT_2019.pdf

FIGURE 2 CURRENT CCS FACILITIES AROUND THE WORLD¹

LARGE SCALE CCS FACILITIES IN OPERATION

© Global Carbon Capture and Storage Institute Ltd. All rights reserved. This content is excluded from our Creative Commons license. For more information, see <https://ocw.mit.edu/fairuse>.

NO.	TITLE	STATUS	COUNTRY	OPERATION DATE	INDUSTRY	CAPTURE CAPACITY (Mtpa)	CAPTURE TYPE	STORAGE TYPE
1	GORGON CARBON DIOXIDE INJECTION	Operating	Australia	2019	Natural Gas Processing	3.4 - 4.0	Industrial separation	Dedicated Geological Storage
2	JILIN OIL FIELD CO ₂ -EOR	Operating	China	2018	Natural Gas Processing	0.6	Industrial separation	Enhanced Oil Recovery
3	ILLINOIS INDUSTRIAL CARBON CAPTURE AND STORAGE	Operating	United States of America	2017	Ethanol Production	1	Industrial separation	Dedicated Geological Storage
4	PETRA NOVA CARBON CAPTURE	Operating	United States of America	2017	Power Generation	1.4	Post-combustion capture	Enhanced Oil Recovery
5	ABU DHABI CCS (PHASE 1 BEING EMIRATES STEEL INDUSTRIES)	Operating	United Arab Emirates	2016	Iron and Steel Production	0.8	Industrial separation	Enhanced Oil Recovery
6	QUEST	Operating	Canada	2015	Hydrogen Production for Oil Refining	1	Industrial separation	Dedicated Geological Storage
7	UTHMANIYAH CO ₂ -EOR DEMONSTRATION	Operating	Saudi Arabia	2015	Natural Gas Processing	0.8	Industrial separation	Enhanced Oil Recovery
8	BOUNDARY DAM CCS	Operating	Canada	2014	Power Generation	1	Post-combustion capture	Enhanced Oil Recovery
9	PETROBRAS SANTOS BASIN PRE-SALT OIL FIELD CCS	Operating	Brazil	2013	Natural Gas Processing	3	Industrial separation	Enhanced Oil Recovery
10	COFFEYVILLE GASIFICATION PLANT	Operating	United States of America	2013	Fertiliser Production	1	Industrial separation	Enhanced Oil Recovery
11	AIR PRODUCTS STEAM METHANE REFORMER	Operating	United States of America	2013	Hydrogen Production for Oil Refining	1	Industrial separation	Enhanced Oil Recovery
12	LOST CABIN GAS PLANT	Operating	United States of America	2013	Natural Gas Processing	0.9	Industrial separation	Enhanced Oil Recovery
13	CENTURY PLANT	Operating	United States of America	2010	Natural Gas Processing	2.4	Industrial separation	Enhanced Oil Recovery
14	SNØHVIT CO ₂ STORAGE	Operating	Norway	2008	Natural Gas Processing	0.7	Industrial separation	Dedicated Geological Storage
15	GREAT PLAINS SYNFUELS PLANT AND WEYBURN-MIDALE	Operating	United States of America	2000	Synthetic Natural Gas	3	Industrial separation	Enhanced Oil Recovery
16	SLEIPNER CO ₂ STORAGE	Operating	Norway	1996	Natural Gas Processing	1	Industrial separation	Dedicated Geological Storage
17	SMUTE CREEK GAS PROCESSING PLANT	Operating	United States of America	1986	Natural Gas Processing	7	Industrial separation	Enhanced Oil Recovery
18	ENID FERTILISER	Operating	United States of America	1982	Fertiliser Production	0.7	Industrial separation	Enhanced Oil Recovery
19	TERRELL NATURAL GAS PROCESSING PLANT (FORMERLY VAL VERDE NATURAL GAS PLANTS)	Operating	United States of America	1972	Natural Gas Processing	0.4 - 0.5	Industrial separation	Enhanced Oil Recovery

LARGE SCALE CCS FACILITIES IN CONSTRUCTION, ADVANCED AND EARLY DEVELOPMENT

NO.	TITLE	STATUS	COUNTRY	OPERATION DATE	INDUSTRY	CAPTURE CAPACITY (Mtpa)	CAPTURE TYPE	STORAGE TYPE
20	ALBERTA CARBON TRUNK LINE (ACTL) WITH NORTH WEST REDWATER PARTNERSHIP'S STURGEON REFINERY CO ₂ STREAM	In Construction	Canada	2020	Hydrogen Production for Oil Refining	1.1 - 1.4	Industrial separation	Enhanced Oil Recovery
21	ALBERTA CARBON TRUNK LINE (ACTL) WITH AGRUM CO ₂ STREAM	In Construction	Canada	2020	Fertiliser Production	0.3 - 0.6	Industrial separation	Enhanced Oil Recovery
22	SINOPEC QILU PETROCHEMICAL CCS	In Construction	China	2020	Chemical Production	0.40	Industrial separation	Enhanced Oil Recovery
23	YANCHANG INTEGRATED CARBON CAPTURE AND STORAGE DEMONSTRATION	In Construction	China	2020 - 2021	Chemical Production	0.41	Industrial separation	Enhanced Oil Recovery
24	WABASH CO ₂ SEQUESTRATION	Advanced development	United States of America	2022	Fertiliser production	1.5-1.75	Industrial separation	Dedicated Geological Storage
25	PORT OF ROTTERDAM CCUS BACKBONE INITIATIVE (PORTHOS)	Advanced development	Netherlands	2023	Various	2.0 - 5.0	Various	Dedicated Geological Storage
26	NORWAY FULL CHAIN CCS	Advanced development	Norway	2023-2024	Cement production and waste-to-energy	0.80	Various	Dedicated Geological Storage
27	LAKE CHARLES METHANOL	Advanced development	United States of America	2024	Chemical production	4.20	Industrial separation	Enhanced oil recovery
28	ABU DHABI CCS PHASE 2 - NATURAL GAS PROCESSING PLANT	Advanced development	United Arab Emirates	2025	Natural gas processing	1.0 - 2.3	Industrial separation	Enhanced Oil Recovery
29	DRY FORK INTEGRATED COMMERCIAL CCS	Advanced development	United States of America	2025	Power generation	3.00	Post-combustion capture	Dedicated Geological Storage or Enhanced Oil Recovery
30	CARBONSAFE ILLINOIS – MACON COUNTY	Advanced development	United States of America	2025	Power generation and ethanol production	2.0 - 5.0	Post-combustion capture and industrial separation	Dedicated Geological Storage and Enhanced Oil Recovery
31	PROJECT TUNDRA	Advanced development	United States of America	2025 - 2026	Power generation	3.1 - 3.6	Post-combustion capture	Dedicated Geological Storage or Enhanced Oil Recovery
32	INTEGRATED MID-CONTINENT STACKED CARBON STORAGE HUB	Advanced development	United States of America	2025 - 2035	Ethanol production, power generation and/or refinery	1.90	Various	Dedicated Geological Storage and Enhanced Oil Recovery
33	CARBONNET	Advanced development	Australia	2020's	Under evaluation	3.00	Under Evaluation	Dedicated Geological Storage
34	QXY AND WHITE ENERGY ETHANOL BOR FACILITY	Early development	United States of America	2021	Ethanol production	0.6-0.7	Industrial separation	Enhanced Oil Recovery
35	SINOPEC EASTERN CHINA CCS	Early development	China	2021	Fertiliser production	0.50	Industrial separation	Enhanced oil recovery
36	HYDROGEN 2 MAGNUM (H2M)	Early development	Netherlands	2024	Power Generation	2.00	Under Evaluation	Dedicated Geological Storage

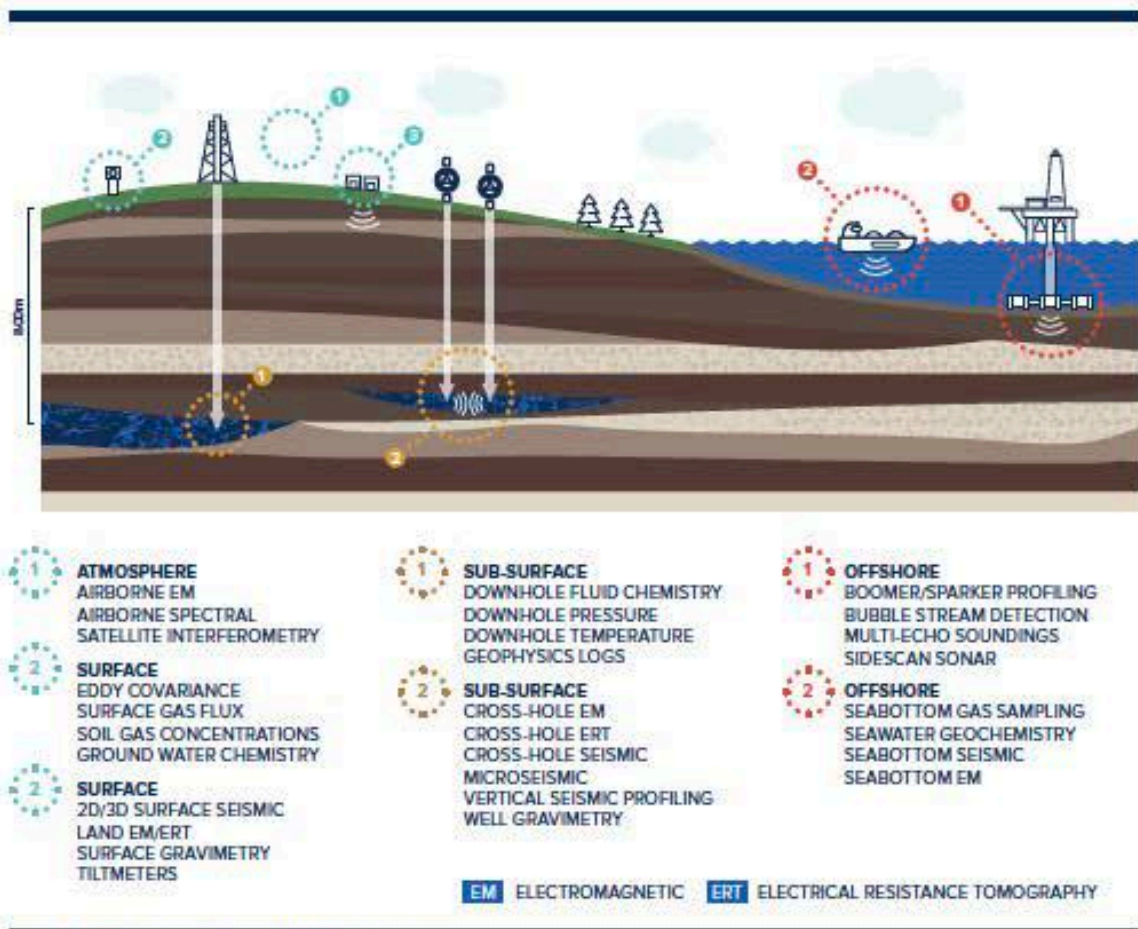


FIGURE 11 A SCHEMATIC OF SELECT MONITORING TECHNOLOGIES AVAILABLE FOR CO₂ STORAGE FACILITIES

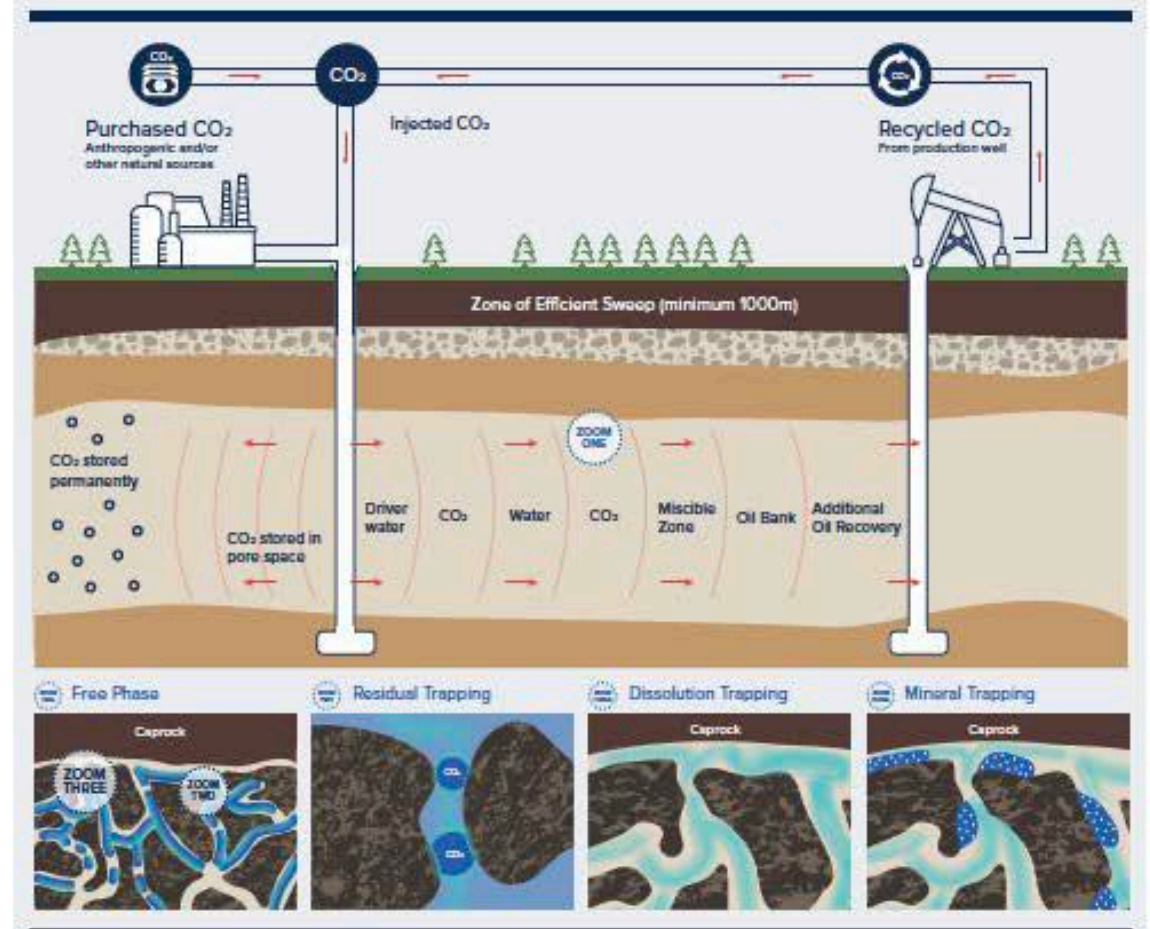


FIGURE 12 SCHEMATIC OF CO₂ EOR AND CO₂ TRAPPING MECHANISMS

© Global Carbon Capture and Storage Institute Ltd. All rights reserved. This content is excluded from our Creative Commons license. For more information, see <https://ocw.mit.edu/fairuse>.

https://www.globalccsinstitute.com/wp-content/uploads/2019/12/GCC_GLOBAL_STATUS_REPORT_2019.pdf

Oil recovery is under:
 Field pressure (primary): 15%
 Water floods (secondary): 30 %
 CO₂ flood (tertiary): 15%

Chemical scrubbing of CO₂ from flue gases has already been demonstrated.

During 82-86, an aqueous solution of MEA was used in: Lubbock Power plant, Texas, NG was fired in a 50 MW plant, producing near 1000 t/d of CO₂, and in a coal-steam generator in Carlsbad NM producing 113 t/d. In both cases, CO₂ was used for enhanced oil recovery (EOR) in nearby fields.

1991, CO₂ scrubbing using 15-20% MEA solutions in the 300 MW Shady Point Combined Heat and Power Plant in Oklahoma has been producing nearly 400 t/d CO₂, which is used in the food industry and in EOR.

A similar operation is done in a Botswana plant burning coal.

Norway Sleipner Vest gas field separates CO₂ from the recovered natural gas to reduce CO₂ concentration in the produced gas from 95% to 2.5%. The separated CO₂ is then injected back into a 250 m deep aquifer located 800 m below the ocean surface.

MIT OpenCourseWare
<https://ocw.mit.edu/>

2.60J Fundamentals of Advanced Energy Conversion
Spring 2020

For information about citing these materials or our Terms of Use, visit: <https://ocw.mit.edu/terms>.

2.60/2.62 lecture 21

Energy system modeling and examples

Xiao-Yu Wu, PhD'17

Postdoctoral Associate at MIT

Assistant Professor at University of Waterloo (starting in May 2020)

April 22 2020

Intended learning outcomes

- After this lecture, students are capable to
- Identify energy systems
- Explain the reason to carry out system analysis of energy systems
- Describe the basic functionality of Aspen PlusTM
- Perform a system analysis using Aspen PlusTM with the help of manual

- Advanced energy systems: innovation and characterization
- System analysis: what we can learn from it?
- Aspen PlusTM overview
- Examples
 - 1. A novel IGCC-CC power plant integrated with an oxygen permeable membrane for hydrogen production and carbon capture (CC)
 - 2. Dynamic modeling of a flexible Power-to-X plant for energy storage and hydrogen production

What is an energy system?

- The energy system comprises all the components related to the production, conversion, delivery, and use of energy

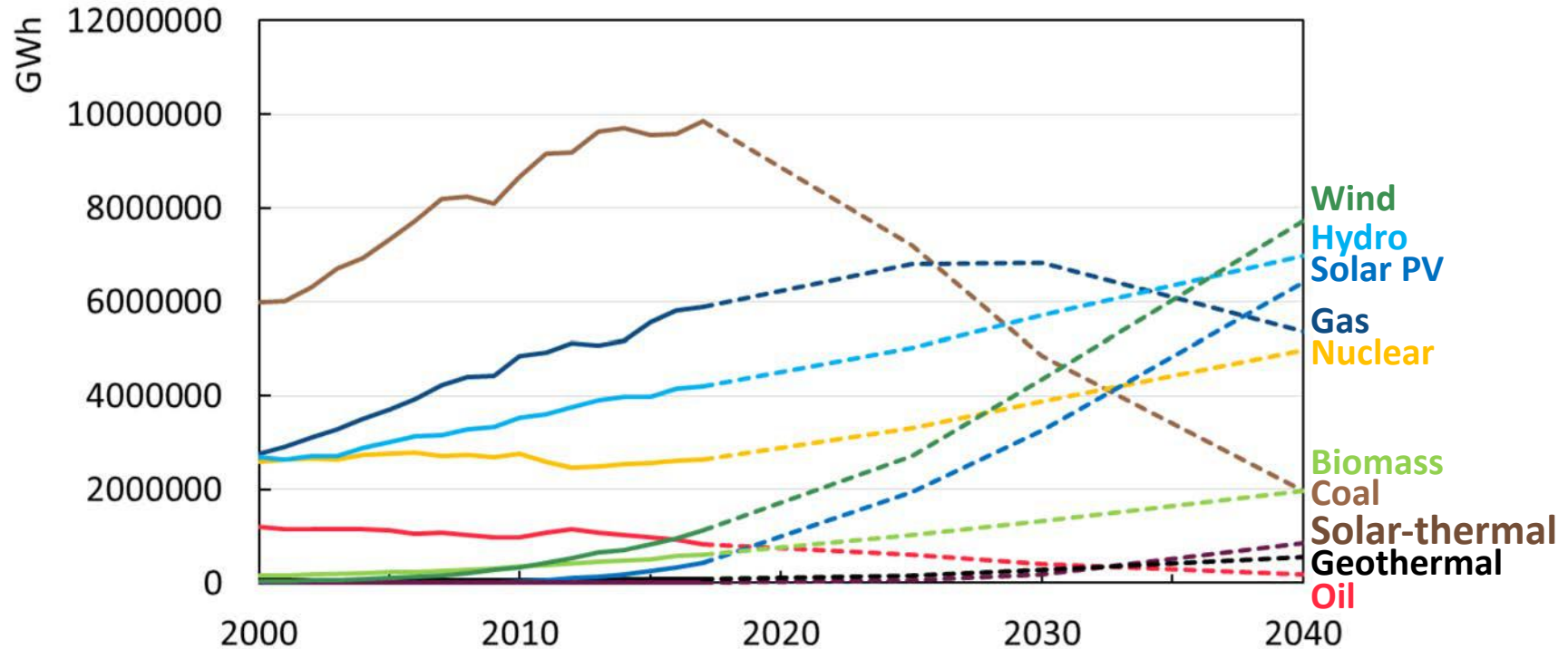
---- Intergovernmental Panel on Climate Change ^[1]



© Source unknown. All rights reserved. This content is excluded from our Creative Commons license. For more information, see <https://ocw.mit.edu/fairuse>.

Energy production: electricity production as an example

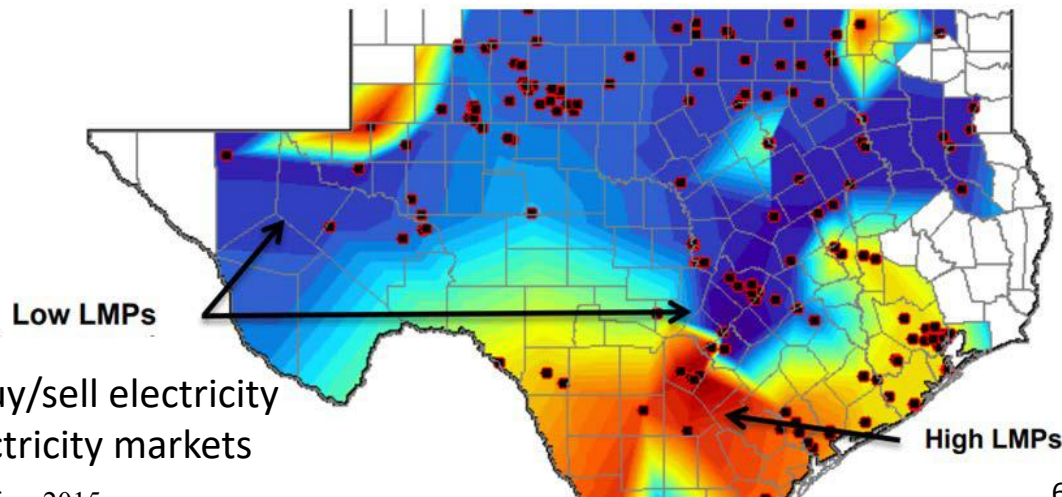
- Global electricity production by source and projection based on sustainable development



Energy transport – electricity transmission congestion

- Electricity transmission has its own constraints -- thermal, voltage and stability limits designed to ensure reliability
- Congestion occurs when lack of transmission line capacity to deliver electricity reliably
- This can impact
 - Electricity price at peak demand
 - Transmission of the cheap renewable electricity
- Solutions:
 - Grid planning
 - Energy storage

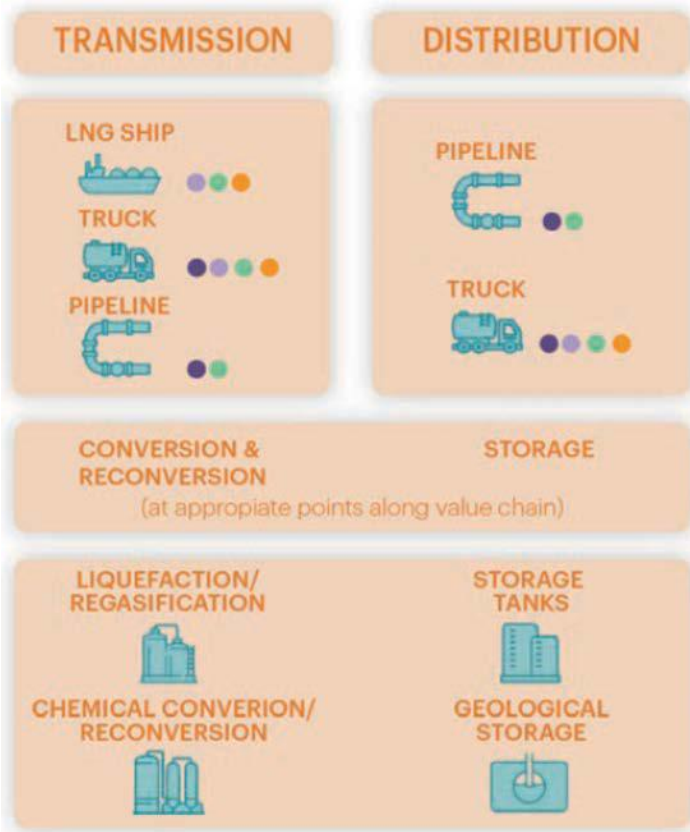
An example: LMP separation in Texas^[1]



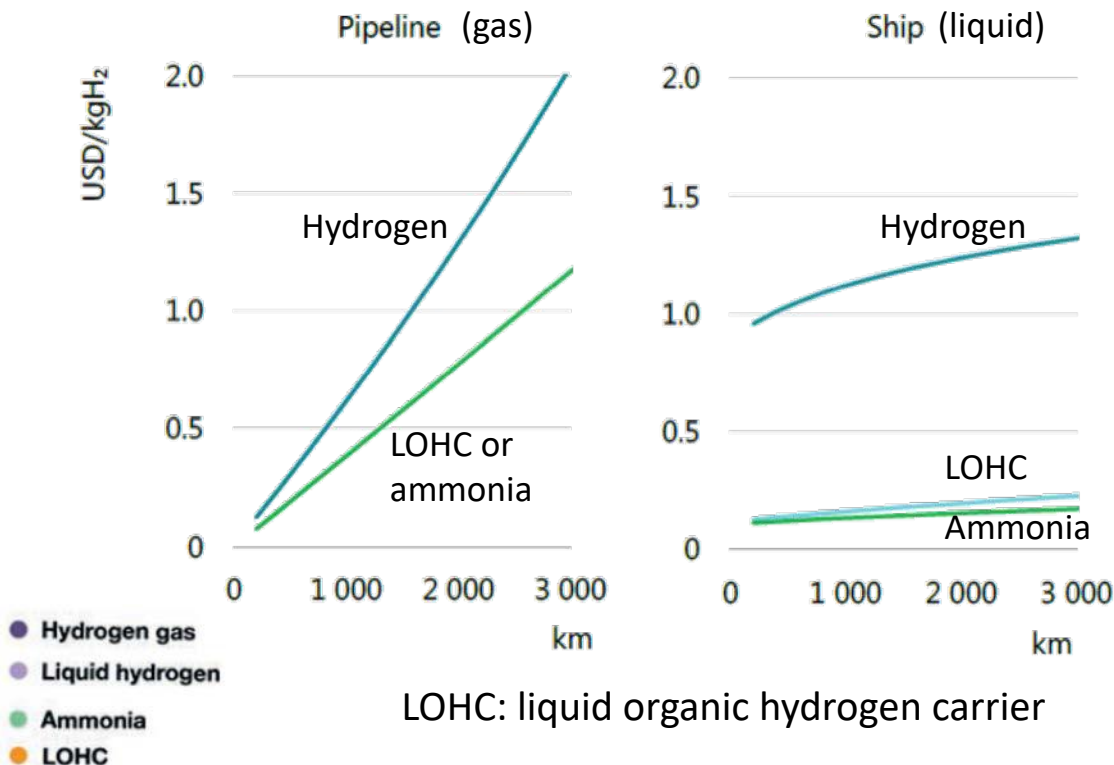
LMP: locational marginal pricing, cost to buy/sell electricity at different locations within wholesale electricity markets

[1] NREL, 'Renewables-Friendly' Grid Development Strategies, 2015

Energy transport – hydrogen transmission and distribution



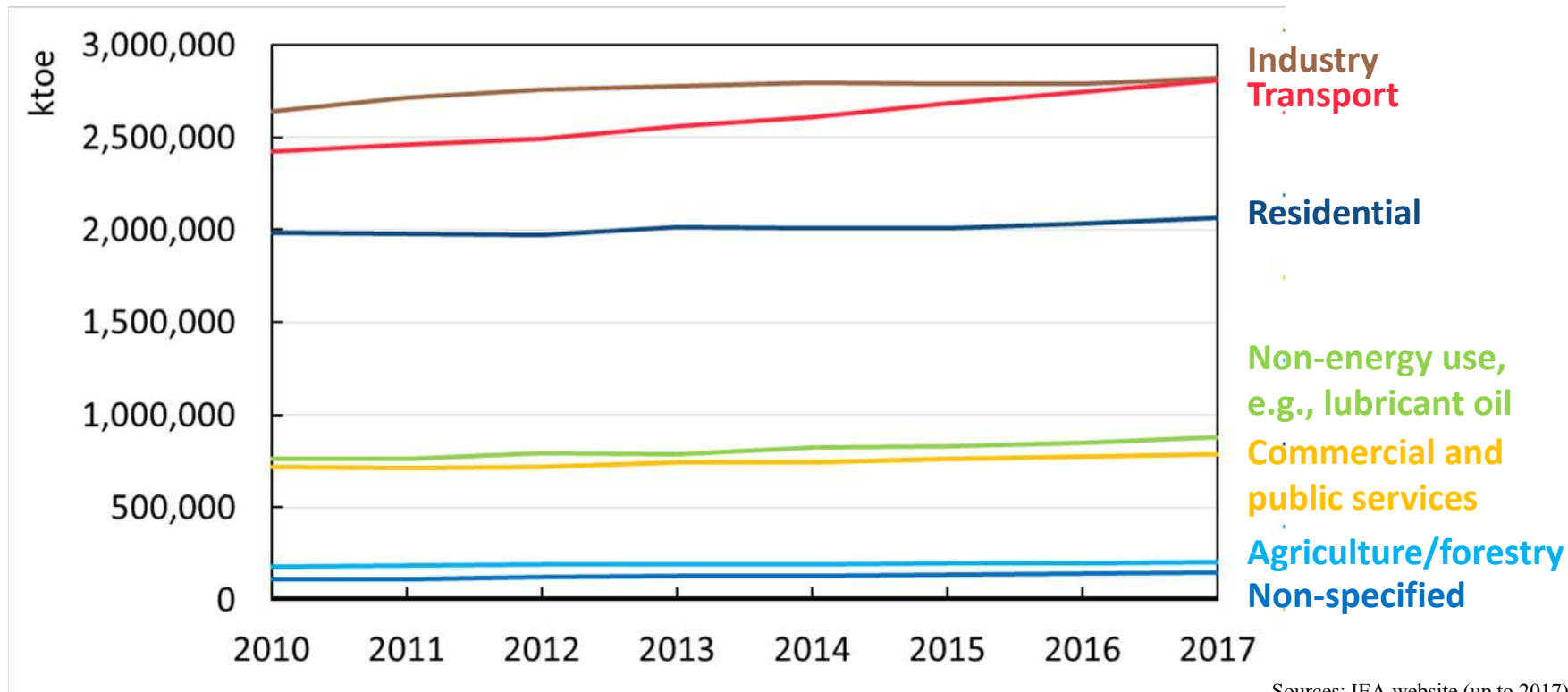
Cost of hydrogen storage and transmission



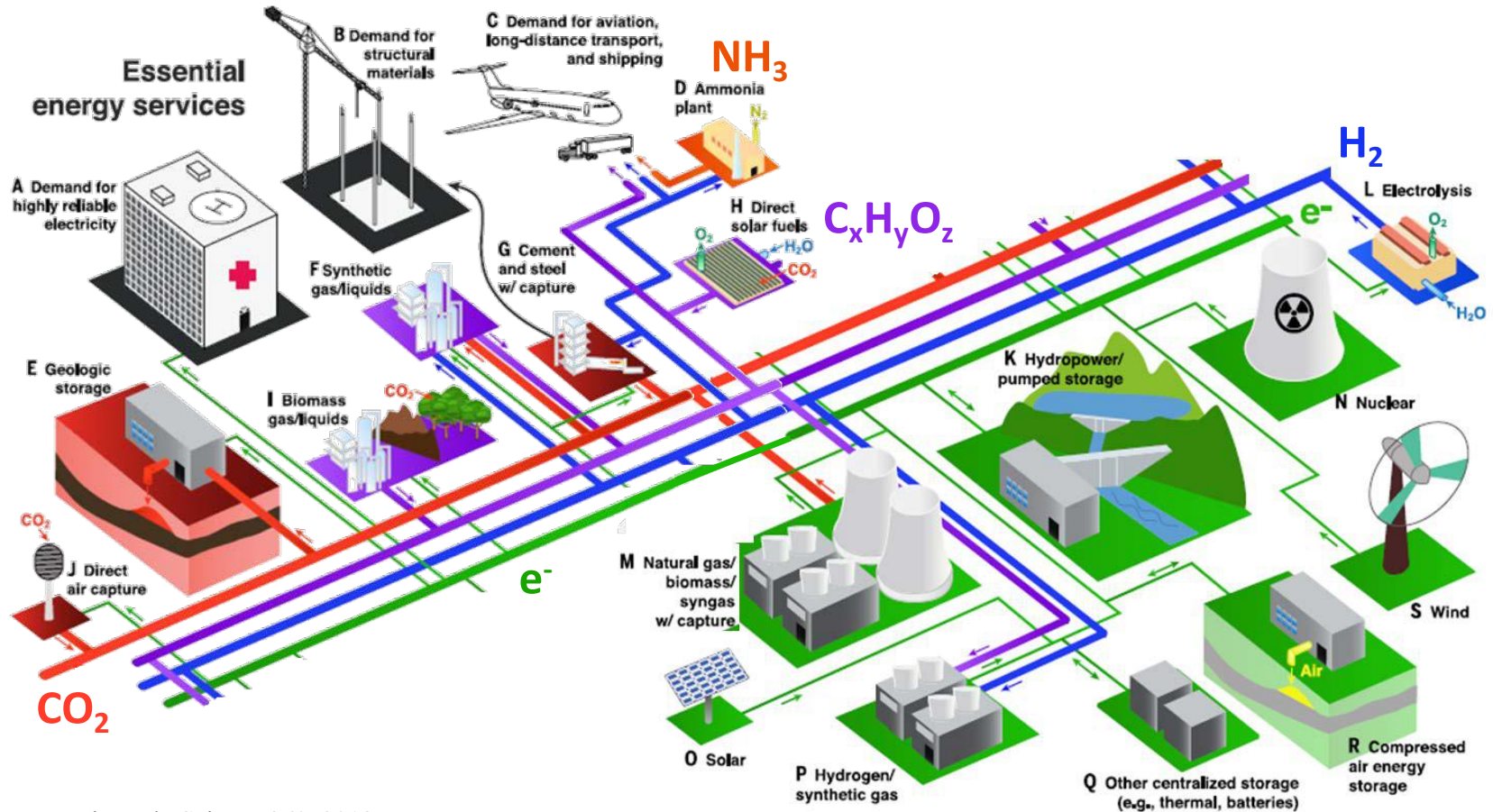
Ref: IEA, The Future of Hydrogen, June 2019

Energy consumption

- Global total energy consumption by sector



Net-zero emission integrated systems

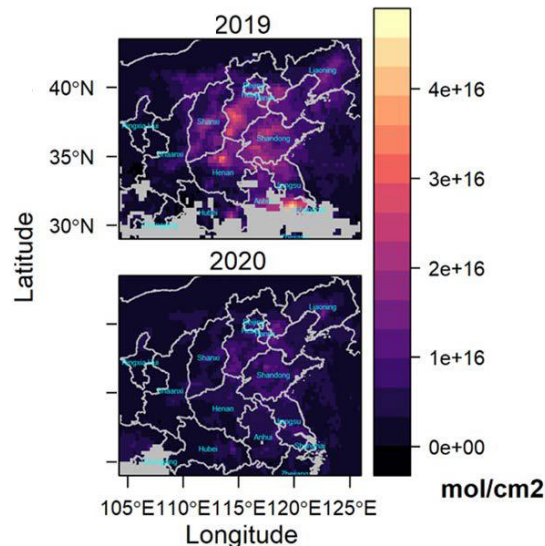


What do we talk about when we talk about energy systems?

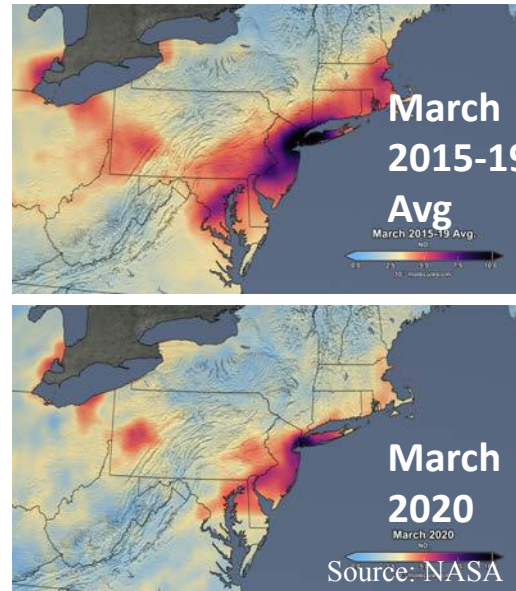
- Energy efficiency: energy consumption and production
- Emissions: GHG, pollutants, waste heat, etc.
- Economics: money flow, etc.
- Societal impacts: health, risks, public perception, etc.
-

- Pollution drops due to the lockdown of cities, decline in industry production and electricity demand
- But meanwhile, people suffers from health problems, job losses, etc.

NO₂ levels in part of China (a week after Chinese New Year)



NO₂ levels in Northeast US in March



System point of view

Emission reduction



Welfare of the people

Energy consumption will ramp up after COVID-19, but in what manners?

- Fossil fuels?
 - Short term incentive due to low prices

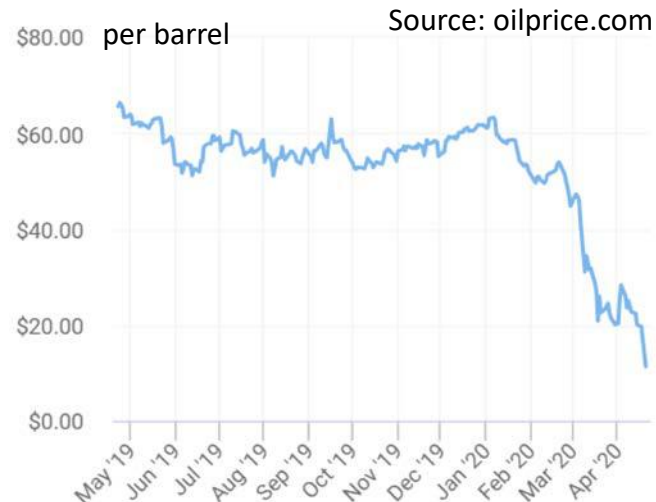
- Renewables?

“Once COVID-19 has been defeated, attracting investments and re-establishing the manufacturing and supply chains for wind and solar power will take much longer than turning up production at oil wells and restarting thermal power plant units.” – *Nature Energy*

- Policies, supply chains, investments, manufacturing capabilities



West Texas intermediate (WTI) price



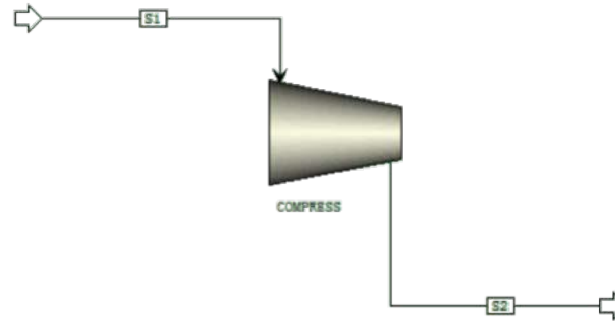
What do we talk about when we talk about energy systems?



- Energy efficiency: energy consumption and production
- Emissions: GHG, pollutants, waste heat, etc.
- Economics: money flow, etc.
- Societal impacts: health, risks, public perception, etc.
-
- **It is useful to obtain these information of the complex energy systems (integrated mechanical, chemical and electrical components) using some modeling softwares**

- With interactive graphical user interfaces (Drag-and-connect)

- Aspen Plus
- Thermoflow
- gPROMS



- Mainly coding

- EES
- Matlab
- Cantera

```
function w = pump(fluid, pfinal, eta)
% PUMP - Adiabatically pump a fluid to pressure pfinal, using a pump
% with isentropic efficiency eta.
%
h0 = enthalpy_mass(fluid);
s0 = entropy_mass(fluid);
set(fluid, 'S', s0, 'P', pfinal);
h1s = enthalpy_mass(fluid);
isentropic_work = h1s - h0;
actual_work = isentropic_work / eta;
h1 = h0 + actual_work;
set(fluid, 'H', h1, 'P', pfinal);
w = actual_work;
```

- A process simulation tool
 - Heat Exchanges
 - Reactors
 - Pressure Changers (Valves, Pumps, Compressors, etc.)
 - Distillation Columns
 - Absorption Columns
 - Extractors
 - Flash systems
 - Separators & Mixers
 - Solid Operations (Crushing, sieving, filtration, etc...)
 - User models (unique for you!)
- Given a process design and an appropriate selection of thermodynamic models, it uses mathematical models to predict the performance of the process

User interface

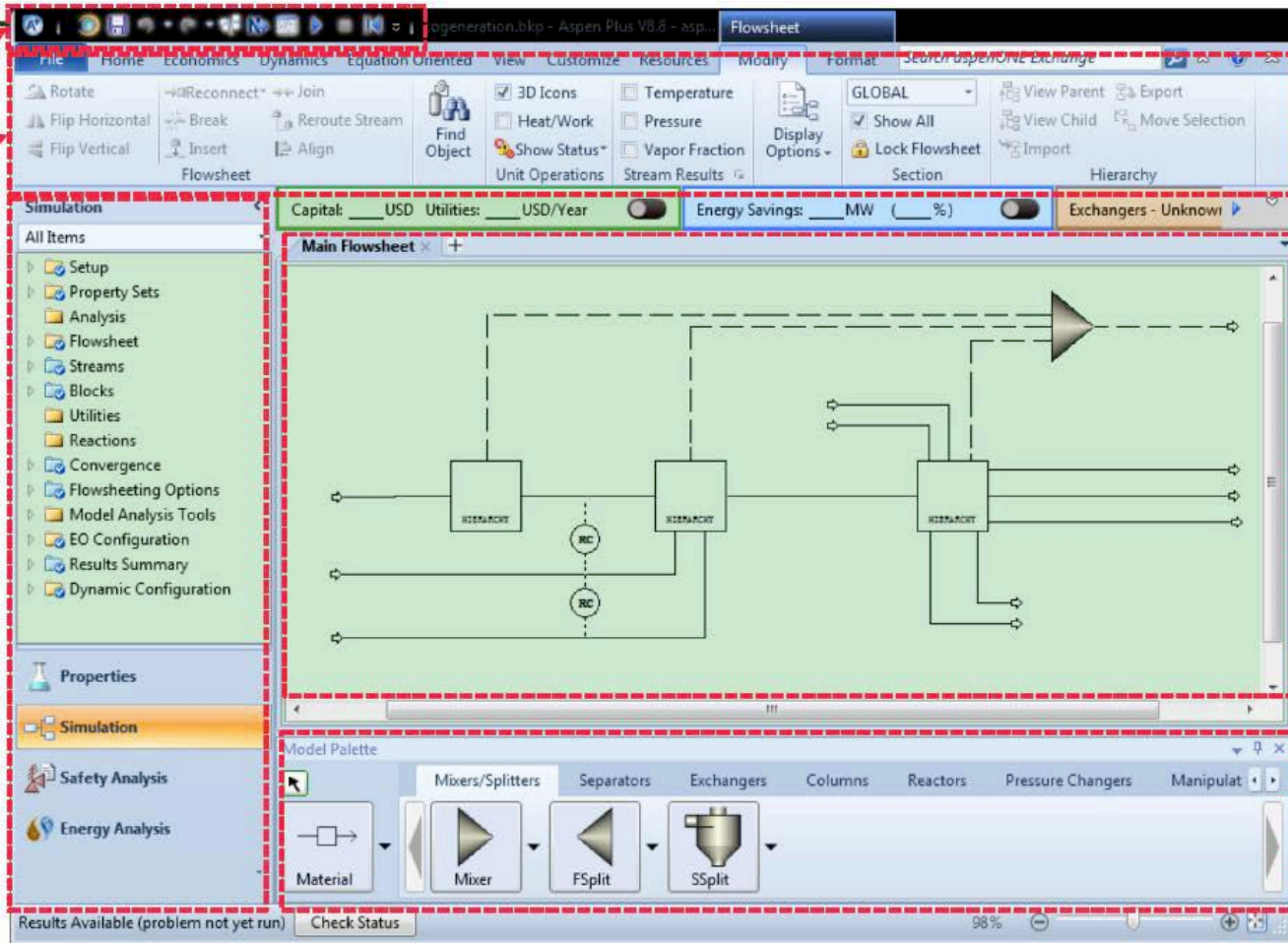
Short-cut

Ribbon

Simulation configuration

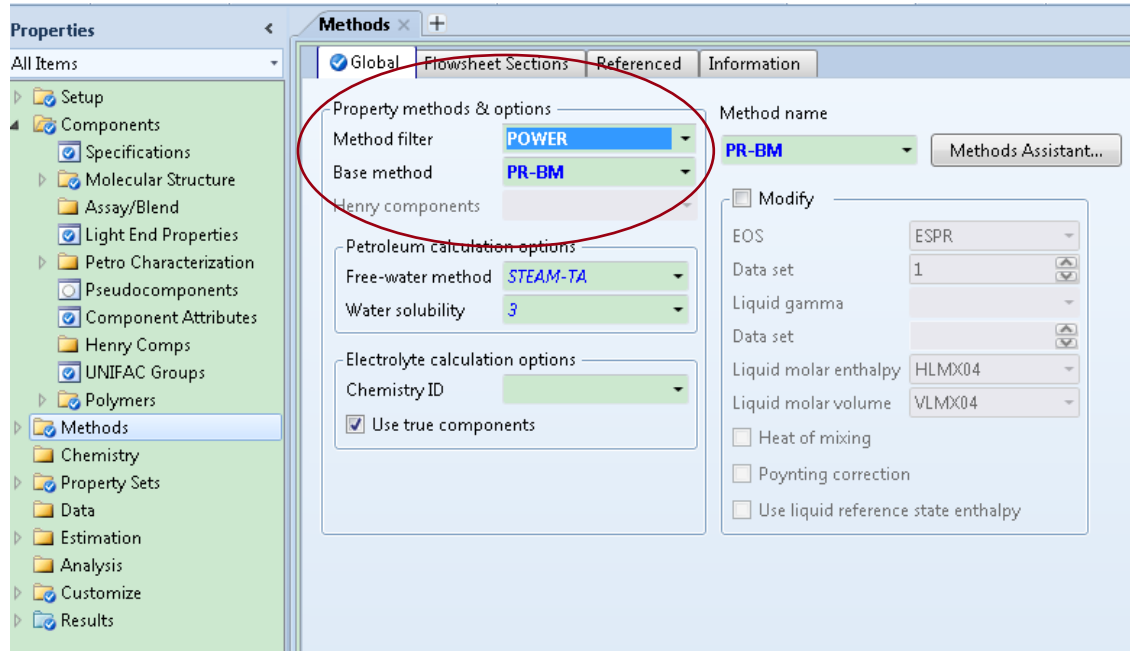
Process flowsheet

Process components

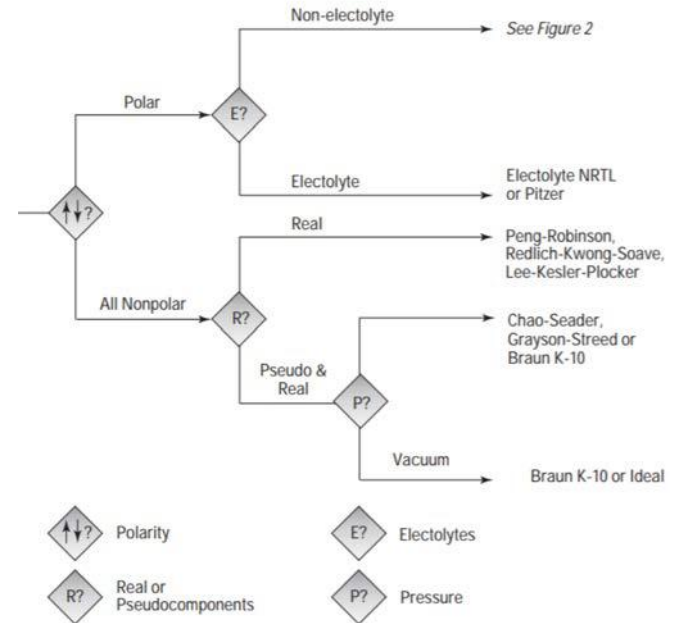


- 1. Define chemical components in the process and select the appropriate thermodynamics model
- 2. Build the process by dragging and connecting components from the palette
- 3. Define the input of the process and the components' parameters
- 4. If there are some constraints in the flowsheet, e.g., temperature, flow rate, and component performance, input them into the flowsheeting options.
- 5. Run the simulation!

Thermodynamics method is important for evaluating the physical properties

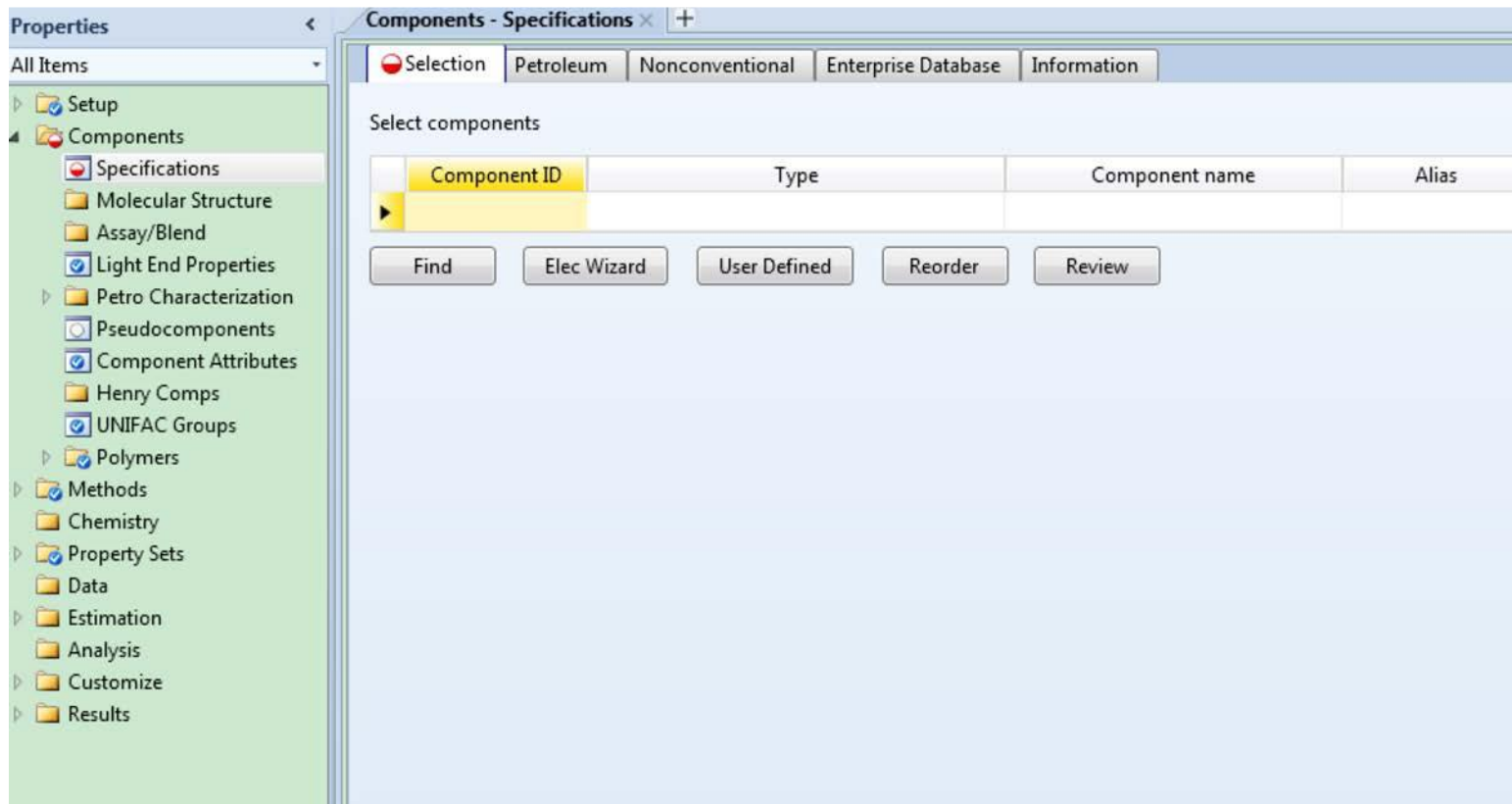


Flow chart for method selection



Ref: Don't Gamble With Physical Properties For Simulations, Eric C. Carlson, Aspen Technology, Inc

First, select components and thermodynamics properties



First, select components and thermodynamics properties

Properties < Components - Specifications x +

All Items ▾


- Setup
- Components
 - Specifications
 - Molecular Structure
 - Assay/Blend
 - Light End Properties
 - Petro Characterization
 - Pseudocomponents
 - Component Attributes
 - Henry Comps
 - UNIFAC Groups
 - Polymers
- Methods
 - Chemistry
- Property Sets
 - Data
- Estimation
 - Analysis
- Customize
- Results

Select components

Component ID	Type	Component name	Alias
H2O	Conventional	WATER	H2O
H2	Conventional	HYDROGEN	H2
O2	Conventional	OXYGEN	O2

Find Elec Wizard User Defined Reorder Review

Then, draw the process flowsheet



The screenshot displays the 'Main Flowsheet' tab in a process simulation software. The interface is divided into three main sections: a sidebar on the left, a top header bar, and a main workspace.

Sidebar (Left): A tree view under the 'Simulation' heading. The 'All Items' dropdown is selected. The tree structure is as follows:

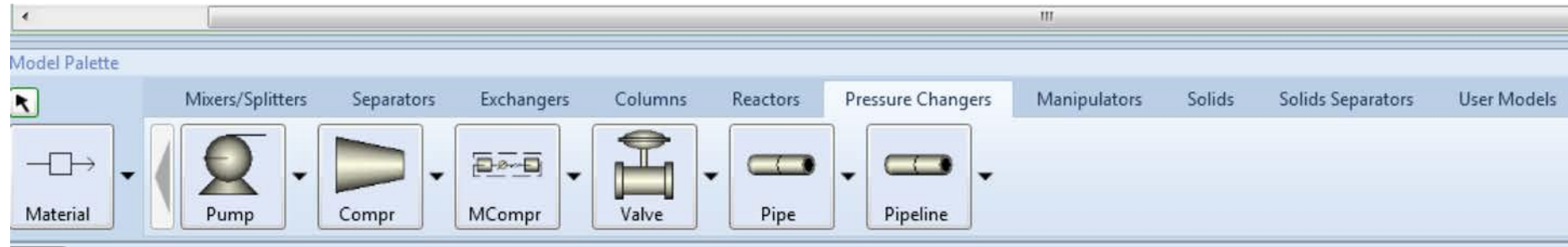
- Simulation
 - All Items
 - Setup
 - Property Sets
 - Analysis
 - Streams
 - Blocks
 - Utilities
 - Reactions
 - Flowsheet
 - Convergence
 - Flowsheeting Options
 - Model Analysis Tools
 - EO Configuration
 - Results Summary
 - Dynamic Configuration

Top Header Bar: Contains three panels, each with a close button (X) in the top right corner.

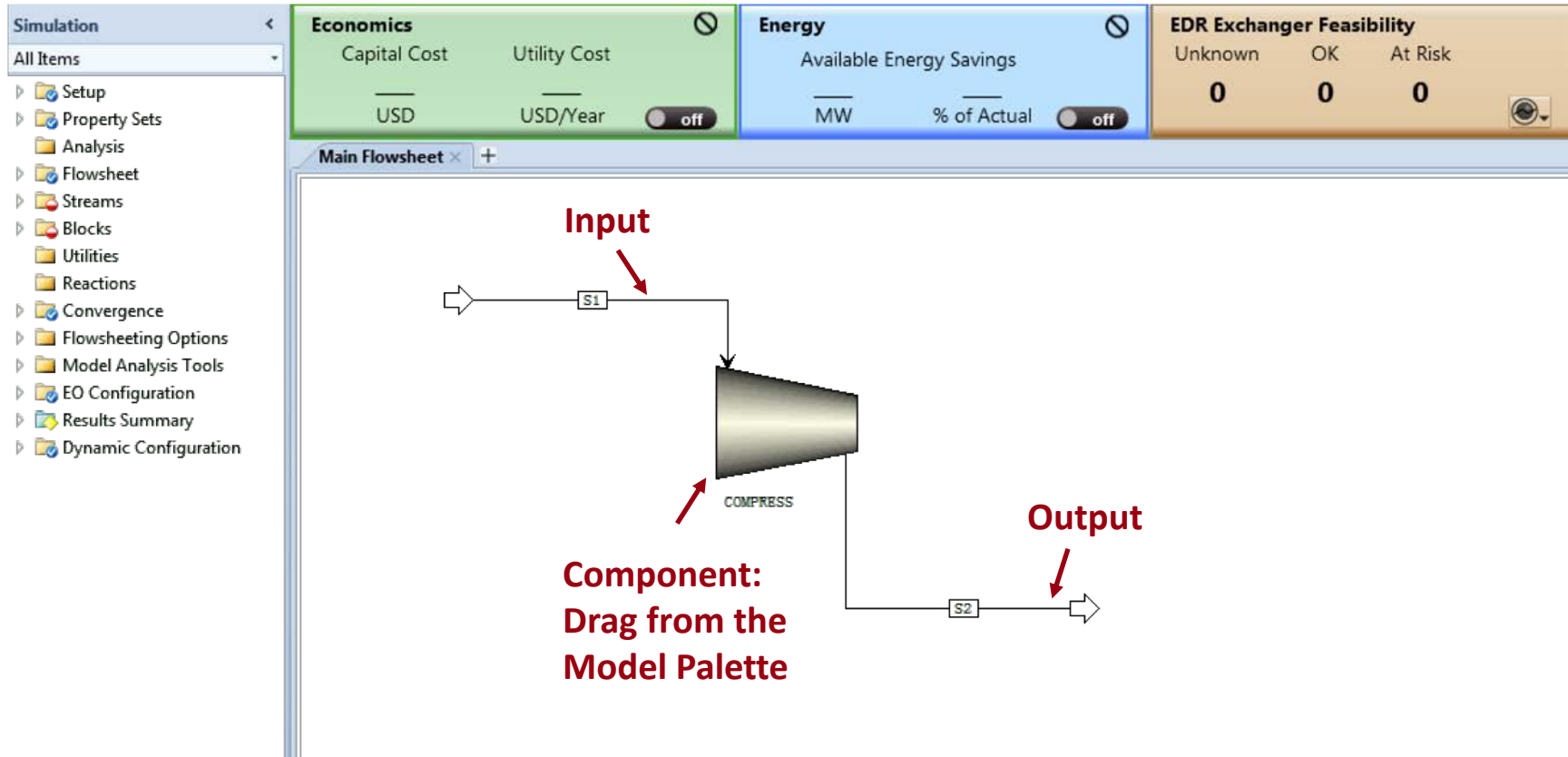
- Economics (Green Panel):**
 - Capital Cost: USD
 - Utility Cost: USD/Year
 - Toggle: off
- Energy (Blue Panel):**
 - Available Energy Savings: MW
 - % of Actual: % of Actual
 - Toggle: off
- EDR Exchanger Feasibility (Orange Panel):**
 - Unknown: 0
 - OK: 0
 - At Risk: 0
 - Toggle: on

Main Workspace: A large empty area for drawing the process flowsheet, with a tab labeled 'Main Flowsheet' and a '+' icon for adding new sheets.

The process components can be added into the process



Then, connect the components



By double clicking the component, you can look at its settings

Main Flowsheet x COMPRESS (Compr) x +

Specifications Calculation Options Power Loss Convergence Integration Parameters Utility Information

Model and type

Model ☒ Compressor ☐ Turbine

Type **Isentropic**


Outlet specification

☒ Discharge pressure **20** **bar**

☐ Pressure increase **bar**

☐ Pressure ratio

☐ Power required **kW**

☐ Use performance curves to determine discharge conditions 

Efficiencies

Isentropic **0.9** Polytropic Mechanical **0.95**

Define the inlet

Main Flowsheet x COMPRESS (Compr) x S1 (MATERIAL) x +

☒ Mixed ☐ CI Solid ☐ NC Solid ☐ Flash Options ☐ EO Options ☐ Costing ☐ Information

Specifications

Flash Type **Temperature** **Pressure**

State variables

Temperature **25** **C**

Pressure **1** **bar**

Vapor fraction

Total flow basis **Mole**

Total flow rate **1** **kmol/hr**

Solvent

Reference Temperature

Volume flow reference temperature

Component concentration reference temperature

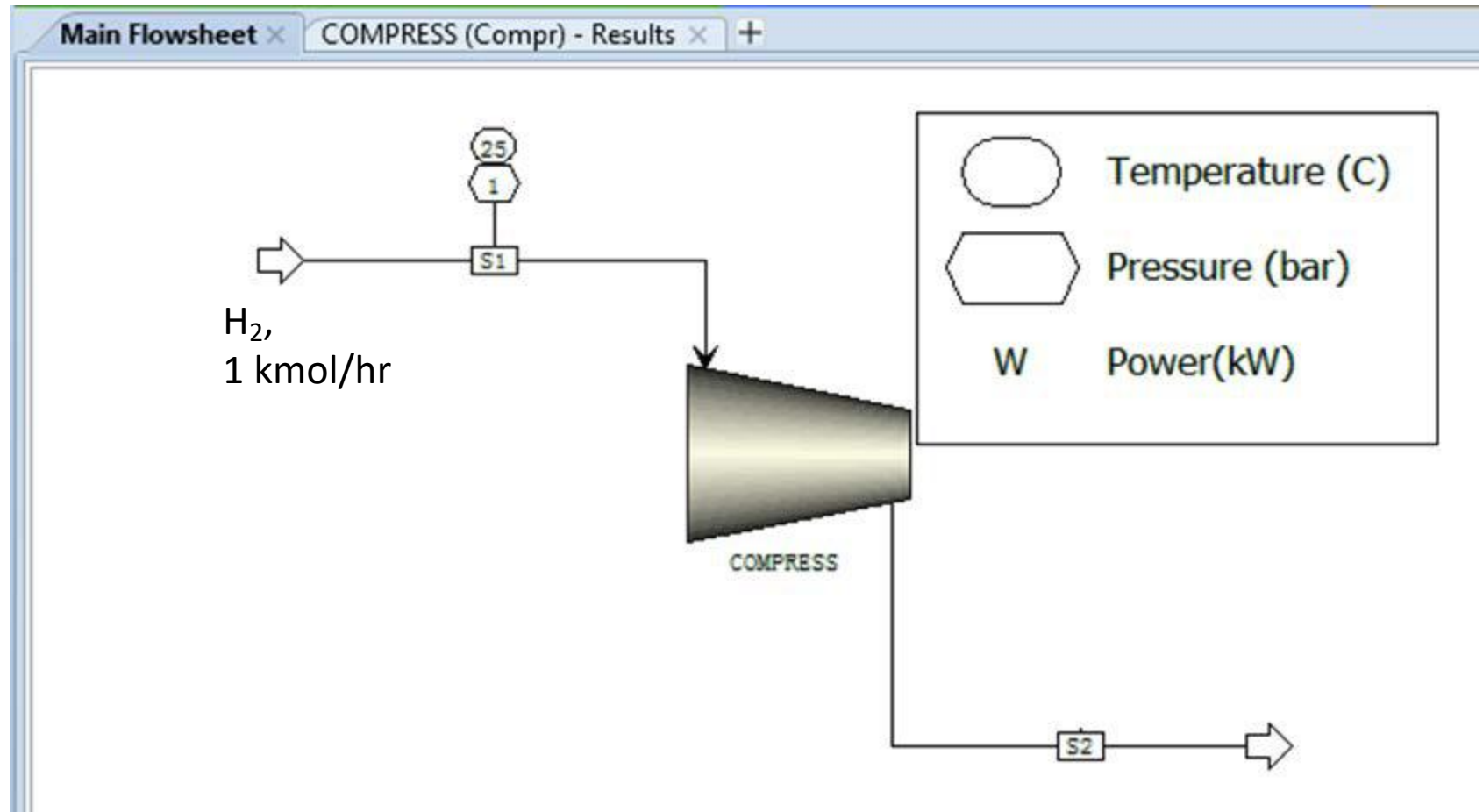
Composition

Mole-Flow **kmol/hr**

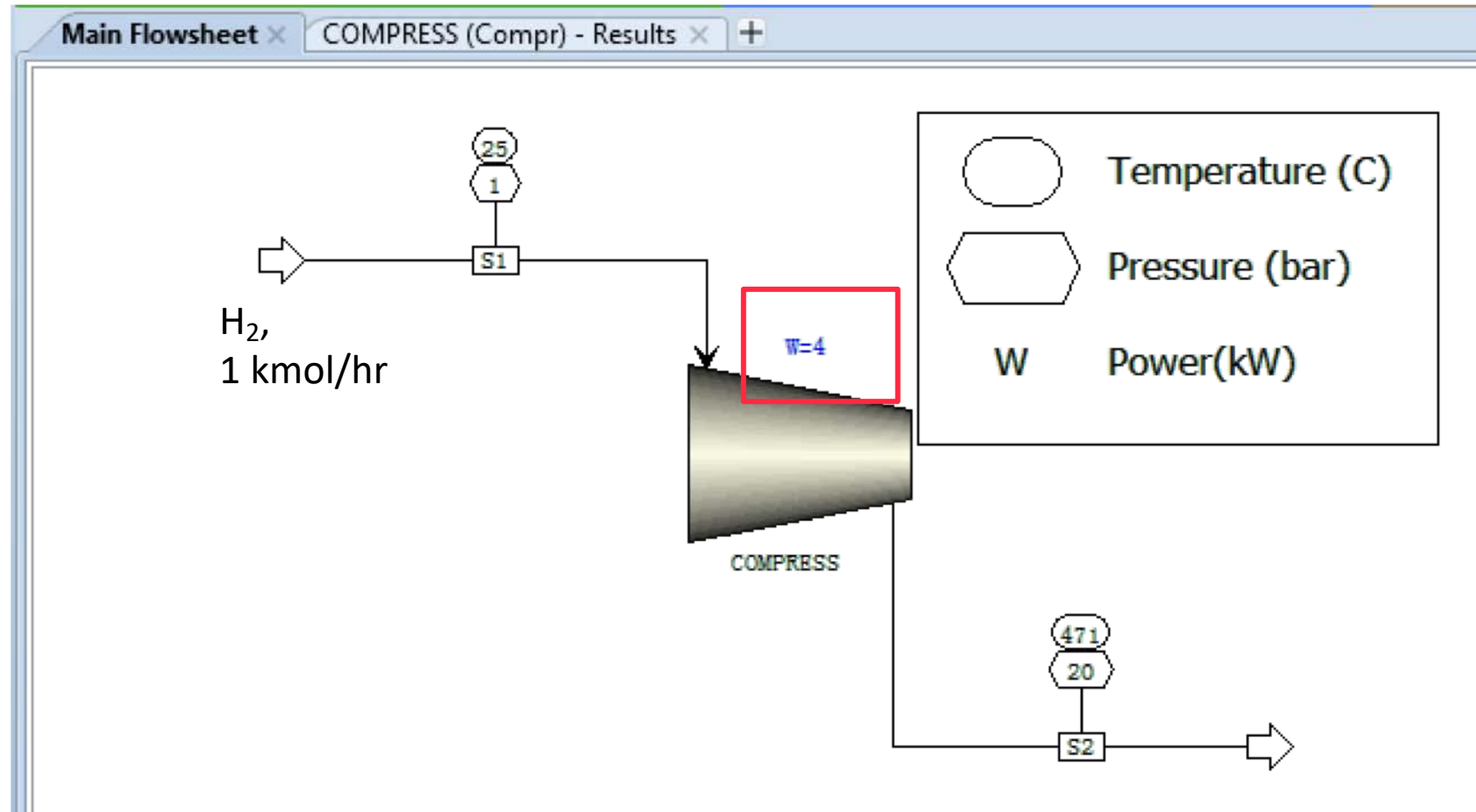
Component	Value
H2O	
H2	1
O2	

Total **1**

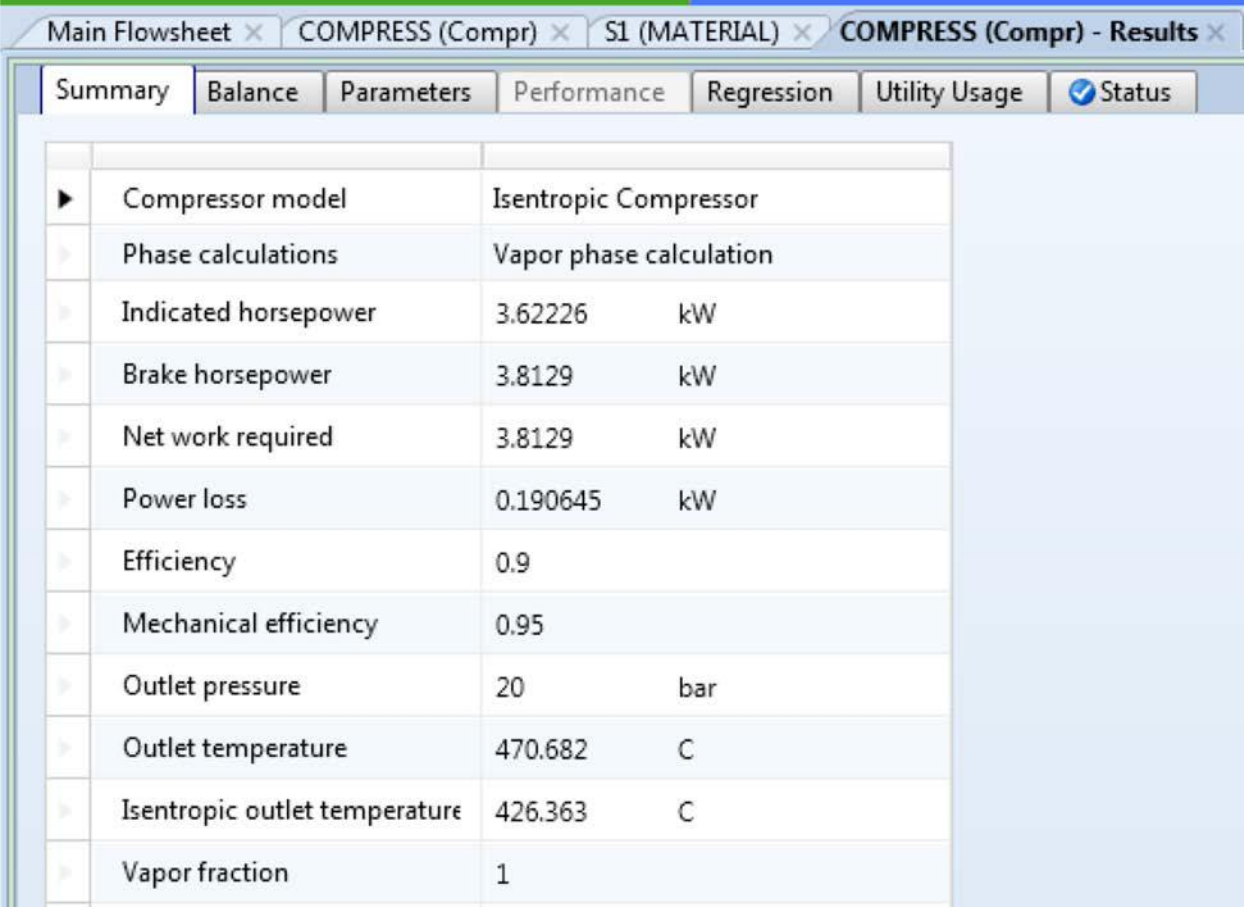
Click run



Results for the hydrogen pressure



More details results can be found by right clicking the component



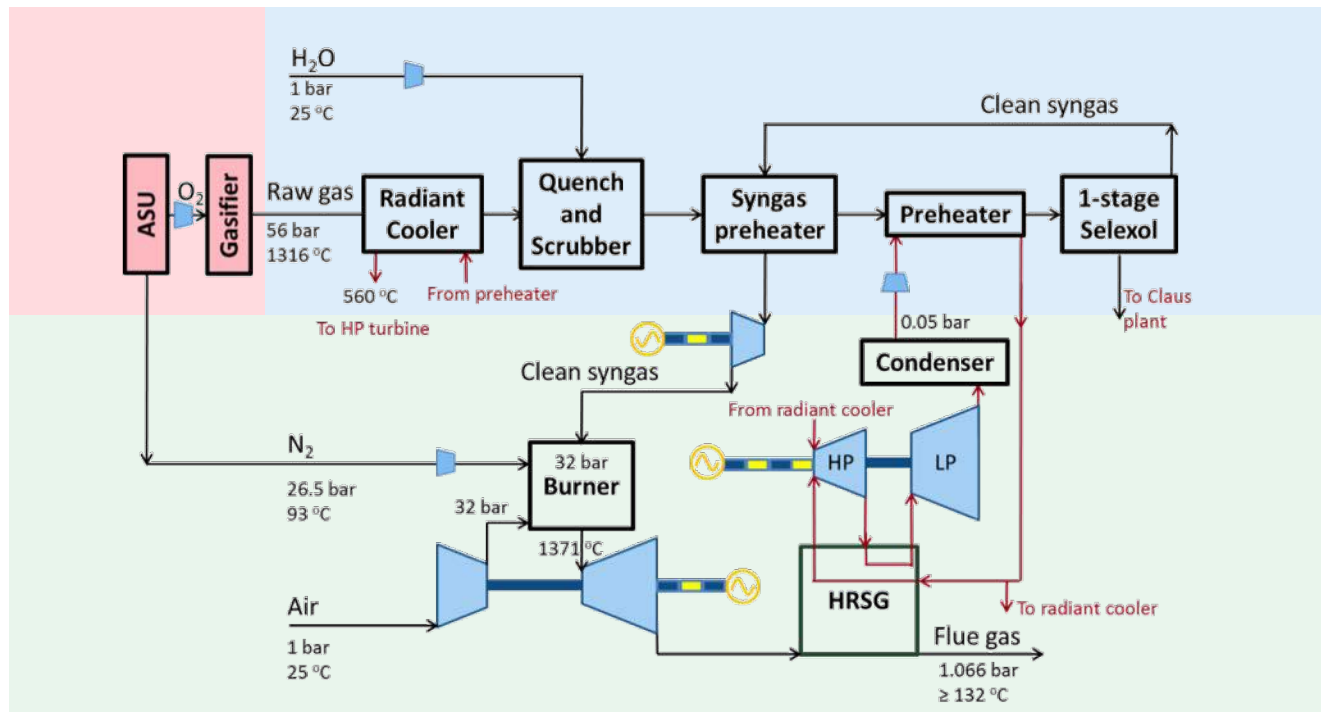
►	Compressor model	Isentropic Compressor	
►	Phase calculations	Vapor phase calculation	
►	Indicated horsepower	3.62226	kW
►	Brake horsepower	3.8129	kW
►	Net work required	3.8129	kW
►	Power loss	0.190645	kW
►	Efficiency	0.9	
►	Mechanical efficiency	0.95	
►	Outlet pressure	20	bar
►	Outlet temperature	470.682	C
►	Isentropic outlet temperature	426.363	C
►	Vapor fraction	1	

Some examples

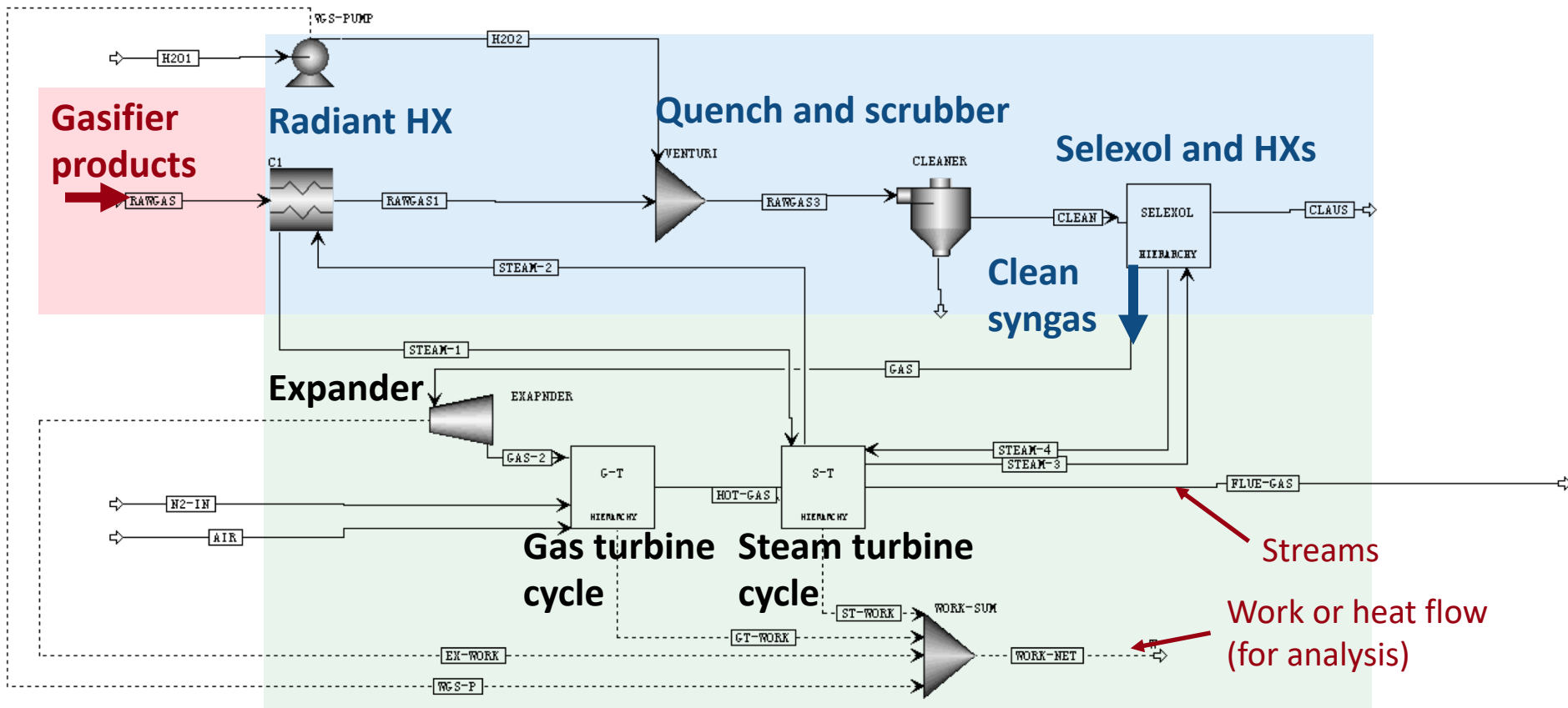
- 1. Thermodynamic efficiency of a novel IGCC-CC power plant integrated with an oxygen permeable membrane for hydrogen production and carbon capture (CC)
(XY Wu, et al., Journal of Advanced Manufacturing and Processing, 2020, under review)
- 2. Dynamic modeling of a flexible Power-to-X plant
(G Buffo, et al., Journal of Energy Storage, 2020, 29, 101314)

Example 1: Energy efficiency analysis (IGCC-CC)

- Conventional Integrated Gasification Combined Cycle (IGCC) plant includes **gasifier**, **syngas cleaning systems**, and a **combined cycle**

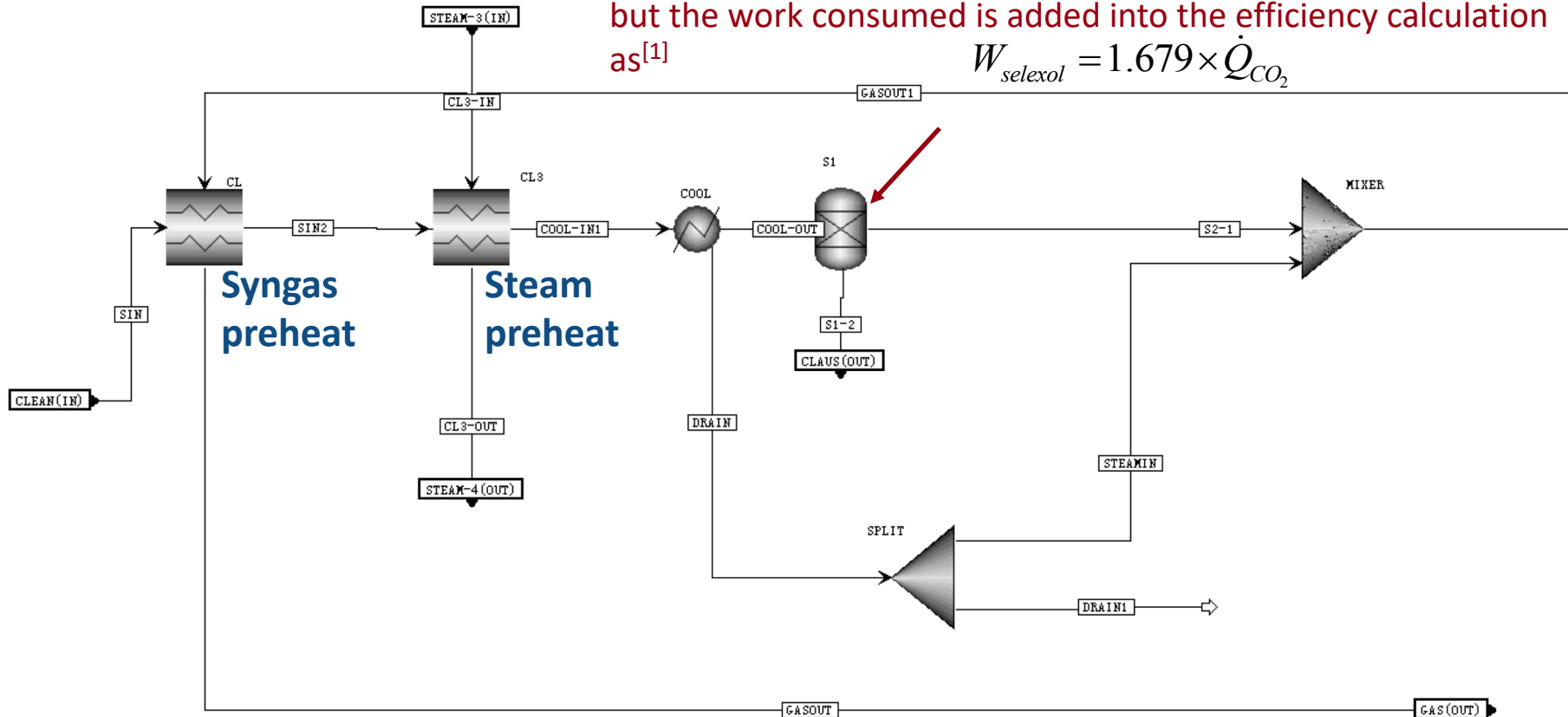


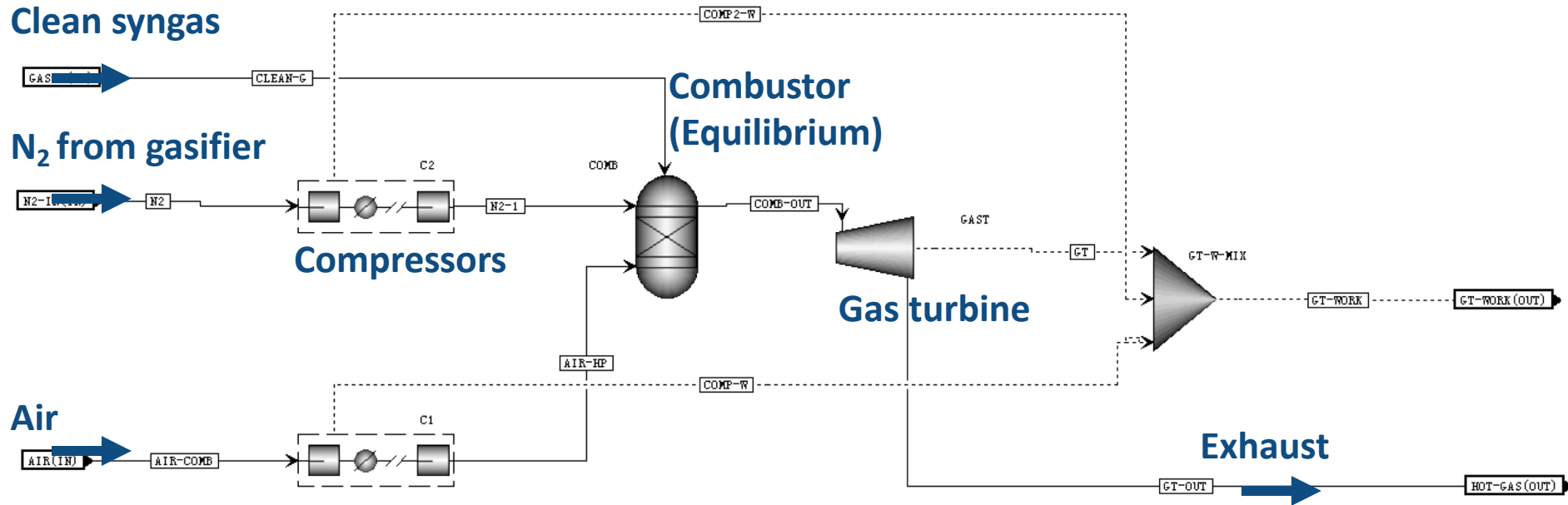
Layout of the Aspen model



The Selexol process is modeled as a separator in Aspen model, but the work consumed is added into the efficiency calculation as^[1]

$$W_{selexol} = 1.679 \times \dot{Q}_{CO_2}$$







Validate the base IGCC model with literature

- The first law efficiency is defined:
$$\eta = \frac{W_{net}}{HHV_{coal}}$$

- The net work output of the cycle is calculated as

$$W_{net} = W_{GT} + W_{ST} + W_{EXP} - \sum W_{pump} + \sum W_{CO_2} + \sum W_{O_2} + W_{Selexel} + W_{aux-gasifier} + W_{BOP} + W_{transformer}$$

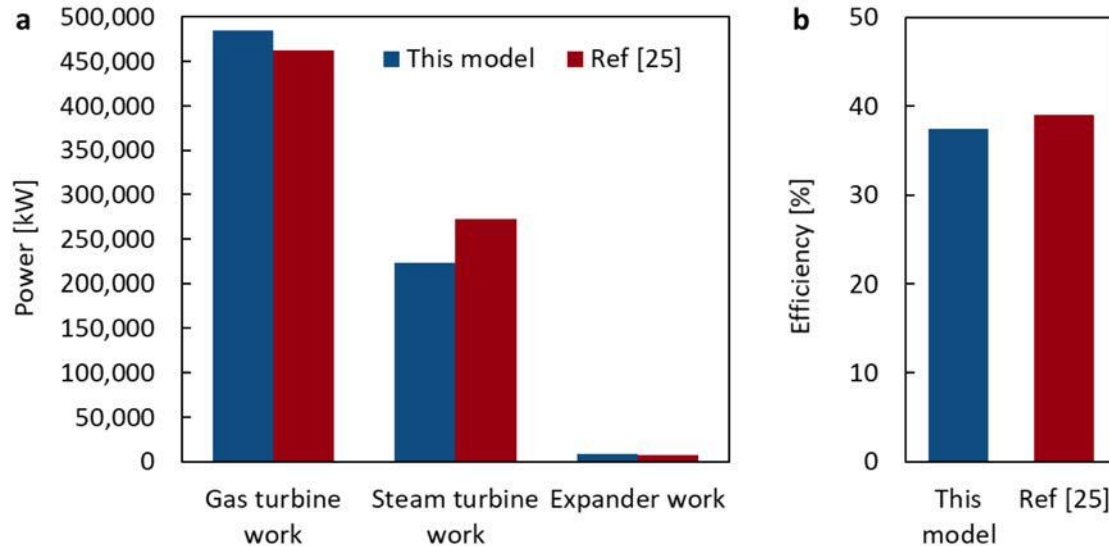
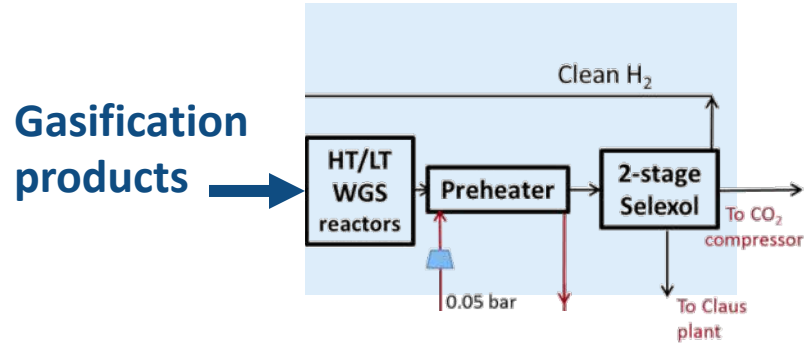


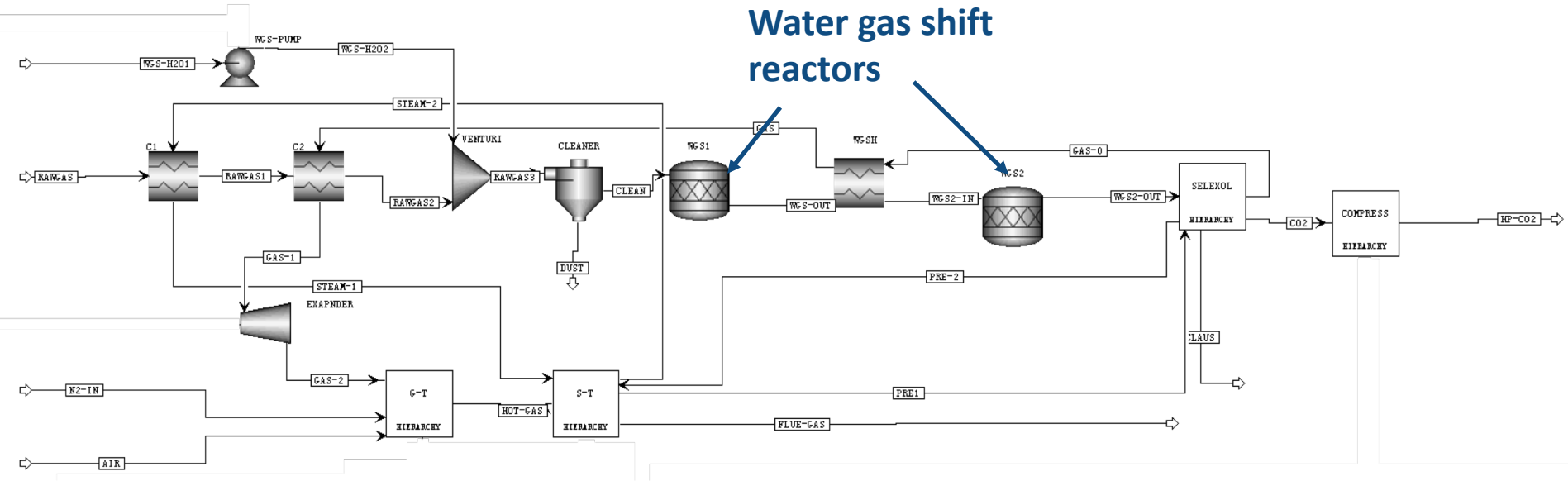
Image courtesy of DOE.

To capture CO₂, water gas shift reactors and acid gas removal systems are installed

- Water gas shift reactor converts CO into CO₂: $\text{CO} + \text{H}_2\text{O} \rightarrow \text{CO}_2 + \text{H}_2$
- Selexol processes separate CO₂ and H₂S

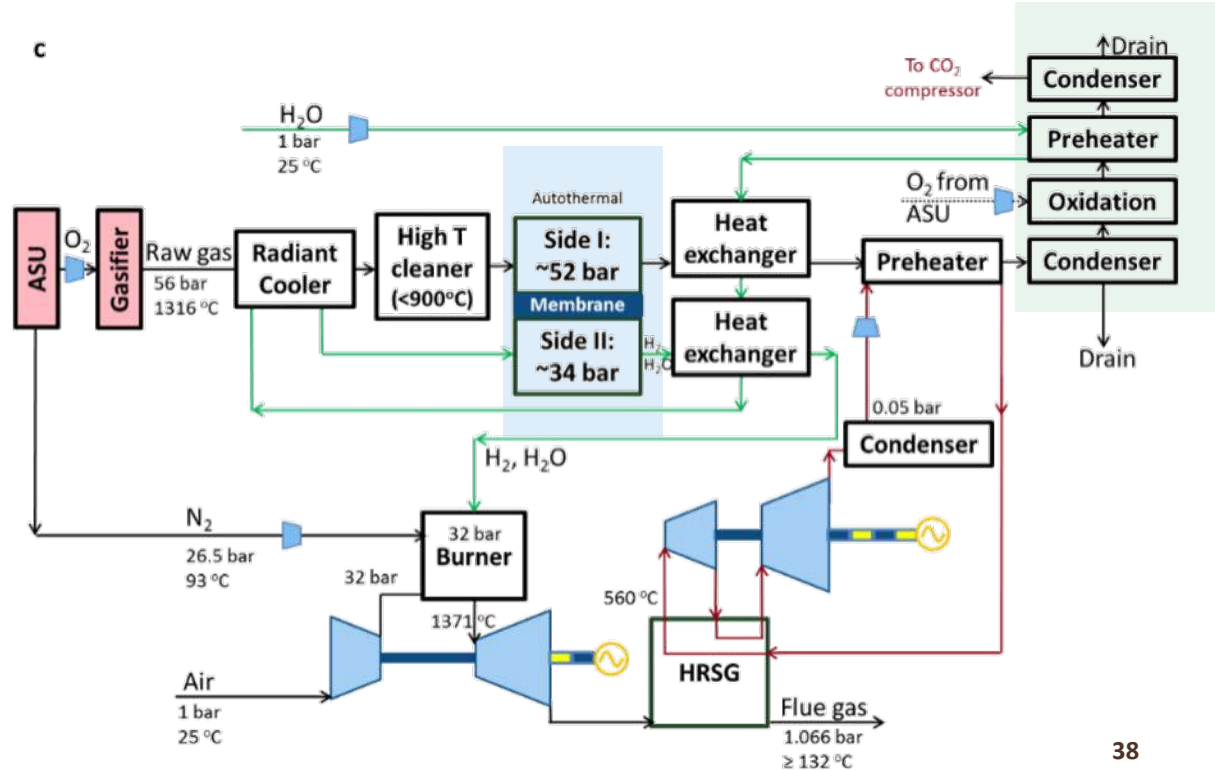
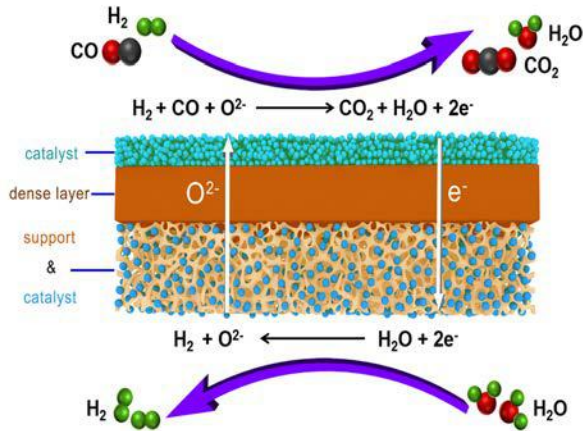


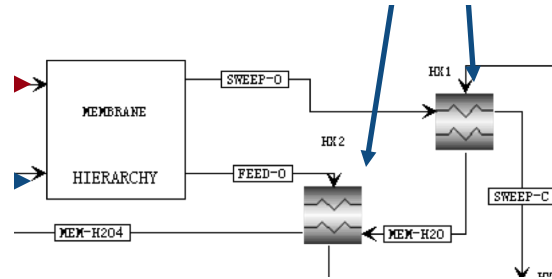
Water gas shift reactors



Instead, IGCC-OTM system uses a membrane to produce high purity H₂ with CC

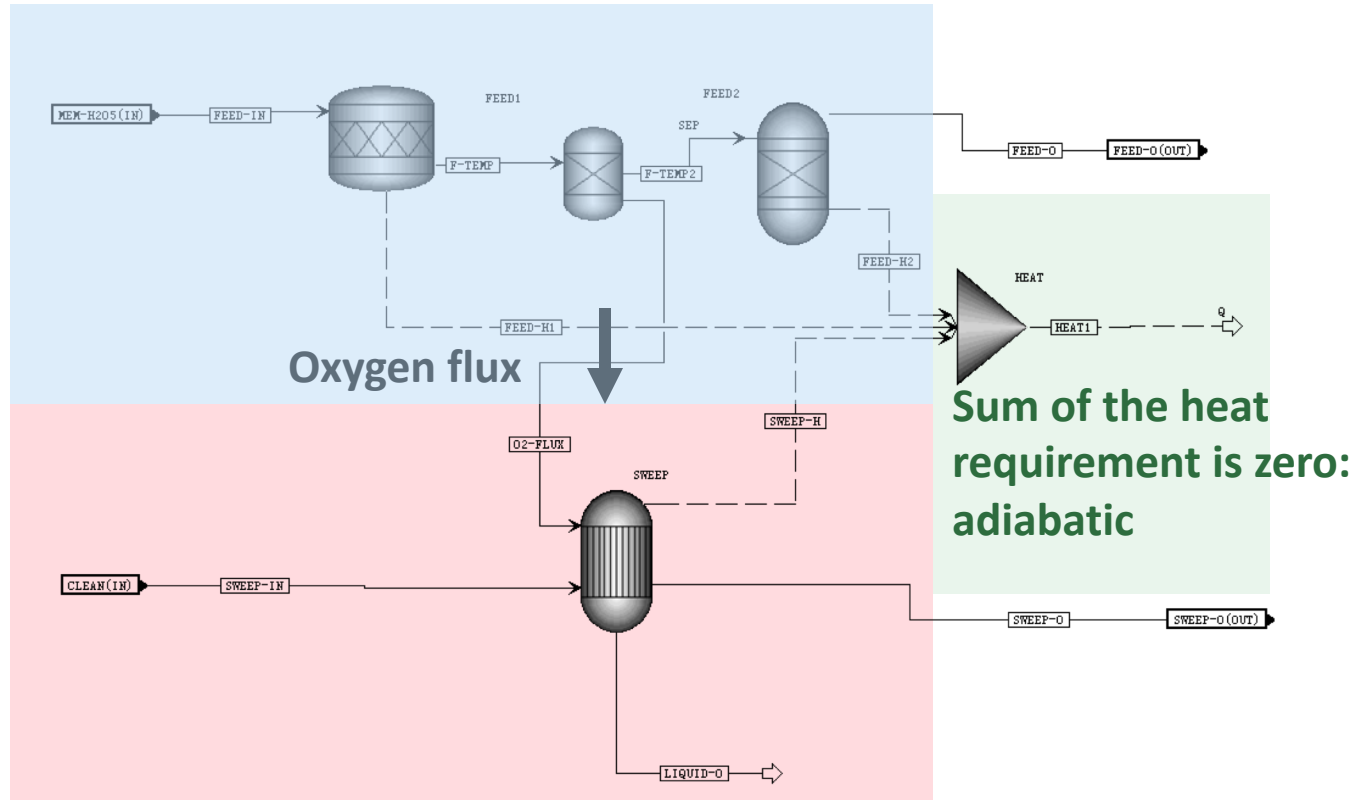
- An oxygen permeable membrane can produce H₂ from water splitting and oxidize the fuel in one unit





Water
splitting
side

Syngas
oxidation
side



Operating conditions

- After connecting all the components in Aspen Plus, the operating conditions and parameters have to be entered

<i>Fuel</i>	
Coal rank	High-volatile A bituminous (Illinois No. 6) HHV (as-received) = 27.135 MJ kg ⁻¹
Raw gas composition	Shown in Table 1
<i>Gasifier</i>	
Technology	GEE gasification technology
T (°C)	1316
P (MPa)	5.6
<i>Gas Turbine</i>	
TIT* (°C)	1371
Combustor pressure (MPa)	3.2
Isentropic efficiency (%)	85

<i>Compressor (air or N₂)</i>	
Isentropic efficiency (%)	84
Heat exchangers	
Minimum internal temperature approach (MITA) (°C)	20 Heat recovery steam generators (HRSG): 10 °C
Pressure drop (%)	5
<i>Steam cycle</i>	
TIT (°C)	560
HP turbine inlet pressure (MPa)	12.5
HP turbine outlet pressure (MPa)	0.568
Turbine efficiencies (%)	90
Pump efficiency (%)	75
Flue gas outlet temperature (°C)	132 (or higher due to constraint of MITA in HRSG)

Selexol process

Work consumption	Calculated from literature
CO ₂ removal efficiency (%)	90
H ₂ S removal efficiency (%)	99.6
H ₂ recovery efficiency (%)	99.4

High temperature gas cleaning

Operating temperature (°C)	~900 °C
----------------------------	---------

Membrane reactor

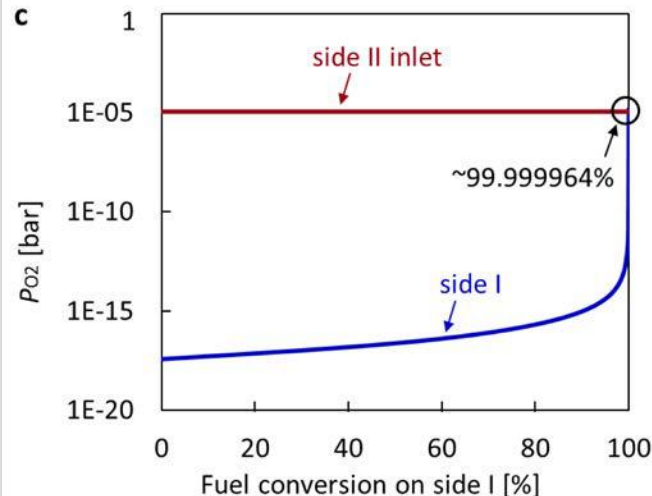
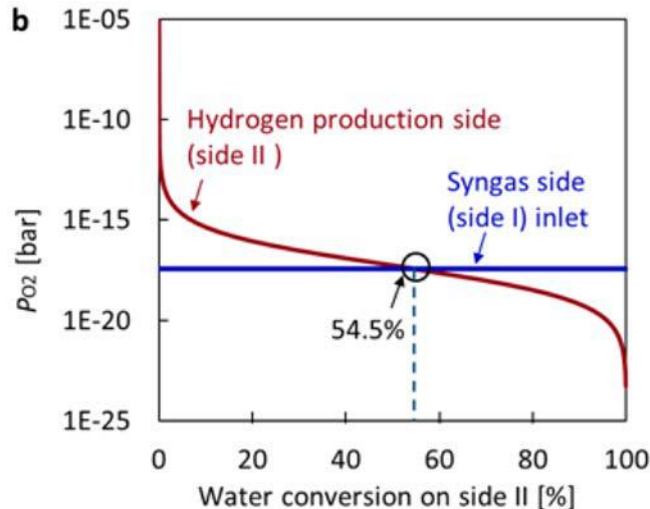
Operating temperature (°C)	850 °C
Raw gas conversion on side I (%)	99**
Water conversion on side II (%)	54**
Reactor design	See Figure 2 (a)

CO₂ compressor

CO ₂ delivery pressure (MPa)	12
Exit CO ₂ stream composition (mol%)	>99% CO ₂ (EOR ready)
Isentropic efficiency (%)	84

Membrane is a user-defined component and its performance has to be determined

- For a counter-flow configuration, the maximum conversion ratios on side I and II are determined

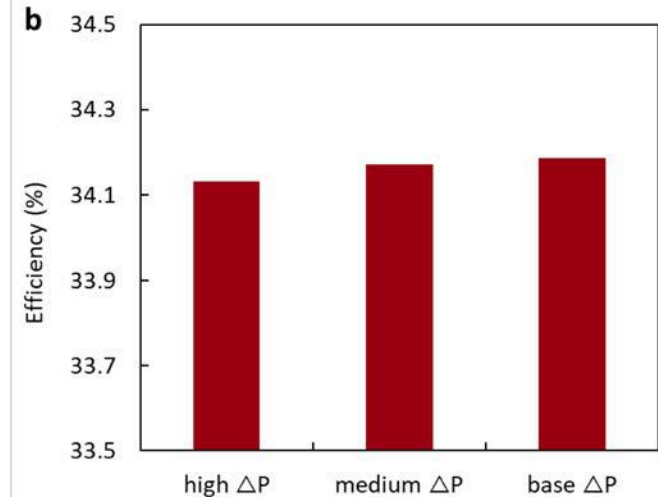
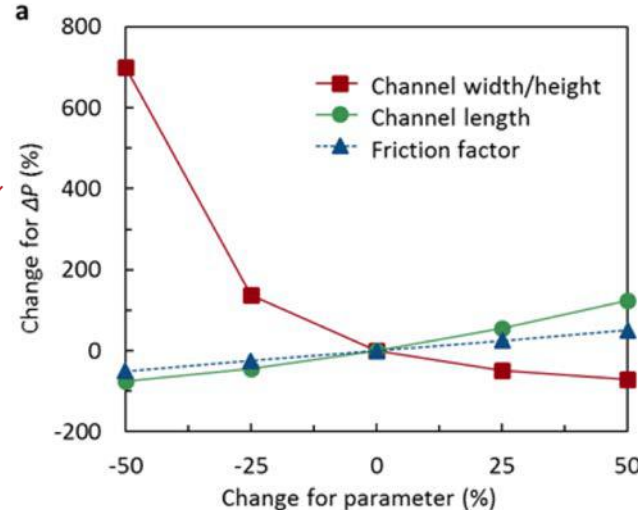
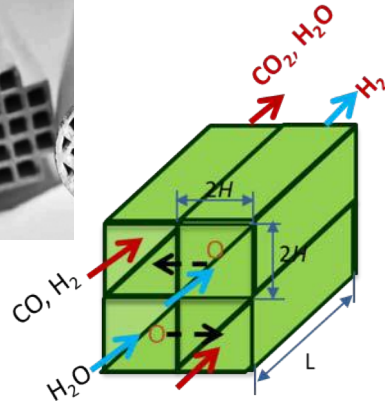


Pressure drop inside the membrane reactor

- A monolith membrane reactor configuration is used to estimate the pressure drop

$$\Delta P_{tot} = \left(\frac{1}{2} \frac{\rho V^2}{D_h} \right) \cdot f \cdot L$$

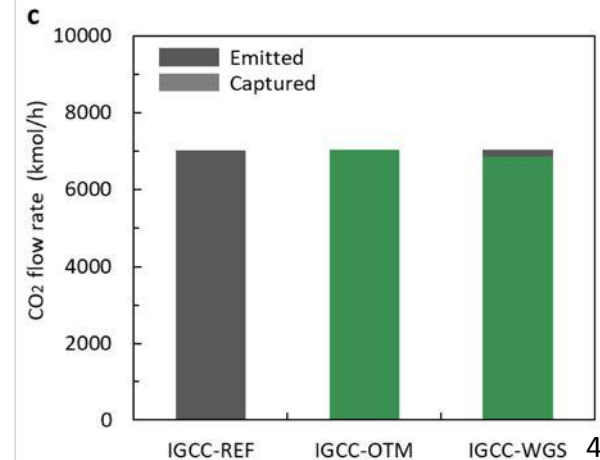
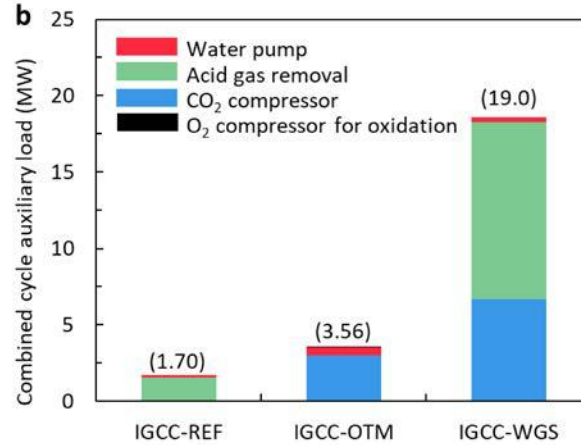
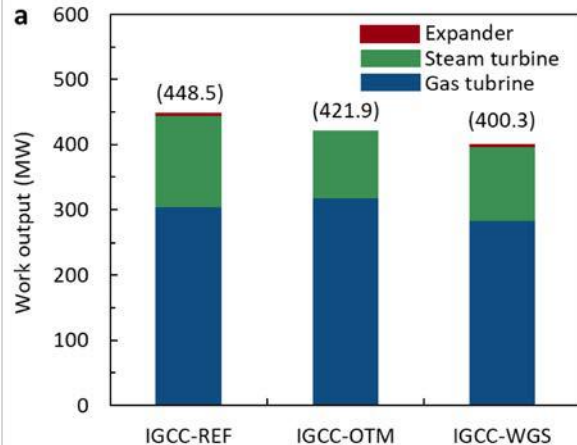
- Sensitivity analysis is carried out to identify the most sensitive membrane parameter and its impacts on the overall efficiency



Performance comparison among the systems

- We can see that the IGCC-OTM can capture more CO₂, while require less auxiliary load than IGCC-WGS
- This leads to higher efficiency of IGCC-OTM than IGCC-WGS (34.2% v.s. 30.6%)
- The specific primary energy consumption for CO₂ avoided (SPECCA) of this novel technology is 1.08 MJ kgCO₂⁻¹, which is 59% lower than that of the IGCC-WGS

$$SPECCA = \frac{\text{Energy consumption due to CC [MJ]}}{\text{reduction in CO}_2 \text{ emission [kg]}}$$

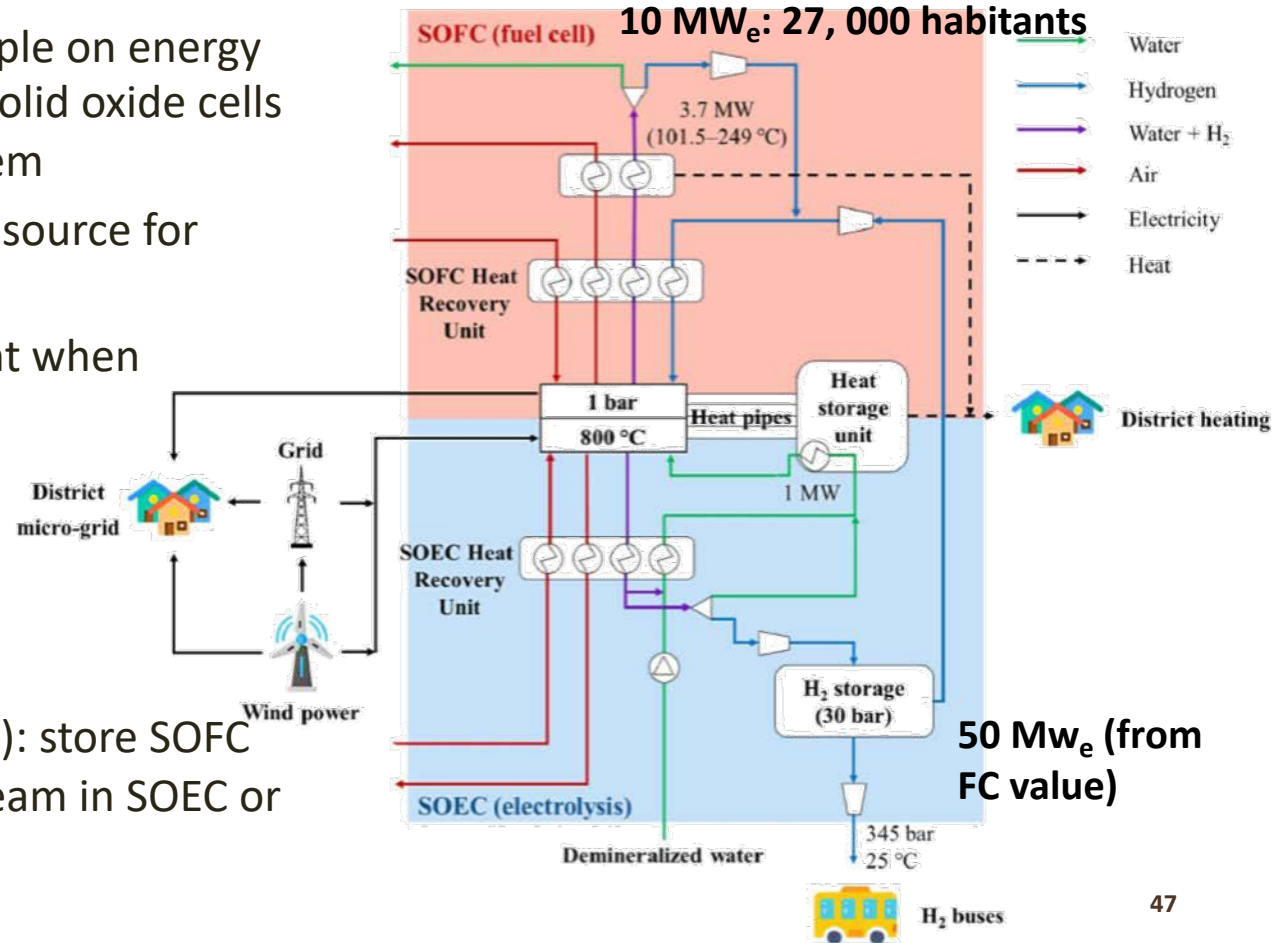


Some examples

- 1. Thermodynamic efficiency of a novel IGCC-CC power plant integrated with an oxygen permeable membrane for hydrogen production and carbon capture (CC)
(XY Wu, et al., Journal of Advanced Manufacturing and Processing, 2020, under review)
- 2. Dynamic modeling of a flexible Power-to-X plant
(G Buffo, et al., Journal of Energy Storage, 2020, 29, 101314)

Example 2: Dynamic simulation

- Here we discuss an example on energy storage using reversible solid oxide cells in a poly-generation system
- Wind power is the major source for energy
- Grid energy is supplement when needed
- Energy consumption:
 - H₂ buses fleet
 - District micro-grid
 - District heating
- Heat storage (molten salt): store SOFC waste heat to preheat steam in SOEC or for district heating



Energy generation

- The wind turbine generation is the kinetic energy of the wind, whose speed distribution follows Weibull distribution:

$$f(x) = \frac{k}{\beta} \left(\frac{x}{\beta} \right)^{k-1} \exp \left[- \left(\frac{x}{\beta} \right)^k \right]$$

The equation is annotated with red arrows and labels:

- Shape factor** points to the parameter k .
- Wind speed** points to the variable x .
- Probability** points to the function $f(x)$.
- Scale factor** points to the parameter β .

Data for an observational site in Nottingham, UK^[1]

	Average wind speed (\bar{x} , m/s)	Shape factor (k)	Scale factor (β , m/s)
Winter	5.51	2.3	6.225
Spring	5.145	2.61	5.798
Summer	4.261	2.76	4.790
Autumn	4.729	2.3	5.351

Demand modeling

- Electricity demand
 - Monte Carlo bottom-up stochastic model
- H₂ bus fleet demand (high priority)
 - 9 kg-H₂/100 km with 10% excess H₂ in the tank for emergency
 - Base case: 1 million km/year (~ Bus 1 mileage)

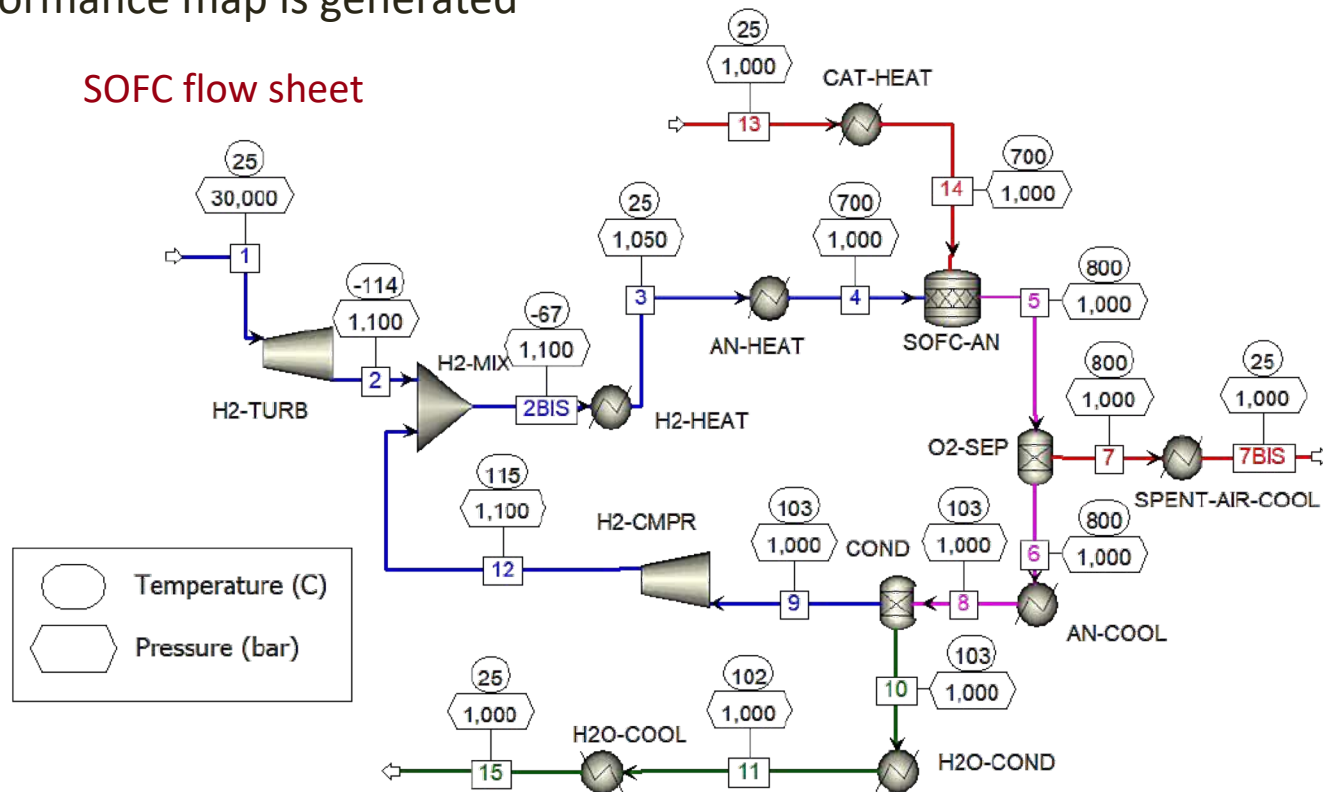
Reference demand of mobility hydrogen.

	Period from September to May		Period from June to August	
	Weekdays	Weekend days	Weekdays	Weekend days
L_d (km)	3544	2102	1581	1032
$H_{2,mob,d}$ (kg)	350.86	208.12	156.46	102.19

- H₂ storage for SOFC (medium)
- District heating demand (low)
 - Stochastic model

- The steady operation of the rSOC plant is modeled using Aspen Plus™
- A performance map is generated

SOFC flow sheet



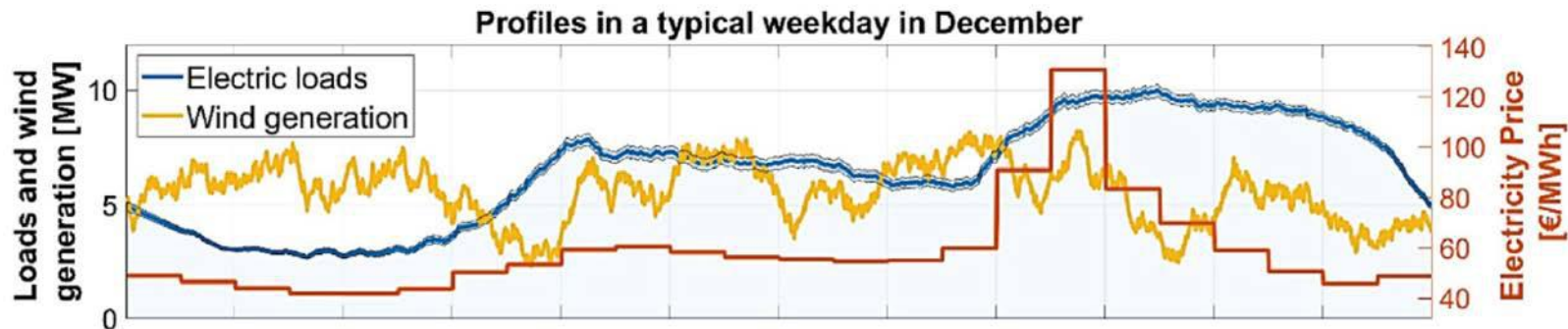
Performance map of the rSOC system

- A time-resolved model can interact with the steady state performance map with the temporal profiles of energy demand of the residential district and wind power generation

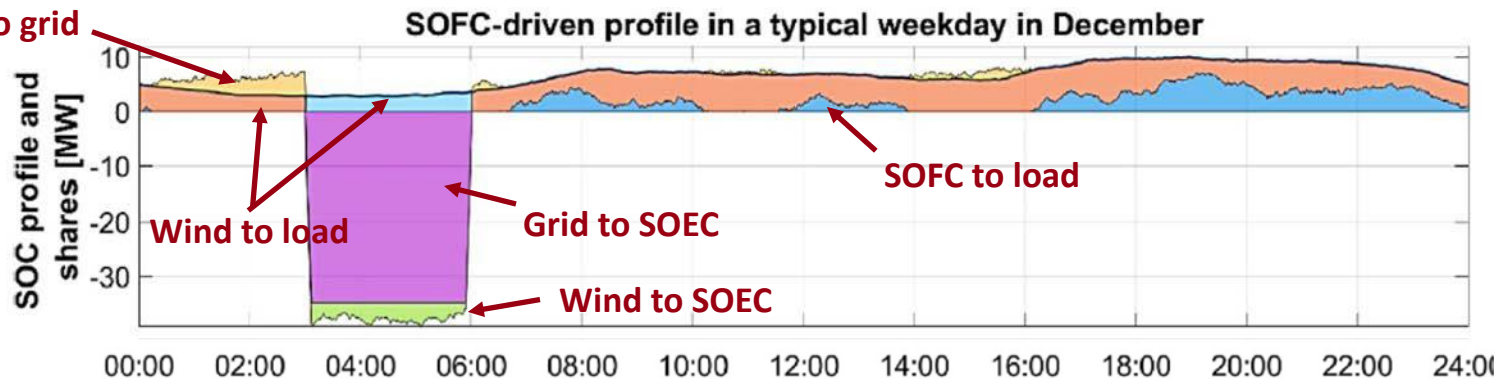
$W_{\text{stack,AC}}$ MW _e	W_{BoP} kW _e	Q_{stack} MW _{th}	Q_{BoP} MW _{th}	P_{H2} MW	η_{EL} %	η_{CHP} %
SOFC subsystem						
2	46	0.82	0.66	3.88	51.55	78.42
4	95	1.86	1.37	8.04	49.75	78.37
6	148	3.18	2.15	12.6	47.62	78.35
8	207	4.88	3.01	17.6	45.45	78.35
10	274	7.13	3.98	23.3	42.92	78.36
SOEC subsystem						
10	-590	-1.69	-0.57	8.45	84.50	75.11
20	-1080	-1.68	-1.05	15.6	78.00	77.05
30	-1510	-0.60	-1.47	21.8	72.67	78.54
40	-1912	1.24	-1.85	27.5	68.75	79.74
50	-2269	3.67	-2.19	32.7	65.40	80.72

System dispatch profile

- SOFC-driven: Maximum SOFC operating hours

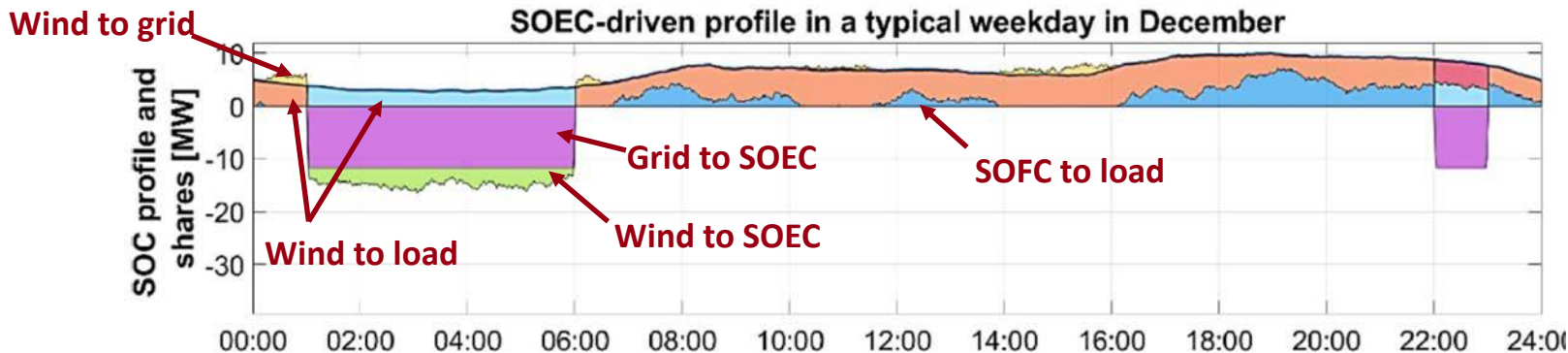
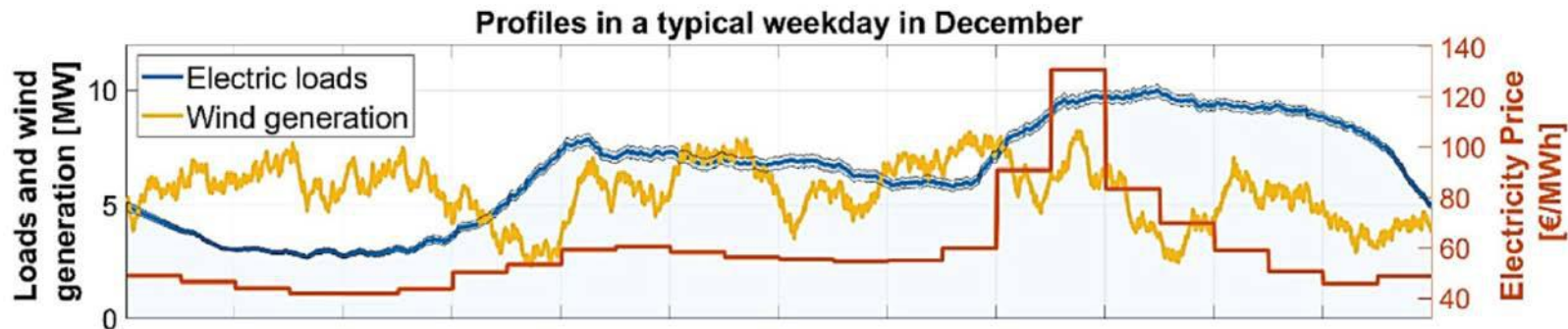


Wind to grid



System dispatch profile

- SOEC-driven: Maximum SOEC operating hours



Based on the operating dispatch profile, some performance criteria can be evaluated

- Capacity factor

$$CF = \frac{\text{Yearly energy produced (consumed)}}{\text{nominal size} \times \text{operating hours}}$$

- Efficiency

- Daily efficiency

$$\eta_{d,p} = \frac{E_{SOFC,d,p} + E_{BOP, SOFC,d,p}}{|E_{SOEC,d,p} + E_{BOP,SOEC,d,p}|} \quad (\text{Energy production is positive})$$

- Annual efficiency

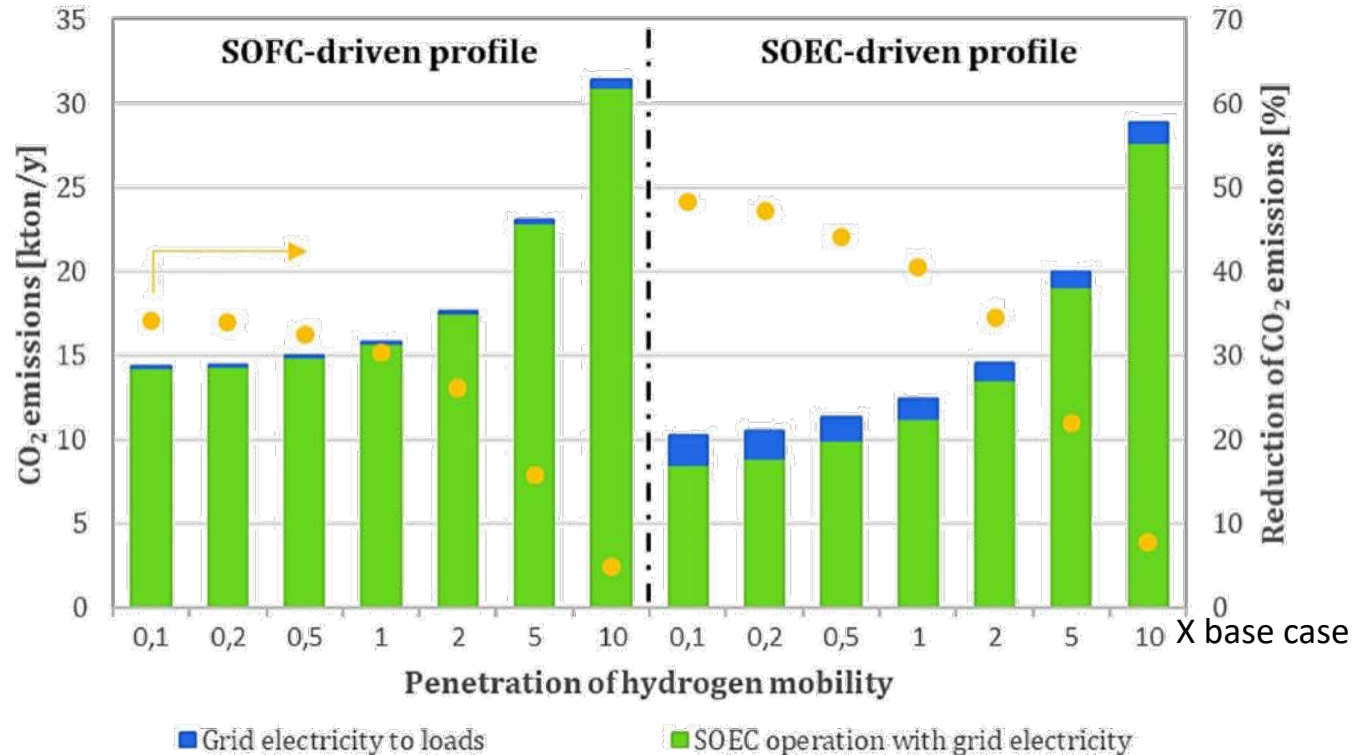
$$\eta_y^* = \frac{(E_{SOFC,load,y} + E_{BOP, SOFC,y}) + H_{2,mob,y} \cdot LHV_{H_2} + E_{DH,y}}{|E_{SOEC,y} + E_{BOP,SOEC,y}|}$$

- Total CO₂ emission

- Emission due to the use of grid electricity
- Emission reduction due to elimination of gas boilers for heating and diesel buses

The potential of CO₂ reduction depends on the hydrogen required for buses

- The system has 30-50% CO₂ reduction potential
- The potential drops when more hydrogen is required for the bus fleet



Base case:
1 million km/year
(~ bus 1 mileage)

- Energy systems: production, conversion, delivery, and use of energy
- System analysis: efficiency, emissions, economics, societal impacts
- Aspen PlusTM: interface and components
- Examples to do thermodynamic analysis and dynamic simulations

Thanks!

2.60/2.62 lecture
Energy system modeling and examples
Xiao-Yu Wu

MIT OpenCourseWare
<https://ocw.mit.edu/>

2.60J Fundamentals of Advanced Energy Conversion
Spring 2020

For information about citing these materials or our Terms of Use, visit: <https://ocw.mit.edu/terms>.

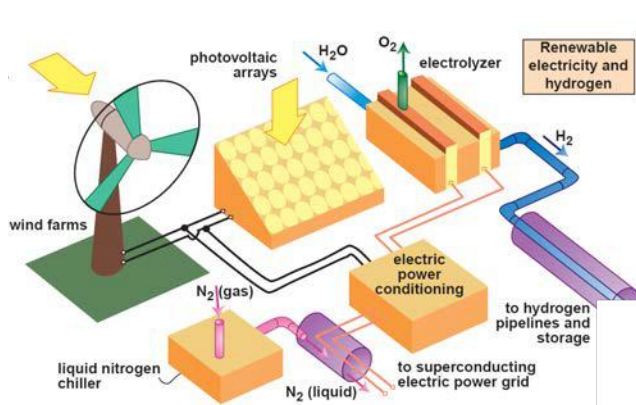
Lecture # 22

Wind Energy

Ahmed Ghoniem
April 27, 2020

- A quick recap, what we covered and what is yet to come
- Wind energy resources and potential
- Wind machines and wind turbine physics

The lecture today is ~ 90 min

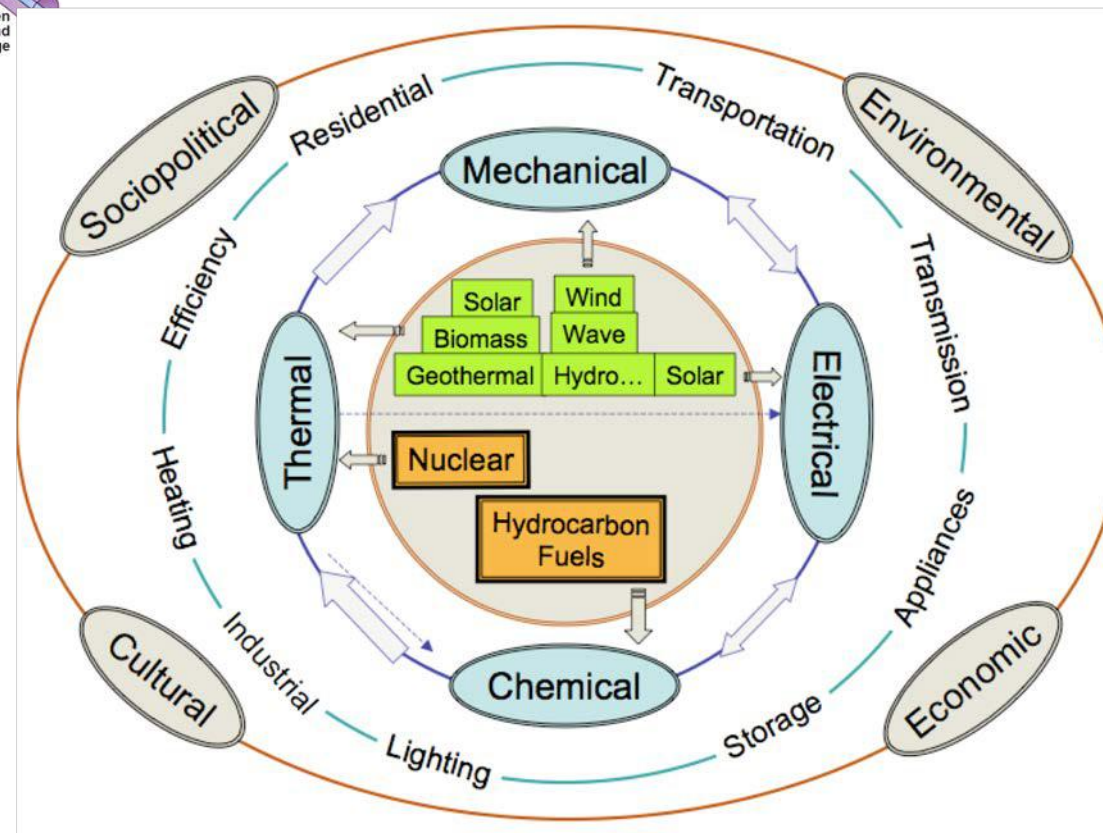


Hoffert et al., Science, 298 (2002)

© AAAS. All rights reserved. This content is excluded from our Creative Commons license. For more information, see <https://ocw.mit.edu/fairuse>.

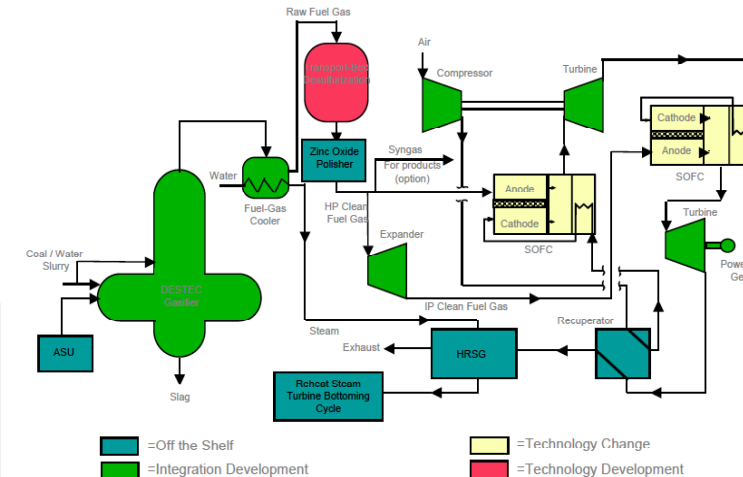


Thermodynamics of the Corn-Ethanol Biofuel Cycle



© Informa UK Limited. All rights reserved. This content is excluded from our Creative Commons license. For more information, see <https://ocw.mit.edu/fairuse>.

Tad W. Patzek (2004) "Thermodynamics of the Corn-Ethanol Biofuel Cycle", *Critical Reviews in Plant Sciences*, 23:6, 519-567, DOI: [10.1080/07352680490886905](https://doi.org/10.1080/07352680490886905).



Fuel cell handbook. Office of fossil energy.

Image courtesy of DOE.

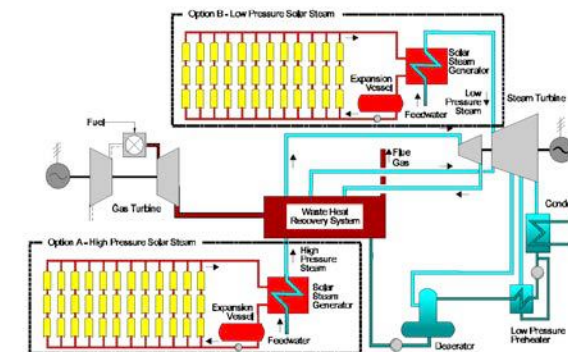


Figure 2. Integrated Solar Combined Cycle System [1].

Mancini TR. An overview of concentrating solar power.

Image courtesy of DOE.

Electrification Worldwide

- Less developed countries have 80% of world's population, consume ~ 30% of total energy
- ~2B people without consistent access to electricity
- The system is moving away from fuels and towards electricity, for many reasons
- Opportunities and challenges

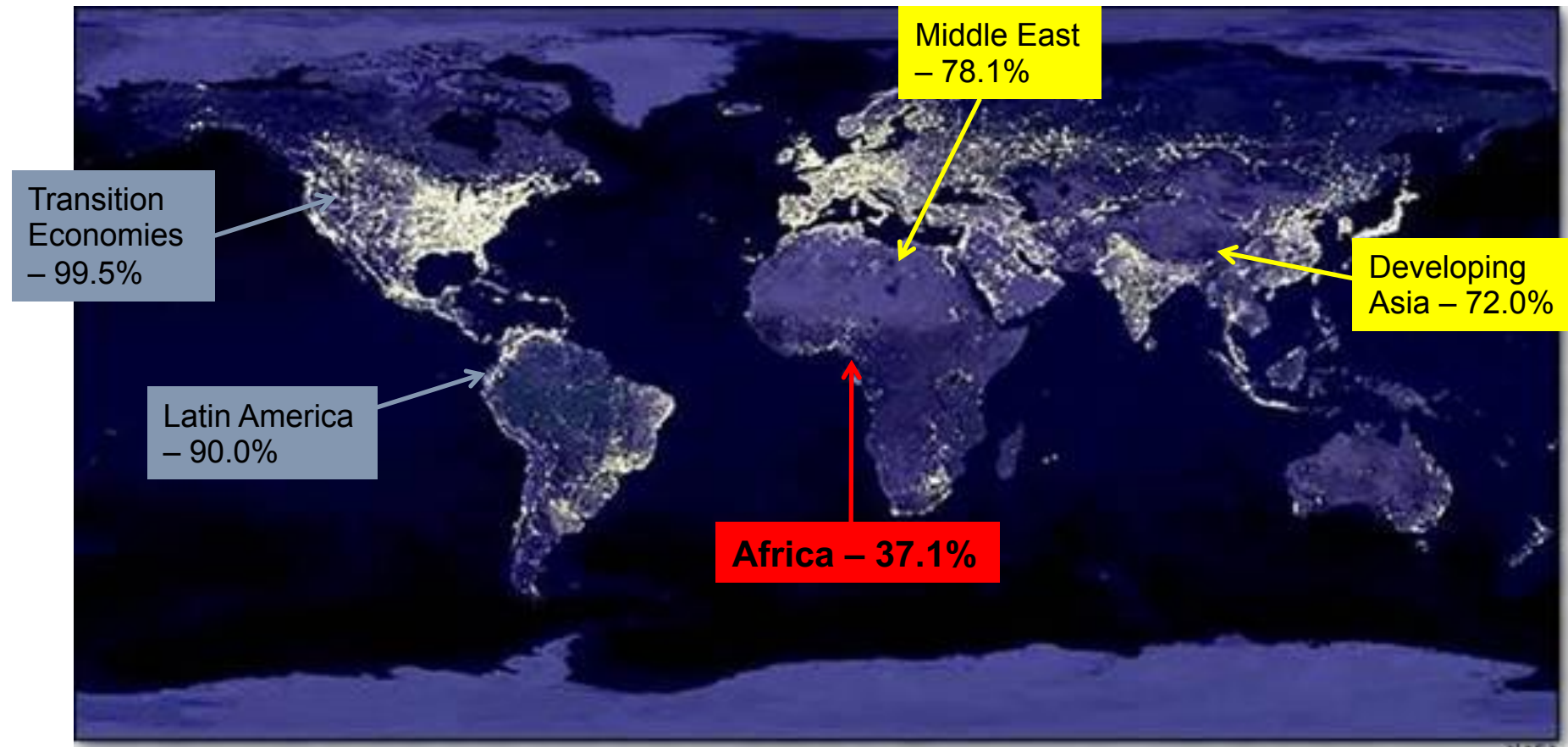
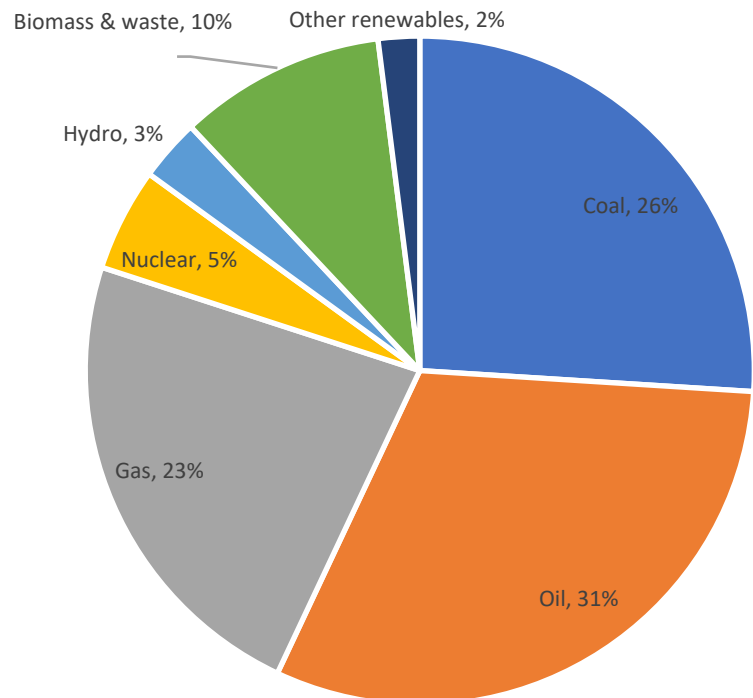


Image courtesy of NASA.

Needs: Energy Consumption

~ 600 EJ (~ 440 EJ in early 2000's) produced by close to 18 TW Power (6.1 TW for electricity generation)



© IEA. All rights reserved. This content is excluded from our Creative Commons license. For more information, see <https://ocw.mit.edu/fairuse>.

World primary energy consumption in 2014, 13,558 Mtoe (was 11,059 Mtoe in 2006). Except for hydropower, primary energy measures the thermal energy equivalent in the fuel that was used to produce a useful form of energy, e.g., thermal energy (heat), mechanical energy, electrical energy, etc. When energy is obtained directly in the form of electricity, efficiency is used to convert it to equivalent thermal energy.
1 toe ~ 42 GJ. IEA World Energy Outlook 2015, p57.

Sankey diagram

US resources, consumption and patterns

~100 EJ/y 2018, <17% of the world total (25% in 2004)

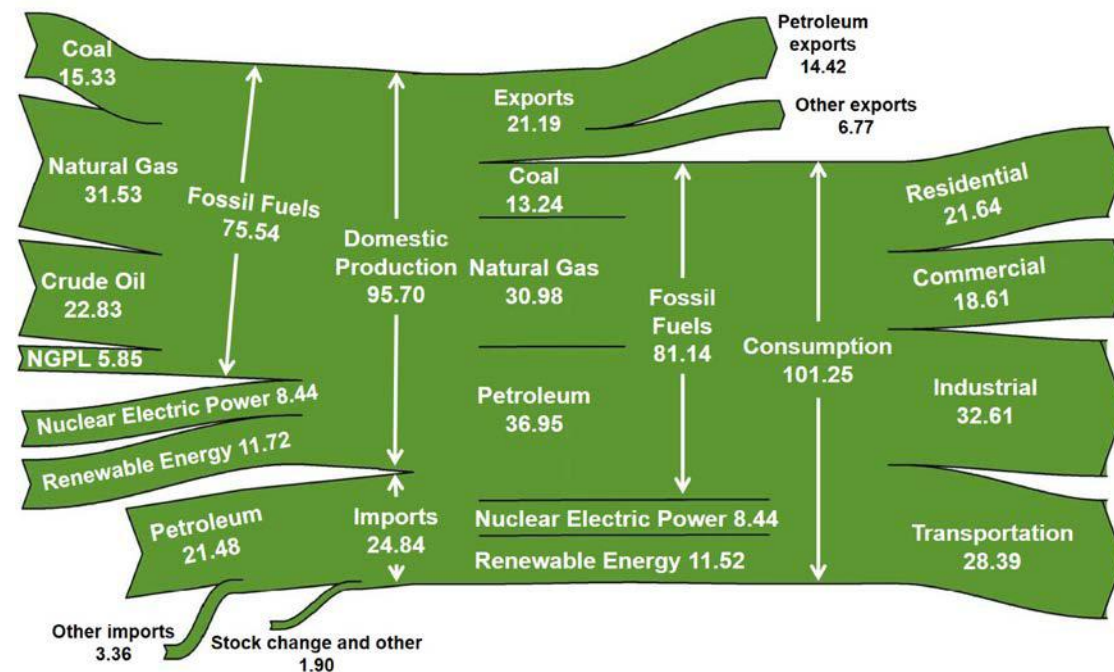
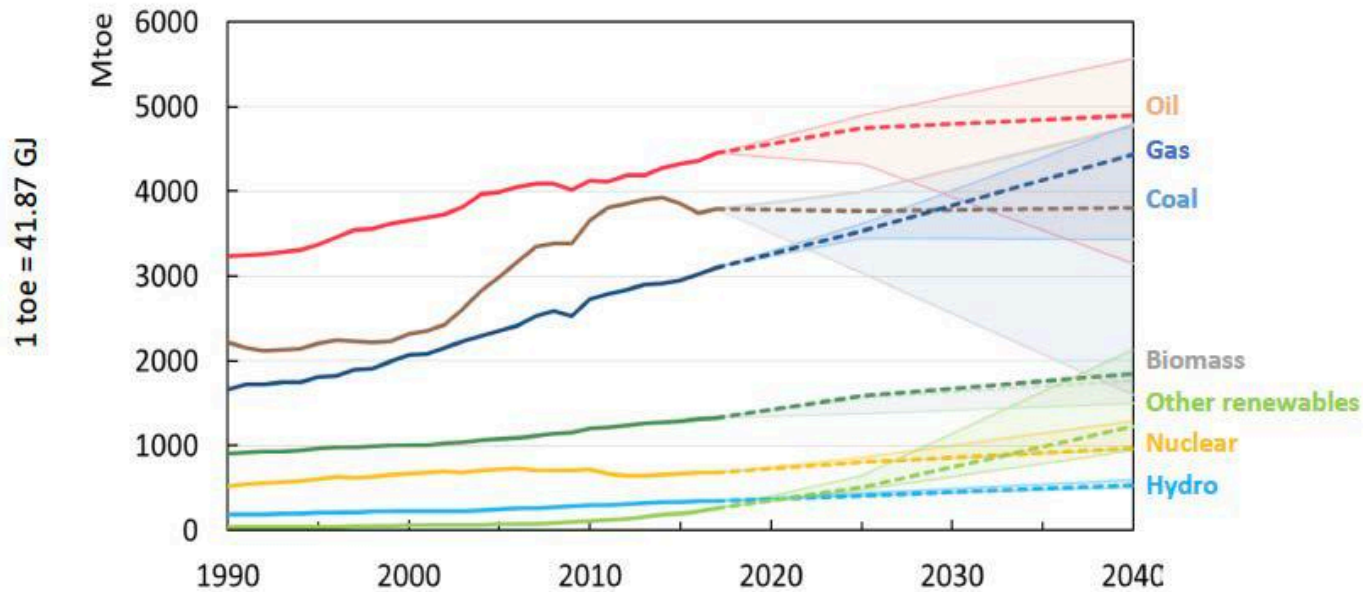


Image courtesy of U.S. Energy Information Administration.

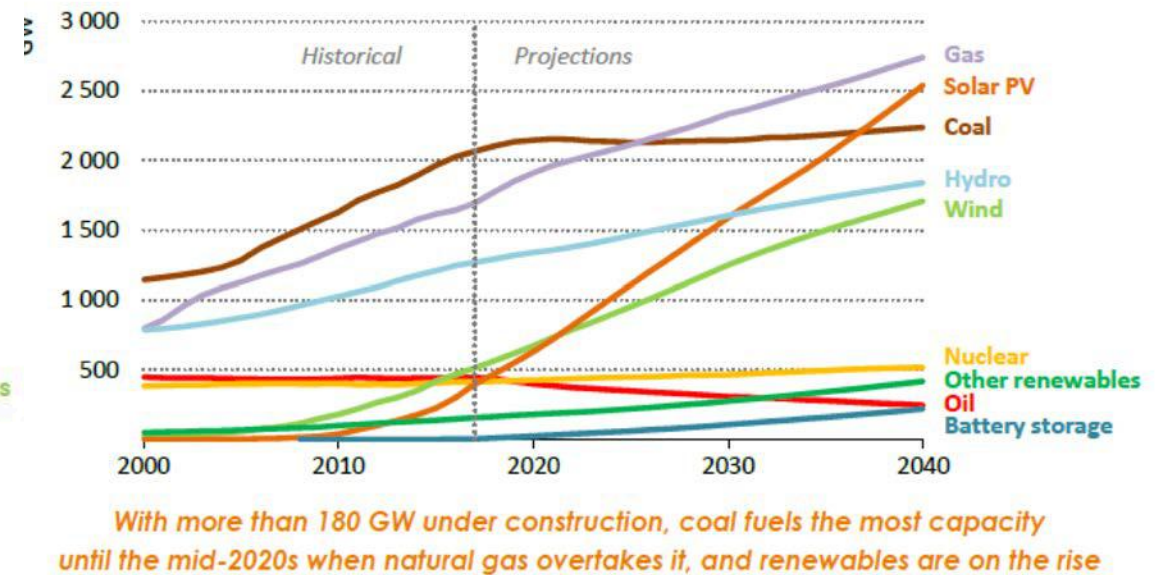
http://www.eia.gov/totalenergy/data/monthly/pdf/flow/total_energy.pdf

World primary energy supply by fuel/source*

The dotted line is the prediction based on new policies to be implemented. The shaded areas show the possible scenarios between current policies and sustainable development. Source: IEA world energy outlook 2018, P38



Installed power (electricity) generation capacity worldwide by source and prediction in the new policies scenario

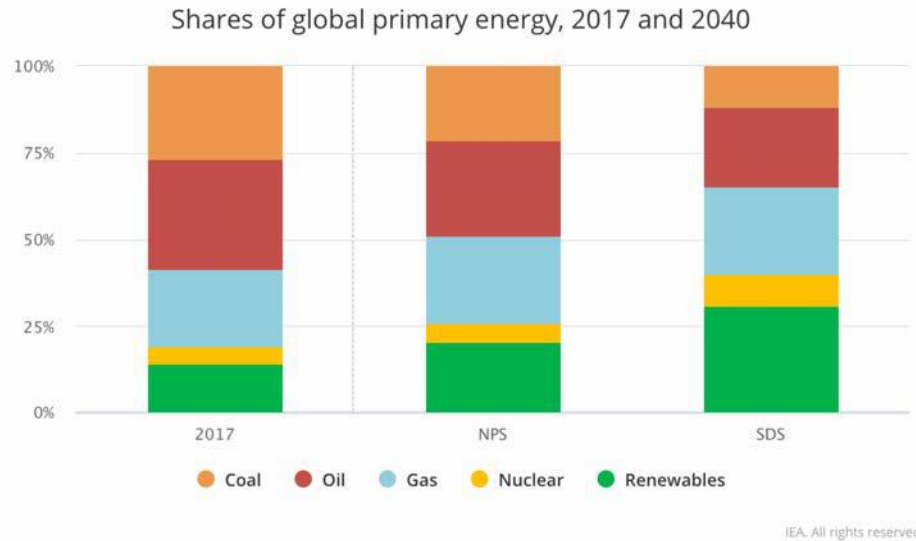


© IEA. All rights reserved. This content is excluded from our Creative Commons license. For more information, see <https://ocw.mit.edu/fairuse>.

Source: IEA world energy outlook 2018, P344

Shares of global primary energy, 2017 and 2040

Source: <https://www.iea.org/weo2018/fuels/>



© IEA. All rights reserved. This content is excluded from our Creative Commons license. For more information, see <https://ocw.mit.edu/fairuse>.

New Policies Scenario (NPS): Global oil demand growth slows but does not peak before 2040.

Sustainable Development Scenario (SDS): Determined policy interventions to address climate change lead to a peak in global oil demand around 2020 at 97 mb/d.

Global Greenhouse Gas Emissions by Economic Sector (2015)

https://www.epa.gov/sites/production/files/2016-05/global_emissions_sector_2015.png

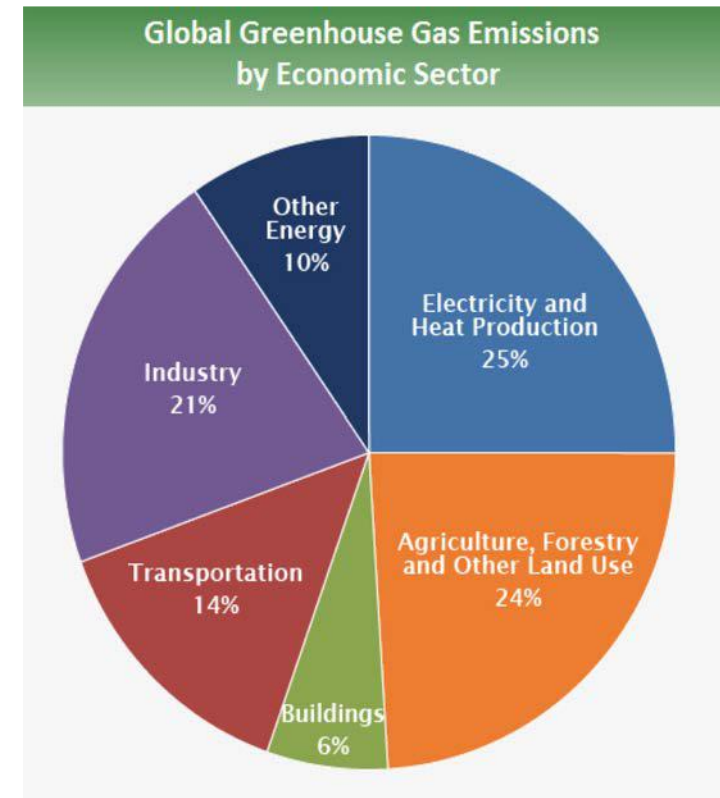
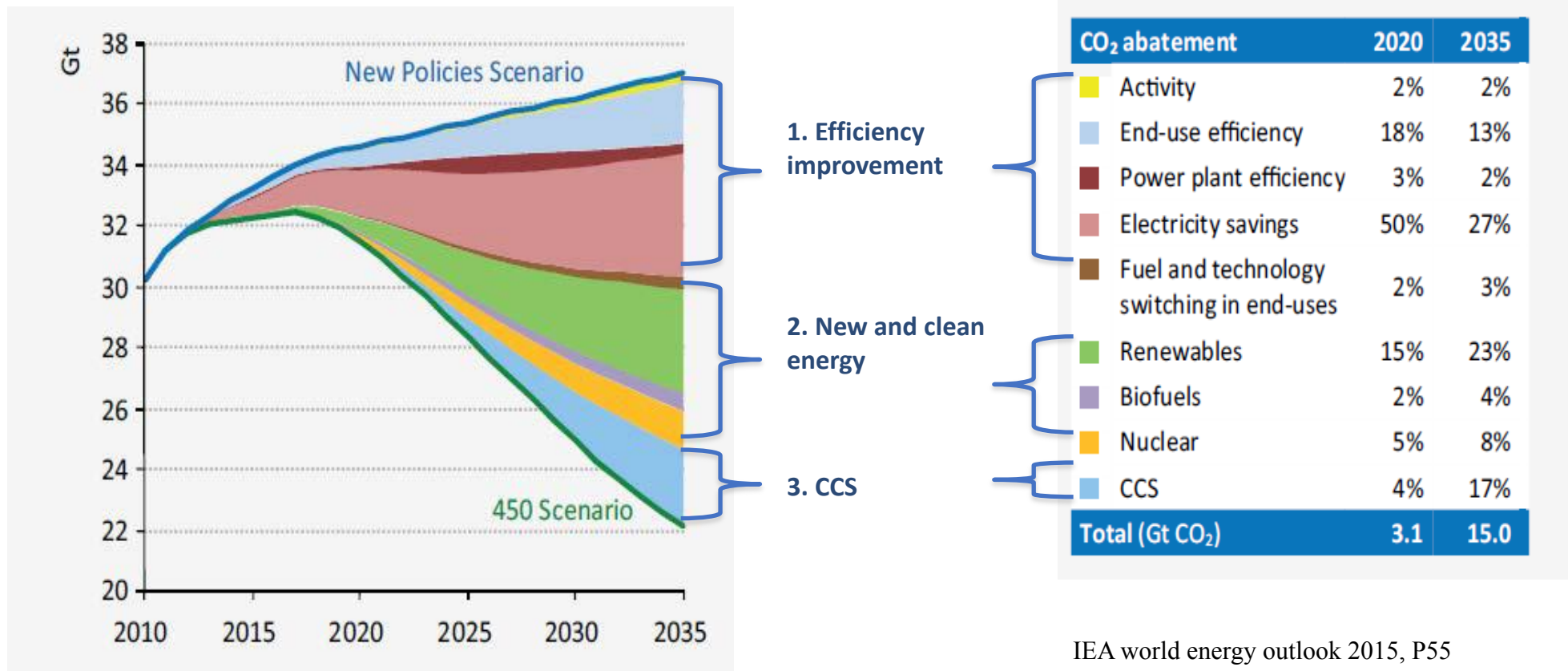


Image courtesy of EPA.

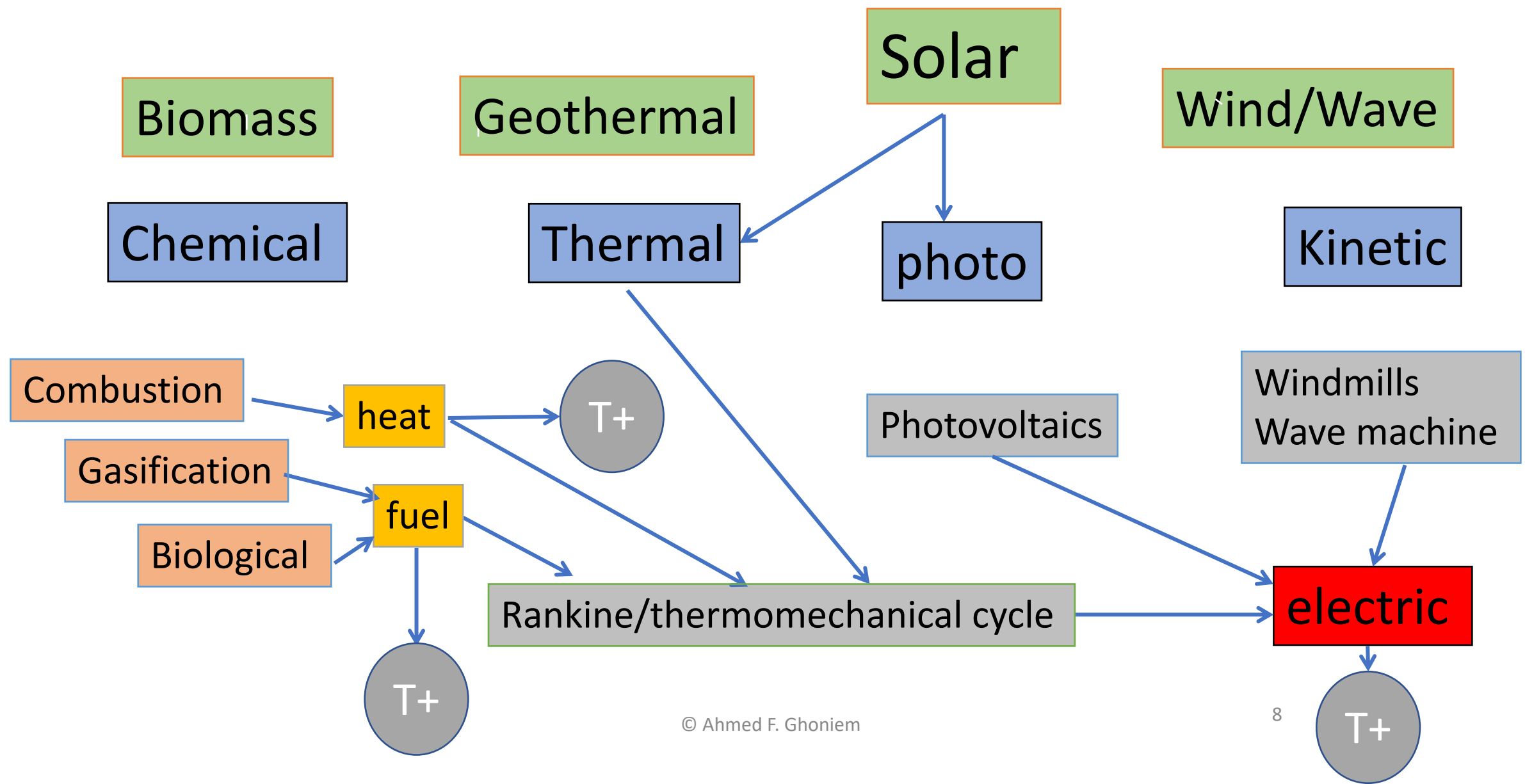
Meeting CO₂ targets using a portfolio of technologies

- New policies scenario: implementing measures affecting energy markets that had been adopted as of mid-2015 (as well as the energy-related components of climate pledges in the run-up to COP21)
- 450 scenario: depicts a pathway to the 2° C climate goal that can be achieved by fostering technologies that are close to becoming available at commercial scale.



IEA world energy outlook 2015, P55

Renewable Sources and Their Utilization



Significant Potential for Wind

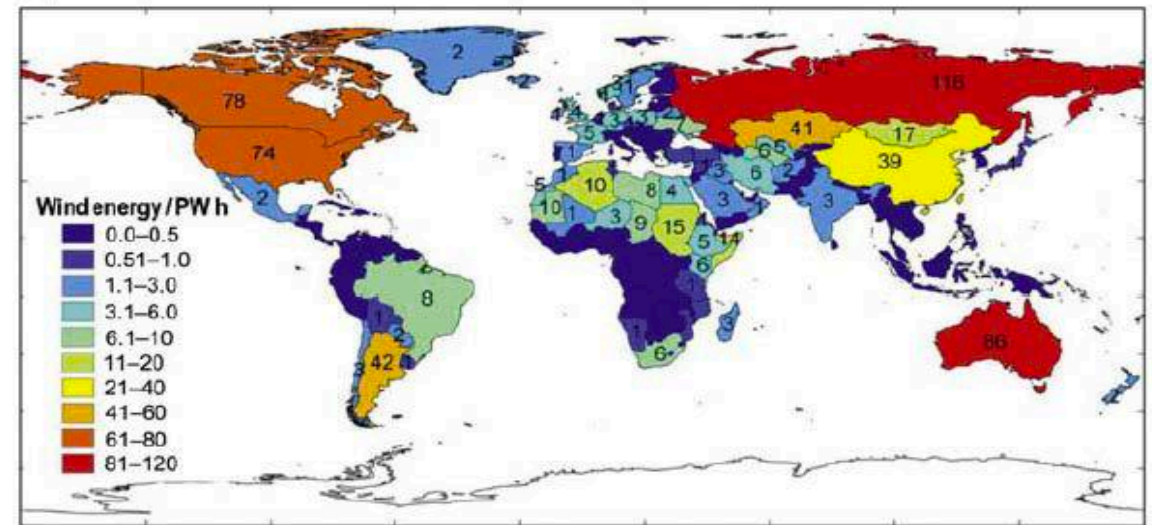
TABLE 4.1 Onshore and Offshore Wind Potential for the 10 Countries Identified as the Largest National Emitters of CO₂ [4]

No.	Country	CO ₂ Emission/ (10 ⁶ Metric Tonnes)	Electricity Consumption/ (TW h)	Potential Wind Energy/(TW h)		
				Onshore	Offshore	Total
1	China	8547.7	4207.7	39 000	4600	44 000
2	United States	5270.4	3882.6	74 000	14 000	89 000
3	India	1830.9	757.9	2900	1100	4000
4	Russia	1781.7	869.3	120 000	23 000	140 000
5	Japan	1259.1	983.1	570	2700	3200
6	Germany	788.3	537.9	3200	940	4100
7	South Korea	657.1	472.2	130	990	1100
8	Iran	603.6	185.8	5600	—	5600
9	Saudi Arabia	582.7	211.6	3000	—	3000
10	Canada	499.1	551.6	78 000	21 000	99 000

Note: CO₂ emission for 2012 and electricity consumption for 2011.

Source: Data from Boden TA, Andres RJ, Marland G. Preliminary 2011 and 2012 global & national estimates. In: Fossil-fuel CO₂ emissions. Oak Ridge, TN: Carbon Dioxide Information Analysis Center; 2013. p. 4 [19] and US EIA. International energy outlook. Washington, DC: U.S. Energy Information Administration; 2013. p. 312 [20].

(A)



(B)

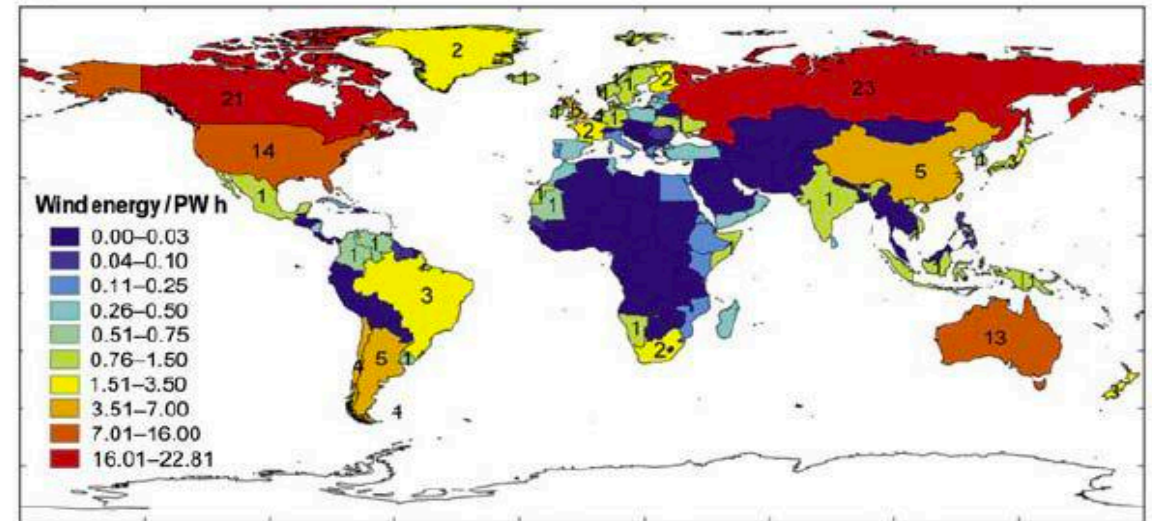
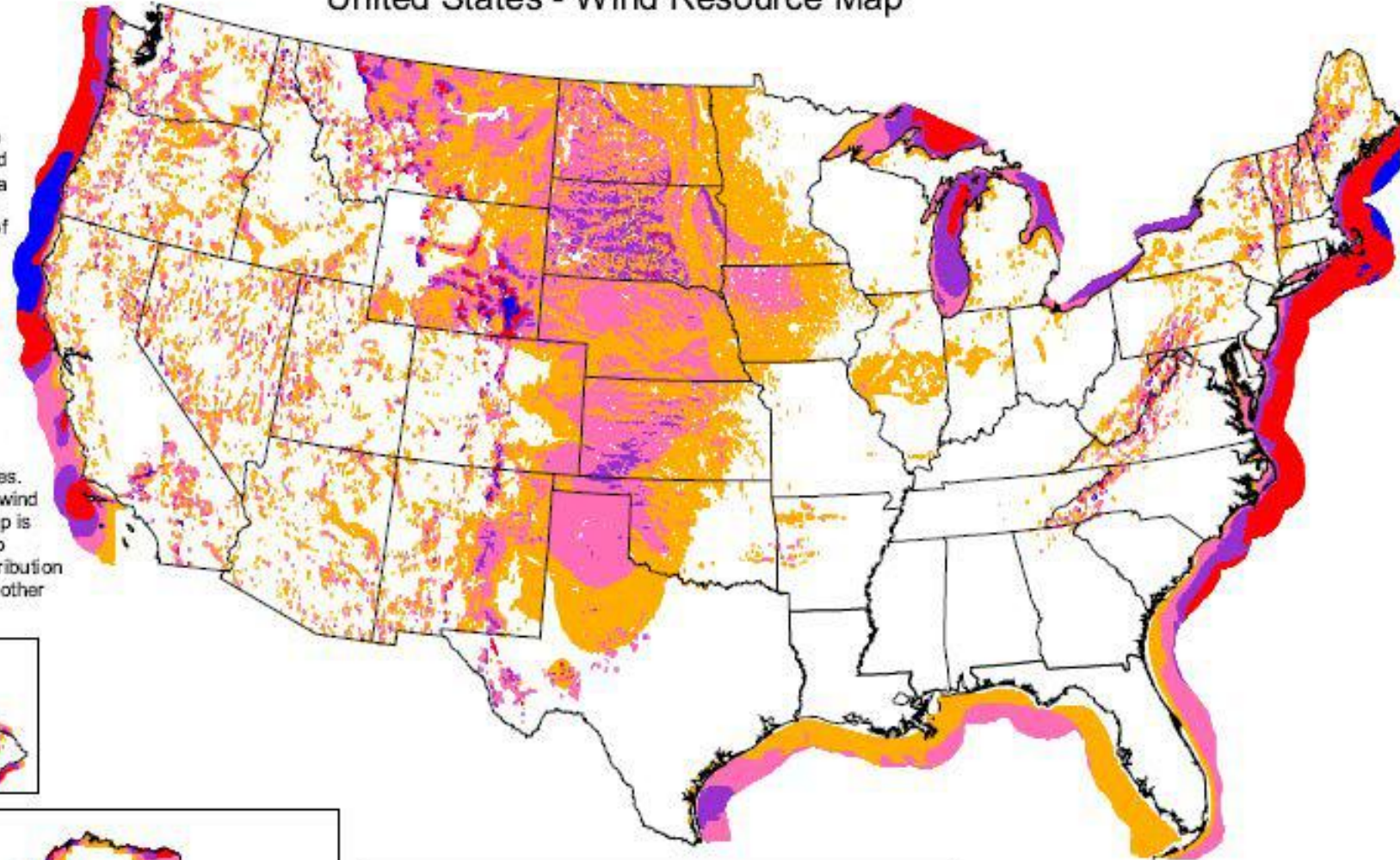
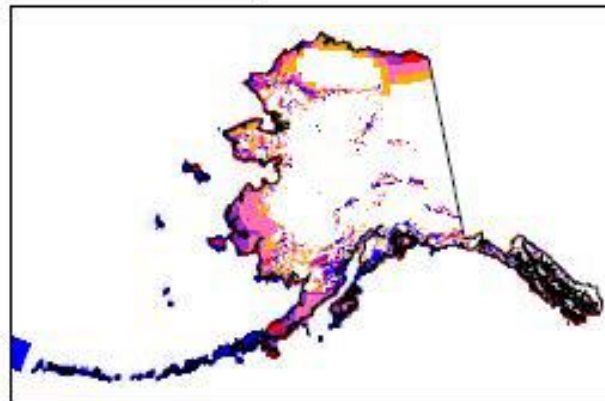
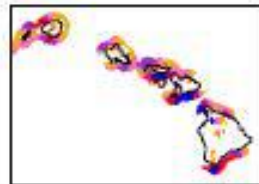


FIGURE 4.4 Annual wind energy potential country by country, restricted to installations with capacity factors greater than 20% with siting limited as discussed in the text: (A) onshore and (B) offshore [4].

United States - Wind Resource Map

This map shows the annual average wind power estimates at a height of 50 meters. It is a combination of high resolution and low resolution datasets produced by NREL and other organizations. The data was screened to eliminate areas unlikely to be developed onshore due to land use or environmental issues. In many states, the wind resource on this map is visually enhanced to better show the distribution on ridge crests and other features.



	Wind power class and potential	Power density at 50 m, W/m ²	Wind speed at 50 m, m/s
	3 Fair	300-400	6.4-7.0
	4 Good	400-500	7.0-7.5
	5 Excellent	500-600	7.5-8.0
	6 Outstanding	600-800	8.0-8.8
	7 Superb	800-1600	8.8-11.1

Image courtesy of NREL, DOE.

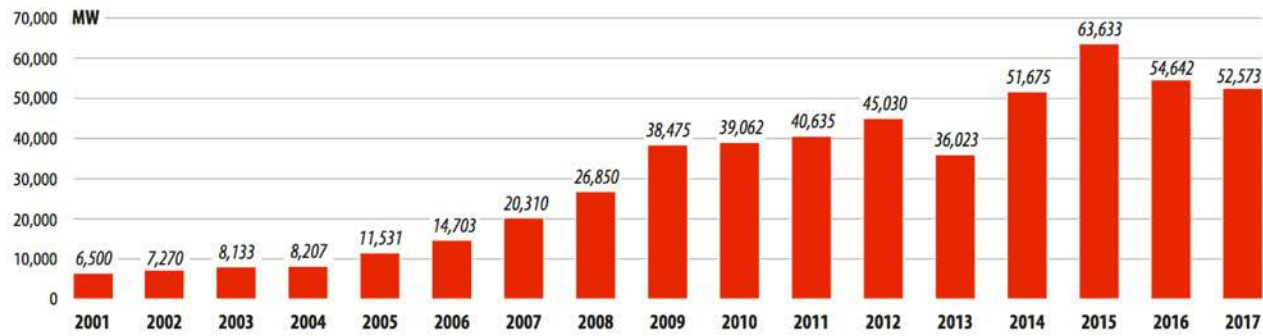


Department of Energy
National Renewable Energy Laboratory

05-MAY-2005 1.1.0

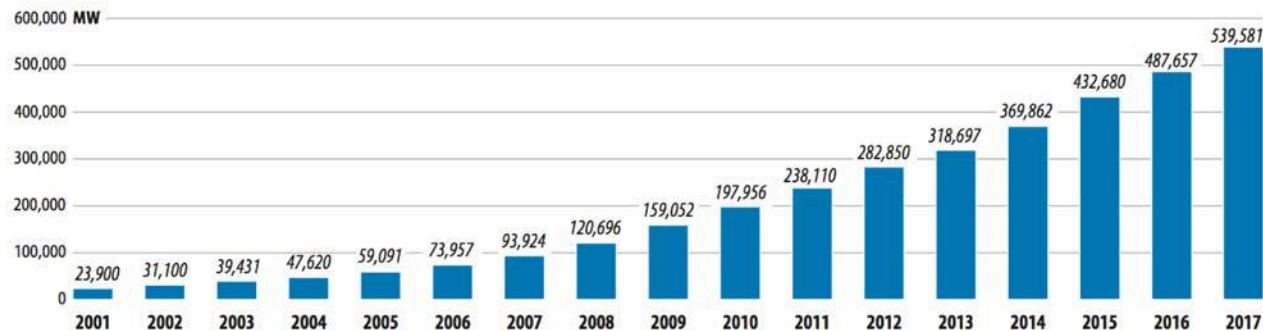
Global Wind Statistics, 2017

GLOBAL ANNUAL INSTALLED WIND CAPACITY 2001-2017



Source: GWEC

GLOBAL CUMULATIVE INSTALLED WIND CAPACITY 2001-2017

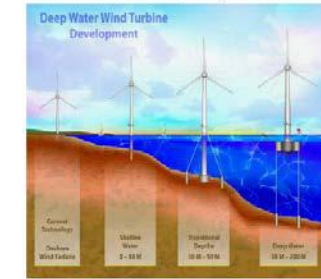


Source: GWEC

© Global Wind Energy Council (GWEC). All rights reserved. This content is excluded from our Creative Commons license. For more information, see <https://ocw.mit.edu/fairuse>.



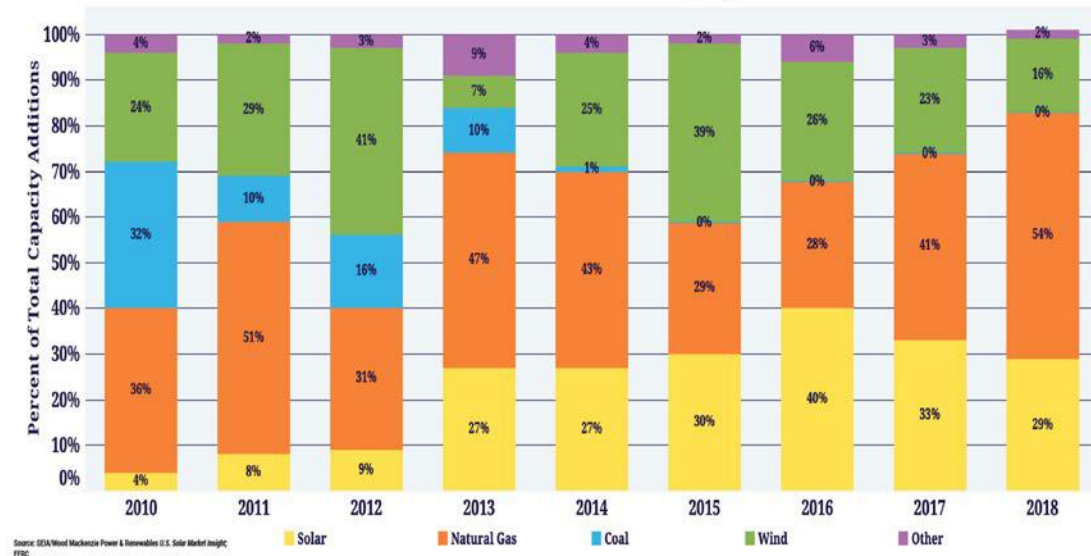
Explore technology pathways for installing and operating large wind power facilities in water depths greater than 30 meters.



© Source unknown. All rights reserved. This content is excluded from our Creative Commons license. For more information, see <https://ocw.mit.edu/fairuse>.

In the US

Annual Additions of New Electric Capacity



Source: EIA/Wood Mackenzie Power & Renewables U.S. Solar Market Insight: PERC



©2019

www.seia.org/solar-industry-research-data

© Solar Energy Industries Association. All rights reserved. This content is excluded from our Creative Commons license. For more information, see <https://ocw.mit.edu/fairuse>.

Extracting Wind Energy

$$P = \frac{1}{2} \dot{m} V_{wind}^2 = \frac{1}{2} \rho_{air} V_{wind}^3 A$$

Take: $\rho_{air} \sim 1.3 \text{ kg/m}^3$, $V \sim 10 \text{ m/s}$, $R_{turbine} \sim 10 \text{ m}$

$P \sim 180 \text{ kW}$ (assuming 100% conversion efficiency)



Old fashion wind mill

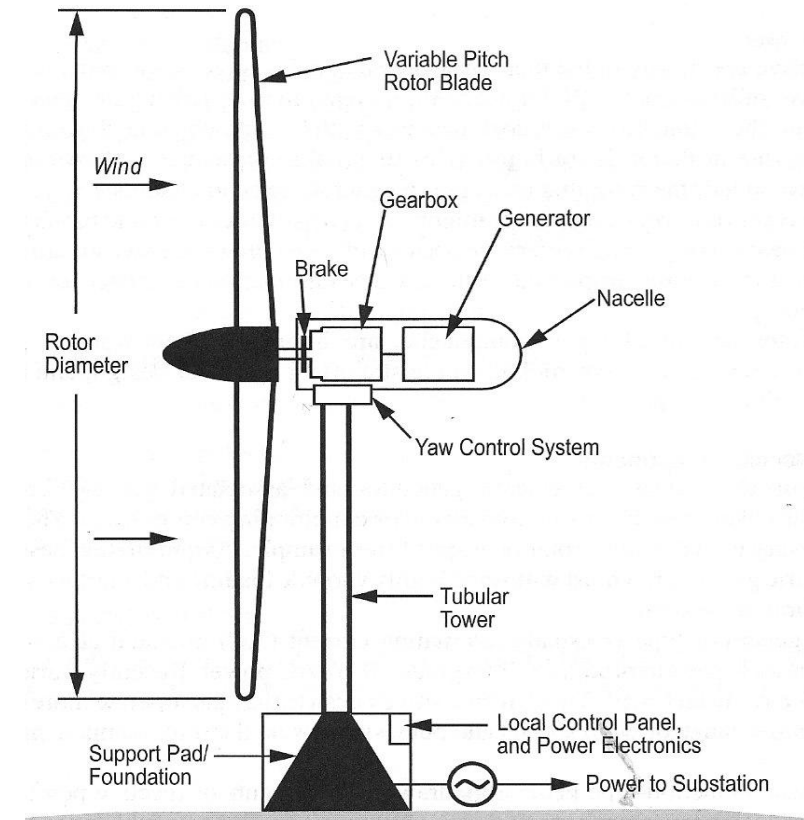


Unusual vertical axis wind machine

MacKay, Sustainable Energy-without the hot air, Cambridge, 2009.



Modern horizontal axis wind turbine (3 blades)



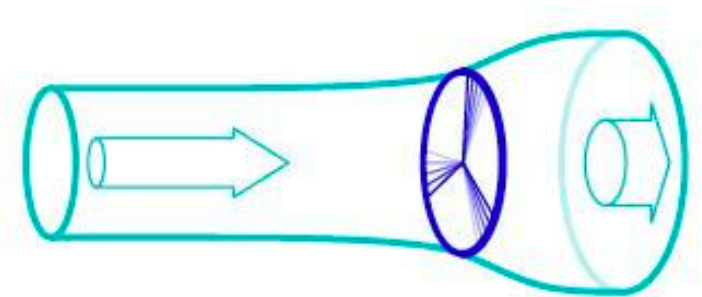
1/18/2019. Rotterdam. GE announced plans this week to erect a prototype of the world's largest wind turbine, the Haliade-X, on the city's outskirts.



What determines the efficiency/coefficient of performance of a wind machine?

Several models can be used to examine how the machine captures energy

- The actuator disk theory is the simplest approach to evaluating the ideal power extracted by a wind machine.
- Assumes ideal conditions with no losses.
- Thrust generated by the turbine is due to pressure change across the disk. The disc obstructs the flow, slowing it down as it approaches the machine
- Assumes that wind *can pass through* the swept area.
- Flow in the wake (or inside the disk) is not rotating!
- Aerodynamics is left out!



mass conservation: $A_\infty U_\infty = A_d U_d = A_w U_w = \frac{\dot{m}}{\rho}$

Bernoulli: $p_\infty + \frac{1}{2} \rho U_\infty^2 = p^+ + \frac{1}{2} \rho U_d^2$

$$p^- + \frac{1}{2} \rho U_d^2 = p_\infty + \frac{1}{2} \rho U_w^2$$

Momentum (across disk): $T = (p^+ - p^-) A_d$

Momentum (entire CV): $T = \dot{m}(U_\infty - U_w)$

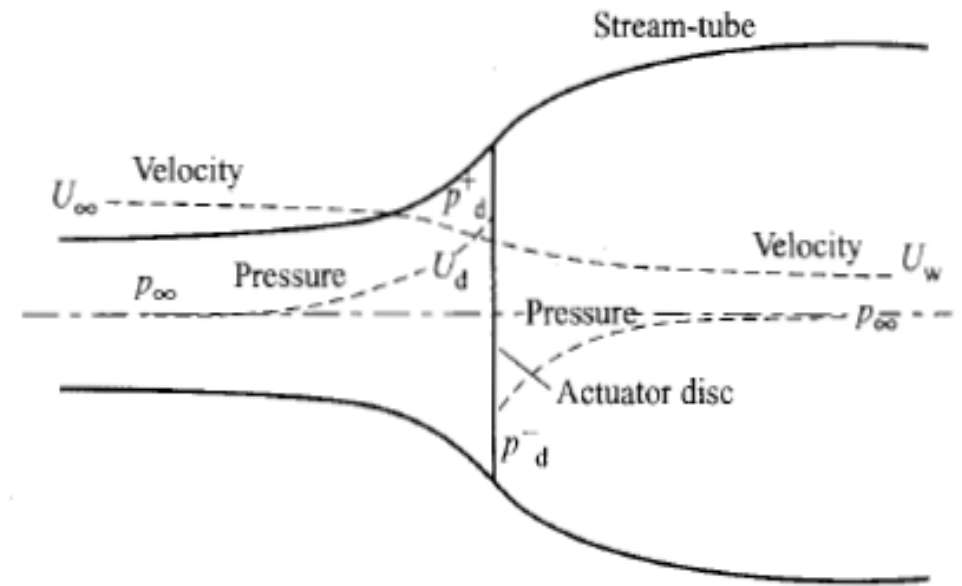
Solve: $U_d = \frac{1}{2}(U_\infty + U_w),$

$$T = 2\rho A(U_\infty - U_d)U_d \quad \text{and} \quad \wp = T U_d = 2\rho A(U_\infty - U_d)U_d^2$$

the power coefficient is $C_p = \frac{\wp}{\frac{1}{2} \rho U_\infty^3 A_d} = 4\alpha(1-\alpha)^2, \quad \alpha = \frac{U_\infty - U_d}{U_\infty}$

for maximum power: $\alpha=1/3$, and $U_d = \frac{2}{3}U_\infty$.

Maximum Power Coefficient, Betz limit (efficiency): $C_p = 0.593$



Modern Wind turbines utilize lifting surfaces (wings) to extract energy:

- Place your hand perpendicular to the wind: you experience “bluffbody or wake drag”
- Place your hand at a small angle with the wind you experience lift force like a wing.
- This is a more efficient way to produce force without blocking the wind.
- Modern wind “turbines” (not old “windmills”) are made of blades that look like wings.



Vesta 7MW turbines, rotor $D = 164$ m, in an off-shore farm.

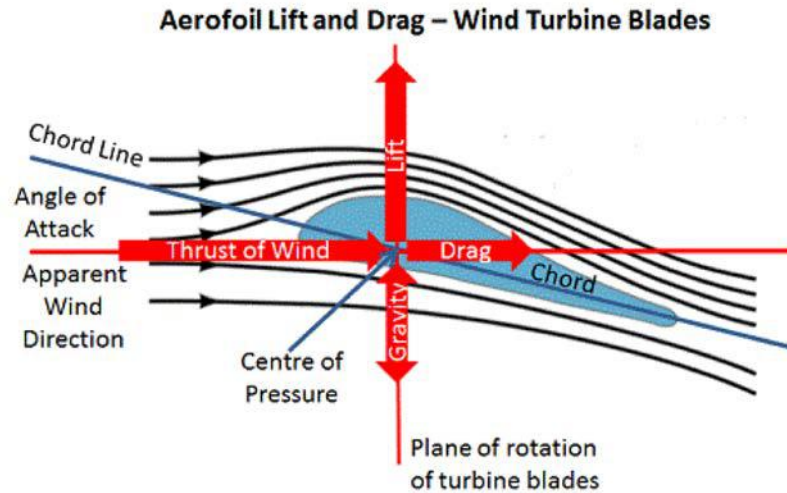
https://www.mpoweruk.com/wind_power.htm



Wind turbines utilize lifting surfaces (wings) to extract energy:

Lift: force perpendicular to the relative velocity

Drag: force in the direction of the relative velocity



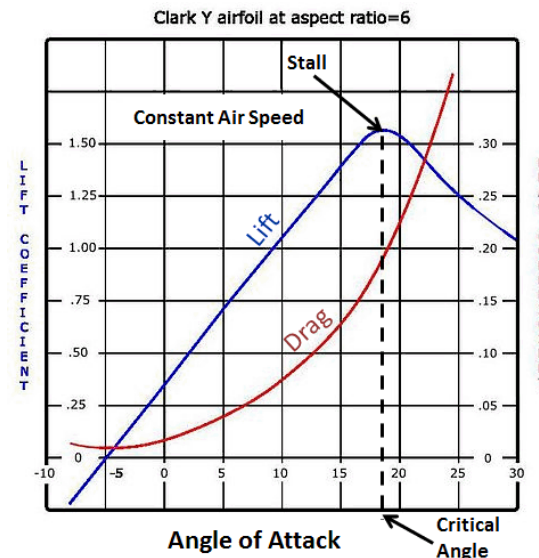
$$L = \frac{1}{2} \rho V_r^2 A_{bl} C_L \left(\alpha, \frac{l}{c}, R_e \right)$$

$$D = \frac{1}{2} \rho V_r^2 A_{bl} C_D \left(\alpha, \frac{l}{c}, R_e \right)$$

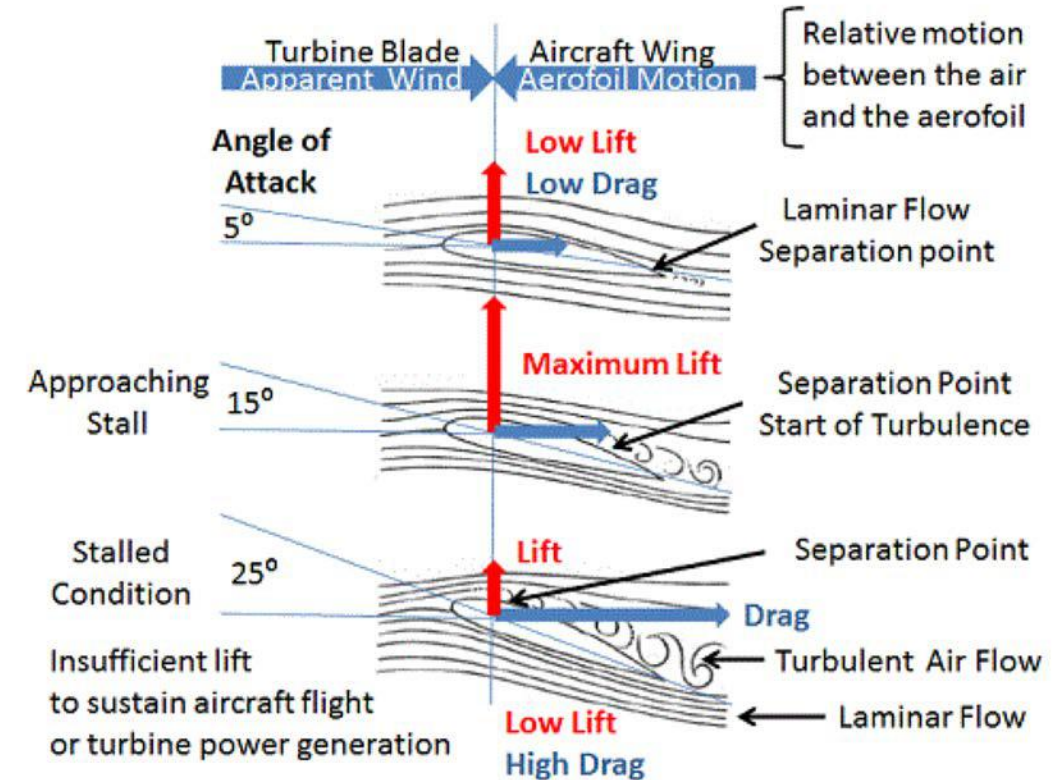
$$A_{bl} = cl,$$

where c is the cord

and l is the thickness



Lift, Drag and Angle of Attack



https://www.mpoweruk.com/flight_theory.htm

The pitch is the angle between the blade velocity (direction of motion) and chord, it is determined by the blade design.

The angle of attack, α , is between the relative wind velocity and the chord determines C_L and C_D .

The angle of attack changes as the wind speed changes.

The complement of $\alpha + \theta$ is β .

$\beta = (90 - (\alpha + \theta))$ determines the forces on the wing and power.

$$\mathcal{P}_{bl} = (\text{torque} \times \omega) = F_V \times (\omega R) = F_V V$$

F_V is the force in the direction of motion of the blade

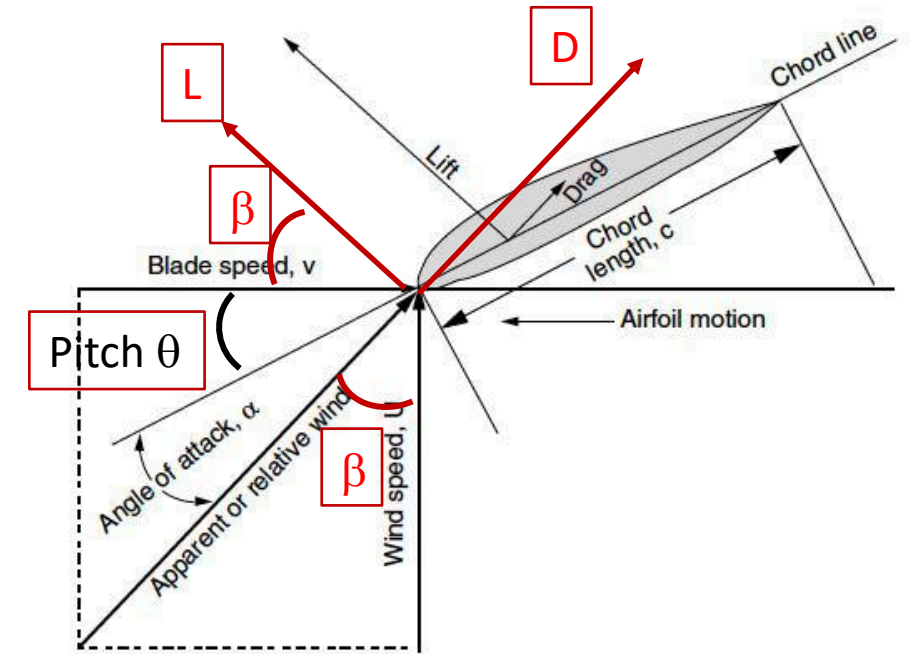
$$F_V = L \cos \beta - D \sin \beta,$$

where $\cos \beta = \frac{U}{V_r}$, and $\sin \beta = \frac{V}{V_r}$ ($\beta = \tan^{-1} \frac{V}{U}$)

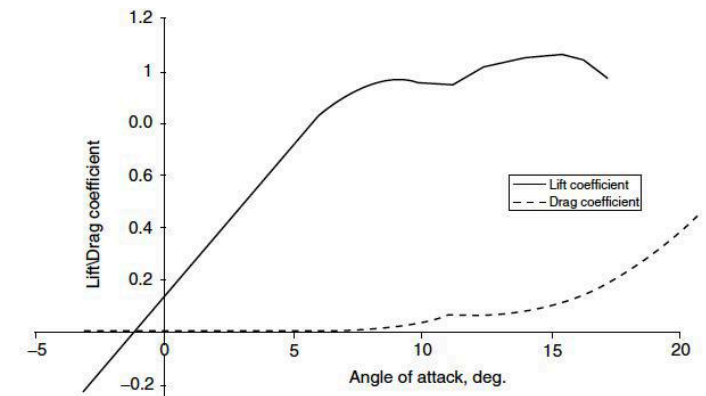
$$F_V = \left(L \frac{U}{V_r} - D \frac{V}{V_r} \right) = \frac{1}{2} \rho V_r U \left(C_L - \frac{V}{U} C_D \right) A_{bl}$$

$$\mathcal{P}_{bl} = F_V V = \frac{1}{2} \rho U^3 A_{bl} \left(C_L - \frac{V}{U} C_D \right) \frac{V}{U} \sqrt{1 + \left(\frac{V}{U} \right)^2} = \frac{1}{2} \rho U^3 A_{bl} C_p$$

Note that the angle of attack (and C_L , C_D) changes with $\left(\frac{V}{U} \right)$



Schematic of translating lift device.



Goswami and Kreith, Energy Conversion, CRC Press, 2008. 18

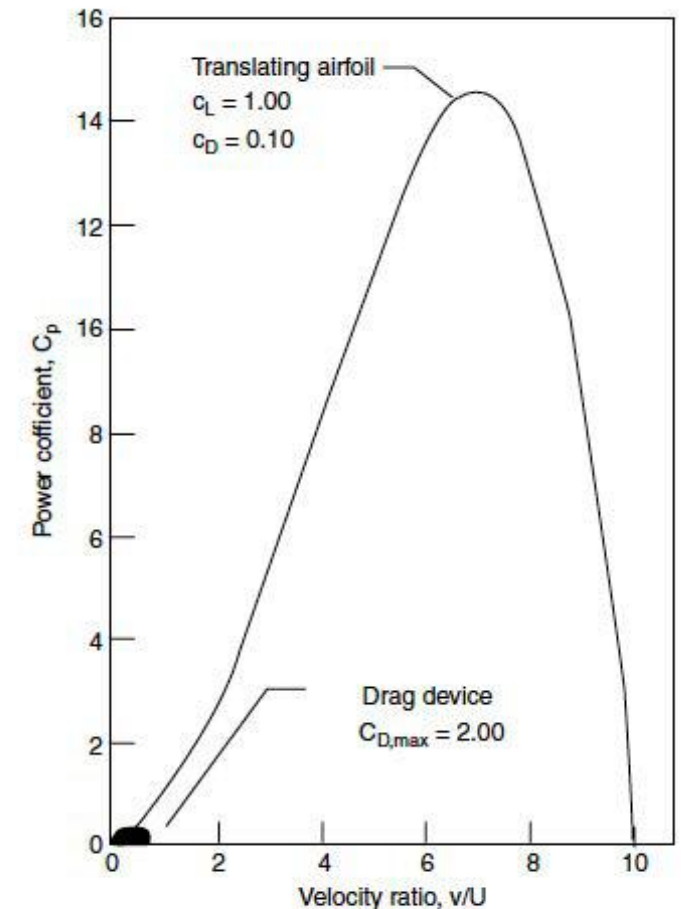
$$(C_p)_{bl} = \frac{F_v V}{\frac{1}{2} \rho U^3 A_{bl}} = \left(C_L - \frac{V}{U} C_D \right) \frac{V}{U} \sqrt{1 + \left(\frac{V}{U} \right)^2}$$

Modern *wind turbine* operate on the principle of lifting surfaces with high C_p , $O(10)$.

(Old *wind mills* operated on the drag force created by a wake and are much less efficient, with $C_p < 1.0$)).

- (V/U) is known as the tip speed ratio (evaluated at the tip of the blade).
- Good wind speed is 5-8 m/s.
- For large turbines, R is 10-100 m, and RPM is 10-30 (with smaller turbines spinning faster). V is 50-100 m/s.
- Should choose blades with high C_L (of the order of 1.0) and low C_D (of the order of 0.1).
- Higher values of V/U raise C_p . *But very high values reduce C_p (see equation and plot)*

Power coefficients for drag-type (old fashion) and lift-type (new designs) machines.



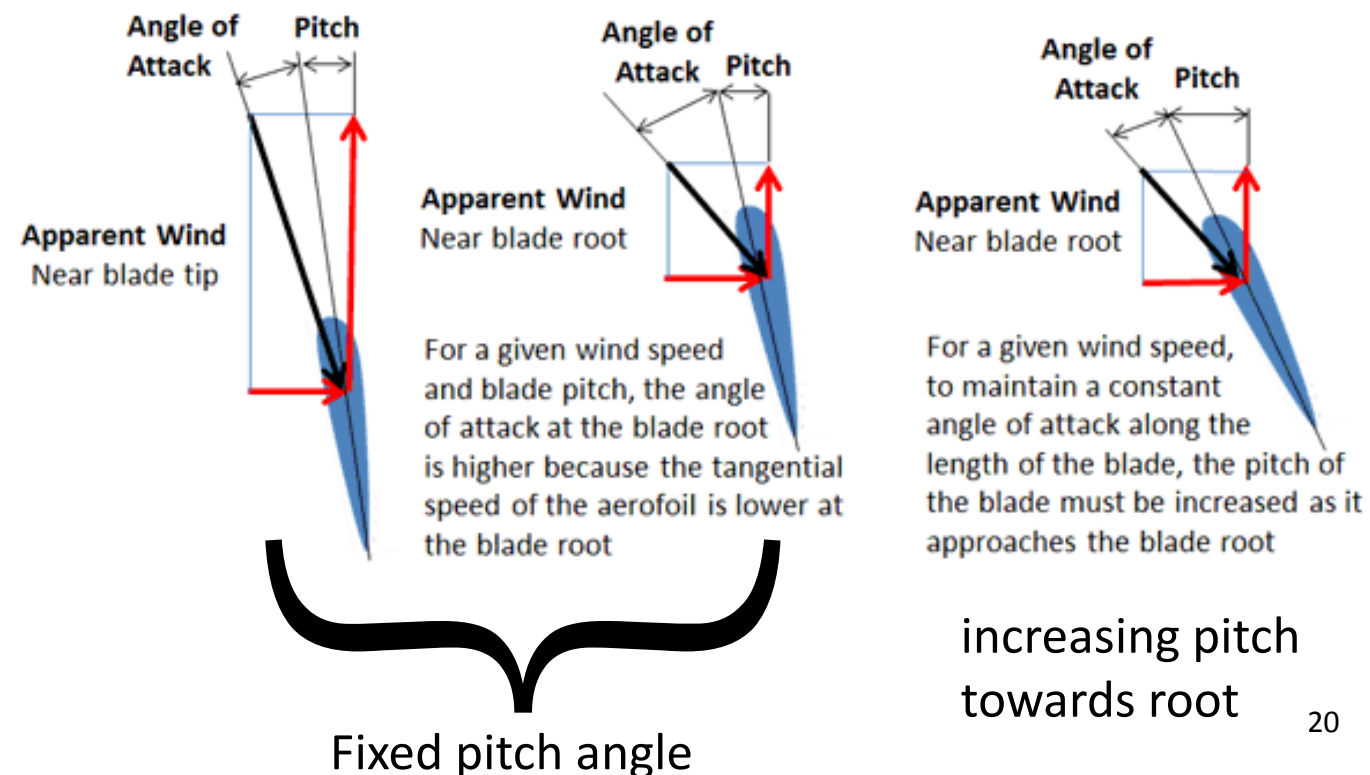
Goswami and Kreith, Energy Conversion, CRC Press, 2008.

- Previous analysis is applicable at some radius along the blade.
- But blade speed increases along r ($V=\omega r$) while U remains constant, causing V/U or α , θ and β to change.
- For a good design, the blade pitch θ must change with radius to maintain optimal $(\alpha+\theta)$ or β almost constant, i.e., must use twisted blades between the root and tip.
- For optimal performance, it is also necessary to vary the overall blade angle as the wind speed changes to maximize C_p , *this is Pitch Control*.
- Speed sensors are mounted on the nacelle to measure the wind speed and adjust the blade pitch.
- It is important that the horizontal turbine axis is always aligned in the wind direction; this is *Yaw Control*.



© The Institution of Engineering and Technology. All rights reserved. This content is excluded from our Creative Commons license. For more information, see <https://ocw.mit.edu/fairuse>.

Angle of Attack and Blade Twist



Almost all modern wind turbine have 3 blades, optimized to operate at highest efficiency at nominal wind speeds

- It is important to keep $(V/U)_{\text{max power}}$ low to minimize stresses on blades, etc. (at $U \sim 10 \text{ m/s}$, $V \sim 100 \text{ m/s}$!)
- “Old fashion” wind mills operate more on the principle of *wake drag* in which the blades are almost perpendicular to the wind.
 - This is less efficient and requires wider blades, and more of them.
 - They also spin slower and generate higher torques; more suitable for mechanical applications.

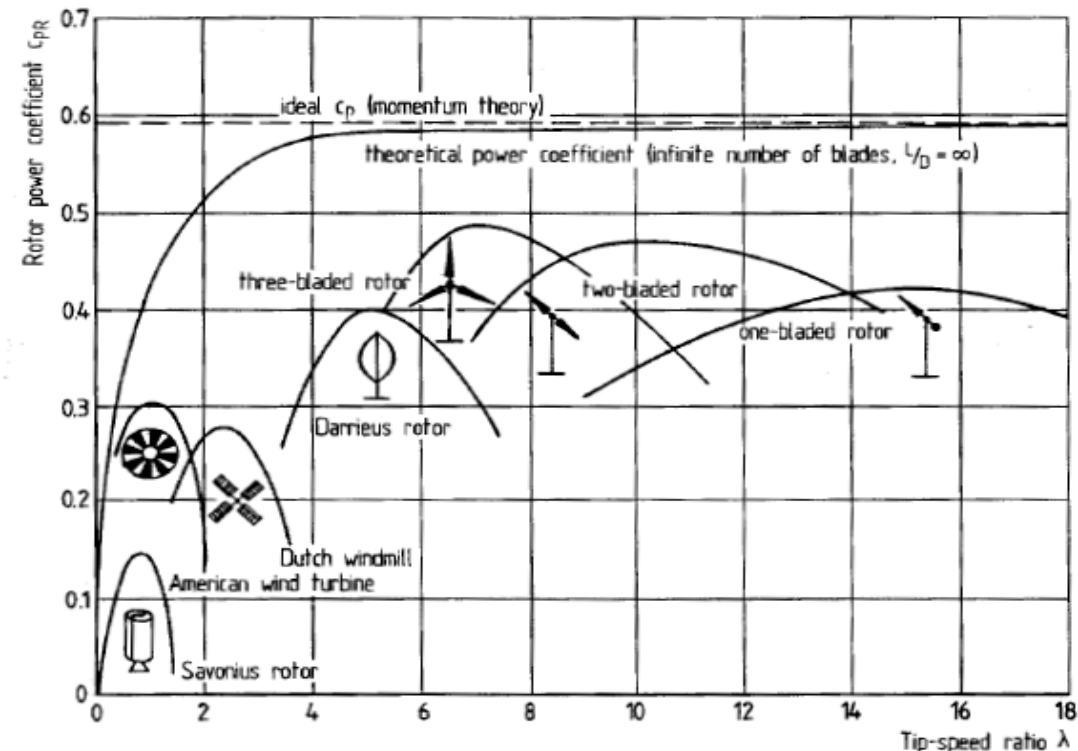


Fig. 5.10. Power coefficients of various of wind rotors [2]

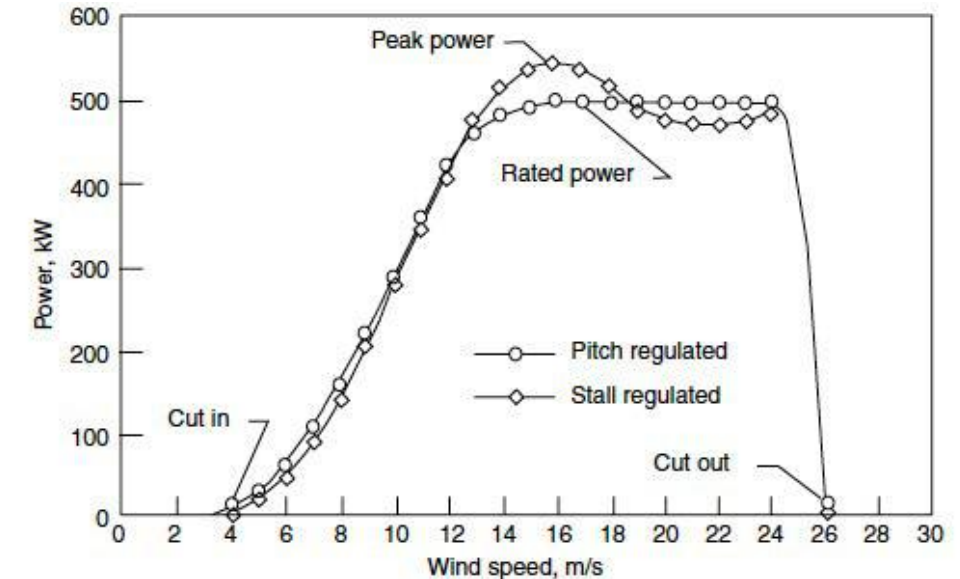
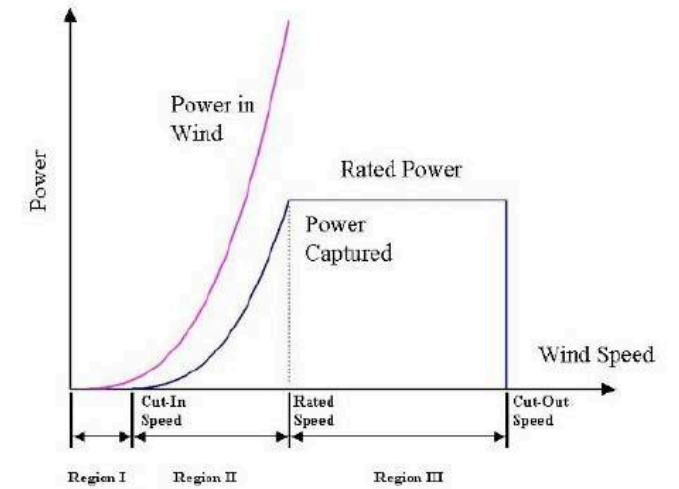
From Wind Turbines by Eric Hau

Wind turbine power-wind speed curve

$$P_{turbine} = \frac{1}{2} C_p \rho U^3 \left(\frac{n_{bl} A_{bl}}{A} \right) A = \frac{1}{2} C_{p,tur} \rho U^3 A, \quad \text{where } A \text{ is the disc area}$$

$$C_{p,Betz} = 0.593, \quad C_{p,tur} = 0.4 - 0.5$$

- Most modern wind turbines operate over a range of wind speed, hence power (depending on the generator, the RPM can be fixed or can vary).
- Must limit the forces on the turbine, and hence the tip speed, to protect the structural integrity, there is a maximum allowable tip speed.
- At this tip speed, the power is nearly constant, determined mostly by the pitch angle of the blade (can force the blade to stall to stop extracting more power) until stall.



Power curve for pitch-regulated and stall regulated wind turbine

$$P_{turbine} = \frac{1}{2} C_p \rho U^3 A, \quad C_p = 0.4 - 0.5$$

- For tall turbines, wind speed changes with height outside the atmospheric boundary layer, but the pattern is seasonal.
- Most of the time, the impact of the change on the power is not as significant because of the change in density.
- For large turbines, the height of the tower is determined more by the size of the blades.

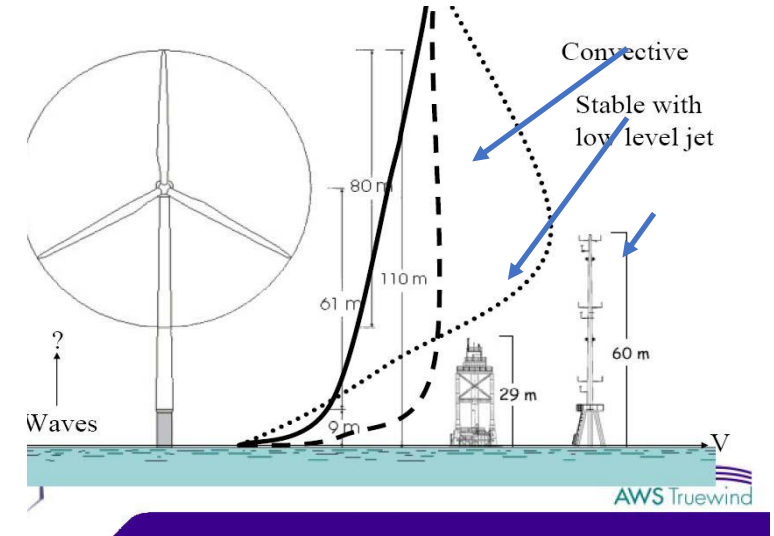
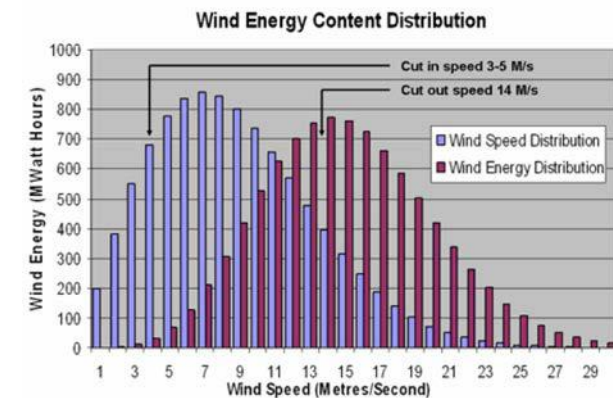
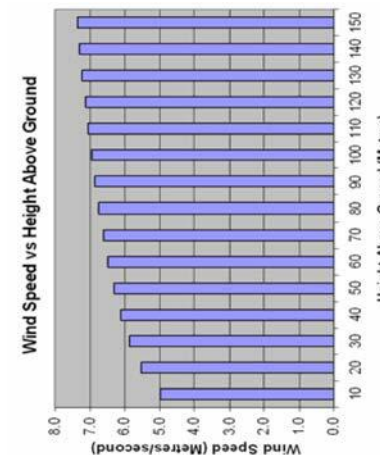


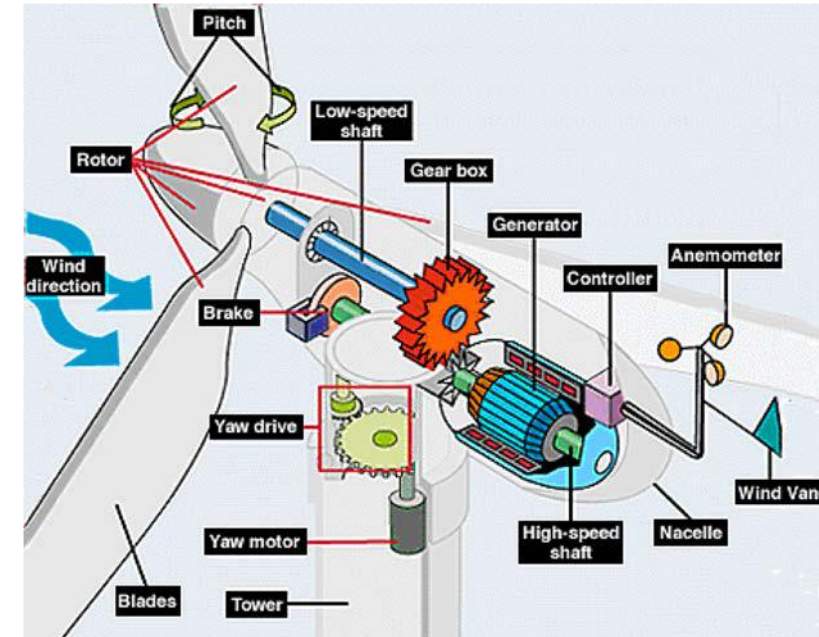
Image courtesy of AWS Truewind, NREL, DOE.



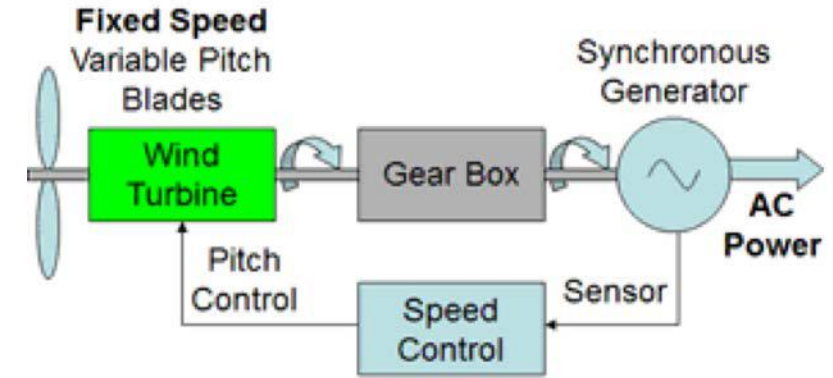
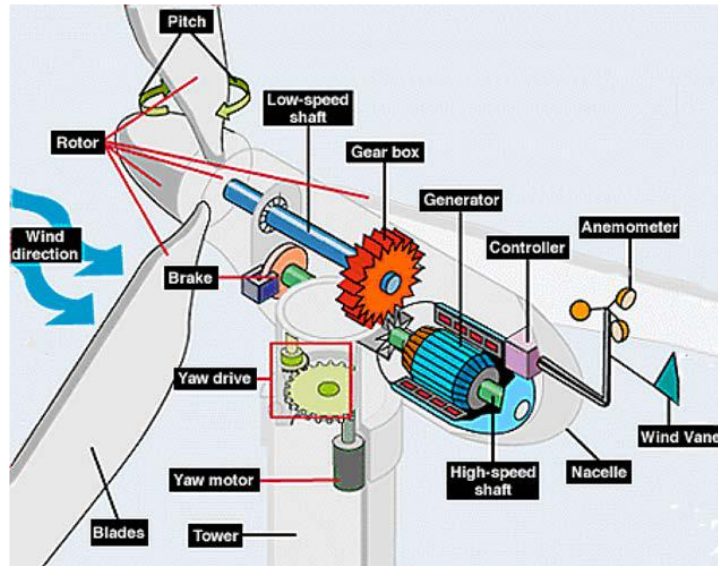
The blue shows the pdf of wind speed, while the red is the power at different wind speeds.

Generators

- Most turbines (especially the larger ones) utilize induction (asynchronous) generators. These generators have simple rugged construction, and can be used as motors (reversing the current) for starting up the turbine.
- Power electronics are used to condition the power (frequency and voltage instabilities) before sending it to the grid.
- The generators can operate with variable speed (in case the rotational speed of the turbine varies in response to changing the wind conditions, again using power electronics to condition the power (especially the frequency of the AC current) before feeding to to the grid.
- Synchronous generators are also used, which can be directly connected with the turbine shaft.

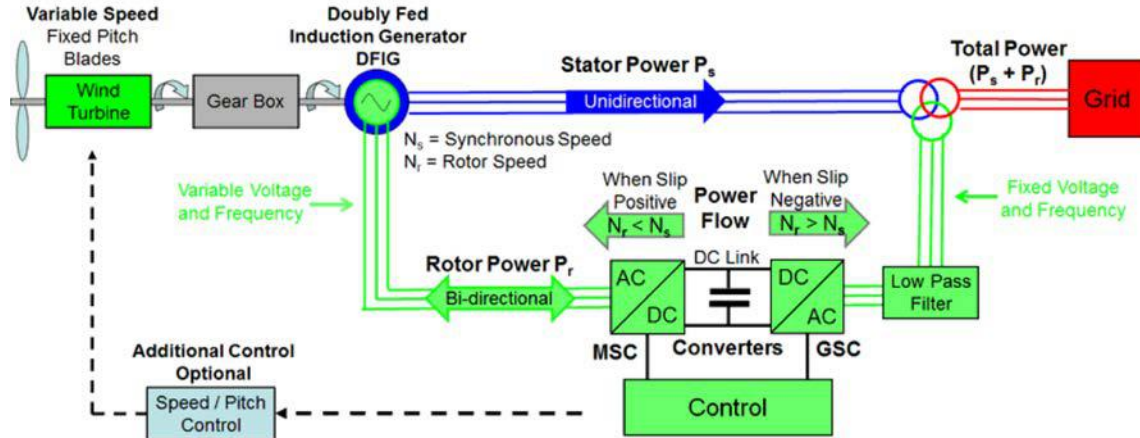


What is inside the nacelle?

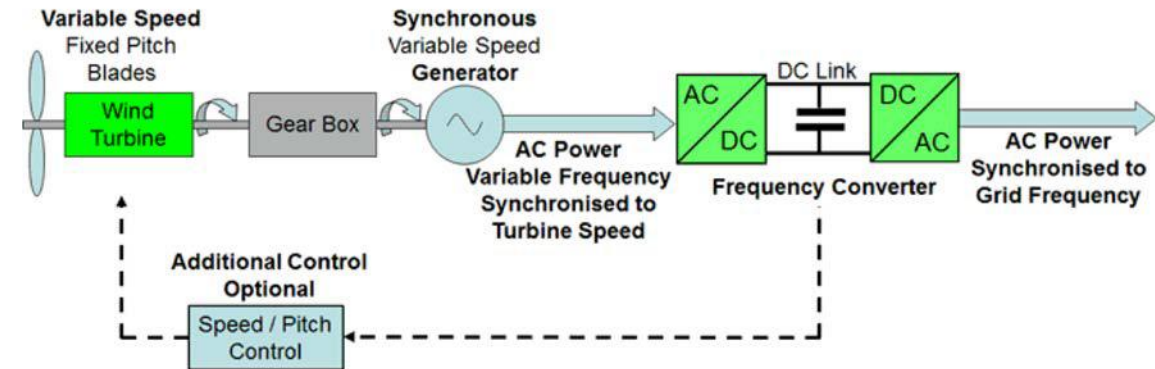


Large Scale Wind Power (Grid Systems)

Asynchronous DFIG Wind Power Generator (Grid Scale)



Large Scale Wind Power with In-Line Frequency Conversion (Grid Systems)



Double fed Induction Generator (DFIG).

Most widely used because of efficiency, simplicity and price.

Can be used as a motor to start the turbine.

Produces high quality power.

https://www.mpoweruk.com/wind_power.htm

25

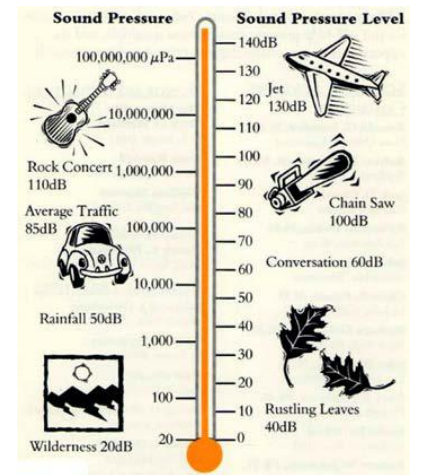
NOISE: Mostly aerodynamic noise are associated with flow over turbine blades:

Jianu et al, World Sustainable Forum, 2011

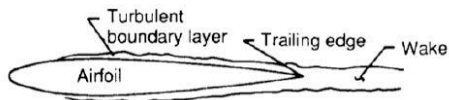
Sound pressure level is defined as:

$$SPL = 10 \log_{10} \left(p_{rms}^2 / p_{ref}^2 \right)$$

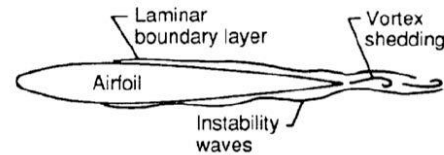
$$p_{ref} = 10 \mu Pa$$



Turbulent boundary layer trailing edge noise [6].



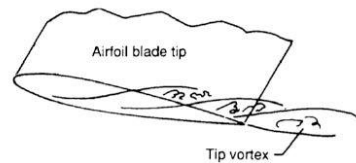
Laminar-boundary-layer vortex shedding noise [6].



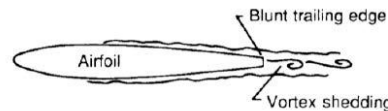
Separation-stall noise [6].



Tip vortex formation noise [6].



Trailing-edge-bluntness vortex-shedding noise [6].



Laminar-Boundary-Layer Vortex-Shedding (LBL VS) Noise

Noise scales with M^5

From Wind Turbines by Eric Hau

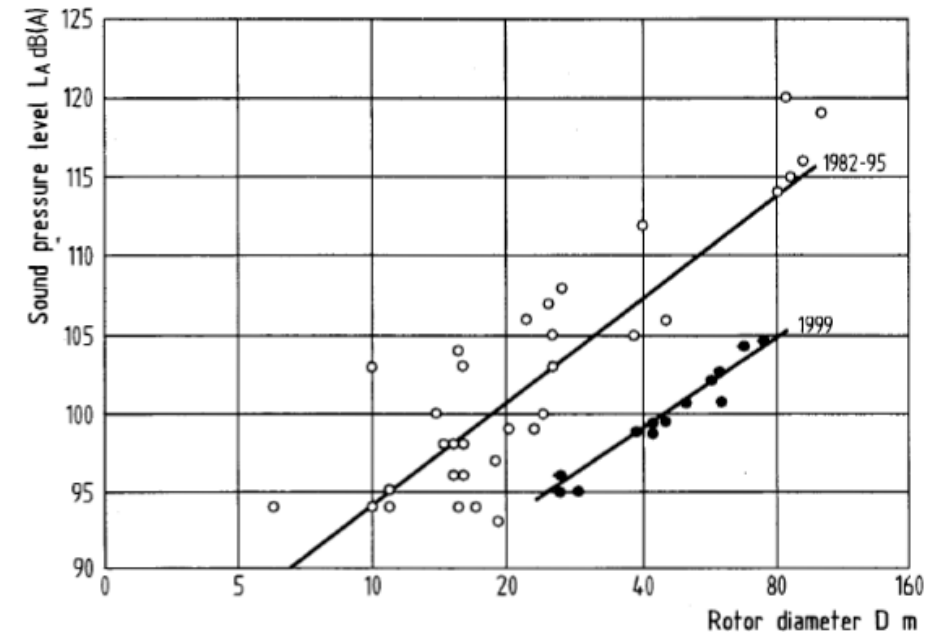
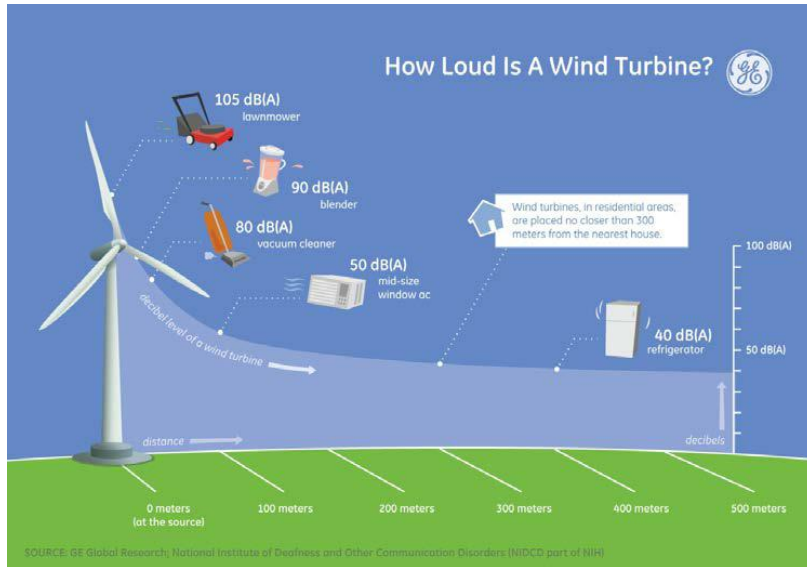


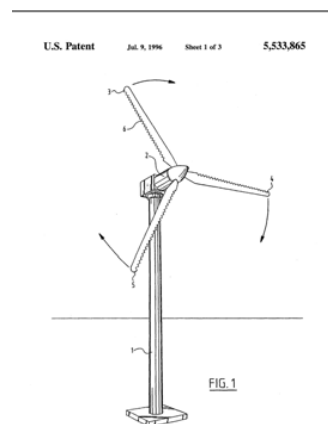
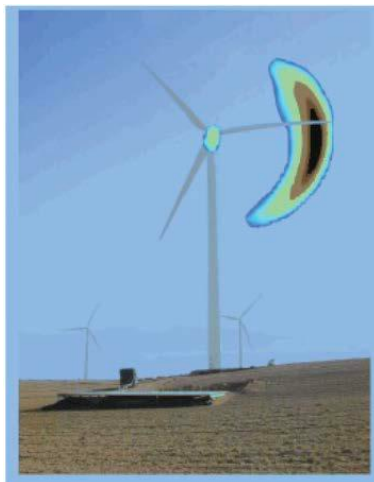
Fig. 17.4. Sound power level of wind turbines [12]

The noise factor



© GE. All rights reserved. This content is excluded from our Creative Commons license. For more information, see <https://ocw.mit.edu/fairuse>.

Emitted mostly from the tip (highest speed)

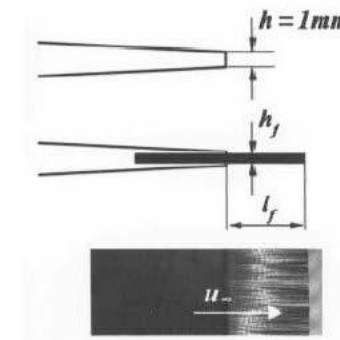


Adding serration to reduce noise



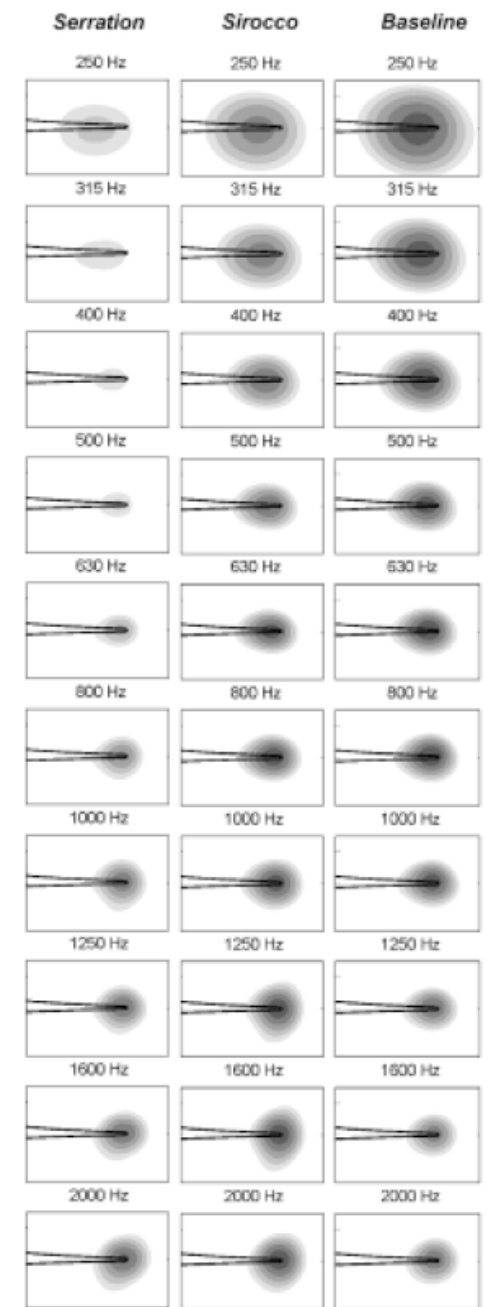
As always with noise, effectiveness depends on frequency

Using brushes can reduce noise by up to 10 dB



Silent rotor by acoustic optimization (SIROCCO)

Jianu et al, World Sustainable Forum, 2011



© Sciforum. All rights reserved. This content is excluded from our Creative Commons license. For more information, see <https://ocw.mit.edu/fairuse>.

Wind Farms and minimizing interference

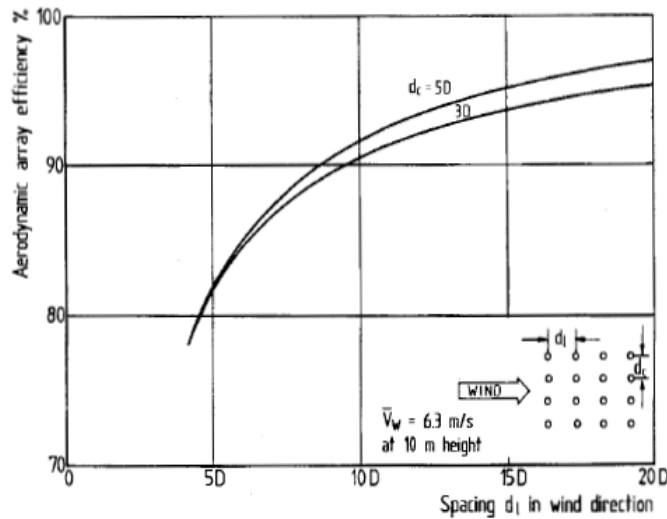


Fig. 16.23. Aerodynamic array efficiency depending on the rotor spacing in wind direction, calculated for a field of 16 wind turbines [21]

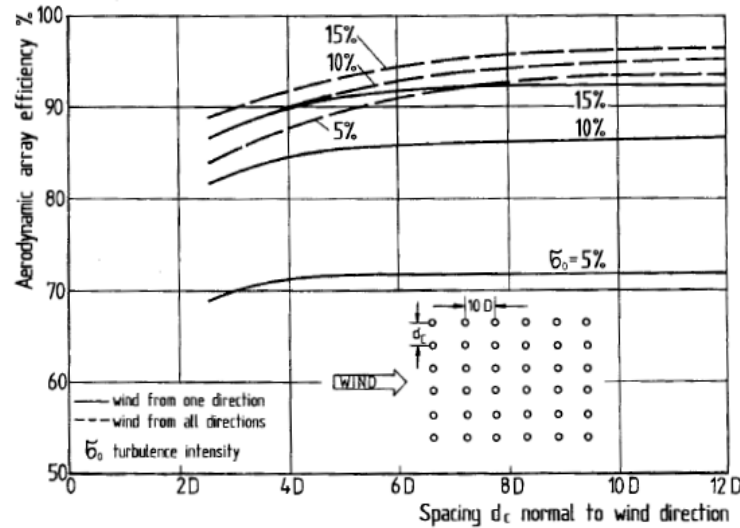


Fig 16.24. Array efficiency depending on the rotor spacing at an angle to the wind and on the turbulence intensity [21]

From Wind Turbines by Eric Hau

© Springer Nature Switzerland AG. All rights reserved. This content is excluded from our Creative Commons license. For more information, see <https://ocw.mit.edu/fairuse>.

- Wakes decay while spreading at a certain angle.
- According to NREL, land required for a single turbine tower (roads, and support structures) is ~ 0.1-0.2 hectares (0.25-0.50 acres).

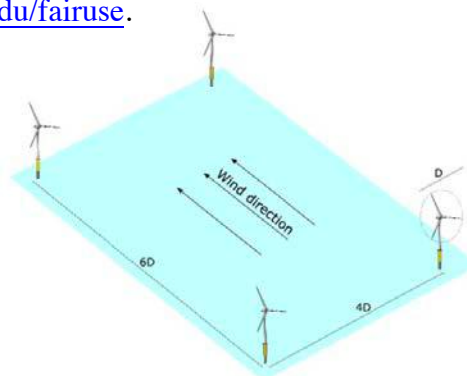


Image courtesy of US Air Force.



FIGURE 12.18 Wake turbulence. Photo credit: Vattenfall Wind Power, Denmark.

© Vattenfall Wind Power, Denmark. All rights reserved. This content is excluded from our Creative Commons license. For more information, see <https://ocw.mit.edu/fairuse>.

© The Associated Press. All rights reserved. This content is excluded from our Creative Commons license. For more information, see <https://ocw.mit.edu/fairuse>.

Off-shore wind

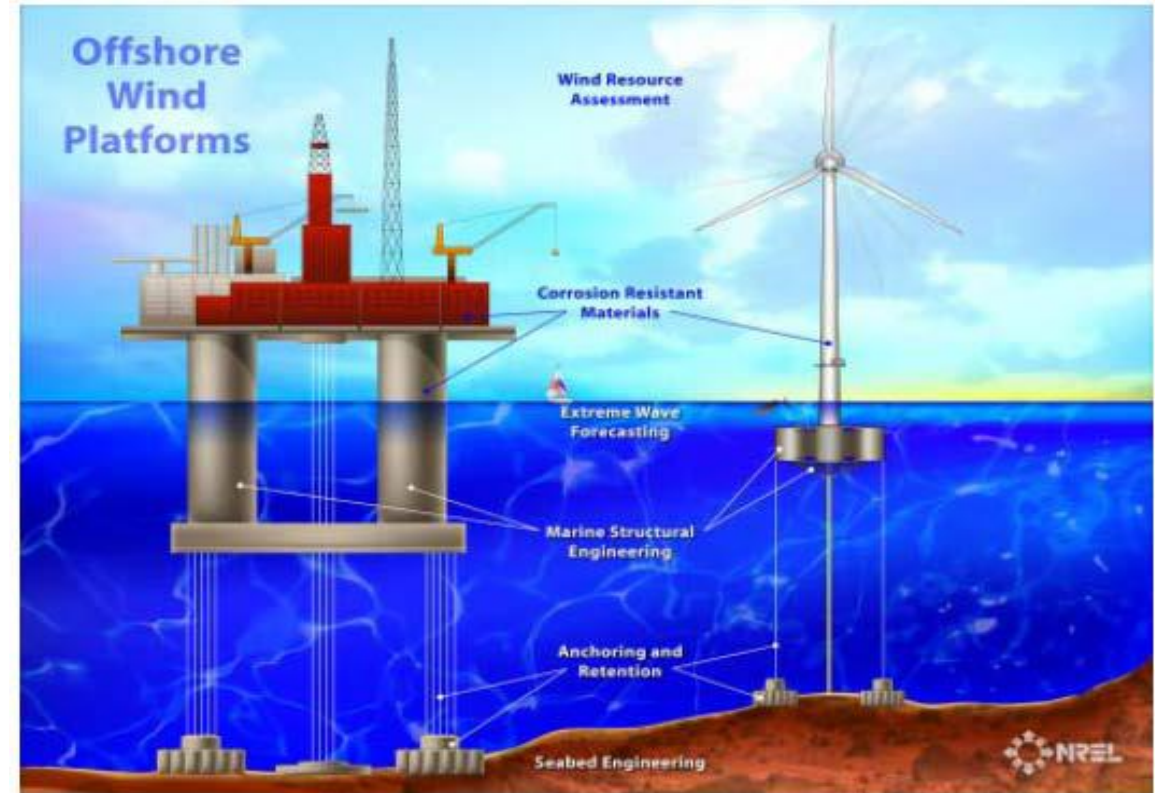
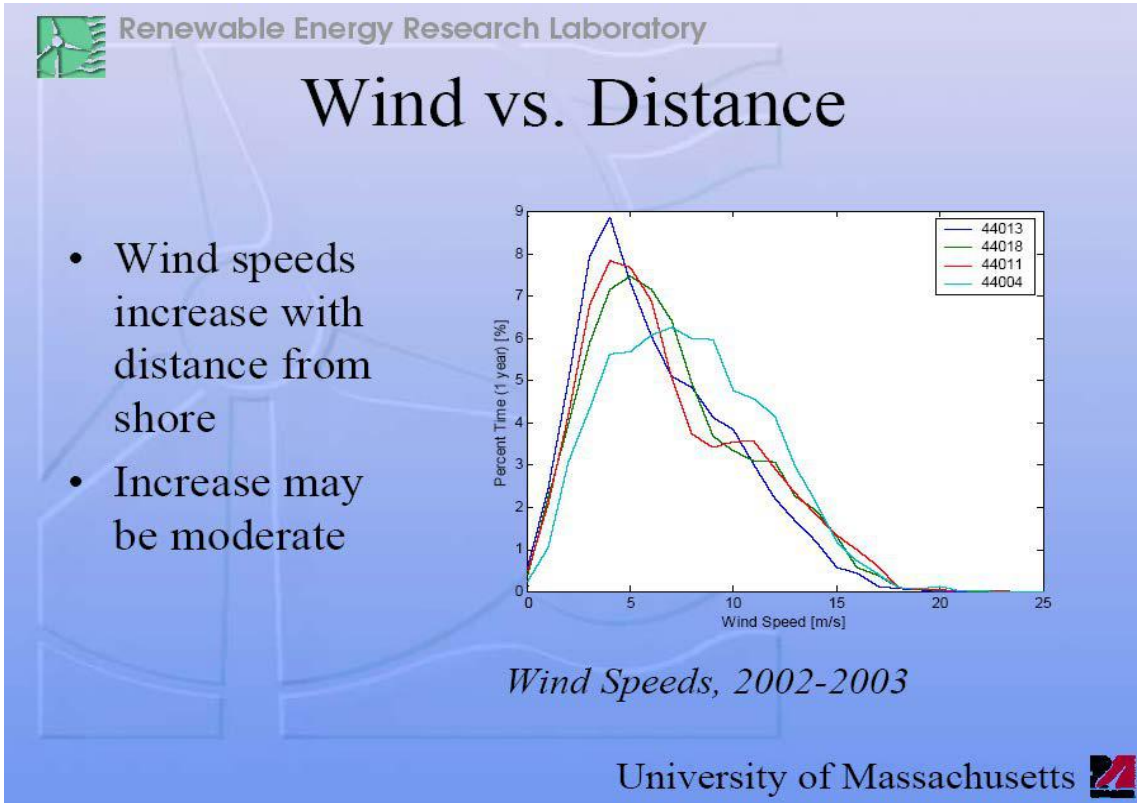


Image courtesy of NREL, DOE.

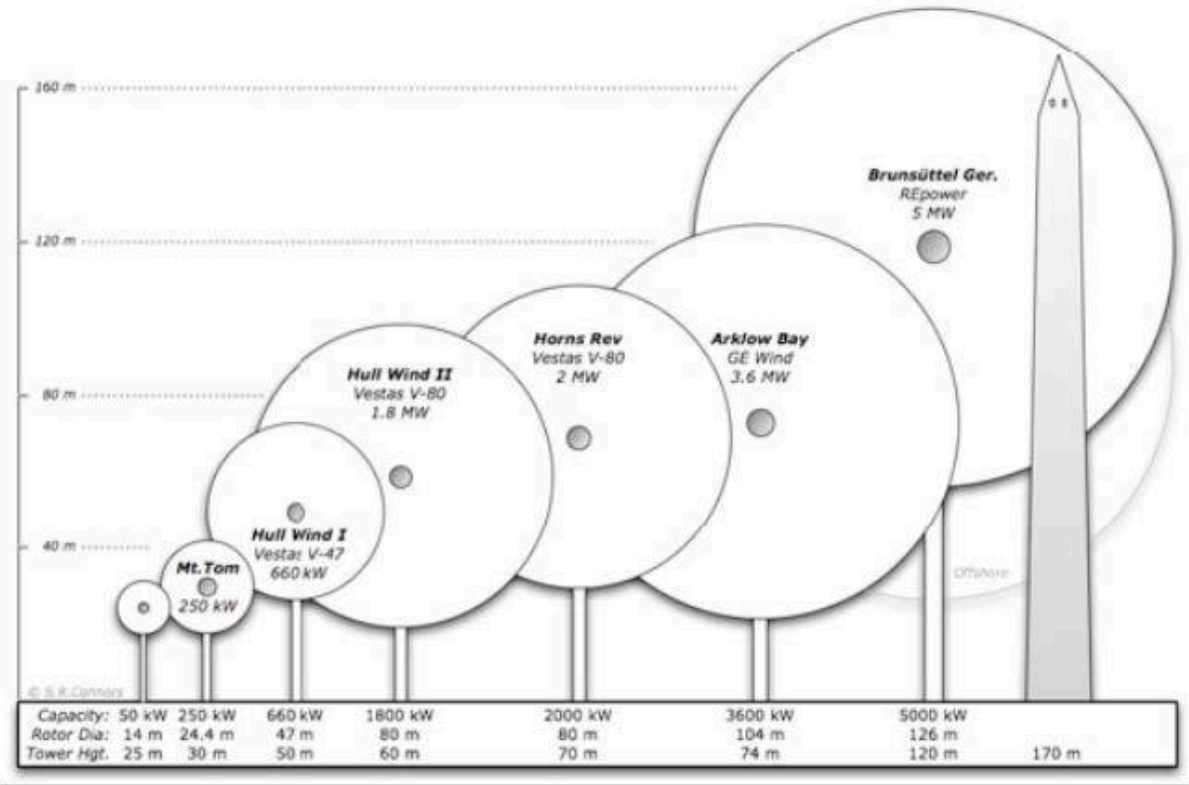
By 2009, 5-7 MW, by 2015, 10 MW, off shore turbine.
 90-100 m high (hub) and 140 m diameter (rotor).
 Mostly floating in 50 m deep water.
 Actively controlled blade pitch for variable wind speed.
 Different sensors and actuators to protect against wind gust and storms, etc.

Offshore GE Wind Energy 3.6 MW Prototype

- Offshore GE 3.6 MW
104 meter rotor diameter
- Offshore design requirements considered from the outset:
 - Crane system for all components
 - Simplified installation
 - Helicopter platform

Boeing 747-400

Image courtesy of NREL, DOE.



© S. W. Conoars. All rights reserved. This content is excluded from our Creative Commons license. For more information, see <https://ocw.mit.edu/fairuse>.



Horns Rev Wind Farm (Denmark) - Rated Power 160 MW – Water Depth 10-15m

Image courtesy of Bureau of Ocean Energy Managment, U.S. Department of the Interior.

Installation must be low cost and weather tollerant.



Vesta 7MW turbines, rotor D = 164 m

https://www.mpoweruk.com/wind_power.htm



Image courtesy of NREL, DOE.

© The Institution of Engineering and Technology. All rights reserved.
This content is excluded from our Creative Commons license. For more
information, see <https://ocw.mit.edu/fairuse>.

MIT OpenCourseWare
<https://ocw.mit.edu/>

2.60J Fundamentals of Advanced Energy Conversion
Spring 2020

For information about citing these materials or our Terms of Use, visit: <https://ocw.mit.edu/terms>.

Energy & Materials

Dr. Georgios Dimitrakopoulos

Research Scientist
Department of Mechanical Engineering
Massachusetts Institute of Technology

2.60 Guest Lecture

Question: How many elements exist in an iPhone???

- An iPhone requires 75 elements!
- Human life requires 30 elements!
- Transistors: Si
- CPU: Si, As, P, Ga, Sb, O
- Reinforced glass: Al, Si, K, O
- Battery: Li, Co, Mn, C
- Electronics wiring: Au, Sn, Ag, Cu
- Color display: Y, Gd, Eu, Tb, Pr
- Touch screen: In, Sn, O
- Capacitors: Ta
- Case: Al

1 H Hydrogen																	2 He Helium						
3 Li Lithium	4 Be Beryllium																	5 B Boron	6 C Carbon	7 N Nitrogen	8 O Oxygen	9 F Fluorine	10 Ne Neon
11 Na Sodium	12 Mg Magnesium																	13 Al Aluminium	14 Si Silicon	15 P Phosphorus	16 S Sulfur	17 Cl Chlorine	18 Ar Argon
19 K Potassium	20 Ca Calcium	21 Sc Scandium	22 Ti Titanium	23 V Vanadium	24 Cr Chromium	25 Mn Manganese	26 Fe Iron	27 Co Cobalt	28 Ni Nickel	29 Cu Copper	30 Zn Zinc	31 Ga Gallium	32 Ge Germanium	33 As Arsenic	34 Se Selenium	35 Br Bromine	36 Kr Krypton						
37 Rb Rubidium	38 Sr Strontium	39 Y Yttrium	40 Zr Zirconium	41 Nb Niobium	42 Mo Molybdenum	43 Tc Technetium	44 Ru Ruthenium	45 Rh Rhodium	46 Pd Palladium	47 Ag Silver	48 Cd Cadmium	49 In Indium	50 Sn Tin	51 Sb Antimony	52 Te Tellurium	53 I Iodine	54 Xe Xenon						
55 Cs Cesium	56 Ba Barium	57 La Lanthanum	72 Hf Hafnium	73 Ta Tantalum	74 W Tungsten	75 Re Rhenium	76 Os Osmium	77 Ir Iridium	78 Pt Platinum	79 Au Gold	80 Hg Mercury	81 Tl Thallium	82 Pb Lead	83 Bi Bismuth	84 Po Polonium	85 At Astatine	86 Rn Radon						
87 Fr Francium	88 Ra Radium	89 Ac Actinium	104 Rf Rutherfordium	105 Db Dubnium	106 Sg Seaborgium	107 Bh Bohrium	108 Hs Hassium	109 Mt Meitnerium	110 Ds Darmstadtium	111 Rg Roentgenium	112 Cn Copernicium	113 Uut Ununtrium	114 Uuq Ununquadium	115 Uup Ununpentium	116 Uuh Ununhexium	117 Uus Ununseptium	118 Uuo Ununoctium						

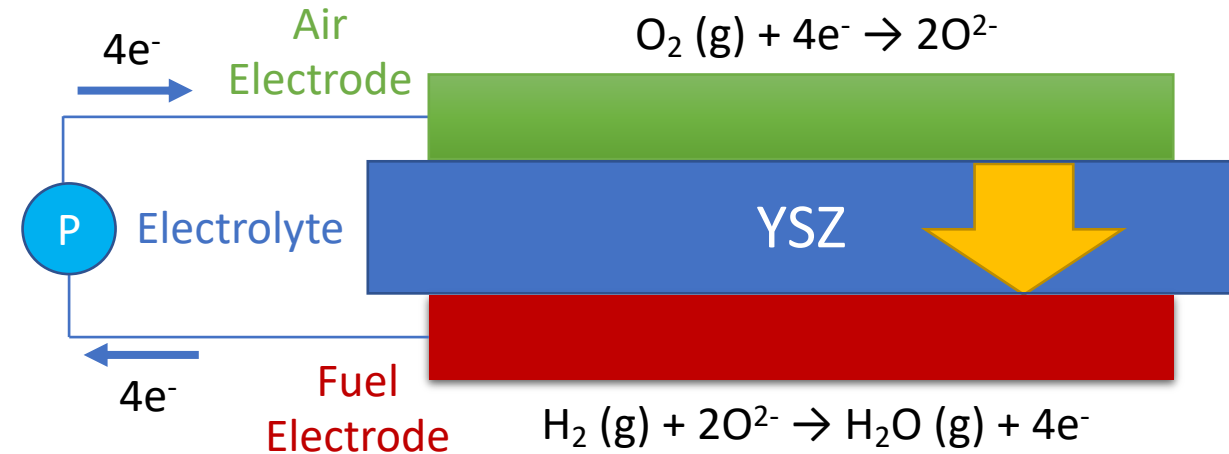
75 / 118

58 Ce Cerium	59 Pr Praseodymium	60 Nd Neodymium	61 Pm Promethium	62 Sm Samarium	63 Eu Europium	64 Gd Gadolinium	65 Tb Terbium	66 Dy Dysprosium	67 Ho Holmium	68 Er Erbium	69 Tm Thulium	70 Yb Ytterbium	71 Lu Lutetium
90 Th Thorium	91 Pa Protactinium	92 U Uranium	93 Np Neptunium	94 Pu Plutonium	95 Am Americium	96 Cm Curium	97 Bk Berkelium	98 Cf Californium	99 Es Einsteinium	100 Fm Fermium	101 Md Mendelevium	102 No Nobelium	103 Lr Lawrencium

Why are materials needed in energy applications?

- Materials are used in almost every energy conversion device.
- Reason:** materials have **properties** that allow an engineer to design a system according to the expected operating requirements
- Take a typical Solid Oxide Fuel Cell (SOFC), for example:
 - Electronic conductivity (electrodes)
 - Ionic conductivity (electrolyte + electrodes)
 - Mechanical strength (electrolyte + electrodes)
 - Catalytic activity (electrodes)
 - Chemical compatibility under operating conditions of interest (i.e. temperature, gas environment etc.)
 - Porosity/densification
 - Electrodes should be porous
 - Electrolyte should be 100% dense
 - Material compatibility (electrodes do not react with electrolyte or with impurities from the gases)
 - Others properties

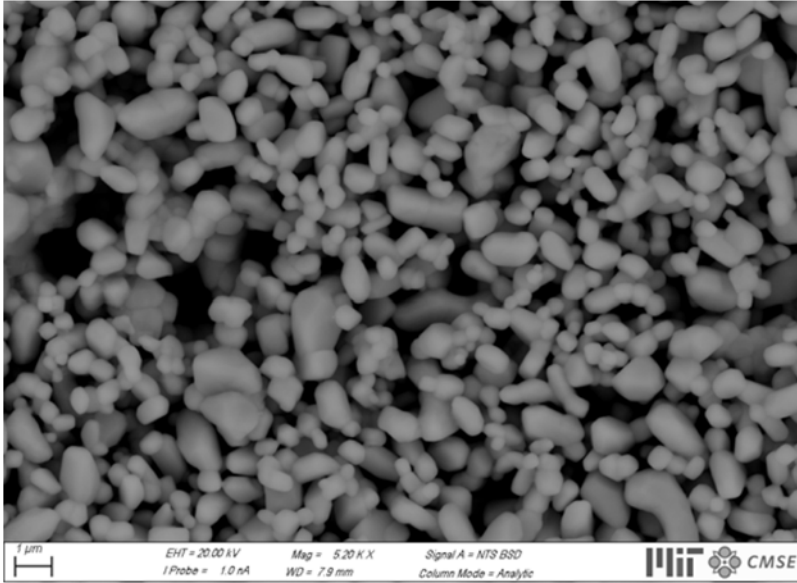
Typical Solid Oxide Fuel Cell



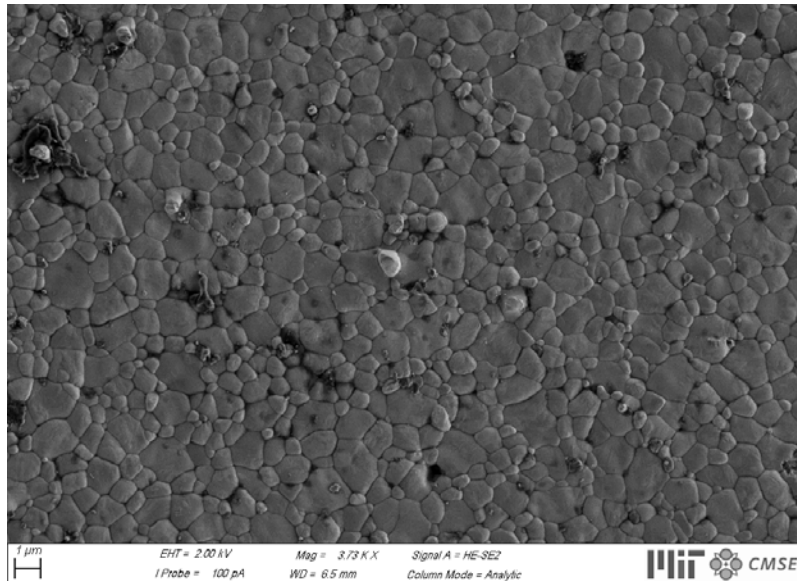
Real Lab Scale Cell

- White: YSZ electrolyte ($\sim 10\text{-}100\mu\text{m}$)
- Black: electrode ($\sim 2\text{-}10\mu\text{m}$)

Solid Oxide Fuel Cells (cont'd)

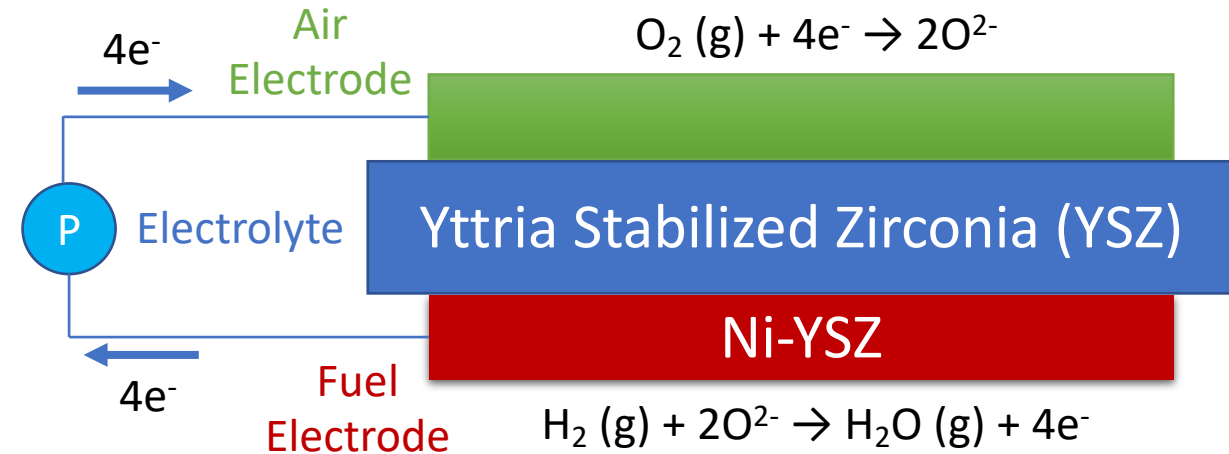


Electrodes should be porous to increase the available surface area for reactions



Electrolytes should be fully dense (i.e. no gaps) to ensure increasing ionic conductivity, mechanical strength and to minimize gas leakage

Typical Solid Oxide Fuel Cell



But what determines the properties of materials???

Elements, composition and bonding (Materials' Science)

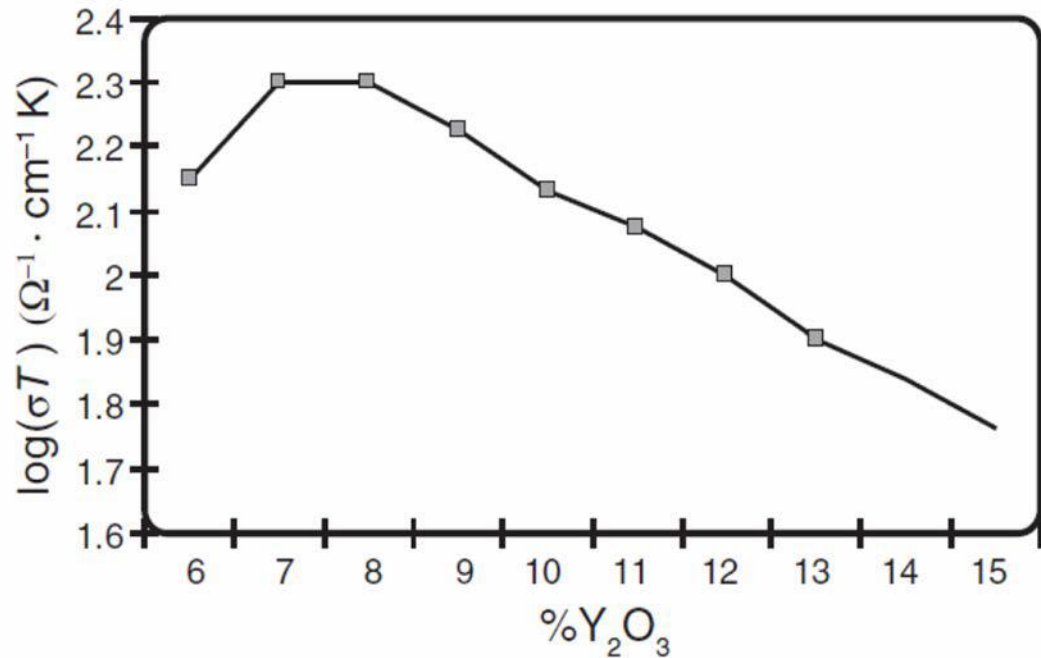
Periodic table of the elements

group	1*																	2	18												
period	1																	2	18												
1	1																	2													
2	3	4													5	6	7	8	9	10											
3	11	12	3	4	5	6	7	8	9	10	11	12	13	14	15	16	17	18													
4	19	20	21	22	23	24	25	26	27	28	29	30	31	32	33	34	35	36													
5	37	38	39	40	41	42	43	44	45	46	47	48	49	50	51	52	53	54													
6	55	56	57	72	73	74	75	76	77	78	79	80	81	82	83	84	85	86													
7	87	88	89	104	105	106	107	108	109	110	111	112	113	114	115	116	117	118													
lanthanoid series 6		58	59	60	61	62	63	64	65	66	67	68	69	70	71																
actinoid series 7		90	91	92	93	94	95	96	97	98	99	100	101	102	103																

*Numbering system adopted by the International Union of Pure and Applied Chemistry (IUPAC). © Encyclopædia Britannica, Inc.

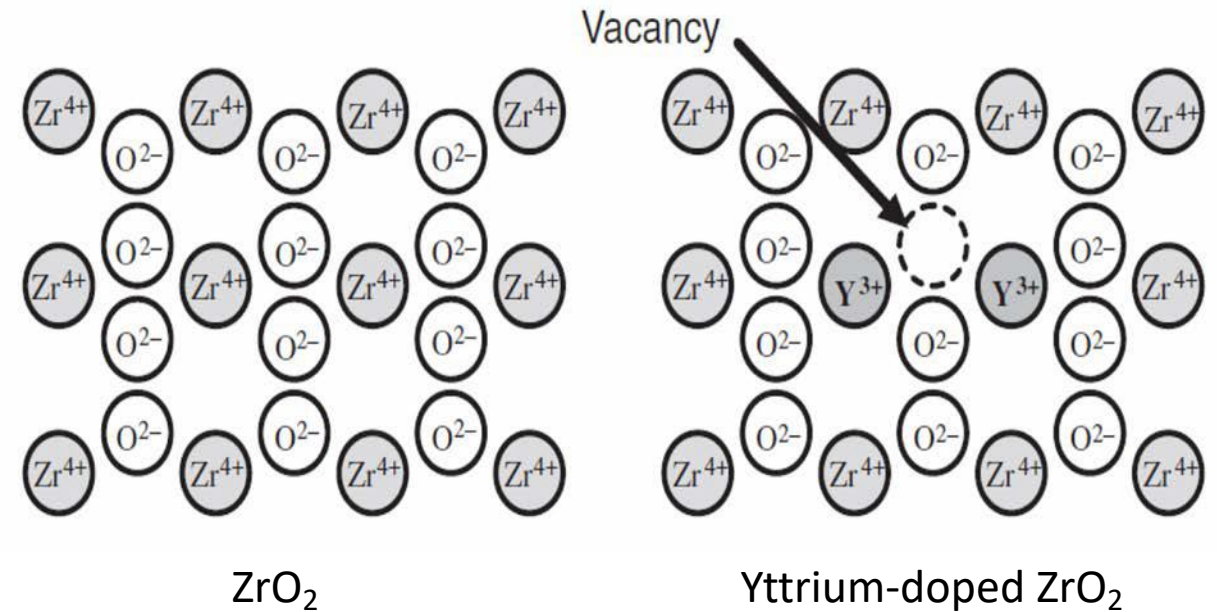
- In general, the properties of materials are dictated by the following characteristics:
 1. The elements in the structure of the material
 2. The amount of elements in the structure (stoichiometry)
 3. The bonding of elements with each other (strong bonds vs. weak bonds)
 4. The defects introduced in the material (vacancies, electron, electron holes etc.)
- What makes things difficult (as well as interesting and challenging!):
 - Designing a material has several constraints (i.e. you cannot make every material you want)
 - Properties change according to the operating conditions (temperature, gaseous environment, applied potential etc.)
 - Designing materials requires the use of characterization techniques (*ex-situ* vs. *in-situ*)

Example 1: Yttrium-doped Zirconium Oxide (YSZ)



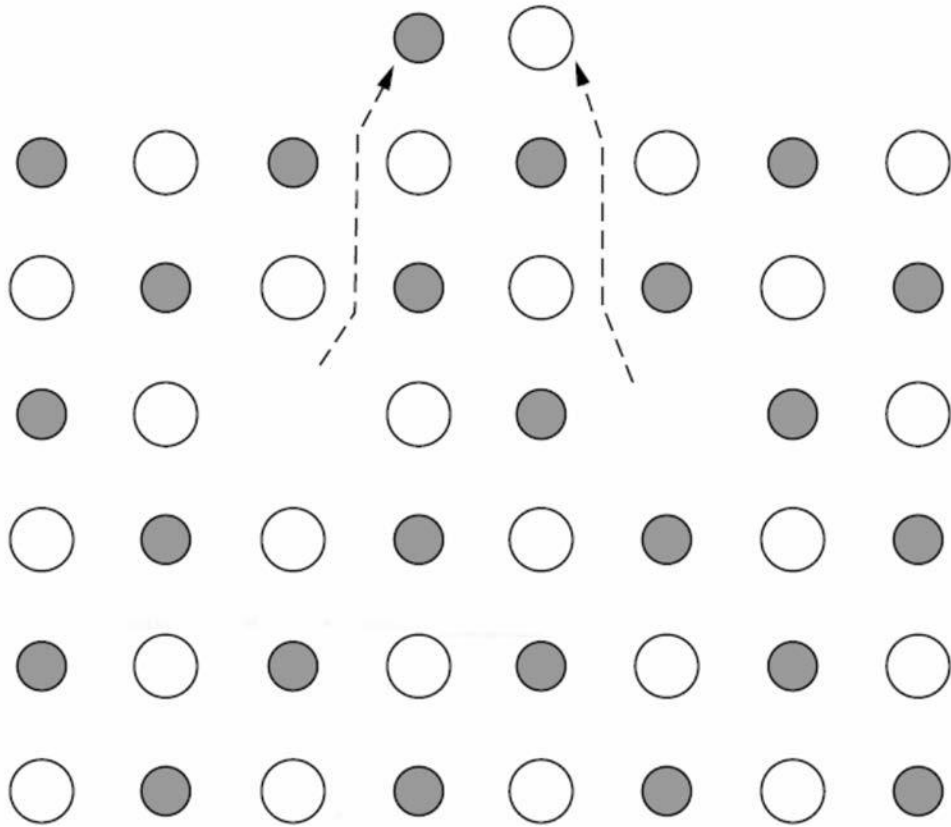
Effect of Y₂O₃ doping in ZrO₂ on the ionic conductivity

Typical electrolyte has 8% Y₂O₃ doping

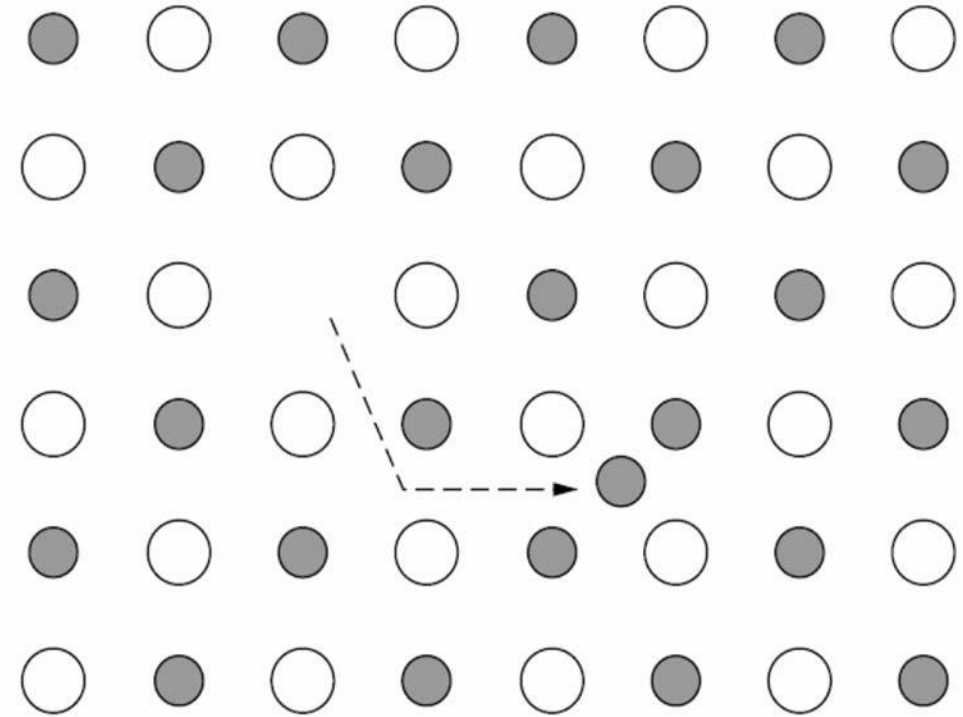


- Charge of Zr: +4
- Charge of Y: +3
- Doping Y for Zr creates a charge imbalance that is compensated by oxygen vacancies (defect species)
- Increasing oxygen vacancies increases the ionic conductivity
- Adding more than 8% Y₂O₃ makes vacancies interact with each other, hence reducing the ionic conductivity

Schottky vs. Frenkel defects (Intrinsic point defects)



Schottky defect: elements leave the crystal leaving behind vacancies



Frenkel defect: an ion leaves its regular lattice site and occupies an interstitial site, leaving behind a vacant site

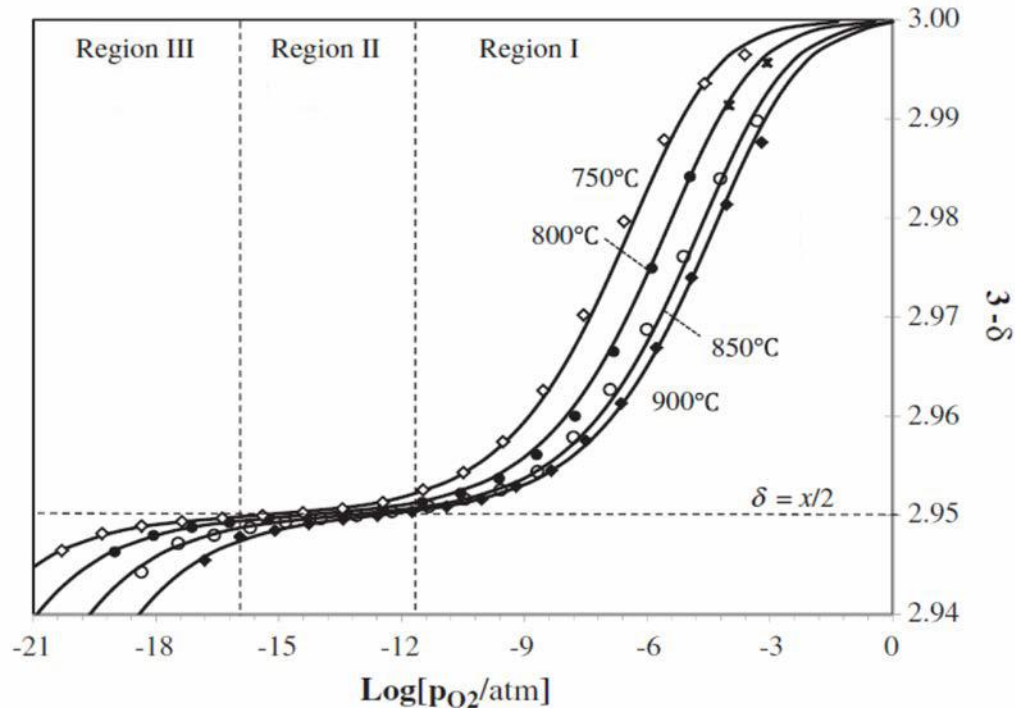
© Informa UK Limited. All rights reserved. This content is excluded from our Creative Commons license. For more information, see <https://ocw.mit.edu/fairuse>.

Example 2: Extrinsic point defects within $\text{La}_{0.9}\text{Ca}_{0.1}\text{FeO}_{3-\delta}$

- Extrinsic defects are caused by external influences, such as changes in the gaseous atmosphere, temperature, dopant etc.
- $\text{La}_{0.9}\text{Ca}_{0.1}\text{FeO}_{3-\delta}$ is used as a ceramic membrane or as a SOFC/SOEC electrode.

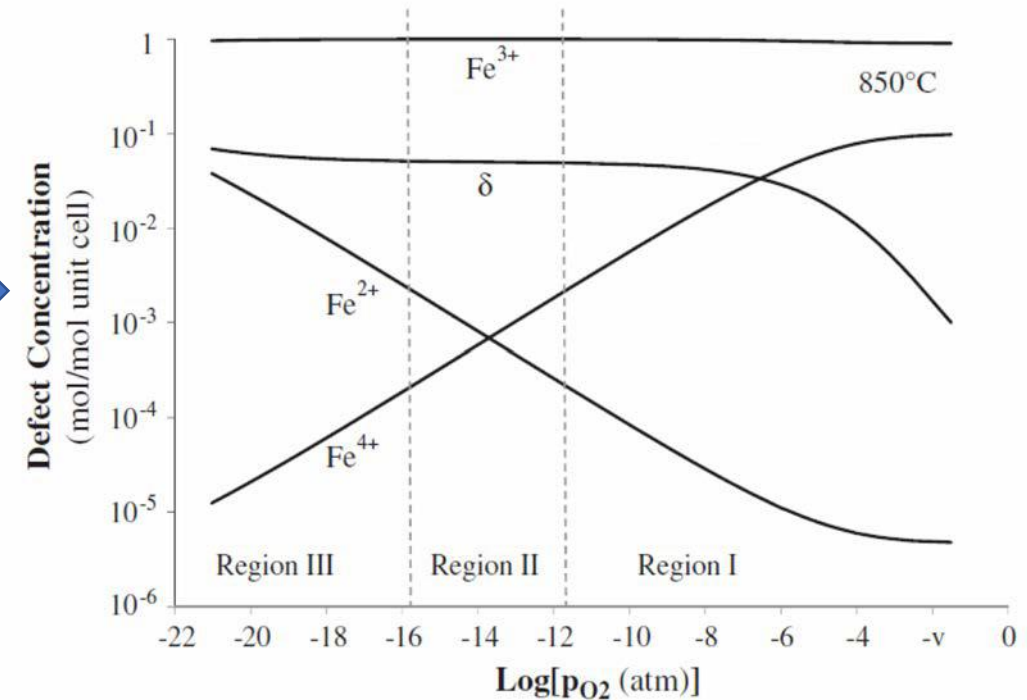
Ceramics loose oxygen from their crystal structure due to favorable thermodynamics:

- as the temperature increases
- as the O_2 partial pressure decreases



Defect
Chemistry
Models

Brouwer Diagram



Courtesy Elsevier, Inc., <http://www.sciencedirect.com>. Used with permission.

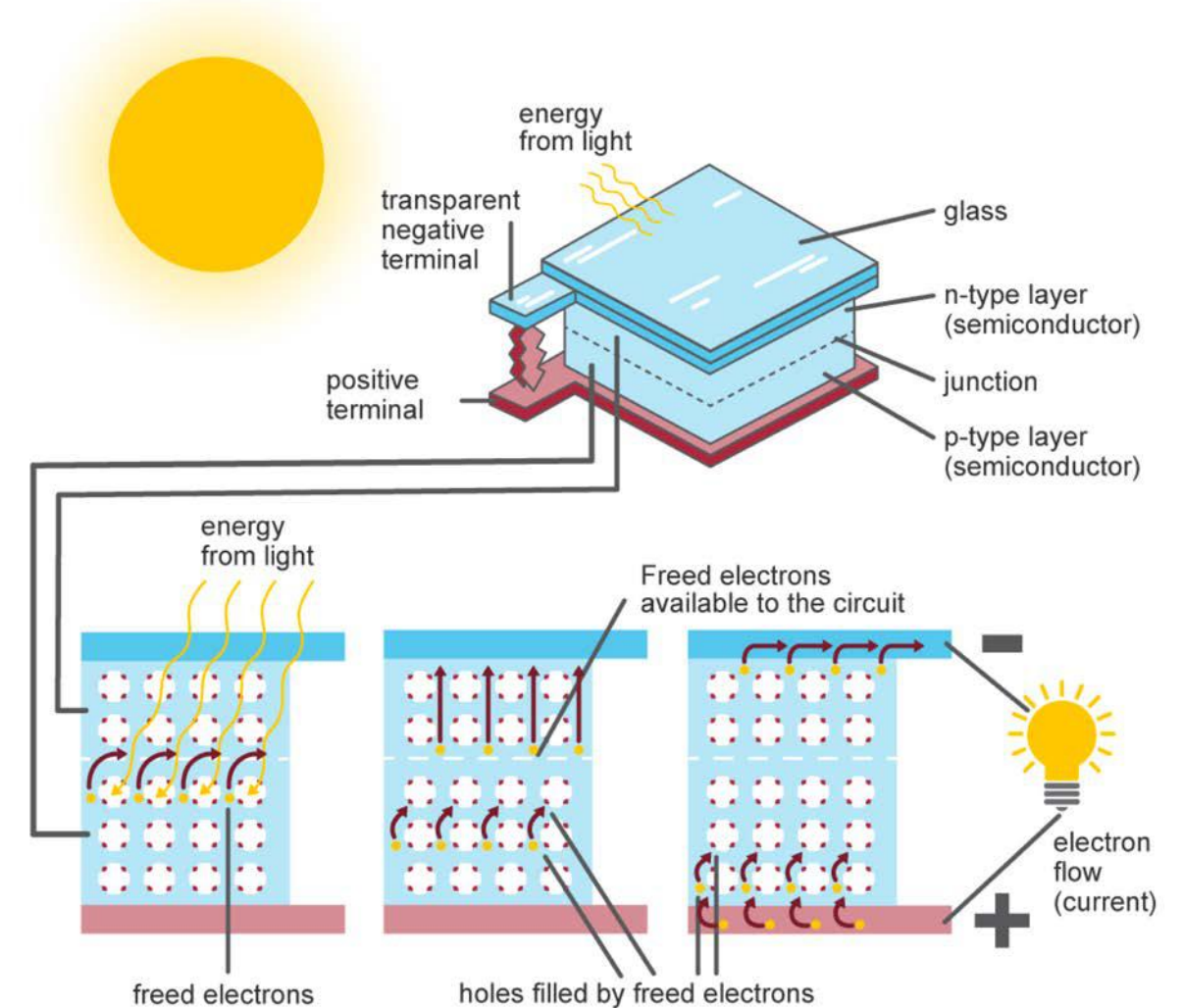
Example 3: Photovoltaics



© iStockphoto LP. All rights reserved. This content is excluded from our Creative Commons license. For more information, see <https://ocw.mit.edu/fairuse>.

Maximum theoretical efficiency = **86.8%**

Inside a photovoltaic cell



Source: U.S. Energy Information Administration

Image courtesy of U.S. Energy Information Administration.

Example 3: Photovoltaics (cont'd)

Best Research-Cell Efficiencies

Maximum theoretical efficiency = **86.8%**

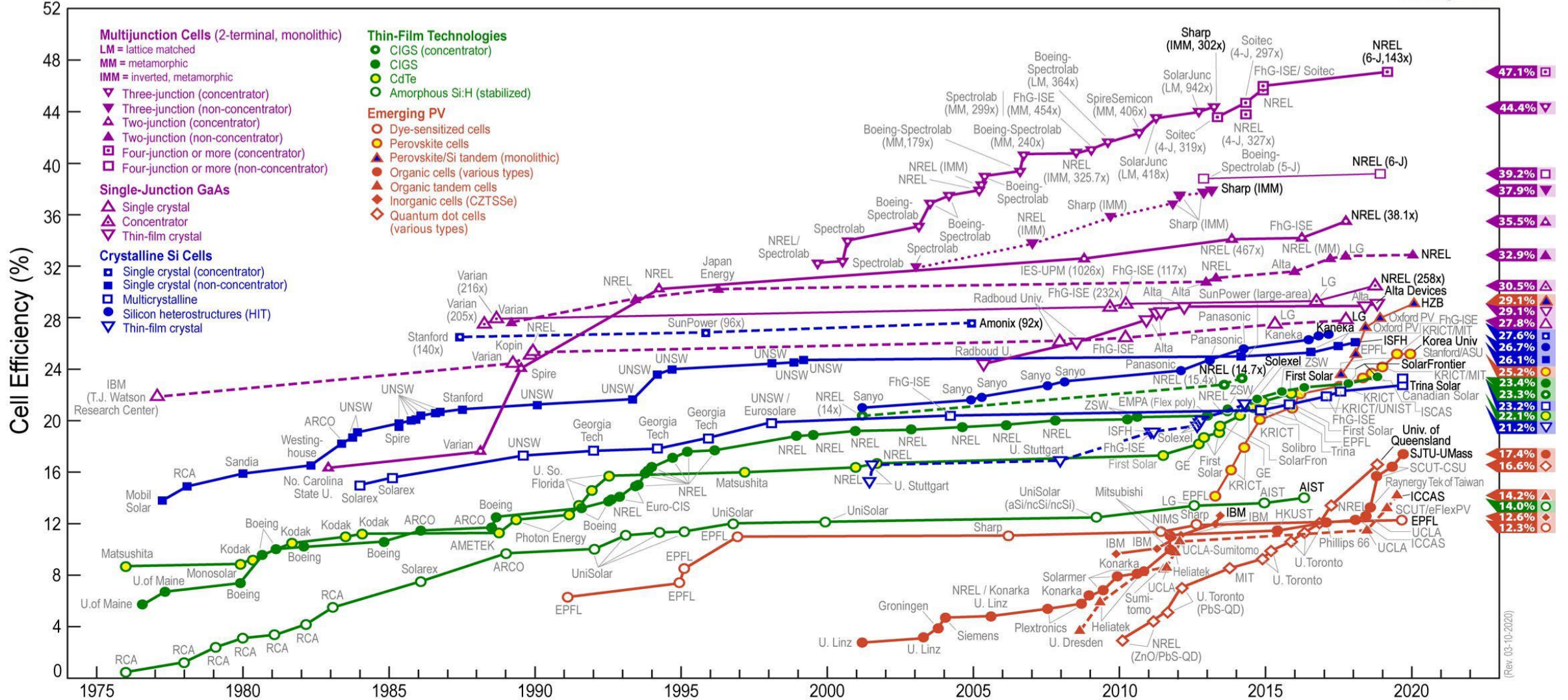
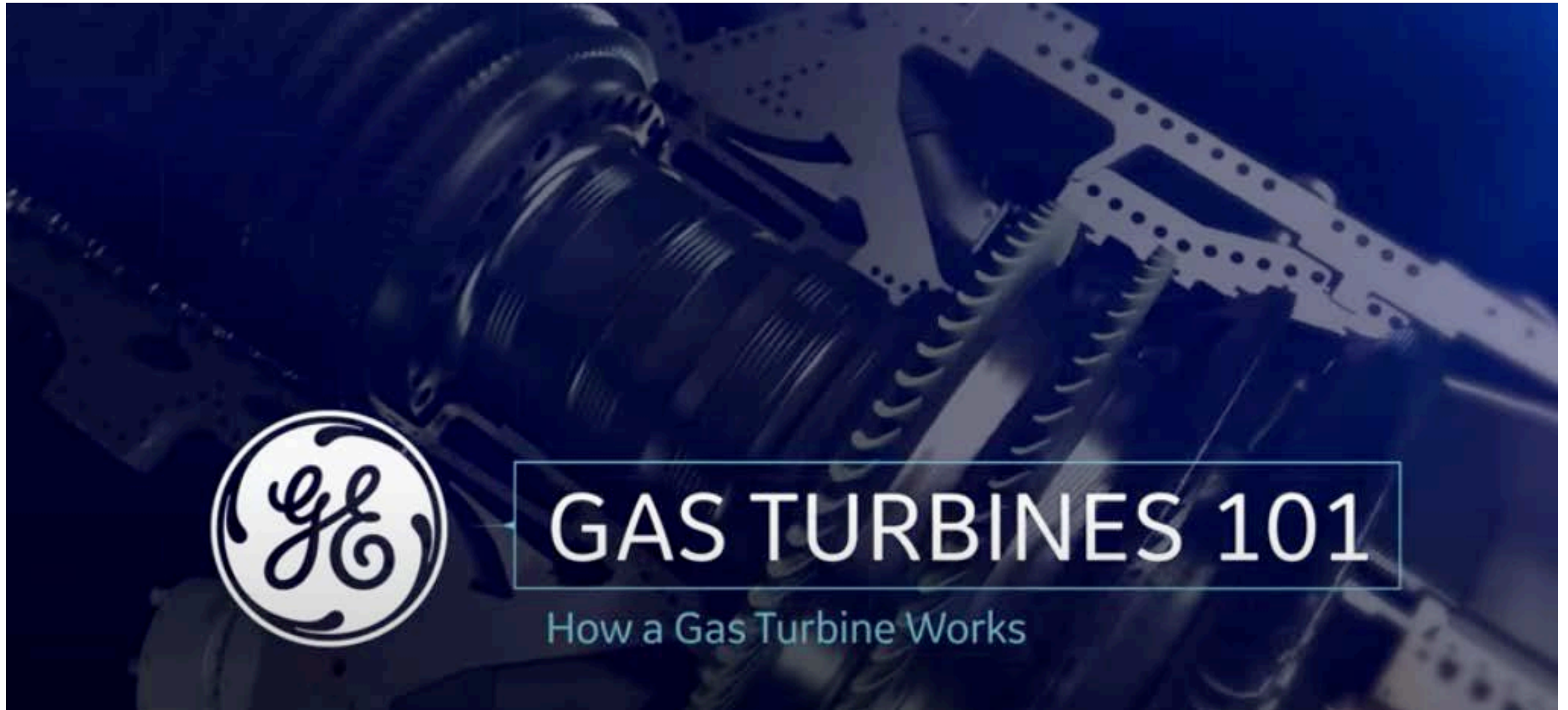


Image courtesy of NREL, DOE.

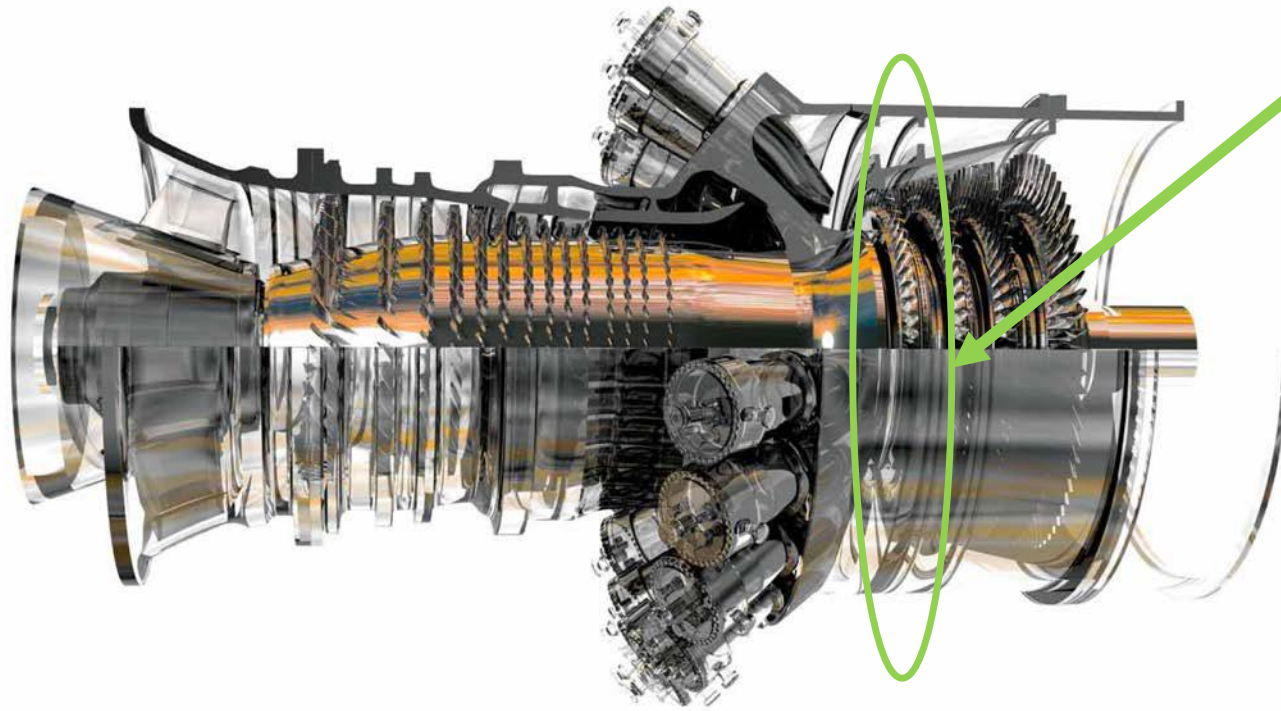
Materials' and Systems' Engineering



© GE. All rights reserved. This content is excluded from our Creative Commons license. For more information, see <https://ocw.mit.edu/fairuse>.

https://www.youtube.com/watch?time_continue=1&v=zcWkEKNvqCA&feature=emb_logo

Example 1: Increasing efficiency while avoiding creep in a gas turbine



GE 9HA Gas Turbine

High-Pressure Stage made of Single Crystals



© GE. All rights reserved. This content is excluded from our Creative Commons license. For more information, see <https://ocw.mit.edu/fairuse>.

A 605 MW General Electric 9HA can achieve a **Combined Cycle Efficiency of 62.22%** with temperatures as high as **1540°C**.

© Pearson Education, Ltd. All rights reserved. This content is excluded from our Creative Commons license. For more information, see <https://ocw.mit.edu/fairuse>.

Example 2: Engineering of the Ni-YSZ anode

- In a Ni-YSZ anode:
 - YSZ provides ionic conductivity
 - Ni provides catalytic activity and electronic conductivity
- However, to create the Ni-YSZ anode, we have to start by mixing Nickel Oxide (NiO) with YSZ
- NiO is a bad electronic conductor and electro-catalyst
- To increase the performance, the NiO-YSZ electrode is heat treated in H_2 so that:
 - NiO transforms to Ni, hence increasing the catalytic activity and electronic conductivity
 - The porosity of the electrode increases (the formation of Ni from NiO leaves behind porosity due to the O removal)

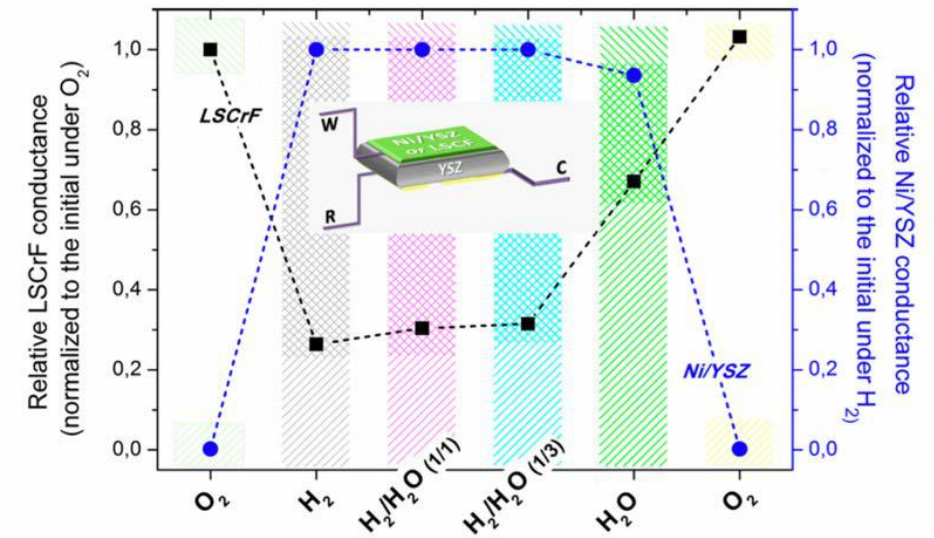
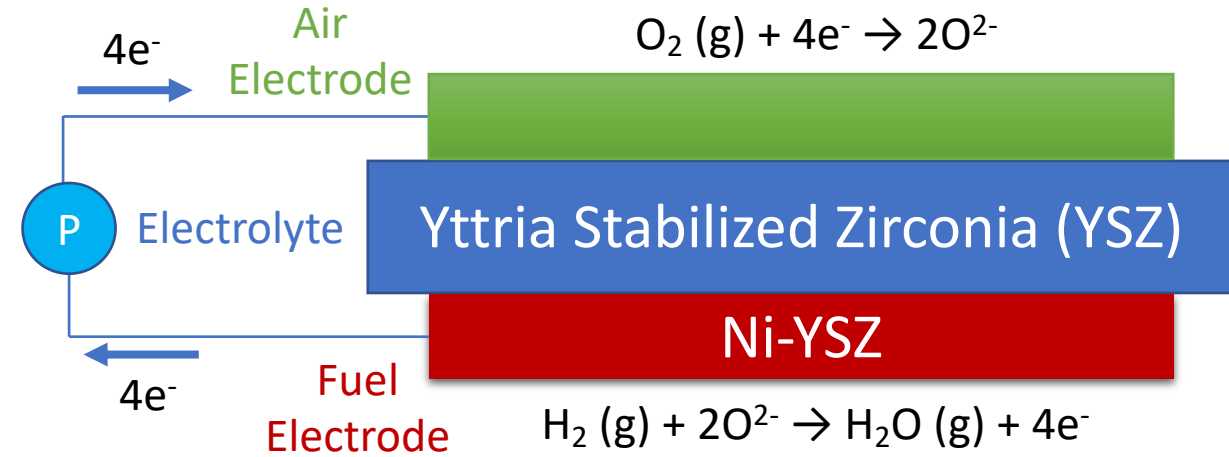


Figure 8. Plot of the reciprocal of the ohmic resistance (electrical conductance) of LSCrF and Ni/YSZ electrodes measured at 500 °C and at open circuit conditions under the indicated gas atmospheres.

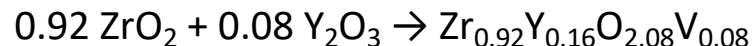
Materials Science & Engineering for Energy Applications

- To design materials and the corresponding energy conversion systems, we need:
 1. To synthesize the material
 2. To characterize the material:
 - a) Crystal structure
 - b) Microstructure
 - c) Properties (electronic conductivity etc.)
 3. To shape materials
 4. To integrate materials with other components of the system
 5. To test the system
 6. **To iterate (at the end and during each step)!!**
 - a) Identify **problems**
 - b) Improve the material and its integration to the system



Material synthesis in powder form (the most important step!!!)

- The synthesis of the material in powder form is the first and most important part of the material design
- This is because the powder characteristics (particle size, morphology and surface area) affect the properties of the material
- To synthesize a material, we need:
 1. The precursors: the raw materials
 2. Mixing of the precursors **remembering that you are inducing a reaction!**
 3. Heat treatment to enable cation diffusion (**Calcination**)
(Cation diffusion is like gas or liquid mixing!!)
- Example: synthesis of 8-YSZ using the solid-state method
 1. Precursors: Y_2O_3 and ZrO_2
 2. Mixing in the appropriate ratio (8% Y_2O_3 and 92% ZrO_2 on molar basis, V stands for oxygen vacancies due to charge imbalance)



3. Increase the temperature to 1400-1500C



Y_2O_3



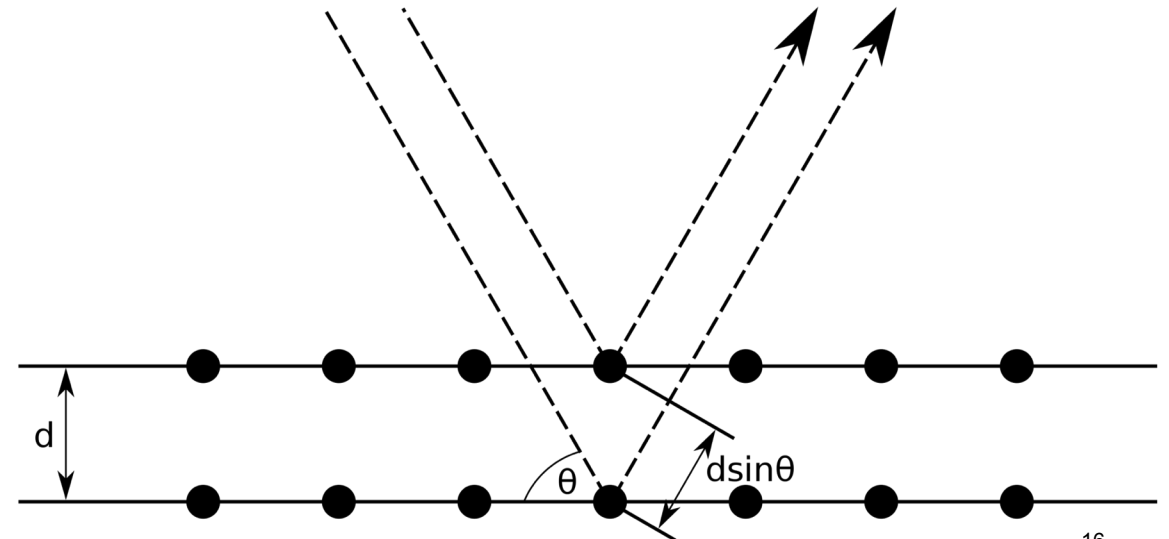
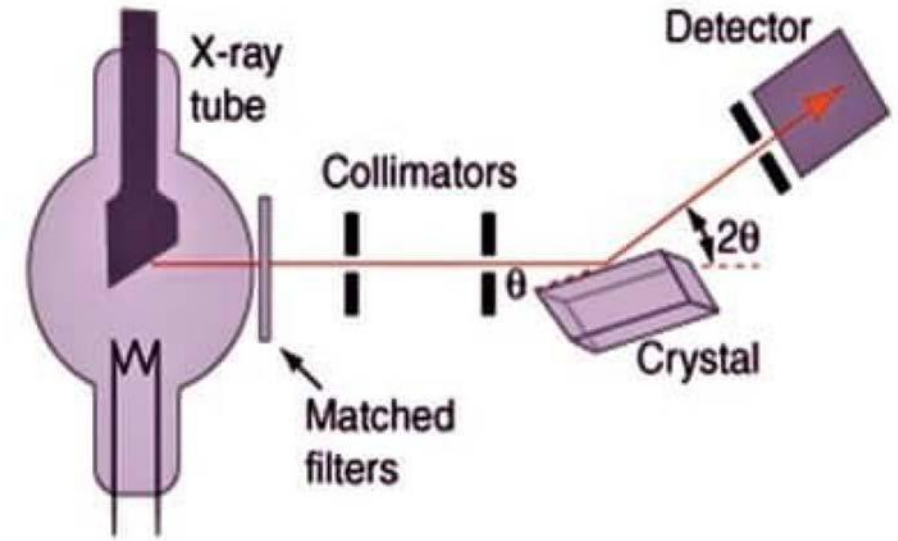
ZrO_2



$\text{Zr}_{0.92}\text{Y}_{0.16}\text{O}_{2.08}\text{V}_{0.08}$

How do we know if a material is synthesized as expected?

- X-Ray Diffraction (XRD)
- XRD allows identification of the phases that exist in the bulk of the material
- Similarly to humans, XRD provides a pattern that is the “DNA” of the material
- Operating Principle:
 1. X-ray's bombard a sample under a specific angle
 2. Electrons are scattered
 3. A detector measures the number of electrons scattered as the angle changes
- Bragg's law: $2d \sin\theta = n\lambda$
 - d : distance between 2 planes
 - θ : incident angle
 - λ : wavelength of the incident wave
 - n : positive integer



Examples of XRD patterns of materials synthesized using the solid-state method

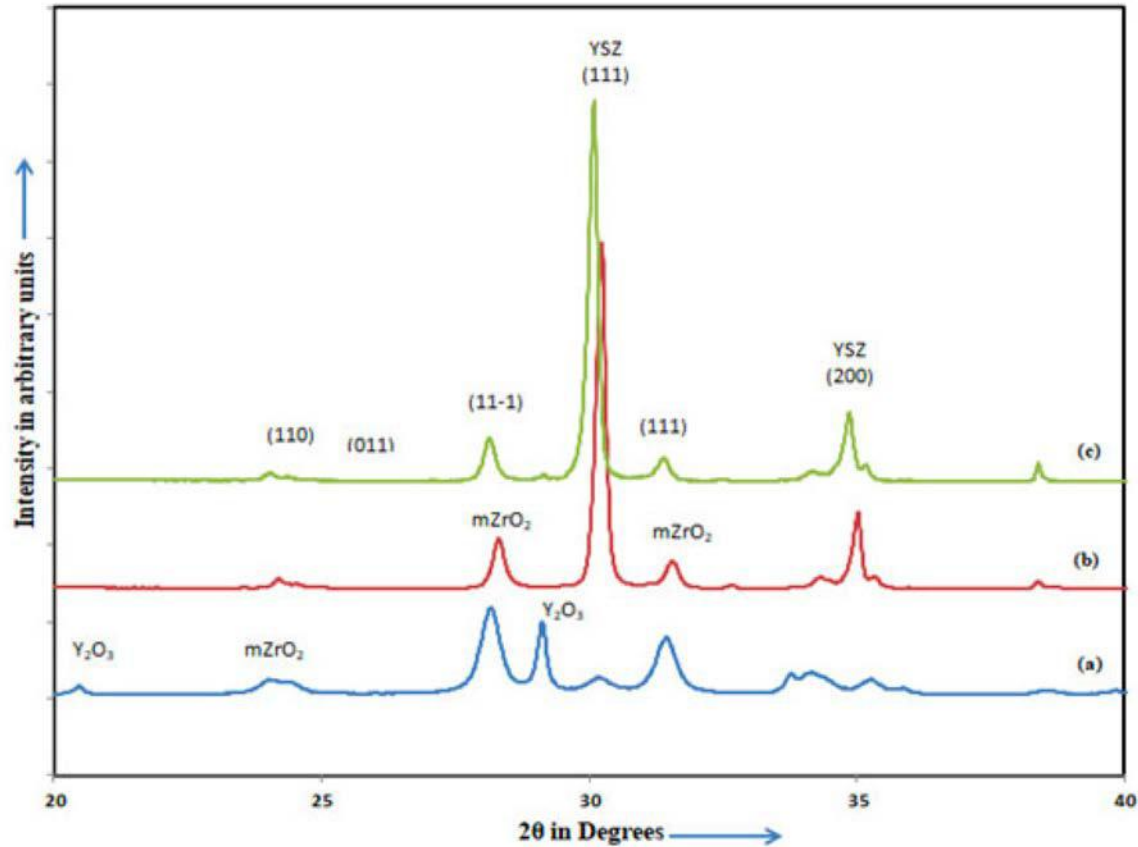
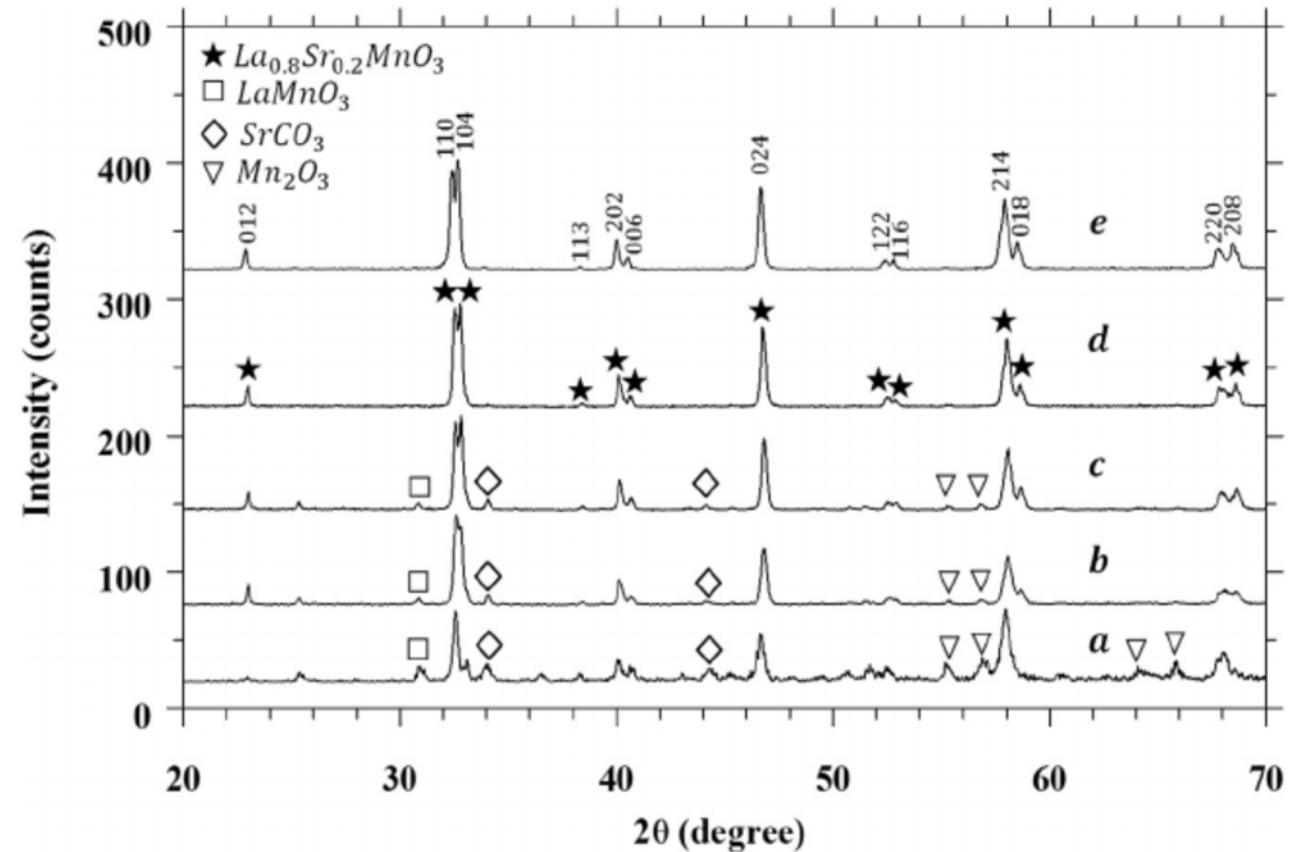


Figure 1: XRD of $(\text{Zr}_{0.92}\text{Y}_{0.08})_{1.00}\text{Ti}_{0.00}\text{O}_2$ (a) precursor (uncalcined product) (b) conventionally sintered at 1400°C for 10 hr (c) microwave sintered at 1400°C for 40 min

© Oriental Journal of Chemistry. All rights reserved. This content is excluded from our Creative Commons license. For more information, see <https://ocw.mit.edu/fairuse>.



X-ray diffraction (XRD) patterns of 20-hour milled powder, followed by heat treatment at (a) 700°C for 1 hour, (b) 700°C for 5 h, (c) 700°C for 10 h, (d) 800°C for 1 h, (e) 800°C for 5 h.

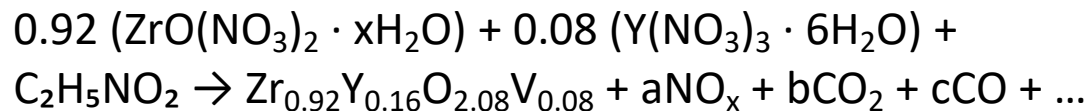
Courtesy Elsevier, Inc., <http://www.sciencedirect.com>. Used with permission.

Dry vs. wet synthesis methods

- Dry methods: manual mixing of powder precursors
- Wet methods: use precursors diluted in H₂O plus a chelating agent to bring cations closer
- Advantages of wet methods
 1. Better control of stoichiometry
 2. Better mixing
 3. Lower calcination temperature
 4. Less contaminations

Example: synthesis of 8-YSZ using a wet method

1. Precursors: Y(NO₃)₃ · 6H₂O and ZrO(NO₃)₂ · xH₂O
2. Use citric acid, EDTA, glycine as a chelating agent



3. Dilute these in purified H₂O and then dehydrate the solution
4. Calcination of the ash at high temperature

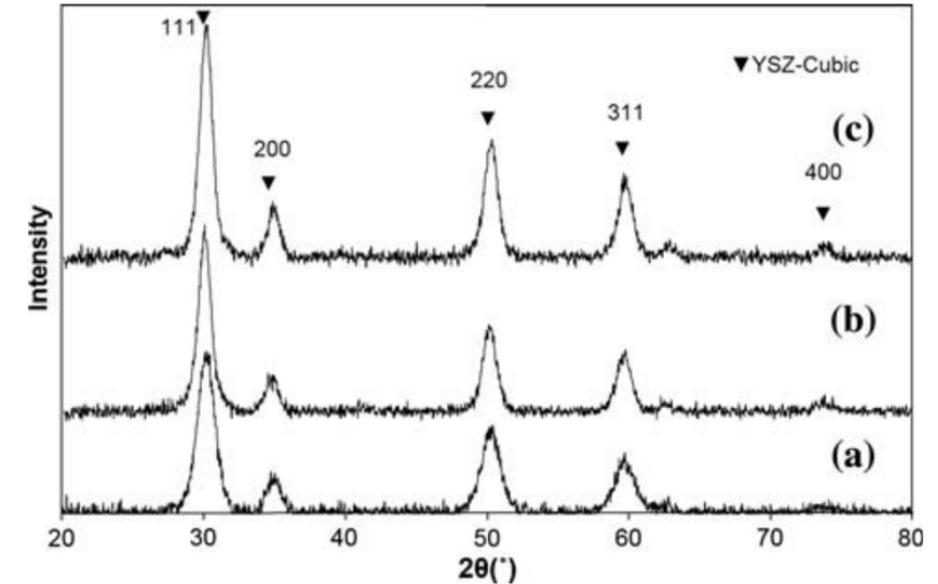


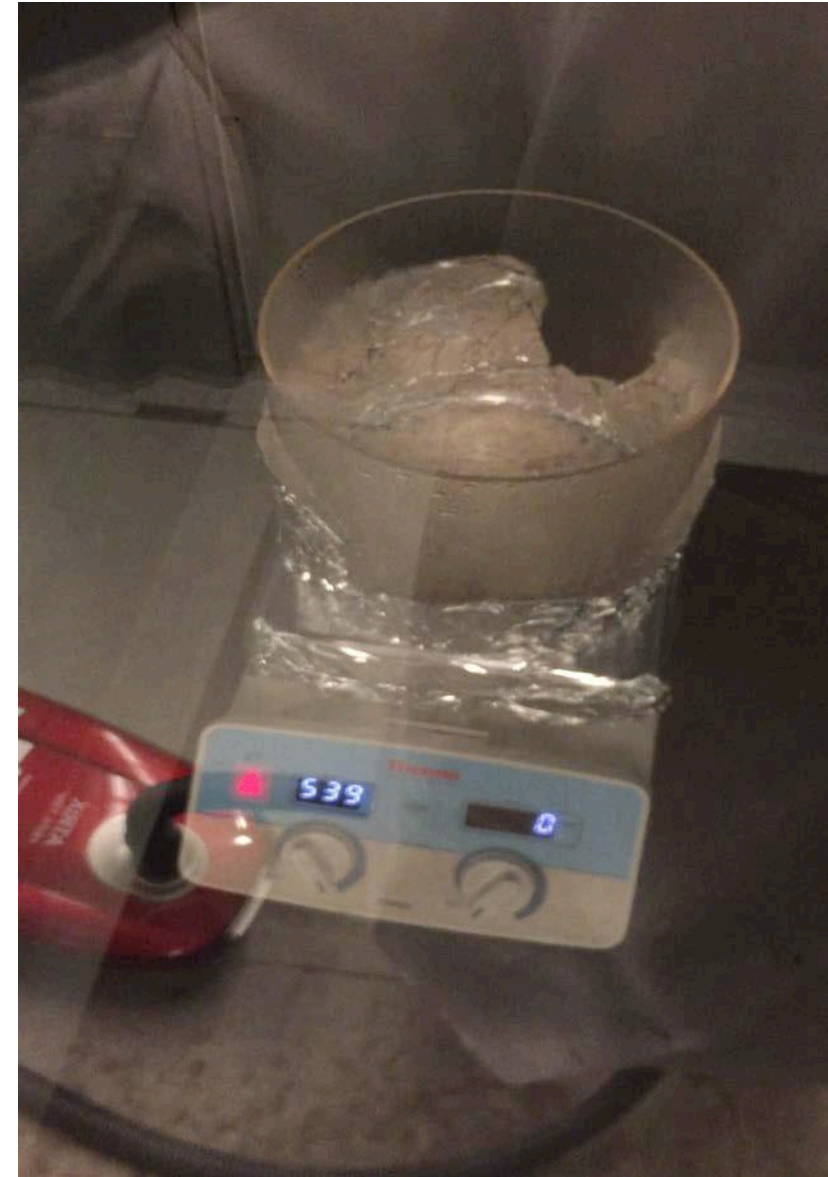
Fig. 6 X-ray diffraction patterns of the YSZ powders prepared from dried gel calcined at **a** 650 °C/2 h, **b** 730 °C/2 h and **c** 800 °C/2 h

© Springer Nature Switzerland AG. All rights reserved. This content is excluded from our Creative Commons license. For more information, see <https://ocw.mit.edu/fairuse>.

- Wet synthesis using Citric Acid and Ethylene Glycol
- YSZ synthesized at 650C!!
- Compare that to the solid state method, which requires calcination temperatures ~1400C!

An example of a wet synthesis method in Prof. Ghoniem's lab

- **Important: do not try this at home!!**
- Materials are synthesized in this way using proper equipment and safety measures
- Synthesis of LSM using glycine as the chelating agent
- First, precursors are mixed to create an aqueous solution
- Then, the mixture is placed on a hot plate (540C) to evaporate the H₂O and combust the mixture
- When most of H₂O has evaporated, autoignition of the solid mixture happens instantaneously (note the flame front)
- Also note:
 - Aqueous solution is white
 - LSM powder (raw ash) is black
- To obtain LSM, the raw ash is collected and calcined at high T (800C, 1h)



Example: synthesis of $\text{La}_{0.8}\text{Sr}_{0.2}\text{CrO}_{3-\delta}$ (LSCr)

- LSCr is used in SOFCs as an interconnect material or as an electrode
- Adjusting the pH of the aqueous precursor solution and the amount of Glycine changes the powder morphology and size
- If a dense material is required, options (a) and (c) are the best
- If a porous material is required, the rest of the options are viable
- To choose the best one, one has to measure the surface area of the material
- Surface area: Brunauer–Emmett–Teller (BET) method

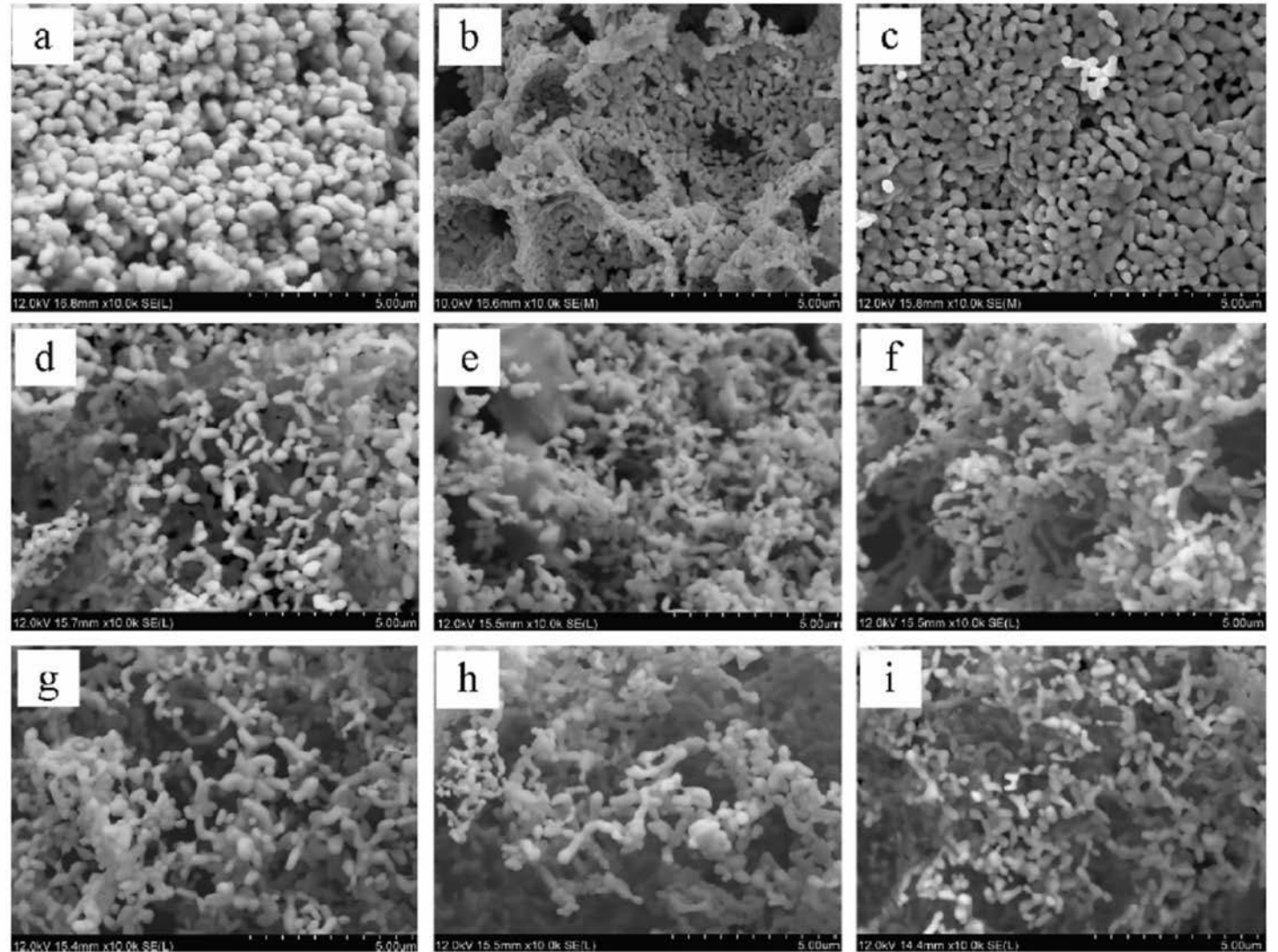


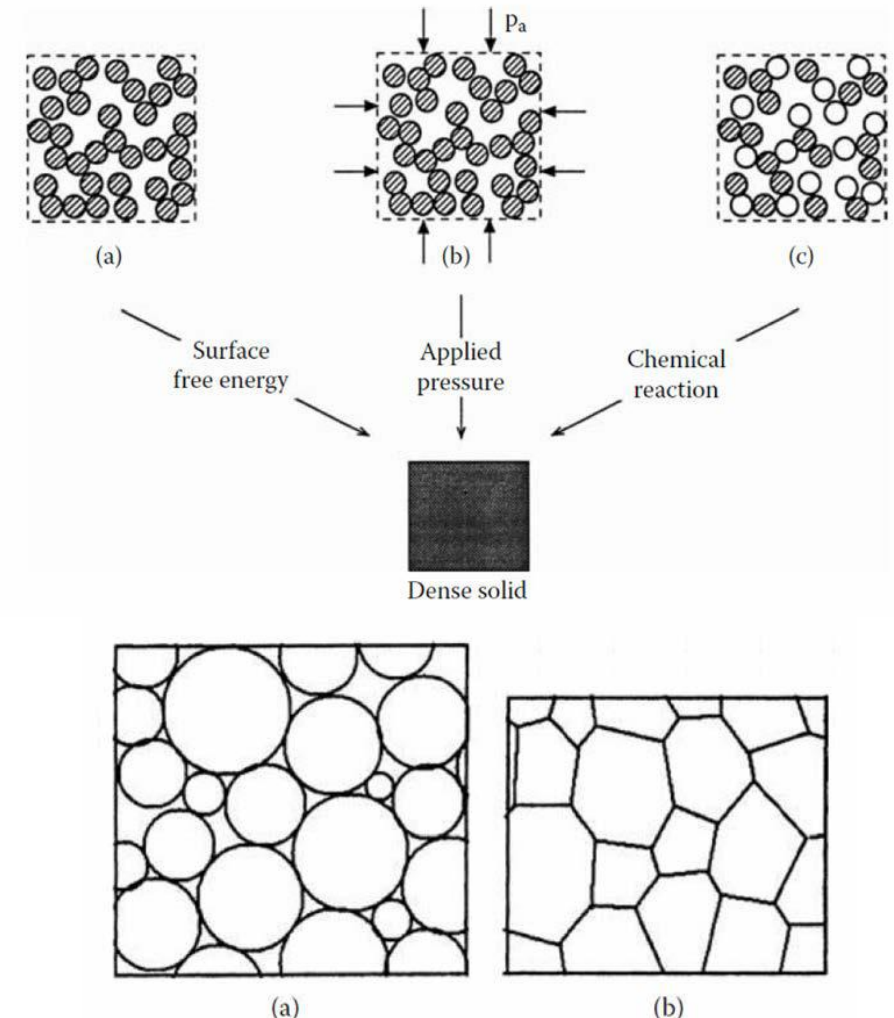
Fig. 5. SEM photographs of $\text{La}_{0.8}\text{Sr}_{0.2}\text{CrO}_3$ powders calcined at 1000 °C with various pH values and glycine-to-nitrate ratios. (a) pH = 3, 1:1 (b) pH = 2, 1:1 (c) pH = 1, 1:1 (d) pH = 3, 1.5:1 (e) pH = 2, 1.5:1 (f) pH = 1, 1.5:1 (g) pH = 3, 2:1 (h) pH = 2, 2:1 (i) pH = 1, 2:1.

Courtesy Elsevier, Inc., <http://www.sciencedirect.com>. Used with permission.

Sintering of ceramics

- To create a useful part, the powder has to be shaped using an appropriate method.
- To achieve high densification of a ceramic part, sintering at high temperatures is required (1200C-1600C depending on the material)
- **Sintering of the part is a major challenge because:**
 1. The material shrinks during the sintering process
 2. Properties of the material depend highly on the microstructure and gran/grain boundary distribution!
- Parameters that affect the sintering of ceramics:
 1. Surface free energy: curvature of particles provides a driving force for densification in order to decrease the surface free energy
 2. Applied pressure: bring particles together while minimizing gaps (can be done before or during the sintering process)
 3. Chemical reaction: change the gaseous environment to make it react with the solid (not frequently employed because the material's microstructure cannot be easily controlled)

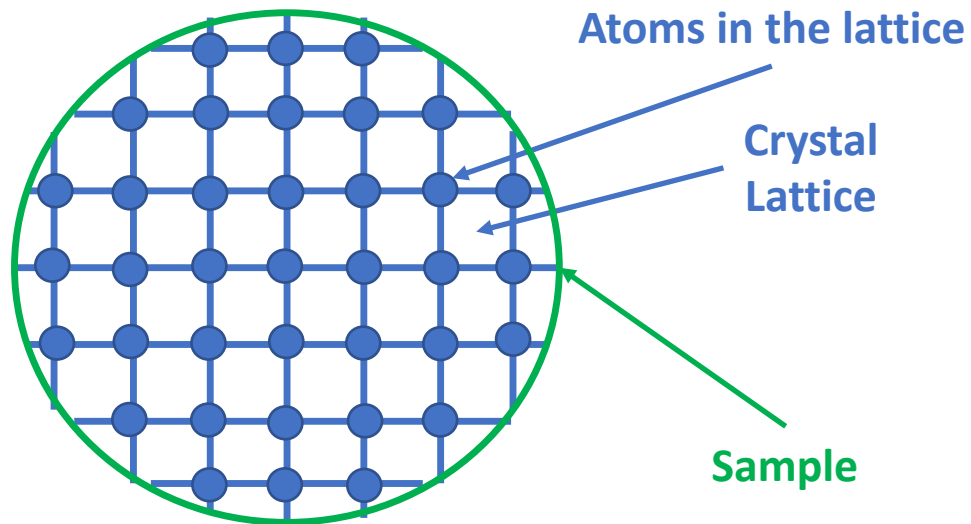
Driving forces leading to sintering of ceramics



Replacement of free surfaces (a) by grain boundaries (b) during the densification of polycrystalline systems.

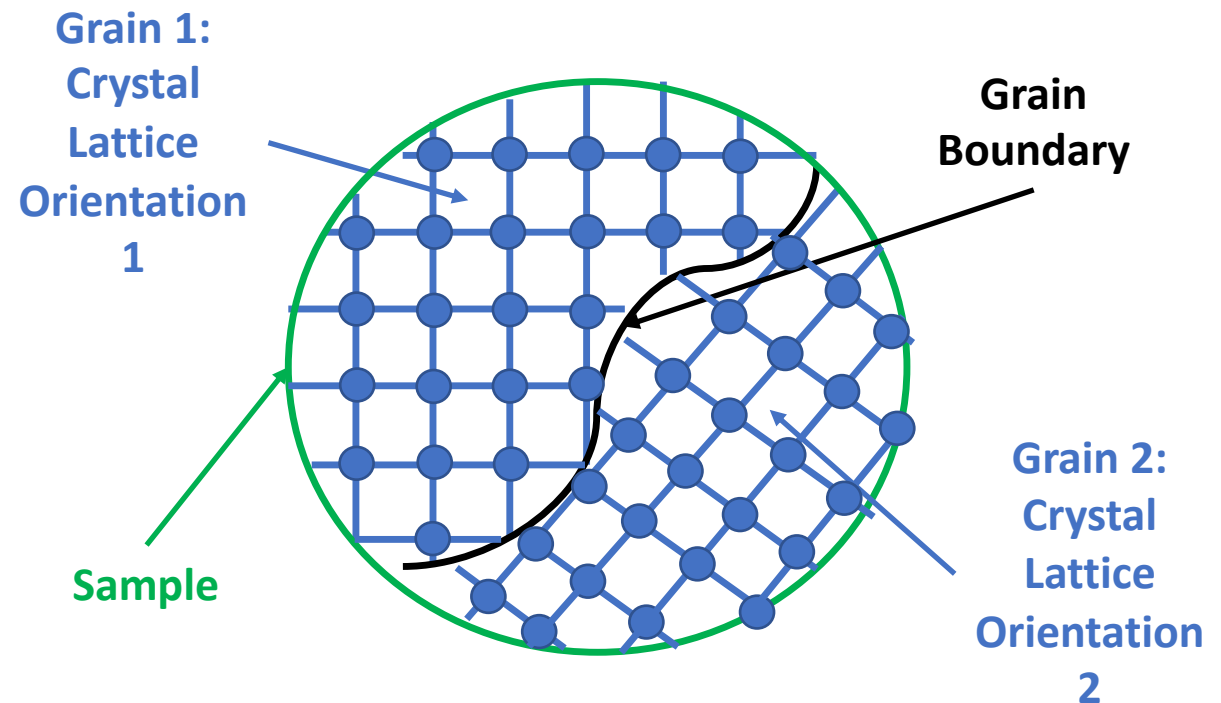
What is a grain boundary???

- Grain boundaries are 2D defects
- They are internal boundaries inside a crystal
- Lattice orientation changes on the grain boundary



Single crystal: **lattice orientation** is the **same** throughout the material

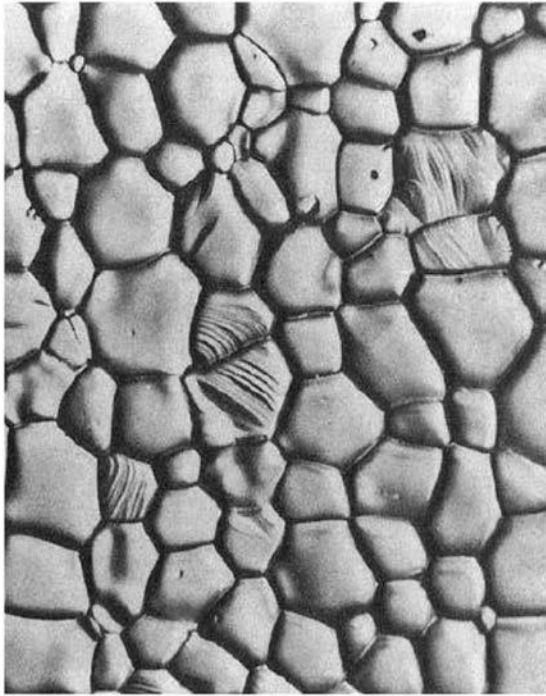
Same lattice – different orientation!!



Polycrystalline material: **lattice orientation** is **different** throughout the material

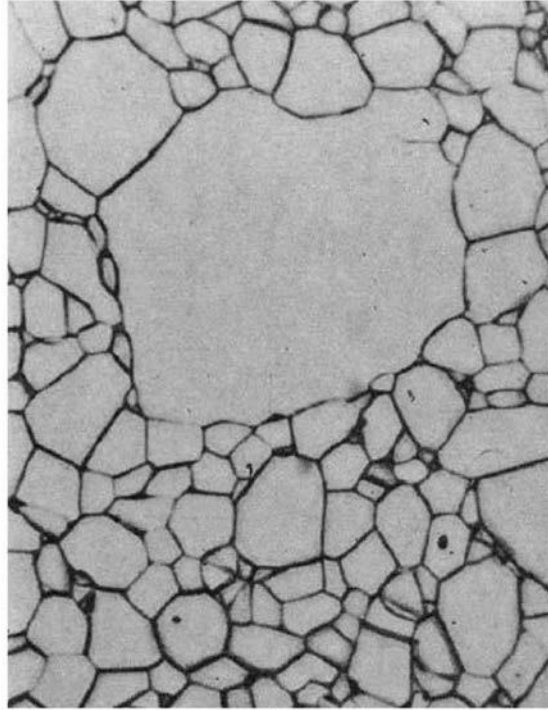
Example 1: Normal vs. Abnormal Grain Growth

Normal



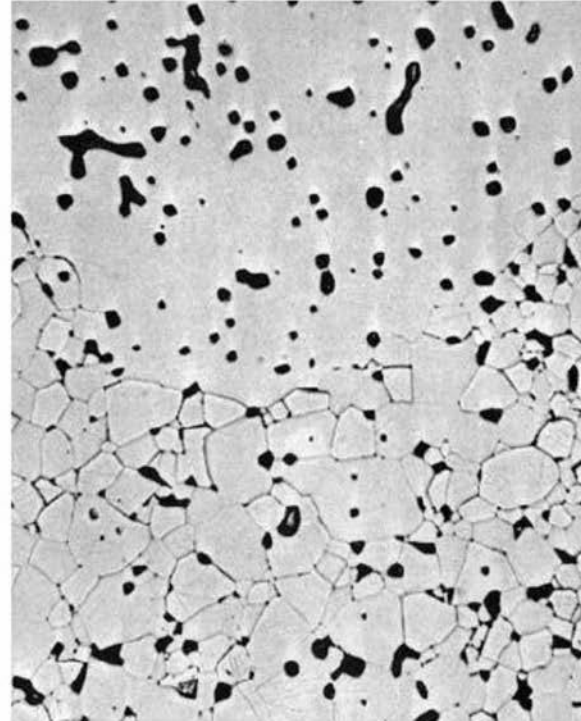
(a)

Abnormal



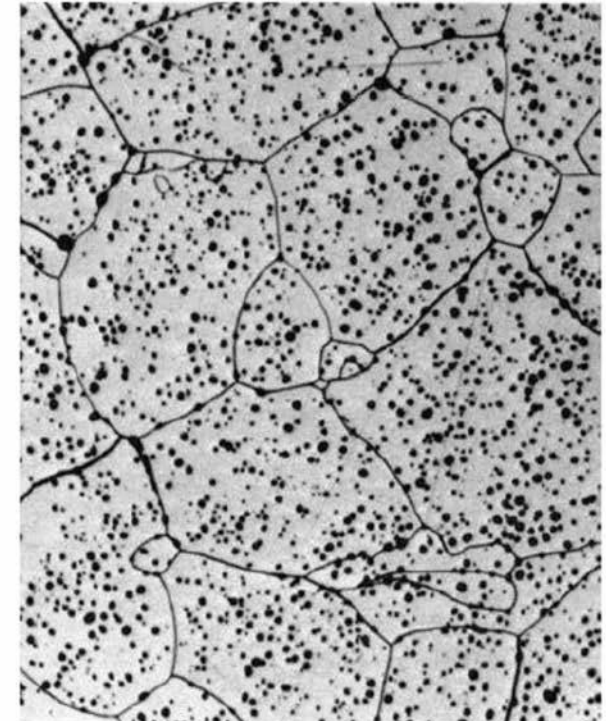
(b)

Abnormal



(c)

Abnormal

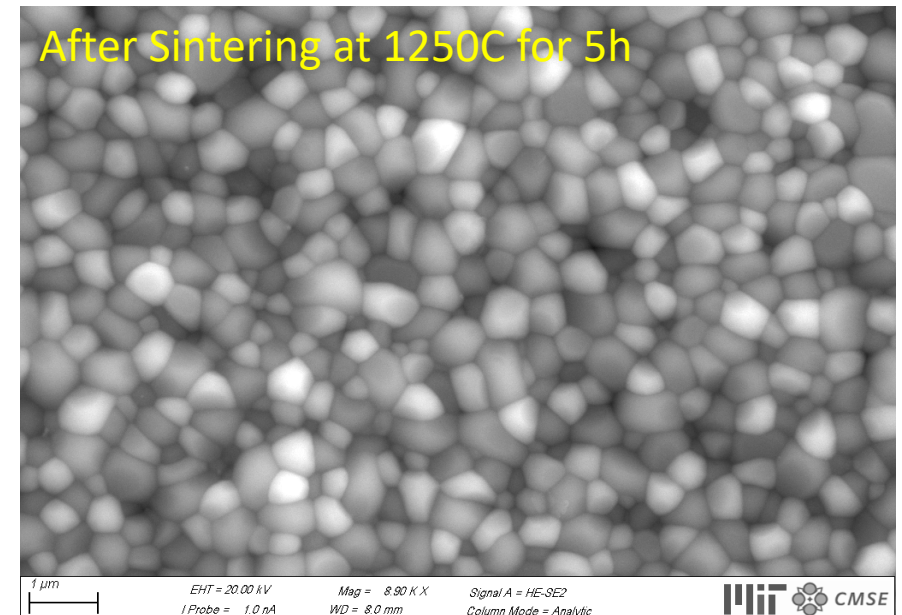
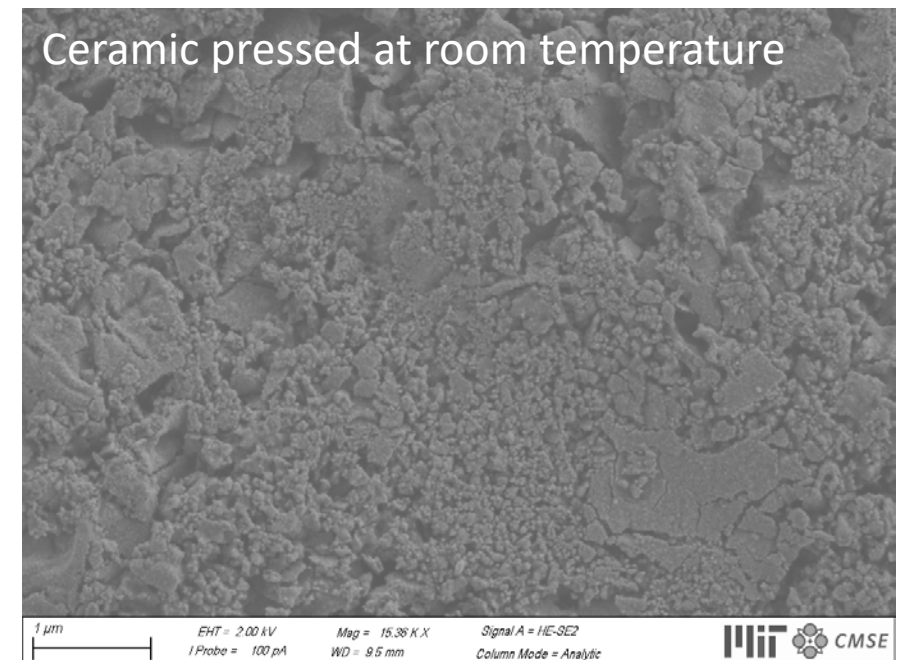


(d)

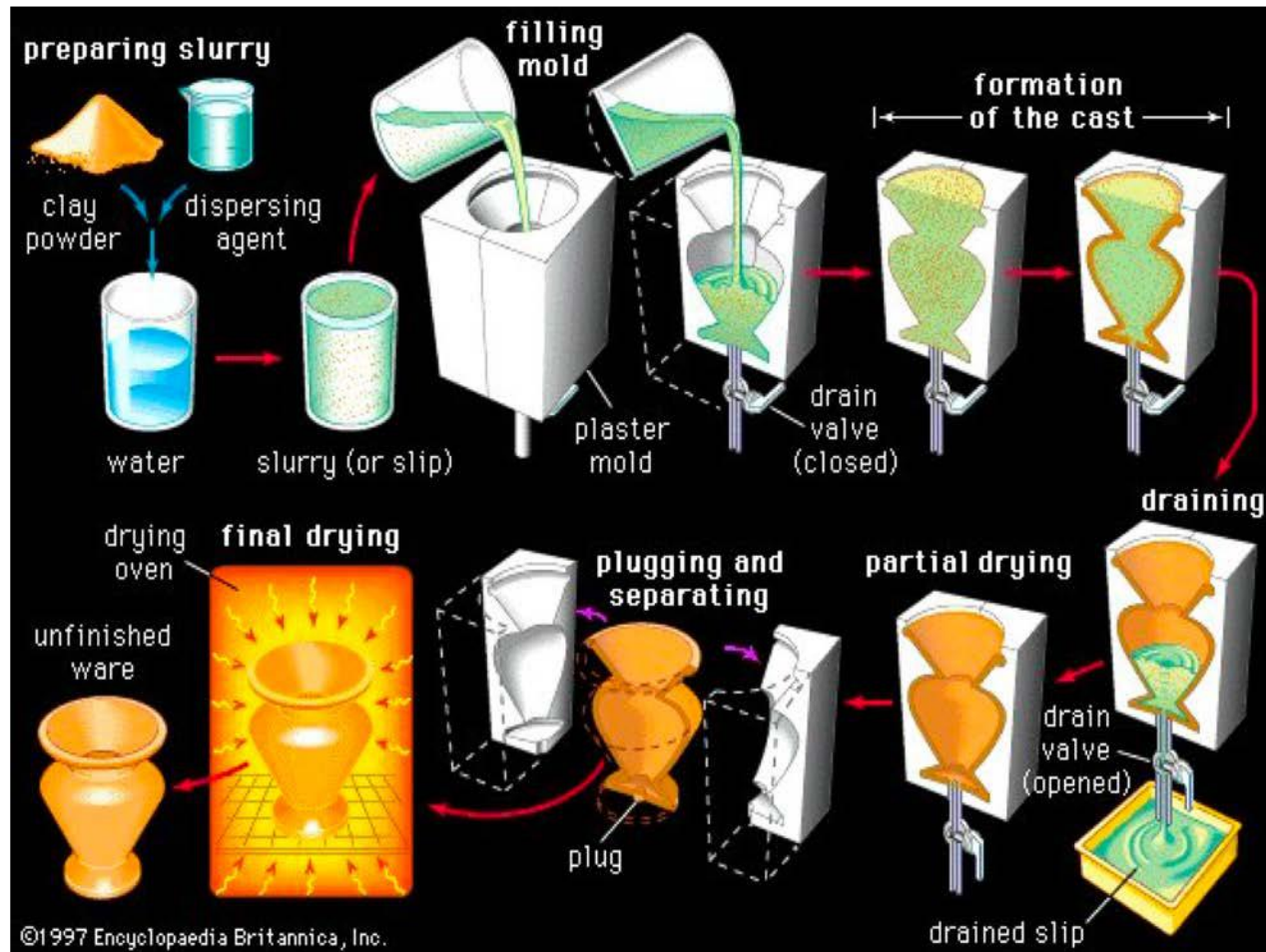
- Abnormal grain growth should be avoided
- It affects the density and the properties of the materials

Shaping of the powder into a useful part

- For dense ceramic oxides, several shaping methods exist:
 1. Casting (industrial scale)
 2. Uniaxial/Isostatic cold/warm pressing (lab scale)
 3. Tape casting (industrial scale – thin flat plates)
 4. Phase inversion method (industrial scale)
 5. Laser sintering (still in lab scale)
 6. Additive manufacturing (early stages, few materials)
- There are 2 methods frequently employed:
 1. Shaping of the powder at room temperature followed by sintering at high temperature
 2. Simultaneous shaping and sintering at high temperatures
- Machining of ceramic oxides using conventional techniques is usually avoided because ceramic oxides are very brittle.



Casting (industrial scale)



Casting of Ceramics

© Encyclopedia Britannica, Inc. All rights reserved. This content is excluded from our Creative Commons license. For more information, see <https://ocw.mit.edu/fairuse>.



Aluminum Oxide (Al₂O₃) Tubes

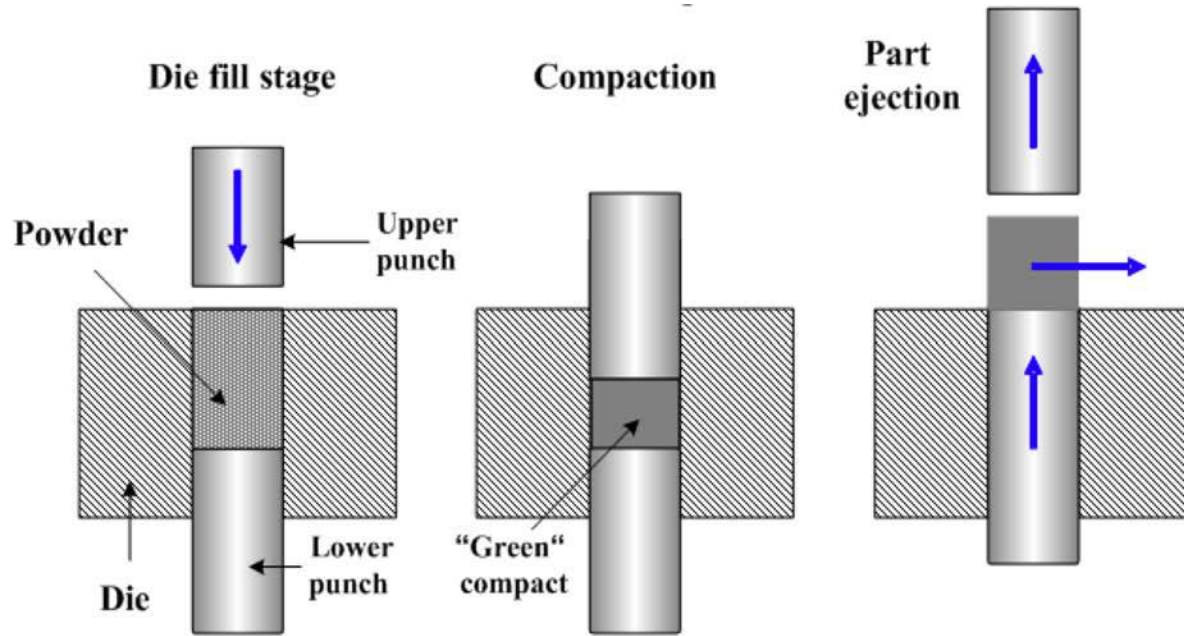
© LSP Industrial Ceramics, Inc. All rights reserved. This content is excluded from our Creative Commons license. For more information, see <https://ocw.mit.edu/fairuse>.



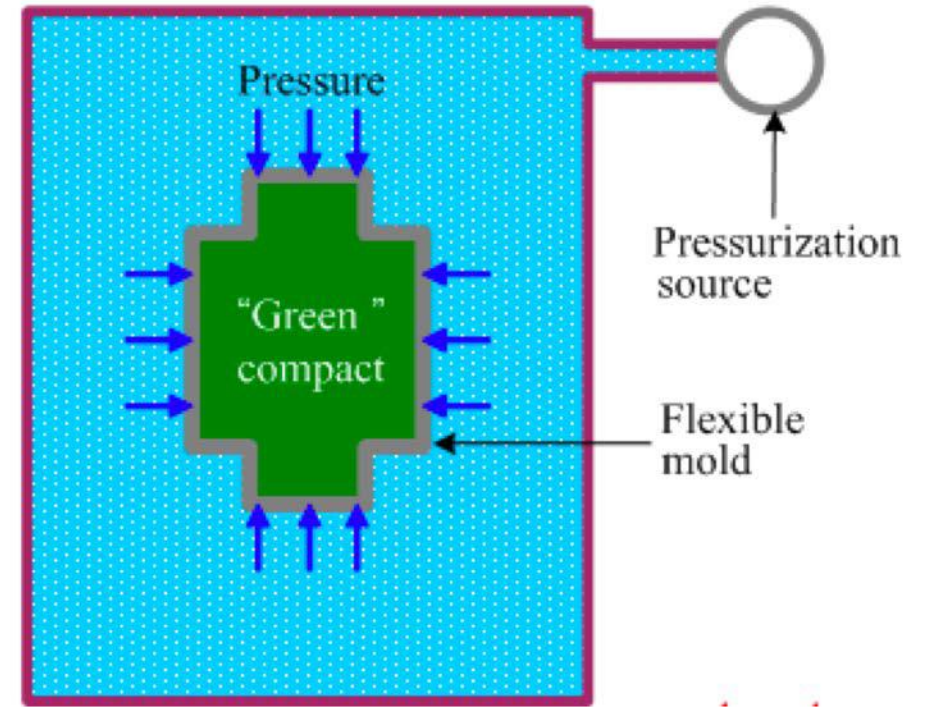
Gas Turbine Blade

© YXLON. All rights reserved. This content is excluded from our Creative Commons license. For more information, see <https://ocw.mit.edu/fairuse>.

Uniaxial/isostatic, cold/warm pressing



Cold uniaxial pressing

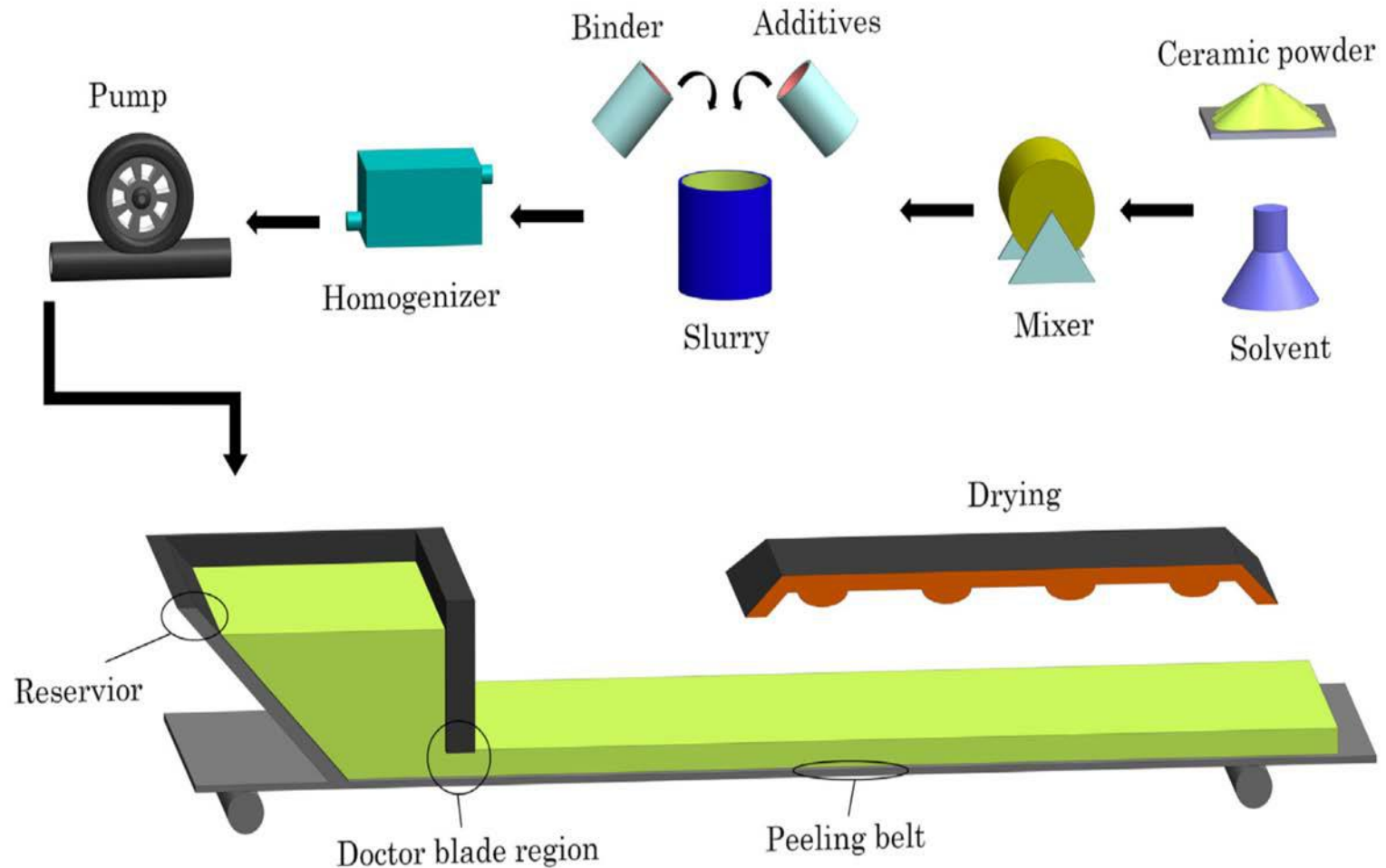


Cold isostatic pressing

- Cold pressing: compaction of powder at room temperature followed by sintering at high temperatures
- Warm pressing: compaction of powder and sintering at the same time













Tape casting

- Tape casting can only produce ceramics in the form of sheets
- Advantages:
 1. Most popular method of ceramic shaping in industry due to low cost
 2. Thickness of ceramics is low ($\sim 5\mu\text{m}$) and can be controlled by the doctor blade in a repetitive manner
 3. Ceramics with different layers can be made
- Disadvantages:
 1. the slurry includes the powder and additives (binder, plasticizer etc.) and the amount of each has to be optimized for each material based on trial and error and experience
 2. Drying and de-binding also has to be optimized
- Electrolytes are mainly fabricated through tape casting



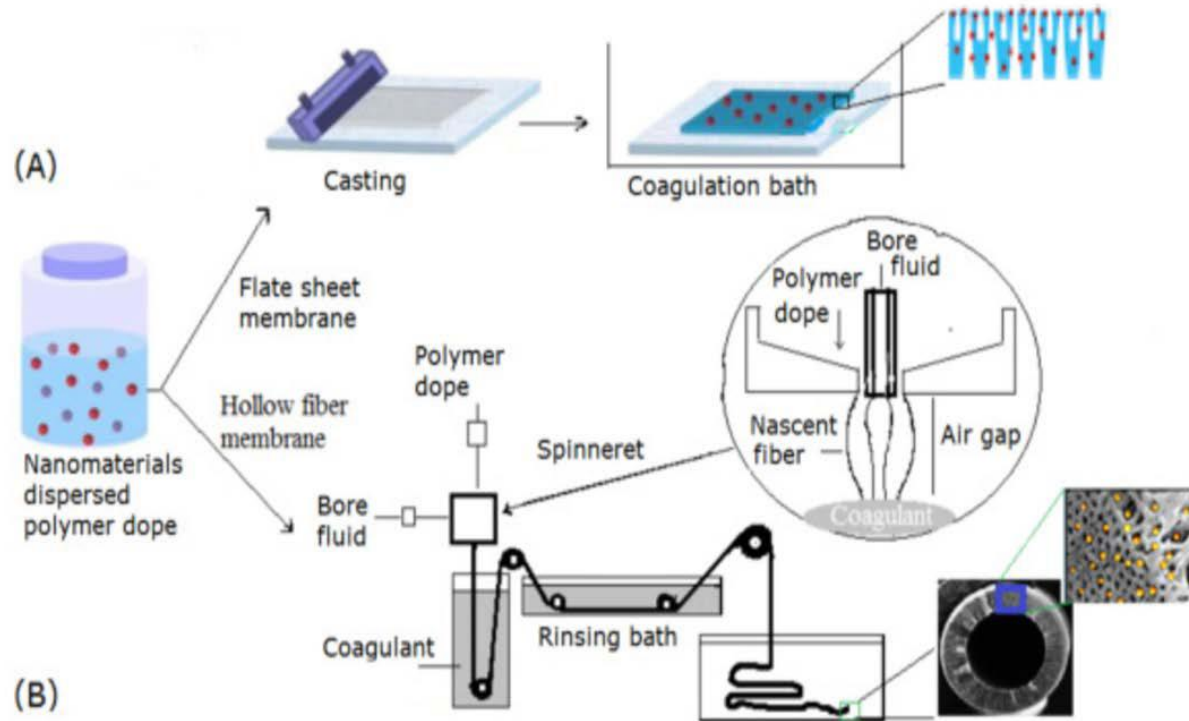
Courtesy Elsevier, Inc., <http://www.sciencedirect.com>. Used with permission.

Example: effect of slurry composition and thermal treatment on final ceramic

	Slurry 1	Slurry 2	Slurry 3	Slurry 4	Slurry 5
TT1					
TT2					
TT3					

© MDPI. All rights reserved. This content is excluded from our Creative Commons license. For more information, see <https://ocw.mit.edu/fairuse>.

Phase inversion

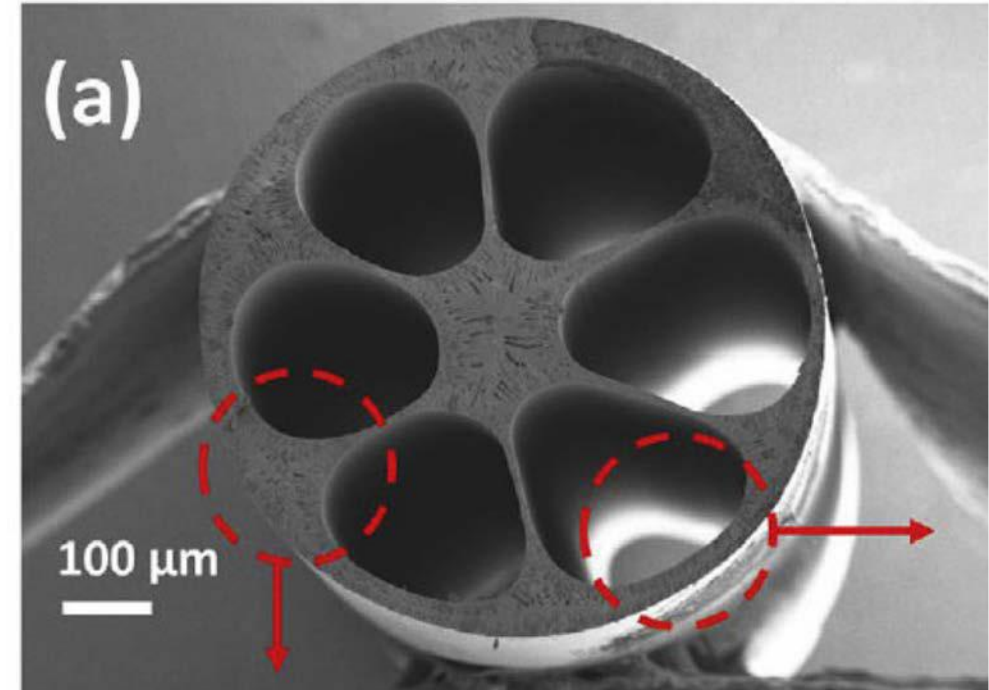


Courtesy Elsevier, Inc., <http://www.sciencedirect.com>. Used with permission.

Phase inversion is suitable for flat or tubular ceramics

Process:

1. Create a suspension of the material including additives
2. Cast the suspension using a blade
3. Immerse into a bath to enable coagulation



A $\text{La}_{0.6}\text{Sr}_{0.4}\text{Co}_{0.2}\text{Fe}_{0.8}\text{O}_{3-\delta}$ membrane used for O_2 separation from air made using the phase-inversion technique.

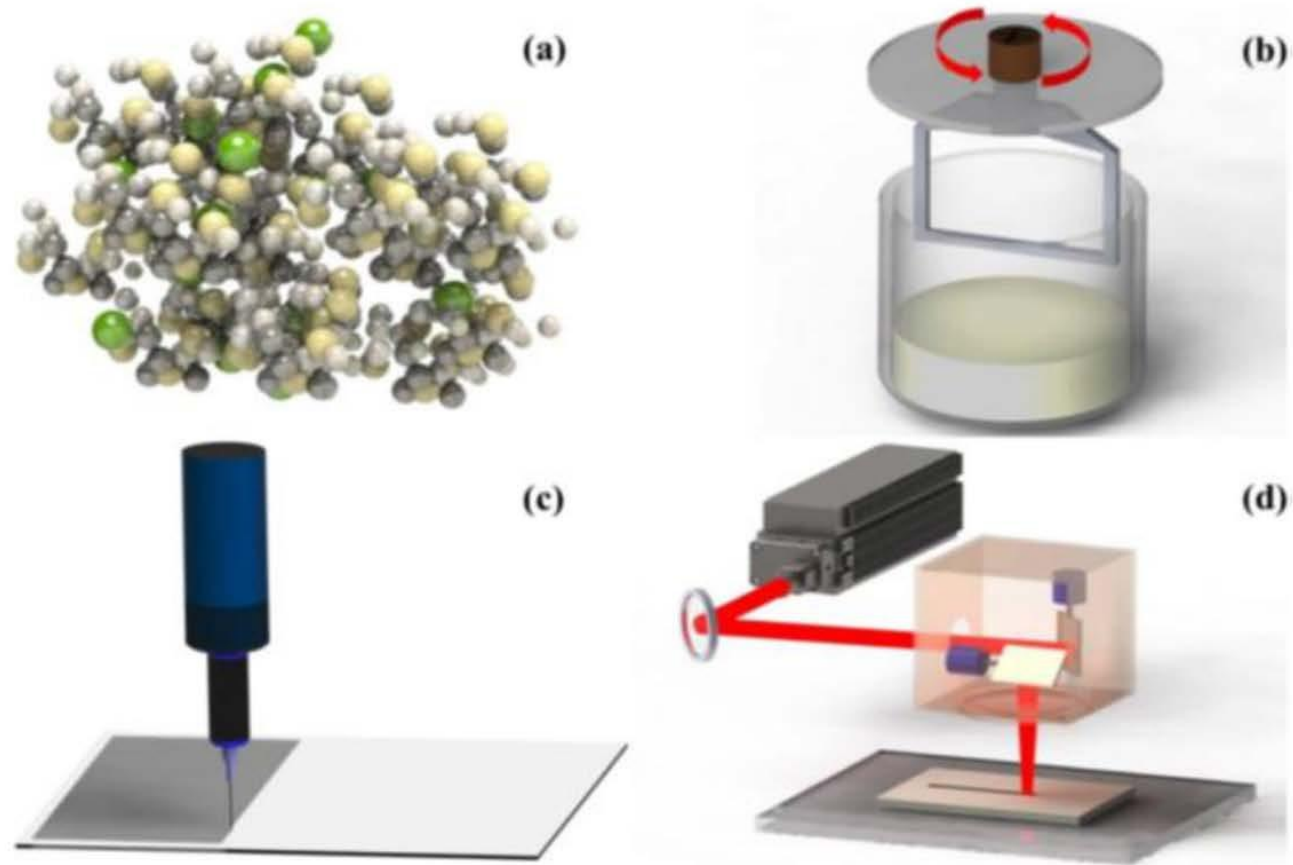
T. Li et. al. J. Membrane Science 578 (2019) 203-208

Phase inversion

YouTube screenshot has been removed due to copyright restrictions.
Please click the link below to see the video.

https://www.youtube.com/watch?v=WTrjqXbzhjE&feature=emb_logo

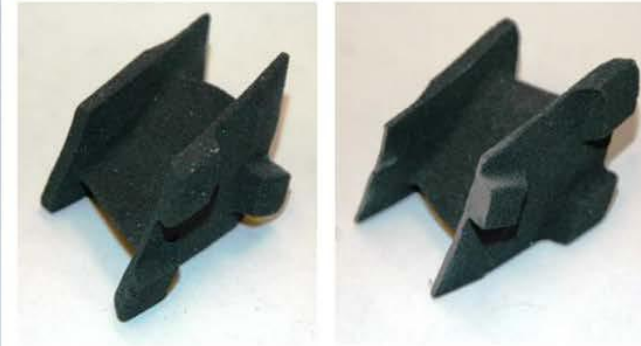
Rapid Laser Reactive Sintering



Schematic description of rapid laser reactive sintering (RLRS) process. (a) Mix precursor solids, (b) prepare precursor paste, (c) deposit precursor layer, and (d) perform RLRS

Courtesy Elsevier, Inc., <http://www.sciencedirect.com>. Used with permission.

Additive manufacturing of SiC turbine nozzle (still on its early stages)



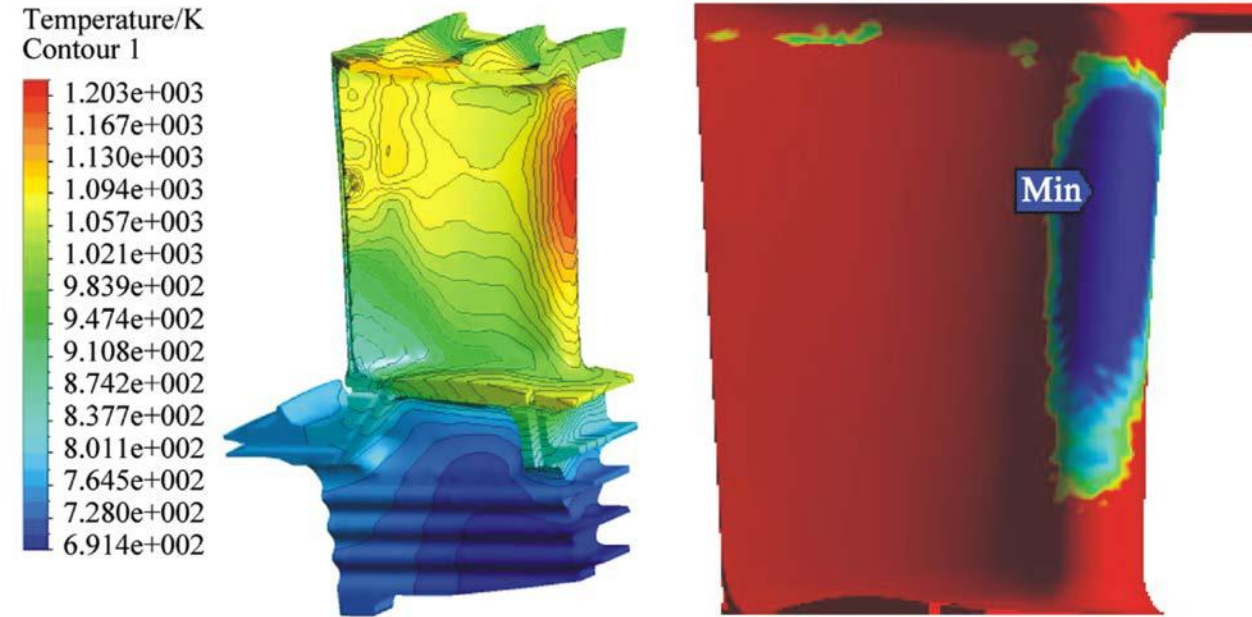
First stage nozzle segments.



© The American Ceramic Society. All rights reserved. This content is excluded from our Creative Commons license. For more information, see <https://ocw.mit.edu/fairuse>.

Computational methods in Material Science

- Given the availability of computational resources, the use of computational models for the prediction of material properties has increased during the last decades.
- Modeling is important because it allows to obtain information that we cannot extract directly through measurements.
- Models exist in all scales depending on the scientific/engineering question that needs to be answered.
- All models are based on assumptions!
- Each model has its own limitations depending on the scale it is formulated for!
- What is important is to know:
 1. The question you want to answer
 2. Which model will give an answer
 3. How fast and/or how accurate will the answer be



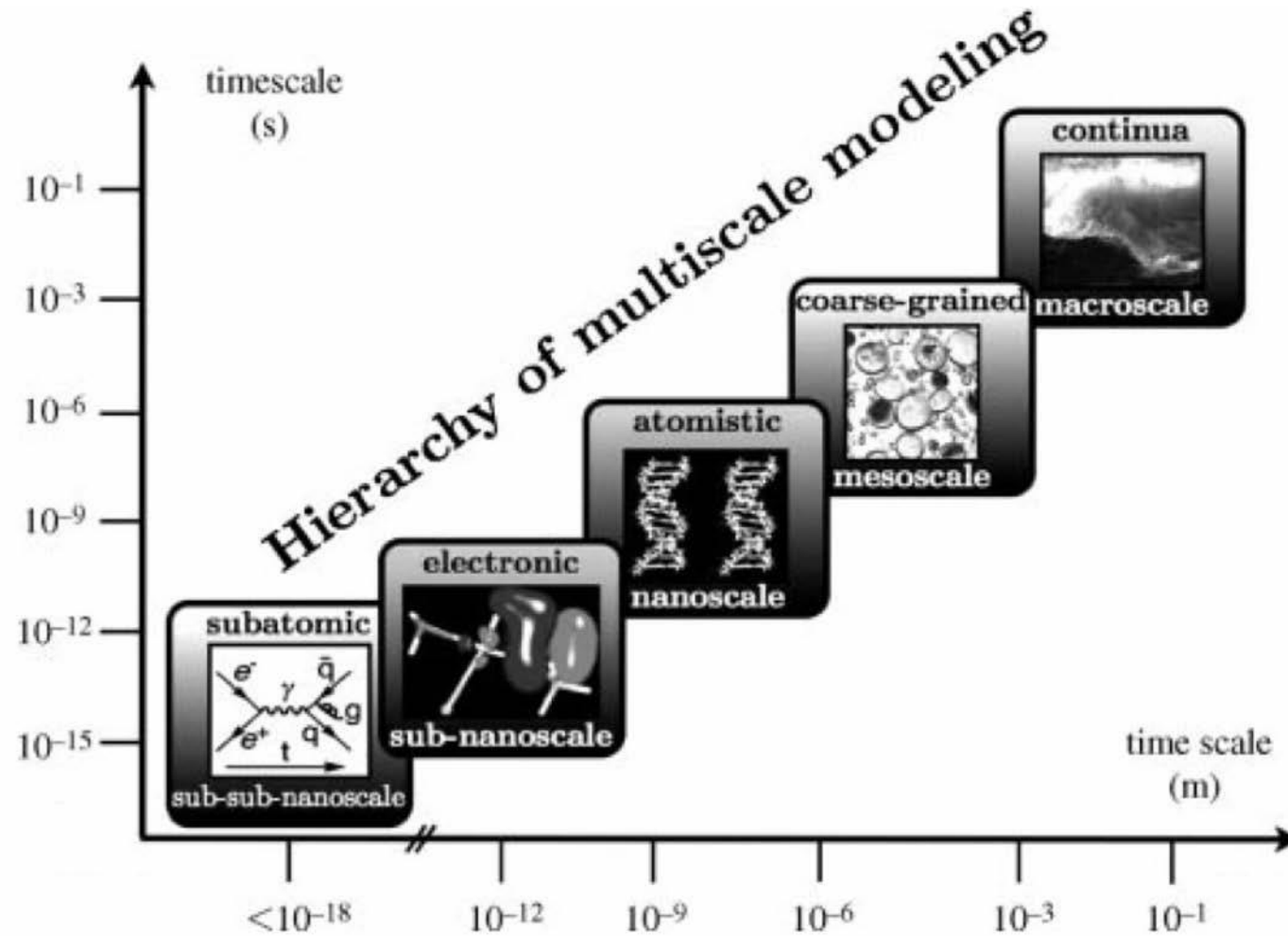
Temperature (left) and creep (right) profiles for a gas turbine blade

M.R. Reyhani et. al. Propulsion and Power Research 2013;2(2):148-161

Courtesy Elsevier, Inc., <http://www.sciencedirect.com>. Used with permission.

If the question is to understand the creep behavior, we will use a continuous model, i.e. we are not going to calculate creep induced by elements in the atomic scale, which will take forever!!

Computational methods depending on the scale of interest



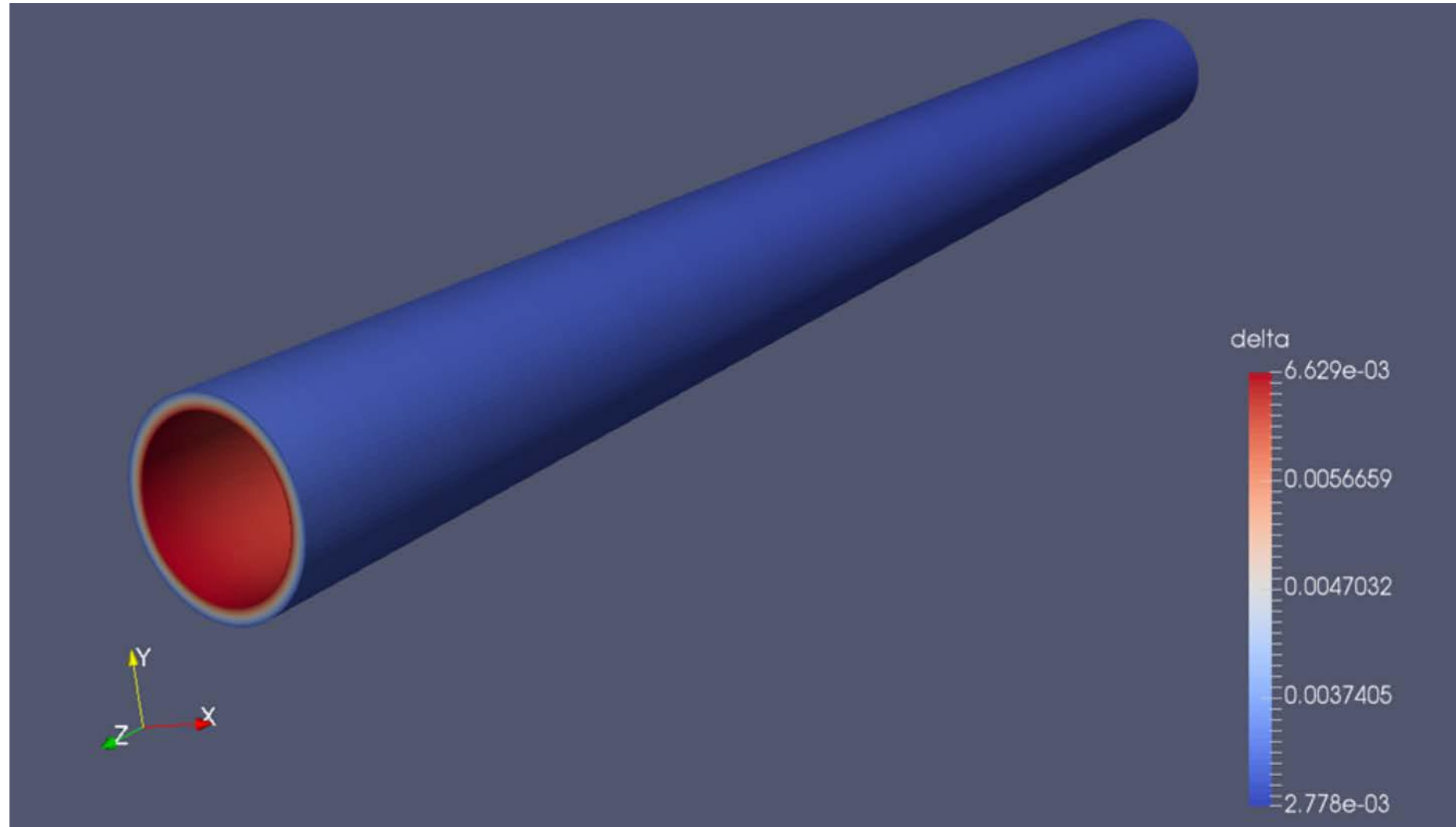
Mechanical Engineers

Material Scientists

Physicists

More detailed models take longer to run!!!

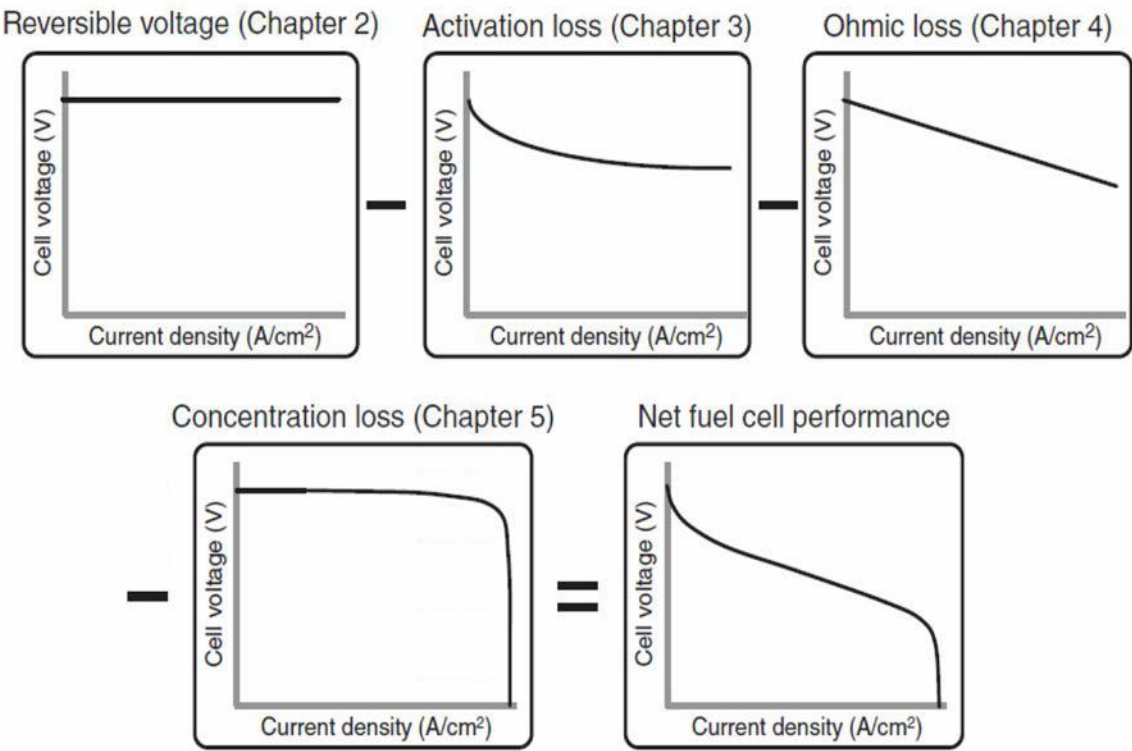
CFD models for design of reactors based on ceramic materials



Design of tubular ceramic membranes using state-of-the-art defect chemistry models

Micro-kinetic models for fuel cells

Simplified modeling of an I-V curve



$$V = E_{thermo} - \eta_{act} - \eta_{ohmic} - \eta_{conc}$$

© John Wiley & Sons, Inc. All rights reserved. This content is excluded from our Creative Commons license. For more information, see <https://ocw.mit.edu/fairuse>.

Heterogeneous reaction mechanism on Ni-based catalysts

	Reaction	A^a	n	E^a
1	$H_2 + (Ni) + (Ni) \rightarrow H(Ni) + H(Ni)$	$1.000 \cdot 10^{-02b}$	0.0	0.00
2	$H(Ni) + H(Ni) \rightarrow (Ni) + (Ni) + H_2$	$5.593 \cdot 10^{+19}$	0.0	88.12
3	$O_2 + (Ni) + (Ni) \rightarrow O(Ni) + O(Ni)$	$1.000 \cdot 10^{-02b}$	0.0	0.00
4	$O(Ni) + O(Ni) \rightarrow (Ni) + (Ni) + O_2$	$2.508 \cdot 10^{+23}$	0.0	470.39
5	$CH_4 + (Ni) \rightarrow CH_4(Ni)$	$8.000 \cdot 10^{-03b}$	0.0	0.00
6	$CH_4(Ni) \rightarrow (Ni) + CH_4$	$5.302 \cdot 10^{+15}$	0.0	33.15
7	$H_2O + (Ni) \rightarrow H_2O(Ni)$	$1.000 \cdot 10^{-01b}$	0.0	0.00
8	$H_2O(Ni) \rightarrow (Ni) + H_2O$	$4.579 \cdot 10^{+12}$	0.0	62.68
9	$CO_2 + (Ni) \rightarrow CO_2(Ni)$	$1.000 \cdot 10^{-05b}$	0.0	0.00
10	$CO_2(Ni) \rightarrow (Ni) + CO_2$	$9.334 \cdot 10^{+07}$	0.0	28.80
11	$CO + (Ni) \rightarrow CO(Ni)$	$5.000 \cdot 10^{-01b}$	0.0	0.00
12	$CO(Ni) \rightarrow (Ni) + CO$	$4.041 \cdot 10^{+11}$	0.0	112.85
	$\epsilon_{CO(s)}$			-50.0 ^c
13	$O(Ni) + H(Ni) \rightarrow OH(Ni) + (Ni)$	$5.000 \cdot 10^{+22}$	0.0	97.90
14	$OH(Ni) + (Ni) \rightarrow O(Ni) + H(Ni)$	$2.005 \cdot 10^{+21}$	0.0	37.19
15	$OH(Ni) + H(Ni) \rightarrow H_2O(Ni) + (Ni)$	$3.000 \cdot 10^{+20}$	0.0	42.70
16	$H_2O(Ni) + (Ni) \rightarrow OH(Ni) + H(Ni)$	$2.175 \cdot 10^{+21}$	0.0	91.36
17	$OH(Ni) + OH(Ni) \rightarrow O(Ni) + H_2O(Ni)$	$3.000 \cdot 10^{+21}$	0.0	100.00
18	$O(Ni) + H_2O(Ni) \rightarrow OH(Ni) + OH(Ni)$	$5.423 \cdot 10^{+23}$	0.0	209.37
19	$O(Ni) + C(Ni) \rightarrow CO(Ni) + (Ni)$	$5.200 \cdot 10^{+23}$	0.0	148.10
20	$CO(Ni) + (Ni) \rightarrow O(Ni) + C(Ni)$	$1.418 \cdot 10^{+22}$	-3.0	115.97
	$\epsilon_{CO(s)}$			-50.0 ^c
21	$O(Ni) + CO(Ni) \rightarrow CO_2(Ni) + (Ni)$	$2.000 \cdot 10^{+19}$	0.0	123.60
	$\epsilon_{CO(s)}$			-50.0 ^c
22	$CO_2(Ni) + (Ni) \rightarrow O(Ni) + CO(Ni)$	$3.214 \cdot 10^{+23}$	-1.0	86.50
23	$HCO(Ni) + (Ni) \rightarrow CO(Ni) + H(Ni)$	$3.700 \cdot 10^{+21}$	0.0	0.0
	$\epsilon_{CO(s)}$			50.0 ^c
24	$CO(Ni) + H(Ni) \rightarrow HCO(Ni) + (Ni)$	$2.338 \cdot 10^{+20}$	-1.0	127.98
25	$HCO(Ni) + (Ni) \rightarrow O(Ni) + CH(Ni)$	$3.700 \cdot 10^{+24}$	-3.0	95.80
26	$O(Ni) + CH(Ni) \rightarrow HCO(Ni) + (Ni)$	$7.914 \cdot 10^{+20}$	0.0	114.22
27	$CH_4(Ni) + (Ni) \rightarrow CH_3(Ni) + H(Ni)$	$3.700 \cdot 10^{+21}$	0.0	57.70
28	$CH_3(Ni) + H(Ni) \rightarrow CH_4(Ni) + (Ni)$	$4.438 \cdot 10^{+21}$	0.0	58.83
29	$CH_3(Ni) + (Ni) \rightarrow CH_2(Ni) + H(Ni)$	$3.700 \cdot 10^{+24}$	0.0	100.00
30	$CH_2(Ni) + H(Ni) \rightarrow CH_3(Ni) + (Ni)$	$9.513 \cdot 10^{+22}$	0.0	52.58
31	$CH_2(Ni) + (Ni) \rightarrow CH(Ni) + H(Ni)$	$3.700 \cdot 10^{+24}$	0.0	97.10
32	$CH(Ni) + H(Ni) \rightarrow CH_2(Ni) + (Ni)$	$3.008 \cdot 10^{+24}$	0.0	76.43
33	$CH(Ni) + (Ni) \rightarrow C(Ni) + H(Ni)$	$3.700 \cdot 10^{+21}$	0.0	18.80
34	$C(Ni) + H(Ni) \rightarrow CH(Ni) + (Ni)$	$4.400 \cdot 10^{+22}$	0.0	160.49
35	$O(Ni) + CH_4(Ni) \rightarrow CH_3(Ni) + OH(Ni)$	$1.700 \cdot 10^{+24}$	0.0	88.30
36	$CH_3(Ni) + OH(Ni) \rightarrow O(Ni) + CH_4(Ni)$	$8.178 \cdot 10^{+22}$	0.0	28.72
37	$O(Ni) + CH_3(Ni) \rightarrow CH_2(Ni) + OH(Ni)$	$3.700 \cdot 10^{+24}$	0.0	130.10
38	$CH_2(Ni) + OH(Ni) \rightarrow O(Ni) + CH_3(Ni)$	$3.815 \cdot 10^{+21}$	0.0	21.97
39	$O(Ni) + CH_2(Ni) \rightarrow CH(Ni) + OH(Ni)$	$3.700 \cdot 10^{+24}$	0.0	126.80
40	$CH(Ni) + OH(Ni) \rightarrow O(Ni) + CH_2(Ni)$	$1.206 \cdot 10^{+23}$	0.0	45.42
41	$O(Ni) + CH(Ni) \rightarrow C(Ni) + OH(Ni)$	$3.700 \cdot 10^{+21}$	0.0	48.10
42	$C(Ni) + OH(Ni) \rightarrow O(Ni) + CH(Ni)$	$1.764 \cdot 10^{+21}$	0.0	129.08

© The Electrochemical Society. All rights reserved. This content is excluded from our Creative Commons license. For more information, see <https://ocw.mit.edu/fairuse>.

Density Functional Theory (DFT)

- In DFT, one solves for the so-called Kohn-Sham equations (not the Schrödinger equation):

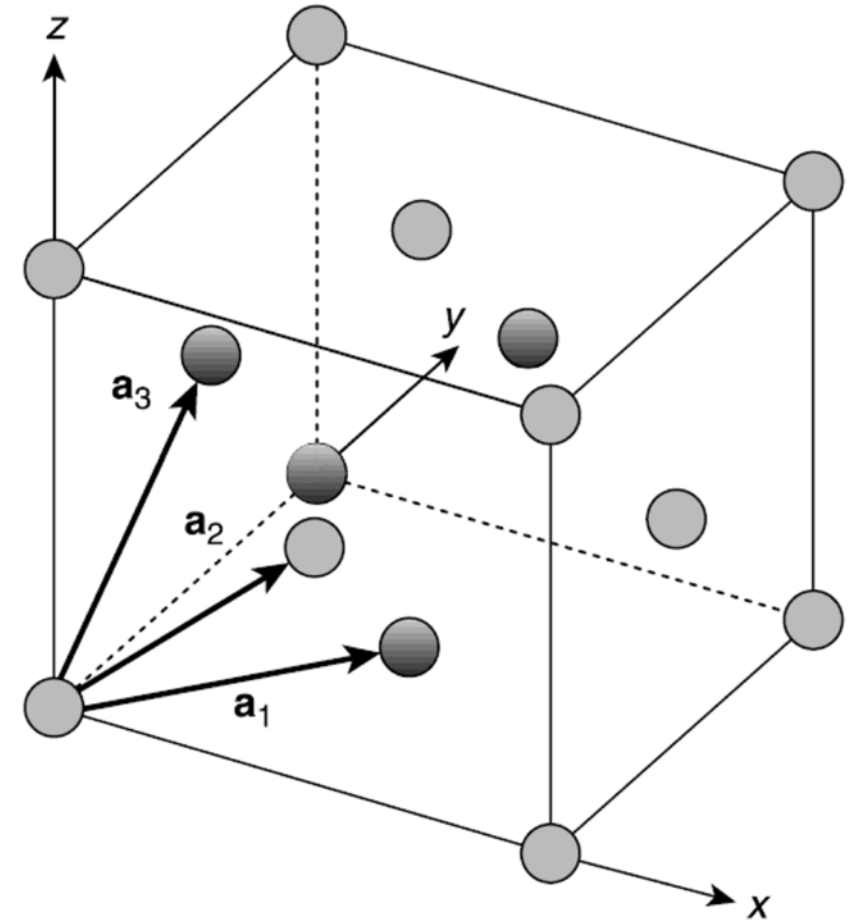
$$\left[-\frac{\hbar^2}{2m} \nabla^2 + V(\mathbf{r}) + V_H(\mathbf{r}) + V_{XC}(\mathbf{r}) \right] \psi_i(\mathbf{r}) = \varepsilon_i \psi_i(\mathbf{r}) \quad (1)$$

Electron Kinetic Energy	Electron- Nuclei Interaction	Electron- Electron Interaction	Exchange- Correlation Functional
-------------------------------	------------------------------------	--------------------------------------	--

- V_H and V_{XC} are a function of the electron density $n(\mathbf{r})$:

$$n(\mathbf{r}) = 2 \sum_i \psi_i^*(\mathbf{r}) \psi_i(\mathbf{r}) \quad (2)$$

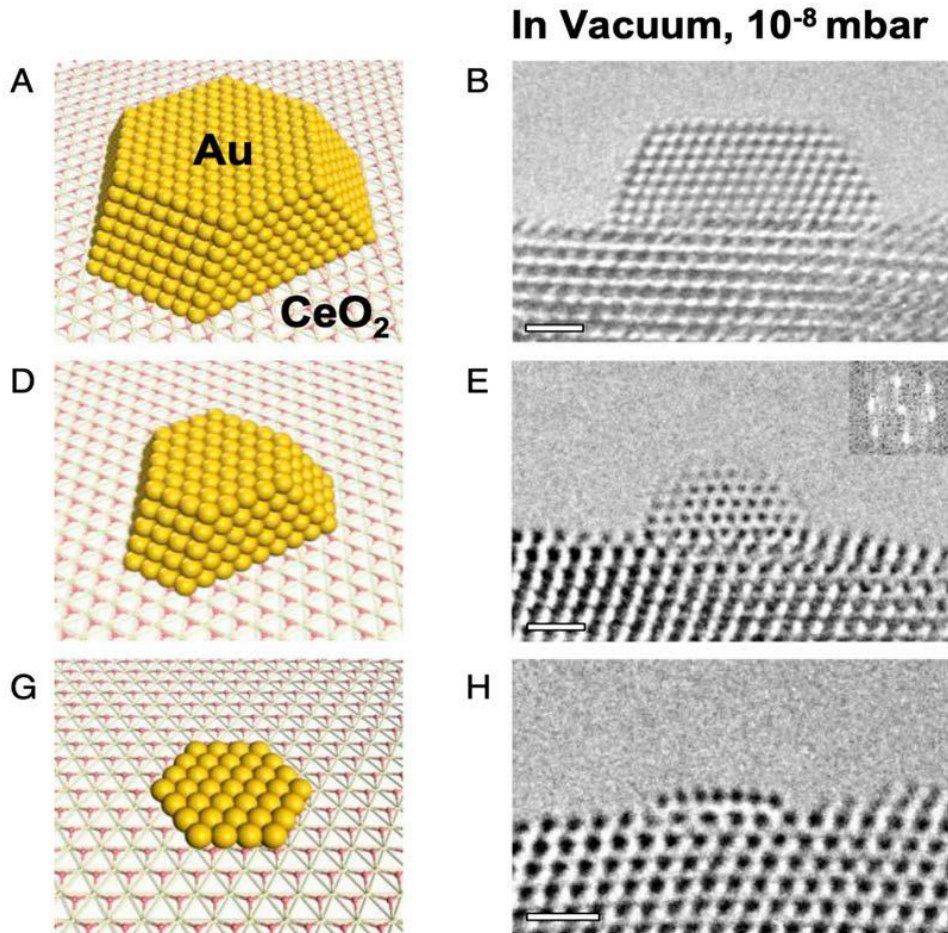
- Iterative algorithm:
 1. Assume an electron density $n(\mathbf{r})$
 2. Solve the Kohn-Sham equations to compute $\psi_i(\mathbf{r})$ using equation (1)
 3. Calculate the updated electron density $n(\mathbf{r})$ using equation (2)
 4. If $n(\mathbf{r})$ of steps 1 and 3 are the same, the ground energy has been determined. If not, $n(\mathbf{r})$ has to be updated and the algorithm is repeated.



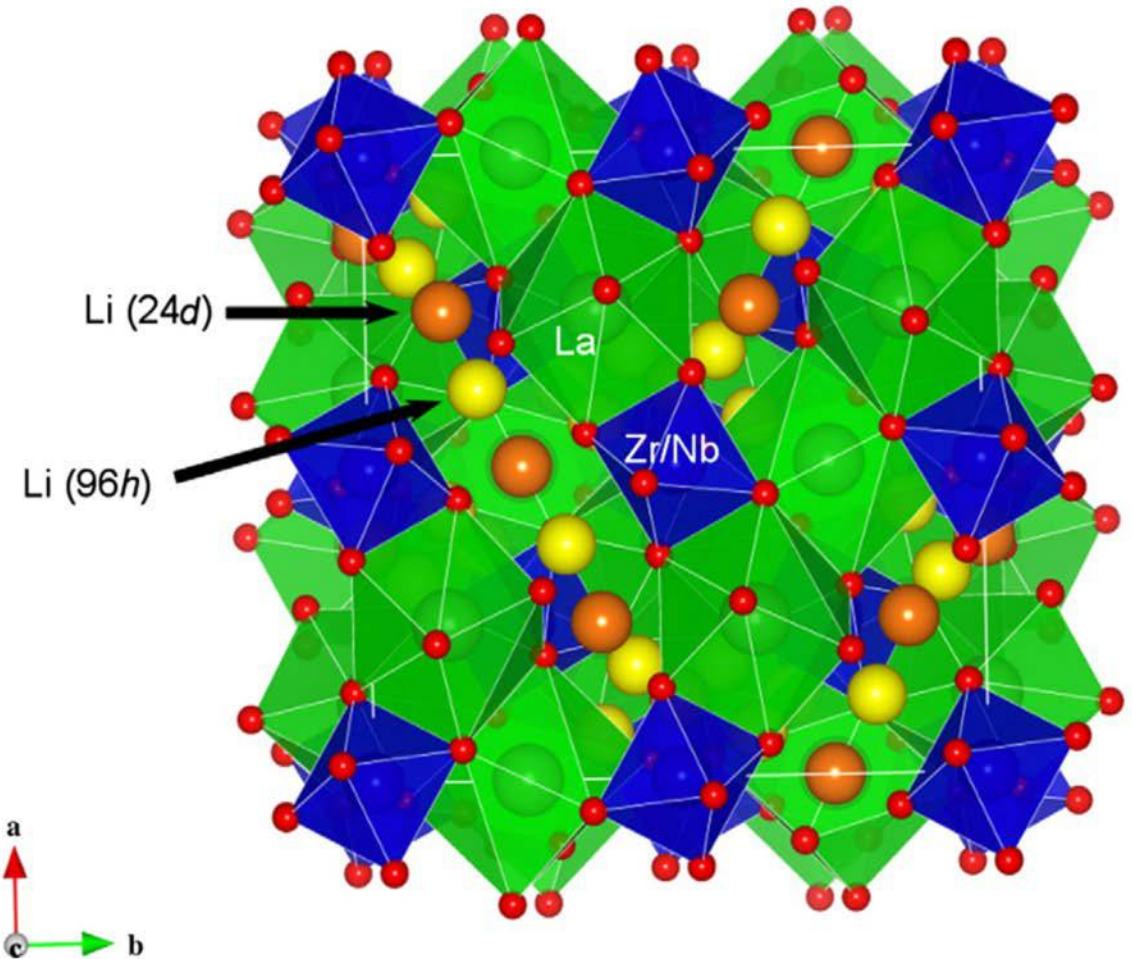
© John Wiley & Sons, Inc. All rights reserved. This content is excluded from our Creative Commons license. For more information, see <https://ocw.mit.edu/fairuse>.

Example 1: DFT calculations for catalysis and Li-ion electrolytes

Gold (Au) clusters on Cerium Oxide (CeO_2)



Lithium garnets (Li-ion battery electrolytes)



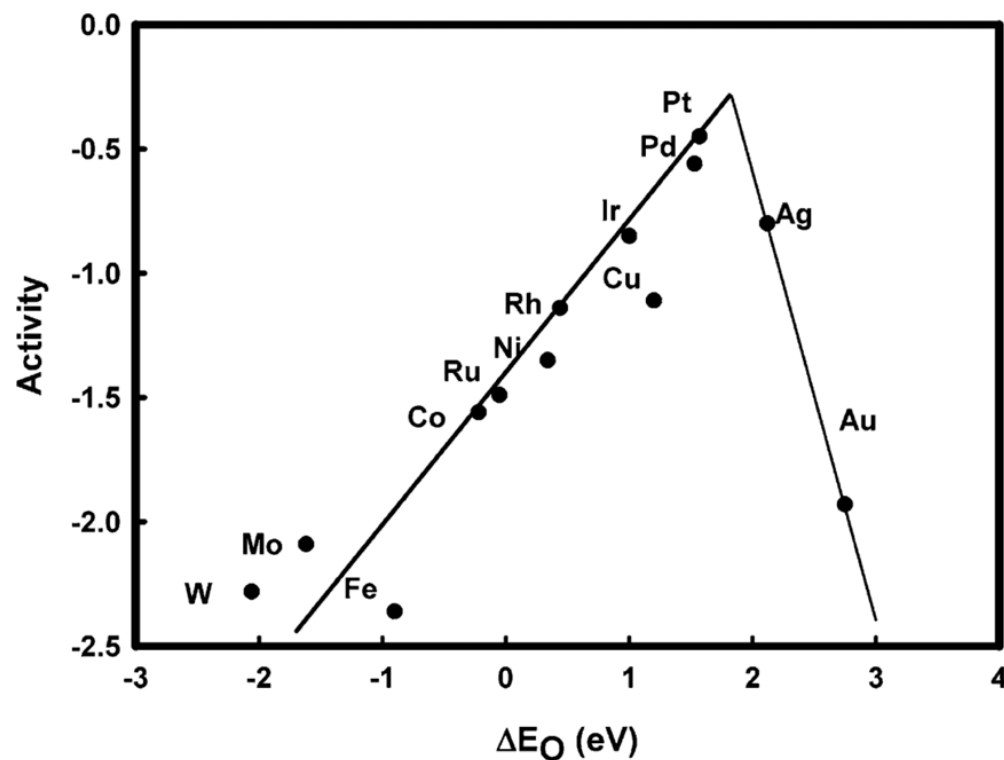
© National Academy of Sciences. All rights reserved. This content is excluded from our Creative Commons license. For more information, see <https://ocw.mit.edu/fairuse>.

Y. He et. al. PNAS 115 (30) (2018) 7700-7705

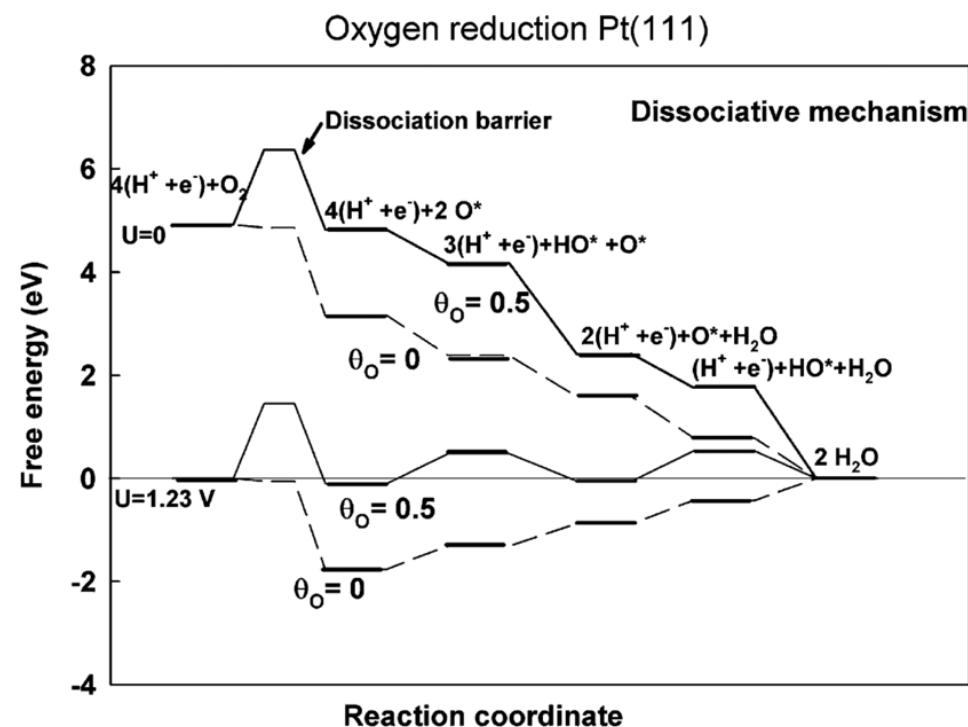
Courtesy Elsevier, Inc., <http://www.sciencedirect.com>. Used with permission.

A. Logéat et al. Solid State Ionics 206 (2012) 33-38

Example 2: DFT Calculations of Oxygen Reduction on Pt



Volcano plot of catalytic activity

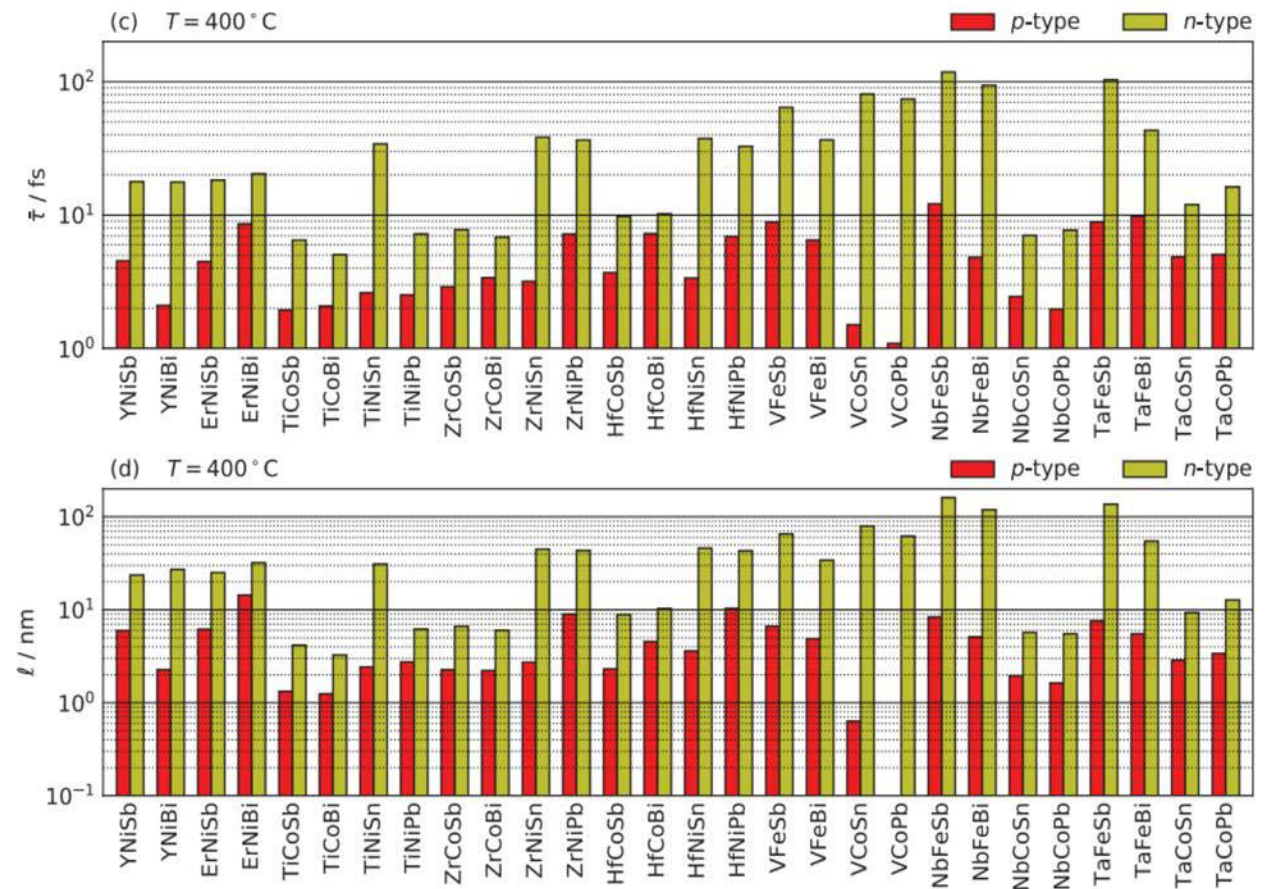
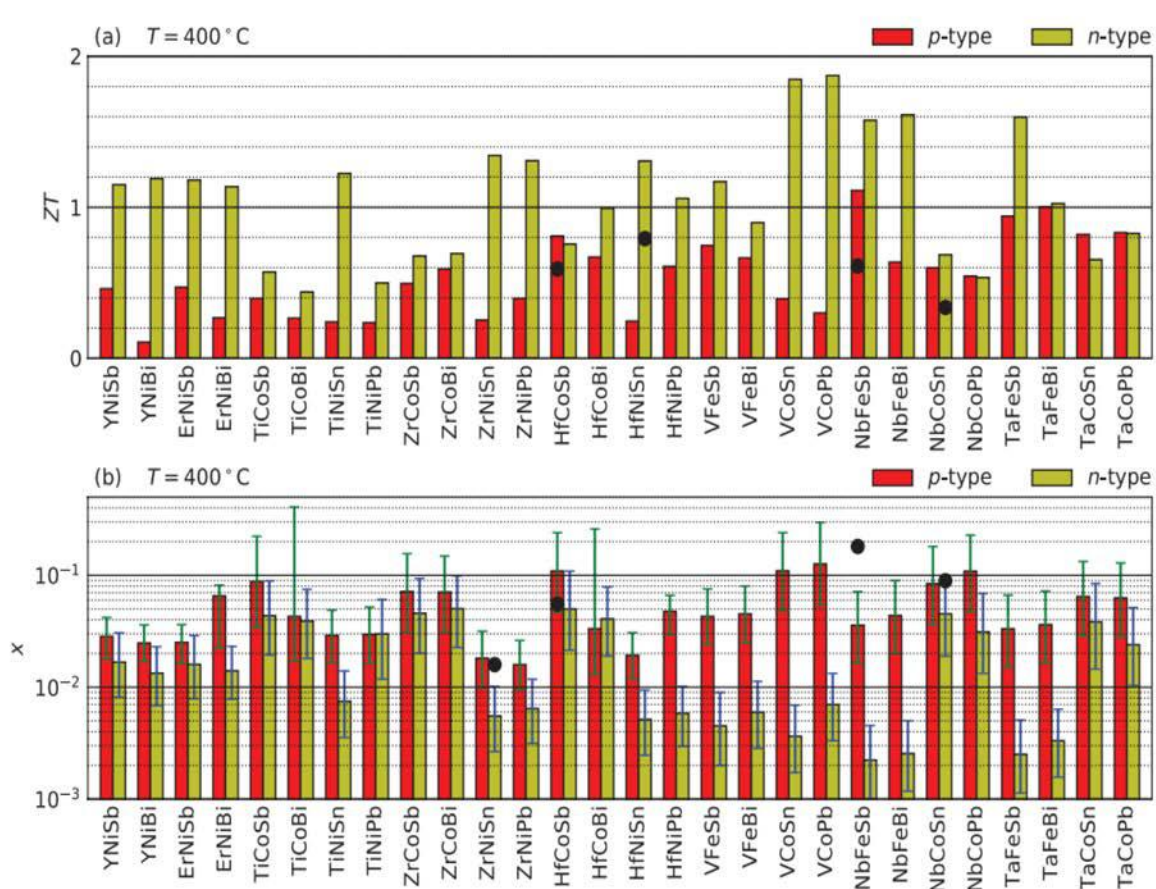


Calculation of intermediate steps of the reaction

© ACS Publications. All rights reserved. This content is excluded from our Creative Commons license. For more information, see <https://ocw.mit.edu/fairuse>.

- DFT can be used to predict properties of materials
- But remember that it has its own assumptions and limitations

High-throughput screening of materials: Thermoelectric materials (1)



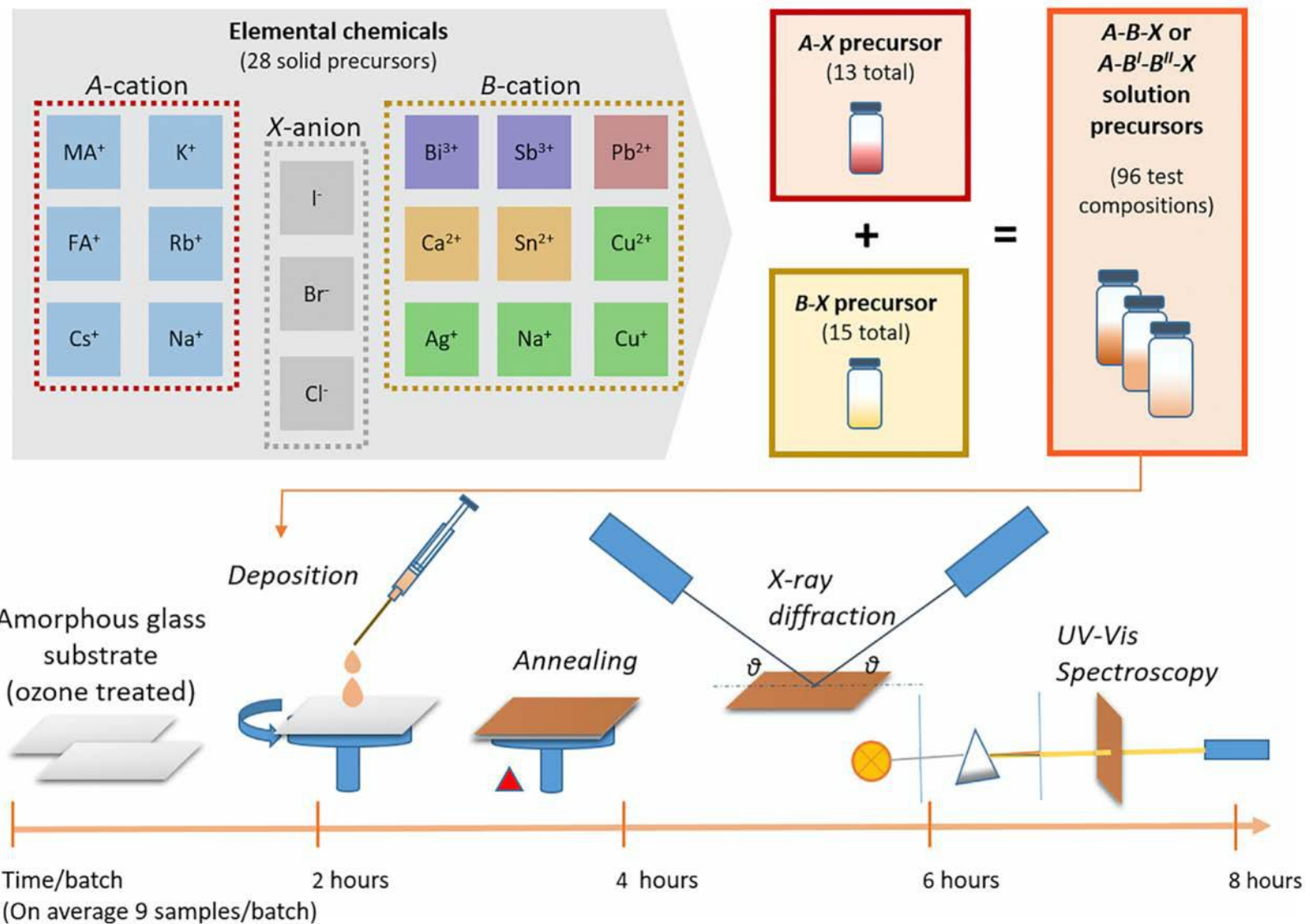
© John Wiley & Sons, Inc. All rights reserved. This content is excluded from our Creative Commons license. For more information, see <https://ocw.mit.edu/fairuse>.

Computational
Screening

Can the predicted materials be
synthesized?

High-throughput screening of materials: Photovoltaics (2)

Experimental Screening



Summary

- Materials are part of every energy conversion technology
- This presentation covered several energy conversion technologies involving the use of materials with focus on ceramic oxides
- Defect chemistry in materials
- Synthesis of materials
- Shaping of materials
- Computational methods
- High-throughput screening



MIT OpenCourseWare
<https://ocw.mit.edu/>

2.60J Fundamentals of Advanced Energy Conversion
Spring 2020

For information about citing these materials or our Terms of Use, visit: <https://ocw.mit.edu/terms>.

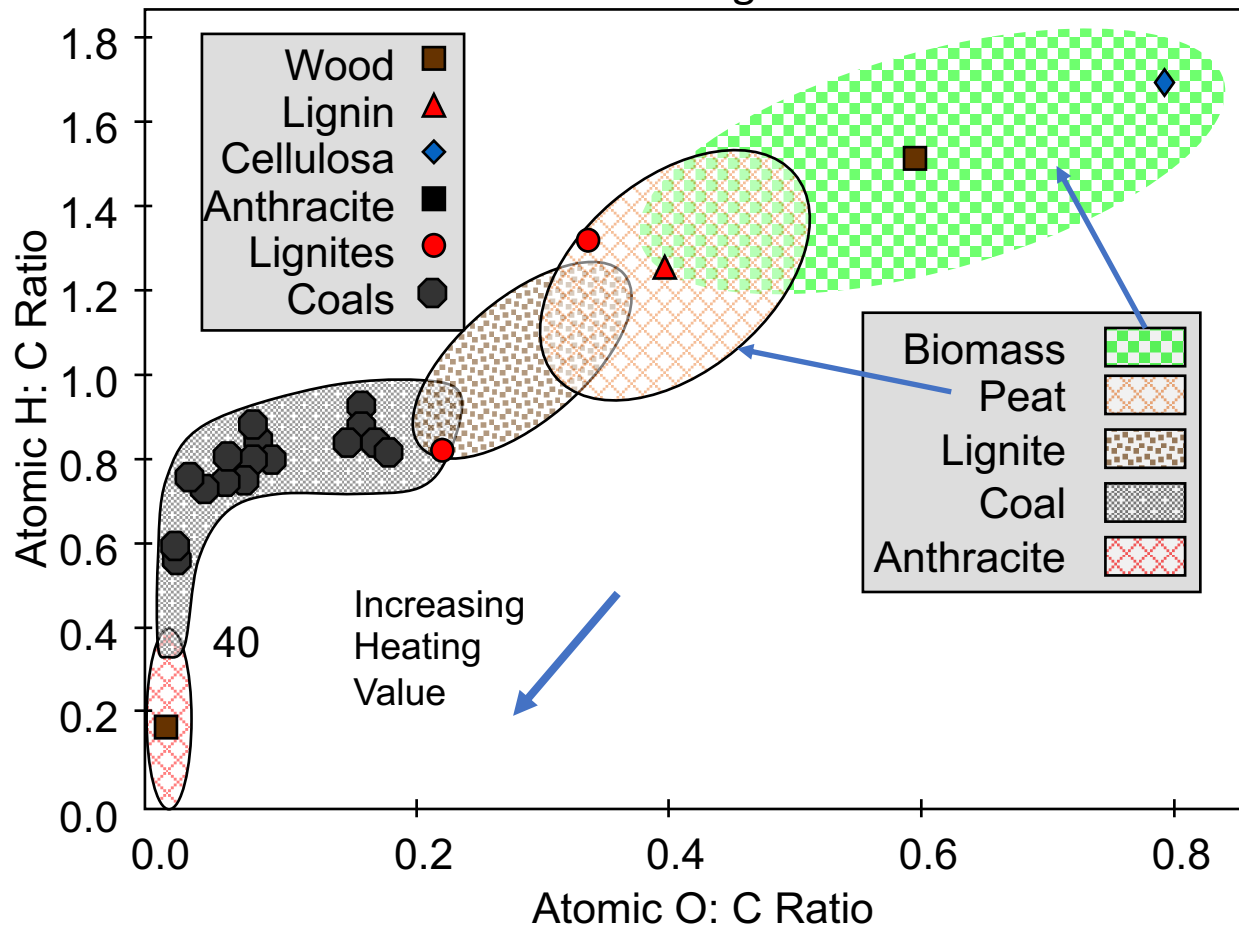
Lecture # 24

BIOMASS ENERGY

Ahmed Ghoniem
May 4, 2020

- Energy properties of biomass
- Some biomass fundamentals
- Fuel production from biomass
- Biomass conversion, biological and thermochemical
- Bioconversion, mass and energy balances
- Does bioconversion of corn to ethanol save energy?

Van Kreveln Diagram



Biomass composition and heating value

Biomass	C (%)	H (%)	O (%)	N (%)	S (%)	Ash (%)	HHV (MJ/kg)
Douglas fir					0	0.8	
Redwood		5.9	40.3	0.1	0	0.2	
Maple		6.0	41.7	0.3	0	1.4	
Sawdust		6.5	45.4	0	0	1.0	
Rice straw		5.1	35.8	0.6	0.1	19.2	
Rice husk		5.7	39.8	0.5	0	15.5	
Sewage sludge							

Ultimate analysis (on dry basis) of some plant biomass including woody and non woody, and sewage sludge, that can be used as fuel

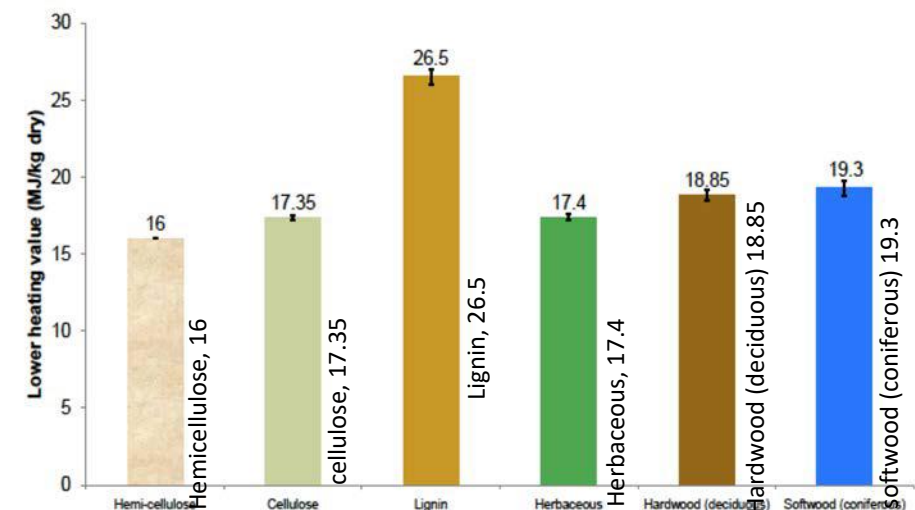
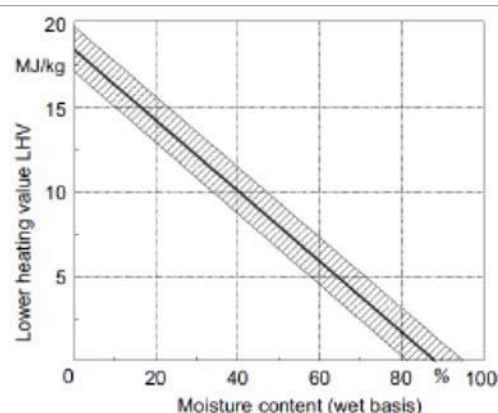


Figure 2-6 LHV of biomass and its cellulosic components (Francescato et al. 2008)



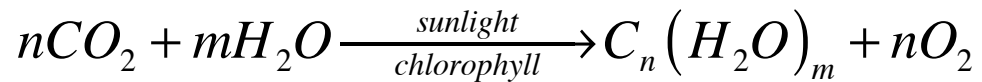
Effect of moisture content on LHV of wood (MJ/kg). (UN Food and Agri. Org.)

© FAO. All rights reserved. This content is excluded from our Creative Commons license. For more information, see <https://ocw.mit.edu/fairuse>.

© Source unknown. All rights reserved. This content is excluded from our Creative Commons license. For more information, see <https://ocw.mit.edu/fairuse>.

Some Biomass Fundamentals

Photosynthesis:



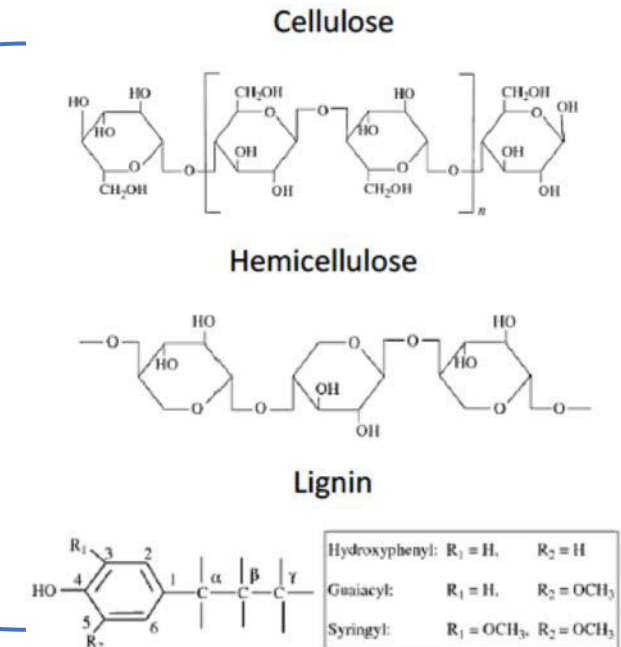
$$\Delta H_r = 470 \text{ kJ / mol}$$

Photosynthesis produces “**carbohydrates**” such as sugar, starch and cellulose from water and carbon dioxide.

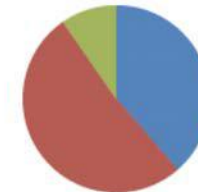
Efficiency of sunlight absorption/conversion during photosynthesis is 0.1-3%, but a fraction of it is lost in other products.

Carbohydrates are also called saccharides. They are sugars or polymers of sugar (defined next).

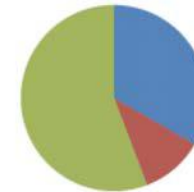
The three primary components of biomass:



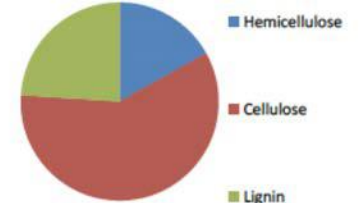
Wheat Straw



Bamboo



Willow

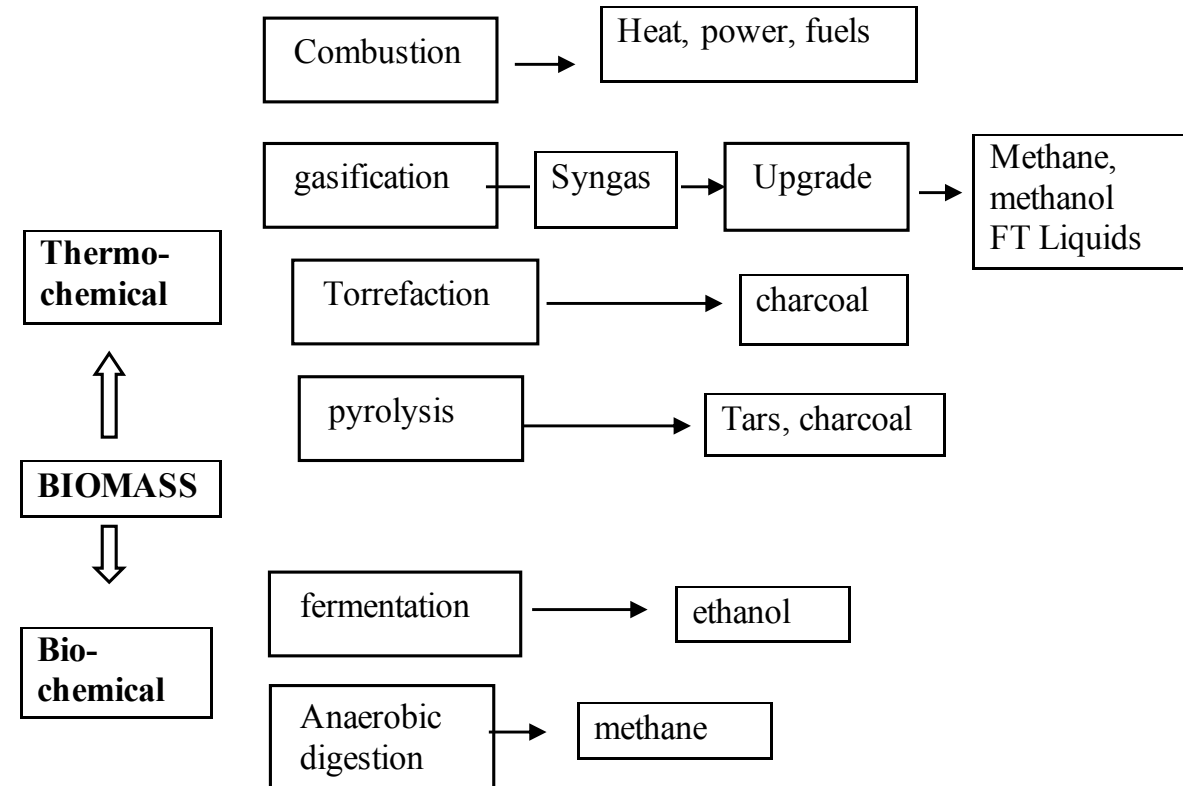


Biomass Utilization: production of heat and fuels

Three major conversion options:

1. Bioconversion to fuel (fermentation and anaerobic digestion),
2. Thermochemical conversion to fuel (pyrolysis and gasification).
3. Combustion to heat.

- Bio conversion is simpler and scalable, but limited to certain biomass components
- Gasification offers improved feedstock flexibility and production of drop-in fuels but is more compatible with larger scale production



Thermochemical processes work with (almost) any biomass:

Combustion is the simplest, but given the low heating value of wood, huge amounts are needed to power a typical power plant. Wood has open pore structure and high moisture content. On a dry basis, the heating value (~15-22 MJ/kg) is: $HHV = -1.3675 + 0.3137Y_C + 0.7009Y_H - 0.0318(1 - Y_C - Y_H - Y_{ash})$

Other *thermochemical* processes including pyrolysis (low temperature torrefaction to solids and intermediate temperature pyrolysis to liquids) and higher temperature gasification, may generally be preferable for recovering the energy of wood and lignin.

Bioconversion works well with sugar and grain crops:

Sugar crops include sugar cane, beet and sweet sorghum. Sugar cane produce nearly twice the energy of beet, measured as unit energy produce/land area, but its growth is restricted to warm climate, good soil and where plenty of water is available. Sugar crops can be more readily hydrolyzed (mixed with water and microbes) to fermentable sugars.

Grain crops include corn, wheat, rice, barley and other cereals. These plant products have high starch contents, which can be hydrolyzed (mixed with water, acids and enzymes) to fermentable sugars.

Property of plant material, as regards their potential for bio conversion:

Carbohydrates in plants are sugars and **polymers** of sugar: starch, hemicellulose and cellulose.

Sugars (oxygenated hydrocarbons) in fruit juices can be fermented (digested biologically) into alcohols.

Starch is granular polysaccharide found in seed, tubers, roots and stem pith; corn, potato, rice, tapioca. 10-20% of starch is soluble in water (alpha amylose) and the rest is insoluble (amylopectin). *It can be hydrolyzed to fermentable sugars using dilute acids and enzymes.*

Dry wood is 66% holocellulosic (combination of cellulosic and hemicellulosic) and 25% lignin, and the rest is resins, gums, tannins and waxes. About 25% of the holocellulose is hemicellulose, the rest is cellulose and some lignin.

Hemicellulose is made of polysaccharides, but they are more soluble than cellulose. *It is amorphous, is dissolved by dilute alkaline solutions, and can be hydrolyzed to fermentable sugars* .

Cellulose is made of fibrous polysaccharides, the main constituent of cell walls, such as cotton, wood, hemp and straw. *They are insoluble and chemically inert, and resist acidic or enzymatic hydrolysis.*

Lignin is not a carbohydrate. It is a polymer of single benzene rings linked with aliphatic chains (mostly phenolic compounds).

Lignin is an important constituent of the walls of woody plants, providing the plant with glue and strength. It is amorphous and more soluble, *but completely resists hydrolysis and is resistant to microbial degradation.* It is removable by steaming or by solvent extraction. Removed lignin can be combusted.

Besides woods and plant crops (fruits, etc.) sources of plant biomass include crop residue, that is, material left after harvest. This material is low on sugar and starch, but high on lignocellulosic material. Thus it may be more suitable for thermal conversion and combustion.

Same is likely to be for switch grass.

Agricultural waste, left over after processing crops include sugar cane bagass, and cotton gin trash. Sold as animal feed, it can also be burned or used in thermal conversion processes.

Aquatic plants including ocean kelp, algae and buckweed. In general, it is more difficult to harvest than other types of biomass, although its growth can be encouraged to grow faster by supplying nutrients such as CO₂.

Municipal solid waste include cellulosic material, may not work well with biochemical conversion processes, but lend themselves well to combustion and thermal conversion.

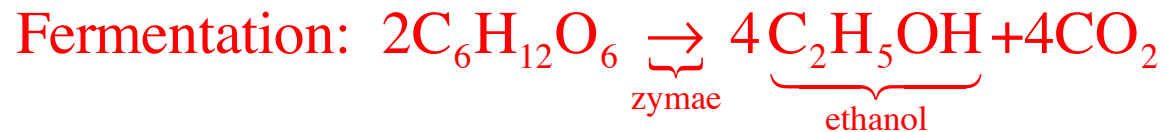
Animal waste is another source of organic biomass, which does not compete with food production, but supplies are limited.

Sugars and fermentation:

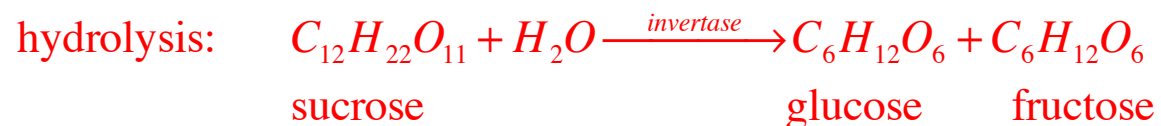
- Sucrose $C_{12}H_{22}O_{11}$ found in plant sap.
- Glucose $C_6H_{12}O_6$ in corn and grape.

Also found in the form of complex isomers in which the primary molecule is arranged in complex patterns, e.g., glucose can be found in D-glucose (dextrose), D-mannose or D-fructose.

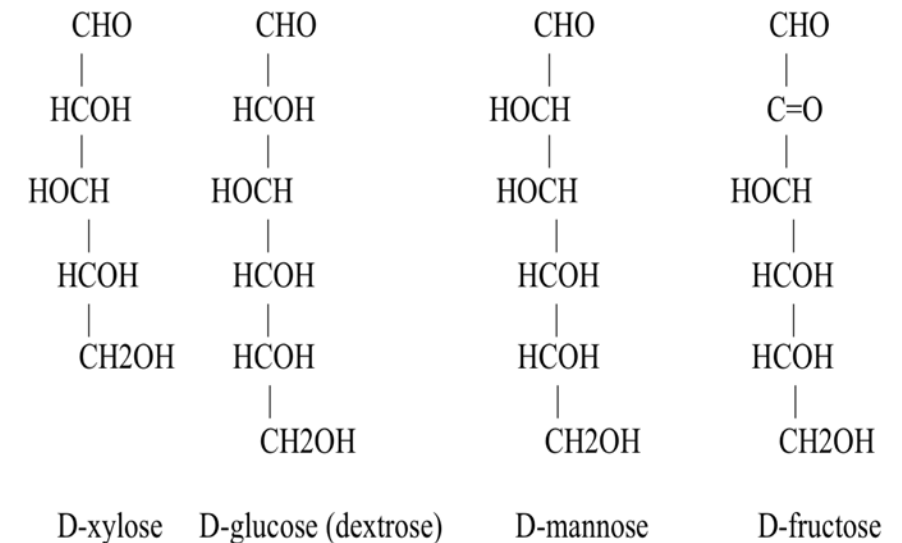
Sugar may be fermentable (that is, can be broken down biologically) or may not be fermentable.



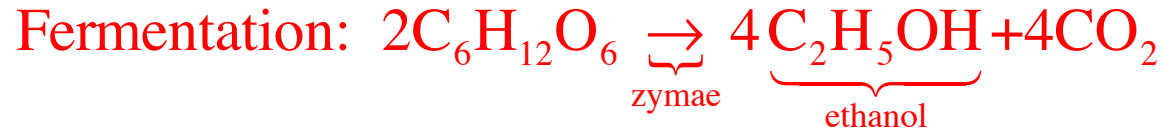
Non fermentable sugars can be made fermentable by hydrolysis in the presence of an acid or an enzyme:



Examples of fermentable (bio-processed) sugars



Bio conversion: Ethanol from Sugar Cane



Glucose is converted to ethanol (after sucrose is broken down by getting dissolved in water)

Two moles of ethanol are produced for each mole of glucose consumed.

The heat of reaction for glucose is 15.6 MJ/kg, or 2.81 GJ/kmol.

The amount of energy in the ethanol is $2 \times 29.7 \times 46 = 2.73$ GJ.

Thus, the theoretical efficiency of conversion is 97.5%. The actual efficiency is lower.

- Fermentation plants receive “burned and cropped” (b&c), or 77% of the raw cane.
- Average b&c production is 58 ton/hectare/year (ton = 1000 kg).
 - Each ton yields ~ 740 kg juice, made up of 135 kg sucrose and water. Sucrose’s HHV is 16.5 MJ/kg
- The residue is wet bagasse, which when dried yields 130 kg of dry bagasse.
- Dry bagasse has HHV of 19.7 MJ/kg that can be extracted by combustion.
- Thus the total HHV of a ton of b&c is $(135 \times 16.5 + 130 \times 19.7) = 4.7$ GJ.
- Per hectare per year, total biomass energy of cane is 270 GJ or 0.86 W/m².
- With average insolation of 225 W/m², the photosynthesis efficiency of sugar cane to energy (ethanol if conversion efficiency is 100%, see next) is 0.38%.

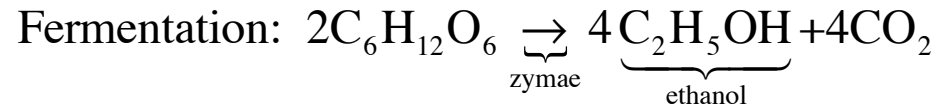
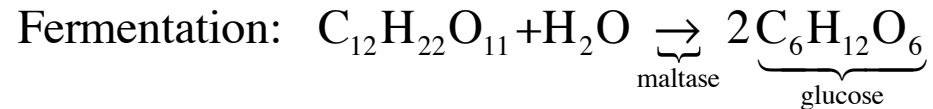
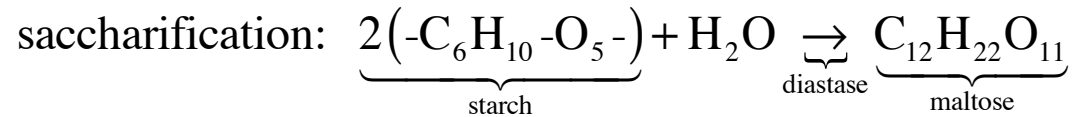
Ethanol from Corn

Conversion occurs in liquid medium using enzymes (proteins, such as glycolysis, produced by living cells) to produce liquid fuels. They have slow kinetics (1-2 orders of magnitude slower than thermal reactions).

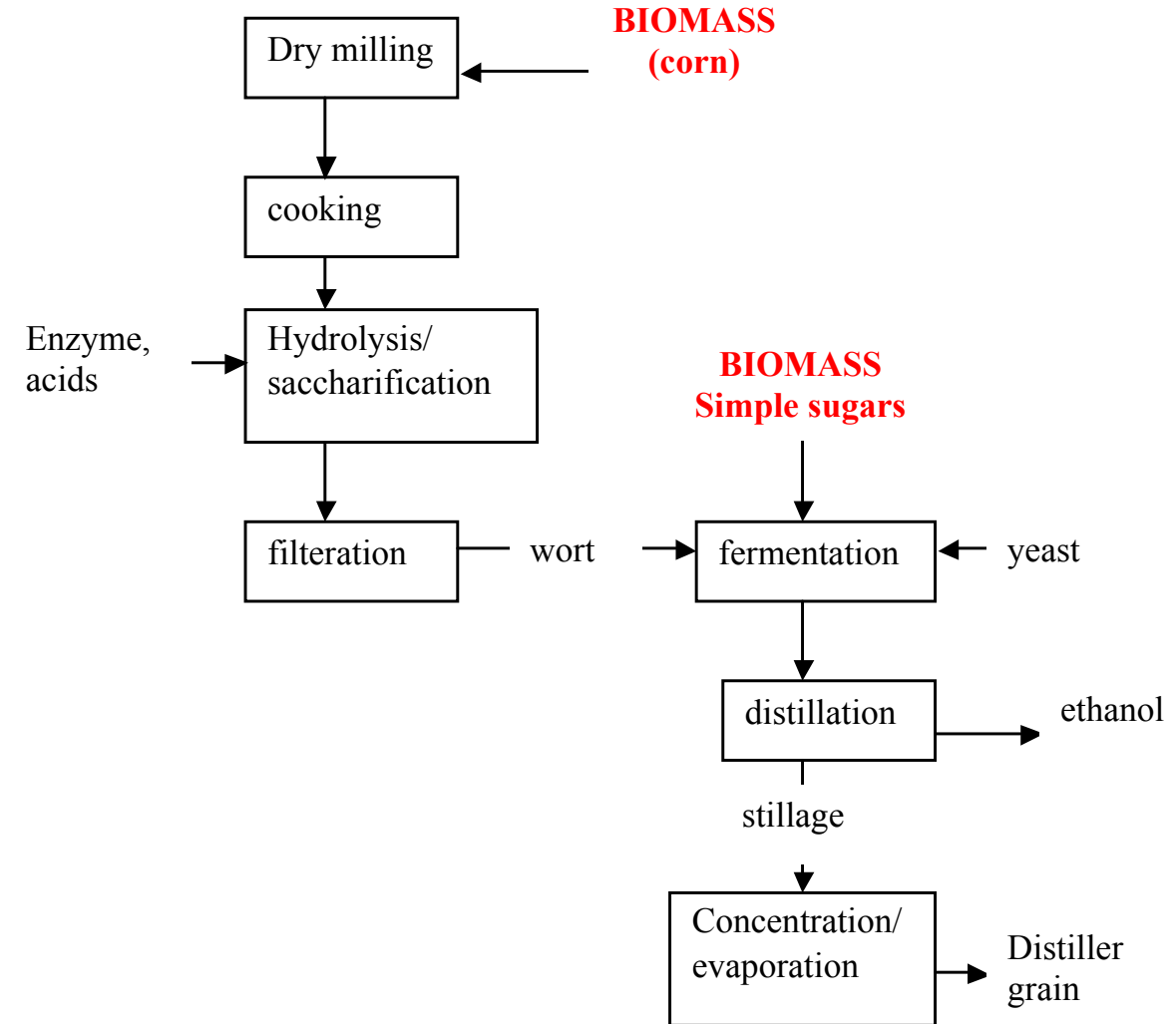
Acids are used for hydrolysis at 140-190 C. Fermentation is exothermic and the environment must be cooled to 30 C.

The final products has ~ 14% alcohol, and must be distilled.

Distillation consumes ~ 7-11 MJ/L of the produced ethanol (nearly 30-45% of the HHV of the product).



Thermal efficiency [ethanol/(corn + heat)] is 46%.



Ethanol from Corn

Is it energy positive or negative?

Using these equations, one can show that for 324 kg of starch used, 184 kg of ethanol is produced.

In practice, $\sim 10\%$ of the starch is converted into other byproducts, such as higher alcohols, glycerin and ethers.

Assuming corn is 61% starch and correcting for the 10 % to byproducts shows that 1 kg of ethanol requires 3.2 kg of corn, or a liter of ethanol requires 2.6 kg corn.

Given the higher heating value of corn, 14.1 MJ/kg, and ethanol, 29.7 MJ/kg, and subtracting the energy for milling, cooking, distillation and recovery of byproducts, an overall thermal efficiency defined as the ratio between the heating value of the produced ethanol divided by the sum of the corn heating value + other energy used, is 46%. The energy used is 65% of that of the enthalpy produced.

To cultivate and harvest the corn crop, these are estimated to be 42% of the energy of the ethanol produced, leading to a negative 7% energy overall.

For the production of ethanol from corn to be energy positive, crop residues and fermentation byproducts must be used to supply some of the heat required.



Thermodynamics of the Corn-Ethanol Biofuel Cycle

© Informa UK Limited. All rights reserved. This content is excluded from our Creative Commons license. For more information, see <https://ocw.mit.edu/fairuse>.

Tad W. Patzek (2004) "Thermodynamics of the Corn-Ethanol Biofuel Cycle", *Critical Reviews in Plant Sciences*, 23:6, 519-567, DOI: [10.1080/07352680490886905](https://doi.org/10.1080/07352680490886905).

True Life Cycle Analysis of corn-to-ethanol, by T. Patzek

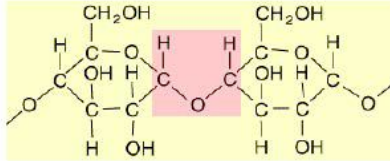


Figure 1: A typical starch molecule is constructed from α -glucosidic bonds (purple background), each of which links two dehydrated glucose molecules. These molecules form either unbranched or somewhat branched polymer chains with up to 360 or 1000 glucose units, respectively (Avers, 1976). In hydrolysis, the glucosidic bonds are broken, and each glucose unit gains one water molecule.

Fuel	Density kg/sm ³	HHV ^a MJ/kg	LHV ^a MJ/kg	HHV ^a MJ/kg	LHV ^a MJ/kg	Source ⁱ
Gasoline	720-800	46.7 ^b	42.5 ^b	46.8	43.6	Table 339
Diesel fuel	840	45.9	43.0	45.3	42.3	Table 350
Methane	0.66 ^d	55.5 ^c	50.1 ^c	55.1(g)		Table 347
LPG ^e	0.58	50.0	46.0			
NG ^f	0.84	48.7	43.9			
Ethanol	787 ^h	29.7 ^g	26.7 ^g	29.6	26.8	Table 353
Corn grain dry		18.8 ^j				
Corn stover ^k		17.7	16.5			
Corn stalks ^l		15.8	14.8			
Corn meal ^m		16.0				
Corn oil ⁿ	909.5	39.5	38.8			

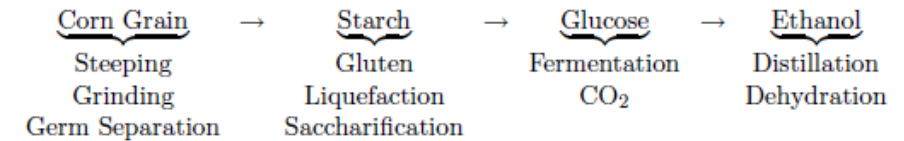


Table 24: The First Law summary of the U.S. corn-ethanol production in 2004

29.6 million hectares	of corn harvested in the U.S.
299.67 million tonnes	of moist corn grain harvested
3.8 million hectares	of U.S. cropland growing corn for ethanol
12.7 %	of all U.S. corn is farmed for ethanol
0.399 liters	of ethanol from 1 kg of corn
12.28 GL/yr	of ethanol produced in the U.S.
3.25 billion gal/yr	of ethanol produced in the U.S.
9.21 GL GE/yr	as ethanol produced in the U.S.
10.16 GL GE/yr	burned to produce this ethanol
1.4 %	of U.S. automobile fuel from ethanol
25.9 million hectares	for 10% U.S. automobile fuel energy
\$1.69 billion/yr	in federal subsidies for ethanol
\$0.32 billion/yr	in average state subsidies for ethanol
\$1.27 billion/yr	in corn-for-ethanol price subsidies
\$3.28 billion/yr	in total ethanol subsidies

GL = Giga Liter = 10⁹ L; GE = Gasoline Equivalent

Agricultural yield= energy of dry corn grain.
 On average it is 125 GJ/ha*.
 For perennial grasses 200-300 GJ/ha-crop
 For sugarcane, 400 GJ/ha-crop

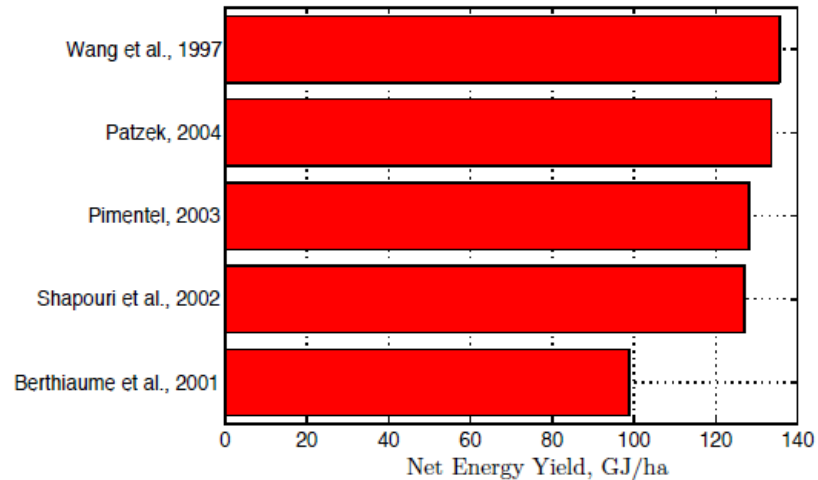


Figure 20: The net energy yield in industrial corn grain production is relatively small, 100 – 135 GJ/ha-crop. The HHV of dry corn grain is 18.8 MJ/kg, based on the mean of the values reported by SCHNEIDER & SPRAQUE (1955), p. 496, 2033 kcal/lb; and MILLER (1958), p. 639, 2059 kcal/lb. 1 thermochemical kcal = 4.184 kJ.

© Source unknown. All rights reserved. This content is excluded from our Creative Commons license. For more information, see <https://ocw.mit.edu/fairuse>.

* 1 ha produces about 8600 kg moist corn x 0.85 = 7300 kg dry corn x 18.8 MJ/kg = 137 GJ/ha
 (1 ha = 10000 m² = 2.47 acres.)
 Or 130 bushels (wet) per acre (with 15% moisture).

Fuels for farming

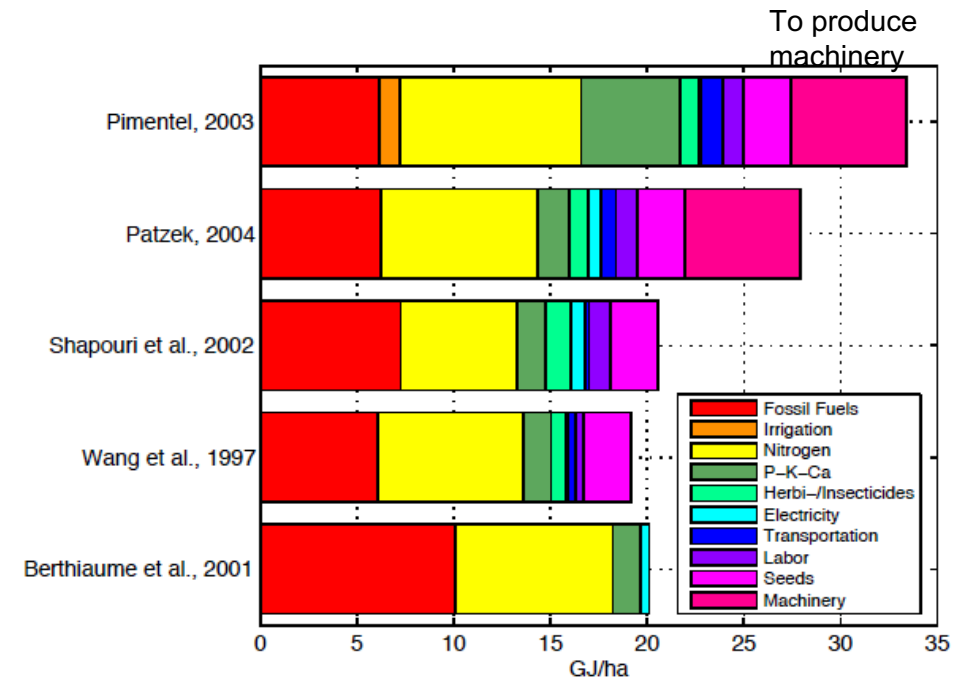


Figure 12: Major fossil energy inputs into corn farming.

Some estimates, like nitrogen and machinery, account for energy used to produce this commodity. P-K-Ca: more fertilizers

Fuels used for ethanol production from corn

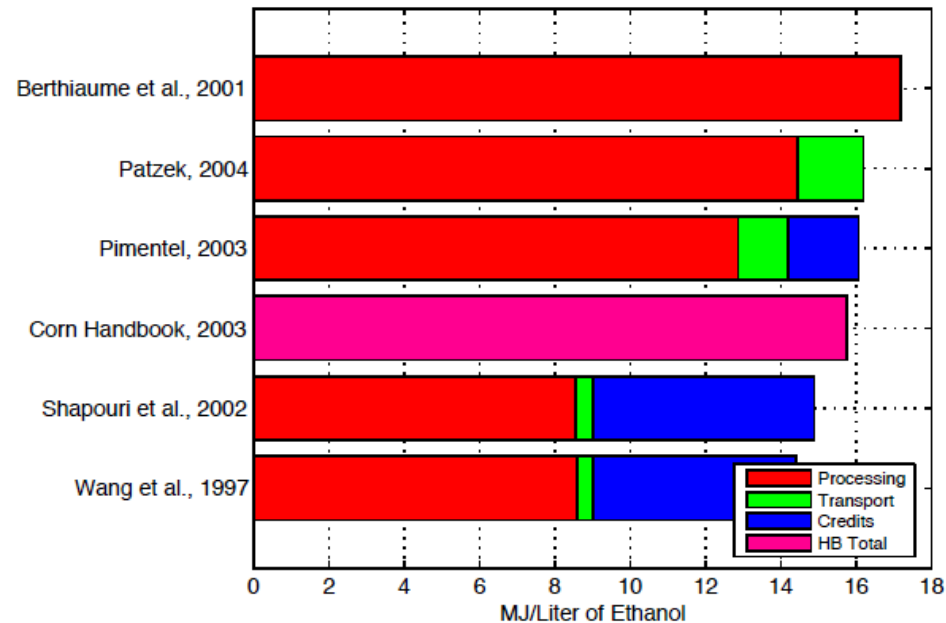


Figure 17: The average fossil energy inputs to ethanol production in a wet milling plant. The length of each bar is the total energy outlay to produce 1 liter of EtOH, and the blue parts denote the size of energy credits assumed by the different authors. The modern dry mill plants use 11.36 MJ/L as steam and 3.12 MJ/L as electricity, 14.5 MJ/L total, not counting transportation costs.

© Source unknown. All rights reserved. This content is excluded from our Creative Commons license. For more information, see <https://ocw.mit.edu/fairuse>.

Taking 16 MJ/L, or 20.3 MJ/kg EtOH (x 2200 kg/ha)
gives 44.7 GJ/ha of fossil fuel requirements to
produce ethanol from corn.
Could be as low as 26 GJ/ha if credit is considered.

Production in terms of corn and ethanol

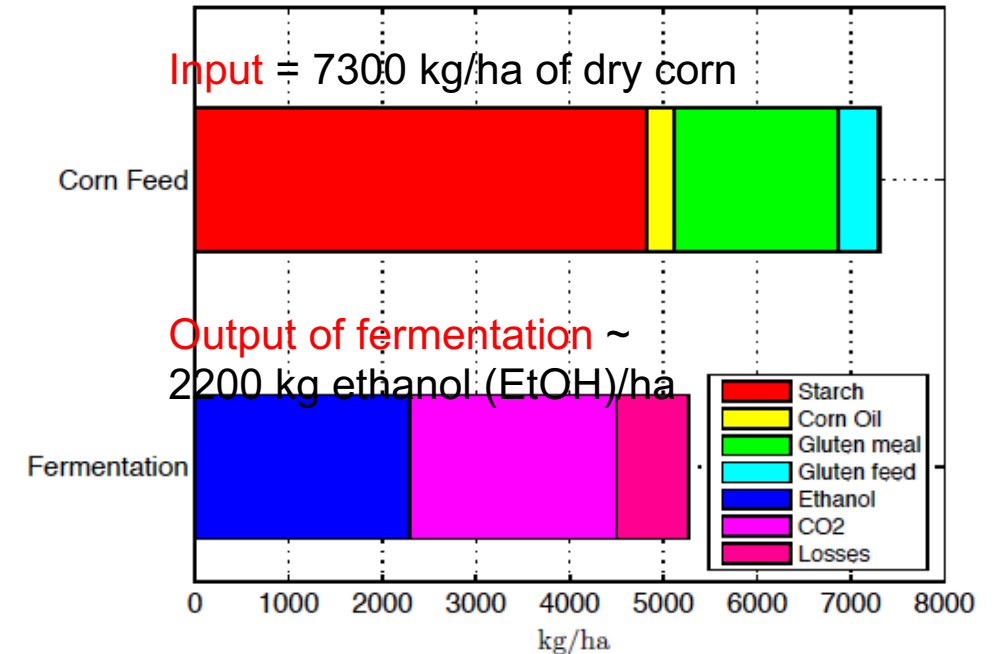


Figure 15: The result of practical corn conversion into ethanol with 16% losses is 0.399 L EtOH/kg dry corn grain = 2.682 gal EtOH/dry bushel = 2.28 gal EtOH/wet bushel with 15% moisture. Note that the dry starch is swollen by a factor of 180/162 caused by hydrolysis to glucose.

Energy input and output

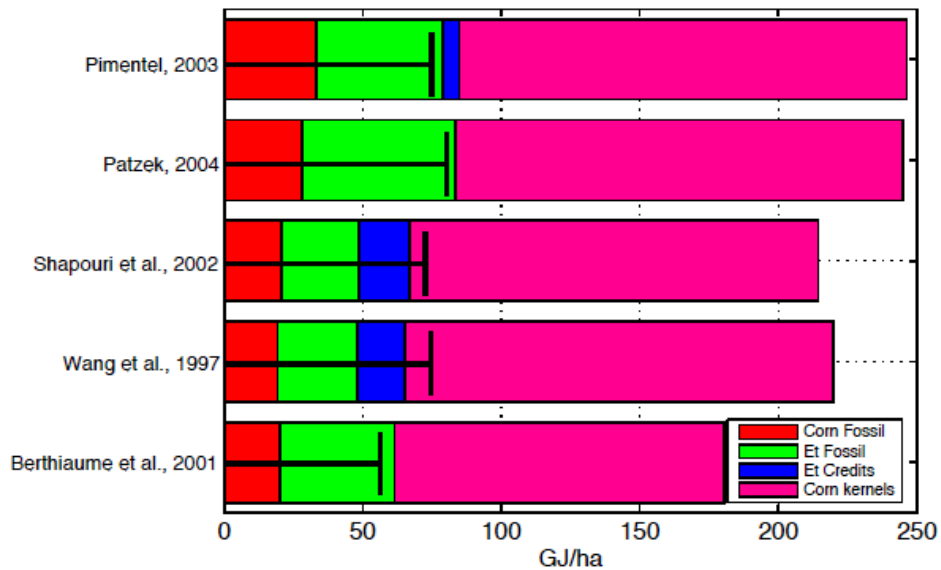


Figure 18: The overall energy balance of ethanol production. The two or three leftmost parts of each bar represent the specific fossil energy used in corn farming and ethanol production. The fossil energy inputs into ethanol production are the sum of the green part and the blue energy credit part for some authors. The rightmost part is the calorific value of corn grain harvested from 1 hectare. The total lengths of the horizontal bars represent all energy inputs into ethanol production. The horizontal lines with the vertical anchors represent the calorific value of ethanol obtained from one hectare of corn. Note that the total energy inputs into ethanol production are equivalent to ~4–5 metric tonnes of gasoline per hectare. The ethanol's calorific value is equal to 1–1.3 metric tonnes of gasoline.

In terms of EtOH, we get 65 GJ/ha.

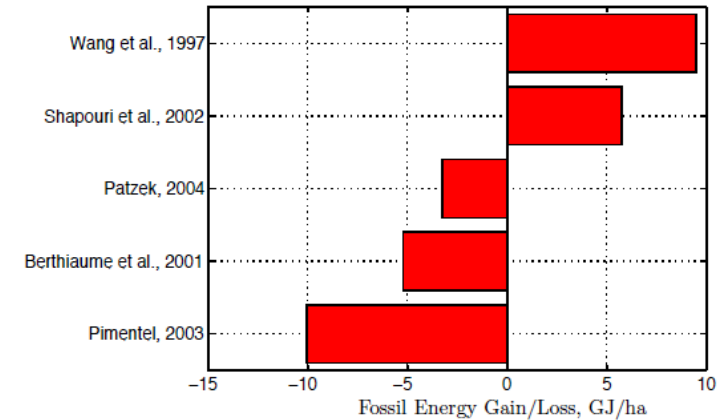


Figure 19: Fossil energy gain/loss in corn ethanol production. Note that the dubious energy credits described in Section 4.4 do not eliminate the use of fossil fuels in the first place, but present alternative useful outcomes of this use.

Farming: 20-33 GJ/ha,
EtOH production from corn, 26-44 GJ/ha,
Total fossil used: 46-77 GJ/ha.

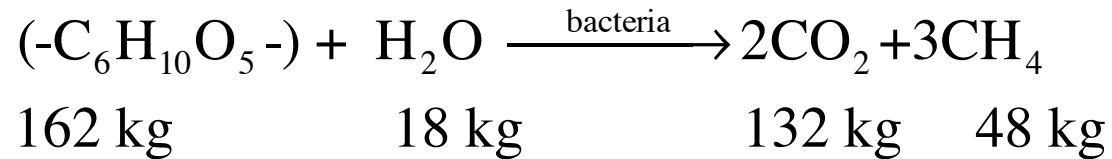
Energy in EtOH (2200 kg/ha x 29 MJ/kg) 63 GJ/ha .

Ideal thermal efficiency of corn to ethanol: 46%
That is, with 137 GJ/ha corn, should 63 yield GJ/ha in EtOH

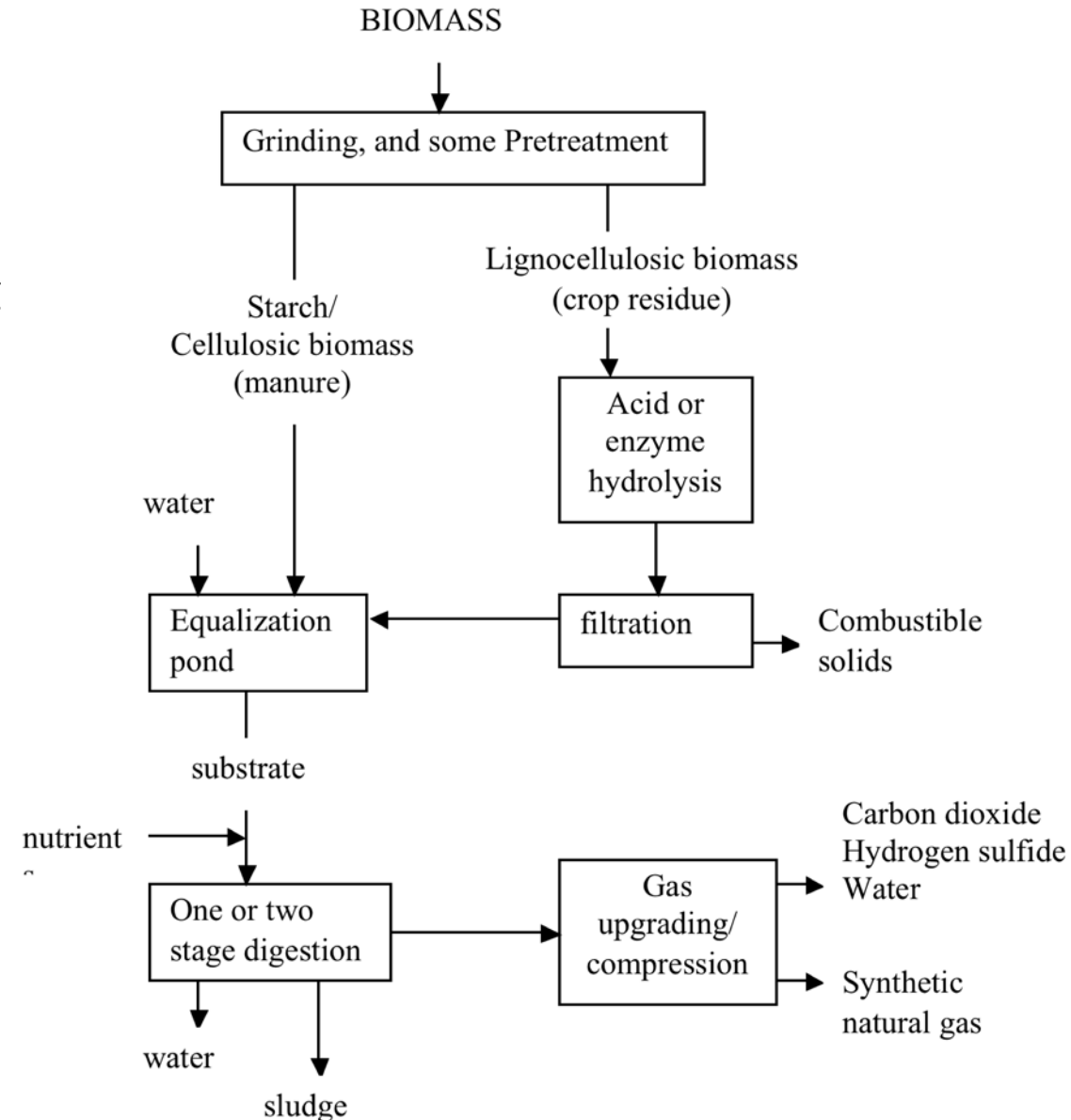
Anaerobic Digestion

Anaerobic digestion:

Decomposition of complex organic molecules to methane and CO₂ through three stages: hydrolysis using bacteria, conversion to fatty acids using bacteria, and finally methanogenesis using bacteria where biogas (CH₄+CO₂) is evolved.



These processes are mildly exothermic, and require temperatures in the range of 45-65 °C. The overall thermal efficiency is 53%.



MIT OpenCourseWare
<https://ocw.mit.edu/>

2.60J Fundamentals of Advanced Energy Conversion
Spring 2020

For information about citing these materials or our Terms of Use, visit: <https://ocw.mit.edu/terms>.

Lecture # 25

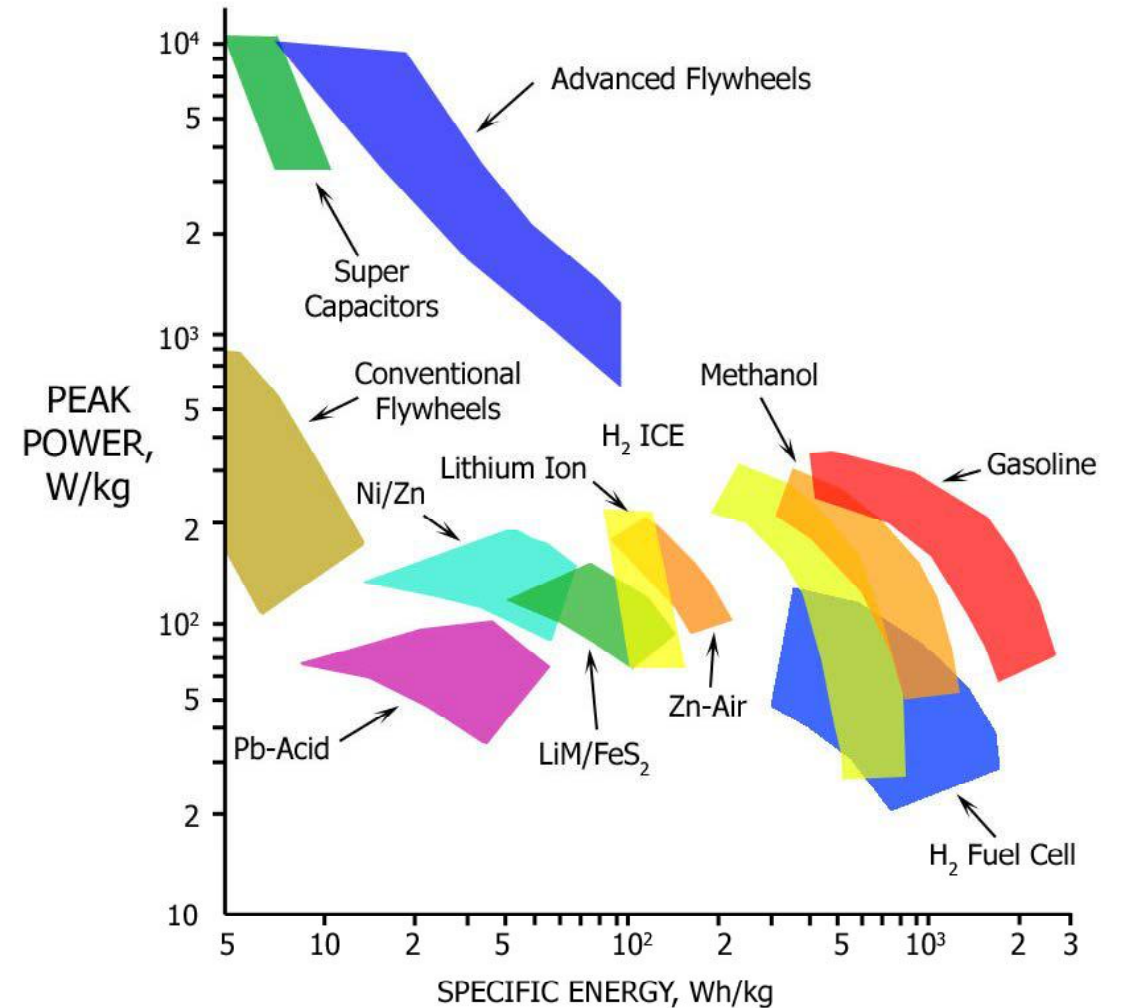
Energy Storage

Ahmed F. Ghoniem

May 6, 2020

- Storage technologies, for grid-level!
- Thermal energy storage, and thermochemical options

- THE RAGONE DIAGRAM, more applicable mobility.
- Specific energy is key, specific power needed for short burst.
- Renewables-powered mobility can be:
 - Battery electric (BEV)
 - Hydrogen ICE or PEM-FC.
- For stationary applications, criteria for selection are different.
- Scale is important



© Walter de Gruyter GmbH. All rights reserved. This content is excluded from our Creative Commons license. For more information, see <https://ocw.mit.edu/fairuse>.

THE RAGONE DIAGRAM. Figure shows approximate estimates for peak power density and specific energy for a number of storage technology mostly for mobile applications.

Energy Storage: a brief comparison

The table shows technologies for stationary and mobile applications including mechanical and electrochemical. Capacitors are integral parts of mobile storage!

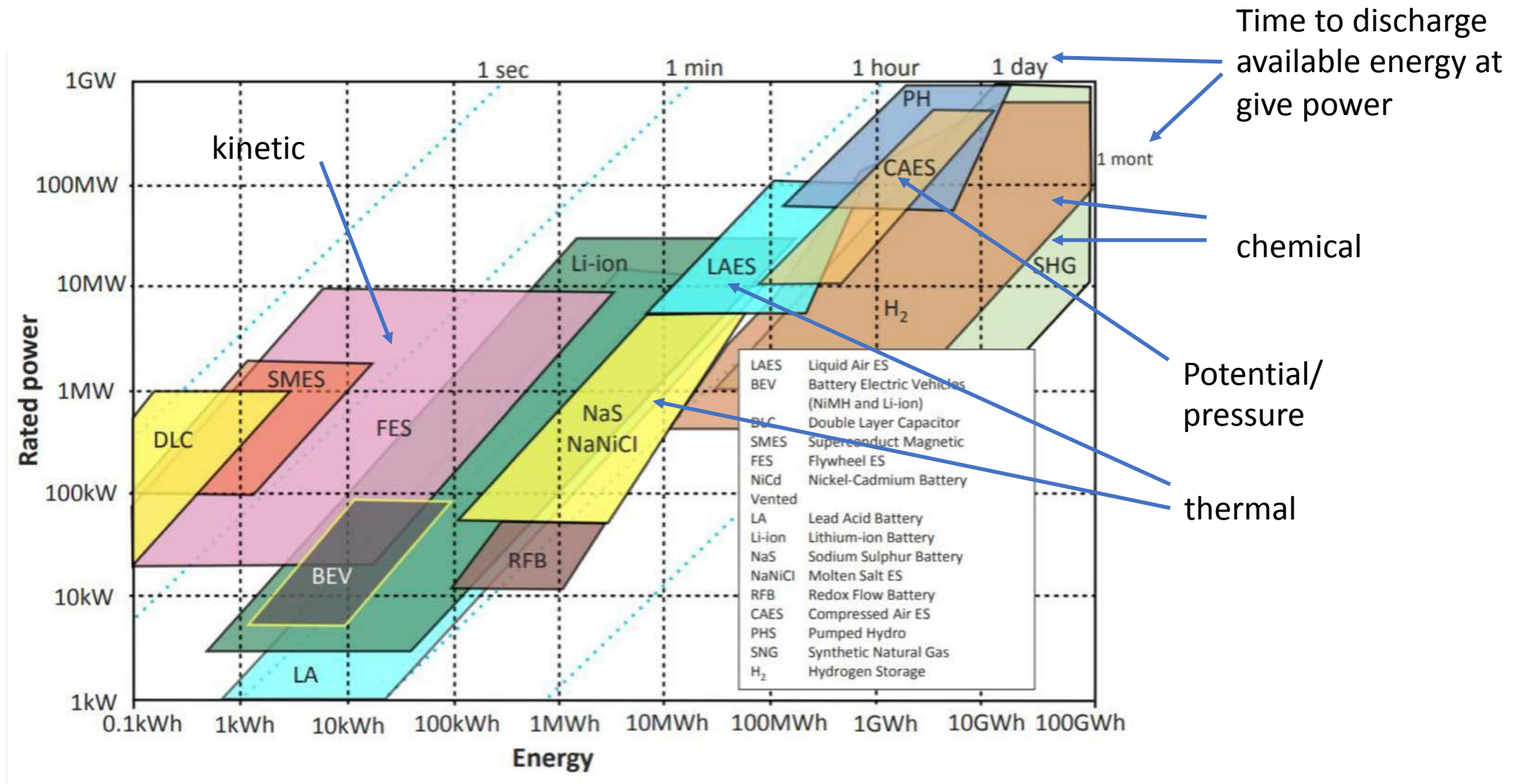
Not inclusive and other options are available and under development.

Does not show thermal (storage) and chemical (hydrogen, fuels and thermochemical) options which are very important.

Prices change constantly but comparison is still reasonable.

Characteristic	PHS	CAES	Batteries	Flywheel
<i>Energy Range (MJ)</i>	1.8x10 ⁶ - 36x10 ⁶	180,000- 18x10 ⁶	1,800 – 180,000	1 – 18,000
<i>Power Range (MW)</i>	100-1000	100-1000	0.1 – 10	1-10
<i>Overall Cycle Efficiency</i>	64-80%	60-70%	~75%	~90%
<i>Charge/Discharge Time</i>	Hours	Hours	Hours	Minutes
<i>Cycle Life</i>	10,000	10,000	2,000	10,000
<i>Footprint/Unit Size</i>	Large if above ground	Moderate if under ground	Small	Small
<i>Siting Ease</i>	Difficult	Difficult- Moderate	N/A	N/A
<i>Maturity</i>	Mature	Development	Mature except for flow type	Development
<i>Estimated Capital Costs - Power (\$/kWe)</i>	600 – 1,000	500-1,000	100-200 (LA)	200 - 500
<i>Estimated Capital Costs - Energy (\$/kWh)</i>	10 - 15	10 - 15	150-300	100 - 800

Energy Storage Capacity



© Source unknown. All rights reserved. This content is excluded from our Creative Commons license. For more information, see <https://ocw.mit.edu/fairuse>.

Chris Mutty and Scott Seo 2019 paper for reference

Storage systems and their utilization

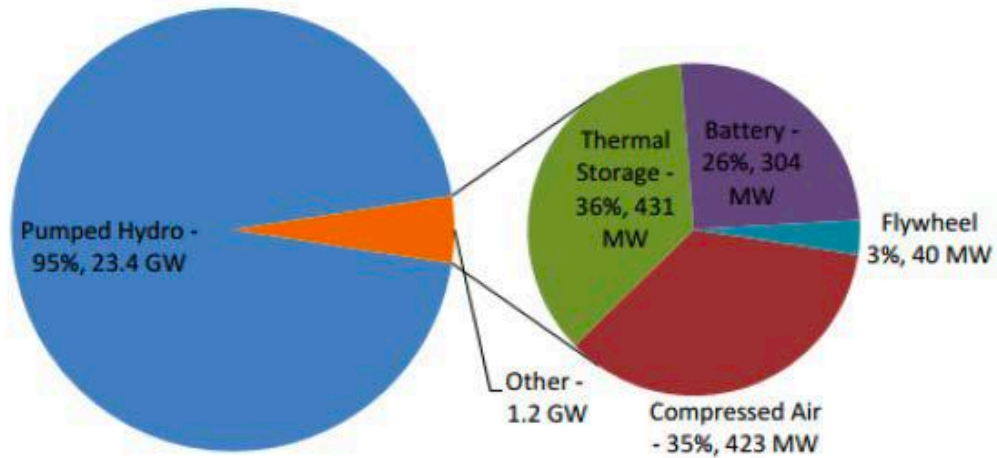


Image courtesy of DOE.

DOE. "Grid Energy Storage":

<https://energy.gov/sites/prod/files/2014/09/f18/Grid%20Energy%20Storage%20December%202013.pdf>

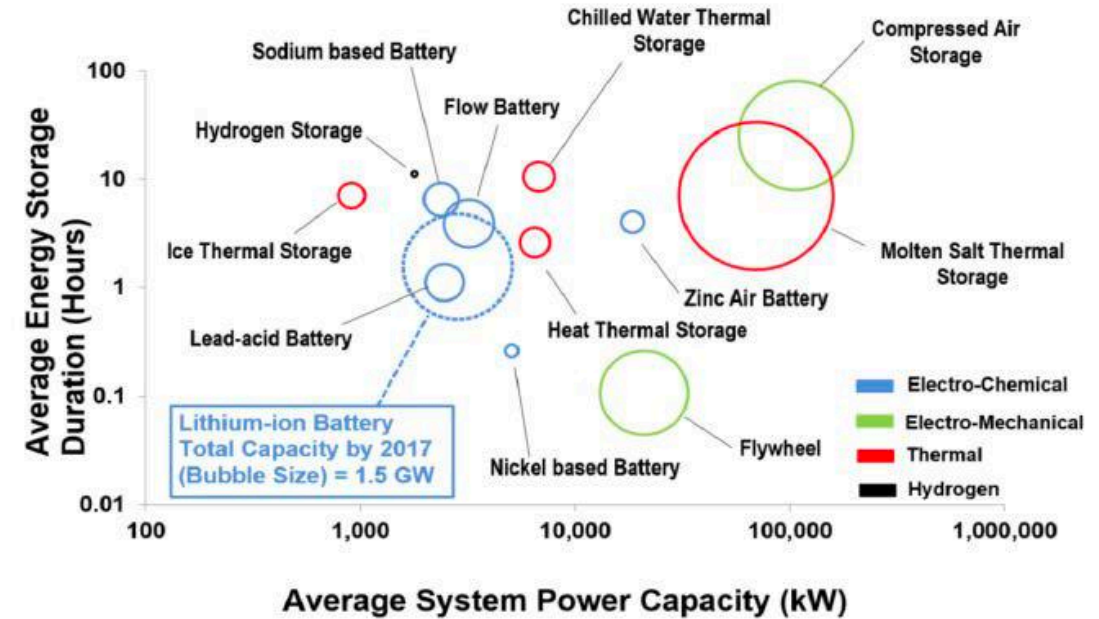


Image courtesy of NREL, DOE.

The power capacity and energy capacity (measured in storage duration) of energy storage plants built between 1958 and 2017. The relative circle size indicates the worldwide installed capacity. Pumped hydro is not shown here due to the large number of plants, but its average size is on the order of 300 MW and 3 GWh (10 hr duration!).

David Feldman, et al. Technical report, National Renewable Energy Lab.(NREL), Golden, CO, US 2016.

Storage systems and their characteristics

An important definition:

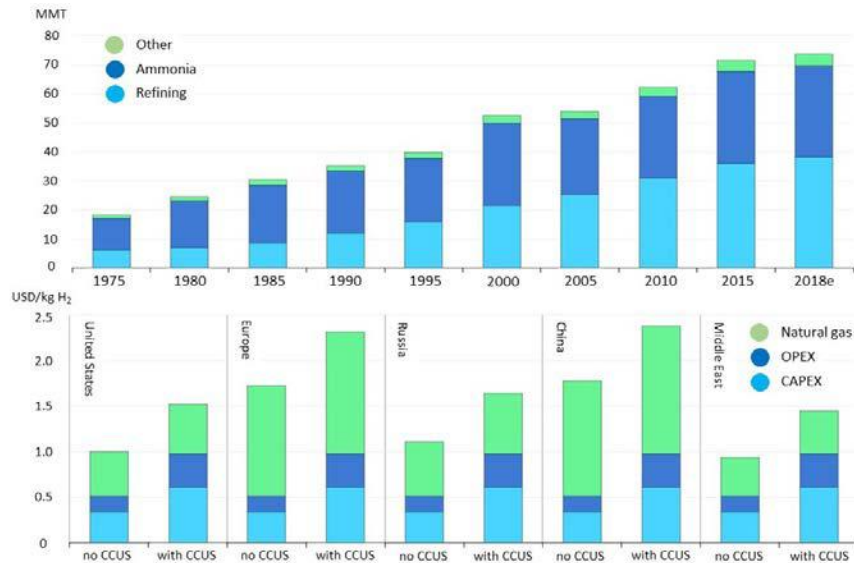
The round trip efficiency:

$$\begin{aligned}\eta_{round} &= \frac{\text{energy recovered during discharging}}{\text{energy added during charging}} \\ &= \frac{\text{energy recovered}}{\text{energy stored}} \cdot \frac{\text{energy stored}}{\text{energy added}} \\ &= \eta_{charge} \eta_{discharge}\end{aligned}$$

Hydrogen Production

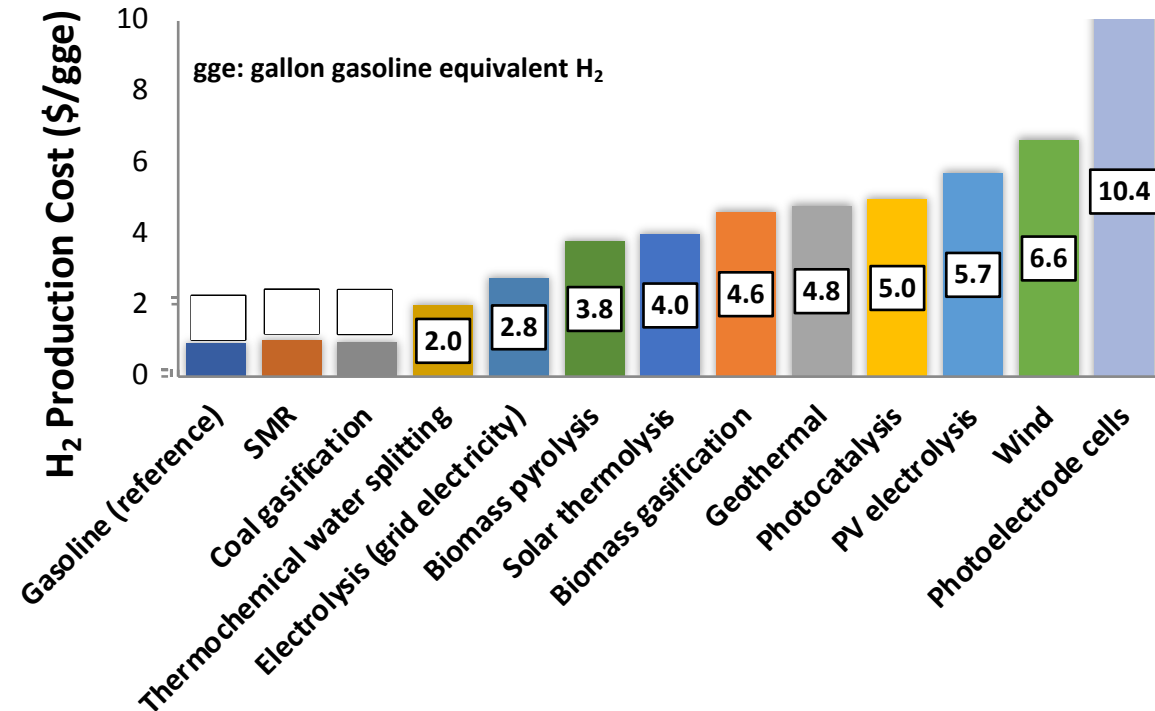
Hydrogen

Worldwide production and cost based on SMR



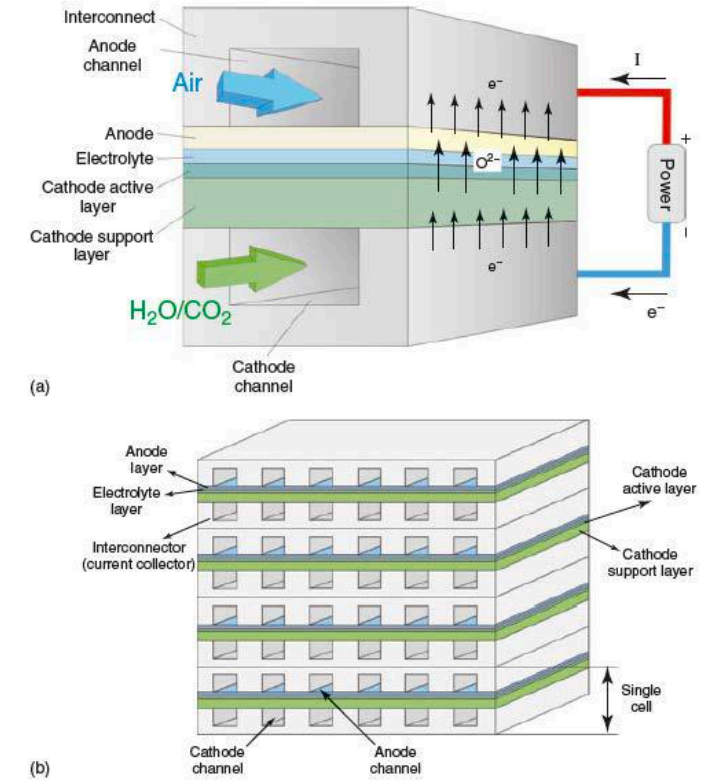
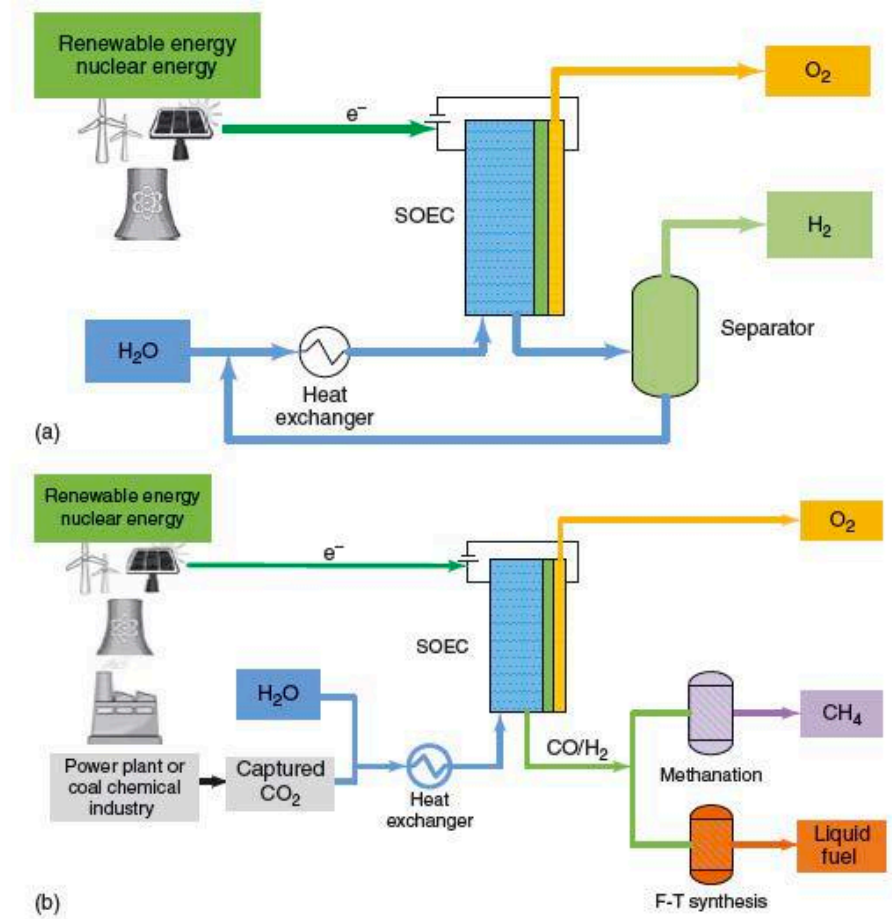
© IEA. All rights reserved. This content is excluded from our Creative Commons license. For more information, see <https://ocw.mit.edu/fairuse>.

IEA Technology Report, June 2019,
<https://www.iea.org/reports/the-future-of-hydrogen>.



- Steam reforming has reached peak efficiency (**70-85%**)
- Novel technology needs to be developed to reach the goal
- Alternatives needed for zero CO₂ emissions

Electrolysis for production of H₂ and/or co-production of H₂/CO and synthesis fuels



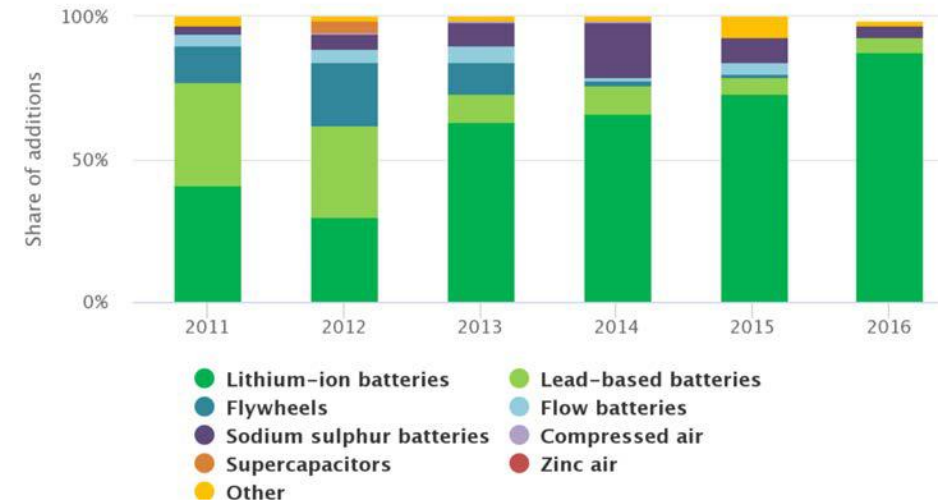
(a) Single element
(b) A stack

© John Wiley & Sons, Inc. All rights reserved. This content is excluded from our Creative Commons license. For more information, see <https://ocw.mit.edu/fairuse>.

Batteries

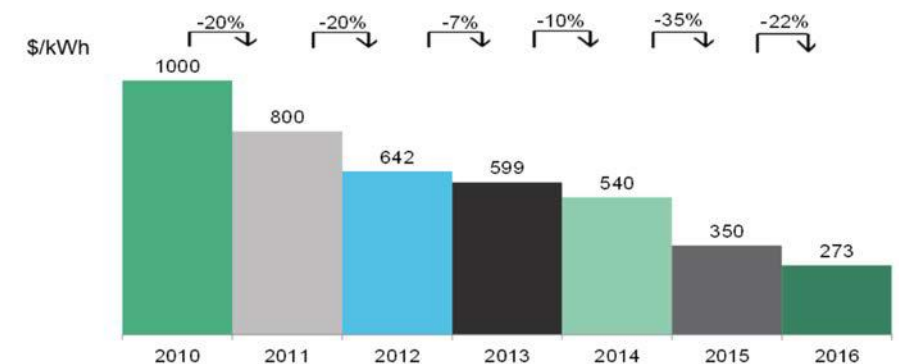
- Similar to fuel cells in that they convert chemical to electrical energy directly, and the secondary type can reverse the reactions
- But they store their chemicals internally in their electrodes (except for flow batteries)
- Have seen a very wide range of applications, at many scales for centuries!
- Still relatively expensive for large scales storage deployment, although convenient.
- Also heavier than ideal in mobile application.
- Must be carefully managed thermally to avoid thermal run away and fires.

Share of annual battery storage additions, by technology



© Source unknown. All rights reserved. This content is excluded from our Creative Commons license. For more information, see <https://ocw.mit.edu/fairuse>.

BNEF lithium-ion battery price survey, 2010-16 (\$/kWh)



© Bloomberg Finance LP. All rights reserved. This content is excluded from our Creative Commons license. For more information, see <https://ocw.mit.edu/fairuse>.

Gravitational Energy Storage: (1) Pumped Hydro Electric Systems (PHS)

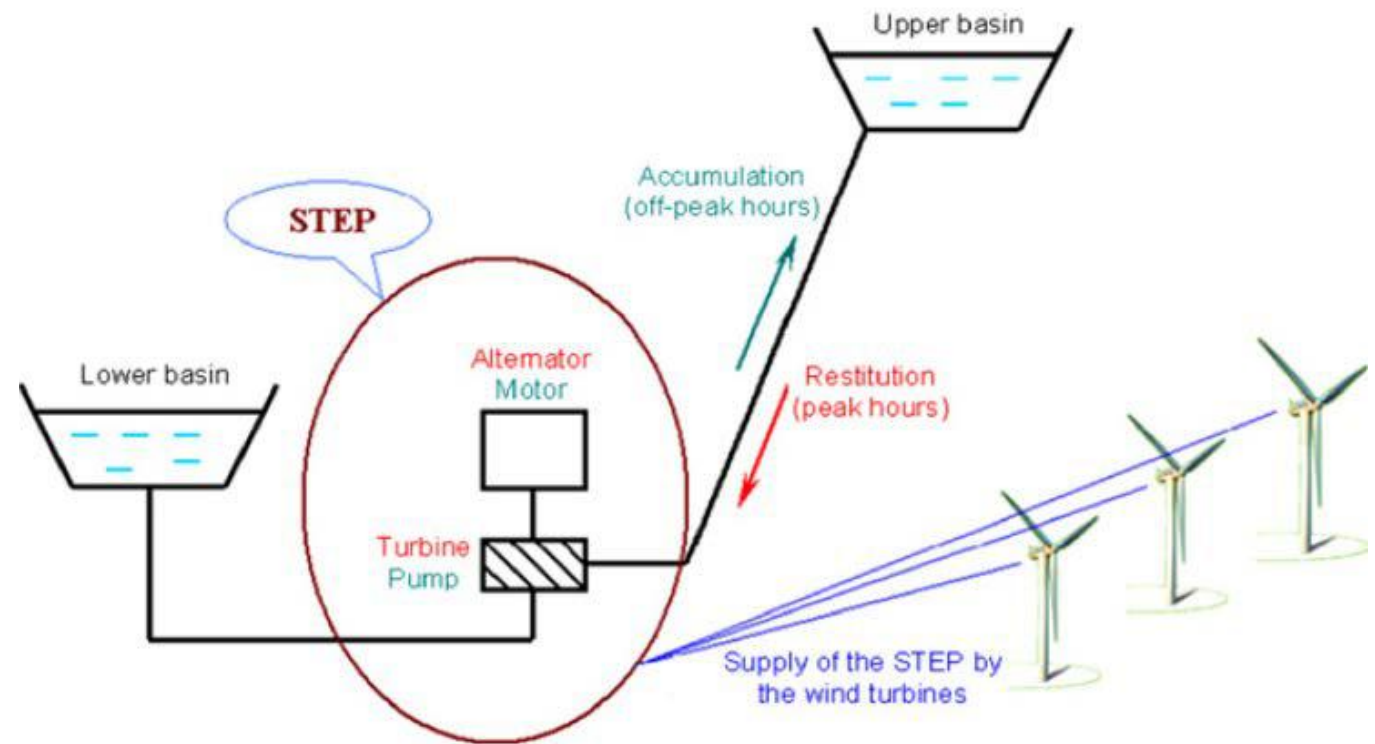
Significant Energy Capacity: $E = Mgh = \rho \nabla_{\text{water}} gH \sim 10^4 \nabla H \text{ J}$

take $H = 10 \text{ m}$, $E = 0.1 \nabla_{\text{water}} \text{ MJ}$

take $\nabla_{\text{water}} = 100 \times 100 \times 10 \text{ m}$, $E = 10 \text{ GJ}$

Power: $\wp = \dot{m}gH$

for the same case, $\wp \sim 0.1 \dot{m} \text{ kJ}$

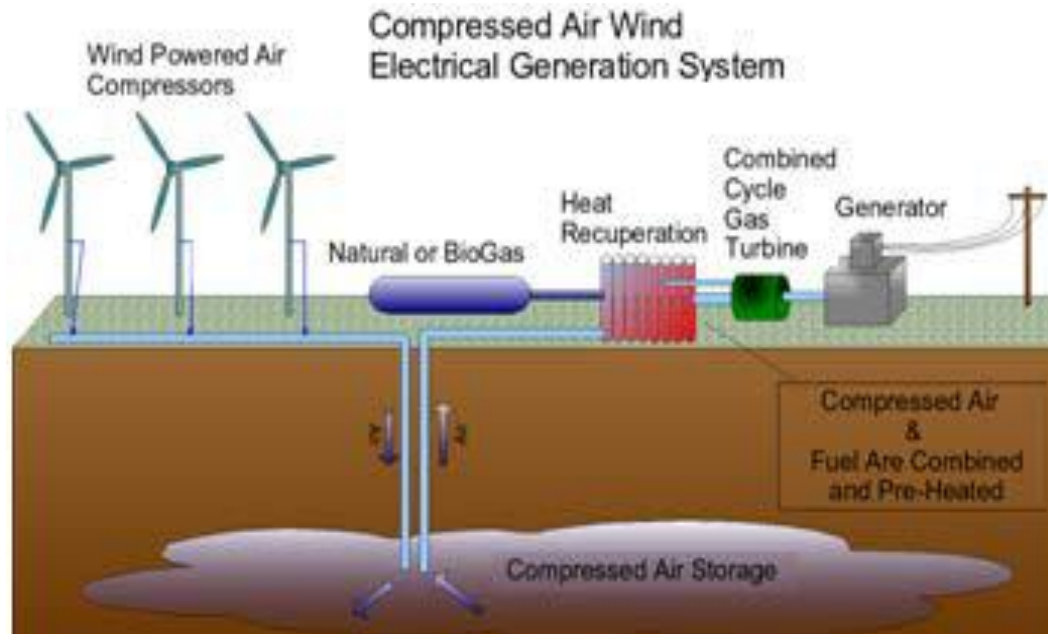


© Allen Institute for AI. All rights reserved. This content is excluded from our Creative Commons license. For more information, see <https://ocw.mit.edu/fairuse>.

Gravitational Energy Storage: (2) moving solids!

Will be covered by some of you in the projects presentations

Energy Storage: Compressed Air Storage (CAES)



© Source unknown. All rights reserved. This content is excluded from our Creative Commons license. For more information, see <https://ocw.mit.edu/fairuse>.

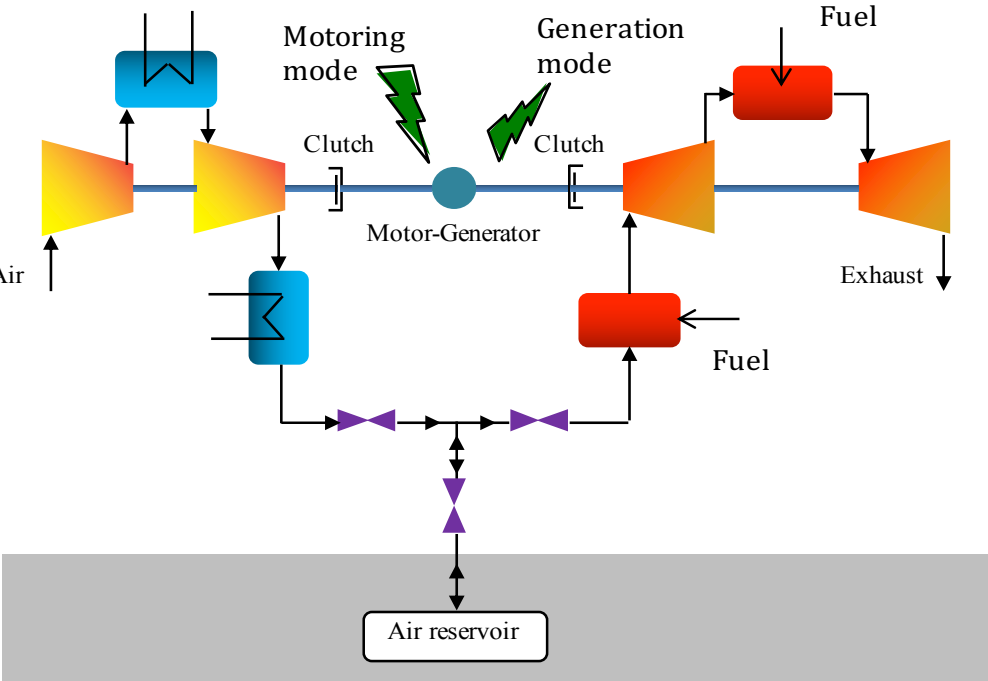


© Applied Energy. All rights reserved. This content is excluded from our Creative Commons license. For more information, see <https://ocw.mit.edu/fairuse>.

Components of a CAES layout system (from Kim et al, Copyright Applied energy, 2012 – Exploring the concept of compressed energy storage (CAES) in lined rock caverns at shallow depth: A modeling study of air tightness and energy balance, Kim, H-M., Rutqvist, J., Ruy, D-W., Choi, B-H., Sunwoo, C., Song, W-K, Applied energy Vol. 92, pp. 653-667, 2012).

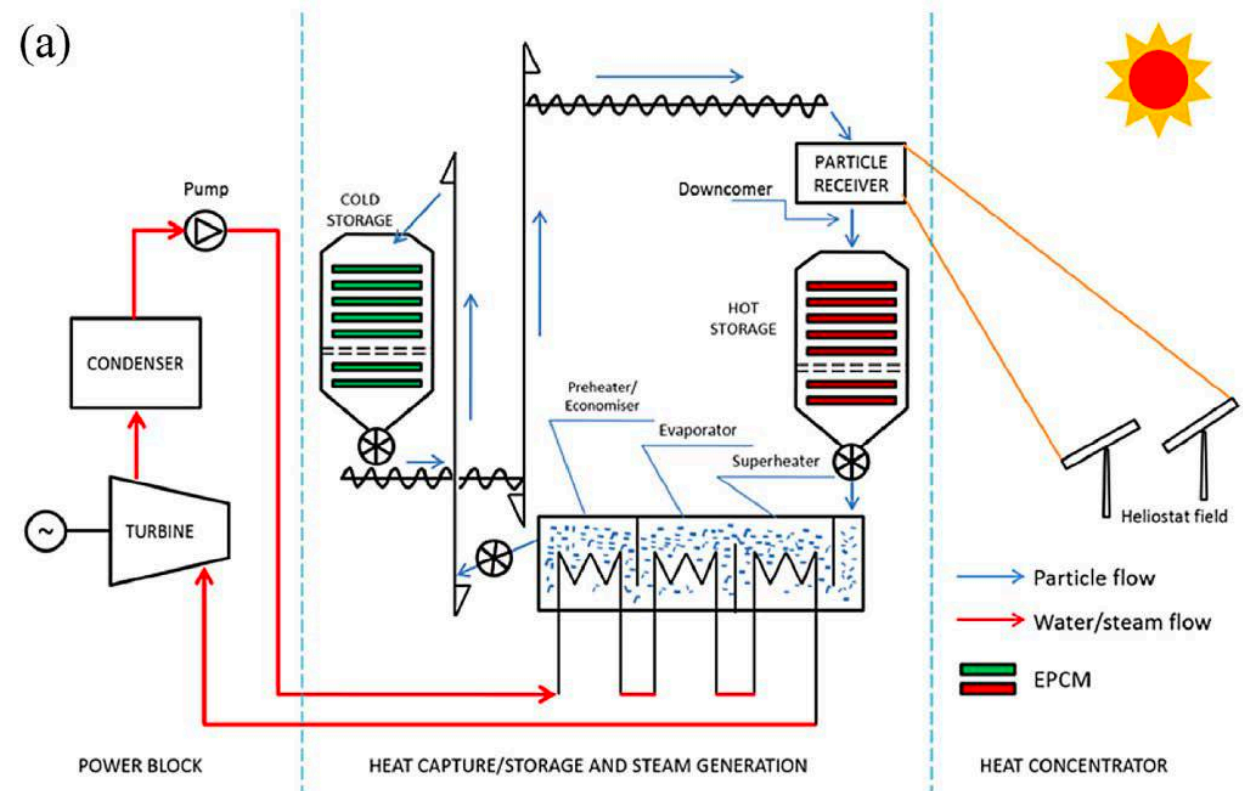
Table Typical performance data of compressed air energy storage (CAES) systems.

	Huntorf, Germany	McIntosh, Alabama	Sunagawa, Japan
Capacity, MW	290	110	35
Generation, hours	2	26	6
Compression, hours	4	1.6	1.2
Volume, 10 ³ m ³	311	538	30
Cavern temperature,	35	35	50
Expander train:			
High pressure			
Inlet pressure, bars	46	45	40
Inlet temp, °C	540	540	800
Low pressure			
Inlet pressure, bars	11	15	15
Inlet temp, °C	670	670	1250
Expander mass flow, kg/s	415	154	47
Recuperator	No	Yes	Yes



Thermal energy storage and recovery

- Should store heat at the highest economically and practically possible temperature to save space and improve the power cycle efficiency (while avoiding corrosion, thermal stresses, chemical transformation, etc.)
- Need a medium to transport the heat, it should have high heat capacity and should be easy to transport, either a fluid or a fluid like medium
- Need a storage medium/tank for the high temperature heat, and another for the low temperature medium.
- The storage medium should have high gravimetric (ρc_p) or volumetric heat capacity. May or may not be the same as the heat transport medium.

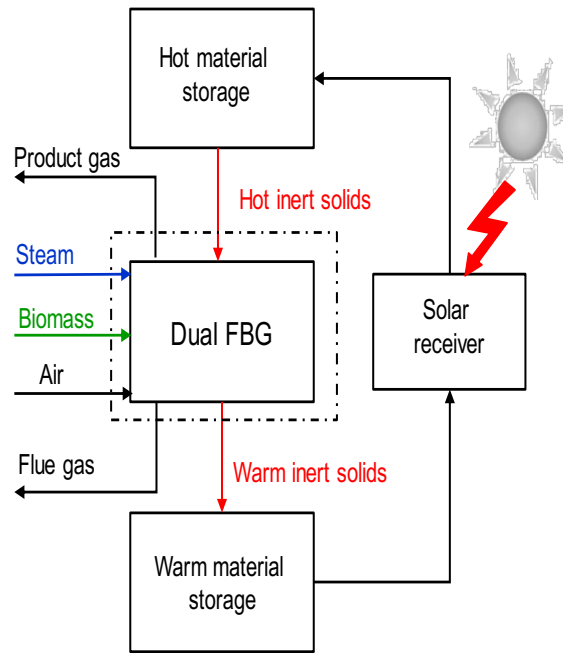


© Pyramid Educational Consultants, Inc. All rights reserved. This content is excluded from our Creative Commons license. For more information, see <https://ocw.mit.edu/fairuse>.

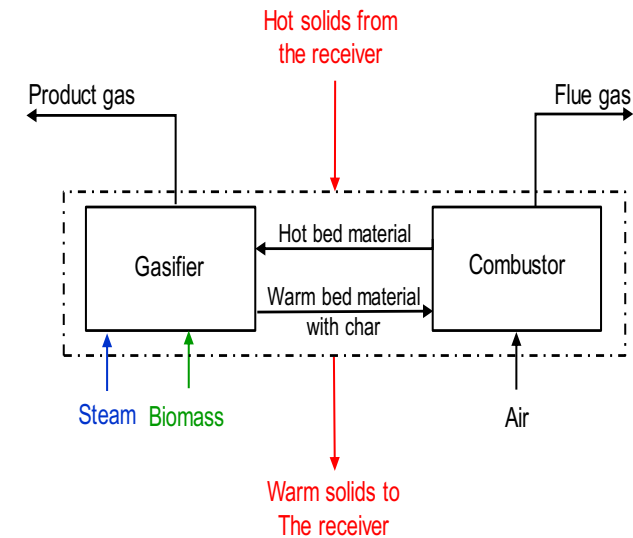
Powder or particulates (50-100 microns) are heated up in the solar receiver and transported/conveyed mechanically and by gravity to a high T storage tank, a heat exchanger to raise steam for the power cycle, then to a low T storage tank before going back to the receiver.

Thermal energy storage in the form of chemical*

- Steam gasification of biomass (or coal or natural gas) is an endothermic process. The produced syngas can be stored for later use.
- Typically the heat added is equivalent to $\sim 25\%$ of the heating value of the original fuel.
- In case of solar energy, it is difficult (expensive) to get solar heat above 700 C, the temperature required for gasification.
- In this case some of the biomass can be burned to provide heat to supplement the solar heat.
- Using a dual bed gasifier makes it possible to separate the combustion (of char) from the gasification (of the volatiles and some char), and hence producing pure syngas (without nitrogen) while using air for combustion.
- Therefore, separate gasifier and combustor are used with “bed” material (sand) circulating in between the two and the solar receiver.



(a)



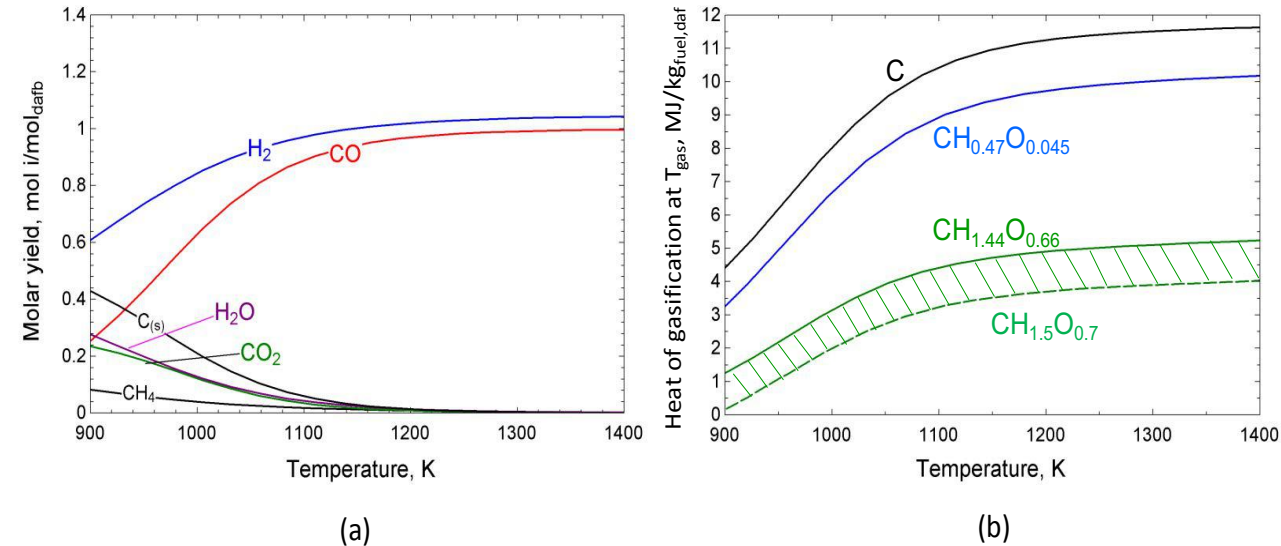
(b)

Layout of a solar-biomass gasification system: (a) Biomass gasifier in a solar loop with a solid particles receiver; (b) Steam gasification in a dual fluidized bed gasifier (SDFBG)

The thermochemistry (mass and energy balance) of biomass steam gasification



- The heat required for gasification increases with temperature, until the fuel is converted in CO and H₂.
- At ~ 1000-1200 K, and for biomass with LHV of ~18-18.5 MJ/kg_{bio} the heat of gasification is 3.5-5.5 MJ/kg_{bio}.
- Thus, gasification stores more energy in the fuel, ~ 20-35% more than the original.
- Heat. Required for biomass (marked in green) is well below that for char (blue) and pure carbon (C in black).
- Clearly, the higher the carbon-to-hydrogen ratio the larger the heat of gasification and the more water is needed.



The effect of temperature on: (a) the molar gas yields of the main species for steam gasification of biomass according to R1 (Tars and other light hydrocarbons are not depicted since their concentrations are very low compared to the rest of species included in the figure). (b) specific heat of steam gasification according to R1 (per kg of daf fuel) for different fuels: carbon, char and biomass (the hatched region in the figure corresponds to a typical biomass). Simulation corresponds to equilibrium predictions with $\text{ER}_{\text{H}_2\text{O}} = 1$.

System operation during the day and night

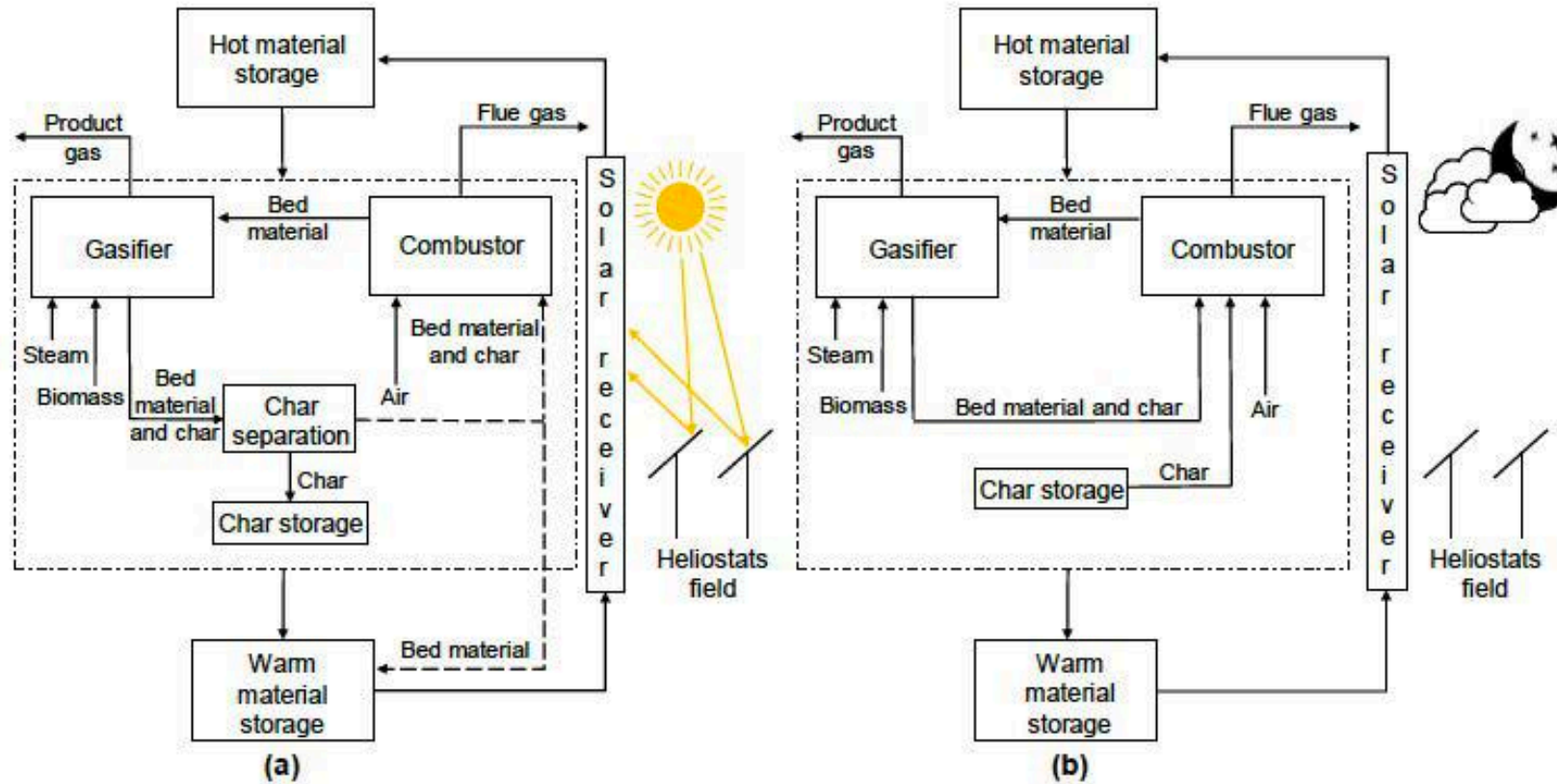


Fig. 2. Operation of the system with char separation and storage: (a) char separation and storage when solar energy is available; (b) discharge of the char storage in absence of solar energy

(Very) High-temperature energy storage

Firebrick resistance heated energy storage “FIRES”

D. Stack (2.62-2016)*

- Firebrick can go up to $> 1600\text{ C}$
- Thermal capacity $\sim 1\text{MWh/m}^3$ or 3.6 GJ/m^3
($DT \sim 1000\text{ C}$ and $mc_p \sim 3.6\text{ MJ/m}^3\text{ K}$)
- [note that for water has high $mc_p \sim 4.2\text{ MJ/m}^3\text{ K}$ but it is DT that makes firebrick superior]
- Can be heated electrically (resistance of inductive heating which is more efficient) to achieve the desired temperature.
- Discharged by blowing cooler air through the honeycomb structure
- Hot air can power a closed Brayton cycle or a ScCO_2 cycle for higher efficiency
- Operating these cycles at higher max temperature improves the storage round-trip efficiency defines as: (electricity out/electricity in).



Figure 8: Firebrick regenerator for a glass furnace¹⁹

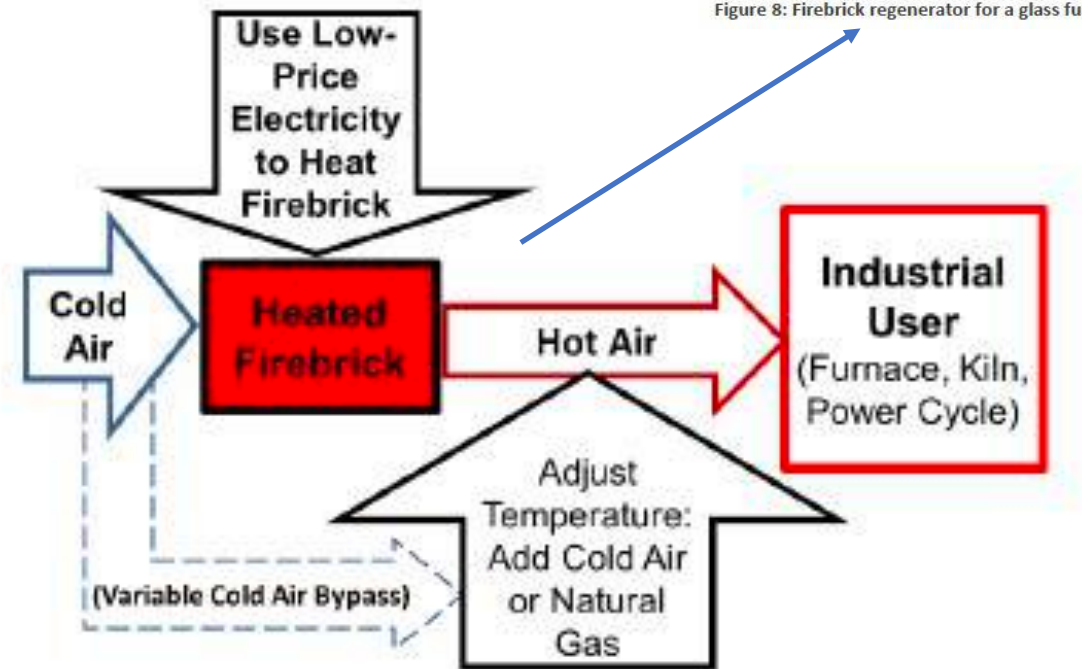


Figure 10: General Schematic of FIRES Implementation

* Also D. Stack M.Sc. Thesis at MIT, same year)

- Same concept proposed for nuclear power plant.
- Air for the Brayton cycle is preheated using molten salt (used to cool the nuclear reactor).
- Next, the warm air is heated by the hot firebricks, before going to the gas turbine.
- When excess electricity is generated (overnight!), it is stored in the form of high T heat in the firebricks.
- For “peak power” or when the firebricks are cold, some natural gas can be used.
- This flexibility can reduce cost.
- Using heat from the firebrick, and hybridizing with natural gas, makes it possible to operate a high efficiency combined cycle (>60%).
- Depending on the thermodynamic cycle used for heat-to-power, the round trip efficiency of firebrick storage is 40-60%.

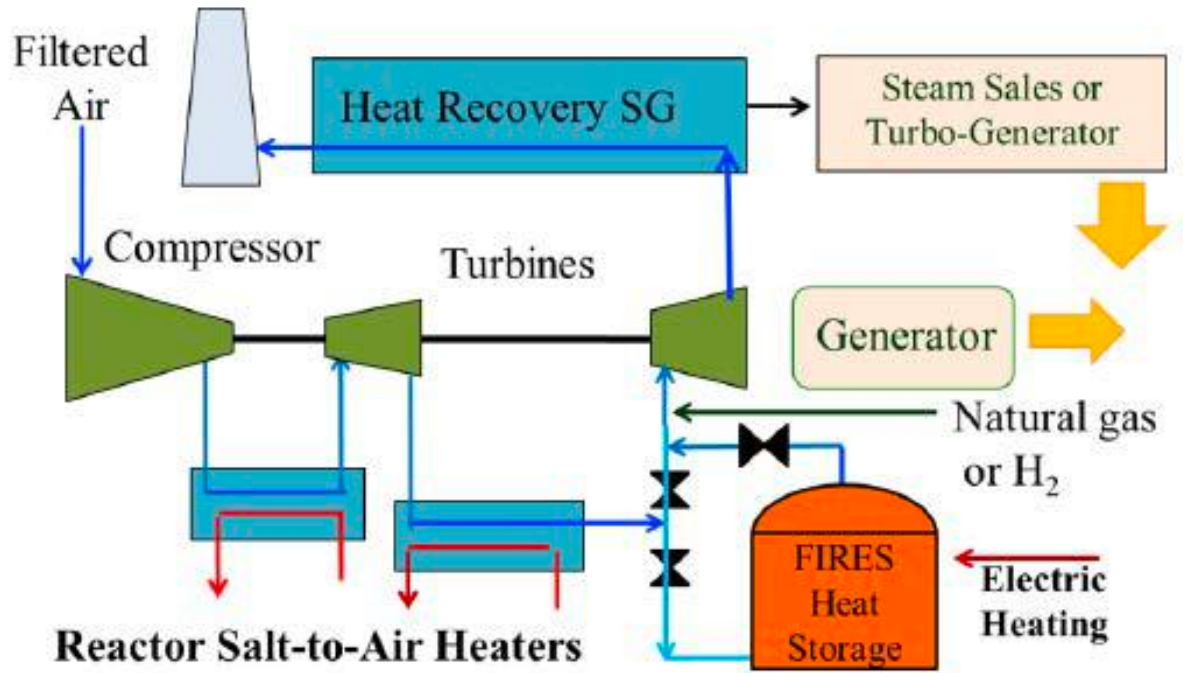
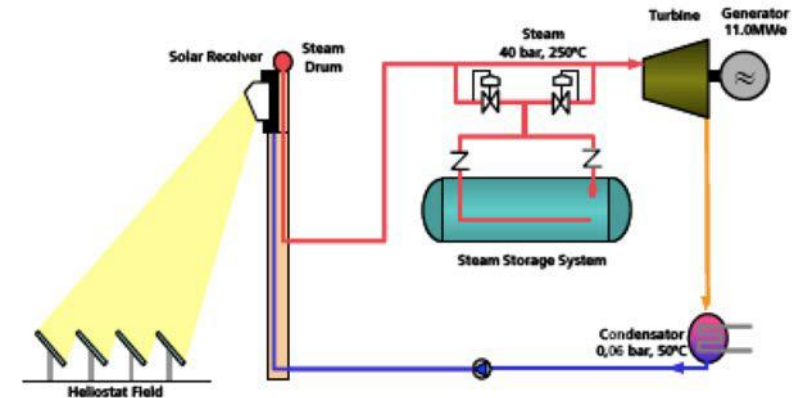


Figure 11: Schematic of FIRES implemented with the FHR NACC²¹

© Source unknown. All rights reserved. This content is excluded from our Creative Commons license. For more information, see <https://ocw.mit.edu/fairuse>.

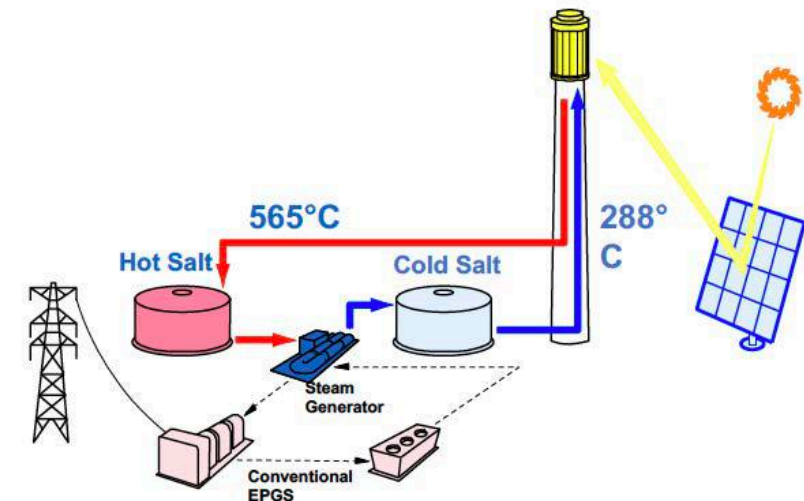
THERMAL ENERGY STORAGE

- A lot cheaper than storing electricity
- Can be deployed at large scale
- Different media can be used at different hot temperature
- Thermal energy can be stored as sensible or latent energy
- Depending on the design, wither the hot working fluid or the hot heat transfer fluid.
- Thermal energy is recovered by either media
- The storage media can be fluid or solid, adding or recovering heat from the storage medium vary.
- In the case of liquid, two tanks, hot and cold, are used, or a single tank with a thermocline.
- Thermal energy storage is compatible with power cycles (mostly steam Rankine cycle, but supercritical CO2 have also been considered)
- It is also possible to store electricity in the form of high temperature thermal energy, and convert that back to electricity at a reasonable round trip efficiency.



© Abengoa. All rights reserved. This content is excluded from our Creative Commons license. For more information, see <https://ocw.mit.edu/fairuse>.

Dispatchable Power Requires Storage



© John Wiley & Sons, Inc. All rights reserved. This content is excluded from our Creative Commons license. For more information, see <https://ocw.mit.edu/fairuse>.

THERMAL ENERGY STORAGE

Characteristics of sensible heat storage solids and liquids

Storage medium	Temperature range		density kg/m ³	heat	heat
	Cold C	Hot (C)		conductivity W/mK	capacity kJ/kg K
Sand-rock-mineral oil	200	300	1700	1	1.36
Reinforced concrete	200	400	2200	1.5	0.85
NaCl (solid)	200	500	2160	7	0.85
Magnesia fire bricks	200	1200	3000	1	1.15
Synthetic oil	250	350	900	0.11	2.3
Silicon oil	300	400	900	0.1	2.1
Nitrate salts (liquid)	265	565	1870	0.52	1.6
Carbonate salts (liquid)	450	850	2100	2	1.8
Liquid sodium	270	530	850	71	1.3
Silicon carbide	200	1400	3210	3.6	1.06
SiO ₂ (cristobalite)	200	1200	2350	0.92	1.13

© Pyramid Educational Consultants, Inc. All rights reserved. This content is excluded from our Creative Commons license. For more information, see <https://ocw.mit.edu/fairuse>.

Phase Change Material (PCM)

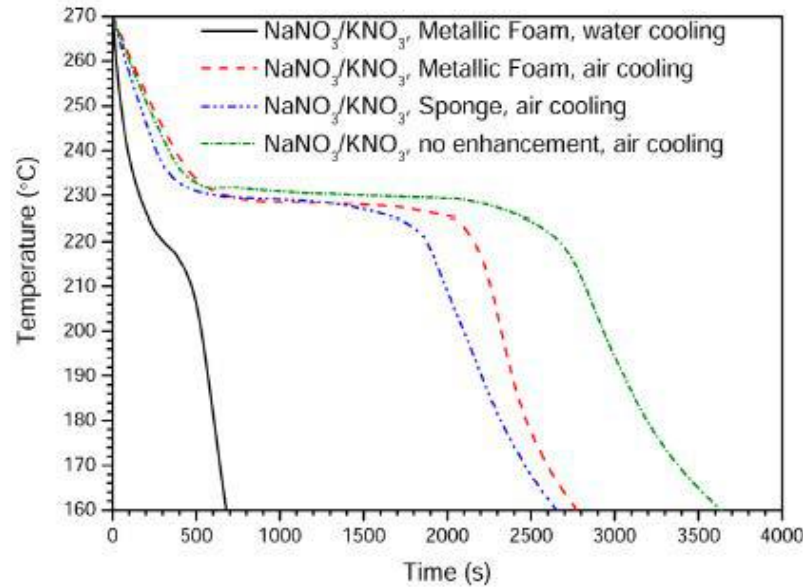


Fig. 11. Temperature vs. time cooling of the E-PCM (nitrates) [27]. Air-cooling of liquid PCM (1) no inserts; (2) metallic sponge; (3) metallic foam. Air-cooling of solid PCM (4) no inserts; (5) metallic sponge; (6) metallic foam; water-cooling of (7) liquid PCM + foam; and (8) solid PCM + foam.

Melting point °C	Heat of fusion kJ/kg	Density kg/m ³	Specific heat kJ/kg K	Thermal conductivity W/m.K
142	84	1990	1.34	0.6
307/308	74	2260/2257	NA	0.5
318	290	2000	1.85	1.0
333/336	266	2110	NA	0.5
350	215	2250	0.96	0.95
380	150	2044	NA	0.5
380	400	1800	0.96	NA
767	790	2100/2670	1.97/1.84	1.7/5.9

Zhang et al., PECS 53 (2016) 1

© Pyramid Educational Consultants, Inc. All rights reserved. This content is excluded from our Creative Commons license. For more information, see <https://ocw.mit.edu/fairuse>.

Hitec: KNO₃—NaNO₂—NaNO₃

NaNO₃

65.2%NaOH—20%NaCl—14.8%Na₂CO₃

KNO₃

22.9% KCl—60.6% MnCl₂—16.5% NaCl

KOH

MgCl₂/KCl/NaCl

80.5% LiF—19.5% CaF₂ eutectic

Thermochemical Energy Storage

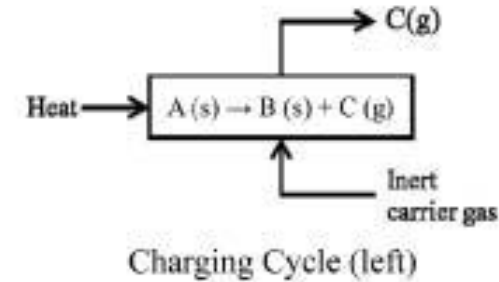
Zhang et al., PECS 53 (2016) 1

The equilibrium T_{eq} for the reaction is T when the driving force for moving the reaction in either direction is zero, corresponding to the equilibrium constant = 1.

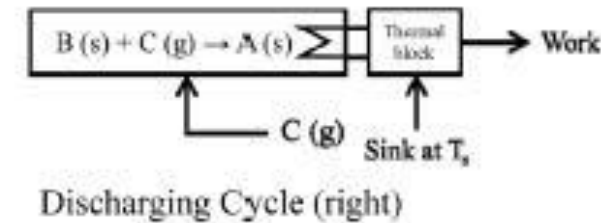
$$\Delta G_R(T_{eq}, p) = 0, \text{ and } T_{eq} = \frac{\Delta H_R(T_{eq}, p)}{\Delta G_R(T_{eq}, p)}$$

at $T < T_{eq}$, reaction releases heat and moves towards reactants

at $T > T_{eq}$, reaction gains heat and moves towards products



Adding heat at high T



Taking heat out at lower T to do work (power cycle)

Possible reaction pairs.

Reaction

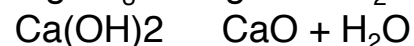
T_{eq} °C
(p=1 atm) ΔH_R (kJ/kg)
at T_{eq}



259 1396



303 1126



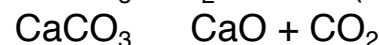
479 1288



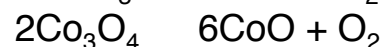
490 868



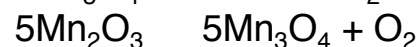
573 137



839 1703



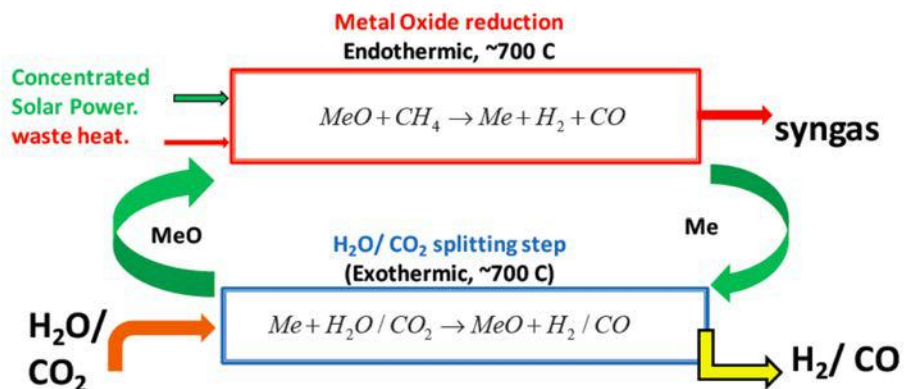
870 844



906 185

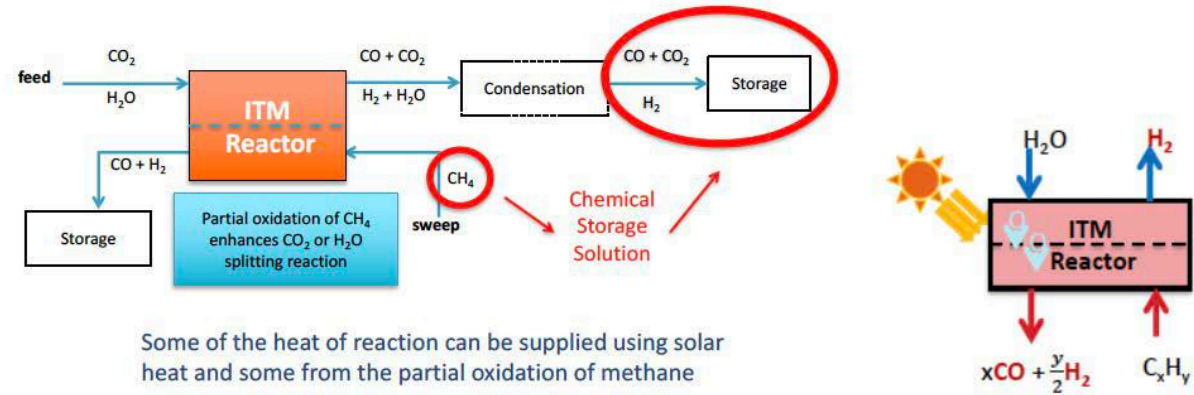


1586 1237



Ripe area for research and development

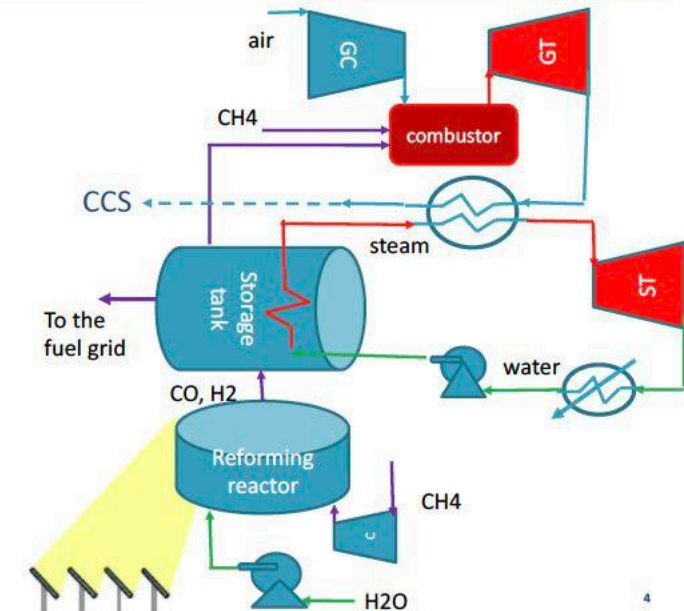
High T Ion (O_2) Transport Membrane Reactors for combined H_2 /Syngas Production; significant synergy



Hybrid Power Plant with integration and co-production

Thermochemical fuel production can extend the storage potential significantly and supply the fuel network

E. J. Sheu, E. M. A. Mokheimer, and A. F. Ghoniem.
Int. J. Hydrogen Energy, 40: 12929, 2015
 E. J. Sheu and A. F. Ghoniem. Receiver Reactor
 Concept and Model Development for a Solar
 Steam Redox Reformer, *Solar Energy*, 2015



Courtesy Elsevier, Inc., <http://www.sciencedirect.com>. Used with permission.

MIT OpenCourseWare
<https://ocw.mit.edu/>

2.60J Fundamentals of Advanced Energy Conversion
Spring 2020

For information about citing these materials or our Terms of Use, visit: <https://ocw.mit.edu/terms>.

Homework 1

2.60/2.62/10.390 Fundamentals of Advanced Energy Conversion
Spring 2020

Total points: 100 (Undergraduate) | 150 (Graduate)

Problem 1. Compressed Air Storage [40 points for Undergrads and Grads]

Compressed air storage (CAS) has been used to store energy (electricity generated by renewable or other sources) in the form of compressed air in underground caverns.

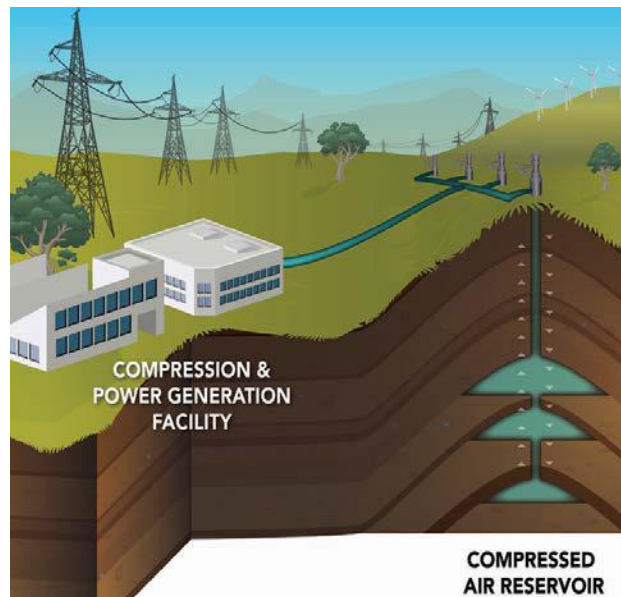


Figure 1: Illustration of a compressed air energy storage system (Courtesy of Pacific Northwest National Laboratory.)

In order to increase the mass of high-pressure air stored in the available volume of the cavern, air may be cooled after compression using a liquid. The heated liquid is then stored in a separate tank. This is the charging process. During discharging, the high-pressure air from the air cavern, and the hot liquid from the tank are used to generate work (electricity) by expanding the air, and extracting heat from the salt tank, respectively, using heat engines interacting with the environment. The overall system (air tank, molten salt tank and heat engines) acts as a giant “thermo-mechanical” battery. In this problem we use an insulated tank to stored high-pressure air, and another insulated tank of molten salt to store the thermal energy, and generic heat engines to generate work from the stored energy.

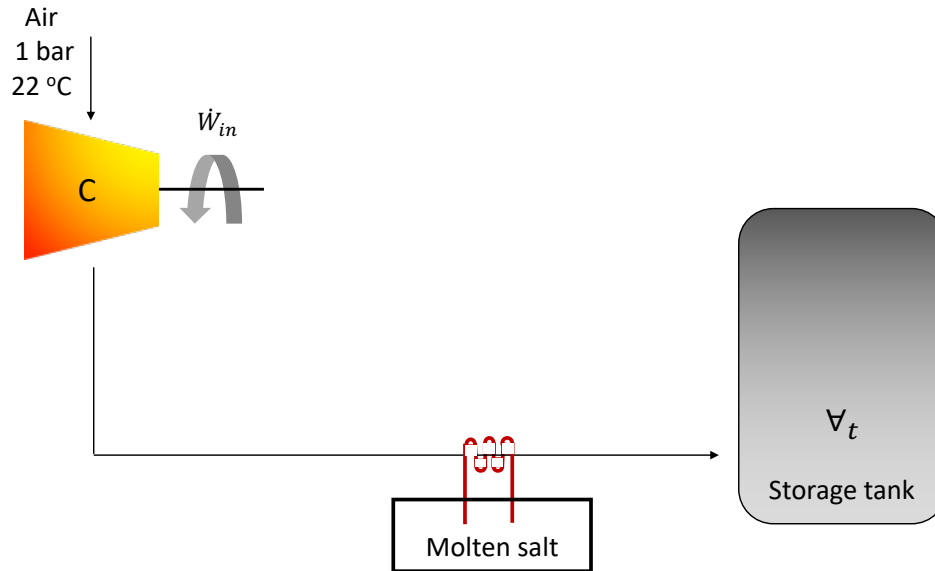


Figure 2: Schematic of the proposed compressed air storage system

The air tank volume is 1000 m³. The molten salt mass in the tank is 100 ton (10⁵ kg). The specific heat of the salt is 1,500 J/kg °K. The conditions of the gas in the tank when fully discharged is $p = 1$ bar and $T = 22$ °C. The temperature of the salt in the tank when fully discharged is 300 °C (to maintain the salt in the liquid phase). When fully charged, the conditions in the air tank are: $p = 100$ bar and $T = 600$ °C. When fully charged, the conditions in the salt tank are: $T = 600$ °C. Atmospheric conditions are $p = 1$ bar and $T = 22$ °C.

Calculate:

- The energy stored in both tanks between the fully charged state and discharged state. [5 points]
- The work required by the compressor train to charge the system of the air tank and the salt tank. The compressor train operates adiabatically. [10 points]
- The maximum work that can be extracted from the molten salt tank starting with the fully charged state. [5 points]
- The maximum work that can be extracted from the gas tank starting with the fully charged state. [10 points]
- Assume that the second law efficiency of the machinery used to extract work from the gas tank is 70% and that of the machinery used to extract work from the salt tank is 60%, what is the round-trip efficiency of this storage system. [5 points]
- How long does it take to charge the system using a wind turbine operating at 1 MW. [5 points]

Problem 2. Claude Cycle [Undergrads: 40 Points | Grads: 50 Points]

A schematic of Claude cycle is shown in **Figure 3**. It is identical to the Linde-Hampson cycle except that the high-pressure hydrogen stream is split after heat exchanger 1. A fraction of the high-pressure hydrogen is expanded to the low pressure in a turbine producing some of the work needed by the compressor. This also makes it possible to eliminate the liquid N_2 bath. Following expansion, this stream is mixed with the gas exiting heat exchanger 3 to provide the cooling in heat exchanger 2. The portion of the high-pressure hydrogen stream bypassing the turbine is cooled in heat exchangers 2 and 3, and expanded through the valve. The liquid is passed to the liquid receiver, and the vapor is recycled to provide cooling for the incoming high-pressure stream of the gas. Assume that:

1. All the heat exchangers are perfectly insulated.
2. The two streams from the make-up gas and the exit of the heat exchanger 1 have the same temperature and pressure.
3. The streams exiting the turbine and heat exchanger 3 have the same temperature and pressure.
4. 50% of the high-pressure hydrogen stream leaving heat exchanger 1 is sent through the turbine, and the turbine isentropic efficiency is 80%.

The states are shown in **Table 1**.

- a. Draw schematically the T-s diagram of the Claude cycle. [10 points]
- b. Calculate the mass of liquid H_2 produced in the hydrogen liquid separator per 1 kg of H_2 at state 2. [5 points]
- c. Determine the pressure and temperature of H_2 at states 1-9. [15 points]
- d. Calculate the work produced by the turbine per 1kg of the produced liquid H_2 . [5 points]
- e. Determine the total work required to produce 1 kg of liquid hydrogen. [5 points]
- f. **(for Grads only)** Determine the second law efficiency of the Claude cycle. [10 points]

State	Temperature [K]	Pressure [atm]
1	298	1
2	298	100
3	160	100
10	125	1

Table 1: Summary of states

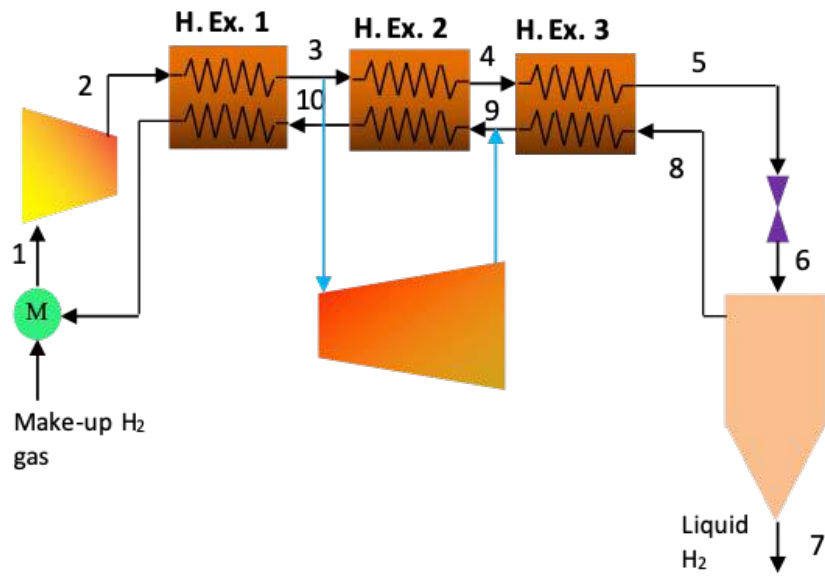


Figure 3: Claude cycle schematic

Problem 3. Desalination [Undergrads: 20 Points | Grads: 60]

Water scarcity is a rising global challenge. The United Nations estimates that 1 in 2 people will experience water scarcity by 2050¹. The magnitude of the challenge prompted the World Economic Forum to classify water crises for the first time as the top global risk facing humanity in terms of impact in 2015².

Tapping into Earth's most abundant resource, desalination, that is the removal of a significant fraction of the salt (NaCl), provides a potential solution. However, seawater desalination is an energy intensive process. At its core, desalination is a separation process that aims to remove salt and produce a stream of pure water using thermal or mechanical energy.

Consider the desalination of seawater at standard temperature and pressure. Seawater is modeled as a 1% concentration by mass of NaCl. We can assume that:

1. The solution is an incompressible liquid with ideal entropy of mixing and zero enthalpy of mixing.
2. The molar heat capacity of seawater is constant and equal to the molar heat capacity of pure water.
3. The density of seawater is constant and equal to the pure water density.

The objective is to produce 1 kg/s of pure water from 2 kg/s of seawater. In the desalination process, there are two outlet streams: the product or permeate (pure water) and the brine or concentrate (the remaining solution).

- a. Calculate the brine flow rate and composition. [5 points]
- b. Calculate the minimal work transfer rate (also known as the least work of separation if expressed in kJ/m³ of product). [15 points]

Note that in a liquid mixture, the entropy of component i is approximately $s_i = s_i^\circ - R \ln X_i$.

Hint: For an incompressible liquid $h = c(T - T_0) + pv$.

¹ "The United Nations World Water Development Report 2018: Nature-Based Solutions for Water.," WWAP (United Nations World Water Assessment Programme)/UN-Water. 2018., Paris, UNESCO, 2018.

² <http://reports.weforum.org/global-risks-2015/executive-summary/>

For Grads only.

Two technologies, thermal and membrane-based, are to be analyzed in this problem.

Technology I: Once-Through Boiling

Once-through boiling is the most basic thermal desalination method, which heats the seawater feed to the boiling point, bringing about fresh water vaporization. You can ignore the boiling point elevation and any change in the enthalpy of vaporization associated with the addition of salt.

- c. Draw a flow diagram for the once-through boiling process. [2.5 points]
- d. Calculate the required heat transfer rate. [5 points]
- e. What work transfer rate could this heat transfer rate produce in an ideal heat engine, assuming that the heat source is at the boiling temperature of water? What is the ratio of this work transfer rate to the minimal work transfer rate? [5 points]
- f. Propose an improvement for this design. [5 points]

Technology II: Reverse Osmosis (RO)

Osmosis refers to the movement of water across the membrane from a region of low salt concentration to that of a higher salt concentration. This transport of water is caused by the buildup of a pressure difference between the two sides of a membrane due to a difference in the chemical potential of water. For more information about osmosis, please refer to Physical Chemistry by P.W. Atkins or <https://en.wikipedia.org/wiki/Osmosis>.

While desalination has historically been a thermal process, the invention of Reverse Osmosis (RO) membranes in the 1960's revolutionized the process. In contrast to osmosis, RO produces fresh water by pumping the seawater to a pressure, P_H , higher than the osmotic pressure as shown in **Figure 4**. The osmotic pressure is given by the Morse equation as:

$$\Pi = 2\hat{\rho}_{sol}RT$$

where $\hat{\rho}_{sol}$ is the molar density of the solute in the brine, R is the ideal gas constant, and T is the temperature.

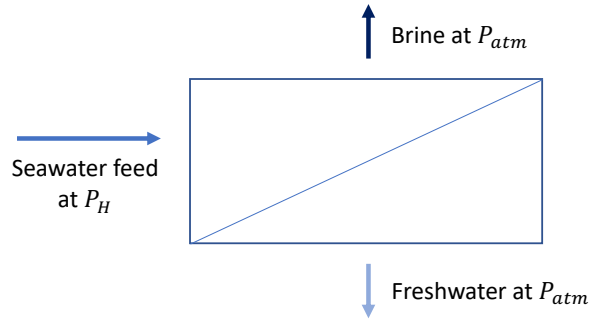


Figure 4: Schematic of the reverse osmosis process

Consider a basic RO process. This consists of a high-pressure pump increasing the pressure of the feed solution from ambient P_0 to the desired operating pressure P_H , and a perfect semipermeable RO membrane through which water can pass, but dissolved ion species cannot.

- g. Draw a flow diagram for the RO process. [2.5 points]
- h. Calculate the minimum pressure for the outlet of the pump and the corresponding work transfer rate. How does this compare to the minimal work transfer rate and why? [10 points]
- i. Calculate the second law efficiency of a RO pump operating at a pressure of 30 bars. [5 points]
- j. Propose an improvement for this design. [5 points]

MIT OpenCourseWare
<https://ocw.mit.edu/>

2.60J Fundamentals of Advanced Energy Conversion
Spring 2020

For information about citing these materials or our Terms of Use, visit: <https://ocw.mit.edu/terms>.

2.62 – Advanced Energy Conversion | Spring 2020

Homework 1 – Solutions

Problem 1

- a) Calculate the energy stored in both tanks between the fully charged state and discharged state:

First, we start by setting a reference state at $T=T_0=22\text{ C}$ and $P=1\text{ atm}$. To simplify the analysis, the specific heats are assumed constant herein. Calculating the energy stored in the thermal mass between its two states:

$$\Delta E_{salt} = M_{salt}c((T_{s2} - T_0) - (T_{s1} - T_0))$$

$$\Delta E_{salt} = (1 \times 10^5 \text{ kg})(1,500 \text{ J/kg}\cdot\text{K})(300 \text{ K})$$

$$\Delta E_{salt} = 4.5 \times 10^{10} \text{ J}$$

Next, we apply a similar approach to calculate the stored energy in the tank:

$$\Delta E_g = ((U_2 - U_0) - (U_1 - U_0))_g$$

$$\Delta E_g = (M_2c_v(T_2 - T_0) - M_0c_v(T_0 - T_0)) - (M_1c_v(T_1 - T_0) - M_0c_v(T_0 - T_0))$$

$$M_0 = M_1 = \frac{P_1 V_t}{RT_1} = \frac{(1 \times 10^5 \text{ Pa})(1,000 \text{ m}^3)}{(287 \text{ J/kg}\cdot\text{K})(295 \text{ K})} = 1,181.1 \text{ kg}$$

$$M_2 = \frac{P_2 V_t}{RT_2} = \frac{(100 \times 10^5 \text{ Pa})(1,000 \text{ m}^3)}{(287 \text{ J/kg}\cdot\text{K})(873 \text{ K})} = 39,912 \text{ kg}$$

$$\Delta E_g = (39,912 \text{ kg} \times 717.5 \text{ J/kg}\cdot\text{K} \times 851 \text{ K}) - (1,181.1 \text{ kg} \times 717.5 \text{ J/kg}\cdot\text{K} \times 0 \text{ K})$$

$$\Delta E_g = 2.44 \times 10^{10} \text{ J}$$

- b) Calculate the work required by the compressor train to charge the system of the air tank and the salt tank. The compressor train operates adiabatically:

To answer this question, we apply the first law of thermodynamics. Assuming the compressor train operates adiabatically:

$$-W + \Delta m_g(h_{in} - h_0) = \Delta E_g + \Delta E_{salt} = \Delta E_g + \Delta E_{salt}$$

$$-W = (2.44 + 4.5) \times 10^{10}$$

$$W = -6.94 \times 10^{10} \text{ J}$$

- c) Calculate the maximum work that can be extracted from the molten salt tank when fully charged:

To find the maximum work extractable, we use the concept of availability:

$$W_{s,max} = \Xi_2 - \Xi_1$$

$$\text{where: } \Xi = (E - U_0) + p(\forall - \forall_0) - T_0(S - S_0)$$

Evaluating this for the molten salt:

$$W_{s,max} = (E_2 - E_1) - T_0 \left(C \ln \frac{T_{s2}}{T_{s1}} \right)$$

$$W_{s,max} = M_{salt} c (T_{s2} - T_{s1}) - M_{salt} c T_0 \left(\ln \frac{T_{s2}}{T_{s1}} \right)$$

$$W_{s,max} = (1 \times 10^5 \text{ kg})(1,500 \text{ J/kg}\cdot\text{K}) \left(300 \text{ K} - 295 \text{ K} \ln \frac{873.15}{573.15} \right)$$

$$W_{s,max} = 2.64 \times 10^{10} \text{ J}$$

- d) Calculate the maximum work that can be extracted from the gas tank when fully charged:

Drawing a control volume around the tank, invoking Equation 2.37 from the text, and following a similar approach:

$$\dot{W}_{g,max} = - \frac{d((E - E_0) - T_0(S - S_0))}{dt} - \dot{m}_{out}((h_{out} - h_0) - T_0(s_{out} - s_0))$$

Maximum work occurs when the air leaves at the dead state (second term goes to zero).

Integrating with time:

$$W_{g,max} = -[(E_{dis} - E_{char}) - T_0((S_{dis} - S_0) - (S_{char} - S_0))]$$

Rearranging:

$$W_{g,max} = (E_2 - E_1) - T_0[(S_2 - S_0) - (S_1 - S_0)]$$

Therefore:

$$E_2 - E_1 = M_2 c_v (T_2 - T_0) - M_1 c_v (T_1 - T_0) = 2.44 \times 10^{10} \text{ J}$$

Likewise:

$$T_0(S_2 - S_0) = T_0 M_2 (s_2 - s_0) = 295 \text{ K} \times 39,912 \text{ kg} \times \left(c_p \ln \frac{T_2}{T_0} - R \ln \frac{P_2}{P_0} \right)$$

$$T_0(S_1 - S_0) = T_0 M_1 (s_1 - s_0) = 0$$

Therefore:

$$W_{g,max} = 2.44 \times 10^{10} \text{ J}$$

$$- (295 \text{ K})(39,912 \text{ kg}) \left(1,004.5 \text{ J/kg}\cdot\text{K} \ln \frac{873.15}{295.15} - 287 \text{ J/kg}\cdot\text{K} \ln 100 \right)$$

$$W_{g,max} = 2.44 \times 10^{10} \text{ J}$$

e) What is the round-trip efficiency of this storage system:

$$\eta_{trip} = \frac{W_{out}}{W_{in}} = \frac{0.6W_{s,max} + 0.7W_{g,max}}{W_{in}} = \frac{1.584 + 1.71}{6.94} = 47\%$$

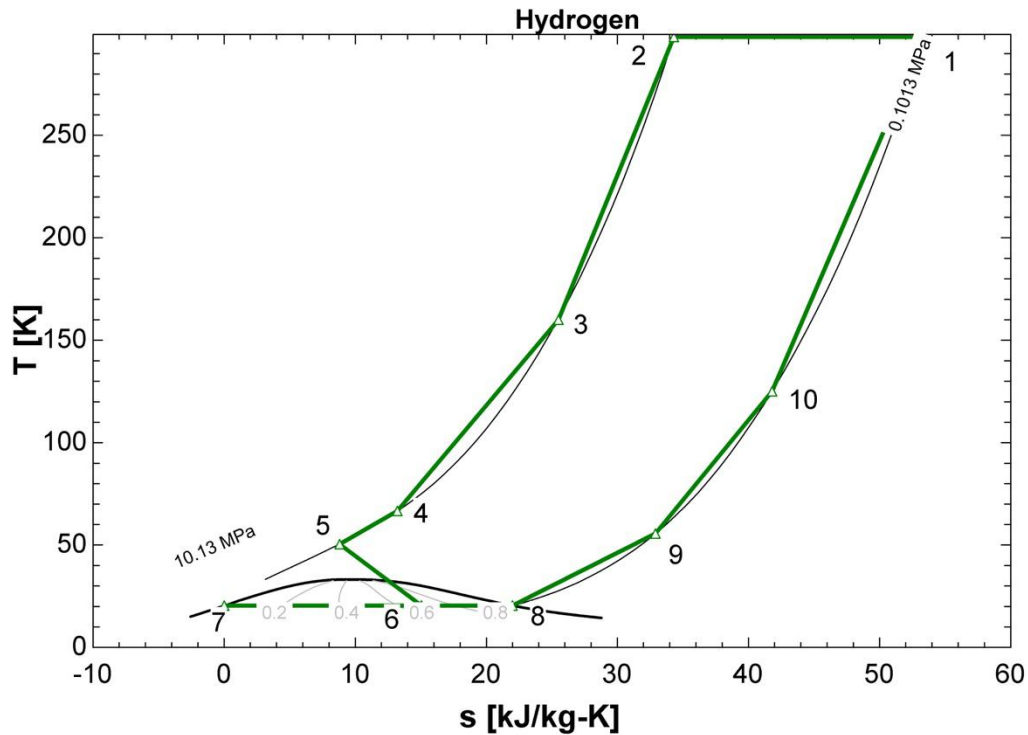
f) How long does it take to charge the system using a wind turbine operating at 1 MW.

$$\Delta t = \frac{W_{in}}{\dot{W}} = \frac{6.94 \times 10^{10} \text{ J}}{1 \times 10^6 \text{ J/s}} = 64,000 \text{ s} \approx 19.2 \text{ hrs}$$

Problem 2

a) Draw schematically the T-s diagram of the Claude cycle:

Using EES, we can plot our states using the Property Plot + Lookup Table (to store states) + Overlay Plot (to add your points from the table):



b) Calculate the mass of liquid H_2 produced in the hydrogen liquid separator per 1 kg of H_2 at state 2:

Start by applying the 1st law to Heat Exchanger 1:

$$\dot{m}_2(h_2 - h_3) + \dot{m}'(h_{10} - h_{11}) = 0$$

Note that:

$$\dot{m}' = \dot{m}_2 - \dot{m}_l$$

Therefore:

$$\frac{\dot{m}_l}{\dot{m}_2} = 1 + \left(\frac{h_2 - h_3}{h_{10} - h_{11}} \right) = 0.1587$$

c) Determine the pressure and temperature of H₂ at states 1-9:

We start from state 7 (saturated liquid):

$$P_7 = P_1$$

$$x_7 = 0$$

State 8 (saturated vapor):

$$P_8 = P_1$$

$$x_8 = 1$$

State 6 (liquid-vapor mixture):

$$P_6 = P_1$$

$$x_6 = \frac{m_v}{m_{tot}} = \frac{m_{tot} - m_l}{m_{tot}} = 1 - \frac{m_l}{m_{tot}} = 1 - 2 \left(\frac{m_l}{m_2} \right) = 0.6826$$

State 9 (Use turbine isentropic efficiency). The only unknown is h_{out} .

$$P_9 = P_1$$

$$\eta_t = \frac{h_{in} - h_{out}}{h_{in} - h_{out,s}}$$

To determine states 4 and 5, we use the other two heat exchangers:

$$0.5\dot{m}_2(h_3 - h_4) + (\dot{m}_2 - \dot{m}_l)(h_9 - h_{10}) = 0$$

$$0.5\dot{m}_2(h_4 - h_5) + (0.5\dot{m}_2 - \dot{m}_l)(h_8 - h_9) = 0$$

Solving the resulting system using EES and summarizing the states in a Table:

State	Pressure [atm]	Temperature [K]	Quality [-]
1	1	298	-
2	100	298	-
3	100	160	-
4	100	66.57	-
5	100	50.42	-
6	1	20.37	0.6826
7	1	20.37	0
8	1	20.37	1
9	1	55.5	-
10	1	125	-

d) Calculate the work produced by the turbine per 1kg of the produced liquid H₂:

$$\dot{w}_t = 0.5 \left(\frac{\dot{m}_2}{\dot{m}_l} \right) (h_3 - h_9) = 3741 \text{ kJ/kg H}_2$$

e) Determine the total work required to produce 1 kg of liquid hydrogen:

$$\dot{w}_c = \left(\frac{\dot{m}_2}{\dot{m}_l} \right) (T_1(s_2 - s_1) - (h_2 - h_1)) = -36,188 \text{ kJ/kg H}_2$$

$$\dot{w}_{net} = \dot{w}_t + \dot{w}_c = -32,448 \text{ kJ/kg H}_2$$

f) Determine the second law efficiency of the Claude cycle:

$$\eta_{II} = \frac{w_{min}}{w_{net}} = \frac{-([h_7 - h_1] - T_1(s_7 - s_1))}{w_t + w_c} = 36.9\%$$

Problem 3

We consider the desalination of seawater at standard temperature and pressure (293 K, 1 atm), modeled as a 1% concentration by mass of NaCl and assume that the solution is an incompressible liquid with ideal entropy of mixing, zero enthalpy of mixing and the molar heat capacity of seawater is constant and equal to the molar heat capacity of pure water.

a) We want to produce 1 kg/s of pure water from 2 kg/s of seawater. From mass balance, the brine flow rate equals to 1kg/s. Seawater is modeled as a solution with 1 wt% NaCl; therefore, 2 kg/s of seawater consists 20g/s NaCl and in the outlet all NaCl goes to the brine. As a result, 1 kg/s brine consists 20g/s NaCl and brine has 2% concentration by mass of NaCl. In terms of water, the seawater feeds in 1.98kg/s of pure water, which is split into 1kg/s of product and the remaining 0.98kg/s go into the brine.

b) The minimal work transfer rate (We will treat NaCl as a single species, which might not be precise since in aqueous solution it dissociates to Na^+ and Cl^-) is

$$\begin{aligned}\dot{W}_{\min} &= \dot{\Xi}_{sw} - (\dot{\Xi}_{brine} + \dot{\Xi}_{prod}) \\ &= (\dot{H}_{sw} - \dot{H}_{brine} - \dot{H}_{prod}) - T_0 (\dot{S}_{sw} - \dot{S}_{brine} - \dot{S}_{prod})\end{aligned}\quad (1)$$

We note that by assumption the enthalpy of mixing is zero. Hence, the first term is zero. Moreover, for the entropic term we can calculate

$$\begin{aligned}\dot{S}_{brine} &= \dot{n}_{H_2O,brine} (\hat{S}_{H_2O,brine} - \Re \ln X_{H_2O,brine}) + \dot{n}_{NaCl,brine} (\hat{S}_{NaCl,brine} - \Re \ln X_{NaCl,brine}) \\ \dot{S}_{prod} &= \dot{n}_{H_2O,prod} (\hat{S}_{H_2O,prod})_{pure\ species} \\ \dot{S}_{sw} &= \dot{n}_{H_2O,sw} (\hat{S}_{H_2O,sw} - \Re \ln X_{H_2O,sw}) + \dot{n}_{NaCl,sw} (\hat{S}_{NaCl,sw} - \Re \ln X_{NaCl,sw})\end{aligned}\quad (2)$$

Combining these equations, we note that the standard entropies cancel out and we get

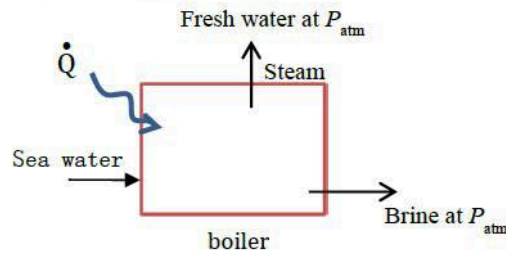
$$\dot{W}_{\min} = -T_0 \Re (\dot{n}_{H_2O,sw} \cdot \ln X_{H_2O,sw} + \dot{n}_{NaCl,sw} \cdot \ln X_{NaCl,sw} - \dot{n}_{H_2O,brine} \cdot \ln X_{H_2O,brine} - \dot{n}_{NaCl,brine} \cdot \ln X_{NaCl,brine}) \quad (3)$$

We now need to calculate the mole fractions of the two species in the three streams. Molar mass of NaCl is 58 g/mol and molar mass of H_2O is 18 g/mol. Since 2 kg/s of seawater consists 1980 g/s H_2O and 20 g/s of NaCl. The mole numbers of H_2O and NaCl in the seawater stream is 110 mol/s and 0.35 mol/s, respectively, and molar fractions are 0.997 and 0.003, respectively. And for the brine, we know that 1 kg/s of brine consist 980 g/s H_2O and 20 g/s of NaCl. The mole numbers of H_2O and NaCl in the seawater stream is 54.45 mol/s and 0.35 mol/s respectively and molar fractions are 0.994 and 0.006 respectively. Then the minimal work transfer rate is:

$$\dot{W}_{\min} = -293 \times 8.314 \times (54.45 \times \ln(0.994) + 0.35 \times \ln(0.006) - 110 \times \ln(0.997) - 0.35 \times \ln(0.003)) = -597.8 \text{ W} \quad (4)$$

Technology I: Once-Through Boiling

f) Flowsheet of the once-through boiling process is presented below:



g) In this process, heat is required to increase the temperature of seawater to boiling temperature and then evaporate it. We assume that the molar heat capacity of seawater is equal to molar heat capacity of pure water and hence equal to $75.33 \text{ J}/(\text{mol}\cdot\text{K})$ and enthalpy of evaporation for the pure water is 40.65 kJ/mol . Therefore heat transfer rate required is

$$\begin{aligned}\dot{Q} &= \dot{n}(\hat{h}_{out} - \hat{h}_m) = \dot{n}\hat{c}_{water}(T_{boil} - T_0) + \dot{n}\Delta\hat{h}_{evap} \\ &= 110.35 \times 75.33 \times 80 + 55.56 \times 40650 \\ &= 2.92 \text{ MW}\end{aligned}\quad (11)$$

h) Assuming that the heat source is at the boiling temperature of water and we have an ideal heat engine, the “Carnot” efficiency of the heat engine is:

$$\eta_{carnot} = 1 - \frac{293}{373} = 0.214 \quad (12)$$

And the work transfer rate is equal to:

$$\dot{W}_{engine} = \eta_{carnot} \dot{Q} = 0.214 \times 2.92 = 0.626 \text{ MW} \quad (13)$$

The ratio of this work transfer rate to the minimal work transfer rate is

$$\frac{\dot{W}_{engine}}{\dot{W}_{min}} = \frac{0.626}{0.598} = 1.047 \quad (14)$$

and thus the second law efficiency of this system is very low.

i) The most basic improvement that can be performed on this design is to recover thermal energy from the outlet streams. Without any heat recovery, the pure water is evaporated and enthalpy of evaporation is totally lost. What we can do is simply to pass the evaporated water from a heat exchanger and recover the heat while the pure water is condensed (which need to do anyways to sell/use the water) and then use the recovered heat to increase the temperature of seawater before feeding it to the boiler. Even further improvement is to reduce the temperature of liquid pure water more after the condensation to recover more thermal energy from the outlet stream.

References

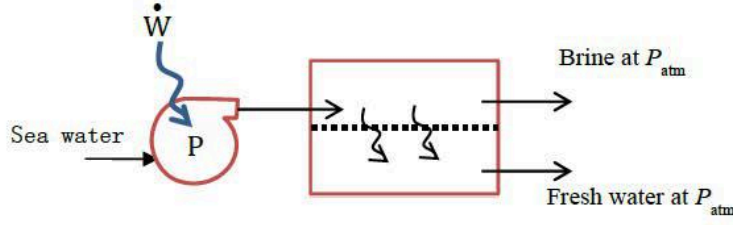
Chase, M.W., Jr. (1998), NIST-JANAF Thermochemical Tables, Fourth Edition, J. Phys. Chem. Ref. Data, Monograph 9: 1:1951.

[http : //en.wikipedia.org/wiki/Osmotic pressure/](http://en.wikipedia.org/wiki/Osmotic_pressure/)

[http : //webbook.nist.gov/chemistry/](http://webbook.nist.gov/chemistry/)

Technology II: Reverse Osmosis

c) Flow diagram of the reverse osmosis process is presented below:



d) The minimum pressure required for the outlet of the pump is the osmotic pressure. The osmotic pressure can be calculated by the Morse equation as

$$P_{osm} = 2\hat{\rho}_{brine}RT, \quad (5)$$

where $\hat{\rho}_{brine}$ is the molar density of the solute in the brine, R is the ideal gas constant and T is the temperature. And $\hat{\rho}_{brine} \approx X_{NaCl}\hat{\rho}_{water}$

Thus, the minimal pressure for the pump is given by:

$$P_{H,min} = 2 \times 0.006 \times 1000 \frac{kg}{m^3} \cdot \frac{1000 mol}{18 kg} \times 8.314 \frac{J}{K \cdot mol} \times 293 K = 16.24 \text{ bar} \quad (6)$$

And the corresponding work transfer rate is

$$\dot{W}_{min} = \Delta\dot{H} = \dot{m}_{seawater} \frac{(P_{H,min} - P^0)}{\rho} = 2 \times \frac{(16.24 - 1) \times 10^5}{1000} = 3048 \text{ W} \quad (7)$$

e) For the actual plant we have

$$\dot{W} = \Delta\dot{H} = \dot{m}_{seawater} \frac{(P_H - P^0)}{\rho} = 2 \times \frac{(30 - 1) \times 10^5}{1000} = 5800 \text{ W} \quad (8)$$

For the second law efficiency for this plant we compare the minimum work in d) and e)

$$\eta_{II} = \frac{\dot{W}_{min}}{\dot{W}} = \frac{3048}{5800} = 52.6\% \quad (9)$$

Or, we can compare the minimum work in b) and e)

$$\eta_{II} = \frac{\dot{W}_{min}}{\dot{W}} = \frac{598}{5800} = 10.3\% \quad (10)$$

MIT OpenCourseWare
<https://ocw.mit.edu/>

2.60J Fundamentals of Advanced Energy Conversion
Spring 2020

For information about citing these materials or our Terms of Use, visit: <https://ocw.mit.edu/terms>.

Homework 2

2.60/2.62/10.390 Fundamentals of Advanced Energy Conversion
Spring 2020

Total points: 100 (Undergraduate) | 150 (Graduate)

(Only use EES for Problem 2)

Problem 1. Carbon Dioxide Emissions [40% for Undergrads and 35% for Grads]

Consider a power plant with a power rating of 100 MWe which can use lignite, methane or octane as fuel. The environment is at standard conditions. Suppose first that the plant has a first law efficiency of 35%, defined based on the lower heating value of the fuels.

- For each fuel, calculate the required fuel flow rate and CO₂ emission rate. Explain their relative values, and comment on which is the best fuel and why.
- Is it reasonable to assume the same efficiency for all fuels? Why?
- Now keep the efficiency the same for lignite but take 52% for octane and 58% for methane. Calculate CO₂ emissions as kgCO₂/MJe for each fuel.
- The plant runs at 75% capacity factor, calculate the total CO₂ emitted yearly from each plant, in kgCO₂.

Now, and for methane only:

- Calculate the adiabatic flame temperature assuming air excess of 35% and that the reaction is complete.
- Based on the adiabatic flame temperature and that of the environment, calculate a maximum first law efficiency using the standard "Carnot efficiency".
- Correct the efficiency to account for the fact that the heat source has finite flowrate, and to allow for a 10K temperature difference between the source, the heat engine and the environment.
- What is the second law efficiency of this plant?

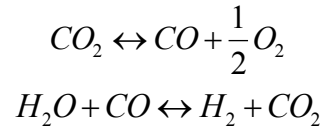
Problem 2. Propane Combustion [40% for Undergrads and 35% for Grads]

Stoichiometric gaseous propane (C_3H_8) air mixture undergoes isentropic compression from STP to 2 MPa, then combustion at constant pressure. During compression the mixture composition is frozen at its initial state. The products of combustion contain only CO_2 , CO , O_2 , H_2O , H_2 and N_2 . The isentropic index is 1.4.

Use EES to:

- Calculate the products temperature without and with dissociation.
- Calculate the products composition with dissociation.

Use the following as the dissociation reactions in the equilibrium calculations, find the equilibrium constant data in the notes or other sources:



- (for Grads only)** Repeat (a) and (b) for the case when the original fuel-air mixture undergoes volume reduction to $1/10^{\text{th}}$ of its original volume (with frozen composition) then constant volume combustion.

Problem 3. Biomass Utilization [20% for Undergrads and 30% for Grads]

Biomass from agriculture and forests is a large source of renewable energy and fuel. It can be burned for heating, electricity generation or to produce biofuels. If used in its raw form, it is carbon dioxide neutral since it is part of the carbon cycle. In this problem we use woody biomass whose chemical formula can be assumed to be $C_6H_{12}O_6$. The original biomass is 85% wood and 15% moisture.

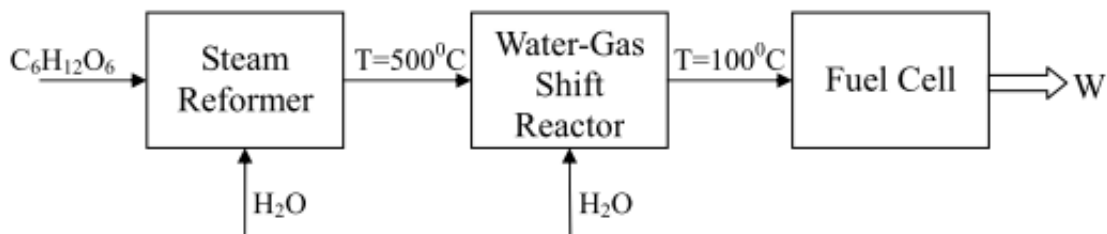
Technology I: Combustion

One way to utilize biomass is to burn it in air in an adiabatic combustion chamber and use the products in a steam cycle to produce work. Biomass and air enter the combustion chamber at atmospheric conditions.

- If the combustion is stoichiometric, calculate the temperature of products assuming complete combustion.
- The combustion products are cooled down to 50°C and 1 atm. The maximum temperature of the power cycle is 550°C . Calculate the maximum possible efficiency for the system, and maximum efficiency of the power cycle (both based on the logarithmic mean temperature).
- If the second law efficiency of the power cycle is 60%, calculate the work produced by the plant per mole of biomass.
- What is the overall fuel utilization efficiency of this configuration?

[For Grads Only] Technology II: Gasification

In this process, one mole of biomass and 6.5 moles of H_2O enter a steam reformer at atmospheric conditions to produce a mixture of CO , CO_2 , H_2 and H_2O at 500°C . Next, the mixture goes through a water-gas shift reactor (WGS) to convert CO to CO_2 . In the WGS, one mole of H_2O (at 25°C) is added for every mole of CO originally in the mixture. The mixture leaves WGS reactor at 100°C . The resulting mixture is used in the fuel cell to generate work. A schematic is shown in the following figure:



- What is the composition of the gas leaving the steam reformer if the temperature of the mixture is 500°C . Assume that this mixture of CO , CO_2 , H_2 and H_2O is at equilibrium.
- What is the heat transfer required in the steam reformer?
- If CO concentration leaving the WGS is negligible, what is the hydrogen concentration in the gas leaving the WGS reactor?

- h. Evaluate the overall process efficiency, including the reforming and WGS process, if no waste heat is recuperated.

The following information might be useful in your calculations:

1. LHV of woody biomass is 21 MJ/kg.
2. Thermodynamic properties:

Enthalpy of formations	Specific heat
$\hat{h}_{f,H_2O(g)}^o = -242 \text{ kJ/mol}$	$\hat{c}_{p,O_2} = 33.4 \text{ J/mol.K}$
$\hat{h}_{f,H_2O(l)}^o = -286 \text{ kJ/mol}$	$\hat{c}_{p,N_2} = 31.1 \text{ J/mol.K}$
$\hat{h}_{f,CO}^o = -110.6 \text{ kJ/mol}$	$\hat{c}_{p,CO_2} = 50.6 \text{ J/mol.K}$
$\hat{h}_{f,CO_2}^o = -393.8 \text{ kJ/mol}$	$\hat{c}_{p,H_2} = 30.0 \text{ J/mol.K}$
$\hat{h}_{f,C_6H_{12}O_6}^o = -1267.1 \text{ kJ/mol}$	$\hat{c}_{p,CO} = 29.3 \text{ J/mol.K}$
	$\hat{c}_{p,H_2O} = 38.2 \text{ J/mol.K}$
	$\hat{c}_{p,C_6H_{12}O_6} = 75.6 \text{ J/mol.K}$

3. Thermodynamic equilibrium constant for WGS reaction:

Table 1: Equilibrium constant values for water-gas shift reaction $CO_2 + H_2 \rightleftharpoons CO + H_2O$	
$Log_{10} K_p(T)$	$T (K)$
-19.6	100
-5.018	298
-2.139	500
-0.159	1000
0.135	1200
0.333	1400
0.474	1600
0.577	1800

MIT OpenCourseWare
<https://ocw.mit.edu/>

2.60J Fundamentals of Advanced Energy Conversion
Spring 2020

For information about citing these materials or our Terms of Use, visit: <https://ocw.mit.edu/terms>.

2.62 – Advanced Energy Conversion | Spring 2020

Homework 2 – Solutions

Problem 1

- a) For each fuel, calculate the required fuel flow rate and CO₂ emission rate. Explain their relative values, and comment on which is the best fuel and why. [10 points]

The powerplant's power rating is 100 MWe and the first law efficiency is 35% = 0.35, which means that the heat input to the plant is $100/0.35 = 286$ MW in each case.

Since the efficiency of the power plant is based on the lower heating value (LHV) of the fuels, the first thing to do is to find out the LHV of each fuel considered. NIST webbook is used here as reference for LHV of fuels (If you are interested in a deeper analysis of heating values of fuel, you can check Chase (1998), which is also used by NIST webbook as reference for heating values of hydrocarbons.) The molar mass of CO₂ is 44 g/mol.

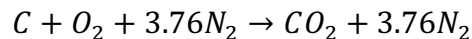
For each fuel, we should calculate the required fuel flow rate and CO₂ emissions.

- (i) **Lignite (C):**

LHV of lignite is 15 MJ/kg and the molar mass is 12 g/mol (we neglect the other components in lignite). In ideal conditions, the required lignite flow rate is:

$$\frac{286}{15} = 19 \text{ kg/s} \quad \text{or} \quad \frac{19000}{12} = 1583.3 \text{ mol/s}$$

The combustion reaction for lignite is:



Therefore, the stoichiometric and complete combustion of 1 mole of lignite forms 1 mole of CO₂ and CO₂ emission is:

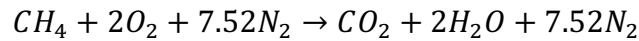
$$1583.3 \times 0.044 = 69.67 \text{ kg/s}$$

(ii) **Methane (CH₄):**

The LHV of methane is 50 MJ/kg and the molar mass is 16 g/mol. In ideal conditions, the required methane flow rate is:

$$\frac{286}{50} = 5.72 \text{ kg/s} \quad \text{or} \quad \frac{5720}{16} = 357.5 \text{ mol/s}$$

The combustion reaction for methane is:



Therefore, the stoichiometric and complete combustion of 1 mole of methane forms 1 mole of CO₂ and the emission rate of CO₂ is:

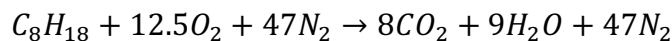
$$357.5 \times 0.044 = 15.73 \text{ kg/s}$$

(iii) **Octane (C₈H₁₈):**

LHV of octane is 45 MJ/kg and the molar mass is 114 g/mol. In ideal conditions, the required flow rate is:

$$\frac{286}{45} = 6.36 \text{ kg/s} \quad \text{or} \quad \frac{6360}{114} = 55.75 \text{ mol/s}$$

The combustion reaction for octane is:



Therefore, stoichiometric and complete combustion of 1 mole of octane forms 8 moles of CO₂ and the CO₂ emission rate is:

$$55.75 \times 8 \times 0.044 = 19.624 \text{ kg/s}$$

As the results show us, the required flow rate is the largest in the case of lignite and the lowest in the case of methane, as a direct consequence of the LHV. In terms of the amount of the fuel required, the order from most to least is lignite, octane, and methane. The same order is valid for CO₂ emission from most to least. The CO₂ emissions of methane and octane are close, while that of lignite is around 4 times higher, which shows lignite is the dirtiest fuel among these three regarding global warming potential.

b) Is it reasonable to assume the same efficiency for all fuels? Why? [2.5 points]

It is not reasonable to assume the same efficiency for all fuels. It is easy to verify that each fuel has a different adiabatic flame temperature. Therefore, even if we assume a similar power cycle for all fuels, they will result in different efficiencies (see discussion in notes). Note also that CH₄ can be directly used in a combined cycle which is more efficient.

c) Now keep the efficiency the same for lignite but take 52% for octane and 58% for methane. Calculate CO₂ emissions as kgCO₂/MJe for each fuel. [5 points]

- **Lignite (C):**

$$\frac{69.67 \text{ kg/s}}{100 \text{ MWe}} = 0.6967 \text{ kgCO}_2/\text{MJe}$$

- **Methane (CH₄):**

$$\frac{\left(\frac{100}{0.58}\right)}{50} = 3.45 \text{ kg/s} \quad \text{or} \quad \frac{3450}{16} = 215.6 \text{ mol/s of fuel}$$

$$215.6 \times 0.044 = 9.49 \text{ kg/s CO}_2$$

$$\frac{9.49 \text{ kg/s}}{100 \text{ MWe}} = 0.0949 \text{ kgCO}_2/\text{MJe}$$

- **Octane (C₈H₁₈):**

$$\frac{\left(\frac{100}{0.52}\right)}{45} = 4.27 \text{ kg/s} \quad \text{or} \quad \frac{4270}{114} = 37.46 \text{ mol/s of fuel}$$

$$37.46 \times 8 \times 0.044 = 13.19 \text{ kg/s CO}_2$$

$$\frac{13.19 \text{ kg/s}}{100 \text{ MWe}} = 0.132 \text{ kgCO}_2/\text{MJe}$$

- d) The plant runs at 75% capacity factor, calculate the total CO₂ emitted yearly from each plant, in kgCO₂. [5 points]

At 75% capacity, the plant now generates 75 MWe. Using the efficiencies specified in part c, we calculate the carbon emissions (CE) as shown:

- (i) **Lignite (C):**

$$\begin{aligned} \text{CE} &= 0.6967 \text{ kg CO}_2/\text{MJe} \times 0.75 \times 100 \text{ MWe} \times 3600 \times 24 \times 365 \\ &= 1.65 \times 10^9 \text{ kg CO}_2/\text{yr} \end{aligned}$$

- (ii) **Methane (CH₄):**

$$\begin{aligned} \text{CE} &= 0.0949 \text{ kg CO}_2/\text{MJe} \times 0.75 \times 100 \text{ MWe} \times 3600 \times 24 \times 365 \\ &= 0.224 \times 10^9 \text{ kg CO}_2/\text{yr} \end{aligned}$$

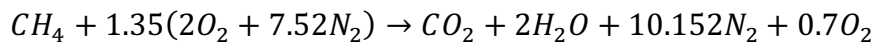
Octane (C₈H₁₈):

$$\begin{aligned} \text{CE} &= 0.132 \text{ kg CO}_2/\text{MJe} \times 0.75 \times 100 \text{ MWe} \times 3600 \times 24 \times 365 \\ &= 0.312 \times 10^9 \text{ kg CO}_2/\text{yr} \end{aligned}$$

Now for methane only:

- e) Calculate the adiabatic flame temperature assuming air excess of 35% and that the reaction is complete: [7.5 points]

Assuming an air excess of 35%, the combustion reaction has the form:



We also assume complete combustion occurs in an adiabatic chamber, so the first law gives:

$$\sum_i \dot{n}_{i,in} \hat{h}_{i,in} = \sum_i \dot{n}_{i,out} \hat{h}_{i,out}$$

where i denotes the species and \dot{n}_i is the molar flowrate of this species. We rewrite this equation as follows:

$$\dot{n}_{\text{CH}_4,in} \hat{h}_{\text{CH}_4,in} + \dot{n}_{\text{O}_2,in} \hat{h}_{\text{O}_2,in} + \dot{n}_{\text{N}_2,in} \hat{h}_{\text{N}_2,in} = \dot{n}_{\text{CO}_2,out} \hat{h}_{\text{CO}_2,out} + \dot{n}_{\text{H}_2\text{O},out} \hat{h}_{\text{H}_2\text{O},out} + \dot{n}_{\text{O}_2,out} \hat{h}_{\text{O}_2,out} + \dot{n}_{\text{N}_2,out} \hat{h}_{\text{N}_2,out}$$

The formation energies of these species can be found in NIST Chemistry WebBook (They use 298.15 K as standard temperature here):

$$H_{f,CH_4}^\circ = -74.87 \text{ kJ/mol} \quad H_{f,O_2}^\circ = 0 \text{ kJ/mol} \quad H_{f,N_2}^\circ = 0 \text{ kJ/mol}$$

$$H_{f,H_2O}^\circ = -241.8 \text{ kJ/mol} \quad H_{f,CO_2}^\circ = -393.5 \text{ kJ/mol}$$

Given the large range of temperature changes from inlet to adiabatic temperature, it is not good practice to assume constant heat capacities for the gases. Therefore, using the equation in NIST Chemistry WebBook, we have the enthalpy relations of the gases:

$$H^\circ - H_{298.15K}^\circ = A \cdot t + \frac{B}{2} \cdot t^2 + \frac{C}{3} \cdot t^3 + \frac{D}{4} \cdot t^4 - \frac{E}{t} + F - H \quad [\text{kJ/mol}]$$

where $t = T[K]/1000$, and the constants are:

	CO ₂	O ₂	N ₂	H ₂ O
T (K)	1200 – 6000	2000 – 6000	2000 – 6000	1700 – 6000
A	58.16639	20.911	35.519	41.964
B	2.720074	10.721	1.1287	8.6221
C	-0.492289	-2.02	-0.196	-1.5
D	0.038844	0.1464	0.0147	0.0981
E	-6.447293	9.2457	-4.554	-11.16
F	-425.9186	5.3377	-18.97	-272.2
H	-393.5224	0	0	-241.8

$$1 \cdot H_{f,CH_4}^\circ = 1 \cdot (H_{f,CO_2}^\circ + H_{CO_2}(T)) + 2 \cdot (H_{f,H_2O}^\circ + H_{H_2O}(T)) + 0.7 \cdot H_{O_2}(T) + 10.152 \cdot H_{N_2}(T)$$

Plugging-in and solving for T:

$$T = 1917 \text{ K}$$

- f) Based on the adiabatic flame temperature and that of the environment, calculate a maximum first law efficiency using the standard “Carnot efficiency”. [2.5 points]

The standard “Carnot efficiency” is stated as:

$$\eta_{carnot} = 1 - \frac{T_0}{T_H}$$

where T_0 is the standard ambient temperature (*environment is usually the cold reservoir*) and T_H is the hot reservoir temperature. Here, we use the adiabatic flame temperature to be T_H , which gives:

$$\eta_{carnot} = 1 - \frac{T_0}{T_H} = 1 - \frac{298}{1917} = 84.5\%$$

- g) Correct the efficiency to account for the fact that the heat source has finite flowrate, and to allow for a 10K temperature difference between the source, the heat engine and the environment. [2.5 points]**

If the heat source has finite flow rate and the corrected Carnot efficiency can be defined as:

$$\eta_{carnot}^* = 1 - \frac{\ln\left(\frac{T_H}{T_C}\right)}{\frac{T_H}{T_C} - 1}$$

where T_H is the adiabatic flame temperature, and T_C is $298 + 10 = 308$ K, since we allow for a 10K temperature difference for the removal of heat to the environment.

Therefore:

$$\eta_{carnot}^* = 1 - \frac{\ln\left(\frac{T_H}{T_C}\right)}{\frac{T_H}{T_C} - 1} = 1 - \frac{\ln\left(\frac{1917}{308}\right)}{\frac{1917}{308} - 1} = 65\%$$

Since we account for the finite flowrate and higher outlet temperature, this efficiency is lower than the ideal case addressed previously.

- h) What is the second law efficiency of this plant? [5 points]**

First, we need to find the heat extracted from the exhaust stream:

$$Q_H = \sum n_i \hat{h}_{i,out} - \sum n_i \hat{h}_{i,in}$$

$$Q_H = n_{CO_2} \hat{h}_{CO_2,out} + n_{H_2O} \hat{h}_{H_2O,out} + n_{N_2} \hat{h}_{N_2,out} + n_{O_2} \hat{h}_{O_2,out} - (n_{CO_2} \hat{h}_{CO_2,in} + n_{H_2O} \hat{h}_{H_2O,in} + n_{N_2} \hat{h}_{N_2,in} + n_{O_2} \hat{h}_{O_2,in})$$

Calculating Q_H (per mole of CH_4) using the definition in Part e:

$$Q_H = 700.8 \text{ kJ}$$

Accounting for the efficiency of the plant from Part g:

$$W_{ideal} = \eta_{carnot} Q_H = 0.845 \times 700.8 = 592.176 \text{ kJ}$$

The actual work of the plant (specified in Part c) per mole of CH_4 is:

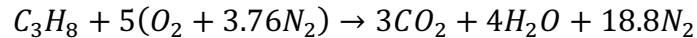
$$W_{actual} = \eta_I Q_H = 0.58 \times 700.8 = 406.464 \text{ kJ}$$

Therefore:

$$\eta_{II} = \frac{W_{actual}}{W_{ideal}} = \frac{406.464}{592.176} = 68.6\%$$

Problem 2

The chemical equation for stoichiometric combustion is air is given by: **[5 points]**



Accounting for isentropic compression (and keeping in mind the composition is assumed frozen), the temperature of the compressed mixture is given by:

$$\frac{T_2}{T_1} = \left(\frac{P_2}{P_1}\right)^{1-\frac{1}{\gamma}} = (20)^{1-\frac{1}{1.4}} = 2.35$$

Therefore:

$$T_2 = 2.35T_1 = 2.35 \times 298 = 701K$$

a) Calculate the products' temperature without dissociation. **[10 points]**

The adiabatic flame temperature may be computed through the conservation of enthalpy:

$$H_R = H_P$$

$$\sum_{react} n_i \hat{h}_i = \sum_{products} n_i \hat{h}_i$$

Taking the temperature of the reactants to be 701 K, and using EES:

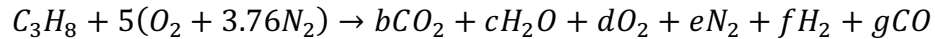
```
Equations Window
"Given: Propane combustion at initial conditions of 2 MPa and 701 K"
"Find: adiabatic flame temperature"
"Solution:"
"1) combustion stoichiometry
C3H8 + 5 (O2 + 3.76 N2) ==> 3 CO2 + 4 H2O + 18.8 N2
2) enthalpy of reactants"
T_o = 701
h_R = ENTHALPY(C3H8,T=T_o) + 5 * ENTHALPY(O2,T=T_o) + 18.8 * ENTHALPY(N2,T=T_o)
"3) enthalpy of products"
h_P = 3 * ENTHALPY(CO2,T=T_a) + 4 * ENTHALPY(H2O,T=T_a) + 18.8 * ENTHALPY(N2,T=T_a)
"4) energy balance"
h_R = h_P
```

Therefore:

$$T_{ad} = 2695.3 \text{ K}$$

b) Calculate the products' composition and temperature with dissociation. [15 points]

Now with dissociation, the combustion reaction takes the form:



Applying mass balances:

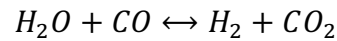
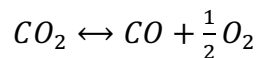
$$\text{C: } b + g = 3$$

$$\text{H: } 2c + 2f = 8$$

$$\text{O: } 2b + c + 2d + g = 10$$

$$\text{N: } 2e = 37.6$$

Note this gives us four equations for 6 unknowns. To solve the system, we need two more equations. We use the dissociation reactions:



Using the definition of equilibrium constant:

$$\frac{P_{CO}P_{O_2}^{1/2}}{P_{CO_2}} = K_{p1} \rightarrow \frac{X_{CO}X_{O_2}^{1/2}}{X_{CO_2}} = K_{p1}\sqrt{p} \rightarrow \frac{gd^{1/2}}{b[b+c+d+e+f+g]^{1/2}} = \frac{K_{p1}}{\sqrt{p}}$$

$$\frac{P_{CO_2}P_{H_2}}{P_{CO}P_{H_2O}} = K_{p2} \rightarrow \frac{X_{CO_2}X_{H_2}}{X_{CO}X_{H_2O}} = K_{p2} \rightarrow \frac{bf}{gc} = K_{p2}$$

Assuming a temperature of 2000 K and referring to the notes:

$$K_{p1} = 10^{-2.884} = 0.0013$$

$$K_{p2} = 10^{-0.656} = 0.2208$$

Using EES, we solve the system of 6 equations and arrive at the following:

$$b = 2.969 \quad c = 3.991 \quad d = 0.02016 \quad e = 18.8 \quad f = 0.009228 \quad g = 0.03109$$

Next, we calculate the temperature in EES as in part (a):

$$T = 2685.49 \text{ K}$$

Updating our guess to $T = 2600$ K, and doing another iteration (to confirm convergence), we arrive at the following:

$$K_{p1} = 10^{-1.219} = 0.06 \qquad K_{p2} = 10^{-0.802} = 0.158$$

Using EES, we solve the system of 6 equations and arrive at the following:

$$b = 2.625 \quad c = 3.912 \quad d = 0.232 \quad e = 18.8 \quad f = 0.08842 \quad g = 0.3755$$

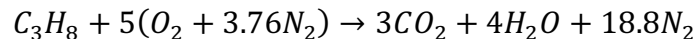
Next, we calculate the temperature in EES as in part (a):

$$T = 2581.047 \text{ K}$$

Of course, this iterative process can be repeated until a smaller tolerance is reached.

- c) Repeat (a) and (b) for the case when the original fuel-air mixture undergoes volume reduction to 1/10th of its original volume (with frozen composition) then constant volume combustion: [15 points]**

Again, the chemical equation for stoichiometric combustion is air is given by:



Accounting for **adiabatic compression** (and keeping in mind the composition is assumed frozen), the temperature of the compressed mixture is given by:

$$\frac{T_2}{T_1} = \left(\frac{V_1}{V_2}\right)^{\gamma-1} = (10)^{0.4} = 2.512$$

Therefore:

$$T_2 = 2.35T_1 = 2.512 \times 298 = 748.5 \text{ K}$$

The adiabatic flame temperature without dissociation may be computed through the conservation of enthalpy (as done previously):

$$H_R = H_P$$

$$\sum_{react} n_i \hat{h}_i = \sum_{products} n_i \hat{h}_i$$

Taking the temperature of the reactants to be 748.5 K, and using EES:

$$T_{ad} = 2733.9 \text{ K}$$

As we can see, adiabatic compression and constant volume combustion lead to higher adiabatic flame temperatures than isentropic compression and constant pressure combustion.

Assuming $T = 2600 \text{ K}$, we arrive at the following:

$$K_{p1} = 10^{-1.219} = 0.06 \qquad K_{p2} = 10^{-0.802} = 0.158$$

Using EES, we solve the system of 6 equations and arrive at the following:

$$b = 2.625 \quad c = 3.912 \quad d = 0.232 \quad e = 18.8 \quad f = 0.08842 \quad g = 0.3755$$

Next, we calculate the temperature in EES as in part (a):

$$T = 2619 \text{ K}$$

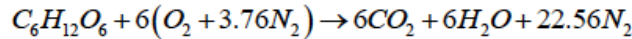
Of course, this iterative process can be repeated until a smaller tolerance is reached.

Problem 3

- a) If the combustion is stoichiometric, calculate the temperature of products assuming complete combustion. [10 points]

Technology one: Combustion

a) If the combustion of biomass is stoichiometric, then the combustion reaction has the form:



Assuming complete combustion occurs in an adiabatic chamber, we can write the first law as follows:

$$n_{C_6H_{12}O_6} \hat{h}_{C_6H_{12}O_6, in} + n_{O_2} \hat{h}_{O_2, in} + n_{N_2} \hat{h}_{N_2, in} = n_{CO_2} \hat{h}_{CO_2, out} + n_{H_2O} \hat{h}_{H_2O, out} + n_{N_2} \hat{h}_{N_2, out}$$

Biomass and air enter the combustion chamber at atmospheric conditions, therefore:

$$n_{C_6H_{12}O_6} \hat{h}_{C_6H_{12}O_6, in} = n_{CO_2} \hat{h}_{CO_2, out} + n_{H_2O} \hat{h}_{H_2O, out} + n_{N_2} \hat{h}_{N_2, out}$$

where for material i ,

$$\hat{h}_i(T) = \hat{h}_{f,i}^\circ + \int_{T_o}^T \hat{c}_{p,i} dT$$

$$\hat{c}_{p,i} = a_i \Rightarrow \hat{h}_i(T) = \hat{h}_{f,i}^\circ + a_i(T - T_o)$$

Using this, we can determine the enthalpy values as:

$$\hat{h}_{C_6H_{12}O_6, in} = -1267.1 \text{ kJ/mol}$$

$$\hat{h}_{CO_2, out} = -393.8 + 50.6(T_{out} - 298) \text{ kJ/mol}$$

$$\hat{h}_{H_2O, out} = -242 + 38.2(T_{out} - 298) \text{ kJ/mol}$$

$$\hat{h}_{N_2, out} = -31.1(T_{out} - 298) \text{ kJ/mol}$$

Hence, per mole of biomass,

$$-1267.1 = 6(-393.8 + 50.6(T_{out} - 298)) + 6(-242 + 38.2(T_{out} - 298)) + 22.56(-31.1(T_{out} - 298))$$

Solving, we get $T_{out} = 2359.7 \text{ K}$

- b) Calculate the maximum possible efficiency for the system, and maximum efficiency of the power cycle (both based on the logarithmic mean temperature). [5 points]

b) Now, we know that:

$$\eta_{car} = 1 - \frac{\ln\left(\frac{T_F}{T^*}\right)}{\frac{T_F}{T^*} - 1}$$

For the steam cycle, $T^* = T_{ambient} = 298 \text{ K}$ and $T_F = T_{turb_max} = 823 \text{ K}$. In addition, for the overall system, $T^* = T_C = 323 \text{ K}$ and $T_F = T_{products} = 2359.7 \text{ K}$. Substituting, we get the maximum possible efficiencies of the system and steam cycle:

$$\eta_{sys} = 1 - \frac{\ln\left(\frac{2359.7}{323}\right)}{\frac{2359.7}{323} - 1} = 0.684 = 68.4\%$$

$$\eta_{steam_cycle} = 1 - \frac{\ln\left(\frac{823}{298}\right)}{\frac{823}{298} - 1} = 0.423 = 42.3\%$$

- c) If the second law efficiency of the power cycle is 60%, calculate the work produced by the plant per mole of biomass. [10 points]

c) First, we have to find the amount of heat addition to the steam cycle:

$$Q_H = \sum n_i \hat{h}_{i,out} - \sum n_i \hat{h}_{i,in}$$

$$\Rightarrow Q_H = n_{CO_2} \hat{h}_{CO_2,out} + n_{H_2O} \hat{h}_{H_2O,out} + n_{N_2} \hat{h}_{N_2,out} - (n_{CO_2} \hat{h}_{CO_2,in} + n_{H_2O} \hat{h}_{H_2O,in} + n_{N_2} \hat{h}_{N_2,in})$$

Hence, per mole of biomass, we get:

$$Q_H = 6(50.6(2359.7 - 323)) + 6(38.2(2359.7 - 323)) + 22.56(31.1(2359.7 - 323))$$

$$\Rightarrow Q_H = 2514 \text{ kJ}$$

Since we calculated the first law efficiency of the steam cycle, we have:

$$W_{ideal} = \eta_{steam_cycle} \cdot Q_H = 1063 \text{ kJ}$$

The second law efficiency of the cycle is given as 60%. Therefore:

$$W_{actual} = 0.6 \times W_{ideal} = 637.8 \text{ kJ}$$

Thus, the actual work produced by the system is 637.8 kJ per mole of biomass.

d) What is the overall fuel utilization efficiency of this configuration? [5 points]

The overall fuel utilization efficiency of the configuration can be calculated (per mole of biomass) as:

$$\eta_{conf} = \frac{W_{act}}{LHV_{C_6H_{12}O_6}} = \frac{637.8}{21000 \times 0.18} = 16.9\%$$

For Technology II: Gasification

e) What is the composition of the gas leaving the steam reformer if the temperature of the mixture is 500°C. Assume that this mixture of CO, CO₂, H₂ and H₂O is at equilibrium. [10 points]

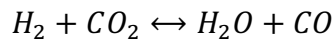
The reaction in the steam reformer has the following form:



Mass balance for C, H, and O gives:

$$a + d = 6 \quad b + c = 12.5 \quad a + c + 2d = 12.5$$

We also the expression for product equilibrium:



At 500 C, K_p of the equilibrium is 0.24 (This can be determined by interpolating the K_p values (not $\log K_p$) using a polynomial expression of order 3 from the range 300 to 1200K. Therefore:

$$0.24 = \frac{ac}{bd}$$

Solving the four equations simultaneously, we have:

$$a = 2.555 \quad b = 9.445 \quad c = 3.055 \quad d = 3.445$$

Therefore, the composition of the gas leaving the steam reformer (in terms of mole fractions) is:

$$X_{CO} = 0.138 \quad X_{H_2} = 0.511 \quad X_{H_2O} = 0.165 \quad X_{CO_2} = 0.1862$$

f) What is the heat transfer required in the steam reformer? [7.5 points]

Writing the first law for the steam reformer, we have:

$$Q_{reform} = a\hat{h}_{CO,out} + b\hat{h}_{H_2,out} + c\hat{h}_{H_2O,out} + d\hat{h}_{CO_2,out} - (\hat{h}_{C_6H_{12}O_6,in} + 6.5\hat{h}_{H_2O,in})$$

where for material i ,

$$\hat{h}_i(T) = \hat{h}_{f,i}^\circ + \int_{T_o}^T \hat{c}_{p,i} dT$$

$$\hat{c}_{p,i} = a_i \Rightarrow \hat{h}_i(T) = \hat{h}_{f,i}^\circ + a_i(T - T_o)$$

and

$$T_{in} = 298 \text{ K}$$

$$T_{out} = 773 \text{ K}$$

We get the enthalpy values as:

$$\hat{h}_{C_6H_{12}O_6,in} = -1267.1 \text{ kJ/mol}$$

$$\hat{h}_{H_2O,in} = -286 \text{ kJ/mol}$$

$$\hat{h}_{CO,out} = -96.7 \text{ kJ/mol}$$

$$\hat{h}_{H_2,out} = 14.25 \text{ kJ/mol}$$

$$\hat{h}_{H_2O,out} = -223.9 \text{ kJ/mol}$$

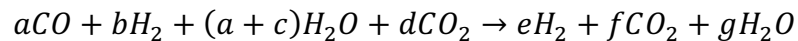
$$\hat{h}_{CO_2,out} = -369.8 \text{ kJ/mol}$$

We already know the coefficient values. Therefore, we get:

$$Q_{reform} = 1055.65 \text{ kJ}$$

g) If CO concentration leaving the WGS is negligible, what is the hydrogen concentration in the gas leaving the WGS reactor? [7.5 points]

H₂O is added to match the moles of CO. We assume that the CO concentration leaving the WGS is negligible. Therefore, the WGS reaction has the form:



The atom balances are:

$$a + d = f \quad a + b + c = g + e \quad 2a + 2d + c = 2f + g$$

We can solve for the three unknowns to get:

$$e = 12 \quad f = 6 \quad g = 3.055$$

Therefore, the hydrogen concentration leaving the WGS reactor is:

$$X_{H_2} = \frac{12}{21.055} = 0.5699 = 56.99\%$$

h) Evaluate the overall process efficiency, including the reforming and WGS process, if no waste heat is recuperated. [5 points]

We can define the overall reformer efficiency as:

$$\frac{e \times LHV_{H_2}}{LHV_{C_6H_{12}O_6} + Q_{reform}} = \frac{12 \times 242}{21000 \times 0.18 + 1055.65} = 0.6 = 60\%$$

MIT OpenCourseWare
<https://ocw.mit.edu/>

2.60J Fundamentals of Advanced Energy Conversion
Spring 2020

For information about citing these materials or our Terms of Use, visit: <https://ocw.mit.edu/terms>.

Homework 3

2.60/2.62/10.390 Fundamentals of Advanced Energy Conversion
Spring 2020

Total points: 100 (Undergraduate) | 150 (Graduate)

Problem 1. Proton Exchange Membrane (PEM) Fuel Cell [30% for Undergrads and Grads]

A PEM (Proton Exchange Membrane) fuel cell operates at 80°C and 2 atm. The fuel is a product of ammonia pyrolysis to N_2 and H_2 . Air is the oxidizer, and the outlet stream consists of nitrogen, oxygen and water (reaction products) as shown in **Figure 1**. Only 65% of the fuel is used (and the rest is recycled). The air flow rate is such that, at the inlet, there is twice as much oxygen as needed to consume all the hydrogen.

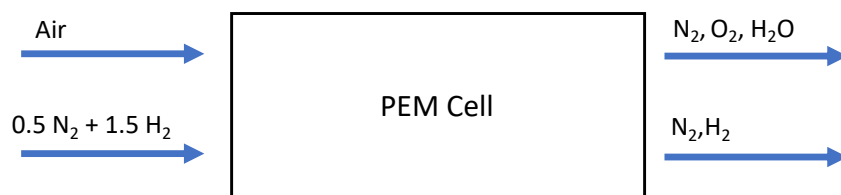


Figure 1 - PEM Fuel Cell

Consider this cell in operation, with a voltage of 0.65V and current density of 600 mA/cm^2 . The effective total area of the cell is 2000 cm^2 . A stack of 200 such cells is used in series for a stationary application (such that their voltages add up).

Please answer the following:

- How much heat is needed to pyrolyze the ammonia?
- Calculate the composition of the two streams at the exit of the cell.
- Calculate the open circuit voltage of this cell based on the concentrations at the exit.
- Calculate the power delivered by the stack of 200 cells in the proposed application.
- What is the mass flow rate of H_2 needed to generate the power?
- What is the cooling rate required to keep the fuel cell at the desired temperature? Note that the inlet and exit streams are all at the same temperature as the cell.

- g. What is the efficiency of the cell?
- h. **(For graduate students only)** If the cell is operating very close to open circuit conditions, is it better efficiency-wise to operate the cell at 10 atm? Assume that the input $\text{H}_2\text{-N}_2$ mixture is available at 1 atm, and an isothermal (and ideal) air compressor is available at 80°C.

Problem 2. Methane Fuel Cell System [30% for Undergrads and Grads]

A fuel cell system is proposed as shown in **Figure 2**. The system utilizes methane and air. All stream conditions are given in the figure. Across the fuel cell, assume that only hydrogen is consumed in the electrochemical reactions with 100% hydrogen utilization. Carbon monoxide passes through the fuel cell without change. Within the cell, O^{2-} ions move through the electrolyte from the cathode to the anode. The flow rate of air at the cathode inlet is determined such that the ratio of the flow rate of the fuel stream (1) to the air stream is stoichiometric. All gases can be treated as ideal gases.

Assume that stream (1) at the exit of the reformer/water gas shift reactor consists of CO , CO_2 , H_2 and H_2O . The products are at thermodynamic equilibrium at the given temperature and pressure. At equilibrium, there are 0.049 kmol/s of CO_2 and 0.284 kmol/s of H_2O within the product stream (1).

- Determine the molar flow rate of methane and water fed to the reformer. Note that the partial pressure based equilibrium constant of the water gas shift reaction at 800 C is $K_p = 0.8879$.
- Calculate the flow rate of hydrogen and the current produced by the fuel cell.
- Determine the heat transfer rate across the reformer/water gas shift reactor.
- Calculate the flow rate of air into the fuel cell.
- Assuming that the product stream (2) of the fuel cell consists of CO , CO_2 , and H_2O , determine the maximum work transfer of the fuel cell.
- Determine the actual work transfer from the fuel cell, assuming a second law efficiency of 70% for the fuel cell.
- Calculate the operating voltage of the fuel cell.

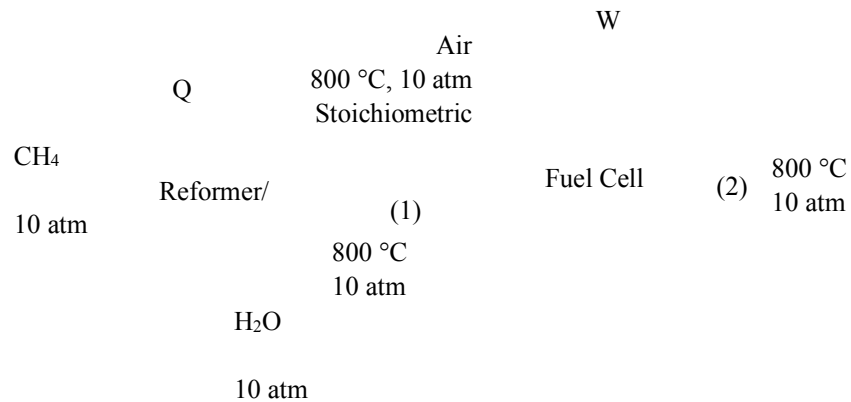


Figure 2 - Methane Fuel Cell System

Problem 3. PEMFC & Water Management [40% for Undergrads and Grads]

Water management is critical for the operation of proton exchange membrane fuel cells (PEMFC). These cells use sulphonate fluoropolymers as an electrolyte (membrane). The most well-known membrane brand is Nafion. For the electrolyte to be a good proton conductor, it should be well hydrated. However, too much water can flood the electrodes blocking gas diffusion through the pores. Therefore, water produced by the electrochemical reaction on the cathode side should be removed by airflow. Even though both the fuel and air streams are mixed with water vapor at the inlet, humidity level is controlled primarily by air stream.

The following figure shows a schematic diagram for the operation of a fuel cell operating on hydrogen produced by steam reforming of methane.

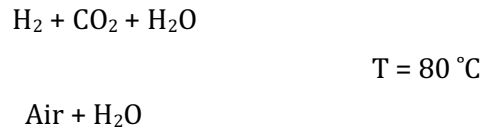


Figure 3 - Proton Exchange Membrane Fuel Cell Setup

We will make following assumptions:

- All streams are at 1 bar and 80C.
- The fuel consists of H_2 and CO_2 with a molar ratio 4:1. The relative humidity of fuel steam is 20%, where the relative humidity is defined as:

$$\phi = \frac{p_{\text{H}_2\text{O}}}{p_{\text{H}_2\text{O},\text{sat}}(T)}$$

- CO , which is poisonous to Pt catalyst, is completely removed from the fuel stream.
- Air stoichiometry, defined as the ratio of inlet oxygen flow rate to the oxygen consumption rate is 2 at the inlet, a very typical value.

$$\lambda = \frac{\dot{n}_{\text{O}_2,\text{inlet}}}{\dot{n}_{\text{O}_2,\text{usage}}}$$

- The inlet air relative humidity is 40%.
- The electrolyte is well hydrated and the level of hydration is constant and steady. In other words, there is no incoming and outgoing water from and to the electrolyte.
- Water produced electrochemically is in the form of vapor.
- All the species are considered as an ideal gas
- Values given at 353K, saturated steam pressure: $0.4708 \times 10^5 \text{ Pa}$:

c_p (Temp range [298K~353K])	Enthalpy of formation (J/ mol)	Entropy of formation (J/ mol-K) @ 1 bar
$\hat{c}_{p,O_2}^0 = 29.55$ $\hat{c}_{p,H_2}^0 = 28.96$ $\hat{c}_{p,H_2O}^0 = 33.59$ $\hat{c}_{p,N_2}^0 = 29.15$	$\hat{h}_{f,H_2O(g)}^0 = -241,826$	$\hat{s}_{f,H_2O(g)}^0 = 188.835$ $\hat{s}_{f,H_2}^0 = 130.68$ $\hat{s}_{f,O_2}^0 = 205.152$ $\hat{s}_{f,N_2}^0 = 191.609$

Answer the following questions:

- Determine the mole fractions at the anode and cathode. What is the theoretical open circuit voltage of this cell?
- What is the open circuit (thermodynamic) efficiency based on the lower heating value of H_2 ? (LHV of H_2 is 120.1 MJ/kg)

A fuel cell stack is used to power a small vehicle that requires 80 kW. Each cell operates at 0.6V, and a typical current density is 1 A/cm². Assume that the surface area of each individual cell is 650 cm², the Faradaic efficiency is 100% and the fuel utilization is 90%.

- How many individual cells are needed to supply the required power for the vehicle?
- What is the total molar flow rate of oxygen?
- What is the composition of the air-side stream at the exit of the stack, expressed in terms of the mole fractions of N_2 , O_2 , and H_2O ?
- When the design exit air relative humidity is 90%, does the current operating conditions satisfy the design target?
- What is the composition at the anode side exit stream?
- What is the molar flow rate of the fuel stream at the inlet?
- What is the first law efficiency of the cell?

$$\eta_1 = \frac{\text{generated power}}{\text{rate of chemical energy in}}$$

- What is the cooling rate required to keep the fuel cell at 80C?
- (Graduate students only)** Derive an expression for the exit relative humidity in terms of the air stoichiometry, λ , the relative humidity of the inlet air stream, ϕ_{inlet} , the water saturation pressure, $P_{H_2O,sat}$, and the pressure P^0 .
- (Graduate students only)** What should be the relative humidity of the inlet air if the relative humidity of the exit air is 90%?

MIT OpenCourseWare
<https://ocw.mit.edu/>

2.60J Fundamentals of Advanced Energy Conversion
Spring 2020

For information about citing these materials or our Terms of Use, visit: <https://ocw.mit.edu/terms>.

2.62 – Advanced Energy Conversion | Spring 2020

Homework 3 – Solutions

Problem 1

- a) How much heat is needed to pyrolyze the ammonia? [5 points]

First, we start by applying an enthalpy balance (first law), assuming we start from ambient conditions ($T_{in} = T_0 = 25^\circ\text{C}$):

$$Q = \sum_{prod} v_i h_i - \sum_{reac} v_i h_i$$

$$Q = \left(0.5 \hat{c}_{p,N_2} (T_{out} - T_0) + 1.5 \hat{c}_{p,H_2} (T_{out} - T_0) \right) - \left(h_{f,NH_3}^o + \hat{c}_{p,NH_3} (T_{in} - T_0) \right)$$

$$Q = \left(0.5 \hat{c}_{p,N_2} (T_{out} - T_0) + 1.5 \hat{c}_{p,H_2} (T_{out} - T_0) \right) - (h_{f,NH_3}^o)$$

$$Q = (0.5 \times 29.15 \times (55) + 1.5 \times 28.96 \times (55)) - (-45,700 \text{ J}) = 48.89 \text{ kJ}$$

- b) Calculate the composition of the two streams at the exit of the cell.
[6 points | 8 points]

Begin by finding the inlet composition on the cathode side. Since the stoichiometry is 2:

$$\dot{n}_{O_2,c,in} = 2 \times \frac{\dot{n}_{H_2,c,in}}{2} = 1.5 \text{ mols/s}$$

$$\dot{n}_{N_2,c,in} = 3.76 \times \dot{n}_{O_2,c,in} = 5.64 \text{ mols/s}$$

The exit conditions on the cathode side are given by:

$$\dot{n}_{N_2,c,out} = \dot{n}_{N_2,c,in} = 5.64 \text{ mols/s}$$

$$\dot{n}_{O_2,c,out} = \dot{n}_{O_2,c,in} - \frac{\dot{n}_{H_2,a,consumed}}{2} = 1.5 - \frac{0.65 \times 1.5}{2} = 1.0125 \text{ mols/sec}$$

$$\dot{n}_{H_2O,c,out} = \dot{n}_{H_2,a,consumed} = 0.65 \times 1.5 = 0.975 \text{ mols/sec}$$

Likewise, the exit conditions on the anode side are given by:

$$\dot{n}_{N_2,a,out} = \dot{n}_{N_2,c,in} = 0.5 \text{ mols/s}$$

$$\dot{n}_{H_2,a,out} = (1 - 0.65) \times \dot{n}_{H_2,a,in} = 0.525 \text{ mols/s}$$

The corresponding exit mole fractions are summarized below:

	Cathode	Anode
H ₂	-	0.5122
O ₂	0.1327	-
N ₂	0.7394	0.4878
H ₂ O	0.1278	-

- c) Calculate the open circuit voltage of this cell based on the concentrations at the exit.
[6 points | 8 points]

To calculate the open circuit voltage, we use the Nernst Equation:

$$\begin{aligned} \Delta \mathcal{E}_{\max}(p^*, T^*) &= \Delta \mathcal{E}^o(T^*) - \frac{\sigma \mathcal{R}T^*}{n_e \mathfrak{F}_a} \ln(p^*) - \frac{\mathcal{R}T^*}{n_e \mathfrak{F}_a} \ln \left(\frac{\prod_{\text{prod}} X_i^{v_i''}}{\prod_{\text{react}} X_i^{v_i'}} \right) \\ &= \Delta \mathcal{E}^o(T^*) + \Delta \mathcal{E}_p(p^*, T^*) + \Delta \mathcal{E}_{\text{conc}}(X_i, T^*) \end{aligned}$$

The equilibrium constant K_p for the reaction $H_2 + 0.5O_2 \rightarrow H_2O$ at a standard pressure of 1 atm and at 80°C is calculated based on Table 3.6 in the notes. Using linear interpolation (note this is a simplification), $K_p = 10^{35.3259} = 2.118 \times 10^{35}$ (no units).

$$K_p(T) = \exp \left(\frac{-\Delta G^o(T)}{\mathcal{R}T} \right)$$

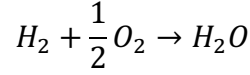
Therefore:

$$\Delta \mathcal{E}^o(T^*) = \frac{\mathcal{R}T^*}{n_e \mathfrak{F}_a} \ln K_p(T^*) = \frac{(8.314 \times 353.15)}{(2 \times 96485.33)} \ln(2.118 \times 10^{35}) = 1.238 \text{ V}$$

Similarly:

$$\Delta \varepsilon_p(p^*, T^*) = -\frac{\sigma \Re T^*}{n_e \Im_a} \ln\left(\frac{p^*}{p_0}\right) = \frac{0.5 \times (8.314 \times 353.15)}{(2 \times 96485.33)} \ln(2) = 0.00527 \text{ V}$$

Given the reaction in the cell:



The last term is calculated as:

$$\Delta \varepsilon_c(X_i, T^*) = -\frac{\Re T^*}{n_e \Im_a} \ln\left(\frac{\prod_{prod} X_i^{v_i''}}{\prod_{react} X_i^{v_i'}}\right) = \frac{(8.314 \times 353.15)}{(2 \times 96485.33)} \ln\left(\frac{X_{H_2, anode} X_{O_2, cathode}^{1/2}}{X_{H_2O, cathode}}\right)$$

$$\Delta \varepsilon_c(X_i, T^*) = 0.00576 \text{ V}$$

Summing up all components:

$$\Delta \varepsilon_{max}(p^*, T^*) = 1.25 \text{ V}$$

- d) Calculate the power delivered by the stack of 200 cells in the proposed application. [2.5 points]**

$$P = j \times A \times V \times n = 600 \frac{\text{mA}}{\text{cm}^2} \times 2000 \text{ cm}^2 \times 0.65 \text{ V} \times 200 = 156 \text{ kW}$$

- e) What is the mass flow rate of H₂ needed to generate the power? [4 points | 5 points]**

To supply a current of $I = 1200$ Amps, the number of moles of electrons needed per second is $N_e = I/F$ (where F is the Faraday number). Since each mole of H₂ supplies $n_e = 2$ moles of electrons, we get:

$$\dot{n}_{H_2} = \frac{I}{n_e F} = \frac{1,200}{2 \times 96485.33} = 0.00622 \text{ mols/s}$$

For a stack of 200 cells, we will need:

$$\dot{n}_{H_2, consumed} = 200 \times 0.00622 = 1.244 \text{ mols/s}$$

However, only 65% of H₂ is consumed (react and contribute electrons to the current) (see Figure 1). Thus, the total mole flowrate of H₂ needed is:

$$\dot{n}_{H_2, supplied} = \frac{1.244 \text{ mols/s}}{0.65} = 1.914 \text{ mols/s}$$

Assuming a molar mass of 2g/mole for H₂, this translates to a H₂ mass flowrate of **3.828 grams/sec.**

- f) What is the cooling rate required to keep the fuel cell at the desired temperature?
 Note that the inlet and exit streams are all at the same temperature as the cell.
 [4 points | 5 points]

Assuming steady state, and ignoring kinetic and potential energy changes, we get the following equation by conserving energy around the fuel cell (the control volume is specified in the figure below). Here $\dot{Q}_{cooling}$ is positive according to the arrow shown in the figure.

$$\dot{Q}_{cooling} + \dot{W}_{elec} = \sum_{inlet} \dot{n}_i h_i - \sum_{outlet} \dot{n}_i h_i$$

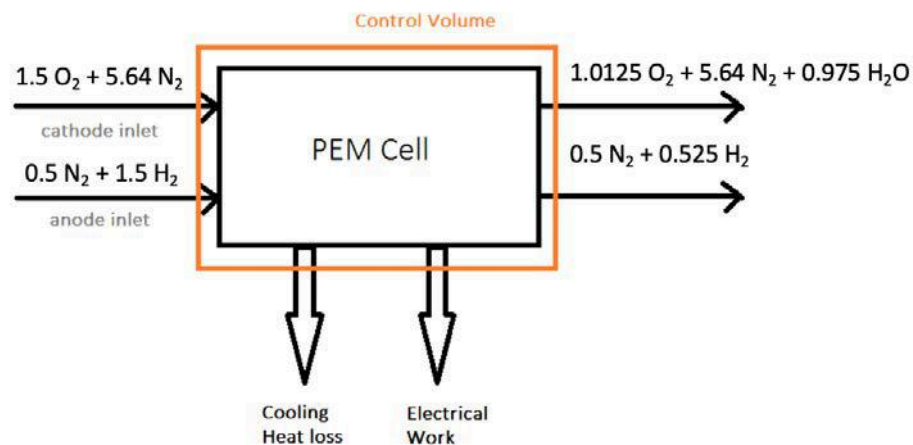


Figure 1 - Control volume to calculate cooling rate

$\dot{W}_{elec} = 156 \text{ kW}$ from part d. The right-hand side is essentially the heat released from the combustion of 1.244 moles of H₂ per second (the number of moles of H₂ participating in electrochemical reactions per second, as calculated in part e). This evaluates to $1.244 \times \text{LHV}_{H_2}$ and $\dot{Q}_{cooling} = 144.8 \text{ kW}$.

g) What is the efficiency of the cell? [2.5 points | 3.5 points]

We use the HHV value for H₂ (since water will be leaving in liquid phase under the specified conditions) and rate of fuel consumed to be more reasonable in the analysis:

$$\eta_{FU} = \frac{\text{Power Out}}{\text{Rate of Chemical Energy In}} = \frac{IV_{act}}{\dot{n}_f \Delta \hat{h}_{R,c}^\circ} = \frac{156000}{(1.244 \times 285800)} = 43.9\%$$

h) Is it better efficiency-wise to operate the cell at 10 atm? [8 points]

If the fuel cell were operated at 10 atm, the open circuit voltage would be increased by:

$$\begin{aligned} \Delta \varepsilon_{p,2}^\circ(p^*, T^*) - \Delta \varepsilon_{p,1}^\circ(p^*, T^*) &= -\frac{\sigma \mathcal{R} T^*}{n_e \mathfrak{F}_a} \ln\left(\frac{p_2^*}{p_1^*}\right) = \frac{0.5 \times (8.314 \times 353.15)}{(2 \times 96485.33)} \ln\left(\frac{10}{2}\right) \\ &= 0.0122 \text{ V} \end{aligned}$$

Therefore, for every 1.5 moles of hydrogen supplied (see Figure 1), we get an additional electric work of $\delta \dot{w} = 1.5 n_e F (d\Delta \varepsilon) = 3,531.4 \text{ W}$.

Corresponding to 1.5 moles of hydrogen supplied, 7.14 moles of air are supplied (see Figure 1). Thus, the compression work (for an ideal, isothermal compressor operating at $T = 80^\circ\text{C} = 353.15 \text{ K}$ and a pressure ratio of 5) is:

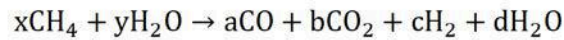
$$\dot{w}_{comp} = \dot{n} R T \ln\left(\frac{p_2^*}{p_1^*}\right) = 7.14 \times 8.314 \times 353.15 \times \ln(5) = 33.74 \text{ kW}$$

Stated differently, we are getting an addition 3.5 kW electric power by supplying 33.74 kW mechanical power to the compressor, which is not desirable.

Problem 2

- a) Determine the molar flow rate of methane and water fed to the reformer. Note that the partial pressure-based equilibrium constant of the water gas shift reaction at 800 C is $K_p = 0.8879$. [7 points | 10 points]

Across the reformer/water gas shift reactor, we can write a chemical reaction equation as,



From the given molar conditions,

$$b = 0.049$$

$$d = 0.284$$

Water gas shift reaction is



Using the thermodynamic equilibrium constant,

$$K_p = \frac{\left(\frac{P_{\text{CO}_2}}{P_0}\right)\left(\frac{P_{\text{H}_2}}{P_0}\right)}{\left(\frac{P_{\text{CO}}}{P_0}\right)\left(\frac{P_{\text{H}_2\text{O}}}{P_0}\right)} = \frac{bc}{ad} = \frac{0.049c}{0.284a} = 0.8879$$

It gives,

$$a = 0.1943c \quad (1)$$

Mass balance gives,

$$\text{C balance: } x = a + b = a + 0.049 \quad (2)$$

$$\text{H balance: } 4x + 2y = 2c + 2d = 2c + 2 \times 0.284 = 2c + 0.568 \quad (3)$$

$$\text{O balance: } y = a + 2b + d = a + 2 \times 0.049 + 0.284 = a + 0.382 \quad (4)$$

We have 4 equations (1 - 4) and 4 unknowns (a, c, x, and y). Combining 4 equations,

$$\begin{aligned} 4x + 2y &= 4(a + 0.049) + 2(a + 0.382) = 6a + 0.96 = 2c + 0.568 \\ 6(0.1943)c + 0.96 &= 2c + 0.568 \end{aligned}$$

Thus,

$$a = 0.0913, \quad c = 0.47, \quad x = 0.1403, \quad y = 0.4733$$

Therefore,

$$\begin{aligned} \text{CH}_4 &: 0.1403 \text{ kmol/s} \\ \text{H}_2\text{O} &: 0.4733 \text{ kmol/s (Ans)} \end{aligned}$$

- b) Calculate the flow rate of hydrogen and the current produced by the fuel cell. [3 points | 5 points]

From the answer to the question 1,

$$\dot{n}_{H_2} = c = 0.47 \text{ kmol/s (Ans)}$$

Using the faraday constant F_a ,

$$I = n_e F_a \dot{n}_{H_2} = 2 \times 96485 \times 0.47 \times 1000 = 90.7 \times 10^6 \text{ A (Ans)}$$

- c) Determine the heat transfer rate across the reformer/water gas shift reactor. [5 points | 7.5 points]

Applying the first law to the reformer/water gas shift reactor,

$$0 = \dot{Q}_1 - \dot{W}_{out} + \sum_{in} \dot{n}_{in} \hat{h}_{in} - \sum_{out} \dot{n}_{out} \hat{h}_{out}$$

Across the reformer/water gas shift reactor, $\dot{W}_{out} = 0$. Thus,

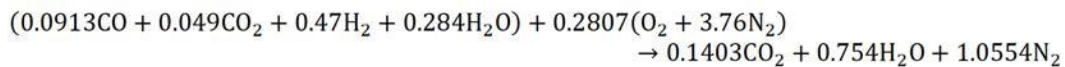
$$\begin{aligned} \dot{Q}_1 &= \sum_{out} \dot{n}_{out} \hat{h}_{out} - \sum_{in} \dot{n}_{in} \hat{h}_{in} \\ &= [\dot{n}_{CO} \hat{h}_{CO} + \dot{n}_{CO_2} \hat{h}_{CO_2} + \dot{n}_{H_2} \hat{h}_{H_2} + \dot{n}_{H_2O} \hat{h}_{H_2O}] - [\dot{n}_{CH_4} \hat{h}_{CH_4} + \dot{n}_{H_2O} \hat{h}_{H_2O}] \\ &= [0.0913 \times (-86410) + 0.049 \times (-356100) + 0.47 \times (22900) + 0.284 \times (-212800)] \\ &\quad - [0.1403 \times (-74610) + 0.4733 \times (-285900)] \\ &= 70772 \text{ kJ/s} \end{aligned}$$

Therefore,

$$\dot{Q}_1 = 70772 \text{ kJ/s (Ans)}$$

- d) Calculate the flow rate of air into the fuel cell. [5 points | 7.5 points]

Because the stream (1)/air ratio is stoichiometric,



Thus,

$$\dot{n}_{air} = 0.2807(1 + 3.76) = 1.336 \text{ kmol/s (Ans)}$$

- e) Assuming that the product stream (2) of the fuel cell consists of CO, CO₂, and H₂O, determine the maximum work transfer of the fuel cell. [6 points | 10 points]

Because only hydrogen reacts as a fuel and the fuel utilization is 100%,

$$\left(\begin{array}{c} (0.0913\text{CO} + 0.049\text{CO}_2 + \mathbf{0.47\text{H}_2} + 0.284\text{H}_2\text{O}) \\ \text{anode inlet} \end{array} \right) + \left(\begin{array}{c} (\mathbf{0.235\text{O}_2} + 0.0457\text{O}_2 + 1.0554\text{N}_2) \\ \text{cathode inlet} \end{array} \right) \\ \rightarrow \left(\begin{array}{c} (0.0913\text{CO} + 0.049\text{CO}_2 + \mathbf{0.47\text{H}_2\text{O}} + 0.284\text{H}_2\text{O}) \\ \text{anode outlet} \end{array} \right) + \left(\begin{array}{c} (0.0457\text{O}_2 + 1.0554\text{N}_2) \\ \text{cathode outlet} \end{array} \right)$$

To get the maximum work transfer, we need to calculate the negative of the change in Gibbs free energy for the given temperature and the pressure. Thus,

$$\begin{aligned} \dot{W}_{\max} &= -\Delta G_{\text{rxn}}(T, p) = -\Delta G_{\text{rxn}}^{\circ}(T) - \sigma \bar{R} T \ln \left(\frac{P}{P_0} \right) - \bar{R} T \ln \left(\frac{\prod_{\text{prod}} X_i^{v''_i}}{\prod_{\text{react}} X_i^{v''_i}} \right) \\ \dot{W}_{\max} &= -\Delta G_{\text{rxn}}^{\circ}(T = 800\text{C}) - \sigma \bar{R} T \ln \left(\frac{P}{P_0} \right) \\ &\quad - \bar{R} T \left(\dot{n}_{\text{H}_2\text{O}, a, \text{out}} \ln X_{\text{H}_2\text{O}, a, \text{out}} + \dot{n}_{\text{O}_2, c, \text{out}} \ln X_{\text{O}_2, c, \text{out}} + \dot{n}_{\text{N}_2, c, \text{out}} \ln X_{\text{N}_2, c, \text{out}} - \dot{n}_{\text{H}_2, a, \text{in}} \ln X_{\text{H}_2, a, \text{in}} + \dot{n}_{\text{O}_2, c, \text{in}} \ln X_{\text{O}_2, c, \text{in}} + \dot{n}_{\text{N}_2, c, \text{in}} \ln X_{\text{N}_2, c, \text{in}} \right) \\ &= 88595 + 4827 - 5977 \\ &= 87445 \text{ kJ/s} \end{aligned}$$

The CO₂ and CO terms cancel out as the total molar flow rate at the anode is constant.

- f) Determine the actual work transfer from the fuel cell, assuming a second law efficiency of 70% for the fuel cell. [2 points | 2.5 points]

$$\dot{W}_1 = \dot{W}_{\max} \times \eta_{\text{II}} = 87445 \times 0.7 = \mathbf{61211 \text{ kJ/s (Ans)}}$$

- g) Calculate the operating voltage of the fuel cell. [2 points | 2.5 points]

Based on the power output \dot{W}_1 ,

$$V = \frac{\dot{W}_1}{I} = \frac{61211 \times 1000}{90.7 \times 10^6} = \mathbf{0.675 \text{ V (Ans)}}$$

Problem 3

- a) Determine the mole fractions at the anode and cathode. What is the theoretical open circuit voltage of this cell? [12 points]

Anode:

Start by using the information we have for water vapor:

$$\phi_{in} = \frac{P_v}{P_{sat}} = \frac{X_v P_0}{P_{sat}} \quad \rightarrow \quad X_{H_2O} = \phi_{in} \left(\frac{P_{sat}}{P_0} \right) = 0.2 \times 0.4708 = 0.09416$$

Given the molar ratio of H₂ to CO₂:

$$X_{H_2} = (1 - X_{H_2O}) \times \frac{4}{5} = 0.7247$$

$$X_{CO_2} = (1 - X_{H_2O}) \times \frac{1}{5} = 0.1812$$

Cathode:

Start by using the information we have for water vapor:

$$\phi_{in} = \frac{P_v}{P_{sat}} = \frac{X_v P_0}{P_{sat}} \quad \rightarrow \quad X_{H_2O} = \phi_{in} \left(\frac{P_{sat}}{P_0} \right) = 0.4 \times 0.4708 = 0.18832$$

Given the molar ratio of N₂ to O₂:

$$X_{O_2} = (1 - X_{H_2O}) \times \frac{1}{4.76} = 0.1705$$

$$X_{N_2} = (1 - X_{H_2O}) \times \frac{3.76}{4.76} = 0.6412$$

Theoretical Open Circuit Voltage:

We do this calculation based on inlet conditions – assuming each stream is pure:

Taking $T_0 = 298$ K, the properties @ (353K and 1) bar are calculated as follows:

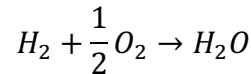
$$h_i = \hat{c}_p(T_i - T_0) + h_{f,i}^o$$

$$s_i = s_i^o + \hat{c}_p \ln\left(\frac{T_i}{T_0}\right)$$

$$g_i = h_i - T_i s_i$$

	Enthalpy (J/mol)	Entropy (J/mol-K)	Gibbs free energy (J/mol)
H2	1592.8	135.5851	-46268.8
O2	1625.25	210.157	-72560.2
H2O	-239978.55	194.5243	-308645.6

In this case, the reaction occurring within the fuel cell is:



$$\Delta \varepsilon_{OC} = \frac{-\Delta G_R^0(353K)}{2F} + \frac{RT}{2F} \ln\left(\frac{X_{H_2,anode} X_{O_2,cathode}^{1/2}}{X_{H_2O,cathode}}\right) = 1.178 \text{ V}$$

- b) Determine What is the open circuit (thermodynamic) efficiency based on the lower heating value of H2? (LHV of H2 is 120.1 MJ/kg) [2 points]**

$$\Delta H_{LHV} = (120.1 \text{ MJ/kg}) \times (2.016 \text{ kg/kmol}) = 242,121.6 \text{ J/mol}$$

$$\eta_{OC} = \frac{\Delta G_R}{\Delta H_{LHV}} = \frac{2F(\Delta \varepsilon_{OC})}{\Delta H_{LHV}} = 93.9\%$$

- c) How many individual cells are needed to supply the required power for the vehicle? [2 points]**

$$Power = N_{cell} jVA$$

$$N_{cell} = \frac{Power}{jVA} = \frac{80,000 \text{ W}}{1 \frac{\text{A}}{\text{cm}^2} \times 0.6 \text{ V} \times 650 \text{ cm}^2} = 205 \text{ cells}$$

d) What is the total molar flow rate of oxygen? [2 points]

$$I = n_e F n_{O_2,consumed} = \frac{Power}{V}$$

$$\dot{n}_{O_2,consumed} = \frac{Power}{V(n_e F)} = \frac{80,000 \text{ W}}{4 \times 0.6 \text{ V} \times 96485 \text{ C/mol}} = 0.3455 \text{ mol/s}$$

Given the air stoichiometry is 2:

$$\dot{n}_{O_2,inlet} = 2 \times 0.3455 = 0.69 \text{ mol/s}$$

The corresponding molar flow rates of N₂ and H₂O at the inlet are:

$$\dot{n}_{N_2,in} = 3.76 \times \dot{n}_{O_2,inlet} = 2.59 \text{ mol/s}$$

$$\frac{\dot{n}_{H_2O,in}}{\dot{n}_{O_2,in}} = \frac{X_{H_2O,in}}{X_{O_2,in}} \rightarrow \dot{n}_{H_2O,in} = \left(\frac{0.18832}{0.1705} \right) \times 0.69 = 0.762 \text{ mol/s}$$

e) What is the composition of the air-side stream at the exit of the stack, expressed in terms of the mole fractions of N₂, O₂, and H₂O? [5 points]

$$\dot{n}_{H_2O,prod} = 2\dot{n}_{O_2,consumed} = 0.69 \text{ mol/s}$$

$$\dot{n}_{H_2O,exit} = \dot{n}_{H_2O,inlet} + \dot{n}_{H_2O,prod} = 1.452 \text{ mol/s}$$

$$\dot{n}_{O_2,exit} = \dot{n}_{O_2,inlet} - \dot{n}_{O_2,consumed} = 0.3445 \text{ mol/s}$$

$$\dot{n}_{N_2,exit} = \dot{n}_{N_2,inlet} = 2.59 \text{ mol/s}$$

Therefore:

$$X_{H_2O} = \frac{\dot{n}_{H_2O,exit}}{\dot{n}_{H_2O,exit} + \dot{n}_{O_2,exit} + \dot{n}_{N_2,exit}} = 0.331$$

$$X_{O_2} = \frac{\dot{n}_{O_2,exit}}{\dot{n}_{H_2O,exit} + \dot{n}_{O_2,exit} + \dot{n}_{N_2,exit}} = 0.0785$$

$$X_{N_2} = \frac{\dot{n}_{N_2,exit}}{\dot{n}_{H_2O,exit} + \dot{n}_{O_2,exit} + \dot{n}_{N_2,exit}} = 0.591$$

- f) When the design exit air relative humidity is 90%, does the current operating conditions satisfy the design target? [2 points]

$$\phi = \frac{P_{H_2O}}{P_{H_2O,sat}} = \frac{0.331}{0.4708} = 70\%$$

Therefore, the relative humidity is lower than the design target.

- g) What is the composition at the anode side exit stream? [6 points]

The molar fraction is independent of the total number of moles (provided the composition remains constant). Take the composition to be that of the anode inlet (Part a) such that $\sum n_i = 1$ mols of mixture (at anode inlet), and account for changes. Given the fuel utilization, we know that:

$$\phi = \frac{\dot{n}_{H_2,inlet} - \dot{n}_{H_2,exit}}{\dot{n}_{H_2,inlet}} = 0.9$$

$$\dot{n}_{H_2,exit} = 0.1\dot{n}_{H_2,inlet}$$

Similarly by mass conservation in the anode:

$$\dot{n}_{H_2O,exit} = \dot{n}_{H_2O,inlet} = \frac{X_{H_2O}}{X_{H_2}} \dot{n}_{H_2,inlet}$$

$$\dot{n}_{CO_2,exit} = \dot{n}_{CO_2,inlet} = \frac{X_{CO_2}}{X_{H_2}} \dot{n}_{H_2,inlet}$$

By the definition of molar fraction:

$$X_{H_2} = \frac{\dot{n}_{H_2,exit}}{\dot{n}_{H_2,exit} + \dot{n}_{CO_2,exit} + \dot{n}_{H_2O,exit}} = \frac{0.07247}{0.07247 + 0.1812 + 0.09416} = 0.208$$

$$X_{CO_2} = \frac{\dot{n}_{CO_2,exit}}{\dot{n}_{H_2,exit} + \dot{n}_{CO_2,exit} + \dot{n}_{H_2O,exit}} = \frac{0.1812}{0.07247 + 0.1812 + 0.09416} = 0.521$$

$$X_{H_2O} = \frac{\dot{n}_{H_2O,exit}}{\dot{n}_{H_2,exit} + \dot{n}_{CO_2,exit} + \dot{n}_{H_2O,exit}} = \frac{0.09416}{0.07247 + 0.1812 + 0.09416} = 0.271$$

h) What is the molar flow rate of the fuel stream at the inlet? [3 points]

$$I = n_e F n_{H_2,consumed} = \frac{Power}{V}$$

$$\dot{n}_{H_2,consumed} = \frac{Power}{V(n_e F)} = \frac{80,000 \text{ W}}{2 \times 0.6 V \times 96485 \text{ C/mol}} = 0.691 \text{ mol/s}$$

Accounting for fuel utilization:

$$\dot{n}_{H_2,inlet} = \frac{\dot{n}_{H_2,consumed}}{0.9} = 0.7678 \text{ mol/s}$$

i) What is the first law efficiency of the cell? [2 points]

$$\eta_l = \frac{\text{generated power}}{\text{chemical energy in}} = \frac{80 \text{ kW}}{LHV_{H_2} \times \dot{n}_{H_2,inlet}} = \frac{80}{240.2 \times 0.7678} = 43.37\%$$

j) What is the cooling rate required to keep the fuel cell at 80C? [4 points]

$$0 = \sum_{in} \dot{n}_i h_i - \sum_{out} \dot{n}_i h_i + \dot{Q} - \dot{W}$$

$$\dot{Q} = \dot{W} + \sum_{out} \dot{n}_i h_i - \sum_{in} \dot{n}_i h_i$$

$$\dot{Q} = \dot{W} + (\dot{n}_{H_2O,produced} h_{H_2O}) - (\dot{n}_{H_2,consumed} h_{H_2}) - (\dot{n}_{O_2,consumed} h_{O_2})$$

$$\dot{Q} = 80 + 0.691 \times (-239.98) - (0.691 \times 1.59) - (0.3455 \times 1.63) = -87.49 \text{ kW}$$

k) Derive an expression for the exit relative humidity: [15 points]

By definition:

$$\phi_{exit} = \frac{\dot{n}_{H_2O,exit}}{\dot{n}_{H_2O,exit} + \dot{n}_{N_2,exit} + \dot{n}_{O_2,exit}} \frac{p^0}{p_{H_2O,sat}}$$

Expanding the terms:

$$\dot{n}_{O_2,consumed} = \frac{Power}{4VF}$$

$$\dot{n}_{N_2,exit} = \dot{n}_{N_2,inlet} = 3.76\lambda\dot{n}_{O_2,consumed}$$

$$\dot{n}_{O_2,exit} = \dot{n}_{O_2,inlet} - \dot{n}_{O_2,consumed} = (\lambda - 1)\dot{n}_{O_2,consumed}$$

To find the last term, we start by defining a ratio of vapor pressures:

$$\psi = \left(\frac{P_{H_2O,in}}{P_{N_2+O_2,in}} \right) = \left(\frac{\phi_{in} P_{H_2O,sat}}{P_0 - \phi_{in} P_{H_2O,sat}} \right)$$

Likewise, using the definition of partial pressure:

$$\psi = \left(\frac{X_{H_2O,in}}{X_{N_2+O_2,in}} \right) = \left(\frac{n_{H_2O,in}}{n_{N_2+O_2,in}} \right)$$

For one mole of oxygen entering, this becomes:

$$\psi = \left(\frac{n_{H_2O,in}}{4.76} \right) \rightarrow n_{H_2O,in} = 4.76\psi \text{ (per mole of } O_2)$$

Accounting for the total amount of oxygen entering:

$$\dot{n}_{H_2O,in} = 4.76\lambda\psi\dot{n}_{O_2,consumed}$$

Also we know that:

$$\dot{n}_{H_2O,produced} = 2\dot{n}_{O_2,consumed}$$

Therefore:

$$\dot{n}_{H_2O,exit} = \dot{n}_{H_2O,inlet} + \dot{n}_{H_2O,produced} = 4.76\lambda\psi\dot{n}_{O_2,consumed} + 2\dot{n}_{O_2,consumed}$$

Substituting back into our starting equation:

$$\begin{aligned}\phi_{exit} &= \frac{\dot{n}_{H_2O,exit}}{\dot{n}_{H_2O,exit} + \dot{n}_{N_2,exit} + \dot{n}_{O_2,exit}} \frac{p^0}{p_{H_2O,sat}} \\ \phi_{exit} &= \frac{4.76\lambda\psi + 2}{4.76\lambda\psi + 2 + 3.76\lambda + (\lambda - 1)} \frac{p^0}{p_{H_2O,sat}} \\ &= \frac{4.76\lambda\psi + 2}{4.76\lambda\psi + 4.76\lambda + 1} \frac{p^0}{p_{H_2O,sat}} = \frac{\lambda\psi + 0.42}{\lambda(\psi + 1) + 0.21} \frac{p^0}{p_{H_2O,sat}}\end{aligned}$$

- I) What should be the relative humidity of the inlet air if the relative humidity of the exit air is 90%? [5 points]**

We start by solving for the ratio of vapor pressures:

$$\phi_{exit} = 0.9 = \frac{2\psi + 0.42}{2\psi + 2.21} \frac{1}{0.4708}$$

$$\psi = \frac{\phi_{inlet} p_{H_2O,sat}}{p^0 - \phi_{inlet} p_{H_2O,sat}} = 0.448$$

Using the definition of the ψ :

$$\frac{1}{\psi} = \frac{p^0 - \phi_{inlet} p_{H_2O,sat}}{\phi_{inlet} p_{H_2O,sat}} = \frac{1}{\phi_{inlet} 0.4708} - 1 = \frac{1}{0.448}$$

$$\phi_{inlet} = 0.657$$

MIT OpenCourseWare
<https://ocw.mit.edu/>

2.60J Fundamentals of Advanced Energy Conversion
Spring 2020

For information about citing these materials or our Terms of Use, visit: <https://ocw.mit.edu/terms>.

Homework 4

2.60/2.62/10.390 Fundamentals of Advanced Energy Conversion
Spring 2020

Total points: 100 (Undergraduate) | 150 (Graduate)

Problem 2. Electrochemical Cells as Sensors and Expanders [50% for Undergrads and Grads]

Electrochemical cells are used extensively as concentration sensors. For instance, as the oxygen sensor of an IC engine. In this case, the products of combustion from the engine are introduced along one electrode of the cell, and air is introduced along the other electrode. The sensor is used to measure the concentration of oxygen in the products given that the oxygen concentration in air is known (0.21). The electrolyte of this cell conducts oxygen ions (O^{2-}). The open circuit potential difference between the two electrodes, which depends on the ratio of oxygen concentration in the two streams, is used to determine the concentration of oxygen in the products.

Please answer the following questions:

- Drive a relation between the open circuit potential of the cell and the oxygen concentration in the products stream. Plot this relation when the cell temperature is 25 C, 100 C and 400 C.
- A similar concept can be used as an isothermal expander (electric work producing machine). In this case, pure hydrogen at high pressure is introduced along one electrode of the cell while the hydrogen concentration is maintained at much lower values along the opposite electrode. The electrolyte conducts hydrogen protons (H^+).

Drive an expression for the open circuit potential and the ideal work of expansion in this case in terms of the hydrogen partial pressure ratio across the electrolyte. Compare this expression with the isothermal mechanical work of expansion across the same pressure ratio. Comment on this result. Calculate the open circuit potential at $T = 30$ C, and hydrogen pressure ratio across the electrolyte of 100 and 10,000.

- As shown in **Figure 1**, it has been proposed to construct a power cycle using (i) isothermal compression between pressures p_1 and p_2 at the initial temperature T_1 , (ii) constant pressure heating at p_2 to T_3 , and (iii) expansion back to p_1 . Drive an expression for the efficiency of this cycle and compare it to that of a conventional Bryton cycle between the same two pressures. Calculate both efficiencies for pressure ratio of 30, $T_1 = 300$ K and $T_3 = 1600$ K.

For graduate students only

- d. How can you improve the efficiency of the cycle proposed in (c) and what is the new efficiency?
- e. Explain how the reverse of the set up described in part (b) can be used as an isothermal electrochemical compressor, in which a voltage is applied to pump the gas (hydrogen in the case of part (b)) from the low-pressure side to the high-pressure side. What is the open circuit voltage required to produce an oxygen stream at 10 bars from air?

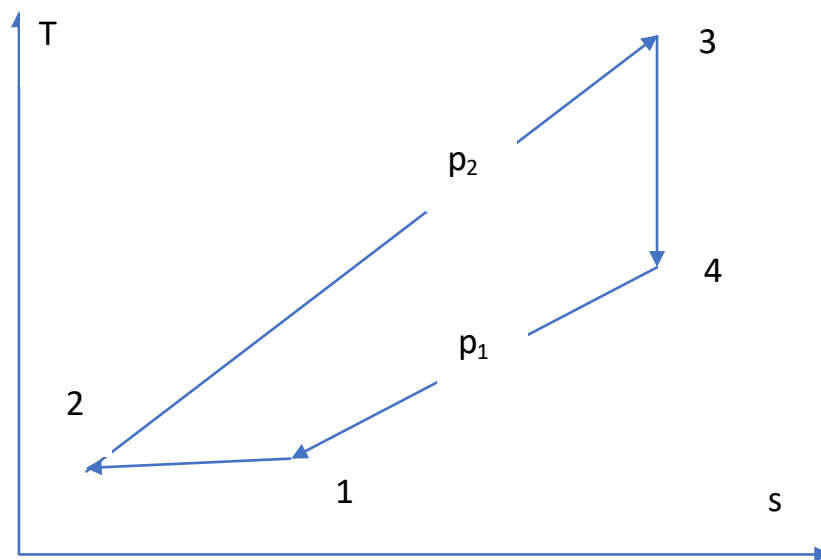


Figure 1 - Proposed Power Cycle

Problem 2. Steam-Injected Gas Turbine Cycle [25% for Undergrads and Grads]

Consider the steam-injected gas turbine cycle shown in the **Figure 2**. Air at 298 K and 100 kPa enters the compressor. The pressure ratio is 9. The turbine inlet temperature is 1423 K. The flue gases leaving the turbine flow through a heat recovery steam generator (HRSG) which produces superheated steam at 700 K. The exhaust gases leave the HRSG at 400 K.

Water at 298K and 100 kPa is pumped to the HRSG. No water recycling from the flue gas is considered. The compressor, turbine and pump operate with isentropic efficiency of 90%, 85% and 70%, respectively. The fuel burnt in the combustor is methane with LHV of 50.05 MJ/kg. The properties of the flow at states 3, 4 and 5 may be modeled as an idea gas of air + steam mixture.

Determine:

- The amount of steam injection and fuel consumption per unit mass of the air.
- The net work produced by the cycle.
- The thermal efficiency of the cycle.
- The simple gas turbine cycle efficiency (without the steam injection).

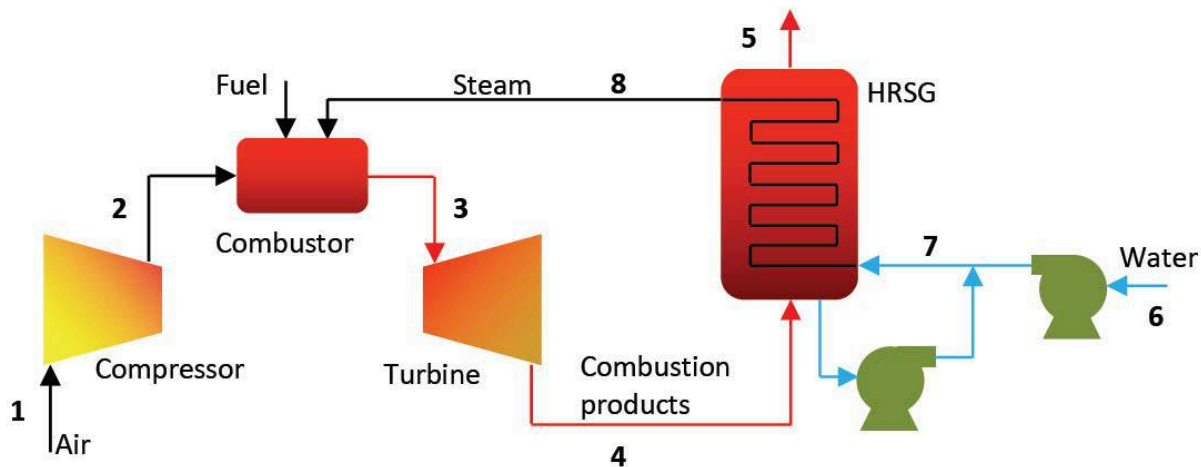


Figure 2 - Steam injected gas turbine cycle

Problem 3. Combined Cycle Power Plant [25% for Undergrads and Grads]

Consider the combined cycle power plant shown in **Figure 3**. Air at 300 K and 100 kPa enters the compressor whose isentropic efficiency is 80%. It is then compressed to 800 kPa, and heated to 1500 K. The hot stream leaving the gas turbine, which operates with an isentropic efficiency of 88%, flows through the HRSG, where it is cooled to 423 K.

Superheated steam at 723 K and 8 MPa enters the steam turbine and it is expanded to 6 kPa. The mass of fuel burnt in the combustor is negligible compared to that of the air. The isentropic efficiencies of the steam turbine and pump are 90% and 70%, respectively.

Determine:

- The amount of steam produced in the HRSG per unit mass of air.
- The work output of the gas and steam cycles.
- The thermal efficiency of gas and steam cycles if they would operate separately.
- The thermal efficiency of the combined cycle.

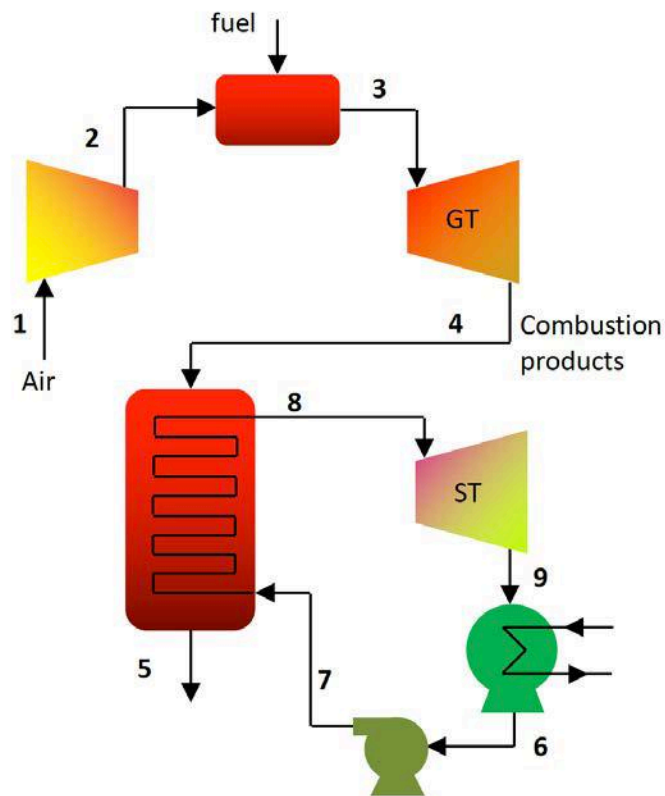


Figure 3 - Combined cycle powerplant

MIT OpenCourseWare
<https://ocw.mit.edu/>

2.60J Fundamentals of Advanced Energy Conversion
Spring 2020

For information about citing these materials or our Terms of Use, visit: <https://ocw.mit.edu/terms>.

2.62 – Advanced Energy Conversion | Spring 2020

Homework 4 – Solutions

Problem 1 (35%)

- a) Drive a relation between the open circuit potential of the cell and the oxygen concentration in the products stream. Plot this relation when the cell temperature is 25 C, 100 C and 400 C? [15 points]

First, we use the Nernst Equation for the reaction noting that no reaction occurs:

$$\chi_{react} = \chi_{prod}$$

$$\begin{aligned}\Delta \mathcal{E}_{\max}(p^*, T^*) &= \Delta \mathcal{E}^o(T^*) - \frac{\sigma \Re T^*}{n_e \mathfrak{T}_a} \ln(p^*) - \frac{\Re T^*}{n_e \mathfrak{T}_a} \ln \left(\frac{\prod_{prod} X_i^{v_i''}}{\prod_{react} X_i^{v_i'}} \right) \\ &= \Delta \mathcal{E}^o(T^*) + \Delta \mathcal{E}_p(p^*, T^*) + \Delta \mathcal{E}_{conc}(X_i, T^*)\end{aligned}$$

Simplifying the equation yields (in terms of the partial pressures):

$$\Delta \mathcal{E} = - \frac{RT}{n_e \mathfrak{T}_a} \ln \left(\frac{p''_{\chi}}{p'_{\chi}} \right)$$

Noting that we have oxygen on both sides and given the oxygen concentration in air:

$$\Delta \mathcal{E} = - \frac{RT}{n_e \mathfrak{T}_a} \ln \left(\frac{p''_{O_2}}{p'_{O_2}} \right) = - \frac{RT}{n_e \mathfrak{T}_a} \ln \left(\frac{p''_{O_2}}{0.21} \right) = - \frac{RT}{n_e \mathfrak{T}_a} \ln \left(\frac{X''_{O_2}}{0.21} \right)$$

Plotting this relationship for the temperatures indicated:

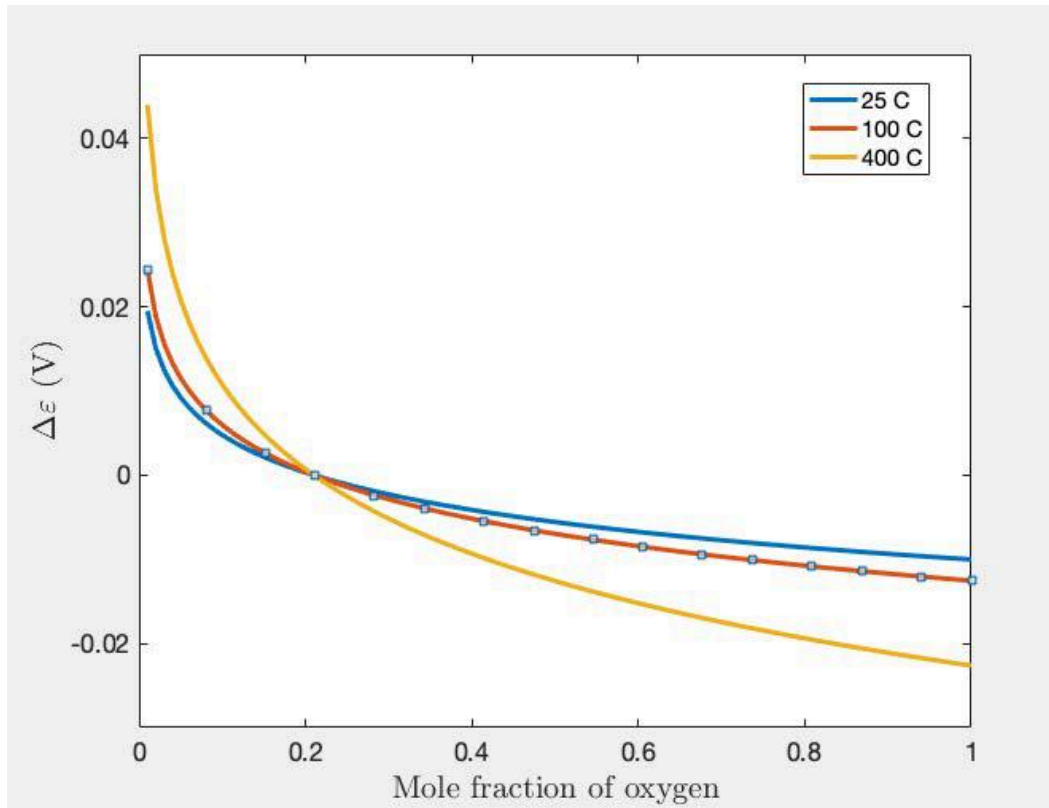


Figure 1 - Open circuit potential as a function of oxygen concentrations in the products stream

Note for one mole of oxygen, 4 moles of electrons are generated ($n_e = 4$). As can be seen, the voltage drops as a function of molar concentration in the products stream. Note the crossover point that occurs at $X''_{O_2} = 0.21$. At that point, a reversal in the voltage sign occurs given the nature of the logarithmic relationship. An increase in temperature amplifies the voltage in either direction (positive or negative).

- b) Drive an expression for the open circuit potential and the ideal work of expansion in this case in terms of the hydrogen partial pressure ratio across the electrolyte. Compare this expression with the isothermal mechanical work of expansion across the same pressure ratio. Comment on this result. Calculate the open circuit potential at T = 30 C, and hydrogen pressure ratio across the electrolyte of 100 and 10,000. [10 points]

For hydrogen, an expression similar to the one presented previously is obtained.

$$\Delta\varepsilon = -\frac{RT}{n_e\mathfrak{T}_a} \ln\left(\frac{p''_{H_2}}{p'_{H_2}}\right)$$

Noting that per molecule of hydrogen consumed two electrons are generated, the work may be expressed as:

$$W = 2\mathfrak{T}_a\Delta\varepsilon = -RT \ln\left(\frac{p''_{H_2}}{p'_{H_2}}\right)$$

Interestingly, we can show that this is the same result as applying the first and second laws of thermodynamics in isothermal expansion.

$$Q = W$$

$$Q = T\Delta S = RT \ln\left(\frac{p_2}{p_1}\right)$$

Calculating the open circuit potential for the conditions specified:

$$\Delta\varepsilon_1 = -\frac{RT}{n_e\mathfrak{T}_a} \ln\left(\frac{p''_{H_2}}{p'_{H_2}}\right) = -\frac{(8.314 \times 303.15)}{(2 \times 96485.33)} \ln(1/100) = 0.06 \text{ V}$$

$$\Delta\varepsilon_2 = -\frac{RT}{n_e\mathfrak{T}_a} \ln\left(\frac{p''_{H_2}}{p'_{H_2}}\right) = -\frac{(8.314 \times 303.15)}{(2 \times 96485.33)} \ln(1/10000) = 0.12 \text{ V}$$

- c) Drive an expression for the efficiency of this cycle and compare it to that of a conventional Bryton cycle between the same two pressures. Calculate both efficiencies for pressure ratio of 30, $T_1 = 300$ K and $T_3 = 1600$ K. [10 points]

The T-s diagram comparing both cycles is shown Figure 2. In this figure, the proposed cycle is given by the states 1-2-3-4, whereas the Brayton cycle is given by the states 1-5-3-4. The efficiency of the Brayton cycle is given in terms of the pressure ratio π_p (refer Chapter 5 in the notes):

$$\eta_{Br} = 1 - \left(\frac{1}{\pi_p} \right)^{\frac{k-1}{k}}$$

For air with an isentropic index of $k = 1.4$, this evaluates to:

$$\eta_{Br} = 1 - \left(\frac{1}{\pi_p} \right)^{\frac{k-1}{k}} = 1 - \left(\frac{1}{30} \right)^{\frac{1.4-1}{1.4}} = 62.2\%$$

For the proposed cycle with isothermal compression, the work of the compression process is given from Part b as:

$$W_c = -RT \ln \left(\frac{P_2}{P_1} \right) = -8.314 \times 300 \times \ln 30 = -8,483.2 \text{ J/mol}$$

Similarly, the work of the turbine is given by (refer to Chapter 5):

$$W_T = \left(\frac{k}{k-1} \right) RT_3 \left(1 - \left(\frac{1}{\pi_p} \right)^{\frac{k-1}{k}} \right) = \left(\frac{1.4}{0.4} \right) \times 8.314 \times 1600 \times \left(1 - \left(\frac{1}{30} \right)^{\frac{0.4}{1.4}} \right)$$

$$W_T = 28,940 \text{ J/mol}$$

Therefore, the efficiency of the proposed cycle with isothermal compression is given by:

$$\eta = \frac{W_T + W_c}{c_p(T_3 - T_2)} = \frac{20,456.8}{29.2 \times (1300)} = 53.89\%$$

The efficiency is **lower** for the isothermal cycle given heat transfer occurring across a considerable temperature gradient from state 2 to 3.

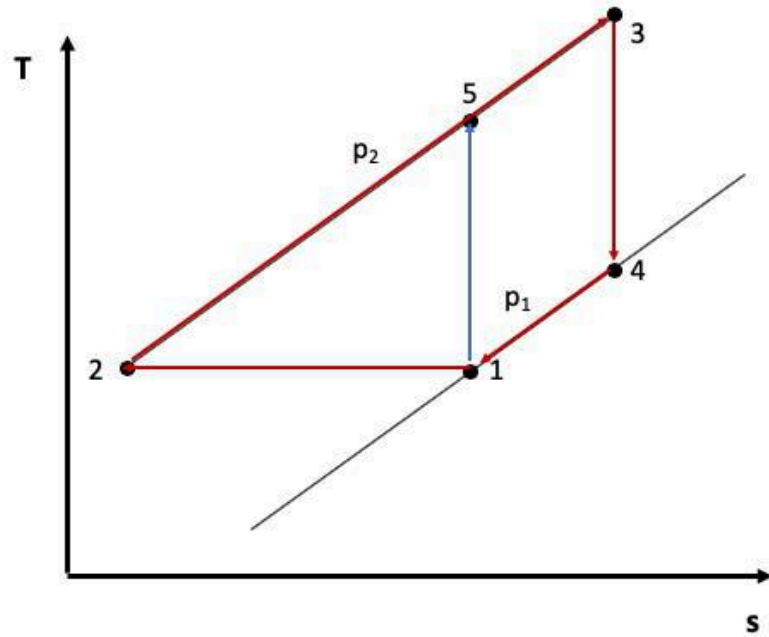


Figure 2 - T-s Diagram for the two cycles under consideration

- d) How can you improve the efficiency of the cycle proposed in (c) and what is the new efficiency? [10 points]

Noting the large input of heat necessary, the cycle may be improved by using regeneration to reduce Q_{in} . This is achieved by recovering the waste heat such that the lowest temperature in the cycle T_4 . This is illustrated in Figure 3, and the resulting efficiency is calculated as follows:

$$T_4 = T_3 \left(\frac{1}{\pi_p} \right)^{\frac{k-1}{k}} = 1600 \times \left(\frac{1}{30} \right)^{\frac{0.4}{1.4}} = 605.5 \text{ K}$$

$$\eta = \frac{W_T + W_c}{c_p(T_3 - T_4)} = \frac{20,456.8}{29.2 \times (994.5)} = 70\%$$

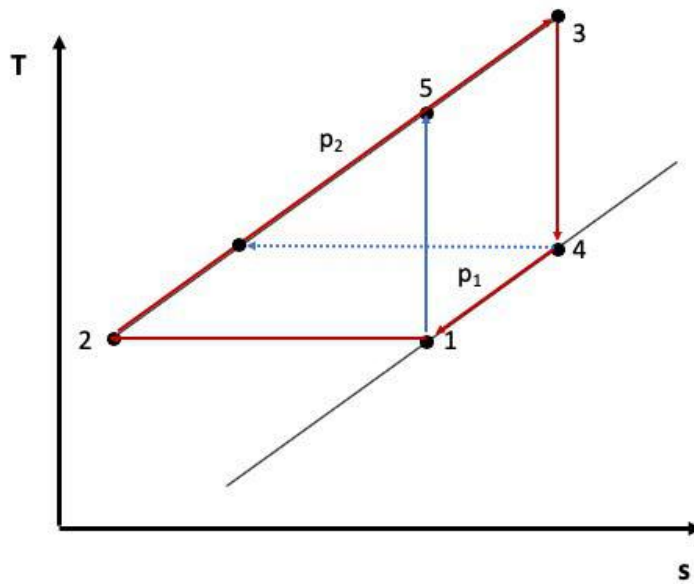


Figure 3 - T-s diagram with improved cycle

- e) Explain how the reverse of the set up described in part (b) can be used as an isothermal electrochemical compressor, in which a voltage is applied to pump the gas (hydrogen in the case of part (b)) from the low-pressure side to the high-pressure side. What is the open circuit voltage required to produce an oxygen stream at 10 bars from air? [7.5 points]

The application of a voltage reverses the driving force across the fuel cell such that hydrogen is transported from low pressure to high pressure and the cell effectively acts as an isothermal electrochemical compressor. The open circuit voltage necessary to produce an oxygen stream at 10 bars from air is given by:

$$\Delta \varepsilon = -\frac{RT}{n_e \mathfrak{F}_a} \ln \left(\frac{p''_{O_2}}{p'_{O_2}} \right) = -\frac{(8.314 \times 303.15)}{(4 \times 96485.33)} \ln \left(\frac{10}{0.21} \right) = -0.025 \text{ V}$$

Problem 2 (32.5%)

- a) Determine the amount of steam injection and fuel consumption per unit mass of the air. [15 points Undergrad | 22.5 points Grad]

We start by fixing some of the states specified before proceeding. While state 1 is given, state 2 can be fixed by determining the temperature at the outlet of the compressor given the inlet conditions and the compression ratio. Hence, using the result from Chapter 5:

$$T_2 = T_1 \left(1 + \frac{1}{\eta_c} \left[(r_p)^{\frac{k-1}{k}} - 1 \right] \right) = 298 \left(1 + \frac{1}{0.9} \left[(9)^{\frac{1.39-1}{1.39}} - 1 \right] \right) = 580.2 \text{ K}$$

Similarly, for the turbine:

$$T_4 = T_3 \left(1 - \eta_T \left[1 - (r_p)^{\frac{1-k}{k}} \right] \right) = 1423 \left(1 - 0.85 \left[1 - (9)^{\frac{-0.29}{1.29}} \right] \right) = 951.53 \text{ K}$$

Furthermore, the conditions at the inlet and exit of the pump are defined using EES such that:

$$h_6 = 104.3 \text{ kJ/kg} \quad \text{and} \quad v_6 = 0.001 \text{ m}^3/\text{kg}$$

As an incompressible fluid, the enthalpy at the pump exit is calculated as follows:

$$h_{7s} = h_6 + v(p_7 - p_6) = 104.3 + 0.001 \times (900 - 100) = 105.1 \text{ kJ/kg}$$

$$h_7 = h_6 + \frac{h_{7s} - h_6}{0.7} = 104.3 + \frac{0.8}{0.7} = 105.4 \text{ kJ/kg}$$

Next, we apply the first law across the combustor to arrive at the expression below. Note that the flow at the exit in state 3 is modeled as an ideal gas mixture of air + steam.

$$\sum_{\text{reactants}} H_i = \sum_{\text{products}} H_i$$

$$\dot{m}_{f,in} LHV_{f,in} + \dot{m}_{air,in} h_{air,in} + \dot{m}_{s,in} h_{s,in} = \dot{m}_{air,out} h_{air,out} + \dot{m}_{s,out} h_{s,out}$$

$$\dot{m}_{f,in} LHV_{f,in} + \dot{m}_{air,2} h_{air,2} + \dot{m}_{s,8} h_{s,8} = \dot{m}_{air,3} h_{air,3} + \dot{m}_{s,3} h_{s,3}$$

Dividing by the inlet air mass flow rate, using the hint provided, and applying mass balance:

$$\alpha \cdot LHV_{f,in} + h_{air,2} + \beta \cdot h_{s,8} = (1 + \alpha)h_{air,3} + \beta h_{s,3}$$

where α is the fuel-to-air mass ratio, β is the steam-to-air mass ratio.

Calculating the enthalpies using EES:

$$h_{air,2} = 586.6 \text{ kJ/kg}, \quad h_{air,3} = 1543 \text{ kJ/kg}, \quad h_{s,3} = 5021 \text{ kJ/kg}, \quad h_{s,8} = 3323 \text{ kJ/kg}$$

Applying the first law to the HRSG, we arrive at the following:

$$\sum_{in} H_i = \sum_{out} H_i$$

$$\dot{m}_{air,4}h_{air,4} + \dot{m}_{s,4}h_{s,4} + \dot{m}_7h_7 = \dot{m}_{air,5}h_{air,5} + \dot{m}_{s,5}h_{s,5} + \dot{m}_8h_8$$

Dividing by the inlet air mass flow rate and rearranging, we arrive at:

$$(1 + \alpha)(h_{air,4} - h_{air,5}) + \beta(h_{s,4} - h_{s,5}) = \beta(h_8 - h_7)$$

The enthalpies are calculated to be:

$$h_{air,4} = 991.3 \text{ kJ/kg}, \quad h_{air,5} = 401.3 \text{ kJ/kg}, \quad h_{s,4} = 3880 \text{ kJ/kg}, \\ h_{s,5} = 2730 \text{ kJ/kg}$$

Solving the enthalpy balance equations of the combustor and HRSG yield:

$$\alpha = 0.03 \quad \text{and} \quad \beta = 0.2939$$

- b) Determine the net work produced by the cycle:**
[10.5 points Undergrad | 15.75 points Grad]

The net work produced by the cycle is given by:

$$W_{net} = W_T - W_c - W_p$$

where:

$$W_T = (1 + \alpha)(h_{air,3} - h_{air,4}) + \beta(h_{s,3} - h_{s,4}) = 903.7 \text{ kJ/kg}$$

$$W_c = h_2 - h_1 = 288.1 \text{ kJ/kg}$$

$$W_p = \beta(h_7 - h_6) = 0.3257 \text{ kJ/kg}$$

Therefore:

$$W_{net} = 903.7 - 288.1 - 0.3257 = 615.27 \text{ kJ/kg}$$

- c) Determine the thermal efficiency of the cycle: [3.5 points Undergrad | 5.25 points Grad]**

$$\eta_{th} = \frac{W_{net}}{\alpha \cdot LHV_f} = \frac{615.27}{0.03 \times 50050} = 40.98\%$$

- d) Determine the simple gas turbine cycle efficiency (without the steam injection):**
[3.5 points Undergrad | 5.25 points Grad]

$$\eta = 1 - \left(\frac{1}{\pi_p} \right)^{\frac{k-1}{k}} = 1 - \left(\frac{1}{9} \right)^{\frac{0.34}{1.34}} = 42.7\%$$

Problem 3 (32.5%)

- a) Determine the amount of steam produced in the HRSG per unit mass of air.
[12.5 points Undergrad | 18.75 points Grad]

We start by applying the first law to the HRSG:

$$\dot{m}_4(h_4 - h_5) = \dot{m}_7(h_8 - h_7)$$

Rearranging:

$$\alpha = \frac{h_4 - h_5}{h_8 - h_7}$$

We proceed to determining the enthalpies using EES and relationships from Chapter 5:

$$T_4 = T_3 \left(1 - \eta_{GT} \left[1 - (r_p)^{\frac{1-k}{k}} \right] \right) = 1500 \times \left(1 - 0.88 \left(1 - 8^{-\frac{0.323}{1.323}} \right) \right) = 975.1 \text{ K}$$

$$h_4 = 1018 \text{ kJ/kg}, \quad h_5 = 424.6 \text{ kJ/kg}$$

For state 6, the liquid water is a saturated liquid at $P_6 = 6 \text{ kPa}$:

$$h_6 = 151.5 \text{ kJ/kg}, \quad v_6 = 0.001 \text{ m}^3/\text{kg}$$

Noting water is incompressible, State 7 is the defined as:

$$h_{7s} = h_6 + v_6(p_7 - p_6) = 151.5 + 0.001(8000 - 6) = 159.5 \text{ kJ/kg}$$

$$h_7 = h_6 + \frac{h_{7s} - h_6}{\eta_p} = 151.5 + \frac{159.5 - 151.5}{0.7} = 162.9 \text{ kJ/kg}$$

State 8 is fixed by $T_8 = 723 \text{ K}$ and $p_8 = 8 \text{ MPa}$:

$$h_8 = 3273 \text{ kJ/kg}, \quad s_8 = 6.557 \text{ kJ/kg} \cdot \text{K}$$

Hence:

$$\alpha = \frac{h_4 - h_5}{h_8 - h_7} = \frac{1018 - 424.6}{3273 - 162.9} = 0.19$$

- b) Determine the work output of the gas and steam cycles:**
[12 points Undergrad | 18 points Grad]

For the gas cycle:

$$W_{net,GC} = W_{GT} - W_c$$

$$W_{GT} = h_3 - h_4$$

where:

$$h_3 = 1636 \text{ kJ/kg}$$

$$W_{GT} = h_3 - h_4 = 1636 - 1018 = 618 \text{ kJ/kg}$$

Similarly:

$$W_c = h_2 - h_1$$

$$T_2 = T_1 \left(1 + \frac{1}{\eta_c} \left[(r_p)^{\frac{k-1}{k}} - 1 \right] \right) = 300 \left(1 + \frac{1}{0.8} \left[(8)^{\frac{0.39}{1.39}} - 1 \right] \right) = 597.1 \text{ K}$$

$$h_1 = 300.4 \text{ kJ/kg}, h_2 = 604.3 \text{ kJ/kg}$$

$$W_c = h_2 - h_1 = 604.3 - 300.4 = 303.9 \text{ kJ/kg}$$

Therefore:

$$W_{net,GC} = W_{GT} - W_c = 618 - 303.9 = 314.1 \text{ kJ/kg}$$

For the steam cycle (note $p_9 = 6 \text{ kPa}$ and $s_{9s} = s_8$):

$$h_{9s} = 2019 \text{ kJ/kg}$$

$$h_9 = h_8 - \eta_{ST}(h_8 - h_{9s}) = 3273 - 0.9(3273 - 2019) = 2144.4 \text{ kJ/kg}$$

$$W_{ST} = \alpha(h_8 - h_9) = 0.19(3273 - 2144.4) = 214.4 \text{ kJ/kg}$$

$$W_p = \alpha(h_7 - h_6) = 0.19(162.9 - 151.5) = 2.166 \text{ kJ/kg}$$

$$W_{net,SC} = W_{ST} - W_p = 214.4 - 2.166 = 212.2 \text{ kJ/kg}$$

The net work output of the combined cycle is:

$$W_{net} = W_{net,GC} + W_{net,SC} = 526.3 \text{ kJ/kg}$$

- c) **Determine the thermal efficiency of gas and steam cycles if they would operate separately: [4 points Undergrad | 6 points Grad]**

The thermal efficiency of the gas turbine cycle alone is given by:

$$\eta_{th,GC} = \frac{W_{net,GC}}{q_{in}} = \frac{W_{net,GC}}{h_3 - h_2} = \frac{314.1}{1636 - 604.3} = 30.4\%$$

The thermal efficiency of the steam cycle alone is given by:

$$\eta_{th,SC} = \frac{W_{net,SC}}{\alpha(h_8 - h_7)} = \frac{212.2}{0.19(3273 - 162.9)} = 35.9\%$$

- d) **Determine the thermal efficiency of the combined cycle:
[4 points Undergrad | 6 points Grad]**

The thermal efficiency of the combined cycle is:

$$\eta_{th,CC} = \frac{W_{net}}{q_{in}} = \frac{526.3}{1636 - 604.3} = 51\%$$

The efficiency of the combined cycle is much higher than that of the simple cycles.

MIT OpenCourseWare
<https://ocw.mit.edu/>

2.60J Fundamentals of Advanced Energy Conversion
Spring 2020

For information about citing these materials or our Terms of Use, visit: <https://ocw.mit.edu/terms>.

Homework 5

2.60/2.62/10.390 Fundamentals of Advanced Energy Conversion
Spring 2020

Total points: 100 (Undergraduate) | 150 (Graduate)

Problem 1. Gas Turbine Powerplant with Pre-combustion Carbon Dioxide Capture [40% for Undergrads and Grads]

A gas turbine power plant operates on pre-combustion CO_2 capture as shown in **Figure 1**. Air at 298 K and 1 bar is used for reforming methane (298 K and 1 bar), and as a working fluid. The reformer operates at 1073 K. The reformate mixture passes through a heat exchanger where it preheats the air compressed to 10 bars, so its temperature reduces to 573 K before entering a shift reactor.

Superheated steam at 573 K reacts with CO of the reformate mixture allowing production of additional hydrogen. The byproducts of the shift reactor leave at 308 K, and then they are directed to a membrane separation unit where CO_2 is separated from the rest of the gaseous mixture. The pressure of the gaseous mixture is increased to 10 bars at the feed of the membrane unit. The permeate is a stream of CO_2 at 1 bar, whereas the retentate is a mixture of hydrogen and nitrogen which flows into the combustor.

The temperature of the combustion products is 1473 K. The isentropic efficiency of the compressors and the gas turbine are 75% and 88%, respectively. The exhaust of the gas turbine is at 1 bar, and it provides the heat requirement of the reformer, shift and steam production. Determine the thermal efficiency of the cycle, and the outlet temperature of the turbine exhaust gas.

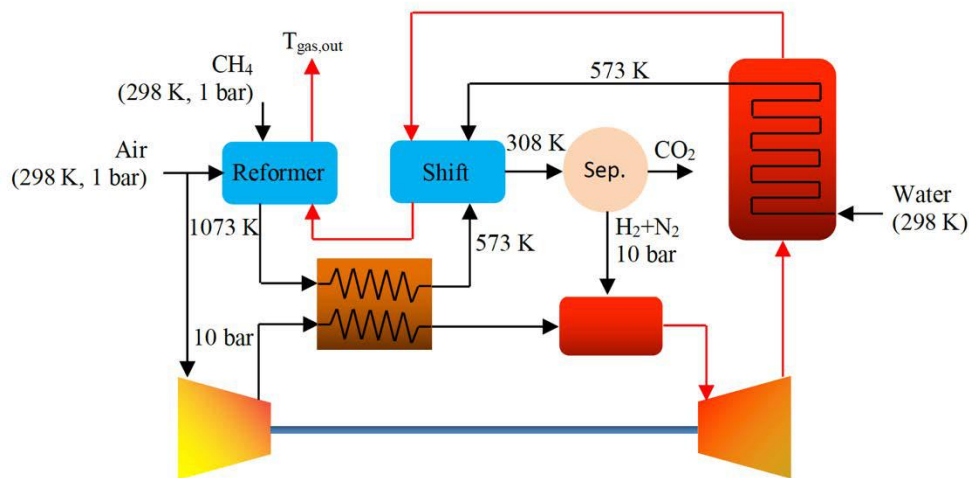


Figure 1 – Gas Turbine Powerplant with Pre-combustion CO_2 Capture

Problem 2. Chemical Looping-based Power Cycle [60% for Undergrads and Grads]

A chemical looping-based power cycle using Ni (metal) and NiO (metal oxide) and methane is schematically presented in **Figure 2**. The dotted line represents the chemical loop of the oxygen carriers (NiO/Ni). In the oxygen reactor, the highly exothermic metal oxidation reaction heats up the air stream, which is utilized to run turbine 1.

In the metal reduction reactor, the endothermic reduction reaction of NiO is used to oxidize methane to CO₂ and H₂O. While these two reactions proceed, the oxygen carriers (Ni/NiO) circulate the chemical loop drawn in dotted line. When the NiO particles are prepared, YSZ (Yttria-stabilized ZrO₂) is added to NiO to improve the reactivity (adding YSZ improves the porosity of the solid particles and raises the oxygen content). The mass ratio of NiO/YSZ is 3:2 when the mixture consists of only NiO and YSZ. To prevent carbon deposition on Ni surface, 3 moles of H₂O is added for each mole of CH₄ in metal oxidation reaction. The degree of reaction, X, is defined at the exit stream of each of the two reactors as follows:

$$X = \frac{m - m_{red}}{m_{ox} - m_{red}}$$

where m_{red} is the mass of the metal when it is fully reduced and m_{ox} is its mass when it is fully oxidized. m stands for the mass of the mixture of NiO and Ni. From experiments, it is shown that $X_{ox}=1$ at the exit of the oxidation reactor and $X_{red}=0.3$ at the exit of the reduction reactor.

The oxidation reactor and the reduction reactor are at 1500K and 900K, respectively. Both reactors are at 20 bars. Only solid particles (a mixture of Ni, NiO, YSZ) circulate through the chemical loop.

Assume that YSZ is ZrO₂ with molar weight is 123.2 kg/kmol. The enthalpy of reaction of metal oxidation reaction is $\Delta h_{ox} = -233.11$ kJ at 1500 K. The enthalpy of reaction of metal reduction reaction is $\Delta h_{red} = 141.38$ kJ at 900 K. The isentropic efficiencies of the compressor and turbines are 80% and 90%, respectively.

Methane is supplied at 20 bars, 300 K, and completely oxidized with NiO. The temperature of CH₄ at inlet of the reduction reactor is 730 K. For each mole of CH₄, 6 moles of air are supplied.

Determine:

- The composition of the chemical loop and the fuel exhaust stream at the exit of the reduction reactor.
- The composition of the chemical loop and the air stream at the exit of the oxidation reactor.
- The temperature of air at the inlet of the oxidation reactor.
- The temperature of the chemical loop at the inlet of the reduction reactor.

- e. The temperature at the exit of heat exchanger 2.
- f. The thermal efficiency of the plant with 100% CO₂ recovery rate, assuming a liquefaction work of 20 kJ per mole of methane.

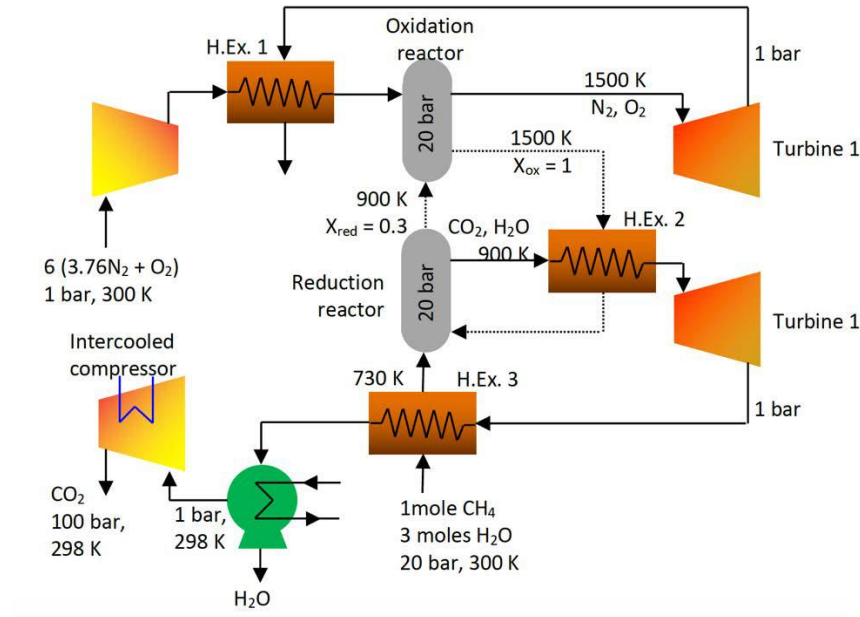


Figure 2 - Chemical Looping-based Power Cycle

MIT OpenCourseWare
<https://ocw.mit.edu/>

2.60J Fundamentals of Advanced Energy Conversion
Spring 2020

For information about citing these materials or our Terms of Use, visit: <https://ocw.mit.edu/terms>.

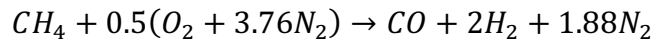
2.62 – Advanced Energy Conversion | Spring 2020

Homework 5 – Solutions

Problem 1 (40%)

A gas turbine power plant operates on pre-combustion CO₂ capture as shown in the figure provided. Determine the thermal efficiency of the cycle, and the outlet temperature of the turbine exhaust gas:

First, we start by noting the reaction occurring in the reformer: [15 points]



Applying the first law to the reformer:

$$Q_R = \sum_{products} H_i - \sum_{reactants} H_i$$

$$Q_R = \hat{h}_{CO}^{1073K} + 2\hat{h}_{H_2}^{1073K} + 1.88\hat{h}_{N_2}^{1073K} - (\hat{h}_{CH_4}^{298K} + 0.5\hat{h}_{O_2}^{298K} + 1.88\hat{h}_{N_2}^{298K})$$

The following thermodynamic properties have been used in the calculation:

Enthalpy of formations	Specific heat
$\hat{h}_{f,H_2O(g)}^o = -242 \text{ kJ/mol}$	$\hat{c}_{p,O_2} = 33.4 \text{ J/mol.K}$
$\hat{h}_{f,H_2O(l)}^o = -286 \text{ kJ/mol}$	$\hat{c}_{p,N_2} = 31.1 \text{ J/mol.K}$
$\hat{h}_{f,CO}^o = -110.6 \text{ kJ/mol}$	$\hat{c}_{p,CO_2} = 50.6 \text{ J/mol.K}$
$\hat{h}_{f,CO_2}^o = -393.8 \text{ kJ/mol}$	$\hat{c}_{p,H_2} = 30.0 \text{ J/mol.K}$
$\hat{h}_{f,CH_4}^o = -74.9 \text{ kJ/mol}$	$\hat{c}_{p,CO} = 29.3 \text{ J/mol.K}$
	$\hat{c}_{p,H_2O} = 38.2 \text{ J/mol.K}$
	$\hat{c}_{p,CH_4} = 46.35 \text{ J/mol.K}$

Taking the ambient conditions as the reference temperature, the heat supplied to the reformer is calculated to be:

$$Q_R = 78,820 \text{ kJ per kmol of } CH_4$$

For each kmol of methane fed to the reformer, 78820 kJ of heat should be supplied for the reforming of methane with air to occur.

Next, we analyze the air compressor using relationships from Chapter 5. The outlet temperature of the compressor is calculated as: [5 points]

$$T_{AC,o} = T_{AC,in} \left[1 + \frac{\left(\frac{p_o}{p_{in}} \right)^{\frac{k_{air}-1}{k_{air}}} - 1}{\eta_c} \right] = 298 \times \left[1 + \frac{10^{\frac{1.388-1}{1.388}} - 1}{0.75} \right] = 657 \text{ K}$$

Similarly, the first law is applied on one end of the heat exchanger yields: [15 points]

$$Q_{HEX} = (\hat{h}_{CO}^{1073K} - \hat{h}_{CO}^{673K}) + 2(\hat{h}_{H_2}^{1073K} - \hat{h}_{H_2}^{673K}) + 1.88(\hat{h}_{N_2}^{1073K} - \hat{h}_{N_2}^{673K})$$

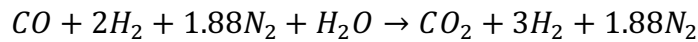
Note the reformat mixture should be leaving the HX at 673K (and not 573 K as mentioned in error by the problem statement).

$$Q_{HEX} = 59,107 \text{ kJ per kmol of CH}_4$$

Applying the first law on the other end of the heat exchanger yields Eq. 1:

$$Q_{HEX} = a(\hat{h}_{O_2}^{T_{HEX,o}} - \hat{h}_{O_2}^{T_{AC,o}}) + 3.76a(\hat{h}_{N_2}^{T_{HEX,o}} - \hat{h}_{N_2}^{T_{AC,o}})$$

In analyzing the shift reactor, we note the reaction occurring: [15 points]



By the first law:

$$Q_s = \hat{h}_{CO_2}^{308K} + 3\hat{h}_{H_2}^{308K} + 1.88\hat{h}_{N_2}^{308K} - (\hat{h}_{CO}^{673K} + 2\hat{h}_{H_2}^{673K} + 1.88\hat{h}_{N_2}^{673K} + \hat{h}_{H_2O}^{573K})$$

$$Q_s = -105,127 \text{ kJ per kmol of CH}_4$$

The heat requirement of the shift reactor is -105,127 kJ for each kmol of methane.

To analyze the separator compressor, we first need to determine the specific heat of the gas mixture: **[10 points]**

$$\hat{c}_{p, mix} = \sum_i \frac{n_i}{n_t} \hat{c}_{p,i} = \sum_i X_i \hat{c}_{p,i} = \frac{1}{5.88} \hat{c}_{p, CO_2} + \frac{3}{5.88} \hat{c}_{p, H_2} + \frac{1.88}{5.88} \hat{c}_{p, N_2} = 33.86 \text{ J/mol} \cdot \text{K}$$

$$k_{mix} = \frac{\hat{c}_{p, mix}}{\hat{c}_{p, mix} - 8.314} = 1.33$$

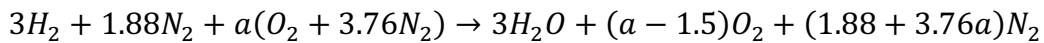
$$T_{Comp,o} = T_{Comp,in} \left[1 + \frac{\left(\frac{p_o}{p_{in}} \right)^{\frac{k_{mix}-1}{k_{mix}}} - 1}{\eta_c} \right] = 308 \times \left[1 + \frac{10^{\frac{1.33-1}{1.33}} - 1}{0.75} \right] = 624.5 \text{ K}$$

The work required by the process is calculated:

$$W_{SC} = (\hat{h}_{CO_2}^{624.5K} - \hat{h}_{CO_2}^{308K}) + 3(\hat{h}_{H_2}^{624.5K} - \hat{h}_{H_2}^{308K}) + 1.88(\hat{h}_{N_2}^{624.5K} - \hat{h}_{N_2}^{308K})$$

$$W_{SC} = 63,005 \text{ kJ per kmol of CH}_4$$

The next step is to analyze the combustor. We start by noting the reaction occurring: **[15 points]**



By the first law, we arrive at Eq. 2:

$$\begin{aligned} 3\hat{h}_{H_2}^{624.5K} + 1.88\hat{h}_{N_2}^{624.5K} + a(\hat{h}_{O_2}^{T_{HEX,o}} + 3.76\hat{h}_{N_2}^{T_{HEX,o}}) \\ = 3\hat{h}_{H_2O}^{1473K} + (a - 1.5)\hat{h}_{O_2}^{1473K} + (1.88 + 3.76a)\hat{h}_{N_2}^{1473K} \end{aligned}$$

Combining Equations 1 and 2 to solve for the unknowns a and $T_{HEX,o}$:

$$a = 5.238$$

$$T_{HEX,o} = 732.1 \text{ K}$$

Analyzing the gas turbine: [5 points]

$$\hat{c}_{p,mix} = \sum_i \frac{n_i}{n_t} \hat{c}_{p,i} = \sum_i X_i \hat{c}_{p,i} = \frac{3}{28.57} \hat{c}_{p,H_2O} + \frac{3.738}{28.31} \hat{c}_{p,O_2} + \frac{21.57}{28.31} \hat{c}_{p,N_2} = 32.11 \text{ J/mol} \cdot \text{K}$$

$$k_{mix} = \frac{\hat{c}_{p,mix}}{\hat{c}_{p,mix} - 8.314} = 1.35$$

$$T_{T,out} = T_{T,in} \left(1 - \eta_T \left[1 - (r_p)^{\frac{1-k_{mix}}{k_{mix}}} \right] \right) = 1473 \left(1 - 0.88 \left[1 - (0.1)^{\frac{1.35-1}{1.35}} \right] \right) = 890.3 \text{ K}$$

$$W_T = 3(\hat{h}_{H_2O}^{1473K} - \hat{h}_{H_2O}^{890.3K}) + 3.738(\hat{h}_{O_2}^{1473K} - \hat{h}_{O_2}^{890.3K}) + 21.57(\hat{h}_{N_2}^{1473K} - \hat{h}_{N_2}^{890.3K})$$

$$W_T = 530,521 \text{ kJ per kmol of CH}_4$$

The net work produced by the power cycle may be calculated according to: [2.5 points]

$$W_{net} = W_T - W_{AC} - W_{SC}$$

where

$$W_{AC} = 5.238(\hat{h}_{O_2}^{657K} - \hat{h}_{O_2}^{298K}) + 19.69(\hat{h}_{N_2}^{657K} - \hat{h}_{N_2}^{298K}) = 282,707 \text{ kJ per kmol of CH}_4$$

Therefore:

$$W_{net} = 530,521 - 282,707 - 63,005 = 184,809 \text{ kJ per kmol of CH}_4$$

For every kmol of methane used in the system, 184,809 kJ net power is produced.

The thermal efficiency of the power cycle is therefore obtained as: [2.5 points]

$$\eta_{th} = \frac{W_{net}}{M_{CH_4} LHV} = \frac{184,809}{16 \times 50050} = 23.1\%$$

To determine the turbine exhaust temperature, we write the following equation: [15 points]

$$3 \left(\hat{h}_{H_2O}^{890.3\text{ K}} - \hat{h}_{H_2O}^{T_{g,out}} \right) + 3.738 \left(\hat{h}_{O_2}^{890.3\text{ K}} - \hat{h}_{O_2}^{T_{g,out}} \right) + 21.57 \left(\hat{h}_{N_2}^{890.3\text{ K}} - \hat{h}_{N_2}^{T_{g,out}} \right) = Q_R + Q_s + Q_B$$

where:

$$\begin{aligned} Q_B &= \left(\hat{h}_{H_2O}^{573\text{ K}} - \hat{h}_{H_2O}^{298\text{ K}} \right) = (\Delta H_v + \Delta H_s) \\ &= (40,650\text{ kJ} + 75.3\{373 - 298\} + 38.2\{573 - 273\}) \\ &= 57,757.5\text{ kJ per kmol of CH}_4 \end{aligned}$$

Therefore:

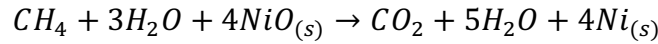
$$T_{gas,out} = 856.4\text{ K}$$

The thermal efficiency is rather low; this is a simple cycle. The poor efficiency is because of the low pressure ratio and lower maximum, temperature in the gas turbine cycle, CO₂ separation and the several heat transfer irreversibility in the heat transfer components. Adding a steam cycle as a bottoming cycle could raise the efficiency.

Problem 2 (60%)

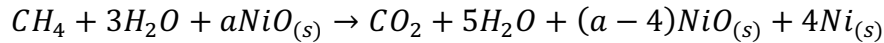
- a) Determine the composition of the chemical loop and the fuel exhaust stream at the exit of the reduction reactor: [25 points]

We start by noting the chemical reaction within the reduction reactor is:



Note that the fuel exhaust stream is $CO_2 + 5H_2O$.

Denoting a as the number of moles entering the oxidation reactor:



Using the definition of the degree of reaction:

$$X_{red} = \frac{m - m_{Red}}{m_{Ox} - m_{Red}} = \frac{[(a - 4)M_{NiO} + 4M_{Ni}] - aM_{Ni}}{aM_{NiO} - aM_{Ni}} = 0.3$$

Noting that $M_{NiO} = 74.7$ kg/kmol and $M_{Ni} = 58.7$ kg/kmol, and solving for a , we arrive at:

$$a = 5.714$$

In other words, 70% of the NiO entering the reduction reactor is reacted with one mole of methane. So, 5.714 moles of NiO enters the reduction reactor and 1.714 moles of NiO leaves unreacted.

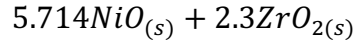
Noting that the mass ratio of NiO to YSZ is 3:2 when $X = 1$:

$$\frac{(nM)_{NiO}}{(nM)_{YSZ}} = \frac{3}{2} \Rightarrow \frac{n_{YSZ}}{n_{NiO}} = \frac{2}{3} \left(\frac{M_{NiO}}{M_{YSZ}} \right) = \frac{2}{3} \times \frac{74.7}{123.2} = 0.4$$

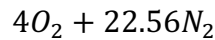
Hence, the number of moles of ZrO_2 is $n_{YSZ} = 0.4 \times 5.714 = 2.3$, and the chemical loop composition is $1.714NiO_{(s)} + 4Ni_{(s)} + 2.3ZrO_{2(s)}$.

- b) Determine the composition of the chemical loop and the air stream at the exit of the oxidation reactor: [10 points]

The composition of the chemical loop into the reduction reactor only includes NiO since $X_{Ox} = 1$. All Ni is oxidized to NiO in the oxidation reactor, and the composition is given by:



For the air stream: $4Ni_{(s)} + 2O_2 \rightarrow 4NiO_{(s)}$. Thus, 2 moles of O_2 (out of the 6 supplied) are used to oxidize Ni(s). The composition of the exit air stream is:



- c) Determine the temperature of air at the inlet of the oxidation reactor: [15 points]

Applying the first law to the oxidation reactor:

$$\begin{aligned} (6h_{O_2}^T + 22.56h_{N_2}^T) + (1.71h_{NiO}^{900K} + 4h_{Ni}^{900K} + 2.3h_{ZrO_2}^{900K}) \\ = (4h_{O_2}^{1500K} + 22.56h_{N_2}^{1500K}) + (5.71h_{NiO}^{1500K} + 2.3h_{ZrO_2}^{1500K}) \end{aligned}$$

$$\begin{aligned} 4\Delta h_{Ox}^{1500K} = (6c_{p,O_2} + 22.56c_{p,N_2})(1500 - T) \\ + (1.71c_{p,NiO} + 4c_{p,Ni} + 2.3c_{p,ZrO_2})(1500 - 900) \end{aligned}$$

The exothermic enthalpy of the reaction is used to heat up the reactants to the oxidation reactor temperature, 1500K. A solution of the above yields:

$$T = 759.5 \text{ K}$$

- d) Determine the temperature of the chemical loop at the inlet of the reduction reactor: [15 points]

Applying the first law to the reduction reactor:

$$\begin{aligned} (h_{CH_4}^{730K} + 3h_{H_2O}^{730K}) + (5.71h_{NiO}^T + 2.3h_{ZrO_2}^T) \\ = (1.71h_{NiO}^{900K} + 4h_{Ni}^{900K} + 2.3h_{ZrO_2}^{900K}) + (h_{CO_2}^{900K} + 5h_{H_2O}^{900K}) \end{aligned}$$

$$\Rightarrow \Delta h_{Red}^{900K} + (c_{p,CH_4} + 3c_{p,H_2O})(900 - 730) = (5.71c_{p,NiO} + 2.3c_{p,ZrO_2})(T - 900)$$

The inlet stream is cooled down to 900 K by the endothermic reduction reaction and by heating up the fuel stream to 900 K. Solving the above equation, we arrive at:

$$T = 1246 \text{ K}$$

e) Determine the temperature at the exit of heat exchanger 2: [10 points]

Applying the first law to heat exchanger 2 yields:

$$(c_{p,CO_2} + 5c_{p,H_2O})(T - 900) = (5.71c_{p,NiO} + 2.3c_{p,ZrO_2})(1500 - 1246)$$

Solving for the exit temperature we arrive at:

$$T = 1392 \text{ K}$$

f) Determine the thermal efficiency of the plant with 100% CO₂ recovery rate, assuming a liquefaction work of 20 kJ per mole of methane: [25 points]

The thermal efficiency of the plant is calculated as:

$$\eta_{th} = \frac{W_{T_1} + W_{T_2} - W_c - W_{liq}}{LHV_{CH_4}}$$

In this calculation, we note (specific heats calculated as in Problem 1):

$$W_{T_1} = n_1 \eta_T c_{p,1} T_{in} \left(1 - \pi_p^{-R/c_p} \right) = 26.56 \times 0.9 \times 32.43 \times 1500 \times \left(1 - 20^{-\frac{8.314}{32.43}} \right) = 623,341 \text{ J}$$

$$W_{T_2} = n_2 \eta_T c_{p,2} T_{in} \left(1 - \pi_p^{-R/c_p} \right) = 6 \times 0.9 \times 42.15 \times 1392 \times \left(1 - 20^{-\frac{8.314}{42.15}} \right) = 141,362 \text{ J}$$

$$W_c = \frac{n_3 c_{p,3} T_{in}}{\eta_c} \left(\pi_p^{R/c_p} - 1 \right) = \frac{28.56 \times 32.56 \times 298}{0.8} \left(20^{8.314/32.56} - 1 \right) = 397,960 \text{ J}$$

Consequently:

$$\eta_{th} = \frac{623,341 + 141,362 - 397,960 - 20,000}{16 \times 50,050} = 43\%$$

MIT OpenCourseWare
<https://ocw.mit.edu/>

2.60J Fundamentals of Advanced Energy Conversion
Spring 2020

For information about citing these materials or our Terms of Use, visit: <https://ocw.mit.edu/terms>.